جامعة قطر
QATAR UNIVERSITY

دولة قطر
وزارة البلدية والبيئة

هيئة الأشغال العامة
Public Works Authority
قطر تستحق الأفضل
Qatar Deserves The Best

Proceedings of the International Conference on Civil Infrastructure and Construction (CIC 2020)

Editor-in-Chief:
Okan Sirin

Editors:
Usama Ebead
Hisham Eid
Murat Gunduz
Mohammed Hussein

دار نشر جامعة قطر
Qatar University Press

جامعة قطر
QATAR UNIVERSITY

هيئة الأشغال العامة
Public Works Authority
قطر تستحق الأفضل
Qatar Deserves The Best

Proceedings of the International Conference on Civil Infrastructure and Construction (CIC 2020)

Editor-in-Chief:
Okan Sirin

Editors:
Usama Ebead
Hisham Eid
Murat Gunduz
Mohammed Hussein

دار نشر جامعة قطر
Qatar University Press

Proceedings of the International Conference on Civil Infrastructure and Construction (CIC 2020)

Editor-in-Chief: Okan Sirin (Qatar University, Qatar)
Editors: Usama Ebead, Hisham Eid, Murat Gunduz, Mohammed Hussein

Doha – Qatar
P. O. Box: 2713 Doha – Qatar
Email: qupress@qu.edu.qa

Foreword of Qatar University President

On behalf of the Qatar University community, we consider it an honor and a privilege to organize the International Conference on Civil Infrastructure and Construction (CIC 2020) alongside the Public Works Authority "Ashghal" and the Ministry of Municipality and Environment, which took place from 2 to 5 February 2020.

The conference is the first and largest of its kind in Qatar and the Middle East. It provides a platform to discuss the next-generation infrastructure and its construction among key players such as researchers, industry professionals and leaders, local government, clients, construction contractors and policymakers of the construction industry. The conference places a special emphasis on important aspects of the industrial sector such as sustainability, innovation and technological impact.

It is with great pleasure that we welcome a large number of technical contributions from academia and industry, both inside and outside Qatar. The conference has accepted 127 papers from 20 different countries. It is also a great pleasure to welcome key figures of this industry in Qatar who are addressing the conference to reflect the major successes Qatar witnessed in the field of infrastructure and construction and share this success with the whole world. I would also like to highlight the contributions of the keynote speakers who represent top international institutions in civil infrastructure and construction.

Finally, I would like to thank the organizing committee of the CIC 2020 conference for their work towards making this conference a great success, the scientific committee for their work in ensuring the highest quality of contributions and the major stakeholders in Qatar for their support and sponsorship. I am also pleased to see the product of this conference as the first proceedings published by Qatar University Press (QU Press), QU's publishing house for peer-reviewed academic and research-based works. Last but not least, I would like to extend my appreciation towards our partners the Public Works Authority of Qatar "Ashghal" and the Ministry of Municipality and Environment who we collaborated with successfully to organize this valuable conference.

Dr. Hassan Al-Derham
Qatar University President

Foreword of the President of the Public Works Authority (Ashghal)

The Public Works Authority 'Ashghal' continues its journey of implementing sustainable infrastructure for the State of Qatar; a journey that has taken Qatar to the level of highly developed countries in the world.

So far, Ashghal has accomplished more than 750 km of highway network, out of which more than 120 km was done in 2019 and more than 50% of materials used in construction were of Qatari origin. Thus, Ashghal has taken a qualitative leap in connecting all regions, enhancing traffic throughout the country. Notably, 95% of the highway networks accomplished by Ashghal link the World Cup stadiums, contributing to the hassle free commutation of football fans to the stadiums, as seen in the recent games conducted, including FIFA Clubs World Cup and the Gulf Cup.

The previous year 2019 was also a year of accomplishments for Ashghal in relation to the completion of more than 400kms of local road networks and an integrated infrastructure to serve many residential areas and more than 1300 housing subdivisions. In 2019, Ashghal also signed seven new contracts, valued at above QAR3.2bn to serve 3090 housing subdivisions, which included five projects to develop roads and infrastructure for citizens' subdivisions.

Another milestone of Ashghal's achievement is the recent completion of land reclamation and rehabilitation project in Karaana Lagoon for removing pollutants and reducing health risks to the environment surrounding the lagoon of natural habitats.

Within the Mesaimeer Tunnel project, Ashghal has started excavation works for the 10-kilometer micro tunneling works. This tunnel will absorb surface water and storm water through the rainwater drainage networks in most areas of Doha city. The waters absorbed will undergo treatment process as per international standards, through Mesaimeer pumping station and outfall, which is one of the longest outfall tunnels in the world.

This year has also witnessed start of another vital project for rehabilitation and development of four drainage pumping stations to increase the capacity of pumping stations by 62% to 211%, in consideration of the current and future needs for sewage flows.

Ashghal also undertakes the tasks of overseeing the executed projects through the operation and maintenance departments of roads and drainage networks. These departments function to monitor and maintain Ashghal assets through dedicated centers equipped with highest level of technology and modern solutions.

Thus, in 2019, Ashghal achieved maintenance and re-pavement of over 455 kilometers of roads through framework contracts for different regions of the country. Within the five-year plan for the period (2018-2022), Ashghal is implementing 25 plans related to assessment and monitoring of road safety including achievement of safety at work sites, managing traffic congestion, implementing intelligent transportation system (ITS), road design safety, traffic safety, as well as asset management. The road operation and maintenance plan also includes the emergency response team to carryout urgent maintenance works, evaluate road signage, ensure pedestrian safety and manage traffic congestion during the hosting of FIFA World Cup Qatar 2022.

Dr. Eng. Saad bin Ahmad Al Muhannadi
President of the Public Works Authority (Ashghal)

Foreword of the Assistant Undersecretary for Urban Planning Affairs – Ministry of Municipality and Environment

The State of Qatar is going through an extraordinary development in building infrastructure for the entire country. The Ministry of Municipality & Environment and other relevant agencies have been collaborating and working together to build sustainable, smart and modern infrastructure in line with the Qatar National Vision 2030 and to achieve the objectives of the Second Qatar National Development Strategy (QNDS-2) 2018-2022. The Ministry plays a big role in the urban planning, environmental and general services sectors through the 8 different municipalities spread across the State of Qatar.

The Urban Planning Sector of the Ministry is committing to urban and infrastructure planning for the country. The Qatar National Development Framework 2032 (QNDF) was prepared by the Urban Planning Sector and approved by His Highness the Emir of Qatar in December 2014. It establishes the spatial framework to achieve national human, social, economic and environmental goals based on the Qatar National Vision 2030 and based on the population and economic projections by the Planning and Statistics Authority.

Moreover, the Urban Planning Sector at the Ministry of Municipality and Environment has completed numerous infrastructure planning studies to aid the infrastructure planning and optimize the efficiency of infrastructure planning in the State of Qatar. Those projects included but not limited to: Qatar Rainfall and Runoff Manual, Assessment of Outfalls in Qatar, Qatar Flood Study, Qatar Geological Mapping – Phase I and Radar Interferometric study for Qatar. Currently, the Sector is carrying out many new infrastructure planning studies such as: The Qatar National Infrastructure Plan and The National Infrastructure Database. These studies will help the industry and the relevant entities in the infrastructure field to improve the infrastructure planning and implementation.

This conference will be a great opportunity for knowledge exchange, sharing success stories and discussing infrastructure and construction challenges. One of the Key outcomes of this conference will be bridging the gap between theoretical research and the practical domain. Currently, the Ministry is working with local and global universities and research institutes on many applied research projects in the infrastructure and construction areas.

The Ministry would like to express its appreciation for all contributions and support received from different agencies and academia in this conference and looks forward to their continued cooperation and commitment in implementing the outcome of this conference.

His Excellency Eng. Fahad Mohd Al Qahtani
Assistant Undersecretary For Urban Planning Affairs
Ministry of Municipality and Environment

Foreword of the Dean of Qatar University College of Engineering

I am pleased to write this foreword for the proceedings of the International Conference on Civil Infrastructure and Construction (CIC 2020). The conference is the outcome of a strong effort by the College of Engineering at Qatar University and the fruitful collaboration with our strategic partners, the Public Works Authority (Ashghal), and the Ministry of Municipality and Environment.

This conference is a major event within the World Congress for Engineering & Technology (WETC-2020) that the College of Engineering is organizing as part of the celebration of its 40th anniversary. Over the past four decades, the College has gained a strong national and regional reputation; this has been achieved through the distinguished dedication of faculty and employees, as well as through the strategic partnership with the main and key industry stakeholders in Qatar. During the past decade, the College succeeded in attracting more than $ 150 million of research funds, which was directed towards addressing various industrial challenges and improving the quality of the various industrial sectors in the State of Qatar.

The International Conference on Civil Infrastructure and Construction (CIC 2020) is one of a number of initiatives that the College has introduced in order to provide the right forum for the exchange of experience, as well as, for the presentation of the latest technology and the state-of-the-art knowledge in the field of infrastructure and construction. The conference is one of the activities that enforce the College effort in supporting the Qatar National Vision 2030 and an important platform to showcase the major advances that Qatar has witnessed in its infrastructure with the international engineering and scientific community. The conference will provide an excellent opportunity for transforming the knowledge to the future generation of engineers in Qatar and, in particular, to the students of Qatar University.

Finally, I would like to thank our organization partners, the supporting companies, the professional partners, the keynote and executive speakers, and the teams who worked hard in organizing this conference. I wish our delegates to have the maximum benefit from the conference besides a pleasant and enjoyable stay for the delegates from outside Qatar.

Dr. Khalid Kamal Naji
Dean of College of Engineering, Qatar University

Sponsors

Platinum

Gold

Silver

Professional Partners

Keynote Speaker

Kancheepuram N. Gunalan,

Ph.D, P.E.
ASCE 2020 President
American Society of Civil Engineers, USA

K.N. Gunalan (Guna) is Senior Vice President of Transportation Alternative Delivery, Americas at AECOM, based in Salt Lake City, UT. Previously, he was vice president at Parsons Brinckerhoff.

Guna has managed large complex infrastructure projects, providing technical advice on civil, structural, geotechnical, pavement, and materials issues on a variety of projects around the world. His collaborative approach has contributed to many successful programs and projects ranging from a few thousand to more than 3 billion dollars.

He has been active in ASCE for many years, including leadership roles as Region 8 director (2009-2012), Region 8 governor (2005-2007), Utah Section president (2002-2003), and Texas Section High Plains Branch president (1992). He served as the chair of ASCE's 2014 Global Engineering Conference in Panama City, Panama, in celebration of the 100th anniversary of the Panama Canal. Most recently, he served as the governor for the Geo-Institute and was a member of the steering committee for the 2017 ASCE India Conference.

Guna has been married for 38 years to Duru. They have a son, Kabilar, and a daughter, Pallavi. He loves to read, travel, and learn about new cultures.

Abstract for Keynote Presentation

Geotechnical Aspects of Mega Transportation Projects in the future

Major transportation projects are being delivered using Public Private Partnerships (PPP) wherein the private sector is primarily focused on mitigating financial risk in meeting long term performance criteria/ requirements of specific elements of work. Additionally, the time provided to develop a technical/ cost proposal for these mega transportation projects is getting shorter and shorter as the agencies are being forced to deliver them in a much accelerated manner. Therefore, development of a successful proposal, delivery and long term performance of mega transportation facilities rely heavily on a very diligent and a pragmatic design by the geotechnical engineer who not only understands how to design the various elements meeting the prescribed performance criteria but also has the experience to predict performance over the life of the contract so as to minimize long term maintenance costs. We have all heard various geo legends say, "a successful practitioner is one who exercises good judgement in addition to having a sound understanding of fundamental behavior of soils in a given environment". This presentation provides a very brief overview on the challenges faced by the geo-professionals on delivery of large, complex projects, sometimes in very challenging geotechnical settings. It also provides a brief insight into what it takes to set up a successful program that can be delivered on time and under budget, including the definition of performance, geotechnical performance criteria and what it takes to understand and develop geotechnical performance criteria.

Keynote Speaker

Randy Black

Chair of 2019 Board of Directors
Project Management Institute, USA

Randy Black is the owner and principal of Edutainer53 Consulting Limited, an Edmonton-based consulting organization focused upon project management, operations consulting and training. He has volunteered with PMI for more than 12 years and served on the PMI Board of Directors since 2016, including service as Board Chair in 2019.

Throughout his 40-year career, he has worked in a variety of industries including telecommunications, IT consulting, e-learning development, project management training and consulting, and PMO management. As a project management consultant and trainer, he has led consulting work in a variety of industries and taught courses as part of executive education training offered through Alberta-based colleges and the University of Alberta.

Mr. Black earned his B.A Sc. In Civil Engineering from the University of Waterloo. Mr. Black holds a Professional Engineering (P. Eng.) designation registered in the Province of Alberta, and has held his PMP® designation since 2004.

Abstract for Keynote Presentation

Welcome to the Project Economy: Global Trends Reshaping the Projectized Future of Construction and Civil Engineering

Major infrastructure and construction projects across the Middle East and around the world continue to drive demand for effective project management skills. In a fast-moving global economy defined by digital disruption, such projects will increasingly demand knowledge of a wide range of emerging capabilities and technologies, including artificial intelligence, machine learning, and agile practices.

In this presentation, Randy Black of the Project Management Institute's Board of Directors will deliver insights from PMI's latest analysis of long-term trends reshaping virtually every sector, especially civil engineering and construction - from shifting global demographics to a growing focus on environmental sustainability. Randy will share his unique perspective on how PMI is advocating for the importance of effective project management to organizations around the world – while enabling individuals to acquire the project skills they need to succeed throughout each step of their career journeys.

Attendees will gain a greater understanding of how to succeed in an increasingly projected environment – and how project teams around the world can work effectively to deliver strategic value for major initiatives, focused on construction, infrastructure, and a wide range of other sectors.

Keynote Speaker

Rachel Skinner

BSc (Hons) MSc (Eng) FREng CEng FICE CTPP MCIHT
Senior Vice President
Institution of Civil Engineers & WSP UK Head of Transport

Rachel Skinner is the Senior Vice President of the Institution of Civil Engineers and WSP's UK Head of Transport. She was recently invited to become a Fellow of the Royal Academy of Engineering and is both a Chartered Engineer and a Chartered Transport Planner. She is an Infrastructure Commissioner for Scotland and a Patron of Women in Transport.

Rachel has authored influential publications on future mobility and place-making, digital potential, industry innovation and collaboration. She leads projects for national, sub-national and local government clients, also for private investors and strategic land-owners, and has a fast-growing portfolio of future mobility projects in the UK and overseas. Rachel has been named in Top 100 Women in Engineering (Financial Times, 2019), as the "Most Distinguished Winner", "Best Woman in Civil Engineering" (European Women in Construction and Engineering Awards, 2017), and as one of the Top 50 Influential Women in Engineering (The Telegraph, 2017).

Abstract for Keynote Presentation

Connectivity, carbon and change: towards better transport outcomes by 2040

Around the world, mobility is changing fast and will continue to evolve across many dimensions of technological change and inter-generational behavioral shift. New urgency around climate change, and the significant contribution of road transport to carbon emissions over recent decades, means that the specific need to decarbonize our existing systems adds fresh impetus, direction and purpose. We have many possible options ahead of us and the long run outcomes to 2040 and beyond – good or bad – that will depend heavily on the strategy and policy mix adopted from now, and the extent to which new technologies are encouraged to engage and support them.

Rachel will explore the new opportunities that exist to address widespread transport challenges such as congestion, safety and urban air quality whilst also seeking the best outcomes to support an agenda for both net zero carbon and an emphasis on equality and 'levelling up'. She will focus on the importance of local context and tailored solutions that consider people, goods and services to create the best possible outcomes for a growing population, thriving places and transport connectivity.

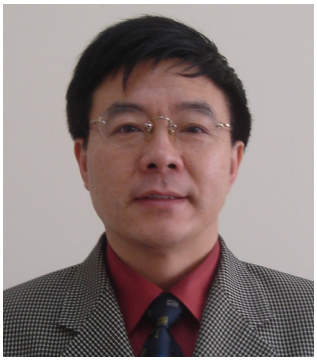

Keynote Speaker

Yaojun Ge

Professor
Department of Bridge Engineering
Tongji University, Shanghai, China
President of the International Association for Bridge and Structural Engineering (IABSE)

Yaojun Ge has been working at Tongji University, specializing in bridge structural analysis, wind engineering, and bridge aerodynamics for more than 35 years. He has contributed to many R&D key projects, including five projects of Natural Science Foundation of China and over 50 major bridge projects, including Shanghai Lupu Bridge as the world's longest arch bridge, Hong Kong-Zhuhai-Macau Bridge as the world's longest sea crossing bridge, Xihoumen Bridge as the world's longest box-girder suspension bridge. He has published 9 books and more than 300 technical papers, and has made over 30 keynote presentations in international conferences. He has received several Chinese National Awards and T. Y. Lin Medal 2016 and ICARO Award from the international community. He has been elected as President of International Association for Bridge and Structural Engineering (IABSE), and is the current President of Bridge and Structural Engineering Institution of China.

Abstract for Keynote Presentation

Scientific Discovery, Technological Innovation and Engineering Creation in Bridge Engineering

Scientific research has the primary goal of advancement and dissemination of knowledge. An important means of accomplishing this goal is through peer-reviewed scientific papers published in science and technology periodicals, such as IABSE's Structural Engineering International. IABSE created the Outstanding Paper Award in 1992 to recognize the authors of papers published in the preceding year's issues of the SEI. In total, 28 scientific papers and eight technical reports have received the award over the past 28 years. The topics covered by these works include structural materials such as carbon fiber reinforced polymer, reinforced and post-tensioned glass and soil-steel systems; new mechanical models including the ones to determine traffic loads on bridges, tension chord models and robustness design models; and structural mechanisms and controls relating to vibration mechanism and control, tuned vibration absorbers and the performance of structural systems in shear. Technological development produces innovative technology, which includes the invention of new techniques, the improvement of existing techniques and the integration of two or more good techniques to produce benefits or value-added results. IABSE does not have any specific award for technological innovation, but some innovative technologies in bridge and structural engineering that were introduced in the technical reports obtained Outstanding Paper Awards and were recognized in the engineering projects that received Outstanding Structural Awards. The highest goal of engineering construction is the creation of new engineering structures, which generally involves the use of new materials, new structural systems or new methods of construction. IABSE established the Outstanding Structural Award in 2000 as one of its highest distinctions. In the past 20 years, 27 bridges and 27 other structures around the world have been recognized as Award Winners or Finalists. Bridges receiving recognition for the use of new materials include the Bras de la Plaine Bridge in the French territory of la Reunion, the Tri-Countries Bridge in Germany and the Viaduct over the River Almonte in Spain. Bridges recognized in the category of new structure creation include the Sunniberg Bridge in Switzerland, the Xihoumen Bridge in China and the Yavuz Sultan Selim Bridge in Turkey. Works recognized for new methods include the Millau Bridge in France, the Rion-Antirion Bridge in Greece, and the Taizhou Bridge in China

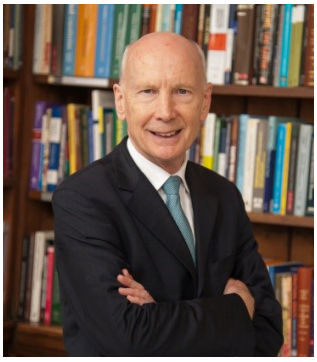

Keynote Speaker

Robert Mair

CBE FREng FICE FRS NAE
Professor
University of Cambridge, UK

Robert Mair is Emeritus Professor of Civil Engineering and Director of Research at Cambridge University, where until recently he was Head of Civil Engineering. He was Master of Jesus College from 2001-2011 and Senior Vice-President of the Royal Academy of Engineering from 2008-2011. He was President of the Institution of Civil Engineers from 2017-18 and is Chairman of the Science Advisory Council of the Department for Transport. Prior to his appointment to a Chair at Cambridge in 1998, he worked in industry for 27 years. In 1983 he founded the Geotechnical Consulting Group, an international consulting company based in London. He has advised on numerous major engineering projects world-wide, and is an international research leader in geotechnical engineering and a world expert on underground construction in soft ground. He was appointed as an independent crossbencher in the House of Lords in 2015 and is a member of its Select Committee on Science and Technology.

Abstract for Keynote Presentation

Smart Civil Engineering infrastructure and Construction

The Lecture will discuss the challenges facing the infrastructure and construction industry, with a focus on the latest developments in Smart Infrastructure, employing recent advances in sensing and digital technologies. Some of the recent work of the Centre for Smart Infrastructure and Construction (CSIC) at Cambridge will be described. CSIC is funded by the UK Government (EPSRC and Innovate UK) and by industry, with around 50 industry partners. Innovative sensor technologies have been deployed on over 100 different sites. Applications of innovative fiber optic sensing to new construction and ageing infrastructure will be presented, with examples of shafts, tunnels, bridges and buildings. The Lecture will demonstrate the huge potential for innovative monitoring of the performance of infrastructure both during its construction and throughout its design life. It will illustrate how sensors, data analytics and smart infrastructure can transform construction, delivering value and greater efficiencies. The vital importance of data analytics to maximize understanding and efficiency of new and existing infrastructure will be emphasized.

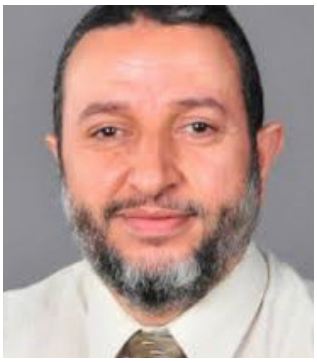

Keynote Speaker

Tarek Zayed

Professor
Department of Building and Real Estate (BRE)
The Hong Kong Polytechnic University

Prof. Tarek Zayed, has a Ph.D., M.Sc., and B.Sc. in Construction Engineering and Management. He has 30 years of professional experience working in the construction industry training and in academic posts in USA, Canada, Hong Kong, and Egypt. Prof. Zayed's research focuses on infrastructure/asset/facility management, simulation and artificial intelligence applications in construction, modular construction, asset performance, scheduling, life cycle cost (LCC) analysis, budget allocation, and risk assessment for construction and rehabilitation of buildings, highways, oil and gas pipelines, water and sewer systems, subway system, and bridges. Recent developments include condition rating, deterioration, LCC and technology-based models for buildings, bridge superstructure, water, sewer, oil and gas pipelines/systems; and tunnels and metro stations. Prof. Zayed published around 400 journals and conference articles and performed research with significant amount of funding from government and private funding agencies. He is serving as associate editor of ASCE's Journal of Pipeline Systems - Engineering and Practice as well as the Canadian Journal of Civil Engineering. Prof. Zayed is also a fellow of the American Society of Civil Engineers (F.ASCE) and the Canadian Society for Civil Engineering (F.CSCE).

Abstract for Keynote Presentation

BIM - Driven Facility Management of Buildings

The primary goal of facility management is to proficiently operate buildings and their services in a safe and comfortable environment for occupants. Traditional facility management faces large number of challenges in managing various types of data related to structural and environmental conditions, deterioration, inspection, maintenance & renewal plans for building components. Building Information Modelling (BIM) has immensely helped in solving facility management problems by generating and managing digital representation of the physical and functional characteristics of a facility. BIM is considered as nD database with immense amount of building information that can be used to expedite the decision making process along the service lives of facilities. BIM poses a lot of difficulties when applied to existing buildings due to incomplete availability of documentation; time consuming surveying to capture required level of details; and high cost of converting existing building data into BIM objects. To overcome difficulties in capturing such data and to reduce facility management efforts/time, research is ongoing to automate converting the existing building data into BIM models, using technologies, such as laser scanning, photogrammetry, etc. The impact of several factors on facility management and the use of BIM in such vital domain will be discussed. Developments for facility management components using various top-notch inspection technologies, on a BIM platform, will be presented. Lessons learnt from the worldwide facility management practices, industry norms, and research gaps will be discussed.

Organizing Committee

Dr. Okan Sirin
Associate Professor, Qatar University
Conference CHAIR

Dr. Hisham Eid
Professor, Qatar University
Member of the Organizing Committee

Dr. Mohammed Hussein
Associate Professor, Qatar University
Member of the Organizing Committee

Dr. Murat Gunduz
Professor, Qatar University
Member of the Organizing Committee

Dr. Usama Ebead
Professor, Qatar University
Member of the Organizing Committee

Eng. Ahmad Al-Ansari
Technical Office Manager, Public Works Authority (Ashghal)
Member of the Organizing Committee

Ms. Fatima Al-Kubaisi
Public Relations Researcher, Public Works Authority (Ashghal)
Member of the Organizing Committee

Dr. Luai M. El-Sabek
Executive Director of Operations, Lean Construction Institute-Qatar
Member of the Organizing Committee

Mr. Ali Feraish Al-Salem
Head of Infrastructure Planning Section, Ministry of Municipality and Environment
Member of the Organizing Committee

Dr. Khaled Al-Akhras
Engineering Advisor, Ministry of Municipality and Environment
Member of the Organizing Committee

Scientific Committee

Dr. Adel Younis, Qatar University, Qatar
Dr. Ahmed El-Refai, Laval University, Canada
Dr. Ahmad Mohammad Ahmad, Qatar University, Qatar
Dr. Ahmed Senouci, University of Houston, USA
Dr. Ala Abutaqa, Qatar University, Qatar
Dr. Alaa Al-Hawari, Qatar University, Qatar
Eng. Ali Kara, Public Works Authority (Ashghal), Qatar
Dr. Ashraf Osman, Durham University, UK
Prof. Aynur Kazaz, Akdeniz University, Turkey
Dr. Bora Gencturk, University of Southern California, USA
Dr. Carlos Oliveira Cruz, Universidade de Lisboa, Portugal
Dr. Charitha Dias, Qatar University, Qatar
Dr. David Segall, New York University, USA
Dr. Deepti Muley, Qatar University, Qatar
Dr. Emad Kassem, University of Idaho, USA
Prof. Esin Ergen, Istanbul Technical University, Turkey
Prof. Eyad Masad, Texas A&M University, USA
Prof. Fares Al Momani, Qatar University, Qatar
Dr. Fernando Matrazo Aguirre, Imperial College, UK
Dr. Ghassan Chehab, American University of Beirut, Lebanon
Prof. Gul Polat Tatar, Istanbul Technical University, Turkey
Dr. Hussain Al-Khalid, University of Liverpool, UK
Dr Ignacio Paya Zaforteza, Universidad Politécnica de Valencia, Spain
Dr. Iman Hajirasouliha, Sheffield University, UK
Prof. Irem Dikmen Toker, Middle East Technical University, Turkey
Dr. Keith Hampson, Curtin University, Australia
Prof. Khaldoon Bani-Hani, Jordan University of Science and Technology, Jordan
Prof. Khaldoon N. Rahal, Kuwait University, Kuwait
Dr. Khaled Hassan, IRD QSTP-LLC, Qatar
Dr. Khaled Shaaban, Qatar University, Qatar
Dr. Khalid Naji, Qatar University, Qatar
Dr. Laurie Koskela, Huddersfield University, UK
Prof. M. Talat Birgonul, Middle East Technical University, Turkey

Dr. Meng Li, Tsinghua University, China

Dr. Mohammad Irshidat, Qatar University, Qatar

Prof. Mohammed Al-Ansari, Qatar University, Qatar

Dr. Mohammed Elshafie, Qatar University, Qatar

Dr. Mohammed Sadeq, Seero Engineering Consulting LLC, Qatar

Prof. Moncef Nehdi, Western University, Canada

Dr. Nan Li, Tsinghua University, China

Dr. Nasser Al-Nuaimi, Qatar University, Qatar

Dr. Neaz Sheikh, Wollongong University, Australia

Dr. Peter McDermott, Salford University, UK

Prof. Rifat Sonmez, Middle East Technical University, Turkey

Dr. Riyadh Al-Raoush, Qatar University, Qatar

Dr. Samir Dirar, University of Birmingham, UK

Dr. Shahram Tahmasseby, Qatar University, Qatar

Dr. Shu-Chien (Mark) Hsu, Hong Kong Polytechnic University, Hong Kong

Dr. Wael Alhajyaseen, Qatar University, Qatar

Dr. Wael Al-Nahhal, Qatar University, Qatar

Prof. Walaa S. Mogawer, University of Massachusetts Dartmouth, USA

Dr. Wei Pan, Hong Kong University, Hong Kong

Dr. Xin Ruan, Tongji University, China

Dr. Ying-Yi Chih, Australian National University, Australia

Dr. Young Hoon Kwak, George Washington University, USA

Supporting Staff

Mr. Abdelazeez Kilayil, Qatar University
Mr. Abdulrahman Abu-Hijleh, Qatar University
Mr. Anas Alsharo, Qatar University
Ms. Aisha Al-Kuwari, Qatar University
Mr. Khaled Rabie, Qatar University
Mr. M. Shekaib Afzal, Qatar University
Mr. Mohammed Amin, Qatar University
Mr. Nasser Al-Nohmi, Qatar University
Mrs. Ratiba Ghachi, Qatar University
Mr. Siju Joseph, Qatar University

Table of Contents

Foreword of Qatar University President 7
Foreword of the President of the Public Works Authority (Ashghal) 8
Foreword of the Assistant Undersecretary for Urban Planning Affairs – Ministry of Municipality and Environment 9
Foreword of the Dean of Qatar University College of Engineering 10

Sponsors and Organizers 11

Keynote Speakers
Kancheepuram N. Gunalan 13
Randy Black 14
Rachel Skinner 15
Yaojun Ge 16
Robert Mair 17
Tarek Zayed 18

Organizing Committee 20
Scientific Committee 21
Supporting Staff 23

Theme 1: Construction Management and Process 37

Performance of University-Construction Industry Collaboration: A Systematic Literature Review and Research Agenda 39
Ziad Al-Gasim, Aslan Amat Senin, Mohd Effandi bin Yusoff

Practical Implementation of Contract Administration Performance Model in Qatar Construction Projects 55
Murat Gunduz, Hesham A. Elsherbeny

Framework for Investigating the Level of Compliance to the OHS Regulatory by the Small and Medium Construction Companies in Oman 65
Mubarak Al Alawi, Mohamed Al Shahri, Amjaad Al Ghafri

Innovative Pavement Materials and Design: Smart Roadways and Smart Road Maintenance for the Future 75
Sherif Hashem, Clinton Cardiño

Unfair Payment Issues in Construction: Re-thinking Alternative Payment Method for Tier-1 Contractors to Subcontractors 84
Laura Peter Swai, Andrew Oyen Arewa, Rex Asibuodu Ugulu

Challenges Facing Building Information Modelling in Construction Industry in Sudan 94
Ahmed Ibrahim, Amged O. Abdelatif

Preventive Approach to Unsubstantiated Claims and Disputes in the UK Construction Industry **98**
Asia Nosheen, Andrew Oyen Arewa, Hafiz Muhammad Akhtar

Utility Impact Assessment of Road Projects in the State of Qatar **108**
Mohammad Mujtaba Hamidy

Project Management: Key Initiatives Case Study **116**
Khaled Al Nass, Lavinia Melilla, Mohamed Tolba

Energy Efficiency in Buildings and Excess Summer Mortality in the UK **122**
Ali Mohamed Abdi, Andrew Arewa, Mark Tyrer, Rex Asibuodu Ugulu

Project Risk Based Evaluation for Infrastructure Works in Qatar: Highway Projects **126**
Nor Rozaini Abd Rahman

Key Lessons Learnt from Stakeholder Management in Design and Build Projects in Qatar **135**
Larno Meyer, Ali Kara

Unique Structural Design and Construction Challenges for Al Bustan South Project in Qatar **143**
Anshuman Ganguli, Ali Kara

The Lean Enterprise at the Design Office **151**
Dawlat Elmosalmi, Mohamed Mohsen Ibrahim

BIM Based Facility Condition Assessment **162**
Faisal Faqih, Tarek Zayed, Ehab Soliman

Effective Project Control within the Context of Lean Construction **172**
Andre F. Koluksuz

How Public Works Authority Has Built a Portfolio Dashboard Through Agility Approach **178**
Abdulrahman Mchaweh

Design and Construction Risk Management of Souq Waqif Station of Gold Line, Doha Metro **182**
Spyridon Konstantis, Spyros Massinas

Variation Orders in Building Projects in Khartoum State-Sudan: The Causes and the Impact on Projects Performance **191**
Eltahir Elshaikh, Salma Mahmoud

The New Construction Approach Adapted by Ashghal for the Public Projects in Qatar 199
Ahmad Al-Buenain, Saeed Al-Muhanadi, Mohammad Falamarzi

Assessment of Response Strategy in Mega Construction Projects 208
Ayman Mashali, Emad Elbeltagi, Ibrahim Motawa, Mohamed Elshikh

Stakeholder Management: An Insightful Overview of Issues 217
Ayman Mashali, Emad Elbeltagi, Ibrahim Motawa, Mohamed Elshikh

Strategies for Communicating Health and Safety Information on Construction Sites in Nigeria 232
Samuel Abiodun Alara, Ibrahim Ibrahim Inuwa

Solar DER Investment for MWANI Qatar Building at Hamad Port 243
Adel Karama

Integrating Building Information Management (BIM) in Civil Infrastructure Coordination: Application at LUSAIL Plaza 252
Mohab Mohamed Abotaleb, Elisabeth Saab, Mohamed AbdelZaher

Risk Management for Qatar Expressway Program 257
Nor Rozaini Abd Rahman

Lean Principles Implementation in Construction Management: A One Team Approach 265
Mahmoud Fahmy

Theme 2: Materials and Transportation Engineering 271

Development of Warm Mix Asphalt with the Aid of Microstructural Characterization 273
Abdullah Al Mamun, Okan Sirin, Eyad Masad

Site-Specific Traffic Loading Estimation Challenges in Structural Pavement Design Process in Qatar: A Case Study 281
Ahmad Al-Tawalbeh, Mohammed Sadeq, Husam Sadek

Vehicle Inspection Policy and Emission Analysis in Kuwait 288
Sharaf Al Kheder, Fahad Al Rukaibi, Ahmad Aiash

Optimum Dispersion Parameters of Carbon Nanotubes: Concrete Strength by Response Surface Methodologies 298
Mohamed Mohsen, Mohamed Al Ansari, Ramzi Taha, Ahmed Senouci, Ala AbuTaqa

Comparison of the Mechanical Behaviour of Railroad Ballast in a Box Test under Sinusoidal and Realistic Train Loadings Using Discrete Element Method 308
Yahia Alabbasi, Mohammed Hussein

Improving Concrete Durability by Using Optimized Aggregate Gradation and Reducing Cement Content 316
Hung-Wen Chung, Thanachart Subgranon, Mang Tia

Advanced Freeze-Thaw Assessment of Internally Integrated Concrete with Sodium Acetate 324
Mazen J. Al-Kheetan, Mujib M. Rahman, Seyed Hamidreza Ghaffar

Reflective Crack Mitigation Using AST Interlayer over Soil-Cement Base for Flexible Pavements 334
Mohammad Reza-Ul-Karim Bhuyan, Mohammad Jamal Khattak

Using Reclaimed Asphalt and Polymer Modified Asphalt (PMA) to Maximize Cost Saving over the Pavement Life-Cycle in Qatar 344
Jean Khnaizer

Producing High Quality Recycled Hot Asphalt with Increased Reclaimed Asphalt Content – Qatar Experience 349
James Maina, Jean Khnaizer

Crowd Dynamics, Management and Control at Tourist Attractions during Special Events: A Case Study at Souq Waqif Using Pedestride® Crowd Simulation Tool 356
Ali Abdelaal, Charitha Dias, Majid Sarvi, Wael Alhajyaseen, Faris Tarlochan

Emerging Transit Technology, Implementing an Urban Gondola System over Al Corniche, Doha, Qatar – A Cost Estimation Study 364
Shahram Tahmasseby

Dosage Optimization of Polypropylene Fiber for Strength Enhancement of Cementitious Composites 372
Mohammad R. Irshidat, Nasser Al Nuaimi, Soheb Salim, Mohamed Rabie

Effect of Alkaline Activators on the Mechanical Properties of Geopolymer Mortar 377
Mohamed Rabie, Mohammad R. Irshidat, Nasser Al Nuaimi

Integrated Accident Resilience Framework (IARF) – A Theoretical Approach Using Spatial and Statistical Analysis 382
Sumanta Ghosh, Srinivasan Manickam, Muhammad Haider

Spatial Impact Network Exposure Model (SINEM) with Integration of Traffic Characteristics and Air Pollution Concentration **393**
Sumanta Ghosh, Rohit Rp

Implementation of Crumb Rubber Modified Binder for Qatar Local Roads Construction Projects **403**
Charles N. Nunoo, Saoud Ali Al-Tamimi

In-Pavement Fiber Bragg Grating Sensor for Vehicle Counting **413**
Mu'ath Al-Tarawneh, Ying Huang

Mechanical and Durability Characteristics of Roller Compacted Geopolymer Concrete Using Reclaimed Asphalt Pavement **420**
Sk Syfur Rahman, Mohammad Jamal Khattak

Crowd Logistics Delivery Determinants: A Stated-Preference Survey **431**
Ali Al-Saudi, Frank Himpel

A Study on Using Reclaimed Asphalt Pavement (RAP) in the Construction of New Roads in the State of Qatar **441**
K. Lakshmi Roja, Eyad Masad

Asphalt Rideability Specification and Construction of Expressways in Qatar **448**
Roger James Hodgson, Ali Kara

Optimizing the Thermal Resistance of Concrete Using The Palm Tree Fronds Fibers **452**
Mohmmad Hany Yassin, Rana Lakys, Taha Ahmed, Shafaq Al-Refaei, Bader Al-Sayed Omar, Rose Shaker Altaher

Application of Vehicle Restraint Systems (VRSs) in the State of Qatar: A Case Study from Northern Roads **462**
Deepti Muley, Shahram Tahmasseby, Bernd Wolfgang Wink, Faris Tarlochan

Modeling Airport Ground Access Mode Choice by Trip Purpose: Business vs. Personal Trips **468**
Gurkan Gunay, Ilgin Gokasar

A Study on the Default Supplemental Adjustment Factors of Progression Adjustment Factor Formula under Non-Lane Based Traffic Condition **477**
Abdullah Al Farabi, Tamal Chakraborty

Novel Method for Assessing Moisture Damage in Asphalt Mixtures **487**
Mohammad Nour Fakhreddine, Ghassan Chehab, Zaher Al Basiouni Al Masri, Mohamad Abiad

Determination of Temperature Zoning for the Great Lakes Region of Africa based on Superpave System **495**
Mukunde Ronald, Ghassan Chehab, Mohammad Nour Fakhreddine

Test Procedures for Advanced Characterization of Bituminous Binders Employed for Pavement Construction in Public Works Authority Road Projects - State of Qatar **502**
Ezio Santagata, Sadegh Yeganeh, Osman Elhusain Mohamed Idris, Moaaz Hashim M.M. Ali, Khalid Mohd I Al-Emadi

Use of Crumb Rubber Modified Binders and Asphalt Mixtures in Public Works Authority Road Projects - State of Qatar **512**
Ezio Santagata, Haissam Sebaaly, Osman Elhusain Mohamed Idris, Moaaz Hashim M.M. Ali, Khalid Mohd I Al-Emadi

Using Ground Penetrating Radar (GPR) to Evaluate Air Voids Content in Hot Mix Asphalt **522**
Pejman Dehdezi

Recycled Concrete Used in Subbase in Potential Use for Road Base and Cement Bounded Material (CBM) **528**
Hassan Haidar Ahmad

Innovation in Road Construction Industry: An Analysis of Different Case Studies **537**
Pardeep Oad, Stephen Kajewski, Arun Kumar

Evaluation of Bond Strength Between Carbon Fiber Reinforced Polymer (CFRP) Composites with Modified Epoxy Resins and Concrete **547**
Mohamed H. Rabie, Eman M. Fayyad, Mohammad R. Irshidat, Nasser A. Alnuaimi, Mohammad K. Hassan

Development and Performance of Cement Bound Materials in Road Pavements **553**
Khaled E. Hassan, Osman El-Hussain, Mohammed bin-Saif Al-Kuwari, Khalid Al-Emadi

Characterization of Asphalt Mixtures in Qatar **560**
Osman El Hussien, Khaled E. Hassan, Khalid Al-Emadi

Modelling the Severity of Plastic Shrinkage in Cementitious Materials **566**
Faez Sayahi, Mats Emborg, Hans Hedlund, Andrzej Cwirzen, Marcin Stelmarczyk

Challenges for the Use of Local Materials in Unbound Road Subbase in Qatar **574**
Moaaz Hashim Mohamedain, Khaled E. Hassan, Osman El-Hussain, Khalid Al-Emadi

Compressive Strength and Hydration of Ravennagrass Baggase Ash Concrete **582**
Ashhabu Elkaseem, Samaila Bawa

An Artificial Intelligence Approach to Estimate Travel Time along Public Transportation Bus Lines **588**
Mohammad S. Ghanim, Khaled Shaaban, Motasem Miqdad

Evaluating the Operational Impact of Left-Turn Exclusive Number of Lanes: A Case Study from Qatar **596**
Khaled Shaaban, Mohammad S. Ghanim

Concept Design of Major Roads and Infrastructure in the Center of Doha City: Phase 4 project **604**
Mohab Zaki

Developing Assessment Framework for Strategic Transportation Projects in Qatar **609**
Anas Mohammad, Nabeel Al Rawi, Osama Freija

Theme 3: Geotechnical, Environmental, and Geo-environmental Engineering **619**

Flood Risk Assessment and Protection Guidelines for Infrastructure Planning in Qatar **621**
Abdullah Al Mamoon

Constructability and Economical Comparison Between Two Proposed Permanent Shoring Systems in Qatar: A Case Study **628**
Mohammed Alfarra, Mohammed Sadeq, Husam Sadek

Resource Recovery from Waste, Water and Wastewaters with Membrane Technologies **634**
Ismail Koyuncu, Bihter Zeytuncu, Mehmet Emin Pasaoglu, Ayse Yuksekdag, Borte Kose-Mutlu

Dynamic Imaging of Hydrate Specific Area Evolution during Xenon Hydrate Formation **640**
Zaher Jarrar, Riyadh Al-Raoush, Khalid Alshibli, Jongwon Jung

Use of 3D Images to Evaluate Formation Damage Induced by Montmorillonite Fines in Porous Media Systems **644**
Jamal Hannun, Riyadh Al-Raoush, Zaher Jarrar, Khalid Alshibli, Jongwon Jung

Enhancement of Naphthalene Biodegradation by Sulfate Application in Brackish Subsurface Systems **649**
Saeid Shafieiyoun, Reem Ismail, Riyadh I. Al-Raoush

Influence of Water Table Fluctuation on Natural Source Zone Depletion in Hydrocarbon Contaminated Subsurface Environments **654**
Reem Ismail, Saeid Shafieiyoun, Riyadh I. Al-Raoush

Embedded Retaining Wall Design and Performance Monitoring for Deep Excavation in Geological Conditions of Qatar **659**
Muhammad Humza, Ghulam Sarwar, Majid Naeem, Gorkem Dora

Investigation of the Effect of the Force-Frequency on the Behaviour of a New Viscous Damper for Railway Applications **666**
Yousif Badri, Mohammed Hussein, Sadok Sassi, Jamil Renno

Influence of Fines on the Compressibility of Surface Sands in Kuwait **672**
Shaikha A. N. AlAbdulmuhsen

Box Jacking/Pushing Method for Tunnel Construction in Rock: Doha Metro, Gold Line Project **680**
Spyridon Konstantis, Spyros Massinas

The Use of Measuring While Drilling and Wireline Logging to Identify the Geological Strata in Qatar **690**
Anna Grace Gravador-Villamor, Fay Pearce

Hydrogen Gas Production from the Injection of Nanoscale Zero-Valent Iron and Sodium Borohydride Solutions: Potential Effects Near Injection Wells **697**
Obai Mohammed, Kevin G. Mumford, Brent E. Sleep

Geotechnical Aspects of Sub-Sea Tunnelling on the Musaimeer Pumping Station and Outfall Tunnel Project **706**
Gary Peach, Mirjana Hrnjak, Ioannis Papadatos, Hernan Vigil

Impact of Ionic Strength on Colloid Retention in a Porous Media: A Micromodel Study 715
Safna Nishad, Riyadh I. Al-Raoush

Treatment of Wastewater Using Reverse Osmosis for Irrigation Purposes 724
MhdAmmar Hafiz, Alaa H. Hawari, Radwan Alfahel

Impact of Draw Solution Concentration on Forward Osmosis Process: A Simulation Study 729
Radwan Alfahel, MhdAmmar Hafiz, Alaa H. Hawari

Utilizing Steel Slag in the Removal of Suspended Solids from Dewatered Construction Water 734
Alaa Al Hawari, Abdelrahman Tariq, Ahmed T. Yasir, Mohamed A. Ayari

Influence of Aspect Ratio on the Bearing Capacity and Correlated Modulus of Subgrade Reaction for Shallow Foundations on Dense Sand 740
Ramez Alchamaa

Predicted and Back-calculated Coefficients of Permeability of Randomly Fractured Rock Mass: A Case Study 748
Hisham Eid, Barry O'Sullivan, Mohammed Elshafie, Reiner Stollberg, Robert Kalin

Fully Softened and Residual Shear Strengths of Midra Shale 754
Hisham Eid

Theme 4: Sustainability, Renovation, and Monitoring of Civil Infrastructure 759

Steel Reinforced Grout for Strengthening of RC T-section Beams Deficient in Shear 761
Tadesse Wakjira, Usama Ebead

Near Surface Embedded Application for FRCM Strengthening of RC Beams in Flexure 769
HossamEldin El-Sherif, Usama Ebead

Life Cycle Assessment for Fiber-Reinforced Polymer (FRP) Composites Used in Concrete Beams: A State-of-the-Art Review 777
Mohamed Ibrahim, Usama Ebead, Mohammed Al-Ansari

Verification of ACI- 549 Code for Flexural Strengthening of Reinforced Concrete Beams Using FRCM 785
Muhammad Shekaib Afzal, Usama Ebead

Effects of Using Seawater and Recycled Coarse Aggregates on Plain Concrete Characteristics **794**
Adel Younis, Usama Ebead

Long-Term Cost Performance of Corrosion-Resistant Reinforcements in Structural Concrete **801**
Adel Younis, Usama Ebead

Positively Shifting the Mindset in Construction Using Non - Biodegradable Materials for Sustainable Construction: An Experimental Study **806**
Faheem Memon

Dune Sand Mortar Effects on Deflections of Repaired Steel Bars-Reinforced Concrete Beams **813**
Madina Djeridane, Ali Zaidi, Mohammed Fatah Lakhdari

Water Supply from Turkey to Cyprus Island with Suspended Marine Pipeline **818**
Izzet Ozturk, Necati Agiralioglu, Omer Ozdemir, Nasir Akinci

Utilizing Recycled Polypropylene Fibres as Reinforcement for Concrete Beams **828**
Khadra Bendjillali, Mourad Hadjoudja, Mohamed Chemrouk

High and Ultra-high Performance Concretes: A Solution to Reinforced Concrete Durability under Harsh Climate of Arabian Gulf **837**
Muazzam Ghous Sohail, Ramazan Kahraman, Nasser Al Nuaimi, Wael Alnahhal, Muhammad Wasee

Accelerated Corrosion Tests on Lapped Spliced Joints in Concrete **846**
Sara Eltayeb-Onsa, Amged O. Abdelatif

Technologies Serving Concrete for Economy, Durability and Sustainability **852**
Yahia Alhassani

Cantilever Beam Metastructure for Passive Broadband Vibration Suppression **857**
Ratiba Fatma Ghachi, Wael Alnahhal, Osama Abdeljaber

Sustainability in Construction: Reduce, Reuse and Recycle for a Greener Qatar **861**
Mohamed Tolba, Lavinia Melilla, Khaled Al Nassa

Concrete Hydration Model Characterization Using Evolutionary Optimization **869**
Qianchen Sun, Mohammed Z.E.B. Elshafie, Yi Rui

Experimental Study on the Performance of Circular Concrete Columns Reinforced with GFRP under Axial Load **877**
Sherif El Gamal, Othman Alshareedah

An Innovative Structural Solution to Failed Stabilized Earth Embankment in Multilevel Interchange **886**
Ali Kara, Tamer Tahoun

Modelling Catchments in Qatar to Assist in Operations **894**
Shirish Gokhale, Anil Kumar Gupta, Nasser Yousef Fakhroo, Kapil Devang, Tim Kelly

Eco-friendly Concrete Using Local Materials From Sudan **900**
Salma Yahia Mohamed Mahmoud, El Tahir Abualgasim Mohammed Alshiekh

Mechanical Properties of Concrete Made with Electric Wires, Steel Fibers, Basalt Fibers and Polypropylene Fibers **909**
Yasmin Zuhair Murad, Haneen Abdel-Jabbar

Climate Change and the Structural Resilience of the Doha Metro **917**
Georgios Nikolis, Petros Chronopoulos, Marin Griguta

Towards Sustainable Public Open Spaces for Promoting Human Comfort, Health and Well-Being: The Case of Oxygen Park in Doha, Qatar **927**
Eman Al-Fadala, Fodil Fadli

Development of a Software for Design and Design Comparison of Prestressed I-Beam for Highway and Railway Bridges Based on International Standards **937**
Mustafa Can Yücel, Dilara Akdoğanbulut, Alp Caner

Vibration Prediction Model for Building Developments Adjacent to Railways **943**
Martin Seiner, Elisabetta Pistone, Günther Achs, Hanno Töll

The Investigation of an Efficient and Effective Proactive Pipeline Integrity System **951**
Masoud Forsat, Abdelmagid S. Hamouda

Integration of Environmental and Sustainability Management Practices into Construction Industry: A Case Study **960**
Gary Peach, Dila Ersenkal, George Daoutis, Sotirios Koropoulis, Pavel Zuzula, Biliana Karamukova

Cut Carbon, Cut Cost – Feasibility of Applying PAS 2080 **969**
Lakshmi Suryan, George Daoutis, Lisa Girrbach

Regulatory Frameworks for the Successful Implementation of Construction and Demolition Waste Treatment Infrastructure **975**
Sam Dowding, George Daoutis

An Analytical Review of Sustainable Green Buildings in Qatar: Implementations in the Architecture, Engineering and Construction (AEC) Sector **979**
Diala Al Midani, Fodil Fadli

East Industrial Pedestrian Bridge: A Case Study of Value Engineering and High Performance Material **989**
Theodoros Tzaveas

Mechanical Performance and Thermo-Physical Properties of Cement Mortar Incorporating Hybrid Slags **997**
Mahad Baawain, Hamada Shoukry, Khalifa Al-Jabri

Structural Efficiency of Steel Stiffening Deck Systems in Suspension Bridges Due to Gravity Loads **1006**
Ahmed Gasim M. Hussein, Mohamed Faisal F. Mohamed

Numerical Study of Four Bolts End-Plate Joint Behaviour for Robustness Assessment **1016**
Bashir Saleh

Latest Advances in Smart Components and Monitoring for Civil Structures **1024**
Thomas Richli, Antonios Chrysovergis, Achilleas Athanasiou, Niculin Meng

Derivation of the Governing Differential Equation of Vibrating Host Plate with Two Piezoelectric Patches **1033**
Wasim Barham, Khaldoon Bani-Hani, Mutaz Mohammad

Theme 1:
Construction Management and Process

Performance of University-Construction Industry Collaboration: A Systematic Literature Review and Research Agenda

Ziad Al-Gasim
eaaziad2@graduate.utm.my
Azman Hashim International Business School, Universiti Teknologi Malaysia, Johor Bahru, Malaysia

Aslan Amat Senin
aslan@management.utm.my
Azman Hashim International Business School, Universiti Teknologi Malaysia, Johor Bahru, Malaysia

Mohd Effandi bin Yusoff
effandi@utm.my
Azman Hashim International Business School, Universiti Teknologi Malaysia, Johor Bahru, Malaysia

ABSTRACT

University-construction industry collaboration (UIC) has become an essential part of driving innovation and fostering construction industry growth. Measuring performance of such collaboration is an emergent field of study. The present research evaluated the literature related to measuring performance of university-construction industry collaboration taking into consideration the publications in selected scientific databases. Findings were discussed and confirmed in the context of Qatar education and innovation ecosystem through semi-structured interviews with two renowned scholars involved in university-construction industry collaboration. This study aims to (1) identify the most cited references in measuring UCIC performance (2) identify UIC performance indicators advocated by top cited references, and (3) refine and map UIC performance indicators in the context of the state of Qatar. The publications reviewed were obtained through a search of the Science Direct, Emerald Insight, Scopus, Web of Science, Springer Link, SAGE, Research Gate, and Taylor & Francis Online. Keywords used in searching for articles included university-construction industry, university-construction business, cooperation, collaboration, relation, performance, and measurement. The study revealed that universities are increasingly focused on measuring performance of collaboration with construction industry. As such, it contributes to a general understanding of measuring UIC performance and defining trends in this research field. It also highlights specifically the challenges for measuring UIC performance in Qatar. In this context, key UIC performance indicators include (1) Number of Publications, (2) Number of Citations (3) Number of Registered Patents, (4) Number of Patent Applications, (5) Number of Training Programs Provided and (6) Number of Innovations.

Keywords: University; Industry; Construction; Cooperation; Collaboration

1 INTRODUCTION

In the age of cyberspace, machine learning, and artificial intelligence, competition has become fierce for universities as well as for construction industry and business actors. Companies are expected to surpass competitors through developing innovative products and services, satisfying customers' requirements, showing business agility, and rapidly

responding to market demands (Ivascu et al., 2016). Universities on the other hand are competing for social reputation and academic excellence in order to attract resources invested in contribution to knowledge and capacity building of the future (Striukova & Rayna, 2015).

A closer look at the economies of developed countries reveals that their innovation level is the result of knowledge creation and its application in industries, which contributes to achieving competitive advantages (Mascarenhas et al., 2018). Therefore, innovation has become a key focus for universities as well as for industry and business actors. However, none of these actors has all skills and resources required to foster innovation agenda. As a result, it is expected to see collaboration for mutual benefits between actors of the innovation ecosystem (Chesbrough, 2012).

University and construction industry can cooperate in different ways. They include, but not limited to, research and development, mobility of academics, mobility of students, commercialization of research results, curriculum development, curriculum delivery, lifelong learning, spinoff and startup formation, and university governance. Davey et al. (2011) found that types of university-industry cooperation that provides straight and measurable benefits having tendency to be the most developed types of cooperation, e.g., research and development, commercialization, and student mobility. Thus, university-industry collaboration, shortly termed "UIC", can take several forms and practice through various activities. Commonly, such collaboration falls under one of three main activities: (1) collaborative training and education, (2) collaborative consulting and services, and (2) collaborative research (Ishengoma & Vaaland, 2016) (Vaaland & Ishengoma, 2016) (Galán-Muros et al., 2017) (Davey et al., 2011).

Indeed, outcome of such collaborations is realized differently by universities and industry. From university perspective, such outcomes are realized by aspects related to enhanced learning environment, increased rates of knowledge creation, and better serving society and regional economies. From the industry perspective, such outcomes are realized by aspects related to improved innovation rates, revenues, and access to resources (Berbegal-Mirabent et al., 2015; D'este & Perkmann, 2011)

Accordingly, UIC is essential to establish and nurture innovation ecosystems that drive country innovation agenda and sustain economic growth (Etzkowitz, 2017). In United States, the notable program to drive UIC is through Bayh-Dole Act (1980) (Hall, 2004). The comparable program in Europe is the Horizon 2020 (Mascarenhas et al., 2018). In Qatar, UIC is driven mainly by the Qatar National Research Fund (QNRF) (Foundation, 2015).

However, the economic dynamic between two major actors of innovation ecosystem faces a dilemma. It consists of two distinguished economies: the knowledge economy and commercial economy. The first is driven by a need for advanced fundamental research or social value through universities and research centers, while the second is driven by the requirements of the marketplace that should be satisfied by business entities (Jackson, 2011). Such dilemma makes measuring UIC performance a challenge for university and construction industry alike.

Indeed, there is a vast literature on the topic of UIC. Additionally, few studies have conducted a systematic literature review to present propositions, findings, and research trends in the field. However, these studies have focused on aspects related to technology

transfer (Agrawal, 2001), UIC governance (Geuna & Muscio, 2009), commercialization (Perkmann et al., 2013), collaboration forms or activities (Rothaermel et al., 2007), university entrepreneurship, and UIC as open innovation (Mascarenhas et al., 2018).

To the best of our knowledge, literature does not include any systematic literature review (SLR) on the subject matter of measuring performance of university-industry relations. Therefore, this research sought to fill this gap in the area and review most relevant literature on measuring performance of UIC. We also conducted semi-structured interviews in order to refine, align, and interpret SLR findings in the context of the State of Qatar.

Therefore, this research, in one hand, contributes to systematic literature review focused on UIC performance. On the other hand, it sheds light on policy and context-related matters for UIC performance in Qatar. In this sense, this research presents a future research agenda for measuring UIC performance. This study aims to (1) identify the main cited references in measuring UIC performance, (2) identify UIC performance matrices advocated by top cited references, and (3) refine performance matrices of UIC in the context of the State of Qatar.

The published articles reviewed were obtained through a search of the Science Direct, Emerald Insight, Scopus, Web of Science, Springer Link, SAGE, Research Gate, and Taylor & Francis Online databases. Keywords used in searching for published articles were university-industry, university-business, cooperation, collaboration, relation, performance, and measurement. Findings are discussed and confirmed in the context of Qatar innovation and education ecosystem through semi-structured interviews with two renowned scholars involved in university-industry collaboration.

The rest of the article is structured as follows: Section 2 provides an overview of methodology used in literature review, Section 3 presents and discusses results, Section 4 presents limitations and recommendations for future research, and finally Section 5 concludes the whole paper.

2 METHODOLOGY

A systematic review of the available academic research was carried out on the topic of UIC. The search for published articles was carried out in Science Direct, Emerald Insight, Scopus, Web of Science, Springer Link, SAGE, Research Gate, and Taylor & Francis Online. We used keywords in searching for articles including university-industry, university-business, cooperation, collaboration, relation, performance, and measurement. Published articles reviewed with 15 years of temporal restriction, i.e., articles published since 2004. This restriction was chosen to reveal most recent trends in this emergent field of research. The temporal selection was also in line with the coverage limitation of Scopus databases, as it is currently limited to articles published since 1995 (Mascarenhas et al., 2018). In addition, top cited articles, e.g., the work of (Agrawal, 2001), were also considered, beyond the temporal restrictions, when repeatedly cited in most recent articles.

The literature research was performed on the period between 10/02/2018 and 10/08/2019. The literature research followed six steps as displayed in Figure 1 below. In parallel, the researcher reached out to two active scholars in university-industry collaboration from Qatar University. The researcher conducted semi-structured

interviews with both scholars in order to reveal country-specific concerns, challenges, and priorities in regard to measuring UIC performance (AlMadeed, 2019; Ben-Ayed, 2018). The interviews were conducted on 19-02-2018 and 07-01-2019. The semi-structured interviews protocol is displayed in Figure 2 (Saunders & Lewis, 2012).

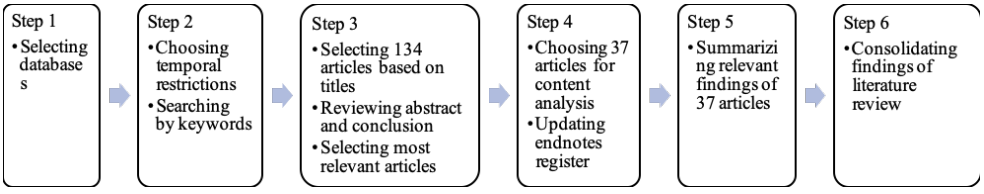

Figure 1: Steps Followed in Literature Research

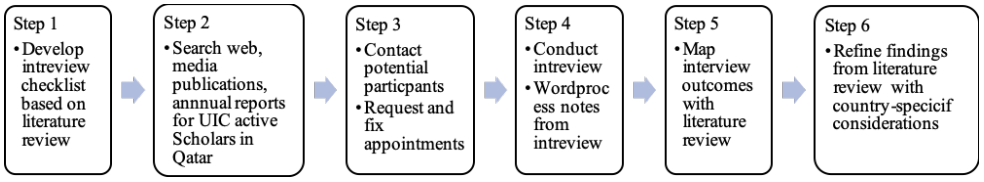

Figure 2: Steps Followed in Conducting Semi-Structured Interviews

3 RESULTS

3.1 Overview of Selected Publications for Content Analysis

In step 4 of the literature review, 37 published articles were selected for content analysis, which included mainly articles in the last 15 years with more focus on most recent publications, as shown in the Figure 3.

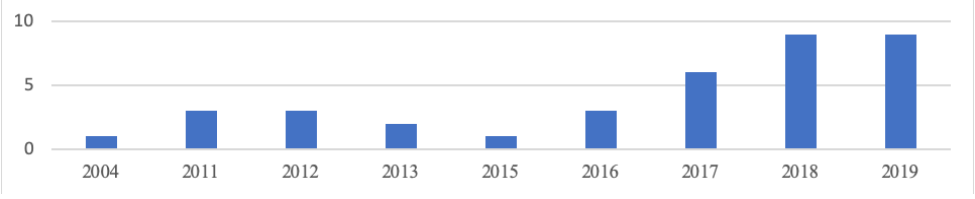

Figure 3: Publication Year of the Selected Articles for Content Analysis

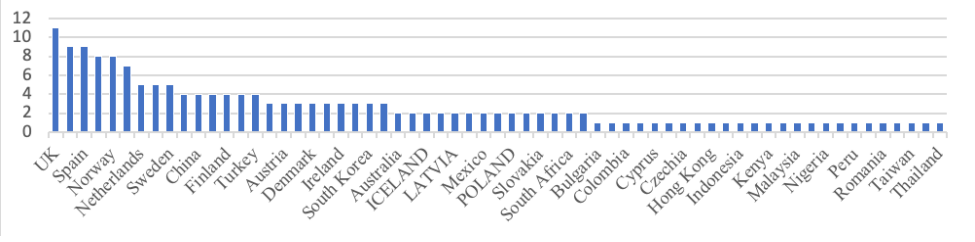

Figure 4: Context of Selected Papers for Content Analysis

From the context perspective, the selected articles covered 63 countries with more articles published in the European context, as shown in the Figure 4. A review of literature published during the last 15 years showed the absence of research related to measuring

UIC performance in Gulf Cooperation Council countries (GCC) and Qatar. This issue provided more rational to conduct interviews and refine findings according to country-specific considerations.

3.2 UIC Performance Explained

University-industry relations influence all three institutional logics involved, i.e., university, industry, and cooperation or collaborative forms of organizing. (Hue Kyung et al., 2016) studied the relationships between the competence factors of universities and the university-industry cooperation performance. Their findings suggested significant influence of university research capacity on driving performance of the UIC in terms of providing full-time faculty members and the size of the Technical Licensing Office (TLO). Hue Kyung et al. (2016) argued that performance in this case is mediated by government funding for research and development activities.

Similarly, Rajalo and Vadi (2017) argued the role of Technology Transfer Offices (TTOS) in establishing successful university-industry partnerships. First, they studied the relationships between TTO age, TTO staff in R&D contracts, and TTO budget with R&D contracts in terms of number and income size. Then, they studied the impact of having a science park on R&D contracts in terms of number and income. Their findings suggested a positive relation between TTO experience and annual budget as well as availability of science parks with income and number of R&D contracts. Another important factor argued by (Rajalo & Vadi, 2017) was the positive influence of university social-capital on setting R&D contracts. Universities with larger social networks, both local and international, are more successful in attracting R&D contracts.

The technology parks influence on university and industry performance differs based on university involvement and its share in the park. For that reason, (Albahari et al., 2017) distinguished four types of parks. The first type, where university is the major shareholder, is called Pure Science Park. The second type, where university is the minority shareholder, is called Mixed Park. The third type, where some university research facilities are located in the park, but university holds no share, is called Technology Park. The fourth type, where the university has no formal involvement is called Pure Technology Parks. Their research findings suggested that the higher involvement of the university, in case of the Pure Science Parks, is correlated with best patenting performance among universities. Unlikely, such involvement is correlated with the lowest product innovation levels measured by sales from new to the market products. On the other side of the spectrum, it was suggested that the lowest involvement of the university, in case of the Pure Technology Parks, is correlated with the lowest patenting performance among universities. On the contrary, such involvement is correlated with best product innovation levels measured by sales from new to the market products. Yet there is no evidence that chance of cooperation between universities and industry, in case of research contracts, is influenced by the degree of university involvement in park shareholding.

Therefore, high level of patent applications and potentially published research, in case of pure science parks does not necessarily lead to increased product innovation. On the other hand, a high level of product and innovation in case of pure technology parks is not necessarily associated with high level of patent applications, nor publication

of studies. These findings illustrate different interest dilemma in university-industry relations. Albahari et al. (2017) suggested that changes to academic reward system shift the academic focus from publishing and patenting to inclusion of commercialization.

Indeed, Muscio et al. (2012) expressed the extent of university-industry collaboration success in terms of capability to attract funding for research activities. He suggested three important elements that can improve such capability. First, previous experience with the business, which builds on recent studies conducted by (Bstieler et al., 2017) regarding the relationship maturity and trust building. Second, ability to produce critical mass of research in a certain sector, which builds on previous studies conducted by (Anatan, 2015) regarding the institutional pressure to improve performance of the university in research activities. And third, the proximity to industrial districts, which build on previous studies conducted by (Villani et al., 2017) regarding different types of distances between university and industry partners, including cognitive, geographical, organizational, and social distances.

The influence of publicly-funded university-industry collaboration on research and development efforts by the industry was investigated by (Scandura, 2016). His findings provided interesting insights into the construction industry. First, university-industry partnerships have a positive impact on the R&D expenditure per employee. Second, university-industry partnerships have a positive impact on the share of R&D employment. In fact, the partnership between university and industry not only enhances the resource utilization for the construction industry, but also encourages the industry to invest more in research and development activities.

University-industry relation is a two-way relationship. Thus, reflection on performance is realized on both sides of the relationship. This is a major outbreak from the traditional role of university knowledge transfer, i.e., a one-way relationship. Striukova and Rayna (2015) investigated the adoption of the open innovation concept by universities. The rise of open innovation in the industry contributed to a "changed paradigm" with respect to university-industry relations. Their findings, in context of UK universities, revealed that universities become a central actor in open innovation ecosystems through acting as reliable intermediary or open innovation hub. This role contributes to performance of both the university and other actors in the ecosystem. Striukova and Rayna (2015) also highlighted the diversity of the institutional logic among universities in terms of norms, values, cultures, and management structures. This, in turn, provides diverse reactions, motivations, and attitudes towards implementation of open innovation.

Similarly, Huang and Chen (2017) studied how to improve academic innovation performance in university-industry collaboration. His findings suggested a positive relationship between both formal management mechanisms and regulation implementation, and academic innovation performance. Both relationships were found to be moderated by the university innovation climate. In this context, formal management mechanism for university-industry relations is related to formal arrangements to control and coordinate university-industry relations under the subject of university. Regulation implementation is related to implementation of specific regulations to foster research and development as well as university-industry relations. Finally, innovation atmosphere reflects the university support for entrepreneurial activities by faculty members, students, and administration staff.

Similarly, in a recent study conducted in Europe, (Galán-Muros et al., 2017) found a positive relationship between four management mechanisms and seven key activities of university-business collaboration. The mechanisms were top management support, communication, incentives, and support structures. The seven key collaboration activities were joint curriculum design and delivery, lifelong learning, student mobility, professional mobility, joint R&D, entrepreneurship, and R&D commercialization of joint R&D results.

Also Perkmann et al. (2013) investigated the role of academic engagement in sustaining university-industry relations. Academic engagement refers to knowledge-related collaboration activities by researchers with industry and non-academic organizations. Perkmann et al. (2013) also distinguished the determinants that lead to academic commercialization from determinants of academic engagement. Commercialization refers to the use of knowledge created by university through patenting, licensing of inventions, and business entrepreneurship. Their findings suggest a positive relationship between some individual determinants and academic engagement. These determinants include gender (male), seniority, previous grant experience from government, previous contract experience from industry, and scientific productivity. In the same sense, Davey et al. (2011) found that academic age (seniority), gender (male), previous business experience, and technology orientation are among the key individual drivers of university-industry relations.

Moreover, Perkmann et al. (2013) argued that some other organizational and institutional determinants positively moderate the relationship between individual determents and academic engagements. These include university focus on applied disciplines. Surprisingly, they debated that quality of the university or department concerned has a negative influence on academic engagement. This finding may be justified by the fact that lower quality departments often have less resources and more reasons to seek engagements and collaborations with the industry.

In addition, Perkmann et al. (2013) asserted that commercialization has a positive relationship with individual determinants, which include gender (male), previous commercialization experience, and scientific productivity. Similarly, some other institutional determinants positively moderate the relationship between individual determinants and academic commercialization. These include quality of the university or department concerned, organizational support, organizational commercialization experiences, peer effects, university focus on applied disciplines, and country specific regulatory policies. Likewise, they argued that academic commercialization often leads to increased secrecy and scientific productivity among academics. Finally, academic engagement often leads to improved collaborative behavior (Corral de Zubielqui et al., 2015).

It should be noted that previous funding experience of academics can be a result of previous none-academic experience. Thus, Gulbrandsen & Thune, 2017 studied the impact of prior none-academic work experience on both external interactions and academic performance. The external interaction in their study refers to activities of dissemination of knowledge, research collaboration, commercialization, and training activities. Academic performance refers to measures of research quality that is represented by publication in highly ranked journals, and research productivity represented by

number of publications. According to their findings, non-academic work experience positively influences external interaction activities among academics. In addition, there was no evidence to suggest that non-academic work experience has a negative effect on academic performance.

To acquire and share knowledge is a key to both university and industry, especially in regard to patenting and licensing new technologies (Azagra-Caro et al., 2017; Clauss & Kesting, 2017). Indeed, university-industry relations influence the performance and outcomes of both institutional logics. From the university side, the intended outcomes include attraction of third-party fund for employees, research, and operational expenses, research papers published, conferences, presentations, and reputation gains among scientific community. From the business side, the intended outcomes include new inventions in products, services and processes, new licenses, and new patents (Clauss & Kesting, 2017).

However, Clauss and Kesting (2017) took into consideration the control factors to examine the impact of knowledge sharing on achieving the objectives of UIC. These control factors include obligation to get external research funding (Goel et al., 2017), professors' attitude towards university-industry collaborations (Lam, 2010), the degree of applied research (OECD, 2002), the number of employees under professors' supervision, professors' years of experience, size of partner organization, and type of partner organization whether it is a private company, public organization, or not-for-profit organization.

Furthermore, relational governance energizes the performance of university-industry relations. Academics and industry counter partners are individuals whose culture, attitudes, behaviors, and mutual experience influence their relationships. The influence can be on issues such as the relationship form, sustainability, and future expectations. In this case, ideas are openly shared, and knowledge is voluntarily combined and created by partners from both institutional logics. Likewise, Davey et al. (2011) maintained that university-industry cooperation is a people business that demands constant dialogue and building of social networks. Consequently, they argued that activities aimed at promoting UIC should focus on improving relationships, commitment, and trust between academics and business. They also believed that focus on transactional mechanisms such as patenting and licensing has a negative influence on building the sense of trust, commitment, and sharing goals among individuals involved in UIC.

3.3 Summary of Key UIC Performance Indicators

Definitions of all performance indicators identified in the content analysis were reviewed, refined, and grouped in order to provide list of distinct indicators, avoid duplications, and remove repetitions. Moreover, measuring UIC performance can take place from university or industry perspectives. Therefore, the performance indicators from each perspective were grouped into two separate lists.

From university perspective, literature review revealed 26 indicators to measure UIC performance. So from university perspective, the most frequent UIC performance indicators include (1) Number of Publications, (2) Number of Registered Patents, (3) Number of Generated Startups & Spinoffs, (4) Income from IP Sales, (5) Number of Patent Applications, (6) Income by type of UIC Activity (Consulting & Services, Research, and

Training & Education), (7) Number of IP Licenses, (8) Number of Occurrences for each UIC Activity (Consulting & Services, Research, and Training & Education), and (9) Impact Factor of Publications.

From industry perspective, literature review revealed 21 indicators to measure UIC performance. So from industry perspective, the most frequent UIC performance indicators include (1) Number of Innovations (Process/Marketing/Product/Organizational), (2) Number of Registered Patents, (3) Income from Innovations (Process/Marketing/Product/Organizational), (4) Number of Patent Applications, (5) Number of Joint Publications, (6) Number of Postgraduate Positions offered within UIC, (7) Number of Joint Supervision to Postgraduate Students, (8) Number of Occurrences for each UIC Activity (Consulting & Services, Research, and Training & Education), and (9) Number of IP Licenses.

Indeed, the above results show different focus for university and industry when measuring UIC performance. These findings are in line with initial discussion stating that universities and industries often operate in different institutional logics (David & van der Sijde, 2015) (Striukova & Rayna, 2015). However, the above results show that both university and industry share some interest when it comes to three key performance indicators. These indicators are (1) Number of Registered Patents, (2) Number of Patent Applications, and (3) Number of IP Licenses. These finding suggests that at the core of mutual benefit foreseen from university-industry relations is driving innovation (Lašáková et al., 2017).

3.4 UIC Performance Indicators and Context-Specific Considerations

The two conducted interviews revealed interesting findings with respect to measuring UIC performance from perspective of Qatar University. In order of significance, both interviews highlighted key indicators to measure UIC performance including (1) Number of Publications, (2) Number of Citations (Local and International), (3) Number of Registered Patents, (4) Number of Registered Applications, (5) Number of Training Programs Provided (to Faculty and Students), and (6) Number of Innovations (Process/Product). (AlMadeed, 2019) (Ben-Ayed, 2018).

The above findings, at least from the interviewees' perspective, provide some key context-specific considerations. In one hand, number of publications, patent registrations, and applications as top UIC performance indicators are in line with previous findings provided by previous literature (Azagra-Caro et al., 2019; Castro et al., 2019; Chen et al., 2019). On the other hand, number of citations is related to previous indicators obtained from literature including citation index (Perkmann et al., 2011) and impact factor of publications (Van Looy et al., 2004); (Aldieri et al., 2018) (Gulbrandsen & Thune, 2017).

Moreover, the indicator of number of innovations (process/product) is also related to previous indicators obtained from literature including number of innovations (process/marketing/product/organizational) (Chen et al., 2019; Von Raesfeld et al., 2012). However, the high importance of this indicator, from the interviewees' perspective, may be related to directions of Qatar National Research Strategy (QNRS) (Fund, 2012) that is aimed at putting Qatar in the world map as a research and innovation hub (Ministry of Development, 2018) (Planning, 2008).

Another interesting finding is the indicator of Number of Training Programs Provided

(to Faculty and Students). From both university and industry perspectives, this indicator is related to Number of Occurrences for each UIC Activity (Rajalo & Vadi, 2017; Clauss & Kesting, 2017; Hue Kyung et al., 2016; Berbegal-Mirabent et al., 2015). The UIC activity in this case is collaborative Training & Education (Ishengoma & Vaaland, 2016) (Vaaland & Ishengoma, 2016).

Historically, university-industry relations have been viewed as means to transfer knowledge from the knowledge economy, i.e., universities, to the commercial economy, i.e., industry and business (Jackson, 2011). As a result, the later indicator may suggest that the interviewees look to industry relations also as means to transfer back knowledge and technology from industry to university members (Paavola & Hakkarainen, 2005) (Etzkowitz, 2017).

In fact, none of the performance indicators obtained from interviews is related to commercialization and revenue generations of university-industry relations. These findings are in contradiction with top UIC performance indicators obtained from literature in relation to Number of Generated Startups & Spinoffs (Castro et al., 2019), Number of and Income from IP Sales (Son et al., 2019; Rossi & Rosli, 2013), Number of and Income by type of UIC Activity (Consulting & Services, Research, and Training & Education) (Rajalo & Vadi, 2017; Clauss & Kesting, 2017). Therefore, a deeper look into motives and drivers of the Qatar National Research Strategy (QNRS) (Fund, 2012) is needed in future research.

4 LIMITATIONS AND FUTURE RESEARCH

This study is limited to a 15-year span of time and publication databases used for searching papers. The key words used in this research provided another limitation to number of generated papers by selected publication databases. Thus, it is recommended for future research to consider a wider literature search in terms of time span, publication databases, and key words.

In addition, only two interviews were conducted with active scholars in university-industry relations. The objective of conducting interviews was to map and refine the findings of literature review with country-specific considerations. Furthermore, both interviews were conducted with scholars from Qatar University. None of the interviewees comes from industry and businesses. Therefore, mapping and refining indicators and country-specific considerations from industry perspective was not possible. Consequently, it is recommended to future researchers to consider a wider representation of scholars and business leaders engaged in university-industry relations in Qatar, or any other context of interest, to get insights that further enable refinement and mapping of findings from literature.

Indeed, this research was mainly a literature review, and country specific considerations were obtained from limited number of interviews. Therefore, results are yet to be confirmed empirically in the context of Qatar. Comparative analysis of UIC performance indicators used across countries is another attractive field for future research.

5 CONCLUSION

First, this study revealed that universities are increasingly focused on measuring

performance of collaboration with industry. The results offered a number of UIC performance indicators, including (1) Number of Publications, (2) Number of Registered Patents, (3) Number of Generated Startups & Spinoffs, (4) Income from IP Sales, (5) Number of Patent Applications, (6) Income by type of UIC Activity (Consulting & Services, Research, and Training & Education), (7) Number of IP Licenses, (8) Number of Occurrences for each UIC Activity, (9) Impact Factor of Publications, and (10) Number of Innovations (Process/Marketing/Product/Organizational).

Second, this study revealed that industry is increasingly focused on measuring performance of collaboration with university. The results presented a number of UIC performance indicators, including (1) Number of Innovations (Process/Marketing/Product/Organizational), (2) Number of Registered Patents, (3) Income from Innovations (Process/Marketing/Product/Organizational), (4) Number of Patent Applications, (5) Number of Joint Publications, and (6) Number of Postgraduate Positions offered within UIC.

Third, university and industry share common interests when it comes to driving innovations as a key motive for university-industry relations. This proposition is supported by the common interests in measuring UIC performance through (1) Number of Innovations (Process/Marketing/Product/Organizational), (2) Number of Registered Patents, and (3) and Number of Patent Applications.

Fourth, this study thus contributes to a general understanding of measuring UIC performance and trends in this emergent field of research. It also highlights the Qatar country-specific considerations and challenges for measuring UIC performance considerations. In such context, the key UIC performance indicators are (1) Number of Publications, (2) Number of Citations (Local and International), (3) Number of Registered Patents, (4) Number of Registered Applications, (5) Number of Training Programs Provided (to Faculty and Students), and (6) Number of Innovations (Process/Product).

Fifth, there is also a need for more research examining a wider range of performance indicators, impacts of research strategies, and related policies. In Qatar, in particular, there is a lack of empirical studies concerning the effects of the Qatar National Research Strategy (QNRS) (Fund, 2012) and impact on what indicators to choose and monitor for UIC performance.

In conclusion, despite numerous studies conducted on measuring performance of UIC, there is still a great deal of research yet to be conducted in order to model, theorize, and empirically test the indicators used to measure UIC performance, in general, and in context of the State of Qatar, in particular.

REFERENCES

Agrawal, A. K. (2001). University–to–industry knowledge transfer: Literature review and unanswered questions. *International Journal of management reviews*, *3*(4), 285-302.

Al-Ashaab, A., Flores, M., Doultsinou, A. & Magyar, A. (2011). A balanced scorecard for measuring the impact of industry–university collaboration. *Production Planning & Control*, *22*(5-6), 554-570.

Albahari, A., Pérez-Canto, S., Barge-Gil, A. & Modrego, A. (2017). Technology Parks versus

Science Parks: Does the university make the difference? *Technological Forecasting and Social Change*, 116, 13-28.

Albats, E., Fiegenbaum, I. & Cunningham, J. A. (2018). A micro level study of university industry collaborative lifecycle key performance indicators. *The Journal of Technology Transfer*, *43*(2), 389-431.

Aldieri, L., Kotsemir, M. & Vinci, C. P. (2018). The impact of research collaboration on academic performance: An empirical analysis for some European countries. *Socio-Economic Planning Sciences*, 62, 13-30.

AlMadeed, D. M. (2019). University-Industry Relations. In Z. Al-Gasim (Ed.), VP of Research & Graduate Studies - Qatar University, Doha.

Anatan, L. (2015). Conceptual issues in university to industry knowledge transfer studies: a literature review. *Procedia-Social and Behavioral Sciences*, 211, 711-717.

Ankrah, S. & Omar, A.-T. (2015). Universities–industry collaboration: A systematic review. *Scandinavian Journal of Management*, *31*(3), 387-408.

Ávila, L. V., Leal Filho, W., Brandli, L., Macgregor, C. J., Molthan-Hill, P. & Özuyar, P. G., et al. (2017). Barriers to innovation and sustainability at universities around the world. *Journal of cleaner production*, 164, 1268-1278.

Azagra-Caro, J. M., Barberá-Tomás, D., Edwards-Schachter, M. & Tur, E. M. (2017). Dynamic interactions between university-industry knowledge transfer channels: A case study of the most highly cited academic patent. *Research Policy*, *46*(2), 463-474.

Azagra-Caro, J. M., Tijssen, R. J., Tur, E. M. & Yegros-Yegros, A. (2019). University-industry scientific production and the Great Recession. *Technological Forecasting and Social Change*, 139, 210-220.

Babić, V. & Savović, S. (2018). University characteristics as the success factor of academic spin-offs. *Zbornik Ekonomskog fakulteta u Zagrebu*, *16*(1), 113-127.

Battaglia, D., Landoni, P. & Rizzitelli, F. (2017). Organizational structures for external growth of university technology transfer offices: an explorative analysis. *Technological Forecasting and Social Change*, 123, 45-56.

Ben-Ayed, P. O. (2018). University-Industry Relations. In Z. Al-Gasim (Ed.), Department of Management and Marketing - Qatar University, Doha.

Berbegal-Mirabent, J., García, J. L. S. & Ribeiro-Soriano, D. E. (2015). University–industry partnerships for the provision of R&D services. *Journal of Business Research*, *68*(7), 1407-1413.

Bstieler, L., Hemmert, M. & Barczak, G. (2017). The changing bases of mutual trust formation in inter-organizational relationships: A dyadic study of university-industry research collaborations. *Journal of Business Research*, 74, 47-54.

Castro, I. J. D., Nagano, M. S. & Ribeiro, S. X. (2019). Elements that influence knowledge sharing in the university-industry-government collaboration: Case studies in Brazil. *Revista de Gestão*, *26*(1), 61-72.

Chen, G., Yang, G., He, F. & Chen, K. (2019). Exploring the effect of political borders on university-industry collaborative research performance: Evidence from China's Guangdong province. *Technovation*, 82, 58-69.

Chesbrough, H. (2012). Open innovation: Where we've been and where we're going. *Research-Technology Management*, *55*(4), 20-27.

Clauss, T. & Kesting, T. (2017). How businesses should govern knowledge-intensive collaborations with universities: An empirical investigation of university professors. *Industrial Marketing Management,* 62, 185-198.

Corral de Zubielqui, G., Jones, J., Seet, P.-S. & Lindsay, N. (2015). Knowledge transfer between actors in the innovation system: a study of higher education institutions (HEIS) and SMES. *Journal of Business & Industrial Marketing*, *30*(3/4), 436-458.

D'este, P. & Perkmann, M. (2011). Why do academics engage with industry? The entrepreneurial university and individual motivations. *The Journal of Technology Transfer*, *36*(3), 316-339.

Dalmarco, G., Hulsink, W. & Blois, G. V. (2018). Creating entrepreneurial universities in an emerging economy: Evidence from Brazil. *Technological Forecasting and Social Change*, 135, 99-111.

Davey, T., Baaken, T., Galan Muros, V. & Meerman, A. (2011). The State of European University-Business Cooperation. Part of the DG Education and Culture Study on the cooperation between higher education institutions and public and private organisations in Europe, 140.

David, F. & van der Sijde, P. (2015). University–Business Co-operation in Indonesian Higher Education for Innovation. In New Technology-Based Firms in the New Millennium (pp. 187-200): Emerald Group Publishing Limited.

Etzkowitz, H. (2017). Innovation Lodestar: The entrepreneurial university in a stellar knowledge firmament. *Technological Forecasting and Social Change*, 123, 122-129.

Fischer, B. B., Schaeffer, P. R., Vonortas, N. S. & Queiroz, S. (2018). Quality comes first: university-industry collaboration as a source of academic entrepreneurship in a developing country. *The Journal of Technology Transfer*, *43*(2), 263-284.

Foundation, Q. (2015). *Qatar Foundation Annual Report_2014-15*. Doha - (Qataro. Document Number).

Franco, M. & Haase, H. (2015). University–industry cooperation: Researchers' motivations and interaction channels. *Journal of Engineering and Technology Management*, 36, 41-51.

Fund, Q. N. R. (2012). *Qatar National Research Strategy 2012*. Doha: Qatar National Research Fund. (Q. N. R. Fund o. Document Number).

Galán-Muros, V., van der Sijde, P., Groenewegen, P. & Baaken, T. (2017). Nurture over nature: How do European universities support their collaboration with business? *The Journal of Technology Transfer*, *42*(1), 184-205.

Garcia-Perez-de-Lema, D., Madrid-Guijarro, A. & Martin, D. P. (2017). Influence of university–firm governance on SMEs innovation and performance levels. *Technological Forecasting and Social Change*, 123, 250-261.

Geuna, A. & Muscio, A. (2009). The governance of university knowledge transfer: A critical review of the literature. *Minerva*, *47*(1), 93-114.

Giannopoulou, E., Barlatier, P.-J. & Pénin, J. (2019). Same but different? Research and technology organizations, universities and the innovation activities of firms. *Research Policy*, *48*(1), 223-233.

Goel, R. K., Göktepe-Hultén, D. & Grimpe, C. (2017). Who instigates university–industry collaborations? University scientists versus firm employees. *Small Business Economics*, *48*(3), 503-524.

Gulbrandsen, M. & Thune, T. (2017). The effects of non-academic work experience on external interaction and research performance. *The Journal of Technology Transfer*, *42*(4), 795-813.

Hall, B. H. (2004). University-industry research partnerships in the United States.

Hansen, I.-E., Mork, O. J. & Welo, T. (2018). Towards a Framework for Managing Knowledge Integration in University-Industry Collaboration Projects. *Paper presented at the European Conference on Knowledge Management*, 994-XIX.

Huang, M.-H. & Chen, D.-Z. (2017). How can academic innovation performance in university–industry collaboration be improved? *Technological Forecasting and Social Change*, 123, 210-215.

Hue Kyung, L., Hyun Duk, Y., Si Jeoung, K. & Yoon Kyo, S. (2016). Factors affecting university–industry cooperation performance: Study of the mediating effects of government and enterprise support. *Journal of Science and Technology Policy Management*, *7*(2), 233-254.

Ishengoma, E. & Vaaland, T. I. (2016). Can university-industry linkages stimulate student employability? *Education+ Training*, *58*(1), 18-44.

Ivascu, L., Cirjaliu, B. & Draghici, A. (2016). Business model for the university-industry collaboration in open innovation. *Procedia Economics and Finance*, 39, 674-678.

Jackson, D. J. (2011). What is an innovation ecosystem. National Science Foundation, 1.

Kruss, G. & Visser, M. (2017). Putting university–industry interaction into perspective: a differentiated view from inside South African universities. *The Journal of Technology Transfer*, *42*(4), 884-908.

Lam, A. (2010). From 'ivory tower traditionalists' to 'entrepreneurial scientists'? Academic scientists in fuzzy university—industry boundaries. *Social studies of science*, *40*(2), 307-340.

Lašáková, A., Bajzíková, Ľ. & Dedze, I. (2017). Barriers and drivers of innovation in higher education: Case study-based evidence across ten European universities. *International Journal of Educational Development*, 55, 69-79.

Leydesdorff, L., Etzkowitz, H., Ivanova, I. & Meyer, M. (2017). *The measurement of synergy in innovation systems: Redundancy generation in a triple helix of university-industry-government relations*. Springer handbook of science and technology indicators. Heidelberg: Springer. Google Scholar.

Li, R. & Fang, W. (2019). University-industry-government relations of the Ministry of Industry and Information Technology (MIIT) universities: The perspective of the mutual information. *PloS one*, *14*(2), e0211939.

Lind, F., Styhre, A. & Aaboen, L. (2013). Exploring university-industry collaboration in research centres. *European Journal of Innovation Management*, *16*(1), 70-91.

Liu, A. M., Liang, O. X., Tuuli, M. & Chan, I. (2018). Role of government funding in fostering collaboration between knowledge-based organizations: Evidence from the solar PV industry in China. *Energy Exploration & Exploitation*, *36*(3), 509-534.

Lotman, J. (2009). *Culture and explosion* (Vol. 1): Walter de Gruyter.

Mäkimattila, M., Junell, T. & Rantala, T. (2015). Developing collaboration structures for university-industry interaction and innovations. *European Journal of Innovation Management*, *18*(4), 451-470.

Mascarenhas, C., Ferreira, J. J. & Marques, C. (2018). University–industry cooperation: A systematic literature review and research agenda. *Science and Public Policy*, *45*(5), 708-718.

Ministry of Development, P. A. S. (2018). *Qatar National Development Strategy 2018-2022*. Doha: Ministry of Development, Planning and Statistics. (P. a. S. Ministry of Development o. Document Number).

Mitchell, T. R. (1982). Motivation: New directions for theory, research, and practice. *Academy of management review*, *7*(1), 80-88.

Muscio, A., Quaglione, D. & Scarpinato, M. (2012). The effects of universities' proximity to industrial districts on university–industry collaboration. *China Economic Review*, *23*(3), 639-650.

OECD. (2002). Frascati Manual: Proposed Standard Practice for Surveys on Research and Experimental Development (6 ed.). Paris: OECD.

Paavola, S. & Hakkarainen, K. (2005). The knowledge creation metaphor–An emergent epistemological approach to learning. *Science & education*, *14*(6), 535-557.

Perkmann, M., Neely, A. & Walsh, K. (2011). How should firms evaluate success in university–industry alliances? A performance measurement system. *R&D Management*, *41*(2), 202-216.

Perkmann, M., Tartari, V., McKelvey, M., Autio, E., Broström, A., & D'Este, P. et al. (2013). Academic engagement and commercialisation: A review of the literature on university–industry relations. *Research policy*, *42*(2), 423-442.

Planning, G. S. f. D. (2008). *The Qatar National Vision 2030*. Retrieved 04 August 2018 from https://www.mdps.gov.qa/en/knowledge/HomePagePublications/QNV2030_Arabic_v2.pdf.

Rajalo, S. & Vadi, M. (2017). University-industry innovation collaboration: Reconceptualization. *Technovation*, 62, 42-54.

Rau, C., Neyer, A.-K. & Möslein, K. M. (2012). Innovation practices and their boundary-crossing mechanisms: a review and proposals for the future. *Technology Analysis & Strategic Management*, *24*(2), 181-217.

Rossi, F. (2010). The governance of university-industry knowledge transfer. *European Journal of Innovation Management*, *13*(2), 155-171.

Rossi, F. & Rosli, A. (2013). Indicators of university-industry knowledge transfer performance and their implications for universities: Evidence from the UK's HE-BCI survey.

Rothaermel, F. T., Agung, S. D. & Jiang, L. (2007). University entrepreneurship: a taxonomy of the literature. *Industrial and corporate change*, *16*(4), 691-791.

Salehi, N. (2013). Mediating Effect of Absorptive Capacity on the Relationship Between Antecedents, Research and Development and Innovation. University Technology Malaysia Johor Bahru.

Salleh, M. & Omar, M. (2013). University-industry collaboration models in Malaysia. *Procedia-Social and Behavioral Sciences*, 102, 654-664.

Saunders, M. N. & Lewis, P. (2012). Doing research in business & management: An essential guide to planning your project: Pearson.

Scandura, A. (2016). University–industry collaboration and firms' R&D effort. *Research Policy*, *45*(9), 1907-1922.

Seppo, M. & Lilles, A. (2012). Indicators measuring university-industry cooperation. *Discussions on Estonian Economic Policy*, *20*(1), 204.

Son, H., Chung, Y. & Hwang, H. (2019). Do technology entrepreneurship and external relationships always promote technology transfer? Evidence from Korean public research organizations. *Technovation*, 82, 1-15.

Striukova, L. & Rayna, T. (2015). University-industry knowledge exchange: An exploratory study of Open Innovation in UK universities. *European Journal of Innovation Management*, *18*(4), 471-492.

Vaaland, T. I. & Ishengoma, E. (2016). University-industry linkages in developing countries: perceived effect on innovation. *Education+ Training*, *58*(9), 1014-1040.

Van Looy, B., Ranga, M., Callaert, J., Debackere, K. & Zimmermann, E. (2004). Combining entrepreneurial and scientific performance in academia: towards a compounded and reciprocal Matthew-effect? *Research Policy*, *33*(3), 425-441.

Villani, E., Rasmussen, E. & Grimaldi, R. (2017). How intermediary organizations facilitate university–industry technology transfer: A proximity approach. *Technological Forecasting and Social Change*, 114, 86-102.

Yalçıntaş, M., Kaya, C. Ç. & Kaya, B. (2015). University-industry cooperation interfaces in Turkey from academicians' perspective. *Procedia-Social and Behavioral Sciences*, 195, 62-71.

Zahra, S. A. & George, G. (2002). Absorptive capacity: A review, reconceptualization, and extension. *Academy of management review*, *27*(2), 185-203.

Zhang, Y., Chen, K. & Fu, X. (2019). Scientific effects of Triple Helix interactions among research institutes, industries and universities. *Technovation*.

Cite this article as: Al-Gasim Z., Senin A. A., bin Yusoff M. E., "Performance of University-Construction Industry Collaboration: A Systematic Literature Review and Research Agenda", International Conference on Civil Infrastructure and Construction (CIC 2020), Doha, Qatar, 2-5 February 2020, DOI: https://doi.org/10.29117/cic.2020.0008

Practical Implementation of Contract Administration Performance Model in Qatar Construction Projects

Murat Gunduz
mgunduz@qu.edu.qa
Department of Civil and Architectural Engineering, Qatar University, Doha, Qatar

Hesham A. Elsherbeny
he1512830@student.qu.edu.qa
Engineering Management Program, College of Engineering, Qatar University, Doha, Qatar

ABSTRACT

Globally, the performance of Construction Contract Administration (CCA) is becoming of significant interest as the industry suffers from notable delays, cost overruns, and disputes as a consequence of poor contract administration practices. In Qatar, the pace of projects will continue after hosting the FIFA 2022 World Cup to achieve the 2030 Qatar National Vision and beyond, therefore, monitoring of the proper CCA implementation and performance is necessary. Due to the wide scope and complicated nature of CCA, there is yet no consensus on how to assess its performance. This study briefly presents a systematic, operational, and multi-dimensional construction Contract Administration Performance Framework (CAPF) consisting of 93 CCA key measures/ tasks categorized in 11 CCA dimensions/process groups. The proposed framework is validated by structural equation modeling and subsequently, the Contract Administration Performance Model (CAPM) model was established. Through this study, the CAPM and its components are briefly explained, and then implemented on a real-world sample of 13 small, medium, and major construction projects in Qatar covering both public and private sectors, and then the performance is benchmarked. It is found that the model provides an operational basis for measuring the CCA Group Performance Indices (GPI), the overall Construction Contract Administration Performance Index (CCAPI) and support the identification of underperforming groups. The benchmarking value for the CCAPI (77.5%) demonstrates that the level of CCA performance is good. Also, the benchmarking values of GPI (range 74.3% to 87.8%) are good, except risk management (GPI= 50.5%), which needs an improvement program.

Keywords: Optimized aggregate gradation; Portland-limestone cement; Cementitious content; Concrete pavement; 3D FEM model

1 INTRODUCTION

According to Jarkas and Mubarak (2016), poor contract administration that reduces liquidity in the markets and employer changes are currently the main causes of disputes. Also, failure to administer, understand, and comply with the contract properly leads to making the dispute difficult (Harris 2013). Furthermore, Arcadis (2017) presents poor contract administration as time-consuming and as the main source of disputes in the Middle East, Europe, Asia, and North America. In 2015, the average global value of disputes was US$46 million, and the average length was 15.5 months versus US$82

million and 15.2 months in the Middle East. In 2016, the average global value of disputes was dropped to US$42.8 million, and the average length was 14 months versus US$56 million and 13.7 months in the Middle East. What's more, several authors study the consequences of poor contract administration and inefficient management of contracts. The consequences are listed as working against sustaining the industry; heavy fine for non-compliance; substantial loss of savings; incur resources waste; delay in time; productive loss; several non-value added activities; poor control of operations; low rate of satisfying customers; unwanted costs; and more risks (Awwad et al., 2016). The importance of contract administration and the consequences of the poor administration in construction projects necessitate an additional urgency to investigate the contract administration process performance and identify the elements that reflect the good contract administration practice. Also, challenges associated with the industry necessitate the need for effective management and proper administration of the contract (Gitonga et al., 2017) and establish an efficient and effective process to maintain a strong relationship between the parties (Bin Zakaria et al., 2013).

2 QATAR CONSTRUCTION

In Qatar, the workload continues to focus on arrangements for the FIFA World Cup 2022 and the related infrastructure projects (AECOM 2016). As a result, several capital investments are being funded, and the construction industry continues to stay as a key element of the nation's plan. Qatar shall continue to invest around $220 billion in capital projects and infrastructure over the next few years. The construction is regarded as one of the largest industries in Qatar; the sector shared 14.5, 15.6 and 17.5% percent of real Gross Domestic Product (GDP) in 2014, 2015 and 2017, respectively, and is still the main contributor to economic growth during the coming years. The construction output is increased from QR 52.5 to 88 Billion for the period between 2014 to 2017, with the highest sectorial growth in the economy by (14.5%) and falls far behind the manufacturing sector with an average annual growth of only 2.6% (Authority 2018). In 2018, the construction sector has contributed to 1.8% of the total expected growth of 2.6%. With an expected growth rate of 5.2%, the construction will contribute to at least 50% of this growth rate between 2018 to 2020. Not only this but construction activities intensively employs around 41% of the total labor force due to the construction boom and speed up large-scale/mega infrastructure projects for the FIFA 2022 session (Statistics 2016, Authority 2018). While the government is committed to allocating 40% of its budget to infrastructure projects, the workload continues to focus on arrangements of sports facilities and the related projects (AECOM 2016).

3 CONTRACT ADMINISTRATION PERFORMANCE MODEL

Gunduz and Elsherbeny (2019) established a systematic, operational, and multi-dimensional construction Contract Administration Performance Framework (CAPF). The framework with detailed measures was developed, investigated, and tested by involving a three-step research design. At the first step, 82 measures under 11 dimensions were determined by literature review, interviews with four construction professionals. In the second step, two rounds modified Delphi study was conducted with 17 construction experts, additional 13 measures were identified, and the collected data were analyzed

for expert's consensuses by employing Spearman rank-order correlation, mode score, mode value, and standard deviation to mean ratio (SDMR). In the third step, the strength of agreement was measured by inter-rater agreement (IRA) analysis, and the agreement level represents 94.6% of the proposed key factors and 100% of the proposed groups. Consequently, a significant consensus was achieved, and construction experts recognized the importance of the identified key factors on the overall performance of the project. At the last step, the model was externally validated through two pilot projects and the results confirmed the generalizability and measurability of the proposed framework for any construction project.

The proposed framework was based on (1) comprehensive literature review on construction contract administrator roles and responsibilities; (2) key success factors for contract administration and management; (3) the obligations of the CCA team under the different forms of contract such as Qatar general conditions of contract: GCC 1987, International Federation of Consulting Engineers (FIDIC): Red Book 1999, American Institute of Architects (AIA): A201-2007, Joint Contracts Tribunal : JCT 2011 , and New Engineering Contract NEC:2005; (4) obligations of the contract administration team under professional service agreements to include Qatar professional service agreement : PSA 2010 (PWA 2010) , and FIDIC White Book 2017; (5) contract administration previous models; and (6) strategies to avoid poor construction contract administration. The proposed framework contained 11 project management process groups and 93 key tasks (measures) affecting the construction contract administration performance as shown in Appendix A.

An on-line questionnaire was distributed to around 1000 practitioners to rate the importance of the CCA measures and process groups, and 336 completed questionnaires were used in data analysis using structural equation modeling. The model achieved the goodness of fit, reliability, validity requirements, as shown in Figure 1. The GPI and CCAPI were calculated from the standardized factor loading- as weighted scores - by the methodology proposed by (Gunduz et al., 2018). As a result, the within-group measures weights are shown in appendix A. The CCAPI index is calculated through Equation 1 where *Pi* represents summations of measures performance within each individual group.

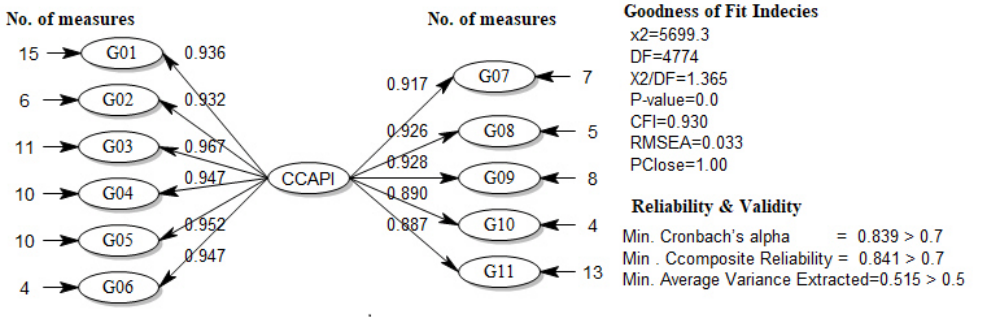

Figure 1: CAPM Second-Order SEM Model

$$CCAPI = [9.15P_1 + 9.11P_2 + 9.45P_3 + 9.26P_4 + 9.31P_5 + 9.26P_6 + 8.96P_7 + 9.05P_8 + 9.07P_9 + 8.7P_{10} + 8.67P_{11}] / 100 \quad (1)$$

4 RESEARCH METHODOLOGY

The study adopted an actual "case studies" research approach. 13 small to major construction projects covering both public and private sectors and different project types are selected. CCA experts completed performance assessment forms and then incorporated data into the CAPM model to calculate the CCA performance for the process groups and the overall project as well. The performance level was benchmarked at the project level and group performance level. Finally, the results have been discussed, and the conclusion is drawn.

5 MODEL IMPLEMENTATION

5.1 Profile of Projects

The CAPM was employed to assess the CCA performance in 13 construction projects. The assessment forms were completed by the CCA experts (minimum 15 years of experience in contract administration) according to a scale between 0 to 100. Where the variables were not implemented, the assessment was recorded as blank, and their relative weights were redistributed to the other measures within the same group. Out of 13 projects, 6 projects were public, and the other 7 projects were private projects. 10 projects represented building type construction (i.e., mega administration building, educational and health facilities, malls and markets, tower, villa compounds, and apartment buildings, drainage, and industrial facilities) and the values of construction ranged between 1000 to USD4million. 3 projects were completed, 3 projects passed testing on completion, and the remaining 7 projects were under construction. Table 1. shows the profile of the 13 projects.

Table 1: Profile of Projects 1 To 13

Project	Sector	Type	Project Value (US Million)
#1	Public	Building	490
#2	Public	Building	232
#3	Public	Building	100
#4	Public	Infrastructure	60
#5	Public	Industrial facilities	38
#6	Private	Building	14
#7	Private	Building	1000
#8	Private	Building	92
#9	Private	Building	75
#10	Private	Building	32
#11	Private	Building	28
#12	Private	Building	15
#13	Private	Infrastructure	4

5.2 Results of Model Implementation

The results of the construction contract administration performance index (CCAPI)

of the 13 projects and the Group Performance Index (GPI) for the 11 groups are presented in Table 2. The CCAPI for project #1 is calculated as 87.0%. The results obtained by calculating the performance level of each process group are quite revealing that the best performance is related to G04-Quality & Acceptance (GPI= 95%) while the worst implemented process group is G10-Contract Risk Management (GPI= 55%). Except for the risk management, no significant differences are observed between the different GPIs. For project #2, CCAPI is calculated as 67.4%. The best performance is related to G01-Project governance and start-up (GPI= 93.9%), while the worst performance is related to G10-Contract Risk Management (GPI= 58.3%). Except for the first group, no significant differences between the different groups are identified. For project #3, CCAPI is calculated as 77.0% and the best performances are related to G09-Claims & Disputes Resolution and G03-Communication & Relationship with GPIs of 86.1% and 85.3%, respectively. On the contrary, the worst groups are G10-Contract Risk Management and G01-Project Governance & Start-up with GPIs of 65.0%, and 67%, respectively. Minor significant differences between groups are observed. For project #4, CCAPI is calculated as 92.5%. The best groups are G05-Monitoring & Reporting, G07-Financial Management, G08-Changes & Changes Control, and G10-Contract Risk Management with ultimate GPIs of 100%. The lowest group is G04-Quality & Acceptance (GPI=78.5%). For project #5, CCAPI is calculated as 87.1% and the best groups are G05-Monitoring & Reporting, G06-Document & Record, and G08-Changes & Changes Control with ultimate GPIs of 100 %. The lowest groups are G03-Communication & Relationship, G04-Quality & Acceptance, and G10-Contract Risk Management with GPIs of range 75.5 to 72.0%.

In the private sector, The CCAPI for project #6 is calculated as 79.7%. The best group is G08-Changes & Changes Control (GPI=100%). The lowest implemented process groups are G10-Contract Risk management and G06-Document & Record with GPIs of zero, and 72.1%, respectively. For project #7, CCAPI is calculated as 86.6%, and the best groups are G06-Document & Record, and G07-Financial Management, with 100% GPIs while the lowest implemented process group is G02-CA Team Management, with GPI of 70.4%. For project #8, CCAPI is calculated as 80.6%, and the best groups are G08-Changes & Changes Control, and G09-Claims & Disputes Resolution with 100% ultimate performance. The lowest implemented process group is G10-Contract Risk Management with GPI of zero and then G11-Contract Close-Out, with only 43.4% performance level. For project #9, CCAPI is calculated as 64.0%. The best groups are G08-Changes & Changes Control and G09-Claims & Disputes Resolution with 85.3% GPIs. The lowest implemented group is G10-Contract Risk Management with only GPIs of 38.9% performance. For project #10, CCAPI is calculated as 73.6%, and the best group is G09-Claims & Disputes Resolution with GPI of 87.5% and then is followed by G07-Financial Management with GPIs of 87.3%. The lowest implemented group is G10-Contract Risk Management, with only 57.2% performance level. For project #11, CCAPI is calculated as 59.6%. The best-implemented groups are G01-Project Governance & Start-up, G02-CA Team Management, and G09-Claims & Disputes Resolution (GPIs= 6.9 to 75%). The lowest group is G10-Contract Risk Management, with only 38.9% GPI. The CCAPI for project #12 is calculated as 67.1%. The best- group is G06-Document & Record with (GPI= 82.5%) and then followed by the G08-Changes &

Changes Control (GPI= 81.0%). The lowest group is G10-Contract Risk Management, with only 57.6% performance level. Finally, the CCAPI for project #13 is calculated as 84.7%. The best groups are G07-Financial Management, G08-Changes & Changes Control, and G09-Claims & Disputes Resolution with an ultimate GPI of 100%. The lowest groups are G05-Monitoring & Reporting and G06-Document & Record (GPIs= 61.1% and 63.0%, respectively).

Table 2: Calculated GPI and CCAPI for Projects 1 to 13

Group	Project													
	#1	#2	#3	#4	#5	#6	#7	#8	#9	#10	#11	#12	#13	Avg.
G01	86.8	93.9	68.0	90.1	86.4	82.3	94.3	84.5	79.6	73.2	76.9	51.4	92.1	81.5
G02	82.0	67.3	73.8	91.3	89.9	84.2	70.4	84.2	43.9	74.2	76.3	63.4	86.9	76.0
G03	92.3	62.3	85.3	79.9	75.5	97.5	91.0	97.7	71.2	61.2	56.9	71.1	73.4	78.1
G04	95.0	67.2	82.7	78.5	75.5	76.4	88.4	88.1	59.1	61.2	45.5	65.5	82.7	74.3
G05	92.6	58.5	80.2	100.0	100.0	86.2	79.2	91.1	64.4	70.9	39.6	63.4	61.0	75.9
G06	92.5	69.9	81.3	94.0	100.0	72.1	100.0	96.1	61.3	86.1	52.6	82.5	63.0	80.9
G07	91.0	61.1	78.9	100.0	85.8	97.4	100.0	95.6	54.2	87.3	65.3	63.0	100.0	83.1
G08	92.0	64.9	78.1	100.0	100.0	100.0	93.9	100.0	85.3	79.7	66.6	81.0	100.0	87.8
G09	90.0	70.2	86.1		87.6	86.5	87.9	100.0	80.5	87.5	75.0	74.5	100.0	85.5
G10	55.0	58.3	65.0	100.0	72.0	0.0	63.6	0.0	38.9	57.2	38.9	57.6		50.5
G11	86.5		67.8		85.1	91.3	83.0	43.4		71.3	61.6	64.3	90.4	74.5
CCA-PI	87.0	67.4	77.1	92.5	87.1	79.7	86.6	80.6	64.0	73.6	59.6	67.1	84.7	77.5
CCAPI Public= 82.4						CCAPI Private = 74.5								

5.3 Discussion of Results

The performance scale is set to a 4-point scale (i.e., excellent performance >=90; good performance 70-89; average performance 50-69; needs improvement/ poor performance 0-49). This scale is adopted by several architects and engineering consultants in Qatar to reflect their performance level. At the project level, the CCAPI benchmarking value for the 13 projects is found to be 77.5%, as shown in Figure 2. The result shows that the highest calculated CCAPI for project #4 is 92.5%, while the lowest calculated CCAPI is 59.6% for project #11. The overall CCAPI values for projects #1, 3 to 8, and 13 exceed the benchmarking value. The CCAPI of project# 10 is slightly dropped below the benchmarked value, while CCAPI of projects #2, 12, 9, and 11 are significantly away from the benchmarking value. Therefore, the management of the last-mentioned projects should focus on improving the performance of the individual process groups to enhance the overall performance. Also, the significant differences among projects necessitate the need to identify the performance of the project team across different groups. It is worthy to note that the CCAPI of public sectors (82.4%) is higher than the private sector (74.5%). This is referred to as the legalization and constraints of rules in the public sector (Patajoki 2013). Following the performance rating scale, it could be concluded that the overall performance of the investigated projects ranged from average to excellent.

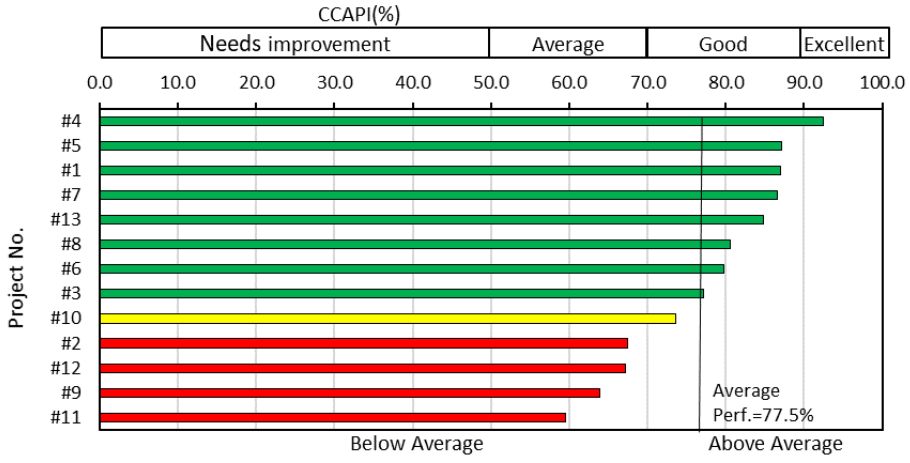

Figure 2: Calculated CCAPI for projects # 1 to 13

At the process group level, as shown in Figure 3, it is worth noting that 5 groups, namely: G01, G03, G06, and G07 to G09 demonstrate average (GPI) higher than the benchmarking value. On the contrary, G08-Changes & Changes Control represents the highest performance (GPI=87.8%) and is followed by G09-Claims & Disputes Resolution (GPI= 85.5%). On the negative side, 3 groups (G02-Contract Administration Team Management, G04-Quality & Acceptance, and G05-Performance Monitoring & Reporting) are slightly below the benchmarking value but within a range of 5%. G10-Contract Risk Management represents the lowest GPI (GPI= 50.5%) among other groups, and therefore, it could be argued that there should be an urgent need to re-structure this process and initiate an urgent continual improvement program for risk management. The literature revealed a similar low performance of risk management in other countries (Surajbali 2016). Following the performance rating scale, it could be concluded that group performance indicators are good except for risk management.

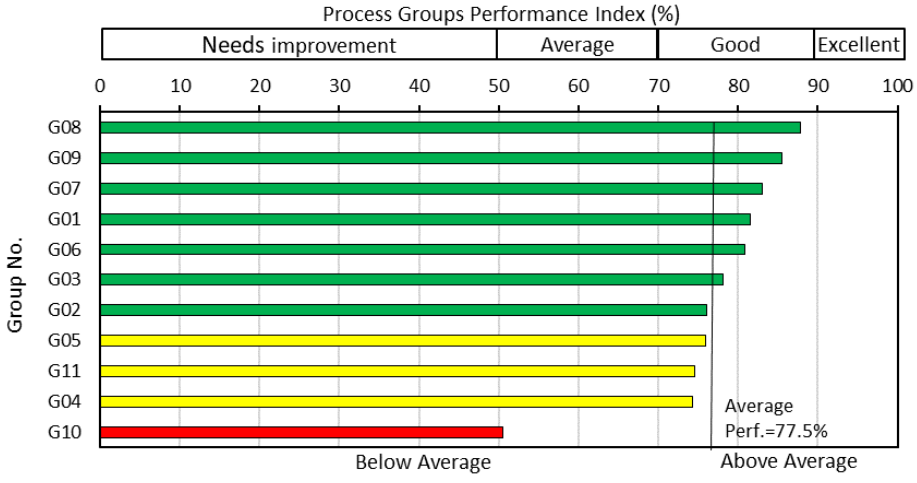

Figure 3: Benchmarking values of the process group

6 CONCLUSION

Based on the authors' established systematic, operational, and multi-dimensional construction Contract Administration Performance Framework (CAPF) and model (CAPM), this study demonstrates the practical implementation of the CAPM for practitioners and researchers to use in calculating CCA Group Performance Indices (GPI) and the overall CCA performance index (CCAPI) for public and private projects of different types and sizes. By using factual data from 13 construction projects in Qatar, the practical implementation of CAPM is demonstrated.

Results from the case study showed that the CAPM implementation has a practical application to identify variations in performance levels among the process groups and project performances, as well. The benchmarking value for the CCAPI (77.5%) demonstrates that the level of CCA performance is good. The CCAPI of the public sector (82.4%) is remarkably higher than the private sector (74.5%). Also, the performance of CCA process groups is good, except risk management, which needs improvement. The CCA performance measurement approach presented in this study can be applied to different construction projects, and the weight of the measures could be changed to cover special projects priorities.

REFERENCES

AECOM (2016). Middle East Handbook: Property and Construction Handbook, *AECOM Middle East*, 1-120.

Arcadis (2017). *Global construction disputes 2017: The higher stakes, the bigger the risk*, pp. 1-29.

Authority (2018). Qatar economic outlook 2018-2020. *Ministry of Development Planning and Statistics*. Doha, 1-50.

Awwad, R., Barakat B. & Menassa C. (2016). Understanding dispute resolution in the Middle East region from perspectives of different stakeholders. *Journal of Management in Engineering*, *32*(6), 05016019.

Bin Zakaria, Z., Binti Ismail S. & Binti Yusof A. (2013). An overview of comparison between construction contracts in Malaysia: The roles and responsibilities of contract administrator in achieving final account closing success. 2013 International Conference on Education and Educational Technologies Rhodes Island, Greece.

Gitonga, J. M., Nzulwa J. & Kwena R. (2017). The effect of critical success factors on the completion of public construction projects in Machakos County Kenya. *Strategic Journal of Business & Change Management*, *4*(3-35): 529-543.

Gunduz, M., Birgonul M. T. & Ozdemir M. (2018). Development of a safety performance index assessment tool by using a fuzzy structural equation model for construction sites, *Automation in Construction*, 85: 124-134.

Gunduz, M. & Elsherbeny H. A. (2019). Operational framework for managing construction contract administration- practitioners' perspective through modified Delphi method. *Journal of Construction Engineering and Management* (in press).

Harris, E. C. (2013). *Global construction disputes: A longer resolution*. Global Construction Report. 1: 17.

Jarkas, A. M. & Mubarak S. A. (2016). Causes of construction change orders in Qatar: con-

tractors' perspective. *International Journal of Project Organisation and Management*, 8(3): 275-299.

Patajoki, U. (2013). *Towards a successful contractual relationship–public service procurement from a small business perspective*. Master, Aalto University.

PWA (2010). Professional services -general conditions of engagement, *Public Works Authority*, Doha, 1-44.

Statistics (2016). Qatar economic outlook 2016-2018. *Ministry of Development Planning and Statistics*. Doha, Qatar, 1-37.

Surajbali, R. R. (2016). Determining contract management challenges relating to supply chain management in the Eastern Cape Department of Education, *Master of Public Administration, North-West University, Potchefstroom Campus*, 1-171.

Cite this article as: Gunduz M., Elsherbeny H. A., "Practical Implementation of Contract Administration Performance Model in Qatar Construction Projects", *International Conference on Civil Infrastructure and Construction (CIC 2020)*, Doha, Qatar, 2-5 February 2020, DOI: https://doi.org/10.29117/cic.2020.0009

APPENDIX A: CONSTRUCTION CONTRACT ADMINISTRATION FRAMEWORK

Weights within Group is shown between brackets.

Framework for Investigating the Level of Compliance to the OHS Regulatory by the Small and Medium Construction Companies in Oman

Mubarak Al Alawi
alawim@squ.edu.om
College of Engineering, Sultan Qaboos University, Muscat, Oman

Mohamed Al Shahri
shahri@squ.edu.om
College of Engineering, Sultan Qaboos University, Muscat, Oman

Amjaad Al Ghafri
s117869@student.squ.edu.om
Tibudin & Partners, Muscat, Oman

ABSTRACT

The construction industry is characterized with a high rate of work-related accidents. Some of the accidents result in severe injuries and sometimes death. One of the reasons for such happenings is due to the noncompliance of the construction companies to the Occupational Health and Safety (OHS) regulatory framework. This paper briefly describes the preliminary results of the first part of an ongoing study. The study is composed of three parts studying the OHS practices in small and medium construction companies in Oman. The three parts are (1) identifying the level of compliance of the small and medium construction companies to the OHS regulatory framework, (2) comprehensively identifying the causation of the non-compliance and the risk generated, and (3) proposing a framework for "Paving Zero Accident Vision" in Oman. Oman's OHS regulatory framework was used to construct an evaluation survey. Sixty small and medium construction companies from two different governorates, Muscat and South Al Batinah, were involved in the study. Three evaluation results related to the construction site fencing, the nature of the project site, and the level of compliance to providing personal protective equipment were reported. The results showed that the 75.5% on an average, the construction companies fenced their construction site; for 59% on average the project site is a construction and an accommodation site at the same time, and the level of compliance to providing Personal Protective Equipment (PPE) is varying in both locations. However, both locations showed similar results in providing ear protection, eye protection, and safety shoes.

Keywords: OHS; Construction industry; Small and medium construction companies

1 INTRODUCTION

The construction industry is characterized with a high rate of work-related accidents that create unpleasant working environment; this statement has been frequently used in Occupational Health and Safety Research, and it has been the driving force in the development of new approaches, techniques to improve the OHS practices in the construction industry. However, leading the way to create a safe working environment is a joint effort between (1) the individual worker, (2) the employing company, (3) the

client, (4) the relevant regulatory, governmental bodies, and (5) the international OHS agencies. Working in harmony and in an integrated way between relevant OHS parties is the key principal to pave the way to Zero Accident Vision (ZAV).

The behavior of the individual construction worker is the performance indicator of how effectively the employing company is managing its designated safety program. In addition, the rate of the construction-related accidents is normally used as an indicator by the relevant OHS regulatory governmental bodies on what degree the company is complying with the OHS regulatory framework. Also, the OHS regulatory frameworks are normally adopted by international OHS agencies. This sequential flow of about OHS facts chain, according to the author's perception, exist globally. Furthermore, it is contained within what is called the *Safety Climate*; safety climate is "the shared perception of values, beliefs, and procedures related to organizational safety" (He et al., 2020). The existence and the level of compliance to the OHS regulatory framework can be considered as the common chain, and therefore knowing to what degree the construction companies are complying with the OHS regulatory framework can help to identify the gaps and challenges the construction industry needs to bridge.

The level of compliance of the construction companies to the OHS regulatory framework differs in terms of the size (Legg et al., 2015). For example, large companies are better managing the OHS safety requirement than the small companies because large companies normally dedicate resources to apply more systematic approaches to health and safety (Hasle et al., 2009). On the other side, it is difficult and expensive for the small and medium companies to cope with the large companies' performance on maintaining a high level of OHS compliance, and they frequently focus their resources on surviving (Lai et al., 2011). This fact hinders spreading the awareness about the prime responsibility of the company, no matter what its size is, which is to maintain the legal requirement of the OHS. Thus, accident in the small and medium companies burden the major work-related accidents rate (Cagno et al., 2013).

It is worth mentioning that non-complying with the OHS regulation is associated with costs, which are the costs that arise from the occurrence of accidents. The cost is classified to tangible and nontangible, and its level of effect extends from the worker going through the family and friends, employer, and finally, the society (Ikpe et al., 2012). The nontangible cost related to society is the reduction of the human potential, and reduction of the quality of life. This kind of cost is not only non-bearable to society but also to the economy, causing imbalanced distribution of local human workers in the construction industry and rebel best talent. Hence, the well-being of the construction industry in general and the well-being of the small and medium construction companies, in particular, is essential.

Therefore, this research aims to investigate the level of compliance of the small and medium construction companies in the context of Oman's construction industry to Oman's OHS regulatory framework. It discusses research plan for ongoing research on studying the small and medium construction companies OHS practices, identifying the causations of not complying with OHS standards, and formulating "Paving the way to Zero Accident Vision" research direction in the future.

2 BACKGROUND

Occupational health and safety for workers has been a vital and crucial factor at all levels of different organizations since the industry revolution (LaDou, 2003). The topic of health and safety compliance to local or global standards has received great attention in past decades. A comprehensive review by Salguero-Caparros et al. (Lai et al., 2011) to address the issues associated with compliance of implementing health and safety regulations. The paper reviewed the published studies that have investigated the interaction between OHS and compliance with legislation, regulation, and rules. Cagno et al. (2013) provided a constructive review of the past decade scientific work that dealt with economic evaluation of OHS. The features of modelling approaches and tools to assess the economic evaluation on small and medium companies were examined and methodological limitations were highlighted as well.

Gunduz and Laitinen (2017) proposed a ten-step occupational health and safety management system (OHS MS) framework for small and medium-sized construction companies to boost the level of OHS. Their study cantered on the small and medium companies within construction industry where most of the accidents occurred. OHSMS frameworks with different steps have been studied and proposed (Zhou et al., 2015) (Zhou et al., 2013). Other studies investigate the influences of adopting human resources skills and their effect on the health and safety outcomes (Lai et al., 2011) (Sunindijo & Zou, 2013). These studies identified and discussed research gaps and corresponding agenda, which can serve as guidance to factors that needed to be considered in future construction safety research and analysis.

The effect of health and safety management within small and medium enterprises have received a lot of attention in the developed countries. However, little attention has been invested in the developing countries. A study by Kheni et al. (2010) was conducted to fill that gap. The research aimed to study the influence of OHS within Ghanaian construction industry. More specifically, the study focused on small and medium construction enterprises to explore the practices and problems that render the effectiveness of implantation OHS standards. The study concluded that effective institutional structure and better socioeconomic environment among other factors are essential in order for better OHS practices within small and medium enterprises. Unnikrishnan et al. (2015) conducted a questionnaire survey to a number of 30 SMEs in India to measure the execution of safety practices within SMEs. The study, also, extended to investigate the obstacles and drivers for implementations of OHS practices. The study found that market competitiveness, better efficiency and rigid laws were among the main drivers for OHS implementation; whereas fiscal constraints, lack of knowledge and training were among the main barriers.

A study by Arewa and Farrel (2012) highlights the compliance of health and safety regulations within SMEs in United Kingdom. Since, the SMEs form around 90% of construction companies and since the OHS regulations are enforced in UK to all enterprises regardless of their nature or size. Therefore, health and safety incidents are more determinately in SMEs compared to the risk that might affect larger enterprises, which increases the financial uncertainties and risks in SMEs. The study emphasized on the relationship between the compliance of health and safety regulations and the financial performances within SMEs. The comprehension of the practitioners within UK

organizations on the anticipated benefits of implementing health and safety standards was also investigated by Chileshe & Dzisi (2012). Health and safety index was proposed to indicate the level of benefits from health and safety implementation and management within the construction industry.

3 METHODOLOGY

This research is conducted in three stages, shown in Figure 1, (1) identifying the level of compliance of the small and medium construction companies to the OHS regulatory framework, (2) comprehensively identifying the causation of the non-compliance and the risk generated, and (3) proposing a framework for "Paving Zero Accident Vision" in Oman. In this section, all of the stages will be briefly explained to show the methodology adopted in this research.

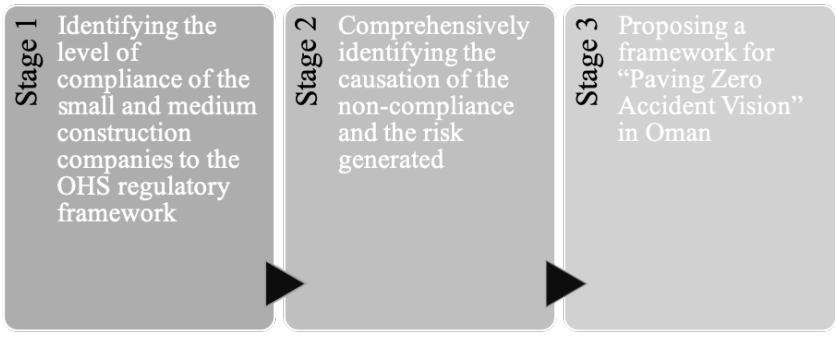

Figure 1: Research Work Sequence

3.1 Identifying the level of compliance of the small and medium construction companies to the OHS regulatory framework

To identify the level of compliance of the small and medium construction companies, first, the OHS regulatory framework adopted in Oman must be studied and used as a benchmark for the evaluation process. The Occupational Health and Safety regulatory framework was released as part of the Labor Law, which was promulgated by the royal decree No.35/2003. The OHS general guidance was published in part six under the title "Industrial Safety". The detailed description of the OHS regulatory framework can be found in the Ministerial Decision 286/2008 of the minister of Manpower (Ministry of Manpower, 2008). The OHS regulatory framework describes the following:

1. Definitions and General Provisions
2. General provisions
3. General Arrangements
4. Utilities
5. Specifications of Work Uniform and Personal Protection Equipment
6. Medical Care
7. Health Friendly Workplaces
8. Protection of women
9. Protection of the Disabled
10. Precautions Against Hazards

The OHS regulatory framework was used to construct a checklist form, and not all ten parts were included rather only the "General Arrangement", "Utilities", "Specifications of Work Uniform and Personal Protection Equipment", "Medical Care", and "Precaution Against Hazards" were adopted. The selection of those parts was because small and medium construction companies are involved in building small to medium construction projects and this research targets only small and medium residential and commercial projects. The checklist form was distributed to 60 small and medium construction companies in two governorates in Oman, Muscat and South Al Batinah (the location is marked by symbol star in Figure 2). The expected results from this stage will not only pinpoint the level of compliance but also it will provide some valuable sight on the safety culture adopted by the companies.

Figure 2: Locations of the Study in Oman (National Survey Authority, Ministry of Defence, 2019)

3.2 Comprehensively identifying the causation of the non-compliance and the risk generated

In this stage of the research, identifying the causation of the non-compliance and the risk generated is the main target. This stage aims to identify what factors cause the low level of compliance or implementation in the small and medium construction companies in Oman. This includes, but not limited, investigating the small and medium construction companies' awareness and understanding of the Occupational Health and Safety in Oman. This stage also aims to investigate ways to mitigate the factors affecting the level of compliance of the OHS regulatory framework.

3.3 Proposing a framework for "Paving Zero Accident Vision" in Oman

At the stage, paving the way to "Zero Accident Vision" will be proposed. A framework on how to move forward in marinating safe and healthy environment will be constructed. At this stage, expert engineers in the area of OHS will play a critical role in setting up

the framework. A panel of experts from different companies representing a variety of industrial sectors will be formed, and rounds of discussion will be arranged to reach consistent agreements on how best to achieve the designated target.

4 DISCUSSION OF RESULTS

This section discusses only partial preliminary results of the first stage of the research. The small and medium enterprises are those having a number of resources less than 200 (Kheni, Gibb & Dainty, 2010). The construction companies in Oman are also categorized according to their capital. There are five categories, Excellent (+250,000 OMR), First (100,000-249,000 OMR), Second (50,000-99,000 OMR), Third (25,000-49,000 OMR), and Fourth (3,000-24,000 OMR) (Ithraa, 2015). The number and the classification of the construction companies involved in the study are shown in Figure 3. The number of small and medium construction companies that participated in the study from Muscat and South Al Batinah governorates is 24 and 36 respectively. Figure 3 shows that the majority of companies in Muscat are under the Excellent class Category; meanwhile, the majority of companies in South Al Batinah are under the First and Fourth class category.

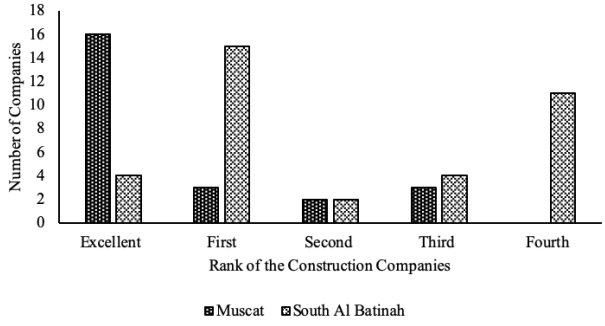

Figure 3: The Number of Construction Companies Studied in Each Class

Figure 4 shows the percentage of construction companies surrounding their construction site with a fence. Although, it is obvious that enclosing the construction site with fence is mandatory in all construction projects and it is one of the conditions which must be maintained to get a construction work permit, however, Figure 4 shows that not all companies are fencing their construction site; only 79% of the construction companies in Muscat and 72% in South Al Batinah have their construction site enclosed with fence. This act creates a new source for hazards to the society where the surrounding neighborhood is exposed to construction hazards. A report in 2015 published by the Muscat Daily with the title "Allegations arise that many construction sites in Muscat are giving safety a miss" highlighted this fact; some big machinery were lying around the construction site and causing serious threat to the residents (Muscat Daily, 2015). This observation raises a question on how the engineering office responsible in managing the project is monitoring and controlling the construction site; answering the question will help to identify one of the root causes of non-compliance to the OHS regulatory framework.

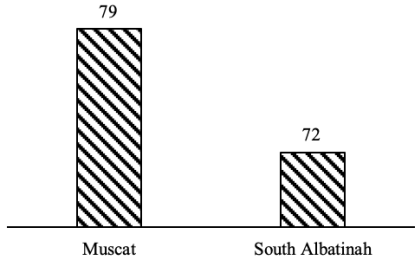

Figure 4: The Percentage of Construction Companies Surrounding their Construction Site with Fence

Figure 5 shows the results regarding the nature of the construction site, whether it is a construction site only or it is both, a construction and an accommodation site. Normally the workers' accommodation is separated from the construction site, and if not, the construction site must maintain certain conditions found in the General Arrangement, Utilities, and Health Friendly Workplace explained in the OHS regulatory framework. It was found that the majority of the construction companies had their construction workers accommodated in the construction site. This observation hints on how the small and medium construction companies are maintaining a healthy workplace. It is worth mentioning that part of the evaluation checklist thoroughly investigates the condition of the accommodation site and on what level it is complying with the OHS regulations. The answer is to be provided on a later stage of this research.

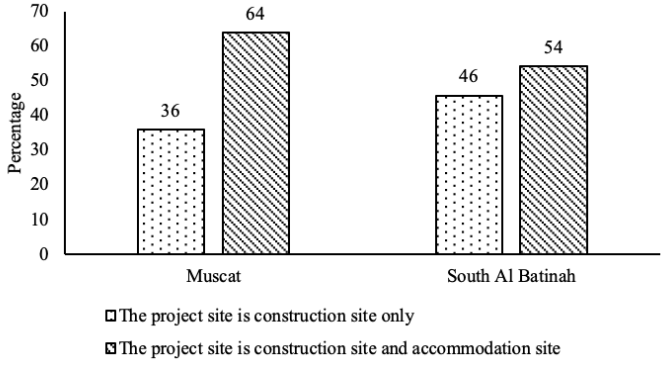

Figure 5: The Distribution of the studied construction companies in terms of the nature of the project site whether it is a construction site only or it is both a construction and an accommodation site at the same time.

Figure 6 shows the level of compliance of the small and medium construction companies towards providing suitable Personal Protective Equipment (PPE) to their construction workers. The results show that a satisfactory level of compliance is maintained by small and medium construction companies in both locations. All companies showed consistent results in both locations regarding safety shoes, head protection, and eye protection. This result is expected since the perception of the OHS in the local market, more specifically, in the small and medium construction companies is all about providing safety shoes,

head protection, and coverall.

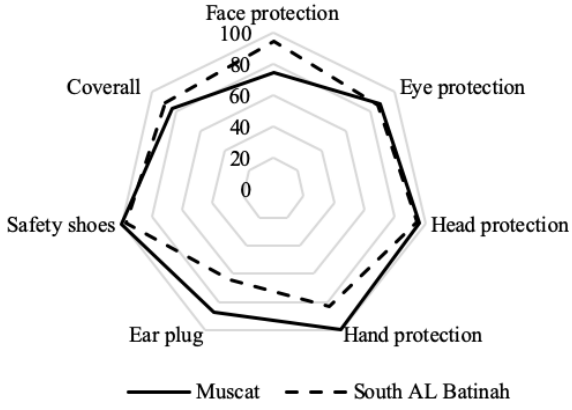

Figure 6: Levels of Compliances of the Studied Construction Companies for Providing Personal Protective Equipment (PPE)

5 CONCLUSION

The level of compliance to the Occupational Health and Safety of small and medium construction companies in two governorates, Muscat and South Al Batinah, in Oman were investigated. The study is conducted in three stages, (1) identifying the level of compliance of the small and medium construction companies to the OHS regulatory framework, (2) comprehensively identifying the causation of the non-compliance and the risk generated, and (3) proposing a framework for "Paving Zero Accident Vision" in Oman, and the partial preliminary results of the first stage was discussed and presented. It was found that not all construction companies surrounding their construction sites with fences resulting are posing hazards not only to the construction workers, but the neighborhood hosting the construction site is also affected.

Furthermore, it was found, the majority of the construction sites are also used as accommodation sites for the construction workers. Thus, raising a question over how these companies are maintaining the health-friendly workplace. The small and medium construction companies were able to maintain a satisfactory level of compliance to provide Personal Protective Equipment to their workers which is a good indication about the awareness regarding the importance of providing a safe working environment to the construction companies. This study pinpointed some negative facts about the OHS practices and bridged the way to the second stage of this research which is to identify the root causation of the non-compliance to the OHS regulatory framework and the risk generated.

The limitations of this research are related to the adequate and representative sample size. The study targets, 269 samples, considering 90% confidence level, and 5% margin of error of a total of 37289 SMEs. In addition, the awareness and the understanding of the respondents about the OHS regulatory framework is challenging and it requires a substantial time to discuss it.

REFERENCES

Arewa, A. & Farrell, P. (2012). A review of compliance with health and safety regulations and economic performance in small and medium construction enterprises. Edinburgh, UK, s.n., pp. 423-432.

Cagno, E., Micheli, G. J., Masi, D. & Jacinto, C. (2013). Economic evaluation of OSH and its way to SMEs: A constructive review. *Safety Science,* Volume 53, pp. 134-152.

Chileshe, N. & Dzisi, E. (2012). Benefits and barriers of construction health and safety management (HSM): perceptions of practitioners within design organisations. *Journal of Engineering Design and Technology, 10*(2), pp. 276-298.

Gunduz, M. & Laitinen, H. (2017). A 10-step safety management framework for construction small and medium-sized enterprises. *International Journal of Occupational Safety and Ergonomics, 23*(3), p. 353-359.

Hasle, P., Kines, P. & Anderson, L. P. (2009). Small enterprise owners' accident causation attribution and prevention. *Safety Science,* pp. 9-19.

He, C., McCabe, B., Jia, G. & Sun, J. (2020). Effects of Safety Climate and Safety Behavior on Safety Outcomes between Supervisors and Construction Workers. *Journal of Construction Engineering and Management, 146*(1).

Ikpe, E., Hammon, F. & Oloke, D. (2012). Cost-Benefit Analysis for Accident Prevention in Construction Projects. *Journal of Construction Engineering and Management, 138*(8), pp. 991-998.

Ithraa (2015). *Setting up a new Business in Oman.* [Online] Available at: https://ithraa.om/ar/Invest-in-Oman/Set-up-a-company.

Kheni, N. A., Gibb, A. G. F. & Dainty, A. R. J. (2010). Health and Safety Management within Small- and Medium-Sized Enterprises (SMEs) in Developing Countries: Study of Contextual Influences. *Journal of Construction Engineering and Management, 10*(136), pp. 1104-1115.

LaDou, J. (2003). International Occupational Health. *International Journal of Hygiene and Environmental Health,* Volume 206, pp. 303-313.

Lai, D., Liu, M. & Ling, F. (2011). A comparative study on adopting human resource practices for safety management on construction projects in the United States and Singapore. *International Journal of Project Management, 29*(8), pp. 1018-1032.

Lai, D., Liu, M. & Ling, F. (2011). A comparative study on adopting human resource practices for safety management on construction projects in the United States and Singapore. *International Journal of Project Management, 29*(8), p. 1018-1032.

Legg, S. J., Olsen, K. B., Laired, I. S. & Hasle, P. (2015). Managing safety in small and medium enterprises. *Safety Science,* Volume 71, pp. 189-196.

Ministry of Manpower (2008). *Occupational safety and health,* Oman: Ministry of Manpower.

Muscat Daily (2015). Allegations arise that many construction sites in Muscat are giving safety a miss. *Muscat: Muscat Daily.*

National Survey Authority, Ministry of Defence, (2019). *Oman Map.* [Online] Available at: http://www.nsaom.org.om/?inc=downloads/maps.

Sunindijo, R. & Zou, P. (2013). Conceptualizing safety management in construction projects. *Journal of Construction Engineering Management, 139*(9), p. 1144-1153.

Unnikrishnan, S., Iqbal, R., Singh, A. & Nimkar, I. (2015). Safety management practices in small

and medium enterprises in India. *Safety and Health Work, 6*(1), p. 46-55.

Zhou, Z., Goh, Y. & Li, Q. (2015). Overview and analysis of safety management studies in the construction industry. *Safety Science,* Volume 72, p. 337-350.

Zhou, Z., Irizarry, J. & Li, Q. (2013). Applying advanced technology to improve safety management in the construction industry: a literature review. *Construction Management and Economics, 31*(6), p. 606-622.

Cite this article as: Al Alawi M., Al Shahri M., Al Ghafri A., "Framework for Investigating the Level of Compliance to the OHS Regulatory by the Small and Medium Construction Companies in Oman", *International Conference on Civil Infrastructure and Construction (CIC 2020)*, Doha, Qatar, 2-5 February 2020, DOI: https://doi.org/10.29117/cic.2020.0010

Innovative Pavement Materials and Design: Smart Roadways and Smart Road Maintenance for the Future

Sherif Hashem
sherif.hashem@ceg-qatar.com
CEG International, Doha, Qatar

Clinton Cardiño
clinton.cardino@ceg-qatar.com
CEG International, Doha, Qatar

ABSTRACT

In an ever-changing world, innovation presents itself as the lifeblood that can make or break any industry or economy. The transportation construction sector is no exception, however, innovation and doing things differently in this sector has been dead slow for centuries, compared to other industries. Automobiles have developed significantly over the years, but the way we build, roadways has not. Innovative vehicles should entail innovative roads to be able to cater them. This paper looks into this subject from a practical perspective with some degree of theoretical depth. It provides a high-level review of a range of cutting technological innovations that can be readily adopted and applied in the State of Qatar and the region in the future. This includes innovative ideas such as solar roadways, plastic roadways, and app-aided road maintenance ignited through the use of the powerful design-build project delivery approach, in addition to addressing the strategic need for building a vivid innovation-driven organizational work culture. The paper is influenced by the author's iconic book 'The Power of Design-Build', USA, (Hashem, 2014), and a number of research and innovation articles and papers in the transportation and infrastructure sector around the world. Daring to adopt innovation and new ideas is a must to advance the roadway construction sector and catch up with the needs and ambitions of the 21st century.

Keywords: Innovation; Design-build; Asphalt; Solar roadways; Plastic roadways; Mobile apps

1 INTRODUCTION

Innovation in pavement design and construction is following the typical axiomatic timeline of innovation of things extending from the far past to the far future, as shown in Figure 1.

Figure 1: The axiomatic innovation timeline

The first asphalt roads were laid thousands of years ago, namely, in Babylon 625 BC, using primitive forms and shapes of road base and a top layer of natural bitumen for waterproofing. The first modern asphalt roads as we know them today were first built in Europe in late 1700's, then enhanced and perfected in early 1800's by the Scottish road engineer J. L. Macadam, after whom the current flexible Macadam pavement is labelled. Surprisingly, despite the exponential growth in technology since the 1800's, we are still building roads using broken stones and asphalt the way Macadam did hundreds of years ago. The only key change that occurred to asphalt pavements ever since, was in early 1900's with the use of refined petroleum instead of natural asphalt. In the meantime, technologies of land transportation developed big time during the same time period, from horse carts and steam powered wagons in the 1700's and 1800's to nowadays 21st century's electrically powered and automatic self-driven vehicles. Figure 2 below provides an overview of the slow pace of technological development in pavement design and construction vs the same in automobiles in recent centuries. The slow development of road pavements has contributed to limiting automobiles safety and maximum driving speeds which are governed by road alignment roughness and quality of pavement. On the other hand, with the steady increase of traffic load, numbers of vehicles and trips, asphalt roads life spans decreases to as low as three to five years before the first maintenance becomes necessary. Cost of road construction and maintenance soars high due to the heavy equipment, hefty materials, intensive labor, and long time required to build roads the old Macadam way. Apart from toll ways and roadside shops, current roadways do not generate income nor have direct ROI, making them a financial burden on governments and taxpayers. Moreover, the environmental impacts and carbon footprints of the current asphalt roads have become just intolerable. The pollution caused by the production of fossil asphalt and that caused by the countless trips of trucks required to transport and compact road construction materials and build asphalt roads is enormous. Moreover, the current asphalt roads are sensitive to road maintenance and hard to maintain. Advancing the ways of design, construction and maintenance of roadways and prolonging roadways service life have therefore become an urgent need. Several groups in the industry realized this fact in recent decades. The academia and research centers recently began to respond with various design-build innovations trying to break the cycle of technological monotony and catch up with the technological revolution going on in the world.

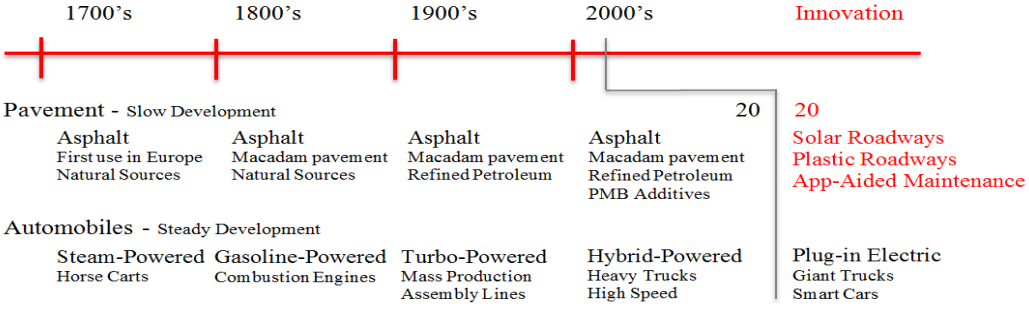

Figure 2: Pavement vs automobiles development timeline

This paper provides a high-level review of a number of recent 21st century emerging innovations, which attempt to change the status quo in pavement design, construction and maintenance done in the near past or for application in the near future. As always, innovation constitutes change, and change is a process that takes time, money, and relentless dedication.

2 PAVEMENT INNOVATIONS FOR THE FUTURE

This chapter presents three innovative concepts related to pavement design, construction, and maintenance management. All three concepts are in final stages of research and development, i.e. although they did not pass the test of time, yet, they are expected to roll out gradually and become popular in the near future. Before final adoption and mass production, innovations shall have to get into cycles of PDCA improvements until deemed and declared fit for purpose. Each concept is presented under a dedicated sub-chapter. Sub-chapters are designed to have three implicit parts into them, namely, background and what the innovation is trying to achieve, a brief system description, and the way forward. Innovations prove that the gap between dreams and reality is achievable.

2.1 Solar roadways – The power of solar energy

The innovative concept of solar roadways which can generate power from the sun has gained popularity in recent years as a smart alternative to the traditional asphalt roads dominating the scene around the world. The key selling point of solar roads is that they can produce clean energy, a precious commodity. The recent emergence of Plug-in Electric Vehicles (EVs) has added fuel to the idea of solar roadways as it provides the answer to the question, how can EVs be charged economically? On the other hand, the solar energy industry is growing steadily, and recently started to extend a hand to the highways industry through intensive research to support the use of solar panels as paving material. The size of the job is hundreds of millions of kilometers of roadways existing or to be built around the world. Solar roadways are still in the offing; however they appear to be here to stay. When fully developed, solar roadways will be able to generate clean electric energy from the sun that is enough to power the ITS system embedded in the pavement solar panels, street lights along the roads, the electrical automobiles driving on the pavement solar panels, and even the buildings and facilities erected along the roads, as shown in Figure 3.

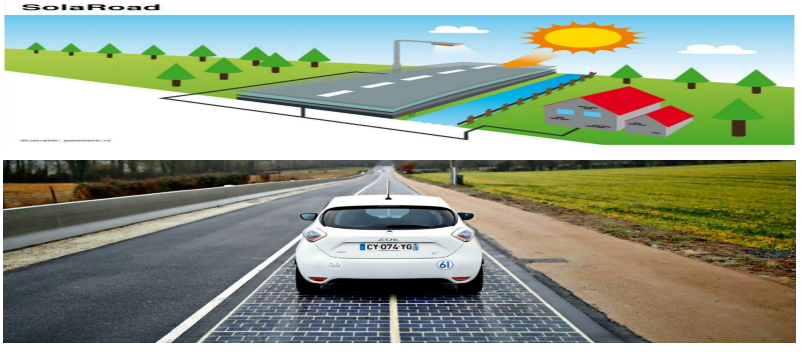

Figure 3: Solar roadways

A pioneer in the field of using solar panels to pave roadways is the USA company Solar Roadways®. The company is working on prototyping solar road pavements built out of a modular system of specially engineered solar panels that can be walked and driven upon. Solar roadways panels contain LED lights to create lines and signage without paint. The panels also have microprocessors, which makes them intelligent. This allows the panels to communicate with each other, with a central control station, and with vehicles and motorists. Solar roadways panels are made of specially formulated tempered glass, which can support traffic loads. Glass has a traction surface that is equivalent to asphalt. Solar roadways are designed to outperform asphalt in many key technical, economical, and performance aspects as shown in Table 1, (Brusaw, 2019).

Table 1: Comparison between solar and asphalt roadways

Surface Features	**Solar Roadways**	**Asphalt Roadways**
Flat place to walk and drive	[redacted]	[redacted]
Rough to allow traction and skid resistance	[redacted]	[redacted]
Can be designed and engineered	[redacted]	[redacted]
Water can be stored, treated or moved	[redacted]	[redacted]
Doesn't soften at high temperatures	[redacted]	
Generates energy	[redacted]	
Intelligent Traffic System	[redacted]	
LED lights for lines and signage	[redacted]	
Remains snow/ice free	[redacted]	
Impervious to potholes	[redacted]	
Modular for faster maintenance	[redacted]	
Requires no paint	[redacted]	
Has ROI	[redacted]	
Facilitates energy independence	[redacted]	
Can charge EVs with clean energy	[redacted]	
Passed the test of time		[redacted]
Mass production and usage experience		[redacted]

Solar roadways are made of photovoltaic solar panels that are able to convert sunrays into electricity by exciting electrons in silicon cells using the photons of light from the sun. Solar panels come in three main types, namely, monocrystalline, polycrystalline, or thin-film. A key factor affecting the feasibility of solar roadways is the efficiency of the solar panels paving the roads. Solar cell efficiency refers to the portion of energy in the form of sunlight that can be converted via photovoltaics into electricity by the solar cell. The efficiency of the solar cells used in a photovoltaic system, in combination with other external factors, determines the electrical energy output of the system. For instance, a solar panel of 20% efficiency and area of 1 m2 would produce 200 kWh at standard test conditions. This output increases when weather is clear and the sun is high in the sky, and will decrease in cloudy conditions or when the sun is low in the sky. Therefore, the use of solar panels in the State of Qatar can be very effective and efficient given the predominantly clear and sunny skies most of the year. According to a study titled, "Assessment of Solar and Wind Energy Potential in Qatar", (Rao & Al-Kuwari, 2013),

the State of Qatar receives an average annual insolation of 2000 kWh/m2/year. That means, the same panel described above can be expected to produce 400 kWh of energy per year. Moreover, the good news is that the solar panels technology is improving steadily over time with solar panel efficiencies of 5-20% in the 1980's, to 30% in the 2000's and recently 45% in 2020 and expected to improve more.

On the other hand, it should be noted that the physical condition of the solar panels forming the road pavement can significantly affect solar panels' efficiency and feasibility of solar roadways. Keeping road pavement and surface clean and intact is therefore of paramount importance. A pilot solar roadway project was launched by The Ministry of Environment in France in 2016 trying to test the system and measure the actual output of solar panels when used as road pavement under real traffic conditions; the WattWay project, (Pasley, 2019), see Figure 2. The WattWay road project was paved by ca 3000 m2 photovoltaic solar panels (3m wide single lane x 1km long). The projected electric energy was ca 150,000 kWh a year, enough to power 15 homes using the rates published by the US Energy Information Administration (Robert, 2018). The output energy however declined in subsequent years due to deterioration of road surface indicating the need for further study, improvement, and testing. The energy output declination could be attributed to a combination of poor quality of both road and solar panels construction.

Conclusion: Solar roadways is an innovative technology, which supports the recent rise of electric vehicles and the global pressing need for sustainability and clean energy. The innovation is still under research and development, however, it can now be applied strategically at small scale e.g. around public facilities such as FIFA 2022 stadiums or public parks, even for pedestrians only, just to show the world commitment to innovation, sustainability and clean energy.

2.2 Plastic roadways – Fast installation and long life

The modern problem of excessive plastic production, combined with the global concern regarding the large cost, long time, disruption to the public and pollution caused by traditional asphalt road construction and road maintenance were the reason why plastic roadways were born.

Plastic roadways is an innovative answer to the long due problems of traditional asphalt and concrete roads. Imagine constructing stretches of roads 'within days' instead of months. Visualize a long-lasting road without a need for regular road maintenance and traffic disruptions. Envision being able to preserve your assets without nuisance while ensuring sustainability and supporting the campaign for a greener environment by recycling plastic wastes.

As shown in Figure 4 below, plastic roadways consist of light, prefabricated, modular and hollow road structure made from recycled plastics with a life expectancy up to three times as long as the traditional asphalt pavement. It is prebuilt and can be easily installed on site preventing excessive disruption to the public or traffic operations. Hollow spaces within the plastic pavement can be used for cables and pressure pipes omitting the need for excavation, and furthermore serves as temporary storage for storm water preventing flooding during extreme precipitation.

Figure 4: Plastic roadways

Plastic roadways' lightweight characteristic, being four times lighter than traditional road structure, reduces the pressure due to construction, which makes it a perfect option on locations with weak or compressible subsoil subject to settlement. The plastic material composition and structure eliminates the risk of cracks and potholes commonly experienced in asphalt pavement, thus reducing the need for road maintenance. Plastic roadways are manufactured from recycled post-consumer plastics, which contributes to solving the global problem arising out of excessive plastic production in an innovative and sustainable way, while ensuring an economically priced road.

Plastic roadways are designed to outperform asphalt roads in many key technical, economical, and road pavement performance aspects, as shown in Table 2 below.

Table 2: Comparison between plastic and asphalt roadways

Surface Features	**Plastic Roadways**	**Asphalt Roadways**
Flat place to walk and drive	[redacted]	[redacted]
Rough to allow traction and skid resistance	[redacted]	[redacted]
Can be designed and engineered	[redacted]	[redacted]
Water can be stored, treated or moved	[redacted]	[redacted]
Doesn't soften at high temperatures	[redacted]	
Impervious to potholes	[redacted]	
Modular for faster installation	[redacted]	
Modular for faster maintenance	[redacted]	
Long life span – up to three times	[redacted]	
Sustainable – made of recycled material	[redacted]	
Light weight	[redacted]	
Passed the test of time		[redacted]
Mass production and usage experience		[redacted]

The Plastic Roadways concept was launched in 2015 by KWS, a Dutch road construction company. In 2016, KWS collaborated with Wavin and Total, all subsidiaries of the Dutch group VolkerWessels, for further development of the concept. On September 11 2018, the world's first plastic road pilot project opened in the municipality of Zwolle in the Netherlands. It was a 30-meter long bicycle path made of recycled plastic, equivalent to more than 218,000 plastic cups. The 30 m stretch was laid in just few hours. On November 22nd 2018 a second pilot project of a similar size was launched. The second pilot project took place in the municipality of Giethoorn, which is also in the Netherlands, taking advantage of the lessons learned in Zwolle. The construction team used lighter equipment during construction, and drove it directly over the placed plastic road elements instead of next to them. Both pilot projects in Zwolle and Giethoorn are being continuously monitored for five years. In the meantime, both pilot projects are regularly evaluated in order to further develop the concept into a product that can be introduced to the market (PlasticRoad, 2019).

Conclusion: Plastic roadways is a promising concept that's aligned with the pressing need to build roads faster and to protect the environment by recycling and reusing non-biodegradable material such as plastic. The innovation is under development; however, it can be applied in small scale projects such as cycle paths, local roads in gated communities, or within FIFA 2022 facilities.

2.3 App-aided maintenance – Every defect counts

After investing billions of dollars in road construction, maintaining the road assets in good and safe condition for as long as possible becomes a challenge and a duty. Record shows that poor maintenance and late reaction to early road defects can shorten service life significantly. A tiny pothole today can be the reason for a major road undermining in a year or less. Depending on traditional routine inspections or seasonal maintenance campaigns have proven deficient. As motorists can confirm, there are numerous cases or road defects, that go unnoticed by authorities for prolonged times leading to major deterioration and the need for costly road reinstatement works along with the associated road closures and disruption to the public. Moreover, the absence of a quick response by road authorities to road defects or even road furniture damages or dislocation can have serious safety consequences and loss of property and human lives.

In recent years, and taking advantage of the current internet based communication revolution, several road authorities around the world started to turn to deploying 'app-aided road maintenance' (all rights reserved as this term is created by the primary author of this paper). The idea is to deploy a mobile application as shown in Figure 5, to be used by the public and reported to road authorities' maintenance teams for review and action. The reporter using their smartphone will identify the defect, take a photo of it, drop GPS pin location, add a brief message, and click send to share the defect report which will be timed and dated automatically. The road maintenance command center will then receive the report in real time, review it, sort it by nature and urgency, add directions as necessary, add time to complete the repair, and forward the report to the engineering teams for action, as shown in Figure 6. The defect can be a pothole, a broken speed hump, a damaged road sign, cracking pavements, excessive road settlement, or similar road defects.

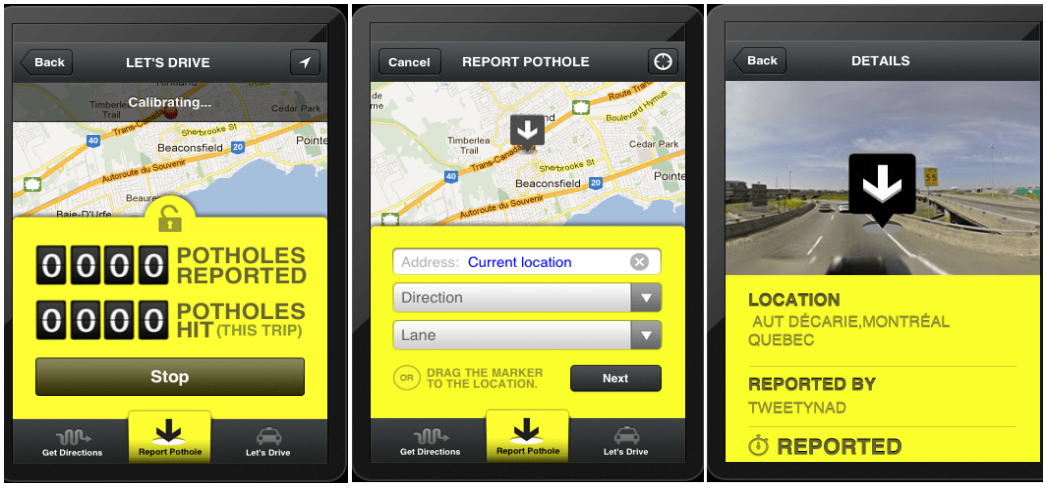

Figure 5: Instant notification app-aided road maintenance technology

Figure 6: Prompt road maintenance on site

In cities such as Singapore, the road transportation authority promises a repair within 48 hours. Singapore is consistently on the top of the list of countries in terms of the road quality as per world ranking published by the World Economic Forum.

Conclusion: Taking good care of public assets so they last longer in a safer and tactful condition is a primary goal for road authorities. Using app-aided technology to achieve this goal is a well-developed concept that is ready for application in the State of Qatar immediately.

3 CONCLUSION

The road industry is moving in the right direction towards advancing pavement design, construction, and maintenance technologies. The innovative technologies presented in this paper are applicable to the State of Qatar and the region; however, such young technologies are still subject to various degrees of research and development. It would be fair to state that status of technological readiness of the innovative concepts presented in this paper would be as shown in Table 3:

Table 3: Innovative concept readiness for application

Innovation	Testing or Demo Purposes, e.g. in facilities of FIFA 2022	Small Scale Application	Large Scale Application
Solar Roadways	Immediately	5 years+	10 years+
Plastic Roadways	Immediately	10 years+	15 years+
App-Aided Maintenance	Immediately	Immediately	5 years+

Innovation is necessary for businesses and economies to progress and flourish. Indeed, innovation is a human obligation for inhabitants of the Earth. The land transportation sector, generally expressed in terms of roadways of different functions and sizes, seems to require a major innovation push that is supported by top-level leadership. Technology is available; it just needs to be used.

REFERENCES

Benedetti, B. (2012). Pothole season…There's an app for that. *Home Technology Montreal*, Montreal.

Brusaw, S. & Brusaw, J. *Welcome to Solar Roadways*, Solar Roadways Website, Idaho.

Fourtane, S. (2019). *Smart Cities: From Plastic Pollution to Plastic Roads*. Interesting Engineering Website.

Greematch.co.uk (2019). How efficient are solar panels? (Greenmatch.co.uk, London).

Hashem, S. (2014). *The Power of Design-Build: A Guide to Effective Design-Build Project Delivery Using the SAFEDB-Methodology*. Business Expert Press, New York.

Marsh, J. (2019). *Solar roadways: what you need to know*, EnergySage Website.

Pasley, J. (2019). *The World's First Solar Road Has Officially Crumbled into a Total Failure*, Business Insider Website.

PlasticRoad (2019). *Construction of 2nd PlasticRoad bicycle path in Overijssel starts*, PlasticRoad Website.

Rao, G. & Al-Kuwari, May Mohd Saeed Al-Alshaikh (2013). *Assessment of Solar and Wind Energy Potential in Qatar*, Qatar Petroleum, Doha, 10/27.

Robertbooker (2018). *How much electricity does an average home need?* Upstart Power Inc., Massachusetts.

Wavin (2018). *Netherlands builds the first PlasticRoad*. Wavin Website.

Cite this article as: Hashem S., Cardiño C., "Innovative Pavement Materials and Design: Smart Roadways and Smart Road Maintenance for the Future", *International Conference on Civil Infrastructure and Construction (CIC 2020)*, Doha, Qatar, 2-5 February 2020, DOI: https://doi.org/10.29117/cic.2020.0011

Unfair Payment Issues in Construction: Re-Thinking Alternative Payment Method For Tier-1 Contractors to Subcontractors

Laura Peter Swai
lauralps006@yahoo.com
School of Energy, Construction and Environment, Coventry University, Coventry, UK

Andrew Oyen Arewa
andrew.arewa@coventry.ac.uk
School of Energy, Construction and Environment, Coventry University, Coventry, UK

Rex Asibuodu Ugulu
rexugulu@gmail.com
School of Environmental Technology / Quantity Surveying Dept., Federal University of Science and Technology (FUTO), Nigeria

ABSTRACT

Recent statistics reveal substantial increase in late payments cases from 18% to 27%; with over £30 billion unpaid invoices to UK contractors. Furthermore, 82% of overdue invoices are monies owed to subcontractor by tier-1 main contractors. Indeed, tier-1 contractors are deemed to be the main elephant in the room despite various contractual, government and private initiatives designed to curb late payment menace. Yet, there is little research concerning use of Alternative Payment Method (APM) to leverage tier-1 contractors paying subcontractors' invoices promptly. The aim of this study is to assess the use APM to enhance pragmatic and sustainable payment practices between tier-1 contractors and subbies. The research question is: what are the industry specific factors that influences unfair payment practices and how can alternative payment method help to leverage fair payments to subbies? The study adopted sequential exploratory design type of mixed method supported by questionnaire and structured interviews. The study population are drawn from experienced industry stakeholders including clients, contractors, designers, professionals in addition to use of computer simulation to validate proposed APM model. Initial findings reveal an optimism bias tendency of most subcontractors agreeing to lengthened and unfair payments terms induced by Tier 1 contractors. The study identified over five industry and business specific influential factors that encourages tier-1 contractors to clinch to unpropitious late payment practices. In specific terms, there are overwhelming evidences that APM has significant potential to minimize late payment in the UK construction industry if there is political, business and legislative will to implement the model.

Keywords: Alternative payment methods; Construction industry; Unfair payment

1 INTRODUCTION

Globally, unfair payment practices such as late payment to contractors, "pay when paid", disparaging rate of items, exclusion of provisional items, imposition of rates and unpaid retentions remains a reoccurring problem in the construction industry. In the UK, subcontractors that carryout works for Tier 1 contractors are disproportionately affected by unfair payment practices. The Federation of Small Business (FSB, 2017)

claims that "in the last five years, two-third of subcontractors in UK construction industry experienced longer payments period of over six weeks". The Euler (2015) report assert that there has been substantial increase in unfair payment cases from 18% to 27%; with over £30 billion unpaid invoices and £7 billion of unremitted retention monies over the past five years. Moreover, 82% of total unpaid invoices are monies owed to subcontractors by Tier-1 contractors. Recent statistics reveal that on average it takes 65 days approximately for tier 1 main contractor to pay subcontractor from the day of receiving invoices (Build UK, 2018). Also "Lost in Transaction: Payment Trends report" (2018) and "Construction Payments Report" (2018) both emphasized the need for genuine review of complex and unfair payment practices in the construction industry. Specifically, Construction Payment report (2018) claimed that the industry is in dire need of Alternative Payment Method (APM) that will synchronize and deliver fair payments to construction supply chain. Yet, there is little research that clearly identifies business and industry specific factors that influences unfair payment practices, and the use of APM to enhance prompt payment of invoices by tier-1 contractors to subbies.

Review of current payment model in the construction sector show a bias design that focuses on boosting Tier 1 contractors' cash flow at the expense of their supply chain. Generically, contractual payments procedures allow for weekly or monthly remittance of money to supply chain; but distribution of payments to subcontractors especially from Tier 1 contractors are often lopsided. The cascade payment method in construction also known as hierarchical contractual framework gives Tier 1 contractor dominant bargaining position over subcontractors' payment. Yet, it is a common practice to see subcontractors that carryout over 74% of major work, wait for 60 days to receive payments (FSB, 2017), due to commercial influence of Tier 1 contractors and archaic payment methods.

2 RELATED LITERATURE

Unfair payment practice in Construction Industry

Unfair payment practices are still common down supply chain in the UK construction industry; despite various regulations such as the Housing Grants Construction and Regeneration Act (HGCRA, 1996), (Late Payment of Commercial Debts Regulation, 2013), and other private initiatives. Recent statistics indicate significant deterioration of payments from Tier 1 contractors to subcontractors, with average payment period of 65 days and in worst scenario 120 days (Build UK, 2018).

Kilgallon (2013) opine that unfair payment practices give rise to additional financing, transactional costs, erode credit rating of affected companies, breed mistrust and adversarialism in supply chain. As a result, clients will experience more expensive projects, with devastating knock-on effect on contractors' cash flow. Latham (1994) stress that unfair payment practices cause significant waste and inhibit productivity through mistrust and confrontation, which ultimately undermines project performance. Uncertainty over how much and when payments are to be made often-lead to big distraction to subcontractors and suppliers that operates with low capital outlays and thin margins.

Build UK (2018) assert that unfair payment practices (especially late payment) contribute significantly to high rate of insolvency; "on average one in ten firms go burst daily in the UK construction industry". Indeed, late payment creates cash flow problems

exacerbated by tough economic climate and banks reluctance to lend in money. Arguably, the demise of Carillion Plc 2017/18 and current Kier financial warnings are concreated to payment issues. Today, late payment to supply chain has become a common characteristic of construction companies that are struggling financially.

Key Definitions

The phrase "unfair payment practice" used in the study is drawn from the UK Department for Business, Innovation and Skills (2017) report titled "Challenging Grossly Unfair Payment Terms and Practices". The report defines "unfair payment" based on Late Payment Act 1998 provision, Section 4 subsection (7A) under three specific aspects as: (i) anything that is a gross deviation from good commercial practice and contrary to good faith and fair dealing; (iii) the nature of the goods or services in question; and (iii) whether the purchaser has any objective reason to deviate from the stipulated/contractual payment term.

The report subsequently identified unfair payment practices as: late payment to contractors/suppliers, "pay when paid", disparaging rate of items, exclusion of provisional remedy, imposition of rates on subcontractors and unpaid retention to contractors as common grossly unfair commercial practices in the UK construction industry. FSB (2017) argued that globally late payment to contractor is the most common unfair payment practices in construction. Ameer (2005) define late payment as failure of paymaster to issue or honor payments as stated in contractual agreement. Zurich index (2017) opine that over half of small and medium sized businesses spend on average £16,000 per year chasing late-payment. Recent survey conducted by BEIS (2018) reveals that 33% of subcontractors had experienced business difficulties as result of late payments.

Ramachandra and Rotimi (2015) suggest that issues of late payments with subcontractor are multifaceted. Abdul Rahman et al. (2010) argued that contractors' poor finance management, disagreement in valuation of work done, use of "pay–when –paid" tactics and insufficient documentation are major causes of late-payments to contractors. Rotimi et al. (2010) claim that the industry payment culture of "work first and then get paid later" is responsible for deferred payment attitude particularly by Tier 1 main contractor. Other authors such Ramachandra (2013) and Danuri et al. (2006) argued that existence of low entry barriers, inadequate capital and the use of "cow boy bullying" tactics by Tier 1 contractors all contributes to chronic unfair payment issues in the industry. Arewa and Farrell (2016) suggest that commercial interest of many Tier 1 contractors' influences unfair payment practices in the construction sector. Indeed, existence of multi-tiered hierarchical structure together with cascade payment obligation places most subcontractors and suppliers at risk of unfair payments practices in the construction sector (Griffiths et al., 2017).

Existing Payment Methods from Tier-1 Contractors to Subcontractors

The Egan (1998) report titled "Rethinking Construction" asserted that current payment methods in construction places a considerable and unfair strain between parties, which in turn affects overall spirit of team working, partnering and supply chain management. Moreover, there is an overwhelming consensus that current payment methods are designed to consider individual project characteristics and cash flows models that favor

Tier 1 contractors compared to subcontractors and suppliers. For example, the use of cost reimbursement payment method to provide compensation for work done by contractors for using their own resources and expertise in terms of buildability, cost of materials and programme, only to be reimburse at a later date is grossly unfair (Master, 2002). Arditi and Yasamis (1998) are of the view that current interim valuation and payment methods in construction industry can best be described as "incentive that compels contractors to perform". Pye-Tait (2016) argue that financial protection methods such as bonds, parent company guarantee, escrow accounts and trust funds are becoming obsolete. However, useful in protecting clients against contractor's insolvency and non-performance, some of these financial instruments usually creates untold financial burden on subcontractors. Moreover, significant of trade credit payment method (pay later after delivery of construction works/materials) cannot be overemphasized, particularly from main contractors' perspective. However, it is important to stress that most Tier 1 contractors see trade credit as a vital business model in sustaining their working capital and profit margins at the detriment of their subcontractors and suppliers.

In the last decade, the use of project bank accounts (PBA) in public projects as a form of payment method is considered a panacea to chronic unfair payment practices in the construction sector. Indeed, PBA provides effective means of addressing waste issue and achieving fair payment through transparency and auditability of its supply chain payments (Kilgallon, 2013). PBA acts as ring fenced electronic bank account in which timely payments are made directly and simultaneously to main contractors and its supply chain. The payment model ensure that clients maintain adequate funds that will cover work in progress and other project commitments. Under a PBA, the subcontractors submit interim application to main contractor showing breakdown of payments claimed by each supplier with the purpose of counterchecking if necessary adjustment are required. Once approved, the client will pay total amount of monies into PBA and direct payments will be made to each subcontractors and suppliers in the supply chain. If the clients want to reduce or adjust payments due to contractor's defaults, the contractor will be required to make a top-up payment into account so that subcontractors and suppliers can be paid on time. To avoid deficit of payments under PBA arrangement, client must ensure that the balance remains at an agreed minimum level (Kilgallon, 2013).

Arguably, the novelty behind aforementioned PBA payment model is that it has been proven to be effective; unlike other payment methods where Tier 1 contractor deliberately withhold payment from subcontractors to boost their working capital and profit margins. In the UK, most payment methods still reflect 19th century business model that enable Tier 1 main contractor to dictate payment terms and disbursement to supply chain. The cascade payment method is for main contractor to receive monthly payments for completed works on site and then distribute those payments to subcontractors and suppliers in the chain. Payment method based on such hierarchical contracting approach per se limits the margin of negotiation between client and subcontractors' thereby putting unnecessary strain between parties.

Danuri et al. (2006) argued that Tier 1 contractors often exert considerable commercial pressure on subcontractors to agree longer payment terms in order to boost their cash flow. For example, many Tier 1 contractor such as Carillion Plc, Interserve and Kier Plc use late payments as a tool for financing their business performance. On the contrary,

most subcontractors are often reluctance to challenge current unfair payment practices, because of clients-contractor relationships and fear of being dropout from the supply chain.

3 RESEARCH METHOD

The research design adopted sequential explanatory type of mixed methods with QUAN → QUAL concept meaning quantitative method is the lead data collection instrument (Creswell, 2015). While, qualitative data are used to support and validate the quantitative findings. The data collection tools for the study includes semi-structured interview and questionnaires. The study questionnaire and interview questions were designed based on existing literature. Pilot studies were conducted to ensure that the data collection tools were designed correctly. Ethnical approval was sought from Coventry University Research Ethics Committee and it was granted, see attached ethics certificate in appendix A. Data collected for the study were obtained from difference location in England and Scotland. The main data collection instruments were designed to answer the study research questions. Stratified random sampling was used to select the study participants for both quantitative and qualitative data. A semi-structured questionnaire was distributed through emails, telephone contact, site visits and through The Chartered Institute of Building (CIOB) and Royal Institution of Chartered Surveyors (RICS) professional networking. All interviews were conducted face-to-face to obtain first-hand information about the research problem.

The population sample consist of, construction clients, commercial managers, contract managers, commercial lawyer, quantity surveyors, managing directors of construction firms and business development manager. For reliability and validity, the study data collection (both questionnaire and interview data) were conducted on one-to-one basis. This method allowed the researchers to probe participants regarding the study aim and research question. On the other hand, the study participants had opportunity to ask questions that were not clear.

Quantitative Data Analysis

Total of 96 questionnaires were administered, 89 were returned and six were considered invalid because they were not completed correctly. Total of 83 questionnaires were used for statistical analysis; performed using SPSS version 25. Cronbach's alpha sigma value of 0.81 was obtained meaning that internal reliability of the quantitative data is very good. Exploratory Factor Analysis (EFA) was used to determine underlying relationship between combinations of factors that influences unfair payment practices in the construction industry. The factor loading was run for both Principal Axis (PA) and Principal Component Analysis (PCA). The communality factor was calculated to be C2 = 0.5842 + 0.4952 = 0.765. Therefore, because the communality factor is close to 1; it indicates that unfair payment variables measured by the study were better explained by the factors. Table 1 illustrates percentage commonality of unfair payment practices claims by construction contractors in the UK construction industry. The greatest percentage score (late payment to contractors) scored 34% (n =83%) was attributed to industry and business factors presented in Table 1 below.

Table 1: Percentage of commonality of unfair payment practices claims by construction contractors

Percentage commonality of unfair Payment Practices		
Variables of unfair payment practices test	**n**	**%**
Late payment to contractors	28	34
"Pay when paid"	3	3
Disparagingly rate of items	8	10
Exclusion of provisional remedy	15	18
Imposition of rates on contractors	10	12
Unpaid retention to contractors	19	23
Total	**83**	**100**

For better understanding of the research problem, construction clients were classified as following: Tier 1 client: major construction clients e.g. government authorities and private institutions; Tier 2 clients: main contractors acting as client to subcontractors) and Tier 3 clients: subcontractors acting as clients to other subcontractors. Using Relative Importance Index (RII) and Quadrant analysis, 42 cases of contractors complains about factors and extent of unfair payment practices were analyzed alongside classification of different clients. Figure 1 illustrate tiers of construction clients with awful unfair payment practices in the UK construction industry. Figure 2 summarizes industry and business specific factors that influences unfair payment practices in the UK construction industry.

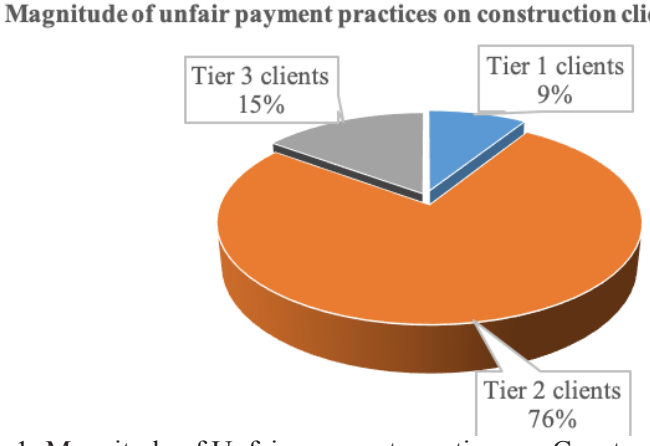

Figure 1: Magnitude of Unfair payment practices on Construction clients

Total of 83 subcontractors that regularly work for main contractors were asked to identify industry and business specific influential factors that encourage Tier 2 clients (principal contractors) to indulge in unfair payment practices without punitive measures. Figure 2 presents key percentages of influential factors that encourages Tier 2 clients to coddle unfair payment practice in the UK construction industry.

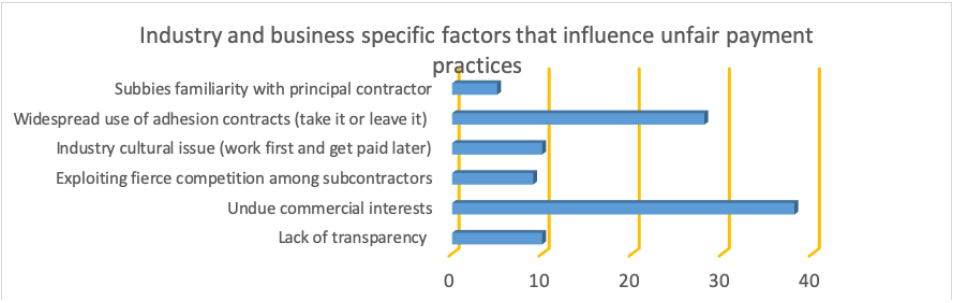

Figure 2: Industry and business specific factors that influences unfair payment practices

Interviews data analysis

Validity of the study qualitative data was upheld in three main areas: selection of participant profile, design of interview questions, and processing/presentation of interview data. Overall, a total of 13 semi-structured interviews were conducted with clients, industry practitioners and construction contractors. The study targeted interviewees with seasoned construction experience. All interviews were recorded using a digital recorder and personal information linked to study participants was removed because of data protection.

Textual excerpts of the interview data were transcribed into manuscript and inputted into Nvivo 12 software. Codes were assigned to key themes to facilitate filtering and sorting of data. The themes from the study aim were used to create codes and sub-codes from the transcribed data. Content analysis was used to analyze the interview data for easy inferences to antecedents of discussions and certain words, themes or concepts spoken between interviewees and interviewer. Excerpts from interviews below were obtained using content analysis; by counting number of processes, extracting systematic and objective meaning from each content via making valid inferences from verbal and archive data. For example, when interviewees were asked to express their view concerning unfair payment practices in the UK construction industry; host of issues were raised about the subject matter. Subsequently, key contents were trimmed for better understanding and spontaneity of interaction between the researcher and study participants. Some textual excerpts are expressed verbatim; as illustrated below for confirmability and better understanding of participants' view points.

"... the culture of 'work first and get paid later' is undeniably the root causes of unfair payment practices ... these problems exist because clients need to be protected from the hands of dodgy contractors; but some clients are exploiting unfair payment for their personal gain" – (Public clients Head of Construction procurement Local Government authority UK)

"…. we have seen different kind of measures and methods implemented by government and private sectors to ensure prompt and timely payments ... but these efforts and procedures still give main contractors a room to wiggle when it comes to real enforcement of payment terms…" (Senior Project Finance Officer to main construction company)

"... the current payment methods in the construction sector are indefensible and long-term pain to subcontractors and suppliers ...." (Director UK Department for Business, Energy and Industrial Strategy)

Interview data presented above suggest that current payment methods in the construction industry are indefensible, unsustainable and subject subcontractors and suppliers to significant financial stress. However, interviewees were asked to explicate how alternative payment methods can bring about feasible and sustainable payment practices particularly between tier-1 contractors and subcontractors.

"... in our previous projects we used project bank accounts to pay contractors and our supply chain which worked perfectly well ... though it had major contractual complications with pay less notice ... the principal contractors never liked it ..." (Senior Commercial Manager Railway infrastructure Project, UK)

"... I can confidently say that most payment methods and regulations have loopholes ... alternative payments method that ring fence payment to supply chain is perhaps the only sustainable solution to this mess" (commercial lawyer – London)

4 FINDINGS AND DISCUSSION

The study literature provided clear understanding of unfair payment practices in the construction industry. Findings from literature and data analysis have unanimous findings. For example, both literature and key findings from the study support the premise that unfair payment practices exist in the industry; and a major issue to both contractors and subcontractor's financial performance. Perhaps, the study literature was grossly limited in terms of scale, extent and industry specific factors that influences unfair payment practices in construction. The study quantitative and qualitative inquiries clearly identified six business and industry factors that influences unfair payment practices as illustrated in figure 1. The study acknowledged that undue commercial interest of main contractors and widespread use of adhesion contracts (take-or-leave) or "back-to-back" types of contractual agreement between Tier 2 contractors and subcontractors as the foremost factors that influences unfair payment in the construction industry. Besides, the study specifically measured type of client's involvement to unfair payment issues. Quantitative findings reveal that 57% of unfair payment cases are akin to late payment (34%) and retentions on subcontractors as illustrated in table 1. However, unfair payment issues certainly go beyond Tier 1 contractors' behavioral issues. Perhaps, subcontractors and other suppliers are complicit as well, because they often exhibit optimism bias tendency by agreeing to lengthened and unfair payments terms induced by them. Moreover, there was unified suggestions from qualitative inquiry that use of PBA (a ring fence payment to supply chain) is perhaps the only sustainable solution to chronic unfair payment problems in the construction industry. However, some study participants believe that there are loopholes to PBA. Thus, the study is proposing an enhance Alternative Payment Method (see figure 3) to enhance prompt payment of invoices from Tier-1 contractors to subcontractors.

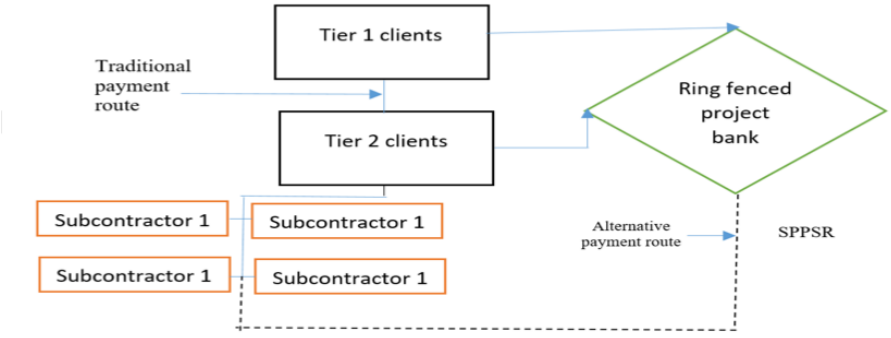

Figure 3: Proposed alternative payment method for construction contractors and suppliers

The main difference between PBA and proposed APM is the introduction of Special Purpose Payment System Regulator (SPPSR) to act as independent regulator. Besides, SPPSR is to act as trustee and guarantor for prompt fortnightly payments to contractors and suppliers. The mandate of the special purpose payment system is to minimize main contractor domineering power over subcontractors' monies and insolvency risks of subcontractors. However, the main contractor still needs to audit and certified interim valuation, before SPPSR releases monies to subcontractors. The proposed initiative is similar to the non-for-profit Tenancy Deposit Scheme (TDS) managed by National Housing Association and regulated by Housing Act 2004. There is need for the proposed APM to be backed by an Act of Parliament; for easy punitive measures against erring tier2 clients.

5 CONCLUSION

The aim of the study is to investigate specific factors that influences unfair payment practices in the UK construction industry. The study identified six business and industry specific influential factors that encourages unfair payment particularly from Tier 2 clients (main contractors) to subcontractors. The factors include: undue commercial interests from Tier 2 clients, lack of transparency, fierce competition among subcontractors, industry culture "work first and get paid later", and widespread use of adhesion contracts "take it or leave it" agreement, as illustrated in figure 2.. Moreover, the quantitative inquiry reveals that late payment (34%) and imposition of rate on subcontractors (23%) are the most common types of unfair payment practices in the construction industry. Findings also show that Tier 2 clients (main contractors) accounted for 86% of unfair payment cases, while 9% and 5% were linked to Tier 3 and Tier 1 clients respectively. Indeed, implication of these findings is that main contractors have and do exert strong commercial influence over their subcontractors and suppliers in the construction industry. Yet, factors that encourages unfair payment practices in the industry are hardly challenged by subcontractors. Ultimately, to minimize unfair payment issues and enhance prompt payment of invoices from tier-1 contractors to subcontractors the study proposed use of APM. The proposed payment method is significant because if its ring fenced, guarantor and legal features. The proposed payment method is still undergoing research development, modification, consultation and subsequent validation with stakeholders.

REFERENCES

Abdul-Rahman, A., Munaaim, M. E. C., Danuri, M. S. M. & Berawi, M. A. (2008). Issues affecting payments in the building and construction industry of a rapidly developing economy. *Building Engineer Journal,* 3-9.

Ameer Ali, N. A. N. (2005) Payment in The Construction industry – towards Zero Default. *QS National Convention 2005*, 10 –11August 2005, Hilton Kuala Lumpur.

Arditi, D. & Yasamis, F. (1998) Incentive/disincentive contracts perceptions of owners and contractors. *Journal of Construction Engineering and Management*, *124*(5) 361-71.

Clough, R. H. & Sears, G. A. (1994). *Construction contracting*. 6ed. John Wiley and Sons Inc. New York Construction Payments Report (2018).

Danuri, M. S. M., Munaaim, M. E. C., Rahman, H. A. & Hanid, M. (2006). Late and non-payment issues in the Malaysian Construction Industry - Contractor's perspective. *In: International Conference on Construction, Culture, Innovation and Management* (CCIM), 26-29 November, Dubai Department for Business, Energy & Industrial Strategy (2017) report titled *"Retention Payments in the Construction Industry a consultation on the practice of cash retention under construction contracts".* Published by GOV.UK. October, pp. 3-5.

Egan, Sir J. (1998) Rethinking Construction. London: Department of the Environment, Transport and the Region.

Euler Hermes (2015). Euler Hermes: UK late payments hit two-year high at 2015 year-end.

Griffiths, R., Wayne, L. & Jeremy, C. (2017). Projects bank accounts: the second wave of security of payment? *Journal of Financial Management of Property and Construction*, *22*(3).

Kilgallon, B. (2013). The Late Show: Project Bank Accounts. *RICS Construction Journal*, pp. 14-17.

Pay safe: *Lost in Transaction Payment Trends* (2018). Available from: Retrieved from https://www.paysafe.com/fileadmin/content/pdf/Lost_in_Transaction_2018_-_Paysafe_-_web_spreads.pdf.

Peter & Arewa (2018). Potentiality of Emerging Technologies to Minimise Late-Payments Quandary in Construction. In: Gorse and Neilson, C, J (Eds) P*roceedings of the 34th Annual ACROM Conference, 3-5 September, 2018,* Association of Researchers in Construction Management, pp. 47-56, Belfast, the UK.

Ramachandra, T. & Rotimi, J. O. B. (2015). Causes of Payment Problems in the New Zealand Construction Industry. *Construction Economics and Building*, *15*(1), pp. 43-55.

The UK Cabinet Office (2013–14) *Sixth Report of Session: Improving government procurement and the impact of government's ICT savings initiatives*. Ordered by the House of Commons Committee of Public Accounts.

Zurich Index (2017) SMEs owed more than £44.5bn in late payments. Retrieved from https://www.zurich.co.uk/en/about-us/media-centre/general-insurance-news/2017/smes-owed-more-than-45bn-in-late-payments [Retrieved on 21July 2019].

Cite this article as: Swai L. P., Arewa A. O., Ugulu R. A., "Unfair Payment Issues in Construction: Re-Thinking Alternative Payment Method For Tier-1 Contractors to Subcontractors", *International Conference on Civil Infrastructure and Construction (CIC 2020)*, Doha, Qatar, 2-5 February 2020, DOI: https://doi.org/10.29117/cic.2020.0012

Challenges Facing Building Information Modelling in Construction Industry in Sudan

Ahmed Ibrahim
ahmedeltigani08@gmail.com
Faculty of Engineering, University of Khartoum, Khartoum, Sudan

Amged O. Abdelatif
Amged.Abdelatif@uofk.edu
Department of Civil Engineering, Faculty of Engineering, University of Khartoum, Khartoum, Sudan

ABSTRACT

Building Information Modelling (BIM) is a valuable and promising approach in Architecture, Engineering and Construction (AEC) industry, which is gradually gaining acceptance by owners, architects, engineers, and contractors as an innovative process of generating and managing building data during its lifecycle. This paper aims to mark the main challenges that are faced by the adoption of BIM and the current BIM maturity level in Sudan. The most challenging issue was found to be the absence of clients demand to implement BIM in their projects. According to this study, the maturity level in AEC in Sudan was found to be Level 1.

Keywords: BIM; Construction industry; Implementation; Challenges; Maturity level

1 INTRODUCTION

The construction industry is one of the most information dependent sectors and relies heavily on traditional means of communications, which needs effective methods for gathering and utilizing performance information on industry, companies, and individual project levels.

Since many years Construction Industry (CI) in Sudan is developing slowly and facing many problems and obstacles, such as: shortage of materials, fluctuation of construction materials' prices, inaccurate estimation of the time, defects during the process of construction, cost overrun, too much pressure on project stakeholders, etc. Recently, many technologies that would improve the construction process were developed, latest and the most popular among them, is Building Information Modelling (BIM), (Khidir M O, 2016).

The adoption of technology in Sudan is moving very slowly, it is affected by economic factors and sanctions. This affects the construction process and adoption of BIM, which is a promising technology lead to transform the construction industry. Therefore, BIM is a working method that requires a new mind set, and mind set change is essential to successful BIM adoption (Mohamed M B, 2015).

Thus, the aim of this study is to identify the main challenges and difficulties facing the implementation and adoption of BIM and to evaluate the status of BIM adoption in Sudan.

2 CHALLENGES

A survey was conducted to gain a better understanding of the background and facts concerning BIM implementation and the challenges that face the organizations to adopt BIM in Sudan.

The questionnaire was broken down into three main sections. The first section focused on general questions related to the type of firm, personal experiences and position of respondents in their organization. The second section focused on the degree of awareness of BIM, and how respondents understand the concept. The third section concentrated on barriers and challenges to BIM and suggested ways to deal with those barriers. The numbers of respondents are 50 in the respective three sections.

Figure 1 demonstrates the main challenges affecting the spread of using BIM suggested by respondents, of which 40% results show that the clients do not demand their work being done by using BIM, while 18% of respondents claim that the most affecting factor is lack of support from managers. 16% is the cost of BIM adoption, 14%, the lack of BIM training and 10%, the lack of BIM experts in the industry, while only 2% claim that the main reason is the lack of knowledge among engineers.

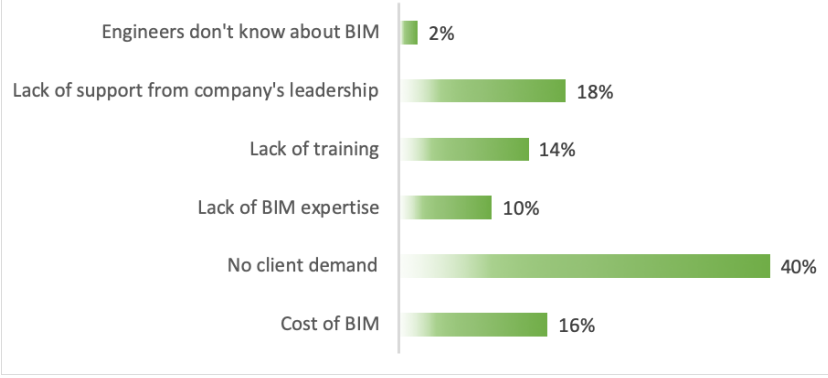

Figure 1: The challenges of using BIM

3 BIM MATURITY LEVEL

Figure 2 shows the ranges of maturity levels of Building Information Modelling (Eastman et al., 2009). The BIM maturity is categorized in four levels:

3.1 Level 0 BIM

Unmanaged Computer Aided Design (CAD) including 2D drawings, and text with the paper-based or electronic exchange of information but without common standards and processes. Essentially this is a digital drawing board.

3.2 Level 1 BIM

Managed CAD, with the increasing introduction of spatial coordination, standardized structures and formats as it moves towards Level 2 BIM. This may include 2D information and 3D information such as visualizations or concept development models. Level 1 can be described as 'Lonely BIM' as models are not shared between project team members.

3.3 Level 2 BIM

Managed 3D environment with data attached, but created in separate discipline-based

models. These separate models are assembled to form a federated model but do not lose their identity or integrity. Data may include construction sequencing (4D) and cost (5D) information. This is sometimes referred to as 'pBIM' (proprietary BIM).

3.4 Level 3 BIM

A single collaborative, online, project model with construction sequencing (4D) cost (5D) and project life-cycle information (6D). This is sometimes referred to as 'iBIM' (integrated BIM) and is intended to deliver better business outcomes.

3.5 Level 4 BIM

Level 4 introduces the concepts of improved social outcomes and well-being.

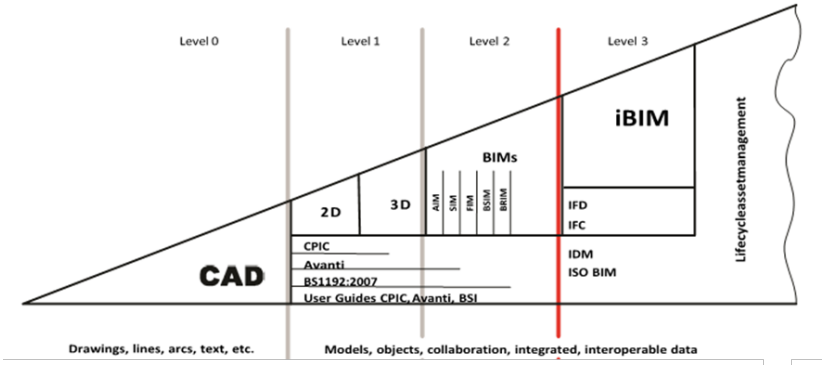

Figure 2: BIM maturity levels (Eastman et al., 2009)

In order to assess the maturity level, interviews with major companies have been conducted in order to investigate the issue of implementing BIM in Sudan, as follows:

- What is the degree of awareness of BIM in Sudan?
- Which level are Sudanese firms in maturity level of BIM?
- How to adopt best practices of BIM in Sudan?

As shown in Figure 3, 80% interviewees see Sudanese companies at BIM maturity Level 1, the remaining 20% mainly at maturity Level 0.

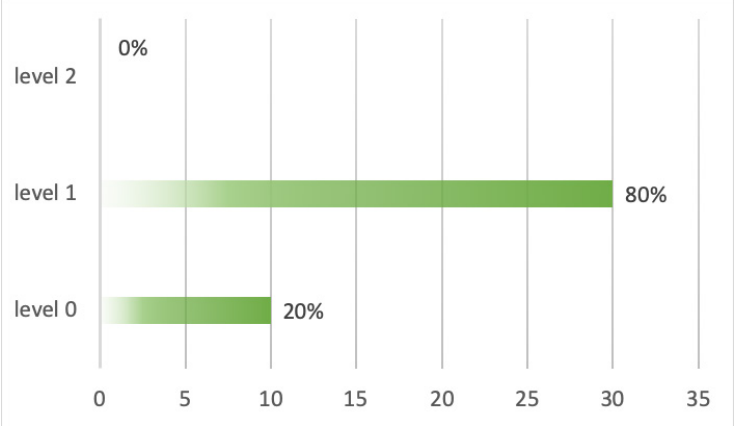

Figure 3: Sudanese construction industry maturity levels of BIM

4 CONCLUSION

The importance of BIM adoption is becoming increasingly recognized by the construction industry all over the world, which has been facing barriers and challenges to increase productivity, efficiency, quality. The paper's aim was to identify the main challenges facing the adoption of BIM in Sudan and the findings indicate that there are numbers of challenges regarding the adoption and implementation. The main challenge was found to be the absence of client demands in the construction industry in Sudan. The paper also assesses the status of BIM in Sudan by using the BIM maturity level gauge. The results revealed that the Sudanese organizations have clear evidence of BIM use in level 1 maturity level.

REFERENCES

Eastman, C., Tiecholz, P., Sacks, R. & Liston, K. (2008). *BIM Handbook*. New Jersey: John Wiley & Sons.

Khidir, M. O. (2016). *Implementation and potential benefits of Building Information Modeling (BIM) in Sudan construction industry* (Sudan University of Science and Technology).

Mohamed, M. B. I. (2015). *A study of project delay in Sudan construction industry* (Partial thesis of Master's degree, Universiti Tunku Abdul Rahman, Malaysia).

Cite this article as: Ibrahim A., Abdelatif A. O., "Challenges Facing Building Information Modelling in Construction Industry in Sudan", *International Conference on Civil Infrastructure and Construction (CIC 2020)*, Doha, Qatar, 2-5 February 2020, DOI: https://doi.org/10.29117/cic.2020.0013

Preventive Approach to Unsubstantiated Claims and Disputes in the UK Construction Industry

Asia Nosheen
nosheen2@uni.coventry.ac.uk
Coventry University, Coventry, UK

Andrew Oyen Arewa
andrew.arewa@coventry.ac.uk
Coventry University, Coventry, UK

Hafiz Muhammad Akhtar
eng_akhtar@hotmail.com
M/s Progressive International (Engineers & Contractors), Lahore, Pakistan

ABSTRACT

Globally, claims and disputes are an unfortunate reality in construction projects. Recent statistics reveal that construction claims in the UK increased by 21% in 2018 compared to other countries such as India (8%), Mexico (3%), Ireland (2%), and Cyprus (2%). Though, construction industry is known for array of standard forms of contract and administrative tendencies; unsubstantiated claims and chronic disputes remain prevalent in the sector. Yet, there is little research on preventive approach to unsubstantiated claims that ultimately lead to disputes. The study advocates the use of Systematic and Technical Appraisal (STA) to prevent unsubstantiated claims and disputes in the construction industry. The study research method is based on qualitative research technique and use of case studies. The research question is: does systematic and technical appraisal of construction claims help prevent unsubstantiated claims and disputes in the UK construction industry? The study population sample is drawn from experienced industry stakeholders including clients, contractors, consultants, experienced quantity surveyors and cost managers in addition to use of construction case studies. Initial findings reveal that claim management processes in the construction sector are far-off from perfection. Other findings reveal that robust systematic and technical claim appraisal process has potential to prevent unsubstantiated claims; which in most cases lead to disputes. The study is part of an on-going PhD study to seek to develop an effective claim management system for the UK construction industry.

Keywords: Claims; Dispute; Systematic and technical claim appraisal

1 INTRODUCTION

In the last two decades, incomplete and unsubstantiated construction claims consistently featured as the second most common reasons for chronic unfair claim issues and disputes in the construction industry. Average value of construction disputes across the globe currently stands at approximately US$43.4 million; with average length of disputes spanning over 14.8 months (ARCADIS, 2018). For example, ARCADIS (2018) report stated that the highest value of construction claim and dispute handled by their team in 2017 was worth of US$400M, and the root causes stem from unsubstantiated

claims. Recent statistics reveal that construction claims in the UK increased by 21% in 2018 compared to other countries such as India (8%), Mexico (3%), Ireland (2%), and Cyprus (2%) (LCIA, 2018). Indeed, unsubstantiated claims in construction businesses are complex issues and often difficult research subject area perhaps, due to unrealistic assumption of claimants, nature of work, dubious rate, inexperience of claim administrator, etcetera. Yet, there is little research on strategic and preventive approach to unsubstantiated claims that ultimately lead to chronic disputes. Therefore, the study seeks to advance knowledge on how to strategically deal with unsubstantiated claims and disputes in the UK construction industry. For better understanding of the research theme; there is need for robust literature review.

2 LITERATURE REVIEW

Construction claims for loss/expenses, extension of time (EoT) and liquidated damages (LD) are important aspect of contract administration; because of its monetary value. A single claim in construction can vary significantly in value usually as low as £250; spanning hundreds and millions of pounds (£) in a single project (LCIA, 2018). Arguably, value of construction claims in a project depends on complexity, alterations and variations to original contract. Claims are common occurrences to both small and large projects. Tochaiwat and Chovichien (2004) argued that claim is simply a process that involves seeking for consideration or changes to an arrangement by contractual parties. Generically, claim is simply a mechanism that allows contracting parties to seek for recompense or compensation such as loss/expenses, EoT and LD if a contractor delays the project. In construction business, claims are often caused by arrays of factors such as variation, instruction, unforeseen circumstances, action or indecisiveness of client's representative. Moreover, claims in construction can also arise from external event such as adverse weather conditions and force majeure. Bonaventura (2015) asserted that *"when a party believes that the other party has not met the contractual obligations or expectations and that they deserve monetary and/or time compensation, they may submit a claim".* Most literature hardly explains unsubstantiated claims and strategic approach to prevent ambiguous contractor's claims. Unsubstantiated claims are vague, abstruse, unsupported with evidence. Professionally, claims are deemed to be invalid or incorrect and should not be processed. Long (2017) stressed that most cases of unsubstantiated claims usually come from construction contractors; and they are leading causes of construction disputes. Arcadis (2018) opined that disputes in construction can only be brought to bare minimum if claims are clearly substantiated and corroborated with sufficient evidence.

2.1 Potential of making unsubstantiated claims valid

The National Economic Development Office (NEDO, 2011) asserted that 60% construction claims are as a result of delays due to groundwork, in a study that involves 5,000 industrial buildings, 8,000 commercial buildings, 200 roads and bridges. Navigant Construction Forum (2012) stated that for fast approval and payment of claims; claimants need to support their claims with proof that are beyond reasonable doubt. Moreover, use of modern technologies and applications such as expensive smart receipts, applied epic, claim center, snap sheet and office lens, claims can be easily managed and supported

with robust evidence. However, it could be argued that these technologies are hardly used in processing construction claims for various reasons such slow adaption of emerging technologies; lack of awareness, technical expertise, and traditional nature of the industry. In addition, emerging technologies do exist; claim administrators do often not accept them for reasons aligned to lack of awareness.

2.2 Importance of substantiated claims in construction

Hameed et al. (2014) asserted that unsubstantiated claims often lead to multifaceted problems in construction such as; (i) creates cash flow difficulties for contactor, (ii) delayed project (iii) disputes (iv) unnecessary administrative costs, etc. From contract perspective, unsubstantiated claim has potential to foil corrupt activities and breaches to a contract. Conversely, claims are significant to construction contract management to promote fairness, transparency and smooth running of construction project. Claim also act as back up to insurance arrangement and enhances confidence in entire contractual processes. More importantly substantiated claims help avert prolong or delay payment or extension of time (EoT); a deep-rooted problem that cut across hierarchies of construction supply chain.

2.3 Factors that influence contractual claims in construction

Claims happen in numerous forms and shape ranging from discrete to relational arrangement. However, there is barely any contract that guarantees non-occurrence of claims and disputes; particularly as it relates to construction projects. However, there is need to understand factors that influence construction claims from a broad point of view. Table 1 below illustrates factors that influence construction claims in different stages of construction circle.

Table 1: Construction stages and likely factors that influence claims

Construction stages		Key factors that influence claims
1.	**Project conception**	▪ Unrealistic assumptions in tendering and contracting stage ▪ Incompleteness of basic engineering package
2.	**Construction**	▪ Unfair contractual clauses ▪ Ambiguity in contracts ▪ Detail contracting vs. non contractual factors ▪ Lump-sum contracts (Risk) ▪ Relational contracts and lack of accountability ▪ Variation ▪ Instructions from PM or contract administrator etc.
3.	**Post construction**	▪ Claim as contractor's right ▪ Problems with payment of retention ▪ Compromising over claims ▪ Personalities ▪ Final account claims

Moreover, World Bank Report (2012) suggested that on a global scale claim management is somewhat influenced by host of factors; particularly in countries known for excellent contract enforceability. Table 2 illustrates (World Bank, 2012) ranking of countries with contract enforceability. The ranking started from number 1 to 257 (denoting 1 as excellent and higher figure as worst along the scale). Factors considered in the (World Bank, 2012) ranking include effective claim management system, ease of

doing business, friendliness to entrepreneurs, openness, fair justice system etc. Similarly, the International Bank for Reconstruction and Development argued that countries with poor contract enforceability ranking are more likely to have checkered history of unsubstantiated claims.

Table 2: World Bank (2012) ranking of countries with contract enforceability

Country	Enforcing Contracts
Luxemburg	1
Germany	6
France	7
United Kingdom	21
Sweden	54
Spain	54
Greece	91
Qatar	95
Brazil	118
Pakistan	154
Italy	158
Angola	181
India	182

2.4 Overview of construction claims and disputes in the UK

Russel (2001) asserted that in the UKthe second and fourth most recurrent matter of litigation between main contractors and employers relate to contractor's claims of extension of time (EoT) and loss and expenses (L&E). This assertion is the same for other countries such as Canada, Australia and USA (Hartman, 1994); (Uher, 1994) and (Paulson, 1992). Wong (2005) stated that disputed construction issues in Singapore are contractor's claims for variation and project delays. Kumaraswamy (2003) stressed that construction claims are usually muddled up by inexperience claim administrators; "fundamental mess while dealing with claims is the existence of conflict of interest between the employer, contractor and claim certifier".

Indeed, 'construction claims can be based on nature of contract itself, common law and quasi-contractual assertion for reasonable (quantum meruit) competition or an ex-gratia settlement request (Kumaraswamy, 2003). Array of court cases relating to construction shows that claim is closely related to dispute; thus, Yates (2003) suggested that claims are resolved problems without turning into disputes.

Vidogah and Ndekugri (1998) are of the view that effective claim management requires a lot of resources like responsible personnel, good documentation and record keeping. For example, project correspondence, amended drawings, specifications, request for information (RFI), cost breakdown and measurement records need to be well documented. Kumaraswamy (2003) opined that claims if managed appropriately can lead to potential improvement to work designs due to cross exchange of ideas between parties. Practically, claims are easy to create but substantiation is often complex

(Chappell, 2014).

Review of literature shows that effective claim management requires detailed attention to avoid potential contractual disputes. This can only be achieved through proper recording of documents and provision of knowledgeable personnel.

Indeed, claims can be problematic to both clients and contractors if they are not dealt in a timely manner. Outcome of claim can be either a settlement or a potential dispute. Purpose of claim management process in construction industry is to acquire certain solution to minimize the impact of claim on project delivery. Vidogah and Ndekugri (1998) stated that claim management is not often recognized as management function due to lack of investment of technical expertise. However, effective claim management can be profitable to a contractor if managed appropriately.

2.5 Effectiveness claim management in construction

The key objective of the claim management process is to resolve claims made by a contractual party in an effective and efficient manner in order to avoid costly, lengthy disputes and to maintain cordial relationship. Arguably, most claims in construction are not taken seriously at project level; thus, it is often associated with disputes. Sun and Meng (2009) observed differences in terminologies used to describe effective claim management in past literature; some authors believe that effective claim management is all about predicted claims, as claims, good change orders or vice versa (Levin, 1998). Thus, all relevant terms, which need clarification with respect to claim management, are discussed. However, Sun and Meng (2009) suggested that effective claim management must entail:

- Speedy decision from the authorized claim administrator;
- Cost saving;
- Fairness;
- Substantiated costs;
- Win-win attributes.

3 RESEARCH METHOD

The research strategy adopted is qualitative method and literature review of initial appraisal of seven construction case studies. The qualitative data were used to gather first-hand information about the research themes and the case studies were used to support and validate the qualitative findings. The data collection tools for the study include semi-structured interview with experienced professionals. The study interview questions were designed based on existing literature. Pilot studies were conducted to ensure that the data collection tools were designed correctly. Ethical approval was sought from Coventry University Research Ethics Committee and it was granted. Data collected for the study were obtained from difference locations in England and Scotland. The main interview data collection instruments were designed to answer the study research objective. Stratified random sampling was used to select the study participants for the qualitative data. Study participants were contacted for interviews through emails, telephone contact, site visits and through The Chartered Institute of Building (CIOB) and Royal Institution of Chartered Surveyors (RICS) professional networking. All interviews were conducted face-to-face, telephone and responses to e-mails.

The study population sample consist of construction clients, commercial managers, contract managers, commercial lawyers, quantity surveyors, managing directors of construction firms and business development managers. For validity, the study data collection was conducted on one-to-one basis. This method allowed the researchers to probe participants regarding the study aim. On the other hand, the study participants had opportunity to ask questions that were not clear.

3.1 Interviews' data analysis

Validity of the study qualitative data was upheld in three main areas: selection of participant profile, design of interview questions, and processing/presentation of interview data. Overall, a total of 13 semi-structured interviews were conducted with clients, industry practitioners and construction contractors. The study targeted interviewees with seasoned construction experience. All interviews were recorded using a digital recorder and personal information linked to study participants was removed because of data protection.

Textual excerpts of the interview data were transcribed into manuscript and inputted into Nvivo 12 software. Codes were assigned to key themes to facilitate filtering and sorting of data. The themes from the study aim were used to create codes and sub-codes from the transcribed data. Content analysis was used to analyze interview data for easy inferences to antecedents of discussions and certain words, themes or concepts spoken between interviewees and interviewer. Excerpts from interviews below were obtained using content analysis; by counting number of processes, extracting systematic and objective meaning from each content via making valid inferences from verbal and archive data. For example, when interviewees were asked to express their view concerning preventive approach to unsubstantiated claims in the UK construction industry; host of issues were raised about the subject matter. Subsequently, key contents were trimmed for better understanding and spontaneity of interaction between the researcher and study participants. Some textual excerpts are expressed verbatim; as illustrated below for conformability and better understanding of participants' views.

"... the culture in construction industry is undeniably the root causes of unsubstantiated claims… these problems exist because of dodgy contractors;… some project administrators maybe exploiting unsubstantiated claims to hold back money from contractors" – (Senior Commercial manager in a Large Construction company, London – the UK)

"…. unsubstantiated claims in construction are mainly caused by poor communication, lack of evidence, poor documentation, lack of systematic digital data capturing, ... Perhaps, the problem can only be cured by having rigorous review and check processes before claims are put forward" – (Managing Director, Medium construction company, Manchester UK)

"... Current claim process in the construction sector are faulty; with little check and balances; as a contractor if you submit a claim and the client project manager is not happy with it; he/she will simply put up flimsy excuses and throw it out; the industry

need Systematic and Technical Appraisal mechanism to evaluate entire process of claim management…." – (Construction Manager, Large Construction Company Milton Keynes – the UK)

Interview data presented above suggest that unsubstantiated claim is a contemporary and genuine problem in the construction industry. However, most participants have mix perception about the research topic; the consensus on the issues is that both claimants and claim administrators usually do not handle unsubstantiated claims in good faith. However, interviewees were asked to expound on how prevent unsubstantiated claims and disputes in the construction industry. Some recorded extracts are expressed verbatim; as illustrated below:

"... in our previous projects we used lot of technologies ... yet we still had problems of unsubstantiated claims, ... to overcome this problem there must be a system or mechanism that will encourage early filing of claims, good claim data base, proper documentation, robust claim identification mechanisms, use of emerging technologies, etc … the industry need to enhance its entire claim management processes*"* (Senior Commercial Manager, Railway infrastructure Project, the UK)

"... I am optimistic that balance communication between claimants and claim examiner and automation of claim management processes will help minimize unsubstantiated claim issues*"* – (Commercial lawyer – London).

"... I can confidently tell you most clients representative – project managers often view claims as dubious exercise that help contractors to make more money in a project; .. ... notwithstanding whether the claim was approved by them ... in an atmosphere of such mistrust pay master is most likely to view contractors' claims as unsubstantiated ..." – (Construction Cost Consultant – London)

To validate the findings from the qualitative inquiry; total of seven selected construction case studies relating to the UK construction industry were sought for better understanding of the problem as illustrated in table 3 below. The seven cases involve: construction projects, specialist contractors, and notable construction clients doing business in the UK. For robust analysis the case studies were drawn cases that were brought formally to competent court of jurisdiction and with clear verdicts. The following criteria were used to select construction cases in table 3: (i) the case relates to the UK construction industry, (ii) clear court verdict on the issue brought before the court, (iii) claim was identified as a major issue of dispute, (iv) judgement was not appealed. The key reason for selecting these seven cases is that there are valuable lessons concerning unsubstantiated claims and nature of construction disputes to be learnt from them.

These measures were taken to enable the researcher gather key lessons about the unsubstantiated claims and how to prevent the issue in the future. Table 3 presents seven case studies regarding nature of construction claims, disputes and key lessons learnt from each case study.

Table 3: Selected construction case laws regarding claims and disputes

S. / No.	Case Study	Year	Nature of construction claims	Key lesson learnt
1.	Costain limited vs Tarmac holdings 2017	2017	Defect and cost related	Adequate and timely communication
2.	Atkins vs Secretary of State for Transport	2013	Defect and cost related	Clarification of lump sum contract
3.	Multiplex Constructions (UK) Ltd vs Cleveland Bridge UK Ltd	2007	Design and cost	Undue influence of lawyer and adherence to use of ADR
4.	City Inn vs Shepherd Construction	2002	Concurrent delays	Lack of clarity regarding contractual provision
5.	Mears Ltd vs Costplan Services (South East) Ltd	2019	Practical completion	Failing to meet PC
6.	Triple Point Technology Inc vs PTT Public Company Ltd	2019	Liquidated damages following termination of the contract	Time management
7.	S&T (UK) Ltd vs Grove	2018	Payment regimes and "smash and grab adjudications"	Payment requirement

4 DISCUSSION AND FINDINGS

Findings from table 3 show that unanimity with the study literature regarding unsubstantiated claims, effectiveness of claim and key lessons learnt from various case studies. Most professionals in the industry believe that balance communication between claimants and claim examiner, early filing of claims, good claim data base, proper documentation, robust claim identification mechanisms, use of emerging technologies are required factors needed to enhance unsubstantiated claims that are often too familiar in the construction industry. Perhaps, unsubstantiated claims issues in construction can be best managed using tactical approach such as timely notification of claims supported by unquestionable evidence. The study identified that over 38% of claims submitted by construction contractors are usually rejected due to lack of verified and corroborated evidence. Findings from the seven case studies reviewed show that time (delay) and variation related claim constitute approximately 52% of most construction claim. Defects and weather related claims consist of approximately 38% of claim. While, design and change order from clients entails approximately 6% of claim and other factors consist of remaining 4% of claims. The study also identified that most construction projects have weak documentation processes; in terms of modern data storage and processing.

5 CONCLUSION

Initial findings reveal that claim management processes in the construction sector

are far-off from perfection. Unsubstantiated claims remain a leading cause of disputes in the construction industry. To prevent unsubstantiated claims there is need for robust systematic and technical claim appraisal (STA) process. The proposed claim appraisal process should entail details record keeping of 4Ms i.e. costs of Materials, Machine, Manpower, and Money. In addition, to update transaction register, training of competent staff to ensure in-depth review of claims, precise and transparent weather recording, information of construction programme. Finally, thorough understanding of relevant compensation events and robust claim management processes (.i.e. identification, notification, examination, documentation, presentation and analysis and timely resolution of claims through negotiation) are vital ingredient to help contracting parties substantiate construction claims. Though, most UK construction projects already use close circuits television (CCTV) cameras/system to monitor production and security properties on site; the same system can be modified to help to corroborate claims.

REFERENCES

ARCADIS (2018). *Global Construction Disputes Report*. ARCADIS.

Bonaventura, H. W. H. (2015). Construction Claim Types and causes for a Large-Scale Hydropower Project in Bhutan 20, 49-63.

Barrie, D. S. & Paulson, B. C. (1992). *Professional construction management: including CM, design-construct, and general contracting*. McGraw-Hill Science/Engineering/Math.

Chappell, D. (2014). *The JCT Standard Building Contract 2011: An explanation and guide for busy practitioners and students*. John Wiley & Sons.

Hameed Memon, A., Abdul Rahman, I. & Faris Abul Hasan, M. (2014). Significant Causes and Effects of Variation Orders in Construction Projects. *Research Journal of Applied Sciences, Engineering and Technology, 7*(21), 4494-4502.

Jack, P., Russell, C. & Bert, B. (2001). Validation of trace-driven simulation models: bootstrap tests. *Management Science*, *47*(11), pp.1533-1538.

Jergeas, G. F. & Hartman, F. T. (1994). Contractors' construction-claims avoidance. *Journal of Construction Engineering and Management*, *120*(3), pp.553-560.

James G. Zack, J. (2013). Delivering Disputes Free Construction Projects: Part-I-Planning, Design & Bidding.

Retrieved from Navigant Construction Forum. Available at: https://conimas.com/pdf/DELIVERING%20

DISPUTE%20FREE%20PROJECTS%20-%20PART%20I%20-%20NCF%20FINAL.pdf [Accessed 25 Nov. 2019].

Kumaraswamy, M. (2003). *Conflicts, Claims and Disputes in Construction*. vol. 4.

London Court of International Arbitration (2018). Construction Claims Guide.

Long, R. J. (2017). Analysis of Concurrent Delay on Construction Claims - 2017 46.

Levin, P. (1998), May. Construction contract claims, changes & dispute resolution. American Society of Civil Engineers.

Sun, M. & Meng, X. (2009). Taxonomy for change causes and effects in construction projects. *International journal of project management*, *27*(6), pp. 560-572.

Tochaiwat, K. & Chovichien, V. (2004) Claim Management Process.

Uher, T. E. (1994). *What is Partnering*. Australian Construction Law Newsletter, 34, pp. 49-61.

Vidogah, W. & Ndekugri, I. (1998) Improving the Management of Claims on Construction Contracts: Consultant's Perspective. *Construction Management and Economics*, *16* (3), 363-372.

World Bank, (2012). *The World Bank Annual Report 2012*. The World Bank.

Wong, Y. L. (2005). *Factors affecting the choice of dispute resolution methods*. (Unpublished bachelors dissertation). National University of Singapore.

Yates, F. (2003). *The occult philosophy in the Elizabethan age*. Routledge.

Cite this article as: Nosheen A., Arewa A. O., Akhtar H. M., "Preventive Approach to Unsubstantiated Claims and Disputes in the UK Construction Industry", *International Conference on Civil Infrastructure and Construction (CIC 2020)*, Doha, Qatar, 2-5 February 2020, DOI: https://doi.org/10.29117/cic.2020.0014

Utility Impact Assessment of Road Projects in the State of Qatar

Mohammad Mujtaba Hamidy
mhamidy@mme.gov.qa
Ministry of Municipality and Environment, Doha, Qatar

ABSTRACT

Qatar has been blessed with large reserves of natural gas and since the past 20 years its leaders have been busy formulating its path to modernization. Henceforth, the sovereign state has been and is still going through tremendous development phase to meet the 2030 vision of making Qatar a world class country and giving its citizens a very high standard of living. This is to be achieved with development in key sectors namely economic, social, environmental and more importantly human development. Moreover, in 2010 Qatar was awarded to host the 2022 FIFA World Cup, which increased the country's pipeline of projects such as stadia, hotels, metro and ports (air and sea). This also led to fast tracking of its stockpile of existing infrastructure projects to meet 2022 deadlines. Accordingly, significant portion of these projects will be constructed within the right of way or road reserve. Although the current practice of road construction and utility installation in Qatar is in-line with world best practices, but such practices were not followed stringently in the past. Moreover, Qatar's cities have gone through an excessive urban densification, which meant that the service providers had to provide greater number of utilities and road authorities had to design and construct complex road networks that involved tunnels, bridges, underpasses and overpasses. These challenges are further compounded by the fact that there are narrow right of ways for the installation of all these utilities in the urban areas. In tackling these challenges, the Ministry of Municipality and Environment (MME) along with road authorities and utility providers have gone through robust review and modification of their practices. As a result, actions were taken and in particular MME developed a process namely, utility impact assessment process that guides the road designers to collaborate with utility designers to achieve a more value engineered outcome.

Keywords: Right of way; Subsurface utilities; Value engineering

1 INTRODUCTION

Qatar is going through an unprecedented development rate that is comparable to some of the major cities that have gone through modernization in recent times and are still going through such as Shanghai and Goughaze. With numerous projects under construction, tender and design also significant portion of projects in the pipeline. It has been reported that $US200 plus billions is being invested in the country's development and with such colossal investment it will naturally lead to tremendous challenges across all governmental sectors, and subsequently it will be a great opportunity for the private sector to embark.

The main driver for this infrastructure development has been Qatar's 2030 Vision that entails modernization of the State across all sectors. However, in this paper we will

focus on the upgrade of road network and more importantly the utility services that are installed below the road networks. At present the traffic volume for the capacity of the road network is excessive, especially in inner urban areas of Doha, which is reflected in the daily commute of the residents. If we compare the infrastructure network to the human circulatory system, highways and roads function as the delivery system, transporting services from one location to another just like the arteries, veins and capillaries that transport nutrients to all parts of the body with the flow of blood. Just like a healthy body requires a healthy circulatory system, so does a healthy city or country require a healthy and smooth-running infrastructure network. The country's decision makers are fully aware of the situation and are taking all the necessary measures not to aggravate the problem further. Hence, a major surgical operation worth $US200 billion plus is planned to make Qatar a world class city comparable to the world's best cities in terms of infrastructure.

2 RIGHT OF WAY CHALLENGES

Right of way or road reserve is generally the space that allows the movement of vehicular traffic as well as non-vehicular traffic (including train, tram, pedestrian, cycle etc… and their associated facilities and appurtenances). The right of way does not only act as a conduit for the movement of traffic but also as a medium to interconnect and deliver all the necessary amenities such as water, electricity, ICT, security and sanitation services to the residents, businesses, institutions and the likes to make the town, city and the entire country function. However, one of the biggest challenges that Qatar is facing is lack of availability of space/corridors for utilities.

The current practice in Qatar is that all utilities in urban areas must be located underground. This is in line with best global standards similar to most advanced cities of the world. At present the standard in Qatar is that each of the utilities have been designated a specific corridor/space within the right of way, whereby the shallower utilities have been located in the edges of the right of way and the deeper utilities (gravity driven) is located more centrally in the road carriageway. If this standard gets enforced and implemented it will lead to an ideal situation. However, such standard was not stringently followed, and utilities were installed within the right of way in a haphazard manner.

To outline some of the challenges it must highlighted that in addition to excessive traffic, the road right of way is extremely congested with subsurface utilities throughout Doha. As a result of proposed road improvements to cater for the greater volume of traffic, the carriageways (vehicle carrying segment of the right of way) will be widened to accommodate greater volume of vehicle movement. With the exception of the deep gravity related pipes, the rest of the utilities are generally placed at the verges of the road and not under the pavements for ease of construction as well as to maintain easy access for operation and maintenance. Given the constraints posed by the road widening the non-gravity utility such as telecommunication ducts, pressured water pipes and electricity ducts will inevitably fall inside the paved roadway, a practice generally not recommended by the respective authorities, due to difficulty in gaining access. In addition, the proposed road configuration is made up of complex set of arrangements at the junctions that may consist of tunnels, underpasses, bridges and flyovers to cater for

free-flowing traffic. This results in installation of utilities at the junctions to be more convoluted as the availability of accessible space for utilities is significantly reduced.

2.1 Overcoming Challenges

To overcome challenges, the State of Qatar has taken number of initiatives and each service agency has developed and modified their procurement process. One of the key organizations in the country is the Infrastructure Planning Department (IPD) of Ministry of Municipality and Environment (MME), whose is responsible to arrange the placement of utilities within a right of way and allot the necessary space for all the services. To carry this work, number of initiatives were introduced that considered the planning and design stages of the project as well the delivery of the project. Furthermore, it must be noted that the urban planning of Qatar is carried out by the Ministry of Municipality and Environment as well, where assigning the land use directly influences and correlates to the space and corridor allocation for the utilities within a given right of way.

The Infrastructure Planning Department of MME has created a flow chart titled "MMUP utility investigation approval procedure". This flow chart enables all the road authorities working on the road project to clearly see the flow of work during the planning and design development of the project. This flow chart can be broken into three major components, namely, "investigation", "assessment" and "approval", as per Figure 1 below.

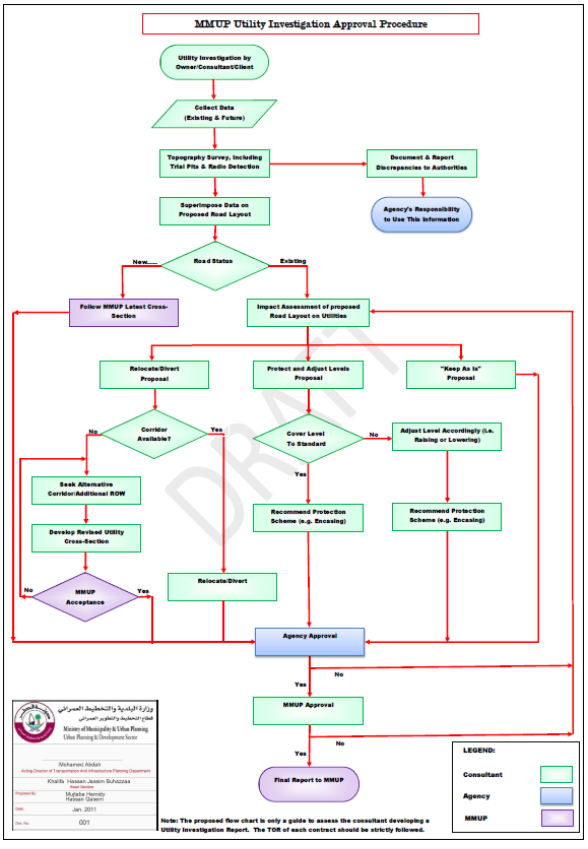

Figure 1: Flow chart for the MMUP utility investigation approval procedure

2.2 Investigation

First let us consider the investigation component. Once the extent of the road project has been defined by the project proponent, usually Public Works Authority (Ashghal) or Ministry of Transportation and Communication (MoTC), then the first essential aspect of the project is to establish an accurate base for the project. Just like traffic engineer carrying a "traffic survey" to capture the existing flow of traffic and in addition obtains the necessary future land-use of the area to establish the future projections of traffic flow, similarly the utility engineer of the project must obtain the latest information for all the utilities. This includes an accurate as built information of the all the existing utilities within the subject road design as well as proposed utility plans. Upon receipt of all the agencies' As Built information it is essential that the responsible engineer engages a licensed surveyor to carry an onsite investigation to verify the location of the agencies As Built information.

It must be emphasized that number of studies and best practices around the world indicate that obtaining accurate As Built information is vital in developing and delivering the most cost effective, timely and less disruptive project. Accordingly, most of the departments of Transportation in US adopt Subsurface Utility Engineering (SUE), which is a well established engineering practice that looks at different stages of the project with different levels of accuracy of the existing assets. This accuracy or perhaps the quality of the information ranges between D to A, where Quality D is desktop information while Quality A involves detailed onsite investigation determining the precise location of the asset's both in XY Cartesian as well in its vertical component.

Given that there is overwhelming number of road and infrastructure projects in Qatar it was IPD-MME's judgement that adoption of SUE practices would've not been practical to incorporate for Qatar's road projects. However, given that the determination of accurate information plays a vital role, carrying adequate field investigation through topographic survey as well more advance form of survey techniques such as radio detection as well as ground penetrating radar and other similar advanced techniques that ascertains an accurate location of below surface utilities were required to be applied. In short MME-IPD encourages the principles of SUE and enforces wherever possible that engineers make appropriate level of analysis on the topographic survey obtained to validate the accuracy of the As Built information. This is achieved through overlaying the As Built information with the surfaced features obtained from the topographic surveys such as manholes, vents, valves, gullies etc…

After the comparison has taken place any the discrepancy between the two set of data is determined, it is the duty of the engineers to report all the inaccurate field data to their respective agency and accordingly the engineer must use the more accurate information of the on-site investigation in developing the design and assessment of the project.

2.3 Impact Assessment

Upon obtaining accurate information the engineer can confidently commence the impact assessment of the proposed road on the existing utilities as well as any future utilities along the subject right of way. How existing and proposed utilities are impacted primarily depend on the actual road design. It must be noted that as part of Public Works Authority (the implementation authority responsible for road and drainage) road

projects, there are two different road programmes, namely the "local road and drainage programme" and the "expressway programme". The general aim of local roads project is to resurface, road widening, improve drainage, allocation of footpath and lighting as well adjustment and installation of the subsurface utilities. However, expressway roads generally take a more extensive design especially around the junction that may include multilevel interchanges which include underpasses, tunnels, ramps and bridges to allow for the free-flowing of traffic movement, in addition there is also metro network and large gravity mains. In carrying the impact assessment of these schemes, the utility and road designers need to make the determination of how the existing utilities will be impacted i.e. for each of the existing utility the design engineer generally has the following main decision to make:

- Keep it in its current location with no adjustment.
- Protect, lower or raise it to meet agency's requirements.
- Or relocate to a more suitable location.

2.3.1 Value engineering the road and utility arrangement

A value engineering exercise needs to be carried out. MME supports proposals that keeps utilities in their existing location as much as possible by adjusting or providing provisions within the road design such as:

i Adjusting the road geometry.
ii Modifying the highway drainage.
iii Appropriate retaining walls selection and design.
iv Appropriate design of batters/slopes/barriers and abutment arrangements to minimize adjustment of existing utilities.
v Protection above water pipes in the proposed paved areas (carriageway or carpark).
vi Concrete protection above electric cables and other ducts (e.g. telecommunication and security ducts).
vii Departures from standard design specifications for road design as well as utility design.
viii Road carriageway or lane width reduction.
ix Consider signal standard changes.
x Increased signal mast arm lengths.
xi Adjust the signal and sign locations.

It is also important that the engineer needs to future proof the construction of the road, where future utilities should be catered for, accordingly it is important that all the planned utilities are incorporated as part of the proposed road project. Therefore a comprehensive utility infrastructure project will be built, the benefit of such practice is cost saving to all the parties where subsurface utilities are placed prior to the pavement construction, which in-turn will not necessitate future road opening (pavement cut), further disruption to the travelling public and subsequently this will decrease the longevity of the road network. Presently, a lot of collaboration between agencies has been carried out to achieve a high-level agreement between road authority and utility agencies that incorporates the utility agencies' future work into the proposed road project. However, such practices are happening only in selected projects and not across all the road projects. However, a more comprehensive agreement can be easily achieved

given that most utility agencies are government owned and the budget for all the projects in Qatar comes from the same source (Ministry of Finance). Accordingly all the parties have vested interests to coordinate their work to obtain the most cost effective result that will also be delivered much more efficiently with better quality and that will last much longer.

2.3.2 Installation of utilities in narrow corridor

One of the key constraints in State of Qatar is the availability of right of way, as the existing right of ways are narrow and acquisition of land in Doha is very expensive and not desirable as it causes significant disruption to the public and potential loss of historical value of the city. Accordingly, the utility engineer must develop out of the box solutions to allow all the utilities to be placed in narrow corridor. To carry out these exceptional designs MME provides some design guides to allow the designer to be more creative to achieve nonstandard solutions. These guidelines include:

i The width of the corridors for utilities shall be reduced and shall only be provided for existing and known future utilities.
ii Greater number of utilities shall be placed under the pavement such as transmission pipes and cables.
iii Shared trenches/common trench for compatible utilities e.g. gas and water.
iv Stacking of utilities over short stretches e.g. transmission cables & large diameter pressure mains below distribution cables & smaller diameter pressure mains.
v Telecommunication ducts above pressure mains or transmission cables where concrete slab is placed between the two for protection.
vi Easement, instead of acquiring land - utility easement can be created to allow utilities to traverse at pinch points.
vii Rerouting of the utilities within secondary minor roads parallel to main traffic routes, this option should be especially considered at junctions.
viii Consideration should be made for power galleries or utility tunnels in lieu of land acquisition and when other options have been exhausted and value engineering has identified tunnels to be an optimal solution in a given case.

2.3.3 Approval process

Upon investigation and assessment of the utilities the project proponent or their assigned consultant must submit appropriate documentation to MME. The approval process of the project prior to implementation is carried out in three stages (i.e. first MME initial approval, second Agencies approval, third MME's pre-construction approval). The first critical stage of the approval involves the corridor allocation for the existing and proposed utilities within the given right of way. This stage requires the approval of MME as the width of the right of way to accommodate the road and utility component of the project solely depends on MME's discretion, whereby MME has to consider that the land acquisition of the project is fully justified for the road elements as well as utilities. Hence once the width of the right of way has been established the approval of how the right of way should be divided among the utilities also lies within MME.

Upon receipt of MME's first initial approval the project proponent must seek NOCs from utility providers. The project proponent is also required to meet agencies' conditions

and all their requirements. Any disagreement or point of contingency between the project proponent and a utility agency should be raised to MME for resolution.

The final stage of approval prior to the implementation of the project is once again with MME where the project proponent must submit all the agencies' approval and if there are any changes in comparison to MME's initial approval, those must be highlighted and documents must be provided to fully justify the proposed changes.

Once the project has been constructed in order to certify and commission the project, MME will also require a completion certificate from the relevant authorities and a copy of the "As Built". The As built plans will be checked against the pre-construction approved documents and in case of any discrepancy between the two submittals, the project proponent is required to provide clarification and justification. If accepted, MME will issue a final approval which will allow the project proponent to request final completion certificate from the concerned municipality.

3 CONCLUSION

In conclusion, Qatar will go through an extraordinary development phase in the coming decade and majority of the projects will involve the improvement of the current right of ways for much needed and improved traffic flow. The improvement of the road will impact the subsurface utilities and will require proper assessment. The high demand for utilities to service a high density development coupled with narrow right of way as well as complex road arrangement, poses a great challenge for all the road, highway and utility engineers to develop an innovative and cost effective solution for the country to function smoothly at its best. MME, Public Works Authority and all the utility agencies have made significant improvements in coordinating, collaborating and communicating across all the ongoing development projects to achieve the desired outcome of building a world class infrastructure for State of Qatar. MME has taken the lead to apply the best practices in optimizing the existing right of ways, through guiding engineers to design and develop a more innovative solutions to overcome the right of way challenges as well as streamlining the overall approval process to fast track the delivery of these projects.

REFERENCES

Avoiding Utility Relocation (2002). *US Department of Transportation Federal Highway Administration*, Washington D. C. Access on Sept 10, 2019 [Online], Available: http://www.dot.ga.gov/PartnerSmart/utilities/Documents/AvoidingUTLRelocations.pdf.

Cesar, Q., Yingfeng (Eric), Edgar, K. & Le, Jerry (2010). Optimizing Utility Owner Participation in the Project Development and Delivery Process, National Technical Information Service, Austin, 161 pages. Available: https://pdfs.semanticscholar.org/0f12/aef23d6f0ede89bcbee346b5407e5730ca1f.pdf

Identification of Utility Conflicts and Solutions (2012). *The National Academies of Science Engineering Medicine*, Washington D. C, 2009. Accessed on Oct 3, 2019 [Online]. Available: https://www.nap.edu/catalog/22819/identification-of-utility-conflicts-and-solutions.

Integrating the Priorities of Transportation Agencies and Utility Companies (2009). *The National Academies of Science Engineering Medicine*, Washington D. C. Access on Oct 3, 2019 [Online]. Available: https://www.nap.edu/catalog/23037/integrating-the-priorities-of-transporta-

tion-agencies-and-utility-companies.

Monri, H. (2015). A Survey of Utility Coordination Practices in the Toronto Area. *Paper of the 2015 Conference of the Transportation Association of Canada Charlottetown*, PEI, pages, 19. Available: http://conf.tac-atc.ca/english/annualconference/tac2015/s23/monri.pdf.

Raymond, S. (1994). Indirect Costs of Utility Placement and Repair Beneath Streets, National Technical Information Service, Minnesota, 56 pages. Available: http://apps.fcc.gov/ecfs/document/view; ECFSSESSION=h00vW0yTFGc9X2SnzkXvxtl4R2P2H1vrp2TNvQR0nmhyZzT520RC!150370719!1967462809?id=6009552992

U.S Domestic Scan Program (2006). Best Practices in Right of Way Acquisition and Utility Relocation. National Cooperative Highway Research Program Transportation Research Board, Cambridge. Access on Oct 3, 2019 [Online]. Available: http://www.trb.org/Main/Blurbs/158478.aspx

Urban Planning Council, Abu Dhabi (2013). *Abu Dhabi Utility Corridors Design Manual*. Access on 5 Oct 2019 [Online]. Available: https://www.upc.gov.ae/en/-/media/upc/feature/tools/ucdm_version-1-en/compressed_ucdm_english.ashx.

Utility Accommodation Policy and Standard (2016) (Revised 01/12/2018). Georgia Department of Transport, 2018 Access: Oct 1 2019 [Online]. Available:http://www.dot.ga.gov/PartnerSmart/utilities/Documents/2016_UAM.pdf

Utility Coordination Manual of Instruction (2017). Utah Department of Transportation, Salt Lake City. Access on Sept 7, 2019 [Online]. Available: https://www.udot.utah.gov/main/uconowner.gf?n=2989808693862464

Utility Investigation Best Practices and Effects on TxDOT Highway Improvement Projects (2013). Texas Department of Transport and the Federal Highway Administration, Austin. Access on 4 Oct 2019 [Online]. Available: http://tti.tamu.edu/documents/0-6631-1.pdf

Utility Relocation and Accommodation on Federal-Aid Highway Projects (2003). Sixth Ed, Office of Program administration Federal Highway Administration, Washington D. C, Access on Sept 10, 2019 [Online]. Available: https://www.fhwa.dot.gov/reports/utilguid/

Utility Policy Manual Ministry of Transportation and Highways, British Columbia, 1995, Access on 5 Oct 2019 [Online]. Available: http://www.th.gov.bc.ca/permits/Utility%20Permit%20Manual.pdf

Cite this article as: Hamidy M. M., "Utility Impact Assessment of Road Projects in the State of Qatar", *International Conference on Civil Infrastructure and Construction (CIC 2020)*, Doha, Qatar, 2-5 February 2020, DOI: https://doi.org/10.29117/cic.2020.0015

Project Management: Key Initiatives Case Study

Khaled Al Nass
kalnaas@ccc.net
CCC, Doha, Qatar

Lavinia Melilla
Lavinia.melilla@arcadis.com
Arcadis, Doha, Qatar

Mohamed Tolba
mtolba@ashghal.gov.qa
Public Works Authority (Ashghal), Doha, Qatar

ABSTRACT

Every project faces risk of delays and disruptions, especially the mega/complex projects of today, which have, amongst others, many interfacing parties engaged. Local roads and drainage projects in general, including DN016, can be considered complex projects due to a number of reasons such as, a) working in residential areas, b) deep excavations, c) number of interfacing parties, d) project duration, e) multifaceted identification for the location of existing underground utilities. The contractor decided to use some tools to help minimize the negative impacts of a number of challenges such as, 1) workface planning by dividing the project into 5 zones and start working in free zones for early zone handover, 2) lean construction to minimize the waste, 3) management processes in order to control the known-unknown challenges and risks and to minimize those and 4) Building Information Model (BIM) for the identification of major and minor clashes to the designer in order to resolve them early as to have a smooth construction flow. In addition, the project management team identified both internal and external stakeholders of the project in order to determine the project requirements and expectations of all parties involved. A dedicated stakeholder manager was appointed to identify and manage the stakeholder issues without affecting the project performance. Although major efforts are done in this regard, many stakeholders residing nearby the construction area are negatively affected from the project execution due to the nature of the project and time constraints. The supervision consultant and the client also directly engaged in managing the stakeholders and ultimately impacted the project. However, further delays were mitigated with the implementation of regular stakeholders' meetings, and work was carried over based on their requirements. Also, the project management decided to have a handing over plan from early stages of the project and to assign a dedicated handing over manager with required resources, and mobilize them very early in the project. The handing over team identified all the handing over procedures and the required documentation with the client.

Keywords: Planning; Workface; Lean construction; Building Information Model (BIM); Risk; Infrastructure

1 INTRODUCTION

Bani Hajer North Phase 2 is part of Ashghal local roads network projects designed at improving the wider infrastructures architecture in the State of Qatar. Roads and infrastructure works in Bani Hajer residential area consist of roads with around 163,000 M2 providing utility services like surface water drainage of length 39,121 and 7 No.

of attenuation tanks with 3,038 LM of micro tunnelling works, TSE network, street lighting, ITS, telecommunication network and landscaping works. The project duration is 16 months with a value of QAR323 million.

2 KEY PROJECT INTIATIVES

The project management has implemented key project initiatives and effectively managed issues throughout the project execution phases. This document outlines the measures and key initiatives that have been implemented for the successful completion of the project:

- Project planning
- Lean construction implementation
- Risk management plan
- Stakeholder management
- Handing over plan

Although these are known project management techniques, the project has utilised and implemented them effectively to mitigate the risk of delays in the project.

2.1 Project planning

The baseline program has been developed for the project, explaining the project construction sequence of works from the date of commencement to completion. The document shows all the coding and work breakdown structure of the schedule from several points of view by highlighting the critical path(s), and the key intermediate milestones. The early part of the project covers the engineering and procurement phases and then the construction phase as well. The schedule ensures the alignment of the engineering and procurement deliverables with the construction sequence.

The project begins with setup and interactive planning to define the optimum construction schedule. The plot plan is broken into Construction Work Areas (CWAs) which are further divided into discipline specific Construction Work Packages (CWPs). Engineering deliverables as EWP (Engineering Work Package) and procurement items as PWP (Procurement Work Package) are defined for each CWP. The CWP sequence defines the timing for development and sequential delivery of engineering and procurement. This helps to organize and deliver all the elements necessary, before the work is started, to enable craft persons to perform quality work in a safe, effective, and efficient manner. This type of planning is defined as Workface Planning or Advanced Work Packaging.

Construction Industry Institute (CII) defines Advanced Work Packaging (AWP) as, "*the overall process flow of all the detailed work packages (construction, engineering, and installation work packages). AWP is a planned, executable process that encompasses the work on EPC project, beginning with initial planning and continuing through detailed design and construction execution. AWP provides the framework for productive and progressive construction, and presumes the existence of a construction execution plan.*"

The construction activities and durations are defined from estimated quantities and preliminary estimates and applying reasonable production rates (based on experience in Qatar) mainly to determine durations.

The utilities storm water drainage, foul sewer, TSE, ITS, Q-Tel, DSSS is grouped into the road works and the scope is detailed for each utility network under the WBS.

The project is divided into five zones. All the roads are grouped into respective zones. The roads are further divided into single phase construction for new roads and two phase constructions for the existing roads.

The single phase construction roads which are new roads are planned to commence immediately once the drawings are submitted and approved. The two phase construction roads with existing traffic are planned to commence once the traffic management plans are submitted and approved for construction.

The project critical path runs on most of the two-phase roads as these needs traffic diversions. The project management identifies that the duration of the project is not enough to complete the project on time considering the criticality of the utilities scope and the sequence of works.

2.2 Lean construction

The following lean concepts implemented in the project are as follows:

A. Construction planning
(i) Utilizing BIM 3D model
(ii) Utilizing clash analysis –BIM model
B. Project execution performance
(i) Issue three months look-ahead
(ii) Identify pre-requisites for the look ahead activities in advance
(iii) Measure the performance of 3 months look ahead- KPIs
(iv) Identify the root causes of the deficiency activities
C. Project execution monitoring and control
(i) Measure the productivities of the direct resources
(ii) Identify root causes for deficiencies
(iii) Target for continuous improvement
(iv) Reduce construction waste
D. Project handing over
(i) Link RFIs to BIM 3D model
(ii) Internal software – ATLAS for handing over

The project planning team utilised the 3D BIM model to analyse the scope of work in detail. Without the use of BIM, the complexity of the underground utilities in the local roads projects cannot be estimated properly in terms of the typical section and the sequence of works.

Salman Azhar (2011) states that, "*Building Information Modelling (BIM) is one of the most promising recent developments in the Architecture, Engineering, and Construction (AEC) industry. With BIM technology, an accurate virtual model of a building is digitally constructed. This model, known as a building information model, can be used for planning, design, construction, and operation of the facility. It helps architects, engineers, and constructors visualize what is to be built in a simulated environment to identify any potential design, construction, or operational issues. BIM represents a new paradigm within AEC, one that encourages integration of the roles of all stakeholders on a project*."

The project management team resolves the utility clashes using BIM before the works

commencing on site. This tool helped avoiding delays in the completion of utilities. The clashes were identified as major, which require design change, and minor, which can be locally resolved on site during construction. Figure 1 below shows a sample for a major utility clash report that requires a design change.

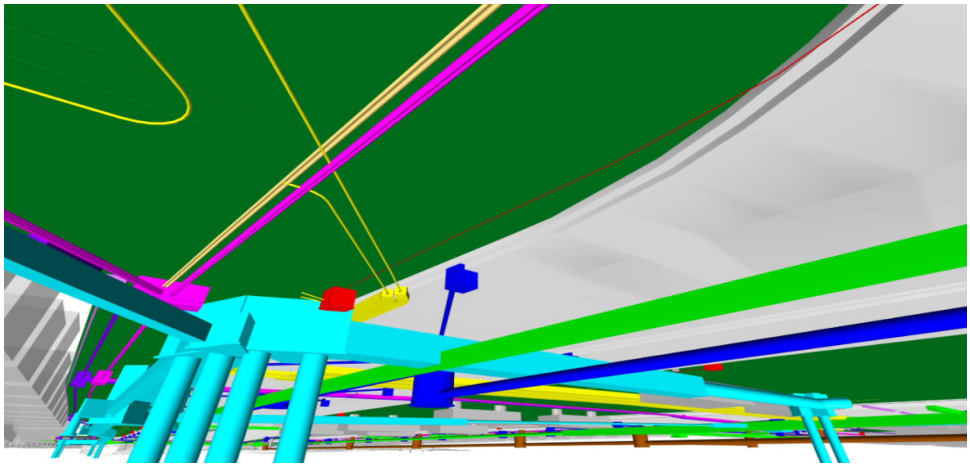

Figure 1: A sample utility clash report from BIM

2.3 Risk management plan

Banaitiene & Banaitis (2012) as per APA, *"risk management is probably the most difficult aspect of project management. A project manager must be able to recognise and identify the root causes of risks and to trace these causes through the project to their consequence."*

Risks were defined for the project with their probability & impact/consequences during brain storming sessions to create the risk register. Based on the P-I Score of each risk, they were categorized as Red Zone, Amber Zone and Green Zone.

- All Risks falling in the Red Zone are treated very carefully by providing risk response plan for each risk. The risk response plans are detailed because the risk response plan could cause some secondary risks. The secondary risks are included in the risk register as secondary risks.
- Risks to be monitored are those falling in the Amber Zone, if during monitoring such risks move to the Green Zone then they will be acceptable but if they move to the Red Zone then they are not acceptable and must be treated.
- Acceptable risks are those falling in the Green Zone.

Risk assessment was carried out on the overall process of risk identification, risk analysis and risk evaluation. Risk treatment carried out to develop strategies and action plans to manage risks as shown in Table 1 below.

Assigned risk manager to continuously manage the risks in the project. Risk register is in the agenda in the weekly progress meeting discussions and the project manager makes sure that all the engineers have input to the risk management in the project.

Table 1: Sample risk register format

Risk ID	Risk Type	Risk Category	Risk Description	Risk Owner	Status	Prob	Impact	Risk Score	Mitigation Action	Mitigation Owner	Mitigation Action Date	Progress Complete	Prob	Impact	Risk Score	Risk Expiry Date
Risk-DN016-P00-14298	Risk	Commercial	The Project May Suffer delay and disruption to expected variation orders	Dennis Rush (GEC/ PMC)	Open	3	4	12	Continuous coordination meeting with GEC. For any changes in scope	Dennis Rush (GEC/ PMC)	30-06-17	90%	2	1	2	31

2.4 Stakeholder management plan

The project management team identified both internal and external stakeholders of the project in order to determine the project requirements and expectations of all parties involved. A sample of the stakeholder register is shown in Table 2 below.

A dedicated stakeholder manager is appointed to identify and manage the stakeholder issues without affecting the project performance. Although major efforts are done in this regard, many stakeholders residing nearby the construction area are affected negatively on the project execution due to the nature of the project and time constraints. The supervision consultant and the client are also directly involved in managing the stakeholders but ultimately impacted the project. However, the project management can strongly say that further delays were mitigated with the implementation of regular stakeholders meetings, and manage accordingly based on their requirements. This is a lesson learnt for the project team and also for the client.

Table 2: Sample of stakeholder register

Issue Detail					Issue Identification				Issue Resolution						Commentary		
Issued ID	Stakeholder	Raised (Yes/No)	Conflict issues (Title of Issue)	Type	Date Raised	Method Raised	Evidence (PMIS EDMS Reference)	Expected duration to resolve the issue (days)	Resolved? (Yes/No)	Date Resolved	Method Raised	Evidence (PMIS EDMS Reference)	Delay in Resolution (Days)	Resolution Weight	Contractor Notes	GEC Notes	PMC Notes
	PWA Public Realm	Yes	PRC 1986: The complainer (MR. Moubarak Al Hajry) is asking the completion of the infrastructure project. PWA Reference complaint number: 08012017-0146	PRC	02/03/2017	Email		1	Yes	03/03/2017	Email		0	1			

2.5 Handing over plan

Handing over of any project is the most hardest and lengthy process among all other processes of the project life cycle. Therefore, the target of the project management was to obtain stakeholders' early acceptance of the project. This meant that all stakeholders accept that the work has been completed in accordance with the project specifications and parameters within the agreed timeframe. In order to make this go smoothly, the stakeholder and project manager must have a well-documented criteria of performance, in place from the beginning of the project. This information should be documented in the project handing over plan which should include all changes requested through the life of the project.

The project management insisted to have a handing over plan from the beginning of the project and assigned a dedicated handing over manager with required resources and mobilized them at the very early stage of the project.

The handing over team identified all the handing over procedures and the required documentation with the client. The team has prepared a detailed program for handing over, identifying all the end users of the project.

The project has utilized the internal software tool ATLAS which is linked with BIM model. The dedicated team decodes all the RFI tags to the BIM elements and identifies the lags time to time in coordination with the QA/QC team to resolve the issues if any arise in this regard.

3 CONCLUSION

Although the construction work was completed on time with opening roads to the traffic, the closing of the project was very time consuming, due to the handover process and procedure. As a way forward and as part of continues development in PWA RPD, new "construction enhancement contracts" call for the handing over to be completed within the project completion date by adding KPIs. Moreover the zone delivery takes into consideration the hand over time. This was agreed with PWA asset affairs, to streamline the process and reduce and risk of delay.

4 RECOMMENDATIONS

The following is recommended to avoid delays in the handing over process:

1) To identify project end-users and list their requirements including the detailed procedures on the list of handing over documents. This will vary from each end-user.
2) To have a contract handing over program binding with the all the end users. This should also dictate the approval durations and approval cycles.
3) To implement and adopt BIM for the handing over. This will simplify the process of documentation and have proper control on the handing over of RFIs, As-built drawings documentation.
4) The paper work of the handing over should be reduced. This is only possible if all the project end users will implement the BIM technology as a procedure in their system.

REFERENCES

Banaitiene & Banaitis (2012). *Risk management in construction projects*, INTECH.

Salman Azhar (2011). Building Information Modeling (BIM): Trends, benefits, risks, and challenges for the AEC industry. *Leadership Manage. Eng.*, *11*(3): 241-252.

Sean, P. Pellegrino (2018). Introduction to CII's advanced work packaging – An industry best practice. Long International, Inc.

Cite this article as: Al Nass K., Melilla L., Tolba M., "Project Management: Key Initiatives Case Study", *International Conference on Civil Infrastructure and Construction (CIC 2020)*, Doha, Qatar, 2-5 February 2020, DOI: https://doi.org/10.29117/cic.2020.0016

Energy Efficiency in Buildings and Excess Summer Mortality in the UK

Ali Mohamed Abdi
abdia7@uni.coventry.ac.uk
Coventry University, Faculty of Engineering, Environment & Computing, Coventry, Cv1 2jh, UK

Andrew Arewa
ab6887@coventry.ac.uk
Coventry University, Faculty of Engineering, Environment & Computing, Coventry, Cv1 2jh, UK

Mark Tyrer
ac5015@coventry.ac.uk
Coventry University, Faculty of Engineering, Environment & Computing, Coventry, Cv1 2jh, UK

Rex Asibuodu Ugulu
rexugulu@gmail.com
Federal University of Science and Technology (FUTO), School of Environmental Technology, Quantity Surveying Department, Nigeria

ABSTRACT

One of the main objective of the building design is to provide comfort and safety to occupants, particularly during adverse weather conditions. In most part of the world, people stay indoors during adverse weather conditions, thus increasing energy consumption. In UK, vulnerable people such as the elderly are highly affected with mortality rate during extreme weather conditions. The 2003 heatwave reached average of 38.5° C in the UK resulting in the death toll of 2,234. The 10 days period of extreme heat is thought to be the warmest about the last 500 years. Across Europe, the 2003 heatwave resulted in 20,000 deaths; in France alone, the number reached 15,000. Similarly, the 2018 summer heatwaves, reached 35.5°C contributing to 863 deaths. Yet, there is little research regarding impact of energy efficiency in building and deaths caused by excessive heatwaves in the UK. The study aims to investigate the impact of energy efficiency in buildings and excessive heatwave deaths among elderly people in the UK. Research question asked is; do energy efficiency programmes and policies contribute to excessive summer deaths in the UK? .The study adopted quantitative research method with participants drawn from low/average income households, in west midlands part of UK, between 2003/04 to 2017/18. Initial findings show that there is a significant relationship between energy efficiency adoption, government policies and excessive summer deaths.

Keywords: Buildings; Energy efficiency; Excess heatwaves; Thermal comfort

1 INTRODUCTION

Majority of people living in cold countries prefer summer weather to winter, however things become uncomfortable when summer temperatures exceed the average normal temperature. The UK has seen some of the hottest summers in recent years with the mean temperature of 17°C and maximum temperature of 38°C. The 2003 and 2018 heatwave led to almost 3000 excess deaths in UK and 80,000 across Europe (ONS, 2019; Taylor *et al*, 2018; Robine et al, 2008). A Prediction by Met Office states that heatwaves of similar

calibre will continue in succeeding years up to 2040s. Consequently, there is growing concern over the impact of these heatwaves especially on vulnerable groups such as the elderly and disabled people. Numerous researches conducted after the 2003 heatwaves found that deaths in care homes increased by 42%. Similarly, in Paris, 92% of deaths reported in 2003 were of the elderly who lived alone (Kovats et al, 2006). Yet, there is scarcity of research regarding extreme heatwaves and excessive summer deaths.

2 OVERHEATING IN BUILDINGS

Current building designs and regulations in UK focus more on retaining heat during winter compared to cooling in the summer period (Lomas & Porritt, 2017). Overheating is notably a major problem in most traditional houses and new houses with poor insulation. The Chartered Institution of Building Service Engineers (CIBSE 2019) defines overheating as "a situation when the local indoor thermal environment presents conditions in excess of those acceptable for human thermal comfort or those that may adversely affect human health". Overheating can have a direct impact on health, safety, comfort and productivity (Taylor et al, 2015). Consequently, the main people affected during extreme summer weather are the elderly people. They are less sensitive to ambient conditions, hence psychologically unable to regulate their body temperature during hot weather leading to morbidity (Astrom et al, 2011). Figure 1 illustrates number of deaths registered in England and Wales.

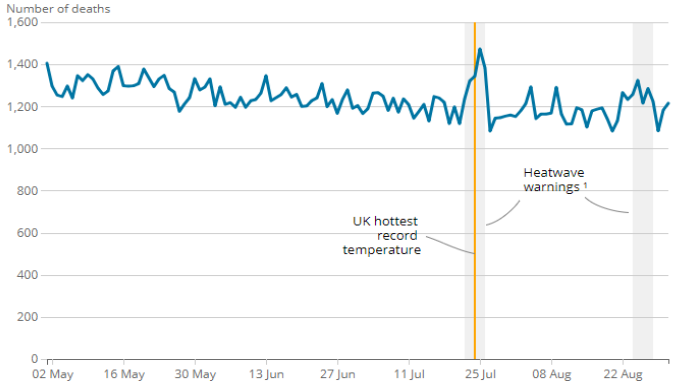

Source: Deaths registered weekly in England and Wales, Office for National Statistics

Figure 1: Summer deaths registered in England and Wales (ONS, 2019).

2.1 Energy Efficiency Policies in UK

Having in place a suitable energy efficiency policy across UK buildings is an important aspect especially when it comes to reducing greenhouse gas emissions, tackling fuel poverty, insulations and reducing energy bills. However, UK has a diverse building stock that requires different energy remedies. UK government statistics reveal that 15% of the existing buildings were built after 1990, meaning that most homes before this period were constructed with none or little information about insulation standards and energy performance (CCC, 2016). In UK, there are various stakeholders responsible for

safeguarding the public against heatwaves; Public Health England (PHE), Department of Health and Social Care (DHSC), Department of Food and Rural Affairs (DEFRA) and the Met Office (Howarth et al, 2019). The responsibility of preparing and publishing the heatwave plan for England is mainly conducted by PHE. Consequently, with the rising risk of unprecedented heatwave event in the future, the country has limited policies that ensure robust safeguards against overheating and adaptation in buildings (CCC, 2019).

3 DATA COLLECTION AND ANALYSIS

Data from the study were collected from the Office of National Statistics (ONS) and Met Office. The ONS data consist of the last five years' summer deaths and the Met office data was sought to determine the average temperature for the period. Months considered for summer temperature are May, June, July and August. Due to limitations, the study data were analysed quantitively using excel and SPSS version 25. The main statistical methods used are Pearson correlation analysis test and Regression analysis. The correlation test looked at the relationship between temperature and summer deaths in the UK. Thus, this produced a score of 0.74 (74%), meaning that there is significant relationship between high temperature in summer months and mortality. Figure 1 shows the relationship between temperature and deaths. Similarly, figure 3 illustrates last five years' summer deaths in UK. Thus, higher the temperature, the higher the number of deaths.

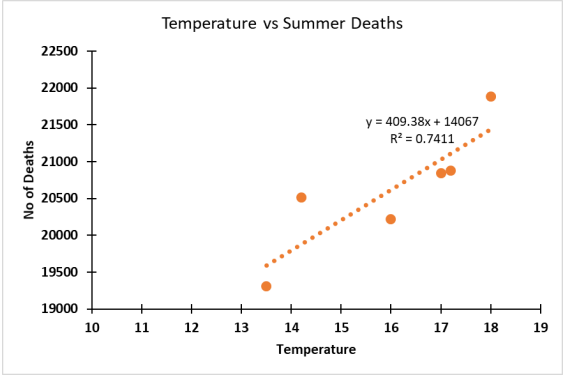

Figure 2: Relationship between Temperature and summer deaths in UK

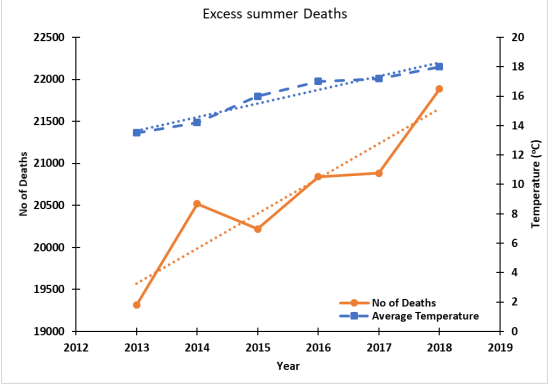

Figure 3: Excess summer deaths for the last five years (ONS, 2019)

4 FINDINGS, DISCUSSION AND CONCLUSION

The study findings and literature reveal that heat related fatalities will continue to increase as temperature rises in the UK particularly during the summer period. Most UK houses have poor insulation and therefore do not retain heat well. Consequently, there are no clear policies or regulations in the UK that aim to raise awareness on the impact of heat related deaths and climate change. Besides, UK building code is not explicit on the use of air-conditioners in residential buildings. Hence, there are fears that installing air-conditioners in residential buildings in the UK will ramp up electricity consumption. Current policies favour winter period where efforts are made to improve energy efficiency of housing stocks and reduction of average heat loss. Similarly, in UK, heat and welfare concerns continue to focus on heat retention rather than summertime comfort. With ever-changing climate and aging population, there is need for alternatives to cooling buildings during summer heatwaves. However, there is little empirical evidence to help identify the best solutions to excess summer heatwaves and deaths. Debates are currently ongoing regarding inventing energy efficient dual heating and cooling systems for buildings in the UK.

REFERENCES

Heat and Preventable Deaths in the Health and Social care System (2019). [pdf] London: Committee of Climate Change. Available at: https://www.theccc.org.uk/wp-content/uploads/2019/07/Outcomes-Heat-preventable-deaths-case-study.pdf [Accessed 25 Nov. 2019].

Hughes, C. & Natarajan, S. (2019). Summer thermal comfort and overheating in the elderly. *Building Services Engineering Research and Technology*, *40*(4), pp. 426-445.

Kovats, R. & Kristie, L. (2006). Heatwaves and public health in Europe. *European Journal of Public Health*, *16*(6), pp. 592-599.

Lomas, K. & Porritt, S. (2016). Overheating in buildings: lessons from research. *Building Research & Information*, *45*(1-2), pp. 1-18.

Ons.gov.uk. (2019). *Number of deaths in the summer period - Office for National Statistics*. [online] Available at: https://www.ons.gov.uk/peoplepopulationandcommunity/healthandsocialcare/causesofdeath/datasets/numberofdeathsinthesummerperiod [Accessed 17 Nov. 2019].

Taylor, J., Wilkinson, P., Davies, M., Armstrong, B., Chalabi, Z., Mavrogianni, A., Symonds, P., Oikonomou, E. & Bohnenstengel, S. (2015). Mapping the effects of urban heat island, housing, and age on excess heat-related mortality in London. *Urban Climate*, 14, pp. 517-528.

Cite this article as: Abdi A. M., Arewa A., Tyrer M., Ugulu R. A., "Energy Efficiency in Buildings and Excess Summer Mortality in the UK", *International Conference on Civil Infrastructure and Construction (CIC 2020)*, Doha, Qatar, 2-5 February 2020, DOI: https://doi.org/10.29117/cic.2020.0017

Project Risk Based Evaluation for Infrastructure Works in Qatar: Highway Projects

Nor Rozaini Abd Rahman
nabdrahman@ashghal.gov.qa
Public Works Authority (Ashghal), Doha, Qatar

ABSTRACT

The implementation of a project for infrastructure works such as highways, bridges, flyovers, underpasses, tunnels, etc. can be complexed and unique. This has always required a proper project management system that includes the conception and initiation, planning, execution, performance/monitoring and close-out phases. The construction risks identification and mitigation processes are critical and essential at the beginning of the project phase i.e. planning phase, in order to deal with the risks and avert them as to minimize effects to the work progress. The construction risks include additional works that could contribute to the project cost overrun and delay the works progress, any political uncertainty including a blockade imposed by a group of countries towards a particular country, and a possibility of introduction of new taxation by the government i.e. Value Added Tax (VAT) which could definitely affect the material, labor, service and machinery prices. This research paper identifies the construction risks which have affected the implementation of certain ongoing and completed infrastructure works undertaken by the Public Works Authority (PWA or ASHGHAL) in Qatar in recent years. The research included and focused on the importance of project evaluation formalization through identification of obstacles and challenges associated with project risks. There could be a possibility that the identified projects were not fully assessing the significant risk factors during the feasibility studies. Based on a literature review, questionnaires, structured interviews, unstructured interviews, and detailed case studies, it has been established that the most critical construction risks were the design changes, additional works, land acquisition, new requirements, contractors' non-performance, and interfacing works. Most of the experts indicated that the design changes could be reduced by defining and establishing detailed scope of works and specifications during the design stage. An early project coordination with the key stakeholders should be implemented to ensure that the detail information, requirements and any future interfacing works are assessed and updated for potential clashes and resolutions.

Keywords: Construction risk; Project evaluation; Infrastructure works; Highway projects; Qatar

1 INTRODUCTION

Highway projects are much more than asphalt, concrete, structure or steel works. They are considered as a backbone of the country economy and development apart from providing better transportation links to the people and end users. Efficient highway networks will enable smooth transportation for the people, goods and services to commute inter and intra states, cities, commercial areas, economic zones, ports and airports. A high

quality highway network system has always been one of the prerequisites for a country to organize any large international events including world sporting championships or tournaments. Qatar is preparing to organize the Federation Internationale de Football Association or International Federation of Association Football (FIFA) World Cup in the year of 2022. ASHGHAL has been mandated to undertake the responsibilities of implementation and completion of the highway projects including the North, South and Orbital expressway programmes with a value of more than USD 8 billion.

2 RESEARCH OBJECTIVE

This research began with the objective of identifying the construction risks in highway projects based on the completed and on-going projects. After analyzing the detail case studies, reviewing the literature and conducting interview with the experts (mostly the highway project engineers and managers), the followings objectives were highlighted:

i. To identify the most critical and extreme construction risk which need to be addressed on priority basis.
ii. To define the mitigation risks in the early stage of the construction works.
iii. To establish the project evaluation process model to be practiced in highway projects in Qatar.

3 RESEARCH METHODOLOGY

3.1 Questionnaires

The data obtained from the literature review and case studies had provided a basis for designing the questionnaires, which were distributed into fifty (50) experts i.e. focusing on the Civil Engineers, Quantity Surveyors and Contract Specialists from PWA. The questionnaires have also been forwarded to PWA' Project Management Consultants (PMC) staff. Out of Fifty (50) experts who were approached directly by the researcher either by-hand or by electronic mail, only 31 responses were received, giving a success rate of 62 per cent.

3.2 Structured Interviews and Unstructured Interviews

Structured Interviews participants were selected and conducted only with the experts who were involved directly in the implementation of highways projects. Some of the questions from the same questionnaires were used to explore more on the construction risk and mitigation plans being implemented in their projects. Therefore, twelve (12) interview sessions involving the middle to upper management personnel from PWA, and PWA's PMC were carried out within the months of October and November 2019.

A second group of unstructured interviews were organized in order to elaborate on certain issues, other than the construction risks, especially related to the blockade, which was considered as a new project risk, and also the probability of imposition of a new taxation i.e. the Value Added Tax (VAT). These would extensively need some mechanisms and methodologies to avoid any potential additional claim from the contractors to PWA in the current scenarios and future contracts.

3.3 Detailed Case Studies

Four mega highways projects were studied and analyzed to determine the construction

risks involved and affected the project implementation related to cost overrun and delays to contracts.

4 FINDINGS

4.1 Case Studies of Four Highway Projects

Project A involved with reconstruction and upgrading the existing highway including interchanges that consisted of tunnels, underpasses, flyovers, junctions and two marine bridges. This project also involved the construction of the Light Rail Transit (LRT), tunnel extension and massive utilities diversion works. Project B's contract associated with upgrading of the existing road related to construction of bridges, tunnels, sub-stations, interchanges, utilities and interfacing works with Qatar Rail.

Project C involved with design, construct and complete the North Road enhancements including to carry out the waterline and Treatment Sewerage Effluent (TSE) works. The scope of works for Project D associated with the construction and upgrading the existing road which included the construction of bridges, underpasses, tunnels, junctions, existing utilities and landscaping works.

Table 1: Risk Assessment of Four (4) case studies for Highway Projects

Descriptions of Construction Risks	Probability Score	Cost Impact & Time Impact (Prolongation Cost)				Level of Risk
		Project A Cost Increase	Project B Cost Increase	Project C Cost Increase	Project D Cost Increase	
Design Changes	4	300-500 mil	20-100 mil	5-20 mil	5-20 mil	Extreme
New Requirements	4	50-100 mil	50-100 mil	5-20 mil	5-20 mil	Extreme
Land Acquisition	4	50-100 mil	5-20 mil	5-20 mil	20-100 mil	Extreme
Interfacing Works	4	50-100 mil	5-20 mil	5-20 mil	5-20 mil	Extreme
Additional Scope of Works	4	100-500 mil	100-500 mil	100-500mil	100-500 mil	Extreme
Non-Performance of the Contractors	3	20-50 mil	5-20 mil	0-10 mil	20-50 mil	High
Availability of Materials, Labors and Machineries	2	5-20 mil	5-20 mil	5-20 mil	5-20 mil	Medium
Physical Geography and Soil Conditions	2	5-20 mil	5-20 mil	5-20 mil	5-20 mil	Medium
Blockade from Neighboring Countries	2	5-20 mil	5-20 mil	5-20 mil	5-20 mil	Medium
Fluctuation of Labor & Materials Price	1	0-10 mil	0-10 mil	0-10 mil	0-10 mil	Low

The researcher has developed the risk assessment as stated in Table 1. This was to identify the level of project risk affected the projects by approaching the most popular method of risk management i.e. the "Risk Matrix" model which adopted the probability/ likelihood of occurrence and the impact/consequences. The risk assessment had been adjusted to suit the information such as the increased of cost considered as an impact to the projects. Furthermore, this method was using both the qualitative variables and quantitative variables. The probability (Score) of occurrence was derived from the opinion, judgement and professional experiences of the experts, questionnaire's result, Variation Order (VO) tracker and the monthly progress report to determine the level of uncertainty and risk associated with the projects. Whereas, to ensure the accuracy

of the cost impact (Cost increase), the information was obtained from the VO detail submission, VO tracker and based on the researcher's observation and evaluation for having five (5) years of working experiences directly involved with contractors' VOs and consultants' addendum for the PWA's highway projects. The result from Table 1 shown that the "Design Changes", "New Requirement' "Land Acquisition", "Interfacing Works' and "Additional Scope of Works are considered the extreme risks.

4.2 The Ranking of Severity Impact of the Construction Risks for Highway Projects

A questionnaire containing a question of severity impact of the construction risks to the implementation of highways projects in Qatar, which includes the respondents' opinion on the risk consequences for construction project performance measures. The result is established based on the construction risks as listed in Table 2; the author developed a method by multiplying the number of respondents to the score number. Based on this approach hierarchical ranking of construction risks in Table 2 shown that the "Design Changes" as the most severe construction risk, followed by the "New Requirements", "Land Acquisition", Non Performance of Contractors" and "Interfacing Works" which were tremendously impacting the cost overrun and caused the delay for the completion of highway projects in Qatar.

Table 2: Severity Impact of the Construction Risk for highway projects in Qatar

No	Descriptions of Construction Risks	Extreme score 4	High score 3	Medium Score 2	Low score 1	Total score	Ranking
1	Design Changes	14	15	2	0	105	1
2	New Requirements	7	18	6	0	94	2
3	Land Acquisition	14	7	6	4	93	3
4	Interfacing Works	4	17	10	0	87	5
5	Additional Scope of Works	4	17	9	1	86	6
6	Non Performance of the Contractors	6	15	9	1	88	4
7	Availability of Materials, Labors & Machineries	3	15	11	2	81	7
8	Physical Geography and Soil Conditions	3	5	15	8	65	9
9	Blockade from Neighboring Countries	3	10	13	5	73	8
10	Fluctuation of Labor & Materials Price	3	1	18	9	60	10

4.3 Construction Risks Identifications and Mitigations Based on Project Stages

The second survey includes the respondents' opinion the possibility of construction risks if they could be identified and mitigated at the early stage to avoid any disruption and obstacles during the construction works. Based on the questionnaires' result as shown in Figure 1, twenty five (25) respondents or 81% clarified that "Land acquisition" matters would need to be justified and resolved during the "feasibility study" stage. Some Twenty three (23) respondents or 74% defined that the risk for "Design Changes" could be identified and mitigated during the design stage. In addition, the majority of respondents agreed that the risks of "New Requirements" and "Interfacing Works" would need to be identified and mitigated during the design stage.

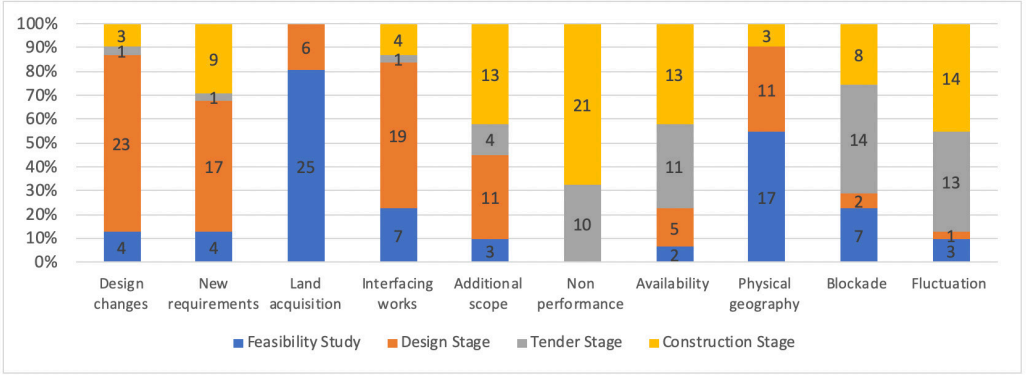

Figure 1: Effective methods of construction risks identifications and mitigations

5 PROJECT RISK IN HIGHWAY PROJECTS

5.1 Design Changes

Design deficiencies in the construction have led lead to major challenges and adverse consequences to the work progress. It was time consuming to correct the design errors, ambiguities and clashes with other existing utilities or structures before any resolutions can be made to replace any part of the design by revising and issuing the new Issued For Construction (IFC) drawings by the design consultant. Despite the revised IFC drawings due to the LRT realignment, this project had also experienced the revised design drawings due to the massive traffic diversions, revised street lighting works, redesign of storm water network, and upgrade of the designed drainage network. Due to the unclear scope of works, specifications were not detailed and new requirements were later received from either from PWA or other stakeholders. According to Oberlander (2000), the lump sum contracts' changes during the construction stage are a major source of cost overrun. For this type of project, it is necessary to ensure a complete design is fully issued to the contractor to keep any changes, thus consequences to the owner, to a minimum as possible during the construction stage.

5.2 Land Acquisition

Land Acquisition issue has caused the disruption to the project program when inability to purchase, own or possess the land would lead to the design changes. For example, a road would need to be diverted or perhaps, to build an underpass or bridge which would affect the project deliverables and cost overrun. Based on the case studies, Project D had been granted a one year of EoT due to the land acquisition issues.

5.3 New Requirements

New requirements were either the implementation of instructions or regulations received from either PWA or other key stakeholders. For example, PWA had instructed the contractors to change the asphalt paving works with Polymer Modified Bitumen (PMB). This issue that was raised by PMC on 21st February 2016 defined that "the contractor is instructed to replace the asphalt concrete wearing course and immediate/ binder course of the main carriageway and branch roads including structure slab portion

with PMB." Another new regulation from a key utility service provider was on the imposed additional requirements on the 66 kV and 132 kV electrical cabling works for Project A which had increased the cost to about USD2.7 million.

5.4 Non Performance of Contractors

The contractor's organization's capabilities especially on financial resources, experiences, competencies, technologies, leaderships and decision makings are vital and essential factors to perform excellently throughout its contract duration to deliver the completed project within the budget and time frame. Referring to the Monthly Project Report for project A, in January 2019, it listed the top critical risk being that the "delay to project delivery due to poor contractor's performance", and stated that, "As the current contract completion date is expired, cumulative program schedule is supposed to be 100%, however, the actual cumulative work progress is around 96%. Delays are observed from four (4) stations and commissioning of utilities, and to make it worst, the sub-contractors in this project were not performing to the expectation.

5.5 Interfacing Works

Integration and interface between other key stakeholders including the Ministry of Municipality and Environment (MME), Ministry of Municipal & Urban Planning (MMUP), Ministry of Transportation and Communication (MoTC), General Electricity and Water Cooperation (GEWC or KAHRAMAA), Qatar Armed Forces, Amiri Guard, Qatar National Broadband Network (QNBN), Ooredoo, Vodafone, Qatar Civil Defense Department (QCDD), Qatar Petroleum, etc. involved utilizing existing utilities, approval processes and new requirements, whichever is applicable. Late approval processes and request for information from stakeholders that include request for as-built drawings, building and road permitting issues, land acquisition and property interfacing matters have contributed to the major delays to the projects.

Based on Monthly Projects Report in September 2018 indicated that the issues concerned for Project C when as-built documents submission was not progressed as per plan due to design issues, uncompleted works and insufficient resources. Zou, Zhang and Wang (2007) stated that "incomplete approval and other documents usually occurs due to management weakness of the project routines or the bureaucracy of government. Clients need to establish a competent team to obtain the approval from government agencies and prepare project documents effectively and efficiently."

5.6 Additional Scope of Works

According to this research, the additional scope of works occurred due to PWA and stakeholders' requirements and additional new scope of works. Based on the Monthly Project Report in September 2018 for Project B, the contractor had been instructed to carry out entrusted works for one of the stakeholders i.e. Qatar Rail, as a variation to the contract. The contractor had been informed that the Site Instruction (SI) for design work had already been issued however; the SI for construction work has yet to be issued by the client to date. According to Atkinson et al. (1997), Takim and Akintoye (2002) successful construction project performance is achieved, when stakeholders meet their requirements, individually and collectively. However, according to Nguyen et al.

(2013), de Wit, (1988) stated that measuring success is complex because it depends on the stakeholders' point of view and it is time dependent. One party may acknowledge project as successful, but another may take the opposite view.

5.7 Availability of Materials, Labors and Machineries

Analysis of the case study of Project A which Monthly Project Report in September 2018, reported that one of the critical risk identified was "availability of construction material especially bitumen." Oberlander (2000) stated that the unsuccessful procurement of material is a common source of delays during construction. A procurement plan must be included in the project schedule to guide the purchase of contractor furnished material.

5.8 Blockade

The sudden political blockade that happened in June 2017 had led to a disruption of work progress to many projects. Purchase Orders (POs) for certain required materials to the suppliers and vendors at those involved countries had to be cancelled and replaced with alternative products from other countries worldwide. For example, vitrified clay (VC) pipes had been replaced with the glass reinforced pipes (GRP) and accessories. The contractors and their new suppliers had successfully arranged the transportation of the alternative products using the diverted routes via sea vessels and airfreights within a few months after the blockade. However, the majority of respondents had agreed that the unexpected blockade could be considered as a moderate project risk.

5.9 Value Added Tax (VAT)

Based on the unstructured interviews with the Contract Specialists of PWA, they had highlighted that lately, the query on VAT has been the most favorite question from the tenderers in their tender submissions. Therefore, the mechanisms and strategies to ensure this issue shall properly be managed if the VAT will ever be enforced are that the proper clauses need to be specified in the general Conditions of Contract (CoC). This pre-empt will minimize, if not eliminate, any additional cost to be incurred to PWA.

6 PROPOSE MODEL OF THE PROJECT EVALUATION PROCESS

Based on the international entry process model by Abd Rahman et al. (2009), the researcher modified and developed the process model to suit this research. The proposed process model of "the highway projects strategic decision process model" as shown in Figure 2 below as a decision guideline for any highway projects implementation. The first stage during the feasibility study is to identify, analyze and resolute for critical issues that related, but not limited to, land acquisition matters, permitting requirements, stakeholders' identification, and potential barriers, bottlenecks or challenges to the projects. If the outcomes are positive, the project will proceed into the next stage i.e. design stage. Design stage is the phase to ensure that the designs, specifications and scope of works are detailed and clearly defined, established and completed before pursuing into the tender stage. The key stakeholders', service providers' requirements, existing utilities, as-built drawings and all other details shall need to be incorporated in the design drawings.

Documentation process during the tender stage including the compilation of the

Bill of Quantities (BoQs), drawings, specifications and all the issues such as embargo, VAT, price fluctuations, as-built drawing with specific version programs shall need to be specified in Condition of Contract (CoC) which shall become a part of the Contract Documents. The selection process of the tenderers/contractors will be carried out based on technical and commercial evaluation. Once the contractor is awarded, the construction stage will start immediately.

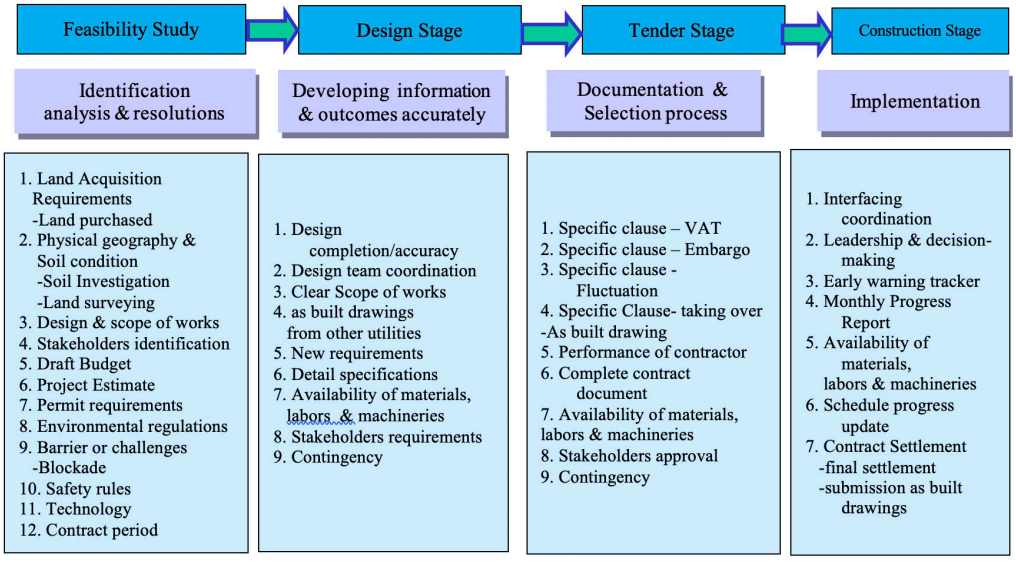

Figure 2: Strategic Decision Process Model for Highway Projects

During construction stage, schedule progress of woks is essential to monitor and control, need to be updated based on actual progress at the site which reflecting labors, materials and machineries resources required. According to Memon, et al. (2006) stated that "project progress monitoring and control is one of the most important tasks of construction project management. Every team member needs to know, in a timely and accurate manner, how is the project progressing, where they are currently in comparison to the initially set plans, whether deadlines are met, budgets are safely measured and followed".

7 CONCLUSION

Construction risks can be controlled and managed efficiently if they are identified, registered and mitigated as early as possible in the project stages. During the feasibility study and design stages, construction risks particularly project requirements and dealing with uncertainty and unpredictable events related to land acquisition matters, coordination with stakeholders, physical geography and availability of materials, labours and machineries are efficiently managed and controlled in order to achieve project success. PWA, PMC, consultants and contractors are recommended to culturally adopt the risk management for every project either minor or mega projects, and risk transfer by shifting to the right contract's strategy especially "Design and Build" type of procurement and ensure that the contractors shall have the right competent personnel to

carry out the works.

A project success is normally measured by the evaluation of time, cost and quality. However, a project can be delayed and over budget but still could be considered as a successful project due to the projects are completed with world class high quality, excellent in terms of safety record, and to the expectations and satisfactions of the PWA and stakeholders. One of the highway projects from the case studies in this paper had won the 6th annual Global Best Project ENR 2018 award by Engineering News-Record (ENR), a reputed engineering and construction industry magazine, in the Road/Highway category. Out of twenty (22) projects from fourteen (14) different countries, Global Best Projects had identified, recognised and honoured the project teams i.e. PWA , PMC, consultants and contractor staff behind their outstanding design and construction efforts in order to complete the most challenging highway projects in Qatar.

REFERENCES

Abd Rahman, N. R., Torrance, J. V. & Torrance, M. H. (2009). *Influential factors impacting international construction*. The Case of Malaysian Contractors, Joint Ventures in Construction, Kobayashi, K., Abdul Rashid, K., Ofori, G., Ogunlana, S., Thomas Telford, London, 90-100.

Memon, Z. A., Abd. Majid, M. Z. & Mustaffar, M. (2006). A systematic approach for monitoring and evaluating the construction project progress. Construction Technology and Management Center (CTMC), Faculty of Civil Engineering, Universiti Teknologi Malaysia, 81310 UTM Skudai, Johor. *Journal - The Institution of Engineers, Malaysia*, (Vol. 67, No. 3).

Nguyen, T. A., Chovichien, V. & Takano, S. (2013). Quantitative weighting for evaluation indexes of construction project success by application of structural equation modeling. *International Journal of Construction Engineering and Management*, *2*(3): 70-84.

Oberlender, G. D. (2000). *Project management for engineering and construction*, Thomas Casson, the USA.

Takim, R. & Akintoye, A. (2002). Performance indicator for successful construction project performance. *18th Annual ARCOM Conference*, 2-4 September 2002, University of Northumbria. Association of Researcher in Construction Management, Vol. 2.545-555.

Zou, P. X. W., Zhang, G. & Wang, J. Y. (2007). Identifying key risk in construction projects: Life cycle and stakeholder perspectives. *Journal of Project Management*, 25 601-614.

Cite this article as: Abd Rahman N. R., "Project Risk Based Evaluation for Infrastructure Works in Qatar: Highway Projects", *International Conference on Civil Infrastructure and Construction (CIC 2020)*, Doha, Qatar, 2-5 February 2020, DOI: https://doi.org/10.29117/cic.2020.0018

Key Lessons Learnt from Stakeholder Management in Design and Build Projects in Qatar

Larno Meyer
lmeyer@ashghal.gov.qa
Highway Projects Department, Public Works Authority, Doha, Qatar

Ali Kara
akara@ashghal.gov.qa
Highway Projects Department, Public Works Authority, Doha, Qatar

ABSTRACT

Stakeholders in the construction industry require accurate, reliable and timely information in order to streamline the design and construction of Projects. Design Bid Build or Design and Build contracts need a process for seeking the latest requirements, interests and existing assets of all the stakeholders involved. This to lead and guide the projects to deliver in a timely, cost-effective and safe manner. This paper summarizes the multi-discipline Stakeholder management challenges and their proactive approach during the execution of the Expressway Programme by Public Works Authority, Qatar illustrated by a case study and actual actions from the industry. Various internal surveys have been undertaken to assess the issues to be resolved. Key to managing the time and cost impacts on the construction projects are identifying the needs of stakeholders, stakeholder communication procedures, their requirements, identification of existing assets, expected future requirements and decisions among the stakeholder. Unique and innovation construction procedures are highlighted in order to overcome construction challenges.

Keywords: Stakeholders management; Stakeholder communication; Qatar expressway programme

1 INTRODUCTION

Qatar Public Works Authority's (Ashghal) Highway Projects Department set out to deliver over 45 major Expressway Road Projects to be completed before the FIFA World Cup in 2022. These projects accounts for over 800 km of new major road network improvements (together with the road improvement works also for the local road projects). These projects were needed to help resolve the traffic congestion due to the increase in population and economic growth of Qatar.

To be able to deliver this large number of major projects in the Expressway Programme within Ashghal various stakeholders had to be consulted to understand their requirements and inputs to each project and to obtain their approvals to proceed into construction. These stakeholders involve both the internal and external groups of people from various departments, ministries, utility authorities and private entities.

2 UNDERSTANDING THE MULTI-DISCIPLINE STAKEHOLDER APPROVAL CHALLENGES

Due to the large number of major projects and stakeholders that must be managed simultaneously, it led to various multi-discipline stakeholder approval challenges across the projects' design and construction interfaces. This formed part of the initial key lessons learnt. The Project Teams should fully understand how the multi-discipline engineering interfaces influence each other during the design development. Each project has Traffic, Roads, Utility and Structure Engineering Teams working along with their Project Management and Project Controls Teams. Projects all have multiple interfaces that need to collaborate effectively during design and construction.

These multi-discipline interfaces include for example, the work on the initial traffic analysis needed to produce concept designs, the road geometry, all the different utility corridors (both new and existing), multiple large structures (bridges and tunnels), limiting land acquisition and environmental impacts, improving road safety, integration with public transport modes, ensuring proper risk management and controlling the overall cost and schedule. Various engineering disciplines therefore needed to work together to complete projects on time and on budget. Each of these engineering disciplines required various stakeholder approvals. It was therefore necessary to identify all the stakeholders for each discipline's approval as early as possible in the Expressway Programme.

3 THE IMPORTANCE OF STAKEHOLDER IDENTIFICATION AND ANALYSIS

Stakeholders are those groups or individuals that can influence and impact a project. On the other hand, they can be affected by a project. Stakeholders can have a positive or negative influence on a project [PMI]. It is therefore important to identify all stakeholders for each project as early as possible and to start engaging with each stakeholder.

Another key lesson was to understand the full scope and scale of all stakeholders involved with Ashghal's projects. For each of Ashghal's projects there can be more 10 internal stakeholders (Departments and Sections) and more than 30 external stakeholders (Ministries, Utility Authorities, Private Entities and their different internal departments). It requires full collaboration with each stakeholder during the duration of the projects from design stage to construction.

After identifying the specific stakeholders, Stakeholder Analysis (Schmeer, 1999) is also required to identify the different types of stakeholders involved and how each stakeholder may influence or impact a project. Some stakeholders have higher levels of power and influence which can approve or oppose decisions on a project. Other stakeholders can help provide expert opinions, inputs and support even if they do not have direct interest in a project's delivery. There are also stakeholders that need to know the progress of work as it can influence their own activities and work to be completed. It is therefore necessary to make use of stakeholder analysis techniques to help understand how to engage and communicate to each stakeholder.

3.1 Stakeholder Analysis Techniques

There are several Stakeholder Analysis Techniques that can be used to understand the interest and influence of each Stakeholder and how to manage each of these stakeholders.

These analysis techniques are also visual mapping tools to help guide the Project Teams on who to focus on as key stakeholders. The Stakeholder Analysis Techniques can include for example:

- 2x2 Grid Analysis (Power / Influence vs. Interest or Influence vs. Impact, Figure 1, (Mendelow, 1981).
- Salience stakeholder analysis (Venn Diagram) (Mitchell, Agle, B. & Wood, D., 1997).
- Stakeholder Circles to reflect the influence of stakeholders on a project (Bourne, Walker, DHT, 2005).

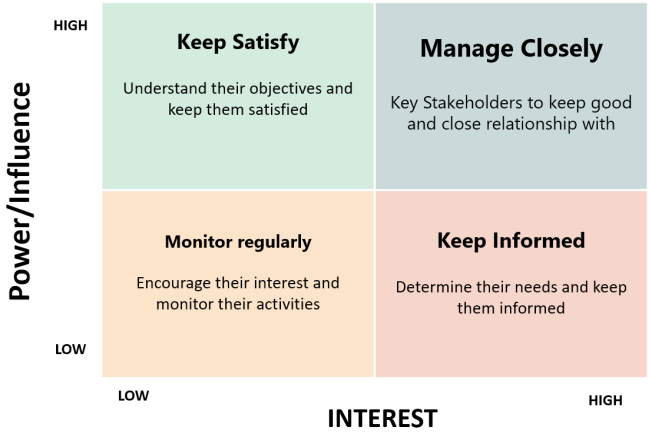

Figure 1: 2x2 Analysis Grid (Power/Influence vs. Interest) (Mendelow, 1981)

4 STAKEHOLDER ENGAGEMENT AND COMMUNICATION MANAGEMENT

4.1 Stakeholder Communication Plans and Procedures

As part of the PMI Project Management Process Groups and Knowledge Area, is the important requirement of Stakeholder Management and Engagement (PMI, Chapter-1, 2017). This also includes Planning the Communication Management (PMI, Chapter-10, 2017) and the specific procedures to follow for each stakeholder identified. The following questions can be asked to obtain an initial understanding of what should be considered in the Stakeholder Engagement and Communication Planning:

- Who are the key stakeholder decision makers to engage and communicate to for approvals?
- What are these stakeholders' requirements and procedures to follow to obtain their inputs and approvals?
- How often to report and follow up with each stakeholder (weekly, bi-weekly or monthly)?

4.2 Implementing Memorandums of Understanding (MoUs)

Various Memorandums of Understanding (MoUs) were implemented between

Ashghal and external authorities to improve the approval processes. These MoUs sets out the agreed principles, accepted expectations and requirements that Ashghal and each Authority will follow. It helped to ensure better collaboration and understanding between all involved using a less formal contractual agreement process. It also helped to define the needs and actions for each stakeholder. These MoUs have been setup following various workshops and discussion. This to obtain the inputs needed to formulate each Memorandum of Understanding.

5 UNDERSTANDING THE COMPLEXITY IN STAKEHOLDER COMMUNICATION

Complexity in project communication results when there are multi-discipline interfaces across multiple stakeholders simultaneously. This while also dealing with changing deliverables to be delivered with available resources. As projects are fast moving and requirement changes are many times undefined, ambiguity and miscommunication or misinterpretation can also result. This increases the complexity of delivering projects in time and on budget.

5.1 Equation to calculate the number of communication channels between stakeholders

In Project Management there is an equation (PMI, Chapter-10, 2013) that defines the number of communication channels (links) between all individuals or groups of people. This equation can help to indicate the complexity of a project, as it reflects on the number of communication channels involved. As the number of communication channels increase, the more complex a project will become. This includes stakeholder communication. Also, more communication channels can result in miscommunication or misinterpretation which can cause delays in project approvals. The following is the equation that can show the number of Communication Channels involved.

Number of Communication Channels (links) = $N(N-1)/2$ (1)

N = number of individuals or groups

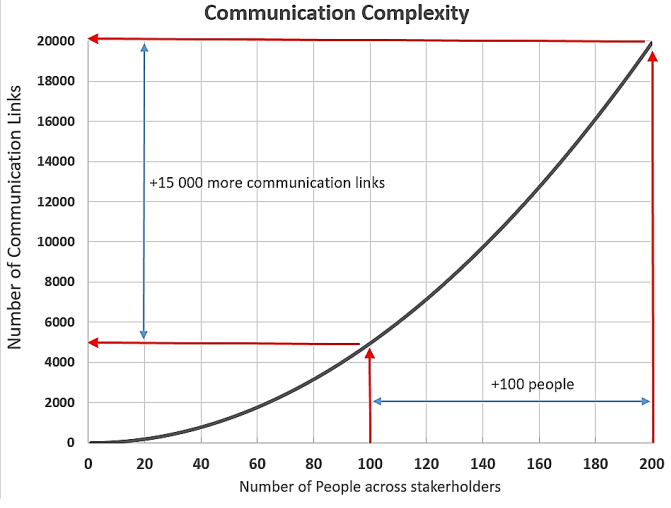

Figure 2: Graph showing the Number of communication channels between stakeholders

The graph in Figure 2, shows that if 100 people are involved across the various stakeholders, then there will be close to 5 000 communication channels (links) created between all the people. Should this number of people double, then the number of communication channels will increase from 5 000 to 20 000 (400%). Therefore, it is important to understand that if more people are involved the complexity in communication will increase. This can contribute to delaying approval processes if not managed well.

5.2 The importance of reducing the number of communication channels between multiple Stakeholders

It is very important to identify the key communication contacts within each stakeholder. This to limit the number of people to communicated to. Channels of communication should be setup through each key communication contact in each stakeholder. This will reduce the number of direct communication links and simplify the complexity of communication across each project.

For example, instead of having to deal directly with more than 100 individual contacts across the different stakeholders, one should aim to focus only of the key decision makers who can report back to their teams. By reducing the number of people to communicate to, the complexity can be reduced. This is return can also help to reduce miscommunication and ambiguity or misunderstandings which can delay approvals.

5.3 The importance of Cultural Awareness and Cross-Cultural Communication Styles

Another key lesson learnt in working in a multi-cultural environment with people coming from across the world, is the complexity in how people communicate and relate to each other. The PMI PMBOK 6th Edition (2017) provides a good summary and states the following: "*Cultural awareness is an understanding of the differences between individuals, groups, and organizations and adapting the project's communication strategy in the context of these differences. This awareness and any consequent actions minimize misunderstandings and miscommunication that may result from cultural differences within the project's stakeholder community. Cultural awareness and cultural sensitivity help the project manager to plan communications based on the cultural differences and requirements of stakeholders and team members*."

6 INNOVATIVE DIGITAL SYSTEMS FOR STAKEHOLDER ENGAGEMENT AND COMMUNICATION DURING THE REVIEW AND APPROVAL PROCESSES

6.1 QDES / QDRS – Stakeholder review and approval system for design

Ashghal's Online Qatar Design Enquiry System (QDES) or also refer to as Qatar Design Review System (QDRS) have been implemented to enhance stakeholder engagement and communication during the approval process. These systems helped to improve sharing information and speed up the coordination between stakeholders.

It provides more transparency of work activities done by various stakeholders across Qatar and helps to identify potential clashes and overlaps. It also provides a paperless web base submission platform that helped to reduce the overall time. The system provides

a time line to follow, which helped to expedite the review process that took longer in the past. Should the time line not being followed, the application is automatically cancelled by system.

6.2 QPro – Road Opening Permits, Approval to work in Right of Way (ROW)

Similar to Ashghal's QDES/QDRS systems, the QPRO system has been created to process Road Opening and Occupancy permit approvals. This applies for all Stakeholders. It is a mandatory process and also applies to the construction phase.

If for example, a Utility Authority wants to implement a new pipe or cable within the Right of Way, they need to obtain from Ashghal a Road Opening Permit approval to do the work within Right of Way (ROW). This process helps to control the work done by the different stakeholders within their respective ROW corridors.

QPRO is dependent on QDES/QDRS system and forms part of the approval process. It is mandatory for all stakeholders to apply for a Road Opening Permit on the QPRO system by using a unique Design Review number for any work associated with excavation.

6.3 IBM BlueWorks – Work flow and Process guidelines

IBM's BlueWorks is a business process-modeling tool that is based on a Flow Chart driven web portal. This tool provides access to all Ashghal's processes and procedures with the related documentation and reference to the internal stakeholders (Departments, Sections) involved. It provides a quick visual step by step process of decision points and approvals needed with the related forms and documents involved.

7 HIGHWAY PROJECT DEPARTMENT CASE STUDY AND LESSONS LEARNT

The following is a case study for the Highway Project Department (HPD). The diagram below Figure 3 indicates the main internal and external stakeholder interfaces and interactions in relation to HPD. This reflects on all approval processed from Concept Design Stage to Preliminary and Detail Design approvals and then the Tendering and Construction Stages.

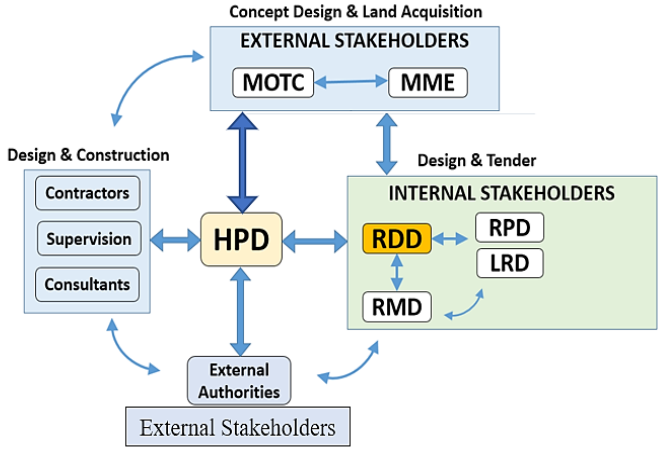

Figure 3: Highway Projects Department (HPD) Case Study

Where:
MoTC – Ministry of Transportation & Communication.
MME - Ministry of Municipalities & Environment.
RDD – Road Design Department.
RPD - Road Projects Department (Local Roads).
LRD – Local Roads & Drainage Department.
RMD – Road Maintenance Department.
External Stakeholders include for example: Kahramaa, MoI, PEO, QP, QRail & Ooredoo.

During the duration of a HPD project, which involves all of these multiple interfaces and interactions with internal and external stakeholder, it became clear that the following issues had to be resolved as part of improving the stakeholder engagement and communication processes:

- Internal and External Stakeholder communication issues between departments/ Sections (misinterpretation / miscommunication issues).
- Missing, unclear or changing standards, requirements and guidelines not fully and officially communicated to all involved and in a timely matter.

An example of where good stakeholder coordination benefited the community and improved safety, is along the new Sabah Al Ahmad Road Corridor between Salwa and Al Waab Roads. To ensure the safety of schoolchildren during the ongoing construction and temporary traffic management, an additional school bus service has been added. This avoided children to cross the Construction Work Zone area and the temporary traffic road diversions.

Also for the Temporary Traffic Management, coordination with MoI Traffic Police made it possible to decide on the most effective way to accommodate the traffic flows during construction in a very restricted urban area.

Other example includes the Memorandum of Understanding (MoU) with Qatar Electricity and Water Co. MoU helped to improve the approval processes for water and electrical utility corridors and electrical substations. Ashghal HPD also holds regular high-level stakeholder coordination meetings where major issues on projects are discussed to obtain high-level approval.

8 CONCLUSION

From the above it is concluded that stakeholder management is vital to the success of any project and even more when there are multiple major projects placed in design and construction at the same time. A large number of people from a diverse background will be involved across both the internal and external stakeholders. Should a multi-discipline project team fail to understand the various interfaces involved across a project (which requires full collaboration with multiple stakeholders), then long costly delays may result.

Project Teams should identify all stakeholders and their influence and interest to a project. In addition, each stakeholder's most current requirements for approval should be checked as early as possible. The project teams should ensure proper stakeholder

communication plans are setup. Moreover, the number of key stakeholder contacts should be limited to avoid introducing unnecessary communication complexity, which can lead to miscommunication and delays in approvals. In addition, the use of information technology and the development of it, help to improve better stakeholder engagement and communication. Successful stakeholder engagement and management will result in the safe, cost and time effective delivery of projects.

REFERENCES

Bourne, L. & Walker, D. H. T. (2005) Visualizing and mapping stakeholder influence. *Management Decision*, *43*(5), 649660.

IBM BlueWorks Business Process Modeling, https://www.ibm.com/products/blueworkslive.

Mitchell, R., Agle, B. & Wood, D. (1997). Toward a Theory of Stakeholder Identification and Salience: Defining the principle of Who and What really counts. *The Academy of Management Review*, *22*(4), pp. 853-886.

Mendelow, A. L. (1981). Environmental Scanning - The Impact of the Stakeholder Concept, *ICIS 1981 Proceedings*, Paper 20.

Project Management Institute, PMI (2013). A Guide to the Project Management Body of Knowledge (PMBOK Guide, 5th Ed), Chapter 10, 10.1.2.1, Newtown Square, Pennsylvania, USA.

Project Management Institute, PMI (2017). A Guide to the Project Management Body of Knowledge (PMBOK Guide, 6th Ed), Chapter 13, Newtown Square, Pennsylvania, USA.

Project Management Institute, PMI (2017). A Guide to the Project Management Body of Knowledge (PMBOK Guide, 6th Ed), Chapter 10, Newtown Square, Pennsylvania, the USA.

Project Management Institute, PMI (2017). A Guide to the Project Management Body of Knowledge (PMBOK Guide, 6th Ed), Chapter 10, 10.1.2.6 (Cultural Awareness), Newtown Square, Pennsylvania, USA.

Schmeer, K. (1999). Guidelines for conducting a stakeholder analysis.

Cite this article as: Meyer L., Kara A., "Key Lessons Learnt from Stakeholder Management in Design and Build Projects in Qatar", *International Conference on Civil Infrastructure and Construction (CIC 2020)*, Doha, Qatar, 2-5 February 2020, DOI: https://doi.org/10.29117/cic.2020.0019

Unique Structural Design and Construction Challenges for Al Bustan South Project in Qatar

Anshuman Ganguli
Anshuman.Ganguli@parsons.com
Parsons International Limited, Tampa, Florida, USA

Ali Kara
akara@ashghal.gov.qa
Highway Projects Department, Public Works Authority, Doha, Qatar

ABSTRACT

The Al Bustan Street South (ABS) Expressway Project features the longest dual carriageway bridges in Qatar spanning 2.6 km each, with a minimum of four lanes in each direction from south of Al Waab Street to south of Rayyan Road. These twin mainline bridges carry the ABS Expressway forming a three-level interchange at Al Waab Street and two-level crossings at Al Rasheeda Street and Snay Bu Hasa. The Al Waab Interchange consists of multiple structures; namely, the mainline bridges at Level +1, the West-South directional ramp at Level +2, and the East-North directional ramp at Level +2. In addition, there are six other on/off ramp structures that tie into the mainline bridges at various locations. While the current construction maintains Al Waab Street at Level 0, in its ultimate configuration, Al Waab Street will contain an underpass at Level -1, resulting in Level +4 interchange. This underpass due to its proximity to the bridge supports requires unique design considering future constructability. The ABS Expressway is part of the prestigious Sabah Al Ahmad Corridor which once constructed will provide a separate north to south route from the Landmark Mall to Hamad International Airport. The appearance of the bridges along the Sabah Al Ahmad Corridor will contain aesthetically pleasing cladding attached to the parapets with artificial green walls running down select piers and MSE Walls. This paper summarizes recent developments in the design and build for the future underpass, which requires special attention in the bridge design while also considering aesthetic features.

Keywords: Design and build; Al Bustan South; Structural design; Construction challenges

1 INTRODUCTION

The Design and Construction of the "Al Bustan Street South (ABS) Expressway Project - P007 C5 P1" commenced on September 2017 and comprised of the following key team members:

- Client: Public Works Authority (ASHGHAL)
- Authority's sub-representative: Parsons International Limited (PIL)
- Construction Contractor: Hyundai Engineering and Construction (HDEC)
- Designers: Parsons International Limited (PIL) & WSP

2 PROJECT DESCRIPTION

The scope of the ABS Expressway Project includes upgrading of ABS from an existing dual carriageway at-grade to dual carriageway at-grade and flyover, with a minimum of 4 lanes in each direction for approximately 3.1 km from south of Al Waab Street to south of Rayyan Road (Junction R6), including 2 to 3 lane service roads running parallel to the mainline bridge along both sides. The 2.6 km twin mainline bridges carry the ABS Expressway forming a three-level interchange at Al Waab Street and two-level crossings at Al Rasheeda Street and Snay Bu Hasa.

The ABS/Al Waab interchange consists of multiple structures; namely, the twin mainline bridges at Level +1, the East-North directional ramp (Ramp 5) at Level +2, and the West-South directional ramp (Ramp 6) at Level +2. The two ramp bridges combine for the total length of 1.5 km. In addition, there are six other on/off ramp structures that tie into the mainline bridges at various locations (Refer to Figure 1 for the Project Layout). While the current construction maintains Al Waab Street at Level 0, in its ultimate configuration, the ABS/Al Waab interchange will have an underpass along Al Waab Street, allowing the free-flow of traffic along Al Waab Street and converting the interchange to become a four-level interchange (Refer to Figure 2 for the Ultimate Design Layout and Figure 3 for Current Interim Construction).

Figure 1 Project Layout.

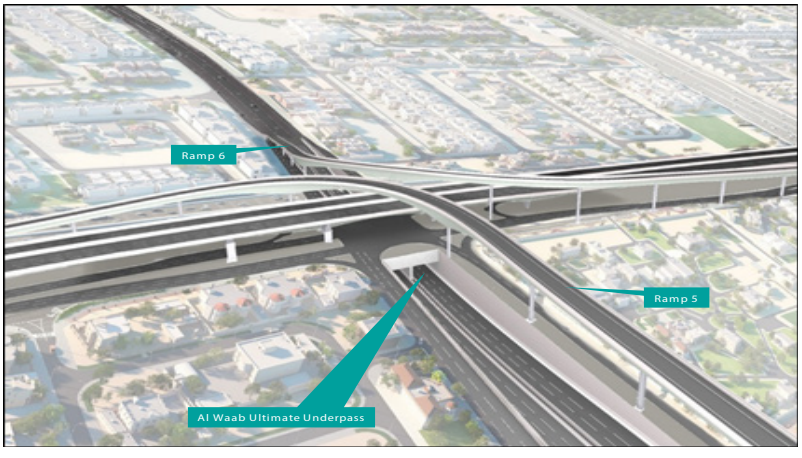

Figure 2 Ultimate Design.

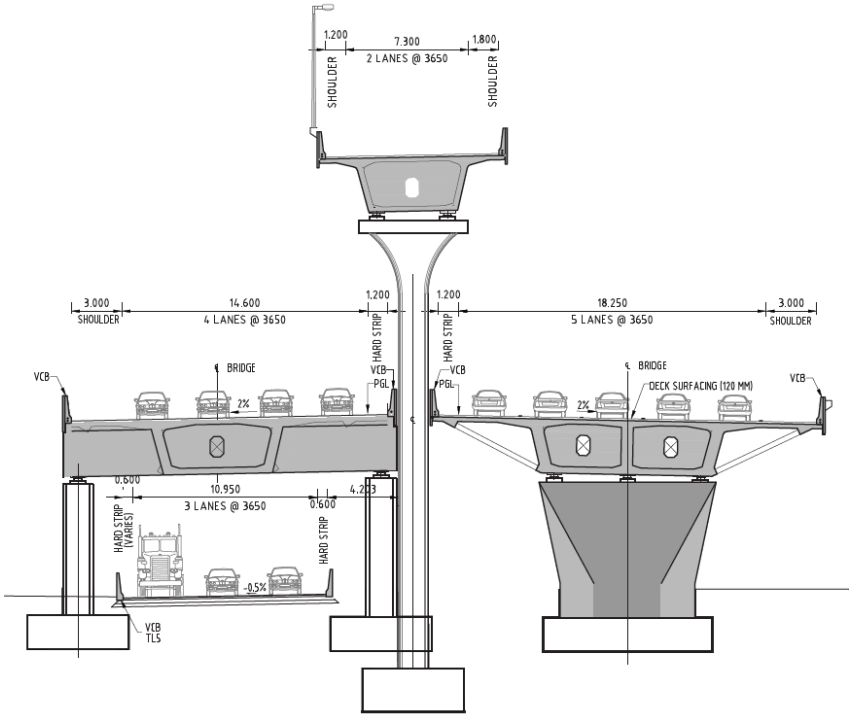

Figure 3 Current Interim Construction.

3 DESIGN

Due to its proximity to the bridge supports, the construction of the future underpass will require special attention in the design. The following measures were taken into account during the development of the bridges' design to allow a safe future excavation of the Al Waab Underpass adjacent to the bridges.

3.1 Pre-Installed Diaphragm Walls

Mechanically Stabilized Earth (MSE) wall embankments are used to support the approaches of the ramp bridges, primarily to fit the ramps in the limited space within the interchange. The alignment of the ramps necessitates the placement of these embankments along the edges of the future underpass. One of such embankments is particularly close to the underpass edge, to the extent that there is no space to install the shoring to support the embankment at the time of the future underpass construction. For this reason, the diaphragm wall will be installed during ongoing construction beneath the MSE wall embankment. As the future excavation takes place, the pre-installed diaphragm will be exposed and retain the MSE wall embankment above during the underpass construction (Refer to Figure 4 for the details of the Pre-installed Diaphragm Walls).

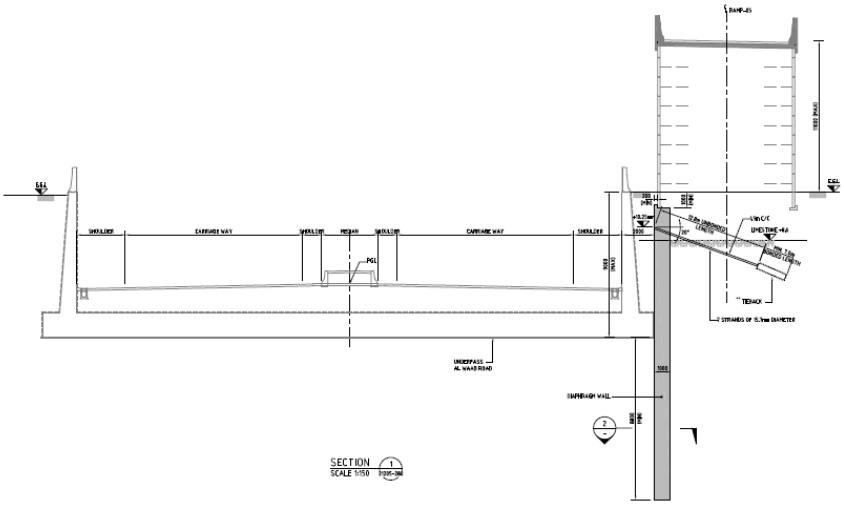

Figure 4 Details of Pre-installed Diaphragm Walls.

3.2 Ramp Bridge Piles Adjacent to the Future Underpass

Some of the ramp bridges' foundations are located closely behind the edges of the future underpass. These piles are close to the extent that their capacity will be impacted by the loss of supporting material due to the underpass excavation. As such, the design of the ramp bridges considers the conditions encountered before, during and after the construction of the underpass. In order to account for these conditions, the bridges are analyzed with variable pile support conditions to represent the various stages throughout the life of the structure. The piles are designed such that their ultimate capacities during and after the construction of the future underpass are derived only from the embedment below the bottom of the future underpass structure (Refer to Figure 5 for the details of Piles Adjacent to the Future Underpass).

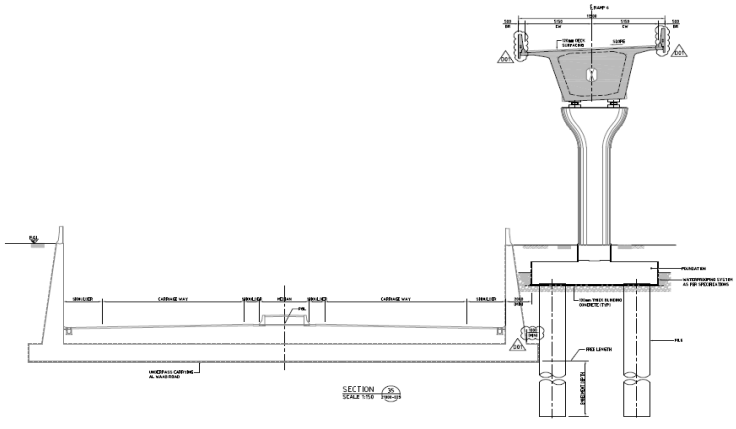

Figure 5 Details of Piles Adjacent to the Future Underpass.

3.3 Foundation Located at Median of Al Waab Street

One foundation, each of Ramps 5 and 6 bridges is located in the median of Al Waab

Street. Similar to the ramp foundations located behind the future Al Waab underpass as described in the preceding section, these foundations will also be exposed due to the future underpass construction. Accordingly, the design of these foundations also incorporates similar considerations regarding the pile analysis and capacities, which are compatible with conditions before and after the underpass construction. In addition, since the underpass construction would expose the piles permanently, the design of these foundations has been made to allow for construction of underpass walls adjacent to the exposed piles. These underpass walls will serve two purposes, one of which is to provide water-tightness to the underpass, which is located below the design ground water level, and the other to visually conceal the exposed piles with smooth walls for aesthetic reasons (Refer to Figure 6 for the details of Foundations at the Median of Al Waab Street).

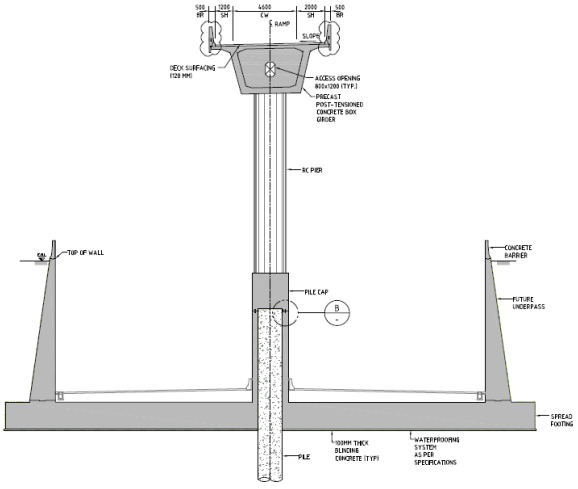

Figure 6 Details of Foundations at the Median of Al Waab Street.

4 CONSTRUCTION

To achieve the fast track delivery method directed by the Client, the Contract mandated all bridge structures to be of precast box-girder construction. This was the method implemented during the construction with the only exception being the spans tying with the ramp bridges that required a variable width box-girder. Balanced cantilever erection method was selected to be the most suitable and efficient method considering the time and site constraints. With a total exceeding 1,100 precast segments of an approximate total length of 4.0 km and the utilization of more than 65 types of formworks, the production, storing, transportation and erection of the segments within a limited time frame and space posed a significant challenge. Further, the scale of the precast segments exceeding a width of 23.0m and a weight of 155 tons for the mainline bridges increased the degree of difficulty of the logistics exceeding the conventional size and weight of precast box-girder segments. In addition, the limited Right of Way availability was also an important consideration, as well as the continuous and uninterrupted traffic flow of Al Waab Street, which was the Clients firm instruction.

Working closely, the Designer and the Contractor approached the Client's Traffic Management Authority and obtained the approval of several Traffic Management Plans,

which allowed the Contractor to divert the traffic and gain access to specified areas to commence construction activities. The complexity of the traffic management plans as well as the short execution duration in coordination with the overall construction schedule formed a difficult challenge for the traffic management team. One of the major Traffic Management Schemes was the four-lane signalized roundabout that replaced the existing at-grade Al Waab junction. However, securing approval of this scheme through the authorities proved difficult and required the upgrade of Mehairja Street, which provided another route to avoid the roundabout. This roundabout allowed the Contractor to construct the +1 level and +2 level substructures and superstructures without impeding traffic flows along Al Waab Street (Refer to Figure 7).

Figure 7 Temporary Traffic Management Map – Al Waab Roundabout & Mehairja Diversion.

5 BRIDGE AESTHETICS ACROSS THE SABAH AL AHMAD CORRIDOR

The Sabah Al Ahmad Corridor is a 25 km stretch of Expressway that provides a new north to south route parallel to Doha Expressway and comprises of the following key projects:

- P008-C2 – E-Ring Road
- P008 C3 - Mesaimeer Road
- P007 C5 P1 - Al Bustan Street South
- P007 C7 P2 - Al Bustan Street North
- P007 C7 P1 – Duhail Interchange and Al Gharrafa Street

Upon completion of the ABS Expressway Project, the Sabah Al Ahmad Corridor will boast the longest bridge in the State of Qatar spanning 2.6 km over Al Waab Street, Al Rasheeda Street, and Snay Bu Hasa (Refer to Figure 8).

Figure 8: Sabah Al Ahmad Corridor.

One of the primary design goals of the bridge designer is to unite the bridge with its immediate environs or set the architectural tone for future development. This approach provides the designer with direction and guidance in the design process and helps assure that the aesthetic properties of the bridges are appropriate and effective. Many of the superstructures in Qatar are used to enhance the appearance of each area by utilizing aesthetics to brighten the visual effect the structure has with the surrounding area. As such, the bridge along the Sabah Al Ahmad Corridor will be enhanced by applying aesthetically pleasing cladding attached to the parapets and MSE Walls. This will be supplemented with decorative lighting along the bridges. In addition, the MSE walls and specific mainline bridge piers will contain arch type cladding that would be decorated with artificial grass and specialized lighting (Refer to Figure 9).

Figure 9: Arch Cladding at Select Piers of Sabah Al Ahmad Corridor.

6 CONCLUSION

In summary, the ultimate challenge of the successful execution of ABS Expressway Project and the greater Sabah Al Ahmad Corridor which features the longest bridge in the State of Qatar spanning 2.6 km, requires the constant coordination of all subcontractors, suppliers and site personnel for the safe execution of this unique project, within the limited time and approved budget by the Client. The collaboration of the experienced personnel from the Designer, Contractor, Authority's sub-representative and Client are

essential for the delivery of a Project of this scale and magnitude. The commitment of the project personnel along with the Client's support resulted in unique design and construction elements that accounted for the Ultimate Al Waab Underpass while proving aesthetically pleasing structures.

REFERENCES

Kara, A. & Al Emadi, Y. (2018). Al Bustan south bridge design and build project, Doha, Qatar. *International Bridge Conference*, Istanbul, Turkey.

Cite this article as: Ganguli A., Kara A., "Unique Structural Design and Construction Challenges for Al Bustan South Project in Qatar", *International Conference on Civil Infrastructure and Construction (CIC 2020)*, Doha, Qatar, 2-5 February 2020, DOI: https://doi.org/10.29117/cic.2020.0020

The Lean Enterprise at the Design Office

Dawlat Elmosalmi
Dawlatmossalamy@hotmail.com
Engineering Consultants Group, Doha, Qatar

Mohamed Mohsen Ibrahim
mohamedmohsenae@gmail.com
Engineering Consultants Group, Doha, Qatar

ABSTRACT

This paper presents the lean practice implementation, which led to a transformation in the design offices/projects explaining how implementing lean principles is affecting the projects at the design phase and also affecting the whole system at the design firm. The paper is divided into two parts; theoretical and practical. The theoretical part will explain lean concept definition, values and wastes, wastes solutions, lean principles and levels of lean implementation. The practical part will present a case study for a successful lean transformation in a consultancy firm showing the challenges faced and the steps for a successful implementation on office activities and on projects as well based on a company's experience and observations reducing wastes and adding value to the work process within the organization to achieve the three parts goal of better, cheaper and faster projects. This research will be enriched by the audiences' interaction, sharing different experiences in lean transformation for maximum benefits.

Keywords: Lean thinking; Culture; BIM; Value; Waste; Design phase; Office activities

1 INTRODUCTION

The Architecture, Engineering, Construction and Operation (AECO) industry is always concerned with improving efficiency, quality and profitability. New innovative processes, such as the lean practice, can give solutions to the trilogy of problems in the AECO industry: time, cost and quality. The integration of the four key functions: process, technology, organization, and information management are required for any enterprise (Arleroth & Kristensson, 2011).

This paper aims to define clearly the concepts of lean thinking, its goals, benefits and challenges faced when first implemented and how to implement it successfully in a consultancy firm by presenting a case study and explaining how lean can be integrated with Building Information Modelling (BIM) achieving less waste and adding value to projects reaching client satisfaction.

2 LEAN CONCEPT

Lean is simplicity in its most valuable form. It has many definitions addressing efficiency, improvement, adding value and eliminating wastes (Womack & Jones, 2005).

2.1 Lean Definitions and History

Lean is the elimination of waste from the production cycle. Value is added at any work

process when waste is removed from the supply chain, leading to lower costs, shorter time schedule and higher profits. Being "lean" is achieved by delivering the right things (including information) to the right location or place in the right amount, at the right time and under the right conditions. Value can be defined as what the customer needs at the end of the process. While waste can be defined as any process or action which takes place in the process but does not add value. Lean as a term was first signified in the manufacturing industry by James P. Womack in his book "Lean Thinking" and the book, "The Machine That Changed the World". It is based on an industrial concept created by the Japanese during the 1900s. The founder of lean production was Toyota in its Production System (TPS). Womack's definition of lean production in 1990 was that it is a method which combines the advantages of craft production and mass production. The manufacturing industry has applied lean thinking successfully; the same principles were applied by lean professionals to the construction industry as a response to address the traditional model shortcomings. It is a fact that there is approximately 30 percent waste in our processes and delivery methods. Also, it is known that manufacturing benefits from repetition, fixed program, controlled environment and known conditions while construction suffers from prototypes at scale 1:1, constant changes, unforeseen costs and increased risks (Badurdeen, 2007) (Arleroth & Kristensson, 2011) (Elmosalmi 2014).

2.2 Wastes classification and solutions

According to lean thinking, there are eight types of wastes, which are connected to each other and interrelated: (1) Overproduction waste is the making or producing more than is needed-leading to excess stocks or fabricating material or ordering it too soon. (2) Waiting time waste is people or equipment waiting for a production process to be completed or resources to arrive. The operator is slower than the production line. (3) Transport waste is moving resources (people/ materials) unnecessarily (ex: lost data because of unorganized data folders, or working space not designed efficiently). (4) Motion waste is a worker who appears to be busy but actually not adding any value. (5) Stocks waste is the material or information stored at office, site or yard, work in progress (processing work), unused tools and data (often held as an acceptable buffer but should not be excessive). (6) Defects (errors) waste is the rework or output that does not reach the required quality standard. (7) Over processing waste is the unnecessary reporting, non-value-added activities or actions, non-value-added reviews. (8) Unused employee creativity waste is wasting time, wasting human resources skills, losing better innovative solutions by not engaging the right persons at the right tasks or outsourcing some tasks because of not knowing the employee's capabilities and skills. There are five waste solutions which are sort, set in order, shine, standardize and sustain. Sort is by separating the tools into two groups: using and not using. Set in order is the items in the "using" group that were set in order. Shine is keeping the area clean and everything in its location. Standardize is to apply the standards to the work area. Sustain is maintaining the gain (Bottirov, 2011).

2.3 Lean thinking principles

Lean thinking principles focus on improving efficiency and productivity by better coordination of information and maintaining better flows. The five lean thinking

principles are, identify customer value, identify the value stream, implement flow, implement pull, and seek perfection. (1) Identify customer value principle is concerned with client identification and understanding about what the client expectations are and what he is willing to pay for. (2) Identify the value stream is both value added, and non-value-added actions required to bring a product through the main flows. (3) Implement flow is to continually deliver the product from start to finish. Synchronize and align so there is only minimum waiting time for work and workers. (4) Implement pull: it means producing only what customer needs at the end of the process or to start new work only when there is a customer demand for it. It results from the fundamental concept of Just in Time (JIT), which states that production should be triggered based on actual demand from customers. (5) Seek perfection (constant pursuit of improvement) is the kaizen concept (the Japanese term for continuous improvement, through a Plan-Do-Check-Act (PDCA) cycle). In lean systems, transparency is required as a main concept, where everyone can see everything, and systems are able to communicate with people, e.g., use of indicators and standards, where immediate recognition of deviations is allowed all the time (Womack & Jones, 1996) (Elmosalmi 2014).

2.4 Lean production methods

There are several lean production methods such as the Lean Operating System (LOS), Cell Production and Kaizen. LOS concept is to create reliability and producing consistent results in the day-to-day operations and in the delivery of projects (monitoring and following up work daily with the team) so that value can be added, and wastes are eliminated. In cell production workers are organized into several teams. Each team is responsible for a particular part of the production process. Each cell is made up of many teams who deliver finished items on to the next cell in the production process. In traditional production, products were manufactured in separate areas as a production line. Cell production can lead to efficient improvements due to increased motivation (team spirit and added responsibility given to cells) and workers sharing their skills and expertise. The Kaizen concept is focusing on engaging employees/stakeholders in developing systems and improving work processes in parallel with their ongoing tasks which helps in improving performance. It also seeks to standardize processes and eliminate or reduce waste (Forbes & Ahmed, 2011) (Elmosalmi 2014).

3 LEAN IMPLEMENTATION

Several requirements are needed at any organization for successful lean implementation; the organization top management and employees should be willing to change, they should have commitment to training and able to learn, they should have a mindset which is quality oriented, they must have commitment to reducing or eliminating waste, commitment to cost and performance measures, willingness to implement lean during the design stages. Also, the organization must enhance the collaborative relationships and its information technology systems. Lean thinking can be applied on many levels as shown in the Figure 1.

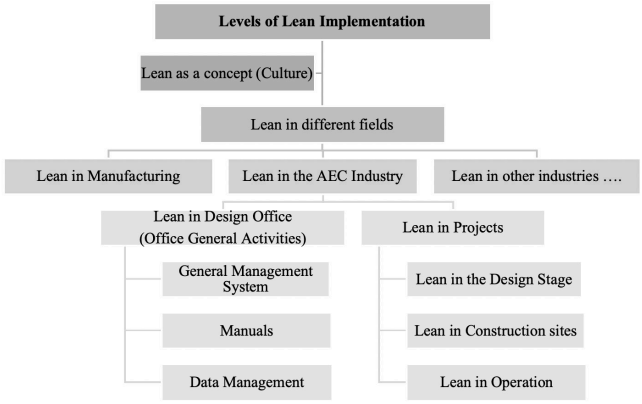

Figure 1: Levels of lean implementation

4 CASE STUDY FOR LEAN IMPLEMENTATION AT THE DESIGN OFFICE

ECG (Engineering Consultants Group) company which has been successfully implementing the lean practice for the past few years in both Egypt and Qatar offices is chosen as a case study to show how lean practice can be implemented in the design office on both levels; the office activities and the projects. Lean can be implemented with a very wide range of benefits at the design office, whether it is a consultancy firm or a design firm. The office activities include but not limit themselves to the company general system of work, the manuals and standards of the company, the administrative processes, the human resources management systems and the data management system.

4.1 Lean drivers (problem identification)

The huge amount of wastes (materialistic and non-materialistic) which the teams were suffering from were the main driver for the lean transformation. In addition, the company's main goal was achieving its clients' satisfaction through better, faster, cheaper delivery of projects while maintaining its employees' satisfaction, development and improvement, and that could not have been achieved successfully without implementing new innovative practices as the lean practice. Examples of the wastes discussed and eliminated after implementing lean practice at office activities are projects waiting for human resources, waiting for software installation, movement as a result of layout of working area, unused data, information, standards, layers, families, reports, and outsourcing in some tasks increasing projects costs and over processing in data transfer between different offices around the world.

4.2 Sources of wastes in the office

The sources of wastes can be classified into people waste, process waste, information waste and asset waste. People wastes are the wastes that happen because of bad human resources; bad leaders and due to lack of training. Process wastes are wastes taking place because of work duplication, improper planning, lacking monitoring and supervision. Information wastes are lost data and material important for accomplishing the work or bad processing of communication data and information. Asset waste is the improper utilization of material and property resources and includes wastes related to excess

inventory, work in process, areas and facilities not properly used. The first step towards lean enterprise is to be fully aware of the wastes existing in the organization. Some of the wastes can be hidden inside long processes so it is necessary to make the entire value stream related to office activities visible by creating the Value Stream Map (VSM) so everyone can discuss the wastes clearly with transparency so that wastes can be easily eliminated (Lareau, 2003).

4.3 Challenges faced

The main challenge was changing the mindset of employees from being production oriented to targeting "continuous improvement" by starting with the right people and involving them in the lean transformation. Examples of the challenges are changing employees' working culture, lack of cooperation from some employees, lack of long-term forecast and investment, fear of admitting the wastes existence, long implementation time and lack of lean knowledge.

4.4 Lean Implementation plan

To transform the organization to a lean one, three main phases took place. First was formulating the idea by discussing it with the top management and learning about lean, then taking the decision by the top management, identifying missions and visions (creating a future vision for development by each department), choosing lean champions, identifying metrics, and giving lean awareness sessions. The second phase is the implementation phase, done by evaluating the organization. It is done by writing Waste Analysis Reports (WAR) for departments (Figure 2), and involves suggesting solutions by the nominated lean candidates, identifying responsibilities (that who is responsible for waste elimination), identifying priorities and capabilities by prioritizing the wastes elimination solutions and put them in order according to capabilities and urgency. Moreover, creating a time line for wastes elimination, implementing lean principles in both office activities and new projects, and wastes elimination. The third phase is evaluation and development by auditing and evaluating, continuing development of teams (targeting more lean certifications), following up to confirm lean commitment.

Table 1: Partial sample of the Waste Analysis Report (WAR)

Wastes	Type	Waste description	Responsibility	Weight (1 to 10)	Phase of Implementation	Solution	Cost of Elimination
Overproduction	Technical	Overproduction as a result of:					
		•Extra Level of Detail (LOD)	CAD/BIM Management+ Project Management	9	1	•Work according to required LOD	x
		•Overproduction as a result of unclear scope of work	Arc+Management	6	2	•Committing to the scope (by conducting Team Leaders and project managers awareness sessions)	x
		•Extra unnecessary data in sheets or information duplication (Ex. Extra dimensions)	Arc	8	1	•Refer to Manuals and Standards (and preparing sessions to architects and monitor their commitment to what they have learnt)	x
		•Delivery methods in BIM	Arc+BIM Management	4	3	•Managing project phases according to process used	x
		•Incoordination	Arc	7	1	•Prototyping in large scale projects should be settled from the beginning of the project.	x
		•Unnecessary submissions (progress print) or Unscheduled submissions	Management	8	1		x

5 CASE STUDY FOR LEAN IMPLEMENTATION ON PROJECTS

Lean thinking can be implemented on all projects at the design stage, the construction stage and at the operation stage. The project selected by ECG to be a case study was a transit-oriented development complex in Doha. It was Detailed Design Scope integrating BIM and lean practices.

5.1 Challenges faced by the project team

The challenges faced by the team of that mega project were design challenges, technology challenges, social and cultural challenges, process implementation, coordination and collaboration, simulation, man-hours budget and resource assignment, waste elimination, resources optimization, quality control and the complex and huge amount of data in assets management life-cycle.

Since all project information is managed by BIM, numerous numbers of BIM models have been produced across different locations accompanied by huge amount of information for different purposes. This information can be classified and sorted with reference to the project stage, phase and use. During the project lifecycle many information exchange issues, related to quality and interoperability may appear. Manual monitoring, reviewing and analyzing of this amount of information became more sophisticated; completeness and accuracy became the major issue of handing over models for each BIM use (Ningappa, 2011).

5.2 Lean implementation plan on the project

The project team used technologies that facilitate lean design through an automated solution, facilitate the aggregation, extraction of important information, reviewing the correctness and completeness of information and helps with decision making on different management levels. The automation process can be classified into four phases: Aggregation, extraction, reviewing & analyzing, and optimization for better decision making. This leads to reduce the duplicative efforts of traditional drafting and traditional coordination methods. BIM allowed the design team to focus more on high-value design earlier through analysis and visualization and deliver the best value to the customer. The applications of BIM helped reduce several kinds of waste. For example, visualization helped reduce confusion, which leads to less error and effectively, leads to less rework. Therefore, less waste due to correction, rework and defects. The tools and techniques used in integrating BIM with lean practice are implementing Common Data Environment (CDE) for design management across different design offices (Figure 3), efficient design coordination, early clash detection for less site wastes in terms of (time, resources & materials), monitoring design productivity, processes and resources efficiently (Figure 4), accurate and automated material take off and cost estimation through the BIM Model, proper phasing and construction planning using 4D simulations, apply production control: utilize a small design batch approach, evaluating against project requirements purpose.

5.3 Detailed sample for technological lean application: Phases of implementation for information management

Aggregation of BIM information: Electronic data management solution and common

data environment implementation should be obligatory; this facilitates managing and controlling the data of all assets. There is now a diversity of EDMS (Electronic Data Management System) & CDEs software, which provide divergent solutions relevant to each project requirements. ECG has managed different projects information utilizing PEER software which is controlled by internally developed electronic data management software complying with ISO BIM requirements, guidelines and project's needs. The elements of the integrated systems are: Data servers, models server, PEER software, and ECG electronic data management system. (Figure 2 illustrates a general workflow for the integrated system).

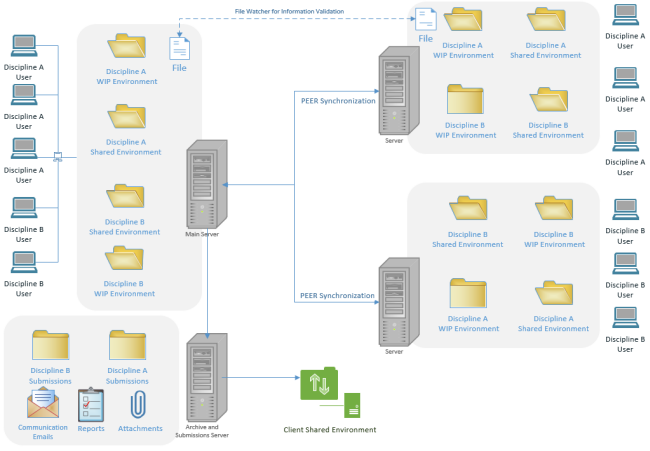

Figure 2: General workflow for the integrated system

Data aggregation from BIM models for check and verification: ECG has elaborated a software for BIM validation and data aggregation using programming codes and Revit API where data can be driven by an automatic process from linked models per request or based on a time interval, this varies based on project and workflow needs.

Instantaneous accessibility of aggregated information for record, check and analyze: The aggregated information earlier demonstrated is saved on the allocated server. The responsibility of processing the received requests from a front-end application falls on a backend server hosted online, which performs as an example the following tasks: insert new project or do modification for the existing one, add/delete users, and get information of diagrams and schedules, etc. Frontend application is responsible to visualize the information in the shape of readable diagrams and schedules with filtering and sorting features (Figure 3).

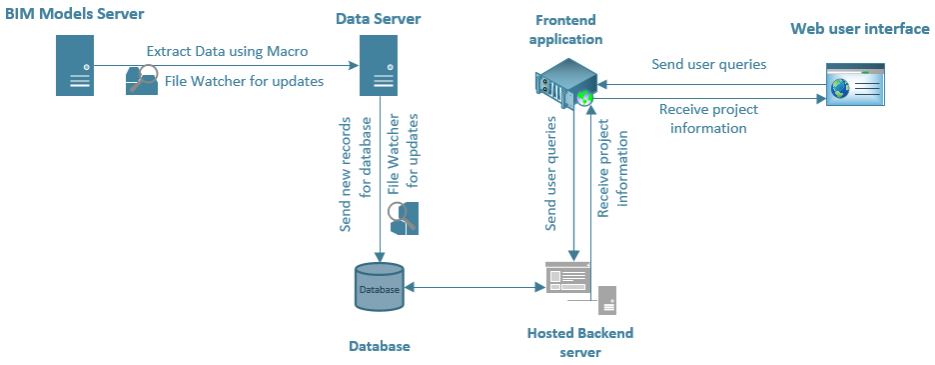

Figure 3: Illustration for the information aggregation and exchange

Design workflows and procedures optimization with reference to aggregated information: The optimization of design workflows and procedures can be achieved if aggregated information is monitored and analyzed for enhanced decision-making and gaining & documenting experience from projects. Sample case, the complexity of architectural BIM models increased suddenly which was a reason for lower production efficiency. When the collected information is analyzed for investigating the reason for that, the following outcomes were noted regarding BIM models' items for number of model categories at each shared version of the model: Count of model elements increased from 72,000 elements (10 months progress) to 208,000 elements (one-year design production duration). This means an increase of 136 thousand elements in 2-months of progress (Figure 4).

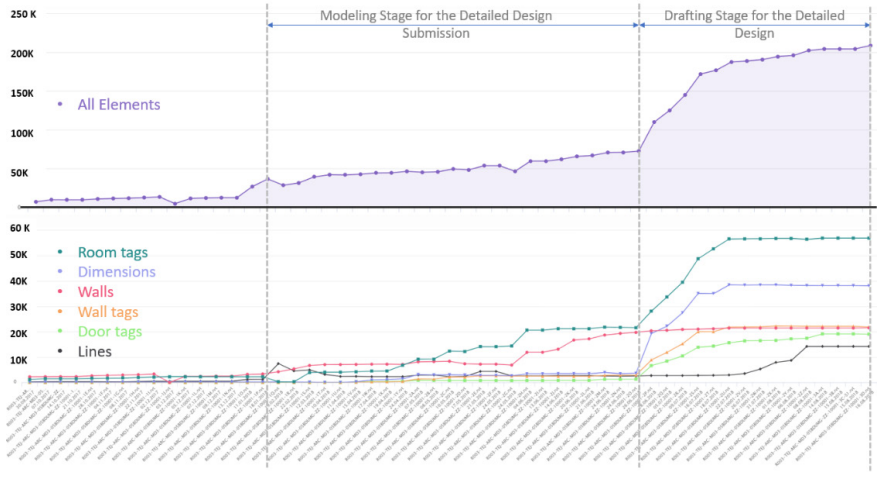

Figure 4: BIM production progress (modelling and drafting) across a year

By analyzing the last arch. model, more than 76 % of the model content was related to 7 element types out of 69 used type as in Figure 5.

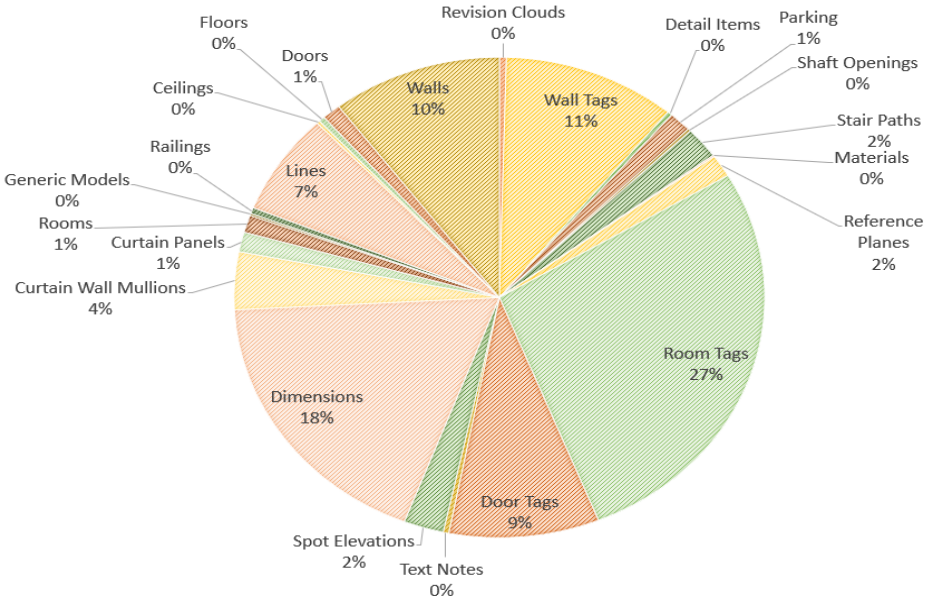

Figure 5: Model content ratios at the latest shared version of the architectural model

One of the most crucial issues for BIM efficient production is to have duplicated model elements. Architectural scope of production was split into two different models managed by two teams (architects & interior designers). When progress was analyzed, a justification was found for design conflicts issues. One of the most critical issues found was ceiling production. A duplication of ceiling elements existed for a duration of 27 days at both models which caused coordination conflicts related to hosting of ceiling elements (spot lights, air terminals, smoke sensors & detectors, and others) on ARC ceiling elements and which was deleted at a developed phase of design production (Figure 6) (Mohsen et al., 2019).

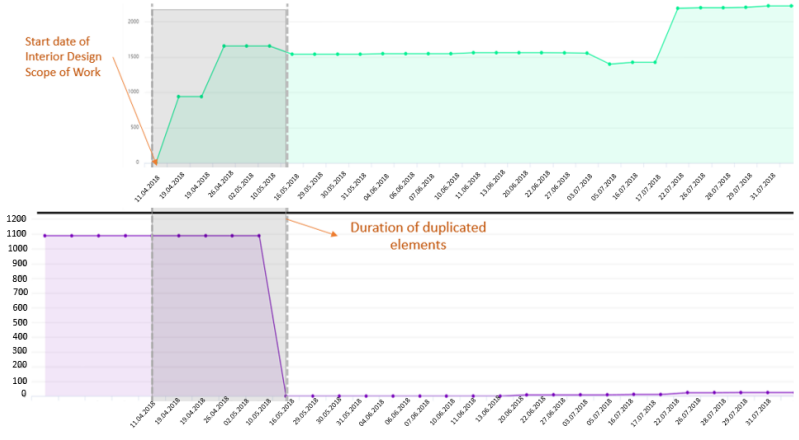

Figure 6: Analysis of the duration of existence of duplicated ceiling elements

6 CONCLUSION

Lean is a way of thinking which can be applied at the design office as well as in construction sites. Being lean is more than just a set of tools and requires a cultural shift among the participating parties—the team must be constantly looking for ways to collaborate and incorporate continuous improvement into the project and in the company as a whole. Applying the lean practice in firms through managing the office activities with lean thinking principles helped in reducing wastes and unnecessary non-value adding activities which costs the company money and act as obstacles in the way of the company's continuous improvement. Also, from practitioners' experience, it was found that to sustain lean operations, the human resources function must support them, beginning with hiring people who are innovative, initiative and can work in a lean working culture.

Managing the projects using lean principles in integration with BIM processes helped in reducing wastes, increasing output value through systematic consideration on customer requirements (by reducing variability, reducing cycle time), simplifying by minimizing the number of steps, increasing output flexibility, increasing process transparency, focusing control on the complete process, building continuous improvement into the process, achieving flow at the value stream. Project quality level has improved significantly when BIM was used as a tool to support implementation of lean thinking on AECO projects. Coordination between different disciplines of the project could be one of the project quality indicators.

The integration of lean practices with BIM in an integrated methodology is inherently the best process for AECO firms to achieve continuous improvement and achieve faster, better and cheaper projects.

REFERENCES

Arleroth, J. & Kristensson, H. A. (2011). *Waste in Lean Construction* (M.Sc., Thesis, Department of technology management and economics). Chalmers University of technology, Gothenburg, Sweden.

Badurdeen, A. (2007). *Lean Manufacturing Basics* (an online book). Retrieved from http://www.leanmanufacturingconcepts.com.

Bottirov, O. (2011). *Lean construction in construction company* (Phd, Viauc University, Department of construction management). Denmark.

Elmosalmi, D. (2014). *Building Information Modeling (BIM) Technology Implementation in Lean Architecture through Managing Human Resource* (M.Sc., Thesis, Department of Architecture). Ain Shams University, Egypt.

Lareau, W. (2003). *Office Kaizen - Transforming Office Operations into a Strategic Competitive Advantage*. Milwaukee: American Society for Quality.

Mohsen, M. & others (2019). *Necessity of Monitoring Vital Bim Information for Optimized Design Process Management*. Witpress, Ltd.

Forbes, Lincoln H. & Ahmed, Syed M. (2011). *Modern Construction: Lean Project Delivery and Integrated Practices*. CRC press, Taylor and Francis Group, LLC.

Ningappa, G. (2011). *Use of Lean and Building Information Modeling (BIM) in the Construction*

Process; Does BIM make it Leaner?' (M.Sc., Georgia Institute of Technology).

Womack, James P. & Daniel T. Jones (1996). *Lean Thinking: Banish Waste and Create Wealth in Your Corporation.* New York: Simon and Schuter.

Womack, James P. & Daniel T. Jones (2005). *Lean Solutions: How Companies and Customers Can Create Value and Wealth Together*. Simon and Schuster, New York, NY.

Cite this article as: Elmosalmi D., Ibrahim M. M., "The Lean Enterprise at the Design Office", International Conference on Civil Infrastructure and Construction (CIC 2020), Doha, Qatar, 2-5 February 2020, DOI: https://doi.org/10.29117/cic.2020.0021

BIM Based Facility Condition Assessment

Faisal Faqih
f.faqih@connect.polyu.hk
Department of Building and Real Estate, Hong Kong Polytechnic University, Hong Kong S.A.R, China

Tarek Zayed
tarek.zayed@polyu.edu.hk
Department of Building and Real Estate, Hong Kong Polytechnic University, Hong Kong S.A.R, China

Ehab Soliman
ehab.solimanmoursi@ku.edu.kw
Civil Engineering Department, College of Engineering and Petroleum, Kuwait University, Kuwait

ABSTRACT

Current practices of using traditional methods of managing data using spreadsheets or hard paper copies for various building data, are commonly being used during building inspection and condition assessment. Building Information Modelling (BIM) can immensely help in solving problems of facility inspection by generating and managing digital representation of the physical and functional characteristics of a facility. This paper describes a model, which is developed to integrate the physical and environmental conditions of a facility on a BIM platform. In this study, factors influencing physical condition and environment condition of the building were identified. Building defects which causes physical deterioration of the building component reduces the ability to perform its intended designed function while environmental condition influences the comfort and health of occupants or users of the building. It is imperative to understand that physical and environment condition of the building are both of vital importance for safety, health and comfort of building users. Factors affecting physical and environment of building were used to develop proposed condition assessment model. Using this proposed model periodic general condition assessment can be performed and correspondingly deterioration graph can be generated for the facility over period of time. Based on inspection data and condition assessment models, building performance can be analyzed for future preventive maintenance.

Keywords: Facility management; Building inspection; Condition assessment; BIM

1 INTRODUCTION

Facility Managers are responsible for management, operation & maintenance of buildings which influences the total life cycle cost of building. International Facility Management Association (IFMA) defines Facility Management as, 'A profession that encompasses multiple disciplines to ensure functionality, comfort, safety and efficiency of the built environment by integrating people, place, process and technology'. Facility Managers are also responsible for health, safety and space management ensuring the owner or organization fulfil its obligation to those who use the workspace and are likely to be affected by its operation. Facility management thus have deep impact on efficiency of the workplace, compliance of regulations, local environment and financially to the

owner or organization. Physical deterioration of building reduces the ability of building to perform it's intended function (Grussing, Uzarski & Marrano, 2009).

Facilities managers need to identify effect of deterioration in order to prepare corrective and preventive maintenance plans. This task is difficult because of the complex interaction and interdependencies between different building components & systems. This research aims to use Building Information Modelling (BIM) as a tool for facility condition assessment by using a model which integrates the physical and environmental conditions as well as solve the problem of management of large amount of data generated in condition assessment of large facility.

The aim of this research is to develop a model for facility condition assessment using Building Information Modelling (BIM) as tool for management of data generated during building inspection. The objectives of this research are to identify critical factors, which affects physical building condition and environmental condition of the building. This study proposes a condition assessment model based on building defects. This study further developed an application program to integrate the physical & environmental conditions of a facility linked with BIM model in Rivet software.

2 RESEARCH METHODOLOGY

The research methodology adopted for this study can be described in following steps, which were carried out as follows: Literature review; Identification of critical factors affecting building condition; Develop condition assessment model; Develop application program as an API for Rivet software; Testing and validation of proposed model. For this study, literature search was carried out in major scientific research databases such as Web of Science, Scopus, ASCE Online Library, Science Direct, Google Scholar etc. as well as repositories of universities. It was imperative to identify first what are the factors which affects the physical and environmental building condition. Condition assessment model was developed after identification of factors, which influence the condition of the building. This condition assessment model was developed into an application program as a API for Rivet software, which is one of the extensively used BIM software package. A 3D BIM model was developed for testing and validation of condition assessment model. The development of condition assessment model is examined, analysed and discussed. This paper is concluded with potential benefits of using BIM for facility condition assessment.

2.1 Literature Review

Literature review reveals that irrespective of age of the building, defects occur in different forms and to various extents in all types of buildings (Buildings Department, 2002; Yacob, Ali & Peng, 2016). Building defects can create hazards leading to serious or fatal injuries. Classification of building defects into categories is useful for identifying the type of defect and to estimate probable causes and its recurrence (Haryati, Kharizam, Zainol & Othman, 2016). Most defects can, at their early stages, be discovered through visible or detectable symptoms. If not promptly rectified, minor defects can develop into serious ones, causing failure or sudden collapse, endangering lives and becoming costlier to rectify (Ahzahar, Karim, Hassan & Eman, 2011; Buildings Department, 2002). Rafaela and Núria (2018) in their study found out that cracking, water leakage

are the most common defects for building elements, while leakage and corrosion were more often found in plumbing system. Sometimes one defect can cause other building defect to appear. Othman et al. (2015) in their study found out that moisture problem in a hospital building has cascading effect and leads to several other building defects such as peeling paint, blistering of wallpaper, staining, discoloration, watermarks, mold growth, corrosion on different building elements such a roof, wall, ceiling and floors. Previous studies have noted common building defects such as cracks, water leakage, corrosion etc. which indicates that these defects across different countries are similar in nature which affect physical building condition, however these defects may originate due to different reasons (Chong & Low, 2006; Kian, 2004; Othman et al., 2015; Suffian, 2013).

2.2 Critical Factors Affecting Building Condition

To identify the current state of the building, building stakeholders conduct condition assessment to make appropriate decision for repair and maintenance. During condition assessment if building defects are just identified without finding the source of the defect will lead to reoccurrence of the defect even after repair. To identify the source of building defects it is essential to recognize the factors, which cause them. Building inspection personnel must know different factors or agents, which influences the condition of the building in order to conduct effective condition assessment. Different research concluded that building defects could be attributed to various factors. This study identifies the factors, which influence physical condition and environment condition of the building. According to ISO 19208:2016, major agents affecting physical condition of building or its components can be classified into five types namely Mechanical agents, Electro-magnetic agent, Thermal, Chemical and Biological agents. While four main categories which influence the environment condition of the building are Indoor Air Quality (IAQ), Thermal environment, Acoustics and Lighting as per (ASHRAE Guideline 10, 2016).

2.3 Factors Affecting Physical Condition of the Building

The soundness of the building is measured by assessing the physical condition of the building. It is important to be cognizant of the factors which influences the building condition in order to assess the correct building diagnosis during condition survey. Various external and factors affect physical condition of the building during its life span. According to ISO 19208:2016 major agents affecting building or its components can be classified into five types namely Mechanical agents, Electro-magnetic agent, Thermal, Chemical and Biological agents. Mechanical loads may include gravity loads like snow loads and dead loads etc. can cause structural failure, loss of function or both. Super imposed forces or restrained deformations such as ice formations, expansion due to heat or contraction due to cold, creep; shrinkage can also cause failure or loss of function or cracks. Building can also be subjected to kinetic energy such as impact loads, storm, or earthquake similarly disturbance from man-made activity such as vibrations from tunneling near building or machine vibrations can also severely affect the strength of the building or its components which may cause structural failure. Solar or ultraviolet radiations, radioactive radiations can cause heating of the building and degradation of building material (Paulo, Branco & de Brito, 2014). Electricity due to lightning can also seriously harm the building in case of lightning strike on the building. Magnetic fields

can also affect the building components. Extreme levels of temperatures such as heat, frost or fire can also severely affect the building's appearance, loss of function or may cause structural failure (Lin & Scott, 2006). Chemical agents source can be waters and solvents from air humidity or ground water (Othman et al., 2015); acids can be from bird droppings, vinegar; salts such as chlorides, nitrates, phosphates; oxidizing agents such as disinfectants, bleach; reducing agent like ammonia, sulphides can also affect the condition of components of building by degrading the building material. Biological agents such as vegetable and microbial agents e.g. plant roots, bacteria, molds and fungi can affect the building or its components. Animals such as rodents, birds, worms or rodents can also affect the building condition by contaminating or degrading the material.

2.4 Factors Affecting Environmental Condition of Building

People spend a large part of their life inside the building hence it is essential to identify the factors which affects the environment of the building. According to ASHRAE Guideline 10 (2016) the four main categories which influence the environment condition of the building are Indoor Air Quality (IAQ), Thermal environment, Acoustics and Lighting. The quality of air inside the buildings is a contributing factor for healthy life and wellbeing of people who spend a large part of their life inside buildings (World Health Organization, 2010). Poor indoor air quality can lead to discomfort, ill health, and, in the workplace, absenteeism and lower productivity (Al Horr et al., 2016). Good indoor air quality safeguards the health of the building occupants and contributes to their comfort and well-being. According to ASHRAE 62.1 (2016) acceptable indoor air quality is defined as "air in which there are no known contaminants at harmful concentrations as determined by cognizant authorities and with which a substantial majority (80% or more) of the people exposed do not express dissatisfaction". Children, elderly and those with existing respiratory or heart disease are more susceptible to the effects of indoor environment quality. Indoor environment condition has several health effects on humans such as sore throat, headache, eyes irritation, nose irritation, dizziness, fatigue etc. after exposure to high concentrations of indoor air pollutants (IAQMG HKSAR, 2019).

Parameters such as temperature, humidity, and air movement are important indoor air quality parameters as they could affect people's perception of the indoor air quality (Arif, Katafygiotou, Mazroei, Kaushik & Elsarrag, 2016). The level of some of the indoor air pollutants could also be affected by temperature and humidity (ASHRAE Guideline 10, 2016). However thermal comfort may differ from person to person based on their gender, age and personal preferences (Arif et al., 2016), according to ASHRAE 55 (2017) thermal comfort is defined as "that condition of mind that expresses satisfaction with the thermal environment and is assessed by subjective evaluation".

Thermal comfort is directly affected by air temperature. There are various factors, which can influence the temperature of a room such as air conditioning, heat sources from solar heat, lighting, computer or any other heat dissipating machines in the room. If a room is considerably large the same room may have different room temperatures based on air conditioning outlet, window location etc. Since the temperature evaluation is subjective, different people may have different level of comfort in the same room with same temperature. This difference in temperature perception of comfort will depend of various factors such as gender, age, season activity level etc.(ASHRAE 55, 2017; Kim,

de Dear, Cândido, Zhang & Arens, 2013; Maykot, Rupp & Ghisi, 2018). Humidity in air affects human body's ability to lose body heat through perspiration, which in turn influences thermal comfort of people. High humidity encourages growth of fungi on building furnishings and fabrics while low humidity can cause eyes, nose throat to dry which can lead to discomfort and irritation (IAQMG HKSAR, 2019). Low humidity in the room can also cause static electricity generation, which can affect electronic components and discomfort among the occupants of the room (ASHRAE 55, 2017).

Building acoustic quality can have great impact on occupant's comfort level. Noise is unwanted sound and its perception is very subjective from person to person. Different factors influence in noise perception such as magnitude, duration or time of occurrence. Music to one's ear may be noise to another. The characteristics of sound in a room is also affected by surfaces in the room that might absorb, reflect, or transmit sound (ASHRAE Handbook, 2017). Adequate and appropriate lighting is required to perform visual tasks efficiently. Good lighting inside the building is also essential for visual comfort of the occupants or users of the building. The degree of visibility and comfort required in a wide range of work places is governed by the type and duration of the activity (BS EN 12464-1, 2011).

2.5 Proposed Condition Assessment Model

In this proposed condition assessment model, each space in a building is assessed simultaneously for both physical condition as well as environmental condition. Each space in buildings can be clustered into groups according to user defined building hierarchy groups such as classrooms, corridors, laboratories, offices, corridors, staircase etc. Same building components may have different relative weightage in different buildings according to their functional use. Hence, there should be flexibility in assigning relative weightage of building components according to the requirements and importance of components of building. In this proposed model user is allowed to define relative weightage of building components according to their importance in the building. Analytical Hierarchy Process (AHP) is used for calculating relative weightage of different building components based on pairwise comparison between them. Proposed condition assessment model is defect-based model in which each building component is assessed based on damage, which has occurred due to various building defects. The condition assessment process of proposed model is as shown in figure 1. The four main assessment criteria considered for this condition assessment model are Safety; Criticality of Element / Component (Importance); Operational Efficiency (Functional use); and Appearance (Aesthetics).

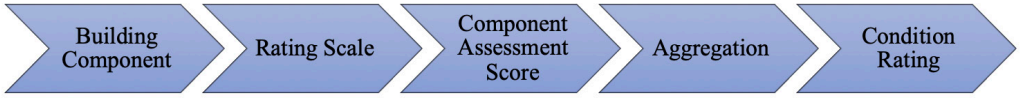

Figure 1: Condition assessment process for proposed model

Scale of 1-10 is used to assess the condition of building component for physical condition based on visual inspection. An average of scores of individual criteria is used for further calculations.

Final consolidated rating is calculated by aggregating the products of individual component ratings with their relative weights as shown in equation 1.

$$R_{Phy} = \sum_{i=1}^{m} S_i W_i \quad (1)$$

where, R_{Phy} = final consolidated physical rating

S_i = Average of score for individual assessment criteria based on scale of 1-10

W_i = Relative weightage of component as defined using AHP

Similarly, for environmental condition assessment for a particular room/space reading from instruments measuring concentrations of carbon dioxide, carbon monoxide, and ozone representing Indoor air quality; humidity and temperature readings; lighting intensity and sound decibels are used for calculation. These reading are converted into Utility Values using from on a common scale of 0-1 by using permissible limits given by respective guidelines and codes as follows: IAQMG HKSAR (2019) for Indoor Air Quality readings, Thermal Comfort as per (ASHRAE 55, 2017), Acoustics as per ASHRAE Handbook (2017) and lighting of room as per (BS EN 12464-1, 2011). Final consolidated rating is calculated by aggregating the products of individual utility values with their relative weights as shown in equation 2.

$$R_{Env} = \sum_{j=1}^{n} U_j W_j \quad (2)$$

where, R_{Env} = final consolidated environmental rating

U_j = Average utility value converted from instrument readings

W_j = Relative weightage of component as defined using AHP

2.6 BIM Application Program

Building Information Modelling (BIM) is the process through which essential facility information is captured, maintained, and shared digitally in a set of integrated BIM models. Inspection of large number of building components is a huge task, sorting them in groups and categories and building hierarchy is required for easier management during condition assessment. Building Information Modelling (BIM) can help immensely in solving problems of facility managers by generation and management of digital representation of the physical and functional characteristics of a facility. To test and validate the condition assessment model for this study, a 3D BIM model of entire floor of a building was created using Rivet software.

The program developed for this study can be accessed as Add-Ins in rivet software, which can retrieve the tagged room from BIM model. After filtering the tagged room, the groups as defined by user can be assigned relative weights according to user defined importance of the space inside the building using Analytical Hierarchy Process (AHP). These relative weights will be further used for calculation. Each space then can be assessed based on four criteria as per proposed model on a scale of 1-10. Similarly, the

environmental readings from the instruments can be entered for the same room/space for IAQ, Humidity, Temperature, Sound levels, and lighting intensity. Additionally, individual remarks and photos of the room/space can be attached along with the readings. On clicking analysis, all the entered values are processed and converted to their respective utility values and final aggregated ratings are calculated and graphically presented.

3 RESULTS

Rivet software by Autodesk was used to create BIM model as this software is widely used in industry. Rivet also has provision for API (Application Programming Interface) which gives user to extract data from BIM model to another program for further analysis. Using C# language in Microsoft Visual Studio, a program was developed and linked with API of Rivet to extract data from existing BIM model. To analyze and run the program requisite input of rating scores of building component and instrument readings for environment condition analysis is required by user. Condition assessment for a particular date of each user-defined groups can be graphically presented. Deterioration of entire facility condition over a period of time can also be generated as shown in Figure 2.

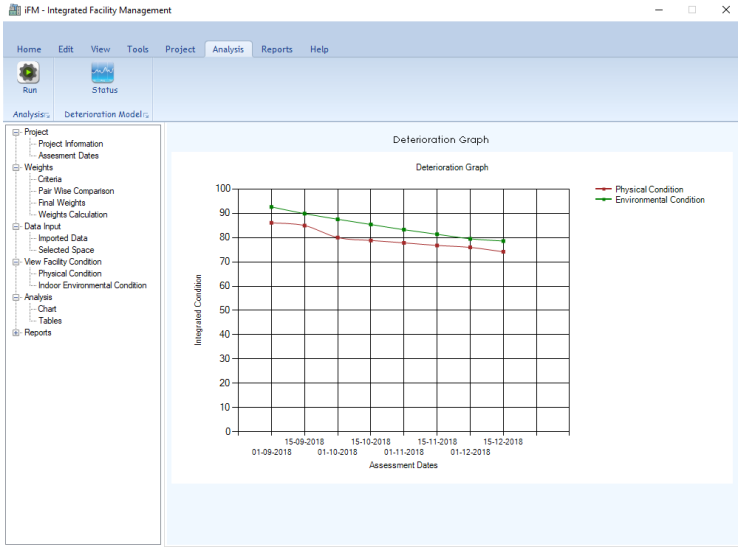

Figure 2: Deterioration graph of facility condition generated from program

The reason to use API of Rivet software for development of computer program is that the same Rivet BIM model can also be used by facility managers for other services such as space allocation management, building services management, clash detection while operation & maintenance of the facility, controlling expenditure cost by managing resources efficiently and also for meeting statutory regulatory compliances. Existing BIM models can be customized according to this program requirement to aid in inspection of building component assessment and correspondingly a deterioration model can be generated for the facility using the program developed. Further deterioration graph can be generated based on condition assessment of different period of time. Deterioration

graph based on condition assessment can serve as a benchmark for comparison for the building at different period of time. Periodic inspection of building and corresponding condition assessment will be useful to quantify the severity of deterioration of building components in order to prioritize interventions and decision making in maintenance during service life of the building. This proposed building condition assessment model can serve as key performance indicators (KPIs) which can help stakeholders to make better choices in operation, maintenance and repair of the building facilities.

4 DISCUSSION

The condition of majority of building starts declining ever since it is started being used due to external factors such as weather or factors such as inadequate maintenance along with general wear and tear (Wahida, Milton, Hamadan, Lah & Mohammed, 2012). There is a complex inter relationship between different building components and systems which depends on intended design of the building as a whole (Uzarski, Hicks & Zahorak, 2002). Buildings are composed of large number of inter-dependant elements, components and systems with complex interrelationship. Physical deterioration of the building reduces its ability to perform its intended designed function while environmental condition influences the comfort and health of occupants or users of the building. It is imperative to understand that physical and environment condition of the building are both of vital importance for safety, health and comfort of building users. In this study, factors influencing physical condition and environment condition of the building were identified and used to develop proposed condition assessment model. These factors individually or in combination of the others may lead to growth of defects in various building elements, which can have cascading effects leading to deterioration of the whole building. It is important to understand factors, which influence building condition to accurately identify probable cause of building defect under consideration for further correct diagnosis during inspection. Building defects if remain unable to detect due to incorrect diagnosis of source of problem may further worsen the condition of the building. In this study, different factors, which influence the condition of the building, were identified and BIM as interface is used to run proposed condition assessment model.

5 CONCLUSION

The aim of present research is to enable sustainable facility management and improve efficiency by integrating the complex interaction and interdependency between physical & environmental conditions of different components & systems of the facility. Cognizance of condition of building periodically can be helpful to building managers to intervene earlier on detection of minor defects. Taking appropriate remedial action as preventative maintenance could reduce time and cost required for major repair costs due to propagation of minor defects into major defects. This study can help building stakeholders and building inspection personnel to conduct condition assessment of the building using BIM as a tool. The computer program developed in this study has an advantage that it can be implemented into existing BIM models in Rivet software for facility condition assessment via Application Programming Interface (API). Future buildings constructed using BIM will generate the necessity of application of BIM in facility management.

REFERENCES

Ahzahar, N., Karim, N. A., Hassan, S. H. & Eman, J. (2011). A study of contribution factors to building failures and defects in construction industry. *Procedia Engineering*, 20, 249-255.

Al Horr, Y., Arif, M., Kaushik, A., Mazroei, A., Katafygiotou, M. & Elsarrag, E. (2016). Occupant productivity and office indoor environment quality: A review of the literature. *Building and Environment*, 105, 369-389.

Arif, M., Katafygiotou, M., Mazroei, A., Kaushik, A. & Elsarrag, E. (2016). Impact of indoor environmental quality on occupant well-being and comfort: A review of the literature. *International Journal of Sustainable Built Environment*, *5*(1), 1-11.

ASHRAE 55. (2017). *Thermal Environmental Conditions for Human Occupancy*. Atlanta, GA: American Society of Heating Refrigerating and Air-Conditioning Engineers (ASHRAE).

ASHRAE 62.1. (2016). *Ventilation for Acceptable Indoor Air Quality*. Atlanta, GA: American Society of Heating Refrigerating and Air-Conditioning Engineers (ASHRAE).

ASHRAE Guideline 10. (2016). *Interactions Affecting the Achievement of Acceptable Indoor Environments*. American Society of Heating Refrigerating and Air-Conditioning Engineers (ASHRAE).

ASHRAE Handbook. (2017). *ASHRAE Handbook, Chapter 8 Sound and vibration*. American Society of Heating Refrigerating and Air-Conditioning Engineers (ASHRAE).

BS EN 12464-1. (2011). *Light and lighting — Lighting of work places Part 1 : Indoor work places*. British Standard Institution.

Buildings Department. (2002). *Building Maintenance Guidebook*. Buildings Department, Hong Kong.

Chong, W. K. & Low, S. P. (2006). Latent building defects: causes and design strategies to prevent them. *Journal of Performance of Constructed Facilities*, *20*(3), 213-221.

Grussing, M. N., Uzarski, D. R. & Marrano, L. R. (2009). Building Infrastructure Functional Capacity Measurement Framework. *Journal of Infrastructure Systems*, *15*(4), 371-377. https://doi.org/10.1061/(ASCE)1076-0342(2009)15:4(371).

Haryati, M. I., Kharizam, I., Zainol, H. & Othman, M. F. (2016). Tracking architectural defects in university building in Malaysia. *MATEC Web Conferences, International Building Control Conference (IBCC)*, *66*, 00017. Retrieved from https://doi.org/10.1051/matecconf/20166600017.

IAQMG HKSAR. (2019). *Guidance Notes for the Management of Indoor Air Quality in Offices and Public Places*. Retrieved from https://www.iaq.gov.hk/media/82253/gn_officeandpublicplace_eng-2019.pdf.

ISO 19208. (2016). *Framework for specifying performance in buildings*. International Organization for Standardization (ISO).

Kian, P. S. (2004). A review of factors affecting building defects in Singapore. *Dimensi Teknik Sipil*, *3*(2), 64-68.

Kim, J., de Dear, R., Cândido, C., Zhang, H. & Arens, E. (2013). Gender differences in office occupant perception of indoor environmental quality (IEQ). *Building and Environment*, 70, 245-256. https://doi.org/https://doi.org/10.1016/j.buildenv.2013.08.022.

Lin, J. & Scott, D. (2006). Assessment of Significances of Building Failure Induced by Foundation Failure: Facade Failure, and Moisture Problem. *Architectural Engineering Conference*, 1-13.

https://doi.org/doi:10.1061/40798(190)26.

Maykot, J. K., Rupp, R. F. & Ghisi, E. (2018). A field study about gender and thermal comfort temperatures in office buildings. *Energy and Buildings*, 178, 254–264. https://doi.org/https://doi.org/10.1016/j.enbuild.2018.08.033.

Othman, N. L., Jaafar, M., Harun, W. M. W. & Ibrahim, F. (2015). A case study on moisture problems and building defects. *Procedia-Social and Behavioral Sciences*, 170, 27-36.

Paulo, P. V., Branco, F. & de Brito, J. (2014). BuildingsLife: A building management system. *Structure and Infrastructure Engineering*, 10(3), 388-397. https://doi.org/10.1080/15732479.2012.756919.

Rafaela, B. & Núria, F. (2018). Building Inspection System for Evaluating the Technical Performance of Existing Buildings. *Journal of Performance of Constructed Facilities*, *32*(5), 4018073. https://doi.org/10.1061/(ASCE)CF.1943-5509.0001220.

Suffian, A. (2013). Some common maintenance problems and building defects: Our experiences. *Procedia Engineering*, 54, 101-108.

Uzarski, D., Hicks, D. & Zahorak, J. (2002). Building and Building Component Condition and Capability Metrics. *Applications of Advanced Technologies in Transportation*, 441-448. https://doi.org/doi:10.1061/40632(245)56.

Wahida, R. N., Milton, G., Hamadan, N., Lah, N. M. I. B. N. & Mohammed, A. H. (2012). Building Condition Assessment Imperative and Process. *Procedia - Social and Behavioral Sciences*, 65, 775-780. https://doi.org/https://doi.org/10.1016/j.sbspro.2012.11.198.

World Health Organization (2010). *Guidelines for Indoor Air Quality: Selected Pollutants*. https://doi.org/10.1186/2041-1480-2-S2-I1.

Yacob, S., Ali, A. S. & Peng, A. Y. C. (2016). Building Condition Assessment: Lesson Learnt from Pilot Projects. *MATEC Web of Conferences, International Building Control Conference (IBCC)*, 66, 72. Kuala Lumpur, Malaysia: EDP Sciences.

Cite this article as: Faqih F., Zayed T., Soliman E., "BIM based Facility Condition Assessment", *International Conference on Civil Infrastructure and Construction (CIC 2020)*, Doha, Qatar, 2-5 February 2020, DOI:https://doi.org/10.29117/cic.2020.0022

Effective Project Control within the Context of Lean Construction

Andre F. Koluksuz
fkoluksuz@ashghal.gov.qa
Public Works Authority (Ashghal), Doha, Qatar

ABSTRACT

Two of the "Lean Thinking" principles relate to managing a project through relationships, shared knowledge and common goals and to removing waste where possible. Success of a project is only possible with the collaboration of all project participants and stakeholders throughout the entire project life cycle. Collaboration starting at the early stages of the project enables the project participants not only deliver what the owner wants, but also allows them to provide advice and help shape expectations throughout the project. In the age of technology, too much unfiltered data and information are produced quickly, making it a challenge to determine what is significant and what is not. As Project Controls is an important element of "Lean Construction" philosophy, it should be subjected to similar scrutiny to explore opportunities for improvement and for minimizing the waste. This paper will discuss how utilizing both the old and new ideas and methodologies such as the Critical Path Method (CPM), Pareto Principle and Last Planner System® (LPS) will help project managers adopt a balanced approach in selecting the optimal processes, methodologies and tools for meaningful project planning, progress monitoring and communicating the right amount of information on a timely basis.

Keywords: Lean thinking; Delay; Pareto principle; Waste

1 INTRODUCTION

According to Lean Construction Institute (LCI), currently, 70% of projects are over budget and delivered late and the results of a recent UK survey indicate that country's 10 biggest contractors made a combined margin of less than half a percent. Evidence from research and observations also indicate that the conceptual models of Construction Management and the tools it utilizes (WBS, Critical Path Method, Earned Value Management) fail to deliver projects 'on-time, at budget, and at desired quality (www.leanconstruction.org).

Findings of a large scale study on Causes of Cost Overrun in Transport Infrastructure Projects" (Flyvbjerg et al, 2004) and based on a sample of 258 rail, bridge, tunnel and road projects covering 20 nations, state that 9 out of 10 transport infrastructure projects fall victim to cost escalation, average escalation being 28%. It further states that this is a global phenomenon, although cost escalation appears to be more pronounced in developing nations than in North America and Europe. Another striking finding of the study is that cost escalation has not decreased over the past 70 years, clearly showing that no lessons are being learned.

2 PROJECT CONTROLS APPROACH

2.1 Main Challenges and Causes of Delay

Lack of "bigger team" spirit, organizational challenges and reluctance to provide honest forecasts and early warnings coupled with dependence on software tools are eroding project managers' ability to utilize judgment and to make sound decisions.

Unrealistic programmes and ineffective controls are being delivered solely to meet contractual requirements rather than being used as a tool for success. Inadequate risk identification and mitigation cause projects to fail or delay due to unforeseen events which are sometimes outside the control of the owner and the contractor.

Results of a study titled "Causes of Delay on Infrastructure Projects in Qatar" (Emam et al., 2015) shows that over 80% of infrastructure projects suffer from delays with an average delay of 25% and the top five factors were: long response times from utility agencies; major changes in design during construction; ineffective planning and scheduling; ineffective control of progress, and; changes in the scope of projects. Top ten causes mentioned in this study are tabulated along with main Lean Thinking principles which can be applied to help eliminate these causes (See Table 1).

A similar study titled "Delays in construction projects: A review of causes, need & scope for further research" based on a wider sample of developing and developed countries, has shown similar factors amongst the top ten causes (Prasad, K and Vasugi, V., 2017).

Table 1 Aligning Lean Principles with Causes of Delay on Infrastructure Projects

Cause of Delay (based on Relative Importance Index, Qatar Study, Emam, H. et al., 2015)	**Applicable LEAN Principle & Methodologies to help eliminate the cause of delay**
Long response time from utility agencies	collaboration, relationship, shared knowledge
Major change in design during construction	shared knowledge, collaboration (early stakeholder involvement)
Ineffective planning and scheduling	LPS (collaboration), minimize waste due to rework of plans/schedules
Ineffective control of progress	LPS (collaboration), minimize waste in performance measurement and reporting
Changes in the scope of the project	collaboration, shared knowledge
Slow decision-making	collaboration, relationship, shared knowledge
Delay in issuing the drawings	collaboration, shared knowledge (work prioritization)
Delay in solving design problems	collaboration, shared knowledge (parallel reviews)
Delay in approving shop drawings and sample materials	collaboration, shared knowledge (parallel reviews)
Difficulties in obtaining work permits	collaboration, relationship

It is telling that only one of the top ten reasons ("delay in issuing the drawings"), is somewhat related to production and none are related to the constructing activities, where, typically most of the focus in the construction industry has been on many projects. Construction management teams need to adopt project control approaches to tackle the true challenges. Implementing schedule risk management processes by way of producing meaningful plans, schedules and performance indicators will better mitigate the impact of uncertainties and help eliminate the main delay causes listed above.

2.2 Utilizing Pareto Principle to Reduce Waste in Project Control

Pareto Principle states that the significant few things will generally make up 80% of the whole, while the trivial many will make up about 20%. The value of the Pareto Principle is that it helps the project team to focus on what matters the most without entirely ignoring the rest. This can be applied to almost anything;

- 80% of problems will be caused by 20% of defects.
- 80% of project activities are delayed by 20% of materials.
- 80% of your results are created in 20% of your time.
- 80% of the project information is relayed with 20% of reports.
- 80% of delays will be the result of 20% of the causes.
- 80% of the desired outcome can be achieved by tackling 20% of the issues and risks.

To demonstrate how a Pareto Chart can be utilized to identify the significant few focus areas for project management teams, the top 20 causes listed in the above-mentioned study and hypothetical quantitative data are used as an example below (Figure 1).

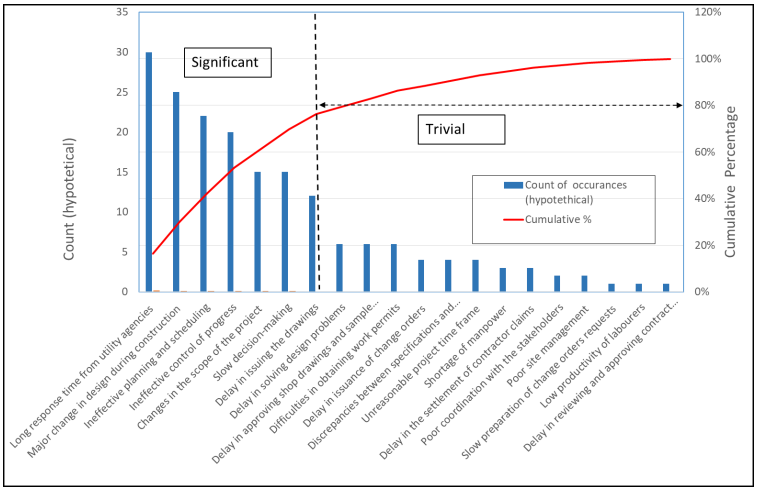

Figure 1: Pareto Chart Example for Delay Causes.

In addition to focusing on the true causes of delay, project management teams should also utilize Lean principles in implementing effective project control processes. These can include manageable size and realistic schedules detailed by phase and developed collaboratively; focusing on the critical and near critical path activities; unbiased and

realistic cost and time forecasts.

There is generally too much focus on physical works (i.e. constructing) and too little focus on less quantifiable factors, which tend to cause biggest delays. Some of those factors are:

- Unstable design and design interfaces.
- Client and/or stakeholder reviews/permits/approvals.
- Interfaces with other project contractors.
- Authority inspections, certifications.
- Test failures and rework in commissioning stage.

Risks and issues are also good candidates for applying Pareto Principle to. While tackling project risks and issues, it is reasonable to assume that most problems arise from few significant risks and issues. Regular risk reviews for large projects are crucial to identify critical programme activities associated with high risks and determine cost and schedule contingencies to mitigate the risk impact along with other mitigation measures to be put in place by the technical teams.

Last but not least, utilizing software tools for Project and Portfolio Management is another area often overemphasized despite lack of evidence that the projects executed globally in the last 20 years had any better success rates than the projects executed pre-technology age. Those who demand 100% functionality, 100% centralized system and 100% automation will fail 100%.

2.3 Last Planner System®

The main benefits of Last Planner System (Figure 2) is that the plans are generated with input from all teams to ensure collaboration and buy-in and designed to define clear outcomes and constraints in each phase to ensure reliable commitments. It also reduces wasted effort by project control teams by passing the responsibility of planning and monitoring of daily/weekly tasks to the site teams who are performing the work.

Establishing the main objective of the project, phase pull planning method, identifying and removing the constraints with make-ready planning are important elements of the LPS.

Along with benefits provided, the Last Planner System® has its shortfalls. Last Planner® does not readily provide a platform to analyse criticality and effect of changes to the master plan. When project teams or corporate management need alternate plans, “what-if” schedules are required to quickly demonstrate the effect. This is when the CPM based schedules will provide a complimentary platform to the LPS. While the ratio is not necessarily 80-20, there is generally smaller core set(s) of tasks, i.e. the “critical and near-critical paths” which are essential to project success. This is where the project teams and the project control staff should focus most of their energy.

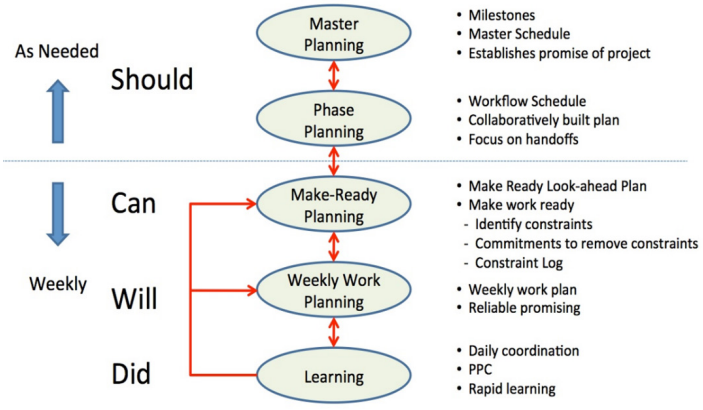

Figure 2: Last Planner System ®.

2.4 Programme Performance Indicators and Reporting

Some of the commonly used schedule performance measurement metrics such as Earned Value, SPI, which can be classified as lagging indicators, have been proven to be misleading and insufficient due to the calculation methods used and its focus on physical construction activities. Using the quantitative SPI without much reference to the schedule floats and criticality of the works can be misleading as it may hide the fact that the right amount of work is being done in the wrong place.

Forward looking (i.e. leading) Key Performance Indicator trends (KPI) such as Variance from baseline dates for Key Milestones, rate of design and material submissions/ approvals/rejections, time taken to obtain permits/approvals, percentage of weekly activities completed, resource assignment against the plan, float erosion would be more meaningful measures of the schedule performance.

On the commercial side, metrics such as turnaround time for payments, claims settlements, variation approvals, tender reviews, and percentage of materials ordered on time would also be better indicators of where the project is heading.

3 CONCLUSION

Given all the evidence and historical data, it is clear that incremental improvements and timid action, rather than a bold new approach to project control, will not make a visible difference in project performance. Construction industry has lost decades doing the same thing over and over again and expecting different results. The humble admission that everyone has their share in failure- albeit at different times and on a different scale- is sorely needed.

There is wealth of statistical and lessons learnt data in the Middle East in general and Qatar in particular thanks to the large number of megaprojects of all kinds having been completed since the awarding of FIFA World Cup to Qatar. This will provide a tremendous opportunity to all the project managers in the region and worldwide to evaluate the best practices in construction management in search of successful project execution.

Foundations of and fundamental thinking behind the Critical Path Method, Pareto

Principle and Lean Construction will help the construction industry immensely in achieving better project performance. Identifying the problems correctly and focusing efforts on the most significant challenges will enable the project control professionals to add more value and will create a positive working environment for all stakeholders and individuals towards the common goal.

REFERENCES

Emam, H., Farrell, P. & Abdelaal, M. (2015). *Causes of delay on infrastructure projects in Qatar*.

Flyvbjerg, B., Skamris Holm, M. & Buhl, S. (2004). What Causes Cost Overrun in Transport Infrastructure Projects. *Transport Reviews*, Vol. 24, No. 1, pp. 3-18.

Prasad, K. & Vasugi, V. (2017). Delays in construction projects: A review of causes, need & scope for further research. *Malaysian Construction Research Journal,* Vol. 23, No. 3, pp.89-113.

Cite this article as: Koluksuz A. F., "Effective Project Control within the Context of Lean Construction", *International Conference on Civil Infrastructure and Construction (CIC 2020)*, Doha, Qatar, 2-5 February 2020, DOI: https://doi.org/10.29117/cic.2020.0023

How Public Works Authority Has Built a Portfolio Dashboard Through Agility Approach

Abdulrahman Mchaweh
Amchaweh@Ashghal.gov.qa
Public Works Authority (Ashghal), Doha, Qatar

ABSTRACT

The aim of this paper is to share PWA experience to develop a Portfolio Performance Dashboard (PPD) that suits its unique requirements. The case study sheds light on the challenges that PWA faced to develop an interim front reporting solution that deals with multiple scattered reporting systems within the different components of the portfolio. This paper demonstrates how PWA adopted Agility project management to develop a short-term dashboard solution for executive management.

Keywords: Dashboard; Reporting; Agility; Business intelligence; Project methodologies

1 INTRODUCTION

Agility software development methodology has been gaining interest within software and solutions developers, due to appeal of the agile methodologies to the bureaucracy of the engineering methodologies (Fowler, 2005).

Using Agile methodology in software development depends on several parameters, including project size, level of complexity, integration with other systems, documentation requirements and budget.

One advantage of using the agility method its ability to predict the customer needs, these needs are traditionally collected through business analysis process, which is independent from development phase, However, agility process is iterative that incrementally develops multiple deliveries of ever-growing functionality (Fowler & Highsmith, 2001; Salah et al., 2014).

PWA in Qatar has been deploying and searching for a PPD for several years, the aim is to have simple, concise, and meaningful information on the status of the portfolio and its major components.

Business intelligence system based on S.A.P was under consideration, but several challenges such as time required designing and implementing, data integration and other issues, called for pragmatic solution that utilizes the available data. Among the options that suite the circumstances were Tableau and Microsoft BI.

2 PROJECT ASSUMPTIONS

Various reasons qualified the selection of Tableau, among those is the management previous experience with the solution, the cost of the solution and the ability to fill the gap as to interim solution until organization set “BI Strategy”.

Among the advantages of the interim PPD is having overarching solution on top of current “Systems structure” without wholesale change that impacts the ongoing operations, and elimination of many reports to C-level.

Development team has taken into considerations the organizations structure and data integration level to design a suitable solution that aimed to:

1. Deliver executive management dashboard within 3 months.
2. Work with the departments that have reasonable performance data.
3. Reflect and agree on simple processes that generate information quickly.
4. Standardizations of key information and terminologies.

3 BUILDING THE PROJECT TEAM

PWA senior management tasked the corporate Project Management Office (PMO) to lead the project development in collaboration with Information technology department to support aspects such as, application Licenses and Dashboard developers.

The selection criteria that qualifies Tableau to build PPD is:

1. Application license is affordable.
2. The solution is applicable to link to several databases such as Excel and Oracle Tableau.
3. Tableau Reader Application for end users is free and could be installed on standard systems in PWA.
4. Intuitive and rich user interface.
5. Previous management experience with the solution.
6. Tableau dashboard to serve as an interim solution.

The core development team consists of planning engineers; project advisor and one Tableau developer. The initial requirements are collected through workshops with senior and middle management; all draft designs were demonstrated using power point slides to effectively communicate initial thoughts without investing time and effort in building modules using sophisticated dashboard solution.

Due to lack of centralized portfolio database that includes program data, commercial aspects and quality parameters, Excel is the most pragmatic tool collect data. The spreadsheets include performance and commercial data in addition to high-level risk, quality and procurement information; however, data collection and data quality remain the key challenges for the project team.

Additionally, the rigid organization structure is a key aspect to important parameters consider in building PPD. The reporting function was assigned to a particular business unit while the information technology department is mandated to deliver (software solutions) irrespective of the projected environment of the organization.

4 PROJECT MANAGEMENT APPROACH TO DELIVER THE SOLUTION

The team lead set a clear plan to deliver the solution to meet tight time constraints using agility process where:

1. Each deliverable was managed as an independent project.
2. User testing process was done during the development phase, the feedbacks and challenges are used as a lesson learned for further development.
3. Started with of 5 Tableau desktop licenses and more added as the development proceeds.
4. Build standards and definitions template and get data owner's buy-in.
5. Assign focal points within the departments to manage data collection, data quality and data acceptance processes.

6. Build data collection templates, a complete workbook is designed, it contained 17 sheets to collect all data sets from different departments.
7. Daily review meeting to review project progress and assign tasks. All tasks managed internally using a shared task list.
8. Adding value to current reports, through linking GIS (data to identify project locations.

5 CHALLENGES DURING THE PLANNING AND IMPLEMENTATION PHASES

Over the project lifecycle, several challenges were identified. Some are unique and related to the organization data 'structure, others are common in fast delivery software projects. Among those are:

1. The developers usually do not understand construction jargons; this creates barriers between the developer and the users.
2. Challenging timeframes to deliver the dashboards solution to management.
3. Bringing the internal departments to speed, arrangements were needed to develop new data sets, agree on definitions, standards, user acceptance and delivery dates.
4. Continuous collaboration and coordination between IT department and reporting team to deliver the solution to the satisfaction of senior management.
5. New requirements, new schemes, new initiatives and new stakeholders.

6 RESULTS

The team was able to deliver the PPD within 3 months and obtain management approval on the final dashboard. During the following year, more than 10 dashboards were developed for highway projects, local roads projects, drainage projects and building departments

The departments showed interest in Tableau, several departments requested to use dashboard to replace current reports and get advantages of rich graphical interface and the ability to connect to several data sources.

The lessons learned from each dashboard used as an input to improve next release of the dashboard and management team was able to augment the knowledge needed to link data sources and capture results.

Senior management and Information technology department considered Tableau as one of the potential solutions to include as a part of the Business intelligence strategy.

7 CONCLUSION

Agility process is gaining interest in software development mainly for fast track projects that have limited resources. This process motivate the teams and provide high learning in addition to its clear advantage in controlling the final product specifications.

However, managing project teams, scope creep and lack of clear business requirements are main obstacles to develop powerful PPD, furthermore, Management support of is key for the success those initiatives.

REFERENCES

Fowler, M. (2005). The new methodology. *Software. World*, Vol. 36, No. 1, pp. 3-6.

Fowler, M. & Highsmith, J. (2001). *The agile manifesto*, pages 3.

Salah, D., Paige, R. F. & Cairns, P. (2014). A systematic literature review for Agile development processes and user centered design integration. *ACM Int. Conf. Proceeding Ser.*, No. May 2014.

Cite this article as: Mchaweh A., "How Public Works Authority Has Built a Portfolio Dashboard Through Agility Approach", International Conference on Civil Infrastructure and Construction (CIC 2020), Doha, Qatar, 2-5 February 2020, DOI: https://doi.org/10.29117/cic.2020.0024

Design and Construction Risk Management of Souq Waqif Station of Gold Line, Doha Metro

Spyridon Konstantis
skonstantis@qr.com.qa
Qatar Rail, Doha, Qatar

Spyros Massinas
smassinas@goldlinemetro.qa
ALYSJ JV, Doha, Qatar

ABSTRACT

The case of redesigning Souq Waqif station by raising the base slab formation level due to significant water inflow during the excavation and dewatering works and the break in activities of two EPB TBMs under adverse hydrogeological conditions is presented. The station is at close proximity with a structure of great heritage value and the monitoring records prior to TBM break in, indicated unacceptable ground deformation values. Back analyses were performed and contingency measures defined and implemented on site. The station redesign had also to take into consideration an adjacent future development affecting the station, the design basement levels of which increased during the station excavation.

Keywords: Station; Water ingress; Ground deformations; Stability; Redesign

1 INTRODUCTION

The Doha Metro Gold Line is part of the Qatar Integrated Railway Project (QIRP) and as shown in Figure 1 it extends from Ras Bu Abboud Station in the east (near Hamad International Airport), crosses Msheireb Major Station and reaches Al Aziziyah in the west (near Aspire Zone). The line comprises approximately 15km of twin bore TBM tunnels, 24 cross passages and a number of underground structures, including 11 stations (Msheireb station was built by others), an underground stabling yard with light maintenance and washing facilities, switchboxes and an emergency exit. The project was awarded to ALYSJ Joint Venture, formed by Aktor of Greece, Larsen & Toubro of India, Yapi Merkezi & STFA of Turkey and Al Jaber Engineering of Qatar.

Souq Waqif station is located on the tunnel section between the Musheireb main interchange and the National Museum of Qatar stations. It is a 226m long and approximately 26m deep station constructed as a single integral reinforced concrete structure with the cut and cover method. In close proximity and inside the construction influence zone of the station and the twin bore tunnels, a Mosque complex structure of great heritage value for the State of Qatar is located (see Figure 2).

During the temporary works and dewatering activities for the station excavation with approximately 2m left until the formation level and prior to the arrival of the two EPB TBMs, significant water inflow occurred mainly from the bottom of the excavation. Given the schedule criticality and constraints for casting the station slab to enable passing through of the TBMs, it was decided to modify the original station design and raise the

base slab formation level. From a tunnel alignment point of view, this was feasible as the TBMs were in a sufficient distance from the station and the alignment could be accordingly adjusted. The station redesign had also to take into consideration the future PEO (Private Engineering Office) development on the north side of the station, which was foreseen to have 4 basements and was planned to be constructed while the station would be operational.

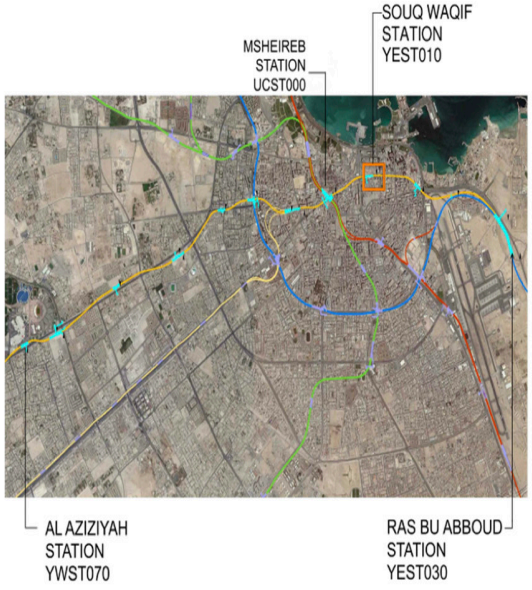

Figure 1: Doha Metro (Gold Line alignment is shown with yellow color)

In addition to the water inflow, ground deformations on the east headwall, near the Mosque occurred which exceeded the predefined trigger levels (Construction impact Stage 3, 2019). In order to ensure the integrity of the Mosque from the induced ground deformations and the safe reception of the two TBMs through the east headwall, a back analysis was performed and contingency measures were defined and implemented on site, as per the response action plan (Konstantis & Massinas, 2017).

Figure 2: Souq Waqif station plan view

2 GEOTECHNICAL AND HYDRO-GEOLOGICAL CONDITIONS

The geological units of the concerned area can be grouped into four main categories from newest to oldest geologically: superficial material (made ground, quaternary deposits and/or residual soil deposits); Simsima Limestone with varying degrees of weathering; Midra Shale and Rus Formation (Geotechnical Interpretive Report, 2019). Due to the presence of limestone type geological units, an assessment on the presence of cavities and voids was made prior to the station excavation based on the information provided by the additional geotechnical investigations, in addition to the geophysical campaign. Small karst features had been identified within the footprint of the station but such features were interpreted to be small and were assessed as unlike to affect the temporary works and construction activities. In Figure 3, the as built hydrological conditions are presented, where the active dewatering was capable to develop a drawdown groundwater depression cone.

On the 25th August 2015, during the excavation works and with approximately 2m remaining ground to be excavated until the base slab formation level was reached, a karstic feature was encountered resulting in excessive water inflows inside the station (Figure 4). This adverse condition posed great difficulties to the continuation of the station excavation and hindered the base slab casting to enable the timely passing through of the approaching TBMs, a critical schedule activity associated with contractual milestones. Prior to encountering the karst feature, the water inflow recorded due to the active dewatering was around 12,000m3/day, whereas post the occurrence of the event, the water inflow recorded was 24,600m3/day as an average value with a recorded maximum of 56,688m3/day.

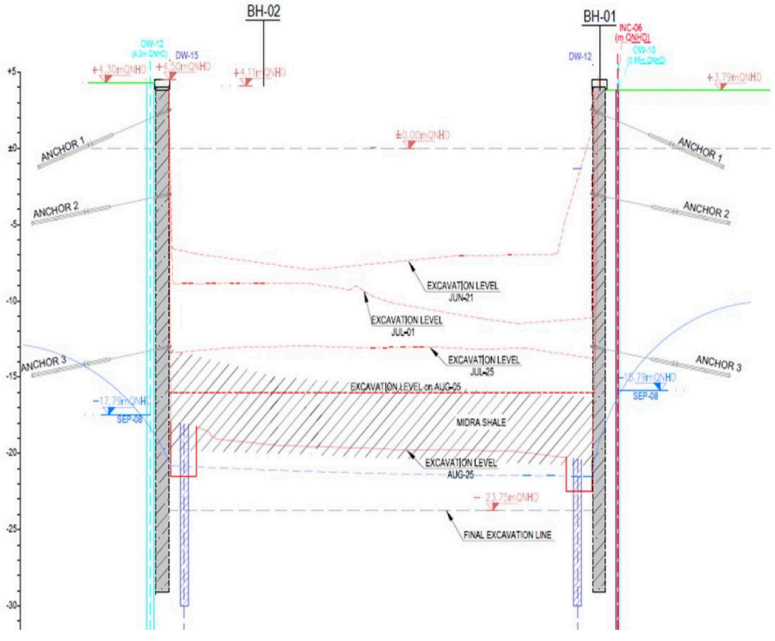

Figure 3: Prevailing hydrogeological conditions and active dewatering with dewatering wells

Figure 4: Water ingress inside the station due to karstic feature

In order to identify the location, extent and condition of the karstic feature, additional geotechnical investigations were carried out, including a thorough MASW geophysical campaign (see Figure 5, left). Following a comprehensive and thorough analysis and interpretation of all the available information, the possible configuration and extent of the karstic feature was determined (see Figure 5, right), which was gradually and carefully filled and sealed with grout. In addition, before the re-commencement of the works and in order to further investigate the possibility of more and possibly interconnected karsts, additional geophysical surveys were executed. As per the results, no further karst features or channels were found.

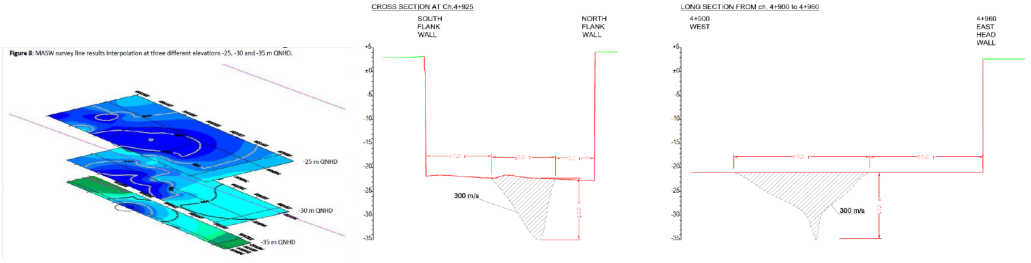

Figure 5: MASW survey line results interpolation at different elevations (left) and configuration and extent of the encountered karstic feature (right)

3 ORIGINAL STATION DESIGN

The original station design foresaw a 3.4m layer of unreinforced concrete over the station base slab to counterbalance the buoyancy effect (see Figure 6). Due to the planned future development next to the station box and the requirement for direct connection of the station's concourse level with the development, there was very limited overburden available for landscape purposes and utilities, which was practically neglected in the flotation checks. In addition and as per the Qatar Rail Employer's Requirements, the groundwater design level was considered to be on the ground surface. That was considered the worst case given the proximity of the station to the sea and the adjacent construction and dewatering works, which were taking place concurrently in the area. In fact and based on past aerial photographs, it was identified that the station was located very close to the original coastline.

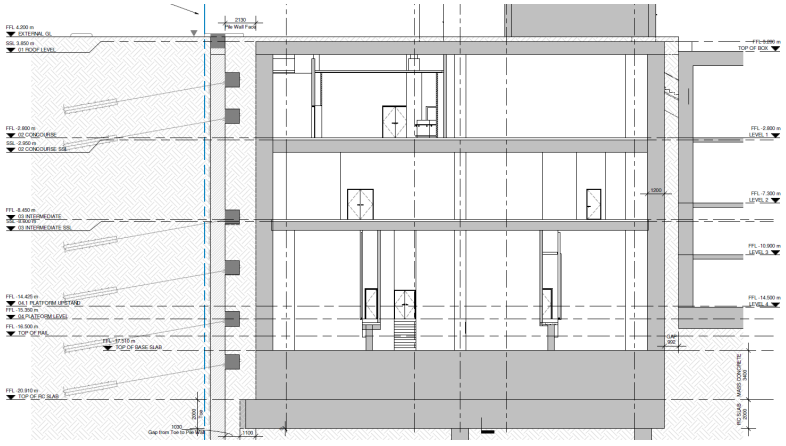

Figure 6: Station cross section of the original design

The station's ELS (Excavation and Lateral Support) was based on the Geotechnical Interpretative Report (GIR) findings and comprised contiguous and soldier anchored pile wall. With regards to groundwater inflow and management, the design assumption was made that the water table draw-down would be achieved with manageable water inflow quantities. Thus no water-tight system was foreseen to be required. Any possible water pressure at the Midra Shale layer would be relieved by systematic installation of drainage holes. As a groundwater control risk mitigation measure, the design specified grouting to be executed in the perimeter of the excavation for void filling. As per the original design, the formation level was foreseen in -22.9m QNHD (Qatar National Height Data). When the karstic featured was encountered, the excavation level in that area had reached approximately -20.5m QNHD.

4 MODIFIED STATION DESIGN

As already mentioned above, the schedule criticality of the passing through of the approaching TBMs necessitated the urgent casting of the station's base slab without delay. Given the prevailing conditions, the risk of reactivating the sealed karstic feature or encountering new ones during the remaining excavation works and thus causing again excessive water inflow in the excavation pit was assessed as high and classified as unacceptable. Therefore the decision was taken to halt the excavation works at the level reached and modify the structural design of the station by raising the base slab to the already excavated level. In order to counterbalance the buoyancy and satisfy the minimum acceptable factors of safety against flotation with the reduced base slab mass, several options were considered and evaluated (see Figure 7).

The option of constructing tension piles was rejected due to the increased construction costs, schedule constraints as well as the durability requirements and the high risk of re-activating the sealed karst or encountering other karsts. Other options considered were the connection of the station concrete structure with the excavation support pile wall with dowels or the construction of a base slab shear key. However both options were also discarded mainly due to the additional construction costs, the questionable durability of the pile temporary wall and the schedule constraints in constructing the shear key.

The option finally adopted was to mobilize the interface resistance between the station and the ground (see Figure 8) and increase the dead weight of the concrete structure by increasing the wall thicknesses, where possible. This option eliminated the schedule risks as any additional works required (e.g. increase of thickness of the concrete walls) could be constructed following the reception, transfer and relaunch of the TBMs.

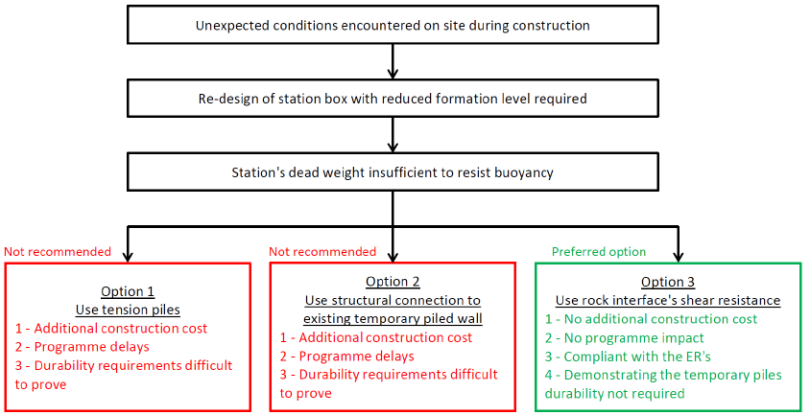

Figure 7: Comparative assessment of alternatives considered to counterbalance buoyancy

At the same time and as the design of the adjacent future development was in parallel progress, it was identified through the stakeholder interface and coordination management that the future structure's design foresaw the excavation formation level at approximately -19m QHND. That meant that when the future development would be excavated next to the operational station, the station box would then be subject to asymmetric lateral loading, with soil and water pressure acting only on one side. The analysis determined that this asymmetric loading and in particular the water pressure would lead to overturning and sliding of the station box with detrimental effects since the potential movement of the concrete box would result in damages to the operational station/tunnel segmental lining interface in a water bearing regime.

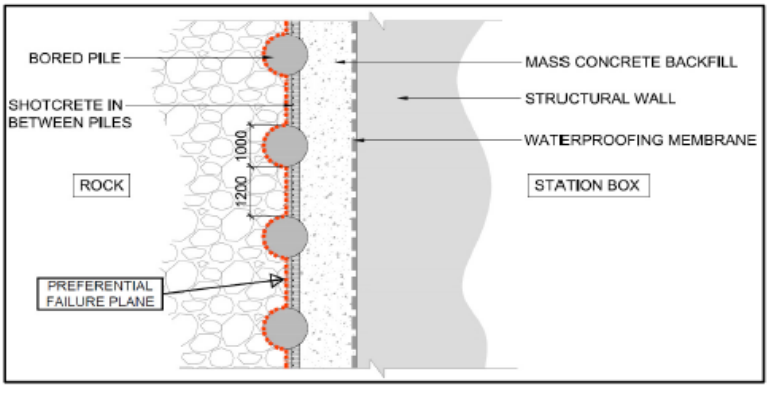

Figure 8: Plan cross section of the station box permanent and temporary works interface

As per the Qatar Rail Employer Requirements and the applicable Qatari Law, any third party structures located inside the Final Rail Route Approval and in particular

the defined Protection Zone must receive a No Objection Certificate (NOC) for any construction works. In this process, certain restrictions and conditions can be set by Qatar Rail in the design and construction execution and method statements of these structures in order to ensure than no adverse impact on the Rail assets will occur.

In order thus to ensure that no asymmetric water pressures would be exerted on the station, the condition was set that continuous dewatering will have to take place during the future construction until the future structure is constructed and the backfill in between the station and the development is in place (see Figure 9).

For the dewatering activities during the excavation of the station box, dewatering wells were installed in the perimeter of the station between the temporary support pile wall and the extrados of the station external walls. The dewatering wells on the south wall were retained with the objective to be handed over to the contractor of the future development to carry out the necessary dewatering works as outlined above.

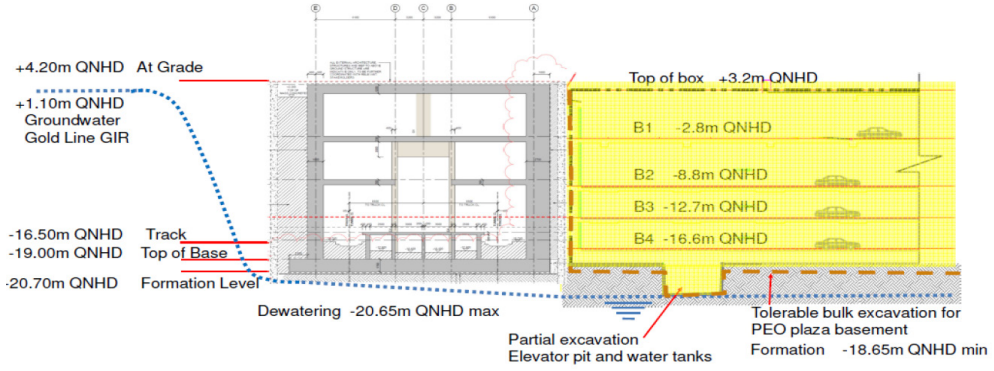

Figure 4: Cross Section of Future Development Excavation and Groundwater Control

Figure 9: Cross Section of future development excavation and groundwater control

Given the criticality of the future dewatering works with respect to the station's structural integrity and robustness, a thorough risk assessment was carried out with the objective to put appropriate measures in place and reduce the risk to As Low As Reasonably Practicable (ALARP). One of the major technical and construction risk identified was the blocking of the retained dewatering wells. Thus, an effort was made, albeit the tight spatial constraints, to configure this area in such a way that new dewatering wells could be installed. In some cases, positions for new dewatering wells were preselected and the installation of the casing in the top meters was carried out to enable insertion of the drilling rig without the need for utility diversions or removal of any other obstacles (see Figure 10).

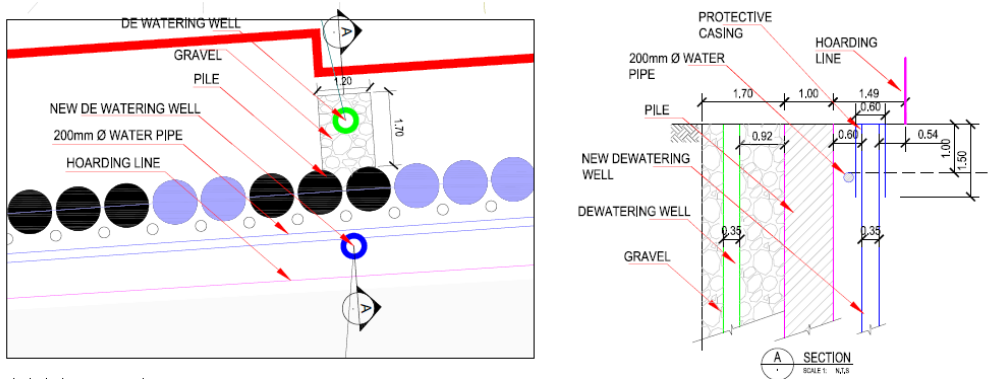

Figure 10: Dewatering wells encasement detail

In addition and in order to ensure that the groundwater flow path shown in Figure 9 will be retained during the future dewatering activities and no water pressure will be exerted on the station base slab, transverse drain channels were introduced and constructed below the slab.

As per the original design, the area between the temporary support pile wall and the external wall of the station would be backfilled with permeable rock type fill material. With this configuration in place, the groundwater would be filtered and led to the pumps inside the dewatering wells and any overpressure would be relieved through the drainage channels below the base slab. However, given the spatial constraints which dictated the backfilling and compaction equipment to be used, the productivity rate was lower than anticipated. Hence in order to improve the backfill construction performance which would also enable the earlier decommissioning of the dewatering system, it was decided by the contractor to replace the rock type fill with lean concrete. The backfill with impermeable material necessitated thus the construction of an encasement around the dewatering well, which was filled with permeable material (see Figure 10 and Figure 11).

Figure 11: Encased dewatering well inside the lean concrete backfill

5 CONCLUSION

Despite the tight and challenging schedule constraints and the significant water inflow which occurred during the excavation works, which necessitated the design modification of the station during its construction, as well as the concurrent ground deformations on the east headwall which exceeded the predefined trigger levels, the base slab was cast on time, the TBMs arrived without any issues and they continued their journey towards their successful final breakthrough which occurred prior to the contractual milestone.

ACKNOWLEDGEMENTS

The authors would like to thank Qatar Rail and ALYSJ JV for their permission to publish this article.

REFERENCES

Construction impact Stage 3 (2019). Risk assessment for Complex Mosque at Souq Waqif Station, Qatar Rail.

Geotechnical Interpretive Report (2019). Souq Waqif Station, Qatar Rail.

Konstantis, S. & Massinas, S. (2017). Qatar Rail, Doha Metro – Gold Line Project / Assessment of TBM breaking-in activity into Souq Waqif station under adverse conditions. *ITA World Tunnel Congress 2017*.

Cite this article as: Konstantis S., Massinas S., "Design and Construction Risk Management of Souq Waqif Station of Gold Line, Doha Metro", International Conference on Civil Infrastructure and Construction (CIC 2020), Doha, Qatar, 2-5 February 2020, DOI: https://doi.org/10.29117/cic.2020.0025

Variation Orders in Building Projects in Khartoum State-Sudan: The Causes and the Impact on Projects Performance

Eltahir Elshaikh
schoolcivil@yahoo.com
Construction Engineering Department, Sudan University of Science and Technology, Khartoum, Sudan

Salma Mahmoud
salmaymm@gmail.com
Civil Engineering Department, University of Science and Technology, Khartoum, Sudan

ABSTRACT

Occurrence of variation orders (VOs) is a common phenomenon in building projects and a challenging feature. Opinions and feedback of the stakeholders of building projects at Khartoum State – Sudan were investigated to identify and rank the key factors that cause VOs and evaluate their consequent impact on projects' performance. 10 projects were thoroughly analyzed to determine how their performance was affected by the occurrence of VOs and in conjunction with this an industry wide survey that was conducted to determine the frequency of occurrence of a previously compiled list of factors. 130 respondents -contractors, consultants, projects' owners and project managers-took part in the survey. Considering the frequency of occurrence and the strength of their impact, the relative importance index from the participants' feedback was calculated allowing the ranking of the factors causing VOs. It was found that the main causes for VOs emerged from the owners' side and are mainly attributed to changing his needs or scope of work. It was also confirmed that there is a significant relationship between the occurrence of VOs and projects' time extension (by 22-200%) and cost overrun (by 2.67-42.86).

Keywords: Variation orders; Khartoum; Sudan; Building projects

1 INTRODUCTION

The building industry is one of the largest industries in the world. Sudan, as one of the developing countries, put some efforts to commit a reasonable share of their annual budgets for the building sector. With best efforts to execute the projects as planned for, the occurrence of VOs is still a common feature and a recurring phenomenon in most if not all building projects stakeholders in Khartoum State Sudan. VOs depict any deviation from the agreed upon (scope, time, cost or quality) among the project's stakeholders (Osman et al, 2010). Concerns and some preliminary, informal investigations with some construction managers in Sudan, revealed that VOs are viewed as a major source of nuisance leading to contract over budget and time extension problems. Consequently, this study was launched to investigate the root causes of VOs in building projects in Khartoum State- Sudan as viewed from the perspective of all the stakeholders and to evaluate their impact on some selected project performance dimensions.

2 PREVIOUS STUDIES

Previous studies that considered the same phenomenon but in their own settings were

consulted. That made it possible to compile a list of factors, which are highlighted as causes of VOs in construction projects. A study in Gaza Strip described 64 factors among which "lack of materials and equipment spare parts, design change by consultant, lack of consultant's experience, design errors and omission, conflicts between contract documents, owner's financial problems, lack of coordination among project parties, and change is specification by owners" were the most significant (Enshassi et al., 2010). With a similar study geared towards the investigation of VOs in highway projects, (Wu et al., 2005) differentiated between external and internal causes where he considered the external causes to include factors such as political, economic, natural environmental aspects and third party. On the other hand, he classified the internal causes as those initiated by the owner, construction design consultant, contractor or other parties.

Studies on VOs in Oman, as described by (Alnuaimi et al., 2010) confirmed that clients' additional works or design modifications come at the top of the list of frequently occurring and most influential factors while adding the unavailability of formal construction manuals and procedures besides some quality related issues as other causes. With a proven adverse impact on project s' performance, VOs effect on productivity and project costs was reported by (Cox, 1997) who viewed then as unwanted but inevitable source for cost escalation, time overrun and declining quality.

3 MATERIALS AND METHODS

To tackle the stated problem and allow measuring the stakeholders' opinions regarding the raised concerns, both qualitative and quantitative approaches were adopted.

3.1 Preliminary Investigation

In the preliminary stage, an in-depth investigation was conducted through the study of 10 building projects developed and executed at the State of Khartoum, Sudan during a range of 8 years covering the period (2007-2015). For each project the contract documents and progress reports were reviewed to provide a clear explanation of the actual deviations that took place and allow spotting the causes and the probable impact on the overall project performance. After defining and meticulously tracking the VOs occurred, the projects' participants were interviewed to give an account on what they think the actual causes and hence the possible consequences as happening within their context.

3.2 Industry Survey

The preliminary investigation was followed by an industry-wide survey to validate the preliminary outcomes from the studied cases and to allow generalizing the results. A questionnaire form was designed, tested and translated then devised as a tool to collect the required data. Part of the questionnaire included a close-ended question comprising 28 factors, previously highlighted in the literature and the studied cases, as the main causes of VOs. Depending on their experience, respondents were asked to state the frequency of occurrence of each of the listed factors against a 5-points Likert scale. Another question was devised to measure the possible impact of VOs on the project performance as viewed by the project participants. The participants responded by weighting the impact on cost and time and the weighted average for their feedback was determined.

3.2.1 Sample Size and Configuration

The survey participants were client, civil engineering contractors, consultants and project managers and were randomly selected from the official reference lists of the Sudanese Contractors Union and the Council of Organizations of Consultants in Sudan. The sample size was determined on the basis of statistical principles for this type of exploratory research following equations (1) and (2) as described in the literature for this type of research (Yin, 2009; Palinkas et al., 2015):

$$n_0 = (P * q) / V^2 \quad (1)$$

$$n = n_0 / [1 + (n_0 / N)] \quad (2)$$

Where:

n_0: first estimate of sample size,

P: the proportion of the characteristic being measured in the target population,

q: complement of 'p' or 1-p,

V: maximum standard error allowed,

N: population size,

n: sample size.

180 responses were targeted from the four major groups who represent the projects' stakeholders. 130 respondents successfully participated in the survey. Table 1 portrays the sample configuration and the response rate.

Table 1: Survey Sample Configuration

Respondents category	Questionnaire		
	Copies distributed	Copies returned	Response rate (%)
Clients	35	23	65.71
Contractors	70	53	75.71
Consultants	60	47	78.33
Project managers	15	7	46.67
Total	180	130	72.2

3.2.2 Data Analysis

The Statistical Package for Social Sciences (SPSS) version 21.0. was used for the analysis of the obtained data where the reliability test was performed to measure the degree to which a research instrument (questionnaire) yields consistent results or data after repeated trials. A commonly accepted rule of thumb for describing internal consistency using Cronbach's alpha as described in the literature by (Kombo & Tromp, 2006) is as stated in Table 2.

Table 2: Cronbach's alpha consistency rule

Cronbach's Coefficient Alpha	Internal Consistency Remarks
$\alpha \geq 0.9$	Excellent
$0.7 \leq \alpha < 0.9$	Good
$0.6 \leq \alpha < 0.7$	Acceptable
$0.5 \leq \alpha < 0.6$	Poor
$\alpha < 0.5$	Unacceptable

The Cronbach's alpha coefficient value for the questionnaire was 0.857. This value according to table 2, indicates that the questionnaire items form a scale that has good internal consistency that could be used as a reliable data collection tool.

(RII) was calculated according to equation (3) as described in (Mohammed et al, 2017)

$$RII = (5x5 + 4x4 + 3x3 + 2x2 + x1)/(5 * N) \quad (3)$$

Where:

X_i: the number of respondents who selected the option of impact;

N: the total number of respondents.

4 RESULTS ANALYSIS AND DISCUSSION

4.1 Preliminary results

Table 3 shows the results that emerged from the studied cases. The calculations of the percentage increase in cost and time due to VOs were presented. It is evident for the investigated projects that a substantial majority (75%) of the recorded causes for VOs were related to the owner's changing needs, scope of work, change of materials prices of in local market, changing government regulations and legislation and change in the project use. I was also found that a direct relationship exists between the presence of VOs and the project's time increase. It was noticed that the projects' durations were extended by (22-200) % due to VOs while the cost analysis exercise showed over budget expenses to increase by (2.67-42.86) % due to VOs.

Table 3: Variation orders and their impact on projects' cost and time

Studies Projects	Causes of Occurrence of Variation Orders	Impact of VOs on the Project Dimensions					
		Cost			Time		
		Initial Contract Cost (Million SDG)	Final Contract Cost (Million SDG)	% of Increase in the contract cost	Initial Project Duration (Month)	Final Project Duration (Month)	% of Increase in the project duration
Project (1)	• Change use of building • Design Changes, • Instability of prices	140	200	42.86	24	42	75
Project (2)	• Client's changing needs • Design Changes • Instability of prices	6,	7.5	25	12	16	33
Project (3)	• Client's changing needs • Design Changes	8	8.42	5.25	18	22	22
Project (4)	• Client's changing needs • Design Changes	2.5	2.85	14	12	21	75
Project (5)	• Changing government regulations and legislation	4	5	25	9	27	200
Project (6)	• Client's changing needs • Change use of building • Design Changes	22	22..91	4.14	20	35	75
Project (7)	• Client's changing needs • Change use of building • Design Changes	17..5	19.9	13.71	12	18	50
Project (8)	• Client's changing needs • Design Changes	140	161	15	18	54	200
Project (9)	• Client's changing needs • Design Changes	6	6.16	2.67	18	30	66.67
Project (10)	• Change the Scope of Work • Design Changes	30	32	6.67	12	22	83

4.2 Industry Survey Results

4.2.1 Frequency of occurrence of the factors causing VOs

Based on the assertion that VOs could be caused by several factors with a variable impact levels, the weighted averages for respondents' opinions made it possible to rank the factors depending on the frequency of their occurrence as depicted in table 4.

The results showed that the most frequently occurring factors causing VOs are:(1) Lack of stability of prices and the exchange rate change, (2) New government regulations, (3) Non availability of construction manual and procedure for construction project in Sudan, (4) Errors and omissions in design ,two factors in the same ranking (5) Owner fails to make decisions or review document at the right time and Owner's needs during the design stage are not well-defined or variably , (7) Owner's financial problems ,two factors in the same ranking (8) Contractors financial difficulties and The lack of coordination between consultant and contractors and subcontractors and (10) Non-use value engineering in design stage to find the best alternatives and providing cost.

Table 4: Factors causing VOs and their impact on cost and time

Factor	Factor Description	Very Often	Often	Sometimes	Seldom	Never	Relative Importance Index
F 1	Owner's financial problems	74	33	15	3	5	0.86
		56.92%	25.38%	11.54%	2.31%	3.85%	
F 2	Change of plan by Owner	75	20	25	9	1	0.84
		57.69%	15.38%	19.23%	6.92%	0.77%	
F 3	Change of Scope by Owner	72	28	21	6	3	0.85
		55.38%	21.54%	16.15%	4.62%	2.31%	
F 4	Owner fails to maintain hold on the project schedule.	69	21	24	12	4	0.81
		53.08%	16.15%	18.46%	9.23%	3.08%	
F 5	Owner fails to make decisions or review document at the right time.	85	24	15	4	2	0.89
		65.38%	18.46%	11.54%	3.08%	1.54%	
F 6	Owner's needs during the design stage are not well-defined or variably.	87	21	15	5	2	0.89
		66.92%	16.15%	11.54%	3.85%	1.54%	
F 7	Change in design by engineer or consultant	64	27	25	8	6	0.81
		49.23%	20.77%	19.23%	6.15%	4.62%	
F 8	Conflict between contract documents	81	19	14	8	8	0.84
		62.31%	14.62%	10.77%	6.15%	6.15%	
F 9	Errors and omissions in design	90	22	9	4	5	0.89
		69.23%	16.92%	6.92%	3.08%	3.85%	
F 10	The scope of work for the contractor is not well defined	80	16	20	7	7	0.84
		61.54%	12.31%	15.38%	5.38%	5.38%	
F 11	Technology changes	72	26	16	7	9	0.82
		55.38%	20.00%	12.31%	5.38%	6.92%	
F 12	The lack of coordination between consultant and contractors and subcontractors	84	17	18	3	8	0.86
		64.62%	13.08%	13.85%	2.31%	6.15%	
F 13	Differing site conditions	76	17	19	5	13	0.81
		58.46%	13.08%	14.62%	3.85%	10.00%	
F 14	Contractors financial difficulties	82	21	15	6	6	0.86
		63.08%	16.15%	11.54%	4.62%	4.62%	
F 15	The required labor skill are not available	76	23	17	12	2	0.84
		58.46%	17.69%	13.08%	9.23%	1.54%	
F 16	The required equipment and tools are not available	72	23	17	11	7	0.82
		55.38%	17.69%	13.08%	8.46%	5.38%	
F 17	Material not meeting the specifications	72	17	14	9	18	0.78
		55.38%	13.08%	10.77%	6.92%	13.85%	
F 18	Contractor desire to improve his financial conditions	72	19	13	8	18	0.78
		55.38%	14.62%	10.00%	6.15%	13.85%	

F 19	construction delay by other contractors working on different contracts	80	21	11	15	3	0.85
		61.54%	16.15%	8.46%	11.54%	2.31%	
F 20	Acceleration of work Safety consideration / emergency field conditions	67	26	14	15	8	0.80
		51.54%	20.00%	10.77%	11.54%	6.15%	
F 21	Weather conditions	70	16	18	17	9	0.79
		53.85%	12.31%	13.85%	13.08%	6.92%	
F 22	Demolition and re-work	60	22	14	13	21	0.73
		46.15%	16.92%	10.77%	10.00%	16.15%	
F 23	Difference between the design and the actual construction on site	76	13	16	9	16	0.79
		58.46%	10.00%	12.31%	6.92%	12.31%	
F 24	New government regulations	99	19	8	4	0	0.93
		76.15%	14.62%	6.15%	3.08%	0.00%	
F 25	Lack of stability of prices and the exchange rate change	107	17	3	3	0	0.95
		82.31%	13.08%	2.31%	2.31%	0.00%	
F 26	Non-use value engineering in design stage to find the best alternatives and providing cost	86	14	14	11	5	0.85
		66.15%	10.77%	10.77%	8.46%	3.85%	
F 27	Non availability of construction manual and procedure for construction project in Sudan	97	16	10	3	4	0.91
		74.62%	12.31%	7.69%	2.31%	3.08%	
F 28	Obstinate nature of owner and consultant	60	17	10	19	24	0.71
		46.15%	13.08%	7.69%	14.62%	18.46%	

4.2.2 Impact of VOs on projects' time and cost performance

With a variable impact level, respondents were asked to give their opinion to help gauging the impact of VOs on projects' performance. The results obtained are as presented in Table 5.

Table 5 shows the respondents' feedback summary on weighting the impact of VOs on projects' performance. That included workers decreased productivity, (2) Increase the cost of the projects, (3) Delay in completion schedule, (4) Disputes between owners and contractor , (5) Decrease in quality of work, (6) Increase in overhead expenses, (7) Increase in duration of individual activities, (8) Demolition and re – work, (9) Delay in payments (10) Hold on work in other areas, (11) Additional money for contractor.

Table 5: Impact of VOs on projects cost and time performance

Impact	very Often	Often	Sometimes	Seldom	Never	Relative Importance Index
Increase the cost of the projects	89	30	11	0	0	0.92
	68.46%	23.08%	8.46%	0.00%	0.00%	
Increase in duration of individual activities	68	33	13	13	3	0.83
	52.31%	25.38%	10.00%	10.00%	2.31%	
Delay in completion schedule	94	17	9	7	3	0.90
	72.31%	13.08%	6.92%	5.38%	2.31%	
Delay in payments	75	18	14	13	10	0.81
	57.69%	13.85%	10.77%	10.00%	7.69%	
Demolition and re – work	78	15	16	15	6	0.82
	60.00%	11.54%	12.31%	11.54%	4.62%	

Decrease in productivity of workers	97	19	11	3	0	0.92
	74.62%	14.62%	8.46%	2.31%	0.00%	
Increase in overhead expenses	82	21	7	15	5	0.85
	63.08%	16.15%	5.38%	11.54%	3.85%	
Decrease in quality of work	91	18	7	6	8	0.87
	70.00%	13.85%	5.38%	4.62%	6.15%	
Disputes between owners and contractor	91	15	12	12	0	0.88
	70.00%	11.54%	9.23%	9.23%	0.00%	
Hold on work in other areas	68	15	19	12	16	0.76
	52.31%	11.54%	14.62%	9.23%	12.31%	
Additional money for contractor	66	13	13	17	21	0.73
	50.77%	10.00%	10.00%	13.08%	16.15%	

5 CONCLUSION

The results obtained from this study displayed the major factors causing VOs, confirmed that they emerged from the owners' side, and are mainly attributed to changing his needs or scope of work. It was also confirmed that there is a significant relationship between the occurrence of VOs and projects' time extension (by 22-200%) and cost overrun (by 2.67-42.86).

REFERENCES

Alnuaimi, S. A., Taha, A. R., Al Mohsin, M. & Al-Harthi, S. A. (2010) Causes, Effects, Benefits, and Remedies of Change Orders on Public Construction Projects in Oman. *Journal of Construction Engineering and Management*, Vol. 136, No. 5.

Arun, C. & Rao, B. N. (2007). Knowledge based decision support tool for duration and cost overrun analysis of highway construction projects. *J. Inst. Eng.* (India), Part AG, Vol. 88, pp. 27-33.

Cox, R. K. (1997). Managing change orders and claims. *Journal of Management in Engineering*, ASCE, Vol. 13, No. 1, pp. 24-30.

Enshassi, A., Arain, F. & AlRaee, S. (2010) Causes of variation orders in construction projects in the Gaza Strip. *Journal of Civil Engineering and Management*, *16*(4), pp. 540-551.

George, D. & Marllery, P. (2003). SPSS for Windows Step by Step: A Simple Guide and Reference.

Kombo, D. K. & Tromp, D. L. A. (2006). (Proposals and Thesis Writing: An Introduction). Nairobi: Pauline's Publications Africa.

Mohammed, E. E., Mohammed, S. Y. & Hassan, A. S. (2017). Factors causing variation orders in building projects in Khartoum State-Sudan. *International Journal of Engineering Sciences & Research Technology*, *6*(11), 117-129.

Mizanur, R. M. D., Dai, L. Y. & Khanh, H. D. (2014). Investigating main causes for schedule delay in construction projects in Bangladesh. *Journal of Construction Engineering and Project Management*, *4*(3), 33-46.

Osman, Z., Omran, A. & Foo, C. K. (2009). The potential effects of variation orders in Construction

Projects. *Journal of Engineering*, 2, 141-152.

Palinkas, L. A., Horwitz, S. M., Green, C. A., Wisdom, J. P., Duan, N. & Hoagwood, K. (2015). *Purposeful sampling for qualitative data collection and analysis in mixed method implementation research*.

Wu, C., Hsieh, T. & Cheng, W. (2005). Statistical analysis of causes for design change in highway construction in Taiwan. *International Journal of Project Management*, Vol. 23, 554-563.

Yadeta, A. E. (2016) The Impact of Variation Order on Public Building Projects. *Journal of Construction Engineering and Management*, *5*(3), 86-91.

Yin, R. K. (2009) *Case Study Research: Design and Methods*. 4th ed. London: SAGE Publications

Cite this article as: Elshaikh E., Mahmoud S., "Variation Orders in Building Projects in Khartoum State-Sudan: The Causes and the Impact on Projects Performance", *International Conference on Civil Infrastructure and Construction (CIC 2020)*, DOI: https://doi.org/10.29117/cic.2020.0026

The New Construction Approach Adapted by Ashghal for the Public Projects in Qatar

Ahmad Al-Buenain
aa1304017@student.qu.edu.qa
College of Engineering, Qatar University, Doha, Qatar

Saeed Al-Muhanadi
sm1805291@student.qu.edu.qa
College of Engineering, Qatar University, Doha, Qatar

Mohammad Falamarzi
mf1407364@student.qu.edu.qa
College of Engineering, Qatar University, Doha, Qatar

ABSTRACT

The purpose of this paper is to review the new strategy adapted by Ashghal to implement lean construction in Qatar to improve project performance and predictability of delivery. This is a significant change programme led by a government delivery entity. In 2017, the Public Works Authority (ASHGHAL) piloted the implementation of lean construction principles within 3 projects. Following realization of tangible benefits through the pilot application, Ashghal made it contractual to implement lean in all future projects. Since then, Ashghal has awarded 26 projects with the enhanced requirements in the construction contracts. The enhanced requirements within the construction contract are intended for improving public satisfaction and project delivery performance. This paper discusses the changes implemented by Ashghal and provides some recommendations. The paper presents findings from Literature reviews, interviews with Ashghal, and site visit to one of the projects undergoing the transformation. Qatar had not implemented lean construction principles at such large scale before 2018. Ashghal has realised various challenges in embedding the new strategy, which will be explored in this paper. Ashghal recognizes that the program requires time and effort, and has invested in building local capability. The enhanced requirements are applicable only to full infrastructure construction projects awarded post October 2018. Thereby the new approach is focused on contractors and supervision consultants' way of delivery. There is scope however to expand the application of lean principles to improve internal processes. Other influencing government agencies could also benefit from this program. Finally, this paper presents the efforts by Ashghal in raising the bar of delivery in the state of Qatar and the region. It is a rare example of a public sector authority leading a major change initiative that can benefit all parties involved and especially in construction, which makes this a very unique and special case that deserves to be written about.

Keywords: Enhancing delivery; Lean construction; Qatar; Public projects; Collaborative planning; Visual management

1 INTRODUCTION

Qatar, the country with one of the highest GDP per capita of 61,000 USD (PSA, 2017). Mainly driven by the large oil and gas reserves that makes it the largest exporter of Liquefied Natural Gas (LNG) in the world, in addition to the small population of approximately 2.7 million, has great ambition for the future. After successfully hosting

2006 Asian games along with other international sporting events, Qatar decided to raise the bar by bidding to host 2022 FIFA World Cup. With large capital from its hydrocarbon sales, Qatar managed to develop a strong and extensive bid with huge developments to make the bid promising and attractive. In December 2010, FIFA announced that Qatar won the bid. This was a great motive to start developing the entire country to host such event. In addition, there was another major motive that made this development ambition double in magnitude, it was Qatar National Vision 2030, launched in 2008, with the aim to drive Qatar towards a knowledge-based economy rather than a Hydrocarbon based economy.

More than USD $200bn was budgeted for the investment in the massive development of new roads, stadiums, facilities, and other major projects in the period between 2011-2022. Most of this budget is dedicated to the transport sector that is required to support FIFA 2022 World Cup and Qatar National Vision 2030 to meet the rapid infrastructure and economic growth (MME, 2016). The largest budget in the transport sector, 40 billion USD, is for Qatar National Rail Scheme, and the second largest budget in the transport sector, 14.6 billion USD, is for the Local Roads & Drainage programme managed by the Public Works Authority, Ashghal. (Ashghal, 2018).

Ashghal is responsible for all infrastructure projects and public buildings in Qatar through their lifecycle from planning to asset management. A number of departments are established to handle this responsibility, these are design, roads, highway, drainage networks, and buildings departments. Large budgets are placed yearly to serve these departments to achieve their objectives, these went up to 18.8 billion Qatari Riyals in 2018 on roads projects and are 23 billion Qatari Riyals in 2019 for roads department (The Peninsula, 2019).

With this rapid and massive development in Qatar's infrastructure, Ashghal perceived that the current construction practices and the overall construction industry is underperforming and is facing issues. Some of these issues are the waste that is present in many forms, for example, over-production, waiting, inventories, defects, skills misuse and others. These issues cause projects to finish late and overbudget. Therefore, Ashghal realises a need for construction enhancement, and they are revising their strategy to improve construction productivity.

The purpose of this paper is to show efforts undertaken by Ashghal in implementing a program to enhance the delivery of construction projects in Qatar, and to analyse the program and the challenges associated with it. The paper aims to give observations and recommendations based on the review.

The paper starts with literature review on lean construction methods, benefits, and challenges. Then the research methodology and Ashghal program will be discussed. Finally, the paper will give conclusion and recommendations.

2 BACKGROUND AND LITERATURE REVIEW

Generally, construction is a project industry whose unique features are associated with one-of-a-kindness of the project, construction site, production set-up and temporary organization. Over the last couple of years, infrastructure construction has continued to grow and equally affected by factors which include but not limited to, economic conditions and government policies. In fact, construction performance of road project

for example affects the productivity of several sectors of the economy. Evaluation of project failure by the Construction Managers Association of America reveals that usually about 50% of the work on the weekly plan are finished by the end of the stipulated week plan and that majority of these planning failures could be mitigated by construction contractors through active management of the variability (Ansah & Sorooshian, 2017).

Down the history, construction has suffered from cost and time overruns. Among the most known example is the Sydney Opera House that costed about $102 million in comparison to the estimated value of $7 million and took a total of 10 years from an initial estimate of 4 years. (Gade, 2016). A good example that drew the attention of lean construction in the UK was the construction of Wembley Stadium. The cost was about two times the estimated cost and construction period as it surpassed the estimated construction time (Gade, 2016).

In addition, lack of reliability often delays smooth flow and results in efficiency losses as far as construction of road projects is concerned. Therefore, there is urgent need for a majority of contractors to adopt lean construction: unlike the traditional road building processes, lean construction minimizes waste of materials, time and ensures the safety of workers at the site; this produces maximum value for client and other relevant stakeholders.

2.1 Lean construction methods

Generally, there exist a number of lean construction methods and techniques: one of the methods of lean construction is lean work structuring (Tauriainen et al., 2016). Unlike the work breakdown structure, the lean work structuring integrates the processes with product design and extends the functions down to the systems, it evaluates when the various chunks of work will be done. Another method is schedules; in this case the phase milestones required to complete the project are often established. Unlike traditional construction management, detailed schedules generated at the beginning of the construction project do assure control of the entire project. Other method is the last planner system of controls.

2.2 Benefits of lean construction

In essence, lean construction has huge benefits; it is important to note that this approach enhances value generation as well as waste productions (Ferng & Price, 2005). Value is usually produced by a methodology and processes, which are aimed at examining and equally clarifying the clients and stakeholders' needs/demands. Other advantages of lean construction include ensuring the delivery of product with a specified budget; minimization of direct costs associated with the construction projects by effective project delivery management and enhanced well-informed decision making at all the levels of the construction project. Furthermore, reduction of potential risk and maximization of reliability and accountability into construction project environment is possible. For instance, in the construction of the Turner Construction Co Tennesse Medical Center, incorporation of the Building Information Modeling (BIM) and lean construction; the cost of the project was reduced by approximately $3million and equally the project was delivered within the shortest time possible. Equally, the incorporation of lean construction management in the construction of Gerona building resulted in a

decrease in the construction time and cost by 25% and 30% respectively.

2.3 Challenges of lean construction

Arguably, there exist quite a number of challenges or limitations associated with the implementation of lean construction strategies and methods. Ansah et al. (2016) found out that some of the barriers linked to the implementation of lean construction include: insufficient technical skills, incomplete designs, poor relationship between the contractors and clients and poorly defined individual duties and responsibilities during the project. Notably, training and educating workers on the various lean methods require a lot of time and commitment and therefore some employee may not be pleased with such changes. In essence, cohesive teamwork among the workers is vital for lean construction and thus if workers are not working in harmony, then chances are that the efficiency of the lean construction may be compromised and result into a breakdown of project schedules. Moreover, in order for the lean construction to work effectively and efficiently, all sections need to be in line with the construction management plan as breakdown in the chain results in failure of the lean methodology.

2.4 Top countries implementing lean construction

As examined by the lean construction Institute (Ansah et al., 2016), lean construction is popular and active in the following countries, namely: United States, United Kingdom, Denmark, Finland, Australia, Brazil, Chile, Peru, Singapore, Ecuador, Venezuela and Colombia. Although survey in the UK and the Netherlands shows that the construction has been slow in adopting the lean construction concepts (Angaya, 2012). Grana Montero, one of the biggest engineering and construction firms in Peru employed lean construction in about nine projects and realized an increase in profit from $3million to $9.5milion. In Sweden, majority of small to medium-size construction firms have specialized in multi-story construction by employing extensive prefabrication strategies (Ogunbiyi et al., 2014). Among the established contractors, who majorly work with a traditional approach, which comprises of huge projects, organization as well as on-site work, a similar trend in specialization is seen. It is important to note that the specialization majorly is concerned with an increased usage of prefabricated construction items and client relationships. Ansah et al. (2016) noted that this specialization trend is attributed by factors such as reduced costs of construction.

3 RESEARCH METHODOLOGY

Methodology is the road to analyze and solve the research questions. In this section, the procedure of making the research and the step by step logic will be described. The purpose of the research is to demonstrate the process of transformation in Ashghal from the traditional construction to the application of lean construction. In order to achieve this study objectives, the researchers did intensive and extensive literature study through journals, conducted meetings with Ashghal management, and performed a site visit to one of the major projects that are implementing new lean strategy.

The literature study done for this project was aiming to gather information about general construction industry around the world, lean construction methods, benefits of lean construction, challenges of lean construction, and top countries in implementing

lean construction. These topics were analyzed carefully in order to understand the situation around the world in implementing lean methods and to be prepared to conduct the research in Qatar.

The researchers focused in this project to meet with the concerned department in Ashghal and the meeting was conducted between the project team and Eng. Ahmad Al-Ansari Technical Office Manager, Jenefer Alam lead for construction enhancements, and Don Ward manager of Construction Excellence international, where the research team adjusted the direction of the study to be a strategic and qualitative analysis due to limited data available when this study was conducted as the enhancements and lean initiative within Ashghal is at early stages of implementation. There is scope to expand this research in future to incorporate tangible benefits this initiative generates for Ashghal and the responses by the market in the state of Qatar.

Finally, the team did a site visit to one of the major projects that implemented the enhanced contracts. The main target of this step was to observe the site and listen to all of the stakeholders such as Ashghal representative, project consultant, and the contractor. In addition, close interacting with the new technique used in the project which was the performance center helped the researchers to know more about Ashghal new style in managing the project. Further details about this visit will be discussed below in this paper.

This paper will discuss all the collected information in the research discussion and the team will show their findings and recommendation to improve the new strategy of Ashghal. Then all the results will be concluded in the conclusion section. Knowing that the targeted audience for this study were chosen to be Ashghal as the whole study was about their strategy and projects as they may benefit from the recommendations. This project focused on lean construction and it's a good opportunity to show how lean construction are implemented at Qatar. In addition, road and infrastructure contractors in the region may know more about lean construction and how to help in improving the new projects while working with Ashghal and lastly, all who are interested to know more about lean construction in Qatar.

4 DISCUSSION

4.1 The need for change

In 2017, ASHGHAL embarked on a fact finding mission to identify the root causes for recurring issues in construction. A task force was established comprising personnel from contractors, supervision consultants, designers and Ashghal. With the help of construction experts brought in from UK and the extensive local knowledge, the task force completed several initiatives and presented their recommendations for improvement, after being in action for ten months. Their proposals were focused at improving public satisfaction and project delivery performance. Along with improvement proposals related to zonal delivery, public engagement, disruption minimization, early engagement; a proof of concept study was run for lean construction principles on three pilot projects.

4.2 Initiative timeline

The proof of concept for lean was established through some key tools such as collaborative planning, minimizing wasted effort, visual management and work study.

For a period of five months the pilot projects were monitored and analyzed and in August 2017, the realized benefits from the pilot projects were concluded. This included improved productivity at no additional cost. Subsequently, the findings and recommendations of the task force were presented to the president of Ashghal and approval was obtained to embed the proposals as new requirements in the construction contract to raise the bar of project delivery. Alongside this, Ashghal incubated Construction Excellence, a non-profit organization, to encourage further sharing of international best practice. In March 2018, Ashghal announced the launch of its enhanced contracts at the second industry briefing. And in October 2018, it awarded the first five contracts with the new authority's requirements (which included Lean), worth QAR 2.7 Billion ($740 million) and of duration up to five years.

4.3 Enhanced contracts

The enhanced contract included authority's requirements such as 1- Zonal Deliver, which obligates the contractors to divide the projects into zones to reduce the disturbance to the residents and to help concentrate resources and efforts. 2- Improved public relations and stakeholder management, enabling better project planning by early engagement. 3- Lean construction principles to reduce wasted efforts, improve collaborative delivery and increase productivity and predictability. 4- logistics, welfare and site housekeeping. 5- improved look and feel of the project site. An incentive was outlined for contractors to get a 40% of the saving through any value engineering proposals.

New KPIs were introduced in the enhanced contract. For 6 disciplines (health and safety and welfare, quality, project delivery, environment and sustainability, public relations and handover) the project would score positive points for leading and proactive indicators, and score negative points for incidents not acceptable by standard. The KPI scores are evaluated yearly and a 5% of the contract value tied to this. Thus, the contractor is motivated to perform on these disciplines and standards. Figure 1 below shows an example KPI score model.

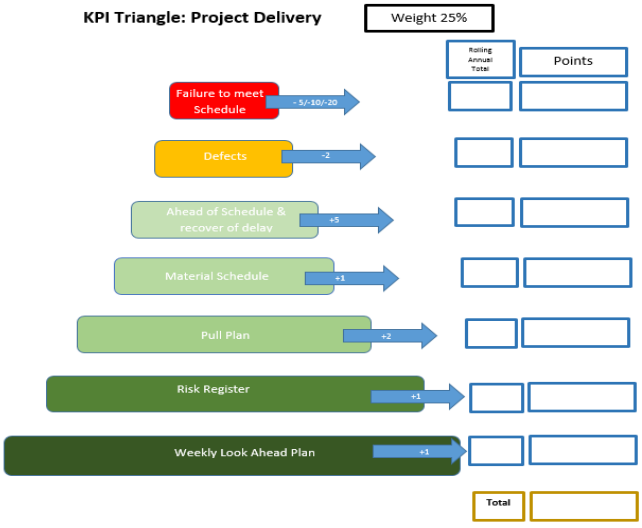

Figure 1: Monthly Performance Tracking Chart

4.4 Construction excellence

Constructing excellence Qatar has been established by Ashghal in collaboration with Constructing Excellence from the United Kingdom. Constructing Excellence is a non-profit organisation which promotes industry best practice, energises collaboration through industry events and seminars, and provides tools for benchmarking project performance. In 2017 Ashghal embedded CE within its Technical office by part funding it. CE went on to expanding the awareness of Ashghal's construction improvement initiatives, including the implementation of the enhanced contracts and lean principles via several industry seminars, jointly hosted with professional institutions and academia. Thus CE helped facilitate the transformation program.

4.5 Training program

To ensure that their new lean construction strategy is understood and that all the stakeholders are aware of the changes and how they should be implemented, Construction Excellence Qatar have developed a training program for all their employees, contractors, Consultants. And other governmental stakeholders. The training program is divided into four different levels that are Intro, users, practitioners, and advanced practitioners. All ASHGHAL's and the stakeholders' staff members are obligated to take the training sessions with the level depending of his/her position and job nature. Figure 2 below shows the detailed structure of ASHGHAL's Lean Construction training program.

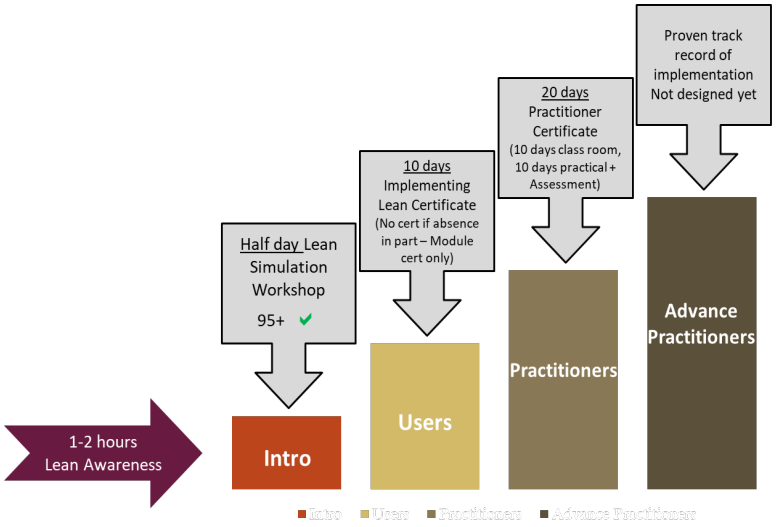

Figure 2: Lean Construction Training Program

4.6 Lean implementation

The new enhanced contracts include minimum requirements that aim in the implementation of lean strategies; these requirements are discussed in this section. The first requirement is to apply visual management by having a project performance center that displays appropriate information at worksite. This center is a place where all plans are displayed, and all equipment's and teams are shown on a map on each day to display where and what they are doing. Figures in the appendix show pictures of the project

performance center that was visited. Another requirement is collaborative planning, this is by doing four weekly, including look ahead plans and pull production planning. The next requirement is the implementation of 5S organization. Final requirement is to have structured problem solving to avoid defects and rework.

5 CONCLUSION

The construction industry is one of the slowest industries around the world to move towards technology or to implement any major changes. Therefore, seeing this kind of efforts being made by a governmental organization is a great sign that the construction industry in Qatar has finally found the needs for change and is going to change and improve soon. Also, this kind of governmental movement is what made Qatar ahead of all its neighbors in the regions since they only have some private companies that have implemented the usage of lean construction in their projects. Finally, the time is early now to say whether this program is successful or if it has improved the level of the projects in Qatar; however, this paper's intention was to show the efforts of the people in ASHGHAL and to increase the awareness in the construction industry that there is still a big room for improvement and change.

6 RECOMMENDATIONS

Although this paper's objectives were to show the efforts and to support this kind of initiatives in the construction industry. There are some improvements that we think are necessary to improve the outcome of this initiative and to enable its full potential. 1- Applying the enhanced requirements on projects with different scopes like infrastructure, highway, and building projects would be more useful to measure and compare the effects of lean construction on each project type. 2- Applying internal changes in ASHGHAL regarding their approval durations and payment period to the contractors. In their initiative ASHGHAL assumes that all the delays are caused by the contractors and consultants however the studies have shown that many delays in construction projects are caused by the owners of the projects. 3- Increasing the collaboration between the different governmental agencies in order to increase the performance of the projects and success of the construction excellence initiative. 4- Using incentive in contracts to motivate the contractors in improving project delivery

REFERENCES

Alam, J, (2018), "Lean Construction, A Strategic Vision for Operational Excellence in Qatar", Warwick Univeristy, DLMBA programme

ANGAYA, A. (2012). *Influence of Lean Construction on The Performance of Housing Scheme Building Projects in Nairobi County*, 2-10.

Ansah, R. H. & Sorooshian, S. (2017). Effect of lean tools to control external environment risks of construction projects. *Sustainable cities and society*, 32, 348-356.

Ansah, R. H., Sorooshian, S. & Mustafa, S. B. (2016). Lean construction: an effective approach for project management. *ARPN Journal of Engineering and Applied Sciences*, *11*(3), 1607-1612.

Ferng, J. & Price, A. D. (2005). An exploration of the synergies between Six Sigma, total quality

management, lean construction and sustainable construction. *International Journal of Six Sigma and Competitive Advantage*, *1*(2), 167-187.

Gade, R. J. (2016). A proposed solution to the problem of construction industry overruns lean construction techniques and linear programming. *Indian Journal of Science and Technology*, 1-12.

MME, (2016). *Qatar National Development Framework*. Retrieved from http://www.mme.gov.qa/QatarMasterPlan/Downloads-qnmp/QNDF/English/English_QNDF.pdf

Meeting with Eng. Ahmad AL-Ansari manager of the president technical office in the public works Authority (ASHGHAL).

Ogunbiyi, O., Goulding, J. S. & Oladapo, A. (2014). An empirical study of the impact of lean construction techniques on sustainable construction in the UK. *Construction innovation*, *14*(1), 88-107.

PSA (2017). *Window on Economic Statistics of Qatar*. Retrieved from https://www.psa.gov.qa/en/statistics/Statistical%2 0Releases/Economic/GeneralEconomicStatistics/windowonstatistics/2017/WinEconomicStat_23th_Issue_Q4_2017_AE.PDF.

Peninsula, (2019). https://thepeninsulaqatar.com/article/30/04/2019/Ashghal-budget-for-road-projects-reaches -QR23-bi llion-in-2019

Tauriainen, M., Marttinen, P., Dave, B. & Koskela, L. (2016). The effects of BIM and lean construction on design management practices. *Procedia engineering*, 164, 567-574.

Cite this article as: Al-Buenain A., Al-Muhanadi S., Falamarzi M., "The New Construction Approach Adapted by Ashghal for the Public Projects in Qatar", *International Conference on Civil Infrastructure and Construction (CIC 2020)*, Doha, Qatar, 2-5 February 2020, DOI: https://doi.org/10.29117/cic.2020.0027

Assessment of Response Strategy in Mega Construction Projects

Ayman Mashali
ayman00067@yahoo.com
Faculty of Engineering, University of Mansoura, Egypt

Emad Elbeltagi
eelbelta@mans.edu.eg
Faculty of Engineering, University of Mansoura, Egypt

Ibrahim Motawa
i_a_motawa@mans.edu.eg
Faculty of Engineering, University of Mansoura, Egypt

Mohamed Elshikh
Mohamed_elshikh@yahoo.com
Faculty of Engineering, University of Mansoura, Egypt

ABSTRACT

Mega Construction Projects (MCPs) that are executed unavoidably face several of the organizational challenges and pressures. Due to the stakeholder pressures in the execution of MCPs, organizations may adopt various strategic responses. **Purpose** – The objective of this paper is to investigate the common response strategies (RSs) applied in MCPs in the State of Qatar, in addition to overcoming the construction problems and enhance performance during the construction stage. **Design/methodology/approach** – A questionnaire survey is carried out among the most important firms in construction industry in Qatar. Three steps are used to finalize and evaluate the questionnaire before proceeding with the full survey, validity, pre-testing and pilot study. Quantitative data analysis is carried through the Statistical Package for Social Science software (SPSS). **Findings** – Results define and demonstrate five different types of RSs. They are ranging from passive to active strategies determined by project organization. The RSs include: adaptation strategy, avoidance strategy, compromising strategy, dismissal strategy, and influence strategy. **Originality/value** – This paper identifies and evaluates the RSs in MCPs that could potentially improve project team more efficiently and effectively.

Keywords: Construction industry; Mega projects; Response strategies; Stakeholder management; Stakeholder categories

1 INTRODUCTION

Recently, Qatar has been booming in development, and the Qatari market is considered a rapidly growing one. Like all countries around the world, the construction industry is considered the most efficient contributor in country's development. The construction industry in Qatar is facing massive challenges due to the huge construction development required for the World Cup 2022 and to achieve Qatar vision 2030. As such, many mega construction projects are to be accomplished to improve the country's infrastructure which comprise numerous international companies and multinational professionals. The rapid development of Qatar MCPs in all zones raised the question of stakeholder management (SM) and response strategy in the development of MCPs. Furthermore, the complex

nature and the scale of these projects requires proper SM process. Whereas, Cleland (1986) introduced the perspective of strategic SM and the concept of stakeholders in the domain of project management, the field of construction industry globally has a weak record of SM over the past decades (Olander and Landin 2005). In this paper, the author focusses specifically on MCPs that comprise numerous participants and are executed in the state of Qatar. Through reviewing the records of MCPs, the most unexpected risks in MCPs executed under difficult environments are identified as: conflicts and incidents related to the stakeholder.

2 LITERATURE REVIEW

2.1 Mega Construction Projects

The definition of MCPs from several viewpoints comprises of complexity, size, cost, and time (Othman, 2013). They can, also, be described as wide-scale, complex undertaken that commonly value 1 billion US Dollars or more, need many years for developing and building, require multiple stakeholders, are transformational, and impact millions of people (Flyvbjerg, 2014). El-Sabek and McCabe (2017) agreed with Flyvbjerg's description of mega projects, whereas Canadian oil and gas construction projects are considered mega when they exceed 300 million Canadian Dollar (Rankin et al., 2008). Moreover, from a contractual context, mega-projects are associated with endemic disputes and large numbers of claims of significant magnitude (Dettman et al., 2010). Also, MCPs are highly large-scale investment projects, commonly valuing more than 0.5 Billion Euro (Travaglini and Dunović, 2016). Nevertheless, the implementation of an international MP in the region with its colossal size, complicated scope, technical aspects, and an international team not familiar with local regulations and culture can result in failures (El-Sabek and McCabe, 2017).

Furthermore, MPs are completely different types of projects in their aspiration level, lead times, complexity, and stakeholder engagement. Indeed, it is their scale and extreme complexity in both technical and human terms that characterize MPs from traditional projects (Marrewijk, 2007 and Flyvbjerg, 2014). Besides, MPs are distinguished by a high degree of uncertainty, because of a mix of public institutions and sub-contractors, which increases their complexity level (Marrewijk, 2007).

2.2 Stakeholder Definitions

The PMBOK (2018) defines the stakeholder as a person, groups, or organizations that may influence, be influenced through an activity, decision, or project result. The stakeholder literature presents different conceptualisation and definitions of stakeholders ranging from wide to narrow views. Freeman (1984) proposed a classic definition of stakeholders that it is any set and individuals who can impact or be impacted through the fulfilment of a firm's objective. However, this definition is wide in meaning and does not define the stakeholders' relationship with their institution. In general, the most common definition of stakeholder is: any individual or group which can influence or is affected by a project.

2.3 Stakeholders Categories

The PMBOK (2018) categorized stakeholders into two categories: (i) Internal

stakeholders include but are not limited to; the sponsor, project staff, supervision team, and contractors, etc. (ii) External stakeholders involve but are not limited to; the suppliers, project's customers, competitors, and government authority, etc. The scientists of project management have categorized stakeholders differently. Most outstanding in the literature were categorizations established on involvement of stakeholders and their relationship nature with the project, the stakeholders' claims and their attitude for the project, the role of stakeholders, and the level of anticipating of stakeholders' attitude (Aaltonen, 2010; Cova et al, 2002 and Moodley et al, 2008).

The primary stakeholder groups are those stakeholders or individuals who are considered as a base to the presence of the organization, and often most of them have some formal contract with the organization as owners, employees, customers, and suppliers. Secondary stakeholders are the group that plays an essential part in giving credibility and acceptance to the organization for its activities and include: communities, governments, and competition (Ayuso et al, 2006; Podnar and Jancic, 2006). Stakeholders are commonly classified by a broad range of attributes, such as interest, attitude, impact, influence, power, urgency, risk, and satisfaction (Mitchell et al., 1997). Miller and Olleros (2001) stated that projects successful display extraordinary SM and maybe follow the process of stakeholder identification, analysis, and classification, besides management strategy formularization.

2.4 Stakeholder Engagement's Levels

Stakeholder Management is categorized in four levels: involve, inform, consult, and collaborate (Chinyio and Olomolaiye, 2010):

Informing-includes providing the stakeholders with practical, real, and topical information to help them understand problems and suggest solutions. Despite this, set of external stakeholders have a lower probability of impact and lower level of impact, they should be aware and informed regarding all decisions taken, which can affect them directly. Taking into consideration that they will not have an effective or positive role in making any decision (Karlsen, 2002).

Consult-is a method to retain stakeholders awareness of the project by obtaining their feedback on decisions, analysis, and alternatives. While the secondary stakeholders with higher probability of impact need to be 'kept on board,' they should be consulted for their opinions over key decisions that can affect them directly or indirectly. It is improbable that the strategy will be changed because of such consultation, but tactics may be well modified to keep higher levels of obligation (Chinyio and Olomolaiye, 2010).

Involve-includes working fair and directs for the stakeholders during the SM process for ensuring that the attention of stakeholders is retained and their ambitions understood and considered continuously. Stakeholders with a top impact level, especially require to be involved in the project for all activities. Nevertheless, project management should deal directly with these stakeholders continuously to meet their requirements and their satisfaction (Chinyio and Olomolaiye, 2010).

Collaborate-*includes partnering by the stakeholders in all of the sides of a decision, including the evolution of alternative approaches as the principal stakeholders have a significant level of influence on project success.* Therefore, these approaches of working as one group to reduce conflict using multiple viewpoints and different perspectives. So,

they should be considered as partners to increase their engagement and obligation. This can be achieved by revising and tailoring project strategy, objectives, and outcomes if necessary, to win their support (Savage et al., 1991).

2.5 Stakeholder Management Strategies

Jawahar and McLaughlin (2001) stated that the strategy used by the organization to deal with any stakeholder is dependent on the significance of the stakeholder to the organization compared with concerned stakeholders. Whereas, the perception of the stakeholder's strategic responses and factors impacting them in the sector of project management is not developed (Aaltonen, 2010). Aaltonen and Sivonen (2009) selected four case construction projects that were included an external stakeholder concerned challenges and that had been executed in developing markets. They described and identified five various types of response strategies, varying from passive to active approaches established by focal project institutions. As the legitimacy and power of stakeholders' claims rise, focal institutions favour to involve extra actively and perform more strategies that are active. Furthermore, Oliver (1991) determined various strategies certain institutions have set as a response arising from pressures of the companies' environment. He provides five various types of RSs: compromise, acquiesce, avoid, defy, and manipulate. Despite this, there are still many investigations needed to build a broad understanding of the project SM strategy.

3 RESEARCH METHODOLOGY AND DATA COLLECTION

In order to realize this study's goal, a survey was conducted to gather information among the most representative firms in Qatar, which play an essential role in the local economy and construction sector. The methodology starts with defining the problem, aim and objective of the study followed by an extensive literature review, a questionnaire based on quantitative approach and analysis using scoring rate from 1 (very low) to 5 (Very High). The quantitative approach is used in this research to collect and understand the opinion and perception of construction professionals towards RSs in MCPs. The data collected from the questionnaire are analysed using SPSS. The questionnaire survey involved the engineers at different levels and types of experience. The sample was randomly selected from different stakeholders including: governmental, semi-governmental, and municipalities; Client/Owner/ Engineer; consultants (supervision and design) and contractors/sub-contractors. The questionnaire was sent to 400 people in different types of organizations and 235 (60% response rate) responses were received which is a satisfactory number of responses (Heravi, 2014).

After designing the questionnaire, pre-testing and pilot study were considered to refine and evaluate it. The questionnaire pre-testing was done by sending the questionnaire to five construction experts and requesting their review and comments. Pre-testing is used to determine the effectiveness of the questionnaire concerning strength, formatting, wording, and order to assure that the questionnaire is clear, simple, and easy to respond. Then, a pilot study is performed to gather data from specific sets of respondents (30 individuals). The pilot study is essential to enhance the validity and performance of the research prior to the factual collection of data starts (Naoum, 2007).

4 RESULTS AND DISCUSSIONS

The analysis is conducted for 235 responses. Figure (1) provides a distribution of the respondents for each party. The majority represents supervision (consultant/designer/ management) (43.4%) and contractors (33.1%) which mainly reflect the construction stage. The high percentage of this category reflects an excellent signal that ensures the goodness of the information obtained.

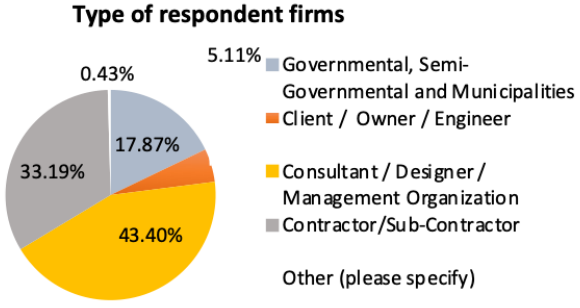

Figure 1: Type of respondent affiliation.

According to Figure (2), further than 70% of the participants are from the senior levels and topmost management, who have managerial and technical skills, who have essential positions that prop the goodness of obtained data. Since this research focuses on SM, the findings of this section emphasize that proper participants in the survey were approached.

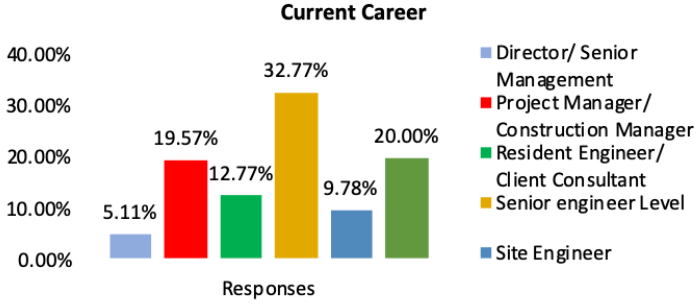

Figure 2: Respondents' roles.

As shown in Figure (3), higher than 15 years' experience in the construction projects of the participants had a good percentage (28%). They act as the leaders and decision-makers of the projects in their organizations. Also, 50.0% of the respondents have prime positions; the highest amount of deep experience increases the level of accuracy of evaluation. It was good for the contributed respondent of juniors to sustain the desired development of the construction project. The variety of experiences will sing the study by various knowledge and information. As shown in Figure (4), more than 88.0% of questionnaires were collected from public/government client organizations. This high percentage reflects the state of construction in Qatar and reflects an accurate assessment

of the current situation in the construction market in Qatar. Moreover, this reflects the high development proceed at this time for construction projects in Qatar.

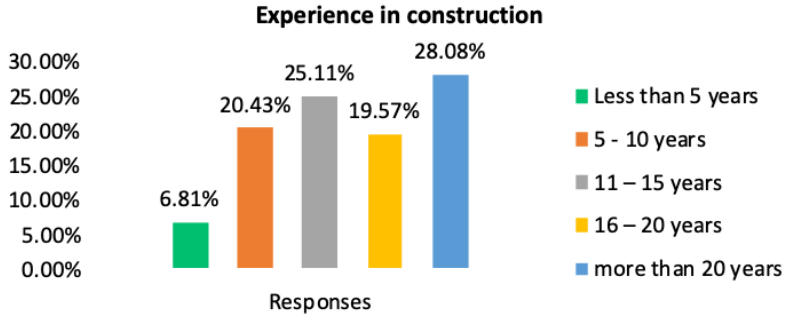

Figure 3: Years of experience.

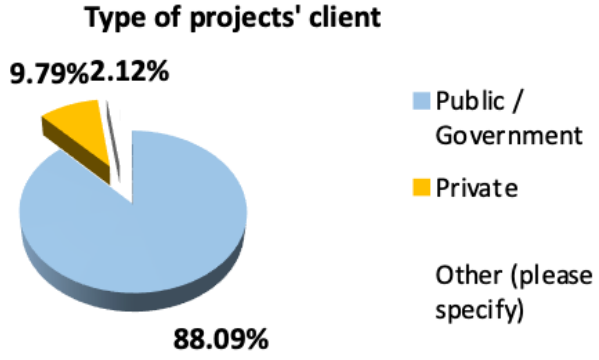

Figure 4: Distribution of client type.

4.1 Type of response strategy to deal with the stakeholder claims

The participants were asked their opinions concerning the types of efficient response strategies for dealing with the stakeholder claims in MPs.

Table 1 Efficient response strategy

Type of Strategy	Mean	Std. Error	Std. Deviation	*RII%	Rank
Adaptation strategy	3.9510	.07898	.94443	79.02	3
Avoidance strategy	3.4056	.09936	1.18819	68.11	4
Compromising strategy	4.1958	.06452	.77149	83.92	1
Dismissal strategy	2.9441	.11086	1.32567	58.46	5
Influence strategy	4.0559	.06259	.74848	81.26	2

*RII: is the relative importance index.

Table (1) shows that the compromising strategy was ranked in the first position, in this set with RII equals (83.92%). The respondents chose this strategy to deal with the demands of the main stakeholders. That is the most preferred strategy in construction projects

because project managers use it in listening to stakeholder claims and requirements, negotiating with them, and presenting possibilities and areas for discussions. This strategy can be considered a lose-lose but useful, where finding a middle ground that satisfies all parties to some degree. Also, in this strategy, no one is delighted with the solution; both parties must abandon something vital to them. That is a lose-lose situation.

The influence strategy was ranked in the second position (RII equals 81.26%). This indicates that the project managers can use this strategy with the main stakeholders to seek to affect their claims in conjunction with the project aim. It requires others to undergo the point of view of one side or another. This is not recommended unless very necessary. Generally, this technique involves pushing one opinion at the expense of another. It is a win-lose situation.

The adaptation strategy was in the third position in this set with RII equals 79.02%. This technique emphasizes agreement rather than differences of opinion. Whereas the project manager can realize that it is better to accept the demand when it is possible and does not have a significant change in the project, this is useful for achieving the project's objectives.

Avoidance/withdrawing strategy is in the fourth position with RII equals 68.11%. This strategy type could be adopted if the need of the stakeholders' claim is above the project capability. Furthermore, the project manager seeks to adopt Avoidance/withdrawing strategy with preventing and covering him/herself from the claims and shifting the liability of the requests to another one in the project.

Avoiding or withdrawing from the conflict or possible conflict and allowing the concerned parties to solve the conflict on their own is strategy not recommended unless it is a very dangerous situation (Lose/Lose).

The dismissal strategy was ranked in the last (RII = 58.46%). Most significant of the participants opposed this strategy. That means that the project managers should transact with stakeholder's matters suitably and properly.

5 CONCLUSION

MCPs are unique due to the enormous stakeholder's relationship networks in the project, with crucial impacts on society and the environment. This study provided an overview of the response strategy dealing with the stakeholder claims in MCPs in Qatar. The compromising strategy is ranked in the first position as a critical factor. Such a result reflects the full agreement of respondents regarding the importance of implementing the strategy based on compromise. Moreover, the respondents considered this approach was useful, and the project managers prefer to use compromising strategies to deal with the primary stakeholder needs, because they can use this strategy for stakeholder negotiating, attending to their requirements associated with the project, displaying opportunities, domain concerning dialogue, obtaining satisfaction, and awarding compensation. Otherwise, the respondents do not accept the use of a dismissal strategy. Additionally, this study mentions that companies may respond to stakeholder pressures in various ways, ranging from passive adaptation strategies to active influence strategies, and it contributes to some understanding of the current challenges for MCPs. Moreover, the selection of the strategy types should be by the engagement methods, information input set, classification, and besides the priority of stakeholders. Formulated strategies

should be fulfilled subsequently. After the strategies being fulfilled, the assessment of the stakeholders' reactions to the selected strategies should be adopted to enhance the aims in the succeeding SM process. Furthermore, this study's results will be valuable for all concerned project stakeholders when considering future execution plans, assist the improvement of researches to overcome the construction obstacles as much as possible to increase the execution level. Moreover, this paper makes a significant contribution by providing a view for implementing a response strategy in MCPs that motivates decision-makers and project players to adopt a compromising strategy in their projects. Although, this paper contributes to a better understanding of the response strategy of MCPs for dealing with project SM challenges; confirming its wide-scale validity to deal with challenges of SM and related response strategy of MCPs requires further research, as clarified by participates.

REFERENCES

Aaltonen, K. (2010). *Stakeholder management in international projects*. PhD thesis, Aalto University, Espoo, Finland.

Aaltonen, K. & Sivonen, R. (2009). Response strategies to stakeholder pressures in global projects. *International Journal of Project Management*, *27*(2), 131-141.

Ayuso, S., Rodrıguez, M. A. & Ricart, J.E. (2006). Responsible competitiveness at the micro level of the firm: Using stakeholder dialogue as a source for new ideas: a dynamic capability underlying sustainable innovation. *Corporate Governance*, *6*(4), 475-490.

Chinyio, E.A. & Olomolaiye, P. (2010). *Construction Stakeholder Management*. Wiley-Blackwell, Oxford.

Cleland, D.I. (1986). Project stakeholder management. *Project Management Journal*, *17*(4), 36-39.

Cova, B., Ghauri, P. & Salle R. (2002). *Project marketing: beyond competitive bidding*. John Wiley & Sons Ltd, Chichester, England.

Dettman, K., Fauchler, D., Bayer, R., Wojtasinski, S. & Mandry, M.J. (2010). In mega projects: Challenges and recommended practices, In P. Levin, ed. construction contract claims, changes, and dispute resolution, Reston VA: *American Council of Engineering*, 469-481.

El-Sabek, L. & McCabe, B. (2017). Coordination challenges of production planning in the construction of international mega-projects in the Middle East. *International Journal of Construction Education and Research*, 1-23.

Flyvbjerg, B. (2014). What you should know about megaprojects and why: An overview. *Project Management Journal*, *45*(2), 6-19.

Freeman, R.E. (1984). *Strategic management: a stakeholder approach*. Pitman, Boston, the USA.

Heravi, A. (2014). *Improving construction management: an investigation into the influences of effective stakeholder involvement on project quality outcomes.* Dissertation, Faculty of Science and Engineering, Queensland University of Technology, Austraila.

Jawahar, I. M. & McLaughlin, G. L. (2001). Toward a descriptive stake-holder theory: An organizational life cycle approach. *Academy of Management Review*, *26*(3), 397-414.

Karlsen, J. T. (2002). Project stakeholder management. *Engineering Management Journal*, *14*(4), 19-24.

Marrewijk, A.V. (2007). Managing project culture: The case of environ mega-project. *International Journal of Project Management*, *25*(3), 290-299.

Miller, R. & Olleros, X. (2001). Project shaping as a competitive advantage, In: Miller R, Lessard DR, editors. *The strategic management of large engineering projects: shaping institutions, risks and governance*, Cambridge, MA: MIT Press, 93-112.

Mitchell, R.K., Agle, A.R. & Wood, D.J. (1997). Toward a theory of stakeholder identification and salience: Defining the principle of who and what really counts. *Acad. Manag. Rev.*, *22*(4), 853–886, 1997.

Moodley, K., Smith, N. & Preece, C.N. (2008). Stakeholder matrix for ethical relationships in the construction industry. *Construction Management and Economics*, *26*(6), 625-632.

Naoum, S.G. (2007). *Research and Writing for Construction Students*. Dissertation, British Library Cataloguing in Publication Data.

Olander S. & Landin, A. (2005). Evaluation of stakeholder influence in the implementation of construction projects. *International Journal of Project Management*, *23*(4), 321-328.

Oliver C. (1991). Strategic responses to institutional processes. *Acad. Manag. Rev.*, *16*(1), 145–179.

Othman, A. (2013). Challenges of mega construction projects in developing countries, Organisation, Technology and Management in Cons. *An International Journal* DOI10.5592.

PMBOK (2018). A guide to the project management body of knowledge (PMBOK), Sixth Edition. *Project Management Institute (PMI)*, the USA.

Podnar, K. & Jancic, Z. (2006). Towards a categorization of stake-holder groups: An empirical verification of a three-level model. *Journal of Marketing Communications*, *12*(4), 297-308.

Rankin, L., Slootman, T. & Jergeas, G. (2008). The industry's perspective on workforce planning for major projects. *AACE International Transactions*, PM.12.1–12.

Savage, G., Nix, T., Whitehead, C. & Blair, J. (1991). Strategies for assessing and managing stakeholders. *Academy of Management Executive*, *5*(2), 61-75.

Travaglini, A. & Dunović, I.B. (2016). *Megaproject case studies: a stakeholder management perspective*, (International Conference on Industrial Engineering and Operations Management), Kuala Lumpur, Malaysia.

Cite this article as: Mashali A., Elbeltagi E., Motawa I., Elshikh M., "Assessment of Response Strategy in Mega Construction Projects", *International Conference on Civil Infrastructure and Construction (CIC 2020)*, Doha, Qatar, 2-5 February 2020, DOI: https://doi.org/10.29117/cic.2020.0028

Stakeholder Management: An Insightful Overview of Issues

Ayman Mashali
ayman.mashali@yahoo.com, amashali@km.qa
Faculty of Engineering, Mansoura University, Mansoura, Egypt / KAHRAMAA, Doha, Qatar

Emad Elbeltagi
eelbelta@mans.edu.eg
Faculty of Engineering, Mansoura University, Mansoura, Egypt

Ibrahim Motawa
i_a_motawa@hotmail.commans.edu.eg
Faculty of Engineering, Mansoura University, Mansoura, Egypt

Mohamed Elshikh
i_a_motawa@hotmail.commans.edu.eg
Faculty of Engineering, Mansoura University, Mansoura, Egypt

ABSTRACT

This paper attempts to contribute towards investigating the existing literature base of stakeholder management (SM), provide a compilation, and define any gaps in this area. Besides, explore different groups of critical success factors (CSFs) and grouping these actors. This study is based on reviewing the literature. Therefore, more than a hundred research papers were searched by the key terms specified in a preceding literature review. Succeeding tours of abstract research surveys resulted in forty-two research papers being picked for the compilation. SM constructs were identified, and the following crucial analysis defined the literature base gaps. The most notable outcomes are the absence of research that has studied BIM-based stakeholder management, especially in mega projects. Additionally, further investigations are still required to study the SM influence throughout the different stages of the project life cycle and study the impact of project type and contract type in SM. However, there is still considerable debate about the SM nature and merits approach. This study presents a comprehensive gathering of all earlier identified SM processes through a structured approach. Additionally, a more realistic and practical methodology for the development and implementation of SM will emerge, and twenty-seven CSFs associated with SM in construction projects are identified. The study is expected to have a theoretical contribution to this subject, especially in the context of the Qatari construction industry.

Keywords: Construction industry; Implementation; Stakeholder engagement; Management; Stakeholder management; Critical success factors (CSFs)

1 INTRODUCTION

The construction industry is highly complicated that requires strict systems to achieve projects efficiently and on time. In trying to maintain competitiveness, there has been a growing necessity in institutions to link the information supplied by every section into a joint entity. The outcome, there was widened research and study concentrating on the execution process and its CSFs (Al-Mashari et al., 2003; Hong & Kim, 2002; Xu et al.,

2002; Ribbers & Schoo, 2002). Nevertheless, it seems that much of the literature has concentrated on SM with too limited concern to stakeholders' perspectives. Concerning a project execution crew, a deeper understanding of SM would make it likely to evaluate the project planning stage and determine if the interests are being managed as efficiently as potential. Finally, this will reinforce the likelihood of gaining more significant success levels and, thus, cost-savings, time-saving, efficiency, and quality in their project. Moreover, different aspects of implementation influence some stakeholder sets more than others, and some sets are higher qualified to remark on particular side than others. Furthermore, the identified gaps of the SM approach, identified by previous researchers, need to be further investigated in terms of how they have been addressed in the SM literature. Based on the outcomes of a full gathering and analysis of SM, this study seeks to introduce a new protocol to other research on SM *prosses* and to uncover the more in-depth application of the broad aspects of SM.

2 STAKEHOLDER MANAGEMENT AND CSFs LITERATURE COMPILATION

As per reviewing the literature for SM and identifying its success factors, the first step was to categorize and group success factors that, fully initially, seemed to indicate a similar phenomenon. Then, a consecutive round of the analysis of the concepts resulted in producing 31 CSFs in total.

2.1 STAKEHOLDERS' DEFINITION AND CATEGORIES

Stakeholder Definitions

PMBOK (2018) defines a stakeholder as an individual, groups, or organizations that may affect, be affected through, or perceive themselves to be affected by a decision, activity, or outcome of a project. The stakeholder literature presented different conceptual and definitions of stakeholders ranging from wide to narrow views. Freeman (1984) proposed a classic definition of stakeholders that it is any group and individuals who can affect or is affected through the fulfilment of an organization's objective. However, this definition is wide in the meaning that it does not specify the relationship between stakeholders and the firm. Also, it does not take a situation whether the claims of the stakeholders are legitimate or not. In conclusion, the most common definitions of project stakeholders broadly, as any individual or organization who can affect or be affected through the project.

Stakeholders Categories

PMBOK (2018), categorized stakeholders into two categories as (i) Internal project stakeholders generally include the project sponsor, project team, support staff, and internal customers for the project. Other internal stakeholders include top management, other functional managers, and other project managers because organizations have limited resources. (ii) External project stakeholders include the project's customers (if they are external to the organization), competitors, suppliers, and other external groups that are potentially involved in the project or affected by it, such as government officials and concerned citizens. Other categorizations in the literature are based on stakeholders' involvement in the project and the character of their relationship with the project, the nature of stakeholders' claim and their attitude towards the project, their role in the

project, and their degree of anticipating behavior (Aaltonen, 2010; Cova et al., 2002 and Moodley et al., 2008).

The primary stakeholder groups are those who are considered as a base to the presence of the organization, and often most of them have some formal contract with the organization as owners, employees, customers, and suppliers. Secondary stakeholders are the group that plays an essential part in giving credibility and acceptance to the organization for its activities and include, communities, governments, and competition (Ayuso et al., 2006; Podnar et al., 2006). Wheeler and Sillanpaa (1997) classified stakeholders into two additional dimensions of social and non-social. Stakeholders are commonly classified by a broad range of attributes, such as interest, attitude, impact, influence, power, urgency, risk, and satisfaction (Mitchell et al., 1997; McElroy & Mills, 2003). Miller et al. (2001) stated that successful projects display exceptional SM and maybe follow the process of stakeholder identification, classification, analysis, and management strategy formularization.

2.2 CRITICAL SUCCESS FACTORS (CSFs) COMPILATION

Numerous researchers have applied the CSFs as a method to enhance the realization of the management process (Yang et al., 2009b; Yu, 2007; Jefferies, 2002). CSFs can be defined as "areas, where outcomes if they are satisfying, will ensure strong competitive achievement for the organization" (Yang et al., 2009a). CSFs are identified from studies on SM, in general, or "the works of those who have discussed a special factor in detail" (Wong & Aspinwall, 2005). Based on an extensive literature review, six groups, comprising 31 factors contributing to the success of SM were identified and proposed as follows:

Group 1: Project Type

Project characteristics are significant to project success (Songer & Molenaar, 1997).

- *Industrial:* Industrial projects are characterized by a high level of complexity (Anderson et al. 2016). While numerous researches evaluate project complexity, little integrated studies present a proper approach for successfully managing the project complexity (Liu et al., 2017). Therefore, there is a significant need for an applicable approach that can simplify the assessment process to manage the project effectively.
- *Infrastructure*
- *Buildings: The construction of buildings suffers from the isolation of construction responsibility from the design phase. Grilo et al., (2007) supported these issues and mentioned that the cause is the contractors' relegation from the design process.*

Group 2: Contract type.

The organization must have a comprehensive construction contract, and the contract must realize an efficient collaborative environment with a balance between vendor and client.

- *Lump Sum*
- *Measurement*
- *Cost Reimbursable*

- *Design-Build (EPC)*: Design-build (D-B) is an undertaking procurement process where one entity or consortium is contractually liable for the construction and design (Songer et al., 1997). D-B is illustrated to be an efficient delivery technique and has become common within the world in the current days (Xia & Chan, 2010). In D-B projects, the pre-qualification of implied tenders is essential for gaining a first evaluation of engaged individuals' fitness for undertaking the project (Lam et al., 2004). Furthermore, conditions, regulations, and laws of settlement and contract documentation must be complete regarding parties' rights and duties to give sufficient information toward the responsibilities at many phases of construction and design (Nguyen et al., 2004).

Group 3: Decision making.

Whereas not broadly cited, this group deserves specific consideration. Moreover, this concept indicates the need for the team to be enabled to make crucial decisions in proper time, to allow effective timing for the implementation (Shanks & Parr, 2000; Chen, 2001; Gupta, 2000).

- *Transparent Evaluation of the alternative solution based on stakeholder concern*: A clear asses of alternate solutions for the improvement of a construction industry based on the concerns of stakeholders would assist the managers to build the foundation of confidence required for a satisfactory SM process (Olander & Landin, 2008).
- *Ensuring effective communication among the project's stakeholder*: The success of a project is connected by efficiently communicate and manage relationships among the different project stakeholders. Therefore, to ensure the project's success, much information needs to be communicated on a steady basis to all major stakeholders, including expectations, goals, and needs. In contrast, communications comprise the processes needed to secure the appropriate and proper generation, collection, distribution, storage, and recovery of all data of the project. Furthermore, efficient communication builds a bridge among different project stakeholders, linking many cultural and organizational backgrounds, various expertise levels, and many views and interests in the project fulfilling (Jergeas et al., 2000; Čulo & Skendrović, 2010).
- *Formulate appreciate strategy to deal with stakeholder*: The strategy of SM is the behavior of wherewith the project directors addresses various stakeholders needs (Karlsen, 2002). Thus, many researchers repeated the urgency to address the implementation strategy by a gradual approach (Cliffe, 1999; Gupta, 2000; Scott & Vessey, 2000; Motwani et al., 2002; Robey et al., 2002; Mandal & Gunasekaran, 2003).
- Additionally, 'Stakeholders' reactions to the strategies' is a vital factor when project managers make decisions regarding the strategies to deal with stakeholders (Freeman et al., 2007). Therefore, the project team must predict stakeholders' behavior in fulfilling strategy (Cleland & Ireland, 2007), where an effective strategy for project management is that ensures the success of the project (Smith & Wilkins, 1996). Besides, it was determined and described five different types, ranging from negative to active approaches used by the construction industry companies. SM strategies are: compromising, adaptation, avoidance, influence and dismissal (Hammad, 2013).

Group 4: The best manages stakeholder team.

The challenges of stakeholder perspectives of unreasonable and wrongly concentrated about a project and its expected outcomes may lead to problems in project implementation (Olander, 2007; Jha & Iyer, 2006). Most of project stakeholders' research on managerial behavior focused on the conceptual development of various managerial frameworks, tools, and processes to identify, categorize and manage project stakeholders and studying the role and value of SM process (Bourne & Walker, 2005; Cleland, 1986; Cleland, 1995; Cleland, 1998; Olander & Landin, 2005).

- *Client Team*: There is a necessity for communication, session and consultation with numerous essential stakeholders, though, especially with the Owner (Al-Mudimigh et al., 2001; Al-Mashari et al., 2003). Organizations necessitate keeping their owners informed of their projects to keep away errors (Holland & Light, 1999; Al-Mudimigh et al., 2001; Mandal & Gunasekaran, 2003).
- *Formulate Project Management Team*: It has declared in the course of the literature that there is a significant want to build a strong and powerful staff that comprises the organization's satisfactory and brightest employees. These employees must own established credit (Cliffe, 1999), and there have to be a pledge to release the employees to the implemented mission on a full-time basis (Siriginidi, 2000b; Shanks & Parr, 2000). The team needs to hold the necessary skills to investigate details when conducting the planning phase (Soh et al., 2000). Once the team has been set up, it would then be primary to teach and train the employees (Bajwa et al., 2004).
- *Supervision Consultant Team*: Several researchers have supported the necessity to add a consultant as part of the execution crew (Trimmer et al., 2002; Motwani et al., 2002; Bajwa et al., 2004; Kalling, 2003). Still, as part of this link, it is essential to manage the transfer of knowledge from the consultant to the firm (Al-Mashari et al., 2003; Skok & Legge, 2002).
- *External Party team*: It is remarked that if a construction authority does not be in complex mega-projects, a third-party will hold the position of the construction authority or a project management firm expert in similar projects type (Adrem et al., 2006). This concept is observed in several airport projects, such as the Doha Airport Expansion project where construction authority control is needed to obtain a balance between stakeholder's interests.
- *Contractor Team*: Designers could gain from the early contractors' engagement who usually aren't engaged in the tender stage previously in design management systems and traditional procurement (Pocock et al., 1997). Subsequently, the contractor's involvement at the design stage owns an essential influence on the ought right-first-time design and will have a favorable influence on efficiency, quality, constructability, and speed construction of the project (Cooper et al., 2005). Also, while contractors come to be involved, they have minimal options since most designs are previously determined (Adrem et al., 2006).

Group 5: Stakeholders' Categories in the Project stages

Most of the researchers investigating SM have mentioned the vital significance of

identifying stakeholders (Karlsen, 2002; Olander, 2006; Walker et al., 2008; Jepsen & Eskerod, 2009). Although the project stakeholders can be divided into many types according to various criteria, the question of "who are the stakeholders?" must be answered earlier (Pinto et al., 2009). Project stakeholders influence the project management procedure (Olander, 2007). Therefore, realizing the stakeholders' impact is significant for planning and implementing enough strict SM processes (Olander & Landin, 2005). Accordingly, if an external SM process conducted properly, it represents an opportunity for project improvement (Oalnder, 2006).

- *Initiation stage*: Numerous researchers indicated that project performance, in terms of time, schedule, scope, quality, and safety, will be enhanced by implementing SM at the early project stages (Chen et al., 2001). Moreover, the project management team should classify project stakeholders in the early project stages to ensure the project success. It is crucial to identify the project stakeholders and to get the stakeholders' engagement process for integrating them into the design and construction activates and to determine the interference among them and the SM problems to improve it (Weshah et al., 2014a). Clear and appropriate stakeholder definition is considered as one of the essential frequent contributors to project success, and it is a product of the initiation phase of project development. Therefore, success throughout the next phases would be highly dependent on the level of the effort spent during this phase. A specific mega-project execution approach is selected at this vital stage in a project's life span (Gabriel, 2015).
- *Planning stage*: The project activities could be secured in an excellent situation by efficient overall management actions in leading, planning, controlling, and organizing (Nguyen et al., 2004; Mandal & Gunasekaran, 2003). The method of planning should be thoughtful of tasks to be fulfilled (Mandal & Gunasekaran, 2003), and subsequently, the planning should include external and internal best practices for execution (Al-Mudimigh et al., 2001). In mega-projects, there is a sequence of phases through which a project develops to its conclusion. In each succeeding phase of a project, new and different activities are developed, with the outcome of one phase becoming an input to the next phase. Different studies have shown that greater efforts in project planning and SM lead to improved project performance (Gabriel, 2015). This stage develops the design in a logical array endeavoring to gain approval on progressing to the execution stage. It is usually improved subsequent signing the project funding and delivering a suitable design solution that fits the client's requirements (Wahab, 2011). The planning stage aims to ensure complete commercial power to move to the execution phase and following achieving the owner is knowledgeable of the works' range, and likely risks can be known (Cooper et al., 2005).
- *Execution stage*: During the execution phase, almost all SM areas have to be considered. This phase consists of two stages: (1) project construction and (2) Monitor and Control on-site. The project team must be familiar with the environmental conditions, local weather, and the geotechnical conditions have to be checked and studied carefully (Cooper et al., 2005; Weshah, et al., 2014a). During this stage, the organization generates alternatives and chooses the preferred alternative. The significance of scope definition and data reliability is higher than in the previous

phase. Also, the project manager and crucial project resources are assigned at this stage (Hussain, 2015). Also, information, data, and feedback are regularly gathered and made available to concerned stakeholders on time (Gabriel, 2015).

- *Monitoring and Controlling stage*: Through this stage, the project has been completely funded, a detailed schedule is in place, and the executive team engagement is high for executing the project according to the project schedule and budget. Where the performance of the project team is measured through the project execution phase adds progress and performance reports go to the client's side, executives, and all project stakeholders (Hussain, 2015). Also, throughout the monitor and controlling process, performance information is gathered, analyzed, and distributed in periodical reports (Gabriel, 2015).
- *Closing stage*: The closing stage includes the owner's operations teams; all the project teams and contractors are released from the project (Hussain, 2015). However, the project handing over is a long process, and especially when there are complicated activities. So, this stage ensures a soft process handing-over. Therefore, as-built designs are documented and handed over to the client representative, whereas preparation workshop will carry out to ensure that the end-users' teams are qualified for operation and maintenance works (Hussain, 2015).
- *Maintenance stage*: The object of this stage is to reveal the maintenance requirements of the completed project. Where it is very significant to the engagement of the facility management in initial design phases, which will secure the maintenance stage limited uncertain. Also, documenting the project's legacy archive duly will succeed in reducing the necessity for surveys of the completed property (Cooper et al., 2005).

Group 6: Management support.

Top management support is crucial for effective SM (Yang et al., 2009b). Therefore, for guaranteeing successful SM, individuals should be ready to participate in power and resource that would help the overall organization's aim (Brooke & Litwing, 1997). Moreover, the commitment and support of senior management were one of the most widely mentioned CSFs. Also, this concept indicated the need to have obliged leadership at the senior management level. Besides, it is referred to the necessity for management to expect any weakness that might be faced (Motwani et al., 2002) and the requirement for top management who would be involved in the strategic planning, but who are likewise technically orientated (Yusuf et al., 2004). Reliable and committed leadership at the top management level is essential to the success of project achievement (Sarker & Lee, 2003).

- *Managing Stakeholders with corporate responsibilities*: Project management indicates the continuous management of the execution plan. Accordingly, it includes not only the planning phases but also the distribution of duties to many members, the definition of critical paths, milestones, training, and planning of human resources, and lastly, the judgment of success measures (Nah et al., 2001). Additionally, there is a necessity to institute a steering panel included top management of various corporate duties, top project management reps, and end-users (Somers & Nelson, 2001, 2004).
- *Flexible project organization*: Flexible project organization is necessitated to

overcome the complicated and doubts of execution (Li et al., 2011), which is confirmed by Olander and Landin (2008), who come to the influence of the flexibility performance of the project to hire employees to realize the aims of the project. As one purpose of SM is to obtain agreement from stakeholders on the project execution, and this will be accomplished if a company is established to include enough resources for communication and interaction with stakeholders.

- *Project manager Competence / Skills*: The project managers should own high and strong leadership skills, technical, business, and managerial competencies (Mandal & Gunasekaran, 2003; Kraemmergaard & Rose, 2002). In most conditions, stakeholders' relationship is managed by projects' managers; therefore, the outcomes of SM are subject to the PMs' relationships, experience, capability, and power (Karlson, 2002). Also, PMs should be skillful communicators and negotiators to be fitted with directing different stakeholder expectations and building a positive culture exchange inside the overall company (Olander & Landin, 2008). Therefore, the PMs role should comprise not only easily a knowledge of the technical certainties at hand but also of the connections among the environment, technology, community, and people in it. Moreover, The PMs should gain knowledge about the project place and engage the local society when planning of the construction project.

3 RESEARCH METHODOLOGY

The full literature review has included copious note-taking that has highlighted all likely sources to SM, through adopting a conceptual analysis approach. CSF can be described as; a reference to any element or stipulation that was considered essential for the stakeholder management successfully implementation. The papers comprising a CSFs' reference of SM implementations were investigated and analyzed to code the specified constructs. Consequently, all CSFs, regardless of the characterize, were noted that the sorting stage would begin to place CSFs in the same categories. Since the purpose of this paper was to obtain a deep understanding of SM issues and different CSFs that previously identified by other researchers. Therefore, a content analysis was a suitable analysis methodology. It is the utmost common method for analyzing texts (Silverman, 2000).

4 ANALYSIS OF SM LITERATURE

The researchers have much usually concentrated on only a particular perspective of the implementation process or a particular SM. Thus, there is limited study documented that includes all essential SM states. Despite methodology, all the previous studies mentioned above have been narrowly concentrated, providing to the readers a constricted yet comprehensive view of a particular success factor. The comparatively weak degree of stakeholder consultation and the shortage of reporting of their personal views, as evidenced in the previous citations, is a vital gap in the existing literature base, and it illustrates the prime shortage of the CSF approach. Besides, there is too small offered in the literature that endeavors to identify or describe the particular tactics needed to manage and fulfil these SM activities successfully. As expressed by the references mentions above, the views on SM and precisely what SM includes vary hugely. These required to be more investigated, thus that these ideas can be better displayed in a way

that makes it achievable for the project manager to execute and control effectively. Moreover, though there is no doubt that SM is a crucial regard, it is not clear exactly how it could be handled.

Table 1: Title of CSFs in literature

CSFs	CSF category	Group No	Group description	
C1	Industrial Project	1	Project Type	
C2	Infrastructure Project	1		
C3	Buildings Project	1		
C4	Others Project	1		
C5	Lump Sum	2	Contract Type	
C6	Measurement	2		
C7	Cost Reimbursable	2		
C8	Design-Build (EPC) Project	2		
C9	Transparent Evaluation of the alternative solution based on stakeholder concern.	3	Decision making	
C10	Ensuring effective communication among the project's stakeholder.	3		
C11	Formulate appreciate strategy to deal with stakeholder.	3		
C12	Client Team	4	The best manages stakeholder team	
C13	"Project Management team" P.M Team	4		
C14	S.C Team	4		
C15	Ex.3rd Party team	4		
C16	Contractor Team	4		
C17	Initiation stage for; a- Internal stakeholder	5	4a- Internal stakeholder	Stakeholders' Categories in the Project stages
C18	Planning stage for; a- Internal stakeholder	5		
C19	Execution stage for; a- Internal stakeholder	5		
C20	Monitoring & Controlling for; a- Internal stakeholder	5		
C21	Closing stage for; a- Internal stakeholder	5		
C22	Maintenance stage for; a-Internal stakeholder	5		
C23	Initiation stage for; b- External stakeholder	5	4b-External stakeholder	
C24	Planning stage for; b- External stakeholder	5		
C25	Execution stage for; b- External stakeholder	5		
C26	Monitoring & Controlling for; b- External stakeholder	5		
C27	Closing stage for; b- External stakeholder	5		
C28	Maintenance stage for; b- External stakeholder	5		
C29	Managing Stakeholders with corporate responsibilities	6	Management support	
C30	Flexible project organization	6		
C31	Project manager Competence / Skills	6		

Based on the extensive literature review of SM, 31 critical success factors are identified in construction projects, and these factors were collected and classified into six groups, as presented in Table 1. Such compilation is based on the range of CSFs/ SM citations. Nevertheless, there was further analysis carried that attempted to expose any apparent gaps in the literature to time. As an outcome, the characteristic apparent from this discussion is the very shortage of in-depth coverage of CSFs. Moreover, added important note was the absence of BIM based-SM cited in the literature. Lastly, the notion of management support, one of the common broadly cited CSFs, and the range of activities comprised of management support are varied.

This paper would help interested professionals to have more information about the potential and the most critical success factors for SM. Where, this information may minimize conflict among different project stakeholders involved in construction projects, which may positively impact project performance. As mentioned above, and based on the review of the literature, the importance for more study about SM and considerations of the possible positive influence of SM in MCPs are highlighted. Also, the perspective on SM that identifies, examines and evaluates this issue is missing in the literature. In order to bridge this gap, this research concentrates on exploring and evaluating SM as the primary step for achieving better outputs.

Nevertheless, further investigations are still needed to improve SM during the different stages of project execution. Also, it is necessary to evaluate and analyze SM and their impact, for managing the stakeholder in MCPs, and the effect of internal and external stakeholders in the construction industry. Furthermore, translating the theoretical findings into an empirical study and show the impact of using the SM on the overall cost and productivity of a project.

5 CONCLUSION

Research on SM implementation and CSFs is a valuable step toward enhancing the chances of project success. A review of the SM and CSFs/implementation shows that, in numerous cases, CSFs are introduced based on a review of limited case studies or the previously published literature. As an outcome, one fundamental limitation of this paper is the occurrence of duplicates in the frequency analysis of the CSFs. Moreover, in cases when past researchers have sought to identify CSFs by their empirical study, they have so often concentrated on only a particular perspective of the implementation or a particular type of CSFs. Whereas, preceding methodology in investigating CSFs have been very alike in the method to the fragmented methodology. Also, it has been exposed that there was no study carried to date that has reflected the significance of CSFs during SM implementation by adopting BIM. That is a significant finding. While management support emerges being one of the common widely cited CSFs, there yet seems to be considerable variance for what exactly is surrounded. Because of the literature limitations mentioned above and according to the suggestions from different studies, there is a necessity to concentrate further research efforts on the investigation of BIM-based stakeholder management, especially in mega projects. Furthermore, to secure that this stakeholder methodology is too broad in its study of CSFs. Lastly, there is a necessity to carry further in-depth study on the concept of SM and what it involves. All of the success factors are significant in their individual. Therefore, the necessity to approach SM implementation from a view is fundamental to the project's success. The gap in this regard to the literature requires to be investigated in deeper detail. Expressly, there is a necessity to identify the strategies to be employed and the explicit tactics to be adopted for managing stakeholders for successful implementation of mega projects.

REFERENCES

A. Smith & B. Wilkins (1996). Team relationship and related critical factors in the successful procurement of health care facilities. *Journal of Construction Procurement*, Vol. 2, no. 1, pp. 30-40.

A. Songer & K. Molenaar (1997). Project characteristics for successful public-sector design-build. *Journal of Construction Engineering and Management*, Vol. 123, no. 1, pp. 34-40.

Aaltonen (2010). *Stakeholder management in international projects* (PhD thesis). Aalto University, Espoo, Finland.

Adrem, A., Schneiderbauer, D., Meyer, E. & Majdalani F. (2006). *Managing airports construction projects*, [Accessed 4 Augutst 2010] Available at: www.Boozallen.com.

Al-Mashari, M., Al-Mudimigh, A. & Zairi, M. (2003). Enterprise resource planning: a taxonomy of critical factors. *European Journal of Operational Research*, Vol. 146, pp. 352-64.

Al-Mudimigh, A., Zairi, M. & Al-Mashari, M. (2001). ERP software implementation: an integrative framework. *European Journal of Information Systems*, Vol. 10, p. 216.

Anderson, S., Vahdat, A., Dao, B., Kermanshachi, S., Shane, J. & Hare, E. (2016). Measuring project complexity and its impact. Austin, TX: Construction Industry Institute. https://www.construction- institute.org/resources/knowledgebase/knowledge-areas/measuring-project-complexityandits-impact/topics/rt-305

Ayuso, S., Rodrıguez, M. A. & Ricart, J. E. (2006). Responsible competitiveness at the micro level of the firm: Using stakeholder dialogue as a source for new ideas: a dynamic capability underlying sustainable innovation. *Corporate Governance*, *6*(4), 475-490.

Xia, B. & Chan, A. P. C. (2010). Key competences of design-build clients in China. *Journal of Facilities Management*, Vol. 8, no. 2, pp. 114-129.

Bajwa, D. S., Garcia, J. E. & Mooney, T. (2004). An integrative framework for the assimilation of enterprise resource planning systems: phases, antecedents, and outcomes. *Journal of Computer Information Systems*. Vol. 44, pp. 81-90.

Bourne, L. & Walker, D. H. T. (2005). Visualizing and mapping stake-holder influence. *Management Decision*, *43*(5), 649-660.

Brooke, K. & Litwin, G. (1997). Mobilizing the partnering process. *Journal of Management in Engineering*, *13*(4), pp. 42-48.

Chen, I. J. (2001) Planning for ERP systems: analysis and future trend. *Business Process Management Journal*, Vol. 7, p. 374.

Cleland, D. I. & Ireland, R. L. (2007). *Project Management: Strategic Design and Implementation,* New York, McGraw-Hill.

Cleland, D. I. (1986). Project stakeholder management. *Project Management Journal*, *17*(4), 36-39.

Cleland, D. I. (1995). Leadership and the project management body of knowledge. *International Journal of Project Management*. *13*(2), 82-88.

Cleland, D. I. (1998). *Stakeholder management. In: Pinto J.* (Ed.), Project Management Handbook, San Francisco, Jossy-Bass, Project Management Institute, 55-72.

Cliffe, S. (1999) ERP implementation. *Harvard Business Review*, Vol. 77, p. 16.

Cooper, R., Aouad, G., Lee, A., Wu, S., Fleming, A. & Kagioglou, M. (2005). *Process Management in Design and Construction*, Blackwell Publishing.

Cova B. & Salle, R. (2005). Six key points to merge project marketing into project management. *International Journal of Project Management*, *23*(5), 354-359.

Čulo, K. & Skendrović, V. (2010) Communication management is critical for project success. *Informatologia*, *43* (3), pp. 228-235.

Lam, E. W. M. & Chan, A. P. C., Chan, D. W. M. (2004). Benchmarking design-build procurement systems in construction. *Benchmarking: An International Journal*, Vol. 11, No. 3, pp. 287-302.

Freeman, R. E. (1984). Strategic Management: A Stakeholder Approach, Pitman, Boston.

Freeman, R. E., Harrison, J. S. & Wicks, A.C. (2007) *Managing for Stakeholders –Survival, Reputation, and Success*. Louis Stern Memorial Fund, US.

Gabriel, E. (2015). *The human factor effect on projects' success* (A Thesis Submitted to The Faculty of Graduate Studies in Partial Fulfilment of The Requirements For The Degree of Doctor 0f Philosophy). Department of Civil Engineering, Calgary, Alberta.

Grilo, L., Melhado, S., Silva, S., Edward, P. & Hardcastle, C. (2007). International Building Design Management and Project Performance; Case Study in Sao Paulo, Brazil. *Architectural Engineering and Design Management,* Vol. 3, pp.5-16.

Gupta, A. (2000), Enterprise resource planning: the emerging organizational value systems. *Industrial Management & Data Systems*, Vol. 100, pp. 114-8.

Holland, C. & Light, B. (1999). A critical success factors model for ERP implementation. *IEEE Software*, Vol. 16, p. 30.

Hong, K. K. & Kim, Y. G. (2002). The critical success factors for ERP implementation: an organizational fit perspective. *Information & Management*, Vol. 40, p. 25.

Hussain, T. (2015). *A Model for Project Governance in Delivery of Oil and Gas Projects in Alberta* (A Thesis Submitted to The Faculty of Graduate Studies in Partial Fulfilment of the Requirements for The Degree of Doctor 0f Philosophy). Department of Civil Engineering, Calgary, Alberta.

Jefferies, M., Gameson, R. & Rowlinson, S. (2002). Critical success factors of the BOOT procurement system: reflections from the Stadium Australia case study. *Engineering, Construction and Architectural Management*, *9*(4), pp. 352-361.

Jepsen, A. L., & Eskerod, P. (2009) Stakeholder analysis in projects: Challenges in using current guidelines in the real world. *International Journal of Project Management*, *27*(4), pp. 335-343.

Jergeas, G. F., Eng. P., Williamson, E., Skulmoski, G. J. & Thomas, J. L. (2000) Stakeholder management on construction projects. *2000 AACE International Transaction*, 12.1-12.6.

Jha, K. N. & Iyer, K. C. (2006). Critical factors affecting quality performance in construction projects. *Total Quality Managemen, 17*(9):1155-1170.

Kalling, T. (2003). ERP systems and the strategic management processes that lead to competitive advantage. *Information Resources Management Journal*, Vol. 16, p. 46.

Karlson, J. T. (2002). Project stakeholder management, *Engineering Management Journal*, *14* (4), pp. 19-24.

Kraemmergaard, P. & Rose, J. (2002). Managerial competences for ERP journeys. *Information Systems Frontiers*, Vol. 4, p. 199.

Li, Y., Lu, Y. & Peng, Y. (2011). Hierarchical structuring success factors of project stakeholder management in the construction organization. *African Journal of Business Management*, *5*(22), pp. 9705-9713.

Liu, H., Jazayeri, E. & Dadi, G. B. (2017). Establishing the influence of owner practices on construction safety in an operational excellence model. *Journal of Construction Engineering and Management*, *143*(6), 04017005. DOI: 10.1061/(ASCE)CO.1943-7862.0001292.

Mandal, P. & Gunasekaran, A. (2003). Issues in implementing ERP: a case study. *European Journal of Operational Research*, Vol. 146, pp. 274-83.

McElroy, B. & Mills, C. (2003). Managing Stakeholders. In: Turner, R.J. (Ed.). People in Project Management, Aldershot, Gower, 99-118.

Miller, R. & Lessard, D. (2001). Understanding and managing risks in large engineering projects. *International Journal of Project Management*, *19*(8), 437-443.

Mitchell, R. K., Agle, B. R. & Wood, D. J. (1997). Toward a theory of stakeholder identification and salience: Defining the principle of who and what really counts. *Academy of Management Review*, *22*(4), 853-886.

Moodley, K., Smith, N. & Preece, C.N. (2008). Stakeholder matrix for ethical relationships in the construction industry. *Construction Management and Economics*, *26*(6), 625-632.

Motwani, J., Mirchandani, D., Madan, M. & Gunasekaran, A. (2002). Successful implementation of ERP projects: evidence from two case studies. *International Journal of Production Economics*, Vol. 75, p. 83.

Nguyen, N. D., Ogunlana, S. O. & Lan, Đ. T. X. (2004) A study on project success factors in large construction projects in Vietnam. *Engineering, Construction and Architectural Management*, Vol. 11, no. 6, pp. 404-413.

Nah, F. F. H., Lau, J. L. S. & Kuang, J. (2001), Critical factors for successful implementation of enterprise systems. *Business Process Management Journal*, Vol. 7, p. 285.

Nguyen, N. H., Skitmore, M. & Wong, J. K. W. (2009). Stakeholder impact analysis of infrastructure project management in developing countries: a study of perception of project managers in state-owned engineering firms in Vietnam. *Construction Management and Economics*, *27*(11), pp. 1129-1140.

Olander S. & Landin, A. (2005). Evaluation of stakeholder influence in the implementation of construction projects. *International Journal of Project Management*, *23*(4), 321-328.

Olander, S. (2006). *External stakeholder management*. (PhD thesis). Lund University, the UK.

Olander, S. (2007). Stakeholder impact analysis in construction project management. *Construction Management and Economics, 25*(3), pp. 277-287.

Olander, S. & Landin, A. (2008). A comparative study of factors affecting the external stakeholder management process. *Construction Management and Economics, 26*(6), pp. 553-561.

Pinto, J. K. & D. Slevin, B. (2009). Trust in Projects: An empirical assessment of owner/contractor relationships. *International Journal of Project Management*, *27*(6), pp. 638-648.

PMBOK, PMI (Project Management Institute) (2018). A Guide to the Project Management Body of Knowledge, Fourth version, Newtown Square, Pa.

Pocock, J. B., Hyun, C.T., Liu, L.Y. & Kim, M. K. (1997). Relationship between project interaction and performance indicators. *Journal of Construction Engineering and Management*, Vol. *122*(2), pp.165-176.

Podnar, K. & Jancic, Z. (2006) Towards a categorization of stake-holder groups: An empirical verification of a three-level model. *Journal of Marketing Communications*, *12*(4), 297-308. pp. 167-175.

Ribbers, P. M. A. & Schoo, K. C. (2002) Program management and complexity of ERP implementations. *Engineering Management Journal*, Vol. 14, p. 45.

Robey, D., Ross, J. W. & Boudreau, M. C. (2002). Learning to implement enterprise systems: an exploratory study of the dialectics of change. *Journal of Management Information Systems*,

Vol. 19, p. 17.

Hammad, S (2013). Investigating the Stakeholder Management in Construction Projects in the Gaza Strip, P 7.

Sarker, S. & Lee, A. S. (2003). Using a case study to test the role of three key social enablers in ERP implementation. *Information & Management*, Vol. 40, p. 813.

Scott, J. E. & Vessey, I. (2000) Implementing enterprise resource planning systems: the role of learning from failure. *Information Systems Frontiers*, Vol. 2, p. 213.

Shanks, G. & Parr, A. (2000). A model of ERP project implementation. *Journal of Information Technology*, Vol. 15, pp. 289-303.

Silverman, D. (2000). *Doing Qualitative Research: A Practical Handbook*. Sage, Thousand Oaks, CA.

Siriginidi, S. R. (2000b). Enterprise resource planning in reengineering business. *Business Process Management Journal*, Vol. 6, p. 376.

Skok, W. & Legge, M. (2002). Evaluating enterprise resource planning (ERP) systems using an interpretive approach. *Knowledge and Process Management*, Vol. 9, p. 72.

Soh, C., Kien, S. S. & Tay-Yap, J. (2000). *Cultural fits and misfits: is ERP a universal solution*? Association for Computing Machinery, Communications of the ACM, Vol. 43, p. 47.

Somers, T. M. & Nelson, K. G. (2004) A taxonomy of players and activities across the ERP project life cycle. *Information & Management*, Vol. 41, pp. 257-78.

Trimmer, K. J., Pumphrey, L. D. & Wiggins, C. (2002). ERP implementation in rural health care. *Journal of Management in Medicine*, Vol. 16, p. 113.

Wahab, H. (2011). *Design process and stakeholder management in airport construction*. (Dissertation submitted in partial fulfillment of MSc Project Management), Faculty of Business, The British University in Dubai.

Walker, D. H. T., Bourne, L. M. & Shelley, A. (2008). Influence, stakeholder mapping and visualization. *Construction Management & Economics, 26*(6), pp. 645-658.

Weshah, N., El-Ghandour, W., Cowe Falls, L. & Jergeas, G. (2014a). A New Approach for Evaluating and Analyzing the Impact of Interface Management (IM) on Project Performance during Engineering / Design Phase using Monte Carlo Simulation. In *Proceedings of the Canadian Society for Civil Engineering Conference Halifax,Nova Scotia, Canada, May 28th -31st, 2014.* (pp. GEN–128–1–10).

Wheeler, D. & Sillanpaa, M. (1997). *The stakeholder corporation: A blueprint for maximizing stakeholder value*. London: Pitman Publishing. © University of Pretoria 128.

Wong, K. Y. & Aspinwall, E. (2005). An empirical study of the important factors for knowledge-management adoption in the SME sector. *Journal of Knowledge Management, 9*(3): 64-82. DOI: 10.1108/13673270510602773.

Xu, H., Nord, J. H., Brown, N. & Nord, G. D. (2002). Data quality issues in implementing an ERP. *Industrial Management & Data Systems*, Vol. 102, p. 47.

Yang, J., Shen, Q. P. & Ho, M. F. (2009a). An overview of previous studies in stakeholder management & its implications for construction industry. *Journal of Facilities Management*, *7*(2), pp. 159-175.

Yang, J., Shen, Q. P., Ho, M. F., Drew, S. D. & Chan, A. P. C. (2009b). Exploring critical success factors for stakeholder management in construction projects. *Journal of Civil Engineering and Management*, *15*(4), pp. 337-348.

Yu, T. W., Shen, Q. P., Kelly, J. & Hunter, K. (2007). An empirical study of the variables affecting construction project briefing/architectural programming. *International Journal of Project Management*, *25*(2), pp. 198-212.

Yusuf, Y., Gunasekaran, A. & Abthorpe, M. S. (2004) "Enterprise information systems project implementation: a case study of ERP in Rolls-Royce. *International Journal of Production Economics*, Vol. 87, pp. 251-66.

Cite this article as: Mashali A., Elbeltagi E., Motawa I., Elshikh M., "Stakeholder Management: An Insightful Overview of Issues", *International Conference on Civil Infrastructure and Construction (CIC 2020)*, Doha, Qatar, 2-5 February 2020, DOI: https://doi.org/10.29117/cic.2020.0029

Strategies for Communicating Health and Safety Information on Construction Sites in Nigeria

Samuel Abiodun Alara
samuelabiodunalara@fpmubieportal.edu.ng
Federal Polytechnic Mubi, Adamawa, Nigeria

Ibrahim Ibrahim Inuwa
iiinuwa@atbu.edu.ng
Abubakar Tafawa Balewa University, Bauchi, Nigeria

ABSTRACT

The construction industry (CI) has earned the notoriety of being a risky or profoundly unsafe industry. Studies have credited the majority of the mishap on construction sites to poor communication of health and safety (H&S) information among all the parties engaged in construction activities. The study assessed strategies for communicating H&S information on construction sites and evaluates factors influencing the choice of communication strategies for H&S information on construction sites. The data for the investigation were gotten using multiple-choice questionnaire administered on 20 construction sites domicile in Abuja, Nigeria. A sum of one hundred (100) questionnaire were administered to respondents; out of which eighty-five (85) were returned speaking to 85% reaction rate. Data received were analyzed using descriptive and inferential statistics at 95% degree of certainty. The study revealed that safety signs and training are most important medium of communicating H&S information on construction sites and shown that cost implication of the strategy significantly influences the choice of communication strategies for H&S information on Nigerian construction sites. The study therefore, recommends that contracting firms be duty-bound to engage signs and symbols in communicating H&S information, as communication that involves images is clearer and can be directly understood. Quantity surveyors should ensure that adequate provision is made in the bill of quantities for implementing H&S procedures on construction sites. Safety awareness ought to be incorporated in the overall procurement procedure, and workers should be consistently train and re-train on H&S procedures.

Keywords: Semiotics; Health and safety information; Communication strategies; Nigeria

1 INTRODUCTION

The construction industry (CI) has earned the notoriety of being a risky or profoundly unsafe industry in light of the fact that it has a poor health and safety (H&S) execution record, with operatives' multiple times bound to experience the ill effects of deadly wounds than those in different sectors everywhere throughout the world (Alhajeri, 2011; Dadzie, 2013; Phoya, 2012). The International Labor Organization (ILO) appraises that in any event 60,000 lethal mishaps occur annually on building sites around the globe, which is one out of six of all deadly construction related mishaps. Besides, it has

been recognized that 25-40% of fatalities on the global workplace related accidents are contributed by construction (International Labor Organization-ILO, 2017).

Several studies led in developed and developing nations corroborate proof of this generally high extent of mishaps on building sites. In Australia, the CI comprises 9% of absolute workforce, yet records a casualty rate double that of other sector, and compensate 11% of every single genuine laborer's remuneration claims (Greuter et al., 2012). In Europe, the CI records 30% of all lethal mechanical mishaps, notwithstanding utilizing just 10% of the working populace (McKenzie et al., 1999). According to BLS (2016) report; in United State of America, fatality rate expanded to 10.1 for every 100,000 full-time comparable (FTC) in 2015 as against 9.8 for every 100,000 (FTC) in 2014. In Saudi Arabia, the CI represents 51.35% out of 69,241 all the mishaps cases documented (General Organization for Social Insurance (GOSI), 2015). In Japan, construction casualties represent 30% - 40% of the overall aggregate of contemporary mishaps, with the absolute being half in Ireland (ILO, 2017). It was likewise affirmed that construction lethal mishaps represent 59% of absolute deadly mishaps in all sectors all over Singapore. In Italy, the deadly mishaps in the CI speak to 25% of the absolute mishaps happening in the sector (Baldacconi & Santis, 2000). In Ghana, it was accounted for that the CI recorded 902 mishap cases containing 56 lethal mishaps and 846 non-deadly mishaps in year 2000 (Danso, 2005). In that equivalent report, it was demonstrated that Kumasi (the provincial capital of Ashanti) alone documented 124 construction mishap from 1999 to 2004. Besides, Laryea and Mensah (2010) uncovered a poor condition of H&S on Ghanaian CI. In Nigeria, the CI is liable for about 7.5% of all work related mishap, 49.5% of these incidents were deadly, 12.2% of fractional handicaps and 7.4% of minor wounds (Umeokafor et al., 2014). The Nigerian CI losses 5 – 7% of her labor force every year to construction mishaps (Olatunji et al., 2007). As indicated by Abdullahi et al. (2015), 76.40% of site operatives in Nigeria had one type of mishaps or the other on building sites.

The issues of mishaps and ill health problems in building and CI are of serious concern globally (Alhajeri, 2011; Dadzie, 2013; Phoya, 2012). Thus several researches have been conducted across the globe to improve on H&S status on construction (Albert et al., 2014; Danso, 2005; Greuter et al., 2012; Hare et al., 2012; Inuwa et al., 2018). Findings from studies carried out to assess the causes of accidents have all pointed to poor communication of H&S information among all the parties engaged in construction activities (Akunyumu, 2017; Kwofie, 2015; Landin & Kindahl, 2013). Albert et al. (2014) discovered that communication is the paramount strategy for risks identification. Communication of H&S has been regarded to be a pivotal point for decreasing mishaps and ill-health complications on construction sites and crucial to attaining acceptable level of efficient and effective H&S on construction sites (Phoya, 2012).

However, in Nigeria, communication on construction sites has been inadequate and declined to worrisome state, over 50% of construction projects in Nigeria failed because of unsuitable communication strategies (Kasimu & Usman, 2013). Besides, for H&S information to be compelling it must be comprehended, which is governed by the strategy utilized (Preece & Stocking, 1999; Vecchio-Sadus, 2007). With expanded budgetary ramifications associated with construction related injuries and the rising quest for zero incident undertakings, researchers are investigating the execution of inventive

H&S communication strategies (Albert et al., 2014; Greuter et al., 2012); including signs and images as a communication strategy (Ogunmola, 2013). However, semiotics; the science underpinning how signs and images are utilized to pass information, is a domain that is yet to be appropriately investigated to reduce mishaps on building sites (Inuwa et al., 2018).

An audit of studies led on communication on building sites in the Nigerian CI fall short of focusing on how semiotics can be utilized to facilitate effective H&S communication on construction site (Olaniran, 2015; Tipili & Ojeba, 2014). Thus this research investigated how semiotics can be utilised to enhance effective H&S communication on construction sites in Nigeria, with the end goal of enhancing H&S management that will diminish the event of mishaps on construction sites. The investigation sketched out the following objectives: to assess strategies for communicating H&S information on construction sites, to evaluate factors influencing the choice of strategies for effective H&S communication on construction sites.

2 LITERATURE REVIEW

2.1 Theoretical construct

This investigation builds on the theory of semiotics as upheld by Charles Sanders Peirce (1839-1914). Semiotics is the umbrella term used to depict the theory or investigation of signs and images as methods for communication. As indicated by Huhtamo (2003), semiotic is a field of study that reviews signs as a fundamental piece of social life and communication; semioticians certify that, we can just know culture (and reality) by methods for signs, through the procedures of signification. Signs incorporate words, signals, pictures, sounds, and articles (Henley et al., 2015). For example, the manner by which the individuals who are hard of hearing convey utilizing communication through sign language shows how people react to semiotics and that signs and images can reverberate the same amount of information as words. Undoubtedly, sometimes semiotics transcends language as a means of communication. In semiotics, the word sign has uncommon importance; for example, side effect is an indication of ailment in a wiped out individual. Thus sign is something which represents something (Crow, 2017). Peirce hypothesis of semiotics hypothesized that a sign can possibly successfully convey a message if the intended interest group for which the message is aimed at comprehends the interrelationship between representamen (signifier), interpretant (signified), and the object inside the setting of a sign (Berger, 2004; Crow, 2017).

Along these lines for a sign to be compelling in imparting a message to an individual (subject) inside the setting of construction industry culture, the individual must: perceive the structure the sign takes (signifier; representamen), comprehends (interpretant) the message the signifier is passing on (connoted; appreciation), and recognize the thought wherein the sign represents; the motivation behind the sign (Object).

2.2 Conceptual Framework

Semiotics in built environment can radically improve the capability of H&S communication strategies and help guarantee that different and more extensive audience can be reached adequately. However, it will take consistent implementation for strategy to establish a clear semiotic association and image will help speed up this process, as

it facilitates memory recall. Semiotics in safety can thus be achieved through leitmotifs (reoccurring images). In addition, for the workers to comprehend what this H&S signs represent, they should above all else recollect (Inuwa et al., 2018). Accordingly, this will improve effective communication on construction sites. The workers applying what he has perceived and recognize from different strategies will manage the worker in acting securely on site. Subsequently, empowering the worker to accomplish the objective of the strategy; preventing and curbing accidents on construction sites. This idea is presented in Figure 1.

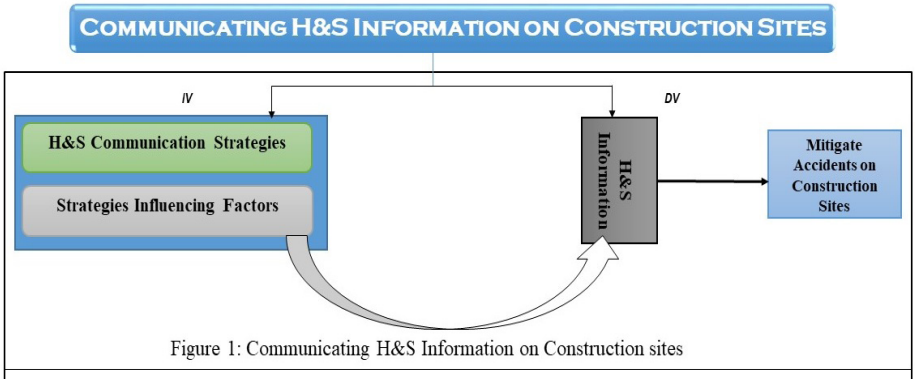

Figure 1: Communicating H&S Information on Construction sites

2.3 Strategies for Communicating Health and Safety Information on Construction sites

For H&S communication to be effective it has to be understood, which is governed by kind of information to be communicated, the target audience, environment where transmission takes place and the strategy used (Preece & Stocking, 1999; Vecchio-Sadus, 2007). The communications strategy of contracting firms; fills in as a suggested structure and activity plan for an association's interchanges and effort endeavors. Studies uncovered that strategies for imparting H&S information on building sites include organization mission statement, strategic plan and policy, checklists manuals and operating procedures, hazards reports, incidents and near-misses, safety induction, training, H&S website, posters, brochures and notice boards, H&S signs, toolbox talks, H&S week and public report (Preece & Stocking, 1999; Vecchio-Sadus, 2007). Vecchio-Sadus (2007) in his studies acknowledged that a number of strategies are required for various organization and choosing the viability of communication of H&S information relies upon the strategy utilized. This strategy will impact whether individuals will comprehend or not and take part in the H&S procedure. The language utilized frequently decide its adequacy, in bid to enhance H&S status of workers on building sites, parties involved need to pay attention to the choice of communication strategies to be used on the sites. Recent developments in the CI have shown the need to assess strategies for communicating H&S information on construction sites in Nigeria for effective H&S communication on site.

2.4 Factors Influencing the Choice of Communication Strategies for Health and Safety

Strategies of communications of H&S information can take many different forms,

with each being appropriate for particular circumstances. It is important to first consider the objective of communication i.e. to persuade; inform; question or instruct the workers on health and safety issues (Preece & Stocking, 1999; Vecchio-Sadus, 2007). This will now be tailored to the strategy that suits the objective of the communication. Studies revealed that choice of communication strategies can be influence by availability of time/ time pressures, literacy skill of site operatives, awareness of information technology, number of recipients, types of information/message, nature of hazard/severity of the risks involved and cost implication of the strategy (Preece & Stocking, 1999; Vecchio-Sadus, 2007) opined that so as to enhance H&S status of workers on building sites, parties involved need to pay attention to the choice of communication strategies to be used on the sites. Recent developments in Nigerian CI have led to a renewed interest on the factors influencing the choice of communication strategies for H&S information in Nigeria. An audit of studies led on H&S management in Nigeria revealed little or no studies led on factors influencing the choice of communication strategies for H&S information on construction sites in Nigeria Accordingly, there is a need to evaluate factors influencing the choice of communication strategies for H&S information on construction sites in Nigeria.

3 METHODOLOGY

This study was led in Abuja, the capital of Nigeria; it has the most elevated convergence of construction activities in the nation, and in that capacity has the most elevated centralization of construction experts (Inuwa, 2014). The experience of the experts' transverses the whole nation. Literatures were explored to identify strategies used for communicating H&S information and factors influencing their choice on construction sites. Afterwards a multi-choice questionnaire was designed to evoke information from respondents on the import of strategies for communicating H&S information on construction sites and evaluates factors influencing the choice of communication strategies for H&S information on construction sites respectively. The investigation utilized purposive sampling to choose key respondents from every one of the classes of respondents to guarantee that the correct respondents with the important information, authority and experience on the topic were satisfactorily chosen. The respondents comprised of construction professionals (management staff/safety officers) carefully chosen from contracting firms; engaged with the administration of 20 on-going government building ventures domiciled in Abuja, Nigeria. One hundred structured questionnaire were distributed to respondents and, accomplishes 85% return rate. This return rate is well satisfactory in the perspective of built environment researchers and sufficient for an important examination (Inuwa, 2014). The study used Cronbach alpha coefficient to test the internal consistency of the questionnaire reliability, the Cronbach's α measure for the questionnaire constructs revealed that the questionnaire is very reliable, since their Cronbach's α exceeds 0.7 (Pallant, 2011). The questionnaire sought information on respondents' profiles. The respondents were solicited to rate the degree of effectiveness of identified strategies in communicating H&S information and indicate the extent to which variables influences contracting firms in choosing a communication strategy that will be most suitable. Respondents view were depended on a 5-point Likert scales: 5(strongly agree/extremely important), 4(agree/very important),

3(neutral), 2(disagree/slightly important) and 1(strongly disagree/not at all important). To empirically assess the effectiveness of identified strategies and to give an understanding with regards to the degree to which each factor adds to conveying H&S information on construction sites in Nigeria; the Relative Importance Index (RII) was utilized. It is a non-parametric statistical technique largely employed by built environment scientists for investigating organized survey reactions for information including ordinal estimation of frames of mind (Kometa et al., 1994). RII was employed for the examination as it is apt for the motivation behind this investigation. In the estimation of the Relative Importance Index (RII), the formula beneath was utilized (see equation underneath):

$$RII = \frac{\sum W}{AN} * 100 \quad (1)$$

Where **W** is the weighting given to each item by the respondents range from 1 to 5; i.e. 5 for highest to 1 for lowest while 'n' is the number for respondents for each weighting. **A** is the highest weight; **N** is the total number of the respondents. RII esteem ranges from ($0 \leq RII \leq 1$). It indicates that higher the estimation of RII, increasingly significant was the communication strategy and vice versa, also the higher the estimation of RII, progressively powerful was the factor in the choice of most suitable communication strategies for H&S information and the other way around. The correlation of RII with the comparing significance level is estimated as per the following range:

From 0.8 to1.0 adjudged High (H), from 0.6 to < 0.8 adjudged High-Medium (H-M), from 0.4 to < 0.6 adjudged Medium (M), from 0.2 to < 0.4 adjudged Medium-Low (M-L), while 0.0 to < 0.2 is adjudged Low (L).

4 RESULTS AND DISCUSSION

4.1 Respondents Demographic Profiles

The significance of statistic data cannot be undermined for an important quantitative investigation. During the research, respondents were requested to provide generation information. As the point of research is centered around the construction stage of the projects, so it was conceived to choose key respondents from every one of the classes of respondents to guarantee that the correct respondents having acceptable expert experience were satisfactorily chosen. Analysis of the feedbacks shows that well over 98% of the participants are within the range of 31 to 35 years and over 50 years of age. This indicates that the vast majority of the participants are sufficiently aged to be safety mindful. Likewise, 93% of the feedbacks are male whereas the residuals are female. This portrays the idea of the CI as male ruled industry. The result of the feedback indicates that over 98% of the respondents have finished their bachelor degree or advanced education. Above 63% of the respondents are project managers, over 8% are architects, over 23% are safety officers, while 4.7% are engineers. This outcome uncovered that these classes of participants are the one's generally engaged with H&S management on construction sites. The participants have more than 15 years' field involvement with the CI. The participants have a mean sum of over 22 years work involvement with the CI. This shows the participants have satisfactory work involvement with the CI, to react to the investigation of this nature.

4.2 H&S Communication Strategies

The first objective was to assess strategies for communicating H&S information on construction sites in Nigeria. The following H&S communication strategies; safety signs and training, organization mission statement, policy and strategic plan, safety induction and toolbox talks, safety week and public report, manuals, checklists and operating procedures, reports of hazards and brochures as well as health and safety website were ranked first, second, third, fourth, fifth, sixth and seventh position respectively. Table 1 summarize the Relative Importance Index (RII) of the communication strategies alongside their equivalent ranking and significance level. It is apparent from Table 1 that ten techniques were evaluated as "High significance levels which are adjudged as of prime significance in conveying H&S information on construction sites while website was ranked as "high medium significance level". These "High" significance markers have Relative Index (RII) in the scope of 0.95–0.85. These high ranked strategies include health and safety signs (RII=0.95), training (RII=0.95), organization mission statement, policy and strategic plan (RII=0.91), safety induction (RII=0.89), toolbox talk (RII=0.89), health and safety week (RII=0.88), public report (RII=0.88), manuals, checklists and operating procedures (RII=0.87), reports of hazards, incidents and near-misses (RII=0.85), brochures, posters and notice boards (RII=0.85) and health and safety website (RII=0.74). They are considered by respondent as important medium of communicating H&S information on construction sites.

The study revealed that safety signs and training are most important medium of communicating H&S information on construction sites with an aggregated relative importance index of 0.95 and was ranked as the top most strategies for communicating H&S information on construction sites in Nigeria, which is in agreement with studies by (Hare et al., 2012) and (Md-Ulang, 2012) however, these studies were conducted in The United Kingdom respectively.

Table 1: Relative Importance Index (RII) of the Communication Strategies

H&S Communication Strategies	N	Mean	RII	Level	Ranking
Organization Mission Statement, Policy and Strategic Plan	85	4.55	0.91	hH	2nd
Safety Induction	85	4.45	0.89	H	3rd
Manuals, Checklists and Operating procedures	85	4.33	0.87	H	5th
Reports of Hazards, Incidents and Near-Misses	85	4.27	0.85	H	6th
Training	85	4.73	0.95	H	1st
Health and Safety Website	85	3.69	0.74	H-M	7th
Brochures, Posters and Notice Boards	85	4.25	0.85	H	6th
Health and Safety Warning Signs	85	4.73	0.95	H	1st
Toolbox Talks	85	4.45	0.89	H	3rd
Health and Safety Week	85	4.38	0.88	H	4th
Public Report	85	4.39	0.88	H	4th

4.3 Factors Influencing Choice of Strategies

Table 2 shows the Relative Importance Index (RII) of factors influencing the choice of communication strategies for H&S information alongside their equivalent ranking and

significance level. From the summary of results in Table 2, it can be observed that all the factors were rated as "High importance levels which are adjudged of prime importance in the choice of communication strategies for H&S information on construction sites in Nigeria. These "High" significance pointers have Relative Index (RII) in the scope of 0.99–0.81. These high ranked factors include cost implication of the strategy (RII=0.99), availability of time/time pressures (RII=0.88), literacy skill of site operatives (RII=0.85), awareness of information technology (RII=0.85), nature of hazard/severity of the risks involved (RII=0.85), types of information/message (RII=0.84) and number of recipients (RII=0.81). They are considered by respondent as important factors in the choice of communication strategies for H&S information on construction sites. Similarly, the investigation revealed that cost implication significantly influences the choice of communication strategies for H&S information with an aggregated relative importance index of 0.99 and was rated as the top most factor that influence the choice of communication strategies for H&S information on construction sites in Nigeria which is in agreement with studies by Windapo (2013), however, this study was led in Western Cape region of South Africa.

Table 2: Factors that influence the choice of communication strategy

H&S Communication Strategies	**N**	Mean	RII	Level	Ranking
Availability of Time/Time pressures	85	4.41	0.88	H	2nd
Literacy Skill of Site Operatives	85	4.27	0.85	H	3rd
Awareness of Information Technology	85	4.27	0.85	H	3rd
Number of Recipients	85	4.05	0.81	H	5th
Types of Information/Message	85	4.20	0.84	H	4th
Nature of hazard/severity of the risks involved	85	4.26	0.85	H	3rd
Cost Implication of the Strategy	**85**	4.93	0.99	H	1st

5 CONCLUSION

The study revealed that safety signs and training are most important medium of communicating H&S information on construction sites which imply that contracting firms ought to engage signs and symbols in communicating H&S Information and continuously train construction operatives on H&S signs and symbols assimilation. Similarly, the study also revealed that cost implication significantly influences the choice of communication strategies for H&S information which implies that contracting firms may not implement H&S communication strategy, if the cost of strategy is a lot when contrasted with their expected profit margin. The study therefore, recommends that contracting firms H&S communication strategy be considered as one of the grounds for awarding contract and ensure strict compliance, as adherence will definitely maximize safety performance of our construction sites. Contracting firms be duty-bound to engage signs and symbols in communicating H&S information, as communication that involves images is clearer and can be directly understood. Quantity surveyors should ensure that adequate provision is made in the Bill of Quantities for health and safety management on construction sites. Safety awareness ought to be incorporated in the overall procurement procedure, and workers should be consistently train and re-train on H&S procedures.

REFERENCES

Abdullahi, U., Anum, I., Adole, A. M. & Williams, F. N. (2015). Artisans Working Conditions In The Nigerian Construction Industry: A Case Study Of Some States In Northern Nigeria. *ATBU Journal of Environmental Technology (A'JET), 8*(1), 16-25.

Akunyumu, S. (2017). *A framework for on-site communication planning for construction managers in Ghana*. (Master of Philosophy Thesis), College of Art and Built Environment, KNUST, Kumasi, Ghana.

Albert, A., Hallowell, M. R. & Kleiner, B. M. (2014). Emerging Strategies for Construction Safety & Health Hazard Recognition. *Journal of Safety, Health & Environmental Research, 10*(2), 152-161.

Alhajeri, M. (2011). *Health and Safety in the Construction Industry: Challenges and Solutions in the UAE.* Coventry University, Coventry.

Baldacconi, A. & Santis, P. (2000). *Risk assessment in construction field in Italy*. Rome, Italy: National Institute for Insurance against injuries at Work.

Berger, A. A. (2004). *Techniques Of Interpretation: Semiotic Analysis Media Analysis Techniques*. SAGE Publications, Incorporated.

BLS (2016). *National Census Of Fatal Occupational Injuries In 2015*. United States of America: Bureau Of Labor Statistics.

Crow, D. (2017). *Visible Signs: Intro to Semiotics From David Crow's Visible Signs.* Retrieved November from http://www.amazon.co.uk.

Dadzie, J. (2013). Perspectives of consultants on health and safety provisions in the labor act: a study into theory and practicals. *Engineering Management Research, 2*(1), 34.

Danso, F. (2005). *Improving safety on building construction site on KNUST campus in Kumasi*, Ghana. (Unpublished BSc Thesis, Faculty of Architecture and Building Technology). KNUST, Kumasi, Ghana.

General Organization for Social Insurance (GOSI) (2015). Annual Statistical Report 1435h: General Organization for Social Insurance (GOSI).

Greuter, S., Tepe, S., Peterson, J. F., Boukamp, F., Amazing, K. D., Quigley, K. & Wakefield, R. (2012). Designing a Game for Occupational Health and Safety in the Construction Industry. *Australian Construction Management,* ACM IE '12, July 21 - 22 2012, Auckland, NZ, New Zealand. DOI: 10.1145/2336727.2336740.

Hare, B., Cameron, I., Real, K. J. & Maloney, W. F. (2012). Exploratory case study of pictorial aids For communicating health and safety for migrant construction workers. *Journal of Construction Engineering and Management, 139*(7), 818-825.

Henley, M., Keddy, M., Kinsman, B., Muggridge, M. & Shields, K. (2015). Semiotic Analysis: A Research Guide. Retrieved March 3, 2018, from Imogen Charles http://fr.scribd.com;presentations.

Huhtamo, E. (2003). Visual Communication and Semiotics. *DESMA 103 Visual Communication Spring,* Retrieved June 12, 2017 from http://www.erkkihuhtamo.com.

International Labour Organisation-ILO (28 April, 2017). One Worker Dies Every 15 Seconds, 153 Have Work-Related Accidents, 2017 World Day For Safety And Health At Work In Abuja, *Vanguard Nigeria*.

Inuwa, I. I. (2014). *Project Planning In Construction Procurement: The Case of Nigerian*

Indigenous Contractor. (PhD Thesis), Jomo Kenyatta University of Agriculture and Technology, Nairobi-Kenya.

Inuwa, I. I., Alara, S. A. & Gambo, N. (2018). Health and safety awareness on construction sites in Yola Metropolis of Nigeria. *Paper presented at the International Conference on Contemporary Issues In Business & Economics (ICCIBE)*, Tasliciftlik Campus, Gaziosmanpasa University, Tokat, Turkey. 235-244.

Kasimu, A. & Usman, M. (2013). Delay in Nigerian construction industry. *Journal of Environmental Sciences and Resources Management, 5*(2), 120-129.

Kometa, S. T., Olomolaiye, P. O. & Harris, F. C. (1994). Attributes of UK construction clients influencing project consultants' performance. *Construction Management and economics, 12*(5), 433-443.

Kwofie, E. T. (2015). *Contribution of unique features of mass housing projects to project team communication performance* (PhD Thesis, College of Art and Built Environment). KNUST, Kumasi, Ghana.

Landin, E. & Kindahl, N. (2013). *Information and communication trends in the Swedish construction industry*. (Msc Thesis, Department of Real Estate and Construction Management). KTH Sweden.

Laryea, S. & Mensah, S. (2010). Health and Safety on Construction Sites in Ghana‖ in The Construction, *Building and Real Estate Research Conference of the Royal Institution of Chartered Surveyors*, 2-3 September 2010, Dauphine Universite, Paris, France.

McKenzie, J., Gibb, A. G. F. & Bouchlaghem, N. M. (1999). Communication of Health and Safety in Design Phase: Implementation of Safety and Health on Construction Sites. *Paper presented at the Proceedings of the 2nd International Conference of International Council for Research and Innovation in Building and Construction (CIB) Working Commission W99*, Honolulu.

Md-Ulang, N. (2012). Communication of construction health and safety information in design.© Norhidayah Md Ulang.

Ogunmola, A. A. (2013). Signs and Symbols as Communication Strategy: A Semiotic Study of Highway Codes in Nigeria. *Journal of New Media and Mass Communication, 19*(1), 62-68.

Olaniran, H. (2015). On the role of communication in construction projects in Nigeria. *Journal of Environmental Science and Technology, 2*(5), 048-054.

Olatunji, O. A., Aje, O. I. & Odugboye, F. (2007). Evaluating Health and Safety Performance of Nigerian Construction Site. *Paper presented at the CIB World Building Congress*, 2007.

Pallant, J. (2011). *SPSS Survival Manual: A Step by Step to Data Analysis Using SPSS*. New South Wales: Allen & Unwin.

Phoya, S. (2012). *Health And Safety Risk Management on Building Construction Sites in Tanzania: The Practice of Risk Assessment, Communication and Control* (Licentiate thesis, Chalmers University of Technology), Gothenburg, Sweden.

Preece, C. & Stocking, S. (1999). Safety Communications Management In Construction Contracting. *Paper presented at the Hughes, W, 15th Annual ARCOM Conference*, Liverpool John Moores University.

Tipli, L. G, Ojeba, P. O. & liyasu, M. S. (2014). Evaluating the effects of communication in construction project delivery in Nigeria. *Global Journal of Environmental Science and Technology*, *2*(5): 048-054.

Umeokafor, N., Isaac, D., Jones, K. & Umeadi, B. (2014). Enforcement of occupational safety

and health regulations in Nigeria: An exploration. *European Scientific Journal,* 3, 93-104.

Vecchio-Sadus, A. M. (2007). Enhancing safety culture through effective communication. *Safety Science Monitor, 11*(3), 1-10.

Windapo, A. O. (2013). Relationship between degree of risk, cost and level of compliance to occupational health and safety regulations in construction. *Construction Economics and Building, 13*(2), 67-82.

Cite this article as: Alara S. A., Inuwa I. I., "Strategies for Communicating Health and Safety Information on Construction Sites in Nigeria", *International Conference on Civil Infrastructure and Construction (CIC 2020)*, DOI: https://doi.org/10.29117/cic.2020.0030

Solar DER Investment for MWANI Qatar Building at Hamad Port

Adel Karama
adelkarama@gmail.com
EllisDon Q, Doha, Qatar

ABSTRACT

This document discusses the benefits of adding a solar distributed energy resource (DER) investment to MWANI Qatar (MQ) building at Hamad Port. The social and environmental aspects of a Solar PV system with battery storage were evaluated besides economic calculations outcome. The calculations show a marvelous 96% CO2 emission reduction with significant battery storage benefits and a 269,676 KWh/yr reduction in electricity leading to a $33,217.52 annual savings. In essence, the State of Qatar is governed by a vision of excellence, innovation and leadership that this investment could be a role model for the country's sustainable future developments.

Keywords: Solar battery; Construction; Distributed energy resource (DER)

1 INTRODUCTION

Hamad Port Project (HPP) is of one of the world's largest Greenfield port developments. Strategically located south of Doha covering 28 square kilometers with a budget of USD $7.4 Billion (New Port Project Steering Committee). It is a megaproject that includes a new port, a new base for the Qatar Emiri Naval Forces and the Qatar Economic Zone (3). The port is managed by MWANI Qatar (MQ), which is in charge for handling Qatar's shipping terminals and seaports. The port contains three iconic buildings that were designed to reflect the advancement technology of the port. One of those iconic buildings is MQ building as shown in Figure 1(MwaniQatar) which is referred to as the "cheese building" due to its triangular design.

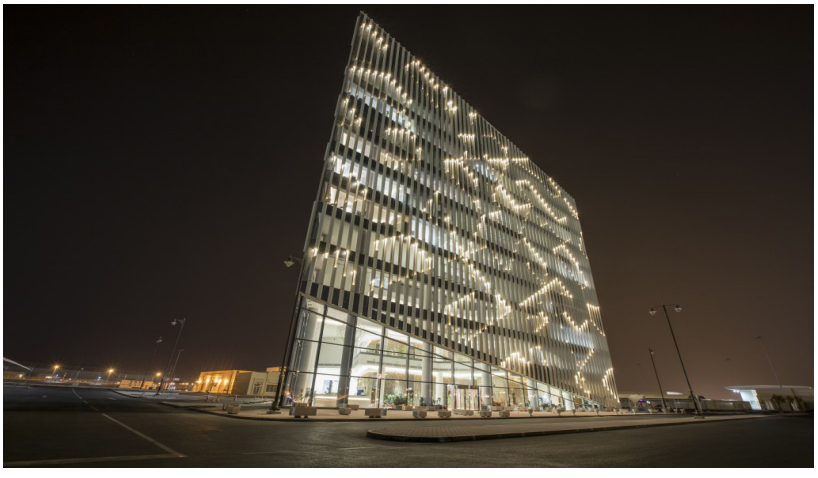

Figure 1: MWANI Qatar Building

Hamad Port is a major green development; hence, distributed energy resources (DER) shall be one of the key sustainable addition for ports buildings. Thus, this paper will evaluate the benefits of adding a solar DER investment to MQ building being the face of the whole port development. The evaluation will include social and environmental aspects besides economic calculations outcome; in addition to the benefits of a battery storage to such investment.

2 TRIPLE BOTTOM FRAMEWORK ANALYSIS, ECONOMIC FACTORS AND INVESTMENT REASONS

The project economic factors will be assumed to be similar to a Commercial Building in Seattle, Washington USA. In this project, the cost of installation of the Solar PV panels is 2.4 $/W, which is based on the Barbose and Darghouth, Tracking the Sun – 2018 Edition for large non-residential systems. Table 1 below shows the inputs used for the building calculations.

Table 1: Input summary

Selected State for calculations	**Washington**
Zip Code	98101
Actual building location	Qatar
Demand Charge	20
Energy Charge	0.12
CO2	0.3 lbs/MWh – 0.0003 Ibs/KWh
CO2 location	Washington, Seattle
Solar	2.4 $/W
Loan Duration	10 years
APR	4%
Federal ITC	30%
Triple bottom line framework analysis location	Qatar
Utility Provider for calculations	Central Electric Networks (CEN)
Utility provider for analysis basis	Kahramaa
PV	Fixed Roof mounted
PV	250 KW
PV Watts location output	98101

The state of Qatar has established country goals represented in Qatar's 2030 vision that Hamad Port is a key investment leader in establishing those goals. Hamad Port is a strategic seaport that is one of the largest green projects in the region. During Hamad Port construction phase, there were major efforts to preserve the natural life, i.e., extensive plants relocation programs were established. Hamad Port Project was able to re-locate thousands of hard corals, soft corals, seagrasses, and mangrove trees. After relocation, the new locations were monitored and found out to have high rate of success, because the plants have grown as planned. In addition, the construction activities were environmentally controlled. Monitoring schemes have been implemented to ensure that the construction activities are following the set plan to preserve the environment. It is worth noting that Hamad Port buildings are designed following the energy conservation and sustainability requirements that all buildings have achieved the targeted ratings using

the locally developed Global Sustainability Assessment System (GSAS), a sustainability rating system (Gulf Organization for Research & Development, GORD). Adding solar panels to MQ building will further enhance Hamad port operations to follow the same environmental goal. Table 2 below shows the calculations outcome for the building before DER implantation and after, using Table 4 & Table 5 monthly electricity consumption and associated costs.

Table 2: Economic results summary table

LCOE of the facility (before PV)	0.16 $/KWh
LCOE of the facility (with PV)	0.245 $/KWh
LCOE of the PV	0.192 $/KWh
Simple payback of the investment	12.64 years
Annual payment of the utility (before PV)	47,586.17 $/year
Annual Payment of the utility (with PV)	14,368.65 $/year
Expected production from PV array size	269,676
Annual energy purchase from the utility (before PV)	298,288 KWh/yr
Annual energy purchase from the utility (with PV)	28,612 KWh/yr
Peak annual demand draw from the utility (before PV)	57.6
Peak annual demand draw from the utility (with PV)	48.6
CO2 emissions (before PV)	89.5
CO2 emissions (after PV)	8.6
Annual cost, if loan is considered	51,782.2

The levelized cost of Energy (lCOE) is a way to describe the present value of the solar investment by calculating the project break-even parameters. The LOCE can guide on which system to select when comparing conventional fuel systems with renewable system but it has a problem which shows in this project. The LCOE went after to 0.245 with PV because due to the simple calculation of LCOE, when you reduce energy and save money the LCOE goes up. In addition, LCOE ignores project risks and other social and environmental considerations.

The project has a recovery period (simple payback) for the PV investment of 12.64 years which is considered high if it is a private investment with profit goals. MQ is a governmental entity where the social and environmental benefits have higher weightage. As a matter of fact, MQ will be saving $33,217.5 (47,586.17-14,368.65) of OPEX cost which is a great incentive. Moreover, the annual energy and the peak consumptions will be reduced by the PV usage, leading to the main investment reason which is an outstanding 96% lower CO2 emission.

In the light of the above, it would not be an exaggeration to say that the social aspect of reducing electricity usage by a clean zero emission energy source is intangible. Hamad

Port covers a huge area of land of approximately 28 km2 and powering such development requires high energy sources. The main energy provider in Qatar is Kahramaa and their power generation comes from fossil fuel sources. Kahramaa has implemented a program called "Tarsheed" that aims to reduce 7% of harmful carbon emissions in Qatar. (Al-Kuwari, 2018). Adding Solar PV will reduce energy consumption, and CO2 emission will be reduced by 96% as calculated which is an important addition to the green port goal and Tarsheed program as well. Adding solar PV satisfies both the environmental sector by lower GHG emissions and the social sector by providing better atmosphere without compromising stable electricity supply.

In other words, such investments are built to show Qatar's efforts following the future vision of clean, developed and environmentally friendly nation.

3 TECHNOLOGY

The weather in Qatar is clear most of the year and Hamad Port is quite far from the city or any populated area and there are no towers or adjacent high-rise buildings to obstruct the sun. Thus, the proposed PV panels are flat fixed panels to maximize the sun exposure and will be placed on the roof of the building. Movable tracking panels will add extra burden on the budget and will not create a huge difference in the local weather conditions.

Kahramaa, the electricity provider in Qatar, does not accept power return to the network; unlike the USA ("Washington State Department of Commerce" & "Net Metering."). This is a major point to consider during the design and planning of this project that extra power cannot be utilized, unless there is a well-established storage system. The power generated by the PV panels shall be consumed 100% within the building; accordingly, the solar PV system was designed to be consumed 100% within the building.

Solar PV panels are quite a new technology in Qatar and there are limited options of suppliers with local experience and local availability to operate the system. To gain the best outcome possible of the PV panels, the same technology that was used in Mshereib Downtown project (MDD) will be considered. The reason behind this selection is that, Msheeib properties, the developer of MDD, is a semi-governmental entity and the selection process follows the same tendering rules as MQ. In addition, the procurement process in a government related project ranges between 6 to 9 months to be able to award a single package because the process should go through tender, technical and steering committees followed by the prime minister's endorsement. Qatar is quite a small country and the delegation of authority is limited to QAR100,000 for project directors. MDD design was well studied and any similar study will most likely yield the same outcomes; the technology and its supporting parameters have been evaluated in a detailed manner allowing the best efficiency possible for the local environment.

As a result, the technology proposed is KIOTO PV model KPV PE NEC 240WP along with SMA solar Technology AG inverter model Sunny Tripower. The system has a maxium power output of 265 Wp with 15.7% panel efficiency and a very high operating temperature range reaching 85 ºC. The Panel dimensions are 1700Hx995Wx7D mm with Polycrystalline cell type 156x156 mm.

Figure 2 shows KIOTO PV panel sample ("ENF Solar"); the project panels are designed to have 3 bypass diodes to reduce the loss and is selected to be poly-crystalline to be more efficient for Qatar's hot weather. The mounting structure is built by HILTI which has a local supplier. As of any design, technology is always meant to deliver the best possible outcome; however, in this project, designers were concerned to not exceed the peak usage of electricity at any point of the day. The proposed technology will be using several locally available equipment to minimize future operational matters with a design that is operated and maintained locally.

Figure 2: KIOTO PV model KPV

4 BATTERY STORAGE

Battery storage is a great addition to the solar energy system; it adds many additional benefits and features. However, storage system has great challenges of how the facility is planning to use it. In other words, controlling the storage battery system is the main factor that drives all features. For instance, if the batteries are not charged when they need to be used, then their great value will be lost. The better the facility controls the storage, the higher the values and benefits. For this project, battery storage control strategies are assumed to be well planned and implemented to optimize the system outcome. Table 3 below shows the benefits of adding solar PV source and their possible effect rate on the building.

Table 3: benefits of adding solar PV to MQ building

Value	Effect
Retail Electric Energy Time-shift	High
Demand charge management	High
Resiliency	Low
Electric supply capacity & Independence	Low
Reserve Power for emergencies	Low
Kahramaa Power return prevention	High

Note: There are many other benefits that were neglected due to the project nature and location. For instance, voltage support which does not apply in Qatar grid

4.1 Retail electric energy time-shift

It involves the storage used to reduce the energy usage and eventually reducing the overall cost of the electricity. The peak time electricity charges are higher than off-peak charges, and the storage can be used to reduce electricity usage during the peak time

of the day while charging during off peak time. Doing so, will result in less cost to the utility by reducing the energy bought from the provider. Accordingly, this is a high relevant value to this project.

The utility calculation of adding a solar PV system resulted in a reduction of energy usage, which is equivalent to $33,217.52.

4.2 Demand charge management

Each facility is being charged for energy usage as well as peak load. Battery storage can add high value to the building by reducing the peak load values that it uses. For this project, the peak load is reduced adding a saving off $856.44 dollars to the bill. Moreover, with battery storage the saving will be much higher by reducing peak loads.

4.3 Resiliency

Qatar weather is stable throughout the year with minimal rain, wind or natural disasters. This value is considered because in the past few years, Qatar has experienced few days with heavy rain and high-speed wind that were not expected or designed for. Those unusual days resulted in electric outages to many areas around the city. Figure 3 below shows Doha city floods due to excess rain that the drainage system was not designed for.

Figure 3: Heavy rain effect (Qatar)

The probability of such incidents is low but its impact is huge; storage system will add great benefit to the facility in such incidents. This is considered to be a low added value to the system because the government has been implementing great measures to upgrade the drainage and storm water systems to minimize the impact of natural disasters.

4.4 Electric supply capacity & Independence

Due to the fact that Hamad Port is a huge area isolated from the city, the electric system design was built with a number of substations to be located around the port area to provide power for allocated areas/buildings. Hamad Port has approximately two major substations distributing the power to 9 smaller substations. As the port is a major development in Qatar, the government added a visitor's center with aquarium after project completion. Adding such a huge building in the electricity grid resulted in an electric shortage and a new substation had to be built. Electric storage can be used to reduce the need to build additional substations, by implementing a well-designed

and controlled storage system, significant energy usage could be reduced in which MQ building can be a valid case to initiate green energy usage.

In addition to the above, Hamad port could eventually reach independence from the grid with vast empty areas that can be utilized for green power. MQ building can be a case study building as well to achieve the independence out of the system and adding a battery storage could make this possible.

4.5 Reserve Power for emergencies

Qatar designed codes and civil defense regulations require each building (or substations) providing power to have a backup generator available to be used during blackout or power issues. Adding a battery storage system, can save the facility, the generators cost and the associated fuel cost. In general, a diesel backup generator from Cummins, the unified brand used at the port, costs approximately US$100,000 due to distinct port specifications that generators have to be sea corrosion coated with high temperature working environment specs. This cost is another added incentive to the storage system.

In addition, replacing the backup generator with a battery storage system will reduce CO2 emission leading to social and health benefits besides the environmental benefits.

4.6 Kahramaa Power return prevention

As mentioned above, Kahramaa does not allow power return to the grid in case of any excess power produced that the design had to be changed in order to account for such restriction. Adding a storage system, will eliminate such restriction in which the PV power could be increased, and further savings could be achieved. In some cases, a zero PV system could be added that could result in almost zero payment for electricity (excluding meter cost) because Qatar does not have a taxation system.

5 CONCLUSION

Hamad Sea Port (HP) is one of the biggest projects in the region that is mainly built to serve Qatar 2022 World Cup needs and is considered one of the key projects in Qatar 2030 Vision. Mwani Qatar (MQ) is responsible for the management and operations of HP and is considered the front face of HP's image. Adding a distributed renewable energy (DER) investment for the MQ building is considered a great overall investment that will not only save energy usage, but will yield benefits to all sectors of economics, society and environment.

The proposed DER is a solar PV system that has 250 KW output. The considered system will use the flat fixed KIOTO PV panels connected to a SMA solar Technology AG inverter model. This type of technology was proven to be effective and locally applicable in a similar mega governmental project, Mshereib Downtown (MDD). The technology and its supporting parameters have been evaluated in a detailed manner allowing the best efficiency possible for the local environment.

A Battery Energy Storage System (BESS) can add many benefits to the solar PV system that makes the investment more appealing for decision makers. The BESS will save bill charges by shifting electric energy consumption out of the peak time and will reduce the peak usages of the facility. Also, it will add reliability and power reserve to

the system during disasters and emergencies. BESS will open the ability to increase the PV output as the excess energy output can be stored creating a further possibility of a stand-alone facility option to be further considered in the future.

In the light of the above, the solar PV investment calculations shown in Tables 2, 4 & 5 indicate savings of $33,217.52 to the facility leaving a stronger overall impact towards the environmental and social benefits. The CO2 reduction is 96%, which is a great start for a small nation like Qatar. Also, this project will add to the environmental requirements dictated by the Ministry of Municipality and Environment (MME) and the energy saving design developed by Global Sustainability Assessment System (GSAS) sustainability rating. As a matter of fact, Qatar is a small rich country and even if the investment did not reach the needed cost saving parameters, the social aspects with their environmental benefits are always more valuable to the country's objectives and goals. The solar PV system for MQ building is a great addition to the ongoing governmental path towards a clean, modern and sustainable nation.

6 APPENDIX

Table 4: Facility without DER

Month		Peak demand (kW)	Monthly energy (kWh)	Demand charge ($)	Energy charge ($)	Total utility bill ($)
1	January	45.8	25,348	$916.96	$3,041.74	$3,958.69
2	February	46.6	22,728	$931.35	$2,727.40	$3,658.76
3	March	45.9	24,994	$917.93	$2,999.28	$3,917.21
4	April	51.4	24,168	$1,028.10	$2,900.21	$3,928.31
5	May	48.5	24,890	$970.23	$2,986.80	$3,957.03
6	June	51.5	24,256	$1,030.18	$2,910.66	$3,940.84
7	July	54.6	25,775	$1,092.74	$3,093.02	$4,185.77
8	August	57.6	26,456	$1,152.01	$3,174.70	$4,326.71
9	September	49.0	24,565	$979.35	$2,947.82	$3,927.18
10	October	46.1	25,181	$922.05	$3,021.68	$3,943.72
11	November	46.7	24,514	$933.64	$2,941.63	$3,875.27
12	December	45.9	25,413	$917.10	$3,049.58	$3,966.68
ANNUAL VALUE		57.6	298,288	$11,791.64	$35,794.53	$47,586.17

Table 5: Facility calculations with PV

Month		Peak demand (kW)	Monthly energy (kWh)	Demand charge ($)	Energy charge ($)	Total utility bill ($)
1	January	45.8	15,989	$916.96	$1,918.67	$2,835.63
2	February	46.6	8,561	$931.35	$1,027.30	$1,958.65
3	March	45.9	4,691	$917.93	$562.91	$1,480.84
4	April	45.4	(4,440)	$908.65	($532.85)	$375.81
5	May	43.4	(6,475)	$868.46	($777.05)	$91.40
6	June	40.8	(9,229)	$816.54	($1,107.50)	($290.96)
7	July	43.6	(10,261)	$872.87	($1,231.34)	($358.47)
8	August	48.0	(6,826)	$959.02	($819.14)	$139.87
9	September	48.6	(1,664)	$971.31	($199.62)	$771.69
10	October	46.1	8,068	$921.37	$968.14	$1,889.51
11	November	46.7	13,319	$933.64	$1,598.26	$2,531.91
12	December	45.9	16,881	$917.10	$2,025.66	$2,942.76
ANNUAL VALUE		48.6	28,612	$10,935.20	$3,433.45	$14,368.65

REFERENCES

Al-Kuwari, Essa (2018). Kahramaa set to award solar power plant tender. *Gulf Times*, 7 Oct. 2018. Retrieved from http://www.gulf-times.com/story/608567/Kahramaa-set-to-award-solar-power-plant-tender.

Energy Independence Act (EIA or I-937). *Washington State Department of Commerce*. Retrieved from www.commerce.wa.gov/growing-the-economy/energy/energy-independence-act/.

ENF Ltd. "ENF Ltd." *ENF Solar*. Retrieved from www.enfsolar.com/pv/panel-datasheet/crystalline/35193.

GSAS: Global Sustainability Assessment System. Gulf Organization for Research & Development (GORD). Retrieved from http://www.gord.qa/gsas-trust.

Mwani Qatar. About Us - Mwani Qatar - Rising to the Challenge. *MwaniQatar*. Retrieved from https://www.mwani.com.qa/English/AboutUs/Pages/default.aspx.

"Net Metering" (2016). Washington Utilities and Transportation Commission. Retrieved from *https://www.utc.wa.gov/regulatedIndustries/utilities/energy/Pages/netMetering.aspx*.

Steering Committee, New Port Project. "Investing in Qatar's Future." New Port Project. Retrieved from http://www.npp.com.qa/overview.html.

Cite this article as: Karama A., "Solar DER Investment for MWANI Qatar Building at Hamad Port", *International Conference on Civil Infrastructure and Construction (CIC 2020)*, Doha, Qatar, 2-5 February 2020, DOI: https://doi.org/10.29117/cic.2020.0031

Integrating Building Information Management (BIM) in Civil Infrastructure Coordination: Application at LUSAIL Plaza

Mohab Mohamed Abotaleb
mabotaleb@QD-SBG.COM.QA
QD-SBG Construction Company, Doha, Qatar

Elisabeth Saab
SElisabeth@QD-SBG.COM.QA
QD-SBG Construction Company, Doha, Qatar

Mohamed AbdelZaher
mohamed.abdelzaher@sph-eag.com
SPH Joint Venture, Doha, Qatar

ABSTRACT

The purpose of this case study is to highlight how the BIM modelling can lead to a smooth construction process for MEP (Mechanical, Electrical & Plumbing), Civil, Architectural, and Landscape works, which can aid the engineers in various project phases. An exploratory approach on a complex mega-project case study (El-Sadek & McCabe, 2017), where the project team was coached on exploring the BIM model to identify any clash and discuss with the technical team to come up with adequate solutions, which was done by holding twice a week regular meetings. This paper introduces the issues appeared during the early phases of the design process and continued all the way through the construction phases. While preparing the composite shop drawings, where each discipline/installation will have a clear corridor without interference with other disciplines/installations, and in a manner sufficient to ensure the avoidance of any clash that may arise during construction. However, what happens if the available corridor for all disciplines is very congested and insufficient to enable the designers from accommodating the space needed into coordination process? This case study triggers the need for identifying a new process in integrating BIM models in the coordination challenges through all the phases of mega-projects, as the complexity associated with mega projects appears to increase from one phase to another. From the lesson learned in this case study readers will know how integrating BIM in the coordination process in complex scale projects can decrease the clashes and improve progress of work during construction phase.

Keywords: LUSAIL; BIM; Coordination; Landscape; Civil; MEP

1 INTRODUCTION

The coordination between different disciplines plays a pivotal role in the success of resolving the provision and delivery of all facilities and especially those intertwining (Yazdani et al., 2015). In turn, identifying and managing interdependencies between the various elements of civil infrastructure works is a key element in establishing full-bodied coordination in the process and delivery of the provision, covering the overall spectrum during all the process from the Issued for Construction drawings (IFC) phase

to the construction phase, passing through the other phases of shop drawings.

The construction industry is unlike any other industry, as there is a strong inter-relation and coordination required across the entire project time. Coordination as a process of getting all disciplines together to enable construction team to perform work in an effective and efficient manner (Alaloul et al., 2016).

It is the guarantee for getting right information at the required schedule in order to improve productivity. Coordination is important for construction projects to manage the interfaces between the stakeholders. To enhance project performance, various coordination methods can be used, but coordination effectiveness needs to be assessed to find out if they are being used appropriately.

2 LUSAIL PROJECT-A BRIEF DESCRIPTION

Lusail Development site is located north of Doha-Qatar, and comprises of residential, commercial centers, hotels and community facilities. To realize their vision, LUSAIL Real Estate Development Company (LREDC), has come up with state-of-the-art discrete engineering projects comprising of various packages. Package **CP07-B** is a part of these projects and aims to establish a foundation for human, economic, social and environmental development, where the top management consists of: Owner: Qatari Diar Real Estate Investment Co. (QD), Client: LUSAIL Real Estate Development Company (LREDC), Main contractor: Qatari Diar (QD-SBG).

The Package CP07-B is divided into five main components: Infrastructure, LRT station, public car park, landscape including urban features, enabling works. The design scope of work under CP07-B comprises the following: Design & build: Road A-1 troughs – 1.5 km long, Road A-1 tunnel (three levels) – 0.5 km long LRT station – structural and civil works, car parks – 2 subterranean multi-story structures (east & west) – 2,200 stalls in total, bridge (at Junction no. 19), pergola (north and south troughs) – 320 m long, substations (7 no., 11 kV), utilities (electrical, mechanical, sewage, irrigation, storm and tunnel drainage network, etc.), At-Grade roads: Gas, district cooling & pneumatic waste collection – design by MARAFEQ / integration by DAR, enabling works (excavation, shoring / dewatering) – design by specialist, Build: Landscape and public realm features (designed by F+P).

3 RESEARCH DESIGN AND METHODOLOGY

This paper focuses only on infrastructure works running between the plaza level and the car parking & the LRT roof deck areas, where it introduces the issues appeared during the early phases of the design process and continued all the way through the construction phases, addresses the BIM for the coordination of architectural, landscape works and civil infrastructure works. Coordination begins at the stages of the design development where all the disciplines are being identified through different computer programs (software). These programs are used for coordination purposes, where all MEP clashes will be identified and sorted out, subsequent to which IFC's and shop drawings will be prepared and issued to the construction team on site for execution.

In the composite shop drawings, each discipline/installation will have a clear corridor without interference with other disciplines/installations, and in a manner sufficient to ensure the avoidance of any clash that may arise during construction. However, what

happens if the available corridor for all disciplines is very congested and insufficient to enable the designers from accommodating the space needed into coordination process? This is where using BIM model in the issued for construction early phases, could not be satisfactory in solving all clashes.

The goal of this paper is to specify, formulate and develop the characteristics of a process using the BIM modeling technologies that will aid the engineers throughout the entire design process, from inception to completion, where it will become an essential tool to sort out all issues that may be encountered to cover the construction phase. The values of reaching this goal is to develop a new procedure for using BIM to its maximum 3D modeling tools that merges different 3D modeling programs to visualize and identify all the clashes during the design phase and extends to the construction phases to assist in resolving the issues that may arise, formulating a coordination platform that could have not been conceived without this technology. The methodology for this paper is a case study, done by exploring the clashes of the infrastructure works between the PLAZA and the roof decks of the car parking & the LRT station, at the LUSAIL project.

4 DEFINING BIM TECHNIQUES IN COORIDNATION PROCESS

The aim of the paper is to define the corridors available/required for the infrastructure works below the plaza, formulating a process for the BIM modelling techniques, through exploring the various computer programs that can be fused into BIM model; identifying a process and highlighting its components for the BIM modelling that can be used from the early phases of design through and up-to the construction phase, through exploring a case study at LUSAIL project.

The coordination between the various systems in such a wide and complexed plaza usually include infrastructure works where the obstacles faced in that design arise due to the presence of a multitude of disciplines including multi MEP utilities, in addition to the impeded civil, architectural and landscape works, especially the involvement of various discipline engineers with different knowledge and experience, where the design/coordination usually passes through a series of processes including workshops and using various computer programs culminating in composite/coordinated design/shop drawings free from clashes, a process that is usually done within the same engineering firm.

This case study introduces the LUSAIL plaza which includes very special landscape/architectural items such as FOG fountains, water features & huge photo cell canopies. In addition, from numerous planter/tree concrete boxes, it includes benches, walls and hand rails, also the buildings above the plaza includes 2 pavilion buildings and 8 pods required for the ventilation of the underground car parking.

Two huge car parks each comprising of 5 stories below the ground level of the plaza with an approximate 40,000 m2 plot area, a backfilled area required for the infrastructure utilities, between the plaza and the car parking roof decks, varying between 2 to 4 m. LRT sub-station passing through the middle of the plaza with 2 entrances leading to the station with an approximate 40,000 m2 plot area, similarity backfilled area required for the infrastructure utilities, between the plaza and the LRT station, varying between 0 m to 4 m. The total area of the plaza is 80,000 m2, bordered by 4 podiums for 4 towers each with basements reaching 25m deep below ground level at the four corners. In addition to the physical limitations mentioned above, there are 3 designers involved in the LUSAIL

projects, contributing towards the design of the plaza (DAR for the underground parking buildings, Foster and Partner for the plaza landscape, Pavilion and Pods & Marafeq/ QRC for the LRT underground station), which hardened the coordination process. Thus it was a massive challenge to coordinate between all these different disciplines, packages and designers, prompting the design and build main contractor (QD-SBG) to assign designer for the preparation of a BIM model addressing all the above issues for the purpose of achieving IFC drawings free from clashes, and thus avoiding any delay that may occur due to miss-coordination during the stages of construction.

4.1 Formulating BIM modelling

Formulating a BIM model through collecting different 3D models from the different designers of the interconnected packages, in addition to build a 3D modelling for the details that have been unexploited or over-looked in the interferences between the different packages, was a great challenge where each designer used different 3D modelling software.

The challenge was finding a software that can fuse all these models into one federated BIM model. This was achieved by using Navisworks software, which allows for an effective identification inspection and reporting of interferences in a 3D project model.

The list of the software used in the archived BIM model is as follows:

Design authoring tools for buildings: Revit, Dynamo, 3DS Max, Sketch Up, Rinho, dRofus, Archicad, Bentley, and Grasshopper. Design authoring tools for infrastructure: AutoCAD Civil 3D, AutoCAD utility Design. Design review tool for building and infrastructure: Navisworks. With the use of the above software all the MEP disciplines were identified, including but not limited to (potable water, irrigation, foul sewer, storm water, gas, low voltage…etc.) also the buildings above, below and through which have been mentioned above.

It was essential for this latest fused model to be shared with all stockholders. Accordingly, the provisions of BS1192 were followed to prepare a Common Data Environment (CDE) to keep all the stakeholders on one sharing platform, in addition to using other platforms to share the fused model, which passed through a group of quality assurance QA/ quality control QC processes.

Later and after the coordination stage was processed where this wasn't only a clash detector from the 3D model but it was included also the clearance required by each system, in addition to the regulation required by the governmental parties. In light of the above a clash matrix was produced, after holding a series of meetings and workshops, a BIM model have reached with an acceptable level of clashes.

4.2 Identifying the new BIM process

After the IFC drawings were received by the main contractor, various packages were prepared and tendered/awarded to qualified subcontractors. Subsequently each subcontractor's engineering technical office and the main contractor's engineering technical office started to issue their shop drawings taking into consideration the coordinated BIM model. During this stage the subcontractors who were using up-to-date systems and cutting edge technologies came up with different routes/corridors for systems and equipment satisfying all the requirements and specification different than

the designed systems shown in the issue for construction stage.

Accordingly, new clashes were identified, which necessitated a new cycle of coordination on the BIM model in order to eliminate these new clashes that arose due to the occurring modifications/ introduction of new systems. Through this process the Level of Details (LOD) has increased considerably from 300 to 400 LOD, by decreasing and eliminating the clashes during the shop drawings stage. This supported the production of shop drawings to be ready for the construction phase.

During the construction phase, new clashes had arisen, as all the coordination, as described above, was done at the level of the engineering office, where the construction engineering team had done some rerouting based on site condition and errors. Moving or relocating any small detail at site will affect the coordinated BIM model. Accordingly, the sharing of the BIM model with the construction staff and engineers was essential and a good practice, where the construction engineers were able to visualize the systems and its adjacent schemes, in addition to the civil concrete works that may clash with the progressed systems. This can be achieved by introducing the site engineers to the BIM model by the mentoring of engineering technical office, which took the decision that the engineers at site should have a platform sharing the BIM model including all the systems (MEP utilities, civil, architectural & landscape works). For the better understanding of the site engineers, where continuous coordination with the engineering technical office through the BIM modelling system had led to a decrease of clashes thus-leading to a smooth construction process.

5 CONCLUSION

The introduction of a new process for the BIM modelling through various phases of the project design and construction can lead to a smooth construction process for all MEP utilities, civil, architectural and landscape works. This can aid the engineers in various project phases using a new process for the 3D BIM modelling thus fulfilling the paper's goal, which is to specify, formulate and develop characteristics of a new process using the advantages of BIM modelling techniques at various project execution phases.

REFERENCES

El-Sadek, L. & McCabe, B. (2017). Coordination challenges of production planning & control in international mega-projects: A case study. *Lean Construction Journal*, pp. 25-48.

Yazdani, Saeid et al. (2015). *Challenges of coordination in provision of urban infrastructure for new residential areas: The Iranian Experience*. Macrothink Institute™, Volume 4, No. 1, p. 48.

Alaloul, Wesam & Liew, M. S. & Wan Abdullah Zawawi & Noor Amila (2016). *A framework for coordination process into construction projects. MATEC Web of Conferences Journal*, Volume 66, p.79, DOI: 10.1051/matecconf/2016660007

Cite this article as: Abotaleb M. M., Saab E., AbdelZaher M., "Integrating Building Information Management (BIM) in Civil Infrastructure Coordination: Application at LUSAIL Plaza", *International Conference on Civil Infrastructure and Construction (CIC 2020)*, Doha, Qatar, 2-5 February 2020, DOI: https://doi.org/10.29117/cic.2020.0032

Risk Management for Qatar Expressway Program

Nor Rozaini Abd Rahman
nabdrahman@ashghal.gov.qa
Public Works Authority (Ashghal), Doha, Qatar

ABSTRACT

The construction of expressway projects associated with the various main risks such as political risks, legal risks, economic risks, cultural risks, and construction risks are considered critical and essential to be identified and mitigated in early stage for every minor or major projects. According to Dziadosz and Rejment (2015), the risk is a measurable part of uncertainty, for which we are able to estimate the occurrence probability and the size of damage. The risk is assumed as a deviation from the desired level. It can be positive or, which most often happens, it can be negative. Therefore, the risks analysis is so important for project selection and coordination of construction work. This paper identifies the level of severity of construction risks which had affected the implementation of the expressway/highway projects in Qatar. This research is also focused on the importance in practising the formality of risk management process by identifying the problems and difficulties associated with the projects risks, which includes obtaining the important information and suggestion the risk response in order to be used on future projects in the particular and focusing the risk mitigation in the early stage is necessary. There could be a possibility that the identified projects were not fully assessing the significant risk factors during feasibility studies, design stage, tender stage and construction stage. Based on a literature review, structured interviews with experts, unstructured interviews and detailed case studies, it was found that major participants agreed that the risk management process was satisfactorily adopted for on-going and previous infrastructure projects in Qatar. The critical construction risk was design changes, new requirements, land acquisition, interfacing works and additional works which had caused the cost overrun and delay the completion works.

Keywords: Construction risk; Risk management; Risk mitigation; Expressway projects; Qatar

1 INTRODUCTION

A high quality highway network system has always been one of the prerequisites for a country to organize any large international events including sporting championships or tournaments. Public Works Authority (PWA or ASHGHAL) is responsible to undertake the implementations and completion of expressway program which covering the North, South, Central, Northwest and Orbital networks approximately 900 kilometre of mainline carriageway, major interchanges, bridges, tunnelling works, bypass includes new and upgraded expressways with value of USD8.1 billion within limited time frame. According to Zou et al. (2007), "managing risks in construction projects has been recognized as a very important management process in order to achieve the project objectives in terms of time, cost, quality, safety and environmental sustainability."

2 PROBLEM STATEMENT

The majority of respondents agreed that the project risks caused the cost overrun and delaying the completion of works. Potential construction risks need to be identified in early stage of construction, and the mitigation risks need to be incorporated in the project risks management process.

3 RESEARCH OBJECTIVE

This research began with the objectives of identifying of construction risks in highway projects based on the on-going and completed projects, the followings objectives were highlighted:

i. To determine the most critical and extreme construction risks which need to be addressed on priority basis.
ii. To define the mitigation risks in early stage of construction works.

4 RESEARCH METHODOLOGY

4.1 Questionnaires

The data obtained from the literature review and one case study had provided a basis for designing the questionnaires, which were distributed into fifty (50) experts i.e. focusing on the Civil Engineers, Quantity Surveyors and Contract Specialist from PWA. The questionnaires have also been forwarded to the PWA's Project Management Consultant (PMC) staff. Out of fifty (50) experts who were approached directly by the researcher either by hand or by electronic mail, only 31 responses were received, giving a success rate of 62 per cent.

4.2 Structured Interviews and Unstructured Interviews

Structured Interviews participants were selected and conducted only for the experts who were involved directly in implementation of expressway projects. Some of the questions from the same questionnaires were used to explore more on the construction risk and mitigation plan being implemented in their projects. Ten (10) interview sessions involving middle to upper management from PWA were carried out between October and November 2019.

4.3 Detailed Case Study

The researcher choose one mega highway project (Project A) which had associated with massive interfacing works particularly when dealing with another key project stakeholders. Project A case was studied and analyzed to determine the construction risks, level of risk involved and to capture the relevant information, obstacles and challenges. And whether the project risk management process had been carried out during the implementation works.

5 FINDINGS

5.1 Case Study of Highway Project

Compared with many other industries, the construction industry is subject to more risks due to the unique features of construction activities, such as long period, complicated processes, abominable environment, financial intensity and dynamic

organization structures (Flanagan & Norman, 1993; Akintoye & MacLeod, 1997; Smith, 2003; Zou et al., 2007). The scope of works for Project A involved with reconstruction and upgrading the existing highway including interchanges that consisted of tunnels, underpasses, flyover, junctions and two marine bridges. This project also involved with the construction of the Light Rail Transit (LRT), tunnel extension and massive utilities diversions. The characteristics for this mega project as shown on Table 1 indicated that the huge additional amount increased 30% of the original contract sum and Extension of Time (EoT) for 1503 days.

Table 1: The Characteristics of Project A

Original Contract Sum	3,574,234,000.00	Start Date	21-May-12
Variation Order (VO)	1,135,860,000.00	Original Completion Date	18-Sep-15
Percentage of VO	32%	Delays to contract	1503 Days
Revised Contract Sum	4,710,094,000.00	Revised Completion Date	30-Oct-19

5.2 Risk Identification of Highway Projects

According to Dziadosz and Rejment (2015), "at the stage of identification we should get the statement of the factors, which are possible to occur in the whole cycle of the project. The most frequently mentioned methods/tools used to identify risk factors are the following: the brainstorming, the Delphic technique, the check-lists, the experts' evaluation, the internal audit in a company, the periodic document reviews, etc." Project Risk identification in this paper is based on one (1) case study i.e. Project A and the feedbacks from the respondents which will be discussed later under the topic of "the Ranking of Severity Impact of the Construction Risks for Highway Projects" in page 4. The risk assessment is developed in order to identify the level of project risk which had affected Project A by approaching the risk management methods i.e. "Risk Matrix" model for analysis the likelihood of occurrence and the impact.

Table 2: Risk Matrix for Project A case study

Descriptions of Construction Risks	Probability	Cost Impact & Time Impact (Prolongation Cost)					Total Score	Level of Risk
		score 5	score 4	score 3	score 2	score 1		
Design Changes	4	300-500 mil					20	Extreme
New requirements	4		50-100 mil				16	Extreme
Land acquisition	4			20-50 mil			12	High
Interfacing Works	4			20-50 mil			12	High
Additional scope of works	4	300-500 mil					20	Extreme
Non Performance of the contractors	3			20-50 mil			9	High
Availability of materials, labors and machineries	2				5-20 mil		4	Medium
Physical geography and soil conditions	2				5-20 mil		4	Medium
Blockade from neighboring countries	2				5-20 mil		4	Medium
Fluctuation of labor & Materials price	1					0-10 mil	1	Low

The probability is derived from opinion, judgement and personal experiences from the experts, detail Variation Orders (VOs) submission and Monthly Project Reports. To ensure the accuracy of the cost impact, the input is based on VOs submission and VOs' trackers. The total score as shown in Table 2 is justified the level of severity on the project risks. Based on total score for project A as shown in Table 2 and Figure 1 indicated that a likelihood of occurrence for "Design Changes", "New Requirements" and "Additional Scope of Works" are almost certain/frequently which the event occurs many times during the construction period. In addition, the cost impact for those extreme categories level of risks also had severely affected cost overrun to project A.

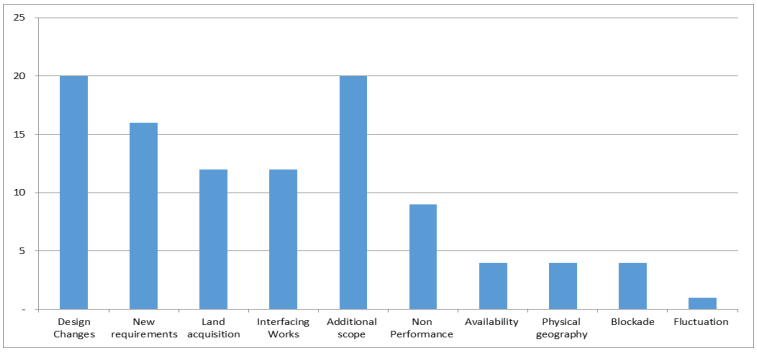

Figure 1: Total Score and Level of Construction Risk for Project A

5.3 The Ranking of Severity Impact of the Construction Risks for Highway Projects

The result is established based on thirty one (31) respondents out of fifty (50) questionnaires been circulated among the experts as listed in Table 3. In order to categorize the ranking for the level of risk, the researcher developed a method by multiplying the number of respondents to the score number. Based on this approach hierarchical ranking of construction risks in Table 3 shown that the "Design Changes" as the most severe construction risk, followed by the "New Requirements", "Land Acquisition", Non Performance of Contractors" and "Interfacing Works" which were tremendously impacting the cost overrun and caused the delay for the completion of highway projects in Qatar.

Table 3: Level of Severity Impact of the Construction Risk for highway projects in Qatar

No	Descriptions of Construction Risks	Extreme score 4	High score 3	Medium Score 2	Low score 1	Total score	Ranking
1	Design Changes	14	15	2	0	105	1
2	New Requirements	7	18	6	0	94	2
3	Land Acquisition	14	7	6	4	93	3
4	Interfacing Works	4	17	10	0	87	5
5	Additional Scope of Works	4	17	9	1	86	6
6	Non Performance of the Contractors	6	15	9	1	88	4
7	Availability of Materials, Labors & Machineries	3	15	11	2	81	7
8	Physical Geography and Soil Conditions	3	5	15	8	65	9
9	Blockade from Neighboring Countries	3	10	13	5	73	8
10	Fluctuation of Labor & Materials Price	3	1	18	9	60	10

5.4 The Implementation of Project Risk Management for Expressway Projects (On-Going and Completed)

The respondents and interviewees are construction industry practitioners, including project managers, senior consultants, senior quantity surveyors and engineers, and top management personnel (i.e. managers and senior associate). They had an average of 15 to 25 years' work experience in the construction sector. The senior positions, long work experience and tertiary educational background infer that the respondents have adequate knowledge of construction projects and the associated risks. Based on their experiences being involved in expressway projects, the experts are requested to rating the implementation of risk management process for on-going and completed expressway projects. Major respondents justified that 29 percent is considered "satisfactory" as stated in Figure 2.

Figure 2: Distribution of respondents on justification, the project risk management had been practiced for on-going and completed highway projects

6 RISK MITIGATIONS FOR HIGHWAYS PROJECTS

Risk mitigation is an action to be implemented but not limited to other option i.e. risk avoidance, risk acceptance, risk eliminate, risk reduce, risk transfer or combination of two or three methods in reducing the risks that had been identified. In addition, each risk needs to be ranked on a scale of probability/occurrence and severity/impact to the projects. Based on the ranking result, level of priority also needs to be considered to mitigate the likelihood of the occurrence or the impact of that particular event. The identified project risk need to be incorporated in the risk register with risk mitigation plan or action should be taken in order to mitigating the risk as shown in Table 4.

Table 4: Risk Register compilation of construction risk that had been identified for expressway program in Qatar

Risk/Issue	Effect	Mitigation/Action
Design Changes		
Discrepancy between Storm Water Contract Drawings & PWA standard Drawings	Delay & time consuming to correct the mistakes and cost impact.	Accuracy and consistency of information in between Contract Drawings, Construction Drawing & PWA standard drawings. Coordination between design team and construction team.
Clash of existing Potable water with proposed Portable water, Medium Voltage (MV), Lower Voltage (LV) existing foul sewer, feeder 1&2 66 kilovolt (kV)	Design error due to absence of structural calculations on water chambers and thrust blocks caused project disruption.	PMC and consultants should be instructed the contractor under specified clause to produce the calculations.

Interfacing Works – Stakeholders		
Delay in submission of wall design due to lack of Design certificate, and CAT 3 certificate.	Delay in getting approval and disruption to the construction works	Expedite the processes in order to obtain the Design certificate and others certificates.
As built document/drawings submission had not been progressed as per plan due to design issues, uncompleted works and insufficient resources.	Delay in getting approval, caused interfacing works and disruption to the construction works	Accurate and sufficient design information. Expedite the progress of works and the submission of As Built document/drawings. Alternative resources need to be arranged.
Delay to securing Ministry of Municipality and Environment (MME). Permit to construct the Site Compound Facilities (Precast/Laydown/hall/workshops, etc.)	Delay in getting approval, caused delay and disruption to the construction works	Consultant to continue to liaise with PWA to determine status of submission and clarification to reduce review process and approval times prior to MME requirements.
New Requirements		
Approval from General Electric (Kahramaa) for new substation including the permit	Delay in getting approval, caused delay and disruption to the construction works	Contractor/Consultant to expedite with Kahramaa the approval of shop drawings and obtain building permit from MME.
Non Performance of the Contractors		
Contractor's rate of progress on remaining utility works remain slow	Delay in completion works	The contractors are advised to increase their supervisory staff and manpower.
Design work had not been approved yet	Delay in getting approval, caused delay and disruption to the construction works	Contractor to expedite final design work and obtain approval from various stakeholders.
Land Acquisition		
Land Acquisition/Demolition permits was pending for hand over/approval	Unable to purchase/own land will cause delay, design changes and prolongation cost also will be claimed by the contractors.	PWA/Consultant/contractor will need to coordinate with the owner/organizations in order to expedite the handover of the related area.
Physical Geography and Soil Conditions		
Unforeseen conditions – damage the utilities	Damage works are required the rectification works which caused delay and disruption to the construction works.	The contractor will be requested to confirm the location and levels of those utilities before the commencement of the works

7 RECOMMENDATION

7.1 Feasibility Study Stage

Based on the structured interview sessions, the author justified that the construction risks for certain project in the expressway program was not properly identified, evaluated and resolute during feasibility study due to the limited time frame. For example, land acquisition issues should be resolved at the early stage before started the construction works. Apart of detail study, adequate ample period of time is essential during feasibility study for focusing potential construction risk which probably will be disrupted the construction works. Risk transfer by shifting the risk to the competent contractor using the right contract strategy particularly "Design and Build" also considered as a strategic option.

7.2 Cost Estimate and Contingency

The design changes, new requirements and additional works had caused the variation orders, which particularly required an additional budget. Most scenarios, the provisional sum and contingency were insufficient to cover the increased cost of actual work done. Cost estimation process is essential to obtain the accuracy of the overall project cost. Therefore, the accuracy of information, rates, scope of works, method of statements, specifications need to be detailed and updated. Engineering design department, stakeholders and PWA requirements, and business support department are responsible for providing the accurate input and information of design factors in order to ensure that an estimator is capable to convert the information and design into the preparation of BoQ. Moreover, to make sure for allocating sufficient provisional sum and contingency. Oberlender (2000) stated that engineering and construction are risk endeavours with many uncertainties, particularly in the early stages of project development. Contingency

is assigned based on uncertainty and may be assigned for many uncertainties, such as pricing, escalation, schedule, omissions, and errors. The practice of including contingency for possible scope expansion is highly dependent on the attitude and culture, particularly that of the business unit, toward changes.

7.3 Design Coordination

Design changes due to design deficiencies take time to correct, and the design errors is leading to variations, ambiguities, major project challenges and will be delayed the progress of works. According to Zou et al. (2007) stated that "Design variations" were popularly arisen in the design phase of a project and may result from issues such as "variations by the client" and defective designs. To avoid defective design, the design team need not only to fully understand what the clients want as defined in the project brief, but also to establish an efficient communication scheme among the designers." Establishing Engineering Design department consisting of building, road, drainage, sewerage, highway, etc. under one roof is necessary and definitely will mitigate conflicts amongst the design team.

7.4 Blockade/Embargo Issues

Political risk can be defined as "the risk of probability of occurrence of some political event that will change the prospects for the profitability of a given investment" (Haendel, 1979; Chua, Wang & Tan, 2003; Abd Rahman et al., 2009). The contractors had submitted the claims to PWA in order to claim the increasing material prices due to the sudden political blockade that happened in June 2017. However, PWA had been specified clearly in General Condition of Contract (CoC) that, "in the event the contractor is unable to source and acquire materials and equipment from countries stated "in the approved manufacturers/suppliers/vendor list due embargo, the contractor shall source and acquire equivalent materials and equipment from other alternative countries accordingly if required without addition cost incurred to PWA."

Unforeseen political risk such as blockade/embargo which need to be seriously managed from top management to the bottom level. PWA and counterparts such as other ministry needs to demonstrate some proactive measures and must lead to minimize the risk and addressed to overcome the impact of material shortages as not to affect the work progress of on-going or future project.

7.5 Strategic Alliances

Identify the primary motivations for organizations to enter strategic alliances to be risk sharing, product rationalization and economics of scale, transfer of complimentary technology/exchange of patents, shaping competition, facilitating international expansion, conformance to host government policy, and vertical linkages (Glaister et al., 1998; Fellows & Liu, 2009). Apart some organizations are focusing to explore/ sharing technology by forming a strategic alliances, another option/reason is to ensure better supply of materials and equipment by considering having a "trading partner" as opportunities particularly for construction firms to create and manage a healthy supply chain, risk reduction and to ensure the project success.

8 CONCLUSION

Based on a project case study analysis, result from questionnaires and the interview sessions with the experts, the results could be justified that the risk management process had been culturally adopted for the previous and on-going projects under the expressway program. However, for certain projects, the risk management implementation including risk mitigations had been approached actively only during the construction stage. Proper risk management processes need to be implemented during the beginning of the projects particularly started from the feasibility study stage and design stage. Project risks need to be identified, ranked the level of risk severity and registered. Furthermore, prioritized the extreme risks, mitigated and managed efficiently. ASHGHAL has its own Risk Management Department and started to adopting the risk management practice currently and also for future infrastructure projects. Apart from risk management department, by establishing the interfacing department in future also could be a strategic solution for managing the interfacing risk. Instead of to ensure that the interfacing matters are identified, assessed for potential clashes and resolutions, the potential interfacing risk for every project could be identified, mitigated, updated and controlled sufficiently.

REFERENCES

Abd Rahman, N. R., Torrance, J. V. & Torrance, M. H. (2009). *Influential factors impacting international construction*. The Case of Malaysian Contractors, Joint Ventures in Construction, Kobayashi, K., Abdul Rashid, K., Ofori, G., Ogunlana, S. & Thomas Telford, London, 90-100.

Dziadosz, A. & Rejment, M. (2015) Risk analysis in construction project – chosen methods. Operational research in sustainable development and civil engineering - meeting of EURO working group and 15th German-Lithuanian-Polish colloquium (ORSDCE 2015): *Procedia Engineering*, *122* (2015), 258-265.

Fellows, R. & Liu, A. M. M. (2009). Construction projects as joint ventures: Issues of culture and risk, joint ventures in Construction. Kobayashi, K., Abdul Rashid, K., Ofori, G., Ogunlana, S. & Thomas Telford, London, 17-29.

Oberlender, G. D. (2000) *Project management for engineering and construction*, Thomas Casson, the USA.

Zou, P. X. W., Zhang, G. & Wang, J. Y. (2007). Identifying key risk in construction projects: Life cycle and stakeholder perspectives. *Journal of Project Management*, 25 601-614.

Cite this article as: Abd Rahman N. R., "Risk Management for Qatar Expressway Program", *International Conference on Civil Infrastructure and Construction (CIC 2020)*, Doha, Qatar, 2-5 February 2020, DOI: https://doi.org/10.29117/cic.2020.0033

Lean Principles Implementation in Construction Management: A One Team Approach

Mahmoud Fahmy
mfahmy@qetaifanprojects.com
Qetaifan Project, Doha, Qatar

ABSTRACT

Lean in construction is a relatively new approach in delivering construction projects. The Lean approach has been introduced to tackle the phenomenal construction projects delays and budget overruns. This paper shall be discussing how the implementation of the Lean approach in construction management processes can improve construction projects' delivery. The paper argues that the Lean approach in the construction industry context revolves around people rather than processes as in the manufacturing industry context. Therefore, the cornerstone of the Lean approach in construction is creating a One Team out of the multiple typical rivals in the construction industry: Owner, architect / engineer, operator and contractor with all taking into consideration the end user. While the 'Lean' concept is manufacturing tackled processes to achieve the 'Lean' goal; in construction the 'Lean' approach is tackling the interaction between people and entities. The interaction between people is addressed by the 'Lean construction' planning tool: The last planner system; while the interaction between entities is addressed by contractual forms of agreement with the most influential being: Alliance contracting. The paper uses a major infrastructure project 'Sydney Desalination Plant' which started in June 2007 and completed in January 2010 as a successful example of Lean approach implementation, although the term 'Lean' was never used then by the parties involved in the project. The paper draws on the first-hand experience of the author in the construction industry including the participation in the delivery of the 'Sydney Desalination Plant' used as example of a Lean project.

Keywords: Lean construction; Alliance contracting; Team collaboration

1 INTRODUCTION

Lean construction is a concept and approach that helps in delivering construction projects. It evolved due to the dire situation of the construction industry where the norm is: projects are delayed, and projects' budgets are overrun. However, it is worth noting that the term 'lean construction' is not limited to the construction phase of a project as the term might be perceived. 'Lean construction' is an overarching concept which encompasses both the design and construction phases of a project. There are number of definitions for 'lean construction' and this paper adopts the definition: "it is a way to design production systems to minimize waste of materials, time, and effort in order to generate the maximum possible amount of value" (Koskela et al., 2002). Meanwhile, it is important to highlight that the 'lean' concept evolved originally from the manufacturing industry to improve the manufacturing processes. While the goal in applying the 'lean'

concept in both industries is one, eliminating waste and maximizing value, the nature of the two industries is different. This paper discusses a major unique characteristic in construction projects setting it apart of the manufacturing industry; which is the human component. In construction projects the direct interface of people of different levels in: intellect, risk appetite, organizational skills and process-driven approach is un avoidable, where in manufacturing to a far extent, automation played a major role in breaking the links of interface between individuals who have high level difference in professional/industry culture. Several 'lean construction' literature and textbooks touched on the fundamental impact of people factor in applying the 'lean' principles. One of many examples is Gary Santorella's book on Lean Culture where he mentions that the main reason for writing the book was "to draw a connection between how construction professionals act as leaders (both positively and negatively) and the subsequent affect their attitude and behavior has on productivity and waste" (Santorella, 2011). Additionally, in the construction industry the interface between multiple entities when each has its own motivation and goals is far complex than in the manufacturing industry where the end product is well defined, and uncertainties are almost eliminated. Therefore, while the 'lean' concept is manufacturing tackled processes to achieve the 'lean' goal; in construction the 'lean' approach is tackling the interaction between people and entities. The interaction between people is addressed by the 'lean construction' planning tool: The last planner system; while the interaction between entities is addressed by contractual forms of agreement with the most influential being: Alliance contracting. Both the last planner system and alliance contracting are founded on 'collaboration', which this paper refers to as 'A One Team Approach'.

2 COLLABORATION

If we to dissect the 'lean' principles in the construction industry, we will recognize that it is founded on the term 'collaboration'. The reason why collaboration falls at the core of 'lean' principles is the nature of the industry, being a people driven industry. However, people are present in any project in two dimensions:

- Individual dimension: Each present by his own set of skills, personality and objectives.
- Entity dimension: Each group of individuals representing the entity, which they belong to.

The 'lean' concept in simple terms is about finding the way (set of processes) which allows project teams to collaborate efficiently in order to eliminate waste and maximize value. The complexity in this simple statement lies in the word 'project teams' i.e. people with their two dimensions present at the project. The first dimension (individuals) is dealt with (firstly) through people skills / soft skills, which cannot be structured in a process to manage the individuals' outcome. Therefore, the 'lean' in construction introduced the 'pull' planning concept opposing the conventional 'push' method as a process to address collaboration at the individual level. The 'pull' planning concept implemented by the 'last planner system' is out of the scope of this paper discussion. However, it is worth noting that 'collaboration', which is the core 'lean principle' is standing on two pillars (as illustrated in figure 1): The collaboration at the individuals' level and the collaboration at the entities level.

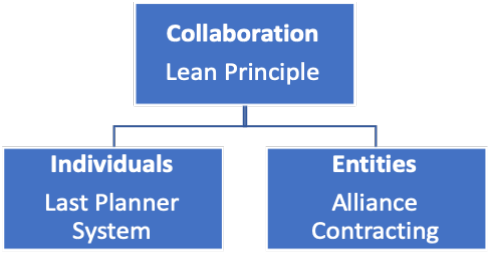

Figure 1: Collaboration pillars

3 TRADITIONAL CONTRACTING

A typical multidisciplinary / mega project involves the following entities:

- Owner
- Architect / Engineer
- Contractor
- Operator / Facility Manager

The traditional forms of contract in the construction industry have been:

- Design – Bid – Build
- Design & Build
- Engineering Procurement Construction (EPC)

All three forms inherently and traditionally dealt with the organizations participating in a project as rivals. The reason being that when a project goes off-track, which is more often than not, each entity strives to prove that the other entity is solely responsible for the unfavorable outcome. This phenomenon is quite understandable for the following reasons:

- Individuals of each entity strive to protect their own entity interest.
- Individuals, regardless of which entity they belong to, strive to depart themselves from the project failures.
- The incidents contributing to the failure of the project are, most often, complex and have the capacity to be interpreted by each entity differently.

Accordingly, the traditional forms of contract launch projects are carried by rival entities rather than collaborating entities.

4 ALLIANCE CONTRACTING

'Alliance contracting', "also known as 'collaborative contracting' is a delivery framework for large multidisciplinary projects, focusing on a co-operative process which aims to promote openness, trust, risk and responsibility sharing, innovation, high performance and the alignment of commercial interests between parties who aim to deliver a project in a collaborative and constructive way," (Walsh, 2015). This offers a different approach, 'the one team approach' by bringing together the entities involved in a project under one umbrella. Accordingly, the 'alliance contracting' addresses the entities dimension by bringing them in a single domain within a framework allowing them to share benefits and risks. Alliance contracting has been implemented in the UK,

Europe, Asia Pacific, Australia & New Zealand with remarkable gains being achieved. Furthermore, there are discussions "that although the volume of alliance activity is growing, the potential benefits of such organizational arrangements are not being realized because participating firms are emphasizing short-term profit sharing and accountancy procedures to the detriment of the more long-term and, ultimately," (Ingirige & Sexton, 2006). This paper is only discussing the first fold of 'alliance contracting', the short-term fold, which in itself serves the 'lean' principles implementation as discussed in the different approach it has towards project problems.

5 APPROACHING PROBLEMS

Clearly, the traditional forms of contract and the 'alliance' form of contract shall result in a completely different approach in dealing with problems facing a project. In traditional contracting, each and every problem facing the project is approached as a dispute between the rival entities. Managing a dispute shifts the focus from resolving the problem to arguing which entity is at fault. While in 'alliance contracting', entities become one team focusing on problems at hand as a challenge facing the project. Table 1: Different approaches in addressing problems provides a comparison between the traditional and the alliance contracting:

Table 1: Different approaches in addressing problems

	Traditional Contracting	**Alliance Contracting**
Project Entities	Rivals	One Team
Problem facing the project	Result in dispute	Treated as a challenge
Goal	Identifying who is at fault	Eliminating the problem
Outcome	Unresolved problem leading to further problems and waste	Moving forward and sharing gain / loss

6 SUCCESSFUL EXAMPLE: SYDNEY DESALINATION PLANT

Since late 1990's 'alliance contracting' has been used in mega construction projects in Australia and New Zealand. A successful example of which is the Sydney Desalination Plant started in June 2007 and completed in January 2010. The project owner, Sydney Water (a government owned entity at the time) made an alliance called 'White Water' with the contractor John Holland and the operator Veolia Water and launched the 1 billion AUD project to build 250 mega litter/day plant (expandable to 500 mega litter/day) , which was a fast track project to tackle the critical low dam levels supplying Sydney with potable water. The alliance then contracted SKM (currently Jacobs) and Maunsell (currently AECOM) JV to undertake the engineering of the project. The project, which successfully provided over 15% of Sydney's potable water supply, was completed on time and under budget by 60 million AUD approximately. Although the term 'lean construction' was never used and the project planning system was the conventional CM method, yet the team collaboration and the one team approach were the main contributors to the project success. That was essentially achieved by introducing the benefit / risk-sharing concept with all entities including the design JV that was not part of the alliance. All entities agreed to bring their teams together, literally all wearing the same alliance shirt, 'White Water'. Each member of the team working on the project belonged to the

project rather than to the entity, he/ she originally came from. Hence, the project was a success.

7 CONCLUSION

Collaboration is an obvious key to projects success. However, implementing collaboration and 'A One Team Approach' cannot be achieved without a proper contract framework, which facilitates the benefit / risk sharing between the entities involved in the project. The most reliable form of contract addressing collaboration, which is backed by record of accomplishment of successful projects, is the 'alliance contracting'. However, the challenge facing the implementation of this form of contract, in many parts of the world, is that the legal frameworks in public sector do not have this form of contracts.

REFERENCES

Ingirige, B. & Sexton, M. (2006). Alliances in construction investigating initiatives and barriers for long-term collaboration. *Research Institute of the Built and Human Environment*, University of Salford, Salford, the UK.

Koskela, L., Howell, G., Ballard, G. & Tommelein, I. (2002). The Foundations of Lean Construction. Research Gate.

Santorella, G. (2011). *Lean Culture for the Construction Industry – Building Responsible and Committed Project Teams*. P. xviii, CRC Press.

Walsh, P. (2015). Alliance Contracting: The Way Forward, Thomson Reuters.

Cite this article as: Fahmy M., "Lean Principles Implementation in Construction Management: A One Team Approach", *International Conference on Civil Infrastructure and Construction (CIC 2020)*, Doha, Qatar, 2-5 February 2020, DOI: https://doi.org/10.29117/cic.2020.0034

Theme 2:
Materials and Transportation Engineering

Development of Warm Mix Asphalt with the Aid of Microstructural Characterization

Abdullah Al Mamun
amamun@qu.edu.qa
Department of Civil and Architectural Engineering, Qatar University, Doha, Qatar

Okan Sirin
okansirin@qu.edu.qa
Department of Civil and Architectural Engineering, Qatar University, Doha, Qatar

Eyad Masad
eyad.masad@qatar.tamu.edu
Mechanical Engineering Program, Texas A&M University at Qatar, Doha, Qatar

ABSTRACT

The polymer-modified asphalt (PMA) reveals different types of advantageous properties depending on the type of polymer. However, one of the unwanted changes in PMA is the required higher temperature for mixing and compaction. To reduce these temperatures, different percentages of warm mix additive (WMA) have been utilized. However, the addition of WMA can lead to different micro-nano structural changes in the PMA and can subsequently affect overall performance of the asphalt pavement. Therefore, understanding the microstructural behavior of the polymer and additive modified asphalt is crucial to achieve the desired performance. This study attempts to substantiate the effect of WMA in three different PMAs and subsequent changes in different properties. These changes can be scrutinized from different perspectives; however, correlating a basic microstructural property to the rheology of asphalt is an effective way to understand the mechanism and predict performance. In this regard, the need for microstructural evaluation in terms of nano-adhesive properties is recommended. It is expected that assessing the adhesive properties by simulating the field condition can address the phase integrity and crystal structure of PMA and subsequent desired performance of the asphalt pavement. Finally, the observed adhesive properties can be further evaluated to find the prospects of other mechanical properties. Therefore, the need for a standard microstructural evaluation method of the adhesive properties has also been addressed in this study.

Keywords: Warm mix asphalt; Multiscale characterization; Polymer modified asphalt; Rheology

1 INTRODUCTION

The polymers used for asphalt modification usually have large chains (straight or cross-linked). The chemical and structural properties of the chains affect the properties of the polymer, as well as polymer modified asphalt (PMA). The most commonly used polymers are elastomers and plastomers. The elastomer improves the elastic properties while the plastomer provides a plastic matrix for the modified asphalt. Based on the type of polymer, asphalt can exhibit different characteristics. One of the significant changes

in PMA is the increased mixing and compaction temperatures for the Hot Mix Asphalt (HMA). These higher temperatures can alter the desired performance of the pavement (Roque et al., 2005). On the contrary, lowering the required temperature for mixing and compaction can result in inadequate volumetric properties and, consequently, poor pavement performance. To overcome these problems, the use of warm mix additive (WMA) in PMA is a viable solution.

The WMA reduces the viscosity of PMA that eventually reduces the required higher temperature for mixing and compaction. Warm mix technologies are categorized into three main types: foaming processes, organic additives, and chemical additives. Chemical additives generally do not require significant modification, and the addition of chemical additives helps to improve the coating of aggregate and compaction of the mixture by lowering the viscosity of the asphalt. In the foaming process, the volume of the asphalt is increased by injecting hot water in a predefined way, and therefore, the expanded asphalt requires relatively low temperature to achieve a similar coating ability. The organic additive helps the binder to flow and melt at temperatures below HMA. The melting point of organic additives is kept higher than the temperature used to avoid permanent deformation (Sadeq et al., 2016). It is observed that the mixing and compaction temperatures of the asphalt mixture can be lowered by 20-30°C using various WMAs (Button et al., 2007).

Although the addition of the WMA in the PMA reduces the required temperatures for the mixing and compaction, it is also expected to affect the rheology (Sadeq et al., 2018) and microstructural behavior (Menapace & Masad, 2017) of the binders, and consequently the response of the mixtures. Since the mixtures with WMA are produced at lower temperatures compared to the traditional HMA, the properties of WMA binders/mixtures are expected to deviate from HMA. In addition, WMA can lead to different micro-nano structural changes in the PMA. Correlating a basic microstructural property to the rheology of asphalt could be an effective way of visualizing the mechanism and performance.

This study attempts to scrutinize the effect of WMA in different PMAs. The scope of the study considers three different PMAs and based on the discussion, the need for an integrated and standard microstructural evaluation has been addressed.

2 POLYMER – ADDITIVE MODIFIED ASPHALT

The study contemplates the effect of organic additives on PMA and includes three different polymers: Styrene–butadiene–styrene (SBS), Low-density polyethylene (LDPE), and crumb rubber (CR). Numerous studies have evaluated the effects of polymers and additives on asphalt binders. In the following sections, the effect of different additives on the desired properties of asphalt binder and mixes are discussed.

2.1 Crumb rubber/additive modified asphalt:

One of the potential polymers for asphalt pavement engineering is crumb rubber (CR). CR is produced from the used tires, which consist of four main components: fiber, steel, carbon, and rubber. Here, the rubber shares the significant (60% of the total weight) portion of the tire (Kim et al., 2012). Several studies have been carried out to better understand the use of crumb rubber modified asphalt (CRMA). It is observed

that the presence of CR can increase the complex modulus and softening point, elastic recovery, viscosity, tensile strength and decrease the ductility, penetration, and phase angle of the CRMA (Cong et al., 2013). Li et al. evaluated the rutting resistance capacity of CRMA using an asphalt pavement analyzer and concluded that the CRMA has better resistance to rutting than the traditional mixes (Li et al., 2016). In combination with different improved properties, it has also been observed that the presence of CR can also increase the mixing and compacting temperatures of CRMA.

The increased mixing and compacting temperatures of CRMA can be counteracted by WMA. WMA additives can reduce the compaction temperatures of CRMA by up to 20–30°C that subsequently reduces energy consumption without jeopardizing the engineering properties (Akisetty et al., 2011). However, the lowered production temperature reduces the aging of asphalt that subsequently may affect the fatigue and rutting properties of asphalt mixture (Cong et al., 2013). A study concluded that Sasobit®-modified CR modified mixtures improved the rutting performance (Fontes et al., 2010) whereas, Sasobit® was found to have insignificant effect on rutting performance for the CRMA (Navarro & Gámez, 2012). The addition of Sasobit® in CR binder showed increased G*/Sinδ (Navarro & Gámez, 2012), whereas, Advera® had an insignificant effect on G*/sinδ (Xiao et al., 2007). Therefore, the addition of WMA in CRMA exhibited a mixed trend and it can affect the rutting performance (G*/Sin δ) of CR modified binder differently. In a study, Xiao et al. (2009) evaluated the fatigue performance of different WMA additives for CRMA and concluded that among Aspha-min, Sasobit and Evotherm, only Aspha-min decreases fatigue cracking resistance.

Therefore, in addition to reducing the mixing and compaction temperature, the warm additive can affect the different properties of CRMA. CR creates a gel-covered particle by interacting with the asphaltenes and light fractions of the asphalt. The subsequent absorption results in the swelling of CR modified asphalt (Wu & Zeng, 2012). The changes in temperature can affect this swelling significantly (Xiao et al., 2007), and subsequently, affect other properties. Such changes dictate the need for microstructural evaluation of CRMA.

2.2 Styrene–butadiene–styrene / additive modified asphalt

In asphalt pavement construction, the most commonly used polymer is Styrene–butadiene–styrene (SBS) (Zhang et al., 2018). It is a block copolymer that makes a coherent bonding with asphalt. The use of SBS in asphalt provides different desired properties such as increased elastic response (Li et al., 2019), lowers the creep stiffness (Iskender et al., 2012), and improved resistance to rutting and fatigue (Kalyoncuoglu & Tigdemir, 2011), etc., yet it also increases the compaction and mixing temperature. Therefore, the use of different warm additive is very common for SBS modified asphalt. The use of WMA (e.g. Sasobit) in SBS modified asphalt can reduce the viscosity depressant characteristics by at least 10oC (Hofsink & Barnard, 2009).In a study, SBS modified binders were incorporated with a different type of additive and it was observed that the production temperature of the WMA was reduced by at least 16oC than the traditional HMA (Wang et al., 2013). Another study concluded that Sasobit can reduce the viscosity of SBS modified asphalt and subsequently reduce the required compaction temperature by 25oC (Li et al., 2016).

In addition to reducing the compaction and mixing temperature, the use of warm additive also affects other properties of SBS modified asphalt. A study investigated the effect of two different additives (Sasobit and Aspha-min) on the performance of SBS modified asphalt by evaluating high failure temperature values from the DSR test (Kim et al., 2010). It was concluded that the additives increase the resistance to rutting at high temperatures. In another study, researchers evaluated the effect of Sasobit and Aspha-min on SBS modified asphalt mixture for different characteristics (Kim et al., 2012). While comparing the performance based on rutting, it was concluded that mixtures with Sasobit outperform all the other mixtures whereas Aspha-min incorporated mixtures were the least effective. However, in terms of fatigue life, SBS modified mixture showed higher fatigue resistance than the similar additive modified mixture at different stress levels (Fakhri et al., 2013).

These changes of SBS modified asphalt due to WMA indicate the microstructural changes in the asphalt. An evaluation of SBS modified asphalt using Transmission Electron Microscopy (TEM) indicates that the morphology and formation of phases may vary following the sources of asphalt and polymer (Yildirim, 2007). Another study concluded that SBS modified asphalt has a tendency of partial miscibility and, in a stagnant condition with a higher temperature it exhibits phase separation phenomena (Jasso et al., 2015). Therefore, the addition of WMA has been reported as a possible reason for forming a kind of gel, crystal or network structure in the SBS modified binder that dictates a further need for microstructural evaluation (Shang et al., 2011).

2.3 Low-density polyethylene / additive modified asphalt

Several studies also recommend using Low-density polyethylene (LDPE) as a plastomer in asphalt modification. Fang et al. (2009) modified the asphalt binder using PVC packaging waste (0-10%wt. of asphalt) and evaluated different properties such as softening point, ductility, elongation and tension, penetration, low-temperature flexibility and found improved performance (Fang et al., 2009). Further microscopic evaluation reveals the development of dissolved and continuous polymer-rich microstructure due to increased polymer. Fang et al. (2012), studied the micro-structure of polyethylene (PE) modified asphalt by Scanning Electron Microscope (SEM) and concluded that the introduction of momtmorillomite improves the dispersion and homogeneity of PE modified asphalt that subsequently results in increased penetration, softening point, with improved ductility.

Ho Susanna et al. evaluated the low-density polyethylene wax materials and concluded that the molecular weight and its distribution significantly affect hot storage stability (Ho et al., 2006). Punith and Veeraragavan evaluated the homogeneity of the PE-modified binder using florescent microscopy scanning and concluded that the blending temperature can affect the penetration and softening point values significantly (Punith & Veeraragavan, 2011). Therefore, it is expected that the use of LDPE can affect the mixing and compaction temperatures. However, to the authors' knowledge, none of the previous studies attempted to study the effect of WMA in LDPE modified asphalt. Therefore, the microstructural evaluation is expected to provide an insight to assess the effect of WMA in LDPE modified asphalt.

3 THE NEED FOR MICROSTRUCTURAL EVALUATION

Different PMAs have provided many remarkable advancements in improving the multi-functional properties and have proved to be promising candidates for high-performance asphalt pavements. However, the addition of WMA can lead to different micro-nano structural changes in the modified asphalt binder. WMA can bring changes in microchemical structure and subsequently reduce the viscosity of asphalt. The microstructure regulates the thermo-rheological behavior along with different mechanical properties such as elasticity, plasticity, and stiffness of asphalt (Das et al., 2013). The addition of additive in PMA also imparts the need for evaluating the phase integrity by microstructural assessment. It is crucial to understand changes in the microstructural behavior of PMA due to WMA to provide desired performance rather than having negative consequences. To this end, scrutiny of microstructural properties of WMA modified asphalt is needed.

4 THE PROSPECT OF MULTISCALE CHARACTERIZATION

The behavior of asphalt depends largely on its intermolecular microstructures and chemical structure. Thus, the evaluation of micromechanical behavior could help in predicting the performance of asphalt mixtures. Different nano and microstructural evaluation techniques have played a significant role in evaluating the properties of modified binder meticulously. In such cases, Atomic Force Microscopy (AFM) has been employed in measuring nano-scale intermolecular forces. In general, the force spectrum technique of AFM is a suitable tool for characterizing the nanomechanical properties of pavement materials. Numerous studies have been carried out to assess different properties - van der Waals forces, friction, contact force- of asphalt using AFM (Mamun & Arifuzzaman, 2018). AFM has also been used in several studies to evaluate the changes in adhesion of modified asphalt binders at the nanoscale. These studies observed that adhesion in asphalt changes due to the presence of polymer and the changes in adhesive properties can affect the phase integrity of modified asphalt (Mamun & Arifuzzaman, 2018). Therefore, evaluation of the adhesive properties of WMA modified asphalt can provide an insight of microstructural properties.

Till date, very few studies have considered the adhesive properties of WMA modified asphalt in microstructural evaluation. Nazzal et al. concluded that the warm mixes increase or decrease the adhesion of asphalt binders in a dry state and wet state, respectively (Nazzal et al., 2015). In another study, AFM has been successfully used to evaluate different nanomechanical properties including adhesion, the cohesion of asphalt binders by evaluating the effect of warm additives (Abd et al., 2018). However, those studies are insufficient to provide an integrated microstructural insight of WMA modified asphalt, since the evaluated adhesive properties have not been correlated with the mechanical properties of asphalt. In addition to that, those studies considered different methodologies to assess the adhesive properties at a certain temperature. However, the nanoscale adhesion and microstructures of the modified binder should be evaluated at different temperatures since the asphalt pavement experiences different temperatures during its service life. The variation in temperature is expected to affect the phase integrity and crystal structure of the modified binder. Therefore, for each PMA, it is imperative to have a comprehensive study of microstructural evaluation by developing

an appropriate methodology for measuring such changes by simulating the real field condition.

5 CONCLUSION

This study discusses the effect of warm mix additive in different PMAs. It is inferred that a comprehensive evaluation at the microstructural level is a prerequisite to understand and estimate the synergy between asphalt and warm additive. Based on it, the following conclusions are drawn:

1. The warm additive can affect different rheological properties of PMA, which is governed by changes in the characteristics of the asphalt microstructure. To evaluate the effectiveness of any warm additive, these changes in asphalt binder should be assessed carefully.
2. In further investigations, different AFM techniques (i.e. force spectroscopy, tapping mode imaging, and nano-indentation) can be employed on warm mix modified asphalt to characterize the micro or nano-scale structures of asphalt.
3. The microstructural evaluation of warm additive modified asphalt can be analyzed from different perspectives; however, correlating the adhesive properties to the rheology of asphalt could be an effective way of visualizing the mechanism and performance.
4. The adhesive property of modified asphalt is one of the basic properties that is expected to subsequently affect the overall performance of the asphalt mixture. Therefore, a standard method should also be developed to measure the change in adhesion/cohesion of the warm additive modified asphalt binder.

REFERENCE

Abd, D. M., Al-Khalid, H. & Akhtar, R. (2018). Adhesion properties of warm-modified bituminous binders (WMBBs) determined using pull-off tests and atomic force microscopy. *Road Materials and Pavement Design*, *19*(8): 1926-1939. Taylor & Francis. DOI: 10.1080/14680629.2017.1374993.

Akisetty, C., Xiao, F., Gandhi, T. & Amirkhanian, S. (2011). Estimating correlations between rheological and engineering properties of rubberized asphalt concrete mixtures containing warm mix asphalt additive. *Construction and Building Materials*, *25*(2): 950-956. Elsevier. DOI: 10.1016/J.CONBUILDMAT.2010.06.087.

Button, J. W., Senior, P. E., Fellow, R. & Estakhri, C. (2007). *A Synthesis of Warm-Mix Asphalt*. Available from http://tti.tamu.edu/documents/0-5597-1.pdf [accessed 15 February 2019].

Cong, P., Xun, P., Xing, M. & Chen, S. (2013). Investigation of asphalt binder containing various crumb rubbers and asphalts. *Construction and Building Materials*, *40*: 632-641. Elsevier. DOI: 10.1016/J.CONBUILDMAT.2012.11.063.

Das, P. K., Kringos, N., Wallqvist, V. & Birgisson, B. (2013). Micromechanical investigation of phase separation in bitumen by combining atomic force microscopy with differential scanning calorimetry results. *Road Materials and Pavement Design*, *14*(sup1): 25-37. Taylor & Francis. DOI: 10.1080/14680629.2013.774744.

Fakhri, M., Ghanizadeh, A. R. & Omrani, H. (2013). Comparison of Fatigue Resistance of HMA and WMA Mixtures Modified by SBS. Procedia - *Social and Behavioral Sciences,* 104: 168-177. Elsevier. DOI: 10.1016/J.SBSPRO.2013.11.109.

Fang, C., Yu, R., Zhang, Y., Hu, J., Zhang, M. & Mi, X. (2012). Combined modification of asphalt with polyethylene packaging waste and organophilic montmorillonite. *Polymer Testing*, *31*(2): 276-281. Elsevier. DOI: 10.1016/J.POLYMERTESTING.2011.11.008.

Fang, C., Zhou, S., Zhang, M. & Zhao, S. (2009). Modification of Waterproofing Asphalt by PVC Packaging Waste. *Journal of Vinyl & Additive Technology, 15*(4): 229-233. DOI :10.1002/vnl.20204.

Fontes, L. P. T. L., Trichês, G., Pais, J. C. & Pereira, P. A. A. (2010). Evaluating permanent deformation in asphalt rubber mixtures. *Construction and Building Materials*, *24*(7): 1193-1200. Elsevier. DOI: 10.1016/J.CONBUILDMAT.2009.12.021.

Ho, S., Church, R., Klassen, K., Law, B., MacLeod, D. & Zanzotto, L. (2006). Study of recycled polyethylene materials as asphalt modifiers. *Canadian Journal of Civil Engineering*, *33*(8): 968-981. DOI: 10.1139/L06-044.

Hofsink, W. & Barnard, M.C. (2009). SMA wearing courses on runways and taxiways: recent experience in South Africa. Available from https://trid.trb.org/view/914660 [accessed 26 February 2019].

Iskender, E., Aksoy, A. & Ozen, H. (2012). Indirect performance comparison for styrene–butadiene–styrene polymer and fatty amine anti-strip modified asphalt mixtures. *Construction and Building Materials*, 30: 117-124. Elsevier. DOI: 10.1016/J.CONBUILDMAT.2011.11.027.

Jasso, M., Hampl, R., Vacin, O., Bakos, D., Stastna, J. & Zanzotto, L. (2015). Rheology of conventional asphalt modified with SBS, Elvaloy and polyphosphoric acid. *Fuel Processing Technology*, 140: 172-179. Elsevier. DOI: 10.1016/J.FUPROC.2015.09.002.

Kalyoncuoglu, S. F. & Tigdemir, M. (2011). A model for dynamic creep evaluation of SBS modified HMA mixtures. *Construction and Building Materials*, *25*(2): 859-866. Elsevier. DOI: 10.1016/J.CONBUILDMAT.2010.06.101.

Kim, H., Lee, S. -J. & Amirkhanian, S. N. (2010). Effects of warm mix asphalt additives on performance properties of polymer modified asphalt binders. *Canadian Journal of Civil Engineering*, *37*(1): 17-24. DOI: 10.1139/L09-118.

Kim, H., Lee, S. -J. & Amirkhanian, S. N. (2012). Influence of warm mix additives on PMA mixture properties. *Journal of Transportation Engineering*, *138*(8): 991-997. DOI: 10.1061/(ASCE)TE.1943-5436.0000406.

Li, J., Zhang, F., Liu, Y., Muhammad, Y., Su, Z., Meng, F. & Chen, X. (2019). Preparation and properties of soybean bio-asphalt/SBS modified petroleum asphalt. *Construction and Building Materials*, 201: 268-277. DOI: 10.1016/j.conbuildmat.2018.12.206.

Li, X., Zhou, Z. & You, Z. (2016). Compaction temperatures of Sasobit produced warm mix asphalt mixtures modified with SBS. *Construction and Building Materials*, 123: 357-364. Elsevier. DOI: 10.1016/J.CONBUILDMAT.2016.07.015.

Mamun, A. A. & Arifuzzaman, M. (2018). Nano-scale moisture damage evaluation of carbon nanotube-modified asphalt. *Construction and Building Materials*, 193: 268-275. Elsevier. DOI: 10.1016/J.CONBUILDMAT.2018.10.155.

Menapace, I. & Masad, E. (2017). Evolution of the microstructure of warm mix asphalt binders with aging in an accelerated weathering tester. *Journal of Materials in Civil Engineering*, *29*(10): 04017162. DOI: 10.1061/(ASCE)MT.1943-5533.0001998.

Navarro, F. M. & Gámez, M. C. R. (2012). Influence of crumb rubber on the indirect tensile strength and stiffness modulus of hot bituminous mixes. *Journal of Materials in Civil Engineering, 24*(6): 715-724. DOI: 10.1061/(ASCE)MT.1943-5533.0000436.

Nazzal, M. D., Abu-Qtaish, L., Kaya, S. & Powers, D. (2015). Using atomic force microscopy to evaluate the nanostructure and nanomechanics of warm mix asphalt. *Journal of Materials in Civil Engineering*, *27*(10): 04015005. DOI: 10.1061/(ASCE)MT.1943-5533.0001254.

Punith, V. S. & Veeraragavan, A. (2011). Behavior of reclaimed polyethylene modified asphalt cement for paving purposes. *Journal of Materials in Civil Engineering*, *23*(6): 833-845. DOI: 10.1061/(ASCE)MT.1943-5533.0000235.

Roque, R., Birgisson, B., Drakos, C. & Sholar, G. (2005). Guidelines for use of modified binders. Available from https://trid.trb.org/view/768711 [accessed 15 February 2019].

Sadeq, M., Masad, E., Al-Khalid, H., Sirin, O. & Little, D. (2016). Rheological evaluation of short- and long-term performance for warm mix asphalt (WMA) Binders. *Springer, Dordrecht*. pp. 129-139. DOI: 10.1007/978-94-017-7342-3_11.

Sadeq, M., Masad, E., Al-Khalid, H., Sirin, O. & Mehrez, L. (2018). Linear and nonlinear viscoelastic and viscoplastic analysis of asphalt binders with warm mix asphalt additives. *International Journal of Pavement Engineering*, *19*(10): 857-864. Taylor & Francis. DOI: 10.1080/10298436.2016.1213592.

Shang, L., Wang, S., Zhang, Y. & Zhang, Y. (2011). Pyrolyzed wax from recycled cross-linked polyethylene as warm mix asphalt (WMA) additive for SBS modified asphalt. *Construction and Building Materials*, *25*(2): 886-891. Elsevier. DOI: 10.1016/J.CONBUILDMAT.2010.06.097.

Wang, C., Hao, P., Ruan, F., Zhang, X. & Adhikari, S. (2013). Determination of the production temperature of warm mix asphalt by workability test. *Construction and Building Materials*, 48: 1165-1170. Elsevier. DOI: 10.1016/J.CONBUILDMAT.2013.07.097.

Wu, C. & Zeng, M. (2012). Effects of additives for warm mix asphalt on performance grades of asphalt binders. *Journal of Testing and Evaluation, 40*(2): 104279. DOI: 10.1520/JTE104279.

Xiao, F., Amirkhanian, S. & Juang, C. H. (2007). Rutting resistance of rubberized asphalt concrete pavements containing reclaimed asphalt pavement mixtures. *Journal of Materials in Civil Engineering*, *19*(6): 475-483. DOI: 10.1061/(ASCE)0899-1561(2007)19:6(475).

Xiao, F., Wenbin Zhao, P. E. & Amirkhanian, S. N. (2009). Fatigue behavior of rubberized asphalt concrete mixtures containing warm asphalt additives. *Construction and Building Materials*, *23*(10): 31440-3151. Elsevier. DOI: 10.1016/J.CONBUILDMAT.2009.06.036.

Yildirim, Y. (2007). Polymer modified asphalt binders. *Construction and Building Materials*, *21*(1): 66-72. Elsevier. DOI: 10.1016/J.CONBUILDMAT.2005.07.007.

Zhang, D., Chen, Z., Zhang, H. & Wei, C. (2018). Rheological and anti-aging performance of SBS modified asphalt binders with different multi-dimensional nanomaterials. *Construction and Building Materials,* 188: 409-416. DOI: 10.1016/j.conbuildmat.2018.08.136.

Cite this article as: Al Mamun A., Sirin O., Masad E., "Development of Warm Mix Asphalt with the Aid of Microstructural Characterization", *International Conference on Civil Infrastructure and Construction (CIC 2020)*, Doha, Qatar, 2-5 February 2020, DOI: https://doi.org/10.29117/cic.2020.0035

Site-Specific Traffic Loading Estimation Challenges in Structural Pavement Design Process in Qatar: A Case Study

Ahmad Al-Tawalbeh
ahmad.altawalbeh@seeroeng.com
Seero Engineering Consulting LLC, Doha, Qatar

Mohammed Sadeq
mohammed.sadeq@seeroeng.com
Seero Engineering Consulting LLC, Doha, Qatar

Husam Sadek
hsadek1@lsu.edu
Louisiana State University, Baton Rouge, Louisiana, USA

ABSTRACT

Upon the design of any pavement structure, three fundamental external design parameters have to be considered throughout the design process: the characteristics of the subgrade, traffic loads, and environmental conditions. This paper focuses on the main challenges being faced to estimate site-specific traffic loading for a pavement design due to the lack of accurate and recent traffic data. A case study for a pavement structural design process for an actual expressway project in the State of Qatar is discussed in this paper. This case study goes through traffic loading calculations inputs; the Average Daily Traffic (ADT), Truck Factor (TF), as well as Heavy Good Vehicle Percentage (HGV%). The challenges of calculating these site-specific traffic loading inputs are discussed through investigation of the accuracy in traffic loading estimation using Qatar Strategic Transport Model (QSTM), and how the model can be incorporated in the design. Besides, limited available Wight-In-Motion (WIM) surveys have been discussed and the paper ends with the conclusion that rich availability of traffic data enhances the accuracy of the pavement structural design. It affects significantly the value engineering practice, and results in sustainable pavement sections.

Keywords: Traffic loading; Pavement structure; Design; Strategic transport model; Qatar

1 INTRODUCTION

The State of Qatar is witnessing dramatic boom in the infrastructure field as part of the governmental 2030 vision and for the preparation of FIFA World Cup Qatar 2022™. According to Qatar Ministry of Finance (MOF) Website (2019), QR16.4 billion budget has been allocated for transportation and Infrastructure projects for Qatar in 2019. Consequently, significant improvement of Qatar's roads network has being achieved. Thousands of kilometres of flexible pavements are being designed and constructed taking into consideration value engineering practices and sustainability measures. Upon the design of any pavement structure, three fundamental external design parameters/ inputs have to be considered throughout the design process; (1) the characteristics of the subgrade layer, (2) expected traffic loads, and (3) environmental conditions. The

accurate estimation of the traffic loading is one of the most critical factors that impact the value engineering results and should be studied extensively along with other pavement design inputs. Availability of the traffic data is dominating the accuracy of the estimated traffic load that results in over- or under-designed pavement structures on roadways. Limited traffic data - in terms of frequency and distribution - creates multiple challenges that all designers would face to come up with a project-customized pavement design. These challenges are presented in this paper and discussed with recommendations to overcome some of them for more robust and economically designed pavement sections.

This paper presents a number of design inputs related to traffic estimation that affects the design decision of the asphalt pavement structure. These inputs are; the Average Daily Traffic (ADT), Heavy Good Vehicle Percentage (HGV%), and Truck Factor (TF). Some of these inputs are defined by following recommended parameters of national and/or international guidelines that were developed in different countries where the road network has different attributes and environmental conditions than Qatar. Having those parameters un-locally defined or refined increases the chance of uncertainty in the design process and risking the sustainability of the pavement structure by providing over- or under-designed sections. Therefore, national or international parameters are generally recommended to be used as references only during a structural pavement design practice and site-specific parameters have to be developed for each project.

To address the objective of this paper, a case study of a certain project in Qatar that went through the traffic load estimation challenges is presented with demonstrated recommendations.

2 LITERATURE REVIEW

In last few decades, many studies have been conducted to determine the sensitivity and traffic inputs in pavement structural design practice. The studies compared using site-specific inputs with default values of the country or state guides. Pavement Design Guidelines Interim Advice Notice 016 Ashghal (2013), recommended to use site-specific WIM if available to determine the actual Equivalent Single Axle Load Factors (ESALF). In a research was conducted in Ohio State to measure the effect of traffic load input level on mechanistic-empirical pavement design (Abbas et al., 2014), the authors recommended to use site-specific axle load spectra when available due to underestimated service life of statewide average axle load spectra. In the US State of Virginia, a study was conducted to analyze Virginia-Specific traffic data for use with mechanistic empirical pavement design guide (Smith and Diefenderfer, 2010). The study recommended using site-specific axle load spectra data for analysis of flexible pavements for users of Mechanistic–Empirical Pavement Design Guide (MEPDG). According to The Federal Highway Administration (FHWA), Traffic Monitoring Guide (TMG) recommends depending on several patterns of traffic fleet as industrial, geographic, agricultural, and commercial patterns, in parallel with

measured or estimated pattern in specific roads in order to define the group of roads based on truck weight (TMG, 2001). Since then, multiple researches and guidelines highlighted the importance of using site-specific pavement design inputs. This paper presents the challenges of implementing site-specific traffic loading inputs for pavement structural design in absence of traffic counting data based on authentic case study in Qatar.

3 TRAFFIC LOAD ESTIMATION CHALLENGES

As mentioned earlier, multiple traffic loading inputs for any pavement design suffer from the risk of inaccuracy that raise couple of design challenges. These inputs are key factors in the design process and below each one of them is discussed in detail.

3.1 Traffic Counts

Under limited traffic count frequency and duration, getting an over- or under-designed pavement section is highly expected due to the wide range of input values that can be selected. The inputs; Average Daily Traffic (ADT), Heavy Good Vehicle Percentage (HGV%), and Truck Factor (TF) are highly affected by the limited traffic counts. In the following subsections, each of the inputs are discussed.

3.1.1 Average Daily Traffic (ADT)

The Average Daily Traffic (ADT) value is a key input in the pavement design process as in other transportation engineering sub disciplines. The ADT is generally calculated from the annual traffic survey considering several periods throughout the year. As mentioned earlier, traffic surveys are conducted for only 1-2 weeks which affect the accuracy of the ADT estimation by ignoring the seasonal variation of the traffic volume in the project area.

3.1.2 Heavy Good Vehicle Percentage (HGV%)

The HGV percentage is a sensitive input in any pavement design process. HGV percentage is commonly calculated based on annual traffic surveys conducted in the project location. When annual traffic surveys are not available, calculating HGV percentage from 1-2 weeks duration traffic survey adds significant risk to the accuracy of the design outcomes.

3.1.3 Truck Factor (TF)

The Truck Factor, which is also known as the "Damage Factor", is generally estimated based on the data collected from the Weight-In-Motion (WIM) surveys. The accuracy of the TF is risked due to the difference in heavy traffic fleet characteristics based on the project area and mobility of the roads. On the other hand, international guidelines recommend values of TF that do not necessarily reflect traffic characteristics in Qatar which witnesses heavy construction activities while the trucks loading regulations are varying based on the country. Interim Advice Notice (IAN) 016 recommends a wide range of TF values for each traffic class, which results in uncontrolled design inputs (Ashghal, 2013). The recommended values show general ranges based on international guidelines. The combined uncertainty of these traffic-related design inputs leads to an enormous risk in the pavement structure analysis and design.

3.2 Strategic Transport Model Deficiencies

The State of Qatar has issued the first strategic transport model in the year of 2013 (MMUP, 2013), with initial roads network and land-uses. The model was developed based on the travel forecasting theory that depends on land-use type for trip generation and land-use's attraction and production for trip distribution. The model is aimed for strategic

decision-making and used for Measure of Effectiveness (MOE) purposes. Accordingly, the model is not accurate for estimating traffic fleet compositions and HGV volume for pavement design purposes. Moreover, the model needs to be continuously updated and disaggregated with plots' land-uses and road network upgrades for simulation that is more accurate. The strategic model considers the operational origin and destination trips from each plot in addition to public transport system trips, but not construction traffic generated due to the development of the plots.

4 TRAFFIC LOAD ESTIMATION RECOMMENDATIONS

The significant impact of the above-mentioned input challenges on the reliability of the designed pavement structure raises the need to propose and recommend solutions for more effective pavement design process. The following section documents the recommended approaches/methods for the mentioned inputs and discuss their impact on the design outcomes.

4.1 Average Daily Traffic (ADT) Estimation

In order to enhance the ADT estimation for a pavement design, Qatar Strategic Transport Model (QSTM), was found to be helpful in estimating the Peak Hour Volume (PHV) for each road link inside a project area. The PHV is used to better estimate the ADT value needed for the project area. The QSTM which was modelled using microsimulation software estimates the overall traffic fleet volume accurately based on many transport planning factors. Besides, the QSTM provides the chance to estimate the diverted traffic volume after upgrading the road network which provides a higher estimation accuracy (MMUP, 2013). In addition, the QSTM considers the variation of PHV along the same highway which facilitates providing several pavement structures for the road alignment while relying on limited number of traffic survey stations and could result in over- or under-estimated traffic load.

4.2 Heavy Good Vehicle Percentage (HGV%) Validation

As mentioned earlier, the QSTM was found to be inaccurate to estimate the HGV volume and traffic fleet characteristics for pavement design purposes. However, the QSTM model can be incorporated by conducting flow bundle analysis of the main HGV generator zones like Cargo Airports, Ports, and Industrial Areas …etc. The ratio of bundle volumes to background traffic volume was found to be very useful to estimate the HGV%. Accordingly, the calculated value can validate the HGV% that is extracted from the traffic survey data.

In addition, the construction traffic can also be a crucial input that impacts the pavement durability if mis-measured. The construction traffic is usually considered as 5% of the ADT value based on the common practice and previous experience. However, the construction traffic can also be refined and validated during the design process. A ratio of construction traffic can be established per unit area for a specific truck class and added to the ADT for a forecasted number of years of development.

4.3 Truck Factor (TF) Estimation

Using the Gross Vehicle Weight (GVW) data extracted from the WIM stations, it was

found to be the most reliable method to estimate the truck factor for a pavement design. The WIM survey represents the only authentic source to calculate the TF in Qatar while finding a weighted average TF of the project's traffic survey. Following the available WIM stations survey values provides Qatar-Specific TF values and controls the selected TF values to be within the 95th percentile truck weight (Ashghal, 2012). This approach reflects to be more realistic and a reasonable range for TF values for design purposes.

5 A CASE STUDY

In this case study, a specific pavement design project for an expressway in Qatar was considered to examine the proposed recommended methodology for input considerations in the pavement design. Accordingly, a comparison between conventional and recommended methodology parameters is conducted. Table 1 shows a description of each methodology inputs.

Table 1: Inputs description for the conventional and recommended methods

Methodology / Input	Conventional Method	Recommended Method
Average Daily Traffic (ADT) in the opening year	Calculated based on 1-2 weeks traffic survey inside the project area	Calculated based on PHV extracted from updated QSTM and Peak Hour Factor (PHF) calculated based on one-week traffic survey inside the project
Truck Factor (TF)	Commonly taken directly as average values from guidelines	Calculated based on 95th percentile TF of WIM survey conducted in several stations along Qatar and applied to project traffic survey volume to calculate weighted average TF
Heavy Good Vehicle (HGV) Percentage	Calculated based on HGV% of available traffic survey inside project location without validation	Calculated based on traffic survey on similar attributes road and validated based on QSTM flow bundle analysis of main HGV generator zones in Qatar

Based on inputs description shown in Table 1, the pavement design parameters are listed in Table 2.

Table 2 Conventional and recommended method input values of an expressway project

Input / Methodology		Conventional Method	Recommended Method
Average Daily Traffic (ADT) in the opening year (veh/day)		84,000	53,000 - 79,000
Truck Factor (TF)	**Class 4**	2.85	1.13
	Class 6	3.75	1.13
	Class 7	3.25	0.93
	Class 8	4.95	0.54
	Class 9	4.63	0.57
	Class 10	5.13	0.62
Heavy Good Vehicle (HGV) Percentage		8.20	9.00

As shown in the Table 2, it can be noticed that the ADT estimation got reduced by considering the PHV extracted from updated QSTM. Moreover, due to the fact that QSTM provides data in several locations, the calculated ADT in Table 2 shows the ranging value that covers the alignments of the studied roads/links. On the other hand, the TF also shows significant difference between both methods which can highly impact

the Equivalent Single Axle Loads (ESALs) calculations (AASHTO, 1993). Finally, the HGV percentage showed higher value than the conventional method since it was estimated and validated by using the QSTM and flow bundle analysis. After fixing the values of Growth Factor (GF) and Lane Distribution Factor (LF), the traffic load in terms of ESALs has been calculated. It is found that using the conventional methodology resulted in higher traffic load up to 88% than the recommended method. One the other hand, it was found that using the conventional method with 95th percentile WIM TFs resulted in higher traffic load up to 36% than the recommended methodology.

The above-mentioned recommendations can lead to more refined design parameters taking into consideration site-specific inputs. The recommended method also represents a validation procedure to justify the selected design inputs and ensure that the final pavement section is not over- or under-designed. The accuracy of pavement design inputs translated in sustainability terms to material resources saving, cost reduction, and longer design life.

6 CONCLUSION

The study presents the main challenges related to the traffic loading estimation that pavement designers are facing in Qatar. The study also recommends few practical solutions to be adopted for more accurate design outcomes. The most crucial design parameters were discussed in the paper and their impact on the final design parameters was shown as a case study. Below are the main findings and conclusions of the study:

- The use of the QSTM and data collected from the WIM stations would positively affect the design inputs and refine them for more economical design thicknesses. It was found that using TF values extracted from WIM surveys along with ADT calculated based on QSTM resulted in traffic load reduction up to 88% in this case study. This reduction is changing whole considerations of the pavement design and decision making during the cost estimation of the projects.
- The use of the QSTM can validate HGV% from traffic survey by conducting flow bundle analysis for zones that generate heavy trucks. The validation empowers certainty in the pavement design process and ensures the reliability of the selected asphalt materials and pavement layers' thicknesses.
- The case study also recommends considering site-specific traffic data when available due to significant impact on sustainability and durability of the pavement structure.

REFERENCES

AASHTO, (1993). *Guide for Design of Pavement Structures (1993 AASHTO Guide)*. American Association of State Highway and Transportation Officials. Washington, D.C., United States.

Abbas, A. R., Frankhouser, A. & Papagiannakis A. T., (2014). Effect of Traffic Load Input Level on Mechanistic–Empirical Pavement Design. *Transportation Research Record: Journal of the Transportation Research Board, 2443*, 63-77.

Ashghal (2013). *Pavement Design Guidelines Interim Advice Notice 016. Revision A1*. State of Qatar Public Works Authority: Doha, Qatar.

Ashghal (2012). *Pavement Design Guidelines Interim Advice Notice 101. Revision 2*. State of

Qatar Public Works Authority: Doha, Qatar.

Federal Highway Administration (FHWA) (2001). *Traffic Management Guide (TMG)*. Department of Transportation, United States.

Ministry of Municipality and Urban Planning (MMUP) (2011). *Guidelines and Procedure for Transport Studies*, Revision 3. Transportation and Infrastructure Planning Department; State of Qatar: Doha, Qatar.

Ministry of Finance (MOF) website (2019). https://www.mof.gov.qa/en/Pages/Data2019.aspx. *Ministry of Finance, Qatar.*

Smith B. C. & Diefenderfer B. K. (2010). Analysis of Virginia-Specific Traffic Data for Use with Mechanistic–Empirical Pavement Design Guide. *Transportation Research Record: Journal of the Transportation Research Board, 2154*, 100-107.

Cite this article as: Al-Tawalbeh A., Sadeq M., Sadek H., "Site-Specific Traffic Loading Estimation Challenges in Structural Pavement Design Process in Qatar: A Case Study", *International Conference on Civil Infrastructure and Construction (CIC 2020)*, Doha, Qatar, 2-5 February 2020, DOI: https://doi.org/10.29117/cic.2020.0036

Vehicle Inspection Policy and Emission Analysis in Kuwait

Sharaf Al Kheder
sharaf.alkehder@ku.edu.kw
Civil Engineering Department, College of Engineering and Petroleum, Kuwait University, Kuwait

Fahad Al Rukaibi
f.alrukaibi@ku.edu.kw
Civil Engineering Department, College of Engineering and Petroleum, Kuwait University, Kuwait

Ahmad Aiash
ahmad.aiash@grad.ku.edu.kw
Civil Engineering Department, College of Engineering and Petroleum, Kuwait University, Kuwait

ABSTRACT

Technical vehicle inspection centers are widespread in Kuwait. All vehicles should pass the test every two years if not older than six years or every one-year for other vehicles. This study provided an insight into the data collected from test centers and the emission test utilized in Kuwait. Data were collected from tests centers in the six governorates. 196 vehicles were tested but only 152 vehicles were utilized for CO emission violation and 157 vehicles for HC emission violation. European standards were selected as limits for emission violation. Independent variables included place of vehicle manufacture, vehicle's age, and odometer reading. A multinomial logit model was used to identify the significant predictors and to determine the correlation between dependent and independent variables. ANN was employed to compare prediction estimates of neural network and multinomial logit. The findings showed that the place of vehicle's manufacture, vehicle's age, and odometer reading were significant regarding violating emission standards of CO. Asian vehicles, vehicles with more than 150,000 km mileage, and vehicles older than 15 years had a higher probability of failing CO test as compared to place of manufacture. In contrast, the odometer reading was the only significant indicator for vehicles that have failed HC test especially those with 150,000 km odometer reading.

Keywords: Inspection test; Emission data; Analysis; Kuwait

1 INTRODUCTION

"The vehicle technical inspection can be defined as a process that is necessitated by governments in different countries, so that the vehicle can be scrutinized to conform with legalized standards" (Al-Kandari, 2017). "This process is sometimes required periodically or when the ownership of the vehicle is transferred to someone else" (Wolfe and O'Day, 1985). The reasons for making vehicle technical inspection as a compulsory test is that pollution can be lessened and set of other standards of the vehicle can be checked (Taneerananon et al., 2005).

Many developed countries are using vehicle technical inspection and maintenance programs to identify high-polluting vehicles. They have also set a procedure to selectively target vehicles that most likely happen to be pollution laws' violators. Most significant

parameters behind the high- pollutants emissions from vehicles were identified as vehicle age, vehicle manufacturer, number of engine cylinders, odometer reading, and whether or not oxygenated fuels were in use (Washburn et al., 2001).

Furthermore, it is worth mentioning that vehicle defects can be considered as one of the contributing factors affecting the environmental quality, even though the scale of the issue is less prominent than human behavior or road environmental factors. However, this technical problem may find a more direct and easier effective solution compared to human behavioral issues. A previous study conducted in Malaysia discussed common vehicle defects contributing to traffic accidents and affecting environment quality. They used a periodical technical inspection database as a basis for their study and determined the common failures affecting the environment and road safety (Solah et al., 2017).

(Millard et al., 2017) "provided an extensive review of the international experience in using vehicles' technical inspection information". Their work investigated the possibility of modelling the relationship between car inspection information and vehicle usage & ownership, energy consumption and vehicle's emission. Their work also consisted of reviewing the international literature on technical inspection and a survey to cognize the international experience in this field. The survey focused on checking odometer readings availability, type of data formatting, car owners' data availability, and data usage. Similar international literature review on technical inspection data can be seen also in the work of (Cairns et al., 2014) and (Chatterton and Anable, 2016).

Reviewing the international literature revealed huge experience in using vehicle technical inspection data for the above-mentioned applications and especially in vehicle emissions' modelling. (Li et al., 2017) performed a study to investigate the social and spatial effects of transforming the private vehicle fleet in Brisbane, Australia. They studied the continuous change in vehicle fleet efficiency (VEF) and investigated their socio-spatial patterns. They found that inner urban locations witnessed higher rate of VFE change. They related this change to the reduction in fuel consumption through adopting a stronger policy that encourages ownership of fuel-efficient cars, which in return will reduce emissions. In France, a strong periodical car inspection system is being implemented that continuously tests the proper functioning of cars' emissions control devices. In 1994, a motivation program for replacing cars with high emission rates was proposed. Yamamoto et al. (2004) examined the effect of the inspection program and the scrappage's fund on cars' transaction timings through building a hazard-based duration model of the household car transaction behaviour. It was shown that upon the availability of scrappage fund, the conditional probability of replacing a 10+ old car had increased by 20%.

In Mexico (Riveros et al., 2002), (I/M) data provided a valuable emission database, carbon monoxide (CO) and Hydrocarbon (HC) emission measurements for about a million vehicles were collected, from Mexico City. The results of analyzing such a big database were helpful in checking anti-pollutant strategies and as a performance index of car-manufacturing quality. In Sweden, Bastian and Börjesson (2015) showed that GDP and petrol cost clarified majority of the tendencies in the travelled vehicle distances. They measured the total distance travelled for the period from 2002 to 2012 by using the distance meter readings taken from the vehicle inspection tests. Results indicated a considerable difference in elasticities among municipalities according to

public transport supply, population density, percent of foreign-born populations and the average income. In UAE, Selim et al (2011) reviewed the mechanical and environmental car inspection programs at different test centers. The results indicated a serious variation between different centers in the country concerning adherence to test regulations and ways of inspection.

In the USA, Cook et al. (2015) used a database of more than 20 million cars in California to stem estimations of VMT and fuel consumption to inspect the spatial spreading of influences for the raise in fuel price besides the effects of applying alternative indicators for policy assessment. Results indicated that the distributions of VMT and fuel consumption varied considerably between different transport regions. Another study done in California Salon et al. (2014) reported on the household car greenhouse gas emissions inventories for eight cities between 2000 and 2005.

Emissions estimations were analyzed and linked to the certified inventory estimations. Binder et al. (2014) examined the relative effect of car and household features on emissions failures in Atlanta, Georgia through connecting the emissions inspection data to a targeted database with info on car owners. Count and hurdle models were used to forecast car emissions failures. Results indicated a clear connection between socio-demographic features and emissions failures. Another study in Massachusetts Ferreira et al. (2012) investigated the relation between costs of crash and the yearly VMT for 3 million passengers' car years of insurance exposure during 2006. Modelling the driver response to pay-as-you-drive insurance indicated that the aggregate VMT and private passenger car greenhouse gas emissions in Massachusetts would fall by 5.0 to 9.5%.

During urbanization, an increase in the numbers of vehicles can be witnessed, which deteriorates air quality. Emission standards became more stringent recently. Inspection programs are increasingly needed to examine vehicles periodically to check their compliance with emission standards. Although traditional technical vehicle inspection programs helped in improving air quality, their suitability had been criticized for many years (Harrington et al., 2000) (Bin, 2003) (Bishop and Stedman, 2008). One of the recent studies Hubbard, (2007), Schifter et al. (2003) showed that the actual number of vehicle on-road emissions were much higher than those measured during emission inspections.

2 DATA DESCRIPTION

The data that were utilized in this study were collected from the six governmental inspection centers in the six governorates of Kuwait including Mubarak Al-Kabeer Governorate, Hawally Governorate, Al-Jahra Governorate, Al Frawaniya Governorate, Al Asima Governorate, and Al Ahmadi Governorate. The data collection was accomplished with the assistance of inspector specialists in 2012 to randomly inspect various types of vehicles with a focus on passenger vehicles. The inspection test evaluated the type and the brand of the vehicle, the date when the vehicle was manufactured, odometer reading, brake condition, tire condition, windshield, fuel tank cap, mirrors, smoke from the exhausts, and emissions data. The data collection started on 1 April 2012 and ended on 26 April 2012. The average daily inspected vehicles in most of the urban inspection test centers were 400 to 500 vehicles per day while the rural centers had between 300 to 400 vehicles per day. As a result, a random sample of 196 different vehicles were inspected

and tested to measure all the previously mentioned aspects. The data were separated into two divisions including vehicles that violated the European test emission standards for the CO gas and the vehicles that violated the same standards but for Hydrocarbon (HC) gas. This is the main reason behind the low number of tested vehicles that were studied in this paper, as only vehicles with specific number of CO and HC violations were included. This, also, can be justified from the number of days that were used to collect this type of data. In Middle east, in general, and in Kuwait, in particular, this type of data is usually hard to be collected from an accessible data base. Then, the data was checked closely to determine if there are any missing values. Due to the undetermined or blanked answers, 152 passenger vehicles were chosen to determine three main factors that may be associated with the increasing emissions volume of CO from the vehicles' exhausts. For the HC, a total of 157 passenger vehicles were utilized for the analysis section of the study. A few numbers of non-passenger vehicles were inspected and tested and part of those vehicles the description data was missing about. Consequently, only passenger vehicles that had a completed test data, used gasoline fuel, and failed the European emission test standards were chosen for this study.

Table 1 and 2 show the overall statistics of the three potential factors that are associated with the increasing emissions volume. Models of the vehicles were classified into three categories including European manufactured vehicles; American manufactured vehicles; and Asian manufactured vehicles. This categorization was established to measure the performance of cars in general, and to establish a preidentified target when the test holders are conducting the test so they can concentrate more on these vehicles. The number of observed vehicles that were considered as European were the lowest in both Table 1 and 2. However, Asian-made vehicles were the highest that violated the standard of emissions for both CO and HC. Also, American vehicles ranked second in emitting CO and HC in high volumes. The age of the vehicle was another chosen predictor to identify its impact on the emissions' rate of CO and HC. The collected sample was fairly distributed between the four categories of vehicle age, which includes vehicles that were 1 to 5 years old, 6 to 10 years old, vehicles between 11 to 15 years old, and vehicles older than 15 years.

Table 1: Descriptive statistics of independent variables related to CO

Variable	**Category**	**Abbreviation**	CO g/km			**Total**
			1 to 4.5	4.6 to 16.5	more than16.5	
Model	European vehicle	MOD1	6	9	2	17
	American vehicle	MOD2	6	20	10	36
	Asian vehicle	MOD3	14	50	35	99
Age	1 to 5 years	AGE1	9	20	2	31
	6 to 10 years	AGE2	9	31	10	50
	11 to 15 years	AGE3	4	20	18	42
	more than 15 years	AGE4	4	8	17	29
Odometer reading	0 to 50,000 km	ODO1	5	7	3	15
	50,001 to 150,000 km	ODO2	11	41	6	58
	more than 150,000 km	ODO3	10	31	38	79

Table 2: Descriptive statistics of independent variables related to HC

Variable	Category	Abbreviation	HC gm/km			Total
			1 to 4.5	4.6 to 16.5	more than16.5	
Model	European vehicle	MOD1	11	2	5	18
	American vehicle	MOD2	18	10	10	38
	Asian vehicle	MOD3	58	27	16	101
Age	1 to 5 years	AGE1	18	6	2	26
	6 to 10 years	AGE2	26	13	9	48
	11 to 15 years	AGE3	29	12	10	51
	more than 15 years	AGE4	14	8	10	32
Odometer reading	0 to 50,000 km	ODO1	9	4	3	16
	50,001 to 150,000 km	ODO2	45	11	4	60
	more than 150,000 km	ODO3	33	24	24	81

3 METHODOLOGY

3.1 Multinomial logit regression

A multicollinearity was tested among the predictors to evaluate the correlations between them. Consequently, a multicollinearity test was performed for both emission cases. The average variance inflation factor (VIF) was 1.158 and 1.078 for CO emission, and HC emission variables respectively. These results show that there are no multicollinearity issues. Additionally, multinomial logit regression does not assume normality, linearity, or homoscedasticity. As a result, multinomial logit regression was chosen in this study to determine the correlations between the independent variables and the dependent variables.

For the multinomial logit equation as per Ma et al. (2014) and AlKheder et al. (2019), each one of the two dependent variables was assigned to y. For CO, the interval from 1 to 4.5 gm/km was assigned to y=1, 4.6 to 16.5 gm/km was assigned to y=2, and lastly the CO emissions that were higher than 16.5 gm/km was assigned to y=3, which was chosen as the reference level in this study. Then y=1 and y=2 were compared to y=3. Similarly, for HC, the interval from 0.100 to 0.300 gm/km was assigned to y=1, 0.301 to 0.450 gm/km was assigned to y=2, and HC emissions that were higher than 0.450 gm/km was assigned to y=3, which was chosen as the base level. Then y=1 and y=2 were compared to y=3. The y=1 and y=2 logit regression functions were as follows:

$$logit\,(p_1) = \ln\left(\frac{p(y=1|x)}{p(y=3|x)}\right) = \alpha_1 + \sum_{i=1}^{m} \beta_{1i}\, x_i \qquad (1)$$

$$logit\,(p_2) = ln\left(\frac{p(y=2|x)}{p(y=3|x)}\right) = \alpha_2 + \sum_{i=1}^{m} \beta_{2i}\, x_i \qquad (2)$$

For both (1) and (2) equations, the value of the ith predictor is x_i, the intercept of the first logit function (1) is α_1, and the intercept for the second logit function (2) is α_2. m is representing the number of variables in both equations (1) and (2). The corresponding coefficient of the first logit function (1) is β_1 and the corresponding coefficient is β_2 for

the second logit function (2). The condition probability of kth outcome category is:

$$p(y = k|x) = \frac{exp(\alpha_k + \sum_{i=1}^{m} \beta_{ki} x_i)}{1 + \sum_{k=1}^{K-1} (\alpha_k + \sum_{i=1}^{m} \beta_{ki} x_i)} \quad (3)$$

The intercept of the kth logit function (3) is α_K, The corresponding coefficient of the k th logit function (3) is β_{ki}, and the number of outcome categories is$K$.

3.2 Multinomial logit regression results

3.2.1 CO results

Table 3 shows the maximum likelihood ratios for the independent variables related to CO gas with different volumes. The results show that all independent variables including the model, age of the vehicle, and odometer reading were found to be significant variables as their p-values were less than 0.05. As a result, all factors were included in the final model.

Table 3: Maximum-likelihood estimations of CO

Variable	Abbreviation	-2 Log Likelihood of Reduced Model	Chi-Square	Degree of freedom	P-value
Model	MOD (Base: MOD3)	105.258	12.977	4	0.011
Age	AGE (Base: AGE4)	113.298	21.017	6	0.002
Odometer reading	ODO (Base: ODO3)	104.727	12.446	4	0.014

Table 4 shows the results after applying the multinomial logit regression for the significant variables. European vehicles were found to be a significant variable in both the first and second set with a positive coefficient in table 4 compared to the reference level, which was Asian vehicles. This indicates that Asian vehicles had a higher probability of involving in emissions violations regarding CO gas compared to European vehicles and related to European standards. Vehicles that were 1 to 5 years old were found to be a significant factor with a positive coefficient in the first and second set compared to vehicles that were older than 15 years old, which was the base level. This indicates that vehicles that were older than 15 years were associated with higher degree of emitting CO emissions. For vehicles that were between 5 to 15 years old, were found to be a significant factor in the first and second set with a positive coefficient compared to the reference level indicating that vehicles older than 15 years had higher probabilities in emitting CO gas higher than the standard limits. Vehicles that were between 10 to 15 years old were found to be significant in the last set with a positive coefficient compared to the base category indicating that vehicles older than 15 years had higher chances in violating CO emissions standards. Lastly, vehicles with more than 50,001 km but less than 150,000 km were found to be a significant factor in the second set with a positive coefficient compared to the reference level. This indicates that vehicles with more than 150,000 km had higher probability of failing the CO emission test standards.

Table 4: Multinomial logit regression model for CO

Variable	Coefficient	Standard Error	Wald Chi-square test	P-value	Odds ratio
1 to 4.5 gm/km vs more than 16.5 gm/km					
Intercept	-3.051	0.836	13.331	0.000	
MOD1	3.305	1.062	9.677	0.002	27.243
AGE1	3.291	1.164	7.987	0.005	26.860
AGE2	2.391	0.907	6.952	0.008	10.923
4.6 to 16.5 gm/km vs more than 16.5 gm/km					
Intercept	-1.952	0.618	9.967	0.002	
MOD1	2.301	0.973	5.598	0.018	9.988
AGE1	2.777	0.961	8.347	0.004	16.066
AGE2	2.315	0.674	11.81	0.001	10.122
AGE3	1.694	0.675	6.308	0.012	5.442
ODO2	1.839	0.594	9.596	0.002	6.293

3.2.2 HC results

Table 5 shows the results of the maximum likelihood tests for HC emissions. Only odometer reading was found to be a significant variable. Consequently, other independent variables were excluded and only odometer reading was included in the multinomial logit regression model for HC gas. In table 6, the results show that vehicles with a mileage between 50,001 to 100,000 kilometres were found to be a significant factor in affecting the vehicle to emit HC gas in higher volumes in the first set with a positive coefficient compared to the reference level, which was vehicles with more than 100,000 kilometres. This indicates that vehicles that had travelled more than 100,000 kilometres had a higher probability of violating the European standards compared to vehicles with 50,001 to 100,000 kilometres mileage.

Table 5: Maximum likelihood estimations for HC

Variable	Abbreviation	-2 Log Likelihood of Reduced Model	Chi-Square	Degree of freedom	P-value
Model	MOD (Base: MOD3)	93.343	5.765	4	0.217
Age	AGE (Base: AGE4)	89.715	2.137	4	0.711
Odometer reading	ODO (Base: ODO3)	104.240	16.662	4	0.002

Table 6: Multinomial logit regression for HC

Variable	Coefficient	Standard Error	Wald Chi-square test	P-value	Odds ratio
0.100 to 0.300 gm/km vs more than 0.450 gm/km					
Intercept	0.318	0.268	1.409	0.235	
ODO2	2.102	0.587	12.836	0.000	8.182

4 CONCLUSION

This study attempts to improve the technical inspection standards in Kuwait by pre-identifying the most polluting vehicles that were emitting harmful gases including carbon monoxides and hydrocarbons. This can help in lessening air-pollution and ameliorate the quality of air. Moreover, the cost of performing the inspection test is mainly accomplished by a governmental sector related to the Ministry of Interior in Kuwait. Special inspectors and public facilities were only utilized for this purpose. Moreover, the time that is wasted due to the long hours required to perform the test, due to the big number of vehicles that need to be tested, is considerably high. This is happening as vehicles to be tested are not pre-identified especially for the emission test as this test is performed randomly or due to visible exhaust smoke from the tested vehicle. Time and money consumed can be both reduced by targeting the most polluting vehicles, thus more efficient tests can be performed.

As a result, a multinomial logit regression was applied so that the correlations between the potential factors associated with the increasing carbon monoxides and hydrocarbons emissions are determined. Three factors were included in this study according to the availability of the data including vehicle manufacture origin, vehicle age, and the odometer reading. Carbon monoxides and hydrocarbons were the dependent variables due to their harmful impact on the air quality. The lack of clear systematic procedures to determine whether the vehicle failed the emission test or passed the test was the reason for following the European standards in determining the failure criteria. For carbon monoxides, all three independent variables were found to be significant in increasing the emission volume. Asian vehicles were found to be the majority of car types in violating the standards compared to European vehicles. The age of vehicle was another significant factor. Vehicles older than 15 years had a higher probability of emitting CO in high volumes, which violates the standards compared to other vehicle categories that were less than 15 years old. Additionally, vehicles with more than 150,000 km mileage were more likely to emit CO emissions higher than the standard limits compared to vehicles with a mileage less than 150,000 km. For hydrocarbons, only the odometer reading was the significant variable in affecting the emissions volume. Similar to CO results, vehicles that had a reading of more than 150,000 km on the odometer had higher probability to fail the test according to the standards.

ACKNOWLEDGEMENT

The Authors would like to thank Kuwait Foundation for the Advancement of Sciences (KFAS) for their generous support.

REFERENCES

Al-Kandari, M. A. (2017). *Legal guide for technical inspection*. National Library of Kuwait, Kuwait.

AlKheder, S., AlRukaib, F. & Aiash, A. (2019). Drivers' response to variable message signs (VMS) in Kuwait, Cognition, *Technology & Work,* pp. 1-15, 2019.

Bastian, A. & Börjesson, M. (2015). Peak car? Drivers of the recent decline in Swedish car use,

Transport Policy, 42, pp. 94-102.

Bin, O. (2003). A logit analysis of vehicle emissions using inspection and maintenance testing data, *Transportation Research Part D: Transport and Environment*, Vol. 8, No. 3, pp. 215-227.

Binder, S., Macfarlane, G.S., Garrow, L.A. & Bierlaire, M. (2014). Associations among household characteristics, vehicle characteristics and emissions failures: An application of targeted marketing data, *Transportation Research Part A: Policy and Practice*, 59, pp. 122-133.

Bishop, G. A. & Stedman, D. H. (2008). A decade of on-road emissions measurements, *Enviromental Science & Technology*, Vol. 42, No. 5, pp. 1651-1656.

Cairns, S., Rahman, S., Anable, J., Chatterton, T. & Wilson, R.E. (2014). Vehicle inspections from safety device to climate change tool, *MOT Project Working Paper* MIS018.

Chatterton, T. & Anable, J. (2016). *Vehicle odometers and other novel methods of examining car ownership and usage* (American Association of Geographers Annual Meeting), San Francisco.

Cook, J. A., Sanchirico, J. N., Salon, D. & Williams, J. (2015). Empirical distributions of vehicle use and fuel efficiency across space: Implications of asymmetry for measuring policy incidence, *Transportation Research Part A: Policy and Practice*, 78: 187-99.

Ferreira, J. & Minikel, E. (2012). Measuring per mile risk for pay-as-you-drive Automobile Insurance, *ITransportation Research Record*, 2297, pp. 97-103.

Harrington, W., McConnell V. & Ando, A. (2000). Are vehicle emission inspection programs living up to expectations?, *Transportation Research Part D: Transport and Environment*, Vol. 5, No. 3, pp. 153-172.

Hubbard, T. N. (2007). Using inspection and maintenance programs to regulate vehicle emissions, *Contemporary Economic Policy*, Vol. 15, No. 2, pp. 52-62.

Li, T., Sipe, N. & Dodson, J. (2017). Social and spatial effects of transforming the private vehicle fleet in Brisbane, Australia, *Transportation Research Part D: Transport and Environment*, 51, pp. 43-52.

Ma, Z., Shao, C., Song, Y. & Chen, J. (2014). Driver response to information provided by variable message signs in Beijing, *Transportation Research Part F: Traffic Psychology and Behaviour*, Vol. 26, No. Part A, pp. 199-209.

Millard, K., Cairns, S., Beaumont, C., Anable, J., Chatterton T. & Wilson, R.E. (2017). International experience of collecting and analysing technical inspection data for private cars, *Published Project Report PPR847, MOT research project (UKRC Energy Programme/EPSRC), TRL Limited (TRL)*.

Riveros, H., Cabrera, E. & Ovalle, P. (2002). Vehicle inspection and maintenance, and air pollution in Mexico City, *Transportation Research* Part D. *7*(1), pp. 72-80.

Salon, D., Cook, J. & Williams, J. (2014). Household vehicle Carbon emissions in California cities, *Transportation Research Board: 93rd Annual Meeting* (No. 14-0630).

Schifter, I., Díaz, L., Durán, J., Guzmán, E., Chávez, O. & López-Salinas, E. (2007). Remote sensing study of emissions from motor vehicles in the metropolitan area of Mexico City, *Enviromental Science & Technology*, Vol. 37, No. 2, p. 395-401.

Selim, M. Y. E., Maraqa, M. A., Hawas, Y. E. & Mohamed, A.M.O. (2011). Assessment of vehicle inspection and emission standards in the United Arab Emirates, *In Transportation Research Part D: Transport and Environment*, *16*(4), pp. 332-334.

Solah, M. S., Hamzah, A., Ariffin, A. H., Paiman, N. F., Abdul Hamid, I., Abdul Wahab, M. A. F., Mohd Jawi, Z. & Osman, M. R. (2017). Private Vehicle roadworthiness in Malaysia from

the vehicle inspection perspective, *Journal of the Society of Automotive Engineers Malaysia*, Vol. 1, No. 3, pp. 2550-2239

Taneerananon, P., Chanwannnakul, T., Suanpaga, V., Khompratya, T., Kronprasert, N. & Tanaboriboon, Y. (2005). An evaluation of the effectiveness of private vehicle inspection process in Thailand*, Journal of the Eastern Asia Society for Transportation Studies*, Vol. 6, pp. 3482-3496.

Washburn, S., Seet, J. & Mannering, F. (2001). Statistical modeling of vehicle emissions from inspection/maintenance testing data: an exploratory analysis, *Transportation Research Part D: Transport and Environment*, Vol. 6, No. 1, pp. 21-36.

Wolfe, A. C. & O'Day, J. (1985). *Cost-effectiveness of periodic motor vehicle inspection, University of Michigan*. University of Michigan, Michigan.

Yamamoto, T., Madre, J. L. & Kitamura, R. (2004). An analysis of the effects of French vehicle inspection program and grant for scrappage on household vehicle transaction, *Transportation Research Part B*, *38*(10), pp. 905-926.

Cite this article as: Al Kheder S., Al Rukaibi F., Aiash A., "Vehicle Inspection Policy and Emission Analysis in Kuwait", *International Conference on Civil Infrastructure and Construction (CIC 2020)*, Doha, Qatar, 2-5 February 2020, DOI: https://doi.org/10.29117/cic.2020.0037

Optimum Dispersion Parameters of Carbon Nanotubes: Concrete Strength by Response Surface Methodologies

Mohamed Mohsen
200202128@qu.edu.qa
Department of Civil and Architectural Engineering, Qatar University, Doha, Qatar

Mohamed Al Ansari
m.alansari@qu.edu.qa
Department of Civil and Architectural Engineering, Qatar University, Doha, Qatar

Ramzi Taha
ramzitaha@gmail.com
College of Engineering, Phoenicia University, Beirut, Lebanon

Ahmed Senouci
asenouci@central.uh.edu
Department of Construction Management, University of Houston, Houston, Texas, USA

Ala AbuTaqa
aa1104819@qu.edu.qa
Department of Civil and Architectural Engineering, Qatar University, Doha, Qatar

ABSTRACT

This paper implements Response Surface Methodologies (RSM) techniques to illustrate the maximum carbon nanotubes (CNTs)-concrete mechanical properties responses to the length, weight fraction and treatment variables. Mixes with different CNTs' content were prepared and tested for flexure, compression and tension. RSM analysis showed that the highest effect on the strengths was due to the CNTs' content variable. The analysis showed that a weight fraction of 0.3 wt.% of non-treated CNTs is required to achieve the maximum flexural, compressive and tensile strengths in a batch as per the predicted model. RSM analysis also showed that maximum flexural strength will be obtained by using 0.2 wt. % non-treated long CNTs, 0.25 wt. % non-treated short CNTs and 0.03 wt. % treated long CNTs, respectively.

Keywords: Carbon nanotubes; CNTs' dispersion; Concrete strength; Response surface Methodologies

1 INTRODUCTION

In the last decade, carbon nanotubes (CNTs) were extensively integrated into cementitious materials studies. Researchers investigated the effect of CNTs' addition on the mechanical, physical, chemical, rheological and microstructural properties of cement pastes and mortars. The major challenge in most studies was about providing an acceptable CNTs' dispersion within the water solution and eventually the cementitious matrix. Many variables affecting the dispersion such as CNTs' weight fraction, aspect ratio, functionalization, mixing procedure and surfactant types, surfactants amount and

sonication energy were investigated (Wang et al., 2013; Chuah et al., 2014; Paula et al., 2014; Siddique et al, 2014; Abu-Taqa et al, 2015; Al-Dahawi et al., 2016; Song et al., 2017; Mohsen et al., 2017; Kramer et al., 2017; Hawreen et al., 2018). Through these studies, the body of knowledge in this field could reach several understandings about the CNTs' amount, CNTs' type and mixing procedures to follow for achieving improvements in the flexural, compressive and tensile strengths of CNT composites. However, up to this moment, a mix design with the optimum length, weight fraction and treatment amount to provide the highest mechanical properties is not observed. In this study, RSM methods are used to investigate the optimum mix proportions to produce the highest flexural, compressive and tensile strength properties. First, CNTs-concrete batches were prepared and tested. Then, Response Surface Methods (RSM) were used to fit a proper model on the collected data.

2 EXPERIMENTAL DESIGN

Table 1 summarizes the tested batches. The testing methodology started with the preparation of the batches and specimens, followed by the measurement of their flexural, compressive and tensile strengths. Then, analyzing the test results using RSM techniques.

2.1 Materials and Equipment

The cement used in this work was Portland cement, CEM I, Class 42.5 R complying with EN 197-1. It was supplied by Qatar National Cement Company (QNCC). The fine and coarse aggregates supplied by Qatar Primary Materials Company (QPMC) were in accordance with ASTM C-33, Standard Specification for Concrete Aggregates. The CNTs used were multi-walled carbon nanotubes (MWCNTs), supplied by Cheaptubes, Inc., and they were differentiated by lengths and treatment type. The surfactant used to disperse the CNTs is a liquid polymer superplasticizer of a polycarboxylate chain, supplied by Sika Qatar L.L.C. The equipment used in this study comprised of a strength-testing machine, supplied by Controls Inc., an 85 liters site concrete mixer and an ultrasonic wave mixer with a commercial name VCX750, supplied by Sonics & Materials, Inc., was used for dispersing CNTs into water.

Table 1: Testing Matrix

Batch #	Batch Name	CNT/Cement Content (wt%)	CNTs Treated	CNTs Length (μm)	Number of specimens
1	0.03 NCNT	0.03	No	10-30	27
2	0.08 NCNT	0.08	No	10-30	27
3	0.25 NCNT	0.25	No	10-30	27
4	0.5 NCNT	0.5	No	10-30	27
5	0.03 TCNT	0.03	Yes	10-30	27
6	0.08 TCNT	0.08	Yes	10-30	27
7	0.25 TCNT	0.25	Yes	10-30	27
8	0.5 TCNT	0.5	Yes	10-30	27
9	0.03 SCNT	0.03	No	0.5-2	27
10	0.08 SCNT	0.08	No	0.5-2	27
11	0.25 SCNT	0.25	No	0.5-2	27
12	0.5 SCNT	0.5	No	0.5-2	27

2.2 Mixing and Testing

The mixing procedure was divided into two processes. The first process included the CNTs dispersion in water using an ultrasonicator, while the second part comprised

of mixing the dispersed solution with cement, coarse and fine aggregate in the concrete mixer. The duration of the whole sonication and mixing procedures was 1 hour. The flexural, compressive and tensile strength testing of concrete-CNTs' samples was conducted according to ASTM C78/C78M−10, ASTM C39/C39M−16 and ASTM C496/C496M−11 standards, respectively.

2.3 Response Surface Methods (RSM) Techniques

The Central Composite Design (CCD) Response Method was used to fit a quadratic model for each phase parameter. This was performed by determining the maximum response of the flexural, compressive and tensile strengths factors using the JMP software. The methodology followed to perform this analysis is as follows:

1- The CNTs' weight fractions, treatment type and length type variables were coded in the (-1,1) interval (Table 2).

2- The factors were modeled by fitting a second order polynomial equation model. Second order polynomial equations were used to express the flexural and compressive strengths as functions of independent variables:

$FS = a_0 + a_1x_1 + a_2x_2 + a_3x_3 + a_{12}x_1x_2 + a_{13}x_1x_3 + a_{23}x_2x_3 + a_{11}x_1^2 + a_{22}x_2^2 + a_{33}x_3^2$ [1]

$CS = b_0 + b_1x_1 + b_2x_2 + b_3x_3 + b_{12}x_1x_2 + b_{13}x_1x_3 + b_{23}x_2x_3 + b_{11}x1^2 + b_{22}x2^2 + b_{33}x3^2$[2]

$TS = c_0 + c_1x_1 + c_2x_2 + c_3x_3 + c_{12}x_1x_2 + c_{13}x_1x_3 + c_{23}x_2x_3 + c_{11}x_1^2 + c_{22}x_2^2 + c_{33}x_3^2$ [3]

where: FS = flexural strength (MPa),
CS =Compressive strength (MPa),
TS = Tensile strength (MPa),
x_1 = CNTs-concrete weight fraction (%),
x_2 = CNTs treatment, and
x_3 = CNTs length.
a_0, a_1, a_2, a3, a_{12}, a_{13}, a_{23}, a_{11}, a_{22}, a_{33}, b_0, b_1, b_2, b_3, b_{12}, b_{13}, b_{23}, b_{11}, b_{22}, b_{33}, c_0, c_1, c_2, c_3, c_{12}, c_{13}, c_{23}, c_{11}, c_{22}, and c_{33} are the response surface coefficients.

3- The response surface coefficients were determined by using a CCD design type with 2 center points.

4- The prediction models, R2 and P values, were recorded.

5- The response surface and contour lines were plotted.

6- The variables resulting in maximum responses were determined by optimizing the Desirability Function.

Table 2: Variables' coding for RSM analysis

Batch	Coded Weight Fraction	Coded Treatment	Coded length	Flexural Strength (MPa)	Compressive Strength (MPa)	Tensile Strength (MPa)
Concrete	-1	0	0	5.73	60.75	4.81
0.03 NCNT	-0.88	-1	1	6.33	70.56	5.45
0.08 NCNT	-0.68	-1	1	7.16	71.16	5.65
0.25 NCNT	0	-1	1	6.54	65.50	4.94
0.5 NCNT	1	-1	1	6.58	69.23	4.88
0.03 TCNT	-0.88	1	1	7.37	74.04	5.77
0.08 TCNT	-0.68	1	1	7.15	67.06	5.52
0.25 TCNT	0	1	1	6.92	67.15	4.90
0.5 TCNT	1	1	1	5.60	65.15	4.63
0.03 SCNT	-0.88	-1	-1	6.30	74.97	5.40
0.08 SCNT	-0.68	-1	-1	5.93	67.60	4.74
0.25 SCNT	0	-1	-1	6.47	63.55	5.50
0.5 SCNT	1	-1	-1	6.82	65.80	4.87

3 RESULTS AND DISCUSSION

3.1 Strength Testing Results

Figures 1, 2 and 3 show the flexural, compressive and tensile strength testing results, respectively. In general, the results indicated that adding CNTs to concrete can increase the flexural, compressive and tensile strengths by 29%, 23%, and 20 %, respectively. Among all batches, it was shown that the batch containing 0.03 wt. % treated CNTs could achieve the highest strength results compared with the control batch on the 90th day. The effect of CNTs' weight fraction on the strength results was noticeable. In flexural strength results (Figure 1), it was shown that long non-treated CNTs (Figure 1a) had an optimum weight fraction of 0.08%, whereas short non-treated CNTs (Figure1b) had an optimum weight fraction was 0.25%. For treated CNT-concrete batches (Figure 1c), the optimum weight fraction was 0.03 wt.%. In compressive strength results (Figure 2) all types of CNTs had an optimum weight fraction of 0.03 wt%, whereas, in tensile testing results (Figure3), the optimum weight fraction was 0.08%.

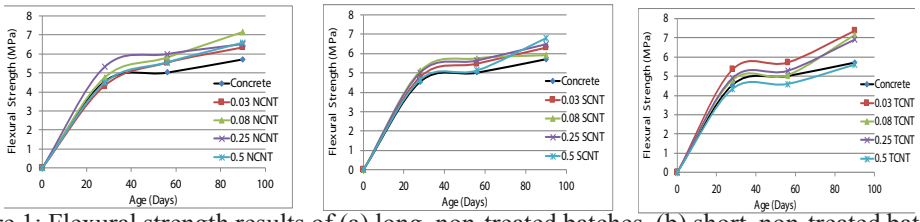

Figure 1: Flexural strength results of (a) long, non-treated batches, (b) short, non-treated batches, and (c) long, treated batches

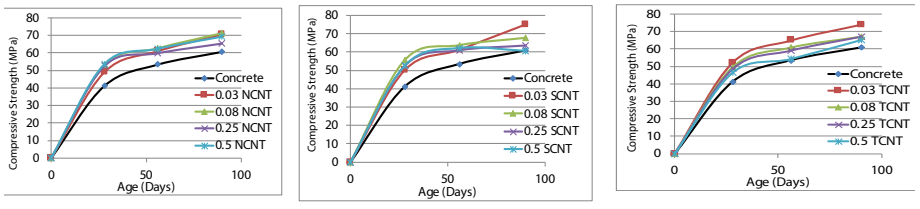

Figure 2: Compressive strength results of (a) long, non-treated batches, (b) short, non-treated batches, and (c) long, treated batches

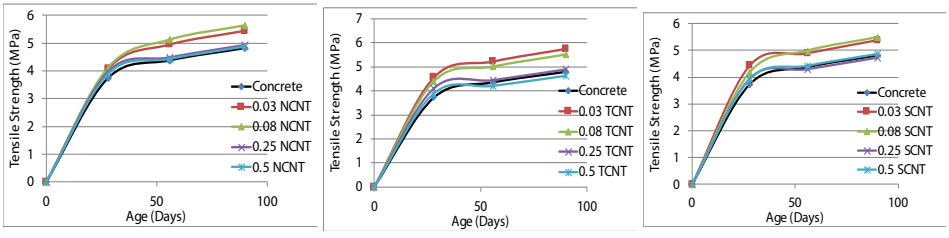

Figure 3: Tensile strength results of (a) long, non-treated batches, (b) short, non-treated batches and (c) long, treated batches

3.2 RSM Analysis

The RSM analysis revealed several observations about the behavior of the mechanical strength functions in terms of the weight fraction, length and treatment variables, and the

effective amount of each variable on the function's response. Figure 4 shows the effect summary of all variables. As depicted, the analysis shows that the largest effect on the strength results was due to the weight fraction variable. The second variable, affecting the strength functions, was observed to be the length factor. Finally, the treatment factor was the least variable affecting the response results. Figure 5 shows the response surface plot of flexural strength against the weight fraction, treatment and length variables. The response chart shows peaks at the mid boundary, where the weight fraction is about 0.25 wt.%. The response surfaces also illustrate that higher results can be obtained for long treated CNTs.

The flexural strength prediction equation was determined as the follows:

$$FS = 7.10 + 0.136x_1 - 0.044x_2 + 0.0023x_3 - 0.190x_1x_2 - 0.295x_1x_3 - 0.0841x_2x_3 - 0.956x_1^2 - 0.1063x_2^2 + 0.29x_3^2 \quad [4]$$

where, FS: Flexural Strength, x_1: Weight Fraction, x_2: Treatment, and x_3: Length

The R^2 and P values of the flexural strength-predicted model were determined as 0.92 and 0.1571, respectively.

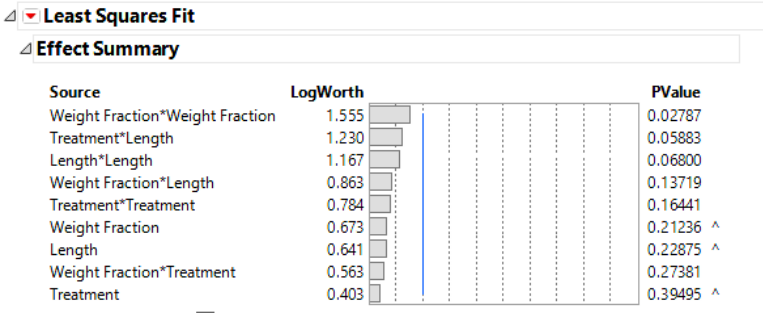

Figure 4: Effect summary of the study variables on the mechanical properties' functions

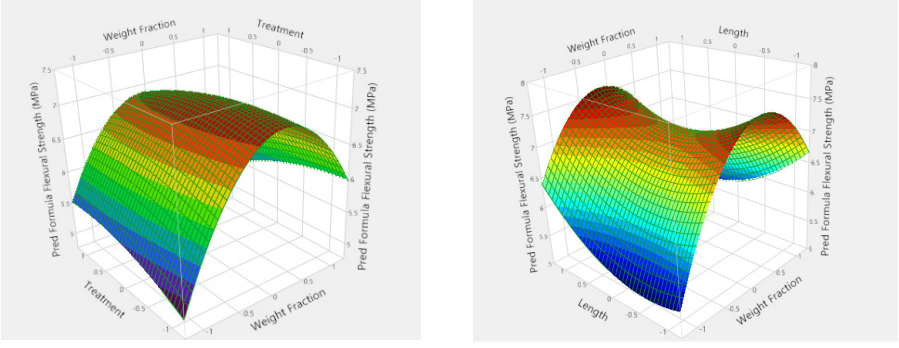

Figure 5: RSM models of flexural strength against (a) weight fraction and treatment, and (b) weight fraction and length

Figure 6 shows the response surface plot of compressive strength against the weight fraction, treatment and length variables. Similar to the response of the flexural strength function, the response chart shows peaks at the mid boundary, where the weight fraction is about 0.25 wt.%. The response surfaces also illustrate that higher compressive strength results can be obtained for long treated CNTs.

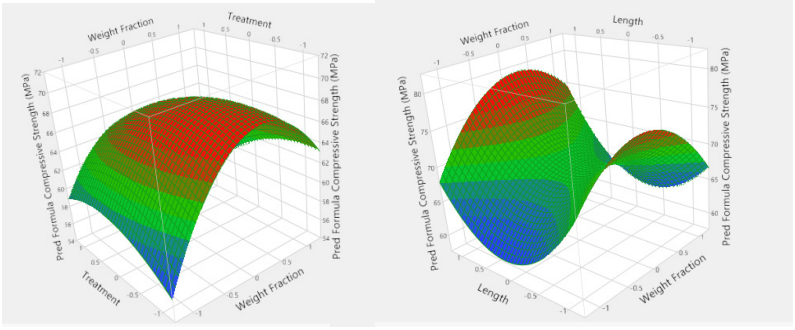

Figure 6: RSM models of compressive strength against (a) weight fraction and treatment and (b) weight fraction and length

The compressive strength prediction equation was determined as the following:

$$CS = 68.56 + 0.73x_1 - 1.02x_2 + 1.23x_3 - 1.615x_1x_2 + 1.571x_1x_3 - 1.579x_2x_3 - 4.787x_1^2 - 1.482x_2^2 + 5.543\ x32 \quad [5]$$

where,

CS: Compressive Strength, x_1: Weight Fraction, x_2: Treatment, and x_3: Length

The R^2 and P values of the compressive strength-predicted model were determined as 0.89 and 0.2155, respectively.

Figure 7 shows the response surface plot of tensile strength against the weight fraction, treatment and length variables. The response chart shows peaks at the mid boundary, where the weight fraction is about 0.31 wt.%. The response surfaces also illustrate that higher tensile strength results can be obtained for long treated CNTs.

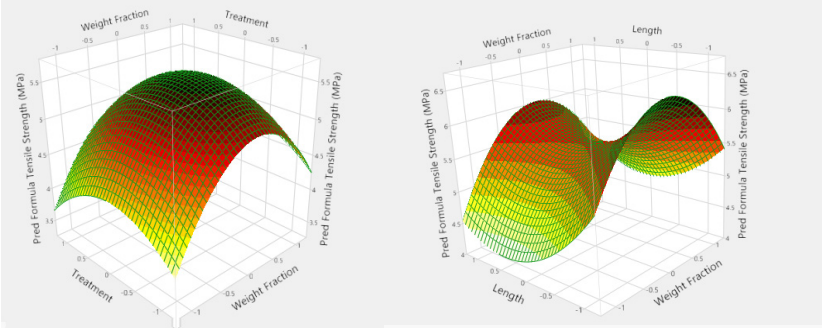

Figure 7: RSM models of tensile strength against (a) weight fraction and treatment and (b) weight fraction and length

The tensile strength prediction equation was determined as the following:

$$TS = 5.57 + 0.165x_1 - 0.071x_2 - 0.179x_3 - 0.0073x_1x_2 + 0.110x_1x_3 - 0.362x_2x_3 - 0.683x_1^2 - 0.363x_2^2 + 0.41x_3^2 \quad [6]$$

where,

TS: Tensile Strength, x1: Weight Fraction, x2: Treatment, and x3: Length

The R2 and P value of the tensile strength-predicted model were determined as 0.89 and 0.2356, respectively.

Figure 8 shows the maximized Desirability Strengths Functions behavior in-terms of the weight fraction, treatment and length variables. By maximizing the desirability function, it was shown that the maximum behavior could occur at a weight fraction of 0.3 wt.% (i.e. coded value = 0.14) using long non-treated CNTs. The maximum predicted flexural, compressive and tensile strengths will be 7.41, 76.91 and 5.93 MPa, respectively. Compared to control concrete, these values indicate 23%, 12% and 25% increase in flexural, compressive and tensile strengths, respectively.

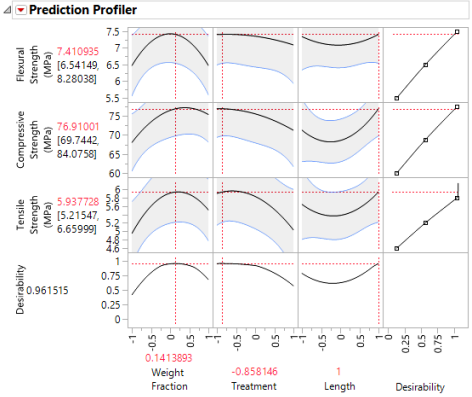

Figure 8: Maximized desirability functions

Figure 9 shows the combined contour profiles of the weight fraction and treatment variables versus the flexural, compressive and tensile strengths for long treated CNTs. The shaded areas show all flexural, compressive and tensile strengths falling below lower strengths limits of 7, 70 and 4.9 MPa, respectively. These maps illustrate the importance of using, a weight fraction variable of 0.2 wt.% (i.e. -0.0731 coded) to maximize the flexural strength while maintaining the compressive and tensile above the lower limits. Figure 10 shows the combined contour profiles of the weight fraction and treatment variables versus the flexural, compressive and tensile strength when short, non-treated filaments were used. The shaded areas shown include all flexural, compressive and tensile strengths falling below lower strengths limits of 7.2, 70 and 5.5 MPa, respectively. It was observed that in order to obtain the maximum flexural strength value with the compressive and tensile above the lower limits, we need to maintain a weight fraction variable of 0.25 wt.% short CNTs (i.e. 0 coded).

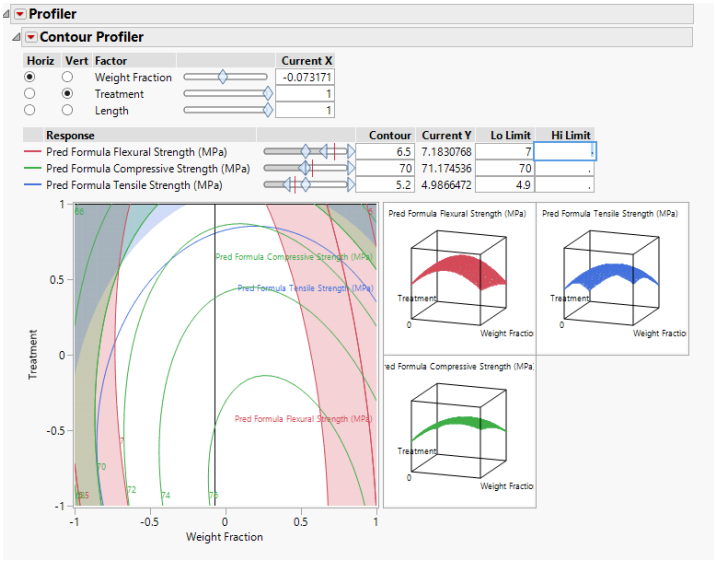

Figure 9: Contour maps of the maximum desirable flexural strength for long treated CNT-concrete batch

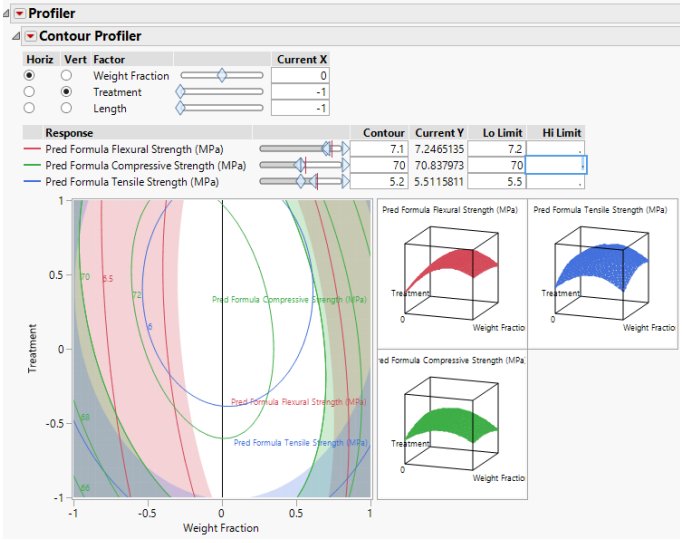

Figure 10: Contour maps of the maximum desirable flexural strength for short-non-treated CNT-concrete batch

4 CONCLUSION

In this research, the effect of multi-walled carbon nanotubes' (MWCNTs) content, length and treatment parameters on the mechanical properties of concrete composites were studied. Several conclusions could be reached as follows:

1. Using CNTs in concrete batches will increase the flexural, compressive and tensile strengths by 29%, 23% and 20%, respectively.
2. The batch of 0.03% treated CNTs appeared to be the optimum concrete batch among all tested mixes, in terms of strength gain and cost savings.

3. RSM techniques proposed empirical formulas to determine the flexural, compressive and tensile strengths of CNTs-Concrete composites.
4. The RSM analysis results showed that the maximum strength properties could be obtained at a weight fraction of 0.3 wt.% with long non-treated CNTs. By applying these variables (i.e. 0.3 wt.%, long and non-treated CNTs), the model predicts increases of 23%, 12% and 25% in flexural, compressive and tensile strengths, respectively, compared to plain concrete.
5. The RSM analysis also showed that the maximum flexural strength properties could be obtained in long, non-treated CNTs and short, non-treated CNTs when weight fractions of 0.2 % and 0.25 % were used, respectively.

REFERENCES

AbuTaqa, A., Al-Rub, R., Senouci, A., Al-Nuaimi, N. & Bani-Hani, K. A. (2015). The Effect of Fiber Geometry and Interfacial Properties on the Elastic Properties of Cementitious Nanocomposite Material, *J Nanomater.*

Al-Dahawi, A., Öztürk, O., Emami, F., Yıldırım, G. & Sahmaran, M. (2016). Effect of mixing methods on the electrical properties of cementitious composites incorporating different carbon-based materials. *Construction and Building Materials*, *104*, 160-168.

ASTM C39/C39M – 17 (2017). Standard Test Method for Compressive Strength of Cylindrical Concrete Specimens, West Conshohocken, PA, 2017, 8 pp.

ASTM C78/C78M – 16 (2016). Standard Test Method for Flexural Strength of Concrete (Using Simple Beam with Third-Point Loading), West Conshohocken, PA, 2016, 4 pp.

ASTM C496/C496M – 11 (2011). Standard Test Method for Splitting Tensile Strength of Cylindrical Concrete Specimens, West Conshohocken, PA, PA, 2011, 5 pp.

Chuah, S., Pan, Z., Sanjayan, J., Wang, C. & Duan, W. (2014). Nano reinforced cement and concrete composites and new perspective from graphene oxide. *Construction and Building Materials*, *73*, 113-124.

Hawreen, A., Bogas, J. A. & Dias, A. P. S. (2018). On the mechanical and shrinkage behavior of cement mortars reinforced with carbon nanotubes. *Construction and Building Materials*, 168: 459-470.

Hu, Y., Luo, D., Li, P., Li, Q. & Sun, G. (2014). Fracture toughness enhancement of cement paste with multi-walled carbon nanotubes. *Construction and Building Materials*, *70*, 332-338.

Kim, H. K., Nam, I. W. & Lee, H. K. (2014). Enhanced effect of carbon nanotube on mechanical and electrical properties of cement composites by incorporation of silica fume. *Composite Structures*, 107: 60-69.

Krämer, C., Schauerte, M., Müller, T., Gebhard, S. & Trettin, R. (2017). Application of reinforced three-phase-foams in UHPC foam concrete. *Construction and Building Materials*, Volume 131, 30 January 2017, Pages 746-757.

Luo, J., Hou, D., Li, Q., Wu, C. & Zhang, C. (2017). Comprehensive performances of carbon nanotube reinforced foam concrete with tetraethyl orthosilicate impregnation. *Construction and Building Materials*, Volume 131, 30 January 2017, 512-516.

Mohsen, M., Taha, R., Abu Taqa, A. & Shaat, A. (2017). Optimum carbon nanotubes' content for improving flexural and compressive strength of cement paste. *Constr. Build. Mater.*, 150 (2017) 395-403.

Paula, J. N. D., Calixto, J. M., Ladeira, L. O., Ludvig, P., Souza, T. C. C., Rocha, J. M. & Melo, A. A. V. D. (2014). Mechanical and rheological behavior of oil-well cement slurries produced with clinker containing carbon nanotubes. *Journal of Petroleum Science and Engineering*, 122 (274-279).

Siddique, R. & Mehta, A. (2014). Effect of carbon nanotubes on properties of cement mortars. Construction and Building Materials. *Construction and Building Materials*, *50*, 116-129.

Song, X., Shang, S., Chen, D. & Gu, X. (2017). Multi-walled carbon nanotube reinforced mortar-aggregate interfacial properties. *Construction & Building Materials*, 133:57-64.

Wang, B., Han, Y. & Liu, S. (2013). Effect of highly dispersed carbon nanotubes on the flexural toughness of cement-based composites. *Construction and Building Materials*, *46*, 8-12.

Cite this article as: Mohsen M., Al Ansari M., Taha R., Senouci A., AbuTaqa A., "Optimum Dispersion Parameters of Carbon Nanotubes: Concrete Strength by Response Surface Methodologies", *International Conference on Civil Infrastructure and Construction (CIC 2020)*, Doha, Qatar, 2-5 February 2020, DOI: https://doi.org/10.29117/cic.2020.0038

Comparison of the Mechanical Behavior of Railroad Ballast in a Box Test under Sinusoidal and Realistic Train Loadings Using Discrete Element Method

Yahia Alabbasi
ya1107037@qu.edu.qa
Department of Civil and Architectural Engineering/ Qatar Transportation and Traffic Safety Center, Qatar University, Doha, Qatar

Mohammed Hussein
mhussein@qu.edu.qa
Department of Civil and Architectural Engineering, Qatar University, Doha, Qatar.

ABSTRACT

A ballasted track is a popular type of railway track and its use is increasing all over the world. A ballasted track consists of different structural elements like rails, fasteners, sleepers, ballast layer, sub-ballast layer and subgrade. A ballast layer is considered as the main structural element of ballasted tracks; it has a significant contribution to track stability and alignment. After service, periodical maintenance of ballast layer is required to maintain its functionality. Ballast maintenance is a cost and time expensive operation. Better understanding of ballast mechanical behavior leads to better ballast design and efficient maintenance. Discrete Element Method has been used extensively in the literature to understand the mechanical behavior of railroad ballast in a box test. Nevertheless, in the literature most of the studies simulate train loading as pure continuous sinusoidal loading unlike the real train loading. This paper aims to investigate the influence of the simulated train loading on the mechanical behavior of railroad ballast after 1000 loading cycles. There are two simulated train-loading cases used in this study for comparison purposes; continuous sinusoidal loading and a more realistic train loading utilizing the Beam on Elastic Foundation theory. The results show a difference of ballast vertical settlement up to 14% between the two simulated train-loading cases.

Keywords: Discrete element method; DEM; Railroad ballast; Ballasted track; Box test

1 INTRODUCTION

The use of railway transportation systems is increasing over the world. In many countries, a railway transportation system has a significant role as a means of transportation. The ballasted tracks have been used since the early commencement of railways. The ballasted track consists of two main structures; super structure and sub structure. The super structure consists of rails, fasteners and sleepers. The sub structure consists of ballast, sub ballast and subgrade.

The ballast element is the main element of ballasted track as it plays a vital role in maintaining the track stability and alignment. After service, periodical maintenance is required, which is an expensive operation (Indraratna, Ionescu & Christie, 1998). Therefore, the research interest and work in relation to ballast mechanical behavior has

been increasing to achieve a better ballast design and cost effective maintenance.

From the literature, Discrete Element Method (DEM) developed by (Cundall, 1971) has been used intensively to understand the mechanical behavior of railroad ballast. DEM is a powerful tool used to understand both the macroscopic and microscopic behavior of railroad ballast. DEM was used commonly for calibration and validation purposes. For example, particle crushing test (Lim & McDowell, 2005), uniaxial test (Chung, Lin, Chou & Hsiau, 2016), triaxial test (Qian, Lee, Tutumluer, Hashash & Ghaboussi, 2018), direct shear test (Gong et al., 2019) and box test (Lim & McDowell, 2005).

In the literature, large number of studies about the understanding of the mechanical behavior of railroad ballast using DEM via box test, simulate the loading coming from train as a pure continuous sinusoidal loading (Hossain, Indraratna, Darve & Thakur, 2007; Ngo, Indraratna & Rujikiatkamjorn, 2016). However, train loading has different shape, where each train car has four axles spaced in different spacing along the train. Each axle applies a load on the ballast layer. The loading from the train is dependent on the number of cars in the train, length of the car, weight of the car and spacing between axles.

The aim of this study is to investigate the influence of the simulated train loading type used in DEM to understand the mechanical behavior of railroad ballast. In this study, EDEM software by DEM Solutions is used for DEM analysis.

2 DEM SETUP

2.1 Material Setup

The first step in setting up the simulation is defining the properties of materials. In EDEM there are two types of materials used in the simulation; bulk and equipment materials. In this simulation, railroad ballast material is the bulk material and the box and sleeper materials are the equipment materials.

In this study, unbreakable spherical ballast shape with a rolling friction resistance approach is used. The main advantage of this approach is the low computational time compared to polyhedrons and multi-sphere approaches. Table 1, summarized the ballast material properties used in DEM model.

Table 1: Material Properties used in DEM

Input used Parameters	Value	References
Passions ratio	0.2	(Ahmed, Harkness, Le Pen, Powrie & Zervos, 2016)
Solid Ballast density	2600 kg/m^3	(Lim & McDowell, 2005)
Youngs Modulus	17.7 GPa	(Irazábal, Salazar & Oñate, 2017)
Coefficient of Restitution	0.4	(Farmer, 1968)
Coefficient of Static Friction	0.6	
Coefficient of Rolling Friction	0.25	(Irazábal et al., 2017)
Contact Model	Hertz-Mindlin	(Ngo Ngoc, Indraratna & Rujikiatkamjorn, 2017)

For the equipment material, there are two equipment materials used in this study. Steel material for the box and concrete material for the sleeper. The simulated box portion of the track used in this study and the geometrical setup in EDEM are shown in Figure 1.

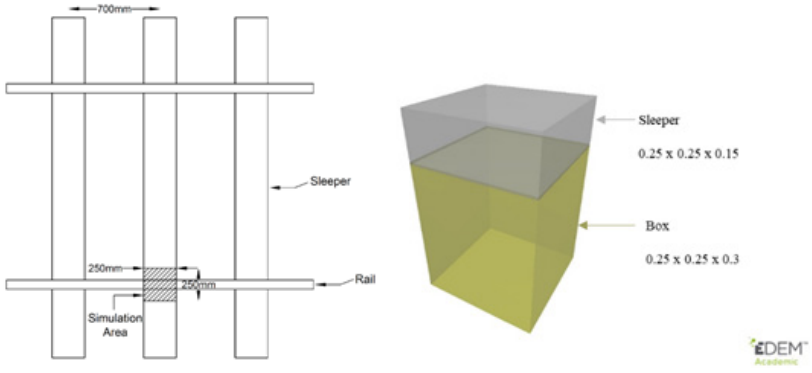

(a) (b)

Figure 1: (a) Box simulation area of a railway track and (b) box geometrical set up used in EDEM (dimensions in meters).

2.2 Control Mode

EDEM software supports displacement control of the geometries. However, it can be customized to support force control mode by the Application Programming Interface (API) through C++, which is the basic language of the software. In this study, force control mode is required to represent the different simulated train loading used in DEM. Therefore, number of C++ codes were used to represent the different input simulated train loading used in EDEM (Alabbasi, 2019).

2.3 Ballast Layer Creation and Preloading

For particle creation, the physical box geometry is used in EDEM as dynamic factory (particles are created during the simulation). The input mass is 29.25 kg which is calculated based on a field bulk density of 1560 kg/m^3 and a box volume of 0.25×0.25×0.3 meters. The boundaries of the steel box are considered as fixed in this simulation to represent the real large-scale box test (Lim & McDowell, 2005).

The particles reached equilibrium, under their own weight, after 3 seconds of simulation time. At the start of the DEM simulation, the ballast material had a void ratio of 0.7 that corresponds to a bulk density of 1531 kg/m^3. Then, ballast layer is preloaded by 2.2 kN that represents the static load from rail and sleeper weights on the simulation box. The calculation of preloading value is based on the common weights of rail and concrete sleepers. The preloading stage is applied and equilibrium state of ballast particles is achieved for 2 seconds of simulation time.

3 LOADING CASES

The train loading for this study is simulated for an infinite train passing the measurement point on the railway track. In this work, two loading scenarios are simulated and used in DEM.

Loading Case 1 represents the more realistic train loading which is simulated utilizing the Beam on Elastic Foundation (BOEF) theory, where rails were modelled as an Euler-Bernoulli beam discretely supported by rail pads to account for sleeper spacing. The rail

pad was modelled as a spring with stiffness constant k_{pad}. The measurement point is the location of the DEM simulation box test as shown in Figure 2. This part is considered as part 1 (Figure 2). In part 2, loading Case 1 is used as an input parameter.

Loading Case 2 represents, the most commonly training load type used in the DEM of railroad ballast in the literature. It is sinusoidal loading type. The usual loading frequency for normal trains is in the range of 8 – 10 Hz and for high speed trains it may extent to 30 Hz; assuming an axle spacing of 2.6 m and a train speed of 75-94 km/hr (Bhanitiz Aursudkij, 2007; B Aursudkij, McDowell & Collop, 2009). For loading Case 2 the frequency used in this study equals to 11.11 Hz assuming a typical axle spacing (L_1) of 2.5 m; and a train velocity of 100 km/hr (Doha Metro maximum train speed).

The simulated train loading for Case 1 and Case 2 are shown in Figure 3. Point A and point B from Case 1 are used as a rang for the sinusoidal loading case for fair comparison purpose; where "A" is the maximum loading point and "B" is the minimum loading point. Point C, represents the flying sleeper phenomena due to the more realistic simulated train loading utilizing BOEF theory. Points A, B and C equal to -5.40×10^4 N, $-2.21\times10\times^3$ N and -696.82 N respectively.

In the field, ballast deformation and degradation occurs after a large number of loading cycles, beyond 100,000 (Hossain et al., 2007). However, the maximum number of loading cycles used in DEM to understand the mechanical behavior of railroad ballast is 4000 for a 3D model by (Ngo et al., 2016). This is due to the huge requirement of the computational time. Therefore, the number of loading cycles used in this study is 1000 loading cycles.

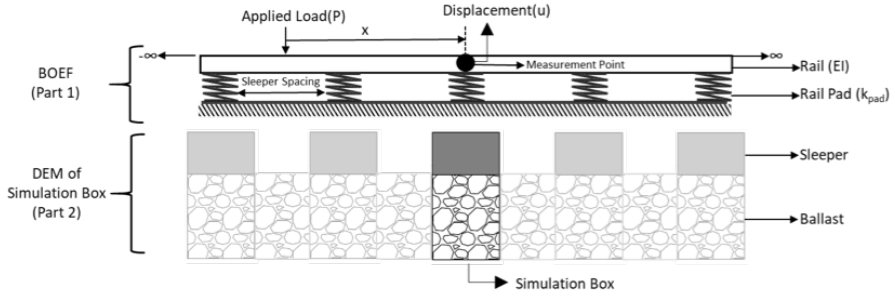

Figure 2: Infinite BOEF model used in this study to simulate train loading

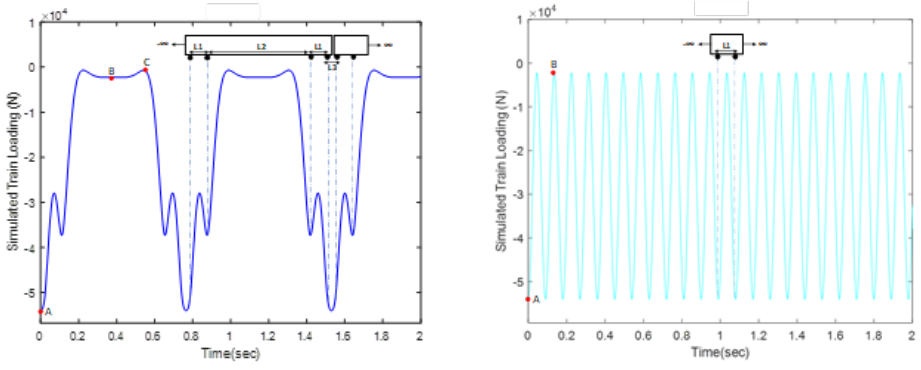

(a) (b)

Figure 3: Loading Cases used in this study; (a) Case 1 and (b) Case 2

4 RESULTS AND DISCUSSION

To investigate the influence of the simulated train loading used in DEM modelling on the macroscopic behavior of railroad ballast, the Absolute Maximum Displacement (AD) of ballast layer versus the number of loading cycles is used as shown in Figure 4. In this study, the displacement of ballast layer is taken as the displacement of sleeper.

A rapid displacement with high rate of change is observed at the initial 10 cycles as shown in Figure 5 (a). This is due to the rearrangement of ballast particles at the initial loading stage. Therefore, the requirement of ballast compaction is significant to reduce the initial settlement of ballast layer before service.

A gradual displacement with almost uniform rate of change is observed at the last 10 cycles as show in Figure 5 (b) because of ballast densification after number of loading cycles. This behavior agrees with the experimental investigations of (Ngo et al., 2016) where under loading cycles ballast layer endures three stages; Initial rapid displacement, gradual displacement and stabilization. In this study, the last stage (stabilization) is not observed because the number of applied loading cycles is low.

To compare the AD between the two loading cases, the difference at each single loading cycles is calculated as shown in Figure 6. It is observed that the type of simulated train loading used in DEM effects the mechanical behavior of railroad ballast. At the initial stage, the difference is maximum – almost 14% - due to the initial rapid displacement of ballast particles resultant of the dynamic effects related to sinusoidal loading as indicated in Figure 6. With the increase of loading cycles, the difference decreases to almost 5% at the last loading cycle due to the particle's rearrangement and densification.

One of the main advantages of DEM is the full insights to the microscopic behavior of discontinues material. In this study, the displacement of each ballast particle at the maximum loads of the 1000th cycle for the two loading cases (Figure 7) is used to observe and investigate the influence of simulated train loading on the microscopic behavior of railroad ballast. The vector represents the particle displacement and its direction.

It is observed for the both cases that at the maximum, load particles move downward and the opposite is at the minimum load of the 1000th cycle. The movement of ballast particles at the maximum and minimum loads agrees with literature (Lim & McDowell, 2005; Lobo-Guerrero & Vallejo, 2006).

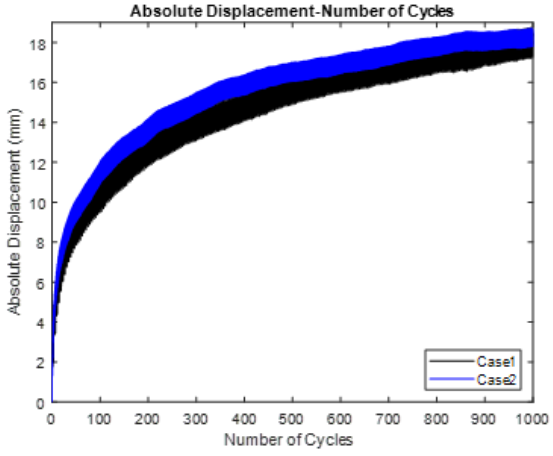

Figure 4: Absolute maximum displacement versus number of cycles for case 1 and case 2.

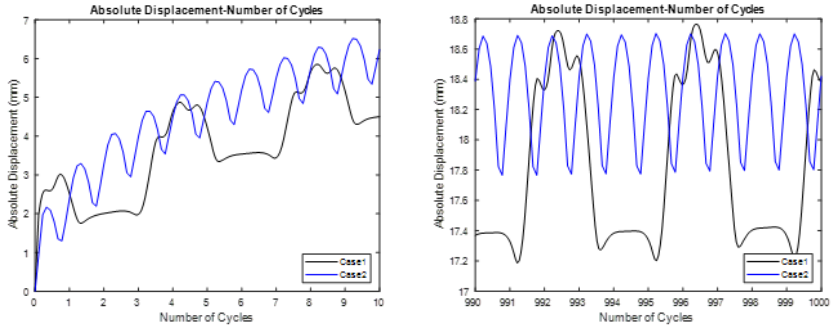

Figure 5: Absolute displacement of ballast layer for the both cases at the (a) initial stage (b) last stage

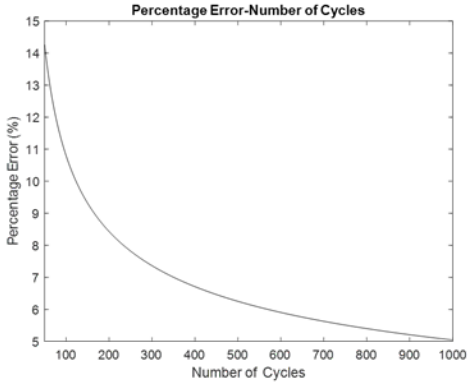

Figure 6: Difference percentage between the AD of ballast of both loading cases at each cycle

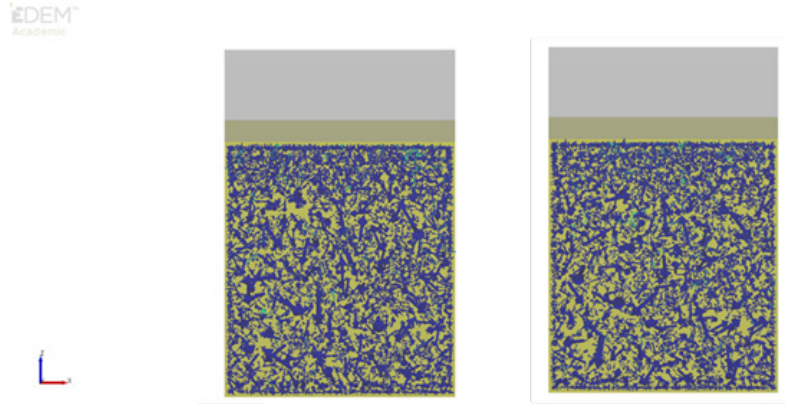

(a) (b)

Figure 7: Particles displacements at maximum loads of the 1000th cycle for (a) Case 1 and (b) Case 2

5 CONCLUSION

The research interest and research work has been increasing throughout the years on understanding the mechanical behavior of railroad ballast for better design and efficient periodical maintenance.

DEM was used extensively in the literature to investigate the mechanical behavior of railroad ballast, most frequently through box test. The train loading was commonly simulated as pure continuous sinusoidal loading. However, trains consist of a number of cars and each car has a number of axles with different spacing in between the axles. Each axle applies a load on the track substructure. The train loading is not a pure continuous sinusoidal; it depends on the train weight, car length, axle number and axle spacing.

This study aims to investigate the influence of simulated train loading to understand the mechanical behavior of railroad ballast using DEM.

In the work presented in this paper, there are two simulated train-loading cases. Case 1 is the train loading simulated utilizing Beam on Elastic Foundation (BOEF) theory, which represents a more realistic train loading. The other case is sinusoidal loading (commonly used in literature).

In this study, the Beam on Elastic Foundation (BOEF) theory is utilized to analytically simulate a more realistic train loading. The numerical Discrete Element Method is used to simulate the behavior of railroad ballast via box test under the two loading cases. The results from the loading cases are compared:

The main findings of this study are briefly summarized as follows:

- DEM is a powerful method in understanding the mechanical behavior of discontinuous material like railroad ballast.
- EDEM software is a useful tool to be used for DEM analysis.
- The type of the simulated train loading used in DEM of railroad ballast effects the mechanical behavior of railroad ballast where a maximum difference of ballast, absolute maximum displacement up to 14% is observed between the two loading cases.

Further investigation is required to account for large number of loading cycles; dynamic loading associated to high train speed, wheel and track irregularities; and particle breakage (permanent deformation).

ACKNOWLEDGMENT

This work has been carried out under a research project entitled “Framework for Research on Railway Engineering” which is supported by a grant sponsored by Qatar Rail with a grant reference number: QUEX-CENG-Rail 17/18.

REFERENCES

Ahmed, S., Harkness, J., Le Pen, L., Powrie, W. & Zervos, A. (2016). Numerical modelling of railway ballast at the particle scale. *International Journal for Numerical and Analytical Methods in Geomechanics, 40*(5), 713-737.

Alabbasi, Y. (2019). *Discrete Element Modeling of Railroad Ballast Under Simulated Train Loading*. (Masters of Science in Civil Engineering Master). Qatar University, Doha, Qatar. Retrieved from http://hdl.handle.net/10576/11684.

Aursudkij, B. (2007). A laboratory study of railway ballast behaviour under traffic loading and tamping maintenance.

Aursudkij, B., McDowell, G. & Collop, A. (2009). Cyclic loading of railway ballast under triaxial conditions and in a railway test facility. *Granular Matter, 11*(6), 391.

Chung, Y. C., Lin, C. K., Chou, P. H. & Hsiau, S. S. (2016). Mechanical behaviour of a granular solid and its contacting deformable structure under uni-axial compression - Part I: Joint DEM-FEM modelling and experimental validation. *Chemical Engineering Science*, 144, 404-420. DOI: 10.1016/j.ces.2015.11.024.

Cundall, P. A. (1971). A computer model for simulating progressive, large-scale movement in blocky rock system. *Paper presented at the Proceedings of the International Symposium on Rock Mechanics*.

Farmer, I. W. (1968). Engineering Properties of Rock–Spon. *Google Scholar*.

Gong, H., Song, W., Huang, B., Shu, X., Han, B., Wu, H. & Zou, J. (2019). Direct shear properties of railway ballast mixed with tire derived aggregates: Experimental and numerical investigations. *Construction and Building Materials*, 200, 465-473. DOI: 10.1016/j.conbuildmat.2018.11.284.

Hossain, Z., Indraratna, B., Darve, F. & Thakur, P. K. (2007). DEM analysis of angular ballast breakage under cyclic loading. *Geomechanics and Geoengineering: An International Journal, 2*(3), 175-181.

Indraratna, B., Ionescu, D. & Christie, H. D. (1998). Shear behavior of railway ballast based on large-scale triaxial tests. *Journal of Geotechnical and Geoenvironmental Engineering, 124*(5), 439-449.

Irazábal, J., Salazar, F. & Oñate, E. (2017). Numerical modelling of granular materials with spherical discrete particles and the bounded rolling friction model. Application to railway ballast. *Computers and Geotechnics*, 85, 220-229. DOI: 10.1016/j.compgeo.2016.12.034.

Lim, W. L. & McDowell, G. R. (2005). Discrete element modelling of railway ballast. *Granular Matter, 7*(1), 19-29. DOI: 10.1007/s10035-004-0189-3.

Lobo-Guerrero, S. & Vallejo, L. E. (2006). Discrete element method analysis of railtrack ballast degradation during cyclic loading. *Granular Matter, 8*(3-4), 195-204. DOI: 10.1007/s10035-006-0006-2.

Ngo Ngoc, T., Indraratna, B. & Rujikiatkamjorn, C. (2017). Micromechanics-Based Investigation of Fouled Ballast Using Large-Scale Triaxial Tests and Discrete Element Modeling. *Journal of Geotechnical and Geoenvironmental Engineering, 143*(2), 04016089. DOI: 10.1061/(ASCE)GT.1943-5606.0001587.

Ngo, N. T., Indraratna, B. & Rujikiatkamjorn, C. (2016). Modelling geogrid-reinforced railway ballast using the discrete element method. *Transportation Geotechnics*, 8, 86-102. DOI:10.1016/j.trgeo.2016.04.005.

Qian, Y., Lee, S. J., Tutumluer, E., Hashash, Y. M. A. & Ghaboussi, J. (2018). Role of initial particle arrangement in ballast mechanical behavior. *International Journal of Geomechanics, 18*(3). DOI: 10.1061/(ASCE)GM.1943-5622.0001074.

Cite this article as: Alabbasi Y., Hussein M., "Comparison of the Mechanical Behavior of Railroad Ballast in a Box Test under Sinusoidal and Realistic Train Loadings using Discrete Element Method", *International Conference on Civil Infrastructure and Construction (CIC 2020)*, Doha, Qatar, 2-5 February 2020, DOI: https://doi.org/10.29117/cic.2020.0039

Improving Concrete Durability by Using Optimized Aggregate Gradation and Reducing Cement Content

Hung-Wen Chung
chweying@ufl.edu
University of Florida, Department of Civil Engineering, Gainesville, Florida, USA

Thanachart Subgranon
tsubgranon@ufl.edu
University of Florida, Department of Civil Engineering, Gainesville, Florida, USA

Mang Tia
tia@ce.ufl.edu
University of Florida, Department of Civil Engineering, Gainesville, Florida, USA

ABSTRACT

This study evaluated the effects of (1) reducing the cementitious content, (2) the use of optimized aggregate gradation (OAG) technique, and (3) the use of Portland limestone cement (Type IL) in Florida Class I pavement and Class IV structural concrete. The potential performance of the pavement concrete mixes was also evaluated using critical stress analysis using a 3D FEM model. The compressive strength, modulus of rupture, modulus of elasticity, Poisson's ratio, splitting tensile strength, coefficient of thermal expansion, rapid chloride permeability, and surface resistivity of the concrete mixes using normal Portland cement (Type I/II) and the concrete mixes using Type IL cement were similar to one another. The results of critical stress analysis indicated that the pavement concrete using Type IL cement had a predicted performance similar to concrete using Type I/II cement. The predicted performance of the pavement concrete was improved when the OAG technique was used. The main findings from this study are as follows: (1) The cementitious content of typical Florida pavement and structural concrete can be reduced by as much as 10 to 15% without loss in workability of the fresh concrete, and without decreasing the strength and durability of the hardened concrete. (2) Portland-limestone cement (Type IL) can be used as a substitute for ordinary Portland cement (Type I/II). (3) The OAG technique can be used to efficiently reduce the cementitious content of the concrete mixes and to improve their performance.

Keywords: Optimized aggregate gradation; Portland-limestone cement; Cementitious content; Concrete pavement; 3D FEM model

1 INTRODUCTION

The concrete industry in Florida and in the U.S. is presently facing two major challenges, namely (1) the rising cost of cement and (2) the shortage of fly ash (ARTBA, 2015). One of the possible solutions to these challenges is using a more effective design method for concrete mixes, in which the cementitious materials content is minimized. Previous preliminary investigations have indicated that most FDOT concrete mixes have an excess of cement paste (Tia et al., 2015). In reality, 10% to 20% of the cement content in most FDOT concrete mixes could be removed without any adverse effects

on the plastic or hardened concrete properties. This reduction in cement content can be maximized when using an intermediate-sized coarse aggregate along with the original aggregate. By adjusting the gradation of the coarse aggregate blend, an optimum packing of aggregate (optimum aggregate gradation, OAG) can be obtained such that the aggregate volume is maximized. The use of OAG along with the reduction of paste (cement) content can improve the properties of the concrete mix, including (1) improved workability of fresh concrete, (2) reduced drying shrinkage, (3) increased resistance to intrusion of chlorides and sulfates (Singh, 2015), (4) reduced heat of hydration, (5) increased thermal conductivity, and (6) reduced coefficient of thermal expansion. The last three property improvements would greatly reduce the tendency for thermal cracking of the concrete (Tritsch et al, 2005).

Using Portland limestone cement (PLC) is an alternative way to decrease the cementitious content of concrete. In U.S., American Society for Testing and Materials (ASTM) allows the ordinary Portland cement (OPC) to contain up to 5% limestone powder in ASTM C150 (ASTM, 2018(a)). According to ASTM C595, blended hydraulic cement can contain up to 15% limestone powder (ASTM, 2018(b)). The reduction in the use of cementitious materials would significantly reduce the cost of concrete and reduce the environmental impact by conserving natural resources, lowering energy consumption, and lowering carbon dioxide emission. This research study was conducted to address this need.

2 LABORATORY TESTING PROGRAM

A laboratory testing program was conducted to evaluate the effects of reducing cementitious material content, the feasibility of using Portland-limestone cement (Type IL), and the benefits of optimized aggregate gradation (OAG) technique on Florida Class I (Pavement) and Florida Class IV (Structural) concrete. The properties of the Type I/II and Type IL cements, which were used in this study are shown in Table 1. The Type I/II cement passed the requirements of AASHTO M85 (AASHTO 2015) and the Type IL cement passed the requirements of AASHTO M 240M/M240 (AASHTO 2018).

Table 1: Properties of Type I/II and IL Cements Used

Test Items		OPC (Type I/II)	PLC (Type IL)
Air Content of Mortar ASTM C185 (%)		4.10	8.00
Blaine Fineness ASTM C204 (m^2/kg)		401.00	522.00
Fineness ASTM C430 (%)		2.80	3.60
Autoclave expansion ASTM C151 (%)		0.04	-.01
Density of Cement ASTM C188 (g/cm^3)		3.20	3.16
Loss on Ignition ASTM C114 (%)		2.00	5.60
Limestone (%)		2.10	12.60
Time of Setting-initial ASTM C191 (minutes)		123.00	105.00
Heat of Hydration ASTM C1702 (Cal/g)		65.00	65.40
Compressive Strength ASTM C109 (MPa)	1 day	14.82	15.43
	3 days	26.82	26.23
	7 days	35.99	33.23
	28 days	49.99	44.29

The mix designs of the pavement concrete mixes which were evaluated are shown in Table 2. The necessary amounts of water-reducing and air-entraining admixtures were

added to achieve the target slump of 0 to 5 cm, and air content of 1 to 6%. The reference pavement mix design is a commonly-used Florida Department of Transportation (FDOT)-approved pavement concrete mixture. The mix had a w/cm ratio of 0.44 and total cementitious materials content of 320 kg/m^3 (540 lb/yd^3) (80% Type I/II and 20% Class F Fly Ash). The cement paste volume (CPV) of the reference mix is 25%, which meets the suggestion of AASHTO Designation PP 84-17. Based on the reference mix, twelve mix designs were developed to evaluate the effects of PLC concrete with OAG technique and reduced cementitious content. Paste contents investigated were 110, 100, 95, 90, and 85 percent (by weight) of the reference paste quantity of the mixture. Three groups of concrete mixtures were developed. The first group is designated as the SC group which used Type I/II cement of various cement contents. The second group is designated as the LC group which used PLC of various cement contents. The last group is designated as the OLC group which used OAG and PLC of various cement contents. A total of thirteen mix designs, and two batches per mix design were evaluated.

Table 2: Mixture Proportions for Pavement Concrete Mixes

Mix Design	Paste Volume (%)	Cement (kg/m^3)	Fly Ash (kg/m^3)	Fine Agg. (kg/m^3)	Intermediate Agg. (kg/m^3)	Coarse Agg. (kg/m^3)
SC110*	27.5	281.9	70.5	785.1	000.0	0985.0
SC	25.0	256.3	64.1	805.4	000.0	1013.0
SC95	23.7	243.5	60.9	828.1	000.0	1038.5
SC90	22.5	230.7	57.7	835.0	000.0	1047.3
LC110	27.5	281.9	70.5	781.2	000.0	0983.4
LC100	25.0	256.3	64.1	811.3	000.0	1020.0
LC95	23.7	243.5	60.9	834.9	000.0	1037.7
LC90	22.5	230.7	57.7	838.9	000.0	1055.6
OLC110	27.5	281.9	70.5	581.9	359.5	0827.6
OLC100	25.0	256.3	64.1	632.9	363.0	0839.5
OLC95	23.7	243.5	60.9	660.7	362.4	0845.2
OLC90	22.5	230.7	57.7	686.0	366.4	0851.0
OLC85	21.5	217.9	54.5	711.3	366.6	0853.7

*Number after mix type indicates % relative cementitious content as compared to the reference mix.

For the SC and LC mixes, the aggregate blend was obtained by combining a size 57 coarse limestone aggregate with a nominal maximum size of 25 mm (1 inch) with a silica sand with fineness of 2.45. The resulting aggregate blend was a gap-graded aggregate. For the OLC mixes, the aggregate blend was obtained by combining the same size 57 coarse limestone aggregate and the same silica sand with an intermediate-size 89 limestone aggregate with a nominal maximum size of 9.5 mm (3/8 inch) using the Coarseness Factor Chart developed by Shilstone (Shilstone 1990). The resulting aggregate blend is a well-graded aggregate with good workability.

The mix designs of the structural concrete mixes which were evaluated are shown in Table 3. The necessary amounts of water-reducing and air-entraining admixtures were added to achieve the target slump of 5 to 10 cm, and air content of 1 to 6%. The reference mixture design is an industrial mixture approved by FDOT. The concrete mix had a w/cm ratio of 0.40, and total cementitious materials content (80% Type I/II and 20% Class F Fly Ash) of 346.5 kg/m^3. The average cement paste volume of the reference mix is

32.0%. Based on the reference mix, twelve mix designs were developed to evaluate the effects of PLC concrete with OAG technique and reduced cementitious content. Paste contents investigated were 110, 100, 85 and 75 percent (by weight) of the reference paste quantity of the mixture. A total of thirteen mix designs, and two batches per mix design were evaluated.

Table 3: Mixture Proportions Structural Concrete Mixtures

Mix Design	Cement (kg/m^3)	Fly Ash (kg/m^3)	Fine Agg. (kg/m^3)	Intermediate Agg. (kg/m^3)	Coarse Agg. (kg/m^3)
SC110*	381.1	95.3	598.7	0.0	965.9
SC100	346.5	86.6	623.8	0.0	1008.7
SC85	294.5	73.6	673.1	0.0	1088.7
SC75	259.9	65.0	706.5	0.0	1131.6
LC110	381.1	95.3	584.3	0.0	943.7
LC100	346.5	86.6	627.4	0.0	1015.3
LC85	294.5	73.6	657.6	0.0	1065.1
LC75	259.9	65.0	687.7	0.0	1113.4
OLC110	381.1	95.3	410.6	143.5	974.4
OLC100	346.5	86.6	445.0	437.1	717.2
OLC85	294.5	73.6	550.6	150.8	1026.2
OLC75	259.9	65.0	592.9	455.3	749.7

*Number after mix type indicates % relative cementitious content as compared to the reference mix.

The tests on fresh concrete were carried out in accordance with ASTM C143 (Slump), AASHTO PP84-17 (Box Test), ASTM C231(Air Content), ASTM C138 (Unit Weight), ASTM C1064 (Temperature), and ASTM C232 (Bleeding). The strength tests on hardened concrete included ASTM C39 (Compressive Strength), ASTM C78 (Modulus of Rupture), ASTM C496 (Splitting Tensile Strength), and ASTM C469 (Modulus of Elasticity and Poisson's Ratio). Concrete cylindrical specimens for compressive strength and splitting tensile strength tests were 10.2 × 10.2 × 20.3 cm (4 × 4 × 8 in.), and concrete beams for modulus of rupture tests were 10.2 × 10.2 × 35.6 cm (4 × 4 × 14 in.). Three specimens for each test at different ages were used. The strength tests on hardened concrete were performed at 7, 28, and 90 days. The Coefficient of Thermal Expansion (COTE) test was performed according to AASHTO T336.

3 EVALUATION OF PAVEMENT CONCRETE MIXTURES

The compressive strength, modulus of rupture, modulus of elasticity, and coefficient of thermal expansion of the pavement concrete mixtures at 28 days are presented in Figures 1 through 4, respectively. The drying shrinkage of the pavement concrete mixtures at 182 days are presented in Figure 5.

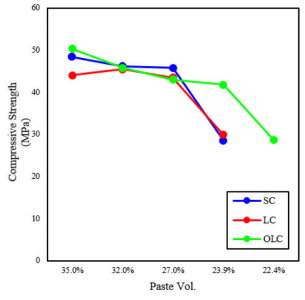

Figure 1 Compressive Strength of the Pavement Mixtures at 28 days

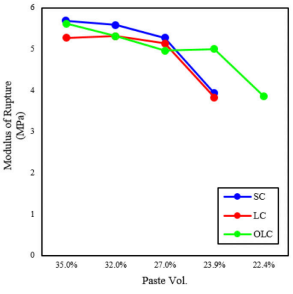

Figure 2 Modulus of Rupture of the Pavement Mixtures at 28 days

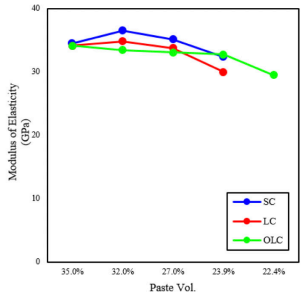

Figure 3 Modulus of Elasticity of the Pavement Mixtures at 28 days

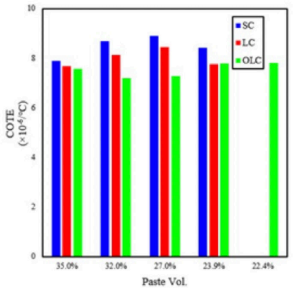

Figure 4 Coefficient of Thermal Expansion of the Pavement Concrete at 28 days

The main findings from the testing program on the pavement concrete mixtures are as follows:

1. The compressive strength, modulus of rupture, modulus of elasticity, coefficient of thermal expansion of the concrete mixes using Type I/II cement, and the concrete mixes using Type IL cement were similar to one another.
2. The concrete mixes using with OAG (OLC mixes) showed lower moduli of elasticity and lower coefficients of thermal expansion, which would result in lower thermal-load-induced stresses in concrete pavement slabs, and thus potentially better performance.
3. The drying shrinkage of the concrete using Type IL cement was slightly higher than that using Type I/II cement.
4. The concrete mixes using OAG showed lower drying shrinkage, which would indicate better performance in structural concrete as well as pavement concrete.
5. The cementitious material content of pavement concrete can be reduced to some extent without loss in fresh concrete workability and hardened concrete strength and durability. When the concrete aggregate gradation was optimized, the reduction in cementitious content could be further increased.

Figure 5: Drying Shrinkage of the Pavement Mixtures at 182 days

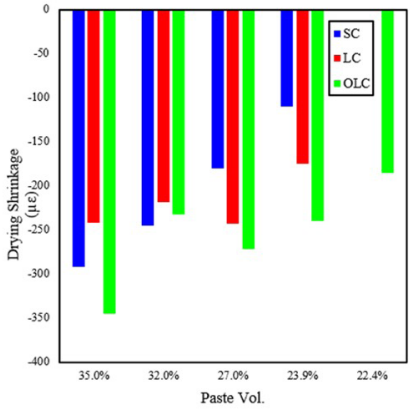

6. Portland-limestone cement (Type IL) containing 12% limestone powder can be used as a substitute for ordinary Portland cement (Type I/II) in pavement concrete with no loss in fresh concrete workability, or hardened concrete strength and durability.
7. The potential performance of the pavement concrete mixes was evaluated using critical stress analysis. A 3D FEM model developed and validated in a previous pavement project (Tia et al 2017) was used for this purpose. The maximum computed stresses under a critical load-temperature condition were divided by the flexural strengths of the respective concretes to determine the stress-to-strength ratios, which were used to evaluate the performance of the concretes from the laboratory testing program. Results of critical stress analysis indicate that when OAG technique was used, the performance of the pavement concrete was substantially improved, and remained unchanged as the cementitious paste volume was reduced to 22.5%.

4 EVALUATION OF STRUCTURAL CONCRETE MIXTURES

The compressive strength, modulus of rupture, modulus of elasticity, and coefficient of thermal expansion of the structural concretes are presented in Tables 4 through 7, respectively. The drying shrinkage of the structural concrete mixtures are presented in Table 8.

Table 4: Compressive Strength of the Structural Concrete Mixtures

(MPa)	Paste Volume (%)											
Curing	35.0%			32.0%			27.0%			23.9%		
Time(days)	SC	LC	OLC	SC	LC	OLC	SC	LC	OLC	SC	LC	OLC
7	35.2	33.2	31.0	40.1	33.0	30.5	42.9	31.6	33.5	47.4	31.6	31.2
28	43.0	41.0	40.7	48.9	43.3	37.8	52.7	39.4	41.0	58.2	39.4	40.3
91	53.2	53.0	51.0	57.8	50.6	47.1	60.5	48.1	51.8	57.0	52.1	50.3
182	54.5	58.4	54.1	64.6	58.4	53.6	65.2	54.5	55.0	63.8	56.3	52.0

Table 5: Modulus of Rupture of the Structural Concrete Mixtures

(MPa)	Paste Volume (%)											
Curing	35.0%			32.0%			27.0%			23.9%		
Time(days)	SC	LC	OLC	SC	LC	OLC	SC	LC	OLC	SC	LC	OLC
7	4.6	4.5	5.0	5.2	4.5	4.6	5.0	4.4	4.5	5.5	4.3	4.3
28	5.3	5.1	5.8	5.4	5.3	5.2	5.9	4.9	5.2	6.2	5.2	5.0
91	5.8	5.7	5.6	6.0	5.7	5.3	5.8	5.6	5.8	6.0	5.7	5.9
182	5.8	5.6	5.5	5.8	5.7	5.3	5.7	5.8	5.8	5.9	5.7	5.9

Table 6: Modulus of Elasticity of the Structural Concrete Mixtures

(GPa)	Paste Volume (%)											
Curing	35.0%			32.0%			27.0%			23.9%		
Time(days)	SC	LC	OLC	SC	LC	OLC	SC	LC	OLC	SC	LC	OLC
7	27.6	28.3	25.2	31.0	28.6	26.5	33.8	30.7	29.0	34.8	29.6	29.6
28	29.6	29.6	28.3	33.4	30.7	27.6	34.5	31.4	32.1	36.9	32.4	31.4
91	32.4	33.1	31.4	36.9	34.1	30.7	37.9	34.8	33.8	39.6	36.5	34.1
182	33.4	35.9	32.4	37.9	35.5	31.4	38.6	36.5	35.2	40.0	38.3	35.2

Table 7: Coefficient of Thermal Expansion of the Structural Concrete Mixture

(με/ºC)	Paste Volume (%)											
Curing	35.0%			32.0%			27.0%			23.9%		
Time(days)	SC	LC	OLC	SC	LC	OLC	SC	LC	OLC	SC	LC	OLC
28	7.59	7.43	7.88	7.53	7.52	7.23	7.60	7.70	7.36	7.32	7.15	7.45
182	7.83	7.86	8.41	8.05	8.17	7.58	8.12	8.53	7.34	8.17	7.88	7.06

Table 8: Drying Shrinkage of the Structural Concrete Mixtures

(με)	Paste Volume (%)											
Curing	35.0%			32.0%			27.0%			23.9%		
Time(days)	SC	LC	OLC	SC	LC	OLC	SC	LC	OLC	SC	LC	OLC
7	55	-13	-70	-10	83	-3	8	10	-13	-2	-2	25
28	93	-17	-100	-10	62	28	110	-68	-30	43	23	-13
91	-260	-340	-522	-233	-298	-383	-185	-397	-347	-203	-272	-426
182	-433	-412	-492	-403	-387	-422	-297	-483	-393	-300	-387	-360

The main findings from the testing program on Class IV (Structural) concrete were as follows:

1. The compressive strength of the concrete using Type I/II cement was slightly higher than that using Type IL cement. However, most of the mixes passed the FDOT specification limits, with the exception of a mix with a low paste volume of 22.4%.
2. The modulus of rupture, modulus of elasticity, and coefficient of thermal expansion of the SC mixes using Type I/II cement and LC mixes using Type IL cement were similar to one another.
3. The concrete mixes using Type IL cement with or without the application of OAG technique showed lower modulus of elasticity as compared with the concrete using Type I/II cement.

4. The drying shrinkage of the concrete might increase when Type IL cement is used to replace Type I/II cement.
5. The cementitious content of structural concrete could be reduced to 25% without loss in fresh concrete workability and strength and durability of hardened concrete. When the concrete aggregate gradation is enhanced by the OAG technique, the amount of reduction in cementitious content could be further increased.

5 CONCLUSION AND RECOMMENDATIONS

The results of laboratory testing program and statistical analysis indicate that the use of Portland-limestone cement (Type IL) as a cement replacement in concrete appears to be not only feasible, but also offers the possibility of improving the performance of concrete. The use of OAG along with the reduction of cement content can improve the properties of the concrete mix.

REFERENCES

AASHTO (2015). AASHTO M240M/M240, Standard Specification for Blended Hydraulic Cement, *American Association of State Highway and Transportation Officials*, Washington D.C.

AASHTO (2018). AASHTO M85 Standard Specification for Portland Cement, *American Association of State Highway and Transportation Official*s, Washington D.C.

ARTBA (2015). Production and Use of Coal Combustion Products in the U.S., *American Road and Transportation Builders Association*, pp. 28, the USA.

ASTM C150 (2018). Standard Specification for Portland Cement, *American Section of the International Association for Testing Materials*, Pennsylvania, the USA.

ASTM C595 (2018). Standard Specification for Blended Hydraulic Cement, *American Section of the International Association for Testing Material*s, Pennsylvania, the USA.

Shilstone, J. M. (1990). Concrete mixture optimization, *Concrete International*, Vol. 10, pp. 33-39.

Singh, H. (2015). Permeability of concrete mix design, proceedings of 6th national conference on Make in India PMs vision: Role of engineering and management innovations to achieve this vision, India.

Tia, M., Subgranon, T., Kim, K., Medina, R. A. & Algazlan, A. (2015). Internally Cured Concrete for Pavement and Bridge Deck Applications, *Research Report, University of Florida*, Florida, the USA.

Tia, M., Kim, K. & Han, S. (2017). Improved analysis tool for concrete pavement, *Research Report, University of Florida, Florida*, the USA.

Tritsch, N., Darwin D. & Browning J. (2005). Evaluating shrinkage and cracking behavior of concrete using restrained ring and free shrinkage tests, *Research Report*, The University of Kansas Center for Research, Kansas, the USA.

Cite this article as: Chung H.-W., Subgranon T., Tia M., "Improving Concrete Durability by Using Optimized Aggregate Gradation and Reducing Cement Content",*International Conference on Civil Infrastructure and Construction (CIC 2020)*, Doha, Qatar, 2-5 February 2020, DOI: https://doi.org/10.29117/cic.2020.0040

Advanced Freeze-Thaw Assessment of Internally Integrated Concrete with Sodium Acetate

Mazen J. Al-Kheetan
mazen.al-kheetan@mutah.edu.jo
Civil and Environmental Engineering Department, Mutah University, Mutah, Karak, Jordan

Mujib M. Rahman
mujib.rahman@brunel.ac.uk
Department of Civil & Environmental Engineering, Design and Physical Sciences, Brunel University, London, UK

Seyed Hamidreza Ghaffar
seyed.ghaffar@brunel.ac.uk
Department of Civil & Environmental Engineering, Design and Physical Sciences, Brunel University, London, UK

ABSTRACT

A new line of research is presented in this study where sodium acetate is used as a protective material for concrete. A newly developed freeze-thaw method that depends on the alteration of temperature and humidity is introduced in this research to investigate the efficacy of integrating sodium acetate with concrete with different water to cement ratios (w/c). Results from the introduced freeze-thaw method were compared with the outcomes of a standard freeze-thaw testing method. The distressed concrete was tested for water absorption and compressive strength after finishing six months of freeze-thaw testing. Results demonstrated the effectiveness of sodium acetate in protecting concrete

Keywords: Fresh concrete; Freezing and thawing; Sodium acetate; Concrete protection

1 INTRODUCTION

Concrete pavement is usually exposed to a combination of mechanical stresses and environmental impacts that accelerate its deterioration rate (Zhang et al., 2017; Al-Kheetan et al., 2019b). The presence of de-icing salts when in contact with the surface of concrete pavement during winter season can increase the damage of concrete, especially after their penetration in the pores with the absorbed water (Farnam et al., 2017; Farnam et al., 2015a; Farnam et al., 2015b; Al-Kheetan et al., 2019a; Sun et al., 2002). Add to that, the freezing and thawing cycles can produce a high pore pressure related to the water phase change inside the pores that work on initiating cracks within the concrete matrix (Li 2017). Accordingly, it is important to protect such structures from all the weathering actions and chemical attacks to keep it in its original form and serviceability (Tang et al., 2015; Mehta and Monteiro 2006).

Many protective materials have been used during the years to reduce the rate of deterioration caused by chloride and water ingress through concrete and to inhibit the freeze-thaw damage (Bertolini et al., 2013; Dry 2000; Lu and Zhou 2000; Al-Kheetan et al., 2017; Al-Kheetan et al., 2018a; Al-Kheetan et al., 2018b; Al-Kheetan et al., 2019c; Al-Kheetan et al., 2018c). Surface applied protective materials like silane and siloxane

were the most widely used materials in this regard due to their high resistance to different environmental impacts and chemical attacks [Al-Kheetan et al., 2019c; Herb et al., 2015; De Vries and Polder 1997; Tittarelli and Moriconi 2008; Brenna et al., 2013; Falchi et al., 2015; Dai et al., 2010). However, few researches considered the protection of concrete pavement, in particular, either by using silane or any other surface applied materials (Al-Kheetan et al., 2019b). This refers to their inconvenient application method that requires closing the roads in front of vehicles and their effect on the frictional properties of concrete pavement (Al-Kheetan et al., 2019b). Accordingly, internally integrated materials were introduced to overcome all the issues associated with the surface applied materials (Cappellesso et al., 2016; Teng et al., 2014; Justnes et al., 2004; Kevern 2010; Ma et al., 2016).

The integration of sodium acetate into concrete for protection purposes is a newly introduced method that aims to improve the drawbacks that are associated with other traditional methods (Al-Otoom et al., 2007). After the mixing of sodium acetate with concrete, in the presence of water, it forms crystals that line the pores of concrete without blocking them. This material is characterised of being hygroscopic, as it works on absorbing water to form crystals that start to grow after the reaction of sodium acetate with water. After the formation of these crystals, they bond with concrete and work on repelling any excess water from the pores due to the development of hydrophobic properties that results from their reaction with cement during the hydration process (Al-Kheetan et al., 2019a).

In this research, two freeze-thaw conditions will be applied to concrete, and the performance of the used protective material, under these conditions, will be evaluated. In the first method, concrete was exposed to fast freeze-thaw cycles while it was immersed in water. This method has been widely used in previous studies but with less number of cycles than it is used in this research, where the number of cycles in this research is the highest until now (Zhang et al., 2017; Shang and Yi 2013; Jianxun et al., 2014; Shang et al., 2012; Wu and Wu 2014). In the second freeze-thaw method, a newly developed method is proposed where concrete is only in contact with air and under the effect of temperature change.

2 MATERIALS AND TEST METHODS

2.1 Materials and specimens

Four concrete mixtures with w/c ratios of 0.32, 0.37, 0.40 and 0.46 were cast following the British Standard BS 1881-125 (British Standards Institution, 2013). A sodium acetate material with some cementitious content was added to all the mixes with two different ratios; 2% and 4% of the cement mass. In addition, a reference mix with 0% sodium acetate was cast for each mix design for comparison. Table 1 shows the proportions of each concrete mix that was used in this study.

Table 1: Mix designs of the used concrete mixtures

Ingredient	Amount (kg/m^3)			
	W/C=0.32	W/C=0.37	W/C=0.40	W/C= 0.46
Cement (CEM II/32.5 N; Sulphates < 3.5%, Chlorides < 0.10%, and initial setting time around 1.25 h)	513	491	450	457
Water	164	182	180	210
Fine aggregate (sharp silica sand with uniform grain size distribution between 1 mm and 300 μm)	658	660	678	660
Coarse aggregate (crushed stones with sharp edges and maximum size of 20 mm)	1068	1070	1092	1073

72 concrete cubes with the dimensions of 100mm x 100mm x 100mm were cast and divided into two groups; 36 cubes were tested for freeze-thaw cycles in air and 36 cubes were tested for fast freeze-thaw cycles in water. From each group, 9 cubes were prepared with 0.32 w/c ratio, 9 cubes with 0.37 w/c ratio, 9 cubes with 0.40 w/c ratio and 9 cubes with 0.46 w/c ratio. For each w/c ratio, 3 cubes were integrated with 2% sodium acetate, 3 cubes with 4% sodium acetate and 3 cubes were used as control.

All concrete samples were cured in a water bath for 28 days. Afterwards, 36 cubes of them were placed in room temperature (21 °C) to dry so they can be tested under the freeze-thaw cycles in air. The other 36 cubes were placed in water for another 7 days until they were fully saturated (to achieve a constant mass).

2.2 Test methods

In the fast freeze-thaw test, cubes were placed in containers filled with water (cubes are immersed in water), and all containers were placed in Weiss-Voetsch Environmental Testing Chamber C340, following the guidelines of the Chinese standard GB/T 50082–2009 (China Academy of Building Research, 2009). Temperature was set to alternate between -10 °C and 6 °C for a duration of 4 hours, representing a full rapid freeze-thaw cycle. The internal temperature of concrete cubes ranged between -6 °C and 4 °C during the freezing and thawing periods respectively. In total, 1080 freeze-thaw cycles during 6 months were carried out in this test.

In the newly developed freeze-thaw test, an environmental chamber that controls humidity and temperature was constructed. The chamber was constructed by utilising an existing industrial freezer as base for the freezing cycles and by introducing heating and humidity units inside the freezer to serve the thawing cycles. Furthermore, the heating and the humidity control units are additionally developed in order to complete the requirements for computer controlled scheduling of 24 hours cycles between temperatures of -20 °C and 20 °C, and constant humidity of 60%. Cubes were placed inside the chamber and it was programmed to run for 6 continuous months with a total of 180 freeze-thaw cycles. The internal temperature of concrete was measured by using

embedded thermocouples and it ranged between 17 °C during the thawing process and -16 °C during the freezing process.

The ability of the sodium acetate compound to preserve concrete from water ingress in harsh environments was assessed by running the ISAT test on the distressed samples (after finishing the freeze-thaw tests). Initial Surface Absorption Test (ISAT) was used to measure the uniaxial water absorption of concrete cubes by following the guidelines of BS 1881-208 (Al-Kheetan et al., 2020; British Standards Institution, 1996).

Mechanical properties of concrete were determined by running the compressive strength test on all the samples after finishing the freeze-thaw cycles, following the British Standard BS EN 12390-3 (British Standards Institution, 2009). Furthermore, the obtained results were compared with the compressive strength results of the samples before running the freeze-thaw tests.

3 RESULTS AND DISCUSSION

3.1 Water absorption (after freeze-thaw)

Concrete samples have shown a general increase in water absorption after the impact of freeze-thaw cycles in water. Figure 1 demonstrates the water absorption rate of concrete after the impact of 1080 cycles under the immersion effect.

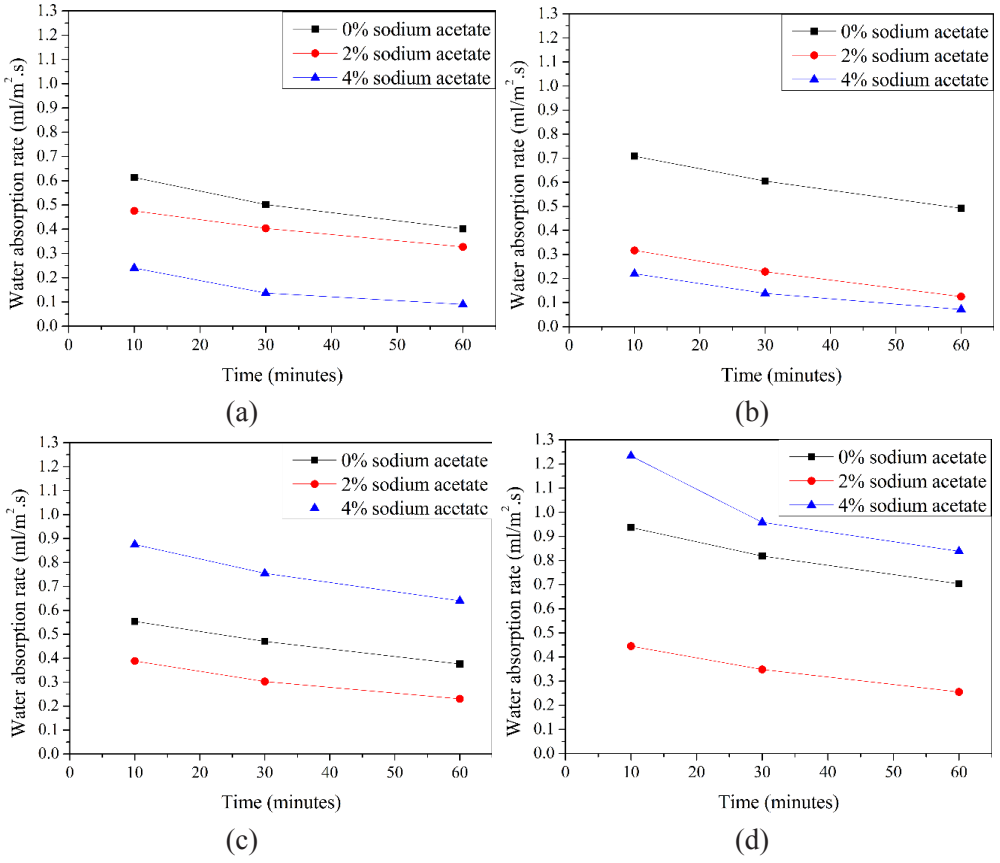

Figure 1: Water absorption of concrete after the impact of 1080 freeze-thaw cycles in water for concrete with w/c ratio of: (a) 0.32, (b) 0.37, (c) 0.40 and (d) 0.46

Concrete samples with w/c ratios of 0.32 and 0.37 treated with 4% sodium acetate show the least water absorption rates among all mixtures. This amount of treatment helped water absorption rate drop by 78% and 85% for mixtures with 0.32 and 0.37 w/c ratios respectively, compared to their control mixtures (Figure 1 a and b). Even when both mixtures were treated with 2% sodium acetate, they have shown a high ability to reduce water absorption. This might be a result of using a compatible amount of water and sodium acetate, where no excess water is present in the mix and the amount of water was suitable to initiate the reaction between sodium acetate and cement, and at the same time water was enough to continue the hydration process.

In the case of concrete with w/c ratios of 0.40 and 0.46 treated with 4% sodium acetate, an obvious destructive effect could be seen from Figure 1 c and d. Water absorption of these two mixes significantly increased, compared to their control and to other mixtures after the impact of freeze-thaw. This might refer to their high porosity when they were first cast and the formation of some microcracks in concrete after the impact of freeze-thaw cycles. Moreover, the high w/c ratio, especially in concrete with w/c ratio of 0.46, and the highly added dosage of the sodium acetate compound will contribute in increasing the formation of the hydrophobic organosilicon content. The presence of this hydrophobic content in large amounts in concrete at early ages will probably work on reducing the needed amount for the hydration process by repelling water out from concrete. This will lead to the formation of some microcracks in concrete during its curing and before initiating the freeze-thaw test. With the impact of the freeze-thaw test, these microcracks will develop into larger cracks, and concrete will absorb more quantities of water.

Referring to the results of water absorption of concrete under the impact of 180 freeze-thaw cycles in air, a clear increase in permeability can be noticed. Figure 2 illustrates the effect of freeze-thaw cycles in air on absorption of water by the concrete.

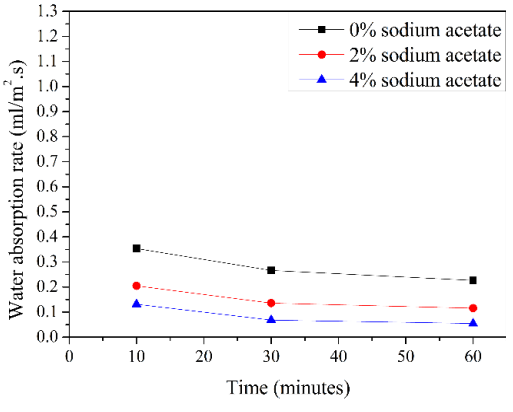

(a)

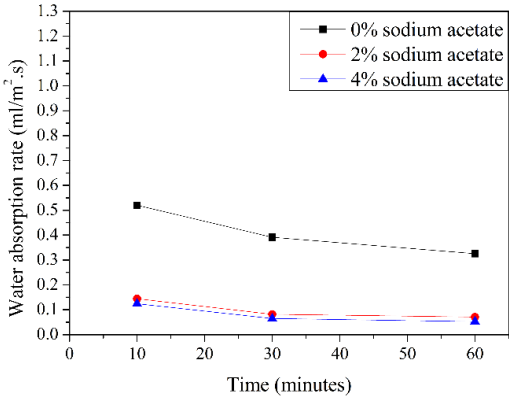

(b)

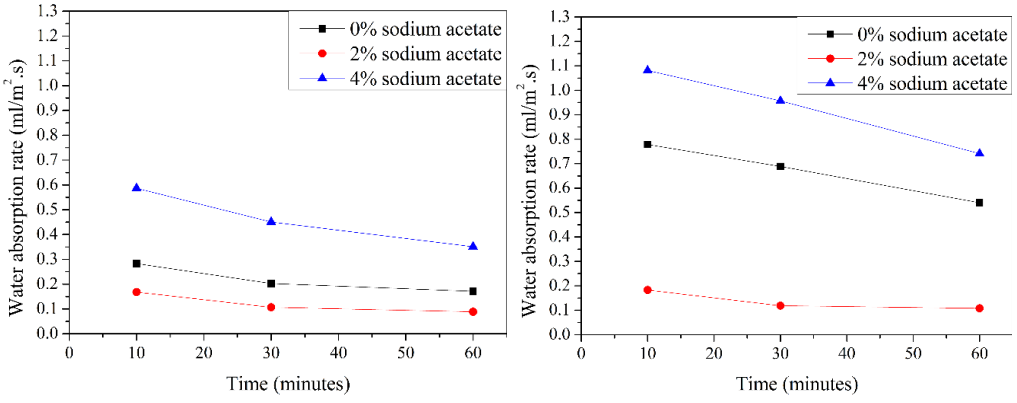

(c) (d)

Figure 2: Water absorption of concrete after the impact of 180 freeze-thaw cycles in air for concrete with w/c ratio of: (a) 0.32, (b) 0.37, (c) 0.40 and (d) 0.46

Water absorption rates under the effect of air have followed a similar trend to that in water but with less absorbing rates. This is expected since the severity of the test in water is higher than that in air.

Similar to the freeze-thaw test in water, concrete with w/c ratios of 0.32 and 0.37 treated with 4% sodium acetate have shown the least absorption rate between all mixes, which refers to the compatibility between the used amount of water and the added percentage of the admixture.

On the other hand, concrete with w/c ratios of 0.40 and 0.46 treated with 4% sodium acetate suffered increase in the absorption rate of water. This issue could be explained by following the same reasons for their high absorption rates after the impact of freeze-thaw cycles in water. In addition, their high tendency to absorb moisture during freeze-thaw in air confirms with the current outcomes, because of the formation of large microcracks and the original high porosity of concrete.

3.2 Compressive strength (after freeze-thaw)

After finishing both freeze-thaw tests, in water and air, all samples have been tested for compressive strength to measure the ability of treatment for preserving the strength of concrete in harsh conditions. Table 2 shows the compressive strength and standard deviation values of concrete after their exposure to cyclic freeze-thaw in water and air.

Table 2: Compressive strength of concrete after the impact of freeze-thaw cycles

		Compressive strength (MPa)											
		Freeze-thaw in water						Freeze-thaw in air					
Sodium acetate %		0%	SD	2%	SD	4%	SD	0%	SD	2%	SD	4%	SD
w/c ratio	0.32	38.7	1.1	42.1	1.5	50.5	0.7	38.8	0.9	47.7	1.6	53.5	0.8
	0.37	31.2	0.9	39.2	1.3	46	2	34.8	2.8	45.2	2.3	50.5	1.3
	0.40	45.5	1.2	36.4	1.2	32.9	0.2	54.4	1.8	42.1	1.9	43.3	0.3
	0.46	36.1	0.8	29.1	1	21.2	0.4	45.1	2.3	37	1.6	30.3	1.6

It is witnessed that concrete under the impact of cyclic freeze-thaw in water suffered from a drop in its compressive strength values when compared to concrete under freeze-thaw cycles in air. Once more, this refers to the severity of the applied conditions in the case of the freeze-thaw test in water. The frost action of the freeze-thaw test in water may damage the internal pores of concrete due to the presence of water inside the pores. The expansion of water inside the pores will damage the pore system and initiate cracks inside the concrete, which in turn will weaken it and reduce its strength.

4 CONCLUSION

The long-term performance of concrete treated with 2% and 4% sodium acetate has been tested through two freeze-thaw tests that operate differently; freeze-thaw under the effect of water and freeze-thaw under the effect of air. Both tests have run for 6 continuous months but with different number of cycles and different speeds. In the freeze-thaw test under the effect of water, saturated concrete was immersed in water and placed under the impact of fast 1080 freeze-thaw cycles during the 6 months. However, in the freeze-thaw test under the effect of air, concrete was under the impact of slow temperature alteration with 180 cycles during the 6 months. Both tests have been destructive to concrete but with severer effect in the case of freeze-thaw cycles in water.

Concrete with low w/c ratios of 0.32 and 0.37 have managed to resist deterioration more than concrete with high w/c ratios of 0.40 and 0.46. Treating the low w/c ratio concrete with the sodium acetate compound has increased its resistance to deterioration unlike the high w/c ratio concrete. Treating high w/c ratio with sodium acetate has increased its deterioration rate more than untreated concrete, and deterioration was noticed to increase with increasing the added dosage of treatment. The opposite was noticed in the low w/c ratio concrete, where increasing the dosage has improved concrete resistance to deterioration. After both freeze-thaw tests have finished, water absorption and compressive strength of the deteriorated concrete were evaluated. All concrete samples have shown an increase in water absorption. However, this increase was minimum in the case of concrete with low w/c ratio, especially when treated with 4% sodium acetate. The maximum absorption rate was noticed in concrete with 0.46 w/c ratio and treated with 4% sodium acetate. Similar results were noticed after testing the deteriorated concrete for compressive strength. However, in the case of concrete that went through the air cyclic freeze-thaw, its compressive strength values did not change and remained similar to original values of non-deteriorated concrete.

REFERENCES

Al-Kheetan, M. J., Ghaffar, S.H., Madyan, O. A. & Rahman, M. M. (2020). Development of low absorption and high-resistant sodium acetate concrete for severe environmental conditions. *Construction and Building Materials,* 230, pp. 117057.

Al-Kheetan, M. J., Rahman, M., Muniswamappa, B. N. & Chamberlain, D. (2019c). Performance enhancement of self-compacting concrete in saline environment by Hydrophobic surface protection. *Canadian Journal of Civil Engineering.*

Al-Kheetan, M. J., Rahman, M. M. & Chamberlain, D. A., (2017). Influence of early water exposure on modified cementitious coating. *Construction and Building Materials*, 141, pp.

64-71.

Al-Kheetan, M. J., Rahman, M. M. & Chamberlain, D. A. (2018a). A novel approach of introducing crystalline protection material and curing agent in fresh concrete for enhancing hydrophobicity. *Construction and Building Materials*, 160, pp. 644-652.

Al-Kheetan, M. J., Rahman, M. M. & Chamberlain, D. A. (2018b). Development of hydrophobic concrete by adding dual-crystalline admixture at mixing stage. *Structural Concrete*, *19*(5), pp. 1504-1511.

Al-Kheetan, M. J., Rahman, M. M. & Chamberlain, D. A. (2018c). Remediation and protection of masonry structures with crystallising moisture blocking treatment. *International Journal of Building Pathology and Adaptation*, *36*(1), pp.77-92.

Al-Kheetan, M. J., Rahman, M. M. & Chamberlain, D. A., (2019a). Fundamental interaction of hydrophobic materials in concrete with different moisture contents in saline environment. *Construction and Building Materials*, 207, pp. 122-135.

Al-Kheetan, M. J., Rahman, M. M. & Chamberlain, D.A., (2019b). Moisture evaluation of concrete pavement treated with hydrophobic surface impregnants. *International Journal of Pavement Engineering.*

Al-Otoom, A., Al-Khlaifa, A. & Shawaqfeh, A. (2007). Crystallization technology for reducing water permeability into concrete. *Industrial & engineering chemistry research, 46*(16), pp. 5463-5467.

Bertolini, L., Elsener, B., Pedeferri, P., Redaelli, E. & Polder, R.B. (2013). *Corrosion of steel in concrete: prevention, diagnosis*, repair. John Wiley & Sons.

Brenna, A., Bolzoni, F., Beretta, S. & Ormellese, M. (2013). Long-term chloride-induced corrosion monitoring of reinforced concrete coated with commercial polymer-modified mortar and polymeric coatings. *Construction and Building Materials*, 48, pp. 734-744.

British Standards Institution BS 1881-125 (2013). *Testing concrete. Methods for mixing and sampling fresh concrete in the laboratory*, British Standards Institution, London.

British Standards Institution BS 1881-208 (1996). *Testing concrete. Recommendations for the determination of the initial surface absorption of concrete,* British Standards Institution, London.

British Standards Institution BS EN 12390-3 (2009). *Testing Hardened Concrete. Compressive Strength of Test Specimens,* British Standards Institution, London.

Cappellesso, V.G., dos Santos Petry, N., Dal Molin, D.C.C. & Masuero, A. B. (2016). Use of crystalline waterproofing to reduce capillary porosity in concrete. *Journal of Building Pathology and Rehabilitation, 1*(1), p. 9.

China Academy of Building Research (2009). *GB/T 50082-2009 Standard for test methods of long-term performance and durability of ordinary concrete,* Ministry of Housing and Urban-rural Development of China, Beijing, pp. 10-14.

Dai, J. G., Akira, Y., Wittmann, F. H., Yokota, H. & Zhang, P. (2010). Water repellent surface impregnation for extension of service life of reinforced concrete structures in marine environments: the role of cracks. *Cement and Concrete Composites*, *32*(2), pp.101-109.

De Vries, J. & Polder, R. B. (1997). Hydrophobic treatment of concrete. *Construction and Building Materials, 11*(4), pp. 259-265.

Dry, C. M. (2000). Three designs for the internal release of sealants, adhesives, and waterproofing chemicals into concrete to reduce permeability. *Cement and Concrete Research, 30*(12), pp. 1969-1977.

Falchi, L., Zendri, E., Müller, U. & Fontana, P. (2015). The influence of water-repellent admixtures on the behaviour and the effectiveness of Portland limestone cement mortars. *Cement and Concrete Composites*, 59, pp. 107-118.

Farnam, Y., Dick, S., Wiese, A., Davis, J., Bentz, D. & Weiss, J. (2015b). The influence of calcium chloride deicing salt on phase changes and damage development in cementitious materials. *Cement and Concrete Composites,* 64, pp. 1-15.

Farnam, Y., Esmaeeli, H. S., Zavattieri, P. D., Haddock, J. & Weiss, J. (2017). Incorporating phase change materials in concrete pavement to melt snow and ice. *Cement and Concrete Composites,* 84, pp. 134-145.

Farnam, Y., Wiese, A., Bentz, D., Davis, J. & Weiss, J. (2015a). Damage development in cementitious materials exposed to magnesium chloride deicing salt. *Construction and Building Materials*, 93, pp. 384-392.

Herb, H., Gerdes, A. & Brenner-Weiß, G., (2015). Characterization of silane-based hydrophobic admixtures in concrete using TOF-MS. *Cement and Concrete Research,* 70, pp. 77-82.

Jianxun, C., Xizhong, Z., Yanbin, L., Xianghui, D. & Qin, L. (2014). Investigating freeze-proof durability of C25 shotcrete. *Construction and Building materials,* 61, pp. 33-40.

Justnes, H., Østnor, T. A. & Barnils Vila, N. (2004). October. Vegetable oils as water repellents for mortars. In *Proceedings of the 1st international conference of Asian concrete federation, Chiang Mai* (pp. 28-29).

Kevern, J. T. (2010). Using Soybean Oil to Improve the Durability of Concrete Pavements. *International Journal of Pavement Research and Technology, 3*(5), pp. 280-285.

Li, K. (2017). *Durability Design of Concrete Structures: Phenomena, Modeling, and Practice.* John Wiley & Sons.

Lu, Z. & Zhou, X. (2000). The waterproofing characteristics of polymer sodium carboxymethyl-cellulose. *Cement and concrete research*, 30(2), pp. 227-231.

Ma, Z., Wittmann, F. H., Xiao, J. & Zhao, T. (2016). Influence of freeze-thaw cycles on properties of integral water repellent concrete. *Journal of Wuhan University of Technology-Mater. Sci. Ed., 31*(4), pp. 851-856.

Mehta, P. K. & Monteiro, P. J. M. (2006). *Concrete: microstructure, properties, and materials*. 3rd edn. New York; London: McGraw-Hill.

Shang, H. S. & Yi, T. H. (2013). Freeze-thaw durability of air-entrained concrete. *The Scientific World Journal.*

Shang, H. S., Yi, T. H. & Song, Y. P. (2012). Behavior of plain concrete of a high water-cement ratio after freeze-thaw cycles. *Materials, 5*(9), pp. 1698-1707.

Sun, W., Mu, R., Luo, X. & Miao, C. (2002). Effect of chloride salt, freeze–thaw cycling and externally applied load on the performance of the concrete. *Cement and Concrete Research, 32*(12), pp. 1859-1864.

Tang, S. W., Yao, Y., Andrade, C. & Li, Z. J. (2015). Recent durability studies on concrete structure. *Cement and Concrete Research, 78,* pp. 143-154.

Teng, L. W., Huang, R., Chen, J., Cheng, A. & Hsu, H. M. (2014). A study of crystalline mechanism of penetration sealer materials. *Materials, 7*(1), pp. 399-412.

Tittarelli, F. & Moriconi, G. (2008). The effect of silane-based hydrophobic admixture on corrosion of reinforcing steel in concrete. *Cement and Concrete Research, 38*(11), pp. 1354-1357.

Wu, Y. & Wu, B. (2014). Residual compressive strength and freeze–thaw resistance of ordinary

concrete after high temperature. *Construction and Building Materials, 54*, pp. 596-604.

Zhang, P., Wittmann, F. H., Vogel, M., Müller, H. S. & Zhao, T. (2017). Influence of freeze-thaw cycles on capillary absorption and chloride penetration into concrete. *Cement and Concrete Research, 100*, pp. 60-67.

Zhang, P., Wittmann, F. H., Vogel, M., Müller, H. S. & Zhao, T. (2017). Influence of freeze-thaw cycles on capillary absorption and chloride penetration into concrete. *Cement and Concrete Research, 100,* pp. 60-67.

Cite this article as: Al-Kheetan M. J., Rahman M. M., Ghaffar S. H., "Advanced Freeze-Thaw Assessment of Internally Integrated Concrete with Sodium Acetate", *International Conference on Civil Infrastructure and Construction (CIC 2020),* Doha, Qatar, 2-5 February 2020, DOI: https://doi.org/10.29117/cic.2020.0041

Reflective Crack Mitigation Using AST Interlayer over Soil-Cement Base for Flexible Pavements

Mohammad Reza-Ul-Karim Bhuyan
mrb4081@louisiana.edu
University of Louisiana at Lafayette, Lafayette, Louisiana, USA

Mohammad Jamal Khattak
khattak@louisiana.edu
University of Louisiana at Lafayette, Lafayette, Louisiana, USA

ABSTRACT

Flexible pavement over soil-cement base deteriorates over time due to reflective cracking caused by the shrinkage of such base. The propagation of the reflective cracks in overlaying hot mix asphalt (HMA) could be mitigated by installing interlayer system. State of Louisiana, USA has been utilizing Asphaltic Surface Treatment (AST) as an interlayer between the soil-cement base and HMA to mitigate reflective cracking. To evaluate the field performance of AST interlayer, flexible pavement projects with and without AST interlayer over soil-cement bases were compared in this study. From the Pavement Management System (PMS) database of Louisiana, 27 AST interlayer projects (70 miles) and 46 No AST interlayer projects (175 miles) were selected for comparison. The service lives of these projects were assessed using the time series cracking, rutting, and international roughness index (IRI) data. It was found that the projects with AST interlayer produced on average 14.3 and 14.7 years of service lives for transverse and alligator cracking, respectively. On the other hand, the average service lives of No AST interlayer projects were 11.6 and 12.5 years for such cracks, respectively. Hence, the AST interlayer projects gained 2.7 and 2.2 years of service life for transverse and alligator cracking, respectively. However, the service life based on rut data showed a loss of 3.2 years for AST interlayer projects (16.2 years). Furthermore, the longitudinal cracking and IRI exhibited no improvements. In summary, AST interlayer can mitigate transverse and alligator cracking but slightly increase the rutting potential of the pavement.

Keywords: Soil-cement base; AST interlayer; Reflective crack

1 INTRODUCTION

Cement stabilized soils are abundantly used in Louisiana as the base of flexible pavements due to its ease of construction, inexpensive nature and load carrying potential. Along with Louisiana, many other US states (TX, CA, MS, VA, NM, GA) are also constructing cement stabilized soil bases for last couple of decades. It's one of the available options for base construction when natural soils are not hard enough to carry extensive traffic load. But as a consequence of cement stabilization, such bases shrink during its long curing and hardening process. Hence, cement stabilized soil-cement bases always develop shrinkage cracks over time. After the construction of flexible pavement with such base, these shrinkage cracks start reflecting from the base to the overlying Hot Mix Asphalt (HMA) surface. For this reason, the cracking potential of such HMA layer

increases substantially and it causes considerable reduction of service lives for such pavements. To increase the service lives of such pavements, many US highway agencies are now striving to control these reflective cracks. (Titi et al., 2003); (Mursalin et al., 2001); (Quintus et al., 2009); Boudreau et al., 2016); (Adaska et al., 2004); (Louw & Jones, 2004); (Metcuff et al., 2001); (Sebesta & Scullion, 2004) and (Wu et al., 2018).

1.1 Reflective Crack Mitigation Techniques

There are many different alternatives for reflective crack mitigation in the existing literature. These alternatives include but are not limited to: Micro-cracking, inverted pavement or stone interlayers stress absorbing interlayers.

1.1.1 Micro-cracking

At the initial curing stage (1 to 3 days) of soil-cement base construction, a network of thin hairline cracks is purposely created by the compaction of high frequency steel vibratory roller. Afterwards, the soil-cement base loses its compressive strength temporarily, but it gains that back within few months. These network of hairline cracks are called micro-cracks which avert the soil-cement base from further crack widening. Hence, the micro-cracked base minimizes or prevents crack reflection from the base. This technique is now currently on the evaluation process in Louisiana, Texas and California. (Louw & Jones, 2004); (Sebesta & Scullion, 2004) and (Wu et al., 2018).

1.1.2 Inverted Pavements or Stone Interlayers

When a pavement is constructed by installing unbound compacted aggregates (4 to 8 inches thick) between the HMA layer and soil-cement base, it is called as an inverted pavement as its cross section looks like an inverted anvil. These aggregates or stones act as an interlayer and delays crack reflection and its propagation. This technique was first augmented in South Africa back in 1970s. Here in this case, unbound compacted aggregate traps the underneath shrinkage crack as it loses the propagation path. Currently, many US states (LA, NC, VA, NM, GA etc.) are evaluating the prospective of stone interlayer as a reflective crack control method for soil-cement bases for flexible pavements. (Boudreau et al., 2016); (Buchanan, 2010); (Vaughan, 2015); (Papadopoulos, 2014).

1.1.3 Stress Absorbing Interlayers

Installing a stress absorbing interlayer between soil-cement base and overlying HMA layer is another technique to mitigate reflective cracking. The shrinkage cracks are temporarily halted by the interlayer membrane and its propagation is delayed for substantial time. In this case, the interlayer member provides a firm base for the overlaying layer by arresting the crack underneath. Paving Fabrics are one example of such interlayers for PCC (Portland Cement Concrete) or granular bases for flexible pavements. (Fyfe, 2010); (Nonwoven, 1997) and (Gibb, 1992). Asphalt Rubber Membrane Interlayer (ARMI) is another example of effective stress absorbing interlayer for PCC or granular bases (West, 1994 & Scofield, 1989). Along with ARMI, several other fiber reinforced stress absorbing membrane interlayer (SAM or SAMI) are being used in USA as an effective interlayer for both PCC and HMA pavements (Metcuff et al., 2001); (Chowdhury & Button, 2007). There is not enough literature for stress absorbing

interlayer utilization for exactly soil-cement bases.

1.2 AST interlayer as a reflective crack mitigation technique in Louisiana

To mitigate or prevent reflective crack propagation on traditional soil-cement pavements, Louisiana have been implementing several techniques since 1990s. One of such techniques is the installation of AST (Asphaltic Surface Treatment) interlayer between cement stabilized soil-cement base and HMA layer. It's worth mentioning here that Asphaltic Surface Treatment (AST) is the application of a layer of liquid asphalt over the top of the soil-cement base followed by one stone thick loose aggregate spread and its compaction. If the process is repeated over the first layer of AST, then it is double layer or 2-course AST. AST is also called as Chip Seal treatment as it is a type of seal by aggregate chips. AST is usually being applied over HMA surface as a preventive type of treatment for long time but its utilization as an interlayer is relatively new and it was not found in the literature. (Nonwoven, 1997); (Gibb, 1992); (Gransberg & James, 2005); (Johnson, 2000); (Bolander, 2005); (Hicks, 2000).

Louisiana started utilizing AST as an interlayer on soil-cement base for flexible pavements from year 2000 as a means of reflective crack mitigation. In this research study, field performance of all those AST interlayer projects (2-course) were evaluated. About 70 miles of AST interlayer projects over soil-cement base were compared with about 175 miles of No AST interlayer projects for cracking, rutting and roughness. From all these comparisons, the extension of service lives was determined which measures the effectiveness of AST interlayer.

2 OBJECTIVES OF THE STUDY

The main objective of this study is to evaluate the actual field performance of AST interlayer and No AST interlayer projects on soil-cement bases for all distresses (cracking, rutting and roughness). This will be accomplished through the determination of service life extension caused by the application of AST interlayer on the soil-cement bases. Thus, this study will compare the service lives of AST interlayer and No AST interlayer projects over soil-cement bases for the above distress types.

3 RESEARCH METHODOLOGY

To achieve the objectives of the study, an orderly research methodology was developed and that is presented below:

3.1 Data Source and Data mining

Office of the pavement management system (PMS) manages Louisiana DOTD's mainframe database that contains the time-series distress data of all flexible pavements. Since 1995, these distress data have been recorded. These distress data include but not limited to following distresses and index: Transverse Cracking (TC), Longitudinal Cracking (LC), Alligator Cracking (AC), Rutting and International Roughness Index (IRI). For each 1/10th mile pavement sections, all these distress data and indexes are recorded. It's worth mentioning here that a soil-cement project could be miles longer and each miles of project would include 10 pavement sections, hence 10 data points for

all distresses. As an example, a 3.5-mile-long project would have thirty-five 1/10th mile sections or data points. For each 1/10th mile sections: TC, LC, AC, Rutting, IRI data are available from year 1995 to 2017 in PMS database. These data could be used for the performance evaluation of those 1/10th mile sections or entire projects.

With the help of the office of PMS, district engineers and information available in Treatment of Projects (TOPS), all the candidate AST interlayer and No AST interlayer projects were identified. Moreover, Traffic data and pavement system data (thickness of HMA and bases) were tabulated for each project.

3.2 Pavement Section Selection

With the help of MATLAB (2016b) and "MS Excel Visual Basics for Application (VBA) 2016", each 1/10th mile sections distress data (TC, LC, AC, Rutting, IRI data) were acquired from the identified candidate projects. All these time series distress data are modelled as a function of time using generic models shown in table 1. Now, as these data did not always behave properly, rational criteria were set for acceptable data selection. Hence, following criteria were augmented for the acceptation of 1/10th mile pavement section for use in these analyses:

1. Minimum three data points. Each 1/10 pavement section must have at least 3 data points as any non-linear model (shown in table 1) could not be fit without 3 data points. Hence, any section that does not have at least 3 data points, were rejected for analyses.

2. Positive gain in distress. After any pavement construction, the distress values should be generally increasing over time. Hence, when the appropriate models(shown in Table 1) were fit to the distress data, the parameters β, ω, θ, or μ should be positive for each 1/10 th mile pavement sections. If the parameters were negative, it means that the pavement is healing over time, which is not reasonable. It may happen because of small treatments which were given to the pavement section that reduces/eliminates the distress data value. Hence, those sections with negative parameters were not included in these analyses. Figure 1 shows an example of accepted and rejected section for the acceptable criteria illustration.

Table 1: Generic Pavement Performance Models (Baladi, 2015)

Form of equation	Pavement distress type (model form)		
	IRI (exponential)	Rut depth (power)	Cracking (Logistic (S-shaped))
Generic equation (modelling)	$IRI = \alpha \exp^{t\beta}$	$Rut = \gamma\, t^{\omega}$	$Crack = \frac{Max}{1 + \exp^{(\theta+\mu t)}}$
Service Life (SL) = Time to reach threshold	$t = \frac{\ln\left(\frac{Threshold}{\alpha}\right)}{\beta}$	$t = exp\left[\frac{ln\left(\frac{Threshold}{\gamma}\right)}{\omega}\right]$	$t = \left[\frac{1}{\alpha}\left(\ln\left(\frac{Max}{Threshold}\right) - 1\right)\right] - \left(\frac{\beta}{\alpha}\right)$
Where, α, β, γ, ω, θ, and μ are regression parameters α,γ, θ are intercepts and β, θ, ω, μ are slopes) t = elapsed time (year), and Max = the maximum value of cracking			

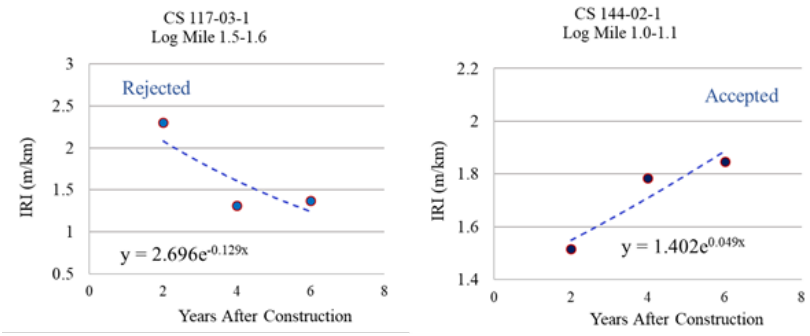

Figure 1: Acceptance Criteria Illustration

Now, any pavement sections have almost zero cracking/rutting and minimum roughness immediately after construction. Hence, one initial data point could be reasonably assumed for a better fit and it also increases the number of accepted data points. Therefore, initial values for distress data were assumed as 0.079 m, 0.67 m/km and 0.0254 cm for cracking, rutting and IRI, respectively. Also, small values (0.3048 m) for cracking are assumed when crack is zero at any year after construction as non-linear model cannot take zero values.

3.3 Service Life Computations

To evaluate the performance of AST interlayer pavements, the service lives of 1/10th mile sections are calculated from table 1 for each distress types (TC, LC, AC, Rutting, IRI). The threshold values of all distress types for SL computations were selected as 3.2 m/km, 1.27 cm, 322.5 m, 322.5 m and 117.7 m2 for IRI, Rut, Transverse Cracking (TC), Longitudinal Cracking (LC), Alligator Cracking (AC), respectively. MATLAB (2016b) and Excel VBA (2016) was utilized to gather and organize all the pavement sections. Using the models shown in table 1, the service lives of all sections were calculated. Its worth mentioning here that any pavement section that generates more than 20 years of service lives by the models, are considered to have only 20 years service life, as the design life of these pavements were only 20 years. Also, all the sections shown here have ESAL: 0-30000, thickness of HMA: 0-4 inches and they have 5 to 7 years of surface age. All AST and No AST soil-cement pavement sections were gathered separately and a histogram of service lives were generated for each of the two categories for comparison. Figure 2 shows the histogram comparison of Transverse Cracking for AST and No AST pavement sections:

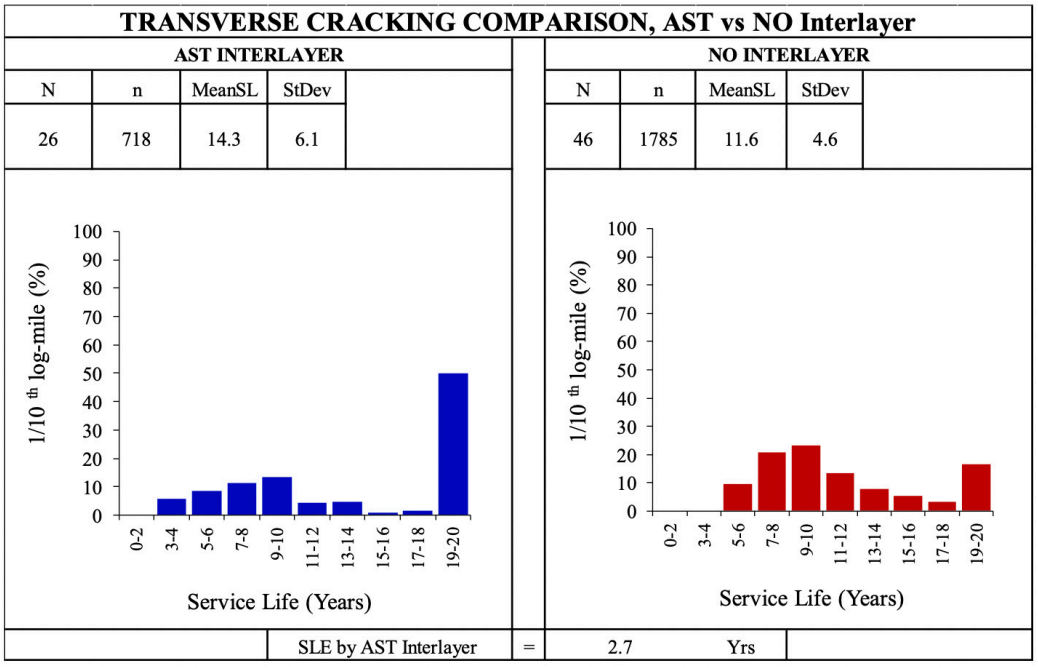

Figure 2: Transverse Cracking Comparison, AST vs No AST interlayer

Percentage of sections are shown at the y-axis of the histogram and service lives (with a bin of 2 years interval) plotted at the x-axis. The arithmetic mean of all service lives of all sections (MeanSL, as shown in the figure 2) were calculated for both AST and No AST sections. Standard Deviation (StDev, as shown in the figure 2) of service lives were also shown in this figure. Here in this figure: N= number of projects available for the group, n= number of accepted 1/10th miles sections for the group. Now, from Figure 2, it is obvious that 26 AST interlayer projects were accepted which includes 718 1/10th miles of sections (=71.8 miles). The arithmetic mean of the services lives of these sections were 14.3 years and these sections have a standard deviation of 6.1 years. For No AST interlayer, 46 projects with 1785 1/10th miles (=178.5 miles) of sections were accepted for analysis and these sections have a MeanSL of 11.6 years.

Finally, Service Life Extension (SLE) is calculated to evaluate the performance of AST interlayer by the following equation:

$$SLE = MeanSLAST - MeanSLNoAST \qquad (1)$$

Here, the Service Life Extension (SLE) for TC is 2.7 years (14.3-11.6=2.7 years) for AST interlayer. It means, on average, AST pavements provide 2.7 years of service life extension when compared to No AST pavements. From the histogram comparison, it is clear that AST pavements are better than No AST pavements as far as TC is concern. Here, 50% of AST section has 20 years of SL whereas only 20% of No AST section has 20 years of service life.

Similar figures were developed for AC and Rutting and shown in the next chapter. SLE is calculated for each of the distress types and the prospective of AST as interlayer

were evaluated from those SLE values. It's worth mentioning here that SLE could be either of positive or negative values. If SLE values are negative, it would mean that AST had reduced the service lives of pavement on average.

4 RESULTS AND DISCUSSION

Figure 3 and Figure 4 show the histogram comparison of AC and Rutting. From figure 3, it is manifest that AST interlayer extends the life of pavements by 2.2 years on average. Moreover, 60% of sections for AST interlayer had minimum 20 years of service life. Whereas, only 30% sections had minimum 20 years of service life for No AST interlayer sections. There are enough data present on both sides in this comparison, hence these results are conclusive.

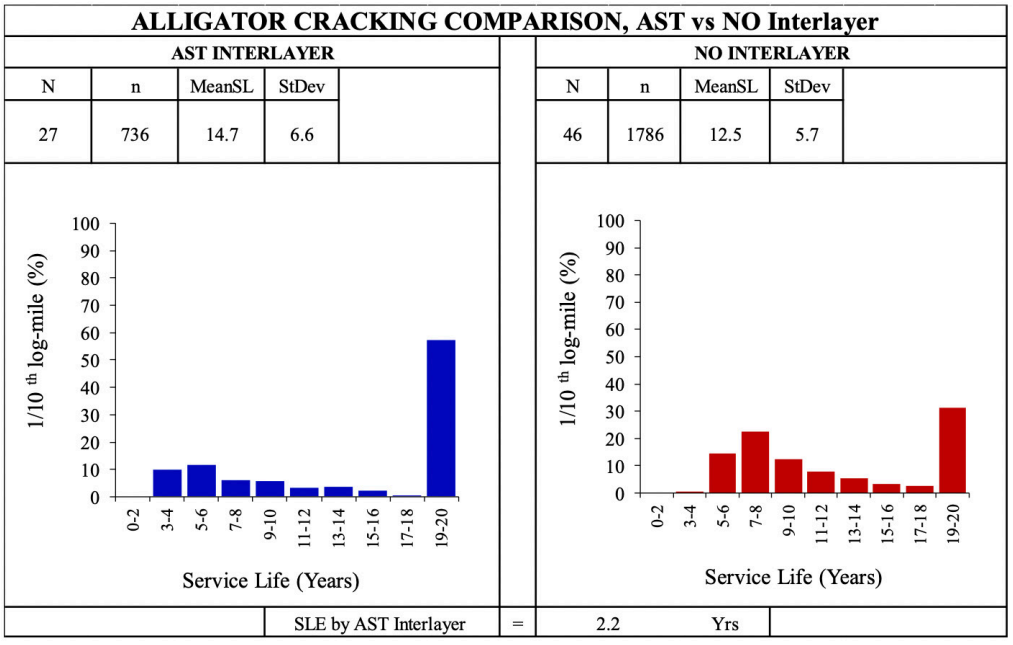

Figure 3: Alligator Cracking Comparison, AST vs No AST interlayer

The rutting potential of AST and No AST interlayer sections were evaluated at figure 4. The AST interlayer sections here behaved worse than the No AST interlayer sections. There is no failure of pavements for No AST sections, as almost 100% sections had minimum 20 years of service lives (MeanSL = 20.0 years). But for AST interlayer sections, only around 60% sections had minimum 20 years of service lives, another 40% (around) sections failed before the pavements design service life of 20 years. These 40% sections service lives are distributed between 5 to 19 years, which could be ascertained from the histogram. As a result, the MeanSL for rutting reduces significantly from 20.0 years to 16.8 years. Consequently, the SLE for rutting became negative: -3.2 years.

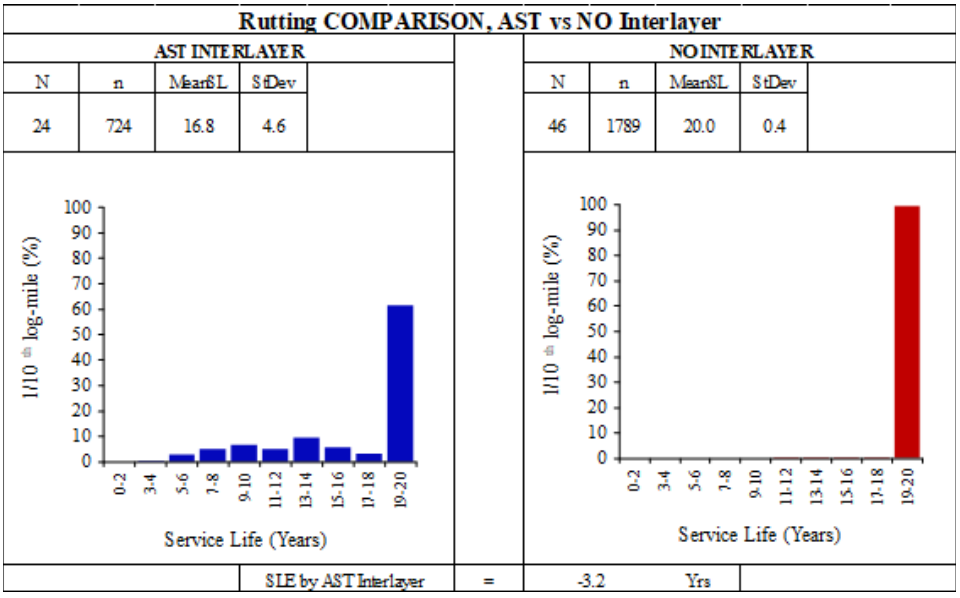

Figure 4: Rutting Comparison, AST vs No AST interlayer

Similar analyses were performed for LC and IRI and it was found that MeanSL for No AST and AST pavements were 16.0 and 15.3 years, respectively for LC; 19.7 and 18.3 years, respectively for IRI. Subsequently, the SLE by AST interlayer is -0.6 years and -1.3 years, respectively for LC and IRI. Hence, roughness and longitudinal crackings are largely unaffected by AST interlayer, as their MeanSL were very similar and SLE values were not large enough.

To summarize, AST interlayer had improved cracking performance of flexible pavements over soil-cement bases, as it extends the service lives of pavement sections by 2 to 3 years (for TC and AC). It also does not change the overall roughness and LC potential of pavement sections. But AST interlayer creates unwanted rutting to the pavement and reduces the service lives for around 3 years for rutting.

5 CONCLUSION

Here in this research, the performance of 70 miles of AST interlayer projects were compared with 175 miles No AST interlayer projects over soil-cement bases. Based on the comparisons, it was found that AST interlayer did mitigate reflective cracking by extending the average service lives of pavements by 2 to 3 years for Transverse and Alligator cracking. In case of longitudinal cracking and IRI, the performance of pavements was largely unaffected by AST interlayer. As far as rutting is concerned, AST interlayer exhibits undesirable rutting in the pavements, and it reduces the service lives by 3 years due to rutting. As these results are supported by more than 70 miles of distress data, the findings of this study are conclusive. Hence, AST interlayer is only recommended as a reflective crack mitigation technique when the rutting of pavements is not a concern for any highway agency.

ACKNOWLEDGEMENTS

The authors would like to thank Mark Martinez, Kevin Gaspard as well as project review committee for their efforts and valuable input to assist in the data acquisition and project identifications. Special thanks to LTRC, DOTD to fund the research project and University of Louisiana to accommodate the research.

REFERENCES

Adaska, W.S. & D. Luhr. (2004). Control of Reflective Cracking in Cement Stabilized Pavements. *In 5th International RILEM Conference, France*, 2004.

Baladi, G. & Khattak, M. J. (2015). Development of Cost Effective Treatment Performance and Treatment Selection Models. *Louisiana Department of Transportation and Development.*

Boudreau, R., Vaughan, K. & Frost, D. (2016). *Interved Pavements.* [TRB Webinar]. Washington, D.C.

Bolander, P. (2005). Seal Coat options: taking out the mystery. *In First National Conference on Pavement Preservation*, Missouri.

Buchanan, S. (2010) Inverted Pavement Systems, South Africa.

Chowdhury, A. & Button, J. (2007) Evaluation of FiberMat® Type B as a Stress Absorbing Membrane, Texas Transportation Institute, Texas A&M University, College Station, Texas.

Fyfe, R. (2010) *Geotextile Reinforced Seals Under Asphalt*. Department of Transport, Energy and Infrastructure, South Australia, New South Wales.

Gibb, I. (1992). Chip Sealing in the Shire of Broome Australia. In Geosynthetics World, London, the UK.

Gransberg, D., James, D. M. B. (2005). *Chip Seal Best Practices. NCHRP Synthesis of Highway Practice*, 342.

Hicks, G.R., Seeds, S.B. & Peshkin, D.G. (2000) *Selecting a preventive maintenance treatment on flexible pavements.* Foundation of Pavement Preservation.

Johnson, A. (2000). *Best practices Handbook on Asphalt Pavement Maintenance*. Center of Transportation Studies.

Louw, S. & Jones, D. (2015). *Pavement Recycling: Literature Review on Shrinkage Crack Mitigation in Cement-Stabilized Pavement Layers*. University of California: Pavement Research Center, Technical Memorandum.

Metcuff, J. B., Roberts, F. L. & Rasoulin, M. (2001) *Construction and Comparison of Louisiana's Conventional and Alternate Base Courses Under Accelerated Loading*. Louisiana Transportation Research Center, Baton Rouge.

Mursalin, M., Titi, H., Martinez, M., Bercel, B. & Keel, G. (2001) *Long Term Performance of Stone Interlayer Pavement*. Louisiana Transportation Research Center.

Nonwoven Paving Fabrics Study, Industrial Fabrics Association International, Austin, TX, 1997.

Papadopoulos, E. G. (2014). *Performance of Unbound Aggregate Bases And Implications For Inverted Base Pavements*. Georgia Institute of Technology.

Quintus, H. L., Mallela, V. J., Weiss, W. & Shen, S. (2009). *Techniques for Mitigation of Reflective Cracks*. Applied Research Associates, Inc.

Scofield L. A. (1989). *The History, Development and Performance of Asphalt Rubber at ADOT.* Arizona Transportation Research Center, Phoenix, Arizona.

Sebesta, S. & Scullion, T. (2004) *Effectiveness Of Minimizing Reflective Cracking In Cement Treated Bases By Microcracking*. Texas Transportation Institute.

Titi, H., Rasoulian, M., Martinez, M., Becnel, B. & Keel, G. (2003). Long-Term Performance of Stone Interlayer Pavement. *Journal of Transportation Engineering*, ASCE.

Vaughan, K. (2015). Inverted Pavement. Vulcan Materials Company, South Africa.

West, K. (1994). *Field Performance of Asphalt-Rubber Interlayers*. Texas Transportation Institute, Austin, Texas.

Wu, Z., Liu, Y. & Intaj, F. (2018) *Minimizing Shrinkage Cracking in Cement-Stabilized Bases through Micro-Cracking*. Louisiana Department of Transportation and Development, Baton Rouge.

Cite this article as: Bhuyan R.-U.-K. M., Khattak J. M., "Reflective Crack Mitigation Using AST Interlayer Over Soil-Cement Base For Flexible Pavements", *International Conference on Civil Infrastructure and Construction (CIC 2020)*, DOI: https://doi.org/10.29117/cic.2020.0042

Using Reclaimed Asphalt and Polymer Modified Asphalt (PMA) to Maximize Cost Saving over the Pavement Life-Cycle in Qatar

Jean Khnaizer
jkhnaizer@hotmail.com
JH Construction W.L.L., Doha, Qatar

ABSTRACT

Low performing asphalt mixes along with poor construction practices reduce the pavement serviceability and lead to early failure under repetitive traffic. Government agencies are sometimes urged to implement maintenance and rehabilitation at earlier stages throughout the pavement lifecycle. As an innovative pavement material solution, Polymer Modified Asphalt (PMA) along with an optimized recycled asphalt (RA) content in the recycled hot-mix asphalt (HMA) provide higher performance for the hot asphalt mixes (HMA) with an upfront saving on the cost of material, and a reduced maintenance cost over the lifecycle of pavement. While the mix performance is driven by various factors, RA characteristics and PMA properties contribute to the performance of HMA. In this study, RA and PMA mixes were produced using an existing target Job Mix Formula (JMF) of a dense graded 19.0 mm Nominal Maximum Aggregate Size (NMAS) and Pen 60/70 neat asphalt binder. Five recycled HMA were produced using respectively RA content ranging from 15 to 35%. PMA was added to every mix at a fixed percentage in order to match mixes using PMB PG 76E-10 (extremely heavy traffic with ESALs > 30 million). The Marshall mix design method was used to verify the properties of the recycled HMA. This paper highlights the benefits of using PMA with RA in Qatar as an ultimate solution that provides durability, values, and reduced maintenance cost over the lifecycle of the pavement.

Keywords: Polymer modified asphalt; Reclaimed asphalt; Pavement life-cycle; Cost analysis

1 INTRODUCTION

The cost of rehabilitation and maintenance of pavement increases especially when the pavement life is shorter than designed, and when it is impacted by various factors such as unanticipated traffic loads and harsh weather conditions that do not align with the appropriate binder grade selection. Moreover, the cost aspects such as material, construction overhead, and maintenance need to be properly assessed to optimize cost over the pavement lifecycle (Chen et al., 2002). Low performing asphalt mixes along with poor construction practices reduce the pavement serviceability and lead to early failure under repetitive traffic. Poor quality pavement causes governments to implement maintenance and rehabilitation at earlier stage throughout the pavement lifecycle (Cooper, 2011).

2 MAIN RESEARCH TOPIC AND WORK METHODOLOGY

Transportation authorities continuously seek innovative solutions and technologies

that increase pavement durability and life. Among those innovative products, Polymer Modified Asphalt (PMA) along with an optimized content of reclaimed asphalt (RA) in recycled hot-mix asphalt (HMA) provide a performing and durable pavement with the advantage of an upfront saving on the cost, and they reduce the maintenance cost over the lifecycle of pavement (Bennert et al., 2014). The main objective of this study was to compare the quality characteristics and cost of production of various mixes using PEN 60/70, PMB and CRMB with recycled HMA in the state of Qatar. However, the study aimed to highlight the upfront costs and reduction of maintenance cost over the lifecycle of pavement associated with each mix. The reduction in maintenance was assumed based on the potential need of performing preventive maintenance throughout the pavement life taking into consideration that the typical failures of the roads in Qatar are either fatigue crack or rutting due to pavement densification under repetitive traffic.

3 THE RESEARCH APPROACH

The thirteen mixes, summarized in Table 1, were developed using PEN 60/70, PMA, PMB 76E-10 and CRMB binder while considering 15 and 30% RA content in mix (Zaumanis et al., 2014) in addition to using rejuvenator (Mogawer et al., 2016) for mixes with 30% RA. Dense graded asphalt mixtures with a 19-mm Nominal Maximum Aggregate (NMAS) were produced to encompass the various asphalt mixes. Four replicates were collected from each mix, and tested according to Marshall method (Asphalt Institute, 2007) and Qatar Construction Specification (QCS, 2014). The Tensile Strength Ration (TSR) and in-place air void were reported and summarized in Table 3. Moreover, the cost analysis per ton of asphalt mix ex-plant was based on the raw material actual rates as of October 2019 (Figure 1). For the Life cycle assessment, samples were tested in accordance with EN 12697-31 by compaction of cylindrical specimens of bituminous mixtures using a gyratory compactor N_{max} = 200 load cycles so that the specimens represented the mixture at the end of its life cycle.

Table 1: Details of HMA Mixes

Mix Detail	Description and Application	Comment
TQ (PEN 60/70)	Highway and Local road, medium to high traffic	Currently Applied
TQ_r (PEN 60/70) +15% RA	Local road, low to medium traffic + 15% RA	Currently Applied
TQ_{rmax} (PEN 60/70) + 30% RA	Local road, low to medium traffic + 30% RA + Rejuvenator	Not applied
PMA (9%)	Highway, medium to high traffic with PMA	Not applied
PMA_r (5%) + 15% RA	Local road, low to medium traffic + 15% RA with PMA	Recommended
PMA_{rmax} (5%) + 30% RA	Local road, low to medium traffic + 30% RA with PMA	Recommended
PMA_{rmax} (9%) + 30% RA	Highway, high traffic + 30% RA with PMA+ Rejuvenator	Recommended
PMB (PG 76E-10)	Highway, medium to high traffic	Currently applied
PMB_r (PG 76E-10) + 15% RA	Local road, low to medium traffic + 15% RA	Not applied
PMB_{rmax} (PG 76E-10) + 30% RA	Highway, high traffic + 30% RA+ Rejuvenator	Not applied
CRMB (PG 76E-10)	Local roads, medium to high traffic	Currently Applied
$CRMB_r$ (PG 76E-10)	Local road, low to medium traffic + 15% RA	Currently Applied
$CRMB_{rmax}$ (PG 76E-10)	Highway, high traffic + 30% RA+ Rejuvenator	Not applied

4 RESULTS AND DISCUSSION

Through trends analysis, PMA_{rmax} (5%) mix had shown the most performing mix providing the most economical rate per ton compared to the mixes using PMB and CRMB. With PMA_{rmax} (5%): the saving is 8.3% saving on cost, 16.9% on aggregates,

and 16.6% saving on bitumen. PMA_{rmax} (5%) and 30% RA is recommended for local road projects as it provides upfront saving and reduction of cost on the future maintenance considering the projected traffic and a minimum 10 years life of pavement. At N_{max}=200, comparison of results in Table 2 comprised only mixes with 30% RA using respectively PEN 60/70, PMB PG 76E-10 and PMA (at 9%).

Table 2: Volumetric Characteristic of PMB and PMA Mixes

Parameter	**PEN 60/70 Mix** TQ_{rmax} (PEN 60/70) + 30% RA	**PMB PG 76E-10 Mix** PMB_{rmax} (PG 76E-10) + 30% RA	**PMA Mix** PMA_{rmax} (at 9%) + 30% RA
Mix Density, G_{mb}	2.674	2.623	2.602
Air Void, V_a, %	1.6	2,7	3,4

Figure 1: Summary of Selected Parameters

Table 3: Summary of Test Results

Mix Designation	Marshall Properties							In-Place Air Void (cores)	Cost of HMA per ton
	V_a	VMA	VFB	Stability	Flow	Stiffness	TSR	Void	QAR
	%	%	%	kN	mm		%	%	149.45
TQ	6.1	14.9	59.0	14.0	2.7	5.2	79.0	6.7	149.45
TQ_r	6.5	15.1	57.1	14.1	2.7	5.2	80.0	6.0	132.64
TQ_{rmax}	7.8	15.9	50.9	14.0	2.5	5.6	85.0	5.4	115.48
PMA (9%)	7.2	16.6	58.0	17.6	2.8	6.0	89.0	7.9	179.45
PMA_r (5%)	7.5	16.2	57.0	17.1	2.7	6.3	92.0	6.5	148.96
PMA_{rmax} (5%)	8.2	15.9	62.0	18.9	2.5	7.6	93.0	5.4	131.62
PMA_{rmax} (9%)	7.8	16.7	61.0	19.2	2.9	6.6	94.0	5.8	143.56
PMB	7.0	15.0	56.0	17.9	3.0	5.9	81.0	6.2	191.07
PMB_r	7.1	15.7	54.8	17.3	2.8	6.2	83.0	5.9	152.09
PMB_{rmax}	7.6	16.0	52.5	17.9	2.8	6.4	85.0	5.4	147.47
CRMB	6.2	15.2	59.4	17.7	2.8	6.3	79.0	7.2	177.98
$CRMB_r$	6.6	15.7	58.0	16.5	2.6	6.3	81.0	6.8	156.55
$CRMB_{rmax}$	7.8	15.9	50.9	17.5	2.9	6.0	84.0	6.6	149.16

5 CONCLUSION

PMA is an innovative technology that maximizes cost saving, extends pavement serviceability, and improves production time and quality of asphalt against the currently available solutions within an economic and ecological perspective (Li et al., 2014). Moreover, PMA enables HMA producers to create mixes with high performance, as well as exhibiting resistance to fatigue and rutting (Becker et al., 2002). Compared to PMB and CRMB mixes, PMA offers equal and higher performance characteristics with the advantages of a considerable cost saving over the lifecycle of pavement assumed based on the in-place air void closer to the end life of the pavement. This indicates that early failure such as rutting is less likely to happen due the lower densification rate under traffic compared to the same mixes using PMB or PEN 60/70 binders.

Combined with RA, PMA offers a great value engineering solution where sustainability, upfront saving, and throughout pavement lifecycle saving are clearly demonstrated and measured. Moreover, PMA allows the reduction in asphalt thickness without reduction in performance of lifecycle of pavement, in addition to the reduction in pollutant emissions such as CO_2, SO_2, NO_x and PM_{10} due to less production and working hours of plant and machinery.

6 RECOMMENDATION

In this study, various laboratory and field tests were conducted to evaluate the effect of PMA solution compared to other traditional and alternative HMA mixes. It was found that PMA with 30% RA in recycled HMA provides an economic solution that can sustain a low maintenance over the lifecycle. However, further investigation to have a reliable performance prediction is needed besides testing the mixtures performance characteristics such as permanent deformation, rut depth, fatigue, modulus and sensitivity to moisture using Superpave method.

REFERENCES

Asphalt Institute (2007). *The Asphalt Handbook: MS-4*. 7th Ed., Lexington, KY.

Becker, Y., Mendez, M. P. & Rodriguez, Y. (2001). Polymer modified asphalt. *Vis. Technol., 9*(1), 39-50.

Bennert. T., Daniel Jo, S. & Mogawer, W. (2014). Strategies for incorporating higher recycled asphalt pavement percentages – Review of implementation trials in northeast states. *Journal of the Transportation Research Board*, 2445, 83-93.

Chen, J. S., Liao, M. C. & Tsai, H. H. (2002). Evaluation of optimization of the engineering properties of polymer-modified asphalt. *Pract. Failure Analysis, 2*(3), 75-83.

Cooper, S. J. (2011). Asphalt Pavement Recycling with reclaimed asphalt pavement (RA). *NWPMA, 18th Annual Fall Pavement Conference*. FHWA, Portland, OR.

EN 12697-31: (2019). Bituminous mixtures - Test methods - Part 31: Specimen preparation by gyratory compactor.

Li, J., Ni, F., Huang, Y. & Gao, L. (2014). New additive for use in hot in-place recycling to improve performance of reclaimed asphalt pavement mix. *Transportation Research Record: Journal of the Transportation Research Board, 2445*(1), 39-46.

Mogawer, W. S., Austerman, A. J., Kluttz, R. & Puchalski, S. (2016). Using polymer modification and rejuvenators to improve the performance of high reclaimed asphalt pavement mixtures. *Journal of the Transportation Research Boar*, 2575, 10-18.

Qatar Construction Specification (2014). Section 6 Parts 5 & 9, Doha, Qatar.

Zaumanis, M., Mallick, R. B. & Frank, R. (2014). Determining optimum rejuvenator dose for asphalt recycling based on superpave performance grade specifications. *Construction and Building Materials*, 69, 159-166.

Cite this article as: Khnaizer J., "Using Reclaimed Asphalt and Polymer Modified Asphalt (PMA) to Maximize Cost Saving over the Pavement Life-Cycle in Qatar", *International Conference on Civil Infrastructure and Construction (CIC 2020)*, Doha, Qatar, 2-5 February 2020, DOI: https://doi.org/10.29117/cic.2020.0043

Producing High Quality Recycled Hot Asphalt with Increased Reclaimed Asphalt Content – Qatar Experience

James Maina
james.maina@up.ac.za
Department of Civil Engineering, University of Pretoria, Pretoria, South Africa

Jean Khnaizer
jkhnaizer@hotmail.com
JH Construction W.L.L, Doha, Qatar

ABSTRACT

Under the Public Works Authority (PWA) maintenance framework contract in the State of Qatar, road rehabilitation and maintenance generate considerable amounts of Reclaimed Asphalt (RA) than can be used in recycled Hot Mix Asphalt (HMA). Therefore, there is a great necessity to develop a national experience to understand the constraints and limitations of increasing RA content in recycled HMA while aligning this with the PWA initiatives on using and increasing RA in HMA. This paper sets out a guideline on how to increase RA content in HMA, considering the RA and virgin material characteristics, setup and capabilities of the asphalt plant. The study aimed to produce several recycled HMA mixes with increased RA contents using a dense-graded 19.0 mm Nominal Maximum Aggregate Size (NMAS) PEN 60/70 mix. Instead of performing design for each RA content, adjustments on the blending proportions were made accordingly as such to meet the same Job Mix Formula (JMF) of an approved HMA mix. Characterizing the RA besides data of the virgin material properties helped in adjusting the proportion during the HMA production as such to meet the control JMF. Qatar Construction Specification (QCS) 2014 was used to benchmark the results of various HMA mixtures that were prepared according to the Marshall mix design method. This paper draws a practical guideline and best practices on how to produce and optimize RA content in recycled HMA, in addition to highlighting and improving key parameters surrounding the production, from milling to laying, to produce stable, workable yet performing mixes.

Keywords: Reclaimed asphalt; Recycled asphalt mix; Job mix formula; Marshall properties

1 INTRODUCTION

Reclaimed asphalt (RA) in recycled hot-mix asphalt (HMA) is an invaluable component of asphalt mixes as it provides economic and environmental benefits. When managed efficiently, the generated RA material creates value for both the client and the contractor, as it aligns with the Public Works Authority (PWA) roadmap for recycling initiatives and the requirements for the Zonal Framework contract for road maintenance. However, it is important to set a general guideline and practical means to design, produce, and place HMA mix with high RA content to improve the experience of using RA in recycled HMA in Qatar. Due to the fluctuation of RA material characteristics as a result of variation in source and cold panning process, additional challenges impact

the consistency of recycled HMA mixes. However, adequate cold planning, stockpiling management, and further processing of RA material prior to recycled HMA production improves its quality and extend visibility to control identified variables.

Additionally, proper evaluation and characterization of RA material allows for a dynamic adjustment during HMA production, which thus enables consistent recycled HMA properties. When properly designed, recycled asphalt mixes are expected to perform equally or better than HMA with 100% virgin material (Reyes-Ortiz et al., 2012). With higher RA content, there are more benefits and value (NAPA, 2015); further challenges related to the rheological properties of aged binder would impact the combined blended binder (AASHTO, 2010).

Alternatively, key production parameters need to be addressed considering the RA characteristics and content in the mix, and the properties of the virgin material to use in the recycled HMA (Willis et al., 2013). In other words, the production parameters need to be carefully examined during every stage of the production process encompassing the cold planning (milling process), management, mix design, plant verification, placing, compacting and quality control.

2 MAIN RESEARCH TOPIC AND WORK METHODOLOGY

While recycled HMA is an economic and strategic choice for road rehabilitation and maintenance, it reduces the utilization of virgin aggregates and binder and provides a sustainable solution for aggregate consumption. Considering that Qatar imports Gabbro and lacks high quality aggregate suitable for HMA, it is important to align the usage of RA with PWA initiatives to use and increase RA in recycled HMA mixes. This research aims to develop an understanding of constraints to increase high RA content in asphalt mix on one hand, and to get insight on limitations in the mix during HMA construction on the other hand. Necessary information, process related parameters and test results were collected from the various activities carried to produce the recycled HMA, starting from cold planning to stockpile management, screening and characterization of RA, production of recycled HMA, and placement and compaction of the recycled asphalt mix.

2.1 Cold planning

Prior to cold planning, coring was performed in different locations of the selected road sections to assess the existing pavement type and the number of layers, thicknesses and the aggregate used in each layer. Knowing the core thickness helped to determine the depth of milling that was carried at 95% of the total asphalt layer(s) thickness as such to avoid contamination with the underneath layer, especially when such layer is an unbound material (roadbase or subbase). The following details were recorded: 1) source (i.e. location, chainage, number of layers, total thickness, age of pavement); 2) date of milling and the generated quantity; 3) milling depth and number of layers; and, 4) stockpile identification number.

2.2 Stockpile management characterization

After milling, the RA material was shifted to the asphalt plant yard and stockpiled as such to avoid segregation and/or contamination with foreign material (Hussain &

Yanjun, 2013). The main RA stockpile collected from milled material was screened to produce two sizes of RA, respectively 0-5 and 5-21 mm. The two screened RA sizes were stockpiled and identified for characterization: gradation, binder content, the grade of recovered binder and moisture content. The characterization data combined with the details of the virgin material were used to determine the right proportion and necessary adjustment to make during the production of recycled HMA.

2.3 Asphalt plant details

The production facility used in this study was a CB 240 AMMANN asphalt batching plant, having a capacity of 240 tons/h and equipped with a ring in dryer to process up to 40% of RA in the mix.

3 THE RESEARCH APPROACH

In this paper, six different recycled HMA mixes were prepared using respectively, 15, 20, 25, 30, 35 and 40% RA content, and they were used in a dense-graded 19.0 mm Nominal Maximum Aggregate Size (NMAS) Pen 60/70 HMA mix. HMA samples were prepared according to the Marshall mix design method (Asphalt Institute, 2007). The main goal of producing the six mixes was based on meeting the limits of the Job Mix Formula (JMF) of an existing mix design used as a control reference to produce and compare results with the ones of the mix using 100% virgin material. The objective of this study is to explore the extent and limitations at the mix level and compliance with QCS, and thereafter to identify the constraints during production and construction of the recycled HMA layers (Willis et al., 2013). The same aggregates, filler type and neat binder source were used to produce the six recycled HMA batches. The virgin aggregate was gabbro imported from Oman, while the neat binder was Pen 60/70 supplied by Qatar petroleum (Woqod).

During the production of recycled HMA, the HotBin aggregate gradation and percentage of neat binder were considered to continuously adjust the recipe to meet the reference control JMF as stipulated in the approved mix design certificate. The recovered binder was PG 70-22, while the extracted aggregate was gabbro. For recycled HMA mixes using RA above 20%, a rejuvenator at 0.1% of the total binder in mix was added during HMA mixing. The rejuvenator improves the binder performance and the asphalt mix workability at higher RA content (Cooper, 2011); thus, it allows to achieve adequate compaction efforts during construction at lower compaction temperature range.

Approximately 200 tons of each mix were produced. Six samples from each mix were collected to assess the Marshall properties (QCS, 2014), binder content and gradation (Figure 1). Moreover, asphalt was paced and compacted in one 70 mm layer. Cores were extracted afterwards from the constructed layer to assess the in-place air void.

4 RESULTS SUMMARY AND DISCUSSION

While the purpose of this study was to increase RA content in recycled HMA, evaluate and optimize the processes surrounding the production (Willis et al., 2013) from milling to asphalt mix production, the goal was to establish a general guideline for best practices to produce consistent and performing recycled HMA with high RA and enable contractors to overcome related challenges (West, 2015). However, it is required

to maintain high-quality control on RA material and exact proportion and adjustment throughout the asphalt production process to help achieve consistent, compliant yet constructible and performing mixes.

Based on the analysis of the trend of results of the six recycled HMA mixes and the mix with virgin material (Figure 2), the following can be drawn: 1) an increased percentage of a known and controlled RA stockpile allowed production of a compliant recycled HMA, 2) RA above 35% content; a mix design is required to yield to a performing and compliant mix, 3) with higher RA content, it is harder to control the blended binder characteristics, 4) It was observed that the air voids (Va) in the lab prepared samples had slightly increased with the increase of RA contents, while the in-place air void of the compacted mat decreased with the increase of RA content. This was caused by the change in the properties of blended binder since the assumption that complete blending would occur between both binders (AASHTO, 2010) was not investigated.

The lab samples were compacted at the same temperature range, assuming that the final blend did not impact the binder grade characteristics; whereas, determining the binder mix and compaction temperature would have helped to achieve accurate results. The compaction at site demonstrated that at a higher RA content, the mixes have an apparently higher binder with thicker film, and this had yielded to lower in-place air voids considering the same compaction efforts for all mixes. The rejuvenator that was used for mixes with high RA 25% and above had improved the mix workability and binder properties, and thus, it improved the compaction efforts to achieve adequate compaction degree at a wider temperature range.

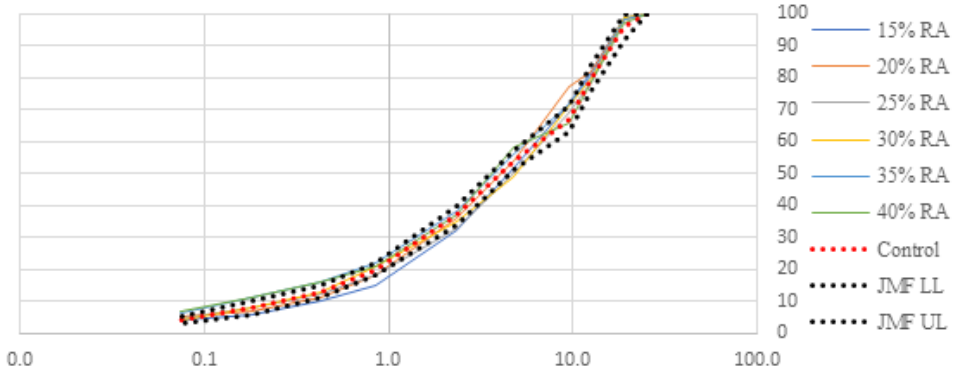

Figure 1: Summary of recycled HMA gradation

5 CONCLUSION

The test results have demonstrated that with a controlled and proper characterization of RA material, a predictive methodology can be developed using this study as a guideline to control the recycled HMA and optimize the RA content. However, the selection of the neat binder grade to use for RA higher than 25% needs to take into consideration the grade of the final blended binder and its appropriateness for the traffic type and suitability to the weather in Qatar.

Prior to milling, the existing pavement should be properly assessed to develop a better understanding of the existing layer thickness and aggregate properties. With

controlled and consistent RA, a percentage up to 30% maximum can be used without compromising the properties of HMA compliance with the QCS (2014). The adjustment of virgin material is necessary during the production of the first batches, especially the neat binder content proportion, in order to make sure that the right amount of binder is added.

Considering the existing plant setup, it was possible to produce a recycled HMA mix up to 40% RA with compliant properties. This is achieved through continuous assessment and control of RA material and proactively adjusting the proportion of virgin material in the plant during production.

Excess of binder and harsher mix with higher RA percentage might reduce the compaction efforts efficiency, thus leading to fluctuating in-place air void.

Generally, mixes with RA between 20 and 30% have performed significantly better than mix with virgin material.

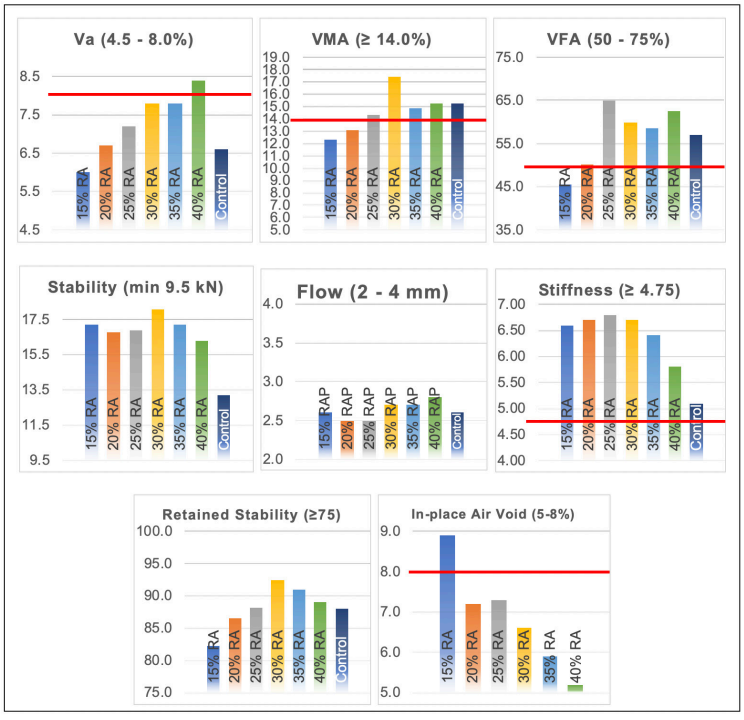

Figure 2: Summary of MARSHALL properties and in-place air void

6 RECOMMENDATION

Best practices and techniques should be used for quality control of RA material during milling, stockpiling, and processing RA (Yousefi, 2013) as elaborated in Figure 3. Fractionation and/or screening helped improve the fractions of RA material, thus allowing to practice additional quality control on the recycled material prior to production.

At RA contents higher than 25%, the workability of the mix becomes harsh; thus, a rejuvenator must be used to avoid excessive compaction efforts to achieve the desired in-place air void. Moreover, rejuvenators lead to adequate compaction at lower temperatures (approximately around 130ºC when Pen 60/70 virgin bitumen is used).

However, softer binder such as 80-100 was not necessary to produce recycled HMA with RA 25% and above in order to maintain the performance of the mix, as the resulting blended binder grade was closer to PG 76-10 which is recommended considering the nature of environment and traffic in Qatar (QCS, 2014).

This study was intended to assess the trends in results, especially the volumetrics in the mixes and in-place air voids when increasing RA in recycled HMA. However, further investigation is necessary to assess the mixtures performance characteristics e.g. permanent deformation, rut depth, fatigue, modulus and sensitivity to moisture.

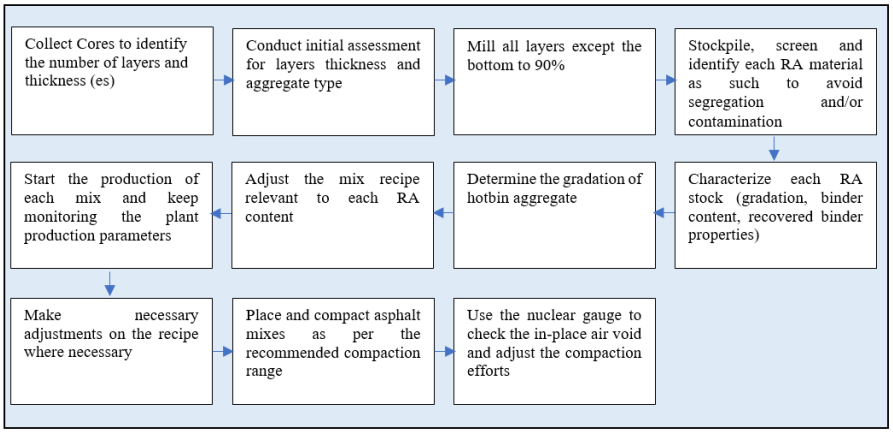

Figure 3: RA cold planning and stockpiling best practice

REFERENCES

American Association of State Highway and Transportation Officials (2010). AASHTO M 323: Standard specification for superpave volumetric mix design. *Standard Specifications for Transportation Materials and Methods of Sampling and Testing*; 30th Ed., AASHTO, Washington, D.C.

Asphalt Institute (2007). *The asphalt handbook: MS-4*, 7th Ed., Lexington, KY.

Cooper, S.J. (2011). Asphalt pavement recycling with reclaimed asphalt pavement (RA). *NWPMA, 18th Annual Fall Pavement Conference*, FHWA, Portland, OR.

Hussain, A. & Yanjun, Q. (2013). Effect of reclaimed asphalt pavement on the properties of asphalt binders. *Procedia Engineering*, Elsevier BV, 54, pp. 840-850.

NAPA (2015). *High RA asphalt pavements: Japan practice — lessons learned*. Retrieved frombhttps://www.asphaltpavement.org/PDFs/EngineeringPubs/IS139_High_RA_Asphalt_Pavements_Japan_Practice-lr.pdf [accessed 02 November 2019].

Qatar Construction Specification (2014). Section 6 Parts 5 & 9, Doha, Qatar.

Reyes-Ortiz, O., Berardinelli, E., Alvarez, A. E., Carvajal-Muñoz, J. S. & Fuentes, L. G. (2012). Evaluation of hot mix asphalt mixtures with replacement of aggregates by reclaimed asphalt pavement (RAP) material. *Procedia - Social and Behavioral Sciences*, Elsevier BV, 53, pp. 379-388.

West, R. (2015). Best practices for RA and RAS management, quality improvement series

129. [pdf] *Lanham: National Asphalt Pavement Association*. Retrieved from https://www.asphaltpavement.org/ [Accessed 03 November 2019].

Widayanti, A., Ria, A. A. S., Jaya Ekaputri, J. & Suprayitno, H. (2018). Characterization of reclaimed asphalt pavement (RAP) as a road pavement material (National Road Waru, Sidoarjo), *MATEC Web of Conferences*. Edited by A. Munawar et al. EDP Sciences, 181, p. 5001.

Willis, J. R. et al. (2013). Improved mix design, evaluation, and materials management practices for hot mix asphalt with high reclaimed asphalt pavement content. Transportation Research Board.

Yousefi, R. F. (2013). *Estimating blending level of fresh and RA binders in recycled hot mix asphalt*. Master of science, University of Wisconsin, Madison.

Cite this article as: Maina J., Khnaizer J., "Producing High Quality Recycled Hot Asphalt with Increased Reclaimed Asphalt Content – Qatar Experience", *International Conference on Civil Infrastructure and Construction (CIC 2020)*, Doha, Qatar, 2-5 February 2020, DOI: https://doi.org/10.29117/cic.2020.0044

Crowd Dynamics, Management and Control at Tourist Attractions during Special Events: A Case Study at Souq Waqif Using Pedestride® Crowd Simulation Tool

Ali Abdelaal
ali.abdelaal@qu.edu.qa
Qatar Transportation and Traffic Safety Center, Qatar University, Doha, Qatar

Charitha Dias
cdias@qu.edu.qa
Qatar Transportation and Traffic Safety Center, Qatar University, Doha, Qatar

Majid Sarvi
majid.sarvi@unimelb.edu.au
The Department of Infrastructure Engineering, The University of Melbourne, Melbourne, Australia

Wael Alhajyaseen
wyaseen@qu.edu.qa
Qatar Transportation and Traffic Safety Center, Qatar University, Doha, Qatar

Faris Tarlochan
faris.tarlochan@qu.edu.qa
Qatar Transportation and Traffic Safety Center, Qatar University, Doha, Qatar

ABSTRACT

Large crowds can be expected at famous tourist attractions, e.g., Souq Waqif, during special events such as the FIFA World Cup 2022. A comprehensive understanding of crowd dynamics is extremely important in order to ensure safety of crowds and efficiency of crowd flows at large gathering spots. Pedestrian crowd simulation tools can be used to evaluate crowd flows and to verify crowd management and control strategies at public infrastructure. The objective of this study is to evaluate safety and efficiency of crowd flows at Souq Waqif, both under normal and emergency situations using Pedestride® Crowd Simulation tool developed at Melbourne University. This simulation model has been calibrated and validated using empirical data collected through controlled experiments and real-world observations. By simulating the increased visitor demand at Souq Waqif as a case study, we aim to highlight any required design modifications and to recommend and verify crowd management strategies in order to mitigate any unfavorable situations, such as stampede during any emergency. The study shows that at increased demands and during emergency evacuation, crowds tend to take similar route. Further, increased demands could elevate the maximum crowd density up to 6 p/m2 at gates and junctions. In order to mitigate such unfavorable situations, dynamic exit signs are needed to direct flows to other clear exits to avoid herding effect.

Keywords: Crowd dynamics; Crowd simulation; Crowd safety; Emergency evacuation; Mega-events

1 INTRODUCTION

Souq Waqif is one of the main tourist destinations in Qatar due to its history, architecture, authenticity, and proximity to other touristic places such as the Museum of Islamic Arts and Cornish. It is also a destination for buying spices, traditional garments, gifts and souvenirs. Literal translation of 'Souq Waqif' is the 'standing market'. It was founded at least 100 years ago and served as a gathering place for locals, Bedouin (nomads) traders, and fishermen. Souq Waqif is located near Msheireb district in Qatar

as shown in Figure. 1. It covers an area of 164,000 m2 at the city waterfront (Furlan and Faggion, 2015). The buildings inside the Souq are constructed from basic materials such as wood, bamboo, straw, and clay with no additional painting as they maintain the natural colour of stones and original building material. The Souq layout makes it appear as a maze with multiple entrances and exits, and relatively complex and irregular network of paths or passages, some of them are open-air. The Main Street and a corridor inside Souq are shown in Figure. 2. Between 2006 and 2008, the Souq went through a major restoration and reconstruction work aiming to preserve the architectural identity of the place that might have transformed due to the rapid development of the city. Moreover, the new Souq includes several additional features such as new art galleries, and a number of restaurants and cafes.

Figure 1: Map of Souq Waqif and surrounding area (Google).

Such a famous destination is likely to be visited by tourists who aim to know about the history of Qatar, try some traditional food, and shop for souvenirs. This type of crowd has distinct characteristics. They might not know the site map, they might not have a specific plan for touring the place, and they will roam the place with the aim of exploration and recreation. Even for some residents, navigating through the very similar corridors of Souq Waqif is a challenge.

Visitors to Souq reported a difficulty in reaching their desired destination due to the limited number of signs. It was also reported that there are no clear indicators of main entrances (Nafi et al., 2015), resulting in a significant need of additional signage at the Souq (Furlan and Faggion, 2015). Another study found that entrances were well defined; however, navigating within the Souq and the very similar looking corridors can be misleading and time consuming when needing to exit quickly (Tannous and Furlan, 2018).

In order to ensure tourists' satisfaction, to enhance the efficiency of visitors' circulation

inside the Souq, and to avoid any unfavourable situations, e.g., stampede during high visitor demand or emergency situations, the crowd flows needs to be managed and guided properly. While some studies have explored the interaction of visitors and traders, and how this impacts time spent inside the market, or increases the density of the crowds in certain locations (Kusuma, 2017; Kusuma et al., 2016a, 2016b), this study aims at analysing the overall behaviour of the crowd during normal and emergency evacuation modes, using a microscopic pedestrian crowd simulation tool.

Figure 2: Main street in Souq Waqif (left, source: The Peninsula, local news agency), and an example of corridors in the Souq (right) (El-Hamalawy, 2015).

2 METHODOLOGY

Pedestride® software (https://www.pedestride.com/) is used in this study to understand Souq visitors' behaviour during an evacuation process. The software utilizes a number of models such as the social force model introduced by Helbing, Farkas and Vicsek (Helbing et al., 2000). The simulation model works at the "operational level" (Haghani and Sarvi, 2018) or the "walking behavior" (Antonini et al., 2006) level, based on the social force model. This model is connected to further superior modelling levels of pathfinding and directional choice, also known as, the "tactical level" (Asano et al., 2010; Bode and Codling, 2013; Haghani et al., 2015, 2018; Haghani and Sarvi, 2016) in addition to a modelling layer for directional choice change. Moreover, the reaction time (also known as, the "strategic level" (Augustijn-Beckers et al., 2010; Lovreglio et al., 2015). The below equation is a simplified version of the model utilized by Pedestride® software;

$$\vec{f}_i = \vec{f}_{des,i} + \vec{f}_{ij(i\neq j)} + \vec{f}_{wall,i} + \varphi\left[\vec{f}_{push} + \vec{f}_{friction}\right] + \vec{\varepsilon} \qquad \text{Eq. 1}$$

Where, $\vec{f}_{des,i}$ is the desired force, $\vec{f}_{ij(i\neq j)}$ is the social interaction force, and $\vec{f}_{wall,i}$ is the force exerted by walls. When the crowd density reaches a higher limit that pedestrians have physical contacts pushing and friction forces are also activated, i.e., $\varphi \neq 0$. Finally, $\vec{\varepsilon}$ represents fluctuation due to randomness.

Map of Souq Waqif was adopted from simplified building geometrical reconstruction (Tannous and Furlan, 2018) and satellite images as shown in Figure. 3. Two areas of the Souq were simulated in this study. In the first case study, 500 agents were distributed over an area of 2260 m^2 resulting in an equivalent pedestrian density of 0.22 p/m^2. The density was almost doubled (0.45 p/m^2) in the second case study by reducing the simulated area

to 1109 m^2 as shown. The other option to increase the density was doubling the number of agents; however, this was not possible due to the software limitation. Corridor width in both case studies ranged approximately from 2.5 to 6 m. It is worth mentioning that at the initiation of the simulation, crowd density in some corridors ranged from 2-5 p/m^2 to simulate peak demand during mega events. This study also investigates the possibility of having certain exits blocked due to an emergency, and how this would affect the evacuation process during higher density.

Figure 3: Area simulated (1st case study area ----, 2nd case study area ---).

3 RESULTS AND DISCUSSION

In general, the design of egress routes in buildings or mega events is based on a number of references that can be categorized into legal regulations, handbooks, and computer simulations. The legal regulations utilize a set of static rules and prescriptive methods. For instance, the number of individuals per room and length of escape route determine the minimum width of doors. This method lacks the dynamics of an evacuation process. On the other hand, handbooks use macroscopic models during evacuation with relevance to time and space. This method can predict the time and location of congestions; however, it treats pedestrians as a body of quasi-constant size and density what gives only a coarse description of the flow. On the contrary, microscopic models simulate individual movement of each pedestrian in order to determine the crowd dynamics on an individual scale, which is used in this analysis.

Multiple reasons could trigger an evacuation, but the most common type is forced evacuation from an enclosed space as a result of a threat like fire or smoke. The simulation assists designers in evaluating their evacuation plans in terms of time needed to completely evacuate a given space, location and number of exits, and possibility of having stampedes. In this study, we considered the evacuation time as the time needed to evacuate 98% of the crowd. The results showed that evacuation time was higher for higher density crowd. The average evacuation time for normal and emergency evacuation in the first case was 55 and 63 seconds, respectively. On the other hand, the second case

study resulted in an average evacuation time of 62 and 77 seconds for the normal and emergency evacuation scenarios, respectively. Despite having multiple routes to exit the Souq, crowds were observed to always take the same exit leading to a peak demand at certain gates, mainly due to herding effect which is a common phenomenon under panic situation. It should be noted that in the exit choice model used in Pedestride we used the default parameters.

Comparing normal and emergency evacuation showed no difference in the rates of evacuation for the first case study as illustrated in Figure. 4. However, when the crowd density was increased in the second case study, a change in the trend between normal and emergency evacuation was observed. Figure. 5 shows that there is almost no difference in percentage of agents evacuated in normal and emergency scenarios up until 20%, then the difference starts to increase and less agents are evacuated for the same evacuation period which indicated a reduced crowd dynamics and possibility of stampeding.

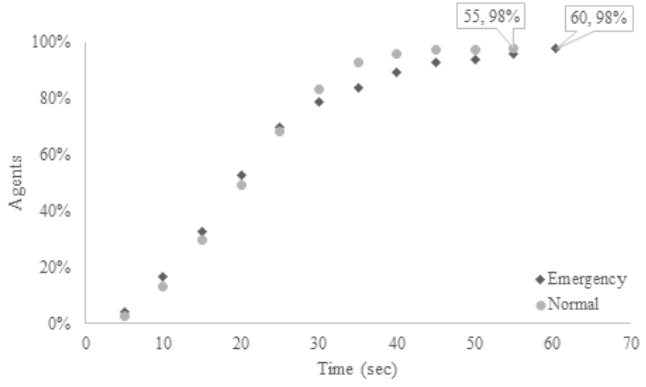

Figure 4: Percentage evacuated over time (0.22 p/m2)

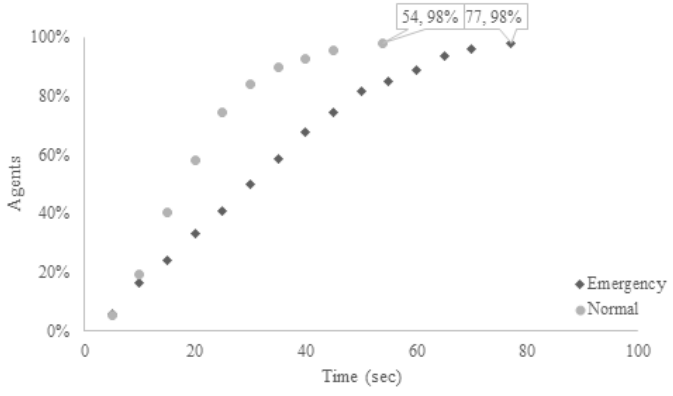

Figure 5: Percentage evacuated over time (0.45 p/m2)

The second part of this study evaluates the impact of blocking certain exits on the crowd evacuation. For the second case study where crowd density was equal to 0.45 p/m2, blocking the east corridor and part of the north corridors resulted in a significantly higher crowd flow towards the south exit, increasing crowd density to almost 6 p/m2 at the junction where crowds from four directions meet.

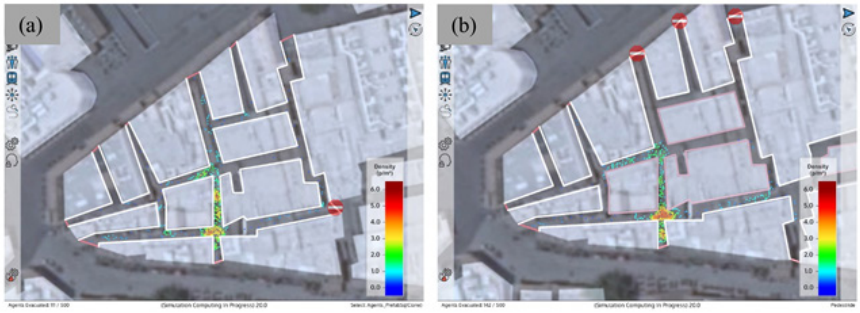

Figure 6: Emergency evacuation at 20 seconds: (a) blocked east corridor, (b) blocked north corridors

Crowd behaviour during evacuation also plays a critical role. Fig. 7 shows the difference between normal and emergency evacuation when east corridor is blocked. In this case, much less congestion is observed at the south exit and crowd could be safely evacuated.

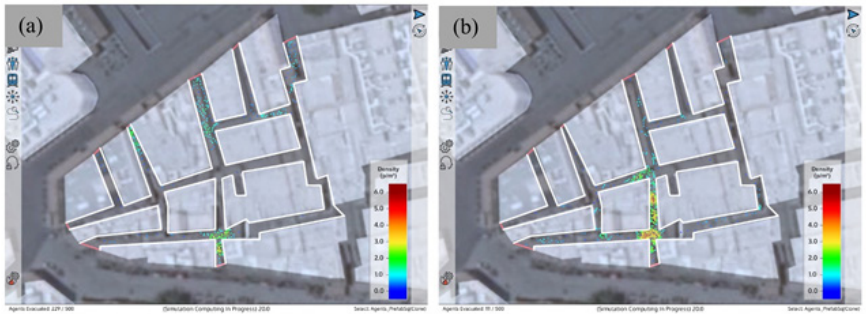

Figure 7: (a) Emergency evacuation and (b) normal evacuation at 20 seconds

Current static exit signs direct the crowd to certain exits as shown in Figure. 8. However, using dynamic signs could mitigate the phenomena observed in Figure. 6. Knowing that crowds may behave in different ways depending on the circumstances of evacuation, these dynamic signs can disseminate variable route guidance information using on-time data on pedestrian density at the different corridors and the clearance of exits which can be collected through the surveillance system. This allows an efficient and safe dynamic crowd management or crowd evacuation process.

Figure 8: Sample exit signs in Souq Waqif (Furlan and Faggion, 2015)

4 CONCLUSION

Souq Waqif is one of the main tourist attractions that is expected to witness an increasing visitor demand during mega events such as FIFA World Cup 2022. The place is characterized by its maze-like layout with multiple entrances and exits, and quite complex and irregular network of paths that visitors can take. Traders on each side of the corridors display their goods, and some restaurants and cafes have an outdoor dining area. All of these factors reduce the effective width of the passageways and adds to the complexity of navigating through the Souq. The study showed that during normal evacuation, crowds can safely exit the Souq even when certain routes are blocked due to the availability of many exit routes. However, during emergency evacuation and due to herding effect, crowds tend to take the same route what leads to stamping and increased crowd density. In order to avoid such unfavourable situations, dynamic exit signage should be implemented to direct the crowds to clear exit routes.

It should be noted that this an initial study and the results obtained give an overview of the issue and suggest primary solutions to it. The collection of Souq Waqif layout and visitor demands was not possible at this stage. However, required data will be collected in the future with the assistance of relevant authorities. In future, we aim to obtain more accurate drawings of the Souq with accurate path dimensions. Moreover, we intend to calibrate and validate the base models, i.e., the force-based behaviour model and the exit choice model, used in Pedestride® software to represent conditions specific to Qatar.

REFERENCES

Antonini, G., Bierlaire, M. & Weber, M. (2006). Discrete choice models of pedestrian walking behavior. *Transportation Research Part B: Methodological,* 40: 667-687.

Asano, M., Iryo, T. & Kuwahara, M. (2010). Microscopic pedestrian simulation model combined with a tactical model for route choice behaviour. *Transportation Research Part C: Emerging Technologies*, 18: 842-855.

Augustijn-Beckers, E.-W., Flacke, J. & Retsios, B. (2010). Investigating the effect of different pre-evacuation behavior and exit choice strategies using agent-based modeling. *Procedia Engineering*, 3: 23-35.

Bode, N. W. F. & Codling, E. A. (2013). Human exit route choice in virtual crowd evacuations. *Animal Behaviour,* 86: 347-358.

El-Hamalawy, H. (2015). Souq Waqif. Available at: https://www.flickr.com/photos/elhamalawy/23733881160.

Furlan, R. & Faggion, L. (2015). The Souq Waqif Heritage Site in Doha: Spatial Form and Livability. *American Journal of Environmental Engineering,* 5: 146-160.

Haghani, M. & Sarvi, M. (2016). Human exit choice in crowded built environments: Investigating underlying behavioural differences between normal egress and emergency evacuations. *Fire Safety Journal* 85: 1-9.

Haghani, M. & Sarvi, M. (2016). Pedestrian crowd tactical-level decision making during emergency evacuations, *Journal of Advanced Transportation.* 50: 1870-1895.

Haghani, M. & Sarvi, M. (2018). Crowd behaviour and motion: Empirical methods. *Transportation Research Part B: Methodological,* 107: 253-294.

Haghani, M., Sarvi, M. & Shahhoseini, Z. (2015). Accommodating taste heterogeneity and de-

sired substitution pattern in exit choices of pedestrian crowd evacuees using a mixed nested logit model. *Journal of Choice Modelling,* 16: 58-68.

Haghani, M., Sarvi, M. & Rajabifard, A. (2018). Simulating Indoor evacuation of pedestrians: The sensitivity of predictions to directional-choice calibration parameters. *Transportation Research Record,* 2672: 171-182.

Helbing, D., Farkas, I. & Vicsek, T. (2000). Simulating dynamical features of escape panic. *Nature,* 407: 487-490.

Kusuma, P. D. (2017). Crowd simulation in souvenir market by using multi agent system. *International Journal of Applied Engineering Research,* 12: 15055-15065.

Kusuma, P. D., SN, A. & Pulungan R. (2016a). Agent-based buyer-trader interaction model of traditional markets. *International Journal of Intelligent Systems and Applications,* 8: 1-8.

Kusuma, P. D., SN, A. & Pulungan, R. (2016b). Agent-based crowd simulation of daily goods traditional markets. *International Journal of Intelligent Systems and Applications,* 8: 1-10.

Lovreglio, R., Ronchi, E. & Nilsson, D. (2015). A model of the decision-making process during pre-evacuation. *Fire Safety Journal,* 78: 168-179.

Nafi, S. I., Alattar, D. A. & Furlan, R. (2015). Built form of the Souq Waqif in Doha and user's social engagement. *American Journal of Sociological Research,* 5: 73-88.

Tannous, H. O. & Furlan, R. (2018). Livability and urban quality of the Souq Waqif in Doha (State of Qatar). *Saudi Journal of Engineering and Technology,* 3: 368-387.

Cite this article as: Abdelaal A., Dias C., Sarvi M., Alhajyaseen W., Tarlochan F., "Crowd Dynamics, Management and Control at Tourist Attractions during Special Events: A Case Study at Souq Waqif Using Pedestride® Crowd Simulation Tool", *International Conference on Civil Infrastructure and Construction (CIC 2020)*, Doha, Qatar, 2-5 February 2020, DOI: https://doi.org/10.29117/cic.2020.0045

Emerging Transit Technology: Implementing an Urban Gondola System over Al Corniche, Doha, Qatar - A Cost Estimation Study

Shahram Tahmasseby
stahmasseby@qu.edu.qa
Qatar Transportation and Traffic Safety Center, Qatar University, Doha, Qatar

ABSTRACT

Urban gondolas are a type of driverless transit vehicles, which are increasingly drawing the attention as a viable mass transit alternative in urban environments and touristic areas. The system is distinctive with high reliability of travel time, because it operates on their own right of. Urban gondolas are also identified with environmental benefits resulting from their low emission, energy use, and noise pollution. They have widely been implemented in touristic areas, mountains and in areas with diverse topography types. The objective of this study is a first step assessment of the potential economic viability of implementing an urban Gondola linking East Mound Skyline View to the promenade side along Al Dafna Park in Westbay Doha, Qatar. The focus of this study is on introducing an appropriate technology plus estimating its associated cost components of implementing such system in Qatar. The (Monocable) urban gondola technology will be investigated in terms of applicability and furthermore, their associated cost components including the capital costs such as infrastructure civil works, as well as operating and maintenance costs (O&M) will be estimated based on the existing benchmarks and similar practices from around the globe. The result of this study could be a basis for an in-depth Cost-Benefit Analysis of implementing emerging transit technologies (e.g. urban gondola) in the State of Qatar.

Keywords: Urban gondola; Cost estimation; Emerging transportation; Operation and maintenance costs

1 INTRODUCTION AND BACKGROUND

A gondola lift, also called a cable car, is a type of aerial lift which is held and driven by cables from overhead. The cable is in the form of a circular steel rope that is strung between two ending points and might also passes over in-between auxiliary towers. The cable is propelled by a bull wheel in a terminal, which is powered up by a diesel-powered or electric-powered engine. Basically, gondola systems are frequently seen as a non-stop/uninterrupted transportation system given their haul rope continual movement and circulating around two terminating points function. The associated capital and operating costs, functionality and capacity of a gondola system may vary based on the combination of cables used for support and/or haulage and the type of grip (detachable grip vs. fixed grip).

In the past, gondolas were conventionally designed and implemented in the ski resorts having mountainous terrain; however, recently they are being designed and used in urbanized areas and considered as a public transportation mode e.g. Metrocable (Medellín), Portland Aerial Tram, Metrocable (Caracas), Cable Aéreo (Manizales) and

Constantine (Algeria) (*SJC Alliance Consulting Services- Creative Urban Projects CUP, 2019*).

The Metrocable systems in Medellin and Caracas are fully integrated with the public transit network. This enables passengers to seamlessly transfer to the local metro lines. The City of London in the UK, built Emirates Air Line (cable car) for the 2012 Summer Olympics which facilitates travel from Emirates Greenwich Peninsula terminal to Emirates Royal Docks terminal in six minutes. *Alshalalfah and Shalaby (2011)* examined the potentiality and feasibility of an urban gondola system to address some of Mecca's transportation issues such as mobility, accessibility, safety and security, equity, sustainability and the economy. Their study demonstrated that depending on the chosen corridor and applied technology, the benefit over cost ratio (BCR) ranges from 1.04 to 4.26. The indirect costs remunerations in that study stemmed from travel time savings, vehicle operating cost savings, GHG (greenhouse gas emission) savings, as well as air pollution savings (i.e. nitrogen oxides, volatile organic compounds, sulphur oxides, PM_{10}, and carbon monoxide).

In 2018, TransLink, the public transit company in Vancouver- British Columbia, examined the feasibility of building a gondola to connect SkyTrain (Production Way – University Station) with Burnaby Mountain, including the main campus of Simon Fraser University (*Ch2M Hill Report 2018*). The introduction of the abovementioned gondola would result in the elimination of the bus service from Production Way-University Station to Burnaby Mountain and its replacement by a gondola service, which would yield to some bus capital and operating cost savings to offset. CH2M estimated that TransLink will be able to recover $34.5 million in capital costs as well as a 25-year reduction of $89.3 million in bus operations. Furthermore, the operating cost of the gondola was estimated to hover around $54.2 million. Including the gondola capital cost, the total cost was approximated $123.4 million. Consequently, by dividing $225.3 million as the estimated total benefits of implementing the gondola over the indicated capital and operating costs for a 25 year period of operation, a BCR of 1.8 was calculated which showed that the overall benefits of the BMGT project would outweigh its costs.

2 GONDOLA SYSTEMS CONSTITUENTS

Nearly all gondola systems are constituted by similar components, despite differences in the applied technique. Basically, gondola systems are constituted from the following fundamental elements:

- carriers (cabins);
- terminals;
- towers;
- ropes; and
- an emergency arrangement for the safe evacuation.

In general, gondolas are considered as a reliable and cost-effective system, thanks to their system energy efficiency. They offer a safe and efficient transport system particularly in hilly terrains. Furthermore, implementing gondola systems as a public transport mode may cut GHG emission and reduce air pollution in urbanised areas. Nonetheless, they might be vulnerable due to the risk of power outages. In case of a hazard e.g. power outage, evacuation is challenging. However, Medellín Metro is ameliorating this problem

by providing a communication system in every vehicle should an emergency occur (*SJC Alliance Consulting Services- Gondola Project Medellin*).

Currently, gondolas that have been used as a mass transit mode in urban areas use one of the following three technologies:

- Monocable Detachable Gondolas (MDG);
- Bicable Detachable Gondolas (BDG); and
- Tricable Detachable Gondolas (TDG, or 3S).

The aforementioned technologies are different in terms of speed, capacity, structure, and operation and consequently capital and O&M costs. In terms of mobility, the applicable capacity of a MDG system hovers around 2,000 to 3,000 pax per hour per direction (pphpd). This figure increases to 4,000 pphpd for BDG and can even reach up to even the nominal capacity of above 5000 pphpd for 3S gondola systems. Practically, reaching to 4000 pphpd is feasible for gondola. For the case of Burnaby, the gondola supplier suggested the aforementioned capacity by presuming cabins travelling with gaps of less than 1 minute and taking 6 to 7 minutes to complete a trip and having capacity of 33 passengers per cabin (*Ch2M Hill report 2018*). Obviously, the capital cost of implementing a 3S gondola system will be a way higher than that of other systems e.g. MDG.

In this case study the MDG system is considered as an appropriate system based on the size of demand catchment area and thus the anticipated patronage. Generally, MDG cabins hold 8 passengers while some systems allowing as few as 4 or as many as 15. As indicated before, this normally amounts to around 2,000-3,000 people per hour per direction, if the cabin cars with the highest capacity are adopted. As indicated before, Monocable Detachable Gondolas (MDG) are likely the most common aerial urban transit system as their low cost has made them an attractive complementation to public transit systems particularly in the developing countries. MDG systems have been installed in South American cities in Colombia, Venezuela, Brazil, as well in Africa Europe and Asia such as in Algeria, England and Singapore respectively. Table 1 summarizes service and technology characteristics of MDG gondola which is suitable for the case study.

Table 1: MDG System and Technology Characteristics

System characteristics	**Description**
Cabin capacity	15 passengers
Service line headway	15 seconds
Service line capacity	Upgradable to 3, 600 persons/hr
Maximum line speed	6 m/s (21.6 km.hr)
Max Distance between Towers	900 meters
Dwell time at terminal [per terminal]	122 seconds
Dwell time at intermediary stations (per station)	42 seconds

3 CASE STUDY- MONOCABLE DETACHABLE GONDOLA (MDG) OVER AL CORNICHE

In this study the proposed gondola system constitutes a single line which connects East Mound Skyline View to the promenade side along Al Dafna Park in Westbay Doha, Qatar, see Exhibit (1) for the proposed line alignment. The length of the line is approximately 2.15 Kms and there will be no intermediary stations along the proposed line.

3.1 Gondola Capital Cost

The cost estimates indicated in this section have been obtained from the existing major vendors of Arial Ropeway Transit technologies in the world [Doppelmayr/ Garaventa Group and Leitner Ropeways]. Hence, the quoted cost estimates alterations are marginal. Generally, the cost components associated with the investment in Gondola can be outlined as follows:

The cost estimates indicated in this section have been obtained from the existing major vendors of Arial Ropeway Transit technologies in the world [Doppelmayr/ Garaventa Group and Leitner Ropeways]. Hence, the quoted cost estimates alterations are marginal. Generally, the cost components associated with the investment in Gondola can be outlined as follows:

- Propulsion, which comprises a major part of the gondola infrastructure costs;
- Infrastructure equipment: include costs of cabins, towers, cables and any other related infrastructure costs such as the cabin carriage, power supply and telecommunication systems;
- Terminal/ in-between stations, the essential costs allocated to build gondolas' basic infrastructure, architectural and civil works. This includes construction of a gondola terminating and/ in-between stations comprise terminal/ intermediary stations capital costs;
- Required civil works i.e. foundations; piling; cupping; and soil tests.
- Reserved generator; The cost of a backup generator comprises a negligible percentage of the total capital cost of a gondola system
- Duty on equipment which represents the expenses of the duty on the electro-mechanical components of the propulsion system at terminals and intermediary stations.
- Contingency plan: based on existing experiences in Gondola systems, the contingency expense is presumed to be 20% of the entire capital cost; and
- Land acquisition, if applicable. In this study the cost of land acquisition was not taken into account

Table (2) outlines the investment and capital costs for the proposed Al Corniche gondola line for the MDG Technology.

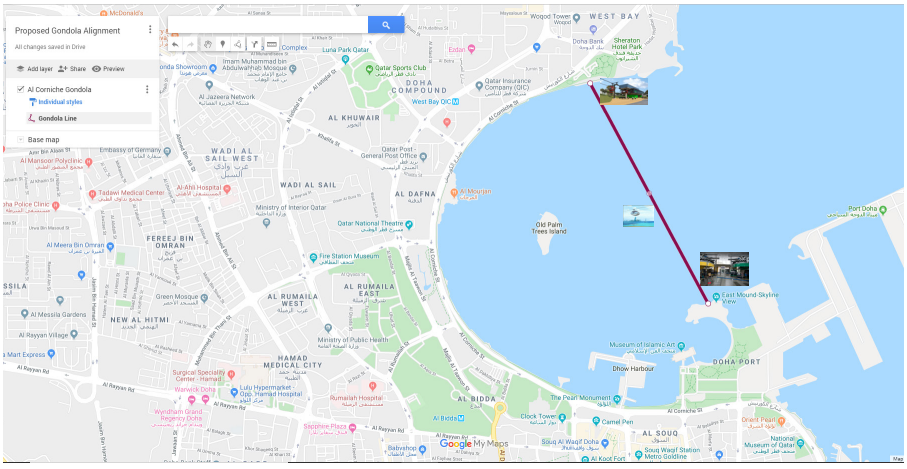

Figure 1: Proposed Gondola Alignment over Al Corniche , Doha, Qatar

Table 2: Capital Cost Components Estimation for the Proposed Gondola Line

Capital Cost Component	Remarks	Cost in QR (M)
Propulsion at terminals	Drive (terminal) + Return (terminal)	7.5
Propulsion at Intermediate Stations	Not applicable	0.0
Terminals Capital costs	Skyline View Terminal + Al Dafna Terminal	5.6
Intermediate stations Capital	Not applicable	0.0
Infrastructure (lines)	QR9.4 M per Km	20.7
Infrastructure civil works	Approximately QR 2.8 M per km	6.2
Backup Generator		0.6
Duty on equipment	Estimated as 10% of the Electro-Mechanical parts associated costs	2.9
Contingency	One fifth of the total capital costs (20%)	8.7
Total Capital Costs		**52.2**

3.2 Operating and Maintenance (O & M) Costs of the Proposed Gondola

The O & M cost for Gondola systems consists of the following components (*Tupper 2009, Alshalalfah and Shalaby, 2011*):

- Energy consumption cost which represents the associated costs of the energy (often electric power or diesel fuel) and water consumption;
- Manpower costs which are generally insignificant due to the automated system as presumed two (2) personnel (incl. a mechanic) are allocated to each station during its 18 hours operation;
- Recurrent maintenance and service costs: the maintenance costs generally range from QR 250 to QR 550 per hour of operations based on 14 hours of operation (Warren, 2011);
- Applicable insurance costs: relatively significant because of the uniqueness of the system; and
- Capital reserve fund costs which is the accrual of a capital reserve fund for future capital expenditures in order to rehabilitate the entire system during its lifetime period.

The total operating and maintenance cost of each Gondola option (annually) is outlined in table (3).

Table 3: O & M Cost Components Estimation for the Proposed Gondola Line per Year

O & M Cost Component per Annum	Remarks	Cost in QR (M)
Energy consumption	Figure is based on similar case studies	1.0
Personnel wage	Assumed QR 140 per hour for mechanics	3.6
Maintenance cost	Assumed QR 420 per hour	2.7
Insurance cost	The figure was derived from a Canadian Gondola case study in British Columbia	0.6
Capital reserve fund	It's presumed over a 25-year period QR11M-16M will be required for the overhaul or improvements of major gondola components	0.5[1]
Total O&M Costs per Annum		**8.4**

4 WAY FORWARD

Following the calculation of the capital, operation and maintenance costs, the next step will be the estimation of the benefits of gondola, which will make conducting a cost –benefit analysis and concluding a comprehensive assessment of viability of implementing such system in Doha, Qatar possible. The project economic efficiency can be examined from the social welfare perspective. The NPV (net present value), and IRR (internal rate of return) are two appropriate economic indicators when it comes to cost-benefit analysis. Calculating the following ex-ante economic benefits is necessary in this regard:

- Estimation of the system patronage: ridership needs to be estimated by applying a methodology based on the transit catchment area concept, and choice behaviour modeling. Conducting a stated preference (SP) survey could be considered as a necessary step in this context to measure the potential riders' tendency and willingness to ride gondola. The estimation of demand at the ex-ante stage should be realistic and thus commensurate with the gondola system capacity (derived from the service frequency, applied technology and the cabin car capacity). As the travel demand for public transport projects is often estimated for a project's lifetime to enable the transport authorities to examine the project economic viability, a thirty-year lifetime window can be deemed for gondola in this case study as a customary figure for gondola technology.
- The estimation of gondola patronage could lead to measure Travel Time Savings and perceived Travel Time Reliability for car and bus users at an aggregate level. It is noteworthy to mention that apart from leisure, the aforementioned metrics are considered as important advantages of riding a gondola from passengers'

1 To build up QR 17 Million over 25 years and considering 2% interest rate , the capital reserve fund is estimated QR 521 K per annum. It was presumed that no capital expenditures would be required for the first 8 to 10 years, ensuring that QR 5.6M to QR 7.0 M would be accumulated by that time to cover such an expense.

perspective. Gondola riders actually benefit from a convenient service line offering very short waiting times, reliable as well as direct service connecting the two sides of Al Corniche without requiring any additional boarding, stopping and alighting. Furthermore, it is never impacted by traffic congestion, traffic signals, road constructions, detours, etc.

- Car operating cost savings given the impacts of gondola on the road network, and
- Environmental benefits, in terms of reduced air pollution emissions.

Finally, the qualitative impacts of factors other than those indicated, which may also be difficult to measure, should be included in project assessment and performance benchmarking. An overall evaluation of Gondola viability over Al Corniche and its surrounding areas needs to be accounted for by qualitatively assessing the following factors:

- Economic efficiency;
- Capacity;
- Convenience and accessibility;
- Operating profitability;
- Sustainability and GHG emissions reduction;
- Visual intrusion impacts;
- Safety, reliability and weather issues.

5 CONCLUSION

In this study, the associated costs i.e. capital, operating and maintenance costs of a Monocable Detachable Gondola (MDG) technology connecting two sides of Al Corniche in Doha, the State of Qatar was investigated. The cost estimation presented in this study, in fact was the first step toward a comprehensive feasibility assessment of implementing an urban gondola, as an emerging transit technology, at the ex-ante stage in the country. It was emphasized that the Cost-Benefit Analysis (CBA) is a relevant method to estimate economic metrics such as Benefit over Cost ratio which help the stakeholders and decision makers in justifying the project viability. Furthermore, it was recommended that the project has to be examined qualitatively by incorporating indirect measures such as sustainability, visual intrusion, convenience and accessibility indices.

REFERENCES

Alshalalfah, B., Shalaby, A. & Othman. F. (2011). *Aerial ropeway transit – Exploring its potential for Makkah.* Center of Research Excellence in Hajj and Morah, University of Toronto.

CH2M HILL Canada Limited (2018). *Burnaby Mountain Gondola Transit – Feasibility Study.* Prepared for TransLink.

SJC Alliance Consulting Services (2019). *Creative Urban Projects CUP.* Accessible at: www.gondolaproject.com

SJC Alliance Consulting Services (2019). *Gondola Project Medellin*. Accessible at: http://gondolaproject.com/medellin/

Tupper. B. (2009). *Proposed Burnaby Mountain Gondola Transit Project,* UniverCity on Burnaby

Mountain.

Warren K. (2011). Keeping the gondola running TMVOA, Mountain Village fund and operate the gondola. Accessible at: https://www.telluridenews.com/news/article_b8ec1825-c8bd-57ea-9a95-10330e9a5803.html

Cite this article as: Tahmasseby S., "Emerging Transit Technology: Implementing an Urban Gondola System over Al Corniche, Doha, Qatar - A Cost Estimation Study", *International Conference on Civil Infrastructure and Construction (CIC 2020)*, Doha, Qatar, 2-5 February 2020,DOI: https://doi.org/10.29117/cic.2020.0046

Dosage Optimization of Polypropylene Fiber for Strength Enhancement of Cementitious Composites

Mohammad R. Irshidat
mirshidat@qu.edu.qa
Center for Advanced Materials, Qatar University, Doha, Qatar

Nasser Al Nuaimi
anasser@qu.edu.qa
Center for Advanced Materials, Qatar University, Doha, Qatar

Soheb Salim
sohebsalim93@gmail.com
Department of Civil and Architectural Engineering, Qatar University, Doha, Qatar

Mohamed Rabie
m.rabie@qu.edu.qa
Department of Civil and Architectural Engineering, Qatar University, Doha, Qatar

ABSTRACT

Concrete is the most commonly used materials for construction in Qatar as well as in the world. Exposure to sever environmental conditions causes physical deterioration of concrete structures and significantly affect the concrete's strengths and modulus of elasticity. In the last decades, many improvements had been made in concrete technology. Most of these improvements focused on the weak point of concrete, which is tensile strength enhancement. One possible method to improve the tensile strength of cementitious composites is incorporation of fibers in the mix. Polypropylene fiber is widely used for this purpose due to their corrosion resistance and relatively low cost. Polypropylene fibers are usually incorporated in cement mortar to control cracks propagation thus enhance its tensile and flexural properties. This research focuses on Polypropylene fiber dosage optimization for strength enhancement of cementitious composites. Four dosages of Polypropylene microfibers; 0%, 0.05%, 0.1%, and 0.2% by weight of cement; were added into cement mortar to explore the optimum dosage that can lead to big enhancement in mechanical strengths of cementitious composites. The mechanical strengths were investigated in terms of compressive and flexural strengths. The results revealed that adding small amount of Polypropylene microfibers could enhance the compressive and flexural strengths of cement mortar. The maximum enhancement in the compressive and flexural strengths was equal to 26% and 19% and was achieved in the case of adding 0.1% and 0.05% by weight of cement, respectively.

Keywords: Polypropylene fiber; Mortar; Optimization; Compressive strength; Flexural strength

1 INTRODUCTION

Concrete is the most common used materials for construction in Qatar as well as in the world. Exposure to sever environmental conditions causes physical deterioration of concrete structures and significantly affect the concrete's strengths and modulus of elasticity. In the last decades, many improvements had been made in concrete

technology. Most of these improvements focused on the weak point of concrete, which is tensile strength enhancement. Failure in cementitious materials is a gradual multi-scale process. When loaded, initially short and discontinuous micro cracks are created in a distributed manner. These micro cracks merge to form macro cracks. To avoid the failure in cementitious materials, the growth of the cracks should be stopped to delay the coalescence of cracks or even to prevent the cracks' initiation at all.

One possible method to mitigate the crack propagation and enhance the tensile strength of cementitious composites is incorporation of fibers in the mix. Polypropylene fiber is widely used for this purpose due to their corrosion resistance and relatively low cost. Polypropylene fibers are usually incorporated in cement mortar to control cracks propagation thus enhance its tensile and flexural properties (Li et al., 2018; Li et al., 2018; Mohseni et al., 2016; Nunes et al., 2019; Szelag et al., 2019; Zanotti et al., 2017).

This research focuses on Polypropylene fiber dosage optimization for strength enhancement of cementitious composites. Four dosages of Polypropylene microfibers; 0%, 0.05%, 0.1%, and 0.2% by weight of cement; were added into cement mortar to explore the optimum dosage that can lead to big enhancement in mechanical strengths of cementitious composites. The mechanical strengths were investigated in terms of compressive and flexural strengths.

2 EXPERIMENTAL PROGRAM

2.1 Materials

Portland cement, locally available silica sand, and tap water were used to prepare the cement mortar used in this research. Commercially available polypropylene micro fibers were used to modify the cementitious matrix. The fibers' length, diameter, and density are two millimeters, thirty-four micrometers, and 910 kg/m3.

2.2 Specimens preparation

Cement mortar was prepared according to the ASTM C305 mixing procedure. Four batches of cement mortar were prepared. One batch was prepared as a control sample of plain cement mortar (water, sand, and cement). The other batches were prepared with various percentages of fibers 0.05%, 0.1%, and 0.2% by weight of cement. A binder/sand ratio of 1:3 and water/binder (w/b) ratio of 0.55 were used to prepare all batches. After mixing, the mortar mixtures were molded into 5 cm cubes for compressive strength and 4 cm x 4 cm x 16 cm prisms for flexural strength tests. Twenty-four hours later, all samples were taken out of molds, and then cured in a bath of lime-saturated water. Twenty-eight days later, the specimens were taken out from the lime-saturated water bath and left to dry, then tested.

2.3 Test procedures

The compressive and flexural strength tests were conducted according to the ASTM C109 and ASTM C348 standards, respectively. Three specimens of each formulation were tested, and the average strengths were calculated.

3 RESULTS AND DISCUSSION

The compressive and flexural strength values of cement mortars as a function of

polypropylene fiber dosage are shown in Figure 1 and Figure 2, respectively. The enhancements in the strengths are tabulated in Table 1. The results reveal that adding polypropylene fibers enhanced the compressive strength of the cement mortar. Maximum enhancement of 26% compared to the control specimen was observed in the case of using 0.1% fibers content. On the other hand, adding polypropylene fibers enhanced the flexural strength of the cement mortar. The enhancement increases with increasing the amount of added fibers. Maximum enhancement of 19% compared to the control specimen was observed in the case of using 0.05% fibers content. The strength enhancement may be attributed to the fact that the polypropylene fibers delay the initiation and propagation of the micro cracks due to the well distributed within the cement mortar. Adding micro fibers may lead to enhance the adhesion between the hydration products and thus improve the mechanical strengths of the mortar.

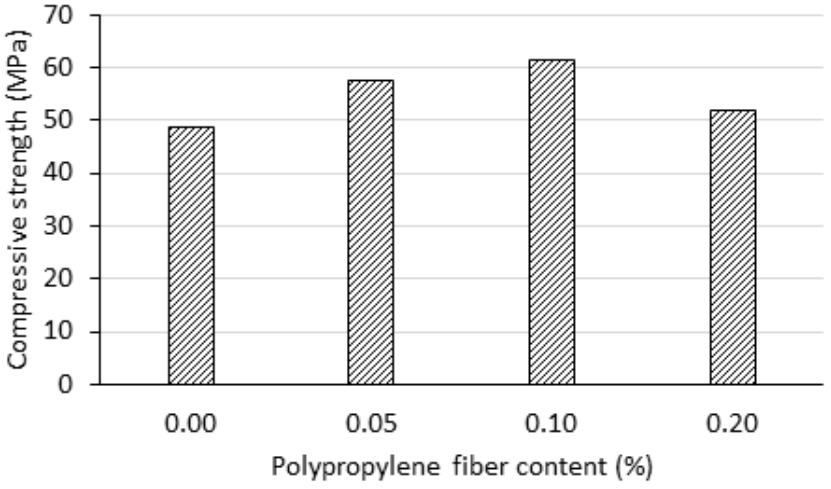

Figure 1: Compressive strength of cement mortar with Polypropylene fibres

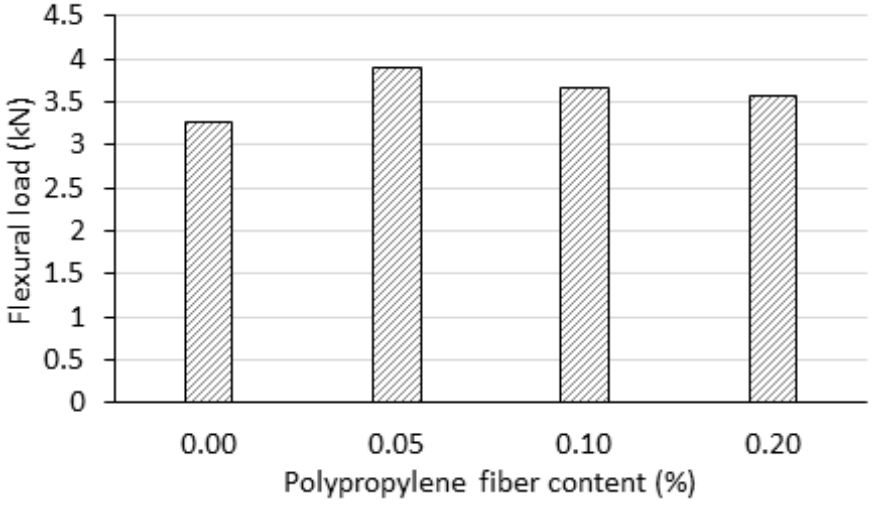

Figure 2: Flexural strength of cement mortar with Polypropylene fibres

Table 1: Mechanical strengths results

Specimen	Compressive strength (MPa)	Flexural capacity (kN)
Control	48.5	3.28
0.05% fiber content	57.5	3.89
0.1% fiber content	61.3	3.67
0.2% fiber content	52.0	3.57

On the other hand, adding polypropylene fibers improved the integrity of the hardened mortar and held the broken parts together after failure as shown in Figure 3.

(a) (b)

Figure 3: Failure mode (a) control specimen (b) mortar with fibers

4 CONCLUSION

1. Adding polypropylene fibers into cement mortar improved its compressive strength. The maximum improvement was noticed in the case of using 0.1% fibers content, which was equal to 26% compared to the control specimen.
2. Adding polypropylene fibers into cement mortar improved its flexural strength. The maximum improvement was noticed in the case of using 0.05% fibers content, which was equal to 19% compared to the control specimen.
3. Cement mortar specimens with polypropylene fibers have ductile failure mode compared to brittle failure for control specimens.

REFERENCES

Li, L. G., Chu, S. H., Zhu, K. L. J. & Kwan, A. K. H. (2018). Roles of water film thickness and fibre factor in workability of polypropylene fibre reinforced mortar. *Cem. Concr. Compos*, 93 196-204. https://doi.org/10.1016/j.cemconcomp.2018.07.014.

Li, L. G., Zhao, Z. W., Zhu, J., Kwan, A. K. H. & Zeng, K. L. (2018). Combined effects of water film thickness and polypropylene fibre length on fresh properties of mortar. *Constr. Build. Mater*, 174 586-593. https://doi.org/10.1016/j.conbuildmat.2018.03.259.

Mohseni, E., Khotbehsara, M. M., Naseri, F., Monazami, M. & Sarker P. (2016). Polypropylene fiber reinforced cement mortars containing rice husk ash and nano-alumina. *Constr. Build. Mater*, 111 429-439. https://doi.org/10.1016/j.conbuildmat.2016.02.124.

Nunes, V. A., Borges, P. H. R. & C. Zanotti (2019). Mechanical compatibility and adhesion between alkali-activated repair mortars and Portland cement concrete substrate. *Constr. Build. Mater*, 215 569-581. https://doi.org/10.1016/j.conbuildmat.2019.04.189.

Szeląg M. (2019). Evaluation of cracking patterns of cement paste containing polypropylene fibers. *Compos. Struct*, 220, 402-411. https://doi.org/10.1016/j.compstruct.2019.04.038.

Zanotti, C., Borges, P. H. R., Bhutta, A. & Banthia, N. (2017). Bond strength between concrete substrate and metakaolin geopolymer repair mortar: Effect of curing regime and PVA fiber reinforcement. *Cem. Concr. Compos*, 80 307-316. https://doi.org/10.1016/j.cemconcomp.2016.12.014.

Cite this article as: Irshidat M. R., Al Nuaimi N., Salim S., Rabie M., "Dosage Optimization of Polypropylene Fiber for Strength Enhancement of Cementitious Composites", *International Conference on Civil Infrastructure and Construction (CIC 2020)*, Doha, Qatar, 2-5 February 2020, DOI: https://doi.org/10.29117/cic.2020.0047

Effect of Alkaline Activators on the Mechanical Properties of Geopolymer Mortar

Mohamed Rabie
m.rabie@qu.edu.qa
Department of Civil and Architectural Engineering, Qatar University, Doha, Qatar

Mohammad R. Irshidat
mirshidat@qu.edu.qa
Center for Advanced Materials, Qatar University, Doha, Qatar

Nasser Al Nuaimi
anasser@qu.edu.qa
Center for Advanced Materials, Qatar University, Doha, Qatar

ABSTRACT

Geopolymerization is a process where silica and alumina rich source materials turn into excellent binding materials by the aid of alkali solutions. Materials such as fly ash are by-products in energy power plants. Fly ash is classified based on its constituent materials. Fly ash class F mainly consists of alumina and silica. Compressive strength of class F fly ash geopolymer mortar is influenced by many factors such as fluid to binder ratio, Na2SiO3/NaOH ratio, curing duration, curing temperatures and molarity of the activator solution. The present study investigates the effect of the fluid to binder ratio and Na2SiO3/NaOH ratio on the compressive strength of geopolymer mortar. The curing temperature was fixed to 80 °C. The curing durations investigated was 24h. For each combination, three cubes with dimensions of 50 x 50 x 50 mm were casted. After heat curing in the laboratory oven, the samples were tested on a universal testing machine for the compressive strength. The results showed very high early compressive strength of 66.39 MPa for samples cured at 80 °C and for a duration of 24 hr. The significance of the present study is that it will allow for establishing methods for production of high strength geopolymer mortar that can be used in civil engineering applications, in addition to the environmental advantages of using such source materials to produce binding materials with outstanding mechanical properties.

Keywords: Geopolymer; Fluid to binder ratio; Activator solution; Na2SiO3/NaOH ratio

1 INTRODUCTION

Cement production process requires immense amount of energy and is accountable for 7% carbon dioxide emissions to the atmosphere. It is estimated that production of 1 ton of cement is equivalent to 1 ton of CO2 (Alnahhal et al., 2017; Ng et al., 2018; Singh et al., 2015). There has been an increasing demand to develop a new binding material that can partially or fully replace cement in mortar and concrete. Geopolymerization is a process where three dimensional polymeric chain rings consisting of Si-O-Al-O are formed by alkali, activating the source material that are rich with silica and alumina (Rattanasak & Chindaprasirt, 2009). Binding materials prepared by the geopolymerization process have proven its competency to provide good binding materials, achieving similar or better mechanical properties than cement-based building materials (Görür et al., 2015).

Activator solutions used in production of geopolymer mortar and concrete are mainly potassium and sodium alkaline solutions. The mechanical strength of geopolymer mortar are affected by many factors such as fluid to binder ratio, curing temperature, molarity of the activator solution and the ratio of the Na2SiO3 to NaOH. Similarly, the mechanical properties of cement-based mortar and concrete are highly affected by w/c ratio (Rattanasak & Chindaprasirt, 2009). Recent literature has proved that fly ash is efficiently activated by sodium based alkaline activators (Singh et al., 2015).

The present study investigates the effect of fluid to fly ash ratio with multiple variations of the ratio between sodium silicate to sodium hydroxide to the compressive strength of geopolymer mortar.

2 MATERIALS AND METHODS

2.1 Materials

2.1.1 Fly ash

Class F fly ash with chemical compositions is mentioned in Table 1 below complying with QCS 2014 standards. Fly ash passing sieve #200 (75 μm) was used in the mix design for geopolymer mortar.

Table 1: Chemical composition of Fly ash %

Oxide	SiO2	Al2O3	CaO	Fe2O3	MgO	SO3	K2O	Na2O	Cl-	LOI
%	49.9	17.1	11.8	7.83	4.9	0.42	0.2772	0.1428	0.011	3.5

2.1.2 Alkaline activators

Sodium hydroxide: 12M Sodium hydroxide (NaOH) solution was prepared by mixing 480 gm of NaOH pellets with purity of 99% in one liter of solution. Sodium silicate: Sodium Silicate (Na2SiO3) solution was prepared by mixing 47% (Na2SiO3) to 53% water. The solutions were prepared separately one day before casting the specimens. Both Sodium hydroxide (NaOH) and Sodium Silicate (Na2SiO3) were mixed together prior to mixing it with source materials to produce GPM.

2.1.3 Sand

Commercially available silica sand with grade of 20-30 sand was used conforming to (ASTM Standard C778 2017) for mortar mixing.

2.2 Experimental program

Eight mix designs were prepared to test the compressive strength of GPM. The proportions of the mix designs are depicted in the Table 2.

Table 2: Mix designs for GPM mortar

Sample ID	Fly ash (gm)	Sand (gm)	Alkaline activator/fly ash ratio	Na2sio3/NaOH ratio	Alkaline activator		
					NaOH solution (gm)	Na2SiO3 solution (gm)	Added water (ml)
F1N1	266.7	733.33	0.4	1	53.33	53.33	20
F1N2	266.7	733.33	0.4	1.5	42.67	64.00	20
F1N3	266.7	733.33	0.4	2	35.56	71.11	20
F1N4	266.7	733.33	0.4	2.5	30.48	76.19	20
F2N1	266.7	733.33	0.5	1	66.67	66.67	-
F2N2	266.7	733.33	0.5	1.5	53.33	80.00	-
F2N3	266.7	733.33	0.5	2	44.44	88.89	-
F2N4	266.7	733.33	0.5	2.5	38.10	95.24	-

Fly ash and sand were mixed for 2 minutes at low speed to ensure a homogenous mixture. The alkaline activators were mixed together and then poured into the mixing bowl. The activators solution was mixed with sand and fly ash for 2 minutes at low speed to allow the polymerization reaction between the source materials and the activator solution. The mix was rested for 30 seconds for scraping the materials stuck in the bowl if any, followed by 2 minutes of mixing at medium speed. The flow table test was conducted according to (ASTM Standard C230, 2014) and water was added to improve the workability if needed. After conducting the flow table test the GPM mix was returned in the mixture and mixed for 15 seconds at medium speed. The GPM mixes were casted in 50 mm cubes according to (ASTM Standard C109, 2019). Casted molds were placed in an oven with the curing temperature and duration fixed for all GPM mix designs at 80 ^{o}C and 24 hours respectively. Both curing temperature and duration were selected based on a preliminary study, with similar values reported in the literature. After 24 hours in the oven, GPM cubes were left for 30 minutes to cool down to room temperature and then tested in a universal compression testing machine.

3 RESULTS AND DISCUSSION

3.1 Compressive strength

The average of three specimen cubes were taken for the compressive strength results shown in Table 3. All specimen experienced similar mode of failure as shown in Figure 1. It was noted during testing that the samples encounter an explosive mode of failure. This might be attributed to the strong geopolymerization chain in binding the constituent materials together (Singh, 2018).

Table 3: Compressive strength of GPM

Sample ID	Average compressive strength (MPa)
F1N1	61.12
F1N2	47.94
F1N3	41.70
F1N4	37.67
F2N1	65.70
F2N2	66.18
F2N3	66.39
F2N4	56.64

Figure 1: Compressive strength of GPM cube.

The effect of the alkaline activator/fly ash ratio was noticeable as there was a decreasing trend in the compressive strength for mix designs with alkaline activator/fly ash ratio 0.40 as the Na2sio3/NaOH ratio increased from 1 to 2.5. On the other hand, for mix designs with alkaline activator/fly ash ratio of 0.5 as the Na2sio3/NaOH ratio increased from 1 to 2, the effect on the compressive strength is negligible. However, for sample F2N4 a slight decrease in the compressive strength was reported.

3.2 Flow table test

The flow table test was conducted for all mixes to check the consistency for GPM. It was noted that as the alkaline activator/fly ash ratio increased from 0.4 to 0.5 the flow table results improved without adding additional water to obtain a consistent GPM mix as shown in Figure 2. The flow table test is summarized in Table 4.

Table 4: Flow table results

Sample ID	Flow table (cm)
F1N1	14.25
F1N2	15.63
F1N3	14.94
F1N4	15.31
F2N1	16.25
F2N2	16.50
F2N3	16.06
F2N4	16.13

Figure 2: Flow table test of GPM

4 CONCLUSION

The effect of alkaline activator/fly ash ratio and Na2sio3/NaOH ratio on the mechanical properties of GPM was investigated and the following conclusions were highlighted:

- The effect of alkaline activator/fly ash ratio is a major contributor to the mechanical properties of GPM, as it increases, the compressive strength increases significantly.
- As the Na2sio3/NaOH ratio increases, the compressive strength decreases at low alkaline activator/fly ash ratio. However, this effect is insignificant at higher ratio of alkaline activator/fly ash.
- The higher alkaline activator/fly ash the more consistent the GPM mixes.
- Maximum early compressive strength of 66.39 MPa was achieved by F2N3 alkaline activator/fly ash of 0.5 and Na2sio3/NaOH of 2.
- Fly ash shows very promising results that will ultimately be used in construction and building materials replacing OPC.

REFERENCES

Alnahhal, M. F., Alengaram, U. J. & Jumaat, M. Z. (2017). Evaluation of industrial by-products as sustainable pozzolanic materials in recycled aggregate concrete.

ASTM Standard C109. (2019). Standard Test Method for Compressive Strength of Hydraulic Cement Mortars (Using 2-in. or [50-mm] Cube Specimens). 1-10.

ASTM Standard C230. (2014). Standard Specification for Flow Table for Use in Tests of Hydraulic Cement 1. 1-6.

ASTM Standard C778. (2017). Standard Specification for Standard Sand.

Görür, E. B., Karahan, O., Bilim, C., Ilkentapar, S. & Luga, E. (2015). Very high strength (120 MPa) class F fly ash geopolymer mortar activated at different NaOH amount, heat curing temperature and heat curing duration. 96, 673-678.

Ng, C., Alengaram, U. J., Wong, L. S., Mo, K. H., Jumaat, M. Z. & Ramesh, S. (2018). A review on microstructural study and compressive strength of geopolymer mortar, paste and concrete. *Construction and Building Materials*, Elsevier Ltd, 186, 550-576.

Rattanasak, U. & Chindaprasirt, P. (2009). Influence of NaOH solution on the synthesis of fly ash geopolymer. *Minerals Engineering*, Elsevier Ltd, 22(12), 1073-1078.

Singh, B., Ishwarya, G., Gupta, M. & Bhattacharyya, S. K. (2015). Geopolymer concrete: A review of some recent developments. *Construction and Building Materials*, Elsevier Ltd, 85, 78-90.

Singh, N. B. (2018). Fly ash-based geopolymer binder: A future.

Cite this article as: Rabie M., Irshidat M. R., Al Nuaimi N., "Effect of Alkaline Activators on the Mechanical Properties of Geopolymer Mortar", *International Conference on Civil Infrastructure and Construction (CIC 2020)*, Doha, Qatar, 2-5 February 2020, DOI: https://doi.org/10.29117/cic.2020.0048

Integrated Accident Resilience Framework (IARF) – A Theoretical Approach Using Spatial and Statistical Analysis

Sumanta Ghosh
s.ghosh@qdcqatar.net; sumantaghosh.76@gmail.com
Qatar Design Consortium, Doha, Qatar

Srinivasan Manickam
srinivasan.m@qdcqatar.net
Qatar Design Consortium, Doha, Qatar

Muhammad Haider
muhammadhaider1997@gmail.com
Qatar Design Consortium, Doha, Qatar

ABSTRACT

Throughout the world, road accidents have become a nightmare for any local government. Data shows that every 24 seconds someone dies on the road (WHO, 2018). Generally, there are multiple factors causing road accidents such as traffic volumes/composition, speed, infrastructure conditions, climatic conditions, and vehicle factors etc. Through this paper, an effort has been made to bring an effective Integrated Accident Resilience Framework (IARF). The framework is in the form of a theoretical method which may help transportation agencies and governments to develop a practical system for crash analysis and mitigation. The Integrated Accident Resilience Framework (IARF) showcased in this paper consists of different stages such as data collection, storage, and analysis, which help to compute correlations between crash causational parameters and crash frequency. The tools used to perform the analysis functions in the framework consist of the GIS platform, as well as the application of the negative binomial regression model. The computed results help identify the major influencing parameters that are linked to traffic accidents and their contribution to crash frequency in black spot locations. This can be used to mitigate future crashes by taking appropriate remedial measures in collision-prone regions. The methodology presented can also be scaled up to a city level network. The entire transportation network can be spatially marked to develop a resilient accident management strategy; even a real-time also.

Keywords: Framework; Accident; Resilience; Parameters; Correlation

1 INTRODUCTION

The World Health Organization recognizes that of all the systems that citizens must encounter in their day to day lives, road transport is the most complex and most dangerous (WHO, 2018). In fact, road accidents are globally the leading cause of death for individuals within the ages of (5) and (29). An approximate 1.35 million deaths occur due to vehicle crashes every year; and following the current trends, this number could rise to 2 million deaths per year by 2030 (WHO, 2018). A fact that is often overlooked is that along with the loss of lives is the economic impacts that accidents have, which is an astonishing 1-3% of a nation's total GDP (WHO, 2015).

Although it is impossible to prevent road crashes completely, effective reformatory actions can assist in reducing crash rates for the future. Traditionally, traffic agencies used methods such as using crash rate to traffic volume ratios at a location to identify possible areas of high collision risk. Thenceforth, other locations with similar traffic/ geometric conditions were compared to improve the investigation. However, such methods of predicting crash frequency and their contributing variables are viewed as outdated, and shortsighted (Al-Marafi et al., 2018). Accurate verification of the causes of crashes at specific locations is vital to identify the major deficiencies of the road network within a study area, and to help take appropriate mitigation measures to tackle them. This requires the development of a practical data collection, storage, analysis, and management system known as an accident resilience framework. The success of an accident resilience framework depends on the ability of transportation agencies, analysts, the police, academicians and local governments to work collaboratively with one another. This is essential to ensure that the whole process of the framework is accurately carried out and that necessary actions are taken based on the conclusions.

2 BACKGROUND RESEARCH

Traffic safety studies aim to associate different variables that may cause accidents to crash frequency. Such variables may be the road geometry, environmental conditions, traffic factors, vehicle factors, and human behavior (Tarko et al., 2008). Early models that were used to predict traffic accidents consisted of simple multiple linear regression which assume a normal distribution of errors. It was later determined by analysts that a Poisson (exponential) distribution would represent a better fit for crash occurrence (Mohammad et al., 2018). However, since crash frequency data tends to be over-dispersed, negative binomial regression models are used in the latest models in order to accommodate for such situations (Zhang et al., 2014). The benefit of using negative binomial distribution is that Poisson distribution restricts the mean and variance to be equal to one another, an assumption that does not always hold true. This can be overcome by using the negative binomial distribution model, which can account for over-dispersion that may exist in crash data counts, and nullify the mean equals the variance condition (Abdulhafedh, 2017). Negative binomial regression models have been used for over decades and still remain the most accepted practice of modelling crash data as of today. Application of the Negative Binomial Distribution model can be found in multiple safety research studies such as "Forecasting Crashes at the Planning Level" (Guevara, 2004), "The Relationship Between Truck Accidents and Geometric Design of Road Sections: Poisson verses Negative Binomial Regressions" (Miaou, 1994), "Accident Prediction Model for Freeways" (Persaud et al., 1993), and "Negative Binomial Regression Model for Road Crash Severity Prediction" (Naghawi, 2018).

In order to develop an accurate statistical model representing crash data, the collection and storage of data is equally as important as the analysis. For this, GIS platforms are a pivotal technique used to visualize and store road accident data (Zhang, 2014). In fact, GIS platforms have been used in several traffic studies such as "Crash Prediction and Risk Evaluation Based on Traffic Analysis Zones" (Zhang, 2014), "A GIS based traffic accident data collection, referencing and analysis framework for Abu Dhabi" (Khan et al., 2004), "GIS for Road Accident Analysis in Hong Kong" (Chan, 2009), and "GIS-

based spatial analysis of urban accidents: Case study in Mashhad, Iran". Safety analysts prefer to use GIS due to its efficiency in handling data, and its numerous spatial analysis techniques which can help identify accident black spot locations such as proximity analysis with buffer operations (Chan, 2009), or using a hotspot analysis (Shafabakhsh, 2017).

3 FRAMEWORK

After examining numerous studies, as mentioned in the literature review, an optimal accident resilience framework is developed. There are two different stages encompassing the accident resilience framework. The first stage, focuses on a procedure for the police to record, store, and maintain data in a database accessible to transportation agencies and analysts. The successful conduction of this stage will be critical for accurate model development as it directly corresponds to the final output results. The second stage highlights the method of how the data can be analyzed using multiple tools to identify and mitigate future collision in accident-prone areas. This stage will be the responsibility of transportation agencies and their analysts working towards a mitigation strategy for accident black spot locations.

The effectiveness of this specific framework lies in its ability to combine both spatial and statistical analysis tools which will provide maximum insight for analysts to dissect the major concerns in prevalent high-risk areas. Due to this, the GIS platform, in conjunction with modern statistical software's are used to produce the final model results. The final model results will clearly specify the contribution of each tested parameter to crash frequency. The accuracy of the results will be validated by the use of multiple methods, e.g. mean absolute deviance; mean squared predictive error etc., to assure that the model measure of prediction is acceptable.

3.1 Accident Resilience Framework - Stage 1

As seen below in Figure 1, the first stage of the accident resilience framework starts at the data collection and storage stage. The responsibility of ensuring that this component of the framework is carried out properly falls on the police or enforcement that arrives at the site of the collision.

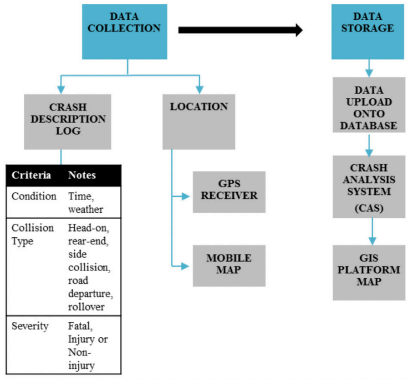

Figure 1: Accident Resilience Framework – Stage 1

3.1.1 STEP 1: Data Collection

The first step involves the completion of a crash description log which clearly notes the type and severity of the collision. Other details such as the time, date, weather/ environmental conditions must also be noted. The second component of the data collection stage consist of recording the exact location of the crash. This can be done in two ways, either by using a GPS receiver, or by pinning the crash location onto a map on a mobile phone. The accuracy of the pinned crash location is crucial as it plays a vital role in examining collision black spots in the analysis stage.

3.1.2 STEP 2: Data Storage

Once the data has been collected, the police must ensure the proper storage of all recorded on-site data. The data will be uploaded by the police onto a centralized database which can be easily accessed by transportation agencies/analysts. This database can be referred to as a "Crash Analysis System" (CAS). The Crash Analysis System will be in the form of a GIS compatible map with geo-referenced locations of all crashes as uploaded by the police, including the details recorded from the crash description log.

Based on a previous literature study, the Highway Safety Information System (HSIS) was a database, which contained accident data for a select group of states in the United States (USDOT, 1999). The HSIS was integrated with a GIS system to develop a crash referencing and analysis system. This improved the ability of analysts and engineers to identify safety deficiencies and perform countermeasure evaluation studies. Furthermore, reporting of accidents was made quicker and more accurate with the combined use of the global positioning system (GPS). Problems were quickly evaluated based on spatial relationships, and even non-traditional data such as land use, zonal ordinance, and population characteristics were fed into the GIS system (USDOT, 1999). Hence, the development of a GIS based crash analysis system is of paramount importance to allow for an effective spatial analysis of crash data for any region. Due to this, the application of GIS has been integrated within our framework. In the next stage, spatial data captured from stage 1 will be further analyzed in the GIS platform, and crash data will be statistically modelled.

3.2 Accident Resilience Framework - Stage 2

As seen in Figure 2 below, the second stage of the accident resilience framework will focus on the analysis of the collected/stored data in a sequential process. The steps involved in this process are briefly explained in the subsequent sections below.

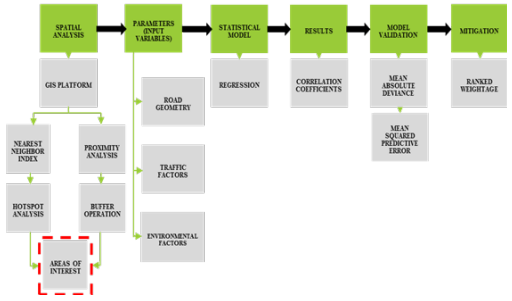

Figure 2: Accident Resilience Framework – Stage 2

3.2.1 STEP 1: Spatial Analysis

The first step of the analysis stage will be completed in the form of a spatial analysis on a GIS platform. The spatial analysis will help in identifying road segments that are prone to frequent collisions, otherwise known as accident black spots (Reshma et al., 2012). This can be conducted in two ways, by conducting a proximity analysis utilizing the buffer operation (Chan, 2009), or by computing the nearest neighbor index followed by a hotspot analysis (Shafabakhsh et al., 2017).

The nearest neighbor index is a calculation of the distance between neighboring feature centroids. It can be easily computed under the pattern toolset in a GIS platform. If the result of the nearest neighbor is a value less than 1, the pattern exhibits clustering. However, if the result is less than 1, the pattern leans towards dispersion. If clustering is present, a hotspot analysis will be conducted in order to identify areas of high collision (hot spot) and low collision (cold spot) frequency. This is done under the spatial statistics tool, and by defining the number of crashes feature as the input parameter. The generated layer will be in the form of hot/cold spots and help in defining segments of interest which will be used as the datasets for statistical modelling in the next stage. However, if the value for the nearest neighbor index is found to be above 1, the data exhibits dispersion and a proximity analysis may be conducted for a more adequate visualization of the data.

The second method of obtaining accident black spots is by conducting a proximity analysis in the form of using the buffer toolset. Aggregation through buffering operation can assist in focusing on disputed locations to undergo mitigation assessments. Larger buffers correspond to areas of higher frequency of collisions within a specified distance. This technique is also showcased in a study conducted in Hong Kong as mentioned in the literature review (Chan, 2009).

Using either, or both methods will assist the user in defining the high-risk road segments for which all input variable information will be needed from the appropriate departments. These details are explained in the next section.

3.2.2 STEP 2: Parameters - Input Variables

The next phase of the framework showcases the parameters to be assessed for their potential contribution to road accidents in the analyzed black spots.

Table 1: Selected Input Parameters and Required Details

Parameter	Source	Details
Road Geometry	• Local Public Works Authority • GIS Map	• Length of Segment (km) • Posted Speed (km/h) • Number of Lanes • Average Lane Widths (m) • Width of Shoulder (m) • Access Point Density (# of points/km) • Average Curvature Radius (m) • Max Curvature Radius (m) • Average Up-Grade (%) • Max Up-Grade (%) • Average Down-Grade (%) • Max Down-Grade (%)
Traffic Factors	• Local Transport Model	• Average AADT per Lane (vehicle/lane) • Heavy Vehicles (%); Speed
Environmental Conditions	• Meteorology Department	• Annual Rainfall at Location (mm)
Crash Data	• Crash Analysis System	• Accident Frequency Per Year (crashes/year)

Once all the high risk road segments have been identified using the method highlighted

in the previous section, their respective geometric, traffic, weather, and crash data are needed. In the case of applying this framework locally, any information regarding the road geometry characteristics can be requested from the local public works authority, traffic factors data can be extracted from the transport model of the region, and climate data can be obtained from the local meteorology department. However, geometric details of roads may also be extracted straight from the GIS map features as a backup if the goal is to perform a quick analysis. A list of parameters that should be tested are specified in Table 1 above. Depending on the available data, parameters to be tested may be added to the users liking. The available input parameters are later modelled through a statistical approach to establish a relationship among the parameters (independent variable) against the number of crashes (dependent variable).

3.2.3 STEP 3: Statistical Model

A comparative assessment among different statistical models has carried out to determine the most suitable crash modelling technique (Mohammad et al., 2018). The best suited statistical model was found to be in the form of negative binomial regression. The general form of the negative binomial regression model has been presented in the equation (1) below:

$$P(y_i) = \frac{e^{-\lambda_i e^{\varepsilon_i}} (\lambda_i e^{\varepsilon_i})^{y_i}}{y_i!} \quad (1)$$

Where $P(y_i)$ is the probability of segment i experiencing y_i accidents in one year and λ_i equals to the number of accidents per year on segment i. ε_i is an error term. The addition of ε_i makes the variance different from the mean, which is a limitation of the Poisson distribution (Mohammad et al, 2018).

The model is to be developed in a software capable of performing negative binomial regression. Several statistical modelling software's are available such as SPSS (Chengye, 2013), amL (Guevara, 2004), R Statistic (Oh et al, 2003), which allow users to input the dependent and independent variable data in a spreadsheet format. The software's are capable of performing a negative binomial regression model of the data and present an output in a tabular format.

Causational parameters such as geometric data, traffic data, and climate data will act as the independent variables for the model as described in the section 3.2.2. Conversely, the crash frequency within the specified road segment will act as the dependent variable. Each year's data for a segment is to be treated as a separate sample. However, the most recent 20% of data should not be used for the model's development as that will be used for validating the prediction performance. The development of the negative binomial regression model helps to define the degree of impact of each input parameter through its computed coefficient value. This has been explained in the next section.

3.2.4 STEP 4: Results

The results of the model will be in the form of a table providing coefficient/estimate values for each parameter along with other computed values such as standard errors, z-values, t-statistics, goodness of fit etc. An example of a set of results are presented in the

study "Modelling Motorway Accidents using Negative Binomial Regression" (Chengye, 2013), and "Negative Binomial Regression Model for Crash Severity Prediction (Naghawi, 2018). The significant takeaway from the results are the correlation/estimate coefficients, which express the significance of contribution of each parameter to crash frequency in the black spots; e.g. a positive coefficient of high magnitude will express a significant contribution to causing road accidents, whereas negative coefficient of high magnitude will express a negative impact on crash frequency. As coefficient values approach 0, the more insignificant the parameter will be in affecting crash frequency.

3.2.5 STEP 5: Model Validation

As stated in section 3.2.3, the latest 20% of the crash data shall not be used in the model development. The latest 20% of data shall be used for the validation of the model. The two techniques used for model validation are the computation of Mean Absolute Deviation (MAD) and Mean-Squared Predictive Error (MSPE), as stated in the study "Validation of FHWA Crash Models for Rural Intersections" (Oh et al., 2003).

The Mean Absolute Deviance calculates the average miss-prediction of the model. A value closer to 0 implies that the model predicts the observed data well on average. The equation for Mean Absolute Deviance (MAD) is given as follows:

$$\text{MAD} = \frac{\sum_{i=1}^{n} |\hat{Y}_i - Y_i|}{n} \tag{2}$$

Where, $\hat{Y}_i$ is the fitted value of Y_i. Variable n is the data sample size.

The second step of validating the model prediction is by computing Mean-Squared Predictive Error (MSPE). The Mean-Squared Predictive Error is an error corresponding with a validation or external data set. The equation for Mean-Squared Predictive Error (MSPE) is given as follows:

$$\text{MSPE} = \frac{\sum_{i=1}^{n} (\hat{Y}_i - Y_i)^2}{n} \tag{3}$$

Based on the magnitude of the deviance between the estimated and actual value of crash frequency, an iterative model building process may be adopted for a more accurate representation. This iterative process may consist of a series of steps including the elimination of skewed datasets, removal of less significant input parameters etc.

3.2.6 STEP 6: Crash Mitigation

A crash mitigation strategy can be formulated based on the results of the regression model. The final estimate/coefficient values for each parameter will clearly specify the affect they have on crash frequency. This will give analysts a clearer picture of the possibilities that may be the common cause of crashes at the collision hotspots. E.g. if maximum curvature is found to cause the biggest increase in crash frequency, analysts can aim to provide proper signage or reduce the speed to ensure drivers can safely manoeuvre around the curves. Similarly, certain contributors may be found to

reduce crash frequency if the calculated coefficient is found to be a negative value. E.g. if the median width value is modelled to have a negative coefficient, it will imply that the presence of a wider median is actually beneficial in mitigating crashes. The crash mitigation strategy will aim to propose mitigations in an order of weightage, with the highest contributors of crash frequency to be mitigated first.

4 BENEFITS OF THE FRAMEWORK

The application of the accident resilience framework proposed in this paper is beneficial for society as it:

a. Promotes the creation of a crash analysis system which will act as a database for future research and development in the area of accident resilience
b. Combines spatial and statistical analysis tools that are best suited to visualize and model crash data, based on modern day research.
c. Is dynamic in nature and allows analysts to choose any accident related parameters to be tested to their liking, based on the depth of available data.
d. Accurately depicts the contribution that tested parameters have on road accidents occurring at black spot locations.
e. Has a quick and cost effective procedure to acquire test results.
f. Allows transportation agencies and analysts to develop mitigation strategies based on a precise and validated model.
g. Encourages a range of stakeholders to cooperate and work in unison to improve safety of the public.

5 FUTURE WORK

The primary focus in this proposed framework is the modelling of total number of crashes and their association with the various parameters that may contribute to their occurrence. The model can help identify hazardous road segments that are in need of being treated through taking the necessary mitigation measures. However, there is still scope for further work to be done on the subject matter of crash data modelling such as correlating zonal based parameters such as demographic, social, and economic factors. Some of these zonal based factors that have not been considered are age, gender, population density, average income per person, occupation types, total time of driving experience, behavioral characteristics etc. However, this will require a detailed survey/ consensus of the population in the study area to obtain an accurate model which can be explained.

Another area that has a potential for more research is the GIS platform. The GIS platform is an effective way to visualize and store crash data. However, GIS data in 3D can be difficult to create and maintain than 2D data. E.g. a road network that is modelled in 3D will contain z-values that would be a lot more complex to maintain than a 2D model. Hence, newer developments in the application of 3D GIS can help create a more comprehensive understanding of a particular area, and in our case, the high-risk collision areas. Moreover, 3D based modelling can help retrieve geometric parameter information such as alignments/grading much faster than having to rely on public authorities to provide the data, which will definitely take much longer and delay the analysis process.

There is room for further development of the framework in terms of its operational

readiness. E.g. Once the final model has been validated to identify the probabilities of crashes in real time, a mechanism/strategy can be developed for authorities such as emergency response teams to reach out to these accident black spots as quickly as possible. E.g. if parameters such as the road curvature, traffic composition, or vertical alignments are computed to have a significantly high contribution to crashes at a location with high validity (95%, 90% or 85% etc.), the spatial model will immediately alarm users that there is a high risk (85%+ probability) of an accident that may occur. This will allow to further enhance the operational strategy for accident response teams and help to ensure that citizens affected by road accidents can be assisted timely and effectively.

It is also worth mentioning that there is a prospect of developing an accident resilience framework for Qatar using the fundamental theoretical model provided in this paper. Such a framework would be particularly beneficial for a booming nation like Qatar that is constantly experiencing a rapid growth in its population, as well as an increase in traffic saturation.

6 CONCLUSION

Traffic accident prediction and safety evaluation is critical in order to combat the ever-growing issue of road accidents. This paper presents a feasible Integrated Accident Resilience Framework (IARF) that is developed combining multiple modern day methods and tools. The framework encompasses a broad series of actions that can be taken by different stakeholders to improve the transport system of society. A set procedure is described of how crash data is to be collected and stored by local police, a step which is critical to act as a baseline for all future studies to be conducted on the subject of crash analysis. The GIS tool is used for spatial analysis as it contains a range of tools to identify high-risk areas that need to be assessed immediately. The two major tools selected for this were the hotspot analysis, as well as the proximity analysis. Both methods are effective ways to visualize the study areas, as well as efficient and quick to perform. Three classifications of parameters to be tested have been included such as road geometry, traffic factors, and environmental conditions. Specific parameters to be tested may be added or deducted based on the depth of available information available to analysts. In terms of the statistical modelling of the crashes, numerous literature reviews were examined which confirmed that that the negative binomial regression was the most widely accepted and best fitting regression for crash data. The results are provided in a tabular format which clearly identify the magnitude of the effect each parameter has on crash frequency in high-risk areas within a region, municipality, city etc. Lastly, a mitigation strategy is developed based on the ranked weightage of which parameters are the largest contributors to crash frequency. When looking at potential future work, there is still room for further research in order to improve the accuracy of the model by weighing in demographic, social and economic factors, as well as incorporating more widely used 3D technology for modelling road networks in GIS. Additionally, there is opportunity to improve the operational readiness of the model by formulating accident response strategies in the case of high alert results from the model. Lastly, there is a definite possibility of implementing a similar accident resilience framework in a growing nation such as Qatar.

REFERENCES

Abdulhafedh, A. (2017). Road crash prediction models: different statistical modeling approaches. *Journal of Transportation Technologies, 07*(02), 190-205.

Al-Marafi, M. N. & Somasundaraswaran, K. (2018). Review of crash prediction models and their applicability in black spot identification to improve road safety. *Indian Journal of Science and Technology, 11*(5), 1-7.

Chan, W. Y. (2009). GIS for Road Accident Analysis in Hong Kong. *A Journal of the Association of Chinese Professionals in Geographic Information Systems, 10*(01), 58-67

Chengye, P. & Ranjitkar, P. (2013). Modelling motorway accidents using negative binomial regression. *Journal of the Eastern Asia Society for Transport Studies*, 10, 1946-1963.

Guevara, F. L. D., Washington, S. P. & Oh, J. (2004). Forecasting Crashes at the Planning Level: Simultaneous Negative Binomial Crash Model Applied in Tucson, Arizona. *Transportation Research Record: Journal of the Transportation Research Board, 1897*(1), 191-199.

Khan, A., Salim A., Kathairi. A. & Garib, A. (2004). A GIS based traffic accident data collection, referencing and analysis framework for Abu Dhabi. *Paper presented in CODATU XI: World Congress: Towards more attractive urban transportation*, Bucharest, Romania.

Miaou, S.-P. (1994). The relationship between truck accidents and geometric design of road sections: Poisson versus negative binomial regressions. *Accident Analysis & Prevention, 26*(4), 471-482.

Mohammed, A., Ambak, K., Mosa, A. & Syamsunur, D. (2018). Classification of Traffic Accident Prediction Models: A Review Paper. *International Journal of Advances in Science Engineering and Technology, 6*(2), 35-38.

Naghawi, H. (2018). Negative Binomial Regression Model for Road Crash Severity Prediction. *Modern Applied Science*, *12*(4), 38.

Oh, J., Lyon, C., Washington, S., Persaud, B. & Bared, J. (2003). Validation of FHWA Crash Models for Rural Intersections: Lessons Learned. Transportation Research Record: Journal of the *Transportation Research Board. 1840*(1), 41-49

Peden, M. M., Organization, W. H. & Bank, W. (2004). *World Report on Road Traffic Injury Prevention*. Chapter 1, Page 3. World Health Organization.

Persaud, B. & Dzbik, L. (1993). Accident Prediction Model for Freeways. Transportation Research Record. 1401, 55-60.

Reshma, E. K. & Sharif, U. (2012). Prioritization of Accident Black Spots Using GIS. *International Journal of Emerging Technology and Advanced Engineering, 02*(09), 117-125.

Shafabakhsh, G. A., Famili, A. & Bahadori, M. S. (2017). GIS-based spatial analysis of urban traffic accidents: Case study in Mashhad, Iran. *Journal of Traffic and Transportation Engineering (English Edition), 4*(3), 290-299.

Tarko, A. P., Inerowicz, M., Ramos, J. & Li, W. (2008). Tool with road-level crash prediction for transportation safety planning. Transportation Research Record: *Journal of the Transportation*

Research Board, 2083(1), 16-25.

USDOT. (1999). *GIS-Based Crash Referencing and Analysis System*. U.S. Department of Transportation Washington D.C.

World Health Organization. (2018). *Global Status Report on Road Safety 2018*. Chapter 1, Page 2. Geneva, Switzerland.

World Health Organization. (2015). *Global Status Report on Road Safety.* Chapter 1, Page 4. Geneva, Switzerland

Zhang, C., Yan, X., Ma, L. & An, M. (2014). Crash Prediction and Risk Evaluation Based on Traffic Analysis Zones. *Mathematical Problems in Engineering*, 2014, 1-9

Cite this article as: Ghosh S., Manickam S., Haider M., "Integrated Accident Resilience Framework (IARF) – A Theoretical Approach Using Spatial and Statistical Analysis", *International Conference on Civil Infrastructure and Construction (CIC 2020)*, Doha, Qatar, 2-5 February 2020, DOI: https://doi.org/10.29117/cic.2020.0049

Spatial Impact Network Exposure Model (SINEM) with Integration of Traffic Characteristics and Air Pollution Concentration

Sumanta Ghosh
s.ghosh@qdcqatar.net / sumantaghosh.76@gmail.com
Qatar Design Consortium, Doha, Qatar

Rohit Rp
rohit.rp@qdcqatar.net / rohitrp.planner@gmail.com
Qatar Design Consortium, Doha, Qatar.

ABSTRACT

The State of Qatar has undergone rapid economic growth and urbanization during the last few decades. This has resulted in an increase in the number of motor vehicles in the country. Therefore, it is vital to monitor and manage the air pollution level in Qatar. Traffic-related air pollutants generally have a significant contribution to air pollution especially in urban areas and they also have an adverse impact on the commuters and abutting street population. Limited study has been carried out in this area and particularly in the context of Qatar. The purpose of this research is to establish a relationship between air pollution concentration and a set of parameters related to traffic and network characteristics; such as traffic volume, speed, VCR, etc. This study aims to develop an area-wide Spatial Impact Network Exposure Model (SINEM) using Geographic Information System (GIS). The SINEM shall be developed to assess the area-wide spatial impact of traffic-related air pollution exposure based on an aggregated approach. This model helps to predict the surrounding network exposure index which helps in the decision-making process. Interestingly, this model also has the potential to scale up as well as convert into a real-time model. It will assist relevant authorities and decision-makers to identify and initialize policy measures to reduce the exposure impact, setting up building regulations, FAR implementation and sustainable master plan development.

Keywords: Traffic pollution; Air pollution; Exposure impact; Spatial assessment; Urban air quality

1 INTRODUCTION

Traffic related air pollution is one of the most significant problems that targets a large number of urban areas (Gwilliam et al., 2004). In many areas, motor vehicle air pollutants such as black carbon (BC), carbon monoxide (CO), nitric oxides (NOx), and particulate matter (PM) have become a dominant source of air pollution (Liu et al., 2019). The increasing congestion and vehicular traffic growth may greatly increase the pollutant emission particularly near the roadways (Zhang & Batterman, 2013).

Air pollution is one of the major challenge for the state of Qatar especially with the upcoming events such as FIFA World Cup 2022 etc. (Charfeddine et al., 2016). Over last few decades, Qatar has been through an accelerated phase of urbanization which has come with a drastic increase in the number of motor vehicles on the nation's roads. The number of registered motor vehicles in Qatar have increased nearly 2.9 times over

a decade (Refer to Figure 1). Therefore, the proper monitoring and management of the air pollution level in Qatar is a necessity. Major initiatives needs to be taken in order to ensure real progress in the environment sustainability pillar as part of Qatar Vision 2030.

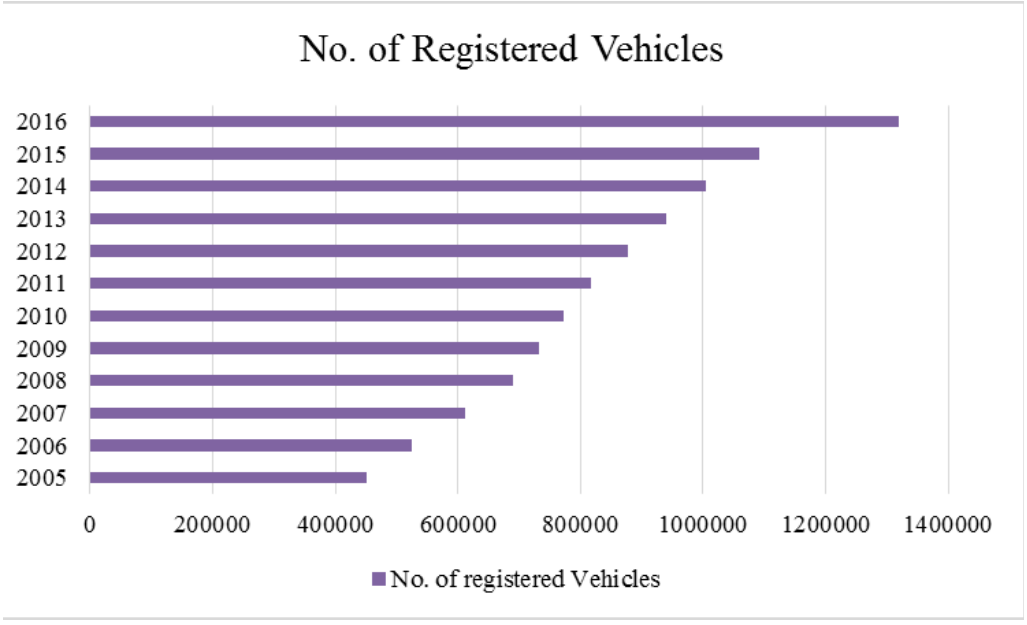

Figure 1: Number of registered motor vehicles (Source: Qatar Planning and Statistics Authority)

Traffic-related air pollutants generally have a significant contribution to air pollution especially in urban areas and have an adverse impact on the commuters and abutting street population. There are several literatures available to investigate the functional relationship between air quality and traffic related air pollution (Kumar et al., 2015). Most research papers that are available either lack in their ability to relate air pollution exposure to traffic characteristics, or they are too complex and not cost effective. Additionally, majority of the research is for exposure appreciation rather than prediction. Limited study has been carried out in this area particularly in the context of Qatar. This paper intends to develop a model framework to establish a relationship between air pollutant concentration and a set of parameters related to traffic and network characteristics; such as traffic volume, speed, vehicle capacity ration (VCR), etc. In the current scenario, implementing monitoring stations at multiple locations within the city are costly and not economically viable. There is a potential opportunity for the integration of the existing available data sources and currently available traffic prediction models such as the Qatar Strategic Transport Model (QSTM) from Ministry of Transportation & Communication (MOTC). The framework presented in this paper aims to develop a prediction model which is an area-wide Spatial Impact Network Exposure model (SINEM) using Geographic Information System (GIS). This model will have the capability to predict the surrounding network exposure index, which assists in the decision-making process and sustainable planning approach.

The paper is organized as follows: Section 1 introduced with the context of the research; Section 2 provides the brief review of the literatures on traffic related air pollution modelling; In Section 3 core elements of the SINEM framework has been explained through schematic flowchart; Section 4 details out the different stages of the SINEM framework with existing data evaluation in GIS platform, model building, prediction and spatial assessment in GIS; Section 5 presents the model benefits and possible interpretations; Section 6 gives the various conclusion of the paper.

2 LITERATURE REVIEW

Sexton and Ryan (1988) has carried out an extensive research on the air pollution exposure models and methods. It is stated that specific emissions sources to the individual exposure are necessary and new models to be developed. However, very few literatures are available for a predictive model for street exposure in particular to traffic related air pollutions. Most of the research works carried out to model the traffic related air pollution and exposure models are limited to pollution concentration, street typology (micro level), specific age group and building height (for example: (Askariyeh et al., 2019); (Valente & Amorim, 2014). However, the congestion period, v/c ratio, speed relation etc., are not taken into account in any of these models. Application of the GIS in air pollution modelling has been carried out by previous researchers (Matejicek, 2005). Considering the specific requirement such as the amount of data, software expertise, implementation cost and marginal benefits, GIS based hybrid model serves the purpose of the exposure modelling at an aggregate level (Jerrett et al., 2005). In context of Qatar, integration of the existing QSTM traffic model with pollution concentration can be better analyzed, and prediction models can be developed which are cost effective and not complex in nature. Also, it is worth mentioning that dynamic prediction models with long term series of data can be better trained with an artificial neural network for improved prediction accuracy (for example (Karimian et al., 2019), (Cabaneros et al., 2017).

3 SPATIAL IMPACT NETWORK EXPOSURE MODEL (SINEM) FRAMEWORK

As shown in the Figure 2, the core elements of the SINEM framework include multiple stages. Initial stages define the spatial and input definition. Spatial definition represents the spatial extent of the model. Input definition defines the dependent (pollution exposure) and independent variables (traffic, environment and study area specific parameters) to be considered for the model. As part of the existing/baseline study, these input variables are to be evaluated and assessed through statistical test to establish the correlation between the dependent and independent variables.

SINEM FRAMEWORK ELEMENTS:

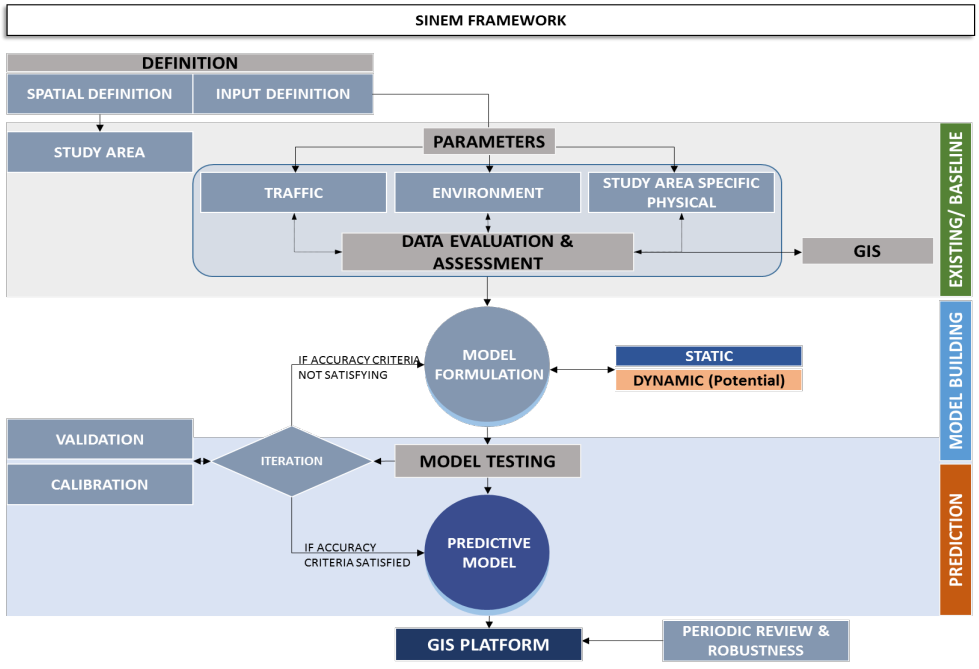

Figure 2: Core Elements of SINEM Framework

GIS has been considered as part of the model building since the digital maps and citywide data base are available for whole of Qatar. ArcGIS software to be utilized for this purpose. As part of the model building process, spatial extent of the study area to be converted into a grid form with 100m by 100m (for city level). According to Shahraiyni, the grid size for the spatial prediction in urban areas should not be less than 100m (Shahraiyni & Sodoudi, 2016). Independent variables are fed into the ArcGIS platform for the entire respective grid. However, the pollution concentration data will be an input to those grids which fall under the survey locations. These grids are to be termed as active grids which inherit the properties of the existing data points. In model building, exposure estimation will primarily be carried out through a static approach using the existing pollution concentration data, as well as both the in-vehicle population and the abutting street population (please refer to Section 4.3). Utilizing the estimated exposure as a dependent variable, multiple regression models shall be developed through an iterative process to attain model accuracy. Training and testing of the model shall be carried out to improve the model prediction accuracy. If the accuracy criteria are satisfied, then the predictive model is to be integrated in the GIS platform to predict the exposure values for those inactive grid cells. It is worth mentioning that in case of a huge data set availability of the pollution concentration, this model can be scaled up to be a dynamic model through application of artificial neural network for improved accuracy and predictions (for example: Karimian et al., 2019).

4 STAGES OF SINEM FRAMEWORK

This section briefly describe the stages involved in the SINEM framework. The prime aim of the model is to establish a relationship between the traffic related air pollution and pollution concentration through an indirect approach and thereby build a predictive model for the population exposure. It can be assessed and visualized in GIS platform (namely ArcGIS), and assist in spatial decision-making.

4.1 Stage 1: Definition & Data Collation

The first stage is to define the spatial extent in line with the objective of the study, which delineates the study area at the scale of microscopic level (zonal level), mesoscopic (city level) or macroscopic (regional level), depending on the objective of the study. As presented in the Figure 3, input variables can be categorized in three forms namely, traffic characteristics (such as link length, traffic volume, number of lanes, v/c ratio etc.), environment (humidity, wind direction etc.) & area specific physical features.

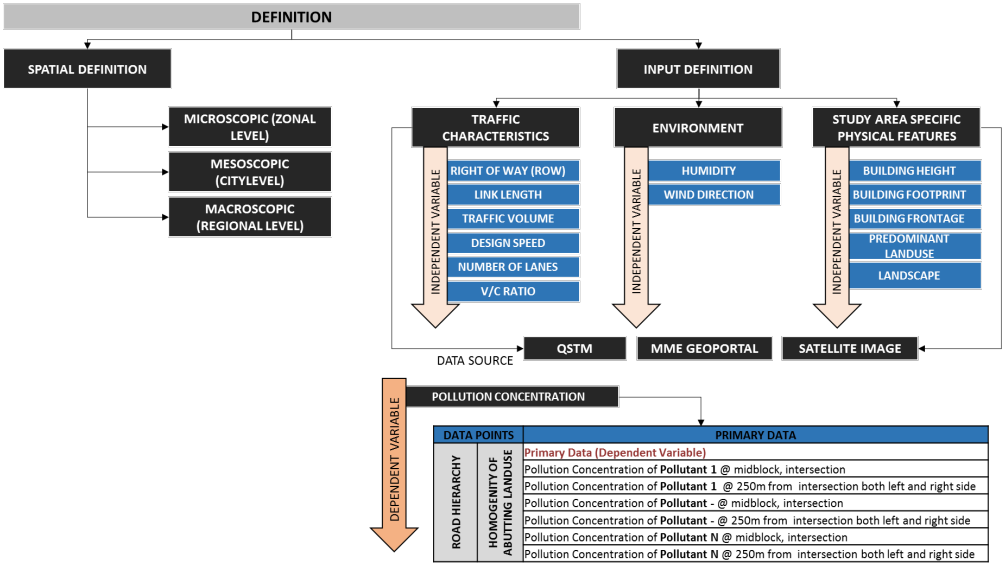

Figure 3: Stage1: Definition and Data Collation of SINEM Framework

Traffic characteristics parameters can be captured through QSTM model and this data can be easily integrated into the ArcGIS. The area specific parameters such as landscape, building footprint, building frontage etc. can be easily extracted through satellite imagery analysis in GIS platform (for example: (Dini & Jacobsen, 2013). Land use information are available through secondary data sources such as the Ministry of Municipality and Environment (MME). However, primary data is also required for the pollution concentration levels. The data sampling is to be carried out on the basis of the road hierarchy and homogeneity of land uses to capture the discrete dataset for modelling exercise.

4.2 Stage 2: Existing Data Assessment & Evaluation

Stage 2 of the framework deals with the data assessment and evaluation as presented

in the Figure 4. Data samples of the pollution concentration of pollutants (P1, P2, Pn) collected as part of the primary survey are to be imported in the ArcGIS platform for the spatial air quality assessment and visualization. Data samples are geo-referenced in the ArcGIS overlaid with network data base link attributes which is extracted from QSTM model. Further, kriging analysis (Tyagi & Singh, 2013) to be carried out to interpolate each pollutant's concentration data samples for the initial review. The existing data range can be classified into high, medium and low categories based on the dataset range. As explained in Section 3, the spatial grid conversion to be deployed and existing survey data points will be inherited in the particular grid cell where the data sample point located. Each grid cell will be having unique numbering and its input data attributes. The active cells with existing data points attributes are fed with all the input parameters and pollution concentration, which is used in the further steps for static model building process to estimate the street exposure.

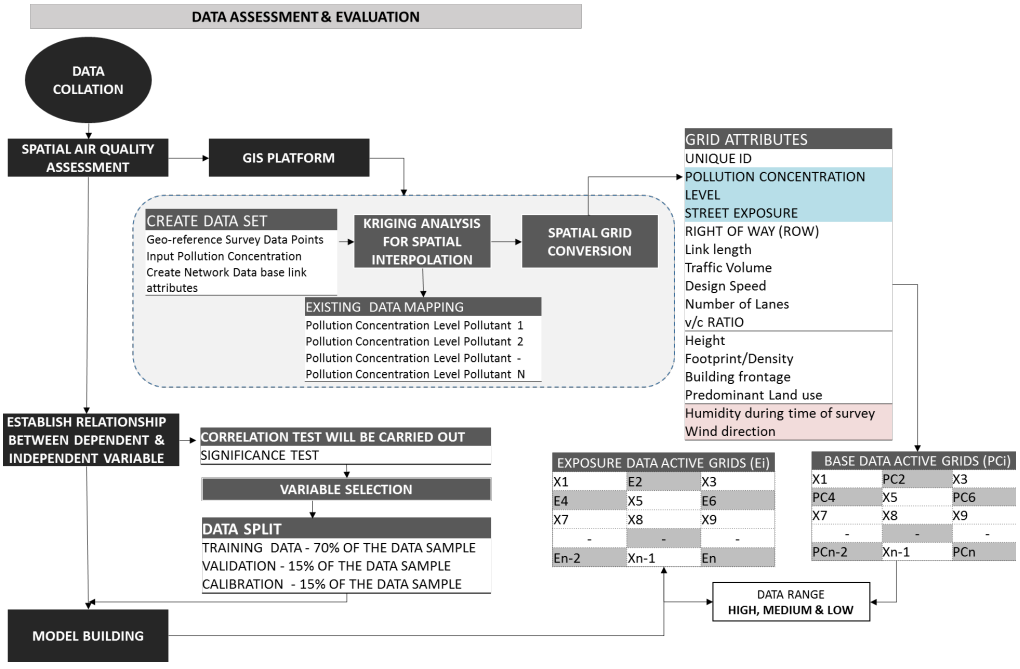

Figure 4: Stage 2: Existing Data Assessment & Evaluation of SINEM Framework

4.3 Stage 3: Model Building & Prediction

Earlier researchers such as Ott (1982), Duan (1982) established simple mathematical formulas to estimate the exposure. Simple Exposure Index does not take into account any traffic-pollution relationships. In general, a simple static exposure model is defined as the ambient air pollution at a geographic location times the total number of people at the location as presented in the equation (1) below. However, some researchers for example: (Kumar et al., 2015)) considered vehicle kilometer travelled to add traffic relation to the exposure model.

$$E\ index = C\ location\ *\ P\ location \quad (1)$$

where,
C location is the concentration level in street, which may be mean, percentile or max values.
P location is the population estimate in that particular location, which is the product of Average Daily Traffic (ADT) and vehicle occupancy.

However, in this framework, the street exposures are estimated as shown in the equation (2) below. Exposure index presented in the equation (2) is a basic mathematical expression, which is product of pollution concentration, street population and average time spent in that particular stretch.

$$E\ street = C\ location * Pstreet * \frac{L}{V} * \frac{1}{L} \quad (2)$$

$$Pstreet = (Nv * Ov) + A\ Pop \quad (3)$$

where,
E street is the street exposure estimate e.g. µg/m3*person*hours/km.
C location is the concentration level in street during the peak hour.
Nv is the number of vehicular traffic during peak hour of type v.
Ov is the vehicle occupancy for the vehicle type v.
A Pop is the abutting street population extracted from QSTM TAZ based on population density.
L is the length of the street.
V is the travel speed of the vehicle type v.
Pstreet is the outdoor street population affected by exposure risk. If we have the data available on pedestrian and bicycle users, can be included in the model.

Stage 3 of the framework which deals with the model building and population exposure is presented in Figure 5. As part of the model building, the exposure estimation for the street within the active grid has been calculated as per using equation (2). The active cells with attribute data to be used as an input for the exposure prediction model building. Shahraiyni & Sodoudi (2016) have carried out an extensive comparative assessment of the different approaches for pollution prediction in urban areas. According to him, the most widely adopted technique for spatial models is the Multiple Linear Regression (MLR) model. However, to capture the temporal variations, Artificial Neural Networks (ANN) have the highest potential for better performance (Karimian et al., 2019). If a huge dataset is available to capture temporal variations, ANN can be deployed in the model for a dynamic prediction model.

In this case, MLR has been considered in the SINEM framework for static modelling for a smaller dataset. Input data is considered based on the correlation test for each pollutant exposure to be considered in the model building. Training and testing of the model shall be carried out with data split proportion of 70% and 30% of the data samples respectively (Dobbin & Simon, 2011). The observed and estimated data has to be tested using statistical approaches such as R squared, the overall F-test and the Root Mean Square Error (RMSE) value for the scatterplot observed and estimate values to evaluate the model fit. If the model fails the test then the model needs to be remodeled with the

best fit function and changes in the parameter coefficient, if required. The predictive model developed needs to be integrated in the ArcGIS to predict the exposure index for the inactive cells. Thus, the model will be capable of fitting the different scenarios, or with the change in the parameters such as ROW, number of lanes, vehicle volume etc. effect on the street population exposure can be estimated and assessed for decision-making.

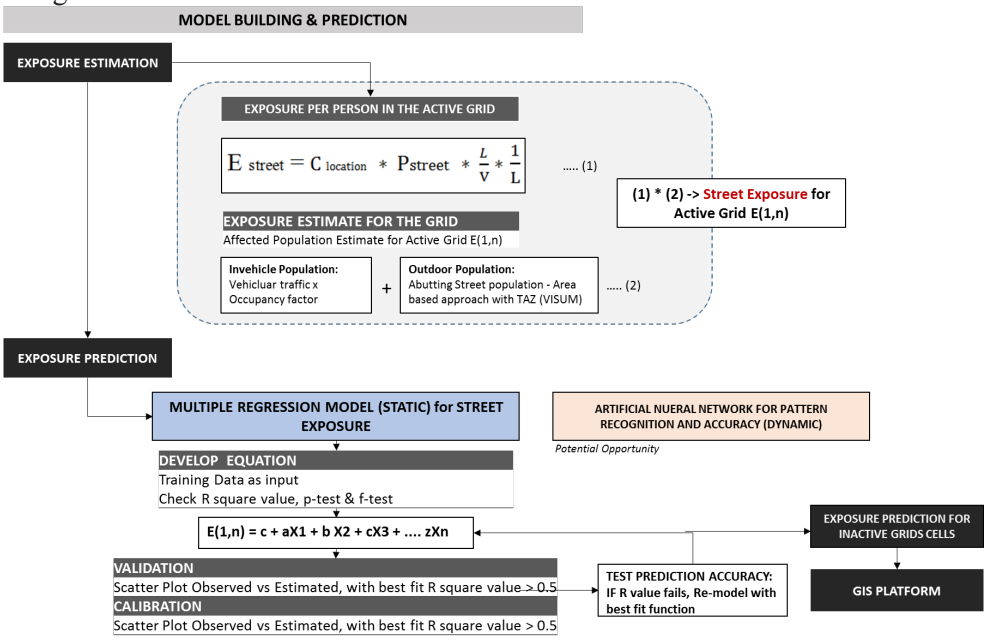

Figure 5: Stage 3: Model Building and Prediction of SINEM Framework

5 ANTICIPATED RESULTS

The key benefits of the SINEM framework are presented below:

a) SINEM helps to understand the exposure levels variation in between and within the different street/network typology.
b) It helps to identify the relationship between each pollutant concentration (traffic related) and traffic/network characteristics.
c) It is a static model in nature but interestingly it can be scaled up to be a dynamic model with increased prediction accuracy using ANN.
d) Allows for the mapping of pollution concentration and exposure level.
e) It has the ability to test different scenarios, which assist in the master planning exercise, policy formulation, building byelaws formulation, FAR implementation and decision making to ensure a sustainable development.

6 CONCLUSION

In the context of the current urbanization rates and increase in the number of vehicles, traffic-related pollution contributes to serious health issues for citizens. It is therefore necessary to monitor and evaluate the traffic-pollution relationships and its spatial impact on the population exposure. In the state of Qatar, majority of the population resides in urban areas. Implementing monitoring stations at multiple locations within

the city to monitor the air pollution levels are not a feasible solution as they are costly and not economically viable. Therefore, the development of a predictive model is crucial for the welfare of society.

This paper presents the integrated modelling framework involving GIS for both exposure assessment and prediction spatially for traffic related air pollutants. The study aims to develop an area-wide Spatial Impact Network Exposure Model (SINEM) integrating traffic-related air pollution using Geographic Information System (GIS). It is a static model integrated into the ArcGIS platform. It makes use of the existing data resources such as satellite imagery, QSTM model, MME GIS portal etc. to capture the input parameters, and thereby it is economically viable and not complex. With the increase of data availability in the future, it can be scaled up to be a dynamic model with the application of ANN for improved accuracy.

REFERENCES

Askariyeh, M. H., Vallamsundar, S., Zietsman, J. & Ramani, T. (2019). Assessment of traffic-related air pollution: Case study of pregnant women in South Texas. *International Journal of Environmental Research and Public Health*, *16* (13), 2433.

Cabaneros, S. M., Calautit , J. K. & Hughes , B. R. (2017). Hybrid artificial neural network models for effective Prediction. *Energy Procedia*. 142, 3524-3530.

Dini, R. & Jacobsen, K. (2013). Delineation of building footprints from high resolution satellite stereo imagery using image matching and a GIS database. International Archives of the Photogrammetry, Remote Sensing and Spatial Information Sciences, XL-1/W1, 81–85.

Dobbin, K. K. & Simon, R. M. (2011). Optimally splitting cases for training and testing high dimensional classifiers. *BMC Medical Genomics*, 4, 31.

Duan, N. (1982). Models for human exposure to air pollution. *Environment International*, 8, 305-309.

Gwilliam, K., Kojima, M. & Johnson, T. (2004). *Reducing Air Pollution from Urban Transport*. Washington, D.C.: The World Bank.

Jerrett, M., Arain, A., Kanaroglou, P. & Beckerman, B. (2005). A review and evaluation of intraurban air pollution exposure models. *Journal of exposure analysis and environmental epidemiology*, 15, 185-204.

Karimian, H., Li, Q., Wu, C., Qi, Y. & Mo, Y. (2019). Evaluation of different machine learning approaches to forecasting PM2.5 mass. *Aerosol and Air Quality Research*, 19, 1400-1410.

Kumar, A., Mishra, R. K. & Singh, S. (2015). GIS application in urban traffic air pollution exposure. *Suan Sunandha Science and Technology Journal*, 2, 25-37.

Lanouar, C., Al-Malk, A. Y. & Al Karbi, K. (2016). *Air Pollution in Qatar : Causes and Challenges*. College of Business and Economics, Qatar University, 1, 1-7.

Liu, S. V., Chen, F.-l. & Xue, J. (2019). *A meta-analysis of selected near-road air pollutants based on concentration decay rates*. Heliyon, 5.

Matejicek , L. (2005). Spatial modelling of air pollution in urban areas with GIS: A case study on integrated database development. *Advances in Geosciences*, 63-68.

Ott, W. R. (1982). Concepts of human exposure to air pollution. *Environment International*, 7, 179-196.

Sexton, K. & Ryan, P. (1988). *Assessment of Human Exposure to Air Pollution: Methods, Measurements, and Models*. In W. AY, B. RR, & K. D, Air Pollution, the Automobile, and Public Health. Washington (DC): National Academies Press (U.S).

Shahraiyni, H. T. & Sodoudi, S. (2016). Statistical Modeling Approaches for PM10 Prediction. *Atmosphere*, 7, 10-13.

Tyagi, A. & Singh, P. (2013). Applying Kriging Approach on Pollution Data Using GIS Software. *International Journal of Environmental Engineering and Management*, 4, 185-190.

Valente, J., Amorim, J. H., Teixeira, R., Pimentel, C. & Borrego, C. (2014). Children's exposure to traffic-related pollution: assessment of CO exposure in a typical school day. *International Journal of Environment and Pollution (IJEP)*, 55, 104-112.

Zhang, K. & Batterman, S. (2013). Air pollution and health risks due to vehicle traffic. *Science of The Total Environment*. 450, 307-316.

Cite this article as: Ghosh S., Rp R., "Spatial Impact Network Exposure Model (SINEM) with Integration of Traffic Characteristics and Air Pollution Concentration", *International Conference on Civil Infrastructure and Construction (CIC 2020)*, Doha, Qatar, 2-5 February 2020, DOI: https://doi.org/10.29117/cic.2020.0050

Implementation of Crumb Rubber Modified Binder for Qatar Local Roads Construction Projects

Charles N. Nunoo
Charles.Nunoo@wsp.com
WSP International / Public Works Authority (Ashghal), Roads Projects Department, Doha, Qatar

Saoud Ali Al-Tamimi
stamimi@ashghal.gov.qa
Public Works Authority (Ashghal), Roads Projects Department, Doha, Qatar

ABSTRACT

The continuous increase in the pile up of used vehicle tires in Qatar poses a challenge contributing to potential environmental pollution problems. The magnitude of this problem can be drastically reduced by processing and recycling these tire wastes into crumb rubber, obtained from grinding up whole scrap tires, and incorporating into conventional asphalt binder to produce Crumb Rubber Modified Binder (CRMB) for asphalt mixes used in pavement construction. Asphalt mixtures which incorporates crumb rubber have been used in different parts of the world, notably USA since the 1960s, ostensibly to solve the associated environmental problems, but with added advantages of improving the overall performance of the asphalt pavement in terms of rutting and crack resistance, increased flexibility and durability. In 2018, the Roads Project Department (RPD) in collaboration with the Quality and Safety Department (QSD) of the Public Works Authority (PWA) in Qatar, undertook a demonstration project which utilized CRMB in the wearing course, in lieu of Polymer Modified Binder (PMB) originally proposed. Preliminary results from this project showed an encouraging prospect for adopting Crumb Rubber Modified Binder technology on local road projects, and eventually on all other roads in Qatar. Consequently, it became imperative for a tentative specification to be quickly put together for use by suppliers and contractors to achieve this goal. The preliminary results of this demonstration project are promising and the ensuing crumb rubber and CRMB guidelines have been useful.

Keywords: Crumb rubber; Crumb rubber modified binder; Polymer modified bitumen; Asphalt mixtures design; Performance test; Environmental pollution

1 INTRODUCTION

Since the 1960s, asphalt mixtures produced with crumb rubber have been used in different parts of the world, notably United States, Canada and many parts of Europe, as a solution for different pavement quality problems and, in the majority of the case, they have demonstrated excellent results by enhancing the overall performance of asphalt pavements. It is well known that the unmodified bitumen has a limited range of rheological properties and durability that are not sufficient to resist pavement distresses, particularly rutting. It has been well-documented around the world including (Harvey et al., 2001) that pavements constructed with CRMB asphalt have demonstrated performance benefits including improved rutting resistance at high temperatures, cracking resistance at low

temperatures and improved durability, as well as functional benefits such as pavement noise reduction. According to Larsen et al. (1988), the bitumen modification provides binders with sufficient increase in consistency at the highest temperature in pavements to prevent plastic deformation, an increase in flexibility and elasticity of binders to avoid crack deformations and loss of aggregates, improvement of bitumen-aggregate adhesion, improved homogeneity, high thermal stability, and aging resistance which helps reduce the hardening and initial aging of the binders during mixing and construction.

Norhidayah et al. (2019) also demonstrated that CRMB asphalt mixtures provide improved temperature susceptibility and flexibility. The modification is achieved by the interaction of crumb rubber (CR) with the conventional asphalt binder at elevated temperatures for a certain period of time. CRMB asphalt mixtures have several advantages over conventional asphalt mixtures including lower susceptibility to varying temperature on a daily basis, more resistance to deformation at higher pavement temperature, proven aging resistance properties, higher fatigue life for mixes, and better adhesion between aggregate and binder. Evidently, CRMB is a proven technology with sound engineering benefits that has been used to build longer lasting, lower maintenance pavements in a cost-effective manner. The main advantages of this technology include its ability to greatly improve the overall performance of the pavement providing increased fatigue resistance, increased flexibility and durability of the pavement, reduction of pavement noise generated into the local residence, and most importantly, increased cost-effectiveness by lowering overall life-cycle cost, and finally reduction of the accumulation of old vehicle tire debris placed at dump sites, thereby eliminating the otherwise nuisance it poses to the environment.

2 MAGNITUDE OF THE PROBLEM IN QATAR

Scrap vehicle tires are being generated and accumulated in large volumes in Qatar causing an increasing threat as a source of environmental pollution. The inappropriate disposal of these tires exacerbates the problems in the immediate and foreseeable future. According to the Qatar Statistics Authority (QSA), at least 500,000 tires are discarded as scrap every year. With the effective age of new tires being about three years in Qatar, the trend is expected to rise. Ironically, though, until recently, there has not been much focus on recycling of used tires in Qatar, which raises more environmental concerns.

In order to eliminate the negative effect of these depositions, in terms of sustainable development, there has been a great interest in processing and recycling these scrap tire wastes into crumb rubber (CR) for incorporation into conventional asphalt binder (60/70 penetration) to produce Crumb Rubber Modified Binder (CRMB), which can then be used for asphalt concrete mixes for pavement construction, as practiced in other countries around the world. With the numerous well documented benefits of crumb rubber for increased fatigue resistance and reduction in ageing of the binder and improving the overall performance of conventional asphalt paving mixes, and in an attempt to mitigate and assuage used vehicle tire menace in Qatar, a concerted effort was taken by PWA and the Ministry of Municipality and Environment to develop a strategy that will encourage the recycling of this scrap tires into road construction, using the existing already proven technologies.

3 CRMB IMPLEMENTATION INITIATIVE FOR PWA ROAD PROJECTS

In line with PWA's strategic objectives for sustainability and preserving the environment, the Roads Projects Department (RPD), in conjunction with WSP International (WSP), undertook an initiative in 2018 to encourage the utilization of crumb rubber as a modifier for asphalt mixes for pavement construction. Accordingly, Nunoo et. al. (2018) submitted a proposal to PWA for the development of a strategy for implementation of this initiative for Qatar local road projects. The proposal was hinged on the aforementioned environmental problem in Qatar and the numerous proven benefits of recycling scrap tires it into asphalt paving mixes for road construction. The objectives established in the proposal included the following:

- Determination of the feasibility of utilizing crumb rubber as modifier for asphalt pavement mixes.
- Ascertaining the cost and benefit of using crumb rubber modified bitumen in lieu of conventional bitumen (60/70) or polymer modified bitumen in asphalt pavements construction.
- Determination of the short-term performance of RPD road projects utilizing CRMB asphalt mixes.
- Collection of useful information and data to facilitate the development of a customized CRMB specifications and guidelines for producers and contractors in Qatar.

To achieve these objectives, the following main tasks were identified:

- Establishment of a preliminary specification for implementing a demonstration project.
- Identification of feasible RPD projects for implementing a demonstration project.
- Identification of CR and CRMB suppliers satisfying the preliminary specification.
- Identification of appropriate contactors with capabilities and expertise to implement CRMB.
- Updating of the contract documents to accommodate the selected demonstration projects.
- Implementation of the pilot projects by selected contractors.
- Monitoring of the pilot projects by QSD, a third-party consultant or institution.
- Production of a final report on the performance and lessons learned.
- Development of specification for widespread utilization of CRMB in Qatar.

4 DEMONSTRATION PROJECT DEVELOPMENT

After several discussions and coordination, the proposal received a positive response and final approval from PWA. Viable local roads projects were identified to serve as demonstration projects with the main objective of evaluating the constructability and short-term field performance of asphalt concrete mixtures containing crumb rubber.

Subsequent to the approval of this initiative, an initial instruction was issued by the president of PWA for CRMB to be use in lieu of PMB on all projects. It became apparent that there was a need for a quick turnaround to develop a tentative specification and procedures for use by CR producers and contractors. A number of discussions were held with representatives from PWA Quality and Safety Department (QSD), about the

best approach for the implementation of the demonstration project in the absence of specification. It was agreed that the implementation should be limited to local roads and in the asphalt wearing course layer. It was also agreed that the demonstration project can use the same mix design as originally developed for the project using PMB. This was based on the consideration that improvement in the properties of these mixtures has been identified as desirable in previous temporary projects in Qatar, including Al Kassarat Street # 1 in the Industrial Area in 2012, and Al Meena Street project in 2013. Unfortunately, these pavements have been reconstructed at various times and so are not available for evaluation and/or verification.

5 DEMONSTRATION PROJECT IMPLEMENTATION

After careful considerations and evaluation of the RPD projects which are scheduled for construction and on the verge of asphalt laying, the Al Kassarat Street # 2 (DS001-Package 2) in the Doha Industrial Area was identified as feasible for the implementation of the demonstration project. This is a six-lane dual carriage roadway with three lanes in each direction. The pavement was designed to accommodate a 20 years design traffic of over 20 million ESALs, and is comprised of 50 mm of dense graded Wearing Course (19 mm nominal maximum aggregate size), over a 70 mm of dense graded Intermediated Course (Base Course Class B), over a 100 mm of dense graded Base Course, over 200 mm of granular Subbase Course, over the prepared Subgrade. The uniqueness of this selection is that, the approximately 1-kilometre length of this project had already been constructed up to the intermediate course, in both directions. One direction of the carriageway had already been paved with PMB asphalt mix wearing course. This unique characteristic of the selected project enabled a better assessment of the success of the demonstration project implementation by comparing results of volumetric and performance tests conducted on cores taken from both the PMB and the CRMB sections in both directions.

A coordinated and collaborative effort was undertaken by WSP with the CR supplier (Al Holdaifi), the CRMB supplier (RAETEX Doha), the selected demonstration project's main contractor (QTCG) and the sub-contractor for the paving works (BOOM Construction). An action plan was developed, with support from QSD for the implementation. This was to ensure that the best possible operational conditions for production, construction, evaluation and material testing were ensured. The CRMB used was produced by the supplier in accordance with the pending version of the revised Qatar Construction Standards (QCS, 2018) and complied with a PG76-10H grade. Meanwhile, the adjacent already constructed PMB Wearing Course segment, in the opposite direction, complied with a PG76-10E grade. It is to be noted that the support for implementation of this demonstration project, by the suppliers and contractors, was undertaken at no additional cost to PWA, as a goodwill gesture to enable this important initiative to materialize.

6 PRELIMINARY TEST RESULTS FROM DEMONSTRATION OF PROJECT

During construction, extra sampling on-site as well as from the plant were collected and specialized tests were performed by QSD, in addition to the standard quality control and quality assurance tests. The preliminary report indicated the following observations:

- The mix design was considered inadequate and asphalt mixture aggregates were not controlled to optimize packing.
- Both the PMB and the CRMB segments did not meet the air voids requirements, probably as a result of the inadequate mix design and/or the level of compaction employed, as it was observed that the steel. breakdown rolling was only two passes and pneumatic tire rolling was prolonged.
- Some level of segregation was observed at the edges of runs, probably due to paver adjustment.
- The mix arrived at a reasonable paving temperature and did not overly smoke but there was some little odor coming from the asphalt fumes.
- All other volumetric properties were in conformance with (QCS, 2014) requirements.

Preliminary performance tests on cores undertaken, including Dynamic Modulus, Flow Number, 4-Point Fatigue Test, Resilient Modulus, Flexural Modulus and Overall Stiffness, to determine the performance comparability of CRMB asphalt with the adjacent PMB asphalt segment. The outcome from the performance test indicated the following characteristics:

- Since the original PMB Marshall design was based on a different aggregate gradation from what was used for the CRMB mix, the Marshall stiffness, stability and flow are considered to be of limited value, even though, they appeared to be in compliance with Qatar Construction Standards (QCS, 2014).
- The performance data showed that the CRMB mix has higher dynamic modulus and higher overall stiffness in all modes of measurement, and therefore very good resistance to deformation and fatigue.
- The CRMB mix also had lower phase angle and hence higher contribution of elastic modulus to the complex modulus, which means better low temperature properties and crack resistance.
- CRMB mixes would potentially have comparable or even better performance than the PMB mixes.
- Results are consistent with international, particularly terminal blend experience from the USA.

It was concluded from the preliminary results, particularly the high in-place air void, that further work is required to improve the mix design by making it essentially performance-based. It was obvious from the results that there was a need for the development of a comprehensive guidelines for asphalt mixtures containing CRMB. To this end, a concerted collaborative effort was quickly set in place to undertake a second demonstration project with a performance-based mix design developed from contributions by QSD, BOOM construction, RAETEX Doha and FUGRO laboratories. The first trial of the initial mix design produced from this effort was implemented on an ongoing paving project. Preliminary results from cores taken after paving showed that the mix design needed to be improved to address some concerns with volumetric properties. However, due to some logistics and other challenges this effort was suspended.

7 DEVELOPMENT OF CR AND CRMB SPECIFICATIONS FOR QATAR

Following the successful implementation of the first demonstration project in 2018, and the second uncompleted attempt to improve on the results of the first, it became

imperative that a new specification needed to be developed or the existing specification revised before attempting to adopt and utilize in a conventional production basis. Accordingly, the QSD took the initiative to compile and issued a tentative guideline for the pre-qualification of CR and CRMB producers together with a guideline for Mix Design and Quality Control of CRMB asphalt mixes. These guidelines were prepared in line with the existing (QCS, 2014) and the pending (QCS, 2018). Essentially, the specifications in the guidelines control CR usage in CRMB production for utilization in a variety of asphalt paving applications. However, the specification does not address any safety or environmental concerns associated with its use. The salient points inherent in these two guidelines and specifications release in 2018 are presented in the next sections.

7.1 Requirements for Prequalification CR and CRMB Producers

The guideline details the requirements for pre-qualification of producers engaged in the production of CR and CRMB for PWA pavement construction projects. The producers' quality management system, general plant information, technical details and quality control plan should be submitted to the PWA Quality and Safety Department to express their desire for pre-qualification.

Crumb Rubber Producers Pre-qualification Requirements

a) The crumb rubber should be derived from car and/or truck tires and should be sufficiently free from contaminants including fabric, metal mineral and other non-rubber substances.
b) When tested in accordance with ASTM D5644 (selected sieves: 30-mesh, 40-mesh, 80-mesh, 200-mesh and 400-mesh), the resulting crumb rubber gradation should be 30 mesh (600 microns) type.
c) When tested in accordance with ASTM D1864, the crumb rubber should contain no more than 0.75% moisture by weight and should be free flowing with oven temperature equal to 105 $\pm 5^{0}$C.
d) Specific gravity of the rubber should be 1.15 ± 0.05, as determined by BS EN 1097-7, making use of a suitable liquid in which the crumb rubber will not dissolve or react (e.g. ethyl alcohol).
e) The crumb rubber should not contain visible nonferrous metal particles and not more than 0.01% ferrous metal particles by weight. Metal particles should be detected and separated by thoroughly stirring a magnet through a 50 g sample and weighing the captured particles. Nonferrous metal particles should be detected by visual inspection.
f) The crumb rubber should contain no more than 0.1% fiber by weight. Method of determining fiber content should be specified by the CR supplier to the CRMB producer.
g) The crumb rubber should contain less than 0.25% foreign contaminant materials (e.g. glass, sand, wood) by weight.
h) Crumb rubber sampling should be conducted from approximately 1-ton quantity in accordance with "California State Transportation Agency – California Test 385 (Section D) dated December 2015" with minimum testing frequency for quality control every 15 tons of production.

Crumb Rubber Modified Binder Producers Pre-qualification Requirements

a) When tested in accordance with ASTM D5546 or AASHTO T44, used to verify the residue of a CRMB placed in an ignition oven or furnace at 400°C for 1 hour, the binder should not contain fibers or discrete particles other than rubber with longest dimensions greater than 250µm.
b) The binder should be graded in accordance with AASHTO M332. However, the solubility test, binder stress sensitivity test and viscosity requirements are waived. The test should be carried out as per AASHTO T315 and T350 and performed with 2 mm gap.
c) The CRMB producer should provide a certificate that indicates the supplier of the CR, type and percentage of CR and any other additives (percentages of CR allowed in the CRMB should be between 10% to 25% by weight) and quality control test results issued by an approved independent third-party laboratory.
d) CRMB producers should provide guidelines to contractors for transportation; storage and handling of their binders (e.g. need for storage in continuously agitated tanks at the modification terminal and the asphalt plant). Recommendations for asphalt mixing and compaction temperature ranges should clearly be specified.

7.2 Requirements for CRMB Asphalt Mix Design Certification

In order for a contractor to obtain asphalt mix design conformity certificate for the production of asphalt for PWA road projects, the following requirements, among others, must be adhered to:

- PG76-10 binders grade to be used in asphalt mixes in accordance with AASHTO M332, with necessary adjustments to account for traffic loading and speed.
- Optionally, the contractor may use the Marshall or Superpave mix design methodology for the asphalt mix design. Albeit, most contractors in Qatar typically use only the Marshall method for their designs.

Table 1: Design Criteria for Marshall CRMB Mix Design

Parameter[1]	BC – A	BC – B	WC
Aggregate Properties	Tables 5.1 and 5.2 (QCS2014)		
Aggregate Grading	Table 5.7 (QCS2014)		
Number of Compaction blows at each end of specimen	75	75	75
Binder Content (% of total mix) inclusive of tolerances	3.2 – 4.4	3.4 – 4.4	3.4 – 4.4
Stability (kN)	12.0 min.	12.0 min.	13.0 min.
Flow (mm)	2 – 4	2 – 4	2 – 4
Marshall Quotient (Stability/Flow) (kN/mm)	5.25 min.	5.25 min.	5.25 min.
Voids in Mix (Air Voids) (%)	4 – 8	4.5 – 8	5 – 8
Voids in Mineral Aggregate VMA (%)	Table 5.9 (QCS2014)		
Voids Filled with Asphalt VFA (%)	50 – 70	50 – 75	50 – 75
Voids in Marshall Specimen at 400 Blows per face at optimum binder content (%)	3.2 min.	3.4 min.	4.0 min.
Retained Stability (%)	75 min.	75 min.	75 min.
Filler/Binder Ratio	0.80 – 1.50	0.80 – 1.50	0.75 – 1.35
Tensile Strength Ratio at 25°C, ASTM D4867 (%)	75 min	75 min	75 min
Rut depth using HWTT[2] at 60°C, Wet, 20,000 passes, AASHTO T324 (mm)	12.5 max.	12.5 max.	12.5 max.

Note:- [1]Unless otherwise stated, relevant ASTM standards shall be followed for testing.

- [2]Hamburg Wheel Tracker Test. Rut depth determined by means of the HWTT as per AASHTO T324 derives from tests carried out on specimens submerged in water.
- Tensile Strength Ratio (TSR) refers to results obtained from Indirect Tensile Strength (ITS)
- tests carried out at 25°C, before and after static water immersion (with no freeze-thaw cycles), as per ASTM D4867.
- BC-A: Base Course Class A, BC-B: Base Course Class B (Intermediate Course) WC-Wearing Course.
- QCS (2014)-Qatar Construction Standards (2014).

8 IMPLEMENTATION OF CRMB ON PWA PROJECTS

In addition to the initial instruction by the PWA president for CRMB to be use in lieu of PMB for all projects, the Roads Projects Department also issued an instruction for CRMB to be used in lieu of the conventional 60/70 bitumen for the Wearing Course mixes for all projects. As a result, the local CR and CRMB producers and contractors engaged in a concerted effort and work collaboratively to acquire the necessary certification and mix design approvals from QSD, based on the guidelines and specifications provided. Currently, two approved local CRMB producers, namely RAETEX Doha and MEMBCO, who obtains their CR from approved local suppliers (Al Holdaifi Recycling Qatar and Bright Future Tire Recycling) have been approved to supply contractors with the required CRMB for their asphalt mixes. The main challenges that the contractors have faced in the development of their asphalt mix designs have to do with the difficulty in satisfying the minimum 75% tensile strength ratio (TSR) requirement shown Table 1. The other challenge has to do with the strong odors that emanate from the asphalt fumes. That notwithstanding, in the last couple of months several contractors, in close co-operation with their respective CRMB producers, have managed to overcome these challenges and develop compliant CRMB asphalt mixes and obtained the required conformity certificates for the production of asphalt mixtures for their respective projects.

In September 2019 the initiative achieved a major milestone as the first CRMB Wearing Course meeting all applicable specifications was successfully implemented on Roads and Infrastructure in North of Al Nasiraiyah RPD project, by BOOM Construction Co. & Lotus Trading & Contracting Co. JV, after a successful plant trial. Many more contractors are expected to be laying CRMB asphalt mixes on several RPD projects in the coming months. Preliminary results show that all Marshall properties, such as air voids, voids in the mineral aggregate (VMA), and voids filled with asphalt (VFA) have been conformed to, for both the loose and compacted mixes. Particularly, air voids between 5.5% to 7.5% have been achieved on two projects executed so far, compared to the high percentages achieved for the demonstration project. Temperature regimes are in the region of 170°C to 178°C at the plant, 165°C to 170°C in truck at site, 160°C to 165°C laying temperatures and breakdown rolling carried out between 165°C. These results are considered very promising.

The PWA (RPD and QSD) will be closely monitoring the implementations of these mixes to ensure that all applicable quality standards and specification are strictly adhered to in order to guarantee the expected short- and long-term performance.

9 CONCLUSION AND RECOMMENDATIONS

The benefits of using CRMB are well documented worldwide with the major driver

for its implementation in Qatar, besides increased fatigue resistance and reduction in ageing of the binder, being the environmental pollution reduction benefits. Currently, the use of CRMB for the Wearing Course is mandated in Qatar for local roads projects and recommended as a substitute for other projects where PMB has been specified. This is considered a major shift in paradigm and considered a very bold initiative by PWA. Even though it is estimated that there is cost impact of using CRMB over conventional 60/70 binders, it is anticipated that the overall benefits and lower lifecycle cost will far outweigh the additional cost impact. It is of paramount importance, though, that the implemented projects be monitored and evaluated diligently by collecting useful information and data that will help in developing a more customized specifications for CRMB producers and contractors in Qatar. To this end, the following recommendations are made by the authors:

1. PWA should develop a strategy to involve other institutions such as Qatar University and Texas A&M University in Qatar to undertake targeted funded research to develop improved mix designs which are essentially performance-based.
2. The long-term performance of these mixes should be monitored annually by a systematic approach to performance testing including the evaluation of the rutting resistance, cracking resistance, and moisture susceptibility of the asphalt mixtures on different segments with various pavement designs and having varying asphalt mix designs and different crumb rubber components.
3. To boost the environmental pollution reduction benefits aspect of this initiative, the requirement in the guidelines for the crumb rubber content in CRMB to be between 10% and 25% by weight must be strictly adhered to and verified prior to issue of conformity certificate.
4. Certification programs should be developed to ensure training of technical personnel of producers, contractors, supervision staff, as well as PWA engineers engaged in the implementation of CRMB.
5. Since current Qatar pavement design is based on the AASHTO empirical design methodology, it will be of immense advantage if the material properties of asphalt mixes with the different grades of CRMB are characterized in terms of their layer coefficient. It is believed that with the expected much higher layer coefficients compared to the conventional asphalt mixes; the pavement designs could be optimized largely which could lead to significant cost savings.
6. Preferably, a performance-based balanced mix design procedure for CRMB asphalt mixtures, which is fast becoming the industry best practice approach, should be evaluated in order to move towards implementation for all asphalt mix designs in Qatar.

ACKNOWLEDGMENTS

The authors would like to thank the president of PWA, Eng. Dr. Saad Ahmed Ibrahim Al Mohannadi for embracing this initiative and giving it the needed support and approvals. Acknowledgement goes to the following individuals at PWA's Quality and Safety Department (QSD) and ANAS S.p.A Qatar Branch for their immense contributions and support, namely; Eng. Khalid Mohd Al-Emadi (QSD Department Manager), Dr. Osman Elhusain Mohamed Idris (QSD Senior Quality Engineer) and Glyn Holleran (former

ANAS Pavement Expert). Particular appreciation goes to Naser Al Bash (Sr. Manager-QA/QC for BOOM Construction Company) and Banji Obikunle (QA/QC Technical Manager for RAETEX Doha). The following PWA Roads Projects Department engineers are also recognized for their valuable support and contribution, namely; Eng. Aly Fahmy (RPD Design Manager) and Eng. Mustafa Shireim (RPD Project Manager) and Roger Hodgson (Senior Materials Specialist at PWA Highway Projects Department).

REFERENCES

Guidelines for Mix Design and Quality Control of CRMB Asphalt Mixes (2018). Published by PWA Quality and Safety Department, Qatar.

Guidelines for Pre-qualification for crumb rubber and crumb rubber modified binder producers (2018). Published by PWA Quality and Safety Department, Qatar.

Harvey, J., Weissman, S., Long, F. & Monismith, C. (2001). Tests to evaluate the stiffness and permanent deformation characteristics of asphalt/binder-aggregate mixes, and their use in mix design and analysis. *Proceedings of the Asphalt Paving Technology*, pp. 572-604.

Larsen, J. E., Wohlk, C. J. & Hall, B. A. (1988). Modified bitumen. *Proceedings of the 14th Australian Road Research Board Conference (ARRB '88)*, Canberra, Australia.

Norhidayah, A. H. et al. (2019). Engineering properties of crumb rubber modified dense graded asphalt mixtures using dry process. *IOP Conference Series: Earth and Environmental Science*, 220.

Nunoo, C., Fahmy, A. (2018). Utilization of Crumb Rubber for Asphalt Pavement Construction on Local Roads and Drainage Projects in Qatar. Proposal submitted to the Public Works Authority (Ashghal), Qatar.

Cite this article as: Nunoo C. N., Al-Tamimi S. A., "Implementation of Crumb Rubber Modified Binder for Qatar Local Roads Construction Projects", *International Conference on Civil Infrastructure and Construction (CIC 2020)*, DOI: https://doi.org/10.29117/cic.2020.0051

In-Pavement Fiber Bragg Grating Sensor for Vehicle Counting

Mu'ath Al-Tarawneh
muath.altarawneh@mutah.edu.jo
Department of Civil and Environmental Engineering, Mu'tah University, Karak, Jordan

Ying Huang
ying.huang@ndus.edu
Department of Civil and Environmental Engineering, North Dakota State University, Fargo, North Dakota, USA

ABSTRACT

Traffic volume studies are conducted to determine the number, movements, and classifications of roadway vehicles at a given location and period. Typically, there are two methods for conducting traffic volume studies: manual and automatic counting. When manual counting is used, a person records the traffic volume on the site or alternatively from video recordings and this estimate can have a large margin of error. Automatic counting is based on measurement technologies, including pneumatic road tubes, inductive loops, infrared, microwave Doppler/radar, passive acoustic, video image detection, and Bluetooth devices. However, they are costly to install and have various limitations, such as high maintenance cost, availability of power source, and dependence on surrounding environment. Currently, weigh-in-motion (WIM) technology has become popular for automatic vehicle counting. In this paper, a three-dimensional glass fiber-reinforced polymer packaged fiber Bragg grating sensor (3-D GFRP-FBG) is introduced for in-pavement vehicle counting. The 3D GFRP-FBG sensor was installed on I-94 freeway, at MnROAD facility, Minnesota. When a vehicle passes over the road, the pavement produces strain signals that are picked up by wavelength changes. These strain peaks can be tracked to achieve vehicle counting. The sensors were laid out 9 feet from the road centerline with 16 feet distance between them to detect all the vehicles travelling on the right side of the road. The feasibility tests show the ability of the sensors to detect vehicles from small cars to semi tractor-trailer. For a 250-second period, the sensor detected 23 vehicles, with a total of 69 axles.

Keywords: Fiber Bragg grating sensor; Vehicle identification; Traffic monitoring; Glass fiber reinforced polymer

1 INTRODUCTION

Accurate traffic volume estimations on various road segments are critical to the appropriate roadway features' geometric design, traffic demand planning, and administrative purposes. In addition, Traffic volume data are essential in many transportations and decision-making models. They are used to estimate vehicle miles travelled (VMT), evaluation of infrastructure management needs such as roadway geometric improvement and maintenance scheduling (Apronti et al., 2016).

Vehicle counting can be defined as the activity of measuring and recording traffic characteristics such as vehicle volume, classification, speed, weight, or a combination

of these characteristics (FHWA, 2013). Typically, there are two methods for counting traffic: manual and automatic counting. When manual counting is used, a person records the traffic volume including vehicle counts at intersections which is a turning movement count, estimation of average daily traffic (ADT) and annual average daily traffic (AADT) on the site or alternatively from video recordings, and the impact of the manual count error is application dependent (Zheng and Mike, 2012). Automatic counting is based on measurement technologies, including pneumatic road tubes, inductive loops, infrared, microwave Doppler/radar, passive acoustic, video image detection, and Magnetometer (Mimbela and Kelin, 2000). The existing automatic counting technologies suffer from the following disadvantages (FHWA, 2013), (Kown, 2003):

1. High cost: Most of the existing technologies require expensive instruments and need significant maintenance and calibration and they are costly to install.
2. Energy efficiency: Most of the existing technologies need to be connected to a power source or a battery in a constant manner.
3. Large scale effectiveness: Majority of the existing technologies cannot be deployed on large scale due to limitations, such as availability of energy sources and high maintenance and installation cost.
4. Stability: Most of the existing technologies show significant dependence on surrounding environment.
5. Telecommunication infrastructure: Most of the existing technologies require a telecommunication platform to transfer data to the diagnose system in order to be analyzed.

In recent decades, weigh-in-motion (WIM) technology has become popular for vehicle counting; there are several in-pavement sensors to be considered including bending plates, piezoelectric sensor, load cells, and fiber-optic sensors.

Table 1 compares the cost, accuracy, sensitivity, and life cycle for these sensors for vehicle counting. The electrical sensors (Piezoelectric sensor, bending plate and load cell) shows significant dependence on surrounding environments, such as moisture. It also shows high electromagnetic interferences (EMI) and relatively short life cycle with a moderate reliability and accuracy.

Table 1 Sensor Comparison (Majumder et al., 2008; Zhang et al., 2007; Lee, 2003)

	Piezoelectric sensor	**Bending plate**	**Single load cell**	**Optic fiber sensor**
Life cycle cost	Low ($5,000)	Medium ($6,000)	High ($8,000)	Low ($1,000)
Accuracy	+/- 15%	+/- 10%	+/-6%	+/- 10%
Sensitivity	High	Medium	Low	High
Expected life	4 years	6 years	12 years	>15 years

Table 1 shows the preference of optic fiber sensor on the electrical sensors. Optic fiber sensor has high reliability and accuracy in addition to some unique advantages, such as small size, lightweight, high sensitivity, immunity to electromagnetic interference, and ability serving in harsh environments (Mall et al., 2008). Fiber Bragg grating (FBG) is

the most common optic fiber sensor which has been widely used for civil engineering applications. However, bare FBG generally is easy to be damaged during installation because it is made up by optic fiberglass. Thus, FBG's sensor needs to be packaged before application. Nowadays, glass fiber–reinforced polymer (GFRP) material has become widely accepted for use in civil engineering applications. It provides a durable and reliable packaging alternative to steel (Oh and Sim, 2004). Hence, the GFRP material can be used to package FBG to improve its ruggedness. The three-dimensional glass fiber-reinforced polymer packaged fiber Bragg grating sensor (3D-GFRP FBG) has been introduced by the author's research team for pavement health monitoring system (Zhou et al., 2012), and low-speed and high-speed WIM measurements (Al-Tarawneh and Hunag, 2017, 2016). In this study, the 3D-GFRP FBG sensor has been applied for vehicle counting.

2 OPERATIONAL PRINCIPLE AND SENSOR DESIGN

2.1 Operational Principle of FBG Sensor

FBG is made by shedding a periodic pattern of intense ultraviolet (UV) light in order to expose the core of single mode fiber, creating a refractive index modulation so called grating. Bragg wavelength form due to reflected light from the periodic refraction change (Al-Tarawneh and Huang, 2016), which can be represented as:

$$\lambda = 2n\Lambda \qquad (1)$$

Where, n is the effective index of refraction, and ʌ is the grating periodicity of the FBG. Bragg wavelength depends on the Brag condition and the wavelength at which this reflection occurs. Light signals at wavelengths other than the Bragg wavelength pass through and only the wavelength matched with Bragg wavelength will be reflected. Figure 1 shows a schematic of the operational principle of an FBG sensor. Due to temperature and strain dependence of the grating period, the Bragg wavelength will change as function of temperature, Te, and strain, ε. The strain-Bragg wavelength relationship for the FBG can be described as (Al-Tarawneh and Huang, 2016):

$$\varepsilon = \frac{1}{(1-P_e)}\left(\frac{\Delta\lambda}{\lambda} - \frac{\Delta\lambda_{Te}}{\lambda_{Te}}\right) \qquad (2)$$

Where, Pe is the optical elasticity coefficient of the optic fiber, λ is the center wavelength from the FBG strain sensor, and λTe is the measured center wavelength from the FBG temperature compensation sensor. When a vehicle axle passes over the road, the pavement produces strain signals that will be picked up by wavelength changes of the embedded 3D-GFRP-FBG sensor. This peak strain signal is related to the passed axle. Thus, the sensor can be applied for vehicle counting.

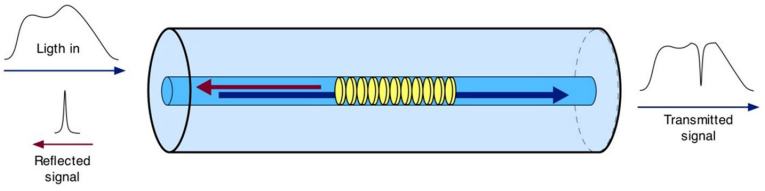

Figure 1: The Operational Principle of an FBG Sensor (Zhang et al., 2016)

2.2 The 3D GFRP-FBG Sensor Geometric Design

Figure 2(a~c) shows the geometric design for the 3D GFRP-FBG sensor. The short-gauged component of the sensor intends to detect the vertical strain while the long-gauged component is used to detect the longitudinal and transverse strains. The longitudinal direction is defined as the direction along the wheel path of the road and the transverse direction is defined as the one along the cross-section of the road. All the three components of the 3D GFRP-FBG sensor share the same diameter of 0.2 in (5mm). The center wavelength of the longitudinal, transverse and vertical gauges in the 3D GFRP-FBG sensor are 1529.138 nm ,1534.518 nm, and 1524.920 nm, respectively.

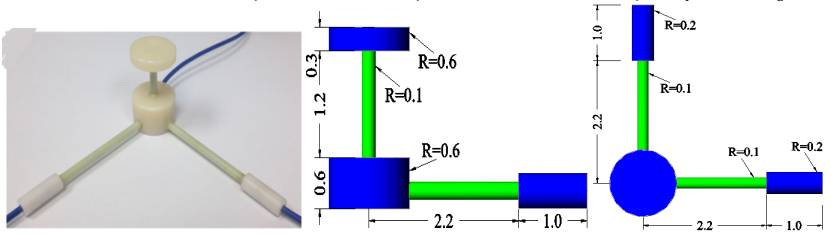

(a) (b) (c)

Figure 2: Geometric Design of The 3D GFRP-FBG Sensor:(a) Photo of The 3D GFRP-FBG Sensor, (b) Elevation View, and (c) Plan View (Unit: in.).

3 SENSOR FEASIBILITY TESTS

In order to validate the feasibility of the 3D GFRP-FBG sensor for vehicle counting, field-testing was performed at the Cold Weather Road Research Facility in Minnesota (MnROAD) facility of Minnesota Department of Transportation (MnDOT). MnROAD consists of two unique roadways: a two-lane low-volume loop that is loaded with a 5-axle 80 kips (36,287 kg) semi-truck and a section of interstate I-94 ‘‘mainline’’ that contains two westbound lanes with live traffic. The 3D GFRP-FBG sensor was installed inside the pavements of Cell 17, which belongs to the interstate I-94 ‘‘mainline’’ westbound lanes as shown in Figure 3 (a). The 3D GFRP-FBG sensor was installed beneath the wheel path on the asphalt pavement as shown in Figure 3 (b), and in Figure 3 (c) for the photo of the sensor installation scene.

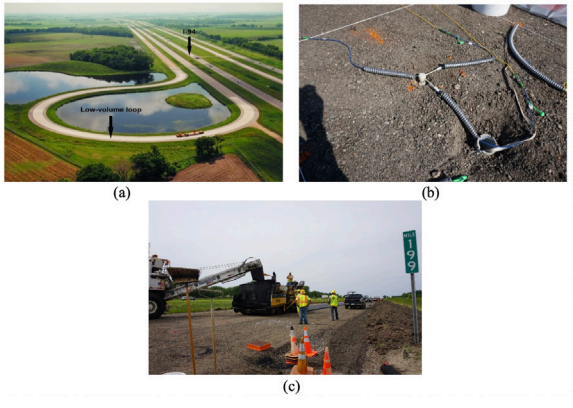

Figure 3: (a) MnROAD Facility, (b) The Sensor Installation Scene, and (c) Installation Scene

Figure 4 shows the detail of sensors layout in Pavement Cell 17 of I-94 at MnROAD, two 3D GFRP-FBG sensors were installed under the expected wheel path, which was 9 feet from the center line of the road. The distance between the two sensors was chosen to be 16 feet in order to detect all the vehicles travelling on the right side of the road (right lane). The temperature compensation FBG sensor was installed to pick up the variation of temperature inside Pavement Cell 17, which is used in Equation 2.

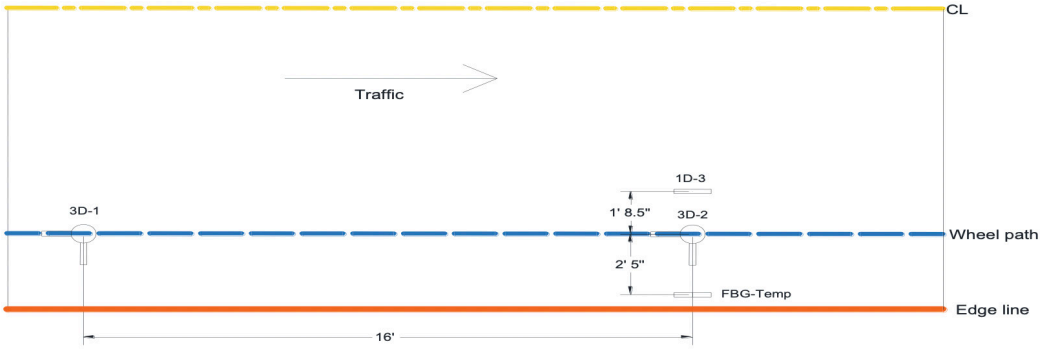

Figure 4: Sensors Layout (3D: Three Dimensions, 1D: One Dimension, CL: Center Line, 1': foot, 1": inch)

After the installation of the sensor, the three components of the sensor were connected to a 5 KHz sampling rate FBG integrator together with a temperature compensation FBG sensor. The FBG integrator was further connected to a personal computer to record the data. The performed sensitivity study in previous study (Al-Tarawneh and Huang, 2016) shows that the longitudinal component has the largest weigh-in motion (WIM) measurements sensitivity among the other components, followed by the vertical component. Thus, both the longitudinal and vertical components are used in this study for vehicle counting.

Figure 5 shows the sensor's responses on its vertical and longitudinal components for a range of vehicle categories including passenger car, two-axle vehicle, three-axle vehicle, and five-axle vehicle. The average speed range for the identified vehicles was between 65 mph and 75 mph. It is obvious that the vertical and longitudinal components responses show the ability of the sensor to detect each axle of the traveled vehicle with different responses proportionate to the tire weight. In addition, over 3 months of testing, the sensors functioning on the I-94 freeway did not appear to have any deterioration in performance. Figure 6 shows the sensor's response on its longitudinal component for a 250-second monitoring period. During this period, 23 vehicles passed over the sensor, with a total of 69 axles. The counting of axles and vehicles was done by tracking the peaks through the sensor's response.

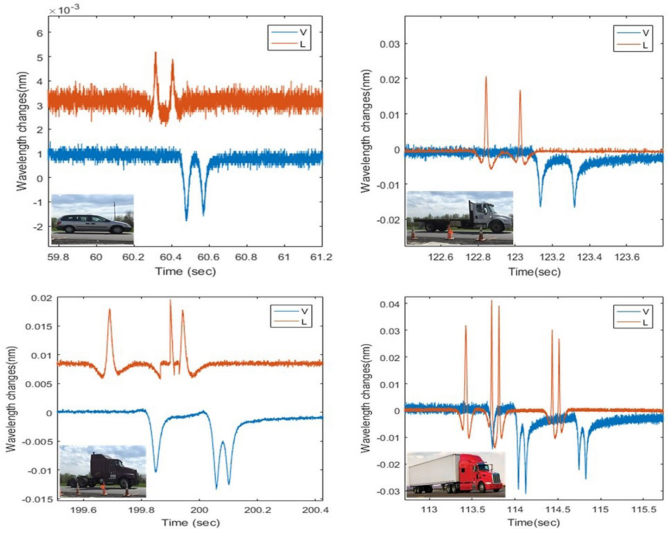

Figure 5: The Responses from Vertical and Longitudinal Components for a Range of Vehicle Categories (V: Vertical, L: Longitudinal)

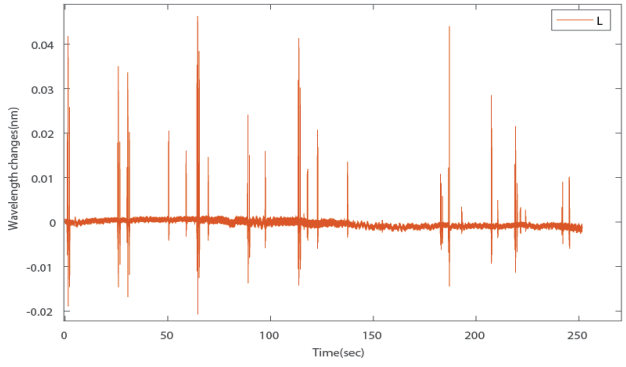

Figure 6: The Responses from Longitudinal Component (L: Longitudinal)

4 CONCLUSION

This study introduced a 3D GFRP FBG sensor for long term and cost-effective vehicle counting. Both of the vertical and longitudinal components of the sensor can be used for vehicle counting, since they have the largest WIM measurements sensitivity. The 3D-GFRPFBG sensors effectively monitored the travelled vehicles on the I-94 freeway, at MnROAD facility, Minnesota. It is obvious that the vertical and longitudinal components responses show the ability of the sensor to detect each axle of the travelled vehicle with different responses proportionate to the tire weight. Vehicle counting can be achieved by tracking the signal peaks through the sensor's response. Vehicles detected include size and weight ranges from small cars to tractor-trailer semi. Future efforts will endeavor to estimate vehicle speeds and to classify vehicles depending on the number of axles and the wheel base. Furthermore, Average Annual Daily Truck Traffic (AADTT) can be calculated since the sensor response appears to be closely proportional to the vehicle weight, which allows the sensor to distinguish truck from a small vehicle.

REFERENCES

Al-Tarawneh, Mu'ath. & Huang, Ying (2017). In-pavement fiber Bragg grating sensors for high-speed weigh-in- motion measurements. *In Sensors and Smart Structures Technologies for Civil, Mechanical, and Aerospace Systems,* vol. 10168, p. 101681Y. International Society for Optics and Photonics.

Al-Tarawneh, Mu'ath. & Huang, Ying. (2016). Glass fiber-reinforced polymer packaged fiber Bragg grating sensors for low-speed weigh-in-motion measurements. *Optical Engineering*, Vol. 55, No. 8, 086107.

Apronti, Dick, Ksaibati, Khaled, Gerow, Kenneth & Hopner, Jaime. (2016). Estimating traffic volume on Wyoming low volume roads using linear and logistic regression methods. *Journal of traffic and transportation engineering* (English edition) 3, no. 6 (2016): 493-506.

Federal Highway Administration (FHWA) (2013). *Traffic Monitoring Guide*. Washington, D.C.

Kwon, J., Varaiya, P. & Skabardonis A. Estimation of truck traffic volume from single loop detectors with lane-to-lane speed correlation. *Transportation Research Record: Journal of the Transportation Research Board*, Vol. 1856, 2003, pp. 106-117.

Lee, Byoungho. (2003). *Review of the present status of optical fiber sensors*. Optical Fiber Technology, Vol. 9, No. 2, pp. 57-79.

Majumder, Mousumi, Gangopadhyay, Tarun, Chakraborty, Ashim, Dasgupta, Kamal & Bhattacharya, Dipak. (2008). Fibre Bragg gratings in structural health monitoring—Present status and applications. *Sensors and Actuators A: Physical,* 147, No. 1, pp. 150-164.

Malla, Ramesh, Sen, Amlan & Garrick Norman. (2008). A special fiber optic sensor for measuring wheel loads of vehicles on highways. *Sensors*, Vol. 8, No. 4, pp. 2551-2568.

Mimbela, Luz Elena & Kelin Lawrence. (2000). Summary of vehicle detection and surveillance technologies used in intelligent transportation systems.

Oh, Hs. & Sim, J., (2004). Interface debonding failure in beams strengthened with externally bonded GFRP. *Composite Interfaces*, Vol. 11, No. 1, pp. 25-42.

Zhang, Lixin, Haas, Carl & Tighe, Susan. (2007). *Evaluating weigh-in-motion sensing technology for traffic data collection*. (Annual Conference of the Transportation Association of Canada), pp. 1-17.

Zhang, Qinghua, Wang, Yuan, Sun, Yangyang, Gao, Lei, Zhang, Zhenglin, Zhang, Wenyuan, Zhao P & Yue Y. (2016). Using custom fiber Bragg grating-based sensors to monitor artificial landslides. *Sensors*, *16*(9):1417.

Zheng, Penguin & Mike, McDonad. (2012). An Investigation on the Manual Traffic Count Accuracy. *Procedia - Social and Behavioral Sciences*, Vol. 43, 2012, pp. 226-231.

Zhou, Zhi, Liu, Wanqiu, Huang, Ying, Wang, Huaping, Jianping, He, Huang, Minghua, & Jinping, Ou. (2012). Optical fiber Bragg grating sensor assembly for 3D strain monitoring and its case study in highway pavement. *Mechanical Systems and Signal Processing*, Vol. 28, pp. 36-49.

Cite this article as: Al-Tarawneh M., Huang Y., "In-Pavement Fiber Bragg Grating Sensor for Vehicle Counting", *International Conference on Civil Infrastructure and Construction (CIC 2020)*, Doha, Qatar, 2-5 February 2020, DOI: https://doi.org/10.29117/cic.2020.0052

Mechanical and Durability Characteristics of Roller Compacted Geopolymer Concrete Using Reclaimed Asphalt Pavement

Sk Syfur Rahman
syfur04016@gmail.com
University of Louisiana at Lafayette, Lafayette, Louisiana, USA

Mohammad Jamal Khattak
khattak@louisiana.edu
University of Louisiana at Lafayette, Lafayette, Louisiana, USA

ABSTRACT

Every year a large quantity of reclaimed asphalt pavement (RAP) is generated in the USA. Utilization of RAP can solve the storage problem, prevent environmental pollution and reduce construction costs. This study focuses on the strength and durability characteristics of RAP mixtures by introducing the concept of roller-compacted fly ash-based geopolymer concrete (RCGPC). Several selected RCGPC mixtures were investigated to evaluate the effect of mixture variables, including sodium hydroxide (NaOH) molarity, sodium silicate (Na_2SiO_3) to sodium hydroxide (NaOH) ratio on the strength, modulus and durability characteristics of the mixtures. The effects of different curing temperature and curing duration on compressive strength were also studied. It was found that the mixtures with Na_2SiO_3/NaOH ratio of 1 yielded about 12 % higher compressive strength than the ratio of 0. Further, the mixtures using 10M NaOH and alkali ratio of 1 produced about 25% higher compressive strength than 8M NaOH which produced about 17 MPa. Similar results were obtained for elastic modulus and split tensile strength of the mixtures. Freeze-thaw durability tests also revealed acceptable results for the RCGPC mixtures. Formation of new geopolymeric compounds and chemical bonds in the newly formed novel RCGPC mixtures were also discovered using XRD analysis. The comparison of mechanical and durability testing further showed that RCGPC performed better than the roller-compacted cement concrete (RCC) using RAP. Based on the results and analysis the developed RCGPC using RAP could be used as a cost-effective solution for the construction of pavement structures.

Keywords: Roller compacted concrete; Geopolymer concrete; Reclaimed asphalt pavement; Pavement; Fly ash

1 INTRODUCTION

Every year vast quantities of construction and demolition (C&D) wastes are generated in the United States (EPA, 2019). Reclaimed asphalt pavement (RAP) is one of the main components of such C&D wastes. The use of RAP can solve storage problems and environmental pollution while at the same time it can reduce construction costs (EPA, 2019; Davorin, 2008 & Ryszard, 2016). However due to the low strength and durability properties of RAP, its usage as a construction material is limited to landfill, low strength base or subbase and replacement of few percentages of natural aggregates in hot mix asphalt (HMA) and conventional Portland cement concrete (Copeland, 2011; Chesner,

2019; Hansen, 2014; Hoyos, 2011; Arulrajah, 2013; Puppala, 2011; Hajj, 2010; Maher, 1997; Ramzi, 1999; Huang, 2006 & Huang, 2005). Although Ordinary Portland Cement (OPC) is being used as a popular binder for a long time, its increasing production generates an enormous amount of CO_2 in the atmosphere, which is also raising environmental concerns (Malhotra, 2010; Naik, 2015 & Salloum, 2007). Geopolymer technology can be a possible alternative to address this issue.

Geo-polymer technology has become a promising technology that provides a mature and cost-effective solution to many problems. Geo-polymeric materials represent an opportunity to simultaneously improve both environmental and engineering performance compared to traditional technologies. Geo-polymer-based materials are environmentally friendly and need only moderate energy to produce. The development of Geopolymer technology could contribute to reducing CO_2 emissions by about 80% as compared to that of ordinary Portland cement with almost no economic sacrifices, while at the same time converting a potentially hazardous industrial waste by-product (fly ash) to a value-added construction material (Davidovits, 2008). The use of RAP in geopolymer can be more beneficial because in this way both waste products RAP and fly ash will be utilized resulting in not only saving the cost but also reducing the amount of CO_2 emission. Recently, RAP is being used in geopolymer concrete by researchers in many ways. They investigated different gradations of RAP, different mix variables like fly ash to alkali activator ratio, the different molar concentration of alkali activator (Delwar, 1997; Hossiney, 2008; Avirneni, 2016 & Horpibulsuk, 2016). However, in none of the above-mentioned studies, the reported improvements in strength and durability were significantly high enough to use RAP alone as a full replacement of natural aggregates.

In this study, the concept of roller-compacted geopolymer concrete (RCGPC) was introduced to improve the strength and durability characteristics of concrete containing RAP as aggregates. Mechanical and durability properties, as well as the morphology of prepared geopolymer mixtures, were investigated and compared with roller-compacted cement concrete (RCC) with RAP.

2 MATERIALS

The chemical composition of Class F fly ash (FA) used in this study is shown in Table 1. This low calcium FA contains 14.82% aluminum oxides and 36.40% silicon dioxide. RAP was secured from a local HMA recycling plant. Chemical analysis of RAP has also been tabulated in Table 1. Sodium hydroxide (NaOH) solutions of 8 and 10 molar concentrations were prepared in the laboratory. On the other hand, a ready-made sodium silicate (Na_2SiO_3) solution was also used as part of the alkali activator. Portland cement Type-II was used for RAP-based RCC specimens.

Table 1: Chemical composition of FA and RAP

Element (%)	FA	RAP
Si	36.40	48.37
Al	14.82	16.63
Fe	12.17	15.33
Ca	13.87	13.30
Mg	0.79	-
S	0.57	-
K	1.59	2.38

A suitable mix-design was developed based on the literature search, which consisted of RAP gradation (Figure 1) recommended by American Concrete Pavement Association (ACPA), 15% fly ash content, 8 and 10 molar concentration of NaOH, and Na_2SiO_3 to NaOH ratio of 0 and 1 by mass. Both accelerated oven and ambient temperature curing methods were adopted to evaluate the mechanical properties of the mixtures.

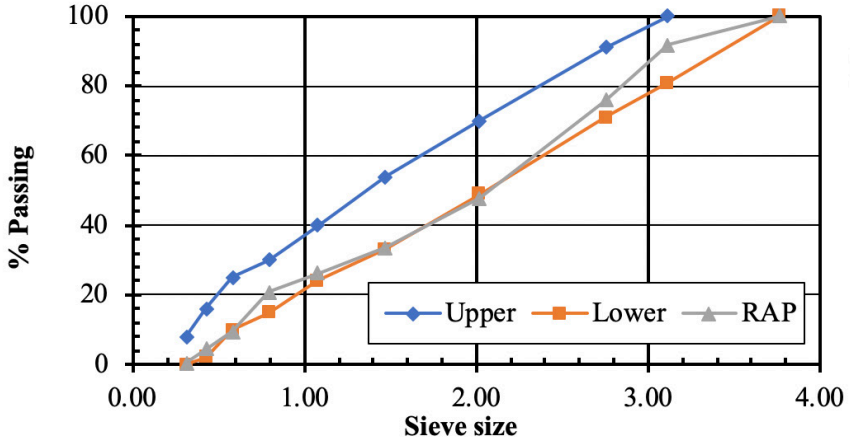

Figure 1: RAP gradation with ACPA recommended upper and lower limits for RCC

3 METHODS

3.1 Maximum dry density (MDD) and optimum alkali content (OMC)

The maximum dry density (MDD) of the mixtures was determined using the modified proctor test (ASTM, D1557). The mixtures were compacted in a cylindrical mold with a dimension of 142.4 mm diameter and 116.4 mm height. The compaction was done in 5 layers, by applying 25 blows per layer, using a 2.5 kg hammer. The height of the fall of the hammer was 45.7 cm. Geopolymer mixtures were prepared using 4 different alkali contents, which were then compacted to determine the dry density of those. However, for RCC mixtures 4 different moisture contents were used. MDD and OMC were determined by plotting a dry density versus alkali or moisture content graphs.

3.2 Experimental design parameters

To find out the optimum oven curing time at 60°C temperature, 3 oven curing periods (24, 48 and 72 hr) were used. To determine the optimum alkali content (OMC) of the mixtures, using modified proctor test, 4 different alkali and moisture contents ranging from 5% to 10% for RCGPC and 5% to 9 % for RCC, respectively, were used. The effect of molarity on compressive and split tensile strengths of RCGPC were evaluated for 8 and 10 molar NaOH concentration. Similarly, the impact of Na_2SiO_3 to NaOH ratio on strengths of RCGPC was evaluated using two different Na_2SiO_3 to NaOH ratio of 0 and 1. For ambient temperature curing 7, 14, 28 and 56 days were also investigated. Loading frequency for dynamic modulus testing was varied as 0.5, 1, 5, 10, and 25 Hz. For durability and morphology analysis the RAP-RCGPC mixture produced from 8 M NaOH, Na_2SiO_3 to NaOH ratio of 1 was used.

3.3 Unconfined compressive strength test

An unconfined compressive strength (UCS) test was performed according to ASTM C39 using Material Testing System (MTS). The compressive load was applied at a continuous rate of 0.51 mm/min until complete failure of the specimen was visible. The data acquisition rate for load and deformation was set as 0.1 per second. The maximum compressive stress at failure was defined as UCS and the slope of the linear portion of the stress-strain curve was termed as elastic modulus (E) of the mixtures.

3.4 Split tensile test

Split tensile strength test was performed similarly to ASTM C496 using Material Testing System (MTS). The load was applied along the diametral axis of the specimen at a continuous rate of 0.51 mm/min until complete failure was observed. Real-time data acquisition at a rate of 0.1 per second was set. This test was used to evaluate split tensile strength (T) of the mixtures.

3.5 Durability test (Resistance to freeze-thawing)

Resistance to freeze-thawing was performed in accordance with ASTM C666 standard procedure. Cylindrical specimens with 100 mm diameter and 200 mm height were subjected to consecutive freeze and thawing cycles. The temperature was increased from -12^{o}C to 12^{o}C within 2 to 5 hr and then decreased from 12^{o}C to -12^{o}C in 2 to 5 hr. The length change of the specimens was measured in every 36 cycles. Each specimen was to be subjected to 300 cycles or 1% length change.

3.6 X-ray diffraction (XRD)

XRD analysis was carried out using the MiniFlex600 XRD machine. The range of diffraction angle, 2θ used in this analysis was varied from 5 to 55^{o}. This test facilitated the identification of chemical compounds formed during geopolymerization.

4 RESULTS AND DISCUSSIONS

4.1 Optimum moisture content

Figure 2 shows the change in dry density with the increase in alkali content for RCGPC and water content for RCC mixtures. The alkali content was varied from 5 to 10 % for RCGPC and water content 5 to 9% for RCC mixtures. İt was observed from the figure that, as the alkali content increased, the dry density also increased and finally reached a maximum value of 6-7% and dropped afterward. Optimum alkali content and maximum dry density (MDD) were found to be 6.3% to 7.2 % and 2056 to 2070 kg/m^3 for RCGPC mixtures, respectively. The RCC mixture using OPC exhibited optimum moisture content (OMC) and MDD of 7% and 2080 kg/m^3, respectively.

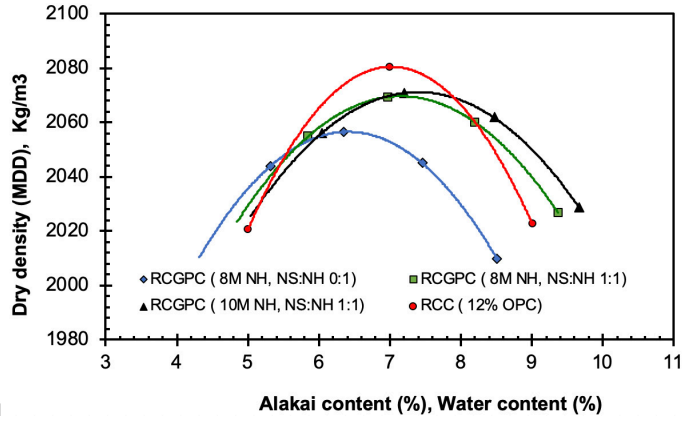

Figure 2: Effect of alkali and water content on the dry density of RAP-RCGPC and RAP-RCC mixtures, respectively

4.2 Effect of curing time

Figure 3 illustrates the effect of oven curing time on the compressive strength development of the RCGPC mixture at 60°C. It was observed from the figure that, as the oven curing time increased, the average UCS also increased until 48 hours of curing, after which no significant increase in UCS was observed. Hence, 48 hours of oven curing at 60°C was considered to be the optimum accelerated oven curing time for RAP-RCGPC mixtures to evaluate the mechanical and durability characteristics of the mixtures.

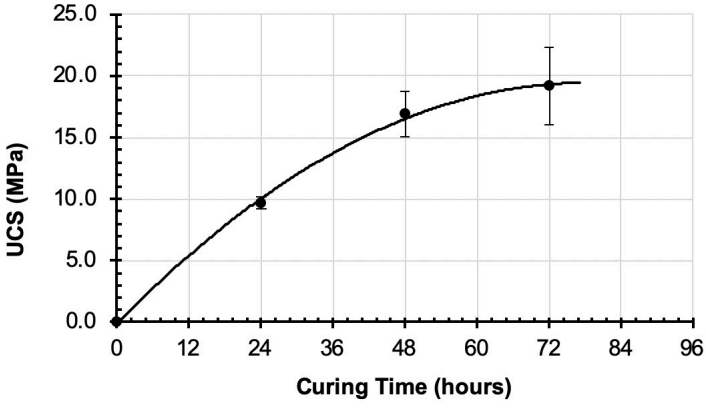

Figure 3: Effect of oven curing time on the UCS of RAP-RCGPC mixtures.

4.3 Effect of NaOH molarity and Na_2SiO_3 to NaOH ratio on UCS

Figure 4 shows the effect of NaOH molarity on the UCS and E of RAP-RCGPC mixtures. It was observed from the figure that, as the molarity of NaOH increased from 8 to 10 molar, the UCS also increased by about 25%. However, the increase in the average E value was only 5%. The heat condition remaining the same, the strength development in geopolymer is mostly dependent on the geo-polymerization reaction between precursor and alkali activator. With the increase of NaOH molarity, increasing alkali solids in the activator solution enhanced the geo-polymerization reaction and

process, which increased the strength and modulus of the final mixture.

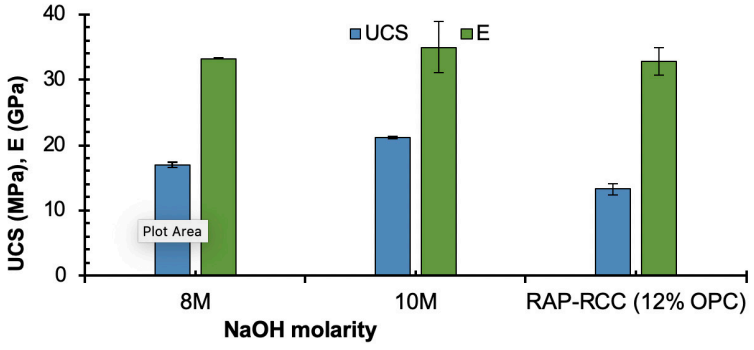

Figure 4: Effect of NaOH molarity on the UCS of RAP-RCGPC mixtures

UCS and E of RAP-RCC using 12% ordinary portland cement (OPC) were found to be about 13.24 MPa and 32.82 GPa. UCS of 8M and 10M RAP-RCGPC were about 28% and 60% more than UCS of RAP-RCC, however, RAP-RCC had shown similar E value as RAP-RCGPC.

Figure 5 displays the effect of Na_2SiO_3 to NaOH ratio on the UCS and E of RAP-RCGPC mixtures. It can be seen from the figure that, as this ratio increases from 0 to 1, the UCS increased by about 12%. The E value also followed a similar trend. The reason behind the high strength and modulus at an equal mass ratio of Na_2SiO_3: NaOH was the dissolution process of alumina and silica tends to be high, which also accelerates the strength development. As a result, the formed bonds were strong enough to enhance initial microcrack resistance (Morsy, 2014). UCS of RAP-RCGPC using 8M NaOH and Na_2SiO_3: NaOH ratio as 0 and 1 are about 14% and 28% more than UCS of RAP-RCC, respectively. However, RAP-RCC has a similar elastic modulus value as that of RAP-RCGPC.

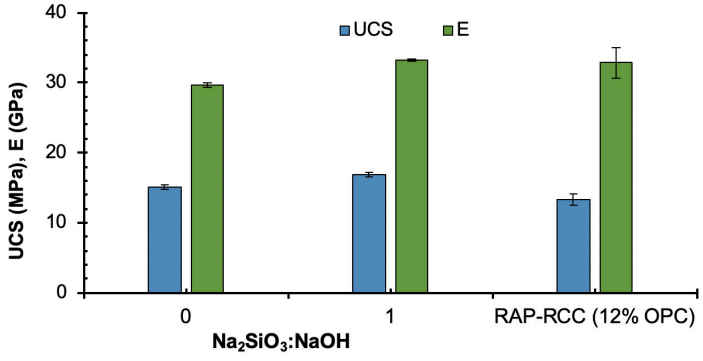

Figure 5: Effect of Na_2SiO_3 to NaOH ratio on the UCS of RAP-RCGPC mixtures

4.4 Effect of ambient temperature curing

Effect of ambient temperature curing period of 7, 14, 28 and 56 days on the strength development of RAP-RCGPC was also investigated. Figure 6 demonstrates the effect of ambient temperature curing days on the UCS and E of RAP-RCGPC mixtures. It can be

seen from the test results that, with the increase in curing days the UCS and E increased. Most of the strength development was observed in the first 7 days (9.8 MPa) of curing, which was around 50% of the 56 days (19.76 MPa) strength.

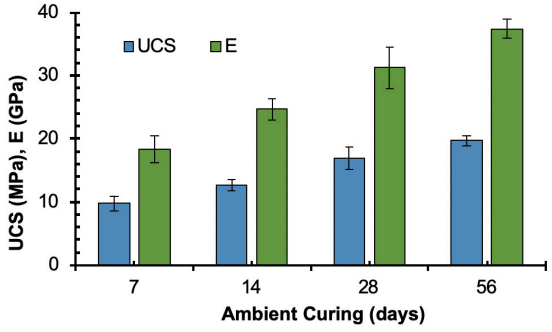

Figure 6: Effect of ambient temperature curing days on the UCS of E RAP-RCGPC mixtures

It was also estimated that 28 days of ambient temperature curing strength was the same as that of the UCS (16.90 MPa) at 60°C accelerated oven curing. It should be noted that the average day and night-time specimen temperatures were recorded around 34.4 ± 5.3°C and 28.8 ± 2.1°C, respectively through these curing days.

4.5 Dynamic modulus (E*)

Cylindrical specimen oven cured at 60°C were subjected to sinusoidal loading for a range of loading frequencies (0.5, 1, 5, 10 and 25 Hz). İt was observed from Figure 7 that, the E* increased by 29% when the loading frequency increased up to 5 Hz, afterward there was no significate change at 10 Hz and then showed a decrease of about 14% at 25 Hz. This indicates that such mixtures exhibited some viscoelastic behavior from 0.5 Hz to 10 Hz at 25°C which may be due to the presence of asphalt coating around the RAP particles. The range of E* was 15 GPa to 21 GPa, which was significantly lower than the E value (33 GPa) of the same mixture.

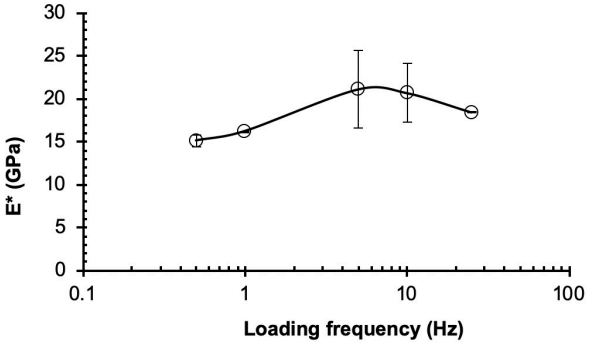

Figure 7: Dynamic modulus of RCGPC mixtures for different loading frequency

4.6 Split-tensile strength

The following Figure 8 (a, b) illustrates the effect of NaOH molarity and Na_2SiO_3 to NaOH ratio on the split tensile strength of RCGPC mixtures. The data in the figure

depicts that as the NaOH molarity increased from 8 to 10, split tensile strength increased about 10%, however when the Na_2SiO_3 to NaOH ratio increased from 0 to 1 with 8M NaOH the there was no significant change in the split tensile strength.

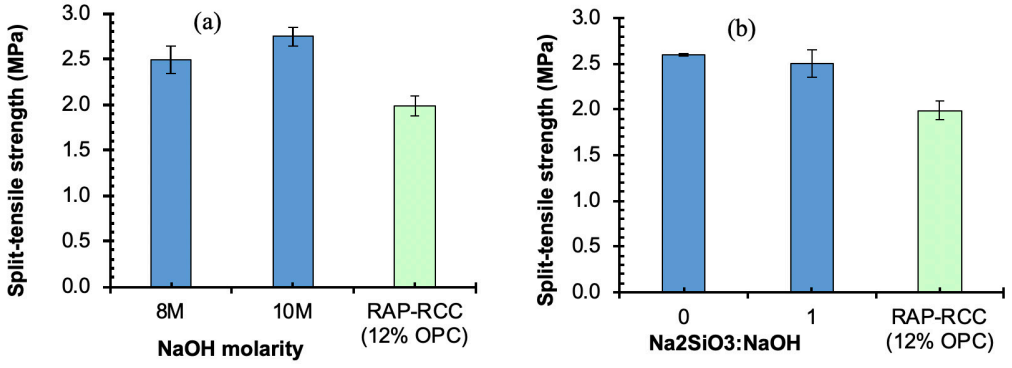

Figure 8. Effect of (a) NaOH molarity (b) Na_2SiO_3: NaOH on the split tensile strength of RAP-RCGPC mixtures

RAP-RCC using 12% OPC exhibited about 2 MPa of split tensile strength which is about 20% and 28% lower than RAP-RCGPC mixture with 8 and 10 NaOH respectively. These results indicated a stronger bond between RAP and geopolymer binders in RCGPC than the cement bond in RCC.

4.7 Durability (freeze-thawing)

The freeze-thawing durability test was performed on RAP-RCGPC specimens. The specimens had been subjected to 300 cycles of freeze-thawing. Length change was recorded every 36 cycles. Dynamic modulus was determined at the end of the 300 cycles. It was found that the average length change and retained dynamic modulus were about 0.4% (criteria:<1%) and 81.14% (criteria: >60%) respectively. So RAP-RCGPC mixtures were considered to be passed in the freeze-thawing durability test.

4.8 X-ray diffraction

Figure 9 illustrates the XRD analysis of the RAP-RCGPC mixture. It was observed from the analysis that quartz, mullite, albite and calcium compound present in the fly ash and RAP were chemically acted by alkali activator (Na_2SiO_3 and NaOH) solution and formed different geopolymer compounds (aluminosilicate), such as Nepheline ($NaAlSiO_4$) and Anorthoclase ($(Na, K)AlSi_3O_8$). Some unreacted crystalline quartz and mullite were also visible in the XRD graph.

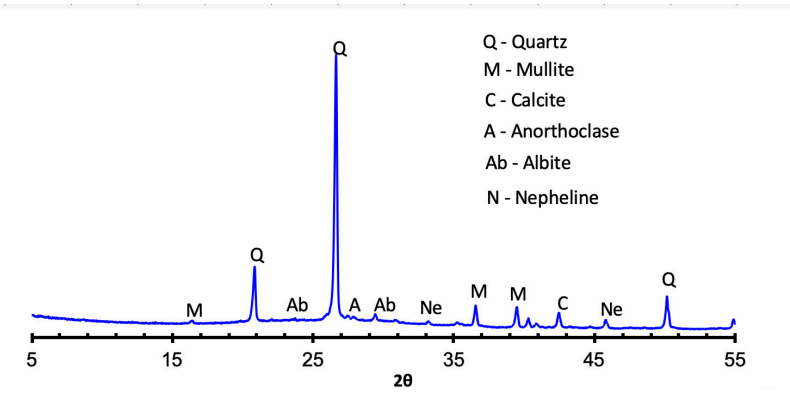

Figure 9: XRD of 8M NaOH with 1:1 Na_2SiO_3 cured at 60^0C

5 CONCLUSION

This study focused on the investigation of the mechanical, durability, and morphology characteristics of the newly synthesized RAP-RCGPC mixtures using appropriate testing methods. Based on the laboratory test results, the following conclusions were drawn:

1. Compressive strength and elastic modulus increased with the increase in oven curing time at 60°C temperature. Accelerated oven curing time of 48 hr at 60°C was considered sufficient to achieve the maximum compressive strength of RAP-RCGPC mixtures.
2. Compressive strength and elastic modulus of RAP- RCGPC mixtures increased with the increase in ambient curing period. Almost 100% of maximum strength (60°C for 48 hr of oven curing) was achieved in 28 days of ambient curing period.
3. It was found that dynamic modulus increased with the increase in loading frequency up to 5 Hz and after that frequency increment did not affect the dynamic modulus significantly. In short, RAP- RCGPC mixture exhibited some viscoelastic behavior at 25°C at l loading frequency ranging from 0.5 Hz to 10 Hz.
4. The split tensile strength of the RAP-RCGPC mixture increased by about 10% when the molarity increased from 8 to 10. However, similar split tensile strength was observed for mixtures containing 8M NaOH with and without Na_2SiO_3.
5. RAP-RCGPC had exhibited up to 60% higher UCS and 28% higher split tensile strength than that of RAP-RCC mixtures using OPC.
6. The XRD test result showed the formation of geopolymer compounds indicating the occurrence of polymerization reaction in RAP-RCGPC mixtures.

Based on the mechanical, durability and morphology analysis, the RAP-RCGPC could be termed as moderate to high strength geopolymer concrete. These mixtures could be used in low volume roads and parking lots as a full-depth pavement or as a strong base with the combination of a hot mix asphalt layer on the top. In this study, the tensile property of the material was evaluated using split tensile testing, however flexural beam testing of such material is recommended to evaluate the modulus of rapture which is an important parameter for pavement design.

ACKNOWLEDGMENTS

The authors wish to express sincere thanks to the University of Louisiana at Lafayette for providing financial support and facility for the research. A special thanks are also extended to Mr. Mark LeBlanc for assisting in experimentation.

REFERENCES

Arulrajah, A., Piratheepan, J. & Disfani, M. M. (2013). Reclaimed asphalt pavement and recycled concrete aggregate blends in pavement subbases: laboratory and field evaluation. *Journal of Materials in Civil Engineering*, 26, 349-357.

Avirneni, D., Peddinti, Pranav R. T. & Saride, S. (2016). Durability and long-term performance of geopolymer stabilized reclaimed asphalt pavement base courses. *Construction and Building Materials*, 121, 198-209.

Chesner, W. H. & Collins, R. J. (2019). *FHWA research and technology, user guidelines for waste and byproduct materials in pavement construction* (FHWA-RD-97-148).

Copeland, A. (2011). *Reclaimed asphalt pavement in asphalt mixtures: State of the practice, Federal Highway Administration* (FHWA-HRT-11-021).

Dachowskia, R. & Kostrzewaa, P. (2016). The Use of Waste Materials in the Construction Industry. *World Multidisciplinary Civil Engineering-Architecture-Urban Planning Symposium*, 161, 754-758.

Davidovits, J. (2008). *Geopolymer Chemistry and Applications*. Second edition, Institute Geopolymer, Saint-Quentin, France.

Delwar, M., Fahmy, M. & Taha, R. (1997). Use of reclaimed asphalt pavements as an aggregate in Portland cement concrete. *ACI Materials Journal*, *94*(3), 251-256.

Environmental Protection Agency (EPA) (2019, June 30). *Construction and demolition: Material-specific data*. www.epa.gov/facts-and-figures-about-materials-waste-and-recycling/construction-and-demolition-material-specific.

Environmental Protection Agency (EPA) (2019, June 30). *Sustainable management of construction and demolition materials*. www.epa.gov/smm/sustainable-management-construction-and-demolition-materials#America.

Hajj, E., Sebaaly, P. & Kandiah, P. (2010). Evaluation of the use of reclaimed asphalt pavement in airfield HMA pavements. *J. Transp. Eng.*, 136, 181-189.

Hansen, Kent R. & Copeland, A. (2014). *Asphalt Pavement Industry Survey on Recycled Materials and Warm-Mix Asphalt Usage*. National Asphalt Pavement Association (NAPA) IS 138(5e).

Hossiney, N., Wang, G., Tia, M. & Bergin, M. J. (2010). Evaluation of Concrete Containing Rap for Use in Concrete Pavement. Pavement Res. Technol. 3(5):251-258

Horpibulsuk H., M. Hoy, Arulrajah, Arul (2016). Strength development of recycled asphalt pavement – Fly ash geopolymer as a road construction material. Construction *and Building Materials*, 117, 209-219.

Hoyos, L., Puppala, A. & Ordonez, C. (2011). Characterization of cement-fiber-treated reclaimed asphalt pavement aggregates: preliminary investigation. *Journal of Materials in Civil Engineering*, 23, 977-989.

Huang, B., Shu, X. & Burdette, E. G. (2006). Mechanical Properties of Concrete Containing Recycled Asphalt Pavements. *Magazine of Concrete Research*.

Huang, B., Shu, X. & Li, G. (2005). Laboratory investigation of Portland Cement Concrete Containing Recycled Asphalt Pavements. *Cement and Concrete Research*. 35(10):2008-2013

Kralj, D. & Markic, M. (2008). Building materials reuse and recycle. *Construction and Building materials*, 4, 409 - 418.

Maher, M. H., Gucunski, N. & Papp, W. (1997). Recycled Asphalt Pavement as a Base and Sub-Base Material, ASTM *Special Technical Publication*, 1275, 42-53.

Malhotra, V. M. (2010). Global warming and role of supplementary cementing materials and superplasticizers in reducing greenhouse gas emissions from the manufacturing of Portland cement. *International Journal of Structural Engineering*, 1, 116-130.

Morsy, M., Saleh, A., Al-Salloum, Y. & Almusallam, T. (2014). Effect of sodium silicate to sodium hydroxide ratios on strength and microstructure of Fly ash geopolymer binder. *Arabian Journal for Science and Engineering*, *39*(6), 4333-4339.

Natik, T. R. (2015). Sustainability of Cement and Concrete Industries. Achieving Sustainability in Construction. https://www.icevirtuallibrary.com/doi/10.1680/asic.34044.0017

Puppala, A. J., Saride, S. & Williammee, R. (2011). Sustainable reuse of limestone quarry fines and RAP in pavement base/subbase layers. J. Mater. Civ. Eng., 24, 418-429.

Ramzi, T. G., Ali, A., Basma, O. & Al-Turk (1999). Evaluation of reclaimed asphalt pavement aggregate in road bases and subbases. Transportation Research Record, 1652, 264-269.

Salloum, T. (2007). Effect of Fly ash Replacement *on Alkali and Sulphate Resistance of Mortars* (MS Thesis). Department of Building, Civil and Environmental Engineering, Concordia University Montreal, Quebec, Canada.

Cite this article as: Rahman S. S., Khattak M. J., "Mechanical and Durability Characteristics of Roller Compacted Geopolymer Concrete Using Reclaimed Asphalt Pavement", *International Conference on Civil Infrastructure and Construction (CIC 2020)*, Doha, Qatar, 2-5 February 2020, DOI: https://doi.org/10.29117/cic.2020.0053

Crowd Logistics Delivery Determinants: A Stated-Preference Survey

Ali Al-Saudi
aalsaudi@mail.hbku.edu.qa
Hamad Bin Khalifa University, College of Science and Engineering, Department of Logistics and Supply Chain, Doha, Qatar

Frank Himpel
fhimpel@hbku.edu.qa
Hamad Bin Khalifa University, College of Science and Engineering, Department of Logistics and Supply Chain, Doha, Qatar

ABSTRACT

Crowd logistics (CL) has the potential to reduce the cost of last-mile delivery and benefit the environment. Consumers' attitudes toward CL are understudied, especially in Qatar, where CL is currently unavailable. The purpose of this paper is to investigate consumers' reactions to the theoretical attributes of a crowd-sourced delivery smartphone application along with customers' willingness to pay for particular features. A stated preference survey was distributed to potential consumers in Qatar and analyzed using a multinomial logit model. Package insurance was identified as the most important attribute, followed by a flexible delivery place and time with GPS tracking and a transparent delivery person profile. Respondents did not want their packages to be delayed by 30 minutes but did not mind a 15-minute delay. This model suggests that consumers are willing to pay up to 13.8 QR for package insurance, implying a lack of trust in CL. This research offers valuable insights for businesses (e.g., to help them design relevant platforms) and policymakers (e.g., to potentially mitigate consumers' trust concerns around using occasional people for delivery). This study also helps fill a gap in CL behavioral studies and confirms extant research findings relative to customers' trust in CL.

Keywords: Logistics; Crowd-sourced; Delivery; Choice; Mlogit

1 INTRODUCTION

An increase in e-commerce has accompanied a growth in freight transport (Frehe et al., 2017). Of all logistics-related activities, transportation is believed to have the most negative impact on the environment (Edwards et al., 2010). In addition to its effects on sustainability, last-mile delivery is the most cost-intensive stage of transportation; it can contribute up to 28% of transportation costs (Odongo, 2018). The high cost and inefficiency of last-mile delivery is attributable to high consumer expectations regarding service quality (Savelsbergh & Van Woensel, 2016). Notably, the last-mile issue is not limited to freight transportation; it applies to the private and public sectors as well (Zellner et al., 2016).

Several companies have sought to address this challenge without compromising service quality; for example, Amazon and Google are testing a same-day delivery service with drones (Brunner et al., 2018). Researchers have also begun to examine routing problems to optimize the delivery process (Savelsbergh & Van Woensel, 2016). The use of electric vehicles or bikes, which have lower emissions than freight vehicles, has also

been found to mitigate adverse environmental effects (Edwards et al., 2010).

Another growing trend related to e-commerce is crowd logistics (CL). This concept has been defined in various ways but generally refers to companies hiring everyday people to assume certain delivery tasks (Odongo, 2018). A more detailed overview of CL is provided in the literature review. Uber is a successful model of CL use (Carbone et al., 2017a). More companies have begun to follow the same business model for passenger transport and for general local delivery, such as DoorDash in the United States, PiggyBee in Europe, and many others (Carbone et al., 2017a). These companies serve as mediators; their primary asset is based on information and communications technology (ICT). Companies' platforms often rely on GPS-enabled devices such as smartphones (Frehe et al., 2017). These platforms must satisfy customers' evolving needs (in this case, consumers are service recipients) (Luisa Dos Santos Vieira et al., 2013). Therefore, it is important to explore these consumers' preferences to provide effective services.

Scholars who have systematically analyzed CL have identified a paucity of acceptance studies (Carbone et al., 2017a). Crowd (i.e., service recipient) behavior relative to CL is thus considered in this paper. Specifically, our research focuses on relationship-influencing factors to clarify CL acceptability and dispersal (Frehe et al., 2017). Despite the lack of literature in this field overall, many studies have addressed CL acceptance, mostly in Europe. However, scarce literature has examined CL acceptance in the Middle East. This paper aims to fill this gap by conducting a stated preference survey on factors affecting potential CL acceptability in Qatar. A given country's jurisdiction can influence CL practices; in the United States, for instance, crowd shippers are subject to labor regulations (e.g., minimum wage and maximum work time) (Castillo et al., 2018). In Qatar, where the survey in this study was conducted, certain stipulations apply. For example, to be an Uber driver, the driver must be employed by a taxi company that is registered in Qatar (Uber, 2019). This parameter violates CL principles, namely the use of occasional (unprofessional) people.

Our study makes two contributions to the literature: (1) we evaluate determining factors of CL use based on potential customers' feedback; and (2) we test customers' choice preferences of the identified determinants. The following literature review presents several influencing factors that were incorporated when designing stated preference attributes and levels for the survey in this study. Our findings should help future investors and stakeholders make decisions regarding the jurisdiction of CL acceptance, particularly in Qatar.

The remainder of this paper is organized as follows. Section 2 presents the literature review. The chosen survey methodology and corresponding data analysis are outlined in Section 3. Results are reported in Section 4, and Section 5 details our conclusions and future work.

2 LITERATURE REVIEW

The term *crowd logistics* combines two terms, *logistics* and *crowdsourcing*. The latter term integrates *crowd* and *outsourcing* (Peiling & Tingting, 2018), in which 'crowd' encompasses a mass of people and 'outsourcing' refers to shifting processes and functions to a third party. The elements of crowdsourcing are as follows: (a) an organization has a pending task; (b) people (i.e., a crowd) are willing to undertake that task; (c) an

online platform is available to facilitate interaction between the organization and crowd members; and (d) both parties receive mutual benefits from this task completion process (Brabham, 2013).

In this paper, we define CL as the outsourcing of logistics services to a crowd via a technological platform to realize economic benefits for all parties (Carbone et al., 2017a). CL is an aspect of the sharing economy, referring to the efficient use of physical assets supported by ICT (Buldeo Rai et al., 2017). CL has been widely discussed within the business domain; however, it has rarely been the subject of academic research (Carbone et al., 2017b). Most studies have explored the topic relative to business models, with comparatively little attention given to CL users' behavior and perceptions (Punel et al., 2018). Scholars have also investigated existing businesses by interviewing professionals (Frehe et al., 2017). Case studies are another means of assessing this phenomenon, especially in terms of identifying research areas and developing corresponding theories (Voss et al., 2002). Overall, however, few systematic studies have considered behavior around shared resources delivery (Stathopoulos & Punel, 2016).

CL allows for greater customization for the customer (Punel & Stathopoulos, 2017), which has been identified as an important factor in customer satisfaction (Ghajargar et al., 2016). For instance, CL firms can offer more affordable pricing compared to traditional shipping couriers (Rougès & Montreuil, 2014) by optimizing resources without increasing infrastructure. CL also has the potential to benefit the environment by reducing the number of trips needed (assuming drivers are already travelling before assigning a job to them) and therefore congestion (Akyelken, 2011).

Crowd shippers are often non-professional drivers (Goetting & Handover, 2016); as such, trust and privacy present obstacles for CL users (Rougès & Montreuil, 2014). Service quality is another challenge because the drivers are occasional (Furuhata et al., 2013). Customers' expectations around service quality are also increasing, such as same-day delivery, package tracking, and overall satisfaction (Stathopoulos & Punel, 2016). These demands may further complicate CL acceptance.

Because CL firms act only as mediators, it is important to study crowd user behavior (Frehe et al., 2017). As noted earlier, scholarship on the acceptability of CL is lacking (Punel & Stathopoulos, 2017). Le and Ukkusuri (2019) studied individuals' willingness to work as crowd shippers using a binary logit model to estimate participants' discrete choices based on 549 survey responses. Ultimately, 78% of respondents reported being willing to work. Punel et al. (2018) used a binary logit model to distinguish preferences among users and non-users of CL, surveying 800 people in several U.S. states. They concluded that young men with full-time jobs were most accepting of CL. Punel et al. (2018) also found that "people with affordability and trust concerns were less likely than others to use CL". Le and Ukkusuri (2018) examined CL by distributing a stated preference survey in the United States and Vietnam. Their findings highlighted package condition and on-time delivery are the two most important attributes: 85% of respondents across the two countries expressed a preference for package insurance, and 67% and 46% preferred on-time delivery in the United States and Vietnam, respectively. Table 1 presents a summary of papers focusing on the behavior of users/potential users of CL.

Table 1 Papers Focusing on CL Behavior

Paper	Most Important Attributes	Sample	Data Collection	Model
Frehe et al. (2017)	Trust, usability, publicity	5 logistics experts*	Expert interviews	
Le & Ukkusuri (2018)	Whether package arrives in good condition (85%); whether delivery is on time (67% USA; 46% Vietnam)	549 U.S. respondents; 509 in Vietnam	Stated preference survey	Descriptive analysis
Punel et al. (2018)	Flexibility	800 U.S. respondents	Stated preference survey	Binary logit model; Biva riate logit model
Stathopoulos & Punel (2016)	Cost, speed	531 U.S. respondents	Stated preference survey	ECRPL**

Note. *Five experts include a CL company founder, innovation expert, senior innovation manager, CEO, and technical director.
**ECRPL = Error component random parameter logit model.

3 METHODOLOGY

3.1 Stated Preference Choice Modelling

We conducted a stated preference survey to examine aspects of CL in Qatar. Attributes included in the survey were drawn from the preceding literature review. Crowd shipping is not currently available in Qatar; therefore, in addition to a literature review of surveys in other countries, we made assumptions when choosing attributes. These assumptions were inspired by other traditional shipping smartphone applications. In this context, 'traditional' means that the shipper/driver is employed by the service provider (i.e., the application). Attributes included in our stated preference survey appear in Table 2.

Table 2 Stated Preference Attributes and Levels

Attribute	Level 1	Level 2	Level 3
Flexibility	Pickup available anytime and anywhere (GPS)	Pickup available anytime and anywhere (without GPS)	Home or office delivery during typical working hours
Delivery Person's Profile	Transparent; includes rating, age, and gender	Anonymous, with; rating only	
Insurance	Yes	No	
Delivery Accuracy	On time	Within 15 minutes	Within 30 minutes
Cost	5 QR	10 QR	20 QR

Random service provider profiles were created, representing all possible combinations of each attribute level. In total, 108 profiles were generated ($3 \times 2 \times 2 \times 3 \times 3 = 108$). Each respondent was presented with three profile options per question and asked to choose their preferred version. Respondents were then presented with 15 random questions out of 36 possible questions. This random design technique is robust because, in this case, each respondent was exposed to random profiles (Rusch, 2015). The survey

was divided into three sections. The first placed respondents in a scenario in which they were required to use a crowd-shipping app. As such apps are not currently available in Qatar, the app structure was developed based on Le, Stathopoulos, Van Woensel, and Ukkusuri's (2019) model. According to this model, the customer decides to use a CS crowd-shipping app. Then, based on certain attributes (e.g., price and rating), the requester chooses an offer. The app in this case is only a platform to determine pricing and routing. Generally, crowd-shipping drivers in CS are classified into three types: (1) traditional professional carriers (e.g., DHL and FedEx); (2) professional drivers who participate in crowd shipping in their free time; and (3) occasional drivers who have no professional shipping experience (Le et al., 2019). An important assumption in this survey was that the driver is an occasional rather than professional driver. This assumption was intended to help familiarize respondents with the crowd-shipping model. When designing the pilot survey, interviews were conducted with three pilot respondents to ensure potential participants would understand the scenario well. The second survey section included demographic items (e.g., respondents' gender and age). The third section presented the stated preference service provider options discussed earlier; a sample question is shown in Figure 1.

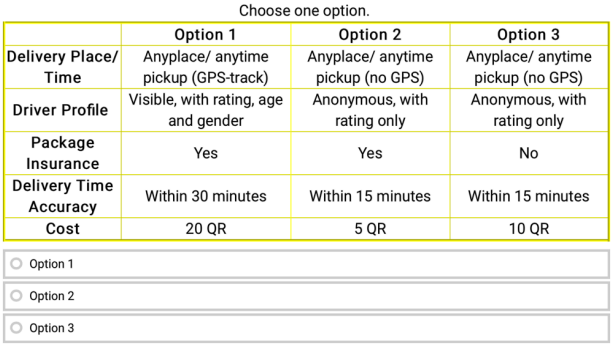
Choose one option.

	Option 1	Option 2	Option 3
Delivery Place/ Time	Anyplace/ anytime pickup (GPS-track)	Anyplace/ anytime pickup (no GPS)	Anyplace/ anytime pickup (no GPS)
Driver Profile	Visible, with rating, age and gender	Anonymous, with rating only	Anonymous, with rating only
Package Insurance	Yes	Yes	No
Delivery Time Accuracy	Within 30 minutes	Within 15 minutes	Within 15 minutes
Cost	20 QR	5 QR	10 QR

Figure 1: Sample Survey Question

3.2 Target Population

The target population for this survey consisted of individuals older than 18 who were living in Qatar. The country is home to two distinct groups: a Qatari and non-Qatari population. The latter group exhibits an unbalanced demographic structure with uneven gender distribution (Planning and Statistics Authority in Qatar, 2018). In 2018, the country hosted 361 female expats for every 100 male expats. This distribution led women to be underrepresented in the survey (39.9% of respondents). However, a U.S. survey indicated that men are 150% more likely than women to use crowd-shipping services (Punel et al., 2018).

3.3 Data Collection

The survey was conducted between July 2019 and October 2019 via www.surveyanyplace.com. The survey link was distributed by email, social media, and link flayers on Hamad Bin Khalifa University campus. Of 381 initial respondents, 280 completed the entire survey. The average completion time was approximately 4 mins (3:57). The 280 responses were sorted in descending order based on completion time. An mlogit model was estimated with an intercept to display preferences for each question's

position. We did not expect respondents to choose an answer based on where it appeared in the option table (i.e., in the top, center, or bottom row). The model revealed that the position of each response option was significant for all responses. Therefore, the responses with the fastest completion time were discarded until 145 responses remained, at which point the position became insignificant (Table 3); each position coefficient demonstrated a high p-value.

Table 3 Preference Estimates by Survey Question Position

Position	Estimate	Std. Error	*z*-value	Pr(>|z|)
pos 2:(center)	0.0279912	0.0666221	0.4201	0.6743772
pos 3:(bottom)	-0.1023388	0.0641355	-1.5957	0.1105633

4 RESULTS

This section presents a detailed overview of our survey results. The *mlogit* package in R software was used to simulate a multinomial regression model to estimate the likely importance of each attribute (Croissant, 2003).

4.1 Descriptive Analysis

Survey results indicated that 57% of male respondents and 54% of female respondents would be willing to work as crowd shippers for a specific amount of money, as listed in Table 4.

Table 4 Respondents' Willingness to Work (Persons)

Age Group	Not Willing to Work		Total	Willing to Work		Total	Grand Total
	Female	Male		Female	Male		
18–24	9	6	15	5	5	10	25
25–34	13	22	35	14	23	37	72
35–44	4	10	14	11	19	30	44
45–54				1	3	4	4
Grand Total	**26**	**38**	**64**	**31**	**50**	**81**	**145**

Respondents' reported incentives to work are listed in Table 5. Of the 81 respondents willing to work, most were interested in earning money. Men were especially interested in supporting the environment, whereas women desired a sense of community.

Table 5 Respondents' Motivations to Work

Gender	Earn Money	Support the Environment	Sense of Community
Male	96%	30%	20%
Female	87%	26%	29%

Note. Some respondents cited more than one reason.

In terms of hypothetical work schedules, slightly more than half (56%) of respondents stated they would work weekly, 19% monthly, and 26% daily.

4.2 Choice Modelling

Survey findings are based on 2,175 different choice tasks. The part worth values in Table 6 represent the mean value of each level (Rusch, 2015).

Table 6 Part Worth for Each Attribute

Attribute	Estimate	Std. Error	*z*-value	Pr(>|z|)
Having insurance	0.958545	0.069602	13.7718	< 2.2e-16
Anyplace/anytime pickup (No GPS)	-0.588422	0.069718	-8.44	< 2.2e-16
Transparent delivery person profile	0.559581	0.054644	10.2405	< 2.2e-16
Home/office pickup during working hours	-0.444719	0.067474	-6.591	4.37E-11
Delivery within 30 minutes of scheduled time	-0.278106	0.068523	-4.0586	4.94E-05
Cost	-0.069051	0.004745	-14.5522	< 2.2e-16
Exact time delivery	0.062655	0.078187	0.8014	0.4229

Log likelihood coefficients are shown in Table 6; attributes not listed in the table are base attributes. Estimates are on a logit scale between -2 and 2, where a higher magnitude indicates that the attribute is more important, and a negative sign indicates that the opposing attribute is more important. All estimates were statistically significant ($p > 0.05$) apart from 'exact time delivery'. Standard values for all attributes were low. Based on these findings, having insurance was reportedly the most important attribute, which is in line with the findings of Le and Ukkusuri (2018). The second most important attribute was 'anytime and anyplace delivery (with GPS)', which allows for greater flexibility according to Punel et al. (2018). Respondents favored a transparent delivery person profile, apparently due to trust concerns as suggested by Frehe et al. (2017). Respondents did not appear to mind a 15-min. delivery delay. Cost was not an important attribute, which may be associated with customers' trust concerns: the hypothetical delivery person was occasional and not employed by the delivery app company, and respondents were willing to pay more.

4.3 Willingness to Pay

Consumers' willingness to pay (WTP) suggested that on average, customers would be equally divided between crowd-shipping attributes at a given price; that is, the price in Qatari Riyal (Table 7) represents the price at which customers appeared indifferent to corresponding attributes.

Table 7 Willingness-to-pay Values

Attribute	WTP in QR
Having insurance	13.8
Having GPS tracking and flexible delivery place	8.5
Transparent delivery person profile	8.1

5 CONCLUSION

Policymakers and businesses can benefit from this study because it delineates initial key factors of Qatar's CL business model. Findings reveal how potential consumers may react to crowd-shipping attributes, how much they would be willing to pay for such a service, and whether they would be willing to work as crowd shippers. The implementation of CL is expected to benefit the environment by reducing road traffic. However, additional research should be conducted using more complex survey techniques, such as an adaptive-conjoint survey. A larger pool of responses would also

result in greater confidence in each attribute. Scholars can use the present findings as a starting point to further explore CL implementation in Qatar. Notably, combining the most important attributes into one business model might not be practical given high associated costs. It is essential to simulate share predictions in a model with a higher number of respondents and without unrealistic profiles. Policymakers may benefit from this research by realizing that introducing the CL model in Qatar will present trust complexities; governmental regulation of CL may effectively reduce consumers' lack of trust.

REFERENCES

Akyelken, N. (2011). Green logistics: Improving the environmental sustainability of logistics. *Transport Reviews*, *31*(4), 547-548. https://doi.org/10.1080/01441647.2010.537101.

Brabham, D. C. (2013). 1 concepts, Theories, and cases of crowdsourcing. In *Crowdsourcing* (p. 168). https://doi.org/10.7551/mitpress/9693.003.0005.

Brunner, G., Szebedy, B., Tanner, S. & Wattenhofer, R. (2018). *The urban last mile problem: Autonomous drone delivery to Your balcony*. Retrieved from http://arxiv.org/abs/1809.08022.

Buldeo Rai, H., Verlinde, S., Merckx, J. & Macharis, C. (2017). Crowd logistics: an opportunity for more sustainable urban freight transport?. *European Transport Research Review*, *9*(3), 1-13. https://doi.org/10.1007/s12544-017-0256-6.

Carbone, V., Rouquet, A. & Roussat, C. (2017a). The rise of crowd logistics: A new way to co-create logistics value. *Journal of Business Logistics*, *38*(4), 238-252. https://doi.org/10.1111/jbl.12164.

Carbone, V., Rouquet, A. & Roussat, C. (2017b). The rise of crowd logistics: A new way to co-create logistics value. *Journal of Business Logistics*, *38*(4), 238-252. https://doi.org/10.1111/jbl.12164.

Castillo, V. E., Bell, J. E., Rose, W. J. & Rodrigues, A. M. (2018). Crowdsourcing last mile delivery: Strategic implications and future research directions. *Journal of Business Logistics*, *39*(1), 7-25. https://doi.org/10.1111/jbl.12173.

Croissant, Y. (2003). Estimation of multinomial logit models in R: The mlogit Packages An introductory example. *Data Management*, 73. Retrieved from http://scholar.google.com/scholar?hl=en&btnG=Search&q=intitle:Estimation+of+multinomial+logit+models+in+R+:+The+mlogit+Packages+An+introductory+example#0

Edwards, J. B., McKinnon, A. C. & Cullinane, S. L. (2010). Comparative analysis of the carbon footprints of conventional and online retailing: A "last mile" perspective. *International Journal of Physical Distribution and Logistics Management*, *40*(1-2), 103-123. https://doi.org/10.1108/09600031011018055

Frehe, V., Mehmann, J. & Teuteberg, F. (2017). Understanding and assessing crowd logistics business models – using everyday people for last mile delivery. *Journal of Business and Industrial Marketing*, *32*(1), 75-97. https://doi.org/10.1108/JBIM-10-2015-0182.

Furuhata, M., Dessouky, M., Ordóñez, F., Brunet, M. E., Wang, X. & Koenig, S. (2013). Ridesharing: The state-of-the-art and future directions. *Transportation Research Part B: Methodological*, *57*, 28-46. https://doi.org/10.1016/j.trb.2013.08.012

Ghajargar, M., Zenezini, G. & Montanaro, T. (2016). Home delivery services: innovations

and emerging needs. *IFAC-PapersOnLine*, *49*(12), 1371-1376. https://doi.org/10.1016/j.ifacol.2016.07.755

Goetting, E. & Handover, W. N. (2016). *Crowd-shipping: Is crowd-sourced the secret recipe for delivery in the future?* (I).

Le, T. V., Stathopoulos, A., Van Woensel, T. & Ukkusuri, S. V. (2019). Supply, demand, operations, and management of crowd-shipping services: A review and empirical evidence. *Transportation Research Part C: Emerging Technologies*, *103*(October 2018), 83-103. https://doi.org/10.1016/j.trc.2019.03.023.

Le, T. V. & Ukkusuri, S. V. (2018). *Crowd-shipping services for last mile delivery: analysis from survey data in two countries*. (18), 1-23. Retrieved from http://arxiv.org/abs/1810.02856.

Le, T. V. & Ukkusuri, S. V. (2019). Modeling the willingness to work as crowd-shippers and travel time tolerance in emerging logistics services. *Travel Behaviour and Society*, *15*(February), 123-132. https://doi.org/10.1016/j.tbs.2019.02.001.

Luisa Dos Santos Vieira, C., Sérgio Coelho, A. & Mendes Luna, M. M. (2013). ICT implementation process model for logistics service providers. *Industrial Management & Data Systems*, *113*(4), 484-505. https://doi.org/10.1108/02635571311322757.

Odongo, B. (2018). *How crowd sourcing is changing the face of last mile delivery: Crowd logistics*. (May). Retrieved from https://www.theseus.fi/handle/10024/149856.

Peiling, Z. & Tingting, L. (2018). Understanding consumer preferences for logistics services within online retailing of fresh products A research conducted on Swedish consumers. *Wired Magazine*. Retrieved from https://www.wired.com/2006/06/crowds/.

Planning and Statistics Authority in Qatar. (2018). Woman and Man in the State of Qatar, a Statistical Profile. In *Qatar, Planning and Statistics Authority in*. Retrieved from https://www.psa.gov.qa/en/statistics1/StatisticsSite/Pages/SocialTopics.aspx.

Punel, A., Ermagun, A. & Stathopoulos, A. (2018). Studying determinants of crowd-shipping use. *Travel Behaviour and Society*, *12*, 30–40. https://doi.org/10.1016/j.tbs.2018.03.005.

Punel, A. & Stathopoulos, A. (2017). Modeling the acceptability of crowdsourced goods deliveries: Role of context and experience effects. *Transportation Research Part E: Logistics and Transportation Review*, *105*, 18-38. https://doi.org/10.1016/j.tre.2017.06.007.

Rougès, J.-F. & Montreuil, B. (2014). Crowdsourcing Delivery : New Interconnected Business Models to Reinvent Delivery. *1st International Physical Internet Conference*, (1), 1-19.

Rusch, T. (2015). R for marketing research and analytics. In *Journal of Statistical Software* (Vol. 67). https://doi.org/10.18637/jss.v067.b02.

Savelsbergh, M. & Van Woensel, T. (2016). City logistics: Challenges and opportunities. *Transportation Science*, *50*(2), 579-590. https://doi.org/10.1287/trsc.2016.0675.

Stathopoulos, A. & Punel, A. (2016). Modeling People's Behavior and Acceptance of Crowdsipping. *Trr*.

Uber. (2019). Uber requirements for drivers in Qatar | Uber. Retrieved April 19, 2019, from https://www.uber.com/en-QA/drive/requirements/.

Voss, C., Tsikriktsis, N. & Frohlich, M. (2002). Case research in operations management. *International Journal of Operations & Production Management*, *22*(2), 195-219. https://doi.org/10.1108/01443570210414329.

Zellner, M., Massey, D., Shiftan, Y., Levine, J. & Arquero, M. J. (2016). Overcoming the Last-

Mile Problem with Transportation and Land-Use Improvements: An Agent-Based Approach. *International Journal of Transportation*, *4*(1), 1-26. https://doi.org/10.14257/ijt.2016.4.1.01.

Cite this article as: Al-Saudi A., Himpel F., "Crowd Logistics Delivery Determinants: A Stated-Preference Survey", *International Conference on Civil Infrastructure and Construction (CIC 2020)*, Doha, Qatar, 2-5 February 2020, DOI: https://doi.org/10.29117/cic.2020.0054

A Study on Using Reclaimed Asphalt Pavement (RAP) in the Construction of New Roads in the State of Qatar

K. Lakshmi Roja
lakshmi.kakumanu@qatar.tamu.edu
Mechanical Engineering Program, Texas A&M University at Qatar, Doha, Qatar

Eyad Masad
eyad.masad@qatar.tamu.edu
Mechanical Engineering Program, Texas A&M University at Qatar, Doha, Qatar

ABSTRACT

In the State of Qatar, road engineers started using RAP in the base course of asphalt pavement from past few years. The use of RAP not only replaces the quantity of virgin aggregate and binder, it also improves the overall stiffness of asphalt mixture due to the addition of aged asphalt binder. Considering the economic and environmental benefits of RAP, in this study, a mix design was developed for asphalt mixtures containing different proportions of RAP and evaluate the performance of RAP blended asphalt mixtures. Based on obtained properties, it was attempted to optimize the use of RAP content in the base course of asphalt pavement. In this study, the asphalt mixtures were produced with three different RAP contents (15, 25 and 35%) and the behavior of these mixtures was benchmarked with conventional mix (0% RAP). The RAP blended asphalt mixtures were tested using several experimental protocols. First, the stiffness modulus of RAP mixtures were determined using AASHTO test method. The high and low temperature distress characteristics of mixtures were determined using Hamburg wheel tracker and semi-circular beam bending test. Based on the stiffness and performance properties, a suitable RAP content and the ways to increase the use of RAP content was recommended.

Keywords: Reclaimed asphalt pavement; Mix design; Rutting; Fracture; Optimum RAP content

1 INTRODUCTION

Large scale road projects are being constructed in the State of Qatar for the past few years. The construction of new road projects requires large quantities of aggregate and binder. Using RAP in the asphalt mix design can be an alternate solution to reduce the consumption of natural resources. Nowadays, the usage of RAP in pavement construction is tremendously increasing due to the benefits of this material in terms of improved performance, cost effectiveness and reduced environmental impact. However, the high and low temperature performance characteristics of RAP blended asphalt mixture are highly dependent on the properties of RAP binder and aggregate. The two major distresses in asphalt pavements are rutting and fatigue cracking. The addition of RAP to virgin asphalt mixture may increase the total stiffness of mix, which may cause higher resistance to rutting and poor resistance to fatigue cracking (Al-Qadi et al., 2007; Shu et al., 2008). While using RAP in the asphalt mix design, it is necessary to balance both high and low temperature distress properties.

To allow high RAP contents in asphalt mix design, few researchers used rejuvenators and adjusted the mix design slightly to improve the resistance to fracture (Mogawer et al., 2015; Menapace et al., 2018). The optimum RAP content can be determined by balancing the performance of asphalt mixtures containing different proportions of RAP at critical pavement service temperatures. The objective of this study was to evaluate the effect of using highly oxidized asphalt on the mixture performance. This objective was achieved by conducting the following tasks:

- Develop a mix design for RAP blended asphalt mixtures and maintain the similar volumterics for virgin and RAP blended asphalt mixtures.
- Evaluate the high and low temperature distresses of asphalt mixtures containing RAP.
- Recommend to the State of Qatar an allowable RAP content that will not impact the durability of asphalt mixtures negatively.

2 MATERIALS AND MIX DESIGN

2.1 RAP characterization

A local contractor in Qatar supplied the RAP material. For asphalt mix design, the RAP material passing 12.5 mm sieve was considered. The RAP binder was extracted and recovered using rotary evaporator as per ASTM D 7906 (2014). The true (continuous) grade of the recovered binder was PG 94-0. These PG high and low temperatures were exact pass/fail temperatures obtained from $G^*/\sin\delta$ values and Bending Beam Rheometer (BBR) testing. The basic properties of the RAP recovered binder and aggregates were determined. From the literature (Sreeram et al., 2018), it was assumed that only 70% of RAP binder was effective for the production of asphalt mixtures.

2.2 Production of asphalt mixtures

A base course class A gradation (Qatar Construction Specification, 2014) with a nominal maximum aggregate size (NMAS) of 25 mm was selected to produce these mixtures. Four types of asphalt mixtures were produced: control mix (0% RAP), 15, 25 and 35% RAP blended mixtures. The superpave mix design was used for all mixtures. A base binder of PG 64-22 (Pen 60/70) grade was selected in this study. For the production of asphalt mixtures, five aggregate stockpiles 37.5-22mm, 22-12mm, 12-8mm, 8-4mm, <4mm and RAP stockpile of <12.5mm and filler material were used.

The virgin aggregates and RAP material were heated separately at 160°C and 110°C respectively and they were mixed with binder at a temperature of 153°C. For testing mechanical properties, asphalt mixtures were short-term aged for 4 hours at 135°C and then increased to a compaction temperature (AASHTO R30, 2011). These samples were compacted using gyratory compactor to a traffic level of >30 million ESAL (N_{design}=125 gyrations). The size of gyratory samples was 150 mm diameter and 165 mm height and the target air voids of 7$\pm$0.5% were used for all tests in this study.

2.3 Mix design

All the mixtures were prepared with binder contents of 2.5, 3.0, 3.5, 4.0 and 4.5%. Based on the values of stability, flow, Voids in Mineral Aggregates (VMA), Voids Filled with Asphalt (VFA) and air void, the optimum binder contents of 0, 15, 25 and 35% RAP

blended mixtures were determined as 3.9, 3.7, 3.5 and 3.5%, respectively. For all the mixtures, the VMA values were maintained in between 12-12.5% and the VFA values were in between 67-70% (as per QCS, 2014).

3 MATERIAL PROPERTY- DYNAMIC MODULUS

The dynamic modulus tests were conducted using an Asphalt Mixture Performance Tester (AMPT) in confined condition (AASHTO T378-17, 2017). The sinusoidal loading waveform was applied with confinement pressure of 69 kPa and the measured strains were in between 85 to 115 microstrain. The tests were conducted at five different temperatures of 5, 15, 25, 35 and 45°C and three frequencies of 0.1, 1 and 10 Hz. The dynamic modulus (|E*|) and phase lag (δ) values were calculated from the ratio of peak stress to peak strain and the time lag between stress and strain curves (AASHTO T378-17, 2017). From the obtained |E*| values, the master curves were constructed at a reference temperature of 35°C as shown in Figure 1. It was observed that the addition of RAP increased the stiffness of asphalt mixtures. However, it is necessary to analyze the performance characteristics of such mixtures to identify an optimum RAP content for asphalt mix design.

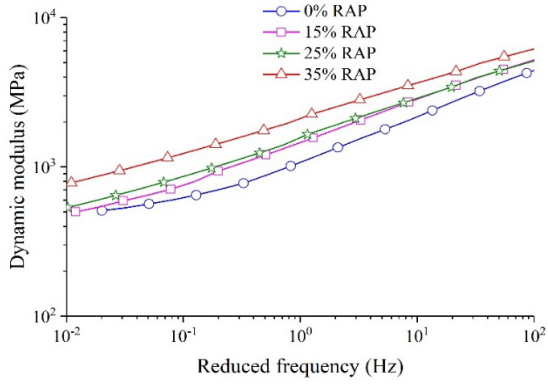

Figure 1: Master curves for RAP blended asphalt mixes

4 RUTTING CHARACTERIZATION

In this study, two test protocols were used to characterize the rutting: Hamburg Wheel Tracker (HWT) and Flow Number (FN) test. In HWT test, a wheel load of 700 N was passed on the surface of the sample in to and from direction at a speed of 52 passes per minute (AASHTO T 324-14, 2014). The rut depth was measured along wheel path using a Linear Variable Differential Transducer (LVDT) and the test was terminated at 20000 passes. For each mix, total of four samples were mounted in the testing device: two on left side, two on right side. The test was conducted in dry condition at 64°C and wet condition at 50°C. The average of maximum rut depth on both left and right sides are plotted in Figure 2 for both dry and wet conditions. The addition of RAP content caused an increase in rut resistance. In dry condition, the final rut depth for 0, 15, 25 and 35% RAP blended mixes was measured as 17.1, 14.1, 8.6, and 6.2 mm, respectively (Figure 2(a)) whereas, in wet condition, the behavior of all the RAP blended asphalt mixes (15, 25 and 35%) was more or less same and the final rut depth was less than 12.5 mm for all the mixes (Figure 2(b)).

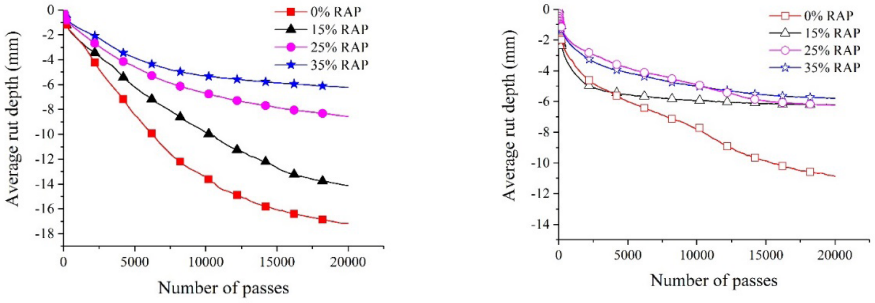

(a) Dry condition (b) Wet condition

Figure 2: Rut depth of asphalt mixtures containing different proportions of RAP

A standard flow number test method was carried out using an Asphalt Mixture Performance Tester (AMPT). A deviatoric stress of 600 kPa was applied with a confinement level of 69 kPa at a temperature of 40°C. The test consists of 0.1 s haversine load and 0.9 s rest period (AASHTO T378-17, 2017). The test was terminated at 10000 cycles. The accumulated irrecoverable deformation at the end of each cycle was recorded and shown in Figure 3. Out of all the mixes, virgin sample (0% RAP) showed more susceptibility to rutting and it has higher percentage of strain. The mix with higher RAP content (35%) has greater rut resistance and the similar observation was seen from wheel tracking tests on mixtures. Flow number is defined as the number of cycles corresponding to the starting of tertiary stage and it can be identified from the rate of change of slope of irrecoverable strain using Francken model (Equation 1) (Francken, 1977).

$$\varepsilon_p = aN^b + c\left(exp^{dN} - 1\right), \quad (1)$$

where, ε_p represents the irrecoverable strain, N represents the number of load cycles and a, b, c and d represents model parameters. The parameters a and b capture the primary and secondary stage and c and d capture the tertiary stage. In Figure 3, it can be observed that there is no sample failure within the test duration (c=0 for no tertiary stage). The first term of equation 1 can be used to capture the primary and secondary stages of (parabolic shape) of three stage creep curve. Parameters a and b derived from the linear portion of primary and secondary stage of the accumulated strain are shown in Figure 3. For all the mixes, irrecoverable strain accumulated at almost same rate. The parameters obtained for 15 and 25% RAP mixes were identical.

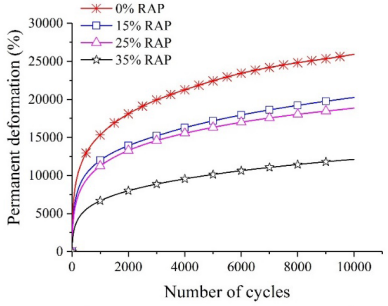

Material	a	b	c	d	R^2
0% RAP	3059	0.233	0	0	0.997
15% RAP	2338	0.234	0	0	0.998
25% RAP	2255	0.231	0	0	0.995
35% RAP	1070	0.263	0	0	0.987

Figure 3: Creep curves for asphalt mixes containing different proportions of RAP and Francken model parameters

5 FRACTURE RESISTANCE

Fracture resistance of asphalt mixtures is an indicator of fatigue behavior that occurs due to the accumulation of tensile strains during repeated loading. In this study, the fracture resistance of RAP contained mixtures was evaluated using Semi Circular Bend (SCB) test. SCB tests were conducted on gyratory samples of thickness 50±2mm and these circular samples were cut into two equal halves. The selected notch depth and width were 16 mm and 3 mm, respectively. A vertical load was applied on these samples with a constant displacement rate of 0.5 mm/min (Sreedhar et al., 2018). When the applied load was below 0.5 kN, the test was terminated. The selected test temperature was 25°C. At least four specimens were tested for each type of mix to check the repeatability.

In the load-displacement curve (Figure 4), the area under curve was calculated using equation 2 which represents the 'work of fracture'. From which, the fracture energy and Flexibility Index (FI) were calculated using equation 4 and 5, respectively. FI parameter is mainly used for fatigue performance evaluation and it is defined as the ratio of the fracture energy (G_f) to the slope at post-peak inflection point of load-displacement curve. FI parameter can dictate the brittleness of material and the lower value of the material shows more brittleness with a higher crack growth rate (Ozer, 2016).

Work of fracture $W_f = \int P\, du$ (in kJ) (2)

Ligment area $A = (r - a) \times t$ (in m^2) (3)

Fracture energy $G_f = \frac{W_f}{A}$ (in kJ/m^2) (4)

Flexibility index $FI = \frac{G_f}{abs(m)} \times 0.01$ (5)

where P = applied load (kN), u = load line displacement (m), r = sample radius (m), a = notch length (m), and t = sample thickness (m), abs(m) = absolute value of the slope at post-peak inflection point of load-displacement curve. From Figure 5, it was observed that the virgin asphalt mixtures (0% RAP) have higher fracture resistance than the RAP blended asphalt mixtures. This could be due to the reason that there is no aged RAP binder in the total mix. As the RAP proportion increased, the virgin binder content was reduced, the fracture resistance of asphalt mixtures was deteriorated.

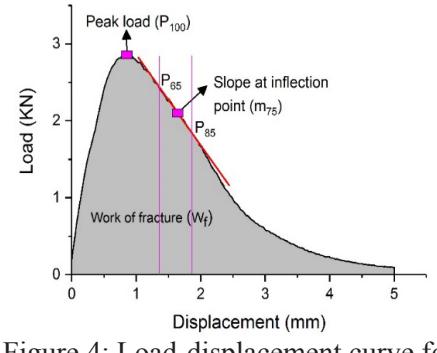

Figure 4: Load-displacement curve for 0% RAP binder (AASHTO TP 124, 2018)

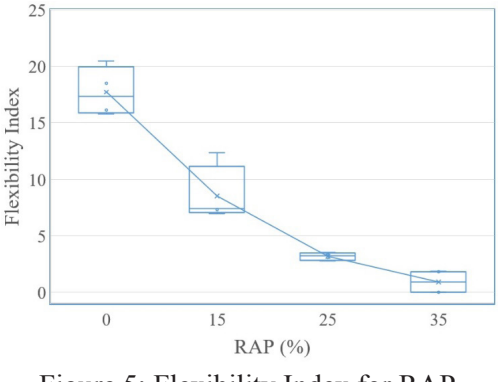

Figure 5: Flexibility Index for RAP blended asphalt mixtures

6 BALANCE OF PERFORMANCE

Figure 6 shows the balancing of rut depth values (HWT dry rut depth) and fracture resistance parameter (SCB FI) of RAP blended asphalt mixtures. In Figure 6, the RAP proportion corresponding to a target rut depth of 12.5 mm was 18%. Hence, a minimum of 18% RAP should be added to avoid failure due to rutting. In fracture test, the target FI value was considered as 8 (Mogawer et al., 2019) From Figure 6, the RAP proportion corresponding to the target FI value was marked as 16%. Qatar has desert hot climatic conditions for many of the days in a year. Hence, it is necessary to make more rut resistant mixtures. In this study, by balancing both rutting and fracture characteristics of asphalt, it is recommended to use up to 20% of RAP without having negative impact on low temperature performance of mixtures.

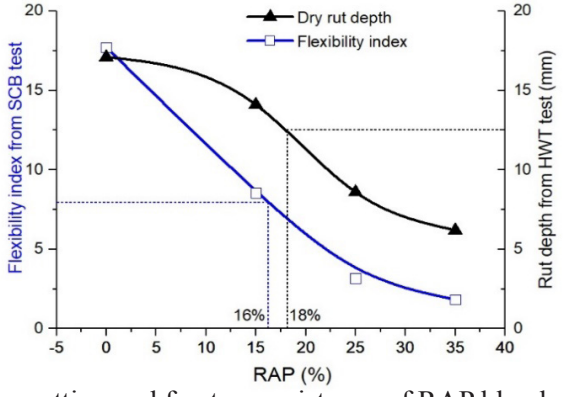

Figure 6: Balancing rutting and fracture resistance of RAP blended asphalt mixtures

7 CONCLUSION

The main objective of this paper was to check the influence of RAP on the performance of asphalt mixtures. The material and performance properties of asphalt mixtures were evaluated using different test protocols. First, the dynamic modulus of RAP contained asphalt mixtures were determined at different temperatures and the high and low temperature distress characteristics of RAP blended asphalt mixtures were balanced. From this investigation, the following conclusions can be drawn:

1. The asphalt mixture blended with higher proportion of RAP (35%) has the highest dynamic modulus values and rutting resistance. However, this mixture exhibited the least fracture performance.
2. For desert hot climatic conditions of Qatar, by balancing both rutting and fracture characteristics of asphalt mixtures, it is recommended to use up to 20% of RAP without having negative impact on low temperature performance of asphalt mixtures. Given the low asphalt contents (typically less than 4% of asphalt content) in mixture designs in Qatar, and the high aging of RAP binders due to high temperatures, it is recommended to limit the RAP content to a maximum of 20% by weight of mix. The use of higher RAP contents would require changes in the asphalt mix design (binder content, gradation) and/or the use of rejuvenating agents.

ACKNOWLEDGEMENT

This investigation was supported by Consortium for Asphalt Pavement Technologies

(CAPT), Texas A&M at Qatar. The authors gratefully acknowledge the support of FUGRO Doha in the sample preparation and basic testing.

REFERENCES

Al-Qadi, M. Elseifi & S. H. Carpenter (2007). Reclaimed asphalt pavement - a literature review, Tech. rep., University of Illinois at Urbana Champaign.

Francken, L. (1977). Pavement deformation law of bituminous road mixes in repeated load triaxial compression. *In Fourth international conference on the structural design of asphalt pavements.* University of Michigan, the USA.

Menapace, I., Cucalon, L. G., Kaseer, F., Arámbula-Mercado, E., Martin, A. E., Masad, E. & King, G. (2018). Effect of recycling agents in recycled asphalt binders observed with microstructural and rheological tests. *Construction and Building Materials*, 158, 61-74.

Mogawer, W. S., Austerman, A., Roque, R., Underwood, S., Mohammad, L. & Zou, J. (2015). Ageing and rejuvenators: evaluating their impact on high RAP mixtures fatigue cracking characteristics using advanced mechanistic models and testing methods. *Road Materials and Pavement Design*, *16*(sup2), 1-28.

Mogawer, W. S., Austerman, A. J., Stuart, K. D., Zhou, F. & Romero, P. (2019). Balanced mix design sensitivity to production tolerance limits and binder source. *Journal of the Association of Asphalt Paving Technologist (AAPT),* Vol. 88. (Under review)

Ozer, H. (2016). Development of the fracture-based flexibility index for asphalt concrete cracking potential using modified semi-circle bending test parameters. *Construction and Building Materials,* 115, 390-401.

Shu, X., Huang, B. & Vukosavljevic, D. (2008). Laboratory evaluation of fatigue characteristics of recycled asphalt mixture. *Construction and Building Materials*, *22*(7), 1323-1330.

Sreedhar, S., Coleri, E. & Haddadi, S.S. (2018). Selection of a performance test to assess the cracking resistance of asphalt concrete materials. *Construction and Building Materials,* 179, 285-293.

Sreeram, A., Leng, Z., Zhang, Y., & Padhan, R. K. (2018). Evaluation of RAP binder mobilisation

Cite this article as: Roja K. L., Masad E., "A Study on Using Reclaimed Asphalt Pavement (RAP) in the Construction of New Roads in the State of Qatar", *International Conference on Civil Infrastructure and Construction (CIC 2020)*, Doha, Qatar, 2-5 February 2020, DOI: https://doi.org/10.29117/cic.2020.0055

Asphalt Rideability Specification and Construction of Expressways in Qatar

Roger James Hodgson
rhodgson@ashghal.gov.qa
Public Works Authority, Highway Projects Department, Doha, Qatar

Ali Kara
akara@ashghal.gov.qa
Public Works Authority, Highway Projects Department, Doha, Qatar

ABSTRACT

Development of an Expressway network with a smooth ride quality is part of the Qatar 2030 Vision. The Public Works Authority (Ashghal) has placed high importance on the asphalt specification and quality of construction of the Expressway network to produce a perceived smooth, uninterrupted ride quality for the benefit of the traveling public. Ashghal has used a robust international specification for the International Roughness Index (IRI) and has required the Contractors and Supervision Consultants on the Expressway projects to produce an exceptional ride quality by training asphalt paving crews, using state-of the art asphalt paving and levelling equipment and quality control testing of the finished pavement. Various obstacles have been encountered in the Ashghal quest to produce world-class asphalt pavements and those obstacles have been overcome. This paper highlights the lessons learned from asphalt construction and aims to deliver to a wider audience the benefits of the Ashghal experience.

Keywords: International roughness index (IRI); Roughness; Pavement; Asphalt; Quality control

1 INTRODUCTION

The Qatar National Vision 2030:

"The National Vision aims at transforming Qatar into an advanced country by 2030, capable of sustaining its own development and providing for a high standard of living for all of its people for generations to come."

In order to achieve the above vision Qatar must balance five major challenges:

- Modernization and preservation of traditions.
- The needs of the present and future generations.
- Managed growth and uncontrolled expansion.
- The size and the quality of the expatriate labor force and the selected path of development.
- Economic growth, social development and environmental management.

To balance the above Qatar's national Vision Rests on the following four pillars:

- **Human Development** - Development of all its people to enable them to sustain a

prosperous society.

- **Social Development** - Development of a just and caring society based on high moral standards, and capable of playing a significant role in the global partnership for development.
- **Economic Development** - Development of a competitive and diversified economy capable of meeting the needs of, and securing a high standard of living for, all its people for the present and for the future.
- **Environmental Development** - Management of the environment such that there is harmony between economic growth, social development and environmental protection.

Therefore, a world-class infrastructural backbone is essential to attaining the vision of economic development. This consists of a comprehensive urban development plan for Qatar that adopts a sustainable policy with regard to urban expansion and population distribution. In establishing a world leading specification for the roughness of the completed asphalt road pavements that have been constructed under the economic development pillar, Qatar has bridged both the Economic and Environmental pillars. Smoother roads lead to reduced fuel consumption, reduced driver fatigue, reduced vehicle wear and tear and reduced induced harmonic compression of the pavement. This resultant virtuous circle of benefits works towards the Environmental Pillar of the Vision.

2 SPECIFICATIONS USED

Qatar's Expressway Programme under the Public Works Authority, is one of World's largest road infrastructure projects currently under construction. It will deliver a world-class new and upgraded road network in line with Qatar National Vision and cater to the 2022 FIFA World Cup. All projects across the Expressway Programme are required to report International Roughness Index (IRI).

IRI is defined as:

- A roughness parameter determined from a measured road profile in both wheel tracks.
- The measured profile is processed using a mathematical transform, which filters and cumulates the wavelengths encountered in the profile.
- Internationally recognized method of reporting detectable surface irregularity relating to the physical responses of vehicles on road surfaces.
- Pavement roughness, defined as an expression of irregularities in the pavement surface that adversely affect the ride quality of a vehicle (and thus the user). Roughness is an important pavement characteristic because it affects not only ride quality but also vehicle operating costs, fuel consumption (Fuel consumption^2 = IRI) and maintenance costs.
- Roughness is also referred to as "smoothness" although both terms refer to the same pavement qualities.

The majority of the Expressway projects that have been constructed to date in Qatar have used the Qatar Construction Specification (QCS) 2010. This Standard did not have a definitive value for IRI and therefore Interim Advice Notes (IAN's) were written to give guidance for the IRI limits to be used during construction for acceptance of the completed asphalt surface.

A typical IAN that was used was IAN 19, titled as "*Amendments to Sections 5 and 6 of QCS 2010".* Sections 5 and 6 being those concerned with pavement construction, roadworks and asphalt works. IAN Specification for the IRI on new pavement construction is:

a) **Flexible Pavement**: Average value over a 400 meter section - 0.90 m/km
b) **Composite and Rigid Pavement**: Average value over a 400-meter section - 1.20 m/km.

The IAN specifies that peak individual value over a 25-meter section shall be 1.5 m/km (Not more than 2 values per 400 meters) for New construction, Reconstruction and Pavement rehabilitation. It came to Ashghal's attention that projects are being affected by inconsistencies in the type and manufacturer of IRI equipment being used and inconsistent Project Specifications where the Supervision Consultants' (SC's) were not fully aware of test requirements.

This includes specifics where SC's were not aware of reported variance requirements in order to confirm accuracy of results being reported or the method of reporting the results. IRI testing has to be reproducible providing a consistent measurement. It was discovered that not all projects analyze and report IRI test results in the same format. Some projects also had different specification requirements. It is important that all profilers are correctly calibrated and consistent testing procedures are adopted on all projects.

3 SPECIFICATION PROBLEMS

Ashghal understands that the Programme Management Consultants (PMC) developed this specification and a very similar specification has been used in the Kingdom of Saudi Arabia (KSA) for some time. It is worth noting here that the 400m treatment length is unusual with respect to other international specifications. It is thought that the 400m treatment length was used in order to assess longer wavelength rideability criteria. Therefore, the 400m length may not be suitable for Qatar Expressways.

Also there was debate if the 400m section should be reported as 400m rolling average (i.e. drop one 25m average section and add one 25m section) or 400m discrete blocks. Analysis of the ASTM standard E1926-08R15 – Computing International Roughness Index, indicates that the averaging of the results should be reported over 25m only. Therefore reporting a rolling average of the 400m sections would result in a doubling of the smoothing, leading to non-representative results and difficulty in pinpointing isolated areas of roughness.

On analysis of the manufacturers internal reporting software on the class 1 laser profilers used, it was apparent that the averaging of individual IRI results has indeed been carried out over 25m sections.

4 INSTILLING THE NEED AND LESSONS LEARNED

It became apparent to Ashghal during construction of the multi-layer asphalt pavements that the level of awareness regarding the importance of meeting the stringent IRI specification and providing a world-class smooth pavement was inconsistent in the

Contractors, Supervision Consultants and the third party testing laboratories. Ashghal therefore, initiated on-site training programmes stressing the importance of meeting the IRI specification and what was expected of the Contractors and Consultants. The outcome was that many of the contractors started to carry out IRI testing on the intermediate asphalt course prior to laying the final asphalt-wearing course. In this way, there was capacity to carry out any repairs or rectification to the underlying layer prior to laying the wearing course.

Asphalt wearing courses were laid using a minimum 9m, but preferably 11 to 13m ultrasonic averaging beams, commonly referred to a "multiplex" levelling system. All third party testing laboratories that carry out IRI were invited to a workshop hosted and arranged by Ashghal to ensure consistency in testing methodology and reporting format.

5 CONCLUSION AND RECOMMENDATIONS

From Ashghal's experience in producing and meeting an IRI Specification, a number of conclusions have been made, they are:

- That there is a need to establish a reference profile against which all the profilographs used for IRI measurement in Qatar can be referenced against. This can set the precision and bias of the profilographs.
- The Specification for IRI should reflect what the owner is expecting to achieve. Using a 400m section for reporting is too long for Qatar, a more realistic section would be 150m, this in-keeping with relevant international standards (Múčka, 2017).
- Rideability can be improved by effective paving plans and by executing the wearing course in long stretches to minimize the number of cold transverse joints.
- Contractors should be made aware of the need to produce smooth pavements at the start of construction and significant financial incentives provided to produce a better than specified IRI.
- Every effort should be made at the design stage to remove ironworks such as handhole covers, personnel access covers for chambers and openings in the carriageway to ensure a smooth running surface.

REFERENCES

American Association of State Highway and Transportation Officials (AASHTO), *Geometric Design of Highways and Streets*, 7th Edition.

Ashghal Interim Advice Note No. 19, revisions 2 & 3, *Amendments to Sections 5 and 6 of QCS 2010*, Public Works Authority, Ashghal.

ASTM Standard E1926-08R15 - Standard Practice for Computing International Roughness Index of Roads from Longitudinal Profile Measurements.

Múčka, Peter (2017) International roughness index specifications around the world. *Road Materials and Pavement Design*, 18:4, 929-965.

Qatar Construction Specification (QCS) 2010.

Cite this article as: Hodgson R. J., Kara A., "Asphalt Rideability Specification and Construction of Expressways in Qatar", *International Conference on Civil Infrastructure and Construction (CIC 2020)*, Doha, Qatar, 2-5 February 2020, DOI: https://doi.org/10.29117/cic.2020.0056

Optimizing the Thermal Resistance of Concrete Using The Palm Tree Fronds Fibers

Mohammad Hany Yassin
m.yassin@ack.edu.kw
Australian College of Kuwait, Kuwait, Kuwait

Rana Lakys
r.lakys@ack.edu.kw
Australian College of Kuwait, Kuwait, Kuwait

Taha Ahmed
t.ahmed@ack.edu.kw
Australian College of Kuwait, Kuwait, Kuwait

Shafaq Al-Refaei
1415432@go.ack.edu.kw
Australian College of Kuwait, Kuwait, Kuwait

Bader Al-Sayed Omar
1211087@go.ack.edu.kw
Australian College of Kuwait, Kuwait, Kuwait

Rose Shaker Altaher
1313084@go.ack.edu.kw
Australian College of Kuwait, Kuwait, Kuwait

ABSTRACT

In the past few years, the issue of global warming has become increasingly visible. Record high as well as record low temperatures are being broken worldwide. Snow is melting in the poles and less sunrays are being reflected causing more temperature to be absorbed by Earth. One of the main reasons of global warming is burning the fossil fuels for producing electrical energy. One of the household items that consumes a lot of electricity is the air conditioner. In the U.S. alone, it is estimated that every air-conditioned house produces two tons of carbon dioxide every year. It is believed that if better insulation systems are used in our houses, especially in the GCC area, the use of air conditioners can be optimized to consume less electricity. The main aim of this project is to come up with an environmentally friendly building insulation system that reduces the electrical consumption used in air conditioners in our houses. PTF was prepared and used as a natural free resource that is available locally in the GCC. Several mixes with different PTF ratios have been prepared and tested for thermal insulation and structural integrity. The results indicate a significant improvement in the R value of concrete. This additive also affected the compressive strength of concrete. It was found that replacing of fine aggregate with less than 1% of PTF will increase the R value of concrete without affecting the strength capacity significantly.

Keywords: PTF; NFRC; Envelop design; Concrete mix; Insulation; Energy efficient design

1 INTRODUCTION

In the past few years, the issue of global warming has become increasingly visible all over the world. Record high as well as record low temperatures are being broken worldwide. Snow is melting in the poles and less sunrays are being reflected causing

more temperature to be absorbed by Earth. One of the main reasons of global warming is burning the fossil fuels for producing electrical energy. One of the household items that consumes a lot of electricity is the air conditioner. In the U.S. alone, it is estimated that every air-conditioned house produces two tons of carbon dioxide every year. As it gets warmer, our home air conditioners work for more hours and consume more electricity, which further increases the global warming problem. An optimal building envelop design which employ the usage of insulating materials with high R value, is the most powerful tool for the designer and the constructor to achieve high energy efficiency in buildings (Papadopoulos et al., 2002). It is believed that if better insulation systems are used in our houses, especially in the Gulf Cooperation Council (GCC) area, the use of air conditioners can be optimized to consume less electricity. The traditional envelop design involves the usage of different insulation techniques and materials that has direct contribution to the global warming and harm the environment. This effect is present during the manufacturing of the insulation material (FPS Health, Food Chain Safety & Environment, 2016) and (U.S. Department of the Interior, 2019) or at the end of the insulation useful lifetime (Dovjak et al., 2017). Consequently, there exists a strong tendency towards preferring "natural" constructional products to the synthetic ones (Dovjak et al., 2017). In the case of thermal insulations. Life Cycle Assessment (LCA) shall be enabled to broaden the meaning of the term "environmentally friendly" (Silvestre et al., 2011). The main aim of this project is to come up with an environmentally friendly building insulation system that reduces the electrical consumption used in air conditioners in our houses. Thermal insulation in concrete building plays an important role in the environment sustainability especially for energy (Shahedan et al., 2017). The use of Natural Fiber Reinforced Concrete (NFRC) walls can result in considerable reduction on the demand on electrical energy for cooling purposes (Al-Jabri et al., 2005). Solar radiation is absorbed by conventional concrete, which stores the heat and releases it later, that can either be during the daytime or night-time (Jhatial et al., 2018). The addition of the fibers in concrete mix will reduces the thermal conductivity (Benmansour et al., 2014) and improve the mechanical properties of concrete such as the tensile and bending strength as well as the ductility cracks propagation resistance [10]. Thus, utilization of Palm Tree Fronds (PTF) as filler in concrete seems to be a very promising option which allows to be applied as thermal insulation materials in buildings (Benmansour et al., 2014). PTF was selected in to be investigated in this research because it is natural free resource that is available locally in the GCC countries.

2 MATERIALS and METHODS

The objective of this research is to enhance the thermal properties of the concrete in order to replace the locally widely available PTF eco-friendly material with the currently used eco-unfriendly insulation substances. Therefore, the focus in this research was mainly on the changes in the R-value of concrete with respect to the added amount of PTF to the concrete mix. However, the effect of this addition on the strength of concrete was also evaluated through structural tests. The results are used as a proof of concept. Nevertheless, a more comprehensive testing program that considers several elements in the mix and their effects on the quality of the concrete product shall be performed. Currently at the civil engineering lab in ACK, several grades of concrete with different

testing techniques are being developed and investigated. The aim of the program is to investigate the effect of adding PTF on the mechanical properties, workability and durability of concrete. In this paper the results of thermal conductivity and compressive strength of concrete cube samples are reported.

2.1 Collection and preparation:

The PTF was collected for free from a local date farm. After drying under sun, the leaves were grinded in a special mill. The grinding was performed in two cycles in order to obtain a powder-like consistency. The consistency of the powder from the first and second cycle is illustrated in Figure 1.

(a) (b)

Figure 1: PTF after grinding (a) first cycle (b) second cycle

2.2 Sieve analysis:

The effect of the size of the PTF powder particles was examined. The powder from the mill came in sizes range between 0.07 and 7 mm. Therefore, two practices were followed in this study. In the first practice, a sieve analysis was conducted on the powder and only powder passed through certain sieve was used in the mix. Where in the other practice the raw powder was used directly without any filtration. Using the data from the sieve analysis, illustrated in Table 1 and Figure 2, it was determined that anything passing sieve *No*. 50 (particle size 0.355mm) would be used as PTF powder for the concrete mix. Overall, PTF fiber to PTF Powder had a yield of 17.8%. This meant, theoretically, that 2.67 kg of PTF Powder could be extracted from an original PTF powder amount of 15kg. Figure 3, illustrates the amount and consistency of PTF powder from sieving 1.7 kg of PTF ground fiber. This method resulted in very small amount of PTF but has slightly improved the results of the strength tests.

Table 1: Sieve analysis results for the ground PTF

Sieve Number	Openings (mm)	Mass of Empty Sieve (g)	Mass of Sieve & PTF (g)	Mass of PTF (g)	Cumulative Mass of PTF (g)	Percent (%)
6	6.300	758.6	798.3	39.7	39.7	72.35
4	4.750	749.1	749.1	0.0	39.7	72.35
8	2.360	443.3	443.8	0.5	40.2	72.01
16	1.180	633.1	637.3	4.2	44.4	69.08
30	0.600	600.4	617.8	17.4	61.8	56.96
40	0.425	334.1	352.9	18.8	80.6	43.87
50	0.355	534.8	552.7	17.9	98.5	31.41
100	0.150	507.0	531.0	24.0	122.5	14.69
200	0.075	488.2	499.0	10.8	133.3	7.17
Pan	-	471.0	481.3	10.3	143.6	0.00

2.3 Water absorption test

Three samples of the powdered PTF were tested for the water absorption as per the ASTM C128-15 standard(C09 Committee, 2015). The samples were dried in the oven for 24 hours prior to the test. The weight of the dried powder was measured using an electronic. The substance was then soaked in water for an hour to reach its saturation level. The saturated PTF mass was then weighed. The difference between the two masses was calculated. The test was carried out for sieved and raw PTF. Lab results indicate high water absorption ratio between 95% -107%. Similar findings were reported in other studies (Saba et al., 2016) & (Ferrández-García et al., 2018). The high-water absorption and low mechanical properties of these natural fibers limit some of their applications (Saba et al., 2016). The large WA will reduce the amount of water in the mix affects both workability and ultimate strength of concrete. In order to maintain the W/C ratio in the concrete mix, the amount of water absorbed by the PTF was calculated and considered during the preparation of the concrete samples. The calculated amount of PTF powder for each set of samples was socked for 24 hours in the equivalent to weight absorbed of water prior to the mixing to avoid adding excessive water to the mix.

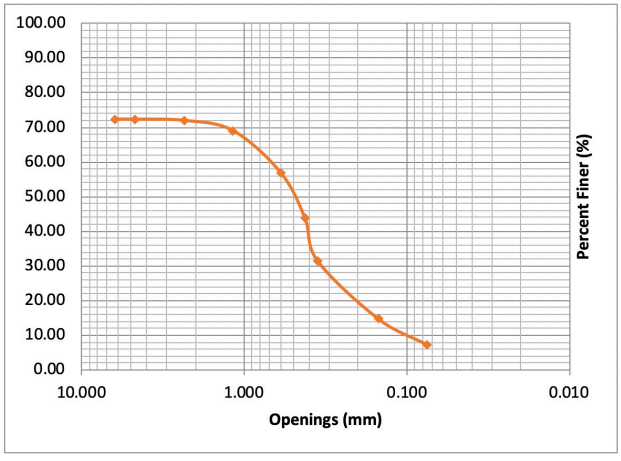

Figure 2: Sieve analysis results for the ground PTF

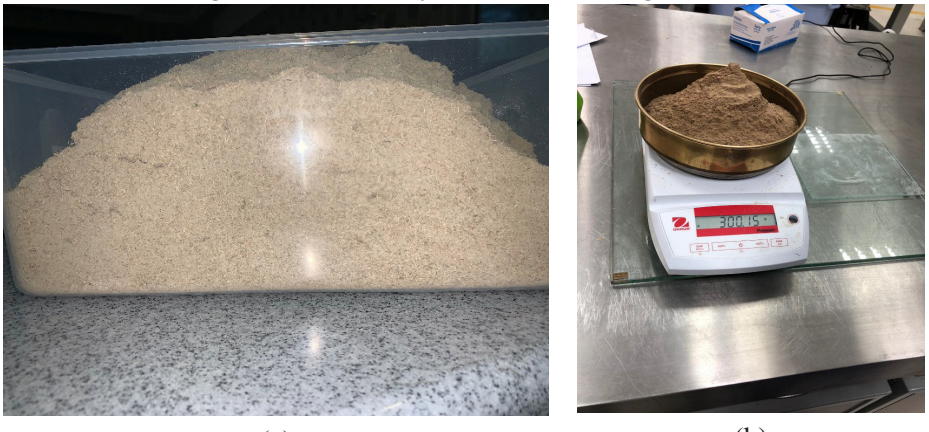

(a) (b)

Figure 3: (a) PTF powder, (b) 300 gr of PTF powder extracted from 1.7 kg of PTF fiber

2.4 Mixing, casting and curing

The dry ingredients were mixed first then water was added slowly with the socked wet PTF. After mixing, concrete workability was checked with the mean of slump test as presented in Figure 4. Concrete was casted into 100×100×100 mm cube as well as 20×40 cylindrical and 100×100×600 beam samples. The number of samples for each test is shown in Table 2. Special 3D printed plastic molds were prepared for the thermal conductivity test as presented in Figure 4 (a). The samples were cured in water under room temperature for 28 days prior to testing.

(a)

(b)

(c)

(d)

Figure 4: (a) 3D printed plastic concrete moulds for thermal conductivity (b) casted cylindrical samples (c) casted cube samples (d) casted beam sample

Table 2: Testing Matrix

PTF %	Cube samples 100 ×100 × 100 (mm) Test: Compressive @ 28	Cylindrical samples 20×40 (mm) Test: Thermal Conductivity	Beam samples 100×100×600 (mm) Test: Flexural Strength
0	3	4	1
1	3	4	1
1.25	3	4	1
2	3	4	1
2.5	3	4	1
3	3	4	1
4	3	4	1
5	3	4	1

(a) (b) (c)

Figure 5: Workability check of concrete with the slump test
(a) concrete sampling (b) placing the concrete in the cone mold (c) measuring slump

2.5 Tests and procedures

Cube samples were tested under compression to check the compressive strength of concrete at age of 28 days. The test was performed at the Civil and Mechanical labs in ACK. The beam samples were tested under pure bending conditions to check the effect of variant percentage of PTF additive on the flexural capacity of concrete. All beam samples have an identical reinforcement as shown in Figure 8.

The cylindrical samples were tested using the G.U.N.T Hamburg WL 420 Heat Conduction testing machine presented in Figure 6. Figure 7 depicts the beam sample dimensions and reinforcement. Samples during and after tests are depicted in Figures 8 and 9.

Figure 6: Preparing Concrete Cylinder with Silicone for Conductivity Test (left) and Thermal Conductivity Test on Concrete Cylinder (right)

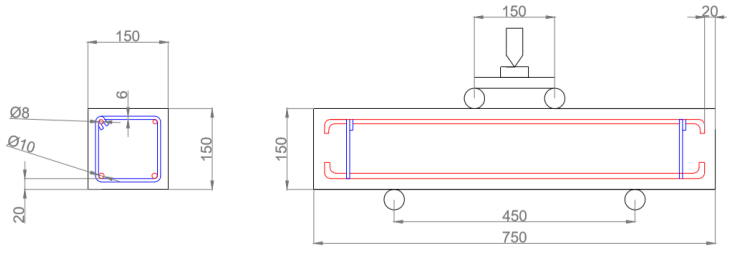

Figure 7: Sketch of concrete beam samples showing section reinforcement, supports span and loading points

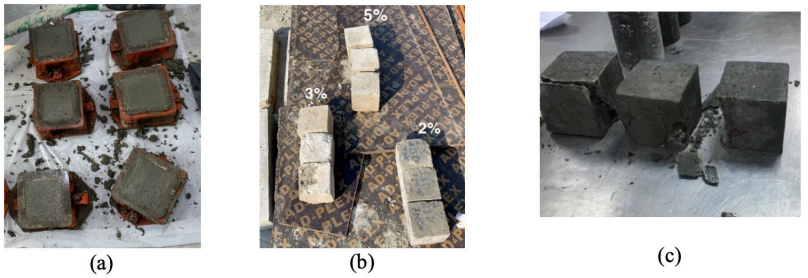

(a) (b) (c)

Figure 8: Concrete cube samples (a) after casting (b) after curing (c) after compressive test

Figure 9: Concrete beam samples during and after test

3 RESULTS AND DISCUSSION

The addition of the natural PTF has noticeably improved its thermal resistance capacity as expected. On the other hand, the compressive strength of concrete cubes and the flexural capacity of the beam samples has shown an inversely proportional reduction with the add percentage of PTF. The results of the thermal conductivity of the concrete has linearly decreased with the increased amount of PTF. This means that thermal resistance of concrete, represented in R-value, is increasing when we add more PTF. However, this thermal resistance enhancement will be on the cost of the structural integrity of the concrete. A summary of averaged results for mechanical and thermal tests is presented in Table 3. The results of the compressive strength are shown in Figure 10 and the results of the measured thermal conductivity with respect to the percentage of PTF in the concrete mix is shown in Figure 11 (a). Figure 11 (b) depicts the increase in the calculated thermal resistance of concrete as a variable of PTF replacement percentage. The thermal conductivity of concrete is normally below 1.9 W/k.m and depends mainly on the density and the water content in concrete (Carman & Nelson, 1921), (Asadi et al., 2018). The high initial conductivity obtained in this research indicates high percentage

of minerals and high water content in the concrete after hardening even for the plain concrete specimens. For the concrete with added PTF, although the thermal resistance was enhanced, the conductivity with low percentage of PTF indicates high water content in the concrete even after 28 days of curing. This water content will potentially decrease with time but other alternatives can be followed to avoid this problem. The other noticed result here is the severe degradation in the compressive strength and flexural strength of concrete specimens after 1% of sand replacement. This is correspondingly can be correlated to the high water content in the concrete which was absorbed by the PTF prior to the mix. The solution for this might be through the chemical treatment of PTF prior to the mix. Machaka and others have reported that treating PTF with NAOH solution prior to the mix will enhance its tensile properties and reduce the water absorption significantly (Machaka et al., 2014). This aspect is being considered in the second phase of this project in ACK.

Table 3: Testing results for several percentages of added PTF powder

PTF%	Averaged Stress MPa	Flexural Strength [kN]	Averaged Thermal Conductivity (W/k.m)	R- Value [m^2.K/W]
0	2923.00	96.52	3.90	0.010
1	20.43	64.61	3.62	0.011
1.25	15.58	49.89	3.50	0.011
2	5.70	5.70	1.60	0.042
2.5	4.25	3.12	0.60	0.067
3	3.10	2.20	0.50	0.080
4	1.42	2.48	0.40	0.100
5	0.20	3.10	0.30	0.120

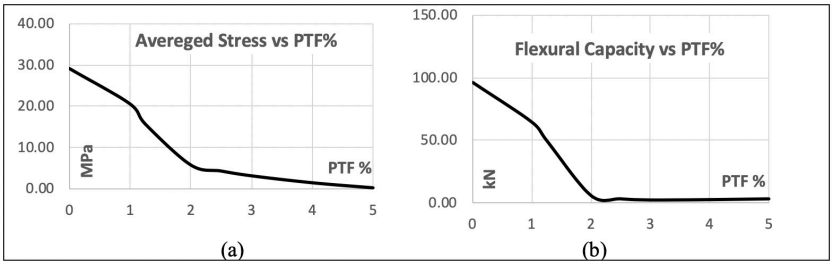

Figure 10: Concrete strength capacity with respect to the percentage of added PTF (a) compressive strength (b) flexural strength

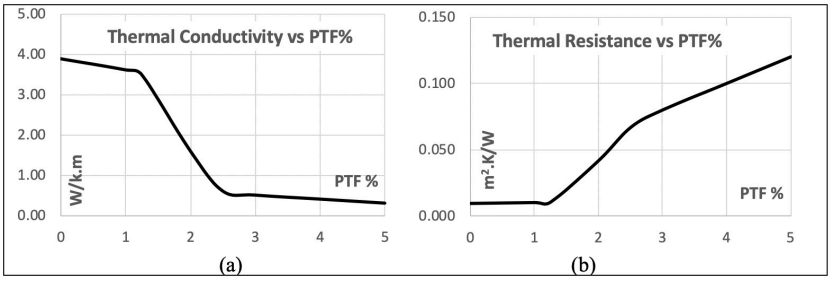

Figure 11: (a) Concrete thermal conductivity with respect to the percentage of added PTF (b) Corresponding concrete thermal resistance with respect to the percentage of added PTF

4 CONCLUSION

In conclusion, PTF powder additive can potentially enhance the thermal and mechanical properties of concrete better than PTF fibers. However, it has high water absorption properties. The high water absorption influences negatively both the mechanical and thermal resistance of concrete. Care shall be taken in order to chemically treat the PTF prior to mixing with concrete. The chemical treatment with NaOH can potential improve the tension capacity of PTF and reduces its water absorption. Thermal conductivity has increased significantly due to the replacement of fine aggregate with PTF however this came on the cost of concrete strength. In this study several PTF replacement percentages was tested. A maximum ratio of 1% was found to be practical. This percentage can be hypothetically increased by treating the PTF to eliminate its water absorption. It is expected that this ratio can be increased sufficiently if the water absorption problem has been controlled by means of chemical pre-treatment of the fibers.

REFERENCES

Al-Jabri, K. S., Hago, A. W., Al-Nuaimi, A. S., Al-Saidy, A. H. (2005). Concrete blocks for thermal insulation in hot climate. *Cement and Concrete Research 35*, 1472-1479. https://doi.org/10.1016/j.cemconres.2004.08.018.

Asadi, I., Shafigh, P., Abu Hassan, Z. F. B., Mahyuddin, N. B. (2018). Thermal conductivity of concrete – A review. *Journal of Building Engineering*, 20, 81-93. https://doi.org/10.1016/j.jobe.2018.07.002.

Benmansour, N., Agoudjil, B., Gherabli, A., Kareche, A. & Boudenne, A. (2014). Thermal and mechanical performance of natural mortar reinforced with date palm fibers for use as insulating materials in building. *Energy and Buildings*, 81, 98-104. https://doi.org/10.1016/j.enbuild.2014.05.032

C09 Committee (2015). Test Method for Relative Density (Specific Gravity) and Absorption of Fine Aggregate. ASTM International. https://doi.org/10.1520/C0128-15.

Carman, A. P. & Nelson, R. A. (1921). Thermal conductivity and diffusivity of concrete / (Bulletin No. 122), University of Illinois Bulletin. University of Illinois, Urbana-Champaign Library.

Dovjak, M., Košir, M., Pajek, L., Iglič, N., Božiček, D. & Kunič, R. (2017). Environmental Impact of Thermal Insulations: How Do Natural Insulation Products Differ from Synthetic Ones? *IOP Conf. Ser.: Earth Environ. Sci*. 92, 012009. https://doi.org/10.1088/1755-1315/92/1/012009.

Ferrández-García, C. E., Ferrández-García, A., Ferrández-Villena, M., Hidalgo-Cordero, J., García-Ortuño, T. & Ferrández-García, M. T. (2018). Physical and mechanical properties of particleboard made from palm tree prunings. *Forests* 9, 755. https://doi.org/10.3390/f9120755.

FPS Health, Food Chain Safety and Environment (2016). The Environmental Impact of Thermal Insulation Materials [WWW Document]. FPS Public Health. URL https://www.health.belgium.be/en/environmental-impact-thermal-insulation-materials (accessed 11.17.19).

Jhatial, A. A., Goh, W. I., Mohamad, N., Alengaram, U. J. & Mo, K. H. (2018). Effect of Polypropylene Fibers on the Thermal Conductivity of Lightweight Foamed Concrete, *MATEC Web of Conferences,* 150, 03008. https://doi.org/10.1051/matecconf/201815003008.

Machaka, M. M., Basha, H. S. & ElKordi, A. M. (2014). The effect of using fan palm natural fibers on the mechanical, *Properties and Durability of Concrete*. IJMSE. https://doi.org/10.12720/ijmse.2.2.76-80.

Papadopoulos, A. M., Karamanos, A., Avgelis, A. (2002). Environmental Impact of Insulating Materials at The End of Their Useful Lifetime 9.

Saba, N., Paridah, M. T., Abdan, K. & Ibrahim, N. A. (2016). Physical, structural and thermomechanical properties of oil palm nano filler/kenaf/epoxy hybrid nanocomposites. *Materials Chemistry and Physics*, 184, 64-71. https://doi.org/10.1016/j.matchemphys.2016.09.026.

Shahedan, N. F., Abdullah, M. M. A. B., Mahmed, N., Kusbiantoro, A., Binhussain, M. & Zailan, S. N. (2017). Review on thermal insulation performance in various type of concrete. Presented at the advanced materials engineering and Technology V: *International Conference on Advanced Material Engineering and Technology 2016*. Kaohsiung City, Taiwan, p. 020046. https://doi.org/10.1063/1.4981868.

Silvestre, J. D., De Brito, J. & Duarte Pinheiro, M. (2011). Life-Cycle Assessment of Thermal Insulation Materials for External Walls of Buildings. https://doi.org/10.13140/RG.2.1.1756.7768.

U.S. Department of the Interior (2019). *Environmental Considerations of Building Insulation National Park Service* – Pacific West Region.

Cite this article as: Yassin M. H., Lakys R., Ahmed T., Al-Refaei S., Omar B. A.-S., Altaher R. S., "Optimizing the Thermal Resistance of Concrete Using The Palm Tree Fronds Fibers", *International Conference on Civil Infrastructure and Construction (CIC 2020)*, DOI: https://doi.org/10.29117/cic.2020.0057

Application of Vehicle Restraint Systems (VRSs) in the State of Qatar: A Case Study from Northern Roads

Deepti Muley
deepti@qu.edu.qa
Qatar Transportation and Traffic Safety Center, Qatar University, Doha, Qatar

Shahram Tahmasseby
stahmasseby@qu.edu.qa
Qatar Transportation and Traffic Safety Center, Qatar University, Doha, Qatar

Bernd Wolfgang Wink
bw.wink@volkmann-rossbach.de
VOLKMANN & ROSSBACH, Montabaur, Germany

Faris Tarlochan
faris.tarlochan@qu.edu.qa
Qatar Transportation and Traffic Safety Center, Qatar University, Doha, Qatar

ABSTRACT

Recent developments within Infrastructural Road Safety and especially in the Sector of Vehicle Restraint Systems (VRS) have enabled Transport Authorities to significantly reduce road fatalities and severe injuries. Predominantly, two authorities have established leading guidelines for VRS installation and maintenance, - the European Union (EU) and the United States. The guidelines for the State of Qatar are based on these two sources. This technical paper briefly reviews the aforementioned guidelines, highlights the additional items in the EU guidelines, and explains the evolution of the State of Qatar guidelines accordingly. Moreover, this paper explains the application of VRS guidelines to the road network of the State of Qatar by presenting evidences from a recent site visit to the highways/expressways in the Northern Part of the Qatari Road Network. The outcomes of the site visit mainly highlight the typical steel VRS applied alongside the road (lateral as well as in central reserve, median), crash cushions, and various terminal systems. The paper is aiming to support designers, planners, auditors, contractors and installers to improve road safety from the VRS point of view.

Keywords: Road safety; Vehicle restraint systems (VRS); EN 1317; MASH; NCHRP 350

1 INTRODUCTION

Traffic accidents and consequent injuries and fatalities are a big and main concern of transport authorities all over the world. To reduce the number of serious injuries and fatalities due to traffic accidents, National Road Safety Strategy (NRSS) of State of Qatar has proposed increased installation of road safety barriers according to the state of the art, and designing of forgiving roads (NRSS, 2013). Furthermore, NRSS drew special attention to the treatment of medians, unprotected obstacles along the roadside, accesses and parking at intersections, and pedestrians exposed to high-speed traffic. The Public Works Authority (PWA), ASHGHAL, consequently decided to implement more advanced Vehicle Restraint Systems (VRSs) on newly designed roads in State of Qatar

(Gulf times, 2016). Generally, VRSs are installed to (1) reduce the impact of collision through deformation to absorb the kinetic energy of the vehicle in a controlled way (tolerable deceleration values of the body), and (2) avoid sudden stopping of the vehicle and redirecting it back to the carriageway (Nyamakope, 2017). This paper presents an overview of guidelines for selection/installation of VRSs for the State of Qatar and explains the application of VRSs on Qatari roads using a case study.

2 GUIDELINES FOR INSTALLATION OF VRS

2.1 Qatar standards

ASHGHAL, the Public Works Authority in the State of Qatar has provided guidelines for the selection and implementation of VRSs for roads in the State of Qatar (PWA, 2015). Generally, authority approves three types of longitudinal barriers, i.e. rigid, semi-rigid, and flexible. The components of VRS include typical VRS for longitudinal protection as well as end terminals, crash cushions, transitions, and gates. It is mandatory to have barriers in accordance with EN1317 (European guidelines), NCHRP 350 and / or MASH (American guidelines) and then get approval from ASHGHAL. Primarily, the VRS should be crash tested in accordance with EN1317. Meanwhile, the VRSs passing the test as per MASH or NCHRP 350 will also be considered. Additionally, the in-service performance as well as availability of spare parts are also evaluated before approving a VRS. The safety performance of the VRS is firstly a result of structural adequacy (containment level), occupant risk (impact severity) and deformation of the system (working width), (see EN 1317 and MASH for details).

2.2 European Union (EU) guidelines

The European mandatory Standard EN1317 captures different components such as typical longitudinal safety barriers, terminals, transitions, removable barrier sections, and crash cushions along with pedestrian parapets (ECS, 2010). The test criteria specified in the standards are based on the “average or most frequent case”. Furthermore, the EU Standard is focused on the collision of a human body [please refer to Acceleration Severity Index (ASI) for details]. The installation guidelines also mention mandatory requirements for maintenance of VRSs, which are not available in the American standards. Overall, the EU guidelines focus on deformable VRSs rather than rigid VRSs.

2.3 American guidelines

The recent American guidelines (MASH) evolved from an older report, called NCHRP 350, which was developed by Transportation Research Board (TRB), recommended testing the roadside features for severe vehicle impact conditions (Ross et al., 1993). Subsequently, MASH guidelines were developed presuming “worst practical conditions”. The parameters such as test vehicle, impact speed and angle combination, test matrix, and point of impact were specified for most critical or worst conditions (MASH, 2009). Overall, the American guidelines are focusing on rigid VRSs rather than deformable VRSs.

2.4 Potentials for the improvement of the PWA guideline

The manuals recommended by ASHGHAL, PWA adopt the EU and American

standards directly without stating any modifications according to local conditions of roads in the country. For instance, the requirements for cross slope varies for various European Union countries but the Qatari guideline does not specify any limits in this regard. Moreover, in the State of Qatar around one-third of total road fatalities are pedestrian fatalities (NRSS, 2013), but no specific requirements for VRS for these cases are set.

Another issue is that the vehicle structure on the roads is different from other developed countries because in the State of Qatar significant number of vehicles are Sport Utility Vehicles (SUVs) or four wheel drive. This implies that the test vehicle should be adjusted according to the local conditions. A study shows supporting evidence by suggesting modifications in VRSs based on the weights of vehicles in the system (Hernández et al., 2018). This fact should become reason for taking more care of the overall height of the VRSs to be installed. This implies that the local / Qatari conditions should be considered carefully when selecting the design and especially the installation height of the VRS to be applied in median and longitudinally.

3 CASE STUDY

The Qatar University team members with the Senior Manager of Volkmann & Rossbach Gmbh & Co. conducted a site visit on 22nd October 2019 to a road network in the Northern Part of the State of Qatar. The route itinerary of the survey mainly constitute sections from Al Khor Coastal Road , Al Khor Link Road, , Al Huwailah Link and Al Shamal Road (Figure 1). Overall, 150 km of road network was surveyed. Table (1) summarises VRSs type (median and longitudinal sections) for the aforementioned corridors. For instance, on Al Khor Coastal Road, the median barrier is rigid (made by concrete). However, longitudinal sections' VRSs are predominantly made of steel.

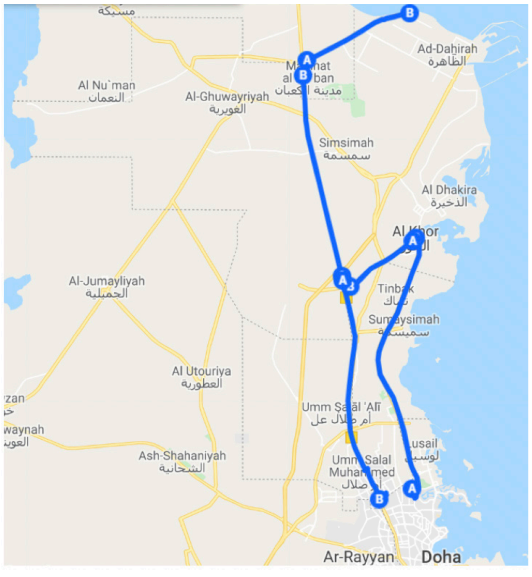

Figure 1: Route traversed for VRS site visit on Oct 22nd, 2019.

Table 1 Overview of VRSs installed on Northern roads in State of Qatar.

Name of road section	Length (km)	Type of VRS installed on	
		Medians	Longitudinal sections
Al Khor Coastal Road	36	Concrete barriers H2 Level	Concrete barriers as well as steel barriers H2/H1 level
Al Khor Link Road	12	Steel barriers H2 level	Steel barriers H1 level Mobile steel barriers H2 level, for temporary applications
Al Huwailah Link	24	Steel barriers H2 level	Steel barriers H1 level
Al Shamal Road	75	Steel barriers H1 level	Steel barriers H1/H2/H4 levels

Note: Various types of crash cushions were observed on the roads. The poles for the bridges are protected by rigid concrete barriers as well as by steel barriers. Gates opening of the VRSs are steel barriers.

Figure 2: Various treatments used along Northern Qatari Roads.

3.1 Survey Findings

- Most of the surveyed sections have advanced, state of the art VRS systems installed to significantly improve the road safety level on these sections of the Qatari Road network (Figure 2(a), (c), (d), (e), (f), (g), and (h)).
- The working width provided along the median of the surveyed roads is in most of the sections complying with the EU – (preferred) standards.
- At some sections, a combination of steel and concrete barriers is observed (Figure 2(e)).
- Some sections were installed with a mobile type of barriers, which were tested for H2 level crash worthiness. These barriers possess highest safety features in spite of being mobile and fixed at the beginning and end-section, only (Figure 2(f)).
- In sections with gantries, light – posts, weigh – stations and pipe / gas –lines below the road, steel VRSs with the highest performance level on global scale (H4b according to EN 1317) have been installed (Figure 2(a) and(g)).
- The bridges pillars are protected by rigid concrete barriers as well as steel barriers.

3.2 Observed Shortcomings

- It was observed on some of the road sections that dangerous hazards like gantries , light –posts etc. are too close to the VRS , mostly because of design – reasons like foundations already made and not changeable anymore, excavation issues, etc., resulting in insufficient space for the efficient working width of the VRS.
- The barriers damaged due to crashes have to be changed or repaired as quickly as possible to ensure that the functionality of VRS is maintained. An observation was made near Ras Laffan site that a heavy accident took place long time ago, but damaged VRS is still not repaired.
- Unprotected concrete blocks were observed at some sections, especially on bridges, which should be replaced with a safer system urgently. Forefront crash cushions installation can enhance the safety of concrete barriers over bridges (see figure 2 (j) for more details).
- Some sections, predominantly ramps were having no VRS or partial VRS installed, please see Figure 2(i) for details.

4 LESSONS LEARNED

The site visit to the roads in northern parts of State of Qatar suggested that the major part of these roads are equipped with very advanced VRSs of highest level on a global scale. The consideration of the following criteria would enhance the road safety level further in the State of Qatar:

- The European and American standards should be applied in consideration of the special, local and fleet related requirements in the State of Qatar.
- The frequency of the maintenance of VRSs should be specified and authorities need to adhere to it consequently.
- The repair or replacement of the damaged VRS units should be undertaken as soon as possible.
- It is recommended that the design and planning of the installation of VRSs should be undertaken at the design stage of the road and not at the audit stage.

5 CONCLUSION

Authorities in the State of Qatar set guidelines for the installation of VRSs predominantly based on the European Union (EN1317) and American (MASH) standards widely practiced in the world. Consequently, the newly developed roads benefit from advanced / latest VRSs, which are designed and installed to enhance road safety and protect the drivers and vehicles from suffering severe damage. Nevertheless, at some sections missing or hazardous segments are observed. These should be corrected to avoid any chance of crucial vehicle crashes. Furthermore, frequent maintenance of these sections should be scheduled and adhered to. It is also recommended that a specific VRS guideline is drafted, based on the country road traffic conditions, posted versus observed speed as well as the vehicle composition in which a significant portion is SUV vehicles.

REFERENCES

ECS (2010). *Road restraint systems part 1 to 3*. European Committee for Standardization, EU.

Gulf Times (2016). https://www.gulf-times.com/story/517778/Safety-barriers-bring-in-drastic-reduction-in-traffic-death-rates, accessed on 26 November 2019.

Hernández, Z. A., Álvarez, F., Alonso, M. & Sañudo, L. (2018). Analysis of the test criteria for vehicle containment systems in the standard EN 1317 regarding the number of vehicles in use. *Transportation Research Procedia*, 33, 315-322.

MASH (2009). *Manual for assessing safety hardware*, American Association of State Highway and Transportation Officials), United States of America. ISBN 978-1-56051-416-9.

NRSS (2013). *National road safety strategy 2013 – 2022*. National Traffic Safety Committee, State of Qatar.

Nyamakope (2017). Vehicle restraint systems and their function: restraining and containing traffic, accessed at http://www.engineersjournal.ie/2017/06/20/vehicle-restraint-systems-function/ on 26 November 2019.

PWA (2015). *Road safety barrier systems – Accepted for use on roads managed by the Ashghal Public Works Authority (PWA)*, Ashghal, State of Qatar.

Ross, H. E., Sicking, D. L. & Zimmer, R. A. (1993) *Report 350 Recommended procedures for the safety performance evaluation of highway features,* Transportation Research Board, National Academy Press, Washington, D.C.

Cite this article as: Muley D., Tahmasseby S., Wink B. W., Tarlochan F., "Application of Vehicle Restraint Systems (VRSs) in the State of Qatar: A Case Study from Northern Roads", *International Conference on Civil Infrastructure and Construction (CIC 2020)*, Doha, Qatar, 2-5 February 2020, DOI: https://doi.org/10.29117/cic.2020.0058

Modeling Airport Ground Access Mode Choice by Trip Purpose: Business vs. Personal Trips

Gurkan Gunay
ggunay@dogus.edu.tr
Dogus University, Istanbul, Turkey

Ilgin Gokasar
ilgin.gokasar@boun.edu.tr
Bogazici University, Istanbul, Turkey

ABSTRACT

Air transportation traffic is increasing, and this results in newer and larger airport investments in outskirts of the cities. Thus, airport ground access is becoming an important topic to focus on. Indeed, there are many studies in this field covering the mode choices of passengers to and from the airports. In this case study, the mode choices of travelers who are residents of Istanbul for access to Sabiha Gokcen International Airport (SAW) are modeled. To collect data, a revealed-preference survey with passengers is conducted at SAW. A literature review indicated that as well as other factors, trip purpose as business or personal affected the airport ground access mode choice. In accordance with this finding, separate mode choice models for both business and non-business passengers, as well as a pooled model for all travelers are built. Multinomial Logit (MNL) is used to model the mode choices. The modes were automobile, taxi and public transit. The results indicated that trip cost to SAW, traveling group size, time difference between the departure time and flight time, and automobile ownership status of the passenger were the explanatory variables for mode choice model. A market segmentation analysis results further showed that building separate models for business and non-business passengers was an improvement over the pooled mode choice model.

Keywords: Airport access; Mode choice; Multinomial logit; Market segmentation; Business vs. Non-business trip

1 INTRODUCTION AND BACKGROUND

Increase in population of the cities causes problems in transportation, since number of trips will increase and result in congestion. Istanbul suffers from traffic problems a lot (TOMTOM 2017); and this suffering affects the trips between the city and its airports. There are many studies focused on the airport access, and this work is a case study related to airport access mode choice.

Istanbul has three airports: Ataturk International Airport (ISL), Istanbul Airport (IST), and Sabiha Gokcen International Airport (SAW). SAW is in the Asian side of the city and 44 km from Taksim, the city center. This makes SAW geographically far from the city center. However, SAW is located next to the major E-80 (TEM) highway, which connects Istanbul to the eastern parts of Turkey. Hence, access to SAW can be considered as easy. SAW was opened in 1999. In 2009, a new terminal with a capacity of 25,000,000 passengers replaced the old terminal. In 2016, 30,000,000 passengers used this airport,

exceeding the capacity. Unlike IST, SAW serves mostly as an origin-destination airport. Locations of IST, ISL and SAW are shown in Figure 1.

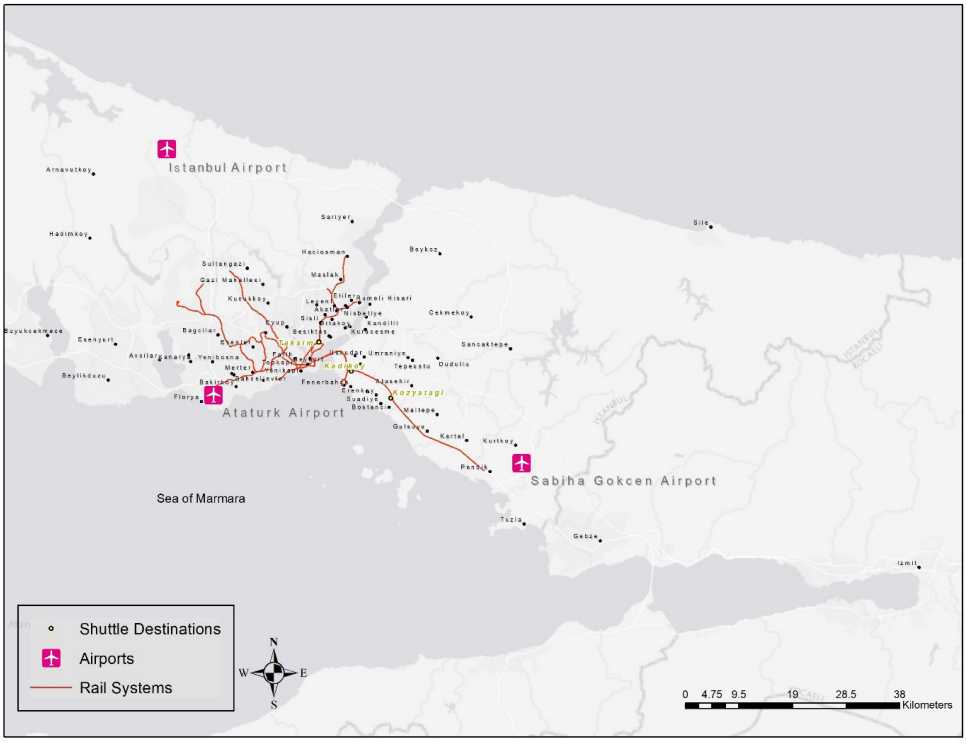

Figure 1: Map Showing IST, ISL and SAW

As it has also been mentioned before, there has been many studies on this field. Different modeling techniques such as Multinomial Logit, Nested Logit and Mixed Logit were applied to model the airport access mode choice behavior of passengers. In those studies, several explanatory variables were determined for airport access mode choice. These variables are namely travel time to the airport, travel cost to the airport, time difference between the departure time and flight time, travel purpose, domestic or international travel, amount of luggage, car ownership status, age of the passenger, gender and income level (Harvey, 1986; Monteiro & Hansen, 1996; Psaraki & Abacoumkin, 2002; Hess & Polak, 2006; Gupta et al., 2008; Tam et al., 2008; Alhussein, 2011; Jou et al., 2011; Akar, 2013; Choo et al., 2013; Zaidan & Abulibdeh, 2018). Travel purpose as business or non-business is particularly important for choosing private vehicle over public transit. It was found that passengers making business trips choose private vehicles to access the airports (Choo et al., 2013; Zaidan & Abulibdeh, 2018). Similarly, increasing number of carried luggage causes shift from public transit to private vehicle modes (Tam et al., 2008; Akar, 2013; Zaidan & Abulibdeh, 2018). However, this effect of luggage was not observed in some other studies; the high number of luggage did not deter passengers from using public transit in those cases (Gokasar & Gunay, 2017). Another factor for airport access mode choice is being close to a transit station. Rail transit is preferred if

the passenger's origin point was located within 1/2 miles from the station (Gokasar & Gunay, 2017).

Several studies developed different models for business and non-business passengers before (Harvey, 1986; Tam et al., 2008; Choo et al., 2013). However, they did not show the importance of segmentation quantitatively. In this study, a market segmentation analysis was made using likelihood ratio test statistic to test the segmentation.

In this case study, it was aimed to show the following:

- A pooled model for airport access mode choice,
- Separate airport access mode choice models for business and personal trip purposes, and
- Superiority of segmented models over the pooled model using likelihood ratio test statistic.

2 DATA AND THEORY

2.1 Data

Data was collected by conducting a survey with passengers at departures hall of SAW during one weekday in January 2015. Two three-hour sessions were held for data collection. The sessions were held during peak hours, 10:00-13:00 and 17:00-20:00. Sampling method was convenience sampling. A total of 251 interviews were collected. In the interviews, information about passengers' type of travel destination as domestic or international, time difference between their departure time and flight time (TDDF), travel purpose as business or personal, traveling group size, number of luggage and trip cost, time and access mode to SAW were collected. In addition to these, demographics of passengers such as age, gender, income level, education level and automobile ownership status were also obtained. Descriptive statistics revealed that 100 (39.8%) of the passengers were business travelers, and the remaining 151 (60.2%) passengers were traveling for personal purposes. 143 (57%) passengers owned an automobile, and automobile ownership was used as a dummy variable in the models. As it will also be explained in Section 3, most of the other variables were revealed insignificant at 95% level of confidence.

2.2 Theory

In this study, to model the airport access mode choice, discrete choice theory was used. Specifically, from the discrete choice modeling family, multinomial logit (MNL) model was applied. Discrete choice models use the maximization of utility, *U,* of users as basis. Below is the mathematical expression for user *i* on the mode *j* in choice set C_i (Ben-Akiva & Lerman, 1985):

$$P_i(j) = \Pr(U_{ji} \geq U_{li}, \forall l \in C_i) \quad (1)$$

The utility function has two parts as deterministic, *V;* and random, ε :

$$U_{ji} = V_{ji} + \varepsilon_{ji} \quad (2)$$

The deterministic part of the utility function is linear; and can be expressed as:

$$V_{ji} = \hat{\mathbf{a}}_{\mathbf{i}} \mathbf{x}_{\mathbf{ji}} \quad (3)$$

, where $\hat{\mathbf{a}}_{\mathbf{i}}$ is the coefficient matrix and $\mathbf{x}_{\mathbf{ji}}$ is the vector of independent variables. Probability of individual *i*'s choosing mode *j* $P_i(j)$ is:

$$P_i(j) = \frac{\exp(V_{ji})}{\sum_{l \in C_i} \exp(V_{li})} \quad (4)$$

In this study, three different MNL models were developed. First one for all passengers, second one for only business passengers and the third one for the remaining passengers; that is, passengers making personal trips. The last two models were segmented models; and the improvement of segmentation over the pooled model was checked using the log-likelihood (LL) values of the three models. The likelihood ratio test statistic (LRTS) was computed, which had a chi-squared distribution. LRTS is used to test the null hypothesis stating that "segmentation did not improve the fit". If the null hypothesis is rejected, then segmentation would not improve the fit. The LRTS formula is given by:

$$LRTS = -2 * LL(\beta) + 2\sum_{G} LL(\beta^{G}) \quad (5)$$

, where $LL(\beta)$ is the log-likelihood of the pooled model and $LL(\beta^{G})$ is the log-likelihood of the model for segment *G*.

Several assumptions about the costs of trip modes were made for modeling purposes. These were explained as the following:

- Cost of automobile: In the models, automobile mode had two types. First, the passenger drove on his/her own. Second type is that the passenger was dropped off at the airport by someone else. Cost of first auto travel type only included the fuel cost. The average fuel cost per km in Istanbul was assumed to be as 0.34 TL (Gokasar & Gunay, 2017). Drop-off travel type involved no cost for the passenger. To incorporate these costs, weighted average was used. Descriptive statistics of the data indicated that 40 % of the auto travelers drove on their own, while the remaining 60% were dropped off. These percentages were used to calculate weighted average of driving and drop-off costs.
- Cost of public transit: Public transit modes were made of shuttle buses and public transit buses. In 2015, average shuttle bus cost was 13 TL between the city and SAW (Havabus, 2017). On the other hand, using public buses involved several connections to access SAW from different locations in Istanbul. At each connection, a fee was paid. The fare structure of public transit system of Istanbul in 2015 is given in Table 1. According to the descriptive statistics, 43% of the public transit users opted for public buses. Again, weighted averages were used. It was assumed that cost of average public bus and connections to other modes would be 6 TL. Weighted average of this cost with the shuttle cost yielded in 10.4 TL.

Table 1: Public Transit Rates in Istanbul in 2015 (IETT, 2015)

	Full	Elderly Passenger	Student
First Ride	2.3	1.65	1.15
1st Connection	1.65	0.95	0.5
2nd Connection	1.25	0.75	0.45
3rd Connection	0.85	0.5	0.4
4th Connection	0.85	0.5	0.4
5th Connection	0.85	0.5	0.4

- Cost of taxi: In Istanbul, the taxi tariff in Istanbul was as the following (Istanbul Metropolitan Municipality Directorate of Public Transportation Services, 2016):

$$R = 3.2 + 2(\text{Distance in km}) + 0.325(\text{Travel time in minutes}) \quad (6)$$

Eq. (6) was used to calculate the taxi cost for passengers, since each passenger's origin in Istanbul and their trip times to SAW were collected during survey. Distances between SAW and the origin points were calculated using Google Maps.

3 ANALYSIS AND RESULTS

Three MNL models were given in this section: Pooled model for all passengers, and two models for business and non-business passenger segments. Table 2 shows the pooled model below. McFadden R^2 was 0.148; and all variables were significant at 95% level of confidence, except automobile ownership and group size for the utility function of public transit. This could be expected though; automobile ownership status not necessarily affects the choice of public transit over taxi. Also, it can be observed that not driving an automobile decreased the choice of automobile over taxi, obviously. Further, travel cost decreased the likelihood of choice of auto or public transit over taxi. As the traveling group size increased, one would less likely choose taxi over automobile. Finally, TDDF was significant for the choice between public transit and taxi. Coefficient of this variable was positive; hence, a passenger is more likely to choose public transit over taxi if they leave for the airport early. It should also be noted that other variables in the data such as income level of the passenger, gender, or amount of luggage were insignificant; hence, they were omitted.

Table 2: Pooled Model

		Model	
Variables Specific to Alternatives		Coefficient	Significance
Travel Cost		-0.014	0.011
Auto	Constant	-0.503	0.485
	No Auto Ownership	-1.225	0.005
	Group Size	0.402	0.048
	TDDF	-0.003	0.560
Public Transit	Constant	-2.867	0.000
	No Auto Ownership	0.198	0.581
	Group Size	0.319	0.106
	TDDF	0.014	0.002
LL(c)		-254.899	
LL(B)		-217.060	
Chi-squared Test Statistic		75.678	
Significance		0.000	
McFadden R2		0.148	
Adjusted McFadden R2		0.133	
Number of Observations		251	

MNL model for business travelers was given in Table 3. This model had interesting results compared to the pooled model: Only the generic variable, travel cost, was significant at 95% level of confidence. It had a negative coefficient, which meant that its increase would result in a decrease in likelihood of choosing auto or public transit modes over taxi. Other variables, which were auto ownership and traveling group size, were insignificant. However, these variables were kept here for consistency between the pooled and segmented models, to compute the LRTS.

Table 3: Model for Business Travelers

		Model	
Variables Specific to Alternatives		Coefficient	Significance
Travel Cost		-0.020	0.026
Auto	Constant	-0.353	0.714
	No Auto Ownership	-0.705	0.322
	Group Size	0.383	0.265
	TDDF	-0.006	0.325
Public Transit	Constant	-2.574	0.012
	No Auto Ownership	0.849	0.172
	Group Size	-0.323	0.436
	TDDF	0.008	0.164
LL(c)		-106.654	
LL(B)		-91.312	
Chi-squared Test Statistic		30.684	
Significance		0.000	
McFadden R2		0.144	
Adjusted McFadden R2		0.104	
Number of Observations		100	

Table 4 shows the MNL model for passengers who make personal trips (non-business passengers). McFadden R^2 was 0.144, and interestingly, unlike the model for business

passengers, travel cost to the airport was insignificant at 95% level of confidence in this model. For the choice of automobile over taxi, not owning an automobile decreased its likelihood, while a large traveling group size increased its probability. On the other hand, a large group is more likely to choose public transit over taxi. About TDDF, similar to the case in pooled model, it can be said that a passenger will leave early if the mode choice is public transit rather than taxi.

Table 4: Model for Travelers Making Personal Trips

		Model	
Variables Specific to Alternatives		Coefficient	Significance
Travel Cost		-0.010	0.182
Auto	Constant	-1.103	0.351
	No Auto Ownership	-1.374	0.020
	Group Size	0.579	0.047
	TDDF	0.001	0.869
Public Transit	Constant	-3.581	0.000
	No Auto Ownership	-0.299	0.531
	Group Size	0.544	0.049
	TDDF	0.021	0.002
LL(c)		-141.714	
LL(B)		-117.626	
Chi-squared Test Statistic		48.175	
Significance		0.000	
McFadden R2		0.170	
Adjusted McFadden R2		0.145	
Number of Observations		151	

Finally, to check if the segmentation improved the fit over the pooled model; the LRTS was computed. Using Eq. (1), the LRTS was revealed 16.243. The tabular value of this statistic for 4 degrees of freedom and 5% level of significance was 9.49; hence, it was smaller than the calculated value. Thus, it was concluded that the null hypothesis "segmentation did not improve the fit" could be rejected at 95% level of confidence. Therefore, segmentation improved the fit over the pooled model.

4 CONCLUSION

In this case study, airport ground access mode choice for SAW Airport in Istanbul was investigated. Three MNL models were built for all passengers, business travelers and passengers making personal trips, respectively. A market segmentation analysis was carried out; and it was understood that building segmented airport access mode choice models proved a better fit than pooled model. Further, the need of segmentation was also visible due to the significant variable types in the segmented models. This is because only trip cost was significant for the MNL model for business passengers, and that variable was insignificant for passengers making personal trips. For the non-business passengers, traveling group size, TDDF, and auto ownership status variables were significant. Hence, this study's results are in conjunction with the work of (Harvey, 1986), (Tam et al., 2008) and (Choo et al., 2013), since they developed different models

for business and non-business passengers. However, this study is different from them in terms of explanatory variables. Those studies used variables related to number of luggage, age of the passenger, and travel time to the airport in addition to the travel cost. However, those variables were insignificant in this study. Further, in this work, market segmentation test was used to show the necessity of segmentation, something the other studies did not use.

Future research may focus on the stated preferences of passengers in case of a new mode's introduction for the trips between SAW and Istanbul. With the help of stated preferences, the interest in the new mode can be understood and strategies related to that mode can be developed accordingly.

REFERENCES

Akar, G. (2013). Ground access to airports, case study: Port Columbus International Airport. *Journal of Air Transport Management,* 30, 25-31.

Alhussein, S. N. (2011). Analysis of ground access modes choice King Khaled International Airport, Riyadh, Saudi Arabi. *Journal of Transport Geography*, 19, 6, 1361-67.

Ben-Akiva, M. & Lerman, S. (1985). *Discrete choice analysis: Theory and application to travel demand*. MIT Press, Cambridge, MA.

Choo, S., You, S. & Lee, H. (2013). Exploring characteristics of airport access mode choice: A case study of Korea. *Transportation Planning and Technology*, 36, 4, 335-51.

Gokasar, I. & Gunay, G. (2017). Mode choice behavior modeling of ground access to airports: A case study in Istanbul, Turkey. *Journal of Air Transport Management*, 59, 1-7.

Gupta, S., Vovsha, P. & Donnelly, R. (2008). Air passenger preferences for choice of airport and ground access mode in the New York City, Metropolitan Region. *Transportation Research Record: Journal of the Transportation Research Board,* 2042, 1, 3-11.

Harvey, G. (1986). Study of airport access mode choice. *Journal of Transportation Engineering,* 112, 5, 525-545.

Havabus (2017). *Havabus*. Retrieved July 23, 2017 (www.havabus.com).

Hess, S. & Polak, J. W. (2006). Airport, airline and access mode choice in the San Francisco Bay Area. *Papers in Regional Science*, 85, 4, 543-567.

IETT (2015). *IETT Public Transit Rates (in Turkish)*. Retrieved February 25, 2017 (http://www.iett.istanbul/tr/main/pages/toplu-tasima-ucret-tarifesi/42).

Istanbul Metropolitan Municipality Directorate of Public Transportation Services. (2016). *Taksi Taşımacılığı Taksimetre Ücret Tarifeleri (in Turkish)*. Retrieved from https://tuhim.ibb.gov.tr/media/2147/taksi-tas-%C4%B1mac%C4%B1l%C4%B1g-%C4%B1-taksimetre-u-cret-tarifeleri.pdf.

Jou, R. C., Hensher, D. A. & Tzu, L. H. (2011). Airport ground access mode choice behavior after the introduction of a new mode: A case study of Taoyuan International Airport in Taiwan. *Transportation Research Part E: Logistics and Transportation Review*, 47, 3, 371-381.

Monteiro, A. B. F. & Hansen, M. (1996). Improvements to airport ground access and behavior of multiple airport system: BART extension to San Francisco International Airport. *Transportation Research Record,* 1562, 38-47.

Psaraki, V. & Abacoumkin, C. (2002). Access mode choice for relocated airports: The New

Athens International Airport. *Journal of Air Transport Management*, 8, 2, 89-98.

Tam, M. L., Lam, W. H. K. & Lo, H. P. (2008). Modeling air passenger travel behavior on airport ground access mode choices. *Transportmetrica*, 4, 2, 135-53.

TOMTOM (2017). *TOMTOM Traffic Index - Full Ranking*. https://www.tomtom.com/en_gb/trafficindex/list?citySize=LARGE&continent=ALL&country=ALL.

Zaidan, E. & Abulibdeh, A. (2018). Modeling ground access mode choice behavior for Hamad International Airport in the 2022 FIFA World Cup City, Doha, Qatar. *Journal of Air Transport Management,* 73, 32-45.

Cite this article as: Gunay G., Gokasar I., "Modeling Airport Ground Access Mode Choice by Trip Purpose: Business vs. Personal Trips", *International Conference on Civil Infrastructure and Construction (CIC 2020)*, Doha, Qatar, 2-5 February 2020, DOI: https://doi.org/10.29117/cic.2020.0059

A Study on the Default Supplemental Adjustment Factors of Progression Adjustment Factor Formula under Non-Lane Based Traffic Condition

Abdullah Al Farabi
a.al.farabi.buet@gmail.com
Department of Civil Engineering, University of Asia Pacific, Dhaka, Bangladesh

Tamal Chakraborty
tamalchakraborty0108@gmail.com
Bangladesh University of Engineering and Technology, Dhaka, Bangladesh

ABSTRACT

A mathematical expression of supplemental adjustment factor (f_{PA}) has provided a way to estimate Progression Adjustment Factor (P.F.) more accurately as the P.F. relies on the f_{PA} value. The mathematical formula of f_{PA} requires traffic parameters that need to be determined from the field survey. As non-lane based traffic behavior is significantly different from lane-based traffic, this study examines the applicability of the default fPA values of Highway Capacity Manual-2000 under the non-lane based traffic condition. Default values for all six Arrival Types (AT1 to AT6) are reviewed against an available mathematical expression. After performing statistical analysis on the collected data, it is found that the HCM-provided default f_{PA} values for AT1, AT3, AT5 and AT6 are consistent with the mathematical expression. However, the supplemental factors for AT2 and AT4 are found to vary significantly from the default values. By considering the mathematical expression as a standard of comparison, a graphical representation of error corresponding to trial f_{PA} value shows that a value of 0.99 for f_{PA} provides the minimum error of P.F. for AT2. Thus, the default value (f_{PA} =0.93) is found to underestimate f_{PA} as well as P.F. by 6.5%. In a similar way, the f_{PA} value for AT4 is found to be 0.96 which is 16.5% less than the default value. So, the default value (f_{PA} =1.15) overestimates f_{PA} and P.F. by 16.5%. Therefore, f_{PA} = 0.99 for AT2 and f_{PA} = 0.96 for AT4 should be used to estimate P.F. in case of non-lane based traffic.

Keywords: Highway Capacity Manual; Progression Adjustment Factor; Default supplemental adjustment factor; Modified supplemental adjustment factor; Non-lane based traffic

1 INTRODUCTION

Highway Capacity Manual (TRB, 2000) provides a mathematical model of control delay which includes a factor termed as Progression Adjustment Factor (P.F.). In fact, from previous HCM (TRB, 1985) to the most updated version, this factor is recognized to incorporate the effects of signal progression on vehicle-delay estimation. This factor is also present in the Canadian Capacity Guide (ITE, 2008) which provided a model to estimate vehicle stops. Now, this P.F. factor includes a supplemental adjustment factor (f_{pA}) in its expression. By addressing the six different Arrival Types (AT), (Akcelik, 1996) provided two distinct lists of the supplemental factors for the uniform delay and the overflow delay component. Later, (TRB, 2000) provided default values of

supplemental adjustment factor (f_{pA}) for six types of arrival (AT1 to AT6) of vehicles. (Strong & Rouphail, 2005) analyzed and explained these f_{pA} factors and they highlighted an underlying assumption that is associated with the HCM provided P.F. formula. Most importantly, they were able to formularize f_{pA} mathematically by eliminating this assumption. Thus, this mathematical formula eliminates the need for using default f_{pA} values. Again, another approach was taken by (Wu, 2014) to modify the Progression Adjustment Factor (P.F.) considering the planning aspects. (Wu, 2014) provided valuable insights into P.F. formulation for default conditions. Nonetheless, default supplemental values of HCM are still useful in determining performance indicators (delays, stops) and it can also be used in planning scenarios. So, the authors of this study have decided to focus on the mathematical expression developed by (Strong & Rouphail, 2005). This expression provides mathematical ground to the f_{pA} factor and the formula is more suitable than default HCM-provided values. However, the f_{pA} formula requires two additional traffic parameters and these parameters need field determination. This aspect has motivated the authors to determine the f_{pA} factors by performing field surveys and assess whether the default values agree with the HCM-provided values. The significance lies in the fact that the traffic condition in non-lane based operation is much different than lane-based disciplined traffic. So, any discrepancy in default values will lead to errors in stops and delay estimation. Besides, previous studies on control delays by (Hadiuzzaman et al., 2014) and (Farabi et al., 2018) used default values of the f_{pA} factors to determine P.F. values. So, the significance is understandable as the default values might have led to errors in delay estimations. Therefore, considering the traffic conditions of the Dhaka city, the authors perform a study to justify whether the default values of HCM supplemental adjustment factor (f_{pA}) provides accurate P.F. for different arrival types, or the mathematical expression by (Strong & Rouphail, 2005) should be used. Also, an approach to modify the default values for non-lane based traffic conditions is taken if found necessary. Therefore, the rest of the paper explains the methods of the study and data collection. After that, a comparative analysis is provided in this study.

2 METHODS OF THE STUDY

Progression Adjustment Factor (P.F.) formula of Highway Capacity Manual (TRB, 2000) is shown in Equation (1).

$$P.F = \frac{(1 - P)f_{pA}}{1 - \frac{g}{C}} \quad (1)$$

Where,

P.F. = Progression Adjustment Factor

$P = R_P \frac{g}{C}$ = Proportion of vehicles in arrival in green

R_P = Platoon Ratio

$\frac{g}{C}$ = Ratio of effective green to Cycle time

f_{pA} = Default Supplemental Adjustment Factor

Equation (1) requires default Supplemental Adjustment Factor (f_{PA}), which can be found in the HCM as shown in Table 1.

Table 1: Default Supplemental Adjustment Factor (f_{PA}) provided by HCM

Arrival Type	AT1	AT2	AT3	AT4	AT5	AT6
Progression Quality	Very Poor	Non-Favorable	Isolated	Favorable	Highly Favorable	Exceptional
P_A	1/3	2/3	1	4/3	5/3	2
f_{pA}	1.00	0.93	1.00	1.15	1.00	1.00

Table 1 lists the default f_{PA} factors for six different arrival types. HCM determines and classifies the arrival types (AT1-AT6) using the Platoon Ratio formula (R_p) and this classification of arrival types can be found in HCM. It can be observed from Table 1 that the f_{PA} factors for AT1, AT3, AT5, AT6 are equal to unity. But, f_{PA} factors for AT2 and AT4 are different from unity. At the same time, Table 1 shows the description of Progression quality and the Platoon arrival ratio (P_A) for every arrival type. P_A is the ratio of the arrival flow rate in green period (v_G) to the arrival flow rate of the cycle (v). The default values of P_A for each arrival type are also provided by HCM.

On the contrary, (Strong & Rouphail, 2005) provided a detailed expression of P.F. by eliminating the underlying assumption of HCM provided P.F. formula. They proved that the P.F. of HCM makes an assumption that the uniform queue dissipation happens at the same time position in a cycle irrespective of signal coordination. By eliminating this assumption, they provided a new formula of P.F. as shown in Equation (2).

$$P.F = \frac{(1-P)}{\left(1-\frac{g}{C}\right)} * \frac{\left(1-\frac{v}{S}\right)}{\left(1-R_p * \frac{v}{S}\right)} * \left[1 + \frac{v}{S} * \frac{\left(1-R_p\right)}{\left(1-\frac{g}{C}\right)}\right] \quad (2)$$

Where,

P.F. = Progression Adjustment Factor (P.F.)

$P = R_P \frac{g}{C}$ = Proportion of vehicles in arrival in green (R_P = Platoon Ratio)

$\frac{g}{C}$ = Ratio of effective green to Cycle time

v = Arrival flow rate (vehicles per hour)

S = Saturation Flow Rate (vehicles per hour)

So, Equation (2) provides an equation of P.F. which includes f_{PA} as a multiplicative term instead of a default value. Therefore, f_{pA} factor is expressed mathematically as shown in Equation (3).

$$f_{pA} = \frac{\left(1-\frac{v}{S}\right)}{\left(1-R_p * \frac{v}{S}\right)} * \left[1 + \frac{v}{S} * \frac{\left(1-R_p\right)}{\left(1-\frac{g}{C}\right)}\right] \quad (3)$$

Equation (2) was derived analytically and it is superior to simplified HCM formula. It requires two additional traffic parameters (arrival flow rate and saturation flow rate) to determine P.F. Also, results given by Equation (2) are more precise than Equation (1). However, on the other hand, it is not sure how much accuracy the Equation (2) provides over Equation (1) in the case of non-lane based traffic.

It is obvious that non-lane based traffic is significantly different from lane-based

traffic. With different compositions of vehicles in traffic stream, saturation flow rates in non-lane based traffic vary greatly. In addition, queue formation and queue discharge are quite different in non-lane based traffic. As vehicles form clusters near the intersection, they tend to utilize gaps to go faster during discharge. So, traffic parameters vary greatly and it is always preferable to determine the traffic parameters by performing site surveys in case of non-lane based traffic. As Equation (2) depends on the saturation flow that needs to be determined from the field, this formula should reflect the field conditions much better if used in the study.

Therefore, Equation (2) is considered as the basis of the study and an analysis to review the existing default f_{PA} factors in comparison to Equation (2) was performed in this study. This comparison provides a justification for the applicability of HCM-provided default values. The above-mentioned procedure of the study is summarized in the general framework shown in Figure 1.

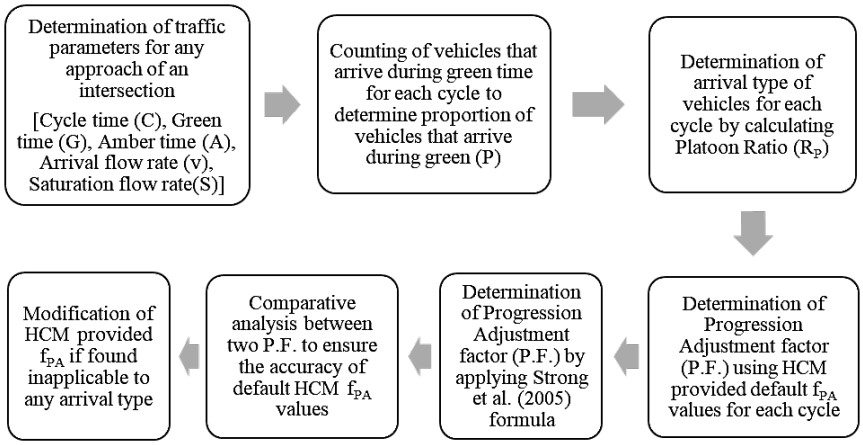

Figure 1: Procedures followed for the study

The procedure in Figure 1 requires various traffic parameters and those parameters were measured in the site. Cycle time, Green time, Amber time needs no special method as they were measured directly. Likewise, vehicle arrival flow and departure flow were performed by counting. Using the counting, arrival flow rate (v) was determined by following the method of (McShane et al., 1990), which is shown in Equation (4).

$$\text{Average Arrival flow rate, } v = \frac{\text{vehicles passed in green + queued vehicles at the end of green}}{\text{Cycle time}} \quad (4)$$

Another important parameter is the saturation flow (S). Saturation flow rate (S) and lost times were determined by Road Note 34 method (Webster, 1963). This method requires Passenger Car Equivalent (PCE) values to determine saturation flow rate. PCE values for this study were taken from (Hadiuzzaman et al., 2008). After determining the saturation flows (in units of PCU per hour) for each green period, it was converted into equivalent vehicles per hour using the procedure described in Canadian Capacity Guide (ITE, 2008) as presented in Equation (5).

$$S_{veh/hour} = \frac{S_{PCU/hour}}{\sum \frac{\%P_k * a_k}{100}} \quad (5)$$

Where,

$\%P_k$ = Percentage of vehicles in category k that arrive

a_k = PCE factor for vehicle type k

3 SITE SELECTION AND DATA COLLECTION

Data for the study were collected from an urban intersection of Dhaka city known as "Hotel Intercontinental" intersection. This intersection is a three-legged intersection. Data were collected from all three approaches (East, North, and South) of the intersection. Video recording method was applied to collect primary data. Data were collected on three different days between 09:30 a.m.-11.00 a.m., 02.00 p.m.-05.00 p.m. and 02.30 p.m.-05.30 p.m. A total of 6 hours of recordings were analyzed.

Now, an important fact to notice about the selected intersection is that the traffic movements of the intersection are controlled manually by Police. As the upstream intersections of the "Hotel Intercontinental" intersection are also maintained manually, there is no proper coordination among the intersections. This fact leads to generation of various arrival types in any approach of the intersection. So, it is quite common to observe different arrival types in this intersection.

4 COMPARATIVE ANALYSIS OF PROGRESSION ADJUSTMENT FACTORS

After video data collection and data transcription from video recordings, Progression Adjustment Factor (P.F.) for each observation was determined. These values are summarized in Table 2 to Table 7.

Table 2: Progression Adjustment Factor for Arrival Type-1 (AT1)

	Arrival Type-1 (AT1)							
Observation No.	**g/C**	**Rp**	**P_A**	**f_{PA} (Strong)**	**P.F. (Strong)**	**f_{PA} (HCM_Default)**	**P.F. using f_{PA} (HCM_Default)**	**Percentage of deviation**
1	0.15	0	0.00	1.43	1.16	1	1.17	0.94
2	0.21	0	0.00	1.59	1.27	1	1.27	-0.25
3	0.13	0.3	0.28	1.22	1.11	1	1.11	-0.04
4	0.24	0.34	0.46	1.47	1.21	1	1.21	0.12
5	0.16	0.47	0.29	1.26	1.1	1	1.11	0.77
6	0.13	0	0.42	1.28	1.15	1	1.15	-0.36
7	0.26	0.3	0.42	1.53	1.26	1	1.25	-0.7
8	0.18	0.43	0.28	1.3	1.12	1	1.13	0.57
9	0.15	0	0.36	1.48	1.15	1	1.17	2.01
10	0.23	0.39	0.36	1.36	1.19	1	1.18	-0.71

Table 3: Progression Adjustment Factor Arrival Type-2 (AT2)

	Arrival Type-2 (AT2)							
Observation No.	**g/C**	**Rp**	**P_A**	**f_{PA} (Strong)**	**P.F. (Strong)**	**f_{PA} (HCM_Default)**	**P.F. using f_{PA} (HCM_Default)**	**Percentage of deviation**
1	0.4	0.76	0.75	1.01	1.18	0.93	1.08	-8.08
2	0.52	0.66	0.65	1.05	1.44	0.93	1.28	-11.2
3	0.57	0.82	0.80	1.05	1.3	0.93	1.16	-11.11
4	0.44	0.56	0.55	1.03	1.38	0.93	1.25	-9.37
5	0.59	0.81	0.79	1.05	1.33	0.93	1.18	-11.05
6	0.32	0.77	0.75	1	1.12	0.93	1.03	-7.31
7	0.41	0.84	0.83	1	1.11	0.93	1.04	-6.76
8	0.49	0.65	0.63	0.91	1.22	0.93	1.25	2.36
9	0.32	0.78	0.75	0.89	0.98	0.93	1.03	4.69
10	0.19	0.6	0.65	0.94	1.04	0.93	1.02	-1.58
11	0.2	0.66	0.62	1.19	1.08	0.93	1.01	-6.74
12	0.23	0.55	0.60	1.23	1.14	0.93	1.06	-7.75
13	0.14	0.53	0.46	1.15	1.07	0.93	1	-7.06
14	0.13	0.7	0.57	1.1	1.04	0.93	0.97	-6.87
15	0.14	0.52	0.42	1.21	1.06	0.93	1	-5.82

Table 4: Progression Adjustment Factor Arrival Type-3 (AT3)

	Arrival Type-3 (AT3)							
Observation No.	**g/C**	**Rp**	**P_A**	**f_{PA} (Strong)**	**P.F. (Strong)**	**f_{PA} (HCM_Default)**	**P.F. using f_{PA} (HCM_Default)**	**Percentage of deviation**
1	0.43	1.01	1.00	1	0.99	1	0.99	0.11
2	0.41	0.91	0.90	0.94	1	1	1.06	6.2
3	0.45	1.08	1.07	1	0.93	1	0.93	-0.07
4	0.57	0.92	0.89	0.97	1.07	1	1.11	3.18
5	0.15	0.88	0.79	1.04	1.02	1	1.02	-0.07
6	0.29	1.09	1.00	0.93	0.96	1	0.96	0.15
7	0.54	0.92	0.75	1.13	1.11	1	1.09	-1.52
8	0.15	1.11	0.94	0.96	0.98	1	0.98	-0.23
9	0.33	1	0.93	1	1	1	1	0

Table 5: Progression Adjustment Factor Arrival Type-4 (AT4)

	Arrival Type-4 (AT4)							
Observation No.	**g/C**	**Rp**	**P_A**	**f_{PA} (Strong)**	**P.F. (Strong)**	**f_{PA} (HCM_Default)**	**P.F. using f_{PA} (HCM_Default)**	**Percentage of deviation**
1	0.37	1.25	1.21	0.98	0.84	1.15	0.98	16.97
2	0.22	1.4	1.23	0.78	0.88	1.15	1.02	14.96
3	0.53	1.37	1.26	0.42	0.52	1.15	0.66	27.61
4	0.42	1.34	1.29	0.62	0.73	1.15	0.87	19.12
5	0.33	1.28	1.13	0.8	0.85	1.15	0.99	16.68
6	0.16	1.23	1.11	0.9	0.96	1.15	1.1	14.73
7	0.72	1.38	1.27	0	0	1.15	0	0.00
8	0.52	1.29	1.18	0.55	0.64	1.15	0.79	22.93

Table 6: Progression Adjustment Factor Arrival Type-5 (AT5)

	Arrival Type-5 (AT5)							
Observation No.	**g/C**	**Rp**	**P_A**	**f_{PA} (Strong)**	**P.F. (Strong)**	**f_{PA} (HCM_Default)**	**P.F. using f_{PA} (HCM_Default)**	**Percentage of deviation**
1	0.08	1.77	1.60	1.02	0.95	1	0.93	-1.85
2	0.46	1.57	1.53	0.94	0.49	1	0.52	6.35
3	0.19	1.58	1.30	0.75	0.86	1	0.86	0.05
4	0.38	1.73	1.61	0.41	0.51	1	0.54	7.21
5	0.3	1.78	1.71	0.51	0.63	1	0.66	3.75
6	0.21	1.51	1.30	0.73	0.88	1	0.87	-1.01

Table 7: Progression Adjustment Factor Arrival Type-6 (AT6)

	Arrival Type-6 (AT6)							
Observation No.	**g/C**	**Rp**	**P_A**	**f_{PA} (Strong)**	**P.F. (Strong)**	**f_{PA} (HCM_Default)**	**P.F. using f_{PA} (HCM_Default)**	**Percentage of deviation**
1	0.26	2.56	3.47	0.26	0.43	1	0.45	5.37
2	0.27	2.25	2.00	0.4	0.52	1	0.55	4.75
3	0.11	4.67	1.80	0.15	0.73	1	0.56	-22.98
4	0.12	2.11	3.45	0.7	0.86	1	0.85	-0.6
5	0.18	2.19	1.87	0.54	0.75	1	0.75	-0.89
6	0.18	2.5	1.85	0.41	0.67	1	0.66	-1.46

Table 2 to Table 7 shows the Progression Adjustment factor (P.F.) for all six-arrival types. Also, Platoon Arrival Ratio (P_A) is shown for each observation. P.F. values were calculated using both the HCM-default f_{PA} and Equation (2). The percentage of deviation of P.F. (by HCM) from the mathematical Equation (2) is shown in the last column of each Table (Table 2 to Table 7).

By analyzing Table 2, It is evident that the HCM formula estimates P.F. much accurately for AT1. The percentage of deviation from Equation (2) lies between -0.71% to 2.01% for AT1. The average deviation is still less than 1%. Therefore, the default HCM value agrees with Equation (2). For AT3, AT5, and AT6, the average deviation of HCM formula is much less than 5%. At the same time, the deviations for these Arrival Types (AT3, AT5, and AT6) are not statistically significant. Therefore, the default HCM values for these arrival types agree with Equation (2).

For AT2, P.F. of HCM deviates from Equation (2) and the deviation ranges between -11.2% to 4.69% as shown in Table 3. The average deviation is -6.24% with a standard deviation of 4.67%. By performing a t-test, it is also found that this deviation is statistically significant. Therefore, HCM formula underestimates P.F. by 6%. On a different note, the average P_A value for the data of AT2 is 0.66 with a standard deviation of 0.12. The average P_A value is found to be equal with the listed value (P_A= 2/3) of Table 1.

Data for AT4 is shown in Table 5. Observation No. 7 in Table 5 provides a zero value of P.F. for both the cases. This is due to the fact that all of the vehicles arrived during the green time. Thus, the proportion of vehicles arriving in green was equal to unity. This unity led to a zero value of P.F. in HCM formula. On the other hand, f_{pA} value using Equation (2) is nearly zero. However, the P.F. still becomes zero as the P value was unity. Now, In the case of AT4, the average value of P_A for the data is 1.21 with a standard

deviation of 0.07. The average value of P_A is found to be lower than the listed value (P_A= 4/3) of Table 1.

The average deviation of P.F. is 16.5% with a standard deviation of 8.01% as shown in Table 5. This deviation is statistically significant enough. So, the HCM formula measures 16.5% higher value than Equation (2).

It is not quite sure about the exact reasons behind the significant differences from the default values of HCM for AT2 and AT4. However, f_{PA} values for AT2 and AT4 are found to provide inaccurate results. Thus, these two values will lead to significant errors in the P.F. calculation. So, a further investigation on the data of AT2 and AT4 is performed to find appropriate values. A trial process is considered and a graph is plotted as shown in Figure 2.

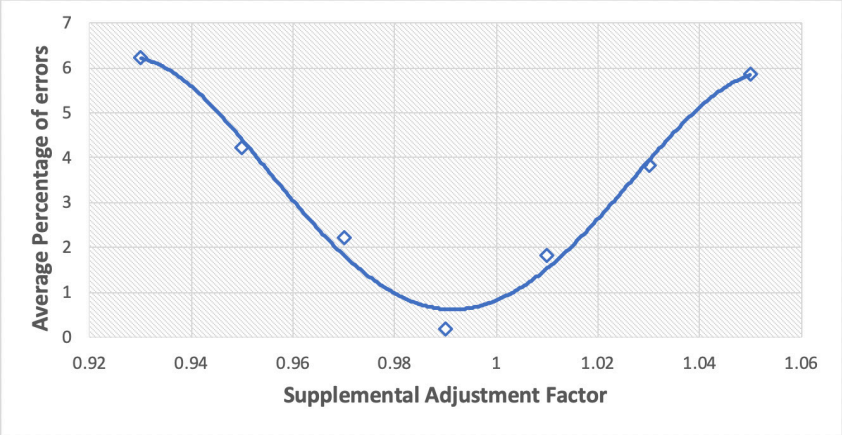

Figure 2: Modification of Supplemental Adjustment Factor Arrival Type 2 (AT 2)

Figure 2 depicts the average of the percentage of errors (deviation from Equation 2 is considered as error) corresponding to trial f_{PA} values for AT2. The process of formulating the graph is as follows: a trial value of f_{PA} is picked (a substitute of the HCM-provided f_{PA} value) and P.F. is calculated for every observation with this trial value (Using the observations of Table 3). Thus, trial P.F. values are found for every observation. These trial P.F. values are then compared with the corresponding actual P.F. of Equation (2). From these comparisons, the percentage of errors were calculated for each observation (similar to the last columns of Table 2-7). Using the percentages, the average of the percentage of errors is determined. For different trial f_{PA} values, this process is repeated. Lastly, a graph of error corresponding to trial f_{PA} value is plotted which is shown in Figure 2.

Figure 2 clearly shows that the percentage of error is minimum at the value of 0.99 (rounded to two decimals). The error increases in both directions from the value of 0.99. Therefore, the default value of f_{PA} should be considered as 0.99 for AT2 instead of 0.93. A similar plot is drawn for Arrival Type 4 using the observations of Table 5 and it is shown in Figure 3.

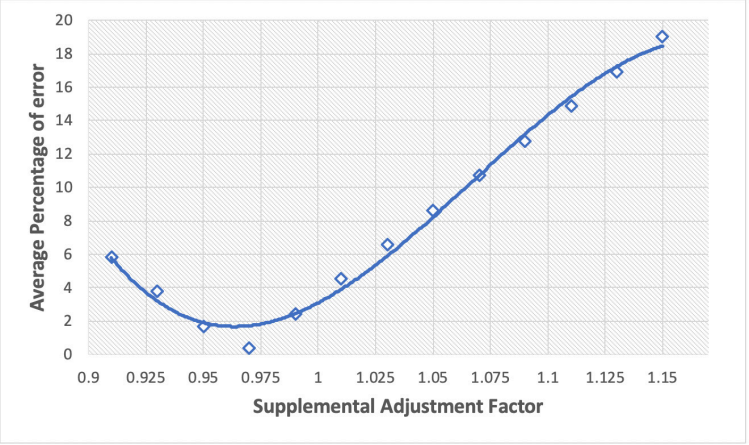

Figure 3: Modification of Supplemental Adjustment Factor Arrival Type 4(AT4)

It can be inferred from Figure 3 that the minimum percentage of error lies between 0.95 to 0.975. By performing mathematical operation on the regressed curve, it is found that the minimum value should be considered as 0.96 for AT4 instead of 1.15.

5 CONCLUSION AND RECOMMENDATIONS

The comparative analysis concludes that the supplemental adjustment factors for Arrival Type 1, Arrival Type 3, Arrival Type 5, Arrival Type 6 of HCM (TRB, 2000) are acceptable. In other words, supplemental adjustment factors for these arrival types (AT1, AT3, AT5, AT6) can be used instead of the complex formula of Equation (2). On the other hand, factors for Arrival Type 2 and Arrival Type 4 have been found to deviate from the exact mathematical expression. Therefore, the modified values may be used instead of HCM-provided values. Therefore, the findings of the study are summarized in Table 8 which shows the updated supplemental adjustment factors.

Table 8: Supplemental Adjustment Factor (f_{PA}) provided by this study

Arrival Type	AT1	AT2	AT3	AT4	AT5	AT6
f_{PA}	1.00	***0.99***	1.00	***0.96***	1.00	1.00

Table 8 provides the values of Supplemental Adjustment Factor (f_{PA}) that can be used in non-lane based traffic condition. However, this study is based on a single intersection of Dhaka city. More extensive research is still necessary to get the exact reasons behind the deviations. More data will eventually lead to accurate determinations of supplemental Adjustment Factors. However, the findings of this study are much useful and significant when estimating performance indicators such as delay, vehicle stops, queue length, etc. So, this study will eventually lead towards accurate determinations of Progression Adjustment Factor (P.F.) in case of non-lane based traffic.

REFERENCES

Akçelik, R. (1996). Progression Factor for Queue Length and Other Queue-Related Statistics. *Transportation Research Record*, *1555*(1), 99-104.

Farabi, A. A., Hadiuzzaman, M. & Hoque, M. S. (2018). A study on The Effect of Non-Lane Behaviour on HCM 2000 Delay Formula, *In Proceedings of 4th International Conference on Advances in Civil Engineering ICACE, CUET*. Chittagong, 887-892.

Hadiuzzaman, M., Rahman M. M. & Karim M. A. (2008), Saturation Flow Model at Signalized Intersection for Non-Lane Based Traffic. *Canadian Journal of Transportation*, Volume 2, Part 1, page 77-90.

Hadiuzzaman, M., Rahman, M., Hasan, T. & Karim, M. A. (2014). Development of Delay Model for Non-Lane Based Traffic at Signalized Intersection. *International Journal of Civil Engineering*, 3, 67-82.

ITE (2008). *Canadian Capacity Guide for Signalized Intersections*. Ed. J W Gough (Canada: Institute of Transportation Engineers).

McShane, W. R., Roess, R. P. & Prassas, E. S. (1990). *Traffic Engineering*. International Edition, Pearson Education International.

Strong, D. W. & Rouphail, N. M. (2005). Incorporating the Effects of Traffic Signal Progression into the Proposed Incremental Queue Accumulation (IQA) Method. Compendium of Papers on TRB 2005 CD-ROM, Transportation Research Board, Washington D.C.

Transportation Research Board (TRB) (1985). Highway Capacity Manual. National Research Council, Washington, D.C.

Transportation Research Board (TRB) (2000). Highway Capacity Manual. National Research Council, Washington, D.C.

Webster, F. V. (1963). *A Method of Measuring Saturation Flow at Traffic Signals*. Road Research Laboratory, Road Note 34, Crowthrone.

Wu, N. (2014). Modifying Progression Adjustment Factor and Upstream Filtering Adjustment Factor at Signalized Intersections in HCM. In *TRB 2014 Annual Meeting*, Preprint No. 14-0414. Transportation Research Board, Washington, D.C.

Cite this article as: Al Farabi F., Chakraborty T., "A Study on the Default Supplemental Adjustment Factors of Progression Adjustment Factor Formula under Non-Lane Based Traffic Condition", *International Conference on Civil Infrastructure and Construction (CIC 2020)*, Doha, Qatar, 2-5 February 2020, DOI: https://doi.org/10.29117/cic.2020.0060

Novel Method for Assessing Moisture Damage in Asphalt Mixtures

Mohammad Nour Fakhreddine
mff17@mail.aub.edu
American University of Beirut, Beirut, Lebanon

Ghassan Chehab
gc06@aub.edu.lb
American University of Beirut, Beirut, Lebanon

Zaher Al Basiouni Al Masri
zsa14@mail.aub.edu
American University of Beirut, Beirut, Lebanon

Mohamad Abiad
ma192@aub.edu.lb
American University of Beirut, Beirut, Lebanon

ABSTRACT

Moisture damage is a major cause of early pavement deterioration and often accelerates other distresses such as rutting, fatigue cracking, and raveling. Water infiltrates into the pavement structure through the cracks and air voids and weakens the adhesive bond between the binder and the aggregates as well as the cohesive bond between the binder particles. Several tests have been adopted to test for moisture susceptibility, most commonly the Modified Lottman (AASHTO, T283) and the Hamburg Wheel Tracking Device (AASHTO, T32404), however, these tests correlate poorly with field results and do not properly replicate the conditions which a pavement structure experiences in the field. Also, the mechanism which determines the mode of failure due to moisture damage, being either adhesive or cohesive, remains largely not understood, and the research tackling this issue is very scarce. The objective of this study is to introduce a new testing procedure based on the pull-off approach and study the factors which influence the mode of failure of the samples, such as the asphalt film thickness and loading rate.

Keywords: Moisture damage; Adhesion and cohesion; Stripping; Asphalt-aggregate bond; Strain rate; Asphalt film thickness

1 INTRODUCTION

Pavements constitute a major part of the transportation infrastructure network in most countries, providing invaluable social and economic benefits. The level of maintenance of a pavement network can have a significant impact on the economy and safety of users; as such, it is necessary to understand the causes of pavement deterioration to extend their lifetime and improve their performance under field conditions. Moisture damage is a major problem that affects the durability of pavements and causes premature deterioration, which in turn significantly increases the annual vehicle operating costs for users (Caro et al., 2008). It also accelerates the occurrence of other major distresses, such as rutting and cracking (Kakar, 2015). Failure can occur due to loss of adhesion and/or cohesion. The loss of adhesion, also known as stripping, is when the interfacial bond between the binder and aggregate surface deteriorates, whereas the loss of cohesion happens within

the binder itself due to the decrease in stiffness (Diab et al., 2014). Moisture damage causes the aggregates to break loose from the structure, which over time, leads to the formation of potholes and cracks; these distresses decrease the safety and rideability of the road in addition to incurring high maintenance bills for municipalities and the users of the road. As such, a reliable and simple procedure that measures the moisture susceptibility of pavements is necessary.

2 LITERATURE REVIEW

The AASHTO T283 is most commonly used to measure the moisture susceptibility of asphalt mixtures. The test consists of placing 3 samples in a water bath for 24 hours at 60 degrees C. The samples are then conditioned at 25 degrees C for 2 hours before being tested in indirect tension at a rate of 2 inches per minute. The results are compared to those of 3 samples which were not subject to moisture conditioning (AASHTO). However, the test uses compacted asphalt cylindrical samples and thus does not isolate the stripping phenomenon at the level of the asphalt-aggregate interface (Al Basiouni Al Masri et al., 2019). The test also uses a fixed conditioning time and load rate, which may not simulate accurate conditions experienced by the pavement in the field. Other tests such as the Hamburg Wheel Tracking Device (AASHTO, T324), Environmental Conditioning System (ECS) (AASHTO, TP34), Asphalt Pavement Analyzer (APA), and Moisture Induced Sensitivity Test (MIST) also exist but are rarely used due to the lack of standardization and complexity of the procedures and sample preparation (Taib et al., 2019).

Researchers have proposed other methods to evaluate moisture sensitivity by using the Dynamic Shear Rheometer (DSR) and different variations of pull-off tests. Cho and Bahia (2010) proposed the wet to dry yield shear stress (W/D YSS) ratio as a parameter to quantify moisture damage by using the Dynamic Shear Rheometer (DSR). They concluded that while the W/D YSS ratio is sensitive enough to measure moisture effects, other factors limit the use of the DSR. Zhang et al. (2016) also used the DSR to control the film thickness of the samples by adding specially manufactured parts for it. The samples were then tested using a Universal Testing Machine (UTM) by also using custom fixtures to hold the samples, which makes the testing setup both very expensive and complicated to use. Rahim et al. (2019) also modified a 10 KN Universal Testing Machine (UTM) and the authors reported that further improvement for the gap assembly is needed for repeatability and practicability reasons. One of the most common tests to evaluate moisture damage is the Bitumen Bond Strength (BBS) test, which uses the Pneumatic Adhesion Tensile Testing Instrument (PATTI). The BBS test consists of pulling a metal stub attached to an aggregate substrate by a film of binder and recording the maximum pulling force. The test was reported by (Moraes et al., 2011) to be successful in measuring the effects of moisture conditioning timing and asphalt modification on the bond strength of asphalt-aggregate systems. The BBS test was used to investigate several issues such as the effect of the bitumen stiffness on the adhesive strength, (Moraes et al., 2012) and the adhesive and cohesive properties of asphalt-aggregate systems using different combinations of aggregates, binders, and mineral fillers (Canestrari et al., 2010; Chaturabong et al., 2018). Despite the popularity of the BBS test, it does have some drawbacks such as using a high film thickness of 0.8 mm, not all elements of the system

being at the same temperature at the time of the sample preparation, and the limitation of the test in terms of output where only the strength can be obtained while other data such as strain cannot (Cala et al., 2019).

Although significant research has been done to evaluate the effect of moisture on the asphalt-aggregate bond using several variations of pull-off and direct tension tests and taking into consideration factors such as binder modification, soaking time, and aggregate mineralogy, little has been done to investigate the effect of test-related factors on the strength of the asphalt-aggregate bond. Such factors include the asphalt film thickness and the rate of loading.

3 OBJECTIVES

The objective of this study is to investigate the factors that affect the asphalt aggregate bond such as the asphalt film thickness and loading rate by running sensitivity analyses. The factors will be tested based on the direct tension test using a simple testing and sample preparation procedure. The results of this sensitivity study on the key affecting factors are used to come up with optimal testing and conditioning procedures that promote adhesive failure. The authors believe that the resulting test procedure will pave the way into really understanding the phenomenon of moisture damage in asphalt pavements through analyzing the load-displacement patterns and observing the modes of failure at the level of the asphalt-aggregate interfacial bond.

4 MATERIALS

For the purpose of the sensitivity study, two types of asphalt binder are used:

1) An unmodified PG64-16 binder

2) A SBS polymer modified PG76-28 binder.

Along with limestone aggregates. Furthermore, limestone filler (less than 75 μm particle size) is mixed with both binders to produce asphalt mastics. As part of the ongoing research, the use of filler material from construction demolition waste (CDW) is being investigated. Finally, the effect of using recycled coarse aggregates, namely recycled concrete aggregates (RCA) and reclaimed asphalt pavement (RAP), on moisture susceptibility of asphalt-aggregate systems is also being studied but is not presented in this paper.

5 SAMPLE PREPARATION AND TEST PROCEDURE

To produce the asphalt-aggregate samples used in the tensile test, limestone cylinders are first produced by coring large limestone blocks obtained from a known quarry. Then, the cylinders are sliced into 5mm-thick aggregate discs, each of which is epoxied into an aluminum endplate. The exposed aggregate surface is cleaned using a clean cloth dipped in a small amount of acetone to remove any residues or oils that might affect the adhesion with the asphalt binder. Meanwhile, asphalt binder is heated until it liquefies, poured in a round silicon mold, and left to cool down at room temperature. In order to control the asphalt film thickness, the zero-gap is defined by fixing two aggregate discs into the tensile machine and lowering the actuator until a 1 N contact load is recorded.

The aggregates are then removed and placed on top of a hot plate to reach the binder application temperature which should be similar to the mixing temperature for an asphalt

mix with the same binder. After the temperature of the aggregates stabilizes, they are quickly fixed in the tensile machine and the binder disc is directly attached to the hot aggregate surface. The actuator is then lowered until the specified film thickness is reached. Finally, the excess binder is trimmed, and the sample is left to cool down to room temperature before testing or removing from the machine. The temperature of the sample is monitored using a thermocouple inserted at the middle of a dummy specimen; it was found that 30 minutes are enough to bring the entire sample back to room temperature. It should be noted that the time between heating the aggregates and lowering the actuator should not be more than 1 minute to avoid excessive loss of temperature of the aggregate surface, which can cause inadequate adhesion with the binder. The sample preparation procedure is visually summarized in Figure 1.

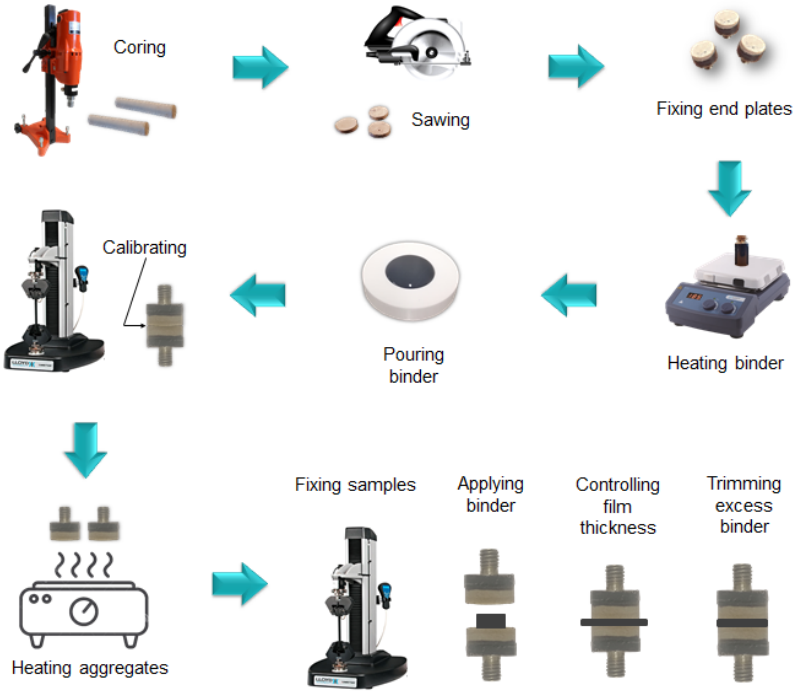

Figure 1: Sample Preparation Procedure

Three replicates of each asphalt-aggregate combination for each testing condition are fabricated using the procedure detailed above.

5.1 Problems Faced with Sample Preparation and Testing

After several trials with the proposed testing procedure, the following challenges were faced and tackled:

- For samples that were tested after moisture conditioning, it was observed that some gained strength. The issue was traced back to the resting time after the samples were fabricated. The asphalt-aggregate bond continued to gain strength even after cooling to room temperature and seemed to stabilize after 24 hours. As such, it is recommended that all samples be left to rest for at least 24 hours before dry testing

or moisture conditioning.

- Due to the viscoelastic nature of asphalt, the binder film decreased in thickness under the weight of the top plate and aggregate over the resting period. The decreased film thickness affected the strength of the bond and thus all samples were modified after fabrication by adding fixtures to their sides so that no load is applied on the asphalt film.
- Some samples exhibited low strength after testing due to the low temperature at which the binder was attached to the aggregate. It is necessary to ensure that the aggregates are sufficiently hot to allow for proper adhesion of the binder to the surface of the aggregates.
- Upon observation of the aggregate surface after testing, it was noticed that some samples were failing in adhesion particularly from one edge of the disk. This was because the surfaces of the 2 aggregates were not completely parallel and thus the sample had a tapered film thickness. The surfaces of the aggregates must be parallel to ensure a uniform film thickness.

6 RESULTS

6.1 Effect of Rate of Loading

The behavior of asphalt, being a viscoelastic material, depends on the strain rate being applied to it. It is known that as the strain rate increases, the stiffness of the binder also increases, and vice versa; and given that a pavement in the field experiences different strain rates depending on the speed of passing trucks and heavy vehicles, then it makes sense to test for different strain rates when checking for the moisture susceptibility of an asphalt mix. To verify that the strain rate influences the strength of the asphalt-aggregate bond and its mode of failure, 3 replicates were tested for each of the chosen strain rates and the results are as shown in Figure 2.

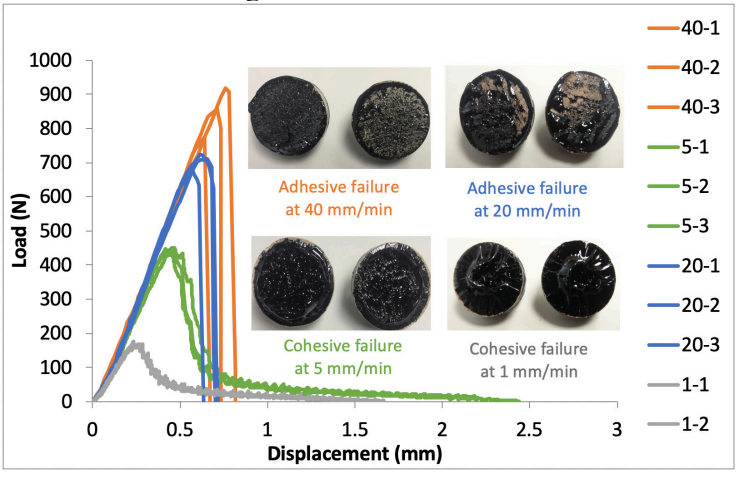

Figure 2: Load vs. Displacement and mode of failure for Different Strain Rates

As the strain rate increases, the strength of the asphalt-aggregate bond also increases. The mode of failure also tends to be adhesive for higher strain rates and cohesive for low strain rates. The test is thus very sensitive to the strain rate and it is a very important factor that can be manipulated to simulate field conditions and promote adhesive failure.

6.2 Effect of the Asphalt Film Thickness

To check the sensitivity of the test for the asphalt film thickness, thicknesses of 0.1 mm, 1 mm, and 1.5 mm were tested for samples using unmodified binder (Figure 3), polymer modified binder (Figure 4) and mastic (Figure 5) using the unmodified binder and limestone filler for a ratio of 1 to 1 by mass. The samples were tested at a strain rate of 20 mm/min.

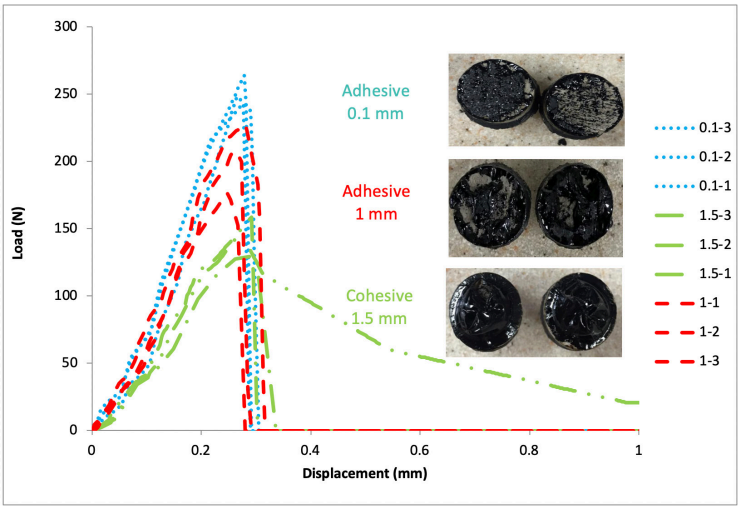

Figure 3: Load vs. Displacement and mode of failure for Different Film Thicknesses using Unmodified Binder

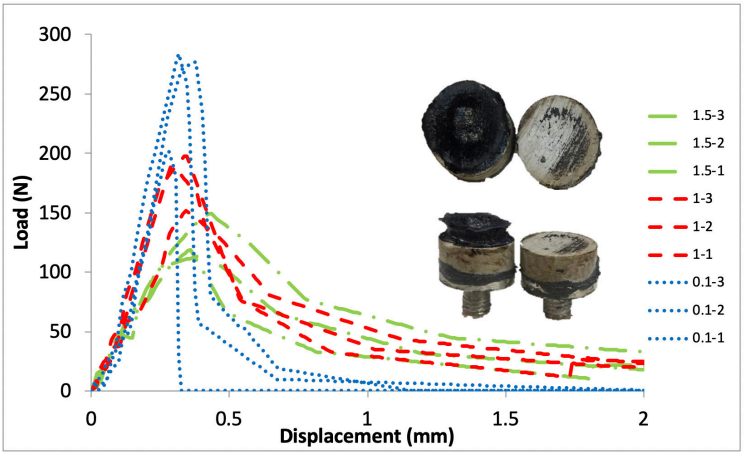

Figure 4: Load vs. Displacement and mode of failure for Different Film Thicknesses using Polymer Modified Binder

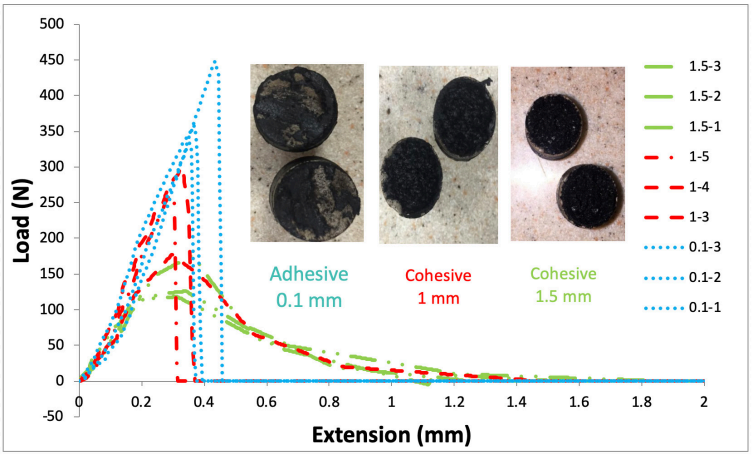

Figure 5: Load vs. Displacement and mode of failure for Different Film Thicknesses using Asphalt Mastic

The results show that as the asphalt film thickness decreases, the strength of the asphalt-aggregate bond increases and the mode of failure tends to be adhesive, while for higher film thicknesses, the strength decreases, and the mode of failure tends to be cohesive. In the case of the polymer-modified binder, the same mode of failure, which was completely adhesive, was observed for all film thicknesses, the authors suspect that the wetting temperature is the main reason behind this observation and will follow up on this issue in future work.

The results agree with (Huang & Lv, 2016) who tested for different stress rates and film thicknesses but using the BBS test; Therefore, the authors were not able to collect load-displacement data, but only the strength of the samples at failure.

7 CONCLUSION

This study confirmed that the asphalt film thickness and loading rate are important factors that must be considered when measuring the moisture susceptibility of asphalt mixes due to their significant effect on the asphalt-aggregate bond. An increase in the loading rate increases strength and promotes adhesive failure, and an increase in asphalt film thickness decreases strength and promotes cohesive failure. The study also proposed a simple testing procedure where film thickness and strain rate can be easily adjusted, and additional data to the maximum strength can be obtained.

The authors believe that strain rate and asphalt film thickness should be included as parameters when testing for moisture susceptibility and will follow up this study with a more detailed one which includes testing of soaked samples.

REFERENCES

Al Basiouni Al Masri, Z., Alarab, A., Chehab, G. & Tehrani-Bagha, A. (2019). Assessing moisture damage of Asphalt-Aggregate Systems using principles of Thermodynamics: Effects of recycled materials and binder aging. *Journal of Materials in Civil Engineering*, *31*(9), 4019190.

Cala, A., Caro, S., Lleras, M. & Rojas-Agramonte, Y. (2019). Impact of the chemical composition of aggregates on the adhesion quality and durability of asphalt-aggregate systems. *Construction and Building Materials*, 216, 661-672.

Canestrari, F., Cardone, F., Graziani, A., Santagata, F. A. & Bahia, H. U. (2010). Adhesive and cohesive properties of Asphalt-Aggregate Systems subjected to moisture damage. *Road Materials and Pavement Design*, *11*(sup1), 11-32.

Caro, S., Masad, E., Bhasin, A. & Little, D. N. (2008). Moisture susceptibility of asphalt mixtures, Part 1: mechanisms. *International Journal of Pavement Engineering*, *9*(2), 81-98.

Chaturabong, P. & Bahia, H. U. (2018). Effect of moisture on the cohesion of asphalt mastics and bonding with surface of aggregates. *Road Materials and Pavement Design*, *19*(3), 741-753.

Cho, D.-W. & Bahia, H. U. (2010). New parameter to evaluate moisture damage of Asphalt-Aggregate bond in using dynamic shear rheometer. *Journal of Materials in Civil Engineering*, *22*(3), 267-276.

Diab, A., You, Z., Hossain, Z. & Zaman, M. (2014). Moisture susceptibility evaluation of nanosize hydrated lime-modified Asphalt–Aggregate Systems based on surface Free Energy Concept. *Transportation Research Record*, *2446*(1), 52-59.

Huang, W. & Lv, Q. (2016). Investigation of critical factors determining the accuracy of binder bond strength test to evaluate adhesion properties of asphalt binders. *Journal of Testing and Evaluation*, *45*(4), 1270-1279.

Moraes, R., Velasquez, R. & Bahia, H. (2012). *The Effect of Bitumen Stiffness on the Adhesive Strength Measured by the Bitumen Bond Strength Test.*

Moraes, R., Velasquez, R. & Bahia, H. U. (2011). Measuring the effect of moisture on asphalt–aggregate bond with the bitumen bond strength test. *Transportation Research Record*, *2209*(1), 70-81.

Rahim, A., Thom, N. & Airey, G. (2019). Development of compression pull-off test (CPOT) to assess bond strength of bitumen. *Construction and Building Materials*, 207, 412-421.

Taib, A., Jakarni, F. M., Rosli, M. F., Yusoff, N. I. M. & Aziz, M. A. (2019). Comparative study of moisture damage performance test. *IOP Conference Series: Materials Science and Engineering*, *512*(1), 12008. IOP Publishing.

Zhang, J., Apeagyei, A. K., Grenfell, J. & Airey, G. D. (2016). Experimental study of moisture sensitivity of aggregate-bitumen bonding strength using a new pull-off test. *8th RILEM International Symposium on Testing and Characterization of Sustainable and Innovative Bituminous Materials*, 719-733. Springer.

Cite this article as: Fakhreddine M. N., Chehab G., Al Masri Z. A. B., Abiad M., "Novel Method for Assessing Moisture Damage in Asphalt Mixtures", *International Conference on Civil Infrastructure and Construction (CIC 2020)*, Doha, Qatar, 2-5 February 2020, DOI: https://doi.org/10.29117/cic.2020.0061

Determination of Temperature Zoning for the Great Lakes Region of Africa Based on Superpave System

Mukunde Ronald
rmm78@mail.aub.edu
American University of Beirut, Beirut, Lebanon

Ghassan Chehab
gc06@aub.edu.lb
American University of Beirut, Beirut, Lebanon

Mohammad Nour Fakhreddine
mff17@mail.aub.edu
American University of Beirut, Beirut, Lebanon

ABSTRACT

Majority of the countries in the Great Lakes region of Africa still rely on the traditional Penetration grading approach for characterizing asphalt binder, as opposed to the more recent and reliable approach of SuperPave (Superior Performing Asphalt Pavements). This paper outlines the steps and criteria of selecting Performance Grade (PG) of bitumen to be used in selected countries of the Great Lakes region, based on the SuperPave approach. In Superpave, high-temperature (HT) Performance Grade required for a given region of project is determined based on a rutting damage model. HT equation is a function of layer thickness, climatic conditions, and latitude of the site (Mohseni et al, 2005); whereas, Low-temperature (LT) Performance Grade is selected using an algorithm developed from LTPP climatic data, and that relates the minimum pavement temperature to minimum air temperature, latitude, and depth (Mohseni, 1998). Study of climatic conditions of selected countries (Uganda, Kenya and Tanzania) in the great lakes region shows that the maximum pavement design temperature is 64 ºC, while the minimum pavement design temperature is -10 ºC. Further, the temperature zoning is distributed into three geographical areas, namely PG 64-10, PG 58-10 and PG 52-10 according to the collected and studied data.

Keywords: Strategic highway research program (SHRP); Superior performance asphalt pavements (SUPERPAVE); Long term pavement performance (LTPP); Performance grade (PG); Great lakes region of Africa

1 INTRODUCTION

Super pave binder specification is based on the performance of asphalt pavement, which is the main difference between this system and other earlier approaches such as Penetration and Viscosity grading (Asphalt institute, 2003). The physical and mechanical properties requirements of asphalt binders are fixed for all performance grades, but in the Superpave method, the maximum and minimum temperatures at which the binder shall meet the requirements are the basis of various grades. AASHTO M320 contains a listing of the more commonly used performance grades (PG), but the PG grades are not limited to those given classifications because the specification temperatures are unlimited (Azari

et al, 2003). The high and low temperatures extended as far as necessary in the standard six increments. This paper explains the steps and criteria of selecting performance grade (PG) with reference to the Strategic Highway Research Program (SHRP) Specification and determination of the Great Lakes of Africa Temperature Zoning. The currently used Penetration grading in this region is empirical and suffers the limitation of accuracy in determining the full effects of variations in environmental and loading conditions on the pavement performance. Registered historical temperature data for ten years was obtained from various weather stations to cover different regions of the selected countries. The selection of performance grade based on SHRP specifications includes three important factors which are: historical temperature data, traffic conditions, and the desired reliability factor. The desired reliability and historical temperature data are of high importance in selecting the temperature zone for the selected country or region. Although other factors such as the traffic condition should be considered when selecting binder grade for the asphalt mix, the Superpave system facilitates the knowledge of the base PG of the asphalt binder to be used in the project area directly from the temperature zoning map.

2 METHODOLOGY

2.1 High pavement design temperature

SHRP developed two models for determining high pavement temperature for PG grading purposes; one based on the rutting damage concept (the rutting damage model) and the other based on adjusting the PG with depth into the pavement (the LTPP High pavement temperature model). The latter was used in this study and is a function of air temperature, latitude and depth (Mohseni et al, 2005) as shown in Equation 1.

$$T_{H.pav} = 54.32 + 0.78\,T_{air} - 0.0025\,Lat^2 - 15.14\log(H+25) - Z\,(9+0.61\,\sigma^2_{Tair})^{0.5} \ldots\ldots (1)$$

Where,

$T_{H.pav}$ = High pavement design temperature.

T_{air} = Average seven-day average high air temperature, ˚C.

Lat = The Geographical latitude of the project.

H = Depth to surface, mm.

$\sigma^2_{T\,air}$ = Standard deviation of the mean low air temperature, °C.

Z = Standard normal distribution value 2.055 for 98% reliability.

2.2 Low pavement design temperature

Low-temperature (LT) performance grade is selected using the algorithm developed from LTPP climatic data. LT algorithm relates minimum pavement temperature to minimum air temperature, latitude, and depth (Mohseni, 1993) as shown in Equation 2.

$$T_{L.pav} = -1.56 + 0.72\,T_{air} - 0.004\,Lat^2 + 6.26\log(H+25) - Z\,(4.4 + 0.52\,\sigma^2_{T\,air})^{0.5} \ldots\ldots (2)$$

Where:

$T_{L.pav}$ = Low pavement temperature at surface, °C.

T_{air} = Low air temperature, °C.

3 RESULTS

The mean and standard deviation for maximum and minimum air temperatures during the specified period (ten years) for all the meteorological stations representing all the regions in the Great Lakes region are tabulated in **Tables 1 to 3**.

Table 1: The mean and standard deviations for high and low air temperatures in Uganda

Region	Station	Mean		Standard deviation (sd)		+2 sd (98% reliability)	
		Highest °C	Lowest °C	Highest °C	Lowest °C	Highest °C	Lowest °C
North	Gulu	34.56	16.67	1.27	0.52	37.09	15.63
	Lira	34.11	16.22	1.14	0.63	36.38	14.96
	Moroto	32.00	16.89	0.88	0.63	33.75	15.62
	Arua	33.78	16.78	0.92	0.67	35.62	15.43
West	Kabale	27.44	14.00	1.42	0.47	30.28	13.06
	Mbarara	27.56	14.00	1.26	0.47	30.09	13.06
	Kasese	27.78	13.11	0.99	0.95	29.77	11.21
	Fort Portal	27.78	13.11	0.99	0.95	29.77	11.21
	Hoima	33.22	16.22	0.82	0.63	34.87	14.96
East & Central	Entebbe	25.11	17.33	0.79	1.48	26.69	14.38
	Kampala	28.22	15.44	1.03	1.07	30.29	13.29
	Jinja	29.89	14.44	1.62	1.08	33.13	12.28
	Kalangala	25.11	17.33	0.79	1.48	26.69	14.38
	Tororo	31.33	14.67	1.07	0.67	33.48	13.32
	Mbale	29.78	14.11	0.94	0.42	31.66	13.27
	Soroti	34.33	16.11	1.27	0.74	36.87	14.64

Table 2: The mean and standard deviations for high and low air temperatures in Kenya

Region	Station	Mean		Standard deviation (sd)		+2 sd (98% reliability)	
		Highest °C	Lowest °C	Highest °C	Lowest °C	Highest °C	Lowest °C
Central	Nairobi	27.50	12.10	1.27	0.57	30.04	10.96
Coast	Mombasa	31.70	22.00	0.82	0.00	33.35	22.00
North East	Wajir	36.40	22.40	0.52	0.70	37.43	21.00
East	Meru	24.40	11.50	0.70	1.35	25.80	8.79
Rift valley	Nakuru	25.30	8.90	1.25	0.74	27.80	7.42
West	Kisumu	30.00	14.10	1.15	0.57	32.31	12.96

Table 3: The mean and standard deviations for high and low air temperatures in Tanzania

Region	Station	Mean		Standard deviation (sd)		+2 sd (98% reliability)	
		Highest °C	Lowest °C	Highest °C	Lowest °C	Highest °C	Lowest °C
Costal	Dar-es-Salaam	31.00	21.20	0.57	0.42	32.14	19.94
Central	Dodoma	32.10	14.00	1.29	0.82	34.67	11.55
North	Arusha	29.90	13.20	1.20	0.63	32.29	11.30
West	Kigoma	26.10	19.40	1.20	1.17	28.49	15.88

SHRP performance-based binder and mixture specifications are developed based on the tests related to the pavement performance under different climatic conditions. **Equation 1** is used to transfer the highest air temperature to high design pavement temperature. Similarly, **Equation 2** is used to determine the low design pavement temperature. The results of design pavement temperatures were used to determine the PG grades for different regions of selected countries in the Great lakes region of Africa.

3.1 East African Temperature Zoning Map

The Great Lakes region of Africa consists of seven countries, Uganda, Kenya, Tanzania, Rwanda, Burundi, Malawi and the Democratic Republic of Congo. The region experiences tropical climate which is characterized by high precipitation throughout the year. Moreover, the air temperatures rarely fall below 10 ºC yet do not go beyond 37 ºC. In this study, three countries were selected as representatives of the region due to their strategic location and varying climatic conditions. Twenty-six weather stations are considered to cover the selected states. As a result of this study, the East African Temperature Zoning map was established, to serve as reference for asphalt PG grade selection in this region according to the Superpave system. The hottest areas reported high pavement design temperature not more than 64 ºC and the rest reported high design temperatures between 52 and 58 ºC.

The following assumptions were used to establish the East African Temperature Zoning Map:

I. The station in any region should be taken as a reference for the whole region;
II. If there are many stations in one region, then the high recorded reading is used; and
III. The regional/ provincial borders are used as separators between zones.

The results of fourteen (14) regions for the three selected countries in the Great Lakes region of Africa are illustrated in **Figures 1 to 4** below;

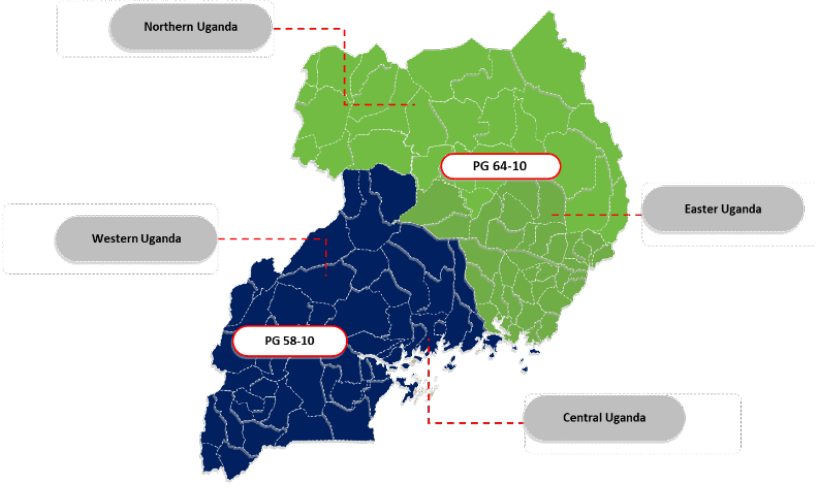

Figure 1: Uganda's PG zoning map

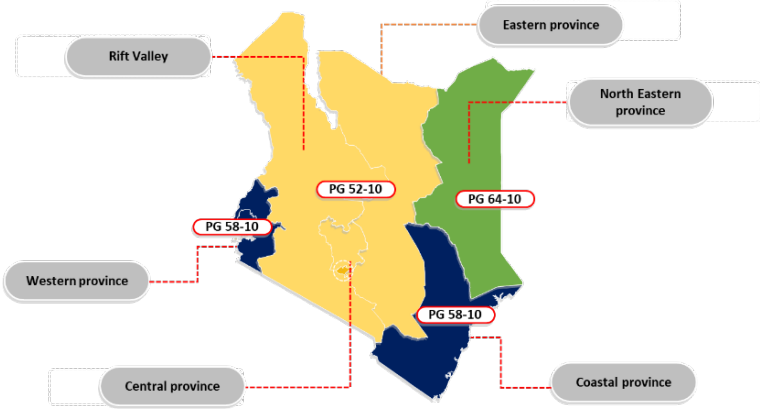

Figure 2: Kenya's PG zoning map

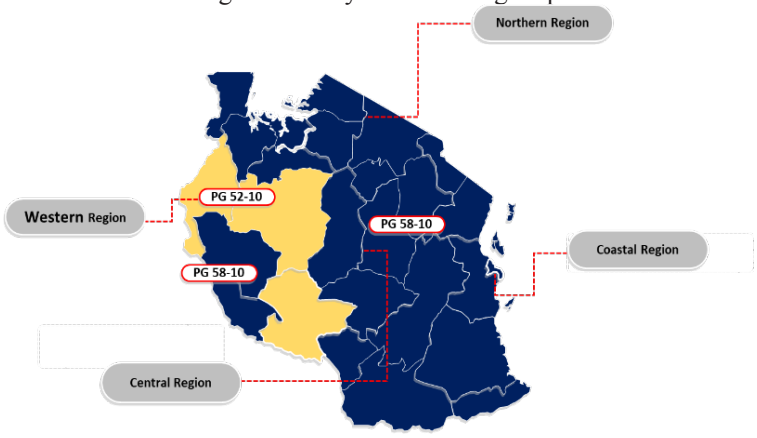

Figure 3: Tanzania's PG zoning map

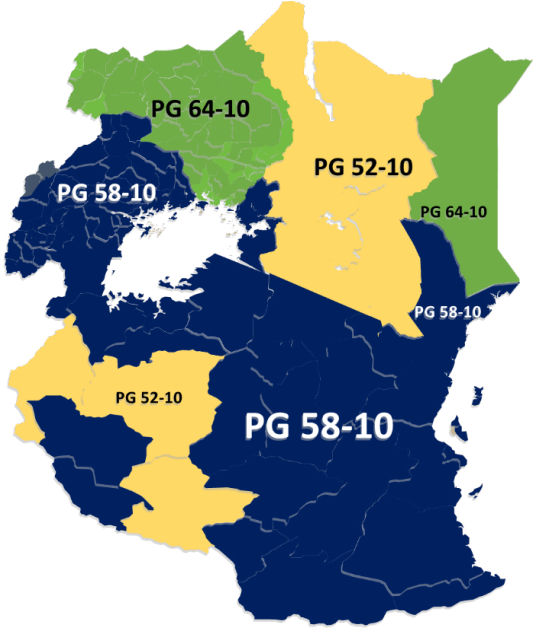

Figure 4: East Africa's PG zoning map

3.2 Incorporating Effects of Traffic Conditions

Final selection of required Performance Grade (PG) for a given project depends on adjusting the base binder grade selected according to climatic criteria to account for desired reliability and traffic conditions. Table 4 includes the Superpave specifications for high-temperature design grade adjustment (grade bump) based on traffic volume and speed. One major drawback is that SHRP does not provide any guidelines regarding the depth of the asphalt layer up to which this bumping should be applied (Chehab et al, 2019).

Table 4: Adjustment to the high-temperature grade of Binder based on traffic speed and traffic level

Adjustment to Binder PG grade [2]					
Traffic loading rate (design speed)	Base Grade	Design ESALs (millions) [1]			
		< 3	3 - 10	10 - 30	>30
Standing (Av. Speed < 20Km/hr.)	**52**	2	2	2	2
	58	2	2	2	2
	64	2	2	2	2
	70	2	2	2	2
Slow (Av. Speed 20 to 70 Km/hr.)	**52**	1	1	1	1 [(3)]
	58	1	1	1	1
	64	1	1	1	1
	70	1	1	1	1
Fast (Av. Speed > 70 Km/hr.)	**52**	-	-	-	1
	58	-	-	-	1
	64	-	-	-	1
	70	- [(3)]	-	-	1

[1.] Design ESALs is the anticipated project traffic level expected on the design lane over 20 years.

[2.] Increase the high-temperature grade by the number of grade equivalents indicated (one grade equivalent to 6°C). The low-temperature grade is not adjusted.

[3.] Consideration should be given to increasing the high-temperature grade by one grade equivalent. Practically, performance graded binders stiffer than PG 82-XX should be avoided. In cases where the required adjustment to the high-temperature binder grade would result in a grade higher than a PG 82, consideration should be given to specifying a PG 82-XX and increasing the design ESALs by one level (e.g., 10 - 30 million increased to > 30 million).

4 CONCLUSION

Based on the comprehensive collected data from the meteorological weather stations in selected Great Lakes region states and the analysis of the data based on the SHRP Superpave system procedure, the following conclusion can be stated:

1. The range of average lowest and highest air temperatures during the specified period is between (8.06 ºC to 18.52 ºC) and (24.40 ºC to 36.41°C) respectively.
2. Based on the weather data analysis, the maximum and minimum air temperatures registered are in North Eastern and the rift valley provinces of Kenya respectively.
3. The study also showed that the base maximum pavement design temperature is 64 ºC and the conservative minimum pavement design temperature is -10 ºC.

4. The temperature zoning in the selected states is distributed into three zones which are PG 64-10, PG 58-10 and PG 52 -10.
5. The PG grade map acts as a reference for pavement design in the selected states. The design traffic conditions should be taken into consideration for pavement design in any of the regions, to know the need for improving the PG grade according to Table 4.
6. Further studies should be carried out for neighboring countries to establish the corresponding PG grades to be used in asphalt pavements.

REFERENCES

Asi, I. M. (2007). Performance evaluation of SUPERPAVE and Marshall asphalt mix designs to suite Jordan climatic and traffic conditions. *Construction and Building Materials*, *21*(8), 1732-1740.

Asphalt Institute (Ed.) (2003). *Performance graded asphalt binder specification and testing* (No. 1). Asphalt Institute.

Azari, H., McCuen, R. H. & Stuart, K. D. (2003). Optimum compaction temperature for modified binders. *Journal of Transportation Engineering*, *129*(5), 531-537.

Chehab, G. R., Hamdar, Y. S., & Haddad, A. J. (2019). Investigating High-Temperature PG Grade Adjustment Recommendations for Airfield Pavements. *Transportation Research Record*, 0361198119838259.

Denneman, E. (2007). Application of locally developed pavement temperature prediction algorithms in performance grade (PG) binder selection.

Design, S. M. (1996). Superpave Series No. 2 (SP-2). *Asphalt Institute, Lexington, KY*.

Mohseni, A. (1998). LTPP Seasonal Asphalt Concrete (AC) Pavement Temperature Models, Report No. FHWA-RD-97-103, Federal Highway Administration, Washington, D.C.

Mohseni, A. Carpenter, S. H., & D'Angelo, J. (2005). "Development of Superpave high temperature performance grade (PG) based on rutting damage (With Discussion and Closure)," *Journal of the Association of Asphalt Paving Technologists, 74*(1), pp. 197– 254, The Association of Asphalt Paving Technologists, Lino Lakes, MN.

Cite this article as: Ronald M., Chehab G., Fakhreddine M. N., "Determination of Temperature Zoning for the Great Lakes Region of Africa Based on Superpave System", *International Conference on Civil Infrastructure and Construction (CIC 2020)*, Doha, Qatar, 2-5 February 2020, DOI: https://doi.org/10.29117/cic.2020.0062

Test Procedures for Advanced Characterization of Bituminous Binders Employed for Pavement Construction in Public Works Authority Road Projects - State of Qatar

Ezio Santagata
ezio.santagata@polito.it
Department of Environment, Land and Infrastructure Engineering, Politecnico di Torino, Turin, Italy

Sadegh Yeganeh
sadegh.yeganeh@polito.it
Department of Environment, Land and Infrastructure Engineering, Politecnico di Torino, Turin, Italy

Osman Elhusain Mohamed Idris
osmane@ashghal.gov.qa
Quality and Safety Department, Public Works Authority (Ashghal), Doha, Qatar

Moaaz Hashim M. M. Ali
moaaz@ashghal.gov.qa
Quality and Safety Department, Public Works Authority (Ashghal), Doha, Qatar

Khalid Mohd I Al-Emadi
kemadi@ashghal.gov.qa
Quality and Safety Department, Public Works Authority (Ashghal), Doha, Qatar

ABSTRACT

This paper illustrates the approach adopted by the Public Works Authority (Ashghal) of the State of Qatar for the advanced chemical and rheological characterization of bituminous binders (both neat and modified). The ultimate objective of testing is to create a database of employed binders, which may be meaningful for the optimization of the selection of materials and for the consequent enhancement of pavement performance. This paper provides an illustration of employed testing procedure and briefly discusses typical experimental results.

Keywords: Road pavements; Bituminous binders; Test procedures; Chemical characterization; Rheological characterization

1 INTRODUCTION

The road infrastructure network of the State of Qatar has grown significantly in the last few decades, and it has become essential to create a database of the main characteristics and engineering properties of available materials. Such a task has been undertaken by the Quality & Safety Department (QSD) of the Public Works Authority (Ashghal) and by ANAS S.p.A. Qatar Branch as part of the ongoing QA/QC Pavement Consultancy Services contract. Considered materials include those of the "standard" type, which are already fully described in current Qatar Construction Specifications (QCS, 2014), and "alternative" materials which have never been employed in Qatar – or only in experimental trials – and that may be considered for future use.

Since the majority of road pavements constructed in Qatar are of the flexible type, major efforts have been made in order to fully characterize bituminous binders employed for the production of wearing, intermediate and base courses for pavements

of all categories. According to the requirements set in (QCS, 2014), these may be either of the "neat" type, or of the "polymer-modified" type (PMBs). However, ongoing developments related to implementation of the so-called "Ashghal Recycling Initiative" (Ashghal, 2018), have recently led to the replacement of PMBs with crumb rubber modified binders (CRMBs) in all projects overseen by the Road Projects Department (RPD) of Ashghal (RPD, 2018).

The State of Qatar does not produce a significant quantity of bitumen from oil refining and therefore has always imported it from foreign Countries. During the entire period of development of the Qatari road infrastructure, bitumen was exclusively imported from a single Country (and a single refinery, which produced it by straight run distillation of a single type of crude). However, since June 2017 bitumen has been supplied from different sources, with the corresponding availability of materials obtained by means of a multitude of crude processing technologies (including air blowing and blending of vacuum tower bottom residues and other petroleum-derived fractions).

As a result of the evolving scenario outlined above, it has become apparent that characterization of bituminous binders employed in the State of Qatar should require the use of advanced testing procedures for the assessment of their intrinsic chemical and rheological properties, which are also affected by ageing. The current characterization approach which is implemented in (QCS, 2014) relies on penetration grading for neat bitumen (as per ASTM D946-15), required to belong to the 60-70 grade, and on the SUPERPAVE system for modified binders (as per AASHTO M 320-17 and AASHTO M 332-14), which have to be classified as PG76-10. While the former system has proven to be scarcely related to actual field performance, the latter one, although conceived with a performance-based character, provides only partial information on the true nature and behavior of bituminous binders, and may therefore fail in capturing relevant differences between products of variable type and origin.

This paper outlines the approach adopted by Ashghal in order to address the issues discussed above, with an illustration of employed testing procedures and typical results obtained in the characterization of different types of bituminous binders, considered in various ageing states. A more comprehensive description of the studies performed on this topic is presented elsewhere (Santagata et al., 2019). Investigations were carried out in the Ashghal Center for Research & Development (ACRD), with the involvement of the Road Materials Laboratory of the Politecnico di Torino, Italy.

2 CHEMICAL CHARACTERIZATION

As part of the advanced approach adopted by the QSD-ANAS team, chemical characterization is carried out, only for neat bitumen, by referring to the classical colloidal scheme proposed by (Nellensteyn, 1928), in which asphaltenes are kept in dispersion in a continuous medium of oils (saturates and aromatics) by means of the peptizing effect of resins which are distributed around asphaltene micelles. The transition of bitumen macromolecules from saturates to aromatics to resins and to asphaltenes occurs with an increase of molecular weight, polarity and aromaticity. The colloidal scheme is a simplification of the true nature of bitumen, which in the reality is formed by a complex and in most part random combination of different macromolecules (Branthaver et al., 1994). Nevertheless, this idealized structure, characterized by given percentages of the

four different fractions, can be of support in comparing bituminous binders of different origin, in assessing the effects of ageing, and in explaining some of the specific features of their rheological behavior (Santagata et al., 2009).

Analyses that are consistent with the scheme illustrated above, also known as SARA analyses, are performed by means of an equipment (Iatroscan, model MK-6) which combines thin layer chromatography (TLC) with a flame ionization detection (FID) technique (Leroy, 1989; Ecker, 2001). The adopted testing protocol, validated in the course of previous research work (Santagata et al., 2015), entails the preliminary preparation of solutions of bitumen in dichloromethane with a concentration of 10 mg/ml. A small quantity of these solutions (1 μl) is injected in porous quartz rods covered by a thin film of silica gel. Identification of the four bitumen fractions is thereafter carried out by immerging the rod tips in a set of tanks containing n-hexane, toluene and a mixture of dichloromethane (95%) and methilic alcohol (5%). Finally, percentages of the four fractions, characterized by different polarity, are assessed by means of the FID unit, which operates by measuring the electrical current produced by combustion in hydrogen flame.

Examples of results obtained from SARA analyses are provided in Figure 1, where there are shown in the form of a bar chart (Figure 1a, which contains the relative percentages of all four fractions) and of a triangular chart (Figure 1b, in which saturates and aromatics are considered as a single fraction). Represented data refer to a single neat bitumen (indicated as bitumen A), considered in its three ageing states: virgin (as drawn from plant storage tanks), short-term aged by means of the Rolling Thin Film Oven (RTFO) test as per ASTM D2872-19 and AASHTO T240-13, long-term aged by means of the Pressure Ageing Vessel (PAV) as per ASTM D6521-19 and AASHTO R28-12. Figure 1 also displays other data which have been considered for comparative purposes. These were obtained for two binders which were extracted (as per ASTM D2172-17) from cores taken from an in-service pavement (bitumen B-C) and from reclaimed asphalt pavement (RAP) material retrieved from the stockpile of a local Contractor (bitumen C-R). Results that refer to this last sample are of special interest since in Qatar the use of RAP in asphalt mixes is being strongly encouraged within the "Ashghal Recycling Initiative". Thus, assessing the chemical nature of bitumen contained in RAP is functional for the prediction of its effectiveness as a binder and for the identification of proper rejuvenating treatments (Cong et al., 2016).

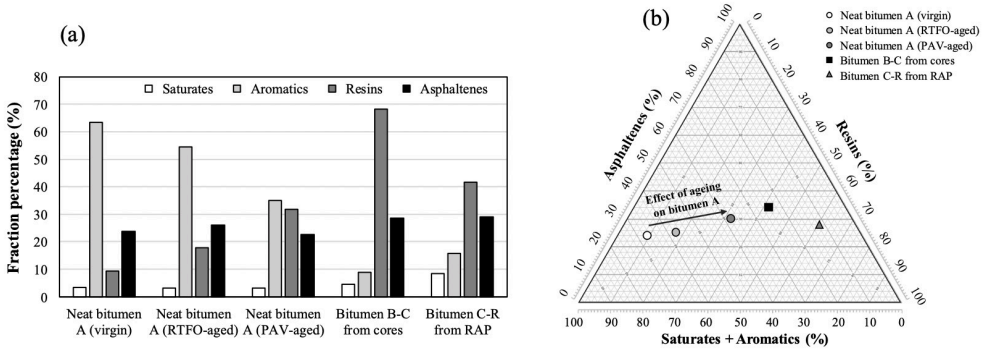

Figure 1: Results of SARA analyses

By considering the results given in Figure 1 it can be observed that SARA analyses clearly describe the evolution of bitumen chemistry as a function of ageing. In particular, as ageing progresses, it causes a gradual reduction of the percentage of dispersing fractions, mainly as a consequence of the transition of part of the aromatics into resins (or asphaltenes) of higher polarity and of the shift of part of the resins to the asphaltene fraction (Eberhardsteiner et al., 2015). Such an evolution is clearly depicted by means of the triangular chart representation, which allows binders coming from different sources and production technologies to be clearly differentiated. Although no information was available on the chemical composition of the bitumen originally contained in the asphalt pavement layer subjected to coring, results obtained on the extracted bitumen are consistent with the observed ageing trends. However, in line with previous findings documented for asphalt mixes employed in Qatar (Sirin et al., 2017), they also suggest that the degree of ageing reached in the field may be superior to that which is mimicked by means of the PAV protocol. Finally, it can be observed that binders contained in RAP, subjected to prolonged ageing, may exhibit a balance between fractions that is completely different from that of all other binders, with an overall reduction of the quantity of oils (saturates and aromatics) and with a significant increase of the percentage of resins. Such an outcome indicates that when using RAP in the production of asphalt mixes it may be necessary to make use of specifically tailored rejuvenating agents, and that for some specific RAP sources the aged binder may be ultimately considered as "black rock" (Chen et al., 2007).

3 RHEOLOGICAL PERFORMANCE-BASED CHARACTERIZATION

According to the approach adopted by the QSD-ANAS team, rheological performance-based tests for the advanced characterization of bituminous binders are carried out by making use of a Dynamic Shear Rheometer (DSR). Employed testing procedures address different aspects of the expected behavior in service, with analyses that are carried out on binders considered in their three characteristic ageing states (virgin, RTFO-aged and PAV-aged).

The following sections contain a description of test protocols and a brief discussion of typical results. Data provided in this paper were obtained by making use of a Physica MCR 302 from Anton Paar Inc., an air-bearing stress-controlled device equipped with a permanent magnet synchronous drive (minimum torque = 0.5 nNm) and an optical incremental encoder for the measurement of angular rotation (resolution = 0.05 μrad).

3.1 Viscoelastic fingerprinting

Viscoelastic fingerprinting of bituminous binders consists in the construction of master curves which provide a full description of their time- temperature- and age-dependent behavior. Such an assessment is of premium importance since parameters obtained from master curve modelling (described in the following) can be related to the synthetic composition parameters derived from SARA analyses (see section 2).

Master curves are obtained by means of frequency sweeps in which the norm and phase angle of the complex modulus is monitored in a wide frequency range (from 1 to 100 rad/s) at temperatures comprised between 4 and 82 °C (with 6 °C increments between each measurement step). Depending upon temperature and frequency, shear

strains applied to test specimens are adjusted in order to focus on linear viscoelastic response. A 25 mm parallel plate system is used with a 1 mm gap between the plates at higher test temperatures (34-82 °C), while the 8 mm parallel plate with 2 mm gap is employed at lower temperatures (4-34 °C).

Temperature-dependent shift factors (a_T) are modelled by referring to the following expression, originally proposed by Williams, Landel and Ferry (Ferry, 1980):

$$\log a_T = \frac{-C_1(T-T_{ref})}{(C_2+T-T_{ref})} \log a_T = \frac{-C_1(T-T_{ref})}{(C_2+T-T_{ref})} \quad (1)$$

where C_1 and C_2 are model parameters, T is the generic test temperature, T_{ref} is the reference temperature at which the master curve is evaluated (usually set at 20 °C for all binders).

Measured values of the norm and phase angle of the complex modulus, shifted to the reference temperature, are fitted to the following expression proposed by Christensen and Anderson (1992):

$$G^*(\omega) = G_g[1 + (\frac{\omega_c}{\omega})^{\frac{Log2}{R}}]^{-\frac{R}{Log2}} G^*(\omega) = G_g[1 + (\frac{\omega_c}{\omega})^{\frac{Log2}{R}}]^{-\frac{R}{Log2}} \quad (2)$$

where G*(ω) and δ(ω) are the norm and phase angle of the complex modulus at the generic reduced angular frequency ω, G_g is the glassy modulus, ω_c is the crossover frequency, and R is the rheological index.

Examples of obtained results are shown in Figure 2 and in Table 1, which refer to tests carried out on two neat binders of different origin (indicated as D and E) considered in their three ageing states, a PMB (binder F-P), and a binder recovered from RAP (indicated as G-R).

From Figure 2a it can be observed that the two neat binders, although being of the same penetration grade (60-70), exhibit a completely different rheological behavior. In particular, when compared to bitumen D, bitumen E possesses a lower stiffness in all ageing states and is characterized by a lower sensitivity to ageing. By referring to Figure 2b, significant differences can also be found when comparing binders of different type and origin. In particular, binders extracted from RAP may be extremely stiff in the entire range of considered frequencies, while the effects of polymer modification can also be relevant, with a significant change of the master curve shape. These observations can be supported by the critical analysis of the fitting parameters provided in Table 1.

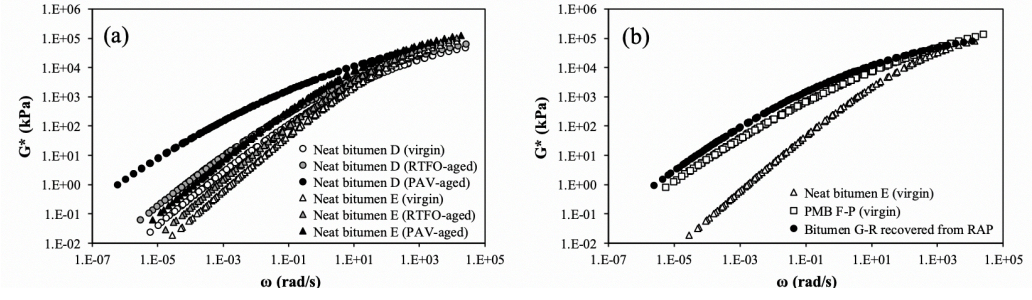

Figure 2: Master curves

Table 1 Master curve parameters

Binder	Type	C_1 (-)	C_2 (°C)	$\log(G_g)$ (kPa)	$\log(\omega_0)$ (rad/s)	R (kPa)
D (virgin)	Neat	15.10	116.87	5.31	1.57	1.65
D (RTFO-aged)	Neat	16.81	126.60	5.53	0.92	1.97
D (PAV-aged)	Neat	31.16	247.87	5.90	-1.55	2.94
E (virgin)	Neat	12.64	110.46	5.42	2.60	1.10
E (RTFO-aged)	Neat	13.98	120.18	5.53	2.28	1.22
E (PAV-aged)	Neat	15.72	127.04	5.60	1.57	1.43
F-P (virgin)	PMB	13.40	89.40	9.93	1.16	6.58
Bitumen G-R	From RAP	23.92	202.49	5.59	-0.61	2.23

3.2 Resistance to permanent deformation

Resistance to permanent deformation is analyzed by performing multiple stress creep recovery (MSCR) tests carried out as per AASHTO T350-19 at temperatures comprised between 52 °C and 76 °C (with 6 °C increments), and two different shear stresses (0.1 and 3.2 kPa). When compared to standard oscillatory tests, MSCR tests are more simulative of in-service loading conditions since they are carried out at higher strain levels, thus allowing a better assessment of rutting potential (D'Angelo, 2009). According to the approach adopted by the QSD-ANAS team, MSCR tests are not simply aimed at identifying temperatures at which AASHTO M 332-14 threshold conditions are met, but rather at giving a full description of the rutting resistance potential in a wide temperature range. Thus, reference is made to the temperature-dependency of percent recovery (R) and non-recoverable shear compliance (J_{nr}), which provide an insight into the degree of elastic response of considered materials.

Examples of obtained results are shown in Figure 3, which refers to tests carried out on two neat binders (indicated as H and I) and two PMBs (J-P and K-P). The two neat binders, of the 60-70 penetration grade and classified as PG64S-22, were of different origin. PMBs, obtained from local Contractors, were reported to contain styrene-butadiene-styrene (SBS) as a modifier and were classified as PG76V-16 and PG76E-22, respectively.

When considering the results obtained at 76 °C (Figure 3a), it can be observed that the two neat bitumens exhibit an almost negligible elastic recovery in the virgin and RTFO-aged state, with no possibility of capturing any significant difference in response. However, in the PAV-aged state they show a different response under repeated loading, the R parameter at 3.2 kPa being equal to 4.25 and 0.76 for bitumen H and I, respectively. Differences between the two PMBs at 76 °C are more noticeable. In particular, it is shown that they are characterized by a different sensitivity to ageing. Additional information on the potential resistance to permanent deformation of the various binders can be extracted from the temperature-J_{nr} plots displayed in Figure 3b. In this case, it is observed that neat bitumens and PMBs can be characterized not only by significantly different values of non-recoverable compliance, but also by a different temperature-susceptibility.

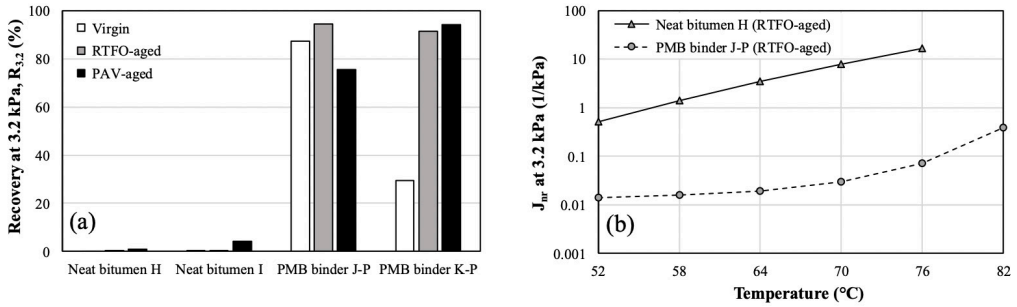

Figure 3: Results of MSCR tests

3.3 Resistance to fatigue damage

Resistance to fatigue damage is investigated by subjecting binder specimens to linear amplitude sweep (LAS) tests as per AASHTO TP 101-14 at 19 °C, with a frequency of 10 Hz and strain amplitudes comprised in the 0.1-30% range. Preliminary characterization in the undamaged state is carried by varying frequency between 0.2 Hz and 30 Hz with an imposed strain of 0.1%.

The final objective of LAS tests is to construct fatigue curves (also known as Wohler curves), which provide a synthetic description of fatigue behavior and allow a straightforward comparison between different materials. These curves are given by the following expression:

$$N_f = \mathrm{A} \cdot \gamma^{-B} \qquad (3)$$

where N_f is the number of loading cycles to failure, γ is initial shear strain, A and B are material-dependent constants derived from fitting of experimental data.

Such an approach to the assessment of resistance to fatigue damage constitutes an improvement with respect to the evaluation of the G*·sinδ parameter referred to in the SUPERPAVE grading system, which shows a poor correlation with field performance as a result of the fact that is obtained in the linear viscoelastic range and after only few cycles of loading (Bahia et al., 2001).

LAS tests have been proposed as an alternative to time sweep tests which have been reported to yield highly variable results (Kim et al., 2006; Botella et al., 2012; Hintz & Bahia, 2013; Santagata et al., 2013). Results recorded during frequency and amplitude sweeps are subjected to Viscoelastic Continuum Damage (VECD) analysis, which eventually leads to the calculation of constants A and B indicated in Equation 3 (Kim et al., 2006; Wen & Bahia, 2009).

Examples of obtained results are shown in Figure 4, in which they are plotted in terms of the N_f/ESALs parameter, given by the ratio between the number of loading to failure (N_f) and the fixed constant (equal to 10^9) provided in AASHTO TP 101-14. Experimental data refer to tests carried out on two neat binders of different origin (indicated as L and M).

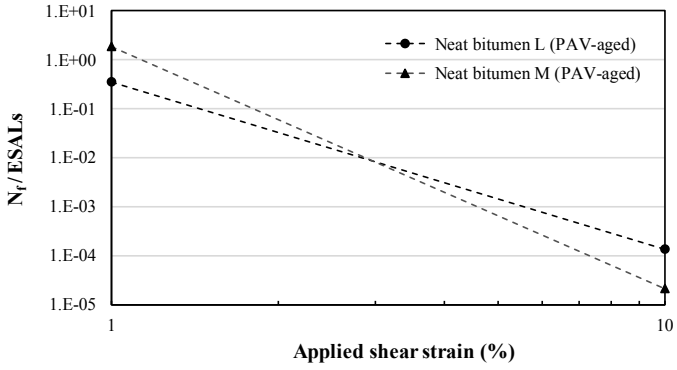

Figure 4: Results of LAS tests

From the analysis of the data presented in Figure 4 it can be observed that the two considered binders display a completely different resistance to fatigue damage, with a relative ranking that depends upon the considered level of strain. Although strain levels typically experienced by bituminous binders in the field are seldom greater than 1% (Masad et al., 2001), such an outcome, which reveals the strong strain-dependency of fatigue resistance, needs to be considered when comparing binders of different origin and type. In particular, it may be of premium interest while analyzing the effects of bitumen modification and of the use of RAP in asphalt mixes.

4 CONCLUSION

Based on the discussion of the results presented in this paper, it can be concluded that the use of advanced chemical and rheological procedures for the characterization of bituminous binders may be of great value in Qatar as a result of the wide variability of available materials. Adopted procedures are capable of highlighting the differences between binders of different origin and type, including those which are modified with polymers or are extracted from pavement layers and RAP samples. The approach adopted by the QSD-ANAS team for binder characterization will be further improved, eventually leading to the fine-tuning of advanced characterization criteria to be included in future specifications. In such a context, the ACRD will have a key role in continuously expanding the chemical and rheological database of bituminous binders employed in Qatar.

REFERENCES

Ashghal (2018). *Roadmap for implementation of Ashghal Initiative of recycling in construction projects* (Circular No (69)). Doha, Qatar, 09/05/2018.

Bahia, H. U., Zhai, H., Zeng, M., Hu, Y. & Turner, P. (2001). Development of binder specification parameters based on characterization of damage behavior. *Journal of the Association of Asphalt Paving Technologists*, 70, 442-470.

Botella, R., Perez-Jimenez, F. E. & Mirò, R. (2012). Application of a strain sweep test to assess fatigue behavior of asphalt binders. *Construction and Building Materials*, 36, 906-912.

Branthaver, J. F., Petersen, J. C., Robertson, R. E., Duvall, J. J., Kim, S. S., Harnsberger, P.

M., Mill, T., Ensley, E. K., Barbour, F.A. & Schabron, J. F. (1994). *Binder Characterization and Evaluation*. Volume 2: Chemistry, SHRP A-368 Report, Strategic Highway Research Program, National Research Council, Washington, D.C., the U.S.A.

Chen, J. S., Huang, C. C., Chu, P. Y. & Lin, K. Y. (2007). Engineering characterization of recycled asphalt concrete and aged bitumen mixed recycling agent. *Journal of Materials Science*, 42, 9867-9876.

Christensen, D. C. & Anderson, D. A. (1992). Interpretation of dynamic mechanical test data for paving grade asphalt cements. *Journal of the Association of Asphalt Paving Technologists*, 61, 67-116.

Cong, P., Hao, H., Zhang, Y., Luo, W. & Yao, D. (2016). Investigation of diffusion of rejuvenator in aged asphalt. *International Journal of Pavement Research and Technology* 9, 280-288.

D'Angelo, J. A. (2009). The relationship of the MSCR test to rutting. *Road Materials and Pavement Design*, 10: sup1, 61-80.

Eberhardsteiner, L., Fussli, J., Hofko, B., Handle, F., Hospodka, M., Blab, R. & Grothe, H. (2015). Towards a micro structural model of bitumen ageing behavior. *International Journal of Pavement Engineering*, *16* (10), 939-949.

Ecker, A. (2001). The application of Iatroscan-technique for analysis of bitumen. *Petroleum and Coal*, *1* (1), 51-53.

Ferry, J. D. (1980). *Viscoelastic properties of polymers*. 3rd edition, John Wiley and Sons, New York, the U.S.A.

Hintz, C. & Bahia, H. U. (2013). Simplification of the linear amplitude sweep (LAS) test and specification parameter. *Journal of the Transportation Research Board*, 2370, 10-16.

Kim, Y., Lee, H. J., Little, D. N. & Kim, Y. R. (2006). A simple testing method to evaluate fatigue fracture and damage performance of asphalt mixtures. *Journal of the Association of Asphalt Paving Technologists*, 75, 755-788.

Leroy, G. (1989). Bitumen analysis by thin layer chromatography (Iatroscan), *Proceedings, 4th Eurobitume Congress* (4-6 October 1989, Madrid, 166-170.)

Masad. E., Somadevan, N., Bahia, H. U. & Kose, S. (2001). Modeling and experimental measurements of strain distribution in asphalt mixes. *Journal of Transportation Engineering*, *127* (6), 477-485.

Nellensteyn, F. J. (1928). Relation of the Micelle to the Medium in Asphalt. *Journal of the Institute of Petroleum Technologists*, 14.

Qatar Construction Specifications (QCS) (2014). Ministry of Municipality and Environment, Doha, Qatar.

Road Projects Department (RPD), Ashghal (2018). *Use of Crumb Rubber in RPD projects* (Circular No. (26)). Doha, Qatar, 28/10/2018.

Santagata, E., Baglieri, O., Dalmazzo, D. & Tsantilis, L. (2009). Rheological and chemical investigation on the damage and healing properties of bituminous binders. *Journal of the Association of Asphalt Paving Technologists*, 78, 567-596.

Santagata, E., Baglieri, O., Tsantilis, L. & Dalmazzo, D. (2013). Evaluation of self-healing properties of bituminous binders taking into account steric hardening effects. *Construction and Building Materials*, 41, 60-67.

Santagata, E., Baglieri, O., Tsantilis, L. & Chiappinelli, G. (2015). Fatigue and healing properties of nano-reinforced bituminous binders. *International Journal of Fatigue*, 80, 30-39.

Santagata, E., Yeganeh, S., Idris, O. E. M., Ali, M. H. M. M. & Al-Emadi, K. M. I. (2019). Chemical and rheological fingerprinting of bitumen employed in the State of Qatar. *Submitted to Construction and Building Materials*.

Sirin, O., Paul, D. K., Kassem, E. & Ohiduzzaman, Md (2017). Effect of ageing on asphalt binders in the State of Qatar: a case study. *Road Materials and Pavement Design*, 18: sup4, 165-184.

Wen, H. & Bahia, H. U. (2009). Characterizing fatigue of asphalt binders using viscoelastic continuum damage mechanics. *Journal of the Transportation Research Board*, 2126, 55-62.

Cite this article as: Santagata E., Yeganeh S., Idris O. M. E., Ali M. H. M. M., Al-Emadi K. M. I., "Test Procedures for Advanced Characterization of Bituminous Binders Employed for Pavement Construction in Public Works Authority Road Projects - State of Qatar", *International Conference on Civil Infrastructure and Construction (CIC 2020)*, Doha, Qatar, 2-5 February 2020, DOI: https://doi.org/10.29117/cic.2020.0063

Use of Crumb Rubber Modified Binders and Asphalt Mixtures in Public Works Authority Road Projects - State of Qatar

Ezio Santagata
ezio.santagata@polito.it
Department of Environment, Land and Infrastructure Engineering, Politecnico di Torino, Turin, Italy

Haissam Sebaaly
h.sebaaly@anas.com.qa
ANAS S.p.A., Qatar Branch, Doha, Qatar

Osman Elhusain Mohamed Idris
osmane@ashghal.gov.qa
Quality and Safety Department, Public Works Authority (Ashghal), Doha, Qatar

Moaaz Hashim M. M. Ali
moaaz@ashghal.gov.qa
Quality and Safety Department, Public Works Authority (Ashghal), Doha, Qatar

Khalid Mohd I Al-Emadi
kemadi@ashghal.gov.qa
Quality and Safety Department, Public Works Authority (Ashghal), Doha, Qatar

ABSTRACT

This paper illustrates the approach adopted by the Public Works Authority (Ashghal) of the State of Qatar for the widespread implementation in road projects of paving technologies related to the use of crumb rubber modified binders (CRMBs). Such an approach has entailed the monitoring of a full-scale preliminary trial, the definition of a prequalification system for crumb rubber and CRMB producers, and the development of mix design and quality control guidelines applicable to CRMB asphalt mixtures. Experimental results obtained in the preparatory phases of work and during the approval process of materials and mixtures are critically presented.

Keywords: Road pavements; Recycling; Crumb rubber; Asphalt; Mix design; Quality control

1 INTRODUCTION

The use of crumb rubber (CR) derived from end-of-life tires (ELTs) as a bitumen modifier has proven to be effective in enhancing the performance characteristics of asphalt mixtures worldwide (Way et. al., 2012). Currently available technologies fall within the category of the "wet processes" by means of which CR is directly incorporated in hot bitumen prior to mixing with aggregates, thereby leading to the formation of a binder characterized by enhanced elasticity and ductility (Bahia & Davis, 1994). Depending upon the quantity of added CR and on the adopted mixing technique, binders may either be of the "asphalt rubber" type (with CR dosages higher than 15% by weight of total binder) or of the "terminal blend" type (with CR dosages of 8-12%) (Bressi et al., 2019).

In the case of "asphalt rubber" binders, the CR-bitumen blend is cured in controlled conditions until the creation on the surface of CR particles of gel-like shells that are

responsible for mutual interactions (Artamendi & Khalid, 2006). The resulting binder is characterized by the presence of clearly visible CR particles and by a very high viscosity, thus leading to the need of either employing the binder immediately after production or keeping it in continuous agitation in properly equipped storage tanks. A further consequence of the peculiar structure of these binders is that their use is generally recommended in gap-graded or open-graded mixtures, which are characterized by the presence of voids in the mineral aggregates sufficient to include high binder volumes.

In case of "terminal blend" binders, a greater degree of digestion of the CR particles takes place in the bituminous medium, usually as a result of a finer grading (Way et al., 2012). The resulting binder is more homogeneous and, provided that its storage stability is initially evaluated, agitation prior to use may not be mandatory. Applications of these binders are similar to those of polymer-modified binders (PMBs), with the possibility of easily including them in dense-graded mixtures. It should be mentioned that the term "terminal blend" (which underlines the location of production) is frequently substituted by the more generic term, also adopted in this paper, "crumb rubber modified binder" (CRMB).

In the specific case of the State of Qatar, in the past there have been several full-scale applications involving the use of CRMBs. However, since these have not been organized as part of a general development program, their outcomes, which have been considered overall positive, cannot be analyzed on a quantitative basis. Furthermore, during the development of the road network, for infrastructures of strategic importance preference has been given to PMBs.

A renewed interest for the widespread implementation of CR technologies in Qatar has recently been stimulated by a scheme called "Ashghal Recycling Initiative", which has been launched by the Public Works Authority (Ashghal) in order to reduce construction costs, increase national self-sufficiency, limit environmental impacts, and enhance overall sustainability (Ashghal, 2018). Such an initiative has ultimately led to the enforcement of the use of CRMBs in lieu of PMBs for all projects overseen by the Road Projects Department (RPD) of Ashghal (RPD, 2018).

Implementation of CRMB technologies in Qatar has been supported by several activities carried out by the Quality & Safety Department (QSD) of Ashghal and by ANAS S.p.A. Qatar Branch as part of the ongoing QA/QC Pavement Consultancy Services contract. In particular, these activities included the preliminary assessment of CR availability, the monitoring of a full-scale trial, and the preparation of two QSD Memoranda, respectively containing specific guidelines applicable to the production of CR and CRMBs (QSD, 2018a) and acceptance criteria to be adopted in the mix design and quality control of CRMB mixtures (QSD, 2018b).

This paper briefly summarizes the abovementioned activities, with the purpose of sharing obtained results and of illustrating the rationale underlying the official documents issued by Ashghal.

2 AVAILABILITY OF CRUMB RUBBER

According to available data, in the State of Qatar there is an estimated annual generation of approximately 1.5 million ELTs (QDB, 2017). These have been for a long time discarded as waste but have then become of major interest for local companies

involved in their processing to produce CR which may be suitable for recycling.

As part of the preliminary activities of the QSD-ANAS team, the facilities of three different local CR producers were inspected, with the relevant assessment of employed technologies and potential productivity. It was found that the various plants combine size-reduction operations with other treatments (e.g. shredding, iron separation, granulation and sieving) in various configurations. However, all plants operate at "ambient" conditions, with no use of alternative techniques such as cryogenic milling or water jet-blasting. It is thus expected that resulting CR particles are irregular in shape and characterized by a significant surface roughness, which may lead to a high surface area available for interacting with bitumen in the production of CRMBs (Thodesen et al., 2009). All plants are capable of processing both truck tires, which are characterized by a higher content of natural rubber, and car tires.

Overall potential productivity of the plants was considered to be adequate for the local paving market, although it is envisioned that further improvements may be needed in the future in order to fully sustain the construction and maintenance of the road network.

3 FEASIBILITY FULL-SCALE TRIAL

In order to directly assess the local feasibility of CR recycling, a full-scale field trial was carried out on a local road, with the production and laying of a wearing course (WC) asphalt mix containing CRMB (50 mm thickness). For comparative purposes, the trial also included a WC asphalt mix with identical composition but containing PMB.

The RPD of Ashghal selected the trial location and organized construction operations. Given the preliminary nature of the activity, the involved Contractor was not required to perform a rigorous mix design of the CRMB mixture. Rather, reference was made to the Conformity Certificate of the mix containing gabbro aggregates and PMB (indicated as a PG76E-10). Target binder content for both mixtures was 3.9% by weight of total mix, while the target particle size distribution curve was of the continuous type, with 19.0 mm nominal maximum aggregate size.

The employed CRMB was produced by referring to the draft version of (QCS, 2018) (Section 6, Part 9), which was made available at the time of the trial. According to the manufacturer, the CRMB contained 11% CR by weight of total binder and was graded as a PG76V-10. The CR used for modification, derived from car and truck tires, was of the -30 mesh type (90-100% passing the 30-mesh sieve, with a 600 μm opening, and 100% passing the 20-mesh sieve, with a 850 μm opening).

Activities carried out by the QSD-ANAS team included critical observation of production and laying operations, and assessment of the most relevant characteristics of the produced mixtures. Experimental analyses were performed in the Ashghal Center for Research & Development (ACRD).

3.1 Composition and quality control testing

Samples of loose mixtures taken on site were subjected to tests for the determination of their composition as per ASTM D2172-17 and ASTM D5444-15. Binder content was found to be very close to target for both produced mixtures. Results of grading analyses were in most part contained within tolerance ranges, with the only exception of filler content, which was slightly lower than expected and reflected into low values of

the filler/bitumen ratio. Such a violation led to high values of the voids content, of the order of 9.0%, both in Marshall specimens and in the field. Nevertheless, the study was continued since it was envisioned that a meaningful comparison between the mixtures could be obtained from performance-based testing (see section 3.2).

Encouraging results were obtained for the CRMB mixture with respect to its potential durability, captured by means of the tensile strength ratio (TSR) evaluated as per ASTM D4867-14. In fact, although the average TSR value was relatively low (equal to 70%) as a result of the high voids content, it was identical to that which was found for the reference PMB mixture.

3.2 Performance-based testing

Performance-based testing of the two mixtures focused on the assessment of stiffness and resistance to permanent deformation. Specimens were compacted in the laboratory by means of different techniques (gyratory compaction as per AASHTO T312-15 and press box compaction as per AG:PT/T220) in order to reach a void content of 7.0 ± 0.5%.

Flexural stiffness tests were performed in the four-point bending configuration at 10 °C and 20 °C by imposing a bending strain equal to 50 microstrain (as per AG:PT/T274). Dynamic modulus tests were carried out in accordance with AASHTO T378-17 at three different temperatures (4 °C, 20 °C and 45 °C) and by considering three different stress states (corresponding to unconfined conditions and to confining pressures equal to 30 kPa and 60 kPa). Given that test results were available at temperatures covering a sufficiently wide range, dynamic modulus data were modelled by means of the approach indicated in AASHTO R84-17. Resistance to permanent deformation was assessed by means of flow number tests (as per AASHTO T378-17) carried out at 45 °C.

Experimental results obtained from stiffness tests clearly indicated that the two mixtures exhibited a similar response under loading. In the case of flexural stiffness (Figure 1), such a similarity was quite remarkable: the maximum recorded percentage difference for all frequencies and temperatures was as low as 3.3%, while the corresponding phase angle values were also very close to each other, with percentage differences never higher than 7.9%. When considering the results of dynamic modulus tests, greater differences were observed between the two mixtures. In particular, the CRMB mixture exhibited higher stiffness and lower phase angle values at all frequencies and temperatures. The percentage difference increased by considering progressively lower frequencies, whereas it was quite variable as a function of temperature. Plots of the dynamic modulus and phase angle, shifted as per master curve construction, are shown in Figure 2, which also displays dynamic modulus master curves. Hence, it was confirmed that in the uniaxial loading mode the CRMB mixture exhibited a stiffer and more elastic response with respect to the PMB mixture, especially at lower frequencies and lower confining pressures. It should be underlined that the dynamic modulus requirement set by (QCS, 2014) for SUPERPAVE mixtures (minimum value of 1,920 MPa at 45 °C and 10 Hz, no confining pressure) was satisfied by both mixtures, with values equal to 3,661 MPa and 2,810 MPa for the CRMB and PMB one, respectively.

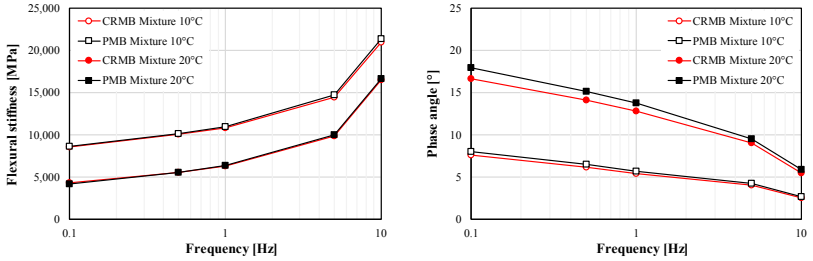

Figure 1: Results of flexural stiffness tests

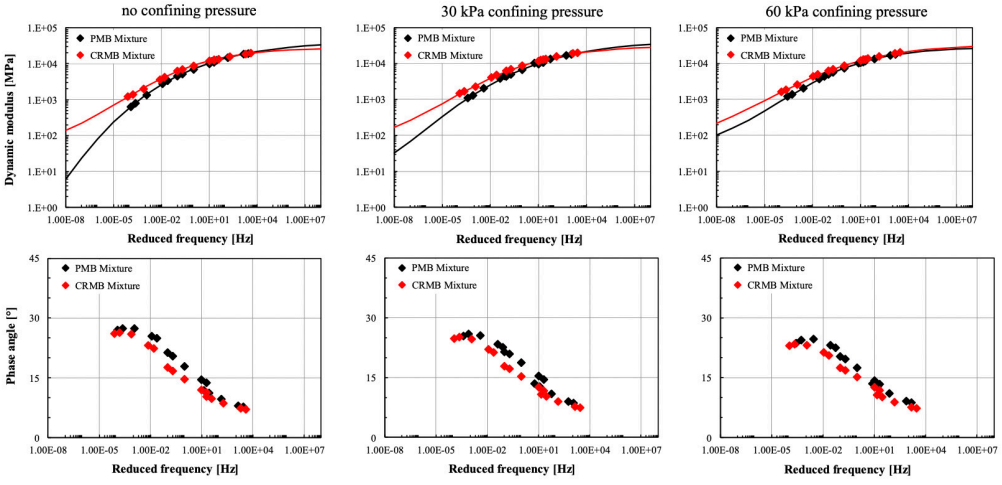

Figure 2: Dynamic modulus and phase angle master curves

Results obtained from permanent deformation tests are synthesized in Table 1, which contains average flow number values and corresponding void contents of specimens subjected to testing. Variation ranges of the measured parameters are also provided. Listed results clearly show that the two mixtures exhibited an equivalent resistance to permanent deformation. In particular, the difference between the average flow number values was equal to 3.4% and the corresponding variation ranges were found to overlap significantly. Finally, it should be emphasized that all flow number values well above the fixed acceptance threshold defined in (QCS, 2014) for the so-called SUPERPAVE mixes, equal to 740 at 45 °C.

Table 1: Results of flow number tests

	CRMB Mixture		**PMB Mixture**	
	Average	Range	Average	Range
Flow number (-)	8,415	8,134 - 8,695	8,140	7,014 - 9,386
Voids content (%)	7.0	6.9 - 7.1	6.8	6.7 - 6.9

Based on the results discussed above, it was concluded that CRMB mixtures, when compacted to target volumetrics, have the potential of being equivalent, and perhaps even superior, to PMB mixtures in terms of their load spreading capacity and resistance to rutting. However, in this stage it was clearly emphasized that further improvements were necessary in order to properly optimize the composition of CRMB mixtures. Thus,

further work was initiated in the ACRD, and is still in progress, for the evaluation of the volumetric and mechanical characteristics of trial CRMB mixtures.

4 QUALITY SYSTEM FOR CRMB MIXTURES

As a result of the preliminary activities described in sections 2 and 3, and by considering the outcomes of ongoing testing in the ACRD, the QSD-ANAS team worked on the fine-tuning of the quality system to be locally adopted for CRMB mixtures. In particular, the existing Ashghal QA/QC system was supplemented with the two previously mentioned QSD Memoranda (QSD, 2018a-b). The contents of these documents, prepared in line with (QCS, 2014) and with the draft of the upcoming (QCS, 2018), are synthesized in the following, with a discussion of key issues which should be addressed by all involved Parties (producers, consultants, contractors, third party laboratories).

4.1 Prequalification of CR producers

The purpose of the prequalification requirements made mandatory in the QSD Memorandum (QSD, 2018a) is to ensure the consistent production of high-quality CR, capable of acting as an efficient bitumen modifier. In such a context, constraints are imposed to CR particle size distribution and to its cleanliness, with a minimum quality control testing frequency of one determination (of each relevant parameter or quantity) for every 15 tons of production. The corresponding sampling methodology has been drawn from the experience of the California State Transportation Agency.

With respect to CR grading, only fine products of the -30 mesh type are allowed for use since they can be dispersed in bitumen more homogeneously, thereby reducing segregation potential. Furthermore, fine CR is more suitable for mixtures as those adopted in Qatar, characterized by a dense aggregate packing and by a rather low binder content.

Although the QSD Memorandum does not introduce any gradation acceptance band, CR producers are requested to report the full particle size distribution by referring to a subset of the ASTM D5644-18 series (30-mesh, 40-mesh, 80-mesh, 200-mesh and 400-mesh). This is due to the fact that surface area is highly affected by finer particles, and it is envisioned that in the future specific measurements of such a parameter may be introduced in the prequalification stage for a better control of CR quality (Santagata et. al., 2012).

With respect to CR cleanliness, various parameters need to be monitored throughout production (by following prescribed procedures) and continuously compared to allowable maximum thresholds or acceptance ranges. Relevant parameters include specific gravity and content of moisture, non-ferrous and ferrous metal particles, fibers, and foreign contaminant materials. It should be noted that most of the requirements have been drawn from those contained in ASTM D6114-19, which have been extensively validated for the assessment of CR products employed for asphalt rubber production.

It should be underlined that there are no restrictions on CR origin, since the QSD Memorandum allows the use of products derived from car and/or truck tires. However, producers need to clearly declare the origin of processed ELTs.

When considering the applications received by QSD since the issue of the Memorandum, it was observed that all local CR producers were able to meet the requirements synthesized above.

4.2 Prequalification of CRMB producers

In line with the high standards required for the prequalification of all manufacturers involved in the pavement construction supply chain, the QSD Memorandum (QSD, 2018a) requires CRMB producers to give full evidence of their quality management system and provide relevant information on their production plant and staff. As in the case of CR, prequalification requirements have the function of ensuring the consistent production of uncontaminated high-quality CRMBs, which have to possess rheological properties that match the prevalent loading and environmental conditions occurring in road pavements in the State of Qatar. Required quality control testing entails the verification of set requirements on each batch, defined as the quantity of binder produced and stored in one tank once the production run into that tank has been completed.

CRMB producers are required to clearly state the source of employed CR, providing all the necessary supporting documents, and to declare the adopted modification dosage, which should be comprised between 10% and 25%. While the lower limit is consistent with the usual formulation of terminal blend binders, the upper one, more typical of asphalt rubber products, allows producers to develop more advanced formulations, thus including the potential introduction of improved technologies which may lead to a reduction of bitumen consumption and to an increase of the cost-effectiveness of production. As a result of the performance-based nature of acceptance requirements, no tests are necessary for the verification of CR dosage. Nevertheless, this type of analysis may be taken into consideration in the future for a critical evaluation of construction costs and in the context of Green Public Procurement policies and of Life Cycle Analyses (Farina et al., 2017). This will require specific research work in the ACRD, which will be carried out by considering relevant investigations documented in literature (Zanetti et al., 2018).

Although purity requirements are already introduced in the CR prequalification process, additional verifications, to be carried out directly on the CRMB, were deemed necessary. These were expressed by referring to the outcomes of a two-step laboratory procedure which combines binder solubility (as per ASTM D5546-09 or AASHTO T44-14) and burning with an ignition oven at 400 °C for 1 hour. The maximum allowable weight of the resulting residue, equal to 1% of the original sample, ensures the absence of contaminants and is consistent with CR requirements and typical CRMB formulations. Furthermore, assessment of the residue after the solubility test may provide information on the degree of digestion of the CR particles during production, thereby allowing a critical assessment of the adopted production technology.

With respect to rheological properties and to the corresponding SUPERPAVE grading, it is well known that the climate encountered in Qatar calls for the use of binders belonging to performance grade PG76-10 (Al-Abdul Wahhab et al., 1997). QCS (2014) contains such a requirement for PMBs, by referring to the original SUPERPAVE scheme implemented in AASHTO M 320-17 and by considering the application of the more recent scheme of AASHTO M 332-14 as an option.

The QSD Memorandum refers to AASHTO M 332-14 for the assessment and grading of CRMBs. However, it removes the requirements therein contained for solubility, non-recoverable creep compliance difference (J_{nrdiff}, which needs only to be reported), and viscosity (once again only to be reported). These modifications to the specification

scheme are respectively due to the specific nature of CRMBs (characterized by the presence of insoluble, not completely digested rubber residues), to the specific non-linear response under oscillatory loading (which makes the current J_{nrdiff} limits not applicable) and to the use of efficient pumping systems in asphalt mix production (which can handle high viscosity binders). Furthermore, in order to account for the presence of undigested rubber particles in the binder, rheological tests for binder grading carried out in the oscillatory mode (as per AASHTO T315-10 and AASHTO T350-19) are required to be conducted with an increased measurement gap of 2 mm. Such a prescription is consistent with current research and has been proven to be effective for the reliable assessment of the rheology of CRMBs.

It should be underlined that the QSD Memorandum explicitly requires CRMBs to be stored in continuously agitated tanks, both at the modification terminal and the asphalt plant. Such a constraint was deemed necessary regardless of CR dosage in order to avoid any risk of segregation, which may jeopardize the successful implementation of CRMB technologies.

Results documented in the applications submitted to QSD for approval indicate that the CRMBs produced by two different manufacturers (containing CR only from truck tires) easily met all the requirements synthesized above. In particular, they were all reported to be PG76E-10 and exhibited viscosity values at 135 °C which satisfied the waived requirement of AASHTO M 332-14.

4.3 Mix design and quality control of CRMB mixtures

The QSD memorandum which focuses on the mix design and quality control of CRMB asphalt mixes (QSD, 2018b) is consistent with QCS 2014. However, additional requirements have been introduced in order to account for the particular nature and behavior of CRMBs.

With respect to mix design, it is left to the Contractor to decide whether to adopt the classical Marshall method, or to adopt the more advanced SUPERPAVE approach. In both cases, as for all other mixtures certified for use in Qatar, approval of the mix design requires a preliminary laboratory study followed by trial batching and trial laying. Quality control is carried out by referring to the sampling and testing frequencies listed in (QCS, 2014), supplemented by further indications which apply to the newly introduced tests described in the following.

Requirements referred to in both the mix design and quality control process are taken from (QCS, 2014), considering those defined for PMB mixtures as prevalent (if present). Additional acceptance limits are introduced for Marshall-designed mixtures with respect to the results of Indirect Tensile Strength (ITS) tests carried out at 25°C, before and after static water immersion (as per ASTM D4867-09). Furthermore, in the case of all mixtures (Marshall- and SUPERPAVE-designed), reference is made to the results of Hamburg wheel-track (HWT) tests carried out on water-submerged specimens (as per AASHTO T324-19). It should be clarified that rather than for the assessment of moisture sensitivity, these procedures were selected for the evaluation of strength and resistance to permanent deformation in extreme conditions, thereby ensuring the identification of durable mixes regardless of the environment in which they are placed. Thus, a minimum TSR value of 75%, slightly lower than those adopted in other specifications, was considered adequate

for such a purpose in the case of Marshall mixtures. The standard limiting maximum rut depth of 12.5 mm was considered for HWT tests: these were preferred to flow number tests in accordance with current international trends.

Results obtained in the prequalification of four wearing course CRMB asphalt mixtures approved by QSD are synthesized in Table 2, where they compared to the acceptance limits. All Contractors chose the Marshall design option. In the mix design phase tests were carried out only by third party laboratories, whereas in the plant verification phase tests were also performed by the ACRD. All mixtures contained gabbro aggregates with a similar continuous total grading (not displayed in this paper).

Table 2: Results of mix design tests (Marshall-designed wearing course asphalt mixtures)

	Acceptance limits	Mixture #1		Mixture #2		Mixture #3		Mixture #4	
		Mix design	Plant trial	Mix design	Plant trial	Mix design	Plant trial	Mix design	Plant trial
Optimum binder content (OBC), %	3.4 - 4.4	4.1	4.1	4.2	4.1	4.0	4.0	4.0	4.2
Air voids (Va), %	5.0 - 8.0	6.2	7.2	5.9	6.5	5.9	6.3	6.0	6.3
Voids in mineral aggregate (VMA), %	≥ 14.0	14.6	15.6	15.8	15.4	15.5	14.3	15.1	14.9
Voids filled with asphalt (VFA), %	50 - 75	58	54	62	58	59	56	60	58
Marshall stability (Sta), kN	≥ 13.0	16.8	13.5	15.7	18.5	19.5	16.9	17.3	15.3
Marshall flow (F), mm	2.0 - 4.0	2.9	2.5	2.7	2.5	2.6	2.64	2.3	2.8
Marshall quotient (Sta/F), kN/mm	≥ 5.25	5.69	5.40	5.86	7.40	7.5	6.40	7.3	5.46
Air voids at 400 blows per face, %	≥ 4.0	4.2	4.4	4.4	4.5	4.4	4.1	4.5	4.9
Retained stability, %	≥ 75	89	94	86.9	90	84	85	96	83
Tensile strength ratio (TSR), %	≥ 75	78	81	77	84	78	79	76	81
Filler to bitumen ratio (F/OBC)	0.75 - 1.35	1.03	0.95	0.90	0.76	1.10	1.25	1.07	1.05
Rut depth from HWT test, mm	≤ 12.5	6.6	4.7	5.6	7.2	3.2	3.7	4.3	3.8

From the analysis of the data listed in Table 2 it can be observed that the considered mixtures were characterized by similar optimum binder content values (comprised in the 4.0-4.2 range), close to those of typical PMB wearing course mixtures employed in Qatar. As a consequence of such a similarity (and of the previously mentioned similarity in aggregate grading), volumetric and mechanical characteristics of Marshall-compacted specimens were also contained in very narrow ranges. All mixtures were characterized by a dense aggregate packing (revealed by the contained values of the voids in the mineral aggregate, VMA) combined with a sufficiently limited volume of binder (indicated by the voids filled with asphalt, VFA), which led to satisfactory mechanical properties. It is interesting to underline that the newly introduced TSR and HWT requirements were met, with average values of corresponding parameters equal to 79.3% and 4.9 mm. Only for one mix (#4) use was made of an anti-stripping agent, employed with a dosage of 0.5% by weight of binder.

5 CONCLUSION

Based on the discussion of the activities presented in this paper, it can be concluded that implementation of CRMB technologies in Qatar is proceeding in accordance with the plans of the “Ashghal Recycling Initiative”. Local CR and CRMB producers have shown to be capable of meeting the recently issued prequalification requirements and several contractors have already obtained official approval of their asphalt mix designs. Ashghal will seek further improvements in the future, by continuously supporting the application of proposed quality control measures and by sustaining research activities carried out in the ACRD.

REFERENCES

Al-Abdul Wahhab, H. I., Asi, I. M., Al-Dubabe, I. A. & Farhat Ali, M. (1997). Development of performance-based bitumen specifications for the Gulf countries. *Construction and Building Materials*, *11*(1), 15-22.

Artamendi, I. & Khalid, H. A. (2006). Diffusion kinetics of bitumen into waste tire rubber. *Journal of the Association of Asphalt Paving Technologists*, 75, 133-164.

Ashghal (2018). *Roadmap for implementation of Ashghal Initiative of recycling in construction projects* (Circular No (69)). Doha, Qatar, 09/05/2018.

Bahia, H. U. & Davis, R. (1994). Effect of crumb rubber modifiers (CRM) on performance-related properties of asphalt binders. *Journal of the Association of Asphalt Paving Technologists*, 63, 414-449.

Bressi, S., Fiorentini, N., Huang, J. & Losa, M. (2019). Crumb rubber modifier in road asphalt pavements: state of the art and statistics. *Coatings*, *9*(6), Article number 384.

Farina, A., Zanetti, M. C., Santagata, E. & Blengini, G. A. (2017). Life cycle assessment applied to bituminous mixtures containing recycled materials. *Resources, Conservation & Recycling*, 117, 204-212.

Qatar Construction Specifications (QCS) (2014). Ministry of Municipality and Environment, Doha, Qatar.

Qatar Development Bank (QDB) (2017). Materials Recovery, Doha, Qatar.

Quality and Safety Department (QSD), Ashghal (2018a). *Pre-qualification of Crumb Rubber and Crumb Rubber Modified Binder Producers*, Doha, Qatar, 13/12/2018.

Quality and Safety Department (QSD), Ashghal (2018b). *Guidelines for Mix Design and Quality Control of CRMB Asphalt Mixes*, Doha, Qatar, 18/11/2018.

Road Projects Department (RPD), Ashghal (2018). *Use of Crumb Rubber in RPD projects* (Circular No. (26)). Doha, Qatar, 28/10/2018.

Santagata, E., Dalmazzo, D., Lanotte, M., Zanetti, M. C. & Ruffino, B. (2012). Relationship between crumb rubber morphology and asphalt rubber viscosity. *Proceedings, 5th Asphalt Rubber Conference*, Munich, Germany, 513-532.

Thodesen, C., Shatanawi, K. & Amirkhanian, S. (2009). Effect of crumb rubber characteristics on crumb rubber modified (CRM) binder viscosity. *Construction and Building Materials*, 23, 295-303.

Way, G. B., Kaloush, K. E. & Biligiri, K. P. (2012). *Asphalt-rubber standard practice guide, Rubber Pavements Association*, Tempe, Arizona, the USA.

Zanetti, M. C., Ruffino, B., Santagata, E., Dalmazzo, D. & Lanotte, M. (2018). Determination of crumb rubber content of asphalt rubber binders. *Journal of Materials in Civil Engineering, 30* (4), Article number 04018041, 1-6.

Cite this article as: Santagata E., Sebaaly H., Idris E. M. O., Ali M. H. M. M., Al-Emadi K. M. I., "Use of Crumb Rubber Modified Binders and Asphalt Mixtures in Public Works Authority Road Projects - State of Qatar", *International Conference on Civil Infrastructure and Construction (CIC 2020)*, Doha, Qatar, 2-5 February 2020, DOI: https://doi.org/10.29117/cic.2020.0064

Using Ground Penetrating Radar (GPR) to Evaluate Air Voids Content in Hot Mix Asphalt

Pejman Dehdezi
p.dehdezi@fugro.com
Fugro, Doha, Qatar

ABSTRACT

Air voids content is one of the most important characteristics of Hot Mix Asphalt (HMA). Air voids content that is either too high or too low can negatively impact pavement life and lead to deteriorations such as fatigue cracking, rutting, raveling, bleeding, and moisture damage. Currently destructive testing, such as coring, is typically conducted to evaluate in-situ air voids content of placed HMA. Asphalt coring, by its nature, is highly localized and therefore can easily miss localize areas of low quality. In addition, in large projects, there are some concerns expressed on the aesthetic deficiencies with respect to the number of cores in the wearing course and the introduction of potential weak spots within the pavement structure. In other methods of air voids determination, such as nuclear density gauge, there are also concerns regarding safety, costs associated with radioactive material licensing and requirements for closing off work areas. In this paper the use of a "GSSI PaveScan RDM" GPR model for non-destructive assessment of in-situ air voids in HMA is investigated. In-situ air voids content can be determined through plotting of dielectric changes with measured cores' air voids content. This technique provides an opportunity for continuous measurement of air voids in HMA and, at the same time, faster and reliable in-situ data for QA/QC. These benefits can significantly accelerate pavement construction and so this paper looks to proliferate the adoption of such practice. The case study on Al Khor Expressway, one of the major expressways in Qatar, has demonstrated good repeatability and correlation with measured air voids content.

Keywords: Ground Penetrating Radar (GPR); Hot Mix Asphalt (HMA); Air voids; Quality assurance; Non-destructive testing

1 INTRODUCTION

The air voids content of HMA, achieved by contractors at the time of construction, is the most important factor that affects the long-term durability of the pavement. The compaction process on site is the practice to control the air voids content of the HMA. In Qatar, properly designed HMA should have an air voids content in the range of 5% to 8% (QCS, 2014).

The primary performance concern of an HMA with low in-place air voids content could be deformation resistance (or rutting). Previous research shows that significant rutting was likely to occur once the in-place air voids fall below 3% (Brown, 1990). On the other hand, the primary performance concern of high in-place air voids content would be reduction in pavement fatigue life. Several researchers have reported that fatigue properties can be reduced by 30 to 40% for each 1% increase in air voids content from

5 to 8% (Linden et.al., 1989). Accelerated ageing, moisture damage, raveling, bleeding, decrease in stiffness and strength are other pavement distresses that would occur as a result of HMA air voids content that is either too high or too low.

Currently destructive methods are the most common methods for determination of density and air voids content in HMA. Many road owners specify destructively cutting cores in the pavement to determine air voids content of HMA. The drawbacks of destructive pavement coring are that the locations are randomly chosen, the process is destructive and relatively expensive, and it is labor intensive. Most importantly, it is time consuming and does not provide immediate feedback to the contractor on the HMA air voids content. Furthermore, aesthetic deficiencies with respect to the number of cores in the wearing course and the introduction of potential weak spots within the pavement structure are of concern.

Other existing technologies such as nuclear density gauges and electromagnetic density indicators (Figure 1) are alternative techniques to pavement coring that are currently used in the United States and Europe. However, these techniques are non-destructive, they can only be used for spot density (or air voids) measurements. Problems reported with these devices are usually caused by large variations in surface texture (Sebesta et al., 2013). In addition, there are particular concerns on using nuclear density gauge such as safety, costs associated with radioactive material licensing and requirements for closing off work areas.

This paper focuses on a case study of using Ground Penetrating Radar (GPR) as an alternate non-destructive evaluation of air voids content in newly constructed HMA. This technique has been used for the first time in the State of Qatar to determine the in-place air voids content of the HMA. The use of GPR as a rapid non-destructive technique can provide real-time information to paving contractors so that corrective action can be taken immediately. It must also be noted that GPR has been used for many years to determine asphalt layer thickness; however, this is the first time that this technique has been used as an alternative to coring and other non-destructive methods (e.g. nuclear and non-nuclear density gauges) to determine in-place air voids of HMA.

Figure 1: Nuclear density gauge and electromagnetic density indicators (Sebesta et al., 2013)

2 METHODOLOGY

GPR is an echo sounding method where a transducer (transmitter/receiver) is

passed over the surface at a controlled speed. Short duration pulses of radio energy are transmitted into the subject and reflections from material boundaries and embedded features such as metalwork or voids are detected by the receiver. Sampling is so rapid that the collected data effectively constitutes a continuous cross section, enabling rapid assessment of density and condition over large areas. By assessing the amplitude, phase, and velocity of the signals from within the material, type and density of materials can be identified.

A case study was conducted on Al Khor Expressway utilizing a "GSSI PaveScan RDM" (Figure 2) GPR model integrated with GPS systems. The project deals with the construction of 34-km ten-lane dual carriageway expressway with 12 viaducts, eight road junctions, pedestrian footpaths, and two cycle lanes. Pavement construction consists of 3 asphalt layers (i.e. wearing course, base course class B, and base course class A) overlying roadbase and subbase layers, each approximately 150 mm thick and overlaying 500 mm of imported subgrade.

Pavescan RDM measurements are dielectric values. Dielectrics can be converted to physical properties (e.g. density and air voids content) by generating a least-squares fit relationship derived from dielectric values and known air voids content obtained over a range of dielectric values. Di-electric properties of HMA were determined through transmitted high frequency radio signal (2 GHz) into the ground (few millimeters below the surface) and receiving pairs of the array. The data was collected at walking speed (approximately 1.5m/s). The overspeed indicator in the status bar will turn red if the operator is walking too fast. A provisional standard has been developed by American Association of State and Highway Transportation Officials (AASHTO, 2019) on "Best Practice for Asphalt Surface Dielectric Profiling System using Ground Penetrating Radar" and the standard's procedure was followed in this study.

A series of core samples at known dielectrics were extracted from the site and air voids content of each core was determined in the laboratory. Air voids content (%) vs. dielectric values were plotted and a least-squares-fit line was used to calculate the air voids content from subsequent dielectric values. The test was conducted on different layers (i.e. wearing course, base course class B, and base course class A as per (QCS, 2014)) and the measurement results on the wearing course are presented in the next section.

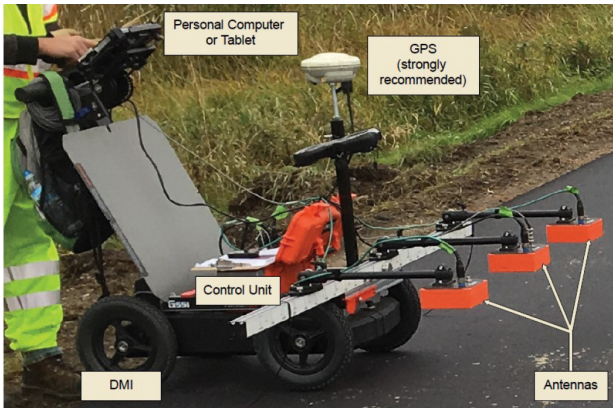

Figure 2: GSSI PaveScan RDM model with three antennas 0.5m apart

3 RESULTS AND DISCUSSION

Figure 3 shows the relationship between dielectric readings taken from the GPR and air voids content measured on 39 extracted pair of core samples from the wearing course layer. A least-squares fit relationship with a coefficient of determination (i.e. R-square, R^2) of 0.79 was generated.

The established relationship between di-electric and air voids was used to calculate the air voids content from subsequent dielectric values. Figure 4 shows an example of data collected on a section of the expressway using GSSI PaveScan RDM. Colorful graphs refer to data collected by 3 antennas. In order to validate the data, additional pairs of cores have been extracted from the site (under each antenna) and their air voids content measured in the laboratory. As shown in Figure 4, the measured air voids content of the core samples are in good agreement with collected GPR data. The difference in di-electric measurements between the 3 antennas, as it is clear in Lane 1 (Figure 4), can also be used as an indication of aggregate segregation on surface of the asphalt layer

Further analyses have been performed to establish the accuracy of the GPR data. A Root Mean Square Error (RMSE) of 0.55 was calculated which proves that the GPR tool can be used as a predictive tool to estimate the in-place air voids content of HMA with an average accuracy of ±0.55. Further study needs to be performed to investigate the effect of HMA temperature, ambient temperature, and presence of moisture on the surface of HMA on the di-electric readings from the GPR.

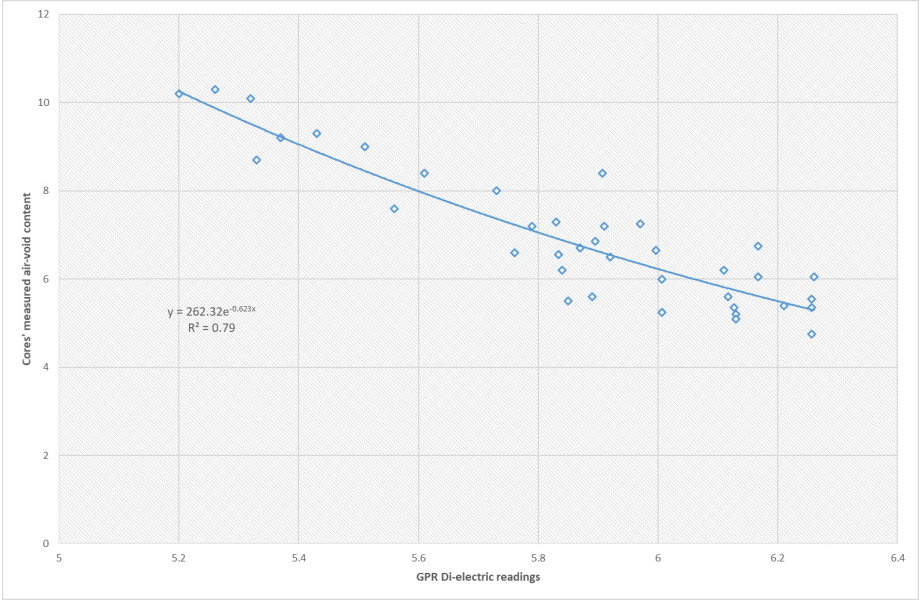

Figure 3: Relationship between GPR di-electric readings and air voids content of extracted cores

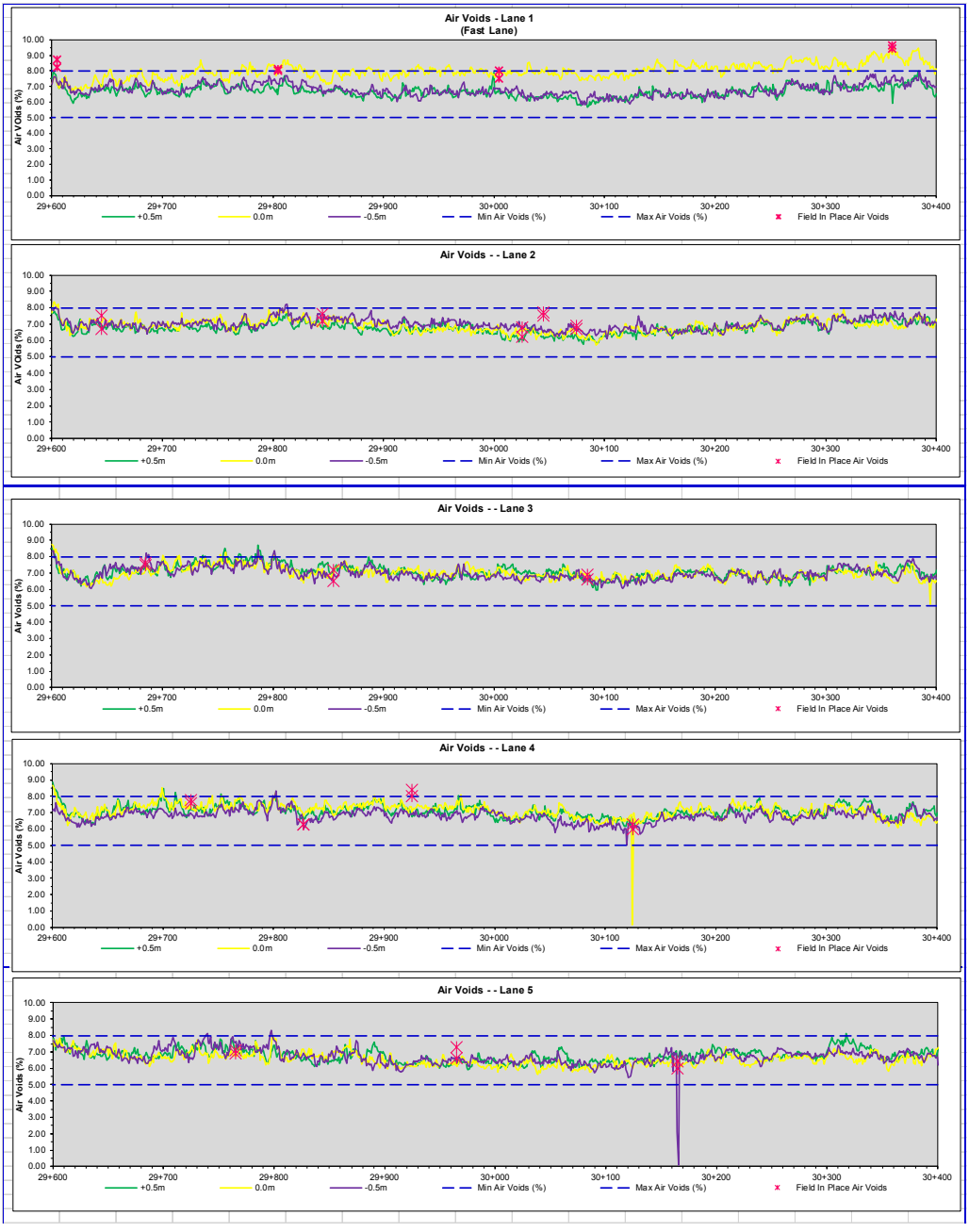

Figure 4: Example of data collected on a section of the expressway using GSSI PaveScan RDM

4 CONCLUSION

Obtaining adequate in-place air voids content is vital for achieving pavement durability for Hot-Mix Asphalt (HMA) pavement. A case study was carried out to use Ground Penetrating Radar (GPR) as an alternative non-destructive evaluation of air voids content in newly constructed HMA. “GSSI PaveScan RDM” GPR model integrated with

GPS systems was utilized to determine in-place air voids content. The data collected by the GPR demonstrated good repeatability and correlation with cores' measured air voids content with a Root Mean Square Error (RMSE) of ±0.55. This technique provides an opportunity for continuous measurement of air voids content in HMA and, at the same time, faster and reliable in-situ data for QA/QC which subsequently accelerate pavement construction significantly.

REFERENCES

American Association of State and Highway Transportation Officials (AASHTO) (2019). Asphalt Surface Dielectric Profiling System Using Ground Penetrating Radar. AASHTO PP 98-19, Washington, D.C., the USA.

Brown, E. R. (1990). *Density of Asphalt Concrete – How Much Is Needed*. Transportation Research Board 1282, TRB, National Research Council, Washington, D.C.

Linden, R.N., Mahoney, J. P. & Jackson, N. C. (1989). *Effect of Compaction on Asphalt Concrete Performance*. Transportation Research Record 1217, TRB, National Research Council, Washington, D.C.

Qatar Construction Specifications (QCS) (2014). Section 6: Part 5, Roadworks, Ministry of Municipality and Environment.

Sebesta, S., Scullion, T. & Saarenketo, T. (2013). *Using Infrared and High-Speed Ground-Penetrating Radar for Uniformity Measurements on New HMA Layers*. (Report S2-R06C-RR-1). Strategic Highway Research Program, National Transportation Board, Washington, D.C.

Cite this article as: Dehdezi P., "Using Ground Penetrating Radar (GPR) to Evaluate Air Voids Content in Hot Mix Asphalt", *International Conference on Civil Infrastructure and Construction (CIC 2020)*, Doha, Qatar, 2-5 February 2020, DOI: https://doi.org/10.29117/cic.2020.0065

Recycled Concrete Used in Subbase in Potential Use for Road Base and Cement Bounded Material (CBM)

Hassan Haidar Ahmad
hhaidarahmad@gmail.com
Al Jaber Hadid Construction, Doha, Qatar

ABSTRACT

Structure life cycle and economic developments in Qatar can lead to reconstruction as well as demolition of structures such as buildings and roads. One of the main wastes from demolition work is concrete and reinforced concrete. Concrete dumped as waste in landfills in Qatar, so this paper will emphasis utilizing the concrete waste through means of recycling and reusing in the road construction market. Qatar's benefit is to decrease pollution, generating economic benefits and become more self-sustainable and save its existing resources. This paper will focus on the fine recycled concrete (FRC) 0-5 mm as a fine aggregate material in the mix design for constructing the base road layers under the Asphalt layers and how using crushed concrete can increase the quality and change the classification of the base aggregate mixes. After the process of concrete crushing, the crushed material will be produced and used as fine aggregate in a fixed amount of fine crushed concrete which can improve the properties of the mix design for base road construction (aggregate base) produced in different production dates. This can decrease the use and import of sand (dune sand and washed sand) from overseas, in the mix designs for Subbase, Road Base and Cement bounded material (CBM) and increase the quality in Qatar. The paper will verify the use of fine crushed concrete (FRC) in the aggregate mixes to upgrade the quality of the fine aggregate material used in the road construction (Goonan, 1998).

Keywords: Recycled concrete; Sub-base; Road base; Cement bounded material

1 INTRODUCTION

Finding purposes for waste materials are more popular by reuse and recycle process. This is due to a shortage of aggregate sources, increasing waste cost, and increasing the demand of material, so crushing the aggregates for the construction purposes makes an impact on resource due to demand of material and environmental degradation, in addition, the recycled materials create many economic and environmental benefits. Fine Crushed concrete can be considered as an alternative solution and a useful source of aggregate for the construction industry in Qatar. International research has been revealed that recycled concrete aggregates can be applied complete or incomplete. However, they had proven that the fine portion of Recycled Concrete makes intangible effects on the mix properties of base aggregate material.

Throughout this study, it is evident that using recycled crushed concrete for the fine portion of the base aggregate design mixes which prove ideal for the full mix by improving the mix design quality. As stipulated by QCS 2014 and the range of materials to be used, crushed concrete can be utilized for subbase road base and CBM; for example,

when using crushed concrete in the 0-5 mm content of a mix design for subbase, the properties improve the whole design to satisfy the requirements for road base and CBM.

Fine recycled concrete classifications should be taken in consideration for the variability of material consistency, performance, and evaluation for the characteristics of an unbounded and bounded material constructed using the fine recycled concrete and subjected to real traffic loading. This paper presents the results for classification tests of six different mixes samples to analyse the feasibility of using the FRC material in unbounded material (subbase & Road base) mixes comparing their classification properties with the original unbound aggregate materials used in Qatar.

2 MATERIAL DESCRIPTION

In this paper, one available fine recycled concrete product, obtained from a crusher plant in Qatar. Material sources are crushed from the waste of concrete of the building. The collected materials are undergone a normal crushing process to produce fine recycled concrete. Table 1 shows the maximum and the minimum percentages of the coarse and fine aggregate that create subbase and Road base as unbounded material. These three aggregate materials sizes were blended in a fixed combined aggregate percentage by weight of the total mix from different date production to form six samples which represent a combination of fine and coarse aggregates Table 2 shows the combined aggregate percentages, original sample was used for the purpose of comparing the properties of the mixes which prove the consistency for the produced material (Kelly & Thomas, 1996).

Table 1: Minimum and Maximum Percentage in Mix

Maximum and minimum limits of each Constituent (percentage by mass)			
	Coarse Aggregate	**Fine Aggregate**	**Fine Recycled Concrete FRC**
Road base & Subbase	70-65	15-14	20-16

*FRC-Fine Recycled Concrete

Table 2: Combined Blending Percentages

Size in mm	**50.0**	**37.5**	**19.0**	**9.5**	**4.75**	**0.600**	**0.075**
Original material (no FRC)	100.0	100.0	75.2	58.7	42.9	15.8	3.5
Mix 1	100.0	100.0	85.9	68.0	44.5	18.1	3.7
Mix 2	100.0	100.0	77.5	59.2	39.5	14.2	3.1
Mix 3	100.0	98.7	76.6	63.4	43.5	20.5	8.9
Mix 4	100.0	98.9	73.7	55.3	41.4	16.8	5.0
Mix 5	100.0	100.0	72.6	60.0	48.7	17.5	2.8
Mix 6	100.0	100.0	84.4	63.6	41.5	18.3	4.6
Average of results	100.0	99.6	78.5	61.6	43.2	17.6	4.7
Minimum as per QCS 2014 S6 p4	100	95	70	50	35	12	0
Maximum as per QCS 2014 S6 P4	100	100	92	70	55	25	8

3 LABORATORY TESTING AND RESULTS ANALYSIS

Usually fine recycled concrete (FRC) materials are highly inconsistent and include different amounts of impurities and their quantities are not cumulative. This makes FRCs have a specific classification property, so to characterize the properties of FRCs through classification tests such as sieve analysis test, Atterberg limits test, Sand equivalent, to investigate the possible range of material properties that lead to pursuing the use specific material in the related mix. The results were compared with the minimum or maximum acceptable requirements for subbase and road base materials as per Qatar Construction Standards (QCS, 2014, section 6 part 4).

4 MATERIAL SIZE DISTRIBUTION TEST

Aggregate size distribution of an unbounded material mix type affects its Atterberg limits, Sand equivalent, and maximum dry density (MDD) so the size distribution of soil aggregate is important because the size of the aggregate determine their susceptibly to movement (erosion) so the gradation results of all six mixes obtained from material size distribution analysis are shown in Figure 1.

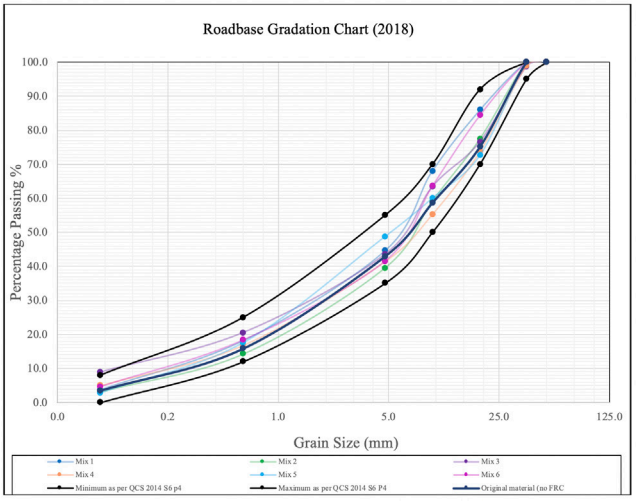

Figure 1: Gradation Curves for The Six Mixes with The Limits Required QCS 2014 S6 P4

As shown from the graph that all samples were equivalent in the size distribution and satisfy the requirements as per QCS 2014 section 6 part 4 (Table 4.4)

5 ATTERBERG LIMITS TEST

The Atterberg limits test is a basic test used to find the critical water contents for fine-grained soil. Casagrande method as per ASTM D4318 was used to determine the liquid limit test (LL) as well as plastic limit test (PL) for the 6 samples with FRC typical sample used, these results help in proposing the design of the road and to show the behavior of soil material in road construction in another word under the layers of road asphalt.

Liquid Limit is the limiting water content at which reactive soil changes from a liquid to a plastic status and the Plastic Limit is the limiting water content at which reactive soil changes from a plastic to a semisolid state so Plasticity Index (PI). The

higher PI the higher clay content.

The liquid limit (LL) and the plastic limit (PL) test values were summarized in Figure 2. According to QCS (2014) specifications, the maximum Liquid limit is 25 % & the plasticity index (PI) is 6 % for Road base and subbase layers and FRCs material show it is Non-plastic.

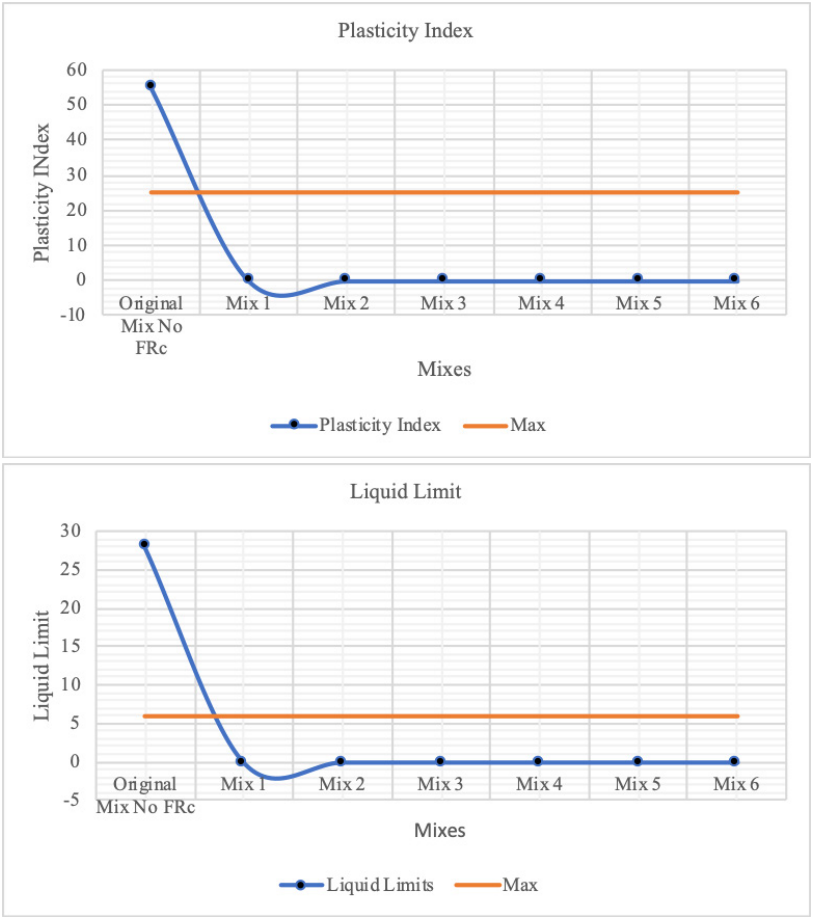

Figure 2: Summary of Plasticity Index and Liquid Limit Tests

As shown from the graph, adding the FRC content substantially improved the samples when compared with the opriginal material where no FRC and all mixes fall below the maximum limit requiored by (QCS, 2014) section 6 part 4 (table 4.1).

6 SAND EQUIVALENT TEST

The sand equivalent test is a test that shows the attributes of the fine clay in the fine aggregate. The sand equivalent test delineates that most of the fine aggregates are mixtures from the fine waste of coarse particles and generally reactive clay and the characteristics of clay-like material present. As a specific description the sand equivalent test, a sample of aggregate will be prepared from the fine aggregate and then added to cylinder with a specific solution to separate the fine and the coarse aggregate of the fine aggregate passing the 4.75 mm then additional separation will be done by adding the

cylinder to a mechanical shaker which will lead to a total separation of dust from the fine aggregate, so the sand equivalent test dominate on calculating the percentage of sand equivalent from the sand reading over the clay reading, so higher sand equivalent reflect to two parts first that the material contains less amount of dust and second the material contain high sand amount in the fine aggregate but this will not clarify the cleanness of the material because there is high sand equivalent for some materials but the clay content is destructive for the material and the mix.

The Sand equivalent test method is done as per ASTM D2419 and it is used for the original material FRC and the 6 mixes and the values are summarized in Figure 3. According to QCS (2014) specification, the minimum limit for Sand equivalent for subbase is 25 % and for Road base is 35 % but all the mixes were done to satisfy subbase and road base mix without any additional charge on the material cost.

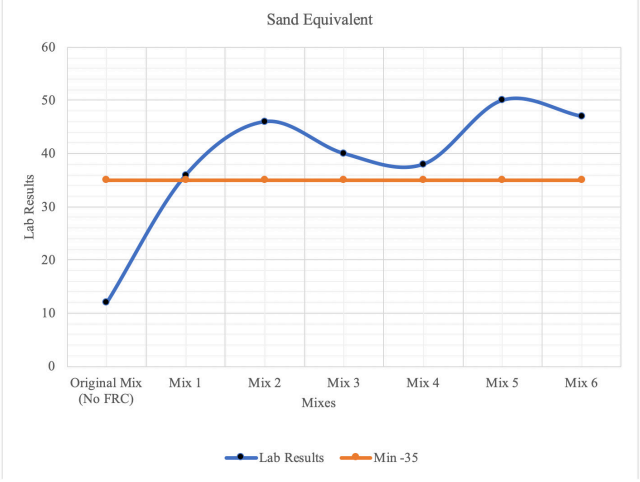

Figure 3: Sand Equivalent Tests Results

7 MAXIMUM DRY DENSITY (MDD) TEST

The compacted soil must be stable enough to carry the traffic load without any undesirable settlements or even deformation of the surface for the compacted soil during the laying process and during the construction period. The compacted soil is tested on-site by the nuclear density machine (NDT) and use the maximum dry density with the moisture content. This soil is compacted with reference to the MDD prepared from a sample collected for the construction site, tested and verified by site laboratory. The percentage of compaction required for the soil is 100 % in the constructed area but sometimes the result of the compaction varies from one location to another location in the same site even if the same material and same mix is used. So, the percentage amount 100 % for compaction which is required by (QCS, 2014) S6P4 should be conducted by the MDD tested from the approved lab and verify the 100 % compaction.

The Maximum Dry Density (MDD) for a soil calculated upon the effect of moisture towards the density of the material. Unbounded material is affected by the variations in the moisture content specified if the mix is a coarser or a finer mix. The standard proctor compaction test in accordance ASTM D1557 was performed on each produced sample.

Optimum Moisture Content (OMC) and Maximum Dry Density (MDD) values for each mix are summarized in Figure 4. The specification of MDD and OMC for Road base and subbase are 2.15 mg/m3 and 2.05 mg/m3, respectively. It can be seen that both MDD and OMC are affected by the mix gradation in case the mix is finer this provide that more fines can absorb more water and can decrease the voids created from the large aggregate sizes, moreover, the fine in the samples are more pointed showing the sensitivity of mixture for water.

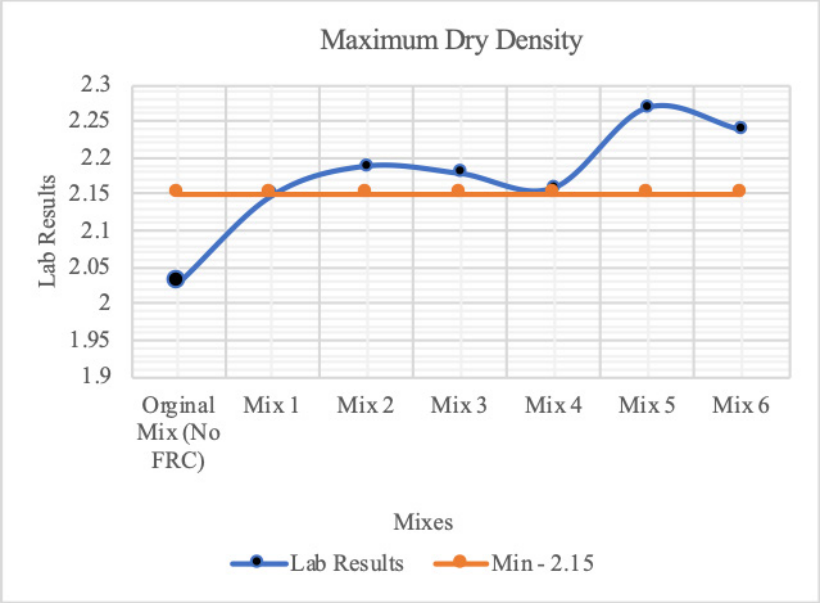

Figure 4: Maximum Dry Density Tests Results

From the graph, adding the FRC to the original material clearly upgraded the MDD from the low unaccepted value as per the minimum limits required in the (QCS,) 2014 section 6 part 4 (Table 4.3)

8 CALIFORNIA BEARING RATIO (CBR) TEST

The Californian Bearing Ratio (CBR) test is a test used to evaluate the strength of cohesive material used for roads and pavements specified in soil material. The results of these tests are used to design the thickness of pavement and its component layers for the type of mix. This is one of the important tests used to create the design for road pavement.

The California Bearing Ratio (CBR) test is a simple strength test that dominates on the bearing capacity of the base material or unbounded material with required material gradation and MDD.

The CBR test is used in pavement construction for the strength measure, elastic modulus and moisture durability for all layers required by the road works. CBR tests were performed as specified in ASTM D1883 on the six samples compacted at their corresponding OMCs.

The CBR values are tabulated in Figure 5, the specification of CBR for road base and

subbase is 80% and 70% respectively.

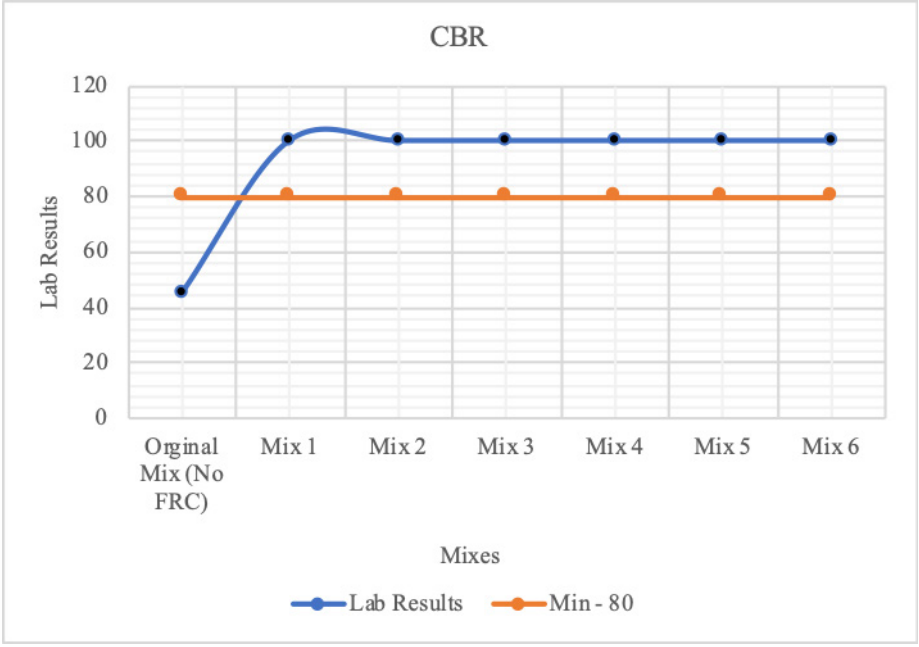

Figure 5: CBR Tests Results

The higher CBR, the higher stability and higher quality however more durability. As presented by the graph that the mix with no FRC material fall beyond the minimum requirement as per (QCS, 2014) section 6 part 4 (table 4.3), while adding FRC material shows that it is the only material that can replace the Gabbro to upgrade and increase the CBR percentage to higher value as per QCS.

9 SOIL CLASSIFICATION

AASHTO as per AASHTO SOIL Classification System (from ASHTO M 145 or ASTM D3282) has classification parameters used to identify various soil mixes based on the gradation and the plasticity index quality test. In highway construction these classifications are used and applied to our original and upgraded sample with FRC material to provide the results as tabulated in Table 3.

Table 3: Classification of the 6 Soil Mixes with *FRC material

AASHTO Classification:	**Table 1**	**Table 2**
	A-1	**A-1-a**
Stone Fragments, Gravel and Sand (Excellent to Good)		

*FRC: Fine recycled concrete

While the original material without the fine crushed, concrete had been classified also to verify the classification type as per Table 4.

Table 4: Classification of The Original Material without *FRC material

AASHTO Classification:	**Table 1**	**Table 2**
	A-2	**A-2-7**
Silty or clayed gravel and sand (Excellent to Good)		

*FRC: Fine recycled concrete

Adding the FRC material not only upgrade the material quality from the failed zone as per (QCS, 2014), also it upgrades the material classification from Silty or clayed gravel and sand to a Stone Fragment gravel and sand.

10 CONCLUSION

As per the material size distribution, Atterberg limits, sand equivalent, maximum dry density and California bearing ratio tests which shows that adding a 20% fine crushed concrete material is a versatile material and it will delineate the capability to increase the quality for the susceptible material as the gradation is in the required minimum and maximum percentage, Atterberg limits upgraded from a high plasticity index to a non-plastic material as the fine crushed concrete material is a non-plastic material, sand equivalent increased from very low percentage to a higher percentage as the sand equivalent for the fine crushed concrete is high as well as the acceptable results for maximum dry density and the CBR which specify the requirements mentioned in (QCS, 2014) section 6 part 4.

It is evident that the various samples with FRC supersede the typical mix (with no FRC) on every level. The comparison was conducted for the results of various testing methods stipulated by the (QCS, 2014) for mix designs. This paper shows in detail that the results for every test conducted prove the mix designs containing FRC to better the typical sample. That is on a technical level, although the benefits stretch to provide environmental, economic, and theoretical Value. With consideration of the growing demand for recycling, waste management and cost control management approaches such as project management, six sigma, and lean construction management. Recycling concrete waste by crushing and utilizing the material not only proves as a solution to reducing pollution and saving resources while also serves as a solution for bettering the quality of mix designs in road construction to improve specifications and meeting regulations. All these benefits come with reduced costs for both the Qatari government and the contractors in Qatar. In laymen terms, we call this a win-win situation and other advantages the crushed concrete can be used as a replacement for washed and dune sand within different mixes for different road construction practices.

REFERENCES

Dickenson, S. E. (1996). *Soils in construction*. Fourth Edition, Chapter 4, page 255, R. R. Donnelley & sons company, New Jersey.

Deal, T. A. (1997). What it costs to recycle concrete: C&D Debris Recycling, V. 4, no. 6.

FOHS, D. G. (1990). Use of waste and by products in highway construction. *Transportation research record*, 1288.

Goonan, T. G. (1998). Aggregates from natural and recycled sources—Economic assessments for construction applications, (U.S. Geological Survey), Circular 1176.

Kelly, T. (1996), Crushed Cement Concrete Substitution for Construction Aggregates—A Materials Flow Analysis, (U.S. Geological Survey), Circular 1177.

Snyder, M. B. (1995). *Use of crushed concrete products in Minnesota pavement foundations*, Technical report documentation, (MN/RC-96/12).

Cite this article as: Ahmad H. H., "Recycled Concrete Used in Subbase in Potential Use for Road Base and Cement Bounded Material (CBM)", *International Conference on Civil Infrastructure and Construction (CIC 2020)*, Doha, Qatar, 2-5 February 2020, DOI: https://doi.org/10.29117/cic.2020.0066

Innovation in Road Construction Industry: An Analysis of Different Case Studies

Pardeep Oad
Pardeep.oad@hdr.qut.edu.au
Queensland University of Technology, Brisbane, Australia

Stephen Kajewski
s.kajewski@qut.edu.au
Queensland University of Technology, Brisbane, Australia

Arun Kumar
arun.kumar@rmit.edu.au
RMIT University, Melbourne, Australia

ABSTRACT

Process improvement and innovation in the field of road construction sector offers significant community and industry benefits, by making an important contribution in economic growth and enhancing the quality of life. However, achieving better innovative practices in order to improve existing construction processes and to heighten competitiveness have gradually become a challenge for the road industry. The use of innovation in this context refers to the use of suitable materials in the construction of road, material such as eco-friendly roads, solar roads and recycled materials. This paper examines 12 different case studies on the uses of new material in road construction and where case studies are from different countries in different context and explores the usefulness of the practices under numerous road situation and conditions. The case studies have been analyzed in the following context: location of the case study, which helps to identify the suitability of road construction material with the weather condition; driving factors, which indicates, how and what selected case studies contribute in the field of innovation; economy and environment feasibility; and barriers in the case studies, which indicates hurdles to implement selected case studies. The study findings indicate that in order to maintain competitiveness, construction industry needs to continuously focus on the improvement of their construction processes and innovative materials. Finding indicates that in most case studies both economic and environmental benefits were realized.

Keywords: Construction innovation; Manufacturing innovation; Road construction; Case study; Project management; Plastic bags; Glass bottle

1 INTRODUCTION

It is widely accepted that innovation is required in the road construction industry as a foundation to competitive benefit for organizations functioning in the road construction industry. However, there is a perception amongst some specialists that the process of innovation in construction industry is uncommon and that the construction industry is slow to change. This type of perception occasionally arises from contrasts of road construction industry to the medical, education, electronics and other business industries in which the implementation and adoption of new theories, products and technologies have been widespread over the past numerous decades (Drejer, 2002).

Despite this opinion, the idea of innovation in road construction industry does occur and the idea has been documented by many developers and researchers (Slaughter, 1998), infect there is continued attention in shaping how to improve innovation in the industry. Panuwatwanich, Stewart, & Mohamed (2009) suggested that the process of innovation in road construction industry is necessary as a foundation of competitive benefit for similar organizations. Aouad, Ozorhon and Abbott (2010) underlined that the competitiveness of organization unavoidably based on regional and national arrangements of innovation in the construction industry, which in alternately depends on government procedures and policies. Consequently, given the continuous and rapid changes and enthusiasm of the commercial environment, protecting competitiveness is thus an important agenda of most organizations in construction industry.

Many researchers have identified that rise in technical knowledge of innovation in the road industry in relation to the road material and road, the growing exchange of information between different developing and developed countries across the globe offer new options and possibilities for the asphalt roadway societies to support the wider realization of innovative service or products used in all designated nations to achieve a practical and cost-effective optimization of road supervision and administration (Lundberg, et at., 2019; Caerteling, et al., 2011; Hausman, 2005; Wolfe, 1994).

This paper examines twelve different cases in context of innovation in roads which include, use of recycled material in road construction industry, development of eco-friendly roads, solar roads, Tron-like and glows in the dark, use of technology in traffic control, precast pre-stressed concrete pavement, toner recycling for roads, extracting energy from roads, foamed bitumen stabilized pavement and use of plastic in road construction.

2 INNOVATION IN ROAD SECTOR: CASE STUDIES AND DISCUSSION

The aim of this paper is to examine different road situations, where innovation has been implemented. The case studies are presented below. Twelve different case studied from different countries are presented.

2.1 Use of recycling material in road industry

In Hamburg, Germany, new policies and procedures have been executed stating that the Hamburg road required to be use recycled materials only. Similarly, there has been a noteworthy growth in the cost of road materials, which were used for the building of bridges and roads, including aggregates and bitumen. Therefore, the management of Hamburg City has involved road construction corporations to carry out development and research to deliver a justifiable solution to supply for the requirements of the new procedure policy, as well as to manage the problems related to the price increment of materials used in road and bridge construction. As a result, an explanation was provided to construct 100 % recycled asphalt pavement (RAP). This solution not only helps to consume fewer energy, but it also minimizes the harmful emissions of gases for example carbon dioxide gas emission. In this context Bitumen is one of the most expensive road materials, which is used for the development of special roads and bridges. Though a meagre 5% of the road material structure is bitumen, this could donate to 60% of development cost of road and bridge. Likewise, bitumen product is an oil based road

product that could not be locally obtained, addition to the high price instability of the road material (Schroeder, 2015).

In San Francisco, Bay Bridge was demolished due to the earthquake in 1989 and the bridge was rebuilding started in 2002, where all recycling materials were used. The rebuilding of bridge took benefit of applying the exclusive properties of ash along with the ground ash generated by the explosion furnaces in regard to improve the strength along with the sturdiness of the road material such as concrete and which used in rebuilding the bridge. This project applied the biochemical properties of ash concrete in regard to uncover the undesirable accoutrements of the sea salt fog and water which has harsh action, as the mechanical demand of the zone of earthquake. The bridge zone, which an immense salt content is made through applying a concrete mixture that comprises 50% fly ash. This leads to the inhibition of bridge cracking afterward the toughening of the cement used in the bridge. The technique is commonly used in the areas where the salty water is commonly found. Moreover, the uses of particles from the fly ash could leads to the enhancement in the mixture usefulness and durability; also the fly ash uses could makes the mixture thicker and stronger as compare to the old-style concrete which used in the old age, making it improved equipped to transmit substantial traffic loads. However, more than 30 concrete mixes designs have been applied for the building of the new bridge, in which more than 50% mixes were from the fly ash. The process of bridge construction also applied slag, which was crushed, granulated from the explosion furnace. This slag was applied in the pier column, which in result the bridge durability and workability improved substantially (Schroeder, 2015).

2.2 First road developed from plastic bags and glass bottles in Australia

In Australia, the city council Downer, Hume and sustainability, Melbourne Victoria both are working with the RED group to do research on building suitable road, which is made of plastic bags and glass (Onkaparinganow, 2018; Department of the Environment and Energy, Australian Government, 2019).

Through associations with clients, the larger industry and other suppliers, Downer council is including better-recycled content in roadway, while attaining lesser greenhouse gas footprint. This research is not only good help the country to control waste, but also helps to develop roads, which are suitable for the environment. The City of Onkaparinga in South Australian (SA) build a first road from plastic bags and glass in the Happy Valley. The council used about 139,000 plastic bags and 39,750 glass of bottles equals diverted from landfill, as shown in figure below (Onkaparinganow, 2018; Department of the Environment and Energy, Australian Government, 2019). The material used in the road is ethylene-vinyl acetate) (PEVA) and glass of bottles, where packaging, of 63,000 glass bottles and soft plastics from roughly 200,000 plastic bags have been obtained.

Figure 1: Road developed from plastic bags and glass bottles in Australia (Onkaparinganow, 2018; Department of the Environment and Energy, Australian Government, 2019)

2.3 The innovative in eco-friendly road solution

In Israel, roads of Haifa and Ra'anana are two different examples of the extemporary use of innovation in road to generate electricity and for collecting the waste-kinetic energy. An Israel firm which is privately owned has formed customized piezotech generators which could be used for the wasted kinetic energy in building roads/bridges and convert it into electrical energy. This technology is being applied in road construction because the kinetic energy that is converted into electrical energy is collected and applied for road signaling systems and lighting the roads. It is also applied for lighting the diodes which produce lights (Probst et al., 2013).

This form of innovation has given numerous benefits to the road building system. This has led to the sole reliance of development of roads based from the parasitic power, as the movement of road traffic on highways generates kinetic energy that is collected in the shape of electrical energy. They give a continuous supply of electrical energy to the bridges and roads regardless of the weather conditions. This is a method of electrical energy to the roads and bridges, which is recognized against any damage and theft. This method has led to the construction of smart and reliable roads in the region, heading to self-competence of bridges and roads, consequently preservation of power also is made feasible (Probst, et al., 2013).

2.4 Solar roads

Many countries around the globe these days are using solar panels, which are organized consecutively and are planned architecturally to drive cars upon the road. These are innovative and revolutionary replacements to the infrastructures, which are, construct of petroleum bi-products and asphalt. Likewise, to support green communities, it is a good alternative as it useful to use fossil fuel to produce energy. The idea of solar roads is to store the energy and then energy can convert into the form of electrical energy. The energy produced could be applied to bright the roads and bridges along with generate power for the local homes and the business. The key breakthrough of this development is the solar panel, which could stores power.

In this context, Netherlands is the first country, where they introduced a bike lane

based on the solar. The path along the road where they installed solar is in Amsterdam with the suburban zones of Wormerveer and Krommenie. This is the first solar path along with road that allocate to bikes only and which harvests power and is paved. The council put this project on trial for six months and result after six months indicates that the solar road system improved performances in context of operational cost and usability of the road.

Moreover, this solar path able to produce about 3,000 kWh electrical energy, that is adequate to brighten a single house for at least year. The Spokesman of this project "Sten-de-Wit" said. 'if the yearly yield of the solar path is decoded, it could produce about 70 kWh meter of electricity every year.' The concept of developing solar paths on side of the roads became very widespread and now The United States of America planning to install solar panels on their all roads and highways (Katharine, 2014). The solar road produce energy, which cost $20 per kilowatt-hour, which is around 13 times higher than the traditional method that cost only $1.53.

2.5 Tron-like and glows in the dark

In the country of Netherlands, roads and bridges development has come another innovatory invention. It is constructing a highway that glows in the dark and is Tron-like, considered being the world's first highway which glows in the dark. Netherlands announced they already started this research project and now they are in the testing phase and this about 500 meters of the N329 Oss freeway that have been prepared for this innovative idea implementation. These roads will not only glow in the dark but also will give weather indications. They named that as a "Smart Highway" and the concept behind this development is the construction of freeways which are sustainable in nature and interactive. These freeways will be painted in a way that could glow without any light, through captivating energy during day time and they estimated paints glow could glow for eight hours (Dube, 2014).

The execution of this research could be an efficient initiative to preserve, very smart in saving cost and energy, as, if this research becomes successful, country could change the local road and streetlights also. These innovative freeways will lead to the formation of safe and maintainable roads. According to Heijman, this technology cloud be an alternative of the lighting posts, which are located alongside the roads of the freeways. Similarly, this development could serve as an improved substitute to roads in the zones where electricity and lighting do not exist (Dube, 2014).

2.6 Use of technology in traffic control

In Sydney, Australia, the Coordinated Adaptive Traffic System known as SCATS has been controlling Sydney traffic effectively. This method has become globally acknowledged, and is being applied in more than 141 cities in different countries around the globe and the method is regulating 32,000 road connections in the world. SCATS has recognized itself widespread and internationally accepted technological systems in order to control traffic. The National ICT Australia (NICTA) is the Center for development and Research in ICT Australia, which was developed in 2004. The NICTA has delivered an innovative solution, which has been well established and successful in the context of controlling traffic. The research group actively involved in discovery innovative

approaches of traffic control on different road situations (Kilby & Johnson, 2010).

2.7 Precast Pre-Stressed Concrete Pavement

From last several years, the United States State Transportation has been working on how to adopt innovative approaches and using systems of road building so that normal traffic flow cannot be disturb. In this context PPCP know as Precast Pre-Stressed Concrete Pavement brought another innovative idea, in which an effective and durable road can be developed without distracting the normal traffic flow. In Texas University, a Center for Transportation Research (CTR) conducted a study on roads feasibilities and result revealed that there was a developed of 0.7 Km of the PPCP pilot plan. This pilot plan was later conducted nearby Georgetown, Texas (U.S. Department of Transportation, 2015; Merritt & Tayabji, 2009).

By means of formed concrete pavement includes the use of advanced methods for road building in regard to build and repair roads and bridges in less period of time. The modules that are assembled and invented anywhere else and afterword transported to the production site and connected. This method is highly reliable, as it involves short time frame for field preserving. This research could be applied effectively for road repair in shorter time frame and its rebuilding and for high traffic situations. Currently, the research is applied for continuous intermittent repairs and rehabilitation (Merritt & Tayabji, 2009; U.S. Department of Transportation: Federal Highway Administration, 2015).

An additional research project was commenced at the center of Caltrans, which was supported by the PPCP system by means of spreading of the worryingly trafficked lanes. The project resulted in addition of 10 feet and 27 feet lane with the existing lane. The key advantage of these pavements in this research project is to improve the road quality and minimize the road development time (Merritt & Tayabji, 2009; Department of Transportation U.S., 2015).

2.8 The Jet Stream Super-Highway

The innovative concept of super highways is based on the automobiles which extract power from the structure of the bridge or roads and take power from the situation (Huang, 2015). These freeways or highways have been designed in a way where wind in the tunnels that lead to the creation of a stream of airflow on a constant basis. The design and shape of these types of roadway is like a half-pipe see through in a cross-sectional sight. These freeways are made up of a sequence of turbines which are motorized by solar electric and road hover in regard to push the airflow in the road trail. Moreover, there is a cycle impact formed by the sketching vents over the sides as a result of airflow being drawn endlessly. Due to the solar panels coating at the upper surface of the road, makes it a very atmosphere friendly. There are electronic sensors that permit communication with the automobiles which are driven on the road, in regard to obtain precise adjustments. This freeway is founded on the idea that the future of the transport in urban zones is based on applying green systems of energy practice along with conservation (Huang, 2015).

2.9 EME2 technology and high modulus Asphalt EME2 Pavement Design

The road construction industry is facing challenges to the design and delivery of high-performance asphaltic concrete in order to carry high traffic load including axle

wheels loading. As the density of traffic is increasing in Australia day by day, there has ascended a requirement for a reliable asphalt materials in regard to manage the changing weather conditions. The EME stand for 'enrobes à module élevé' and it is a French word, which is also known as "high-modulus". This technology is being applied widely in the country of France, where it the technology was originated. The technology of EME is divided into two grades, namely: EME Class 1 and EME Class 2.

The difference among these two grades is that the EME Class 1 include higher binder content in the material in context of richness modulus; the EME2 mixtures are founded on richness modulus along with the requirements for features like water sensitivity, stiffness, wheel tracking, and fatigues. The EME class 2 is usually applied on roads where traffic load is high. The key features of EME are that it is moderately stronger as well as rigid. Also, reduces the pavement thickness without major any big change in the roads strength (Petho & Bryant, 2015; Petho, Beecroft, Griffin & Denneman, 2014). Moreover, central laboratory and Colas' in Paris, both companies have been able to evaluate the mix designs by using Strain Alleviating Membrane Interlayer (SAMI) bitumen and local aggregates to guarantee that the proposed mix design should fulfil the France requirements.

2.10 Foamed asphalt stabilized roadways

An initiative of the Austroads (Australia) since 2012 is testing the Foamed Bitumen Stabilized Pavement (Rose & Manley, 2012). The objectives of Arena Evaluation of Foamed-Bitumen-Stabilized-Pavements are: 1) development of the measures for Austroads in regards to the design of new materials for roads, and the roadway of structural reintegration and handling of the Australia roads; 2) identification and examination of the modes of distress of the FBS roadways; 3) development as well as coordination of the nation-wide mixes design for Foamed-Bitumen-Stabilized materials.

Figure 2: Twelve case studies from different countries

2.11 Plastic roads

The Netherlands is country where some developer doing a pilot study on the construction of new types of road, which is easy to construct and much more reliable, using recycled plastic. (Koudstaal & Jorritsma, 2015). They will bear higher variation of temperature and need comparatively fewer maintenance. The data that is collected from numerous real-world case studies from different countries as shown in figure 2. Moreover, these case studies have been analyzed in the context of demonstrated drivers, economic benefits, environmental/sustainability benefits and barriers to innovation for each case.

3 CONCLUSION

It is widely accepted that Government agencies in the road construction and management industry sector aim to achieve value for their investment as they procure road construction industry services. As Government announces any road construction project and seeks procurement for services, several contractors apply, and it is complex to assess innovation in these proposals on a comparative basis. This requires several factors such as: clear project definition, what is new (innovation), previous experience for the proposed project. However, it is not easy to assess innovation on a comparative tender assessment basis.

The aim of this paper is to analyze different case studies in the context of innovation in the road construction industry.

REFERENCES

Aouad, G., Ozorhon, B. & Abbott, C. J. C. I. (2010). Facilitating innovation in construction: directions and implications for research and policy. *10*(4), 374-394.

Austroads (2014). *Design and Performance of Foamed Bitumen Stabilized Pavements: (Progress Report 2*, AP-T275-14). Sydney: Austroads Ltd.

Bain, R. (2001). Moveable barrier technology-the key to the dynamic highway? *42*(10), 340-342.

Caerteling, J. S., Di Benedetto, C. A., Dorée, A. G., Halman, J. I. & Song, M. (2011). *RETRACTED: Technology development projects in road infrastructure: The relevance of government championing behavior*, *31*(5), 270-283.

Drejer, A. J. E. J. O. I. M. (2002). Situations for innovation management: towards a contingency model. *5*(1), 4-17.

Dube, D.-E. J. G. N. (April, 2014). Netherlands test-drives world's first glow-in-the-dark highway. 15. Retrieved from http://globalnews.ca/news/1272844/glow-in-the-dark-highway-of-the-future/

Department of the Environment and Energy, Australian Government (2019). *Australia's first road built with soft plastics, glass and toner*. Retrieved from https://www.environment.gov.au/about-us/partnerships/case-studies/australia-first-road-built-soft-plastics.

Hausman, A. J. I. M. M. (2005). Innovativeness among small businesses: Theory and propositions for future research. *34*(8), 773-782.

Huang, D. (2015). Jet Stream Super-Highway. Retrieved from http://psipunk.com/jet-stream-super-highway-by-david-huang/.

Katherine, J. (2014). Netherlands Is The 1st Country To Open A Solar Road For Public Use. Retrieved from http://www.collective-evolution.com/2014/11/09/netherlands-is-the-first-

country-to-open-solar-road-for-public/

Kilby, P. & Johnson, F. (2010). RTA and NICTA: Innovating on Successful Traffic Management. *Paper presented at the 17th ITS World Congress ITS Japan ITS America*, ERTICO.

Koudstaal, A. & Jorritsma, S. (2015). Plastic Road. Retrieved from *VolkerWessels*, http://en.volkerwessels.com/en/about-us/profile/profile

Lundberg, M., Engström, S., & Lidelöw, H. J. C. I. (2019). *Diffusion of innovation in a contractor company*. Construction Innovation.

MacDonald, F. (2015). The solar road in the Netherlands is working even better than expected. Retrieved from http://www.sciencealert.com/solar-roads-in-the-netherlands-are-working-even-better-than-expected.

Merritt, D. K., McCullough, B. F., Burns, N. H. & Rasmussen, R. O. (2004). Construction of the California precast concrete pavement demonstration project. Retrieved from http://www.fhwa.dot.gov/pavement/concrete/pubs/if06010/ch1.cfm

Merritt, D. K. & Tayabji, S. (2009). *Precast Prestressed Concrete Pavement for Reconstruction and Rehabilitation of Existing Pavements*. Retrieved from Federal Highway Administration. http://www.fhwa.dot.gov/p...e/pubs/if09008/if09008.pdf.

Merritt, D. K. & Tyson, S. S. (2006). Precast Prestressed Concrete Pavement–A Long-life Approach for Rapid Repair and Rehabilitation. *Paper presented at the Proceedings, International Conference on Long-Life Concrete Pavements* (pp. 497-512).

Orta, M., Lemus, E. J. G. J. O. M. & Research, B. (2015). Leading Innovation Change in Today's Competitive Environment. *15*(2), 35.

Onkaparinganow. (2018). First South Australian road built with plastic bags and glass.

https://www.onkaparinganow.com/spring-2018/first-south-australian-road-built-with-plastic-bags-and-glass/#.

Panuwatwanich, K., Stewart, R. A. & Mohamed, S. J. C. I. (2009). Validation of an empirical model for innovation diffusion in Australian design firms. *9*(4), 449-467.

Petho, L., Beecroft, A., Griffin, J. & Denneman, E. (2014). *High modulus high fatigue resistance asphalt (EME2) technology transfer* (1925037932). Retrieved from https://http://www.onlinepublications.austroads.com.au/items/AP-T283-14.

Petho, L. & Bryant, P. (2015). High modulus asphalt (EME2) pavement design in Queensland. *Paper presented at the AAPA International Flexible Pavements Conference, 16th*. Gold Coast, Queensland, Australia.

Probst, L., Monfardini, E., Frideres, L., Demetri, D., Schnabel, L., Alain, K. & Clarke, S. (2013). *Business Innovation Observatory Environmentally friendly technologies and energy efficiency*. In: European Union.

Rose, T. M., Manley, K. J. C. M. & Economics. (2012). Adoption of innovative products on Australian road infrastructure projects. *30*(4), 277-298.

Schroeder, R. (2015). *The use of recycled materials in highway construction*. Public Roads Retrieved from https://http://www.fhwa.dot.gov/publications/publicroads/94fall/p94au32.cfm.

Slaughter, et al. (1998). Models of construction innovation. *124*(3), 226-231.

Solar Roadways. (2016). Solar roads. Retrieved from http://www.solarroadways.com/.

U.S. Department of Transportation: Federal Highway Administration. (2015). *Construction of the California Precast Concrete Pavement Demonstration Project*. Washington, D.C.: Retrieved

from http://www.fhwa.dot.gov/pavement/concrete/pubs/if06010/ch1.cfm.

Wolfe, R. (1994). Organizational innovation: Review, critique and suggested research directions. *31*(3), 405-431.

Cite this article as: Oad P., Kajewski S., Kumar A., "Innovation in Road Construction Industry: An Analysis of Different Case Studies", *International Conference on Civil Infrastructure and Construction (CIC 2020)*, Doha, Qatar, 2-5 February 2020, DOI: https://doi.org/10.29117/cic.2020.0067

Evaluation of Bond Strength Between Carbon Fiber Reinforced Polymer (CFRP) Composites with Modified Epoxy Resins and Concrete

Mohamed H. Rabie
m.rabie@qu.edu.qa
Department of Civil and Architectural Engineering, Qatar University, Doha, Qatar

Eman M. Fayyad
emfayad@qu.edu.qa
Center for Advanced Materials, Qatar University, Doha, Qatar

Mohammad R. Irshidat
mirshidat@qu.edu.qa
Center for Advanced Materials, Qatar University, Doha, Qatar

Nasser A. Alnuaimi
anasser@qu.edu.qa
Department of Civil and Architectural Engineering / Center for Advanced Materials, Qatar University, Doha, Qatar

Mohammad K. Hassan
mohamed.hassan@qu.edu.qa
Department of Civil and Architectural Engineering, Qatar University, Doha, Qatar

ABSTRACT

Rehabilitation and strengthening of concrete structures are becoming more significant in civil engineering applications. The use of externally bonded Fiber Reinforced Polymers (FRP) is one of the methods to strengthen and rehabilitate reinforced concrete members, providing noticeable improvement to their capacity in resisting load. Carbon Fiber Reinforced Polymer (CFRP) is used along with epoxy resins to evaluate the bond strength of two commercially available epoxies (EPON 828 and EPON 862) between CFRP and concrete. In addition, three new combinations that resulted from mixing the two epoxies were examined. The mechanical properties of epoxy resins are significantly weaker than this of the CFRP making the epoxy characteristics the determining factor in the quality of the bond strength. Three-point flexural test was conducted to examine the bond strength between the CFRP composites and concrete. Further, differential scanning calorimetry was conducted to examine the glass transition temperature of the resultant epoxies. The results showed that the optimum composition was a mixture of 70% of epoxy 828 and 30% of epoxy 862. Therefore, achieving better bond strength and high glass transition temperature, resulting in CFRP composite with higher fire resistance.

Keywords: CFRP; Epoxy composition; Bond strength; Concrete

1 INTRODUCTION

Recently, the need to develop the economic and efficient methods to strengthen the reinforced concrete has received considerable attention. The use of Carbon Fiber Reinforced Polymer (CFRP) composites to increase the rigidity of the concrete structure against the harsh environment was identified as a possible alternative to other strengthening methods (Issa & Asce, 2004). The alternative methods such as adding

of unstressed or pre-stressed steel, installation of external pre-stressed reinforcement, increasing cross-sections are expensive and not enough efficient. Nevertheless, addition of CFRP materials do not corrode because they are a combination of carbon fibers and an epoxy resin matrix that have very high strength and rigidity in the fiber direction and outstanding fatigue characteristics.

Epoxy resins are thermosetting polymers, which are cross-linked using hardeners (curing agents). The most common curing agents for epoxy resins are polyamines, amino amides, and phenolic compounds (Forrest, 2005).

Generally, significant advances characterize the epoxy like excellent adhesion, good strength, low shrinkage, good corrosion resistance, resistance to moisture, thermal and mechanical shock and processing versatility (Zhipeng et al., 2014). Therefore, they are used in many applications as encapsulating materials, adhesive, high performance coatings and so many applications. Several types of epoxy resins are present based on their weight per epoxide and viscosity. Epoxy 828 has viscosity range from 110-150 P at 25 °C and 185-192 weight per epoxide whereas epoxy 862 is characterized by lower viscosity, 25–45 P at 25 °C and lower weight per epoxide, 165–173.

The present study investigates the adhesion of five different epoxy compositions through three-point flexural test. Epoxy 828 and epoxy 862 commercially available were used to produce three different mixtures of epoxies with variable percentages. Differential Scanning Calorimetry (DSC) was conducted to evaluate the glass transition temperature of five epoxy compositions.

2 MATERIALS AND METHODS

2.1 Materials

A total of ten concrete prisms divided into two patches were prepared using ready-mixed concrete. The mix design per cubic meter used to prepare the concrete prisms is composed of 831 Kg of sand, 693 Kg of course aggregate, 455 Kg of fine aggregate, 340 Kg Portland cement and w/c ratio of 0.47. Compression test was performed on two concrete cylinders with a dimension of 100 x 300 mm in accordance with ASTM C39. The average 28-day compressive strength is equal 43 MPa.

Commercial Carbon Fiber (CF) sheets purchased from SIKA group were placed in the tension side of the concrete prisms. Furthermore, a total of five compositions of Epoxy resins were prepared. Two of them were commercially available as Bisphenol A (Epon 828) and Bisphenol F (Epon 826) and diethylenetriamine as a hardener. The remaining three were prepared by mixing Bisphenol A (Epon 828) and bisphenol F (Epon 826) using different ratios. Table 1 summarizes the percentage used to prepare the five epoxy samples.

Table 1: Epoxy compositions

Sample number	Sample code	Epon 828 (%)	Epon 862 (%)
1	BISA	100	0
2	70A/30F	70	30
3	50A/50F	50	50
4	30A/70F	30	70
5	BISF	0	100

2.2 Experimental program

2.2.1 Bond strength

Ten concrete prisms were prepared with geometry shown in Figure 1a. All concrete prisms were of a length of 50 cm with a rectangular cross section of 10 cm x 10 cm. A saw cut with a depth of 2.5 cm was made at the center of the concrete prism to allow for using three-point bending loading scheme (Tatar & Hamilton, 2016). The CFRP sheets were applied in the tension side of the concrete prism. The dimensions of the CFRP are L x W = 20 x 2.5 cm as shown in Figure 1d.

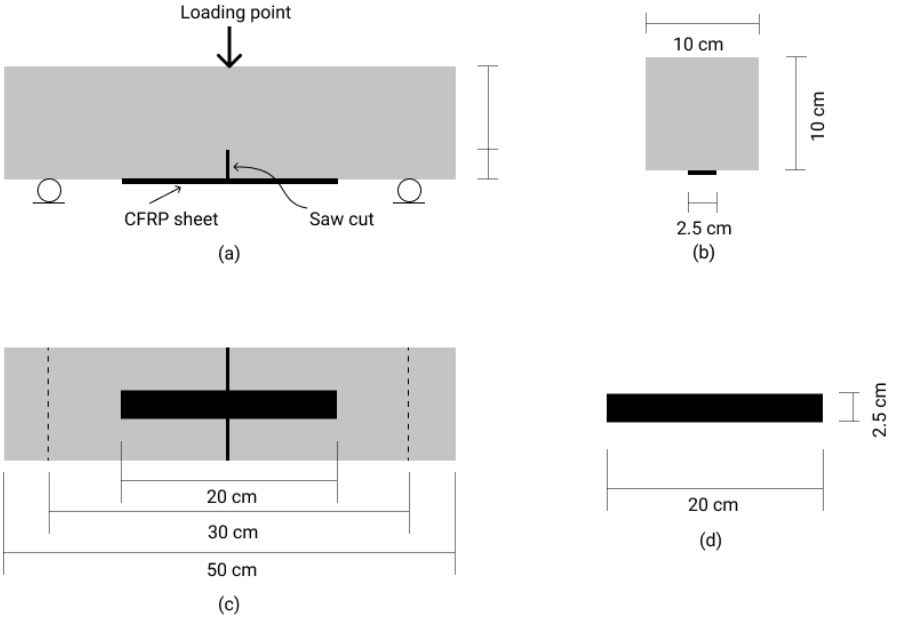

Figure 1: Concrete prism dimensions: a) side view, b) cross section, c) bottom view, d) CF sheet

2.2.2 Differential scanning calorimetry

Measurements of differential scanning calorimetry are carried out using DSC 8500 by Perkin Elmer. DSC is used to examine many epoxy adhesion properties such as initial and final glass transition temperatures, heat curing, and the final material's specific heat. 10 ^{o}C / min as a heating rate was used on temperature range from 20 to 150 ^{o}C. (McKeen, 2014).

3 RESULTS AND DISCUSSION

3.1 Bond strength

Flexural test was performed on ten concrete prisms as detailed in the aforementioned section. The results are summarized in Table 2. The result showed that the maximum load was resisted by Bisphenol F (BISF) with an average load of 16.39 kN. Sample four ranked second in resisting the load applied to the concrete prisms with an average load of 16.28 kN. These results indicate the bond strength between the CFRP and the concrete prism. The higher the load resisted the stronger the bond between CFRP and the concrete prism. Figure 2 and Figure 3 show the set-up of the testing machine and the load vs.

displacement curves for the sample of the tested specimens.

Table 2: Bond strength

Sample	Sample code	Average load (kN)
1	BISA	15.28
2	70A/30F	16.25
3	50A/50F	15.21
4	30A/70F	16.28
5	BISF	16.39

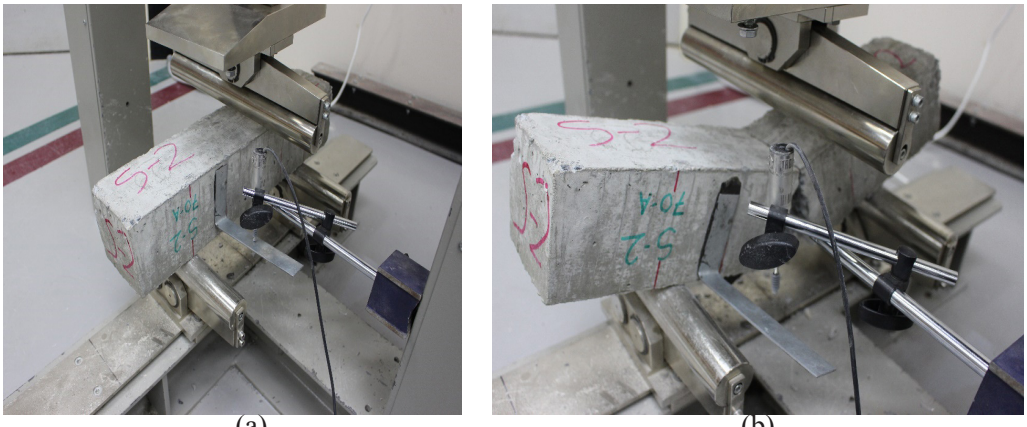

(a) (b)

Figure 2: Three-point flexural test

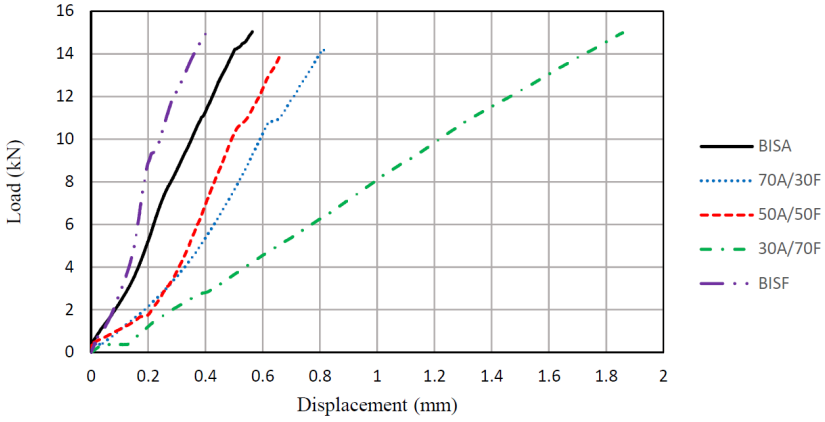

Figure 3: Load vs. displacement

3.2 Differential scanning calorimetry

Figure 4 shows the DSC heat-cool-heat of the different five compositions of CFRP samples at a heating rate of 10 °C/min during temperatures range from 20 to 150 °C. DSC was utilized to determine the glass transition temperature (Tg), which ranged from 104 to 130 °C in the heating curve, as shown in Figure 4 and ranged from 110-130 °C in the cooling curve. Tg is the temperature where the epoxy adhesive transitions from a glassy hard material to a rubbery soft material (Al-Tamimi et al., 2014). It is documented that the extreme environmental temperatures affect the durability of the bond strength

between externally bond CFRP plates and the concrete prism (Abbas, 2010). As the temperatures close to the transition temperature (Tg) of CFRP, the durability of their bond strength diminishes (Gamage, Wong, and Al-Mahadi, 2005).

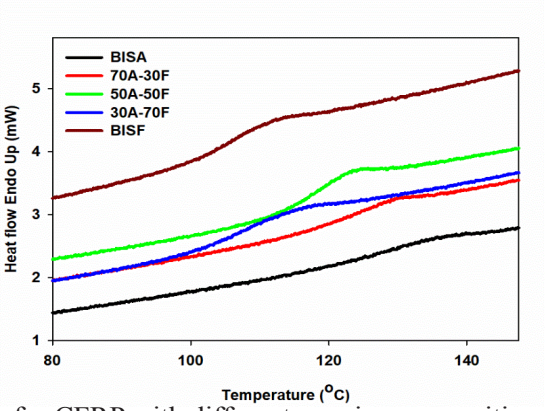

Figure 4: DSC curves for CFRP with different epoxies compositions Tg in the heating curves

It is observed that DSC curve of BISA shows a glass transition around 130 °C, which is the highest Tg value whereas the BISF possessed the smallest one compared to all the used compositions, as shown in Figure 4. The DSC results are summarized in Table 3. The different compositions of BISA and BISF [70A/30F, 50A/50F and 30A/70F] possessed Tg of 122, 117 and 108 °C, respectively. As expected, adding of BISF to BISA results in CFRP networks with lower Tg compared to the use of BISA only. However, all different composition still have high Tg value compared to other composites. In addition, the 70A/30F composition shows higher Tg value than the other two compositions, 50A/50F and 30A/70F. This indicates the well cross-linked of 70A/30F epoxy composition with the carbon fiber since it has a higher crosslink density.

Table 3 DSC summary results

Sample code	Area (mJ)	ΔH (J/g)	Peak	ΔC_p J/g °C	T_g (°C)
BISA	72.933	8.8404	57.07	0.161	130.45
70A/30F	66.910	9.0175	57.94	0.197	122.48
50A/50F	75.697	7.9098	57.47	0.351	117.36
30A/70F	77.604	10.0135	57.52	0.319	108.05
BISF	237.051	27.596	58.37	0.386	104.99

4 CONCLUSION

The bond strength between CFRP laminate and the concrete was evaluated using three-point bending test for total of five epoxy compositions. Further investigation of the glass transition temperature epoxy compositions was evaluated using DSC and the following conclusions were highlighted:

- Epoxy composition BIS A owned glass transition temperature higher than that of Epoxy composition BIS F. In the case of resin made of a mixture of the two types of epoxy, the 70A/30F composition shows higher Tg value.

- Epoxy composition BIS A resin has a melting temperature of 57 °C. Replacing Epoxy BIS A with Epoxy BIS F in different percentages (30, 50 and 70 %) leads to increase in the crystallization melting temperature of the hard chains of CFRP composites.
- The new epoxy compositions slightly affected the bond strength between CFRP composites and concrete.

Future research might study the temperature as a factor affecting the epoxy properties.

REFERENCES

Abbas, Basim M Mahdi (2010). *Durability of CFRP-concrete bond under sustained load in harsh environment*. Civil Engineering, MONASH University.

Al-Tamimi, Adil K., Rami A. Hawileh, Jamal A. Abdalla, Hayder A. Rasheed & Riadh Al-Mahaidi (2014). Durability of the bond between CFRP plates and concrete exposed to harsh environments. *Journal of Materials in Civil Engineering*, *27* (9): 04014252. https://doi.org/10.1061/(asce)mt.1943-5533.0001226.

Forrest, M. J. (2005). *Coatings and Inks for Food Contact Materials*. iSmithers, Rapra Publishing.

Gamage, J. C. P. H., Wong, M. B. & Al-Mahadi, R. (2005). Performance of CFRP strengthened concrete members under elevated temperatures. *Proceeding of the International Sysposium on Bond Behaviour of FRP in Structures (BBFS 2005)*, No. Bbfs: 113-18.

Issa, Camille A. & Asce, F. (2004). Carbon fiber reinforced polymer strengthening of reinforced concrete beams : experimental study, 10 (December): 121-25.

McKeen, Laurence W. (2014). Introduction to the effect of heat aging on plastics. *The Effect of Long Term Thermal Exposure on Plastics and Elastomers*, 17-42. https://doi.org/10.1016/b978-0-323-22108-5.00002-3.

Tatar, J. & Hamilton, H. R. (2016). Comparison of laboratory and field environmental conditioning on FRP-concrete bond durability. *Construction and Building Materials*, 122: 525-36. https://doi.org/10.1016/j.conbuildmat.2016.06.074.

Zhipeng He, Yue Wang, Tingting Zhao, Zichuan Ye, He Huang (2014). Ultrasonication-assisted rapid determination of epoxide value in polymer mixtures containing epoxy resin. *Analytical Methods*, *6*(12): 4257-61.

Cite this article as: Rabie M. H., Fayyad E. M., Irshidat M. R., Alnuaimi M. A., Hassan M. K., "Evaluation of Bond Strength Between Carbon Fiber Reinforced Polymer (CFRP) Composites with Modified Epoxy Resins and Concrete", *International Conference on Civil Infrastructure and Construction (CIC 2020)*, Doha, Qatar, 2-5 February 2020, DOI: https://doi.org/10.29117/cic.2020.0068

Development and Performance of Cement Bound Materials in Road Pavements

Khaled E. Hassan
khassan@irdme.net
Infrastructure Research & Development (IRD QSTP-LLC), Doha, Qatar

Osman El-Hussain
osmane@ashghal.gov.qa
Quality and Safety Department, Public Works Authority (Ashghal), Doha, Qatar

Mohammed bin-Saif Al-Kuwari
msakuwari@mme.gov.qa
Environmental and Municipal Studies Institute, Ministry of Municipality & Environment, Doha, Qatar

Khalid Al-Emadi
kemadi@ashghal.gov.qa
Quality and Safety Department, Public Works Authority (Ashghal), Doha, Qatar

ABSTRACT

The use of cement bound materials (CBMs) for road construction in Qatar is relatively new. CBM improves the structural capacity and durability of pavement, but considerations should be made to the setting time and strength development in hot arid environment, such as in Qatar. The paper presents a laboratory development and performance characteristics of CBM mixtures, with environmental and economic benefits through the use of local and recycled materials. The developed mixtures showed full compliance with the grading, strength and durability requirements of the Qatar Construction Specifications (QCS, 2014). Site data from Ashghal projects indicated the difficulty of producing consistent strength in practice, with the potential of increased strength and associated risk of reflection cracking in the asphalt overlaying. Recommendations are made to improve the construction practice and specification of cement and other hydraulically bound materials to enhance the service life of pavement and support the government strategy of sustainable construction.

Keywords: Cement bound materials; Compressive strength; Construction specification; Durability; Local and recycled materials

1 INTRODUCTION

The use of Cement Bound Materials (CBMs) in road construction has the two-fold benefit of increasing the bearing capacity and enhancing the durability of pavements. CBMs are part of the Hydraulically Bound Materials (HBM) family and generally made with a variety of materials including primary, secondary and recycled aggregates. The binder could be a Portland cement or other slow-hardening industrial by-products of Fly Ash (FA) or Ground Granulated Blast Furnace Slag (GGBS) with an alkali activator (Hassan et al., 2004). CBMs are generally classified based on compressive strength or a combination of tensile strength and modulus of elasticity (BS EN 14227-1, 2013). The Qatar Construction Specification (QCS, 2014): section 6: part 6 classifies CBMs based on their 7-day compressive strength (CBM 1 to CBM 4) with grading, performance and durability requirements.

CBM is generally used as a structural layer within the semi-rigid pavement with an asphalt overlay. The combination of a bound structural layer and an asphalt surfacing has great potential to provide long-life pavements with minimum maintenance. The CBM substrate is relatively strong, durable and provides a good load distribution to the underlying foundation, whereas the asphalt surfacing provides improved riding quality and a protective layer to the structural layer. Higher strength CBM results in increased stiffness, with greater tendency for wide cracks that could reflect through the asphalt overlay (FEHRL, 2009; Hassan et al., 2008).

The first use of CBMs in Qatar was in 2013 as a remedial work for the Corniche project, near the seafront, to overcome durability issues with existing pavement. As bound pavement subbase/base layers, their benefits of increased pavement stiffness, improved distribution of traffic loading, and protection to the pavement foundation were recognized compared to unbound pavement layers. The use of CBMs continued in Qatar over the last few years to include major expressway projects and the new Orbital Highway & Truck Route project with high traffic loadings.

This paper presents a laboratory development of CBM mixtures using local and recycled materials available in Qatar. The strength and durability performance of CBMs were compared to the requirements of QCS 2014. Site data of compressive strength were obtained from Ashghal to assess the performance of CBMs in service. Recommendations are made to improve the wider use of CBMs in Qatar, with consideration of local conditions in Qatar, to support the government strategy of sustainable construction and development.

2 LABORATORY DEVELOPMENT OF CBM MIXTURES

CBM mixtures of CBM 1, CBM 2, CBM 3, and CBM 4 were developed in the laboratories of ReadyMix Qatar. The development was based on the use of 100% local and recycled materials. Details of the CBM mix design and properties are given in Table 1. The Portland cement was supplied by the Qatar National Cement Company (QNCC), and complies with the requirements of the QCS 2014 and BS EN 197-1 (2011), minimum grade of 42.5. The coarse aggregate consisted of 75% local limestone, obtained from sand and rocks crusher, and 25% Recycled Concrete Aggregate (RCA), supplied by Beton concrete. Washed sand from QNCC was used as fine aggregate. The amount of mixing water ranged from 110 to 120 l/m^3, and a superplasticizer based on synthetic polymer was used in the range of 0.6 to 3.75 l/m^3 with increasing content for the various CBM mixtures.

Table 1: CBM mix design and properties

Material/Property		**CBM 1**	**CBM 2**	**CBM 3**	**CBM 4**
Mix design	Portland cement (kg/m^3)	80	120	150	190
	Coarse aggregate (kg/m^3)	1500	1480	1480	1475
	Fine aggregate (kg/m^3)	690	710	690	650
	Water (l/m^3)	120	110	110	115
Properties	Fresh density ((kg/m^3)	2302	2300	2331	2386
	Average 7-day strength (MPa)	5.70	8.30	12.70	19.60
	Minimum 7-day strength (MPa)	5.50	8.00	12.20	18.60
	Retained strength (%)	97	95	96	93
QCS 2014: Min average 7-d strength (MPa)		**4.5**	**7.0**	**10.0**	**15.0**
QCS 2014 Min individual, MPa		**2.5**	**4.5**	**6.5**	**10.0**

Figure 1 shows the grading of CBM materials, together with the grading envelope specified in the QCS 2014. The results show that both CBM 1 and CBM 2 have almost

the same grading, and falling within the specified grading envelope in the QCS 2014. Similarly, CBM 3 and CBM 4 have identical grading, and fit nicely within the mid-range of the specified limits. It is clear that the grading envelope for CBM 1 and CBM 2 provides a wider grading range for the use of different materials.

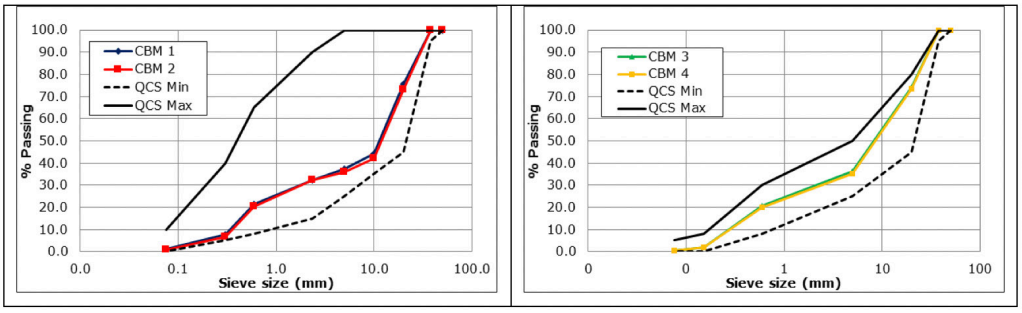

Figure 1: Grading of CBM mixtures with QCS 2014 limits

After mixing, the fresh CBM material was poured into cube molds (150mm) and compacted in two layers using a vibrating hummer, following the procedure described in BS EN 13286-51 (2004). The surface of the casted cubes was levelled and covered with wet hessian and polyethylene sheets overnight. On the following day, the cube specimens were removed from molds and cured in sealed plastic bags until required for testing at 3, 7, and 28 days. Sixteen cubes were prepared for each mix. The fresh density was determined by weighing the cube molds before and after filling with CBM materials, and the average values are given in Table 1. The values ranged from 2300 to 2386 kg/m^3, with increased density for higher cement content.

The cubes were tested for compressive strength as per BS EN 12390-3 (2019) at the age of 3, 7, and 28 days and the results are presented in Figure 2. The QCS 2014 specifies a minimum average 7-day compressive strength for the various CBM mixtures. Table 1 shows that the average 7-d strength for all CBM mixtures exceeded the minimum specified values. The QCS 2014 also specifies a minimum individual value for each CBM type, and all the developed CBMs satisfied the minimum strength requirements of the QCS 2014.

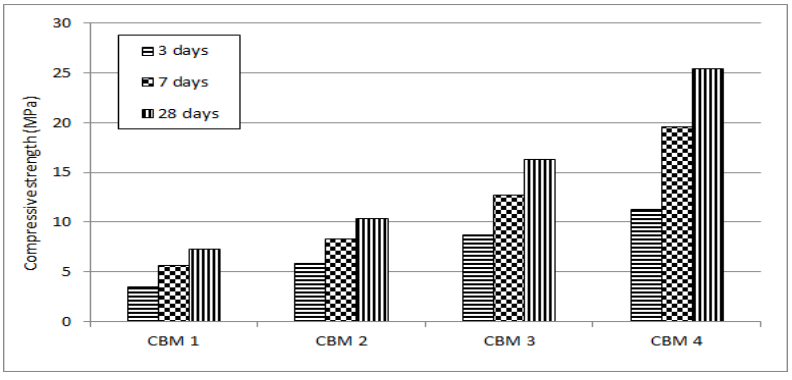

Figure 2: Average 7-day compressive strength of CBM mixtures

The QCS 2014 also specifies a retained strength value of a minimum 80%, as

determined from the ratio of the average compressive strength after immersion in water to the average control strength. The retained strength provides an indication of the durability of CBM mixture when exposed to water. The results in Table 1 show retained strength values ranging between 93 to 97% for the development of CBM mixtures, much exceeding the minimum specified limit. In general, the strength and durability results obtained from the laboratory development show that local and recycled materials could be effectively used for the production of CBM materials with full compliance with the QCS 2014 requirements.

3 SITE data

While the QCS 2014 specifies minimum average and minimum individual compressive strength values at the age of 7 days, project specifications tend to specify a range of compressive strength values at the same age. Most of the projects specified a 7-day compressive strength values between 3.0 and 7.0 MPa, with the preference towards the lower specified value to minimize the occurrence of reflective cracking. The Ashghal QSD team (Quality and Safety Department) provided site data on the 7-day compressive strength of CBM materials constructed in various projects and the results are given in Table 2 under the heading of CBM. Loose CBM materials were collected during construction, compacted on site into cubes (150mm), and tested for compressive strength at the age of 7 days. Table 2 also provides construction data on the 7-day compressive strength of core samples extracted from the laid CBM.

Table 2: CBM average 7-day strength values from site data

CBM Type	CBM	CBM 3
Average compressive strength, MPa	4.5	8.5
Min compressive strength, MPa	0.7	7.0
Max compressive strength, MPa	12.7	9.1
Project specified Minimum strength, MPa	3.0	QCS 2014
Project specified Maximum strength, MPa	7.0	-

Site data for the different CBM projects showed a wide variation of the 7-day compressive strength achieved on site. The CBM average 7-day compressive strength was 4.5 MPa, well within the specified range of 3.0 to 7.0 MPa. However, the minimum 7-day strength was 0.7 MPa, much lower than the minimum specified value for the project of 3.0 MPa. The maximum was 12.7 MPa exceeding the maximum specified strength value of 7.0 MPa. The CBM results indicate the difficulty of achieving a consistent strength for the specified low strength CBM.

The core results of CBM 3 satisfied the minimum individual strength but not the average strength requirement. However, core strength results are expected to be lower than cube strength for the same materials. The CBM 3 results also show a small variation between the minimum and maximum strength values achieved on site, between 7.0 and 9.1 MPa, and indicating strength that is more consistent for CBM made with higher cement content.

4 DISCUSSION OF RESULTS

The laboratory development of CBMs demonstrated the potential use of local and recycled aggregate materials with full compliance with the QCS 2014 requirements. CBMs were made with coarse aggregate of 25% RCA and 75% local limestone, and the cement content varied from 80 kg/m^3 for CBM 1 to 190 kg/m^3 for CBM 4. The developed mixtures satisfied the strength requirements and achieved high values of retained strength, indicating good durability and resistance to water damage. During the laboratory development, it was noticed the low cement content of 3% in CBM 1 was not adequate to coat all the aggregate particles. However, for CBM 2 and above (cement content of 5% and above), the mix looked more homogeneous with adequate binder. Site data also indicated the inconsistent compressive strength, especially for CBMs with low cement content.

CBM layers are expected to crack after construction due to shrinkage and thermal movements, and the intensity of cracks is expected to exceed in hot environment, such as in Qatar. The QCS 2014 specifies that after compaction and immediately before overlaying, the CBM surface shall be well closed and free from movement, cracks, loose materials, ruts, or other defects. It also specifies that all defected areas shall be removed, to the full thickness, and replaced with new CBM layer.

While the tendency is to produce low strength CBMs to minimize the risk of reflection cracks in the asphalt overlay, there is a need to provide consistent strength and uniform support to the pavement across its whole length. The UK Specification for Highway Works (Highways England, 2016), Volume 1, Series 800 specifies induced cracks for all HBMs that are expected to reach a compressive strength of 10 MPa at 7 days. Transverse cracks are induced in the fresh CBM/HBM by grooving the layer between ½ to 2/3 of its thickness, and filling the grooves with a bitumen emulsion before final compaction (Figure 3). The transverse cracks will not prevent the CBM from shrinkage and thermal movements, but will accommodate them to minimize the effect of reflection cracking. The technology is relatively cheap, has been successfully used in the UK, and could be implemented in the following revisions of the QCS.

Figure 3: Induced cracks (left) and filling the grooves (right) of CBM

Another factor contributing to the inconsistent strength of CBM is the setting time of Portland cement and inadequate curing on site. The QCS 2014 specifies that laying

and compaction of the CBM shall be made within 2 hours from mixing the cement with water, and a minimum curing period of 7 days immediately after compaction. The hot weather in Qatar could greatly accelerate the rapid hardening of cement and evaporation of mixing water, and hence influence the strength and cracking of CBMs. Cement replacement materials, such as FA and GGBS, provide alternative Portland cement with improved performance and impact on the environment. The use of FA and GGBS increases the setting time of the binder due to slow-hardening and provides with more homogeneous mixtures with consistent strength and support to the pavement structure.

There is no doubt that the use of CBMs in construction will enhance its structural capacity and durability towards more sustainable construction. Qatar relies mainly on imported aggregate for pavement construction with large volume of construction waste accumulated in landfill sites (Hassan et al., 2015). The importance of sustainability in the development of Qatar was made clear in the Qatar Second National Development Strategy (2018-2022) with a specific target to use 20% of recycled materials within the total materials used in construction projects.by 2022 (PSA, 2018). The versatility of CBMs and ability to accommodate a range of recycled materials with improved performance will support the government strategy of sustainable development with protecting the environment.

5 CONCLUSION

- Mixtures of CBM 1, CBM 2, CBM 3, and CBM 4 were successfully developed in the laboratory with 100% local materials in Qatar.
- The CBM mixtures were made with 75% limestone aggregate and 25% Recycled Concrete Aggregate (RCA) and Portland cement.
- The laboratory mixtures satisfied the grading and strength requirements of the QCS 2014 with retained strength exceeding 90%, indicating good durability and resistance to water damage.
- Site data of 7-day compressive strength showed a high variation of the results, especially for CBM with low cement content.
- To minimize the risk of reflection cracking, improvement in construction practice could be achieved by inducing transverse cracks when the 7-day strength exceeds 10 MPa.
- Recommendations are made for the use of cement replacement materials to improve the performance of CBMs in service.

ACKNOWLEDGEMENTS

The authors would like to acknowledge the Qatar National Research Fund (QNRF) for funding this project (QNRF NPRP: 7 – 795 – 2 – 296). The authors would like also to thank Ready-Mix Qatar for their technical assistant in the development of the CBM mixtures in the laboratory.

REFERENCES

BS EN 12390-3 (2019). Testing hardened concrete. Compressive strength of test specimens. British Standards Institution, London, the UK.

BS EN 13286-51 (2004). Unbound and hydraulically bound mixtures. Method for the manufacture of test specimens of hydraulically bound mixtures using vibrating hammer compaction. British Standards Institution, London, the UK.

BS EN 14227-1 (2013). Hydraulically bound mixtures. Specifications: Cement bound granular mixtures. British Standards Institution, London, the UK.

BS EN 197-1 (2011). Cement, composition, specifications and conformity criteria for common cements. British Standards Institution, London, the UK.

FEHRL (2009). ELLPAG Phase 2: A guide to the use of long-life semi-rigid pavements. Forum of European National Highway Research Laboratories, *FEHRL Report* (2009/001). Brussels (ISSN 1362-6019).

Hassan, K. E., Nicholls, J. C., Harding, H. M. & Nunn, M. E. (2008). Durability of continuously reinforced concrete surfaced with asphalt. *TRL Report* (666). TRL Limited, Crowthorne, the UK.

Hassan, K. E., Elghali, L. & Sowerby C. R. (2004) Development of new materials for secondary and recycled aggregates in highway infrastructure. *TRL Report* (598). TRL Limited, Crowthorne, the UK.

Hassan, K. E., Reid, J. M. & Al-Kuwari, M. S. (2015). Use of recycled and secondary aggregates in Qatar – Guidance document. *TRL Published Project Report* (PPR736). TRL Limited, Crowthorne, the UK.

Highways England (2016). UK Specification for Highway Works, Series 800 Road Pavements – Unbound, cement and other hydraulically bound mixtures. Manual of Contract Document for Highway Works, Volume 1. Highway England, London, the UK. (http://www.standardsforhighways.co.uk/ha/standards/mchw/vol1/pdfs/MCHW%20800.pdf).

PSA (2018). Qatar National Development Strategy 2018-2022. General Secretariat for Development Planning currently called the Planning and Statistics Authority (PSA). Doha, Qatar.

QCS (2014). Qatar Construction Specifications. Ministry of Municipality & Environment, Qatar Standards, Doha, Qatar.

Cite this article as: Hassan K. E., El-Hussain O., Al-Kuwari M. B.-S., Al-Emadi K., "Development and Performance of Cement Bound Materials in Road Pavements", *International Conference on Civil Infrastructure and Construction (CIC 2020)*, Doha, Qatar, 2-5 February 2020, DOI: https://doi.org/10.29117/cic.2020.0069

Characterization of Asphalt Mixtures in Qatar

Osman El Hussien
osmane@ashghal.gov.qa
Quality and Safety Department, Public Works Authority (Ashghal), Doha, Qatar

Khaled E. Hassan
khassan@irdme.net
Infrastructure Research & Development (IRD QSTP-LLC), Doha, Qatar

Khalid Al-Emadi
kemadi@ashghal.gov.qa
Quality and Safety Department, Public Works Authority (Ashghal), Doha, Qatar

ABSTRACT

The State of Qatar went through a massive road construction program in the last decade as part of the ongoing development of its infrastructure and road transport network. Construction of roads in Qatar generally utilizes imported materials such as aggregate and binders as a result of the scarcity of local construction materials. Characteristics of asphalt mixtures are studied in this research program in order to evaluate mixtures properties in terms of aggregate packing, binder content, voids, mixture density, maximum density and Marshall Stability. Actual mixtures used in the Public Works Authority road projects were analyzed in the research program. Mixtures were prepared following the Qatar Construction Specifications (QCS, 2014). Combined aggregate gradations for different asphalt mixtures were compared with maximum density envelopes for different maximum aggregate sizes. Moreover, regression analysis was used to evaluate the strength of correlations established between different asphalt mixtures properties. The analysis of these mixtures is outlined in terms of general characteristics and consequently, recommendations are given to improve asphalt mixtures performance.

Keywords: Asphalt mixtures; Characterization; Qatar construction specifications

1 INTRODUCTION

The economic and social development witnessed in Qatar over the past two decades is associated with improved connectivity through a world-class transport road network for the transportation of people and goods. Traffic volumes and loads continue to increase with high demand for improved quality of roads. Asphalt pavement is widely used for road construction in Qatar, and the country relies mainly on imported aggregate and bitumen binder for its infrastructure development. The properties of asphalt materials could vary widely from different sources and during transportation to Qatar, and hence more emphasis is made on the quality of asphalt mixtures and performance criteria.

Asphalt mix design has changed immensely in recent years with more emphasis on end performance testing. The basics of mix design is primarily focused on the Marshall design methods (Asphalt Institute, 2014) of achieving the optimum binder content for a specific grading curve of the aggregate and ensuring a minimum air voids content. The Qatar Construction Specifications (QCS, 2014) adopted the Marshall Mix design and

provides additional performance criteria based on the Superpave mix design of rutting, fatigue and aging. The Qatar General Organization for Standardization and Metrology (Qatar Standards) issues confirmation certificates of the asphalt mix design for use in pavement projects in Qatar.

The paper reviews the conformity certificates, issued by Qatar Standards for various asphalt mixtures with analyses of the different properties, with the aim of improving the effectiveness of the current specification of asphalt mix design. Recommendations are made to improve the production and construction practice of asphalt mixtures in Qatar to ensure improved long-term performance and sustainability of the road infrastructure in Qatar.

2 DATA COLLECTION

The Qatar General Organization for Standardization and Metrology issued conformity certificates for 191 mixtures. The breakdown of the conformity certificates are as follows:

a. 80 wearing course mixtures.
b. 58 base course class B mixtures.
c. 53 base course class A mixtures.

Wearing course has Nominal Maximum Aggregate Size (NMAS) of 25.0mm, while base course class A has NMAS of 37.5mm and base course class B has NMAS of 25.0mm. Generally, the conformity certificates include combined mixture gradations and Marshall properties such as stability, flow, Marshall quotient, binder content, voids in mix, voids in mineral aggregate, voids filled with asphalt, voids at 400 blows, retained stability and filler to binder ratio. The data were manually transcribed from scans of conformity certificates and supplied in a spreadsheet for analysis.

3 DATA ANALYSIS

The data provided was analyzed with the IBM SPSS statistics computer program. Regression analysis was carried out using a single independent variable and multiple independent variables. The Marshall data from the conformity certificates was analyzed for all layers combined and for each layer separately:

a. Using regression analysis to develop a linear model of each dependent variable in terms of all the other independent variables.

b. Using regression analysis to model the relationship between each dependent variable with all the independent variables other than the verification values.

3.1 Aggregate gradation

Combined gradations of mixtures are plotted out together with the QCS 2014 specification limits and the 0.45 Fuller curve (Fuller & Thompson, 1907), in Figure 1 for the wearing course mixtures, in Figure 2 for base class B mixtures and Figure 3 for the base class A mixtures. It can be seen that all the data fall within the relevant permitted envelope, as would be expected given that the data came from conformity certificates. However, the proportions tend to be nearer the upper limit for the coarser sieve sizes and nearer the lower limit for the finer sieve sizes, which is not unusual elsewhere in the world. Figure 3 shows that one gradation of base course class A was out of QCS 2014 limits. Generally, combined gradations for base course Class A showed more diversity compared to other courses, which were following same trends.

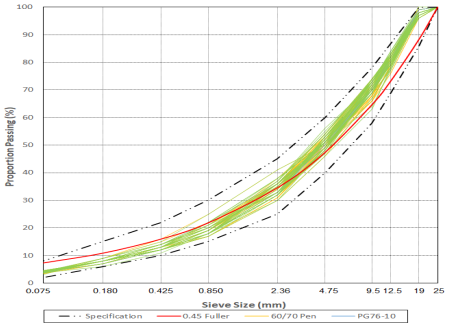

Figure 1: Gradations of asphalt concrete mixtures for surface course

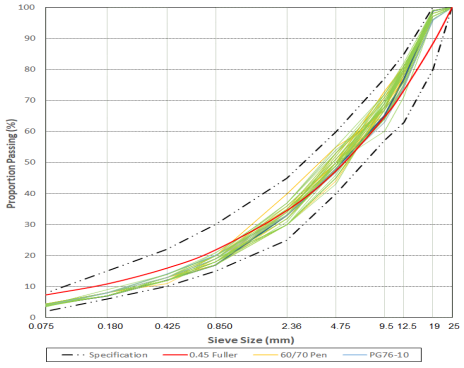

Figure 2: Gradations of asphalt concrete mixtures for base class B

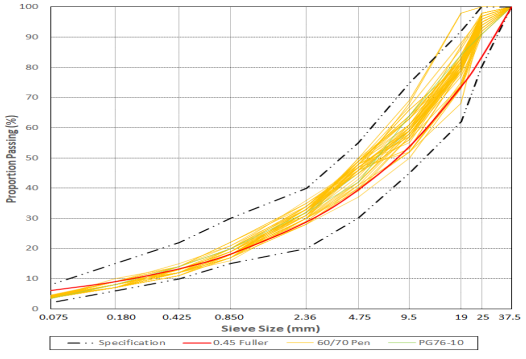

Figure 3: Gradations of asphalt concrete mixtures for base class A

The extent to which the curves cross the sieve sizes relative to the specification range was assessed by the ratio of the value less the lower specification limit and the difference between the two specification limits. The statistics show that the values are all between 0.0 (i.e. on the lower limit) and 1.0 (i.e. on the upper limit). These statistics confirm the visual observation from Figure 1 to Figure 3 that the proportions tend to be near unity for the coarser sieve sizes and smaller for the finer sieve sizes.

3.2 Binder content

It is assumed that the target binder content on site is the Optimum Binder Content (OBC) calculated in the Marshall Mixture design process. Based on that assumption, the

statistics of the binder content found on the conformity certificates are given in Table 1.

Table 1: Statistics of optimum binder content (%) from conformity certificates

Statistic	All layers	Wearing course	Base Class B	Base Class A
Limits	–	3.5 – 4.0	3.7 – 4.1	3.3 – 3.7
Mean	3.77	3.89	3.79	3.58
Standard deviation	0.162	0.130	0.074	0.072
Coefficient of Variation	4.29 %	3.36 %	1.95 %	2.03 %
Range	3.1 – 4.0	3.1 – 4.0	3.7 – 4.0	3.5 – 3.9

The mean values of OBC for the wearing course and base class A layers are nearer to the specification upper limit than the lower limit, whereas the mean value for the base class B layer, with the highest limits, is nearer to the specification lower limit than the upper limit. When those higher limits are applied to the wearing course results, only one addition case fails. Given that, the gradations are also nearly identical for the wearing course and base class B, with most of the certificates for one layer being capable of being applicable for the other. However, the use for different nominal mix designation is attributed to the fact that base course class B is routinely used as a single layer asphalt course for temporary roads, which are constructed under Road Improvement Works (RIW) program by Public Works Authority (Ashghal).

3.3 Air voids content

The statistics of the air voids content of the mixtures (voids) found on the conformity certificates are given in Table 2.

Table 2: Statistics of air voids content (%) from conformity certificates

Statistic	All layers	Wearing course	Base Class B	Base Class A
Specification limits	–	5.0 – 8.0	4.5 – 8.0	4.0 – 8.0
Mean	6.39	6.53	6.40	6.16
Standard deviation	0.421	0.397	0.375	0.412
Coefficient of variation	6.59 %	6.09 %	5.87 %	6.69 %
Range	5.0 – 7.8	5.5 – 7.8	5.3 – 7.3	5.0 – 7.0

The variation is quite extensive, with a coefficient of variation around 6% or more. Despite the variability, all the results comply with the QCS 2014 requirements for the tightest limits imposed on wearing course mixtures. The implication of high air voids contents on the durability of mixtures is considered detrimental even at 8% (Nicholls, 2017).

3.4 Mix density

The statistics of the mix density found on the conformity certificates are given in Table 3. The mix densities have a limited range with coefficients of variation at around 1%. This lack of variation is, presumably, the result of the limited sources of aggregate or at least the similarity in the density between different sources. Nevertheless, the variability that is present can still have an influence on some of the properties of the mixture.

Table 3: Statistics of mix density (Mg/m³) from conformity certificates

Statistic	All layers	Wearing course	Base Class B	Base Class A
Mean	2.557	2.545	2.559	2.570
Standard deviation	0.0340	0.0426	0.0276	0.0147
Coefficient of variation	1.33 %	1.68 %	1.08 %	0.57 %
Range	2.241 – 2.736	2.241 – 2.726	2.518 – 2.736	2.546 – 2.614

3.5 Maximum density

The statistics of the maximum density (Gmm) found on the conformity certificates are given in Table 4. The variability and range are similar to that of the mix density (subsection 3.4), which would normally be expected.

Table 4: Statistics of maximum density (Mg/m³) from conformity certificates

Statistic	All layers	Wearing course	Base Class B	Base Class A
Mean	2.726	2.717	2.723	2.744
Standard deviation	0.04308	0.05366	0.01636	0.04086
Coefficient of variation	1.58 %	1.97 %	0.601 %	1.49 %
Range	2.330 – 2.908	2.330 – 2.904	2.678 – 2.777	2.688 – 2.908

3.6 Marshall stability

The statistics of the Marshall stability (Stability) found on the conformity certificates are given in Table 5. The range is fairly wide, with coefficients of variation of about 10%. However, all the results comply with the QCS 2014 requirements.

Table 5: Statistics of Marshall stability (kN) from conformity certificates

Statistic	All layers	Wearing course	Base Class B	Base Class A
Specification limits	–	≥ 11.5	≥ 9.5	≥ 9.5
All binders				
Mean	16.06	16.46	16.13	15.38
Standard deviation	1.813	1.9099	1.8163	1.4641
Coefficient of variation	11.29 %	11.61 %	11.26 %	9.52 %
Range	11.2 – 20.0	12.3 – 20.0	11.2 – 19.4	12.1 – 19.0
Penetration grade bitumen				
Mean	15.12	15.11	14.55	15.37
Standard deviation	1.518	1.583	1.416	1.477
Coefficient of variation	10.04 %	10.47 %	9.73 %	9.61 %
Range	11.2 – 19.1	12.3 – 19.1	11.2 – 17.1	12.1 – 19.0
Performance grade binders				
Mean	17.30	17.50	17.09	15.8
Standard deviation	1.380	1.435	1.287	Single value
Coefficient of variation	7.98 %	8.20 %	7.53 %	Single value
Range	13.5 – 20.0	13.5 – 20.0	13.5 – 19.4	15.8

When comparing the statistics for the mixtures with performance graded binders against the conventional penetration grade bitumen, there is an average increase of about 2kN but the minimum value is from a performance grade binder. Therefore, it would appear that an enhancement of the Marshall stability generally results from the use of performance grade bitumen, but not always.

4 CONCLUSION AND RECOMMENDATIONS

Combined gradations tend to be near the upper specification limit for the coarser sieve sizes and nearer the lower specification limit for the finer sieve sizes.

The 0.45 Fuller curve is contained within the specification envelope but lies close to the lower limit for the coarser sieve sizes and close to the upper limit for the finer sieve sizes with the mixture gradations being noticeably above it at the coarse end and below it at the fine end.

The mixture density and maximum density values have limited ranges with coefficients of variation at around 1%.

The range of air voids content of the mixture values is wide, producing coefficients of variation of around 6% whilst they are in full compliance with QCS 2014 requirements.

The Marshall stability values have wide range, producing coefficients of variation of about 10%, but all the values comply with QCS 2014 specifications.

The current gradations of asphalt supplied in Qatar, as represented by the conformity Certificate data, do not respect the restricted zone concept. It is recommended to study the effect of this zone on asphalt laying and performance.

Ideally, it would be better to move towards performance evaluation of Marshall Mixtures for mix design purposes and include tests such as wheel tracking and indirect tensile strength to evaluate mixtures' performance.

REFERENCES

Asphalt Institute (2014). *Mix design methods for asphalt concrete and other hot-mix types*. MS-2, 7th Edition, Asphalt Institute, Lexington, the USA.

Fuller, W. B. & Thompson, S. E. (1907). The laws of proportioning concrete. *Transactions of the American Society of Civil Engineers*, 59, pp. 67 172, Reston, Virginia: American Society of Civil Engineers.

Nicholls, J. C. (2017). *Asphalt mixture specification and testing*. CRC Press, London.

QCS (2014). Qatar Construction Specifications. Qatar General Organization for Standardization and Metrology (Qatar Standards), Doha, Qatar.

Cite this article as: El Hussien O., Hassan K. E., Al-Emadi K., "Characterization of Asphalt Mixtures in Qatar", *International Conference on Civil Infrastructure and Construction (CIC 2020)*, Doha, Qatar, 2-5 February 2020, DOI: https://doi.org/10.29117/cic.2020.0070

Modelling the Severity of Plastic Shrinkage in Cementitious Materials

Faez Sayahi
faez.sayahi@ltu.se
Luleå University of Technology, Luleå, Sweden

Mats Emborg
mats.emborg@ltu.se
Luleå University of Technology, Luleå, Sweden

Hans Hedlund
hans.hedlund@ltu.se
Luleå University of Technology, Luleå, Sweden

Andrzej Cwirzen
Andrzej.cwirzen@ltu.se
Luleå University of Technology, Luleå, Sweden

Marcin Stelmarczyk
marcin.stelmarczyk@ltu.se
Luleå University of Technology, Luleå, Sweden

ABSTRACT

Plastic shrinkage cracking in cement-based materials occurs between the mixing and the final setting of the mixture, where rapid evaporation of the mixed water is the main cause behind the phenomenon. The induced cracks may impair the durability and sustainability of the structure by facilitating ingress of harmful materials into the concrete bulk. In this paper a new model for estimating the cracking severity of plastic cementitious materials is presented based on the mixture's initial setting time and the amount of the pore liquid evaporated from within the concrete mass. Results of experiments performed by the authors in another study, in addition to results of tests performed by other researchers are used to control the validity of the model. It is concluded that the model can anticipate the cracking severity of plastic concretes with good precision. The new method can provide practical tools for designers and contractors to predict and compare the cracking risk of the concretes prior to casting.

Keywords: Plastic shrinkage cracking; Initial setting; Evaporation; Bleeding; Modelling

1 INTRODUCTION

Plastic shrinkage cracking in concrete occurs shortly after casting and before the final setting of the mixture, while the concrete still has low tensile strain capacity (Lerch, 1957; Ravina & Shalon, 1968). The aesthetics, durability and serviceability of a structure may be dramatically impaired, as cracks provide passages for harmful materials to reach the concrete interior and cause long-term damage. The physical aspect of plastic shrinkage is manifested in evaporation of the capillary water and the consequent build-up of a hydraulic pressure, also known as capillary pressure inside the pore network (Powers, 1968).

After placing the concrete in the mold, its solid particles settle under gravitational forces, making the pore liquid to move upwards to the surface, i.e. *bleeding* regime (Lura

et al., 2007). This accumulated surface water eventually evaporates, after which menisci form inside the concrete's pores, i.e. *drying* regime (Lura et al., 2007). At this point, a negative capillary pressure builds-up inside the concrete bulk, which applies tensile forces on the solid particles. Cracks may form once the accumulated tensile stresses surpass the relatively low tensile strength of the fresh concrete (Powers, 1968).

Capillary pressure build-up in the pore network and accordingly the evolution of tensile stresses inside the concrete bulk depend on several parameters, such as w/c ratio and permeability. On the other hand, development of the tensile strength is consistent with the hydration rate, which depends on the binder type and w/c ratio.

The mechanism of plastic shrinkage in the drying state of cementitious materials have been investigated in a number of studies, e.g. (Powers, 1968; Dao et al., 2010; Wittmann, 1976; Radocea, 1992) based on which several models were developed. However, it seems that these models sometimes cannot explain some particular cases of plastic shrinkage cracking, where for example, concretes exhibit higher cracking tendency despite of their lower evaporation compared to other mixtures.

This paper presents a new model to predict the severity of plastic shrinkage cracking in cement-based materials, based on the concrete's tensile stress-strength ratio, which in turn is defined as function of the water evaporated from inside the concrete pore network, drying time, and the initial setting time. The model predicts and/or compares the cracking risk of concretes prior to placement, and identifies the one with the least cracking tendency.

2 MODEL DERIVATION

Drying time, i.e. when all the bleed water accumulated at the surface evaporates (Kwak & Ha, 2006) is the beginning of a period during which the potential for plastic shrinkage cracking gradually increases. This is when the tensile stresses start to develop inside the concrete bulk, brought by the beginning of the capillary pressure build-up (Boshoff & Combrinck, 2013). Hence, the longer *critical period*, t_{cr}, i.e. the period between the drying time and the mixtures initial set, see Fig. 1, the higher the cracking potential and vice versa (Sayahi et al., 2019). The critical period is defined as:

$$t_{cr} = t_{ini} - t_d \tag{1}$$

and

$$t = t_d \quad \text{when} \quad \frac{E}{B} = 1 \tag{2}$$

Where t_{cr} is the critical period (min), t is time (min), t_{ini} is the initial setting time (min), t_d is the drying time (min), E is the evaporation (kg/m^2), and B is the bleeding (kg/m^2).

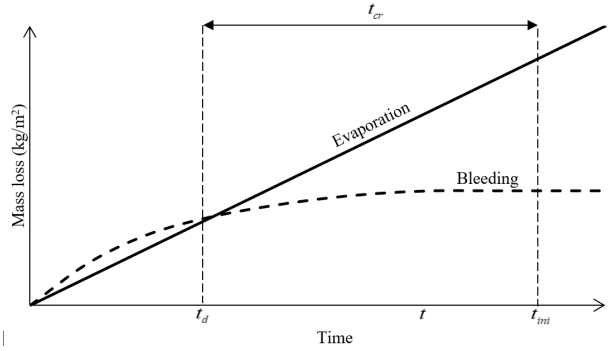

Figure 1: Drying time and critical period, from (Sayahi et al., 2019)

Assuming that cracking tendency of plastic cement-based materials increases with a higher rate of capillary pressure build-up, alongside delayed initial set and longer critical period, the following similarity is proposed:

$$C_s \sim t_{ini} \times \frac{dP}{dt} \times (t_{ini} - t_d) \tag{3}$$

Where C_s is the severity of plastic shrinkage cracking (kg.h/m^2), and P is the capillary pressure (Pa).

If the geometry of a pore is assumed constant, the rate of capillary pressure build-up will be a function of time, evaporation, W_e (the volume between curves 1 and 3 in Fig. 2), and the upwards transferred water, W_b (the water volume between curves 2 and 3 in Fig. 2) (Radocea, 1992; Sayahi et al., 2019).

$$\frac{dP}{dt} = f(W_e, W_b, t) \tag{4}$$

Where W_e is the total amount of the evaporated water in a single pore (kg/m^2), and W_b is the total amount of the upwards transferred water in a single pore (kg/m^2).

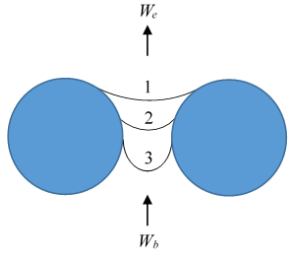

Figure 2: Water evaporation in a pore, based on (Radocea, 1992)

In such a case, according to (Radocea, 1992):

$$\frac{dP}{dt}\frac{dW_r}{dP_r} = \frac{dW_e}{dt} - \frac{dW_b}{dt} \tag{5}$$

Where W_r is the amount of the evaporated water in a sample with no W_b, and P_r is the

pressure in a sample with no W_b.

In Eq.5, dW_r/dP_r, is the tangent to the PW´-curve in Fig. 3, which is always positive, until the air-entry point is reached. Hence, the change of the pressure rate is similar to the way that the difference between the rates of W_e and W_b differs, which in turn is similar to the change of the pore liquid evaporation rate from within the concrete mass.

$$\frac{dP}{dt} \sim \left[\frac{dW_e}{dt} - \frac{dW_b}{dt} \right] \sim \frac{dW_p}{dt} \tag{6}$$

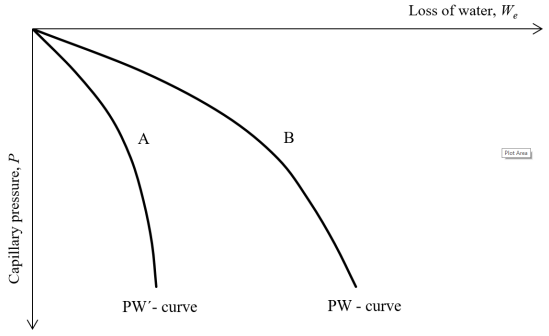

Figure 3: Capillary pressure build-up in A) a saturated sample where $W_b = 0$ and B) a saturated sample where $W_b > 0$, based on (Radocea, 1992).

Where W_p is the amount of the capillary water evaporated from inside the concrete pore network (kg/m^2). Accordingly, the following model is proposed for anticipating the cracking severity in plastic cement-based materials:

$$C_s = t_{ini} \times \frac{dW_p}{dt} \times (t_{ini} - t_d) \tag{7}$$

According to Boshoff and Combrinck (2013):

$$W_p(t) = E(t) - B(t) \quad , \quad t \geq t_d \tag{8}$$

Where $W_p(t)$ is the amount of the water evaporated from inside the pore network at time t (kg/m^2), see Fig. 4, $E(t)$ is the total evaporation at time t (kg/m^2), and $B(t)$ is the total bleeding at time t (kg/m^2).

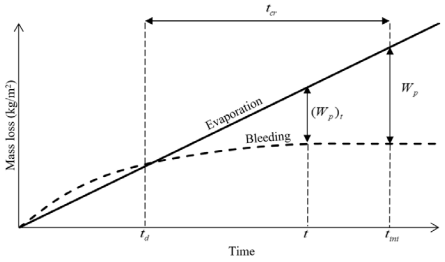

Figure 4: Definition of $W_p(t)$, from (Sayahi et al., 2019)

In eq. (7), the product of the multiplication of (dW_p/dt) and ($t_{ini} - t_d$), is the total amount of the water evaporated from inside the pore system at the initial set. Thus:

$$C_s = W_p \times t_{ini} \quad , \quad t = t_{ini} \tag{9}$$

or

$$C_s = \left[E(t) - B(t)\right] \times t_{ini} \quad , \quad t = t_{ini} \tag{10}$$

Using the new model, it is possible to explain the difference between the cracking tendency of mixtures with equal amount of evaporation. By multiplying the total W_p in t_{ini}, the new model emphasizes on the role of the initial setting time in the cracking tendency of plastic cementitious materials. Accordingly, in Fig. 5, the second concrete with the delayed initial setting is more prone to plastic shrinkage cracking in comparison to the first concrete with the faster setting.

To estimate the evaporation rate Uno's formula (Uno, 1998) or the ACI nomograph (ACI 305R, 1999) can be used. Bleeding, on the other hand, may be predicted according to models proposed by several researchers (Kwak & Ha, 2006; Josserand et al., 2006; Morris & Dux, 2010).

The initial setting time may be experimentally determined before the placement by using Vicat needle apparatus or ultrasonic waves (Carette & Staquet, 2015), or after casting by determining the inflection point of the internal temperature curve.

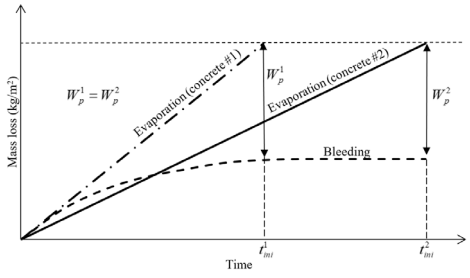

Figure 5: Cracking potential of concretes with equal W_p, but different initial setting times, from (Sayahi et al., 2019)

One limitation of the proposed model is that the restrain degree of the concrete is assumed constant for all the specimens. In addition, the effect of hydration, i.e. autogenous shrinkage, is neglected and it is assumed that the cracking occurs only due to the drying of the mixed water.

3 MODEL VERIFICATION

Some experimental data presented by the authors in (Sayahi et al., 2016) are used to verify the practicality of the model. The tests were performed using self-compacting concretes (SCC) in a mold manufactured according to the NORDTEST-method (Johansen & Dahl, 1993). The bleeding was measured according to (EN 480-4, 2005). Fig. 6 plots the calculated C_s versus the measured average final crack areas, which seem directly proportional. The only mixture that falls way out of this range has a w/c ratio of 0.55. This particular mixture is still in the optimum crack reducing w/c ratio range, defined by (Sayahi, 2019), i.e. 0.45 < w/c < 0.55, and thus, does not affect the cracking tendency.

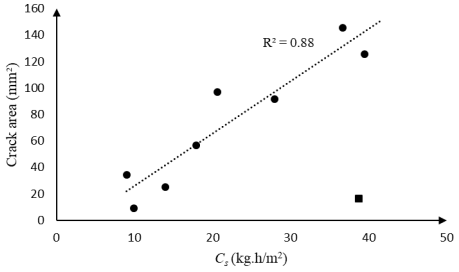

Figure 6: Cracking severity versus the measured average crack area, according to the new model, from (Sayahi et al., 2019)

Ghourchian et al. (2018) studied the influence of different Portland and blended cements on the cracking of plastic vibrated concrete (VC), during which they used an (ASTM C 1579-13, 2013) mold. By applying the model on the reported data by (Ghourchian et al., 2018), a linear correlation between the crack area and C_s was detected, see Fig. 7. Thus, it was concluded that the model is applicable for both SCC and VC.

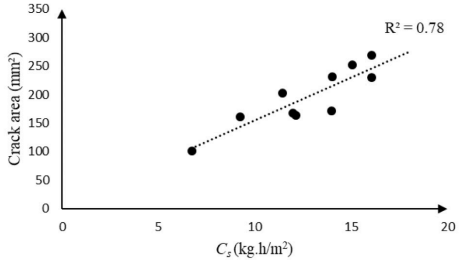

Figure 7: Cracking severity versus the measured average crack area, according to the new model and based on the data reported by (Ghourchian et al., 2018) from (Sayahi et al., 2019)

Maritz (2012) investigated the plastic shrinkage cracking of VC by focusing on evaporation and bleeding. He also used a mold manufactured according to (ASTM C 1579, 2013). The quantified crack areas are plotted in Fig. 8 versus the calculated C_s.

The difference in the values of the measured crack areas, in Fig. 6 to Fig. 8, is caused by the variation of the restrain degree, since different molds were used in the above mentioned studies. Thus, it should be remarked that the new model is only applicable on a group of equally retrained specimens.

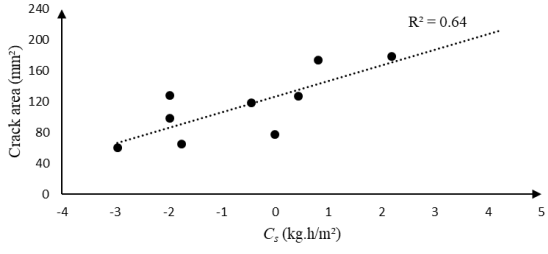

Figure 8: Cracking severity versus the measured average crack area, according to the new model and based on the data reported by (Maritz, 2012) from (Sayahi et al., 2019)

The negative C_s values in Fig. 8 mean higher bleeding compared to evaporation at the initial setting time. In such a case, the cracking may be attributed to initial plastic settlement of the vertically restrained specimens (Boshoff & Combrinck, 2013).

Moreover, by comparing the value of C_s in SCC (Fig. 6) to that of VC (Fig. 7 and Fig. 8), it can be seen that C_s depends also on the concrete type. SCC has relatively lower bleeding capacity compared to VC, based on which the observed dependency of C_s may be explained. Accordingly, the new model gives higher values of C_s for SCC in comparison to VC, which confirms that mixtures of high cement content are more susceptible to plastic shrinkage cracking.

It ought to be mentioned here that the model is a simple method to estimate the cracking severity, in which some parameters such as the effect of admixtures are not included. Thus, more experiments are needed to develop a more comprehensive version of the model.

4 CONCLUSION

The new model may estimate the cracking severity in plastic cementitious materials, based on the amount of the water evaporated from within the pore network and the initial set of the mixture. Accordingly, the following concluding remarks can be made:

- The model predicts the severity of plastic shrinkage cracking in cementitious materials, even before placement.
- The cracking severity in plastic cement-based materials is directly proportional to the product of the amount of the water evaporated from within the pore system, and the initial setting time.
- The model works regardless of the concrete type, i.e. SCC or VC.
- The model can only estimate the cracking severity of equally restrained elements.
- The severity of plastic shrinkage cracking may be reduced by lowering the evaporation-bleeding ratio and/or accelerating the mixtures initial set.

ACKNOWLEDGMENT

The authors appreciate the financial support provided by the Development Fund of the Swedish Construction Industry, SBUF.

REFERENCES

ACI 305R-99 (1999). *Hot Weather Concreting. Manual of Concrete Practice*. Farmington Hills: American Concrete Institute.

ASTM C1579-13 (2013). *Standard Test Method for Evaluating Plastic Shrinkage Cracking of Restrained Fiber Reinforced Concrete (Using a Steel Form Insert)*; ASTM International, West Conshohocken, PA.

Boshoff, W. P. & Combrinck R. (2013). Modelling the severity of plastic shrinkage cracking in concrete. *Cement and Concrete Research*, 48, pp. 34-39.

Carette, J. & Staquet, S. (2015). Monitoring the setting process of mortars by ultrasonic P and S-wave transmission velocity measurement, *Const. Build. Mater.*, 94, 196-208.

Dao V., Dux, P., Morris, P. & O'Moore, L. (2010). Plastic shrinkage cracking of concrete.

Australian Journal of Structural Engineering. Vol. 10, No. 3, pp. 207-214.

EN 480-4: (2005). Admixtures for Concrete, Mortar and Grout. Test Methods, Determination of bleeding of concrete, BSI.

Josserand, L., Coussy, O. & de, Larrard F. (2006). Bleeding of concrete as an ageing consolidation process. *Cem. Concr. Res.,* 36 1603-1608.

Johansen, R. & Dahl, P. (1993). Control of plastic shrinkage of cement. *Proceedings of the 18th Conference on Our World in Concrete and Structures*. Singapore, 1993.

Lerch, W. (1957). Plastic shrinkage. *ACI Journal*, *53*(8): 797-802.

Lura, P., Pease, B., Mazzotta, G. B., Rajabipour, F. & Weiss, J. (2007). Influence of shrinkage-reducing admixtures on development of plastic shrinkage cracks. *ACI Materials Journal*, Vol. 104(2).

Morris, P. H. & Dux, P. F. (2010). Analytical solutions for bleeding of concrete due to consolidation. *Cem. Concr. Res., 40* 1531-1540.

Powers, T. C. (1968). Properties of Fresh Concrete, p. 301, John Wiley and Sons, Inc., New York.

Ravina, D. & Shalon, R. (1968). Plastic shrinkage cracking. *ACI Journal*, *65*(4): 282-291.

Radocea, A. (1992). *A study on the mechanism of plastic shrinkage of cement-based materials*. Chalmers University of Technology.

Sayahi, F. (2019). *Plastic Shrinkage Cracking in Concrete: Mitigation and Modelling*. (Doctoral thesis). Luleå University of Technology, 2019.

Sayahi, F., Emborg, M., Hedlund, H., Cwirzen, A. & Stelmarczyk, M. (2019). The severity of plastic shrinkage cracking in concrete: A new model. *Magazine of Concrete Research*. https://doi.org/10.1680/jmacr.19.00279.

Sayahi, F., Emborg, M., Hedlund, H. & Löfgren, L. (2016). Plastic shrinkage cracking in self-compacting concrete: A parametric study. *International RILEM conference on Materials, Systems and Structures in Civil Engineering*, MSSCE 2016, pp. 609-619.

Uno, P. J. (1998). Plastic shrinkage cracking and evaporation formulas. *ACI Mater Journal*, Vol. 95, pp. 365-375.

Wittmann, F. H. (1976). On the action of capillary pressure in fresh concrete. *Cem. Concr. Res*. 6, 49-56.

Cite this article as: Sayahi F., Emborg M., Hedlund H., Cwirzen A., Stelmarczyk M., "Modelling the Severity of Plastic Shrinkage in Cementitious Materials", *International Conference on Civil Infrastructure and Construction (CIC 2020)*, Doha, Qatar, 2-5 February 2020, DOI: https://doi.org/10.29117/cic.2020.0071

Challenges for the Use of Local Materials in Unbound Road Subbase in Qatar

Moaaz Hashim Mohamedain
moaaz@ashghal.gov.qa
Quality and Safety Department, Public Works Authority (Ashghal), Doha, Qatar

Khaled E. Hassan
khassan@irdme.net
Infrastructure Research & Development (IRD QSTP-LLC), Doha, Qatar

Osman El-Hussain
osmane@ashghal.gov.qa
Quality and Safety Department, Public Works Authority (Ashghal), Doha, Qatar

Khalid Al-Emadi
kemadi@ashghal.gov.qa
Quality and Safety Department, Public Works Authority (Ashghal), Doha, Qatar

ABSTRACT

Current practice in Qatar is to blend local limestone with dune sand for use in unbound pavement applications. Dune sand is used to improve the properties of fine aggregate and compliance with the QCS 2014 requirements of plasticity and sand equivalent. The material has been successfully used for many years but currently facing the challenge of limited dune sand supply and recent government restrictions on its use in construction. The paper presents data on the properties of limestone obtained from different sources, tested in accordance with the QCS 2014 requirements. Variation of limestone source and the presence of clay particles greatly affected its suitability for use in unbound pavement applications. Improvement could be achieved by adjusting the grading of the material. Recommendations are made to revise the QCS 2014 specifications within the context of international specifications, when the unbound material is placed in a dry environment and away from the water level to enhance the wider utilization of local materials and sustainable construction in Qatar.

Keywords: Local limestone aggregate; Pavement; Unbound subbase; Properties; Specifications

1 INTRODUCTION

Local limestone is currently used as unbound road base and subbase materials in Qatar. Qatar is underlain by geologically young rocks, principally of weak limestone with occasional bands of clay, and hence the properties of limestone could vary from different locations or even within the same source. The material has been successfully used in unbound pavement layers for many years. Due to the varying clay type and content, the material is generally blended with dune sand, gabbro fines and/or cement to improve its properties (Hassan et al., 2015). The road subbase acts as a platform for the construction of the upper pavement layers and provides protection of the subgrade material. It is generally made of a compacted granular material with improved properties and quality compared to the subgrade. The Qatar Construction Specification (QCS, 2014) specifies physical and chemical properties for unbound road subbase materials.

This paper covers the characterization of granular subbase materials, being used in selected Ashghal pavement projects. Samples were collected from five (5) sources and tested for compliance with the QCS 2014 requirements. Recommendations are made for the development of performance data to support the wider use of local materials in construction.

2 MATERIALS AND TESTING PROGRAMME

Samples of granular materials were collected from different sources in Qatar between October 2018 and February 2019. A total of five (5) sources for subbase materials (S1 to S5) were considered in the investigation. Six (6) samples were collected from sources S1 to S3, whereas three (3) samples were used from sources S4 and S5. The materials tested in this investigation were claimed to be compliant with the QCS 2014 requirements for use in unbound subbase application. Although no information was provided on the composition of the supplied materials, it is believed that all the materials were composed of local limestone mixed with different quantities of dune sand in the range of 5-20% by weight.

The testing programme followed the compliance tests given in the QCS 2014, Section 6, Part 4 for unbound road subbase materials. Testing was conducted in the Ashghal Research & Development Centre in Najma, and included:

1. Grading (ASTM D6913, 2017) and Fines Content (ASTM D1140, 2017).
2. Sand Equivalent (ASTM D2419, 2014).
3. Liquid Limit (LL) and Plasticity Index (ASTM D4318, 2017, Method A for the LL).
4. Maximum Dry Density and Optimum Moisture Content (ASTM D1557, 2012).
5. CBR and Swelling (ASTM D1883, 2016).
6. Loss of Abrasion (ASTM C131, 2014).
7. Fractured Faces (ASTM D5821, 2017) and Flat and Elongated Particles (ASTM D4791, 2019).
8. Soundness (ASTM C88, 2018).

3 RESULTS

A summary of the test results is given in Table 1, together with the QCS 2014 specified limits. Each value represents the average of 6 tested samples for sources S1, S2, and S3, whereas the average of 3 tested samples for S4 and S5.

3.1 Grading and Fines Content

Sieve analysis testing (Grading (ASTM D6913, 2017)) and Fines Content (ASTM D1140, 2017)) was conducted on the materials received from the five (5) sources and the average grading results are shown in Figure 1. The grading results showed good compliance with the grading envelope specified in the QCS 2014. The average grading curves show that materials from sources S1, S2, S3, and S5 showed full compliance with the grading envelope whereas only S4 marginally failed to meet specific sieve sizes. The S4 curve shows almost a single size grading with a slightly higher value for coarse aggregate (sieve 25mm) than the maximum specified, and a marginally lower value for fine aggregate (sieve 2mm) below the minimum specified limit. The S4 material would

have benefited from the addition of dune sand to improve its grading and compliance with the QCS 2014.

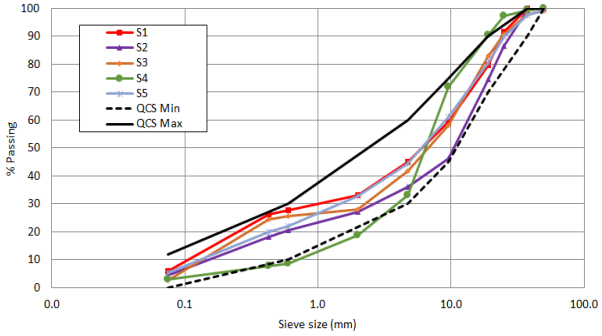

Figure 1: Sieve analysis of subbase materials from different sources

Materials from sources S1 and S3 showed signs of gap grading, presumably due to the addition of an excessive amount of dune sand. The S5 grading fell within the mid-range of the QCS 2014. Maintaining a continuous grading curve within the overall grading envelope is important to ensure good compaction of the subbase. Improved quality control for the production of local limestone, including blending with other materials to improve plasticity and SE requirements, could easily produce compliant gradings for unbound subbase applications.

Table 1: A summary of subbase results from different sources

Parameter	S1	S2	S3	S4	S5	QCS 2014 limits
Sand equivalent, %	70	20	23	45	33	25 min
Liquid limit, %	NP	NP	NP	NP	NP	25 max
Plasticity index, %	NP	NP	NP	NP	NP	6 max
MDD, Mg/m^3	2.08	2.32	2.03	2.04	2.16	2.05 min
OMC, %	8.0	4.7	8.4	9.2	6.9	-
CBR, %	212	177	106	110	122	70 min
Swell, %	0.0	0.5	0.3	0.0	0.0	1.0 max
Loss by abrasion, %	31	26	33	20	23	40 max
Fractured faces, %	100	100	100	100	100	50 min
Flat and elongated, %	0	0	0	1	0	15 max
Soundness, %	4.2	0.9	11.9	2.2	2.1	20 max

3.2 Sand Equivalent, Liquid Limit and Plasticity Index

In general, high plasticity values could lead to problems due to swelling and shrinkage, while aggregates with low plasticity tend to be highly susceptible to changes in moisture content. The QCS 2014 specifies a minimum value of 25 for the Sand Equivalent (SE) of unbound subbase materials (ASTM D2419, 2014). The results in Table 1 for sources S1, S4, and S5 satisfied the QCS requirement, whereas samples from source S2 and S3 failed the test.

In contrast to the SE, the plasticity parameters of Liquid Limit (LL) and Plasticity Index (PI) show that all the tested samples are Non-Plastic (NP). Comparing the SE and plasticity results with sieve size analysis show that source S1 exhibited the highest sand content, passing 4.75mm, as well as the highest contents of particles passing 0.425 and 0.075mm. These materials gave the highest values of SE with NP behavior. Source S3 also showed NP behavior with similar grading of fine aggregate to source S1, even with

less fines passing 0.075mm, but gave low SE values. The comparisons indicate no direct relation between the grading of fine aggregates and the SE and plasticity results.

3.3 Maximum Dry Density and Optimum Moisture Content

The Maximum Dry Density (MDD) is obtained in the laboratory at the Optimum Moisture Content (OMC). The OMC in turn depends on the grading and fines content of the material, as a finer grading tends to increase the OMC due to the increased surface area of the particles. The presence of swelling clay would also increase the demand of moisture. For the unbound subbase materials, the QCS specifies a minimum value of MDD of 2.05 Mg/m^3, a field density of 100% of the MMD, and in place moisture content within ±2.0% of the OMC. The results in Table 1 show that the MDD results ranged from 2.03 to 2.32 Mg/m^3 for the subbase samples tested from different sources. The highest MDD was found for source S2, which also exhibited the lowest OMC of 4.7%. The low OMC of source S2 does not match with the failed SE results, which indicate the presence of expansive clay. The highest OMC of 8.4% and 9.2% are found for sources S3 and S4 respectively, which are associated with the lowest values of MDD below the minimum specified limit of 2.05 Mg/m^3.

3.4 CBR and Swelling

The load-bearing capacity of pavement layers is generally determined from the CBR, which is an important parameter for pavement designs. The results of CBR and swelling are also summarized in Table 1. For unbound subbase materials, the QCS 2014 specifies a soaked CBR of minimum 70% and a maximum swelling of 1.0% (ASTM D 1883, 2016). The CBR values ranged from 106 to 212% for the samples tested from different sources, at least 50% above the minimum specified value. The swelling was relatively small for all tested specimens, maximum 0.3%. Source S2 was the only exception to give a slightly higher value of 0.5%, still below the maximum QCS specified value of 1.0%.

The compliance of the swelling and plasticity results with the QCS 2014 specification contradicts the SE results, especially for sources S2 and S3, which failed to meet the QCS requirement for SE. This finding may raise a question on the suitability of the SE test to assess the quality of fines for unbound pavement materials.

3.5 Loss by Abrasion

Aggregate abrasion characteristics are important for pavement materials to provide adequate resistance to crushing, degradation and disintegration under traffic loadings. The abrasion results are given in Table 1 for the subbase samples tested from different sources. The QCS 2014 specifies a maximum loss by abrasion of 40% for unbound subbase materials (ASTM C131, 2014).

The results show that all tested materials complied with the QCS requirement. The highest values (31 and 32%) were for materials supplied from sources S1 and S3, respectively. The lowest loss by abrasion value of 20% was for source S4.

3.6 Flat and Elongated Particles and Fractured Faces

Flat and elongated particles tend to fracture more easily than cubical and circular aggregate particles, and are more difficult to compact on site. Fracture faces are more

related to the angularity of coarse aggregate, which is important to ensure adequate aggregate interlock and prevent excessive deformation under loadings. The flat and elongated particles were 1% or less for all materials supplied from different sources and far lower than the maximum 15% specified in QCS 2014 (ASTM D4791, 2010). The fractured faces were 100% for all tested samples, doubled the QCS 2014 minimum specified value of 50%.

3.7 Soundness

The soundness of aggregate is related to its durability to resist disintegration by weathering due to wetting and drying and freeze-thaw actions. For subbase materials, the QCS specifies a maximum permissible weight loss of 20% after the soundness test (5 cycles of magnesium sulfate) (ASTM c88, 2018). The results in Table 1 show soundness values between 1 to 12%, lower than the maximum specified value. The highest soundness of 12% is found for materials supplied from source S3, which also exhibited the highest loss of abrasion.

4 DISCUSSION OF RESULTS

Qatar lacks quality aggregate and the construction industry relies mainly on imported aggregate for use in asphalt and concrete. Local limestone, blended with dune sand, has been successfully used for unbound pavement applications. Due to the limited availability of dune sand, the government has recently restricted its use in construction, and therefore there is a need to revise the compliance of local materials with construction specifications and to consider other options to widen the use of local resources. The results in Table 1 for subbase materials showed high variability of the properties of local limestone supplied from different sources. In terms of compliance, the most critical properties that could influence the acceptance or rejection of local limestone materials are the sand equivalent (SE) and plasticity (LL and PI), which are related to the quality of fines.

Two (2) sources, out of the five (5) sources investigated, were found to be non-compliant with the QCS 2014 requirements for SE. The non-compliant SE results were contradictory to the plasticity results. Materials from S2 and S3 failed the SE requirement, while the properties of plasticity and swelling were compliant. If expansive clay is present in the material, it would be expected that the material would exhibit high plasticity, absorb more water to reflect high OMC, and show high swelling values.

The LL and PI are widely used worldwide in pavement specifications to classify fine grained soils into different degrees of plasticity, ranging from low for silty soils to extremely high for clayey soils. The decision of whether to reject a subbase material marginally failing the SE should be discussed within the overall material compliance with other requirements and project-specific conditions. Road Note 31 (TRL, 1993) recommends higher LL and PI limits than currently specified in the QCS 2014, for granular subbases in arid and semi-arid climates, provided that the subbase is at least 1m above the groundwater level. Assuming the subbase material is used in a site where the ground water is low, there could be a case to consider relaxing QCS 2014 plasticity requirements for this specific site/project.

As defined in ASTM D2419 (2014), the SE test gives an indication of the relative

proportions of clay-size or plastic fines and dust in granular soils and fine aggregates that pass the 4.75-mm (No. 4) sieve. The suitability of the SE test to assess the quality of fines has been investigated by different researchers. Felekoglu (2008), reported that the SE test cannot differentiate between clay and silt particles, and that the Methylene Blue (MB) test is more appropriate for assessing the quality of fines. Similarly, Black (2009) indicated the same downsides of the SE test, and concluded the application of the SE test alone could lead to the acceptance of an unsuitable or to the rejection of suitable aggregates. Nikolaides et al. (2007) studied the properties of aggregate from different sources in Greece and found that aggregates that do not satisfy the SE requirement could still be suitable for use in highway engineering. They recommended the importance of including the MB test for assessing the quality of fines.

Recycled materials of excavation and construction waste could provide a sustainable alternative for unbound pavement layers. Recycled materials were used for the construction of an access road to the Rawdat Rashid landfill site in 2014, with satisfactory performance (Hassan et al., 2015). The road comprised of three adjacent subbase sections of excavation waste, crushed concrete, and a control section made of local limestone with 20% dune sand. Both the excavation waste and control subbase sections failed the SE. In-situ testing of density, surface modulus and rutting indicated excellent performance for the three subbase sections. As per the UK Specification for Highway Works, the three subbase sections would be suitable for traffic loading up to 80 million standard axles (Highways England, 2016).

There is no evidence from the results presented in this report that materials failing to meet the SE will not perform in service. It is therefore recommended to consider assessing the performance of subbase constructed with materials that failed the SE, and compare it with the QCS 2014 requirements. Such a revision of the national construction specifications will ensure that local materials are effectively used in construction and support the government strategy of sustainable development.

5 CONCLUSION AND RECOMMENDATIONS

This paper presents the characterization of unbound subbase materials for use in pavement construction. Based on the results, the following conclusions and recommendations are made:

- The properties of local limestone varied widely for materials supplied from different sources, with general compliance with the QCS 2014 requirements for use as unbound subbase.
- Materials failed to meet with the QCS specifications mainly in relation to the grading and sand equivalent.
- The non-compliant grading was related to specific sieve sizes, slightly outside the specified envelope, which could be adjusted at production with improved quality control.
- The use of dune sand to improve the quality of fine particles could put the grading marginally out of specifications, particularly for sieve sizes 0.6 and 0.425mm.
- Inconsistent results were obtained from the plasticity and SE results for assessing the quality of fine particles in unbound materials.
- Unbound subbase materials, which failed the sand equivalent, exhibited accepted

swelling results, with no evidence of harmful and expansive clay.

- Subbase materials satisfied the QCS 2014 requirements of CBR, loss by abrasion, particle shape and soundness.
- More work is required to improve the production of unbound subbase materials, mainly grading, and to assess the suitability of the SE as a pass/fail test in QCS 2014.

REFERENCES

ASTM C131/C131M (2014). Standard Test Method for Resistance to Degradation of Small-Size Coarse Aggregate by Abrasion and Impact in the Los Angeles Machine. ASTM International, the USA.

ASTM C88 (2018). Standard Test Method for Soundness of Aggregates by Use of Sodium Sulphate or Magnesium Sulphate. ASTM International, the USA.

ASTM D1140 (2017).Standard Test Methods for Determining the Amount of Material Finer than 75-μm (No. 200) Sieve in Soils by Washing. ASTM International, the USA.

ASTM D1557 (2012). Standard Test Methods for Laboratory Compaction Characteristics of Soil Using Modified Effort (56,000 ft-lbf/ft^3 (2,700 kN-m/m^3)). ASTM International, the USA.

ASTM D1883 (2016). Standard Test Method for California Bearing Ratio (CBR) of Laboratory-Compacted Soils. ASTM International, the USA.

ASTM D2419 (2014). Standard Test Method for Sand Equivalent Value of Soils and Fine Aggregate. ASTM International, the USA.

ASTM D4318 (2017). Standard Test Methods for Liquid Limit, Plastic Limit, and Plasticity Index of Soils. ASTM International, the USA.

ASTM D4791 (2019). Standard Test Method for Flat Particles, Elongated Particles, or Flat and Elongated Particles in Coarse Aggregate. ASTM International, the USA.

ASTM D5821-13 (2017). Standard Test Method for Determining the Percentage of Fractured Particles in Coarse Aggregate. ASTM International, the USA.

ASTM D6913 / D6913M (2017). Standard Test Methods for Particle-Size Distribution (Gradation) of Soils Using Sieve Analysis. ASTM International, the USA.

Black, M. P. (2009). Geologic inventory of North Island aggregate resources: Influences on Engineering Materials Properties. Geology, School of the Environment, The University of Auckland, North Island. Available at https://www.aqa.org.nz/uploads/files/North%20Island%20Geological%20Inventory%202009.pdf.

Felekoglu, B. (2008). A comparative study on the performance of sands rich and poor in fines in self-compacting concrete. *Construction and Building Materials*, Vol. 22, Issue 4.

Hassan K. E., Reid, J. M. & Al-Kuwari, M. S. (2015). *Use of recycled and secondary aggregates in Qatar – Guidance document*. (TRL Published Project Report PPR736). TRL Limited, Crowthorne, the UK. Available at http://www.trl.co.uk/reports-publications/report/?reportid=7013.

Highways England (2016). UK Specification for Highway Works, Series 800 Road Pavements – Unbound, cement and other hydraulically bound mixtures. Manual of Contract Document for Highway Works Volume 1. Highway England, London, the UK. Available at http://www.

standardsforhighways.co.uk/ha/standards/mchw/vol1/pdfs/MCHW%20800.pdf.

Nikolaides, A. S., Manthos, E. & Sarafidou, M. (2007). *Sand equivalent and Methylene blue value of highway engineering*. Aristotle University of Thessaloniki, Department of Civil Engineering, Thessaloniki, Greece.

QCS (2014). Qatar Construction Specifications. Ministry of Municipality & Environment, Qatar Standards, Doha, Qatar.

TRL (1993). *A guide to the structural design of bitumen-surfaced roads in tropical and sub-tropical countries*. (TRL Overseas Road Note 31). TRL Limited, Crowthorne, the UK.

Cite this article as: Mohamedain M. H., Hassan K. E., El-Hussain O., Al-Emadi K., "Challenges for the Use of Local Materials in Unbound Road Subbase in Qatar", *International Conference on Civil Infrastructure and Construction (CIC 2020)*, Doha, Qatar, 2-5 February 2020, DOI: https://doi.org/10.29117/cic.2020.0072

Compressive Strength and Hydration of Ravennagrass Baggase Ash Concrete

Ashhabu Elkaseem
elkaseem77@gmail.com
Department of Civil Engineering, Hassan Usman Katsina Polytechnic, Nigeria

Samaila Bawa
muazubawaf@gmail.com
Department of Civil Engineering, Hassan Usman Katsina Polytechnic, Nigeria

ABSTRACT

The paper presents the findings of the effect of revennagrass baggase ash concrete compressive strength using compression machine and hydration behavior with the aid of non-contact electrical resistivity measurement device. The result indicates that concrete containing 20% of Revennagrass Baggase Ash recorded the highest compressive strength for 1day, 3days, 7days and 28days respectively. This indicates that, the higher the increase in baggase ash the more the concrete strength up to 20% as the maximum dosage. The reverse is the case in terms of setting time, where the increase in the percentage addition brings about delay in setting time of concrete.

Keywords: Compressive strength; Baggase ash; Electrical resistivity; Admixture

1 INTRODUCTION

In the process of an investigation it reveals that, using waste materials always brings about positive impact for the development of any environment technically and economically (Guilherme et al., 2009). Many forms of pozzolanic materials such as fly ash, rice husk ash, silica fume to mention a few, have been used to serve as additives to our construction materials and this helps in the reduction of danger and hazard to the environment for leaving them as wastes. Sugarcane baggase ash was found to be suitable after investigation as a good pozzolanic material as it records the presence of high amorphous silica and silica content among its chemical composition (Martirena et al., 1998; Singh, 2000; Ganesan, 2007). In this study, concrete with and without revennagrass baggase ash was subjected to investigation from casting to a period of 24hours using noncontact electrical resistivity measurement device and thereby comparing the result in terms of hydration and strength development.

2 MATERIALS AND EXPERIMENTS

2.1 Materials

Materials used in this study were ordinary Portland cement from Dangote Cement Company, Nigeria. Revennagrass baggase ash, referred to as RBAC sample was collected in Funtua Farm of Katsina State, Nigeria and burnt in boilers at a temperature ranging from 600 to 900^{o}C. The chemical composition for the cement and revennagrass baggase ash is as shown in Table 1 and 2 respectively. Then distilled water was used for mixing throughout the experiment.

Table 1: Chemical composition of Portland cement

OXIDES	0 [%]
SiO_2	20.02
Fe_2O_2	1.39
Al_2O_2	3.29
CaO	69.66
MgO	1.43
Na_2O	0.03
SO_2	3.79
K_2O	0.04
L.O.I	0.7

Table 2: Chemical composition of revennagrass baggase ash

OXIDES	0 [%]
SiO_2	59.12
Fe_2O_2	7.51
Al_2O_2	18.01
CaO	8.42
MgO	4.44
Na_2O	0.81
SO_2	2.02
K_2O	5.01
L.O.I	3.5

Table 3: Mix proportion for different concrete

Sample	w/c	Mix ratio	% Addition of baggase ash
RBAC0	0.50	1 : 2 : 4	0
RBAC1	0.50	1 : 2 : 4	10
RBAC2	0.50	1 : 2 : 4	20
RBAC3	0.50	1 : 2 : 4	30

2.2 Experiments

Three different tests were conducted on the concrete with zero percentage addition of revennagrass baggase ash and similar tests were conducted to sample with percentage addition of revennagrass baggase ash. The constituents mix ratio was shown in Table 3. The test procedures were as follows:

2.2.1 Electrical resistivity

The procedure for the determination of resistivity of concrete with zero percentage addition of revennagrass baggase ash and that with the percentage addition of 10%, 20% and 30% respectively, represented symbolically as RBAC0, RBAC1, RBAC2 and RBAC3 was performed using non-contact electrical resistivity measurement device. Mix was casted in mold and the cubes were tested for resistivity after the period of 24hrs hydration. The same test was performed on the concrete at different percentage addition of revennagrass baggase ash, then finally data was collected, analyzed and presented in

our findings based on electrical resistivity measurement (Zongjin et al., 2003).

2.2.2 Compressive strength

Same samples were prepared and casted in 150x150x150mm molds and transferred to curing tank after period of 24hrs for curing before the test. The samples were later subjected to compressive strength test using compression testing machine for a period of 1day, 3days, 7days and 28days respectively. The result is as shown in the result section.

2.2.3 Setting time

Setting time test was conducted to determine initial and final setting time for all samples with the aid of Vicat apparatus (ASTM C191-92, 1993).

3 RESULTS AND DISCUSSION

3.1 Electrical resistivity

Figure 1 presents electrical resistivity development (P (t) curve for different samples with and without percentage addition of revennagrass baggase ash during the first period of 24hrs, it can be observed that, the cement with RBAC3 recorded the highest resistivity and RBAC0 with the lowest, this shows that, the higher the baggase ash the more the resistance up to 30% as in Figure 2.

Four periods were identified from a sample resistivity derivative curve on the bases of critical points pm, pa and pi which classified the hydration process. The periods include dissolution period donated with (I), induction period (II), acceleration period (III) and finally deceleration period (IV) and this conforms to similar results by Zongjin et al. (2003) and Xiaosheng et al. (2008). It was also observed that, more the percentage addition the less the conductivity of electricity as a result of pores decreasing within the cement paste. Another observation made on the curve is the inflection point, the delay was observed for the final inflection to occur as the percentage of revennagrass baggase ash decreases as in the case of RBAC3 at 16.38hrs, which appears earlier than RBAC2 and RBAC1 at 18.45 and 19.47 hrs. respectively.

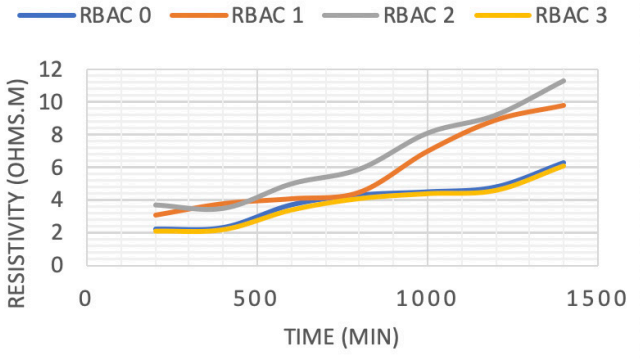

Figure 1: Electrical resistivity of baggase ash concrete for 24 hrs.

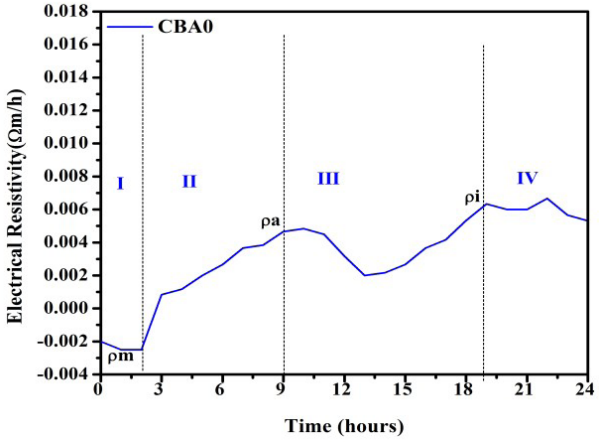

Figure 2: Samples resistivity derivative curve

3.2 Compressive Strength

The result which was presented in Figure 3 revealed that as it was observed in the previous study [4], RBAC2 has the highest compressive strength for 1day, 3days, 7days and 28days respectively. This shows direct effect of baggase ash to concrete strength.

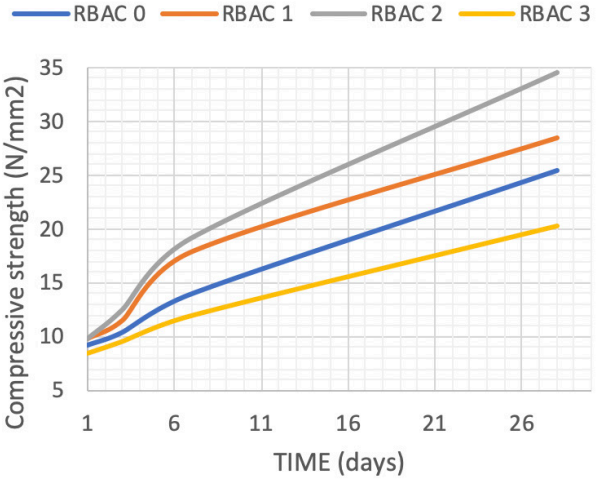

Figure 3: Compressive strength at various percentage additions

3.3 Setting time

It was observed that, there is a delay in the setting time of cement with the percentage addition of revennagrass baggase ash compared to that of zero percent addition as shown in Figure 4. It indicates that, baggase ash can be used as a retarder in concrete.

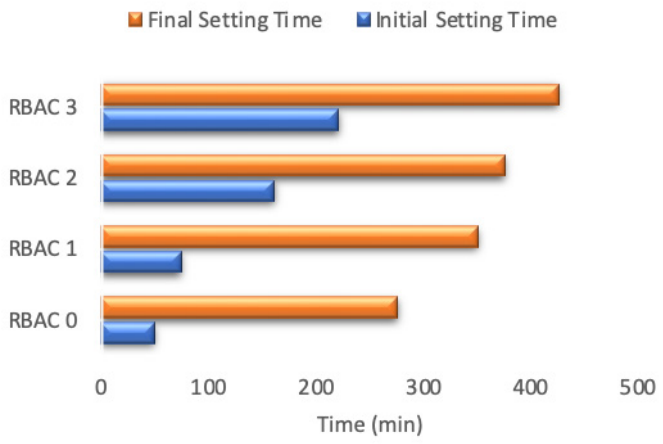

Figure 4: Initial and final setting time at various percentage addition of RBAC

4 CONCLUSION

This paper presents the findings of the effect of revennagrass baggase ash on concrete compressive strength and also examines hydration behavior using non-contact electrical resistivity measurement device. The result shows that, increase in the percentage addition of revennagrass baggase ash has direct bearing on increase in concrete compressive strength up to 20%. This shows that, where revennagrass baggase is available, the use of its ash would substitute the expensive conventional admixtures in concrete industry. Also the delay observed in the setting time of cement with the percentage addition of baggase ash shows the suitability of the baggase ash to serve as retarder in concrete. This would allow for steady strength development in the concrete.

ACKNOWLEDGMENT

The authors wish to acknowledge the efforts of Hassan Usman Katsina Polytechnic and Tertiary Education Trust Fund Nigeria (Tetfund) for sponsoring this research.

REFERENCES

American Society of Testing Materials (1993). Standard test method for setting time of hydraulic cement, C191-92, 866-868.

Ganesan, K., Rajagopal, K. & Thangavel, K. (2007). Evaluation of bagasse ash as supplementary cementitious material. *Cem. Concr. Compos*., *29*(6), 515-524.

Guilherme, C. C., Romildo D. T. F., Luís M. T. & Eduardo de M. R. F. (2009). Ultrafine grinding of sugar cane bagasse ash for application as pozzolanic admixture in concrete. *Cem. Concr. Res*., *39*(2), 110-115.

Martirena, J. F. M. H., Middeendor, B., Gehrke, M. & Budelmann, H. (1998) Use of wastes of the sugar industry as pozzolana in lime- pozzolana binders: Study of the reaction. *Cem. Concr. Res*., *28*(11), 1525-1536.

Singh, N.B., Singh, V.D. & Rai, S. (2000). Hydration of bagasse ash-blended Portland cement.

Cem. Concr. Res., *30*(9), 1485-1488.

Xiaosheng, W., Lianzhen, X. & Zongjin, L. (2008). Electrical measurement to assess hydration process and the porosity formation. *Journal of Wuhan University of Tech*., *23*(5): 761-766.

Zongjin, L., Xiaosheng, W. & Wenlai, L. (2003). Preliminary interpretation of Portland cement hydration process using resistivity measurements. *Material Journal*, American Concrete Institute, *100*(3): 253-257.

Zongjin, L., Lianzhen, X. & Xiaosheng, W. (2007). Determination of concrete setting time using electrical resistivity measurement. *Journal of materials in civil engineering*, *19*(5), 423-427.

Cite this article as: Elkaseem A., Bawa S., "Compressive Strength and Hydration of Ravennagrass Baggase Ash Concrete", *International Conference on Civil Infrastructure and Construction (CIC 2020)*, Doha, Qatar, 2-5 February 2020, DOI: https://doi.org/10.29117/cic.2020.0073

An Artificial Intelligence Approach to Estimate Travel Time along Public Transportation Bus Lines

Mohammad S. Ghanim
mohammad.ghanim@jacobs.com
CH2M HILL International B.V., Doha, Qatar

Khaled Shaaban
kshaaban@qu.edu.qa
Department of Civil and Architectural Engineering/Qatar Transportation and Traffic Safety Center, Qatar University, Doha, Qatar

Motasem Miqdad
mm080855@qu.edu.qa
Department of Civil and Architectural Engineering, Qatar University, Doha, Qatar

ABSTRACT

Public transportation sectors have played significant roles in accommodating passengers and commodities efficiently and effectively. The modes of public transportation often follow pre-defined operation schedules and routes. Therefore, planning these schedules and routes requires extensive efforts in analyzing the built environment and collecting demand data. Once a transit route is operational as an example, collecting and maintaining real-life information becomes an important task to evaluate service quality using different Key Performance Indicators (KPIs). One of these KPIs is transit travel time along the route. This paper aims to develop a transit travel time prediction model using an artificial intelligence approach. In this study, 12 public bus routes serving the Greater City of Doha were selected. While the ultimate goal is to predict transit travel time from the start to the end of the journeys collected over a period of one-year, route-specific inputs were used as inputs for this prediction. To develop a generalized model, the input variables for the transit route included the number and type of intersections, number of each type of turning movements and the built environment. An Artificial Neural Networks (ANN) model is used to process 78,004 valid datasets. The results indicate that the ANN model is capable of providing reliable and accurate transit travel time estimates, with a coefficient of determination (R^2) of 0.95. Transportation planners and public transportation operators can use the developed model as a tool to estimate the transit travel time.

Keywords: Public transportation; Artificial neural networks; Travel time prediction

1 INTRODUCTION

The population in the State of Qatar has increased dramatically during the last few decades and the lifestyle for the people living in the country became a car-dependent one (Shaaban & Khalil, 2012; Shaaban & Khalil, 2013). These conditions caused a substantial pressure on the transport system. Moreover, the current National Vision 2030 for Qatar calls for a reliable multimodal transport system to support the national economic and social development of the country. Furthermore, Qatar is currently planning to host different major events in the near future including the FIFA World Cup

2022 event. Therefore, it is necessary to have an efficient, accessible and sustainable transport system in the country (Shaaban & Hassan, 2014; Shaaban & Maher, 2019).

Previous studies indicate that efficient public transportation is one of the methods to improve traffic congestion (Beaudoin, Farzin, & Lawell, 2015, Dewan & Ahmad, 2007; Shaaban & Khalil, 2012). In Qatar, the public bus service provides an affordable and clean mode of transport to many people (Shaaban & Khalil, 2012; Shaaban & Khalil, 2013). Mowasalat, the only public transport bus system operator in the country, manages more than 45 bus routes around Qatar. Some of these routes connect the city of Doha with other cities.

Nevertheless, the reliability of the bus system, which is defined as the abidance of the bus arrival time to the announced scheduled timings, is considered an issue. The public bus users have reported the need to improve the reliability of the existing bus system (Shaaban & Khalil, 2012; Shaaban & Khalil, 2013). This problem could be tackled using different methods, including improving route planning and scheduling (Nam & Park, 2018), using more realistic and empirical models (Li et al., 2018), improving quality control (Friman & Fellesson, 2009), using Automated Vehicle Location (AVL) systems (Hickman, 2004), and notifying the users of actual or better estimation of arrival time using Advanced Traveler Information Systems (ATIS) (Kumar et al, 2005).

The purpose of this study is to develop a prediction model that can be used by public agencies and transport operators to provide more accurate travel and arrival times for the bus system. The development of such a model using historical data for different routes in Qatar can be useful to improve the travel time reliability issue. The model can be utilized for planning and ATIS purposes. Such a model could resolve the current gap that public transport bus operators in Qatar have to deal with due to the lack of regionally developed models needed to estimate realistic travel time based on empirical efforts.

2 RESEARCH OBJECTIVE

Some of the key performance indicators that are often used in evaluating the quality of public transportation services are schedule adherence (Levine et al., 2000), transit travel time (Kumar at al, 2019), service frequency (Ingvardson et al., 2018) , and out-of-pocket cost (Koppelman, 1983). It can be noticed that accurately predicting transit travel time contributes towards improved service quality. While those travel time values can be estimated at the planning stage, comparing those values against the operational ones can lead to an improved planning process. The improvement process can be further appreciated if prediction models based on real-life observations are readily available. Furthermore, such models can be integrated within the Intelligent Transportation Systems (ITS) framework (Shaaban & Khalil, 2012; Shaaban & Khalil, 2013).

The research objectives can be addressed by implementing the following procedures:

- Collect, process, and analyze historical bus journey trips at selected sites, covering differently built environmental conditions.
- Identify the potential quantified input variables that can be used to estimate the transit travel time for different routes.
- Develop transit travel time prediction model using artificial intelligence techniques and methods based on the previously collected and processed input variables.

3 RESEARCH METHODOLOGY

Public transportation data were collected from two different sources. The first one was Mowasalat, which is the governmental entity in Qatar that manages and operates the public bus system in Qatar. The second source was collecting additional data manually as shown in Table 1. The collected data considered the characteristics of the bus routes in terms of both fixed features (such as route length, number of turning movements, number and type of intersections) and traffic-related features (such as the day of the week and peak periods). It should be noted that the research team could not get other useful data (such as number of and rates of passenger ridership and boarding and alighting passengers at bus stops) due to logistics and security reasons. Accordingly, this study utilized the available data only.

Table 1: Description of the independent variables

Variable	Variable Type	Encoding Description
	Input Variables	
Distance	Numerical	Distance as recorded by AVL; rounded to nearest 1 km
Month	Binary	12 Columns (one for each month) were defined at which each column accepts either 0 or 1 as value
Weekday	Binary	7 Columns (one for each weekday) were defined at which each column accepts either 0 or 1 as value
Weekend	Binary	1 = Weekend (Friday or Saturday) 0 = All other days
Peak	Binary	4 Columns (AM, MD, PM, and Off-Peak) were defined at which each column accepts either 0 or 1 as value
Starting Time	Numerical	The timing bus started the trip, rounded to nearest 30 mins for ease of analysis and interpretation
Through	Numerical	Number of Movements per trip/route
Left	Numerical	Number of Movements per trip/route
Right	Numerical	Number of Movements per trip/route
U-Turn	Numerical	Number of Movements per trip/route
CBD	Binary	3 Columns (Inner-CBD, Outer-CBD, and Non-CBD) were defined at which each column accepts either 0 or 1 as value
Road Class	Binary	1= Major roads (arterials, expressways...etc.) 0= Local Roads
Land use	Binary	4 Columns (Residential, Commercial, Industrial, and Mixed-use) were defined at which each column accepts either 0 or 1 as value
Stops	Numerical	Number of Stops per Route/Trip
Signals	Numerical	Number of Traffic Signals per Route/Trip
Roundabouts	Numerical	Number of Roundabouts per Route/Trip
	Output Variable	
Travel Time	***Numerical***	Trip duration in minutes rounded to 1 min

After grouping and filtering the collected data, the average transit travel times are used for matching records. For instance, if multiple records have identical input variables but their outputs are different, then the average values of these outputs are used after achieving a 95 percent confidence level that there are no statistical differences between these outputs. Then the outliers are excluded from the analysis.

After filtering the data records, it was found that 78,004 of valid data records were available for the analysis. Due to the nature of the independent variables (which has both numerical and categorical variables), an artificial intelligence approach, Artificial Neural

Networks (ANN), has been used to process and model valid records. This approach has been used due to its capability of analyzing big data and understanding the underlying relationship between the independent variables (Jun Lee & Siau, 2001; Ghanim & Abu-Lebdeh, 2018; Ghanim & Shaaban, 2018). The ANN approach performs well in predicting various combinations of input variables that were not previously observed in the analyzed data (Yahia & El-taher, 2010). ANN techniques have several applications in transportation-related studies and research, as can be found in (Ghanim, Abu-Lebdeh et al., 2013a; Ghanim, Abu-Lebdeh et al., 2013b; Ghanim, Dion et al., 2014; Ghanim & Abu-Lebdeh, 2015).

Inspired from the natural neuro-system that exists in humans, ANN processes the stimuli (i.e., inputs) and transfers them into reactions (i.e., outputs) (Yahia & El-taher, 2010). A typical ANN model consists of three different layers. The first layer is for the input variables, where the inputs are usually normalized via transfer functions to avoid any potential bias of the input vectors. The second layer is the hidden layer, which consists of several neurons that would receive the weighted signals from the input layers and transfer other sets of weighted signals to the third layer (i.e., the outputs layer). The third layer processes all the signals received from the neurons in the hidden layer and transfers those signals into an output vector.

The valid records were randomly divided into three different groups. The first one is the training group that is used to train and calibrate the weights between the three different layers through an iterative process. The second group is the validation group that is used to monitor the convergence process of the overall training process, and hence avoiding the model "overfitting" during the training process. The third group is the testing group, which is an independent set of data that were not previously experienced through the ANN model development. In other words, the testing group is used to evaluate the performance of the trained ANN model.

- **Training records:** 54,602 records, which are approximately 70% of all the valid records, and used to train the ANN.
- **Validation records:** 11,701 records, which are approximately 15% of all the valid records and used to validate and monitor the performance of the ANN training process.
- **Testing records:** 11,701 records, which are approximately 15% of all the valid records and used to evaluate the prediction performance of the trained ANN model.

Several training and learning algorithms were evaluated, and the selected one was Levenberg-Marquardt algorithm due to its fast convergence. The hidden layer that was used in the final ANN model consists of 10 neurons. Signals from the input layer are transferred to the output layer using the hyperbolic-tangent transfer function, while a linear transfer function is used to transfer the signal from the hidden layer to the output layer.

Figure 1 and Table 2 summarize the performance of the developed ANN model in predicting the route transit travel time for the different conditions.

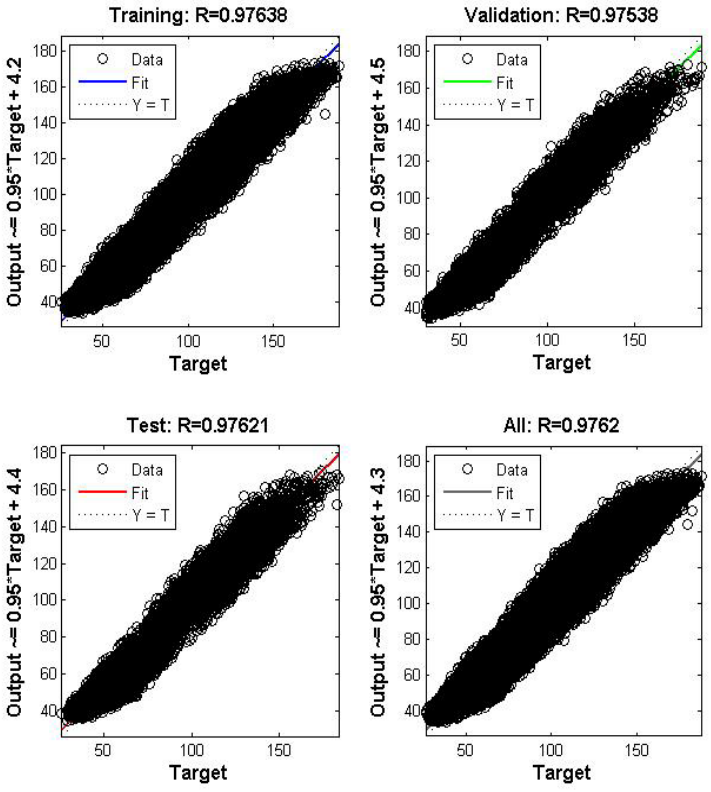

Figure 1: Performance of ANN for training, testing and validation datasets

Table 2: Performance measures for the developed ANN model training process

Number of Epochs	R	R^2	Mean-Squared Error (min^2)	Mean of Absolute Error (min)	Standard Error (min)
123	**0.9762**	**0.9530**	**55.21**	**5.94**	**0.13**

4 VALIDITY OF TRANSIT TRAVEL TIME DEVELOPED MODEL

Following the development of the ANN prediction model, its prediction accuracy has been evaluated by comparing the observed travel time to the predicted ones of the testing group (recall that the testing group has 11,701 records that are used only to assess the performance of the developed model, and they were not part of the learning process at any stage).

To do so, two histograms were created. The first one shows the number of records where the error in predicting the journey's transit travel time is within a given time range. The second histogram shows the number of records where the error is within a given percentage of the trip's observed travel time, as can be seen in Figure 2 and Figure 3.

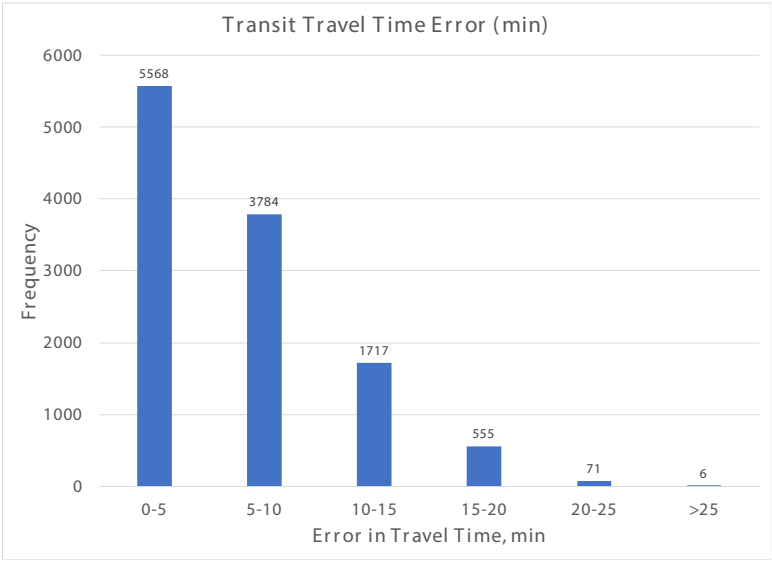

Figure 2: Performance of ANN for training, testing and validation datasets

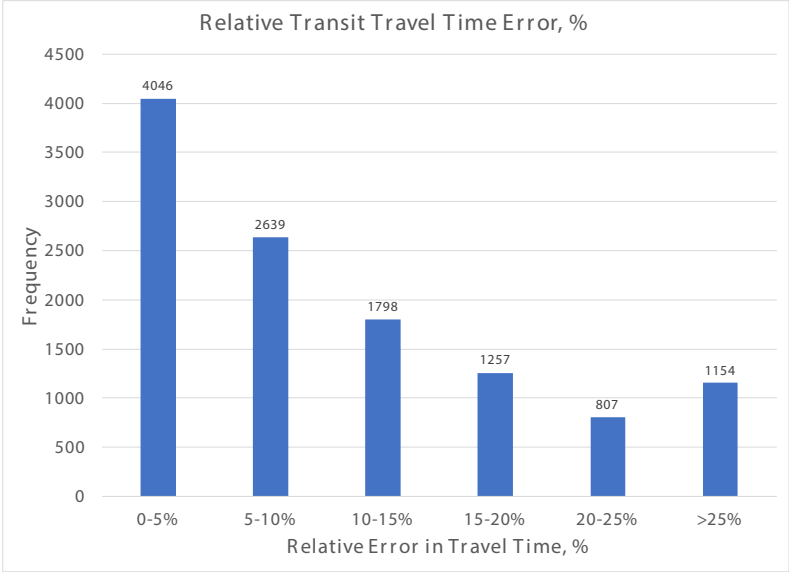

Figure 3: Performance of ANN for training, testing and validation datasets

Figure 2 and Figure 3 clearly reveal that the developed model is performing well in providing a reliable estimate of travel time. For instance, for approximately half of the transit trips, the prediction error is less than five minutes, and around 95% of the trips have an error of 15 minutes or less.

In terms of the percentage error of travel time prediction, more than two-third of the records have an error of 15% or less, with only 10% of all the trips having experienced an error that is more than 25% of its travel time. This observation is an indication that another input variable describing the trip length (i.e., short or long trip for instance) can

be introduced to improve the prediction capabilities of the model.

5 CONCLUSION AND RECOMMENDATIONS

The objective of this research is to evaluate the potential implementation of ANN in predicting model the travel time of different bus routes using a set of variables describing the route characteristics. The model can be later used as a tool by public transportation operators and planners. To do so, a one-year worth of data from 12 different routes were collected, processed and modeled.

Approximately 150,000 records were analyzed. The sum of 78,004 records were found valid and used in the analysis. An ANN model is developed to predict the travel time along the transit route. The results show that the ANN was able to provide a reliable estimation of travel times.

One of the key limitations of this study is the absence of traffic volumes or other traffic congestion indications along the transit travel routes due to the unavailability of such data. Nonetheless, the developed model furnishes the overall framework that can be enriched when traffic information or congestion level indicators are nested in the future.

While the study shows promising results regarding the use of the developed model by stakeholders to plan different public transit routes, there is a significant potential of expanding the scope of this study, where more information about ridership can be integrated into the model. It can also be expanded to be integrated within a real-time advanced traveler information system or an advanced public transportation system.

ACKNOWLEDGMENT

The authors acknowledge the valuable cooperation of Mowasalat in making their data available. All views and results presented in the paper are solely the authors'.

REFERENCES

Beaudoin, J., Farzin, Y., & Lawell, C. (2015). Public transit investment and sustainable transportation: A review of studies of transit's impact on traffic congestion and air quality. Research in Transportation Economics, 52, 15-22.

Dewan, K. & Ahmad, I. (2007). Carpooling: a step to reduce congestion. *Engineering Letters 14*(1): 61-66.

Friman, M., & Fellesson, M. (2009). Service supply and customer satisfaction in public transportation: The quality paradox. Journal of Public transportation, *12*(4), 4.

Hickman, M. (2004). Bus automatic vehicle location (AVL) systems. In Assessing the Benefits and Costs of ITS (pp. 59-88). Springer, Boston, MA.

Ghanim, M., Abu-Lebdeh, G., and Ahmed, K. (2013a). Microscopic Simulation Study of Transit Signal Priority Implementation Along an Arterial Corridor, *5th International Conference on Modeling, Simulation, and Applied Optimization. Hammamet*, Tunisia.

Ghanim, M., Abu-Lebdeh, G. & Ahmed, K. (2013b). Modeling Historical Traffic Data using Artificial Neural Networks, *5th International Conference on Modeling, Simulation, and Applied Optimization*. Hammamet, Tunisia.

Ghanim, M., & Abu-Lebdeh, G. (2018). Projected state-wide traffic forecast parameters using artificial neural networks. IET Intelligent Transport Systems, *13*(4), 661-669.

Ghanim, M. S. & Abu-Lebdeh, G. (2015). Real-time dynamic transit signal priority optimization for coordinated traffic networks using genetic algorithms and artificial neural networks. *Journal of Intelligent Transportation Systems*, *19*(5): 327-338.

Ghanim, M. S., Dion, F. & Abu-Lebdeh, G. (2014). The impact of dwell time variability on transit signal priority Performance. *Canadian Journal of Civil Engineering*, *41*(2): 154-163.

Ghanim, M. S. & Shaaban, K. (2018). Estimating turning movements at signalized intersections using artificial neural networks. *IEEE Transactions on Intelligent Transportation Systems*, *20*(5): 1828-1836.

Ingvardson, J. B., Nielsen, O. A., Raveau, S., & Nielsen, B. F. (2018). Passenger arrival and waiting time distributions dependent on train service frequency and station characteristics: A smart card data analysis. Transportation Research Part C: Emerging Technologies, 90, 292-306.

Jun Lee, S. & Siau, K. (2001). A review of data mining techniques. *Industrial Management & Data Systems*, *101*(1): 41-46.

Koppelman, F. S. (1983). Predicting transit ridership in response to transit service changes. Journal of Transportation Engineering, *109*(4), 548-564.

Kumar, P., Singh, V., & Reddy, D. (2005). Advanced traveler information system for Hyderabad City. IEEE Transactions on Intelligent Transportation Systems, *6*(1), 26-37.

Kumar, B. A., Jairam, R., Arkatkar, S. S., & Vanajakshi, L. (2019). Real time bus travel time prediction using k-NN classifier. Transportation Letters: The International Journal of Transportation Research, *11*(7).

Levine, J., Hong, Q., Edward Hug Jr, G., & Rodriguez, D. (2000). Impacts of an advanced public transportation system demonstration project. Transportation research record, *1735*(1), 169-177.

Li, Z., Hensher, D. A., & Ho, C. (2018). An empirical investigation of values of travel time savings from stated preference data and revealed preference data. Transportation Letters, 1-6.

Nam, K., & Park, M. (2018). Improvement of an optimal bus scheduling model based on transit smart card data in Seoul. Transport, *33*(4), 981-992.

Shaaban, K. & Hassan, H. M. (2014). Modeling significant factors affecting commuters' perspectives and propensity to use the new proposed metro service in Doha. *Canadian Journal of Civil Engineering*, *41*(12): 1054-1064.

Shaaban, K. & Khalil, R. F. (2012). Proposed policies to support the new metro system in Qatar. *Procedia-Social and Behavioral Sciences*, 48: 2315-2324.

Shaaban, K. & Khalil, R. F. (2013). Investigating the customer satisfaction of the bus service in Qatar. *Procedia-Social and Behavioral Sciences*, 104: 865-874.

Shaaban, K. & Maher, A. (2019). *Using the theory of planned behavior to predict the use of an upcoming public transportation service in Qatar*. Case Studies on Transport Policy, https://doi.org/10.1016/j.cstp.2019.11.001.

Yahia, M. & El-taher, M. (2010). A new approach for evaluation of data mining techniques. *International Journal of Computer Sciences*, *7*(5): 181-186.

Cite this article as: Ghanim M. S., Shaaban K., Miqdad M., "An Artificial Intelligence Approach to Estimate Travel Time along Public Transportation Bus Lines", *International Conference on Civil Infrastructure and Construction (CIC 2020)*, Doha, Qatar, 2-5 February 2020, DOI: https://doi.org/10.29117/cic.2020.0074

Evaluating the Operational Impact of Left-Turn Exclusive Number of Lanes: A Case Study from Qatar

Khaled Shaaban
kshaaban@qu.edu.qa
Department of Civil and Architectural Engineering/Qatar Transportation and Traffic Safety Center, Qatar University, Doha, Qatar

Mohammad S. Ghanim
mohammad.ghanim@jacobs.com
CH2M HILL International B.V., Doha, Qatar

ABSTRACT

Left-turning movements can significantly reduce the overall capacity of signalized intersections due to the queueing built up. Intersections with heavy left-turning volumes tend to use multiple lanes to accommodate left-turn movements, such as double and triple left-turn lanes. This study compares the potential impact of different left-turn configurations for saturated/near saturated levels. A signalized intersection located in the city of Doha, Qatar, is selected to be examined and evaluated. A microscopic simulation approach is used to replicate the existing conditions before implementing different traffic demands, left-turn bay configurations, and traffic control parameters. The results suggest that signalized intersections, in general, and left-turn movements, in particular, benefit from multiple left-turn lanes. However, the anticipated operational benefits vary depending on several factors, such as the demand for left-turn movements and the length of the left-turn bay. The findings obtained from this study could be helpful for planners and decision-makers to decide the type of left-turn lane treatment needed to increase the capacity for different conditions. This work can be extended to mathematically quantify the expected operational improvements at signalized intersections

Keywords: Micro-simulation; Traffic signal; Intersection; Left turn; Traffic operations

1 INTRODUCTION

Major intersections with high left-turning volumes are often seen along urban corridors, which cause major congestion and lower capacity problems along these corridors (Saha et al., 2017; Ghanim & Shaaban 2019; Ghanim & Abu-Lebdeh 2016). One of the solutions to improve these conditions and avoid increasing the green time for the left turning movement is increasing the number of left-turn lanes per approach at the intersection to two or three left-turn lanes (Spring & Thomas, 1999; Sando & Mussa, 2003; Yang & Zhou, 2011; Qi et al. 2016).

Adding these lanes has many advantages, including a reduction in the queues and delay for the left turning movements and a reduction in the length of the left-turn lanes since vehicles will be stored in multiple lanes instead of a single lane. However, a proper decision is needed when deciding between dual and triple left-turn lanes because of the major difference in land-use needs and construction costs. Few studies investigated and compared the effects of the geometry of the turn lane and traffic signal characteristics on

the operations of dual and triple left-turn lanes, especially in the case of near-saturation conditions. In general, most of the studies focused on investigating the saturation flow rate when studying double and triple left-turn lanes.

In regard to dual left-turn lanes, Capelle and Pinnell (1961) reported that the capacity of the inside and outside lanes are 12% and 5% below the through lane capacity. Nicholas (1989) investigated the efficiency of dual left-turn lanes and reported that the overall capacity increased by 17.5% in the case dual left-turn lane. In regard to triple left-turn lanes, Leonard (1994) found that the saturation flow for the inside, middle, and outside lanes is 1,946, 1,950, and 1,891 vehicles per hour green per lane (vphgpl), respectively. The results indicated a significant difference for the outside lane compared to the other two lanes. Stokes (1995) reported no significant difference between the saturation flow rate of the inside, middle, and outside left-turn lanes. Moreover, the same study reported no difference between the left-turn and through lane saturation flow rates. Ackeret (1996) reported that the saturation flow is 1,825, 1,809, and 1,773 vphgpl for the outside, middle, and inside left-turn lanes, respectively. This research uses different geometric design and traffic volume scenarios in order to identify the best cases to use dual or triple left-turn lanes in near-saturated conditions at signalized intersections.

2 RESEARCH OBJECTIVES

The objective of this research is to evaluate the potential benefits of converting an exclusive single left-turn lane into double or triple lanes configurations at signalized intersections and to identify the level at which it would be beneficial to increase the number of exclusive left-turn lanes. Ultimately, the outcomes of this study can be further employed to quantify the expected level of improvements that the number of exclusive left-turn lanes has on the operational performance of signalized intersections.

3 METHODOLOGY

In order to meet the previously mentioned research objectives, an intersection in the city of Doha, Qatar, is selected. The intersection is a four-leg intersection that is currently operational and signalized. The aerial image of the intersection can be seen in Figure 1. Turning movement counts were collected at different peak periods and have been used later for the calibration process. A microscopic environment is used to calibrate the intersection before different scenarios are tested and examined. Traffic simulation modeling is a well-known tool that enables the simulation and analysis of various traffic conditions in a safe and cost-effective way. To accomplish the objectives of the study, traffic simulation models are used to model and analyze the different left-turn treatments for various traffic and geometric conditions.

Figure 1: Aerial Image Showing the Study Intersection

3.1 Geometric Layout

As can be seen in Figure 1, the intersection consists of four approaches. Each approach consists of the exclusive left-turn bay (with various lengths and number of lanes), three lanes for through movements, and channelized right-turn lane.

In this research, the geometric configurations of the northbound only (i.e., the south approach) have been manipulated. Currently, this approach has three lanes for left-turn movements, and the bay length is 300 meters of storage. The geometric configurations of this lane have been modified to accommodate different scenarios as follow:

- The number of lanes of the exclusive left-turn bay (single, double and triple lanes)
- The length of the exclusive left-turn bay (300, 200, and 100 meters)

3.2 Traffic Controller

Since the volume-to-capacity (g/C) ratio depends on the cycle length and effective green, three cycle lengths were examined 90, 120, and 150 seconds. Meanwhile, the effective green is kept constant at 30 seconds. This way, the effective-green-to-cycle ratio (g/C) ratio will be 0.2, 0.25, and 0.33. A yellow interval of four seconds and an all-red interval of one second are also used.

3.3 Traffic Volumes

A wide range of left-turn traffic demand has been used to cover unsaturated, near-saturated and over-saturated traffic conditions. Accordingly, the left-turn volumes are: 200, 300, 400, 500, 750, 900 and 1000. While these numbers represent the demand, depending on the congestion level, part of the demand was able to pass through the intersection, as will be illustrated later. Different turning movements can be estimated

based on traffic design hour factors (Ghanim & Abu-Lebdeh, 2019; Ghanim, 2011). The following assumptions are further made to assure an experimental controlled environment. First, the right-turn movements are ignored (i.e., 0% for right-turn movements). Secondly, only passenger cars were considered to overrule the impact of heavy trucks.

3.4 Calibration of Simulation Environment

There are different microscopic traffic simulation packages available in the market, including CORSIM, Paramics, SimTraffic, and VISSIM (Holm et al., 2007; Chen et al., 2016; Nyame et al.; 2018; Shaaban & Kim, 2016; Sun, 2018). These packages are capable of modeling different types of intersections with different variety of geometry and traffic characteristics in order to conduct traffic operations studies including unsignalized intersections (Kaysi & Alam, 2000; Chowdhury et al.; 2005; Liu et al., 2012), signalized intersections (Shaaban & Ghanim, 2018, Ghanim & Shaaban, 2019, Shaaban et al., 2019a), and roundabouts (Bared & Afshar, 2009; Shaaban et al., 2019b; Elhassy et al., 2020). These packages provide a reliable technique for a detailed analysis of different scenarios and strategies. In this study, VISSIM was selected to compare and evaluate the performance of the different proposed alternatives. The intersection has been calibrated to reflect the recommendations of the Ministry of Transport and Communications in Qatar.

4 SIMULATION RESULTS

The simulation results of 540 scenarios are collected and summarized. For each scenario, a total of 10 multiple runs are averaged to represent one scenario. The results are analyzed, and the average delay (in seconds per vehicle) values are presented and discussed in this paper.

4.1 Single Lane vs. Double Lane Comparison

The first comparison in this research is a comparison between having a single left-turn lane or double left-lanes to accommodate the left-turning movements. Figure 2 summarizes the finding in terms of average delay and left-turn hourly discharge rate. The results also aggregated to show the cases associated with two g/C values, 0.2 and 0.25. Moreover, three storage lengths are considered (100, 200, and 300 meters). As for the single-lane scenarios, it can be seen that they can accommodate traffic up to a certain limit before the delay values significantly increase, indicating a grid-lock. The limits are 400 veh/hr for a g/C ratio of 0.2 and 500 veh/hr for a 0.25 ratio of g/C regardless of the left-turn storage length. It both cases, the saturation flow rate is 2,000 vehicles per hour. With respect to the discharge rates, a similar trend can be seen, where the single-lane configurations reach the capacity at earlier traffic demand. It should be noted that for the lowest traffic demand of 200 veh/hr, traffic delay is already exceeding 50 seconds.

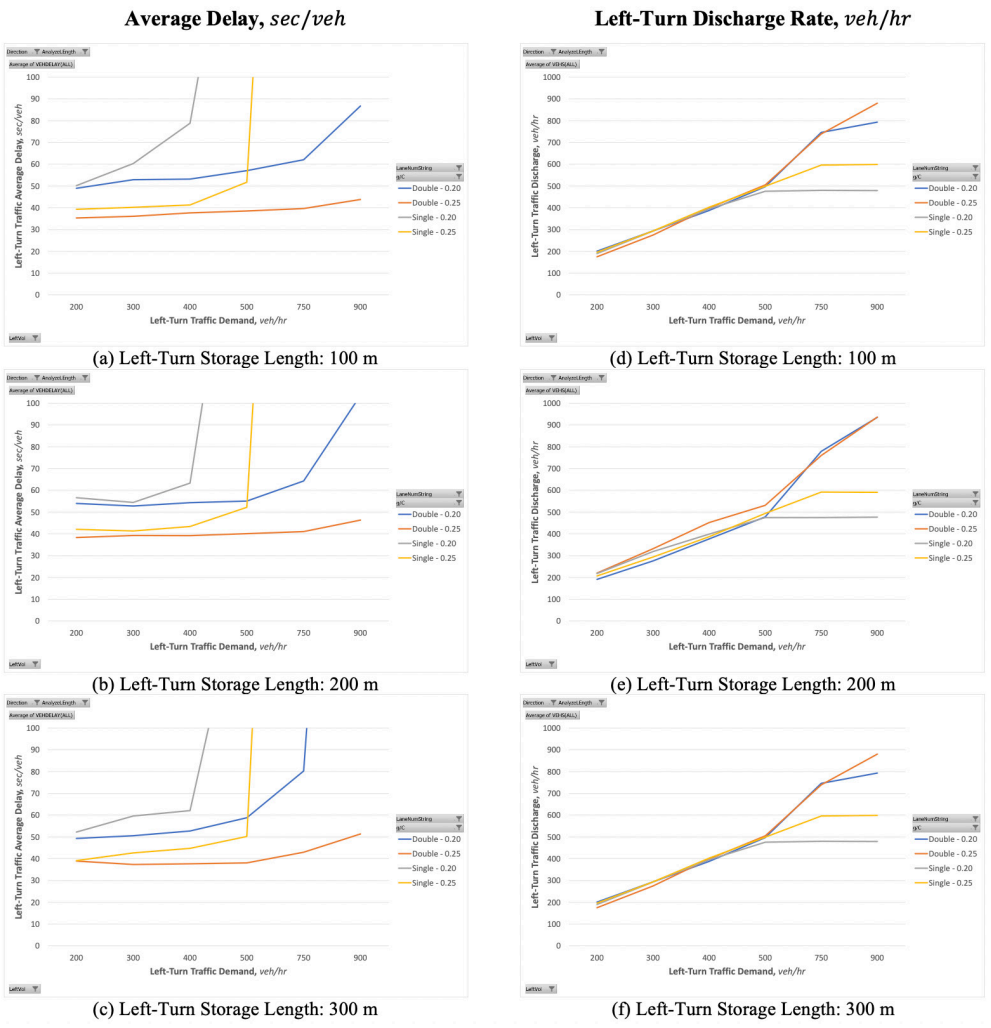

Figure 2: Left-Turn Movement Average Delay and Discharge Rate (Single Lane vs Double Lanes)

4.2 Double Lane vs. Triple Lane Comparison

The second comparison illustrated in this research is the comparison between the double and triple left-turn lanes. Unlike the single lane, both lane configurations (i.e., double and triple lanes) resulted in lower delay values and accommodated higher discharge rates. Because of this, a third g/C ratio of 0.33 is introduced to represent the operational performance at a higher demand rate that reaches 1,500 veh/hr. The simulation results are summarized in Figure 3.

Contrary to the expected, both double and triple lanes configurations perform similarly at low traffic volumes. For instance, and for g/C ratio of 0.25, it can be seen that the average delay is between 35 and 40 *sec/veh* for both configurations regardless of the storage length. This observation can be attributed to the fact that there is a significant variation in lane utilization. While the queue length is relatively low (due to the low

arrival rate), there was a significant gain of using the third lane in the triple lanes configurations. However, by increasing traffic demand, it can be seen that double lanes configuration starts to experience significant delay increase when the demand exceeds 750 veh/hr (for g/C of 0.2 and 0.25) and 900 veh/hr (for g/C of 0.33).

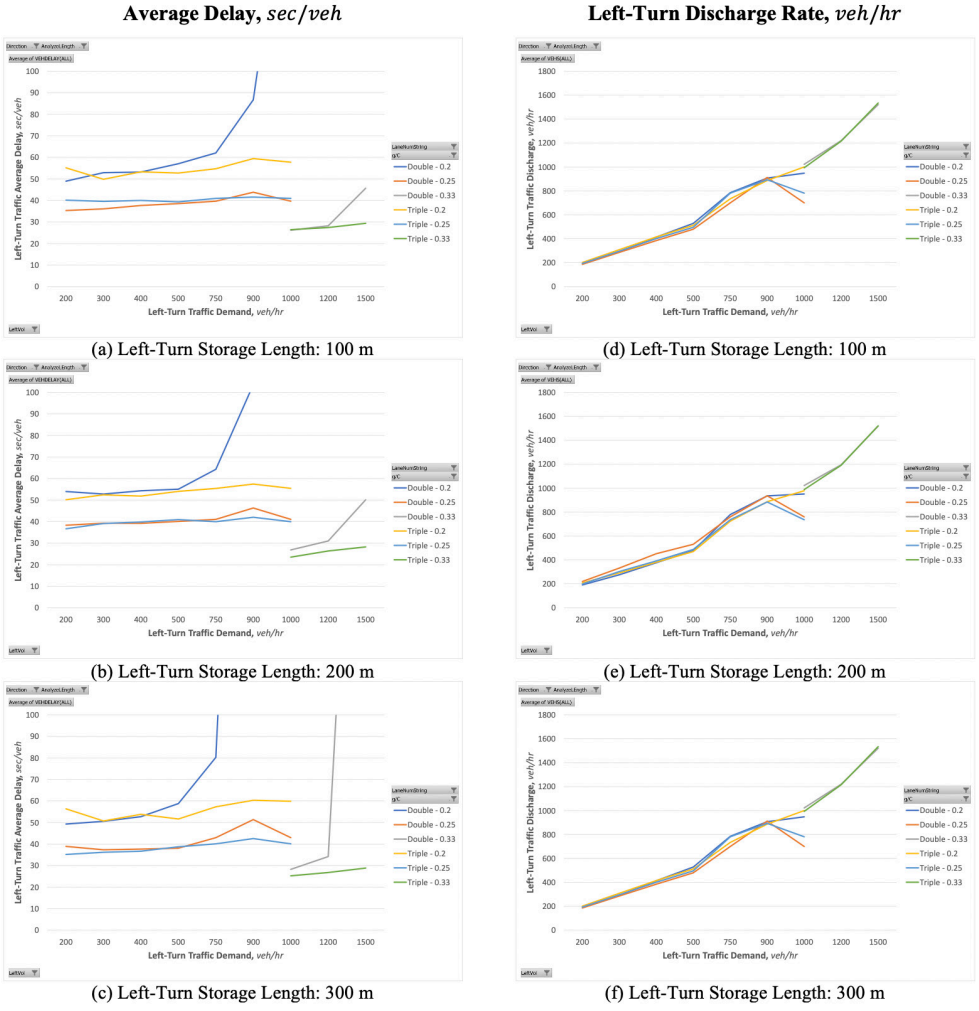

(a) Left-Turn Storage Length: 100 m

(d) Left-Turn Storage Length: 100 m

(b) Left-Turn Storage Length: 200 m

(e) Left-Turn Storage Length: 200 m

(c) Left-Turn Storage Length: 300 m

(f) Left-Turn Storage Length: 300 m

Figure 3: Left-Turn Movement Average Delay and Discharge Rate (Double Lanes vs Triple Lanes)

5 CONCLUSION AND RECOMMENDATIONS

The objective of this research is to evaluate the potential benefits of converting left-turn exclusive single lane bay into double or triple lanes configurations at signalized intersections. To do so, different left-turn demand levels and signal timing parameters were simulated and evaluated. A total of 540 scenarios were developed and analyzed using a VISSIM as a micro-simulation testbed.

The simulation results show that the operational benefits associated with lane configurations for exclusive left-turn bay depend on the level of left-turn demand. The results also reveal that the left-turn demand of 400 veh/hr can be considered as the

highest demand level for single lane configurations. The double lanes is recommended for left-turn demand that does not exceed 750 veh/hr. While the study shows promising results regarding the benefits of multiple left-turn lanes, there is a significant potential of expanding the scope of this study to include additional variables such as the percentage of heavy vehicles and lane width.

REFERENCES

Ackeret, K. W. (1996). *Analysis of saturation flows at single, dual and triple left-turn lanes* (Ph.D. dissertation). Univ. of Nevada, Las Vegas.

Bared, J. G., & Afshar, A. M. (2009). Using simulation to plan capacity models by lane for two- and three-lane roundabouts. Transportation research record, *2096*(1), 8-15.

Capelle, D. G., & Pinnell, C. (1961). Capacity study of signalized diamond interchanges. *Highway Research Board Bulletin*, 291, 1-25.

Chen, Y., Chen, G., & Wu, K. (2016). Evaluation of performance of bus lanes on urban expressway using paramics micro-simulation model. *Procedia Engineering*, 137, 523-530.

Chowdhury, M., Derov, N., Tan, P., & Sadek, A. (2005). Prohibiting left-turn movements at mid-block unsignalized driveways: Simulation analysis. *Journal of transportation engineering*, *131*(4), 279-285.

Elhassy, Z., Abou-Senna, H., Shaaban, K., & Radwan, E. (2020). The Implications of Converting a High-Volume Multilane Roundabout into a Turbo Roundabout. *Journal of Advanced Transportation*, 2020.

Ghanim, Mohammad. (2011) "Florida Statewide Design-Hour Volume Prediction Model". in 90th Annual Meeting of the Transportation Research Board. Washington, D.C.

Ghanim, M. & G. Abu-Lebdeh. (2016). "Improving Signalized Intersections Performance for Better Built Environment". International Journal of Sustainable Society. 2016. *8*(2): 145-152.

Ghanim, M. S. & K. Shaaban (2018). "Estimating Turning Movements at Signalized Intersections Using Artificial Neural Networks." *IEEE Transactions on Intelligent Transportation Systems*, *20*(5): 1828-1836.

Ghanim, M. & G. Abu-Lebdeh (2019). "Projected Statewide Traffic Forecast Parameters using Artificial Neural Networks." *IET Journal of Intelligent Transportation Systems*, *13*(4): 661-669.

Ghanim, M. S., & Shaaban, K. (2019). A case study for surrogate safety assessment model in predicting real-life conflicts. *Arabian Journal for Science and Engineering*, *44*(5): 4225-4231.

Holm, P., Tomich, D., Sloboden, J., & Lowrance, C. F. (2007). Traffic analysis toolbox volume IV: Guidelines for applying CORSIM microsimulation modeling software (No. FHWA-HOP-07-079). United States. Department of Transportation. Intelligent Transportation Systems Joint Program Office.

Kaysi, I., & Alam, G. (2000). Driver behavior and traffic stream interactions at unsignalized intersections. *Journal of Transportation Engineering*, *126*(6), 498-505.

Leonard, J. D. (1994). "Operational characteristics of triple left turns." *Transportation Research Record*. 1457, Transportation Research Board, Washington, D.C., pp. 104–110.

Liu, P., Qu, X., Yu, H., Wang, W., & Cao, B. (2012). Development of a VISSIM simulation model for U-turns at unsignalized intersections. *Journal of Transportation Engineering*, *138*(11), 1333-1339.

Nicholas, A. C. (1989). Exclusive Double-Left-Turn-Lanes Delay and Accidents. *Operations Review*, *6*(1).

Nyame-Baafi, E., Adams, C. A., & Osei, K. K. (2018). Volume warrants for major and minor roads left-turning traffic lanes at unsignalized T-intersections: A case study using VISSIM modelling. *Journal of traffic and transportation engineering (English edition)*, *5*(5), 417-428.

Qi, L., Zhou, M., & Luan, W. (2016). Impact of driving behavior on traffic delay at a congested signalized intersection. *IEEE Transactions on Intelligent Transportation Systems*, *18*(7), 1882-1893.

Saha, A., Chandra, S., & Ghosh, I. (2017). Delay at Signalized Intersections under Mixed Traffic Conditions. *Journal of Transportation Engineering, Part A: Systems*, *143*(8), 04017041.

Sando, T., & Mussa, R. N. (2003). Site characteristics affecting operation of triple left-turn lanes. *Transportation research record*, *1852*(1), 55-62.

Shaaban, K., & Kim, I. (2015). Comparison of SimTraffic and VISSIM microscopic traffic simulation tools in modeling roundabouts. *Procedia Computer Science*, 52: 43-50.

Shaaban, K., & Ghanim, M. (2018). Evaluation of transit signal priority implementation for bus transit along a major arterial using microsimulation. *Procedia Computer Science*, 130: 82-89.

Shaaban, K., Khan, M. A., Hamila, R., & Ghanim, M. (2019a). A Strategy for Emergency Vehicle Preemption and Route Selection. *Arabian Journal for Science and Engineering*, 1-9.

Shaaban, K., Abou-Senna, H., Elnashar, D., & Radwan, E. (2019b). Assessing the impact of converting roundabouts to traffic signals on vehicle emissions along an urban arterial corridor in Qatar. *Journal of the Air & Waste Management Association*, *69*(2): 178-191.

Spring, G. S., & Thomas, A. (1999). Double left-turn lanes in medium-size cities. *Journal of Transportation Engineering*, *125*(2), 138-143.

Stokes, R. W. (1995). "Capacities of triple left-turn lanes." Rep. to Institute of Transportation Engineers Technical Council Committee 5P5A., Washington, D.C.

Sun, D. Z. (2018). Using Micro-Simulation VISSIM to Study the Effectiveness of Left-Turn Waiting Area Implementation. *Applied Mechanics and Materials* (Vol. 876, pp. 187-191). Trans Tech Publications.

Yang, J., & Zhou, H. (2011). Integrating left-turn lane geometric design with signal timing. *Journal of Transportation Engineering*, *137*(11), 767-774.

Cite this article as: Shaaban K., Ghanim M. S., "Evaluating the Operational Impact of Left-Turn Exclusive Number of Lanes: A Case Study from Qatar", *International Conference on Civil Infrastructure and Construction (CIC 2020)*, Doha, Qatar, 2-5 February 2020, DOI: https://doi.org/10.29117/cic.2020.0075

Concept Design of Major Roads and Infrastructure in the Center of Doha City: Phase 4 project

Mohab Zaki
Mohab.zaki@motc.gov.qa
Ministry of Transport and Communication, Doha, Qatar

ABSTRACT

Doha, the Capital City of Qatar. A cosmopolitan, diverse and ever-growing international hub in the Arabian Gulf. It's recent and continuous rapid expansion necessitates the careful planning of its roads infrastructure. This challenging task is been managed by the Ministry of Transport & Communications (MOTC). The Ministry's Land Transport Sector has developed the Concept Design of Roads & Infrastructure for Phase 4 Project which includes Design of Haloul Road" as Package 26 and Design of C-Ring Road, D-Ring Road, Al Muntaza Street, Al Mansura Street, Najma Street, Rawdat Al Khail Street, Al Khalidiya Street and Airport Street as Package 27. Following a detailed study, the Land Transport Planning Department (LTPD) developed a solution that provides optimum mobility, safety, accessibility and efficiency of traffic movement in and around the project area by assessing and designing public realm improvements which will provide additional traffic capacity to accommodate the city's future growth, as well as improve the urban environment through a series of landscaping enhancements.

Keywords: Land transport; Highway design; Public realm; Safety; Traffic

1 INTRODUCTION

Several main and vital roads within Doha Metropolitan Area are currently experiencing delay and operating close to or beyond their capacity during peak hours due to congestion and traffic volume increase now and years to come. The shortage in existing road parking and the discontinuity of footways, unsafe pedestrian crossings and cycle paths, and poor urban environment are also contributing to the current problem.

The purpose of the project is to assess and design a major public realm improvement that works within the city of Doha, which will provide additional traffic capacity to accommodate the city's future transport growth and improve the urban environment through a series of landscaping improvements. These objectives can be achieved by improving the subjects shown in the following figure (1):

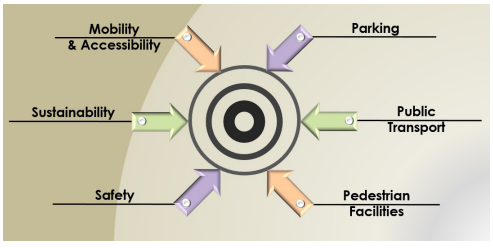

Figure 1: Phase 4 Project Objectives

The Ministry of Transport & Communications (MOTC), Land Transport Planning Department (LTPD)'s method of planning and design of roads is a global, comprehensive approach that considers several dimensions, such as serving road users from motorists, pedestrians and cyclists and ensuring sustainable road network, emphasizing urban design and parking improvements, optimizing use of public transport, protecting the environment, and upgrading infrastructure. One of the many concept design projects managed by Land Transport Planning Department (LTPD), Ministry of Transport and Communications (MOTC), is: "Phase 4 project – Concept Design of Major Roads and Infrastructure in the Center of Doha City" which consists of two packages as shown on Figure (2):

- Package 26 – Design of Haloul Road.
- Package 27 – Design of Major Roads in the Center of Doha City.

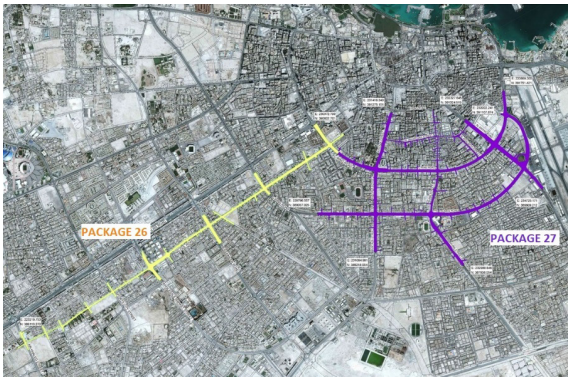

Figure 2: Phase 4 Project (Package 26 and Package 27)

2 PROJECT DESCRIPTION

Phase 4 project consists of two packages:

- Package 26 – Design of Haloul Road corridor between Ain Khaled Street in the southwest and C-Ring Road in the northwest, parallel to the Salwa Road Expressway. The total length of the proposed improvement is approximately 8.60kms and the proposed junction improvements at 14 locations (3 major junctions & 11 minor junctions)
- Package 27 – Design of Roads in the Center of Doha including the C and D Ring Roads, Al Mansoura, Al Muntaza, Najma, Al Khalidiya and Al Matar Streets. The Total length of the proposed improvement is approximately 20.45kms and the Junction improvements at 18 key junction locations (7 major junctions & 11 minor junctions).

3 PROJECT STAGES AND DEVELOPMENT OF DESIGN

The project is undertaken in the following three stages:

3.1 Stage – 1: Investigations and Studies:

The following investigations and studies were carried out to form the basis for the development of design options:

3.1.1 Topographic Surveys.

3.1.2 Transport Studies: A comprehensive traffic assessment study was carried in order to analyze the impact on the transportation system, which considered all future developments within and around the project area. The Transport Investigation and Study included the following:

a. Traffic Surveys
b. Land Use Survey
c. Strategic Modeling
d. Traffic Impact Assessment Analysis

3.1.3 Ground Investigations

3.1.4 Hydrological and Drainage Studies

3.1.5 Environmental Impact Assessment

3.1.6 Urban Design and Landscape related survey data

3.1.7 Utilities Investigations and Assessment

3.2 Stage – 2: Development of Concept Design Options:

During the first stage of the project, several road design options were developed following the (MOTC, 2015), Qatar Highway Design Manual (QHDM, 2015). After careful assessment, the following three design options were finalized:

3.2.1 Options Development:

a. *Option (1) Full Traffic Demand Design:* This option is to meet all the traffic demand requirements.

b. *Option (2) Constrained Design:* This option considers all network constraints, including Qatar Rail, highway boundaries, buildings, Private lands, and developments.

c. *Option (3) Balanced option:* This design uses the information and understanding derived from the options 1 and 2 analysis in order to arrive at a balanced option which considers traffic requirements and constraints equally.

3.2.2 Options Evaluations:

The three (3) best possible options were shortlisted considering key features, advantages, disadvantages, impact on services, preliminary estimated costs, accessibility to side roads and private properties, impact on the right of way etc. Further a qualitative assessment was carried out to select the preferred option as presented in the following figure (Figure 3).

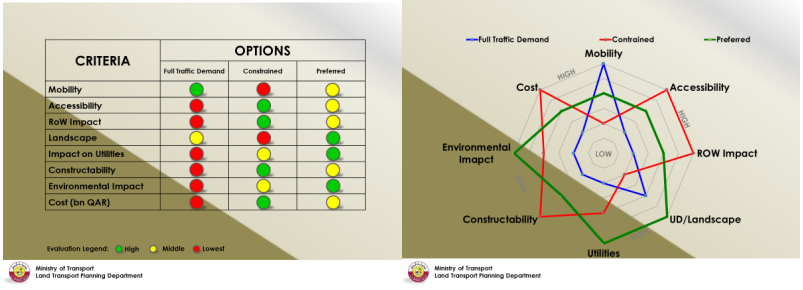

Figure 3: Qualitative Assessment of Three Options

3.2.3 Selection of Option:

Balanced Design (blended between constrained and full traffic demand) was recommended as preferred option to proceed to the next stage, which is the Concept Design.

3.3 Stage (3) Development of Concept Design for Preferred/Recommended Option:

Based on the selected option layout, further detailed traffic assessment study and analyses were carried out. This helped to refine and validate the design using VISSIM micro-simulation modelling, weave and ramp analysis using Highway Capacity Manual (HCS) and additional Synchro junction modelling. The detailed Transport Study included VISUM modelling (QSTM, 2013), traffic circulation and connectivity, parking study, pedestrian and cyclist study (GPTS, 2011).

3.4 Project Design Considerations

While developing the concept design layout and profile, the design team undertook several refinements to the design with paying more attention to minimize the land acquisition without affecting the level of service (LOS) of junctions and corridors (GPTS, 2011), avoid/minimize departures from design standards, improve accessibility, increase parking, improve traffic safety, provide pedestrian accessibility with safety, enhance landscaping, and to minimize impact to existing utilities.

3.5 Other Project Design Components

In addition to the geometric layout and profile, the project included other components that are needed to cover all aspects of road concept design such as geotechnical, earthwork, surface water drainage, foul sewerage and treated effluent (TSE), road signs and markings (QTCM, 2015), road safety audit (RSA), street lighting, structure, construction phasing strategy, pavement, intelligent transport systems (ITS), traffic signal, and urban and landscape design.

4 CONCLUSION

The Phase 4 project – Concept Design of Major Roads and Infrastructure in the Center of Doha City is a major part of Doha as envisioned in the year 2031 successfully planned and delivered by the Ministry of Transportation and Communications. The completed design improved performance when compared to reference case by improving road capacity and travel time 38%- 46%, improving pedestrian facilities by proposed 16no's at grade pedestrian crossing at signals and one (1) grade separated pedestrian crossing, maximizing the parking by proposing on-street parking at six (6) locations and off-street parking at two (2) locations, maximizing the landscaping, foot paths, planting areas and pedestrian shade provisions, improving accessibility and circulation in the project area, mapping and integrating the utilities impacts with appropriate solutions, improving the traffic safety and efficient traffic operations, and improving and enhancing the urban environment.

REFERENCES

Qatar Highway Design Manual (QHDM) (2015). The Ministry of Transport & Communication (MOTC), Land Transport Planning Department, Doha, Qatar.

Qatar Traffic Control Manual (QTCM) (2015). The Ministry of Transport & Communication (MOTC), Land Transport Planning Department, Doha, Qatar.

Qatar Strategic Transport Model (QSTM) (2013). The Ministry of Transport & Communications (MOTC), Land Transport Planning Department, Doha, Qatar.

Guidelines and Procedures for Transport Studies (GPTS) (2011). The Ministry of Municipality and Urban Planning (MMUP), Transportation and Infrastructure Planning Department, Doha, Qatar.

Cite this article as: Zaki M., "Concept Design of Major Roads and Infrastructure in the Center of Doha City: Phase 4 project", *International Conference on Civil Infrastructure and Construction (CIC 2020)*, Doha, Qatar, 2-5 February 2020, DOI: https://doi.org/10.29117/cic.2020.0076

Developing Assessment Framework for Strategic Transportation Projects in Qatar

Anas Mohammad
anas.mohammad@motc.gov.qa
Ministry of Transport and Communication, Doha, Qatar

Nabeel Al Rawi
nabeel.alrawi@motc.gov.qa
Ministry of Transport and Communication, Doha, Qatar

Osama Freija
osama.freija@motc.gov.qa
Ministry of Transport and Communication, Doha, Qatar

ABSTRACT

This paper presents Transportation Assessment Framework and process for selecting, defining, and naming assessment criteria to be used in transport appraisal. The approach is based on a review of national and international practices in transportation planning and appraisal around the world but is adapted to attend the needs and particularities of the Qatar transportation system, according to Transportation Master Plan for Qatar (TMPQ) vision and objectives. The TMPQ vision is derived from four key strategic themes: development, sustainability, livability and culture. The outcome of the research is a comprehensive list, developed using this framework, of 37 transport assessment criteria encompassing direct project impacts, indirect societal impacts, and environmental impacts. This list can serve as a starting point for planners wishing to conduct appraisal for strategic transport projects. A Cost-Benefit Analysis (CBA) procedure and parameter are also developed as part of TAF for a more detailed assessment of the Preferred Scenario(s), covering the impacts (costs and benefits) which can be quantified and monetized. An Excel-based CBA tool is developed and applied to produce the main economic indicators for the preferred scenario, which form part of the assessment criteria that can be monetized.

Keywords: Transport; Master plan; Sustainability; Assessment; Framework

1 INTRODUCTION

The Transport Assessment Framework is developed to provide the overarching framework that recommends an integrated set of strategic transportation initiatives for all transportation modes across Qatar. The objectives of this paper is to present the development of Transport Assessment Framework (TAF) for the Transportation Master Plan for Qatar (TMPQ). The TAF sets out the methodology, approach, criteria, tools and parameters for the assessment of transportation plans, projects or schemes considered in the context of the TMPQ. The ultimate aim of the TAF process is to establish a consistent basis which enables the selection of schemes (or a combined set of schemes known as Scenario), based on the comparative assessment of alternative scenarios, resulting in an optimized solution which provides the greatest amount of benefits for the Qatari society as a whole.

The TAF process will enable the comparative assessment of different scenarios developed to address future transportation provision for Qatar. Hence, it is intrinsically related to the definition of the vision and objectives for the TMPQ, ensuring that decisions are made in line with and to support the strategic vision and objectives. The TAF approach and procedures can be standardized for the assessment of any plan, project or scheme. It can also be customized to address the specific requirements of government agencies and private developers in Qatar in order to appraise their transportation and urban development schemes.

2 REVIEW OF THE EXISTING NATIONAL TAF PRACTICES & INTERNATIONAL BENCHMARKING

The TAF approach is based on a review of national and international practices in transportation planning and appraisal around the world but is adapted to attend the needs and particularities of the Qatar transportation system, according to its specific vision and objectives.

2.1 NATIONAL APPRAISAL PRACTICES FOR STRATEGIC TRANSPORT PLANNING

This section presents an overview of the existing assessment frameworks and practices applied in recent transportation studies in Qatar.

Testing of Scenarios, Policies and Regulations report in the Transportation Master Plan for Qatar, (UPDA, 2008), set out three different transportation scenarios, combining highways, public transport and demand management measures. These scenarios were tested against a Do-Minimum scenario using WebTAG of the UK Department for Transport, along with the package tools such as the TUBA and CBA for a comprehensive economic appraisal. No specific framework had been developed for Qatar on that occasion. Expressway road program proposed the infrastructure improvements priorities were assessed using the Qatar Strategic Transport Model (QSTM), which provided the congestion index for each scenario under consideration. The congestion indices were used to compare the performance of the highway network between scenarios. Although this approach can be considered acceptable for the purposes of what was required at that time, this did not constitute a specific framework to be applied for all type of transportation projects.

In (MOTC, 2017), Qatar Bus Routes and Operations Study (QPROS), the development of the bus network was devised through the use of a bespoke Bus Planning Tool developed from QSTM, which allowed the testing of alternative scenarios. Once the optimum future bus network was agreed, supporting documentation was prepared including financial and implementation plans and the inputs for the business investment case. A Cost-Benefit Analysis (CBA) model was developed, whereby estimates for each scenario under consideration have been made for the Transport User Benefits (Passenger Hours); Total Fare Revenue (QAR); Depot and Stations Cost (QAR); Stops and Bus Priority Cost (QAR); Fleet Cost (QAR); and Operations and Maintenance Cost (QAR). All scenarios have been ranked on the basis of the respective Benefit Cost Ratios (BCRs). This is a standard approach for the assessment of monetized impacts of transportation projects, however it does not capture other important implications such as accessibility,

emissions, accidents, fuel consumption, integration, security, urban realm and cultural norms.

2.2 INTERNATIONAL BEST PRACTICES FOR STRATEGIC TRANSPORT APPRAISAL

The benchmarking cities have been selected at previous stages of the TMPQ process. The international best practice review examined different approaches adopted elsewhere, which can be summarized as:

- Auckland, (NZ Transport Agency, 2015) – the approach adopted is an MCA focused on the prioritization of options but offers limited information about the estimating methods for the 28 indicators.
- Atlanta – the approach is based on an MCA and CBA process, which seems to be an appropriate way to structure the TAF.
- San Diego – the approach is also based on MCA and CBA tools.
- London – the approach used is that applicable to the entire UK, described by WebTAG. It contains a very comprehensive set of tools for modelling and appraisal, including a comprehensive CBA. The results of the appraisal process are helpfully summarized by Appraisal Summary Tables (AST).
- Abu Dhabi – the approach adopted is also based on an MCA, which includes economic and financial impacts.

3 THE RECOMMENDED TAF DEVELOPMENT APPROACH

The recommended approach for TAF development is based on a review of national and international practices in transportation planning and appraisal around the world, but is adapted to attend the needs and particularities of the Qatar transportation system, according to its specific vision and objectives. It also considers the vision and objectives for transportation system in Qatar. The TMPQ vision statement is derived from four key strategic themes: development, sustainability, livability and culture, as stated "An Integrated and Sustainable Transportation System that Supports the Economy and better Quality of Life while Preserving National Identity". The Table 2 below shows the general and specific objectives of the strategic transportation system in Qatar. The principles underlying the conception of TAF are:

- **Multimodal approach:** A multimodal network planning approach focused on meeting people's mobility needs and freight transportation users' requirements. Strategic transportation planning and investment decisions must be made from an integrated multimodal perspective, whereby TAF enables the assessment of schemes from all modes as well as a combination or package of schemes from different modes.
- **Holistic perspective:** It is important to account for the interaction between land use and transportation planning, bringing together economic, social and environmental considerations. TAF also needs to complement and enhance existing assessment practices in Qatar. In addition, TAF needs to incorporate a way of measuring or qualifying the effects of soft transportation initiatives, such as policies, regulations and governance.
- **Integration of stakeholder requirements and contributions:** Relevant stakeholder requirements play an important role throughout the TAF development. A joint

approach between the national government administrations involved in the planning, regulation or provision of transportation services should be adopted to facilitate the decision-making process.

- **Objective-led and responsive:** The development and assessment of schemes or plans must be driven by strategic and specific objectives, so that outcomes are aligned with the wider vision and objectives for transportation in Qatar, and be responsive to address the identified challenges in the transportation system.
- **Transparent and unbiased process:** The guidance should be structured, standardized, transparent, objective and unbiased, supported by both quantitative data and qualitative information, to ensure consistency in the assessment and inspire confidence in the process.
- **Broad applicability:** TAF needs to be suitable to be applied to a wide range of land use and transportation projects, of different natures (i.e. infrastructure, services, and facilities), sizes and at different stages of development, from strategic planning to feasibility.
- **Ease of understanding:** TAF guidelines should be implementable by various government and private organizations, hence need to be clear, specific and descriptive. Results must be presented in a way that is easily understandable to professionals outside the transportation planning field and to the general public.

4 THE TAF PROCESS & PROCEDURES

TAF has a role over different parts of the developing transport scheme/scenarios, as illustrated in the following Figure.

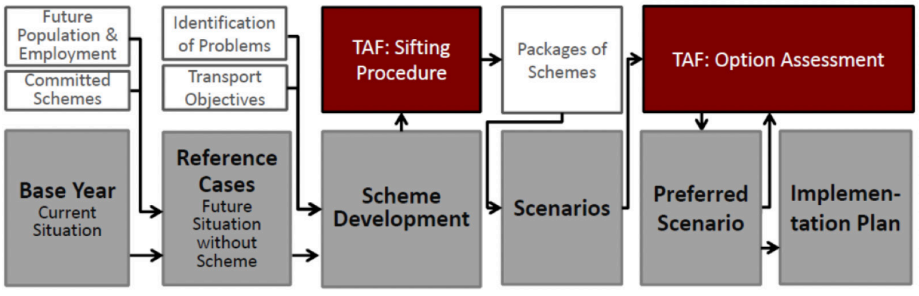

Figure 1: The Role of the TAF in the Transport Schemes Development Process (TMPQ, 2020)

4.1 Scheme Development

This step produces a range of transportation solutions for all modes, which has to be identified to address existing transport challenges and future mobility requirements, as well as to improve efficiency, reliability, safety or reduce congestion and externalities such as pollution and fuel consumption. A long list of proposed schemes/options (including physical measures and policy interventions) shall be developed, considering schemes proposed by stakeholders, government agencies, private developers and a wide range of other initiatives put forward for consideration. These schemes/options have to be developed to a level that enables them, where possible, to be tested, quantified, mapped, costed and simulated using the strategic transportation model (if applicable).

The following information shall be reported about each scheme i.e. description, metrics, mode type, classification, scheme objective, challenges, source, feasibility, risk …etc.

4.2 The Sifting Procedure

TAF has a role in "Scheme Development" by establishing a set of sifting criteria used to narrow down an initial long list of options, actions, measures, initiatives and policies into a more focused (or short) list of schemes to be further tested, refined and assessed as illustrated in below Figure. It also provides a framework for the analysis of the alignment of the proposed schemes against the specific objectives of the TMPQ, which is one of the sifting criteria. This procedure is essentially a qualitative process based on professional judgement and a certain degree of subjectivity.

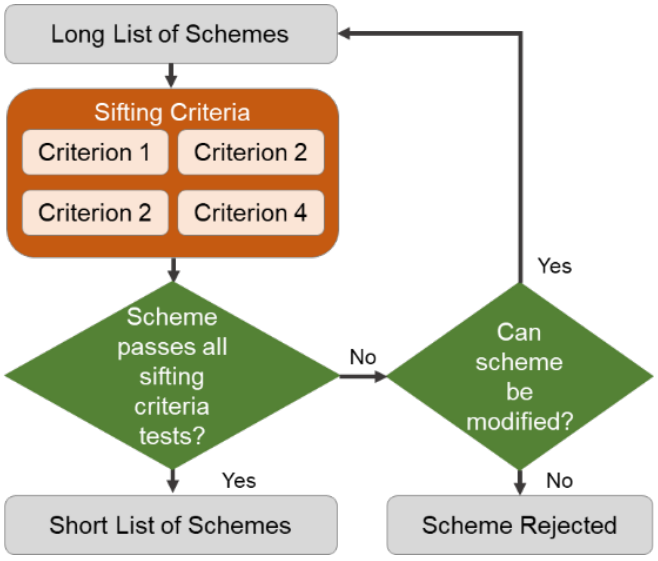

Figure 2: The Sifting Procedure (TMPQ, 2020)

The proposed FOUR sifting criteria are as follows:

a) **Criteria No. 1:** Schemes that are outside the sphere of analysis and intervention, or outside the scope of the land transport, would not qualify for progressing to the next stage of assessment:

- Schemes are related to air transport and airports, other than their accesses and connections with the surface transportation network;
- Schemes are related to maritime transportation and interventions in ports, other than their accesses and connections with the surface transportation network, except those involving the development of infrastructures and facilities for the provision of maritime bus and taxi services between different parts of the country;
- Schemes are related with transportation by ducts and pipelines; or
- Schemes are related to logistics and freight facilities or logistic centers, other than their accesses and connections with the surface transportation network.

b) **Criteria No. 2:** Schemes that are not sufficiently aligned with the specific objectives for the transportation system, would not qualify for progressing to the next stage of

assessment. This sifting criterion verifies the extent to which each scheme is capable of enhancing the performance of the transport network under at least one of the specific objectives of TAF. Qualitative (or more subjective) assessments have been made using on a five-point scale intended to measure the comparative magnitude and direction of the impact assessed against each specific objective. Table below shows the ranking used to test the qualitative alignment of scheme impacts against the objectives of the transport system.

Table 1: Qualitative Scheme Assessment against the Specific Objectives (TMPQ, 2020)

Assessment	Description	Points (Scale)
HIGHLY POSITIVE	The scheme has a significantly beneficial impact in relation to a specific objective	+2
POSITIVE	The scheme has a slightly beneficial impact in relation to a specific objective	+1
NEUTRAL	The scheme has no significant impact in relation to a specific objective	0
NEGATIVE	The scheme has a slightly adverse impact in relation to a specific objective	-1
HIGHLY NEGATIVE	The scheme has a significantly adverse impact in relation to a specific objective	-2

c) **Criteria No. 3** "**FEASIBILITY, RISK AND ACCEPTABILITY":** Under this sifting criterion, schemes that are considered not technically or environmentally feasible or which reveal a high risk of implementation should need to be reconsidered or rejected. This might be the case of proposals involving, for instance:

- The implementation of untested transportation solutions with high technological and regulatory risks;
- A level of investment that is significantly disproportional or not possibly justifiable in relation to expected social benefits or levels of patronage; or
- A severe degree of objection that can be expected from members of the public, government agencies or other stakeholders.

d) **Criteria No. 3 "REDUNDANCY OR BETTER COVERED BY OTHER SCHEMES":** Schemes which can be considered redundant for being more appropriately covered or more effectively addressed by any other more relevant schemes may be removed from consideration, subject to convincing explanations and reasoning being provided. The aim is to remove solutions which are the not most suitable for the local conditions in Qatar or which would overlap in scope, geography or aims with other more pertinent solutions.

4.3 Scenario Development

The schemes shall be grouped into coherent packages, or scenarios. Accordingly, numerous or endless combination of schemes can be developed. Therefore, in order to identify the group of schemes to be included for next step of scenarios assessment, a prioritization exercise needs to be carried out, evaluating the schemes against a set of criteria. The criteria used for this exercise for highway and public transport are summarized in below Table.

Table 2: Evaluation Criteria for Highway and Public Transport Schemes (TMPQ, 2020)

Mode	Criteria
Highway	Connectivity to new developments
	Dependency on other schemes
	Level of service (V/C)
	Traffic volume served by the scheme
	Total vehicle-km
	Strategic routes
	Connectivity to major developments, key locations and centers
	Support for truck movements
	Alignment against planning objectives
Public Transport	Dependency on other schemes
	Level of service (V/C)
	Population / employment catchment
	Connectivity to major developments, key locations and centers
	Ridership (PT passenger volume)
	Total passenger-km
	Alignment against planning objectives

4.4 The Scenario/Options Assessment

Once the Scheme successfully passed the sifting procedure and added to the focused (or short) list of schemes. In the context of the TMPQ, these options will effectively be the future transportation scenarios. Hence, the assessment will be carried out in aggregate terms for the impacts of each scenario, which comprise different integrated and coherent packages of schemes combined.

This stage of TAF uses a standardized multi-criteria assessment (MCA), which is tailored for the purposes and objectives of the TMPQ, for the scenarios/options assessment. This section defines the scope, criteria, and level of analysis required for the assessment of any transportation interventions in Qatar. The assessment of future options/scenarios will be made by comparisons of their impacts ("With Schemes") against the Reference Case ("Without Schemes") for the ultimate horizon year (2050). A comprehensive range of qualitative and quantitative assessment indicators were developed which is illustrated as an Appraisal Summary Table (AST). The AST facilitates the presentation of the impacts from different scenarios using a standard format, which will support and facilitate decision making on the selection of the preferred scenario as shown in the Figure below (Figure 3).

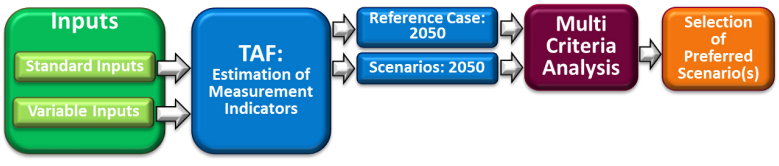

Figure 3: The MCA Process within TAF (TMPQ, 2020)

Table below presents the AST which includes a summary of the assessment of several indicators that were defined based on the possible ways of measuring the degree of fulfilment of the specific objectives of the transport system in Qatar. Individually, each indicator can only provide an indication of an aspect or a perspective for a specific impact, but collectively these indicators have been developed to represent a meaningful and sufficiently robust assessment framework. The ASTs ensure that the differences in performance between the alternative transportation scenarios can be clearly identified. Their standardized format provides ease of understanding and interpretation by decision makers. Whenever possible, the assessment indicators have been defined by transportation mode, by passenger/freight or by any other relevant classification and also how each indicator is expected to be measured, if quantitatively by either the QSTM, by other means (e.g. GIS) or by estimates made without the use of the model) or qualitatively.

MOTC developed a full description for the required data (variables, assumptions and standard inputs or parameters) and the methodology for the estimation of the proposed assessment indicators used to evaluate the contribution of alternative scenarios towards achieving each specific objective mentioned earlier.

The assessment of qualitative indicators is made by qualitative statements with a description the extent to which proposed measures within the scenario evaluated are expected to impact. A five-point scoring scale defining the degree of its contribution will be produced in order to compare the impacts between scenarios in the same way as used in the alignment of schemes against objectives, described in Table 2 in section 4.1. The AST does not identify the relative importance of the various objectives, indicators and associated impacts. This subjective aspect regarding the weighting between objectives and indicators is left to decision makers, with the AST only representing a summary of the expected set of impacts.

4.5 Cost Benefit Analysis

Cost-benefit analysis (CBA) is a process used to analyze decisions, whereby costs and benefits of an option/scenario are converted into the same monetary basis and added up to reflect the overall impact, highlighting the overall balance between costs and benefits. Such normalization of impacts measured in monetary units allows for better informed decision-making. Costs will include items such as capital expenditures and the annual operating and maintenance costs. Benefits will include revenues together with a monetized estimation of the social impacts accrued to users and non-users such as journey time savings, vehicle operating cost savings, monetary valuation of changes in emissions (by pollutant) and fuel consumption and monetary valuation of changes in traffic accidents (by severity type). A CBA for Qatar was developed to be applied to the Scheme/Scenario(s), for which assessment results are required for all horizon years. The CBA components include input and parameters such as Capital expenditures; Optimism bias; Annual operating and maintenance costs; Revenues from public transport fares, tolls and parking; User benefits (Travel time savings; and Vehicle operating cost savings), Non-User benefits (Changes in emissions and fuel consumption; Changes in energy consumption; and Changes in traffic accidents). The parameters of CBA and input values described above were developed based on existing data and a research market. The outcome of CBA using this tool will assist the calculation of Benefit-Cost Ratio, Net

Present Value and Internal Rate of Return.

Table 3: AST Measurement Indicators for Scenario/Option Assessment (TMPQ, 2020)

General Objectives	Specific Objectives	Measurement Indicator (Changes in Relation to the Reference Case)	Measurement Type: Quantitative Model	Quantitative Other	Qualitative
1. Provide an Efficient & Integrated Transportation System	1.1. Improve Operational Efficiency of the Transportation System	Total distance traveled by mode (vehicle-km/year) Average passenger travel distance by mode (km/journey) Average passenger travel speed by mode (km/h)	✓		
	1.2. Reduce the Amount of Time Spent by Passengers Traveling	Total pass-h by mode (pass-hours/year) Average journey time by mode (minutes/journey)	✓		
	1.3. Seek Reliable Movement of Goods	Number of goods vehicle hours under congested and uncongested conditions (# hours) Percentage of goods vehicle hours under congested conditions over the total hours traveled (%)	✓		
	1.4. Seek Reliable Movement for Travelers	Number of passenger-hours under congested and uncongested conditions for road vehicles (# hours) Percentage of passenger-hours under congested conditions over the total passenger-hours (%)	✓		
	1.5. Improve Integration Between Different Services and Modes	Number of trips and average number of trips that entail ≥1 transfers (#) Average time spent in transfers (hours)	✓		
		Qualitative statements that summarize the extent to which proposed measures are expected to impact in overall levels of network integration between services and modes (both physical improvements and policy-based improvements)			✓
2. Promote Transportation Mobility & Accessibility	2.1. Increase the Availability and Attractiveness of Public Transport	Market share of Public Transport by mode (%)	✓		
		Population within a certain distance of a PT service (number of residents)		✓	
	2.2. Improve Access to Essential Destinations	Accessibility index to employment, health and education destinations by car and Public Transport (index)		✓	
	2.3. Provide an Affordable Transportation Experience	Average journey cost by mode (QAR/journey) Market share of the different modes per population group / level of income (%)	✓		
	2.4. Improve Non-Motorized Mobility Options	Number of trips made by walking & cycling (#) Percentage of trips made by walking & cycling (%)	✓		
		Pedestrian and Cycling Activity – qualitative statements that summarize the understanding of the scale and impact of any pedestrian and cycle related improvements			✓
	2.5. Ensure Acceptable Travel Conditions by all Modes for all Travelers	Levels of Service on all modes (roads and public transport): • *For roads: Km of network operating under different Levels of Service (km)* • *For PT: km of PT network operating under different Levels of Service (km)*	✓		
3. Ensure a Safe & Secure Transportation System	3.1. Reduce Number and Severity of Accidents	Number of expected accidents: total number of accidents by level of severity and road type (number of accidents)	✓	✓	
	3.2. Ensure Safe and Secure Transportation System	Qualitative statements that summarize how security and/or personal safety is anticipated to be improved by the proposed measures included in each alternative scenario.			✓
4. Protect the Environment & Ensure Sustainable Development	4.1. Reduce Transportation Related Local & Global Emissions	Estimation of the annual quantities of CO_2, NO_x, CO, HC, PM emissions (tones/year)	✓	✓	
	4.2. Enhance Transportation Energy and fuel Efficiency	Estimation of the annual fuel consumption by mode (liters/year) Estimation of the annual energy consumption by mode (megajoules/year)	✓	✓	
	4.3. Protect the Streetscape and Urban Realm	Qualitative statements that summarize the extent to which the proposed measures scheduled in each alternative scenario would impact sensitive parts of the urban area.			✓
	4.4. Ensure Sustainable Development	Qualitative statements that summarize the extent to which the proposed measures scheduled in each alternative scenario would contribute to encouraging sustainable development.			✓
5. Support Economic Development	5.1. Improve Access to the Workforce	Number of employees located within a predetermined travel time catchment, by private vehicles and public transport, for selected employment locations (#)	✓	✓	
	5.2. Improve Access to International Markets	Goods - Average travel times for goods to the airport and ports (hours/journey) Business Travelers - Average travel times between the Central Business District and the airport using both private and public transport (hours/journey)	✓		
	5.3. Improve the Travel Experience for Tourists	Average travel times between main tourist O-D pairs (tourist attractions, hotel areas, HIA, Doha and Hamad Ports) by taxi and PT (minutes/journey) Average travel costs between main tourist O-D pairs (tourist attractions, hotel areas, HIA, Doha and Hamad Ports) by taxi and PT (QAR/journey)	✓		
	5.4. Improve Integration between Transportation & Land Use Planning	Qualitative statements that summarize the extent to which integration between the transportation system and land use will be improved and the impacts this may have in generating additional economic activity			✓
6. Maximize Quality of Life & Preserve Qatari Values	6.1. Promote Transportation Systems that Enhance Quality of Life	Qualitative statements that summarize the extent to which the proposed measures scheduled in each alternative scenario would contribute to increase the availability of travel options and / or increase traveler comfort and convenience			✓
	6.2. Promote Transportation Systems that Preserve Qatari Norms and Culture	Qualitative statements that summarize the Qatari based social and cultural impacts associated with any transportation related infrastructure, service and / or policy improvements scheduled in alternative testing scenarios.			✓
CBA	Ensure Value for Money	Total capital expenditure by scenario by implementation phase (QAR) Annual operating and maintenance costs (QAR/year) Total revenues (QAR/year) Total value of the time savings by passengers by mode (QAR/year) Total vehicle operating cost by mode (QAR/year) Total monetary valuation of changes in emissions (QAR/year) Total monetary valuation of changes in fuel consumption (QAR/year) Total monetary valuation of changes in accidents (QAR/year) Based on the results of the Social Cost Benefit Analysis - CBA: • *Benefit-Cost Ratio* • *NPV and IRR*	✓	✓	

5 CONCLUSION

This paper presented the Transportation Appraisal Framework (TAF) development and stages in Qatar, which has been conceived for the purposes of transport schemes option/scenario assessment within the TMPQ. It sets out the parameters and methodology for the assessment of options, which can also be used for the assessment of any other transportation intervention requiring approval and/or funding in Qatar to provide the greatest amount of sustainable benefits for the Qatari society as a whole. This paper makes three practicable contributions:

1. A framework for systematically defining and naming assessment criteria to be used as a consistent basis of the comparative assessment of alternative scenarios,
2. A viable list of AST criteria that is readily applicable to all transport projects.
3. A clear procedure and process to use TAF for developing and assessing transport scheme/scenarios.

Developed TAF in Qatar is a form of Multi-Criteria Assessment (MCA), which in this case is structured into 6 General Objectives, 22 Specific Objectives plus the CBA, with a total of 37 indicators in addition to those economic and financial indicators from the CBA. The results of the MCA for each scenario are summarized in the Appraisal Summary Table (AST) in relation to the "without project" situation (Reference Case). The trade-offs between the various assessment indicators for each scenario/option under consideration are used for the analysis of the comparative performances of the different scenarios with the objective of supporting decision-making. The implementation of TAF and CBA is undertaken by MOTC.

The ultimate outcome of scenario/option assessment is the selection of the preferred scenario/option, which will be that representing the highest amount of benefits for Qatar, taking into account the trade-offs between a wide range of impacts for each scenario on transportation objectives and the corresponding costs and risks.

REFERENCES

Auckland Regional Land Transport Plan 2015-2025 (RLTP), NZ Transport Agency, Kiwi Rail, Auckland Council and Auckland Transport. Retrieved from: https://at.govt.nz/media/1191335/Regional-Land-Transport-Plan-Adopted-Version-July-2015.pdf.

Qatar Bus Routes and Operations Study (QBROS) (2017). MOTC.

Qatar Strategic Transport Model v2.0, VISUM (2018). MOTC.

Transportation Master Plan for Qatar (TMPQ) (2008). Urban Planning & Development Authority (UPDA).

Transportation Master Plan for Qatar (TMPQ) (2020). Ministry of Transport and Communication (MOTC).

WebTAG, Transport analysis guidance (TAG) (2013). UK Department for Transport. Retrieved from: https://www.gov.uk/guidance/transport-analysis-guidance-webtag.

Cite this article as: Mohammad A., Al Rawi N., Freija O., "Developing Assessment Framework for Strategic Transportation Projects in Qatar", *International Conference on Civil Infrastructure and Construction (CIC 2020)*, Doha, Qatar, 2-5 February 2020, DOI: https://doi.org/10.29117/cic.2020.0077

Theme 3:
Geotechnical, Environmental, and Geo-environmental Engineering

Flood Risk Assessment and Protection Guidelines for Infrastructure Planning in Qatar

Abdullah Al Mamoon
amamoon@gmail.com
Ministry of Municipality and Environment, Doha, Qatar

ABSTRACT

This paper presents key features of "Flood Assessment and Protection Guidelines" (FAPG) prepared by the Ministry of Municipality and Environment (MME), Qatar. It is intended that the FAPG will provide guidance and assistance to a wide range of entities including government agencies, developers, engineers, planners and policy makers for locating flood prone areas across Qatar, assessing potential flood hazard and subsequent mitigation. A flood modelling was carried out using two-dimensional rain on grid (RoG) hydraulic modelling approach. A series of flood risk maps covering both rural and urban areas of Qatar were then prepared as per the degree of flood risk to people, property and infrastructure. These maps have been provided as digital flood inundation layers in an interactive GIS web-based flood mapping portal.

Keywords: Flood risk; Mitigation; DEM; Planning; Qatar

1 INTRODUCTION

Qatar lies in the northern hemisphere desert (FAO, 2008). Although countries with arid climate receive very little rainfall, occasional flash flooding due to short duration and high intensity rainfall is not uncommon (Mamoon e al., 2014). For example, a devastating flood in Nov 2009 in Jeddah, Saudi Arabia caused deaths of over 100 people and major destruction of urban infrastructure (Al-Saud, 2010). Storm events in Qatar typically consist of relatively high intensity rainfall bursts over short duration. A significant rainfall event on October 19, 2018 in Qatar caused widespread flooding of highways, underpasses and many parts of Doha city (Mamoon & Rahman, 2018).

Flooding within the state of Qatar can be attributed to the nature of storm events coupled with environmental characteristics including relatively flat topography and a lack of well-defined overland flow paths. In urban areas within Qatar, overland flows resulting from significant rainfall events generally make their way to the urban road and drainage network (Figure 1).

The main challenges in flood modelling in the arid regions include lack of recorded flood data, infrequent occurrence of floods and lack of defined water courses (Xao Lin, 1999; Sen, 2008; Morin et al., 2009; Mamoon et al., 2015). Flood assessment in Qatar involves several major challenges (Mamoon et al., 2015):

- Availability and accessibility of relevant GIS and terrain data in Qatar.
- Quality of topographic data for the development of an accurate digital terrain model (DTM). Current terrain data available for Qatar is limited to 1.09 m vertical accuracy for urban areas and 1.58 m accuracy for rural areas.
- Lack of available historical rainfall and flood data for flood model parametrization

and calibration (Mamoon et al., 2013; 2014).

- The complexity of the study area which includes relatively low design rainfall intensities, poorly defined flow paths and potential for high transmission losses typical of arid regions (Pilgrim et al., 2009).

Figure 1: Flooding in Doha, (a) Trapped rainfall-runoff collecting on the low point of a main road in Doha; (b) Example of road drainage network exhibiting capacity exceedance/overflow.

Qatar is currently in the midst of a rapid infrastructure development. As development continues to progress, concern has been raised amongst decision makers on the potential environmental risk and socio-economic damage that may be caused by both frequent and significant flood events. In order to develop an effective planning framework that aims to address flood hazards in Qatar, The Ministry of Municipality and Environment carried out a comprehensive national flood study (MME, 2017) in line with the Qatar National Vision 2030 and fulfilling the objectives of the Qatar National Development Strategy 2017-2022. Consequently, using the results and recommendations of this study, a national flood code guideline titled "Flood Assessment and Protection Guidelines" was developed (MME, 2019).

This paper presents some important features of FARG and describes how these can be applied for adaptation and effective flood management in Qatar.

2 STUDY AREA

Qatar is located on the north-eastern side of the Arabian Peninsula (Figure 2). It has a land area of 11,571 km^2. The average annual rainfall in Qatar is found to be in the range of 55.5–99 mm (Mamoon & Rahman, 2016). Rainfall in Qatar mainly occurs in the period from October to May showing a higher degree of spatial and temporal variability with respect to intensity and duration (Mamoon et al., 2014). A sharp gradient in average annual rainfall was noticed, with north having higher values than the south (Mamoon et al., 2016).

3 DEVELOPMENT OF "FLOOD ASSESSMENT AND PROTECTION GUIDELINES" (FAPG)

The FAPG entails development of a set of flood codes based on the results and

recommendations of Qatar's National Flood Study (MME, 2017). The purpose of flood codes is to identify rural and urban areas of Qatar that are at risk of flooding and regulate development occurring in these areas to ensure development does not cause or increase risks and/or hazards associated with flooding to people, property and infrastructure.

3.1 Data Collection and Review

A significant amount of data was collected for the flood study that includes climate, rainfall, topography, soils, historical flooding, infiltration, tidal levels, land use, infrastructure and storm water management etc.

A detailed gap analysis was undertaken to identify any major data gaps, additional data requirements and limitations. Current terrain data available for Qatar is limited to +/- 0.27 m vertical accuracy for urban areas and +/-1.58 m accuracy for rural areas. In light of the stated accuracy of the topographic data in rural areas, the flood levels estimated by 2D hydraulic models will have an accuracy limitation of at least +/- 1.58m in the vertical. In areas of relatively flat terrain, this inaccuracy will translate into a relatively greater uncertainty in horizontal flood inundation extent.

3.2 Flood Modelling

A detailed computer modelling of flood behavior for a range of design flood events is crucial for preparation of flood risk inundation maps that would assist in development of land use planning solutions. Two alternative flood modelling approaches are compared on a pilot catchment situated in Qatar. The first method involved the application of a coupled hydrologic/hydraulic modelling approach, whilst the second method was based on a 2 dimensional (D) 'rain on grid' hydraulic modelling approach. In the 'rain on grid' approach, design storm events (rainfalls) are directly applied across the two-dimensional hydraulic modelling domain of the study area to simulate the dynamic propagation of flood water across the study area (Figure 2).

An assessment of the results from the two methods demonstrated that the 2D 'rain on grid' hydraulic modelling approach was the preferred method for implementation in Qatar as this needed less data and provided a more realistic simulation of the rainfall runoff process, higher resolution model outputs, and greater efficiency and potential for automation in model setup phase.

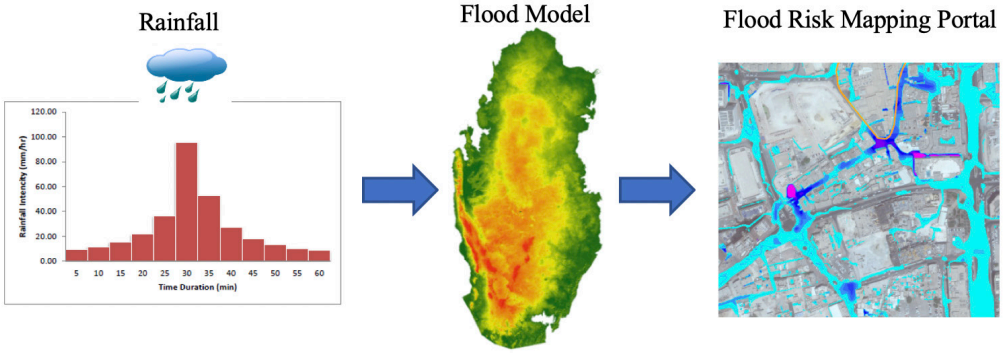

Figure 2: Rain on Grid method

3.2.1 Model Setup and Design Event Analysis

Hydraulic modelling was undertaken using two-dimensional (2D) TUFLOW GPU (Graphics Processing Unit) software. In order to model the required study area at a sufficient level of resolution, the State of Qatar has been delineated into 10 sub-catchments with a flood model developed for each sub-catchment (Figure 3a). Key features of the model include a detailed digital elevation model (DEM) with a cell size of 5m x 5m, a land use layer, building representation, walls/fences and cross drainage infrastructure.

The flood models were validated against the 25th December 2015 storm event in Qatar and a sensitivity analysis was undertaken to confirm the validity of key model parameters. Based on a review of modelled results against limited on ground flood records, the nature and pattern of flooding estimated by the flood model was found to be generally consistent with that experienced on ground.

Design event flood modelling was undertaken for the 10% AEP (10 year ARI) and 1% AEP (100 year ARI) design events for storm durations ranging from 15 minutes to 120 minutes. Flood modelling results for these design events are provided in the form of flood level, depth, velocity and hazard maps.

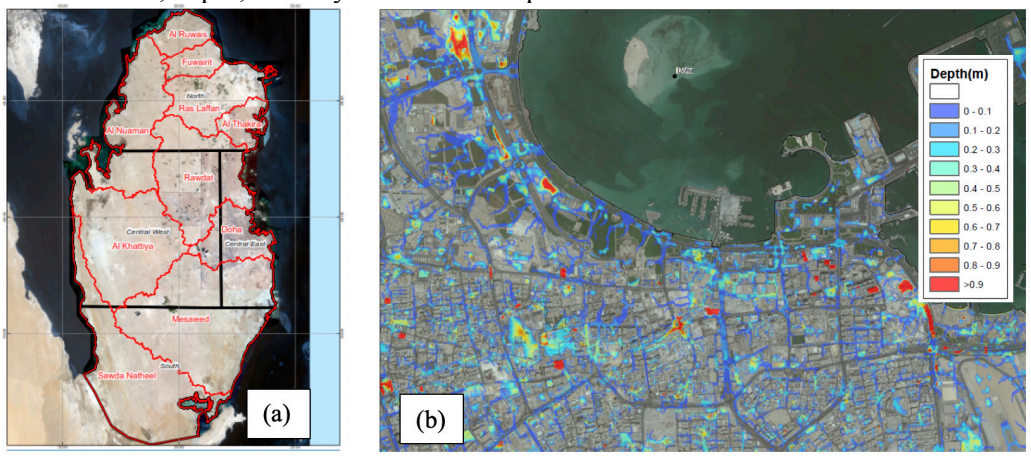

Figure 3: Flood Maps, (a) Flood Model Extent; (b) Flood Hazrad Overlay Map showing depths.

An analysis of flooding for the Probable Maximum Flood Event (PMF) was also undertaken. A climate change assessment was also undertaken to estimate and map the nature of flood risk for Year 2050 and Year 2100 future climate scenarios.

3.3 Flood Risk Assessment

Flood risk is a function of the likelihood of an event occurring and the potential impact (consequence) of the event on receptors. To estimate the degree of flood risk to people, property and infrastructure, flood inundation maps were prepared that illustrate the spatial variation of flood depth, velocity and flood hazard (depth x velocity) for each of the design events modelled (Figure 3b). These maps have been provided as digital flood hazard layers in the Qatar Flood Mapping Portal. Four flood hazard categories have been used to define the degree of flood hazard associated with each design flood event. Table 1 illustrates the depth, velocity, and depth velocity product associated with

each flood hazard category.

Table 1: Flood Hazard Overlay Categories

Items	Low Hazard	Medium Hazard	High Hazard	Extreme Hazard
Depth (m)	<0.30	0.31 to 0.60	0.61 to 1.20	>1.2
Velocity (m/s)	<0.38	0.39 to 0.80	0.81 to 1.50	>1.5
Depth x Velocity (m^2/s)	<Medium	D+0.64*V <0.82	D+0.69*V <1.38	>High
Typical means of egress	Sedan	Sedan early, but 4WD or trucks later	4WD or large trucks.	Large trucks.

3.4 Qatar Flood Portal

In order to illustrate the nature and risk of flooding, an interactive GIS web based flood mapping portal (Qatar Flood Mapping Portal) was developed (Figure 4). The Portal provides a broad scale understanding of the range of potential flood conditions that could occur across the State of Qatar.

The portal's functionality enables the user to open up a high-resolution map of Qatar, zoom in on a particular catchment area and visualize (and query) the flood level, depth, velocity and degree of flood risk at any property location within Qatar for any of the design flood events that were modelled. The Portal also includes flood inundation maps for a range of potential future climate conditions.

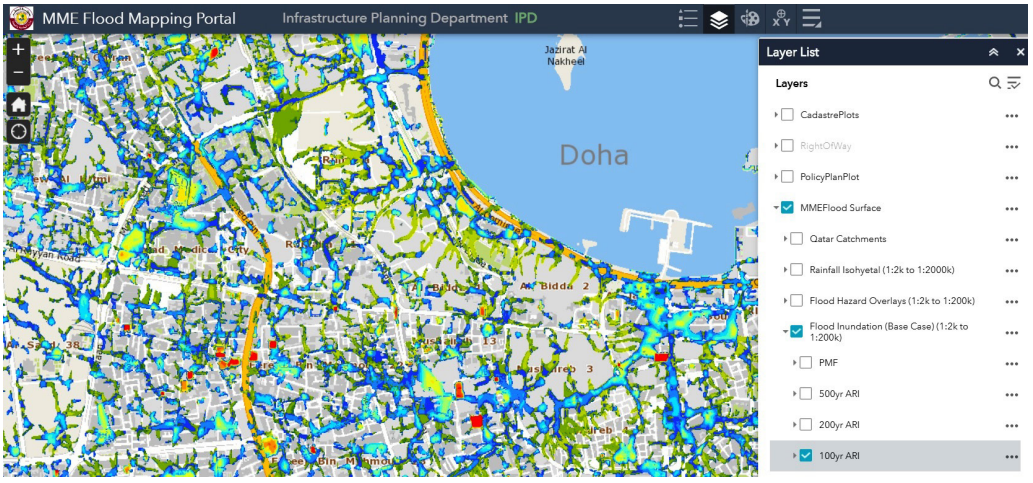

Figure 4: Qatar Flood Portal

In instances where a detailed understanding of local flood conditions is required (e.g. when undertaking detailed design of infrastructure or assessing the potential impact of a development), it is recommended that site-specific flood modelling of the local catchment be undertaken.

4 FLOOD CODES

This code applies to assessing any type of development that lies within a flood

affected area covered by the Flood Hazard Overlay (MME, 2019). Flood Code sets out performance requirements and acceptable solutions during the building permit and development application process. All development-related proposals in Qatar are to be evaluated against the following criteria:

- Whether the cumulative impact of development is likely to cause or increase the adverse impacts of flooding to people, property and infrastructure.
- Whether the development is likely to cause or worsen flood hazard.
- Whether the risks associated with the development are fully known, quantifiable and capable of mitigation to MME's satisfaction.
- Whether flood mitigation works, intended to reduce flood risk, hazard and damage, do so without adversely affecting other land and/or premises, property and infrastructure.
- Whether extra burden is placed on the State of Qatar's emergency management response efforts during a flood emergency.

5 CONCLUSION

Qatar Ministry of Municipality and Environment has developed a national flood code titled "Flood Assessment and Protection Guidelines" for flood risk assessment and development control in Qatar. A flood modelling was carried out using two-dimensional TUFLOW software employing 'rain on grid' hydraulic modelling approach. A series of flood hazard overlay risk maps covering both rural and urban areas of Qatar were prepared using four flood hazard categories namely low, medium, high and extreme. These maps have been provided as digital flood inundation layers in an interactive GIS web-based flood mapping portal that enables the user to conduct flood risk assessment at any location across the State of Qatar. The climate change effect on flooding has also been incorporated in flood inundation maps. The FAPG provides clear procedures and technical guidance, assistance, and the necessary requirements in dealing with floods to a wide range of entities such as; government agencies, developers, urban planners, engineers, and decision makers, for locating and protecting flood prone areas and assessing potential flood risks and required mitigation.

REFERENCES

Al-Saud, M. (2010). Assessment of Flood Hazard of Jeddah Area 2009, Saudi Arabia. *Journal of Water Resources and Protection,* 2, 839-847.

Food and Agricultural Organizations (FAO), United Nations (2009). AQUASTAT, (Water report 34).

Mamoon, A. A., Jeorgensen, N. E., Rahman, A. & Qasem, H. (2013). *Estimation of Design Rainfall in Arid Region: A Case Study for Qatar Using L Moments*, 35th IAHR World Congress. September 8 to 13, Chengdu, China, 1-9.

Mamoon A. A. & Rahman A. (2016). Rainfall in Qatar: Is it changing? *Natural Hazards*, Sept 2016. DOI: 10.1007/s11069-016-2576-6.

Mamoon, A. A., Joergensen, N. E., Rahman. A. & Qasem, H. (2016). Design rainfall in Qatar: sensitivity to climate change scenarios. *Natural Hazards, 81*(3), 1797-1810.

Mamoon, A. A. & Rahman. A. (2018). Qatar Rainfall and Runoff Characteristics – A New Direction of Engineering Education and Practice in Qatar, Proc. *1st International Conference on Advancement in Engineering Education (iCAEED 2018)*, Sydney, Australia. pp. 186-195, ISBN: 978-0-6480147-9-9.

Mamoon, A. A., Jeorgensen, N. E., Rahman, A. & Qasem, H. (2014). Derivation of new design rainfall in Qatar using L-moments based index frequency approach. *International Journal of Sustainable Built Environment*, *3*, 111-118.

Mamoon, A. A., Regan, B., Sylianteng, C., Rahman, A. & Abd Alkader, A. A. (2015). *Flood Study in Qatar – Challenges and Opportunities*, 36th Hydrology and Water Resources Symposium, Hobart, Australia.

Ministry of Municipality and Environment (MME), (2019). *Flood Assessment and Protection Guidelines.*

Ministry of Municipality and Environment (MME), (2017). *Flood Study for the State of Qatar.*

Morin, E., Jacoby, Y., Navon, S. & Bet-Halachmi, E. (2009). Towards flash-flood prediction in the dry Dead Sea region utilizing radar rainfall information. *Advances in Water Resources*, *32*, 1066-1076.

Pilgrim, D., Chapman, T. & Doran A. (2009). Problems of Rainfall-Runoff Modelling in Arid and Semiarid Regions. *Hydrological Sciences Journal, 33*, 4, 379-400.

Sen, Z. (2008). *Wadi Hydrology*. The USA: CRC Press.

Cite this article as: Al Mamoon A., "Flood Risk Assessment and Protection Guidelines for Infrastructure Planning in Qatar", *International Conference on Civil Infrastructure and Construction (CIC 2020)*, Doha, Qatar, 2-5 February 2020, DOI: https://doi.org/10.29117/cic.2020.0078

Constructability and Economical Comparison Between Two Proposed Permanent Shoring Systems in Qatar: A Case Study

Mohammed Alfarra
mohammed.alfarra@seeroeng.com
Seero Engineering Consulting, Doha, Qatar

Mohammed Sadeq
mohammed.sadeq@seeroeng.com
Seero Engineering Consulting, Doha, Qatar

Husam Sadek
hsadek1@lsu.edu
Louisiana State University, Baton Rouge, Louisiana, USA

ABSTRACT

This paper introduces the constructability and economic feasibility study of using one of the proposed two types of permanent shoring system for a highway project in Qatar. The cast-in-situ cantilever retaining wall and the contiguous piles wall were suggested and designed to be used as a permanent retaining system at a multi-level intersection. In this study, the construction complexities of using the cantilever retaining wall system are illustrated and compared to the contiguous piles wall. Besides, the impact on the Right-of-Way (ROW) of the road, excavation process, traffic circulation, and existing utilities are discussed. The paper summarizes the difference in the required construction materials and excavation quantity for the proposed shoring systems at the same retained elevation. Furthermore, the design of both systems is performed based on the local and international guidelines and regulations of the shoring system design in Qatar. The study has shown that both suggested systems are providing the same finishing quality while the contiguous piles system is more effective in minimizing economic and site preparation challenges. It also provides safer utilities handling and faster construction sequencing without cost increases.

Keywords: Shoring system; Contiguous pile wall; Cantilever retaining wall; Qatar

1 INTRODUCTION

Qatar is witnessing a significant upgrade in the infrastructure and transport systems, especially in highways and multi-grade intersections. These multi-grade intersections are usually supported by retaining structures that come as a part of the contractor's role to construct within the limited Right of Way (ROW). Retaining structures are commonly used to retain soil, rock, or water and to withstand their lateral pressures. Using these walls supports roads at different levels, accommodates extra lanes for the roads, and stabilizes slopes. There are various types of retaining wall structures that are used for different objectives, such as; gravity, cantilever, counterfort, piled, sheet pile, anchored, and Mechanically Stabilized Earth (MSE) retaining walls (Standard Specification for highway bridges, 2002).

In the planning stage of any project, the selection of the optimum retaining wall system is not an easy task since it depends on many limitations as safety, economy,

constructability, right of way, underground utilities, and stability.

In this paper, two permanent shoring options were proposed, designed, and compared for a multi-grade intersection project in Qatar. The difference in the level is 10 m between the ground level and a bypass road. The project is located in a fully developed area in Doha city, which added some complexity in choosing the most suitable retaining wall system. The proposed retaining system is very close to the Right of Way (ROW), and existing utilities are crossing the proposed location of the shoring system. The main contractor of the project was recommended to substitute the cantilever retaining wall system with a contiguous piles wall system. Since the proposed retaining structures will be fabricated and cast in the site, more challenges are expected during the construction process. The objective of this paper is to discuss the constructability and economic aspects of both systems. Their effects on the ROW and existing utilities are evaluated to adopt the most feasible option.

2 GEOTECHNICAL PARAMETERS AND SITE CONDITION

The geotechnical investigation of the project site was reviewed to determine the soil properties. Furthermore, the topographical survey, geometric layouts, and excavation levels were used to identify the final retaining systems' lengths and the height of piers on top of the cap beam. It is worth mentioning that the whole shoring system length is within the Quaternary Deposit (QD) and Simsima Limestone (SL) layers. The design ground profile and the geotechnical parameters provided in the geotechnical investigation report are summarized in Table 1.

Table 1: Design ground profile and geotechnical parameters

Layer Lithology	Depth [m]		Specific Gravity (γ) [kN/m³]	Internal angle of friction (ϕ) [deg]	Cohesion of Soil (C) [kPa]	Module of Elasticity (E) [MPa]	Poisson's ratio (v)
	From	To					
QD	0.00	0.80	18.0	35.0	0.0	25.0	0.2
SL	0.80	12.70	25.0	45.0	190.0	2,600.0	0.3

Although the geotechnical investigation report mentioned that the groundwater table level is not at the level of the piles wall, it was assumed that the level of the groundwater table is one meter below excavation levels for conservative considerations. Besides, based on the local guidelines, it has been assumed that the controlled backfill will have the properties presented in Table 2 (Interim Advice Note No. 009, Revision No. A2, 2016).

Table 2: Geo-mechanical parameters of backfill and subgrade material

Layer Lithology	Specific Gravity (γ) [kN/m³]	Internal angle of friction (ϕ) [deg]	Cohesion of Soil (C) [kPa]	Module of Elasticity (E) [MPa]
Backfill & Subgrade Material	20.0	35.0	0.0	40.0

On the other hand, the conditions of the project site are very complicated due to the underground utilities, including electrical high voltage cables, which are crossing the location of the shoring system at the intersection. Moreover, the proposed retaining walls are very close to the ROW, and that affects the traffic flow and the excavation process.

Figure 1 describes the approximate shape for each system considering the right of way and existing utilities location. It is obvious that the excavation limit of the cantilever retaining wall exceeds the ROW and influences the traffic circulation. However, proposed contiguous piles wall system provides more flexibility in the excavation stage and maintains a comfortable distance to ROW, which does not affect the existing utilities or traffic plan.

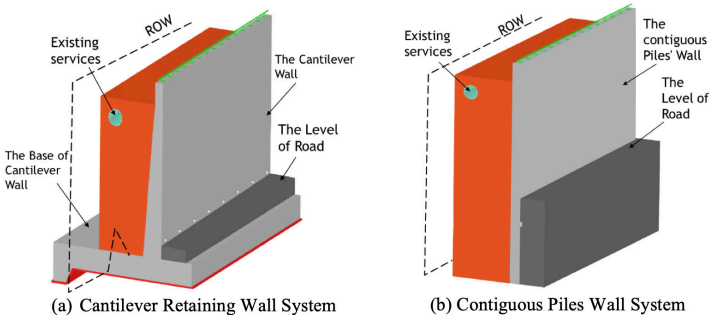

(a) Cantilever Retaining Wall System (b) Contiguous Piles Wall System

Figure 1: The excavation and utilities challenges for both proposed permanent shoring systems

3 COMPARISON BETWEEN TWO PROPOSED SHORING SYSTEMS

Two options of retaining systems are assessed from an economic and constructability perspective to select the most effective retaining structure that can be built rapidly while offering a safe and long-lasting solution. In this project, the proposed systems have been designed using the same assumptions and criteria following the local and international codes (Interim Advice Note No. 009, Revision No. A2, 2016; BS5400, 1990). At the end of the construction stage, the suggested two systems should have the same finishing quality.

3.1 Effect of the Retaining System Type on the Right of Way (ROW) and traffic flow

The retaining walls are usually designed to hold consolidated and unconsolidated soil or water with different levels near to roads and highways. Hence, it is essential to select the ease construction and safer system to avoid any risks or disruption on the traffic plan. As shown in Figure 1, the base of the cantilever retaining system is too wide and overlaps with the ROW. As a result, the equipment used for the excavation process will impact the flow of the traffic. Moreover, Temporary Traffic Management (TTM) plans will be required to avoid any obstruction, risk, or delay on the vehicles or pedestrian movements. On the other hand, the contiguous piles wall system requires limited space for construction compared to the cantilever retaining wall system, which minimizes the interaction with the traffic flow.

3.2 Effect of the Retaining System Type on the quantities of construction materials and cost

As the proposed permanent shoring system will be constructed on four approaches of the multi-grade intersection with an approximate length of 1.7 km, the cost is an

essential factor in adopting the optimum type of the retaining systems. Besides, both retaining walls are designed using the reinforcement concrete and steel rebars available in Qatar. The final cross-sectional of the cantilever retaining wall is presented in Figure 2, while Figure 3 shows the final dimensions of the contiguous piles wall system based on the approved design by the relevant authorities and after carrying out all the required design checks.

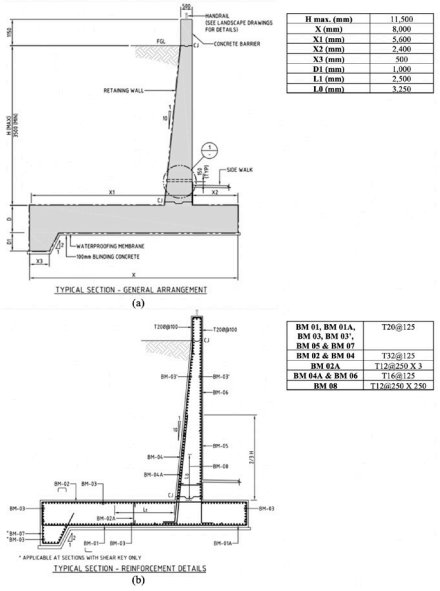

Figure 2: The proposed cross-sectional of the cantilever retaining wall system

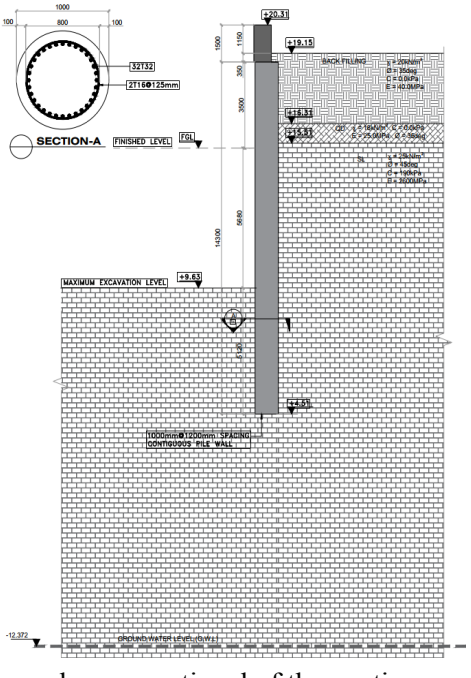

Figure 3: The proposed cross-sectional of the contiguous piles wall system

Based on the cross-section of the proposed permanent shoring systems, the required construction material and excavation quantity of the two options for the same retaining height (level) are presented in Table 3.

Table 3: The required construction materials for both options

Item	Reinforcement Steel (kg/m)	Concrete (m^3/m)	Excavation Quantity (m^3/m)
Cantilever Wall	3056	26	99
Piles Wall	3718	13	9

In addition to the fact that the contiguous piles wall system provides an effective solution to avoid clashes with the underground utilities during the excavation stage and maintain the traffic flow and timeframe without any delays, it also reduces the material and construction cost dramatically.

As shown in Table 3, the proposed contiguous piles retaining system minimizes the quantity of the required concrete to the half, while it almost requires a similar quantity of the steel rebars for the cantilever retaining wall. On contrast, the contiguous piles system decreases the excavation quantity by about 90% compared to the other option due to the excavation methodology. Vertical drilling is used for contiguous piles system, while a deep rectangular area must be excavated for the base of the cantilever retaining wall as shown in Figure 1a. Accordingly, the required construction cost will be noticeably dropped when the contiguous piles system is used as a permanent system in such site conditions.

3.3 Effect of the Retaining System Type on the underground utilities

Great attention is usually paid to the relocation of existing underground utilities and excavation phase of any project site, especially when it has chemicals, flammable materials, or high voltage electrical cables. As part of the constructability evaluation of the proposed system, it was found that using the cantilever retaining wall system might be difficult due to the existing underground utilities, which include high voltage electrical cables and pipelines. These utilities must be relocated into another path that may lead to disruption of service to residential areas surrounding the project. The proposed contiguous piles wall system offers a better solution, by having the piles constructed away from the crossing underground utilities. Furthermore, no influences on the accessibility of domestic services should occur.

3.4 Effect of the Retaining System Type on the project timeframe

Due to the continuous development of the roads, highways, and infrastructure networks in Qatar, most of the planned and ongoing projects must be completed following the Qatar National Vision 2030. In addition, the construction companies are always implementing proper scheduling for the construction activities of their projects. Thus, adopting the ease of construction retaining system is necessary to comply with the timeframe of the execution plan. As a result of the effects of the cantilever retaining wall system on the ROW and the existing underground utilities, it seems that this option should be avoided to complete the construction within a reasonable timeframe. Accordingly, using the

contiguous piles wall system provides more flexibility in the excavation process, which means more time and effort will be saved.

4 CONCLUSION AND RECOMMENDATIONS

This paper evaluated and compared the constructability and economic aspects for two proposed retaining systems to adopt the most effective option as a permanent shoring system. The cantilever retaining wall and piles retaining wall systems have been evaluated in terms of their impacts on the construction process and the required quantities. The selection of one of the suggested systems was not an easy task due to the complicated site conditions.

Based on the comparison of this study, it can be concluded that using the contiguous piles retaining wall system as a shoring system of multi-grade highway intersection is more economical than the cantilever retaining wall. Furthermore, the contiguous piles wall system shows effectiveness in the construction process, timeframe, handling utilities, and excavation procedure.

On the other hand, the selection of the contiguous retaining wall system reduces the quantities of the overall materials needed for the construction, which directly impacts the project budget and cost.

REFERENCES

BS5400: Steel, concrete and composite bridges (1990). British Standards Institution.

Interim Advice Note No. 009, Revision No. A2 (2016). Public Work Authorities (Ashghal).

Standard Specification for highway bridges (2002). American Association of State Highway and Transportation Officials (AASHTO). Washington D.C, the USA.

Cite this article as: Alfarra M., Sadeq M., Sadek H., "Constructability and Economical Comparison Between Two Proposed Permanent Shoring Systems in Qatar: A Case Study", *International Conference on Civil Infrastructure and Construction (CIC 2020)*, Doha, Qatar, 2-5 February 2020, DOI: https://doi.org/10.29117/cic.2020.0079

Resource Recovery from Waste, Water and Wastewaters with Membrane Technologies

Ismail Koyuncu
koyuncu@itu.edu.tr
National Research Center on Membrane Technologies, Istanbul Technical University, Maslak, 34469, Istanbul, Turkey
Environmental Engineering Department, Istanbul Technical University, Maslak, 34469, Istanbul, Turkey

Bihter Zeytuncu
bihtzeytuncu@itu.edu.tr
National Research Center on Membrane Technologies, Istanbul Technical University, Maslak, 34469, Istanbul, Turkey
Environmental Engineering Department, Istanbul Technical University, Maslak, 34469, Istanbul, Turkey

Mehmet Emin Pasaoglu
mpasaoglu@itu.edu.tr
National Research Center on Membrane Technologies, Istanbul Technical University, Maslak, 34469, Istanbul, Turkey
Environmental Engineering Department, Istanbul Technical University, Maslak, 34469, Istanbul, Turkey

Ayse Yuksekdag
yuksekdaga@itu.edu.tr
National Research Center on Membrane Technologies, Istanbul Technical University, Maslak, 34469, Istanbul, Turkey
Environmental Engineering Department, Istanbul Technical University, Maslak, 34469, Istanbul, Turkey

Borte Kose-Mutlu
kosebo@itu.edu.tr
National Research Center on Membrane Technologies, Istanbul Technical University, Maslak, 34469, Istanbul, Turkey
Civil Engineering Department, Yeditepe University, Istanbul, Turkey

ABSTRACT

In this study, critical elements (Boron (B) and Rare Earth Elements (REE)) recovery is studied with membrane technologies. Concentrated boron can be recovered by using different technologies. Membrane technologies such as reverse osmosis have a potential to concentrate the boron. pH of the solution is very important if reverse osmosis is applied. Removal of boron at pH levels of 7 and 10 increases from 80% to 97% with reverse osmosis membranes. Another critical element is rare earth elements in the World. Rare earth elements (REE) is a group of elements that involve lanthanides, scandium and yttrium. A successful REE transport for wastewater was observed compared with the concentrate flow of the acidic waste slime.

Keywords: Shoring system; Contiguous pile wall; Cantilever retaining wall; Qatar

1 INTRODUCTION

Nowadays, wastewater treatment plants have started to be considered as resource recovery facilities. Expectations from resource recovery facilities are water reuse, chemical recovery (such as phosphorus, nitrogen etc.), energy recovery and critical elements recovery (boron, rare earth elements, etc.)

In areas where water scarcity is important in the world, the reuse of water is becoming more and more important. Practice of recovering nutrients (N and P) from wastewater

and converting them into an environmental friendly fertilizer is also getting very important. Nutrient recovery provides a self-sustainable solution to WWTPs and helps to meet discharge limits. PO3 precipitation from wastewater is less energy intensive and economical (Theregowda et al., 2018). Energy positive wastewater treatment plants are also getting very important for sustainable wastewater management.

Critical elements are getting more and more vital with the increased requirement of these elements and the development of advanced technologies. There are 27 critical elements according to European Union science hub raw materials information system (EU CRM list, 2017). Boron and REE are listed as possible critical raw materials for important industries by the European Union and the United States. In addition to this, some REEs were mentioned as "critical REEs". The supply of these elements, especially is limited.

Turkey is ranked top with its share of almost 73% in the global boron reserve standing in the world. There are four main boron production facilities in Turkey (Etimaden, 2019). High boron containing groundwater negatively affects agriculture due to the irrigation in a near basin. Boron concentration is changing around 50-150 mg/l in geothermal water and 3000-6000 mg/l in groundwater. Removal of boron can be provided by several technologies such as adsorption, coagulation, ion-exchange, electrocoagulation and membranes processes such as electrodialysis, Reverse Osmosis (RO) and Membrane Distillation (MD). Concentrated boron can also be recovered by using different technologies.

Rare Earth Elements (REE) is a group of elements involving lanthanides, scandium and yttrium. REEs have various important uses and applications, which make REEs more essential. REEs are needed for a wide variety of products such as catalysts, hybrid vehicles, batteries, mobile phones, plasma televisions, disk drives, catalytic converters and fluorescent lamps. The industrial application demand for rare earth metals is increasing in the world.

The aim of this study is to execute the boron and REE potential of waste and wastewater and recover of these chemicals by advanced membrane separation techniques.

2 MATERIALS AND METHODS

High boron containing spring waters were collected from area of the Eti Maden Boron manufacturing facility in Emet-Kutahya, Turkey. In the experiments to adjust pH of water, high purity sodium hydroxide was used. Brackish Water (BW) and Seawater (SW) RO membranes were used in this study. RO membranes systems were performed as single and double stages with different combinations. The feed solution was first passed through UF and NF membrane to reject the colloidal materials and suspended solids as seen in Figure 1. After that two stages, RO membranes were obtained in the pilot scale system (Zeytuncu et al., 2019).

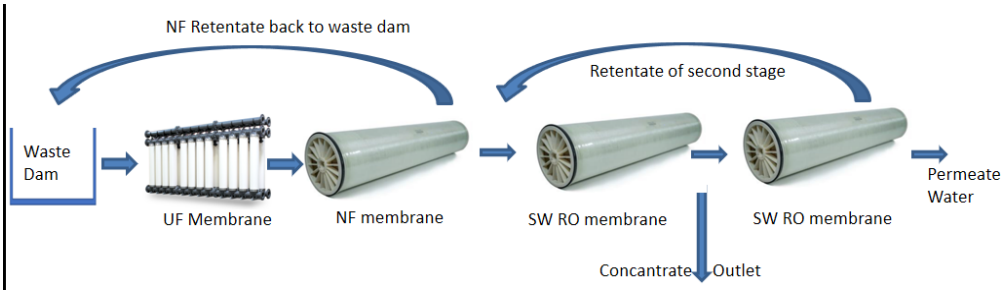

Figure 1: Flow chart of RO membrane system for boron removal from spring water

Boron concentration was analyzed by an inductively coupled plasma optical emission spectrometer (ICP-OES, Perkin Elmer). Other parameters such as pH and temperature were measured by portable meters. The percentage removal of boron is defined as per following equation:

$$\text{Removal} = (1 - C_p/C_f) \times 100\% \quad (1)$$

where C_f and C_p are the component concentration in the feed and permeate, respectively.

Wastewater and waste slime of the boron deposit site of Turkey were investigated for the recovery of REEs. A microwave digestion system (Berghof, Germany) was preferred for the preparation of acidic leach solution for the waste slime under 210 °C temperature for 30 min. Both wastewater and waste acidic leach solutions were analyzed by using inductively coupled plasma (ICP, Perkin-Elmer, USA) to determine the major, trace and REE contents of samples. An X-ray fluorescence (XRF) (Bruker S8 Tiger, USA) analysis was carried out for waste slime, additionally. Two different membrane systems were combined to recover the REEs. First, a NF process was used to concentrate the leach solution of waste slime. On the other hand, the wastewater was concentrated by a pilot-scale cross-flow NF system in the mining plant. The concentrate flows of each NF process were fed to the SLM system as the second step of the recovery process which consists of an H-type microbial fuel cell reactor. Di-2-Ethylhexyl phosphoric acid (D2EHPA, 97% purity) dissolved in kerosene (10% v/v) was used as an organic phase while 5 M HNO_3 was used for the stripping of REEs. Samples were taken from each phase at t=0 and t=3 h for the determination of REE and major element concentrations. Distribution coefficients of each REE were calculated according to the following equation (Yuksekdag et al., 2019).

$$D = [Me]_{strippant}/[Me]_{feed} \quad (2)$$

3 RESULTS AND DISCUSSIONS

3.1 Boron removal and recovery

In this study, first single stage BWRO and SWRO processes were applied to remove boron from spring water containing approximately 3000 ppm of boron concentration at pH 7. After this study, 2 pass processes (SWRO/SWRO, BWRO/SWRO, SWRO/

BWRO and BWRO/BWRO membrane systems) were examined at pH of 7 and 10. The results of boron removal are given in Table 1. The boron removal by single stage process is not good enough to meet irrigation criteria. At single stage BWRO the maximum boron removal was found to be as 58 % at pH of 7 while 88 % of boron removal was achieved for single stage SWRO membrane. Although the removal efficiency is around 88% with SWRO, problems such as clogging of membranes and low performance were encountered due to the hardness of the water. However, since it was seen that one stage would not be sufficient, so, two-stage studies were performed. When double stage RO membrane combinations were investigated one by one, it was seen that the most efficient result for boron removal was obtained by double SWRO membrane. Boron removal rates for double pass of SWRO membranes were given in Table 1. While first stage pH is 7 here, second stage pH is around 10. In SWRO/SWRO membrane system, the boron removal was gained 98.3 % which was the most efficient result. It can be said by these results, that double pass SWRO is essential to meet the required criteria. Figure 2 shows the effect of pH on the boron removal in double pass RO membrane system. It is obvious that pH has an important role to play in boron removal performance. Boron removal increased from 80 % at pH 7 to more than 97% at pH 10 owing to the increasing amount of borate ions while rising the pH. More than 98 % of boron removal can be achieved at a pH level of 11. Removal efficiency is increased especially after pH=9 (Zeytuncu et al., 2019).

Table 1: Boron removal results in double stage RO configuration (Zeytuncu et al., 2019)

	1. Stage			2. Stage	
	pH	**Boron removal, %**		**pH**	**Boron removal, %**
Single BWRO	7.05	58.0	-	-	-
Single SWRO	7.05	88.0	-	-	-
First Stage SWRO	7.05	80.0	**Second Stage SWRO**	10.55	98.3
First Stage BWRO	7.05	83.0	**Second Stage SWRO**	10.55	97.7
First Stage SWRO	7.05	82.0	**Second Stage BWRO**	10.55	96.5
First Stage BWRO	7.05	82.0	**Second Stage BWRO**	10.55	93.3

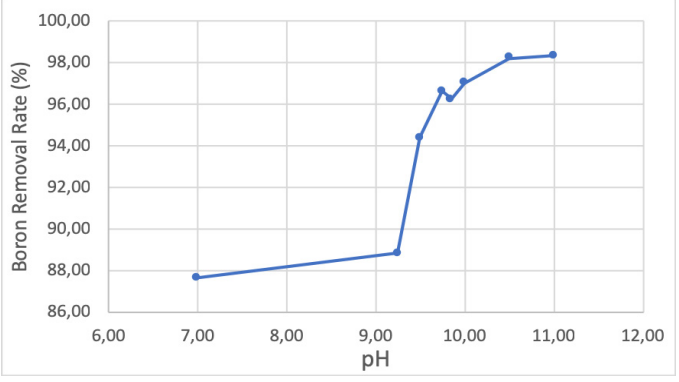

Figure 2: Boron removal for double pass RO membrane systems (Zeytuncu et al., 2019)

3.2 Rare earth elements recovery from wastes

According to the results obtained from three different digestion methods, the highest total REE concentration was achieved by using 6 mL HNO3 + 1 mL HF acid mixture which was around 22 ppm (wt/wt) for the REE recovery studies (Figure 3). Individual concentrations of the top four elements for waste slime are Ce, La, Y, and Nd respectively. On the other hand, Y concentration of wastewater was 25 ppb in 27 ppb (wt/v) total REEs. At the end of the NF process, a 70% rejection and 40% REEs concentration ratio was obtained. As a result of the SLM process, it was confirmed that the distribution coefficients of rare earth elements for wastewater were higher than the acidic leach solution.

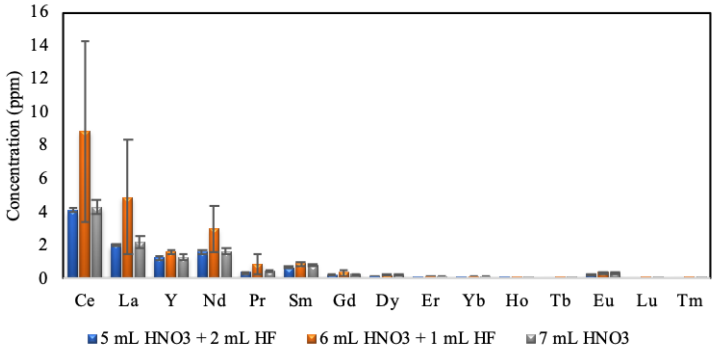

Figure 3: REE concentrations of waste slime (wt/wt)

4 CONCLUSION

It is obvious that pH has an important role to play in boron removal performance. Boron removal increased from 80 % at pH 7 to more than 97% at pH 10 owing to the increasing amount of borate ions while rising the pH. Concentrate stream can be further concentrated with evaporation-crystallation process and boric acid can be recovered from the final concentrate. It has a big economic value.

Rare earth element potential of waste and wastewater of boron mining plant were detected in Turkey. The top four elements with the highest concentration are Ce, La, Y, and Nd respectively. A more successful REE transport for wastewater was observed compared with the concentrate flow of the acidic waste slime. It shows that wastewater of the boron deposit site should be considered as a secondary source for the recovery of REEs.

ACKNOWLEDGMENTS

This study was financially supported by The Scientific and Technological Research Council of Turkey (TUBITAK) (Project no:117Y357), Istanbul Technical University (ITU) Scientific Research Project (Project ID: 41893) and Eti Mining Operations General Directorate. The authors would also like to thank Geochemistry Research Laboratory for XRF analysis.

REFERENCES

Etimaden (2019). Boron as the Rising Value of Turkey. Etimaden Publications, Turkey.

EU CRM List (2017). Study on the review of the list of the critical raw materials – Final Report by British Geological Survey, Bureau de Recherches Géologiques et Minières, Deloitte Sustainability, Directorate-General for Internal Market, Industry, Entrepreneurship and SMEs (European Commission), TNO. EU Publications.

Theregowda, R. B., Gonzalez-Mejia, M., Garland, J. & Ma, X. (2018). Nutrient recovery from municipal wastewater for sustainable food production systems: An alternative to traditional fertilizers, *AWWA Sustainable Water Management Conference.*

Yuksekdag, A., Kose-Mutlu, B., Wiesner, M. R. & Koyuncu, I. (2019). Toward Resource Recovery from Wastewater: Rare Earth Element Potentials and Membrane Technology for the Separation, *International Water Association (IWA) Membrane Technology Conference & Exhibition for Water and Wastewater Treatment and Reuse (IWA-MTC 2019).* Toulouse, France.

Zeytuncu, B., Güçlü, S., Eryıldız, B., Yüksekdağ, A., Korkut, S., Türken, T., Paşaoğlu, M. E., Kaya, R., Kazak, A., Ceylan, M., Ünlü, Mİ., Ün, S., Yılmaz, S., Çeliker, A. & Koyuncu, İ. (2019). *Boron Removal from High Boron Containing Water Sources by Membrane Technologies*. International Symposium on Boron – BORON 2019, Nevşehir, Turkey.

Cite this article as: Koyuncu I., Zeytuncu B., Pasaoglu M. E., Yuksekdag A., Kose-Mutlu B., "Resource Recovery from Waste, Water and Wastewaters with Membrane Technologies", *International Conference on Civil Infrastructure and Construction (CIC 2020)*, Doha, Qatar, 2-5 February 2020, DOI: https://doi.org/10.29117/cic.2020.0080

Dynamic Imaging of Hydrate Specific Area Evolution during Xenon Hydrate Formation

Zaher Jarrar
zjarrar@vols.utk.edu
Civil and Environmental Engineering, University of Tennessee, Knoxville, TN 37996, USA

Riyadh Al-Raoush
riyadh@qu.edu.qa
Department of Civil and Architectural Engineering, Qatar University, Doha, Qatar

Khalid Alshibli
alshibli@utk.edu
Civil and Environmental Engineering, University of Tennessee, Knoxville, TN 37996, USA

Jongwon Jung
jjung@chungbuk.ac.kr
School of Civil Engineering, Chungbuk National University, Cheongju, Chungbuk, South Korea

ABSTRACT

Gas hydrates are ice-like structures formed under high pressure and low temperature conditions. They are considered as a potential energy source due to their abundance and the increase in energy demand worldwide. A fundamental understanding of hydrate formation and dissociation kinetics is essential in order to improve gas productivity from natural hydrates reservoirs. This paper investigates the evolution of hydrate specific area during the process of hydrate formation using dynamic 3D synchrotron microcomputed tomography. Xenon hydrate was formed inside a high-pressure low-temperature cell, filled with silica sand partially saturated with water. The cell has a height of 70.2 mm and an inner diameter of 9.7 mm, and is capable of sustaining an internal pressure of 150 MPa. During hydrate formation and dissociation, full 3D images are acquired at a time resolution of 45 seconds and a spatial resolution of 5.38 μm/voxel. The reconstructed images were enhanced and segmented, and direct volume and surface area measurements were obtained. Initially, the specific area of hydrate increased with increasing hydrate saturation up to a certain hydrate saturation threshold (9% hydrate saturation). After this threshold, hydrate specific area started to decrease with increasing hydrate saturation. This is an indication that the small crystals of hydrates tend to merge and form larger crystals during the process of hydrate formation.

Keywords: Gas hydrates; Synchrotron micro-computed tomography; Dynamic imaging; Hydrate formation

1 INTRODUCTION

Gas hydrates are ice-like structures formed under high pressure and low temperature conditions where gas (guest molecules) is trapped within a crystal structure of water (host molecules). They are considered as a potential energy source due to their abundance and the increase in energy demand worldwide (Sloan & Koh, 2008). A fundamental understanding of hydrate formation and dissociation kinetics is essential in order to improve gas productivity from natural hydrates reservoirs. This paper investigates the

evolution of hydrate specific area during the process of hydrate formation using dynamic 3D synchrotron microcomputed tomography. Xenon hydrate was formed inside a high-pressure low-temperature cell, filled with silica sand partially saturated with water. The cell has a height of 70.2 mm and an inner diameter of 9.7 mm, and is capable of sustaining an internal pressure of 150 MPa. During hydrate formation, full 3D images were acquired at a time resolution of 45 seconds and a spatial resolution of 5.38 μm/voxel, and direct measurements of hydrate volume and surface area were obtained from the segmented images.

2 METHODOLOGY

In this study, pink beam synchrotron microcomputed tomography (PSMT) was used to obtain high-resolution 3D images during hydrate formation. In pink beam tomography, a glazed mirror and an x-ray absorbing foil are used to obtain an x-ray beam with 1000 times higher flux than a monochromatic beam (Rivers, 2016). PSMT images were acquired at beamline 13D, Advanced Photon Source (APS), Argonne National Laboratory (ANL), Illinois, USA.

Xenon hydrate was formed inside a high-pressure low-temperature cell, filled with silica sand partially saturated with water. The cell has a height of 70.2 mm and an inner diameter of 9.7 mm, and is capable of sustaining an internal pressure of 150 MPa. During hydrate formation, full 3D images were acquired at a time resolution of 45 seconds and a spatial resolution of 5.38 μm/voxel. The reconstructed images were enhanced and segmented using Avizo commercial software, similar to the procedure described in Jarrar et al. (2018). A sample xy slice of one of the images is depicted in Figure 1, with hydrates shown as bright voxels.

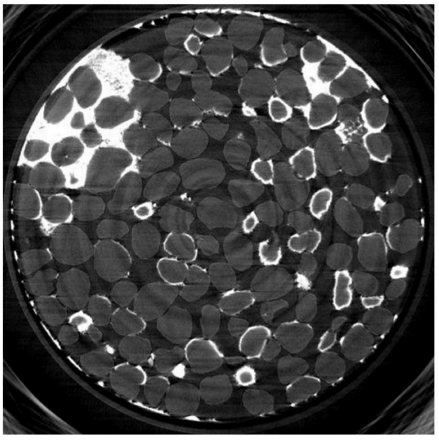

Figure 1: Sample xy slice of one of the images during hydrate formation with hydrates shown as bright voxels.

3 RESULTS

The segmented images were used to directly measure the change of hydrate volume and surface area during hydrate formation. Figure 2 shows the change of hydrate specific area (area/volume) with hydrate saturation during Xenon hydrate formation. Each point in Figure 2 represents measurements obtained from a full segmented 3D image. Initially,

the specific area of hydrate increased with increasing hydrate saturation up to a certain hydrate saturation threshold (which corresponds to about 9% hydrate saturation). After this threshold, hydrate specific area began to decrease as hydrate saturation increases. This is an indication that the small crystals of hydrates tend to merge, forming larger crystals during the process of hydrate formation.

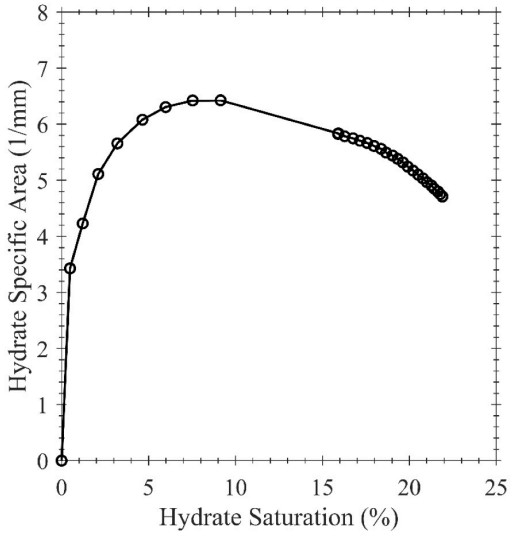

Figure 2: Change of hydrate specific area with hydrate saturation during Xenon hydrate formation.

4 CONCLUSION

Xenon hydrate was formed inside a high-pressure low-temperature cell, filled with silica sand partially saturated with water. The cell has a height of 70.2 mm and an inner diameter of 9.7 mm, and is capable of sustaining an internal pressure of 150 MPa. During hydrate formation, full 3D images were acquired at a time resolution of 45 seconds and a spatial resolution of 5.38 μm/voxel, and direct measurements of hydrate volume and surface area were obtained from the segmented images. The specific area of hydrate initially increased with increasing hydrate saturation up to a hydrate saturation threshold of 9%, after which, hydrate specific area began to decrease as hydrate saturation increased. This indicates that the small crystals of hydrates tend to merge, forming larger crystals during the process of hydrate formation.

ACKNOWLEDGMENTS

This publication was made possible by partial funding from NPRP grant # NPRP8-594-2-244 from the Qatar national research fund (a member of Qatar Foundation) and the Institute for a Secure and Sustainable Environment (ISSE), University of Tennessee-Knoxville, USA. Any opinions, findings, and conclusions or recommendations expressed in this material are those of the authors and do not necessarily reflect the views of funding agencies. This paper used resources of the Advanced Photon Source (APS), a U.S. Department of Energy (DOE) Office of Science User Facility operated for the DOE Office of Science by Argonne National Laboratory (ANL) under Contract

No. DE-AC02-06CH11357. The PSMT images presented in this paper were collected using the x-ray Operations and Research Beamline Station 13-BMD at Argonne Photon Source (APS), ANL. We thank Dr. Mark Rivers of APS for help in performing the SMT scans. We also acknowledge the support of GeoSoilEnviroCARS (Sector 13), which is supported by the National Science Foundation, Earth Sciences (EAR-1128799), and the DOE, Geosciences (DE-FG02-94ER14466).

REFERENCES

Jarrar, Z. A., Al-Raoush, R. I., Hannun, J. A., Alshibli, K. A. & Jung, J. (2018). 3D synchrotron computed tomography study on the influence of fines on gas driven fractures in Sandy Sediments. *Geomechanics for Energy and the Environment*, 100-105.

Rivers, M. L. (2016). High-speed tomography using pink beam at GeoSoilEnviroCARS, Developments in X-Ray Tomography X, Stock. Muller, R., Wang, B. & SPIE, G.

Sloan, E. D. & Koh, C. A. (2008). *Clathrate hydrates of natural gases*. CRC Press, Boca Raton, FL, the USA.

Cite this article as: Jarrar Z., Al-Raoush R., Alshibli K., Jung J., "Dynamic Imaging of Hydrate Specific Area Evolution during Xenon Hydrate Formation", *International Conference on Civil Infrastructure and Construction (CIC 2020)*, Doha, Qatar, 2-5 February 2020, DOI: https://doi.org/10.29117/cic.2020.0081

Use of 3D Images to Evaluate Formation Damage Induced by Montmorillonite Fines in Porous Media Systems

Jamal Hannun
jh1300283@qu.edu.qa
Department of Civil and Architectural Engineering, Qatar University, Doha, Qatar

Riyadh Al-Raoush
riyadh@qu.edu.qa
Department of Civil and Architectural Engineering, Qatar University, Doha, Qatar

Zaher Jarrar
zjarrar@vols.utk.edu
Civil and Environmental Engineering, University of Tennessee, Knoxville, TN 37996, USA

Khalid Alshibli
alshibli@utk.edu
Civil and Environmental Engineering, University of Tennessee, Knoxville, TN 37996, USA

Jongwon Jung
jjung@chungbuk.ac.kr
School of Civil Engineering, Chungbuk National University, Cheongju, Chungbuk, South Korea

ABSTRACT

Formation damage costs oil and gas industry $140 billion/year in lost productivity, this is a key challenge to Qatar, the world's largest LNG exporter. During production from a well, multiphase flow foster drag forces to mobilize fine particles from within the subsurface. Fines' migration can alter the gas flow, clogging pores and disconnecting gas pathways. Understanding fines influence is a complex challenge due to the reservoirs' porous media heterogeneity. Microtomography of sand sediments provides a standardized approach to study the fines impact. X-Ray microtomography of two repacked sand cylinders was carried at Argonne National Lab synchrotron. Rounded silica sand was mixed with hydrophilic swelling montmorillonite clay. High and low fines concentrations were mix¬¬ed with the sand then deposited into five layers. Initially, samples were fully saturated, then gas was injected, the sediments were scanned before and after injection. At first, fines were suspended in the brine, but after injection were retained on the gas-brine interface, and their concentration in the brine increased. Gas injection divided pores and throats, reducing their average size. Contrarily, main gas pathways increased in size but were disconnected in the sediment with high fines concentration. Fines caused increased capillary pressure and lowered the sediment permeability.

Keywords: Geopolymer; Fluid to binder ratio; Activator solution; Na2SiO3/NaOH ratio

1 INTRODUCTION

Multiphase flow of brine and gas in unconsolidated sandy porous media, have an influence on broad set of natural and industrial activities at the subsurface. Methane hydrate, fracking, rainwater and contaminants transported in the vadose zone, are all applications that are dominated by multiphase flow mechanisms in the subsurface.

Dominantly, capillary forces control the horizontal flow of fluids in sandy sediments. The physics of fluids are governed by pore sized pathways, the geometry of these pathways can affect the flow mechanisms. During gas production from deep rock formations, spontaneous imbibition drives the flow, this flow is governed by the pore volumes in the rock formation and is not caused by pressure gradient within the reservoir. Over time, formation damage occurs within rock pores changing their size, this can seize the spontaneous imbibition, causing the need for injection wells to continue production. Understanding the different mechanisms of formation damage is fundamental in planning any activity that involves the multiphase flow of fluids in the subsurface. It is reported that formation damage costs the oil and gas industry $140 billion/year in lost productivity (Byrne, 2012). Lost productivity is a key challenge to Qatar, the world's largest LNG exporter. During production from a well, multiphase flow foster drag forces to mobilize fine particles from within the subsurface. Fines' migration can alter the gas flow, clogging pores and disconnecting gas pathways, changing pathways size and geometry. Understanding fines influence is a complex challenge due to the reservoirs' porous media heterogeneity. The study of homogenous sand sediments provides a standardized approach to benchmark and understand the fines impact. Understanding the quantitative and qualitative effects of fines in the subsurface is fundamental to advance current gas recovery systems and evolve sustainable production technics. Also, it is crucial to conduct such studies in three-dimensional sediments, microtomography is a powerful method that enables accurate reconstruction of real sediment morphology.

2 METHODOLOGY

X-ray microtomography of two repacked sand cylinders was carried at Argonne National Lab (ANL) synchrotron. Rounded silica sand was mixed with hydrophilic swelling montmorillonite clay. High and low fines concentrations were mixed with the sand then deposited into five layers, into two different acrylic cylinders. Initially, samples were fully saturated, then CO_2 gas was injected, the sediments were scanned before and after injection. The scan was done using high brilliance X-rays generated from the synchrotron facility at beamline 13D, Advanced Photon Source (APS), (ANL), Illinois, the USA. A monochromatic beam was pointed towards the sample as it rotated, the scan time took 15 minutes for each sample. Gas was injected, then imaged in the quasi-static state. A scan resolution of 3.9 micron per voxel was chosen for this study, this resolution can resolve the movements of clusters of fines, whether suspended in brine or attaching to the sand interface, changing the pore morphology.

Using the resulting 3D X-ray grayscale images, sand, brine, gas, and fines were binarized to observe the qualitative changes due to the transport of fines. The segmented images were then used to observe changes in the gas flow pattern. As fines concentration increases, capillary flow mechanisms can be altered due to changes in pore morphology (Al-Raoush et al., 2019). These changes can be visually examined by visualizing the 3D gas volume.

Then pore networks were generated to study the quantitative changes in the porous media morphology. A pore network algorithm that uses the maximum spheres approach was used for this analysis (Fouard et al., 2006). The algorithm starts by constructing a skeleton of the porous media that represents the central line of the flow paths, then the

intersection points are grown to spheres in 3D, the inscribed sphere radius increases up until it touches a sand grain. Figure 1 shows a vertical section of the media, (a) is void space in blue, (b) is a distant map used for pore network generation, colored blue toward red as the distance between central line and grains increases (indicating bigger pore radius). Changes in the average pore size are then examined to study the impact of swelling hydrophilic montmorillonite clay on the porous media, due to multiphase flow of the injected gas.

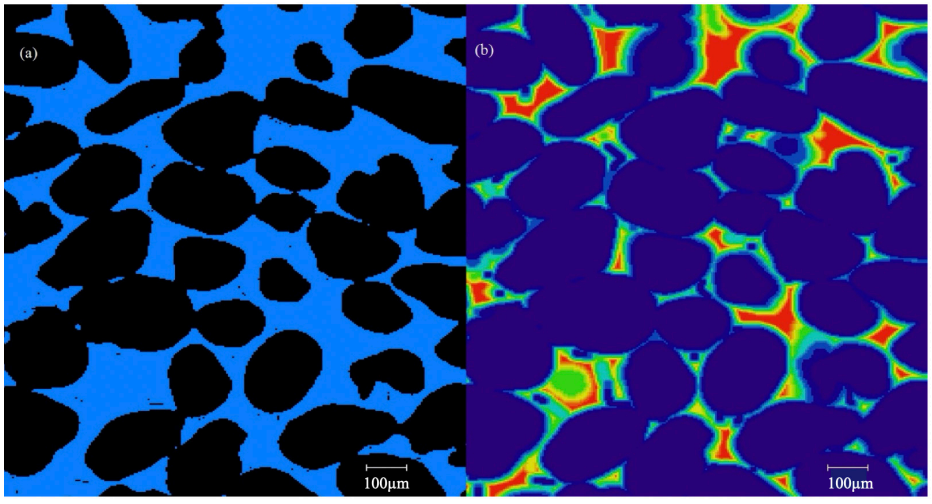

Figure 1: Vertical section of the sediment pack, (a) void space, (b) distant map

3 RESULTS

The results for the two systems, low and high fines concentrations showed a change in gas flow patterns and average pore sizes. The gas flow pattern in the 2% montmorillonite (concentration by weight of sand in the system), was a capillary flow in which a connected gas ganglion was observed, this was validated by visualizing the gas volume. In the other sample with 5% montmorillonite, the gas body was observed to disconnect after CO_2 injection, this can be related to the mobilization of fines clogging the pore throats. The generated pore networks provide a measure for the size change of all the pores in the system. Comparing the change of the average pore size after CO_2 injection, can provide a justification for the gas pathways disconnection in the 5% sample. Table 1 shows how fines reduced the pores and throats sizes causing detachment in the gas ganglion.

These results using maximal ball based pore networks are similar in behavior to other results obtained using grain-based algorithms (Hannun et al., 2019). Figure 2 illustrates the generated maximal ball pore network, (a) is the void space, (b) pore network and (c) is an overlap showing how the network fits the void space. The fines transported in the subsurface can alter the pores morphology, this change is the main cause in altering gas flow patterns.

Fines were suspended in the brine, but after injection were retained on the gas-brine interface, and their concentration in the brine increased. Fines caused increased capillary pressure and lowered the sediment permeability. This is primarily due to the decrease of

pore sizes after the migration of the swelling hydrophilic clay.

Table 1: Change in average pore radius at different fines concentrations due to CO_2 injection

Fines Type	Fines%	Injected CO_2 (ml) [Change in Average Pore Radius]	
Montmorillonite	2	0 [100%]	1.5 [99.98%]
Montmorillonite	5	0 [100%]	1.5 [97.80%]
Gauge CO_2 Pressure psi(kPa)		4(27.6)	6(41.4)

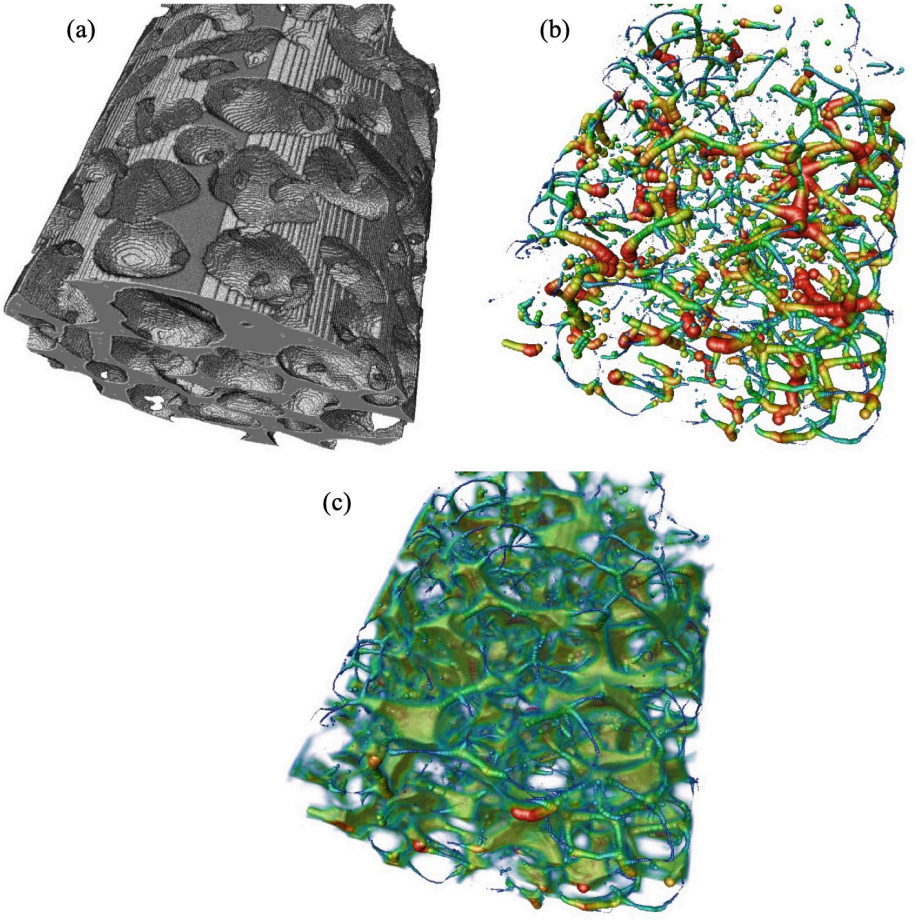

Figure 2: Maximal ball pore network, (a) the void space, (b) pore network, (c) overlap displaying; the network fitting the void space, blue to red are small to large pores respectively

4 CONCLUSION

Synchrotron microtomography of two sand samples was used to study the formation damage caused by fines' migration. Unconsolidated sand was mixed with low and high concentrations of montmorillonite clay, the samples were fully saturated then gas

was injected to cause fines' mobilization. Using 3D X-ray image, pore networks were generated to provide a measure of the change in pore morphology due to fines' migration. Gas injection divided the pores and throats, reducing their average size. For the system with high fines concertation, the average pore radius was reduced by 2.2%, compared to 0.02% in the system with lower fines concentration. This reduction of the throat radius resulted in increased capillary pressure and reduced permeability.

ACKNOWLEDGMENTS

This research was made possible by the National Priorities Research Program (NPRP) grant #NPRP8-594-2-244 from Qatar national research fund (a member of Qatar Foundation). The findings achieved herein are solely the responsibility of the authors. The SMT images were collected using the X-ray Operations and Research Beamline Station 13-BMD at Argonne Photon Source (APS), Argonne National Laboratory. The authors thank Dr. Mark Rivers of APS for help in performing the SMT scans. They also acknowledge the support of GeoSoilEnviroCARS (Sector 13), which is supported by the National Science Foundation, USA, Earth Sciences (EAR-1128799), and the US Department of Energy (DOE) and Geosciences (DE-FG02-94ER14466). Use of the Advanced Photon Source, an Office of Science User Facility operated for the DOE Office of Science by Argonne National Laboratory, was supported by DOE, USA under contract no. DE-AC02-06CH11357.

REFERENCES

Al-Raoush, R., Hannun, J., Jarrar Z., Alshibli, K. & Jung, J. (2019). Impact of fines type on gas flow using 3D micro-computed tomograph. *SPE Kuwait Oil & Gas Show and Conference*. Society of Petroleum Engineers, Mishref, Kuwait. https://doi.org/10.2118/198106-MS.

Byrne, M. (2012). *Formation damage – any time, any place, anywhere*. http://www.afes.org.uk/uploads/files/Formation%20Damage%20%E2%80%93%20Any%20Time.pdf.

Fouard, C., Malandain, G., Prohaska, S. & Westerhoff, M. (2006). Blockwise processing applied to brain microvascular network study. *IEEE Transactions on Medical Imaging*, *25* (10), 1319-28. https://doi.org/10.1109/TMI.2006.880670.

Hannun, J., Al-Raoush, R., Jarrar Z., Alshibli, K. & Jung, J. (2019). Pore networks to characterize formation damage due to fines at varied confinement and sand shape. *Third EAGE WIPIC Workshop: Reservoir Management in Carbonates*, Nov. 2019, Volume 2019, European Association of Geoscientists & Engineers, Doha, Qatar. p.1-4, https://doi.org/10.3997/2214-4609.201903116.

Cite this article as: Hannun J., Al-Raoush R., Jarrar Z., Alshibli K., Jung J., "Use of 3D Images to Evaluate Formation Damage Induced by Montmorillonite Fines in Porous Media Systems", *International Conference on Civil Infrastructure and Construction (CIC 2020)*, Doha, Qatar, 2-5 February 2020, DOI: https://doi.org/10.29117/cic.2020.0082

Enhancement of Naphthalene Biodegradation by Sulfate Application in Brackish Subsurface Systems

Saeid Shafieiyoun
saeid.s@qu.edu.qa
Department of Civil and Architectural Engineering, Qatar University, Doha, Qatar

Reem Ismail
ri1607496@qu.edu.qa
Department of Civil and Architectural Engineering, Qatar University, Doha, Qatar

Riyadh I. Al-Rauosh
riyadh@qu.edu.qa
Department of Civil and Architectural Engineering, Qatar University, Doha, Qatar

ABSTRACT

Anaerobic biodegradation is the most dominant mechanism in the petroleum hydrocarbon contaminated subsurface systems. Due to depletion of terminal electron acceptors such as sulfate, anaerobic degradation of organic contaminants can be restricted. Hence, engineered sulfate application has been proposed as an effective remediation strategy to enhance the activities of sulfate reducer bacteria (SRB) in the contaminated subsurface systems. However, biodegradation process is significantly affected by environmental conditions and sulfate application in the contaminated saline and brackish coastal regions is unknown. A series of flow-through reactors (FTRs) representative of dynamic anaerobic subsurface conditions were conducted using undisturbed soil samples collected from brackish (semi)-arid coastal environments in Qatar. Dissolved naphthalene as one of the most dominant petroleum hydrocarbons that can be found in most of the contaminated sites was injected into FTRs under different salinity conditions. The relevant geochemical indicators as well as soil adsorption and dissolved phase concentrations were measured. The results confirmed development of reducing conditions as well as SRB activity under experimental conditions. Salinity did not restrict bioremediation and dissolved naphthalene degradation was more stable and enhanced under brackish water conditions because microbial cultures within the undisturbed soil were adapted to the brackish water conditions at the field sampling environment. This paper will provide an overview of the flow-through experiments and key findings.

Keywords: Naphthalene biodegradation; Sulfate reducing conditions; Salinity; Brackish groundwater

1 INTRODUCTION

Release of petroleum hydrocarbons in the subsurface systems is one the most important environmental issues that can result in soil and groundwater contamination (Al-Raoush, 2014, Shafieiyoun et al., 2018). Anaerobic biodegradation is the dominant process in contaminated systems but due to depletion of dissolved oxygen (DO) and other electron acceptors during natural attenuation, remediation will last for a long period of time. Sulfate injection is one of the recent treatment methodologies to enhance biodegradation mechanisms. Previous studies indicate that microbial activities can be

limited in the saline and brackish environment (Thamer et al., 2013; Abed et al., 2015). Hence, in this study the effect of salinity on engineered sulfate injection as a remediation strategy was investigated.

2 MATERIALS AND METHODS

None-contaminated undisturbed soil samples were collected from a shoreline known as Sumaysimah beach in the State of Qatar. Groundwater pH and EC values at the sampling location were ~7.5 and ~4000 µS/cm that categorized it in the range of brackish water.

Six flow-through reactors (FTRs) were constructed similar to Pallud et al. (2007) by a Plexiglas ring of 10 cm length and 4.7 cm inside diameter. The nominal pore volume (PV) was 52 mL. FTRs were flushed upward by a peristaltic pump at a nominal rate of 2.7 mL/hr to be in the range of groundwater flow rate at the sampling location. The influent and effluent solutions were sampled regularly and analyzed for the concentrations of naphthalene and sulfate. In addition, pH, EC, Eh, and DO of the samples were also measured.

FTRs were injected by a synthetic influent solution containing back ground levels of $MgCl_2$ (89 mg/L), KCl (24 mg/L), and $CaCl_2.H_2O$ (243 mg/L) on the basis of groundwater analyses were added that were dissolved in argon purged Milli-Q water (DO < 0.8 mg/L). Dissolved naphthalene concentration in the influent solution was 4 mg/L during the first injection episode but later during the second injection episode increased to 13 mg/L to explore the effects of higher levels of contamination on microbial activities. Sulfate concentration during both injection episodes was 150 mg/L to be more than stoichiometric requirement for the biodegradation process. The influent solution was transferred into the 1 L Tedlar bags which served as the reservoir for the FTRs.

Two FTRs were flushed by a low salinity argon purged influent solution containing background nutrients, sulfate, and naphthalene (identified as LS1 and LS2) and two FTRs were flushed by a high salinity argon purged influent solution containing background nutrients, 1300 mg/L NaCl, sulfate, and naphthalene to be in the range of brackish water similar to the sampling location (identified as BW1, BW2). To investigate the soil adsorption, one FTR (identified as Biocide) was flushed identical to the LS FTRs and just 275 mg/L HgCl2 biocide (Van De Graaf, 1995) was added to the influent solution to inhibit biodegradation. The last FTR was flushed identical to the LS FTRs but just naphthalene was replaced by 100 mg/L lactate as a preferred carbon source for bacteria (Acton & Barker, 1992) to control/compare the sulfate reducing bacteria (SRB) development (identified as Lact).

FTRs were operated at ambient temperature in the following sequence of steps for three months:

1. Three PVs of argon purged Milli-Q water containing background nutrients were injected.
2. 5 PVs of argon purged 100 mg/L of NaBr solution was injected for tracer test analyses.
3. ~50 PVs (one month) influent solution with ~4 mg/L naphthalene concentration was injected and then FTRs were stopped for one week under anaerobic saturated condition. Then FTRs were again flushed with ~50 PVs (one month) of ~13 mg/L

naphthalene solution. Naphthalene concentrations of 4 and 13 mg/L were chosen according to field conditions (Shafieiyoun et al., 2018). Lactate concentration was 100 mg/L in the Lact FTR.

3 RESULTS AND DISCUSSIONS

The results from tracer tests indicated the effective porosity for the LS1 and LS2 FTRs are 37 and 44%, respectively, for BW1 and BW2 FTRs are 28 and 32%, respectively, and for the Lact and Biocide FTRs are 39 and 62%, respectively. The differences between the effective porosities are because undisturbed soil samples were employed in this study.

Sulfate concentration in the Lact FTR decreased to < 20 mg/L indicating the development of sulfate reducing bacteria (SRB) under experimental conditions. For the LS and BW FTRs, sulfate concentration decreased to ~135 mg/L which is in the range of theoretical stoichiometry for naphthalene degradation under sulfate reducing conditions. No significant change was observed between the influent and effluent EC values. In the Biocide FTR, no physical changes were observed but the soil color in the Lact FTR became black after two weeks which can be attributed to the production of iron sulfide during SRB activities. The soil color in the LS and BW FTRs also became darker after one month of flushing.

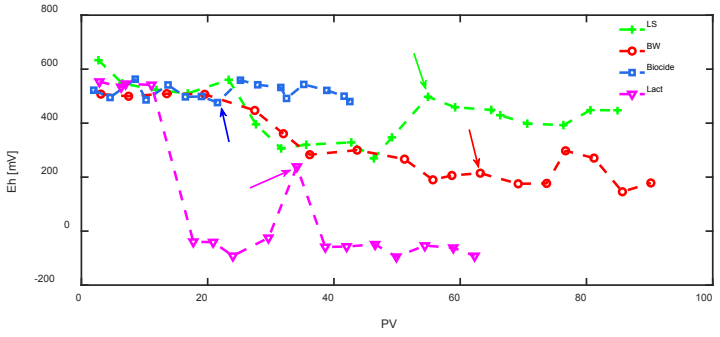

Figure 1: Effluent Eh values under low salinity (LS), brackish water (BW), biocide injection, and lactate injection (Lact). Each arrow represents the first sampling at the beginning of the second injection episode.

The color change in the FTRs was coincident with reduction in the Eh profiles (Figure 1). The Eh profile is an indicator for the redox potential and in the influent solutions was > +500 mV. Eh values did not change in the effluent of the Biocide FTR compared to the influent solutions and remained constant indicating that microbial activities were successfully restricted. As expected, the redox potential initially dropped in the Lact FTR after ~15 PVs (two weeks) and rapidly reached to -40 mV indicating the enhancement of reducing conditions. Following the initial rapid drop, the effluent Eh from the Lact FTR gradually decreased to -90 mV after 25 PVs that was followed by minor fluctuations until the end of the experiments (62 PVs). The peak at 34 PV is following the second injection episode and can be attributed to two weeks of no flow condition. However, following the second injection episode, again redox potential in the

Lact FTR decreased. The Effluent Eh values in the LS FTRs dropped to +300 mV after 25 PVs and following the second injection episode increased to 400 mV after introducing the higher naphthalene concentration. For the BW FTRs, effluent Eh dropped to 200 mV after 20 PVs and following the second injection episode fluctuated in the range of 200 to 300 mV. A notable decrease in the effluent Eh values of the LS and BW FTRs compared to the Biocide FTR indicated the development of reducing conditions. The results from the LS and BW FTRs indicated that reducing and microbial activities were more stable under brackish water conditions which is similar to the sampling location conditions.

Effluent naphthalene concentrations are presented in Figure 2. For the Biocide FTR, effluent naphthalene concentration initially increased from 20% to ~85% of the injected concentration due to saturation of soil sorption capacity. Following the second injection episode, due to an increase of injected naphthalene concentration, sorption capacity increased and effluent concentration decreased to ~58%. However, after saturation of the sorption capacity, effluent naphthalene concentration again increased to 85%. For the LS and BW FTRs, effluent naphthalene concentration during the first injection episode initially increased from ~5% to ~40 % due to saturation of sorption capacity while biodegradation and microbial community was not still developed. After ~20 PVs, effluent naphthalene concentration for the LS and BW FTRs reached to a maximum and then decreased until the end of the first injection episode. While during the first injection episode, the LS and BW FTRs showed similar behavior, following the second injection episode, the LS FTRs were disturbed but the BW FTRs remained stable. The effluent naphthalene concentrations from the LS FTRs increased to ~20% following the second injection episode suggesting that microbial activities and biodegradation were significantly disturbed by an increase in the injected naphthalene concentration. In the case of BW FTRs, effluent naphthalene concentrations after second injection episode remained below the method detection limit (MDL). It can be hypothesized that as opposed to the conventional idea that salinity can restrict biodegradation (Abed et al., 2015), the results from this study indicated that treatment efficiency was higher under brackish conditions probably because microbial community in the undisturbed soil sample was adopted to the higher salinity at the sampling location.

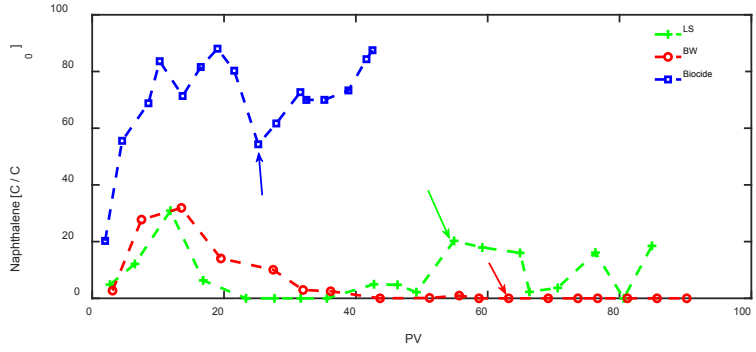

Figure 2: Effluent naphthalene concentrations under low salinity (LS), brackish water (BW), and biocide injection. Each arrow represents the first sampling following the beginning of the second injection episode.

4 CONCLUSION

Our findings indicated that while for the low naphthalene concentration (3.5 mg/L), biodegradation under anaerobic sulfate reducing conditions is not significantly affected by salinity, for the high naphthalene concentration (13 mg/L) reducing conditions, microbial activity, and treatment efficiency was more enhanced under brackish water conditions probably because microbial community in the undisturbed soil samples employed in this study were adopted to the brackish water conditions at the sampling location.

ACKNOWLEDGMENT

This publication was made possible by funding from NPRP grant # NPRP9-093-1-021 from the Qatar national research fund (a member of Qatar Foundation).

REFERENCES

Abed, R. M. M., Al-Kharusi, S. & Al-Hinai, M. (2015). Effect of biostimulation, temperature and salinity on respiration activities and bacterial community composition in an oil polluted desert soil. *Int. Biodeterior. Biodegradation*, Vol. 98, pp. 43-52.

Acton, D. W. & Barker, J. F. (1992). In situ biodegradation potential of aromatic hydrocarbons in anaerobic groundwaters. *J. Contam. Hydrol.*, Vol. 9, No. 4, pp. 325-352.

Al-Raoush, R. I. (2014). Experimental investigation of the influence of grain geometry on residual NAPL using synchrotron microtomography. *J. Contam. Hydrol.*, Vol. 159, pp. 1-10.

Pallud, C., Meile, C., Laverman, A. M., Abell, J. & Van Cappellen, P. (2007). The use of flow-through sediment reactors in biogeochemical kinetics: Methodology and examples of applications. *Mar. Chem.*, Vol. 106, No. 1-2 SPEC. ISS., pp. 256-271.

Shafieiyoun, S., Thomson, N. R., Brey, A. P., Gasinski, C. M., Pence, W. & Marley, M. (2018). Realistic expectations for the treatment of FMGP residuals by chemical oxidants. *J. Contam. Hydrol*.

Thamer, M., Al-Kubaisi, A. R., Zahraw, Z., Abdullah, H. A., Hindy, I. & Khadium, A. A. (2013). Biodegradation of Kirkuk light crude oil by Bacillus thuringiensis, Northern of Iraq. *Nat. Sci.*, Vol. *5*, No. 7, pp. 865-873.

Van De Graaf, A. A., Mulder, A., De Bruijn, P., Jetten, M. S. M., Robertson, L. A. & Kuenen, J. G. (1995). Anaerobic Oxidation of Ammonium Is a Biologically Mediated Process. *Appl. Environ. Microbiol.*, Vol. 61, pp. 1246-1251.

Ward, D. M. & Brock, T. D. (1978). Hydrocarbon Biodegradation in Hypersaline Environments. *Appl. Environ. Microbiol.*, Vol. 35, pp. 353-359.

Cite this article as: Shafieiyoun S., Ismail R., Al-Raoush I. R., "Enhancement of Naphthalene Biodegradation by Sulfate Application in Brackish Subsurface Systems", *International Conference on Civil Infrastructure and Construction (CIC 2020)*, Doha, Qatar, 2-5 February 2020, DOI: https://doi.org/10.29117/cic.2020.0083

Influence of Water Table Fluctuation on Natural Source Zone Depletion in Hydrocarbon Contaminated Subsurface Environments

Reem Ismail
ri1607496@qu.edu.qa
Department of Civil and Architectural Engineering, Qatar University, Doha, Qatar

Saeid Shafieiyoun
saeid.s@qu.edu.qa
Department of Civil and Architectural Engineering, Qatar University, Doha, Qatar

Riyadh I. Al-Raoush
riyadh@qu.edu.qa
Department of Civil and Architectural Engineering, Qatar University, Doha, Qatar

ABSTRACT

Most of the prediction theories regarding dissolution of organic contaminants in the subsurface systems have been proposed based on the static water conditions; and the influence of water fluctuations on mass removal requires further investigations. In this study, it was intended to investigate the effects of water table fluctuations on biogeochemical properties of the contaminated soil at the smear zone between the vadose zone and the groundwater table. An automated 60 cm soil column system was developed and connected to a hydrostatic equilibrium reservoir to impose the water regime by using a multi-channel pump. Four homogenized hydrocarbon contaminated soil columns were constructed and two of them were fully saturated and remained under static water conditions while another two columns were operated under water table fluctuations between the soil surface and 40 cm below it. The experiments were run for 150 days and relevant geochemical indicators as well as dissolved phase concentrations were analyzed at 30 and 50 cm below the soil surface in all columns. The results indicated significant difference in terms of biodegradation effectiveness between the smear zones exposed to static and water table fluctuation conditions. This presentation will provide an overview of the experimental approach, mass removal efficiency, and key findings.

Keywords: Water table fluctuation; Hydrocarbon degradation; Biodegradation

1 INTRODUCTION

Groundwater is one of the most valuable natural resources available on earth. Its existence is vital to life and a fundamental part of our natural environmental cycles of carbon, nitrogen, oxygen, water and nutrients. Accidental spills of petroleum products, such as crude oil, gasoline, and diesel fuel are a common source of groundwater contamination especially in coastal areas. With the development of petroleum industry, petroleum hydrocarbons have become one of the widest spread pollutants. Contamination by crude oil poses serious social, economic and environmental problems worldwide as they gradually change the composition of soil and groundwater. The pollution by organic compounds affects the nature of plants and animals, and human health (Newton, 1990; Zhou, 1995).

When a non-aqueous phase liquid (NAPL) distributes in the subsurface systems, a hot spot will be created at the smear zone between the vadose zone and the groundwater table that is exposed to groundwater fluctuations. The transition zone separating soil from water table is a dynamic part of groundwater contamination. The fluctuations of water table driven by seasonal changes in recharge and discharge or by sea elevation in coastal environments cause temporal differences in local redox conditions (Haberer et al., 2012; Rezanezhad et al., 2014). The NAPL distribution in soil and groundwater is affected by different parameters such as the volume of non-aqueous phase liquid (NAPL), magnitude and speed of water table, the soil media, and fluid properties (Dobson et al., 2007; Oostrom, 2007). The objective of this work is to address the relation between the water table fluctuations on the hydrological and biogeochemical processes, which influence the degradation and mobilization of petroleum hydrocarbons, under conditions relevant to coastal aquifers in the semi-arid environments.

2 MATERIAL AND METHODS

The setup of the experiment contained four soil columns. Two of them were fully saturated under static condition while the other two soil columns were under water table fluctuations. All columns were made of hard acrylic (length is 60 cm, inner diameter is 7.5 cm, wall thickness is 0.6 cm). The water level in the soil columns was controlled by changing the water level in an equilibrium column. One equilibrium column controlled the water level in static soil columns (identified as static1 and static2) and each of the fluctuation columns (identified as fluc1 and fluc2) were separately connected to an equilibrium column. Each equilibrium column was connected to one Tedlar bag as the water storage. A multi-channel pump (9-channel Tower II pump, CAT. M. Zipperer, GmbH) was used to transfer water from the Tedlar bags to the equilibrium columns.

The soil for this experiment was collected from Simaisma beach in the northeast side of Doha, Qatar. The soil was synthetically contaminated by Toluene and Naphthalene following Brinch et al., 2002. Water table regime for the two static columns was maintained at the top of the soil surface (no change). While for the other two columns (fluctuating), an oscillating water table regime was imposed (fluctuating water table). The water level fluctuated between the soil surface (0 cm) and 40 cm below the soil surface, with an imbibition/drainage period lasting for 2.5 days and then 1 day under static conditions.

Aqueous samples were collected through two ports at the middle (30 cm below soil surface) and at the bottom (50 cm below soil surface). Each week samples were collected and analyzed for the concentrations of organic compounds, sulfate, and dissolved inorganic carbon (DIC) followed by the measurement of Eh, pH, DO and EC.

3 RESULTS AND DISCUSSION

The soil oxidation–reduction potential (ORP) is influenced by water table fluctuation unlike the static water table. The dissolved oxygen in all columns indicated a reduction after 20 days of the beginning of the experiment. The ORP of the 4 columns is illustrated in Figure 1. In the static water columns, ORP reduced with time from around 250 mv at the beginning of the experiment at both -30 and -50 cm and reduced to around 114 mv after 100 days. While for the fluctuating columns, values reduced from 300 mv at

the beginning of the experiment at -30 and -50 cm and reduced to 100 mv. In the static columns, ORP at -30 and -50 was approximately the same from the beginning till 100 days of the experiment for both columns. However, for the fluctuating columns, ORP at -50 cm was slightly lower than ORP at -30 cm at the beginning of the experiment, but after 60 days, ORP at the -5 and -30 were intersecting. This reduction in ORP is a strong indication of the reducing condition inside the columns although it does not reach to a negative value.

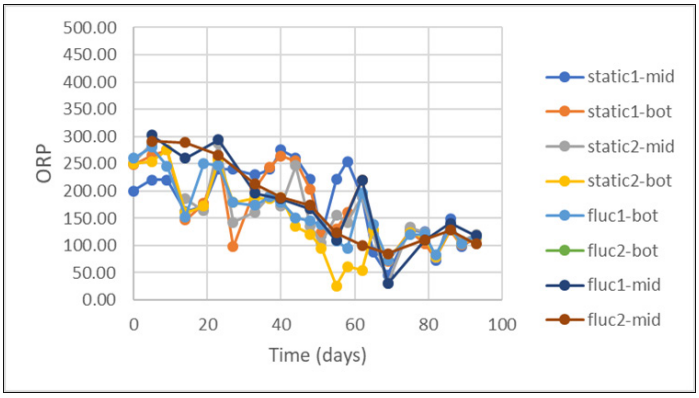

Figure1: ORP values from the middle (mid) and bottom (bot) of the columns under static conditions (static1 and static2) and under water table fluctuation condition (fluc1 and fluc2).

Significant change on the concentration of sulfate is observed in Figure 2. For the static 1 and 2 the concentration at -30 cm was reduced from 450, 330 mg/L to 165, 135 mg/L, respectively. Similarly, the sulfate concentration at -30 cm for the fluctuation 1 and 2 was reduced from 345, 325 mg/L to 230, 215 mg/L respectively. While for the bottom part (-50) of fluctuation 1 and 2, the concentration was reduced from 220, 295 mg/L to 130, 130 mg/L respectively. In general, the reduction percentage of sulfate in static columns (-30), fluctuating (-30), fluctuating (-50) was ~60%, ~ 33%, and 45%, respectively. The sulfate-reducing bacteria obtained energy by oxidizing organic compounds that exist in petroleum hydrocarbon while reducing sulfate (SO_4^{2-}) to hydrogen sulfide (H_2S). The reduction in sulfate concentration in the columns was expected as a result of sulfate reducing bacteria being enhanced and activated.

Toluene concentrations are presented in Figure 3, the results showed no change in concentration due to the large organic mass in soil. Another reason could be that the microbial community in the soil was still undeveloped.

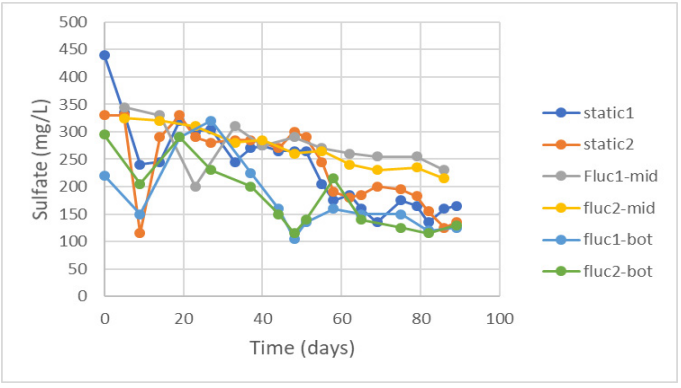

Figure 2: Dissolved sulfate concentrations in the middle of the columns under static conditions (static1 and static2) and from the middle (mid) and bottom (bot) of the columns under water table fluctuation condition (fluc1 and fluc2).

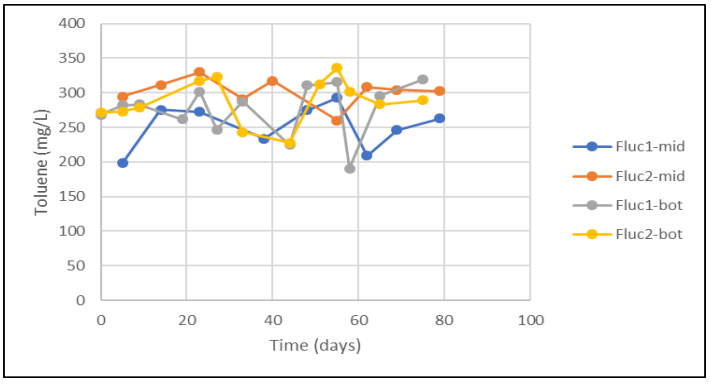

Figure 3: Dissolved toluene concentrations in the middle and bottom of the columns under water table fluctuation conditions (fluc1 and fluc2).

4 CONCLUSION

In this study, the variation in petroleum hydrocarbon concentrations (toluene and Naphthalene) due to water table fluctuation and degradation were experimentally studied. The results showed that, the degradation of toluene was occurring in both static and fluctuation columns. Sulfate consumption was a strong indication of anaerobic hydrocarbon degradation under the experimental conditions.

The results indicate that there is a significant variation in the redox potential and microbial activities at the smear zone under water table fluctuation conditions. While similar sulfate concentrations were observed in the static columns and the bottom parts of the fluctuating column, at the middle of the water fluctuation columns sulfate concentrations were higher. This can result in enhanced microbial community and biodegradation that could be attributed to the sulfate mobilization as well as sulfur oxidation during fluctuation process.

ACKNOWLEDGMENT

This publication was made possible by funding from NPRP grant # NPRP9-093-1-021

from the Qatar national research fund (a member of Qatar Foundation). We acknowledge that all the Gas Chromatography analyses were accomplished in the Central Laboratories unit, Qatar University.

REFERENCES

Dobson, R., Schroth, M. H. & Zeyer, J. (2007). Effect of water-table fluctuation on dissolution and biodegradation of a multi-component, light nonaqueous-phase liquid. *Journal of Contaminant Hydrology, 94*(3-4), 235-248.

Haberer, C. M., Rolle, M., Cirpka, O. A. & Grathwohl, P. (2012). Oxygen transfer in a fluctuating capillary fringe. *Vadose Zone Journal*, *11*(3).

Newton, J. (1990). Remediation of petroleum contaminated soils. *Pollut Eng*, 2, 46-52.

Oostrom, M., Hofstee, C. & Wietsma, T. W. (2007). Behavior of a Viscous LNAPL Under Variable Water Table Conditions Behavior of a Viscous LNAPL Under Variable, 0383.

Rezanezhad, F., Couture, R. M., Kovac, R., O'Connell, D. & Van Cappellen, P. (2014). Water table fluctuations and soil biogeochemistry: An experimental approach using an automated soil column system. *Journal of Hydrology*, 509, 245-256.

Zhou, Q. X. (1995). *Ecology of combined pollution.* China Environmental Science Press, Beijing, 127-128.

Cite this article as: Ismail R., Shafieiyoun S., Al-Raoush R. I., "Influence of Water Table Fluctuation on Natural Source Zone Depletion in Hydrocarbon Contaminated Subsurface Environments", *International Conference on Civil Infrastructure and Construction (CIC 2020)*, Doha, Qatar, 2-5 February 2020, DOI: https://doi.org/10.29117/cic.2020.0084

Embedded Retaining Wall Design and Performance Monitoring for Deep Excavation in Geological Conditions of Qatar

Muhammad Humza
Muhammad.humza@parsons.com
Parsons International Limited, Doha, Qatar

Ghulam Sarwar
Sarwar.Ghulam@parsons.com
Parsons International Limited, Doha, Qatar

Majid Naeem
Majid.naeem@ammico.biz
Ammico Contracting Company, Doha, Qatar

Gorkem Dora
Gorkem.dora@ammico.biz
Ammico Contracting Company, Doha, Qatar

ABSTRACT

Embedded retaining walls such as diaphragm walls and secant bored pile walls have become viable water-tight earth retaining and stabilizing systems for deep excavation in urban areas. In this article, the design aspects of a diaphragm wall are presented, and its performance is assessed and comparison of predicted wall movements with the observed behavior is discussed. The geotechnical analysis and design of retaining system was performed by finite element analysis using PLAXIS with linear elastic perfectly plastic constitutive model. Structural calculations for the support system were done using structural program Staad Pro. A monitoring program was adopted to monitor the performance of the designed retaining system. Design methodology and discussion on understanding of performance monitoring presented in this paper provides a reference for the future design and safe economical construction of similar structures in geological conditions of Qatar. It also provides basis for the potential refinement of the monitoring techniques of embedded retaining walls in Qatar.

Keywords: Deep excavation; Embedded retaining wall; Finite Element analysis; Performance monitoring

1 INTRODUCTION

Embedded retaining walls such as diaphragm walls and secant bored pile walls have become viable water-tight earth retaining and stabilizing systems for deep excavation in urban areas. The advantage of diaphragm wall over the other retaining walls is its use as temporary retention system as well as permanent wall and foundation system. The advantage of a diaphragm, wall over a secant pile wall is the reduced number of joints in the wall which ultimately improves the wall water tightness. Diaphragm walls are installed using trench cutter in the rock formations of Qatar in a series of discrete panels typically ranging in length from 2.8m to 7.0m. Adnan et. al. (2019) presented the case study to show diaphragm wall performance supported by steel struts in rock formations of Qatar. The focus of this paper is on performance monitoring and techniques being used for the monitoring of braced excavations in Qatar.

2 PROJECT BACKGROUND

The project presented for this case study was in Lusail area of Qatar. The 17.5m deep excavation was carried out for the construction of four (04) basements. No critical structures were present adjacent to the excavation except asphalt roads; however, the site was about 140m away from the Arabian Gulf as shown in Figure 1. Therefore, diaphragm wall was used as a water-tight earth retaining system in the proximity of sea. The retaining system was supported by steel struts due to regulations of statutory authority since the installation of ground anchors is prohibited.

Figure 1: Project layout plan

3 GEOLOGICAL CONDITIONS

At depths relative to civil engineering, the geological formations in Qatar peninsula belong to Palaeogene to Quaternary age (Cavellier et al., 1970; Fourniadis, 2010). Within Doha, mainly made ground and residual soils are present on or close to the ground surface, however, marine sediments are found at coastline of Qatar. The main geological formations, in stratigraphic succession, are upper Dammam formation (Simsima Limestone member), Lower Dammam formation (Dukhan Limestone and Midra Shale member) and Rus Formation. The rock units of these formations are mainly comprised of limestones, shales, siltstones, claystones, marls and gypsum. The Simsima Limestone member is present over 80% of the land surface of Qatar. Therefore, most deep excavations, within Doha, have been carried out in Simsima Limestone member. It has been the main founding stratum for most structures due to its presence at shallower depths, thickness and its geotechnical properties. Nevertheless, there is a spatial variance in the thickness and geological characteristics of subsurface formations owing to depositional factors, in particular, near coastlines of Qatar where thick marine deposits are encountered. Therefore, deep excavations and foundations require special attention in the design and method of construction in the marine deposits. For this project, geotechnical parameters were derived from traditional site investigation and laboratory testing program and the derived design parameters are summarized in Table 1.

Table 1: Geotechnical design parameters for FE analysis

Material	Elevation (m QNHD)	Unit Weight (kN/m³)	Cohesion (kPa)	Friction Angle (degrees)	Modulus, E (MPa)
Quaternary Deposits	2.65 to 1.95	18	0	35	25
Weathered Simsima Limestone	1.95 to 0.65	22	95	40	350
Simsima Limestone	0.65 to -10.55	24	95	45	350
Rus Formation (Decomposed)	-10.55 to -24.35	21	0	37	120
Rus Formation	-24.35 to bottom	22	55	24	180

4 DESIGN METHODOLOGY

Finite Element Method (FEM) using 2D PLAXIS was used to analyze the complexity of the interaction between the ground and the retaining structure and to design a retaining structure in detail before construction. PLAXIS is a two-dimensional (plain strain) finite element program, specifically developed for the analysis of deformation and stability in geotechnical engineering problems. The analyses were performed using linear elastic-perfectly plastic Mohr-Coulomb (MC) constitutive model with effective stress parameters. Though, soil response to loading is nonlinear, inelastic and highly dependent on the magnitude of stress, the linear elastic model was used for rock formation because of its simplicity and rock deformation modulus can easily be determined through lab and field testing that is used as primary loading stiffness parameter in MC model.

Three design sections were analyzed according to varying excavation geometry as shown in Figure 1. The finite element models analyzed for section 1, section 2 and section 3 are presented in the Figure 2. The 0.8m thick diaphragm wall was modelled as a plate element. Surcharge load of 20 kPa was considered for all sections. Diagonal steel struts at section 1 and section 2 modelled as fixed-end anchor and installed at 6.15m below the existing ground with 10m spacing between two struts. Diaphragm wall at section 3 supported by inclined steel struts. Inclined steel strut was modelled as node-to-node anchor. The modelled construction sequence was followed at site during the construction.

For section 3 (Figure 2b), the supporting piles were installed at 6.15m below the existing ground level. Excavation was then carried out leaving the rock berm against the wall in section 3. The inclined struts were installed in a way that one end of inclined steel struts rest on concrete Waller beam whilst other end on concrete square cap supported by a pile by creating a slot inside the berm.

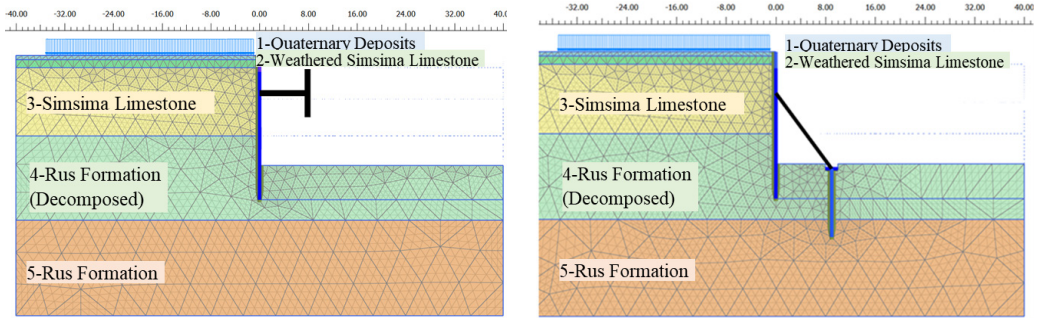

a) Section 1 & 2 b) Section 3

Figure 2: Finite Element models (a) Section 1 & 2 and (b) Section 3

RC Waller beam with strut spacing modelled in STAAD Pro as shown in the Figure 3. Strut forces obtained from Plaxis (2D) for unit spacing are applied at Waller beam. Bending moment, shear fore and deflection of Waller beam and axial force of each strut were determined from STAAD Pro. model.

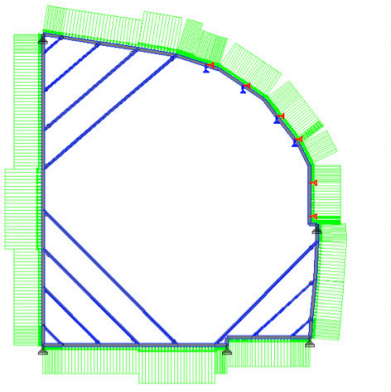

Figure 3: Structural model for Waller beam and struts

5 PERFORMANCE MONITORING

The FE analysis was performed to predict the stresses, strains and resulting deformations in the embedded retaining wall. The deformation results were used to establish estimates of performance that could be compared with field measurements, as a means of determining if the behavior of the wall was within what would be considered the normal range.

Qatar Construction Specifications 2014 (QCS, 2014) states, "*A plan of monitoring shall be established (including necessary instruments and procedures) enabling the comparison of the actual behavior to the acceptable limits. The monitoring shall allow early detection of nonconformities, allowing enough time for corrective actions to be taken successfully"* when setting criteria to enable monitoring during construction. QCS further specifies, for tunneling works, the contractor to submit detailed instrumentation plan, techniques and instrument types and also guidance on the zone of influence is provided. However, influence zone, monitoring techniques and instrument types to be used for monitoring of deep excavations are not explicit and clearly defined. In the absence of particular specifications, by the design consultant or owner, for the instrumentation and monitoring of deep excavations, the contractor usually proposes monitoring regime that is the bare minimum and may not enable the comparison of the actual behavior to the acceptable limits, as specified by QCS.

5.1 Monitoring regime

Optical survey was used to monitor embedded wall movements by the survey targets being mounted near the top of wall. The monitoring scheme used in this selected case is shown in Figure 4. Optical surveys may give reasonable results if they are performed carefully but the problem with optical surveys is that measurements can only be recorded at the location of survey points, as such this technique is not capable of measuring the deflections throughout the wall depth. Secondly, the optical survey is not able to capture

early detection of induced ground movements due to deep excavation that would occur before the installation of survey targets.

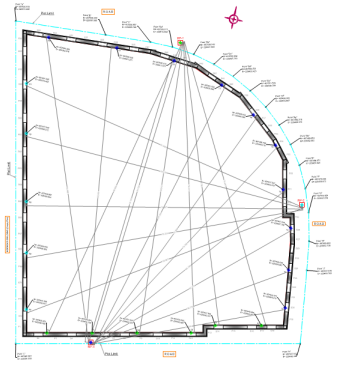

Figure 4: Monitoring regime

For monitoring of deep excavations, detailed instrumentation and monitoring plan should be established. Humza (2019) suggests defining zone of influence and review levels. Review levels are pre-determined values which are established by the designer as a control procedure for monitoring and checking the performance of the designed / impacted structure during excavation work. The review levels are comprised of Alert Levels (AL) and Work Suspension Levels (WSL) and these levels are proposed based on the prediction from the FE analyses. The review levels are set as:

Alert Level = 70% of design value.

Work Suspension Level = 100% of design value.

In general, more commonly used instruments for ground monitoring as well as to reveal the effects of excavation works on the existing buildings are inclinometers, extensometers, ground settlement markers, building settlement markers, tiltmeters and vibration monitors. However, for the deep shaft excavation advanced instrument types such as fiber optical sensors have been used (Schwamb et. al., 2014).

5.2 Comparison of predicted and observed behavior

Figure 5 illustrates the comparison between observed and predicted lateral wall movements using FEM models at the final excavation stage of three sections. The maximum lateral wall movements are 0.14%H, 0.10%H and 0.11%H for section 1, 2 and 3 respectively (H = depth of excavation). The predicted movements compare reasonably well with the observed magnitude at the points where survey targets were installed. However, the predicted magnitude of wall movements is higher at the excavation base, where the movements could not be captured by optical survey. At the base of excavation, predicted movements indicate bulging behaviour, which is well established phenomenon for the braced excavations (Clough & O'Rourke, 1990). Moreover, the main factors responsible for the ground settlement trough behind the retaining wall are the magnitude and shape of deformation of a retaining wall (Ou, 2006). The optical survey technique may be used to measure a cantilevered deformation pattern such as produced in excavation with cantilever wall and also at the early construction stages

before installation of struts as a back-up reference, However, this technique is unable to measure the bulging pattern of wall deformation near the excavation base at the final excavation stage. Therefore, an appropriate monitoring instrument such as inclinometer is recommended to use for performance monitoring of the embedded walls.

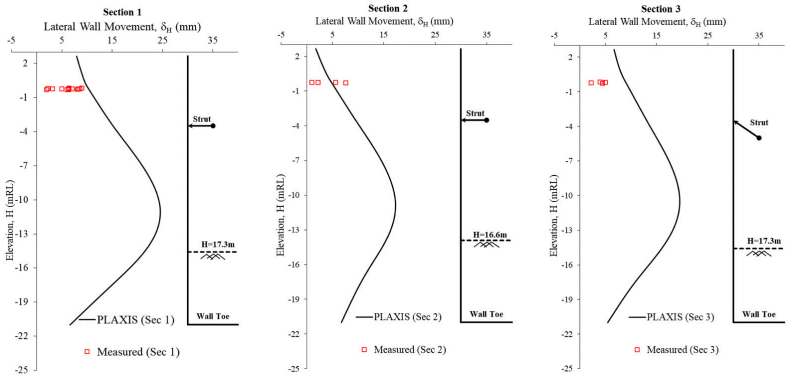

Figure 5: Comparison between observed and predicted lateral movements using PLAXIS

Figure 6 shows the predicted surface settlement using MC model. In general, its use leads to settlement troughs shallower and wider than those observed experimentally (Humza, 2010), signifying the limitation of the model in predicting surface settlement. For this project, surface settlement was not measured since no critical structures were present in the surroundings.

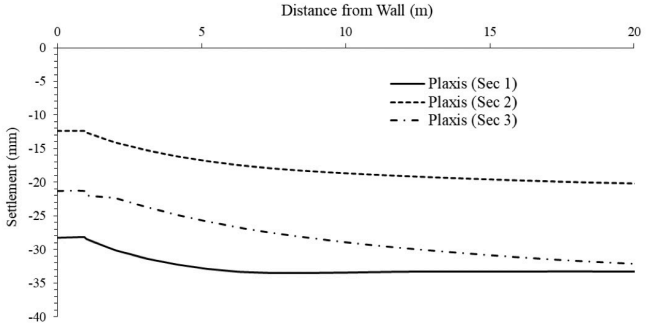

Figure 6: Predicted settlement by PLAXIS

6 CONCLUSION

This paper presents design methodology as a guideline to engineers for the stress and deformation analysis using finite element method for effective designing of embedded retaining wall supported by inclined and diagonal struts for deep excavation. The following points can be concluded:

- The finite element methods can be used effectively for the stress and deformation analysis not only to capture complexity of the interaction between the retaining structure and ground conditions in Qatar but also to establish a site-monitoring control system. The site-monitoring control system should then be implemented by chalking out a proper instrumentation program during construction.
- Although the predicted deflection behavior of diaphragm wall shows good agreement

with observed behavior measured at the top of wall, but the monitoring technique commonly used in local industry is not capable of determining shape of lateral wall movements.

- In order to assess the performance of braced excavations, an appropriate monitoring technique and instrument type is recommended to use that is capable of measuring the deflection profile throughout the depth of embedded wall.

Based on this study, authors suggest design consultants and authorities to make performance monitoring of deep excavation a statutory compulsion and specify the type, quantity and monitoring frequency of an appropriate instrument such as inclinometers for the lateral wall deflection profile. This shall allow early detection of nonconformities, allowing enough time for corrective actions to be taken successfully especially for the deep excavation nearby existing buildings and structures.

REFERENCES

Adnan A.M. et. al. (2019). Diaphragm wall supported by ground anchors and inclined struts: A case study. *International Journal of GEOMATE*, Vol. 16, 57, 150-156.

Cavellier, C., Salatt, A. & Heuze, Y., (1970). Geological description of the Qatar peninsula, Explanation of the 1/100,000 geological Maps of Qatar, Bureau de recherches geologiques et minieres, Paris, France.

Clough, G.W. & O'Rourke, T.D. (1990). Construction induced movements of in-situ walls. *Proceeding of ASCE Conference on Design and Performance of Earth Retaining Structures*, ASCE Geotech. Spec. Publi. No. 25, New York, 439-470.

Fourniadis, I. (2010). Geotechnical characterization of the Simisma Limestone (Doha, Qatar), *Geoenvironmental Engineering and Geotechnics: progress in Modeling and Application*, GeoShanghai 2010, He Q and Shen SL (eds) ASCE, Reston, VA, USA, Geotechnical Special Publication no. 204, 273-278.

Humza M. et al. (2010). Numerical modeling of diaphragm wall behavior in Bangkok soil using Hardening Soil model. *The 4th International Conference on Geotechnical Engineering and Soil Mechanics*, Tehran, Iran 2010, Publication no. 660.

Humza M., (2019). Serviceability limit prediction, monitoring and performance of Open Cut Slope. *Proceedings of 15th International Conference on Geotechnical Engineering*, Lahore, Pakistan.

Ou, C. Y. (2006). *Deep Excavation: Theory and Practice*, Taylor and Francis. London.

Qatar Construction Specification (2014). Ministry of Municipality and Environment, Qatar.

Schwamb, T. et. al. (2014). Fibre Optic Monitoring of a deep circular excavation. *Proceedings of Institution of Civil Engineers, ICE Geotechnical Engineering*, Vol 167, issue GE2, 144-154.

Cite this article as: Humza M., Sarwar G., Naeem M., Dora G., "Embedded Retaining Wall Design and Performance Monitoring for Deep Excavation in Geological Conditions of Qatar", *International Conference on Civil Infrastructure and Construction (CIC 2020)*, Doha, Qatar, 2-5 February 2020, DOI: https://doi.org/10.29117/cic.2020.0085

Investigation of the Effect of the Force-Frequency on the Behaviour of a New Viscous Damper for Railway Applications

Yousif Badri
yousif.badri@qu.edu.qa
Department of Mechanical and Industrial Engineering, Qatar University, Doha, Qatar

Mohammed Hussein
mhussein@qu.edu.qa
Department of Civil and Architectural Engineering, Qatar University, Doha, Qatar

Sadok Sassi
sadok.sassi@qu.edu.qa
Department of Mechanical and Industrial Engineering, Qatar University, Doha, Qatar

Jamil Renno
Jamil.Renno@qu.edu.qa
Department of Mechanical and Industrial Engineering, Qatar University, Doha, Qatar

ABSTRACT

The primary purpose of this work is to experimentally investigate the damping coefficient of a viscous damper, intended to be used in railway applications to reduce noise emission. The viscous shock absorber used in this study is a commercial vehicle damper to which minor modifications were added. This investigation was focused on detecting the variation in the damping coefficient value over a wide range of frequencies. The experimental setup tends to simulate the railway vibration represented by a strong steel metal sheet structure attached to a shaker from its lower side. The shaker itself is connected to the damper rod through a dual acceleration-force sensor. A sinusoidal load with wide range of frequencies was applied by the shaker to the top of the damper's rod. Both acceleration and force time-responses were collected, stored and analyzed to extract the Force-Displacement and the Force-Velocity graphs. Based on the damping coefficients obtained for the different values of excitation frequencies, the results show that the damping coefficient is not constant and depends on the excitation frequency.

Keywords: Damping coefficient; Excitation frequency; Force Vs Velocity; Suspension systems; Transmission oil; Viscous damper

1 INTRODUCTION

A suspension system represents a critical element, whether dealing with automobiles, power transmissions, building, or rail tracks. It is used to prevent discomfort damage, outright structural failure, and even noise (Li & Darby, 2006). A viscous damper usually consists of a cylinder filled with hydraulic oil and separated into two chambers by a piston, itself attached to a moving rod. The movement of the piston in compression or rebound forces the oil to move back and forth through a set of annular orifices on the piston head. This forced passage of oil, which comes from the pressure difference between the two chambers, dissipates the energy of vibration due to the head-loss (Agrawal & Amjadian, 2015).

Many authors have shown how the use of dampers, with a variety of shapes and

designs, could enhance the dynamic stability of structures and minimize their vibration motions. In automotive industry, for example, the viscous damper is mainly used to reduce the vertical oscillations and to maintain handling and ride features to an optimal predefined level. Another promising application of viscous dampers is for railway systems. Kaewunruen & Remennikov (2008) investigated the railway track component dynamic properties. Both the superstructure and substructure of the rail parts generated vibration due to the movement of the rain on the track. Rail pads are usually responsible for reducing the high-frequency forces and transferring the stress from all the rail parts to the sleepers. The modal testing of the previous work showed that the track resonant frequencies are within 40Hz and 1500Hz for the three modes. Also, (Rådeström et al., 2017) provided a full study for implementing fluid damper to reduce the vibration of railway bridges. They generate a model for the bridge sustaining the HSLM-train. Dellner damper was used as a proposed suspension system for the railway bridge. The specification table of the damper showed different damping coefficient values (C) for each stroke length of the piston damper and applied force. Each damping coefficient value was separately implemented in the bridge model to choose the best damping value. Rådeström et al. (2017) did not mention the effect of changing the force excitation frequency on the damping value. The previous gap of knowledge represented a starting point for this work.

Changing the force excitation frequency is a common procedure for the experimental investigation of viscous dampers. G R Iglesias et al. (2014) investigated the behavior of magnetorheological (MR) fluid damper under different force frequencies with changing the current value that excites the damper fluid. The range of frequencies for the previous study started from 1.5 to 12 Hz. It showed that increasing the force-frequency increases the damping coefficient value.

2 EXPERIMENTAL SETUP

The dynamic testing of a viscous damper requires the use of a conventional axial fatigue machine or, in some applications, a specific damper testing machine. In the absence of such equipment, one should look for a convenient way to move the rod of the damper and collect the generated data. In the present investigation, the experimental setup consisted of a viscous damper, for everyday automotive use, attached to a metallic structure. The metallic frame is attached to a shaker on its base support. The shaker moving stinger is connected to the piston rod through a small metallic coupling device. A force-acceleration sensor is attached between the piston rod and the shaker stringer to report both acceleration and force.

2.1 Structure and damper design

At the earliest stages of the present study, a Toyota Landcruiser 2006 commercial shock absorber was chosen. The maneuver of the damper showed an excessive stiffness of the rod because of the internal pressure and the viscosity of the oil. To allow manual handling in the lab, we had to empty it from its original oil and fill it with a low viscosity one. Hydraulic Toyota transmission oil PT088-86806-06ATF was found to be an appropriate substitution for the damper original oil. The most important physical properties of the steering oil are illustrated below in Table 1 (Kemp & Linden, 1990).

Table 1: Physical properties of transmission oil ATF

Property	Value
Specific Heat, J/kg.K	2010
Density, g/cm 3	0.8530
Kinematic Viscosity, mm2/s	33.87
Specific Gravity	0.855
Copper Corrosion Rating	48 (ASN D 130)

The supporting structure (Fig. 1) is a metallic carbon steel frame, made from 1cm thick plates. The 3D structure design was conducted by using SolidWorks 3D software then exported to a water jet cutting machine to provide the exact dimensions.

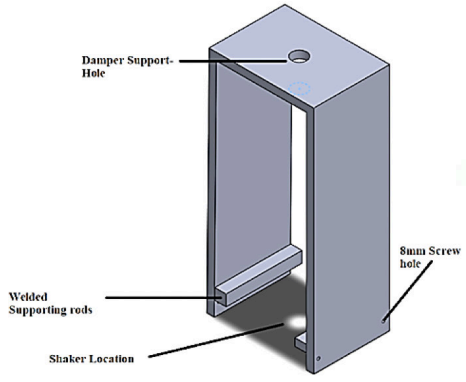

Figure 1: Metallic support for the damper and the shaker

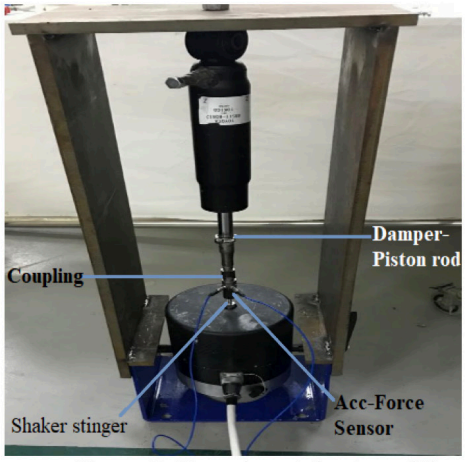

Figure 2: Experimental setup of the viscous damper attached to the shaker

2.2 Shaker test setup

For dynamic testing of mechanical structures, we need an excitation source, a device to measure the response, and a digital signal processor to analyze the system response. In this experiment, the excitation source is represented by a signal generator and a shaker, Model 2100E11 TMS, with maximum output force 440-N. To secure a stable position of the damper, its body was mounted between the two jaws of a vice, itself fixed on a heavy metallic bench. A dual force-acceleration sensor, Model 288D01, was installed between the damper rod and the shaker stringer.

Once the system is correctly installed in a vertical and stable position, the piston rod was driven vertically into a sinusoidal motion. The sensitivity range of the data acquisition system was set to 10.2 (mV)/(m/s²) for the sensor acceleration channel, and 22.4 mV/N for the force channel. The signal generator was set to generate a sine wave with 3V amplitude and send to an amplifier with 24dB gain. During the testing, a continuous reading of the force and the acceleration was achieved, as illustrated in Figure 2.

3 RESULTS AND DISCUSSION

The ideal force vs velocity graph for viscous damper will be more like Figure 3(a). Due to the nonlinear behaviour of the fluid and the hysteresis effect in a real case, the below graph will have an approximate vertical elliptic shape as shown in Figure 3(b). Brigley et al. (2007) conducted an

experimental investigation for the MR isolator damper. The investigation showed that the elliptic shape of the ordinary viscous damper in Figure 3(b) will tend to rotate clockwise when decreasing the MR fluid stiffness, by changing its excitation current. The damper hydraulic oil under study will follow the previous concept of the effect of fluid stiffness on generating the Force-Velocity graph.

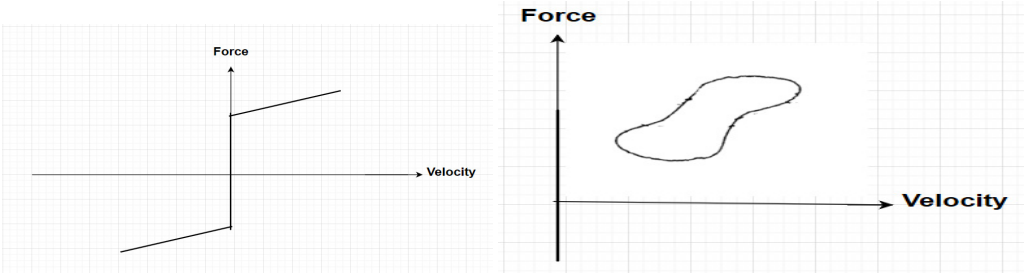

(a) (b)

Figure 3: Force Vs Velocity of the viscous damper, (a) Non-Hysteresis (b) Hysteresis

In order to evaluate the damping coefficient of the modified fluid damper, different excitation frequencies were selected at the signal generator, starting from 1Hz to 10 Hz. At the lowest frequency, the damper will complete its extension and compression stroke with the full designed stinger/shaker stroke length. The results of the acceleration conducted from the sensor were numerically integrated, using MATLAB, to evaluate the corresponding velocity values. Figure 4 depicts the variation of force with respect to speed variation when the excitation frequency is 1 Hz. One can see that the behavior of the damper is nonlinear, although the stroke length is too small (2cm).

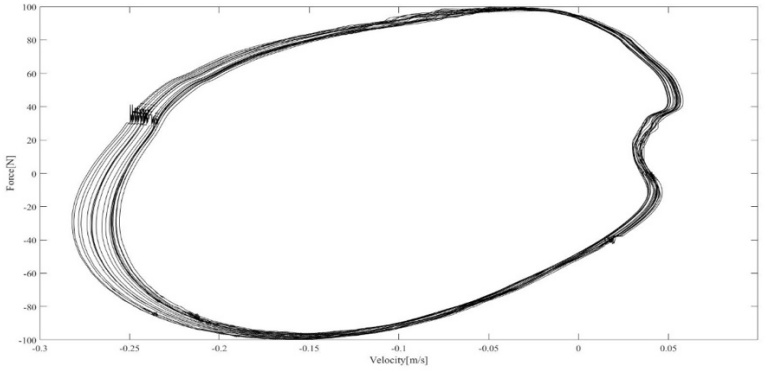

Figure 4: Force Vs Velocity of the piston rod at 1 Hz excitation frequency

The hydraulic oil stiffness is lower than the ordinary viscous damper oil. The low stiffness value tends to rotate the Force-Velocity graph clockwise with a small angle. The enveloped shape that described the extension and extraction process of the viscous damper piston is due to the hysteresis effect as illustrated above in Figure 4. The relation between the damping force and the motion velocity is usually represented by a linear equation, in the form of:

$$F = C\,V \tag{1}$$

where F is the driving force, V is the moving velocity of the rod, and C is the damping coefficient.

Due to the nonlinear behaviour of the system, the calculation of the damping value C, for each frequency, required a linear interpolation for the force-velocity graph data. After conducting such a procedure, the different values of C are shown in the following Table 2.

Table 2: Excitation frequency and damping coefficient values

Frequency (Hz)	**Damping Coefficient C (N.s/m)**
1	220
3	290
5	290
8	530
10	1100

One can see that the damping value, which represents the overall interaction between the oil rheological properties and the damper internal design, is heavily dependent on the excitation frequency. At the range between 1 and 6 Hz, the damping value is quasi-stable. However, starting from 7Hz, the amount of damping increases significantly, as shown in Figure 5.

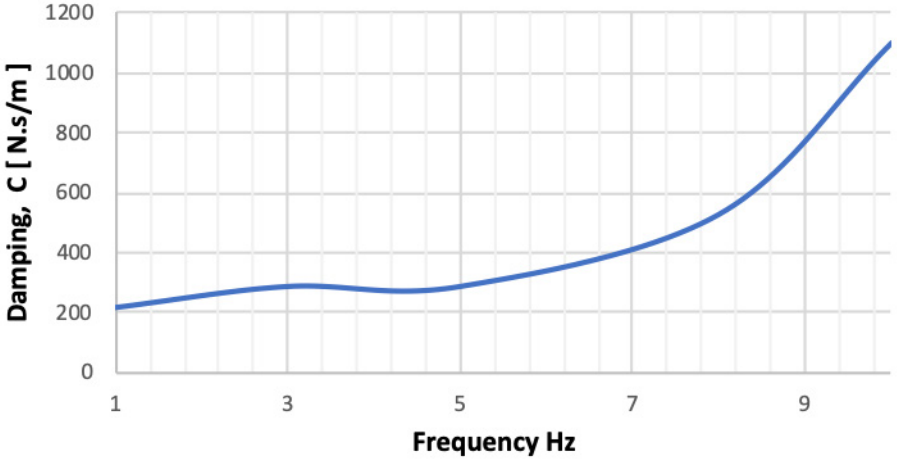

Figure 5: Damping coefficient vs excitation frequency

4 CONCLUSION

This research paper investigates the performance of a modified viscous damper excited by a sinusoidal force. The excitation frequencies were varied from 1 to 10Hz while the force magnitude was kept constant at 440 N. The experimental investigation led to the following conclusions:

1. Contrarily to what is commonly admitted, the damping coefficient is not constant. Indeed, the passage of the oil, the main cause for damping, through the piston head

annular holes is a complex phenomenon that depends not only on the hole geometry but also on the type of oil (mainly its viscosity) and its flow across the piston holes.

2. The damping coefficient was found to be quasi-constant over a frequency range between 1 and 6 Hz. Beyond that limit, a considerable increase is observed.

REFERENCES

Agrawal, A. K. & Amjadian, M. (2015). In Innovative Bridge Design Handbook, chapter 20, Elsevier, The City College of the City University of New York.

Brigley, M., Choi, Y. T., Wereley, N. M. & Choi, S. B. (2007). Magnetorheological isolators using multiple fluid modes. *Journal of Intelligent Material Systems and Structures*, *18*(12), 1143-1148.

Iglesias, G. R., Ahualli, S., Echávarri Otero, J., Fernández Ruiz-Morón, L. & Durán, J. D. G. (2014). Theoretical and experimental evaluation of the flow behavior of a magnetorheological damper using an extremely bimodal magnetic fluid. *Smart Materials and Structures*, *23*(8).

Kaewunruen, S. & Remennikov, A. M. (2008). New Research on Acoustics, chapter 5*,* Nova Science Publisher, New York.

Kemp, S. P. & Linden, J. L. (1990). *Physical and chemical properties of a typical automatic transmission fluid*. SAE Technical Papers.

Li, K. & Darby, A. P. (2006). An experimental investigation into the use of a buffered impact damper. *Journal of Sound and Vibration*, *291*(3-5).

Rådeström, S., Ülker-Kaustell, M., Andersson, A., Tell, V. & Karoumi, R. (2017). Application of fluid viscous dampers to mitigate vibrations of high-speed railway bridges. *International Journal of Rail Transportation*, *5*(1), 47-62.

Cite this article as: Badri Y., Hussein M., Sassi S., Renno J., "Investigation of the Effect of the Force-Frequency on the Behaviour of a New Viscous Damper for Railway Applications", *International Conference on Civil Infrastructure and Construction (CIC 2020)*, Doha, Qatar, 2-5 February 2020, DOI: https://doi.org/10.29117/cic.2020.0086

Influence of Fines on the Compressibility of Surface Sands in Kuwait

Shaikha A. N. AlAbdulmuhsen
engshaikhaa@hotmail.com
University College London, London, UK

ABSTRACT

Influence of fines on the strength and compressibility of compacted fill soil is very important in determining its behavior under applied loads. In Kuwait, fill soil is usually backfilled from excavated surface soils that consists of windblown dune sand with fines content usually varying from 5% to 15% with an average of 10%. However, it exceeds the upper range at some sites. This sand is used as backfill in compacted layers around foundations and below ground slabs. This paper investigates the influence of fines on the compressibility of surface sands. Laboratory consolidation tests were carried out on two types of sand samples with different fines contents to determine the compressibility parameters that included the compression index (C_c), the swell index (C_s), and the coefficient of consolidation (C_v). The influence of relative compaction on the compressibility parameters of both sands was also examined. Results indicated that the compression index (C_c) values decreased from 0.082 to 0.016 for sands with 7.3%, and from 0.089 to 0.016 for sands with 14.6 % fines, when the relative compaction increased from 80 to 100%. The swell index Cs also decreased with increasing relative compaction for both sands. Moreover, with increasing fines, the compressibility increased as demonstrated by the larger values of Cc at all degrees of relative compaction except at 100% and that the coefficient of consolidation Cv decreased with increasing fines, which means that as the fines increase the time required to achieve a certain degree of consolidation will also increase.

Keywords: Compressibility; Fines; Compression index; Swell index; Coefficient of consolidation

1 INTRODUCTION

Generally, natural sands consists of fines and sands in different proportions. The fines content affects the engineering properties of sands. The soil profile in Kuwait consists of a surface layer of windblown dune sand underlain by cemented sands (Ismael, 1985). It varies in thickness from 0 to 7 m and consists of fine or fine to medium sands with some fines (Ismael et al., 1987). The fines are calcareous and softer in nature. The percent of fines usually varies from 5% to 15% with an average of 10%. However, it exceeds the upper range at some sites. This sand is used as backfill in compacted layers around foundations and below ground slabs. The influence of fines on the strength and compressibility of surface sands compacted to different relative compaction (Rc) is very important in determining its behavior under applied loads (Ismael, 2006). The fines may also affect the compressional characteristics of coarse-grained soils (Çabalar, 2008). Further, compressibility characteristics deliver essential information of soil behavior. There are only few studies that have reported on the behavior of granular sandy and/or

clayey soil with different fines contents.

Kim et al. (2005) performed a series of triaxial compression tests on soil mixed with various silt contents, and the results showed that the critical state friction decreased with the increase in fine aggregate content. Phan et al. (2016) investigated the effects of fines content on the engineering properties of sand - fines mixtures based on laboratory tests. They reported that as the fines content increased, all parameters of deviator stress, volumetric strain, shear stress, internal friction angle, and cohesion increased. Moreover, as the fines content increased, soil type with constant void ratio also showed degradation in the cohesion, internal friction angle, and critical state in the consolidated undrained shear test.

In this study, laboratory consolidation tests were carried out on samples of sand with two different fines content to determine the compressibility parameters. These include the Compression Index (Cc), the Swell Index (Cs), and the Coefficient of Consolidation (Cv). Consolidation tests were performed on samples compacted to different relative compaction specified from the modified proctor compaction test. The influence of relative compaction on the compressibility parameters of both sands was also examined.

2 METHODOLOGY

The natural sand used in the tests was collected from the surface of a selected test site in AI-Rai area in Kuwait city, where the fines content is almost 15%. Bulk soil samples collected from excavated test pits were taken to the laboratory at Kuwait University for analysis and testing. The basic properties of the remolded soil sample were determined by conducting sieve analysis, consistency tests and compaction tests in the laboratory. Sieve analysis indicated that the percentage of fines in the soil was 14.63%, which is approximately the maximum value of fines usually encountered for surface sand in Kuwait city (Ismael et a1., 1986). The fines are calcareous and softer in nature. Another soil sample was prepared by washing some part of original soil through sieve # 200, and then adding the isolated fines based on weight calculations, so as to make the percentage of fines in the soil to be 7.3% (50% of 14.63). For example, for every 92.7 kg of soil particles that remain in sieve # 200, 7.3 kg of fines were added. Figure 1 shows the grain size distribution for sand with 14.63% fines and sand with 7.3% fines.

After the sieve analysis tests, samples from both sets of soils were tested to determine the Atterberg limits (liquid and plastic limit), specific gravity, optimum water content and maximum dry density. The liquid limit and plastic limit for the sand with 14.63% fines was found to be 23 and 18, respectively. The sand with 7.3% fines is considered as non-plastic. According to the Unified Soil Classification System (ASTM 0-2487), the soil with 14.63% fines is classified as silty clayey sand (SC-SM), and the soil with 7.3% fines is classified as poorly graded sand with silt (SP-SM). In addition, the specific gravity for the sand with 14.63% fines was 2.61 and for the sand with 7.3% fines was 2.645.

The Modified Proctor Compaction test (ASTM D-1557) was conducted on samples of both sets of soils to determine the max dry density ($\gamma_{d\ max}$) and optimum water content (w_{opt}). In order to determine the consolidation parameters, five one-dimensional consolidation tests were conducted on soil samples with different degrees of relative compaction, for each set of soils. The laboratory consolidation tests were carried out

according to ASTM D-243, on the compacted soil samples with 14.63% fines at 80%, 85%, 90%, 95% and 100% relative compaction at moisture contents corresponding to the wet side of the optimum water content. These tests were repeated on samples with 7.3% fines.

3 RESULTS AND DISCUSSION

Figure 2 shows the compaction curves for sands with 14.63% and 7.3% fines. For the sand with 14.63% fines, the maximum dry unit weight was found to be 2033 kg/m^3 and the optimum water content was 9.4%. The corresponding values for the sand with 7.3% fines were 1954 kg/m^3 and 9.8%, respectively.

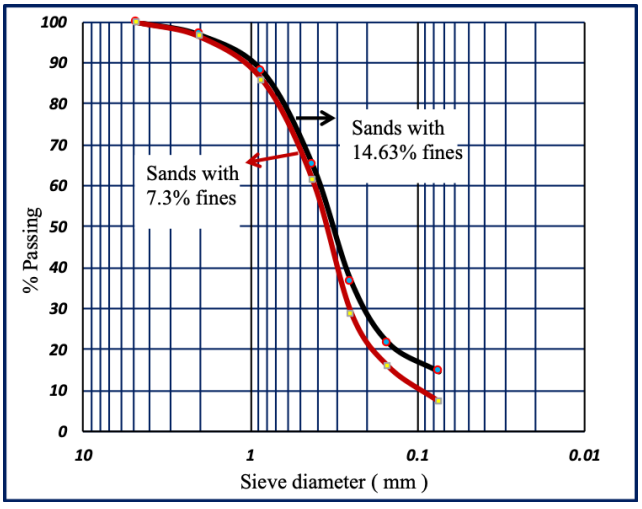

Figure 1: Grain Size Distribution curves for the test samples

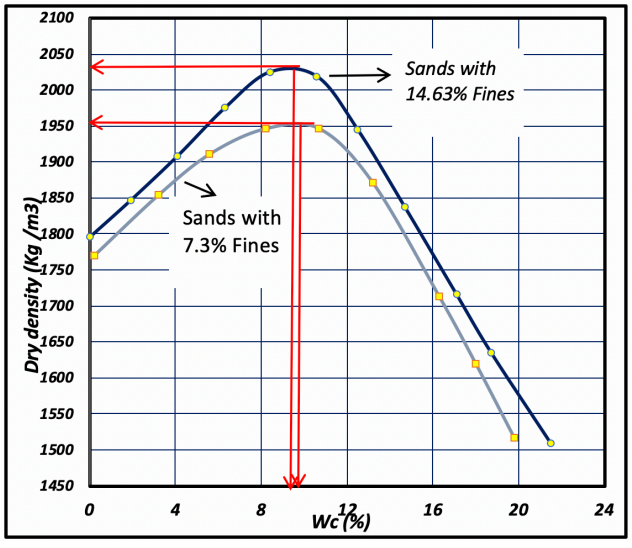

Figure 2: Compaction curves for the soil samples

Table 1 shows a summary of the consolidation test results and Table 2 shows the variation of the coefficient of consolidation with the applied pressure increment for the different relative compaction values. Figure 3 shows comparison between the Compression Index (C_C) and Swelling Index (C_S) with increasing relative compaction. The average Coefficient of Consolidation (C_v) values with respect to relative compaction for the soils with 7.3% and 14.6% fines, are plotted in Figure 4. Figures 5 and 6 show the e-log σ' curves at different relative compaction for sands with 7.3% fines and 14.6% fines, respectively.

Table 1: Summary of the consolidation test results

Relative Compaction (Rc %)	Water Content Wc (%)		Initial Void Ratio (e_{0})		Dry Density $\gamma_{d\text{-}max}$ (kg/m^3)		Compression Index (Cc)		Swelling Index (Cs)		Avg . Cv (mm^2 / min)	
	Sands with 7.3% fines	Sands with 14.6% fines	Sands with 7.3% fines	Sands with 14.6% fines	Sands with 7.3% fines	Sands with 14.6% fines	Sands with 7.3% fines	Sands with 14.6% fines	Sands with 7.3% fines	Sands with 14.6% fines	Sands with 7.3% fines	Sands with 14.6% fines
80	19	18.85	0.702	0.642	1563.2	1626.4	0.082	0.089	0.008	0.009	670.0	667.3
85	17.3	16.75	0.601	0.545	1660.9	1728.1	0.043	0.068	0.009	0.008	679.6	672.5
90	15.4	14.8	0.513	0.459	1758.6	1829.7	0.023	0.035	0.008	0.008	689.8	674.6
95	13.5	12.75	0.433	0.383	1856.3	1931.4	0.018	0.023	0.007	0.007	692.0	690.5
100	9.8	9.4	0.361	0.313	1954.0	2033.0	0.016	0.016	0.007	0.006	694.6	695.1

Table 2: Variation of coefficient of consolidation with applied pressure

Rc %	**80%**		**85%**		**90%**		**95%**		**100%**	
Pressure **(kpa)**	Sands with 7.3% fines	Sands with 14.6% fines	Sands with 7.3% fines	Sands with 14.6% fines	Sands with 7.3% fines	Sands with 14.6% fines	Sands with 7.3% fines	Sands with 14.6% fines	Sands with 7.3% fines	Sands with 14.6% fines
6	700.4	700	699.4	700.5	701.6	688	701	546.5	702.44	703
12	697.3	695.6	695.5	696.6	699.4	686	699	688.2	701.5	702
25	690	682.8	689.5	689.1	696	683	696.4	731.2	699.4	700
50	678	661.6	682.3	678.9	690	678	652.8	737.4	696.2	697
100	662	640	673.9	665	686.9	671.5	732	687.3	692.3	693
200	644	656.7	664.5	648	680.6	663	684	680.5	687.8	688
400	623.4	634.6	652.2	629.7	674.4	652.5	678.5	762.7	682.7	683

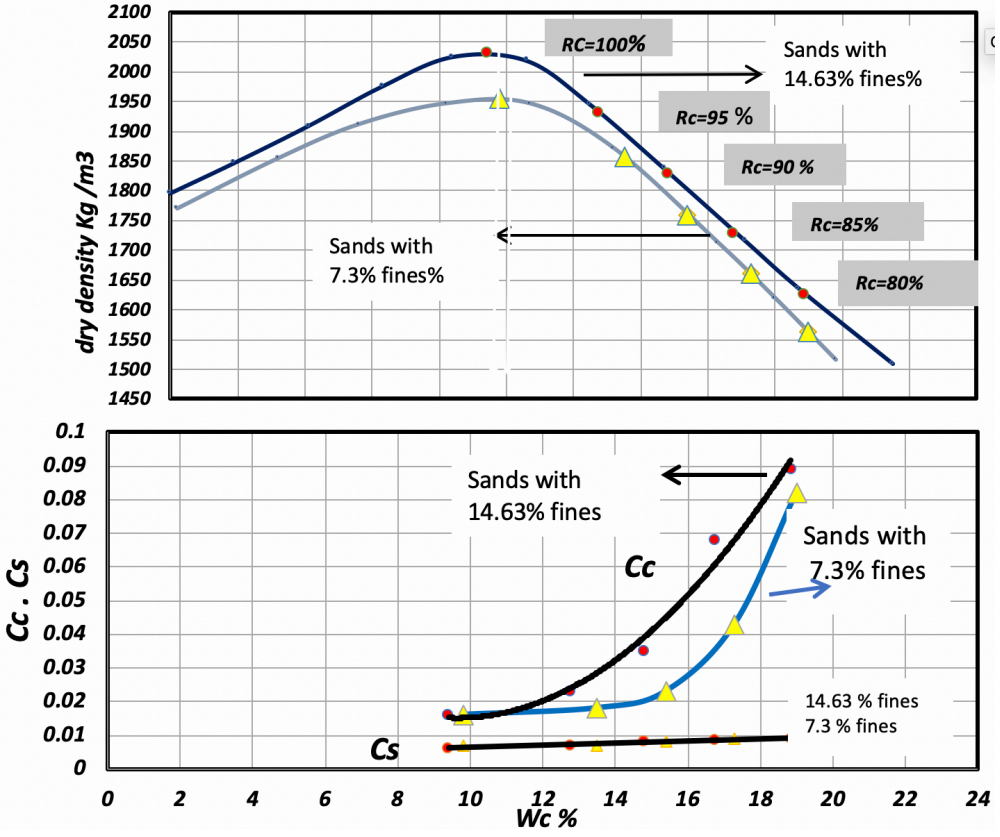

Figure 3: Comparison between the Compression Index (Cc) and Swelling Index (Cs) values

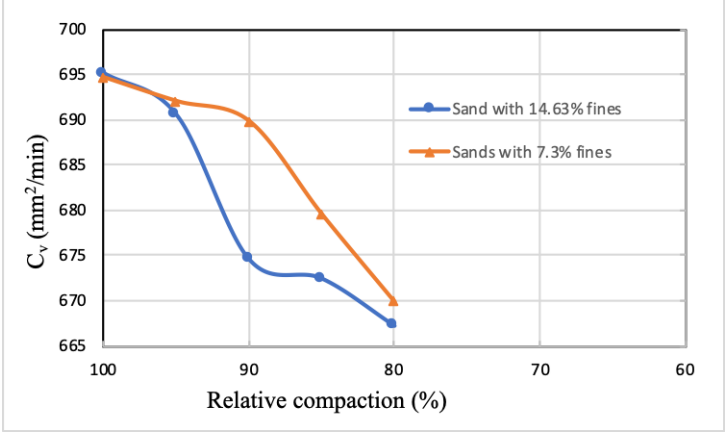

Figure 4: Variation of Coefficient of Consolidation (C_V) with the relative compaction

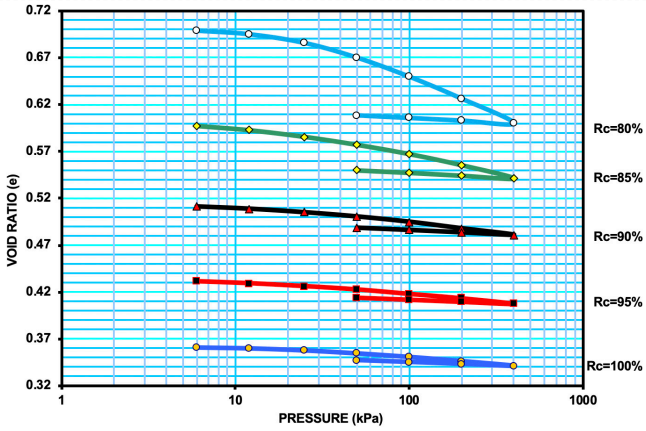

Figure 5: e-log σ' curves at different relative compaction for sand with 7.3 % fines

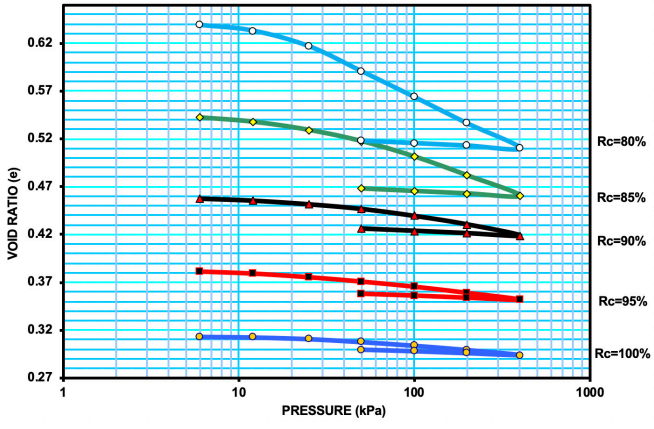

Figure 6: e-log σ' curves at different relative compaction for sand with 14.63 % fines

As represented in Table1, for both sets of soil samples (with 14.63% fines and 7.3% fines) the Compression Index (Cc) decreased sharply as the relative compaction increased from 80% to 90%, and decreased at a slower rate as the relative compaction increased from 90% to 100%. This decrease in compression index values indicates that the compressibility decreased and stiffness increased as the relative compaction increased. The ratio of C_c at 90% to Cc at 80% is 0.28 and the ratio of Cc at 100% to Cc at 90% is 0.69 for the test soil with 7.3% fines. Similar observations were made for the samples with 14.6% fines. The Swelling Index (Cs) decreased slightly as the relative compaction increased as shown in Table 1 and Figure 4.

A summary of the pre-consolidation pressure values σ_c as determined at different relative compaction values is given in Table 3. From Table 3 it is clear that σ_c remained nearly the same except at 80% relative compaction for the sand with 14.6% fines where a significant decrease occurred.

Table 3: Variation of pre-consolidation pressure with relative compaction

Relative Compaction (Rc %)	Pre-Consolidation Pressure, σ_c' (kPa)	
	Sands with 7.3% fines	Sands with 14.6 % fines
80%	40	27
85%	45	48
90%	42	50
95%	43	43
100%	38	45

The above results show the important effect of fines on compressibility. As the fines increase the compression index increases at all values of relative compaction except at the 100% value. A possible explanation is that the decrease with low void ratio makes the effect of increased fines within the range of this project insignificant. Increased compressibility leads to larger settlement under the applied loads as the settlement is directly proportional to C_c.

Looking at the coefficient of consolidation C_v, it is evident from Figure 5 that C_v is lower with increased fines content at all relative compaction except 100%. It is known that for a given degree of consolidation, the time is inversely proportional to the coefficient of consolidation. Thus, it is clear that with lower values of C_v with higher fines, the time required to achieve a given degree of consolidation will be longer due to the lower permeability and the plastic nature of the soil containing larger fines content. As indicated in Figures 6 & 7, the void ratio also decreased with increase in relative compaction.

4 CONCLUSION AND RECOMMENDATION

A laboratory-testing program consisting of compaction and consolidation tests was carried out on two sets of sands with fines content of 14.7% and 7.3%. The following conclusion were made based on the laboratory test results:

i. For both sands, compressibility decreased as the relative compaction increased from 80% to 100%. The Compression Index Cc and the Swell Index Cs decreased with increasing relative compaction.
ii. The Compression Index (Cc) values decreased from 0.082 to 0.016 for sands with 7.3%, and from 0.089 to 0.016 for sands with 14.6 % fines, when the relative compaction increased from 80 to 100%.
iii. The average Coefficient of Consolidation (Cv) increased from 670 to 695 mm^2/min for both types of sands with increasing Relative Compaction (Rc).
iv. With increasing fines, the compressibility increased as demonstrated by the larger values of C_c at all degrees of relative compaction except at 100%.
v. The Coefficient of Consolidation C_v decreased with increasing fines. This indicates that as the fines increase the time required to achieve a certain degree of consolidation will also increase.

It is recommended to carry out the same tests on soils with fines content up to 30% to confirm the findings of this study.

REFERENCES

Çabalar, A. F. (2008). Effect of fines content on the behavior of mixed samples of a sand. *The Electronic Journal of Geotechnical Engineering*, Volume 13D. Available on line at: http://ejge.com/2008/Ppr0835.pdf.

Ismael, N. F. (1985). Allowable pressure from loading tests on Kuwaiti soils. *Canadian Geotechnical Journal*, *22* (2): 151-157.

Ismael, N. F. (2006). Influence of fines on the properties of arid climate sand deposits, *proceedings of the 4th international conference on unsaturated soils, Conference*. Arizona, USA. April 2-6.

Ismael, N. F., Al-Khalidi, O. & Mollah, M. A. (1987). Saturation effects on calcareous desert sands. Transportation Research Record, 1089 pp.

Ismael, N. F., Jeragh, A. M., Mollah, M. A. & Al-Khalidi, O. (1986). A study of the properties of surface soils in Kuwait, *Journal of the Southeast Asian Geotechnical society*, Bangkok, Thailand, *17*(1): 67-87.

Kim, D., Sagong, M. & Lee, Y. (2005). Effects of fine aggregate content on the mechanical properties of the compacted decomposed granitic soils. *Construction and Building Materials*, *19*(3):189 -196.

Phan, V. T. A., Hsiao, D. H. & Nguyen, T. L. (2016). Effects of fines contents on engineering properties of sand-fines mixtures. *Sustainable Development of Civil, Urban & Transportation Engineering Conference*. Procedia Engineering, 142:212-219. Elsevier Ltd.

Cite this article as: AlAbdulmuhsen S. A. N., "Influence of Fines on the Compressibility of Surface Sands in Kuwait", *International Conference on Civil Infrastructure and Construction (CIC 2020)*, Doha, Qatar, 2-5 February 2020, DOI: https://doi.org/10.29117/cic.2020.0087

Box Jacking/Pushing Method for Tunnel Construction in Rock: Doha Metro, Gold Line Project

Spyridon Konstantis
skonstantis@qr.com.qa
Qatar Rail, Doha, Qatar

Spyros Massinas
smassinas@goldlinemetro.qa
ALYSJ JV, Doha, Qatar

ABSTRACT

The case of a box pushing tunneling method in rock, on Doha Metro Gold Line project, successfully implemented to connect multiple entrance structures of Sport City station under a live traffic junction, in a heavy urban environment and under very shallow overburden is presented. Due to the size of the underpasses, the need to maintain uninterrupted traffic and the time-consuming utility diversions and reinstatement, the use of conventional NATM and Cut and Cover methods were assessed as either non-feasible or of high risk. The dimensions of the unsupported span, the encountered geotechnical conditions, the development of the settlements at road level and the box advance rate are presented.

Keywords: Tunnel; Box pushing; Rock; Ram forces; Advance rate

1 INTRODUCTION

The Doha Metro Gold Line Underground project is part of the rail network developed for the State of Qatar and was commissioned on 21 November 2019. The line crosses the center of Doha (see Figure 1) and includes 11 underground stations (Msheireb interchange station is constructed by others), underground stabling facilities, approximately 15 km of 7.1 m diameter twin tunnels excavated with 6 EPB TBMs and 24 cross passages. The project was awarded to ALYSJ Joint Venture, formed by Aktor of Greece, Larsen & Toubro of India, Yapi Merkezi & STFA of Turkey and Al Jaber Engineering of Qatar. Sport City station, one of the major Gold Line stations, is located next to a major highway junction along Al Waab Street and in close proximity to the Khalifa Stadium. It has been designed and constructed as an event station to serve major athletic events and thus cater for the increased ridership. The configuration of the station required pedestrian access to be provided to the station via subways passing under each of these roads and hence the construction of three pedestrian underpasses serving the three quadrants of the junction (see Figure 2).

The subway dimensions were selected to cater for the peak pedestrian traffic flows expected during sporting events and allow the installation of travellators and Mechanical, Electrical and Plumbing (MEP) equipment. The required internal dimensions and lengths of the subways were, Subway 1: 13.1m width, 7.9m height and 80m length, and Subways 2 & 3: 7.9m width, 6.9m height and 50m length each.

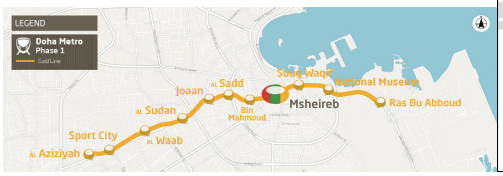

Figure 1: Gold Line overview map

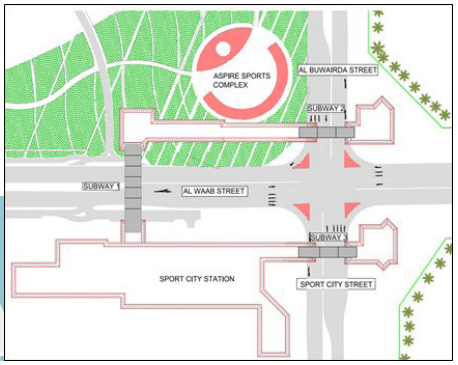

Figure 2: Sport City station configuration

1.1 Geology

The geological model of the area was developed based on ground investigation boreholes. The profile consisted of made ground and residual soil deposits to a maximum depth of 2.6 to 3 m (locally in areas of existing utilities the depth was up to 4m), followed by the upper Dammam formation and the Midra Shale below the base of the subways. The Dammam formation consists of the Simsima limestone which can be met on site in different weathering conditions (from slight to moderate - extremely weak to very weak and moderately strong, light yellowish brown to greyish brown, dolomitic Limestone with pockets of silt/clay). The subways were constructed inside the moderate weathered Simsima limestone having a Young's modulus of 1GPa and a GSI range from 45 to 55. Figure 3 presents the geological profile along subway 1. The overburden height in Subway 1 varied from 3.5m to maximum 5m, while under Al Waab street the mean overburden height was only 4m. In Subway 2 the overburden height was 6m and in Subway 3 it varied from 4m to 6m.

1.2 Existing utilities

Existing services were identified above the subways and within the zone of influence of the works, including TSE, foul sewer and potable water pipes, either INR, ductile iron or HDPE, ranging in diameter from 300 to 800mm (see Figure 4). The identified utilities were documented, assessed for adverse impact, continuously monitored and protected when deemed necessary. In one case, a steel utility bridge was constructed to support a pipe, transversely crossing the underpass.

1.3 Original design

As per the original design proposed by the Contractor, the cut and cover construction method was to be adopted for each of the subways, which however inevitably involved implementation of temporary traffic management schemes, lanes closures and diversions. Due to the close proximity of the station to the highway junction, a preliminary traffic impact assessment report indicated that this would lead to significant traffic disruptions not only at the Sport City junction but also in the surrounding areas and in part due to other concurrent construction activities across the city. That would lead to non-compliance with the contractual requirement to 'KEEP DOHA MOVING' (Qatar Railways Company, Employers Requirements) and hence, alternative solutions were sought and considered

to avoid traffic disruptions and public nuisance and disturbance. The first construction method considered was the mined tunnel construction with conventional method (SCL/SEM/NATM), however this was excluded as an option due to geometrical constraints arising from the large size of the subways and the limited available ground cover (very low overburden height) of soil type formations. From a geological and geotechnical perspective, the underpasses would be excavated and constructed inside weathered and relatively weak limestone rock overlaid by made ground.

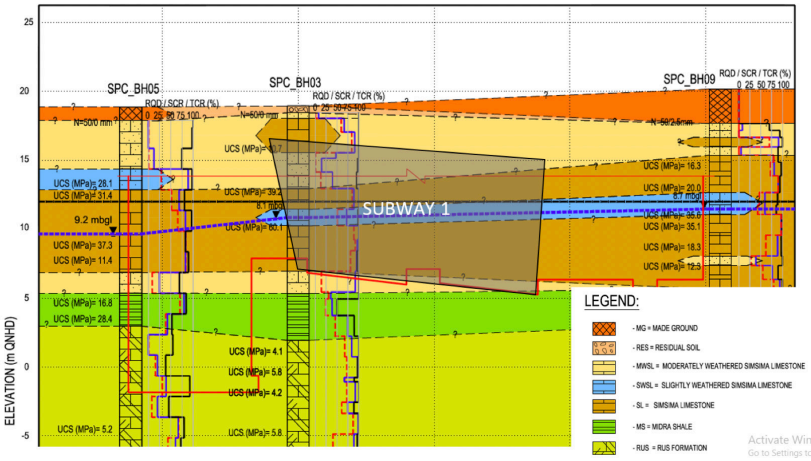

Figure 3: Geological profile along subway 1

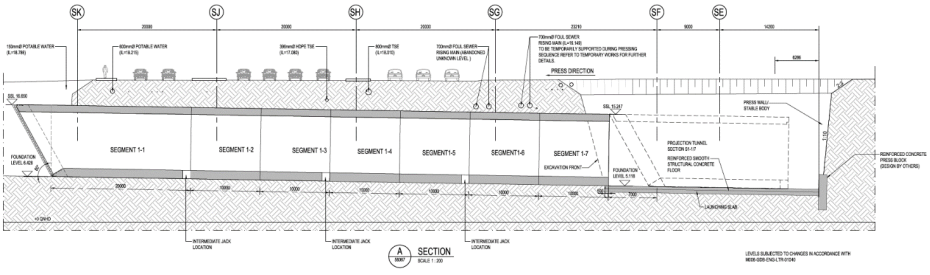

Figure 4: Longitudinal section of Subway 1 with utilities location

Design and construction related issues aside, a major constraint and decisive factor was also the very tight construction schedule with limited available activities duration and float. Following a rigorous comparative risk assessment, the box jacking/pushing method was selected for the three subways passing below the highways (see Figure 2), which was awarded by the Contractor to a specialist subcontractor, Petrucco of Italy. Most if not all of the recorded box jacking/pushing cases are in soil formation and therefore the prevailing ground conditions (weak rock) in Sport City resulted in a unique construction method (excavate and push rather than push inside the ground and excavate inside the box), a first in the Middle East region, and as per authors' knowledge unique worldwide. In the following, the design scheme and construction sequence is presented, together with detailed design inputs for the jacking loads, settlement analysis, ground

stability and structural analysis. In addition, the challenges faced during construction are also presented, including settlement protection of utilities, effects of over excavation and lessons learnt. The subways were successfully constructed between 2016 and 2017 with no disruption to traffic.

2 DESIGN SCHEME AND GENERAL CONSTRUCTION SEQUENCE

The three jack box tunnels, consisting of a number of precast reinforced concrete segments, were constructed in launch pits positioned in such a way that they were laid either along the alignment of the pedestrian walkway or were located within the subway entrance profile. This allowed the excavation space to be re-used and reduced the construction programme. During construction of the jack box subways, several segments were under construction simultaneously to reduce the total construction time. The segments were constructed sequentially and once completed, they were laterally jacked to the excavation face from where they were jacked into their final position (see Figure 5).

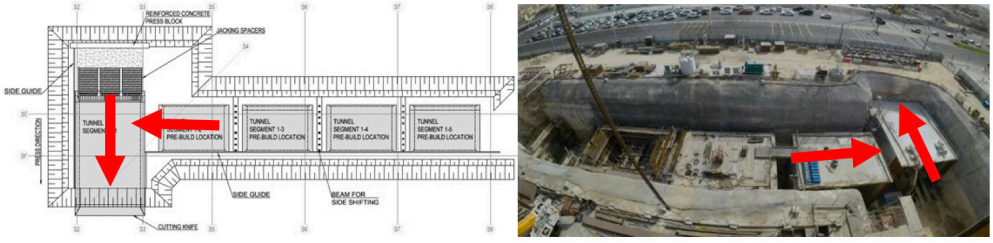

Figure 5: Subway 1 construction: Segments layout drawing and Box jacking sequence (left) and aerial photo (right)

A summary of the construction sequence is as follows; 1) Excavate the launch pit to formation level and cast smooth concrete slab; 2) Cast first segment, reaction block and jack installations; 3) Excavate front face, lay sand on the base, shotcrete for any over excavation, and begin pushing sequence. Install ground beams as required to control alignment. Excavation was limited to 500mm advancement length under the existing utilities in close vicinity with the box roof (until the segment overcame the full width of the utility pipes trenches). For more competent rock (see Figure 6) the excavation length increased up to 1m and even to 2m. Over excavation was limited up to 20mm when underpassing critical utilities, while above 50mm, shotcrete was applied before jacking. The face was excavated in phases before the next push, i.e. first the left and right parts and then the middle part which acted as a buttress (see Figure 7). Above steps were repeated; 4) Concurrent with first segment pushing, next segments were cast in the launch pit (see Figure 5); 5) Dismantle the jack array and slide laterally the next segment into position; 6) Reassemble the jacking array and begin the pushing sequence again. Steps were repeated until all segments were in the final position; 7) Cast box segment stich details; 8) Connect jack box subways to cut and cover station box and entrance structures.

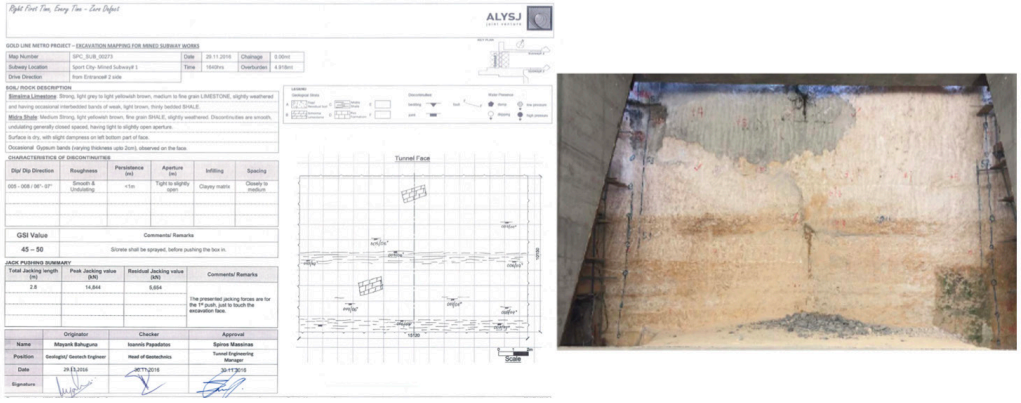

Figure 6: Example of Face Mapping on Subway 1 for good rock conditions at the face

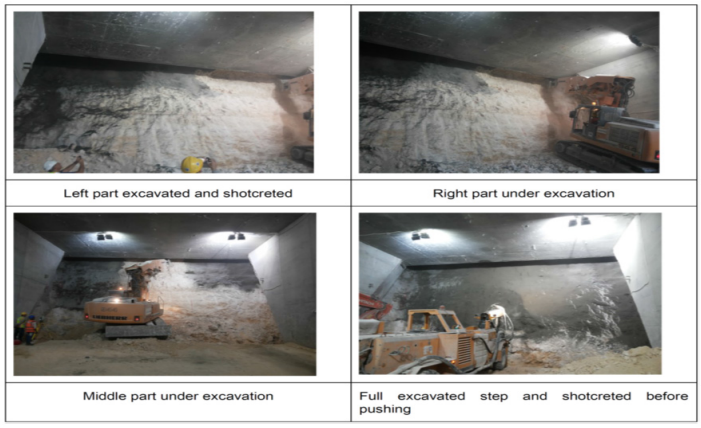

Figure 7: Excavation sequence with shotcrete application to control over-excavation

3 CONCRETE SEGMENTS DETAILS

A major risk associated with the box pushing method is the potential for the box segments to be "trapped" due to the friction between the segments and ground, resulting in major impacts for the construction programme. Several measures were adopted to reduce this risk. Firstly, intermediate jacks were located between the box segments to allow the segments to be pushed individually (intermediate jacking stations every 20m of underpass), reducing the loads and providing construction flexibility. The adjoining segments were also connected with 20mm thick steel plates anchored into the segment with shear studs that could slide freely to open and closed positions (see Figure 8). The steel plates acted to restrain the segments from becoming misaligned and in addition assisted to avoid the segments jack-knifing.

A protection shield (see Figure 9, left) all around the front part of the first segment was constructed. This shield was designed to reinforce the front part against any falling rocks and accidental damages during the excavation. The shield arrangement allowed the construction teams to reach the whole perimeter of the excavation using hammers or mills or use small hand-hammers to refine the excavation profile. It was also designed to be easily removable and allow the teams to reach the structural couplers that were

positioned underneath it without damaging or cracking the concrete structure.

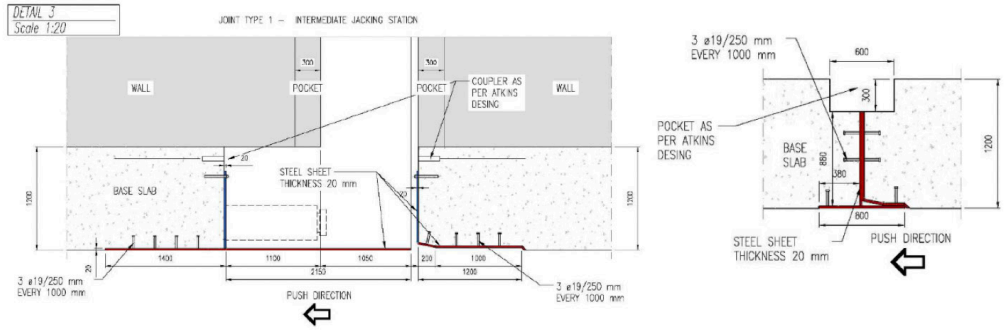

Figure 8: Detailed arrangement for intermediate (left) and non-intermediate (right) jacking station

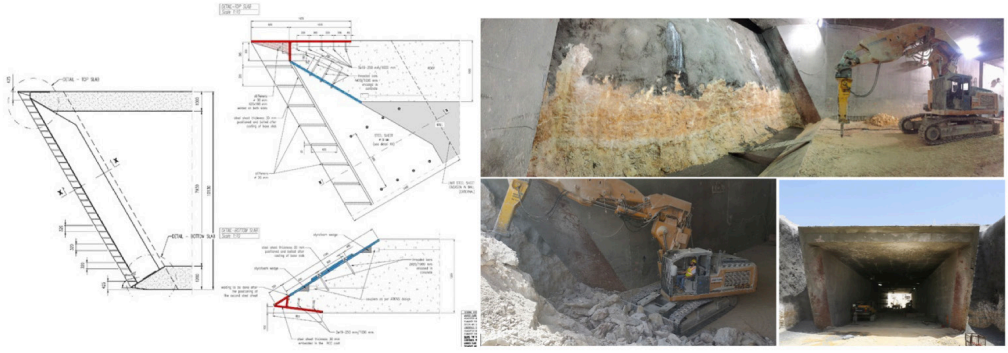

Figure 9: Detailed arrangement of front shield (left) and photographs during construction (right) (Inside subway 1, top; final breakthrough, bottom; protection shield is visible at the front part)

4 JACKING LOADS

In order to minimize or even eliminate the risk of the segments being 'jammed' during the pushing operations (which would have very adverse impact on the construction progress), it was considered necessary to be conservative with the determination of the maximum capacity for pushing the segments and hence ensure that there would be sufficient jacking force with available safety margin. This was achieved by calculating the maximum jacking forces based on the frictional resistance of the ground applied to the roof, walls and base slab i.e. the total perimeter. Based on the experience presented by Petrucco, a coefficient of friction of 0.5 was adopted and applied. The front segment S1 was placed 3m away from the entry point into the ground in order to verify the adopted friction coefficient. The hydraulic jacks were grouped and housed together in steel cradles and positioned to apply loads only to the base slabs. Figure 10 presents the recorded forces of the jacking rams (main rams with counteraction on the reaction wall and intermediate rams between the segments every 20m). The 'saw' scheme of the recorded values is due to overcoming the friction before sliding of the segment in each jacking step.

5 DETAILED DESIGN OF THE CONCRETE SEGMENTS

The relatively high ground stiffness, compared to the more softer ground conditions where the jack box method is traditionally used, meant that the construction methodology and design would have to be modified. Firstly, it would not be possible to push the cutting knife of the first pushed segment into the ground during the pushing sequences. The excavation had therefore to take place in advance of the cutting knife and be larger than the box perimeter to facilitate the jack box pushing sequence. The over excavation could have adverse impact on the surface settlements and it was intended therefore to be limited. The proposed solution was to limit the advance excavation and to use shotcrete to fill any over excavations around the perimeter. This sequence of events required a design verification that the ground would be self-supporting and the magnitude of the surface settlements within acceptable limits. In addition and due to the use of shotcrete for over excavation limitation, additional design verifications had to be carried out for the worst case of shotcrete bonding to the box perimeter. A 3-D solid element soil-structure interaction Finite Element Model (FEM), incorporating all construction sequences, was adopted in the commercially available software LUSAS (see Figure 11, left). A shear strength reduction analysis was adopted to verify the factor of safety of the cutting face slope with a factor of safety of 1.25. The results of the analysis proved that a 300 to 500mm excavation advancement would provide adequate safety and limit settlements to within acceptable limits. For face stability, a 60 slope was recommended to be adopted, however it was also proven through the analysis that a 75 slope could also be safely adopted, to allow for construction tolerances and provide a safe minimum angle.

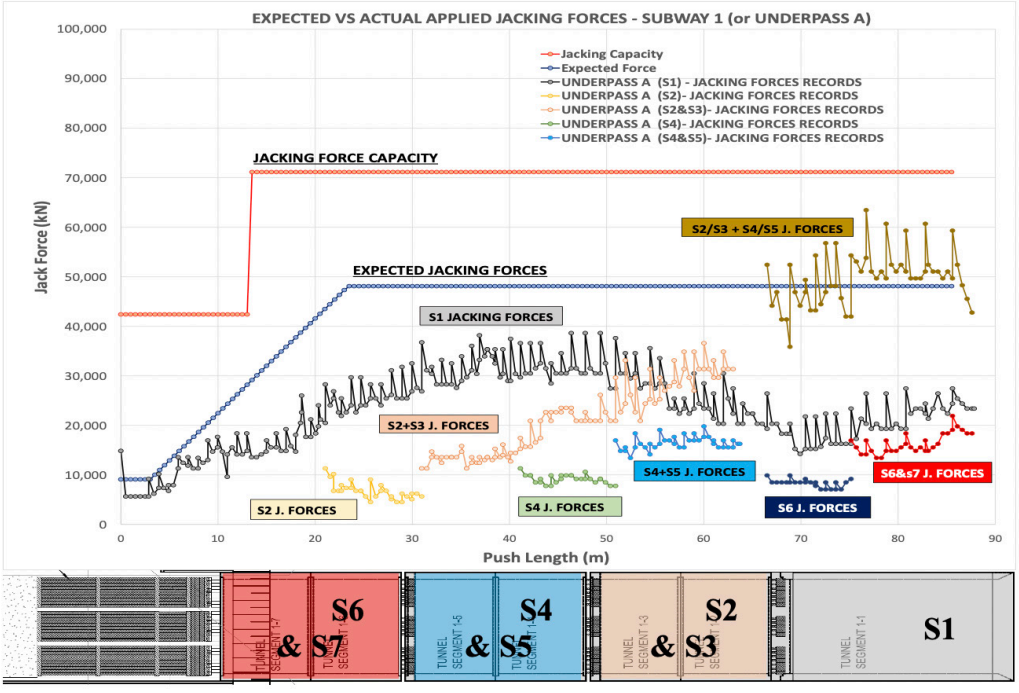

Figure 10: Hydraulic jacks – Designed vs Actual applied forces in each jacking station

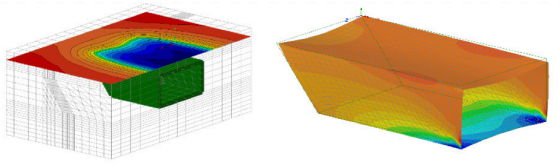

Figure 11: Soil-structure interaction model showing vertical displacement contours (left), and, 3D shell element model showing axial stresses induced by jacking loads (right)

A series of numerical analysis was carried out with a variety of geotechnical parameters to create an envelope of the stress state in the concrete segments. For example the case of no lateral ground loads due to over excavation has been examined. This load combination was critical for the design of the roof slab to limit the crack widths within contract's specifications. To cover the case with full lateral loads due to grouting through grout sockets embedded in the walls, roof and base slabs, another load combination with a K=0.9 was adopted. It is noted that contact grouting was applied in the perimeter only after the final breakthrough. To verify the global behavior of the box segments subjected to the maximum capacity of the jacks, a second 3-D model was built, adopting shell elements (see Figure 11, right). The loads were applied to the base slab and the frictional resistance to the perimeter of the model. Subsequent stress checks were made to ensure that the section did not exceed the allowable tensile capacity of the concrete and bursting reinforcement was added to each base slab (EN 1991-1-2004, Design of Concrete Structures). As mentioned above, additional design verifications were carried out for the worst case of shotcrete bonding to the box perimeter. The minimum concrete cover to reinforcement was 55mm as required for durability on the external face. An additional 30mm was provided as sacrificial concrete for abrasion based on previous experience, equating to a total cover of 85mm.

6 INSTRUMENTATION AND MONITORING (I&M)

Due to the criticality of the box pushing operations being continuously carried out under a busy carriageway and live utilities with limited overburden, a robust real-time instrumentation and monitoring regime was installed, comprising level points installed near utility trenches, extensometers and asphalt road points (see Figure 12, left).

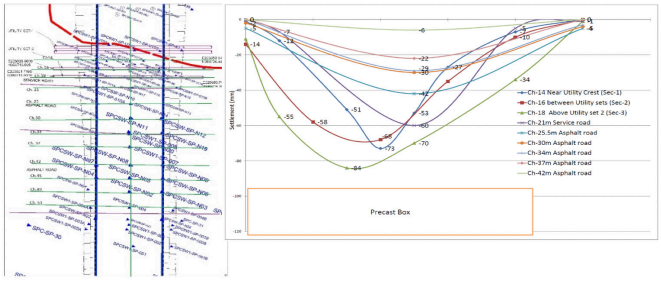

Figure 12: I&M Plan with settlement section lines (left) and measured surface settlements transverse to the box pushing operation (right) – subway 1

Prior to the commencement of the box pushing operations, it was identified through site surveys and determined from the analysis, that the first set of utilities to be encountered located below the service road (see Figure 4) would require appropriate protection as diversion was not an option due to schedule constraints. Further investigations and liaison with the utility owners, revealed that only one set of utilities was live and had to be protected. It was consequently decided to protect these live utilities and suspend them from a utility steel bridge, given also the poor compaction level of the trench backfill identified through site investigations. As foreseen and anticipated (see Figure 12, right and Figure 13), the backfill of these utilities trenches exhibited increased settlements - mainly attributed to the low rock cover in this area and possibly the dynamic compaction of the backfill during the hammer and roadheader excavation. However, no adverse impact was experienced by the live utilities protected by the steel bridge.

From the ground settlement results, it can be seen from the section lines above the asphalt road where the rock cover was in the order of 3-4 m (excluding the sections above the utilities and adjacent to these due to the proximity interaction) that the overlying rock exhibited a 'bridge' response with a remarkable deformation line similar to a loaded 'restrained beam'. In the very limited cases where ground deformations exceeded the allowable limits or caused damage to the surface areas and paved roads, those were reinstated by ALYSJ JV.

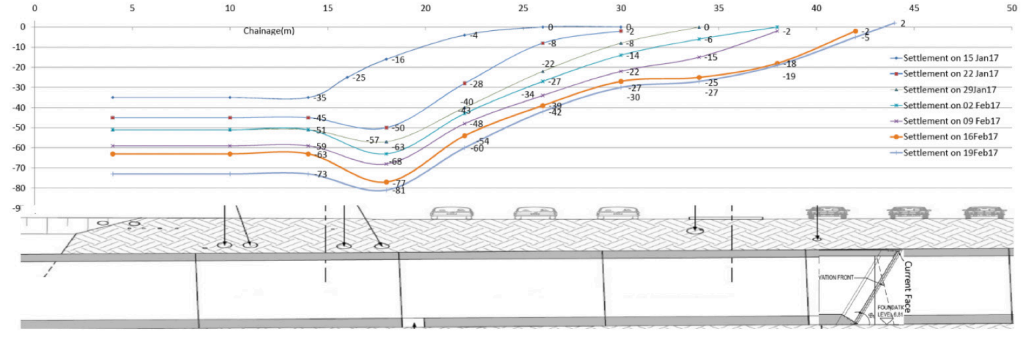

Figure 13: Measured surface settlements along subway 1

The over-excavation above the roof of the pre-cast boxes, was the main parameter for controlling the development and the magnitude of the surface settlements. The rock quality (moderate weathered Simsima limestone with Young's modulus stiffness of 1 GPa and GSI range of 45 to 55) proved competent with increased "stand up time" while the maximum actual over-excavation varied between 50mm and 100mm.

7 CONCLUSION

Despite the tight and challenging schedule constraints and the low cover, the box pushing operations were concluded successfully and the settlements and ground deformations were within the acceptable levels. It was remarkable to observe the behavior of the rock mass for the unsupported length. Through the application of the box pushing construction method, there was no disturbance and negative impact on the high traffic volume and the construction works were completed prior to the contractual milestone.

ACKNOWLEDGEMENTS

The authors would like to thank Qatar Rail and ALYSJ JV for their permission to publish this article.

REFERENCES

EN (1991-1-2004). Design of Concrete Structures.

Qatar Railways Company, Employers Requirements.

Cite this article as: Konstantis S., Massinas S., "Box Jacking/Pushing Method for Tunnel Construction in Rock: Doha Metro, Gold Line Project", *International Conference on Civil Infrastructure and Construction (CIC 2020)*, Doha, Qatar, 2-5 February 2020, DOI: https://doi.org/10.29117/cic.2020.0088

The Use of Measuring While Drilling and Wireline Logging to Identify the Geological Strata in Qatar

Anna Grace Gravador-Villamor
ag_gravador@yahoo.com
Fugro Peninsular Services Co., Doha, Qatar

Fay Pearce
f.pearce12@gmail.com
Fugro Peninsular Services Co., Doha, Qatar

ABSTRACT

In the field of engineering and construction in the Middle East, it is a common practice to economize a geotechnical investigation using a conventional scope, based on the lowest price. This tends to compromise the project integrity by either under- or over-designing the structure. However, a carefully considered ground investigation and engineering evaluation should be practiced in the early stages, to reduce the unknowns related to geology, ground strength and behavior, ultimately optimizing the geotechnical design, and project constructability and efficiency. This begs the question of whether 'cheap and conventional' can ever equate to 'quality' and what can be done to improve the geotechnical investigations. This paper focuses on ground investigations on rocks and presents the key advantages of utilizing instrumented drilling boreholes in combination with rotary coring boreholes, to collect accurate and good quality data on an accelerated schedule. The study identifies the bias of a conventional geotechnical investigation, highlighting how this can be reduced through the use of instrumented drilling and wireline logging, and how the data collected can define the typical trends observed in the Qatar stratigraphy through correlation from instrumented and rotary coring boreholes drilled in several locations across Qatar. The findings have significant implications on revolutionizing the current ground investigations in Qatar, providing a geotechnical investigation alternative that delivers more complete and high-quality data.

Keywords: Geotechnical investigation; Quality geotechnical data; Diagraphy drilling; Instrumented drilling; Wireline logging

1 INTRODUCTION

Due to the rockhead in Qatar being generally shallow, the key geotechnical investigation problems encountered are associated with rocks, and comprise the following: (a) efficient determination of the site stratigraphy / geology, (b) the degree of natural fracturing of rocks, (c) rock quality / strength, (d) groundwater and ground hydraulic conductivity, and (e) storage of samples. As there is a general tendency in Qatar for conventional geotechnical investigations, assumed to be applicable across all project sites, the above-mentioned key problems relate to traditional scoping that generally involves rotary coring through rocks. This investigation method is largely influenced by the driller's ability to maximize core recovery, and therefore depends on the geotechnical engineer to establish rock parameters based on biased and discrete laboratory testing.

This paper describes the use of diagraphy / instrumented drilling (monitoring while drilling, MWD) and wireline logging, and how the data collected from these geotechnical investigation methods can aid in: (a) defining the typical trends observed in the Qatar stratigraphy through correlation from instrumented and rotary coring boreholes drilled in several locations across Qatar, and (b) providing a geotechnical investigation alternative that delivers more complete and high quality data for rocks.

2 GEOTECHNICAL INVESTIGATIONS USING MWD AND WIRELINE LOGGING

2.1 MWD

MWD (BS EN ISO 22475-15, 2016; Measuring While Drilling) is the continuous monitoring of drilling parameters with time/depth, carried out using rotary open hole drilling techniques with fluid flush, and a purpose-built logging unit with a corresponding operating software package. MWD has input and output parameters recorded at every 1cm intervals that are characterized by speed and velocity: rotation speed and penetration speed; and those which are characterized by force: thrust on bit and torque. The rotation speed and thrust pressure is set at a constant rate, with the fine feed fully open, and hold-back pressure off, allowing for the monitoring of the rigs response to the geology and the identification of any free falls while drilling.

Various formulae are used to derive the interpreted parameters from the input and output parameters: (a) Exponential Method (E-Method), the ratio between the log value of velocity and log value of force, (b) Ease-to-drill (Bingham, 1965; Girard et al., 1986), the ratio between the velocity parameter and the force parameter, (c) specific energy (Teale, 1965), the amount of energy to excavate a cubic meter of material, (d) drilling resistance (Falconer et al., 1988; Girard et al., 1986), the correlation between values of strength and the drilling parameters.

The success rate of this method, relies heavily on the understanding of the method, acquisition tools (type of rig, type of bit, etc.), acquisition procedure, interpretation of the results, and the understanding and continuous collaboration between the driller/s, geotechnical engineer/s and/or engineering geologist/s.

2.2 Wireline logging

Wireline logging tools, namely Calliper (CAL) and Natural Gamma Ray (NGR), are recommended to be used with MWD. These tools are used after the borehole is completed to record the borehole diameter (CAL), and the natural radiation retained in the rock (NGR).

Calliper logging can be used to detect cavities and zones of fracturing, as well as the relative strength and homogeneity of the rock. NGR logging can be used to detect depths at which clay is present, and to distinguish the Midra Shale marker bed.

2.3 Stratigraphic Interpretation of Qatar

Through interpretation of the MWD and wireline logging results, and correlation with rotary cored boreholes, the geologist/engineer is able to: (a) to distinguish changes in rock formations, (b) to determine the strength parameters of the various rock layers, (c) to identify fractures, and (d) to identify cavities (Gui et al., 2002). The interpretation

is highly dependent on the engineer's / geologist's ability to understand the geology in which the investigation is taking place, and the ability to recognize the changes in the interpreted parameters with depth and how this corresponds to the changes in geology. This is why it is recommended to have coring boreholes in the investigation (the number is dependent on the number of MWD boreholes).

Data from 9 sites across Qatar (Figure 1) was allowed for the particular characteristics of the Qatar stratigraphy to be analyzed. In general, the Qatar geology follows the sequence of the Damman Formation (Simsima limestone (Umm Bab Member), Dukhan limestone and the Midra Shale formation), the Rus formation, and the Umm Er Radhuma formation. Spatial variations of the sequence are observed, with some units absent.

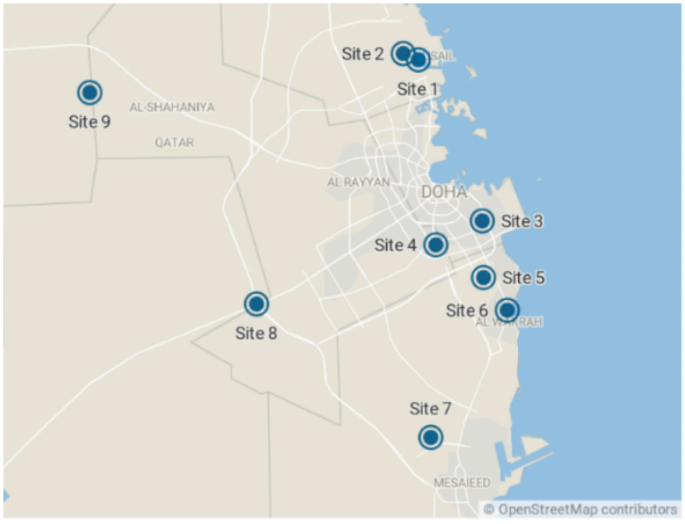

Figure 1: Project sites with MWD

2.3.1 Simsima limestone (Umm Bab formation)

The Simsima limestone is a highly heterogeneous rock both vertically and laterally over short distances. The formation tends to be separated into Weathered Simsima Limestone (WSL), Simsima Limestone (SL) and Basal Simsima Limestone (BSL). The characteristics of the Simsima limestone vary greatly, however through the use of MWD it is possible to discern the strength and stability of the rock. Figure 2 illustrates a sample interpretation of Simsima limestone (Umm Bab formation) geologies.

The WSL is typically moderately weak to strong, dolomitized and highly fractured limestone, and can be identified by the heterogeneous behavior in the ease-to-drill, specific energy, penetration speed and calliper readings. The specific energy and hard-to-drill can be high due to the strength of the dolomitic limestone. Increased penetration rates, ease-to-drill and torque identify the weaker siltstone/silt and/or claystone/clay layers. Due to the highly fractured nature of the WSL unit, there is usually low recovery of samples and hence, limited tests carried out and rock strength data available.

The SL can either be a competent massive limestone, exhibited by very uniform readings in the penetration speed, specific energy and ease-to-drill. Where the SL has mottling of siltstone and claystone of varying degrees of induration, the readings become

more heterogeneous, with the specific energy and hard-to-drill sometimes being greater than that observed in the WSL. In places, the SL is a limestone in a siltstone/claystone matrix, where the MWD can identify this through greater penetration speeds, an increase in the ease-to-drill, and a decrease in the specific energy and force vs. velocity ratios, and thus determined as a weaker rock unit.

The BSL tends to exhibit homogenous readings, with constant penetration speed, torque, specific energy (usually lower than the SL) and a constant force vs velocity ratio.

2.3.2 Dukhan Limestone (DLS)

Usually the DLS unit is characterized by low penetration speeds, low torque values and high specific energy and hard-to-drill values, and generally more uniform calliper readings. These diagraphy results correlate with the literature on the DLS described as a strong, micro-crystalline, partly recrystallized and dolomitized limestone (Cagatay & Namik, 1990), fossiliferous and slightly clayey.

2.3.3 Midra Shale (MSH)

Generally, the MSH is interbedded shale and limestone, of varying thickness depending on the location in Qatar. The shale beds are typically distinguished by a characteristic low and curved E-method and specific energy values, attributed to the low strength of the shale units. The shale units exhibit high torque values and the specific energy values tend to be greater than that observed in the BSL, not because the formation is stronger but as a result of the friction on the drill bit. Sharp spikes in the E-method, specific energy and hard-to-drill parameters indicate the higher strength limestone beds. Here the use of NGR is an important tool in identifying the MSH, as typical characteristic peaks of 50-60 API are observed at this marker bed. Figure 2 illustrates a sample interpretation for Midra Shale in comparison with other geologies.

2.3.4 Rus Formation (RUS)

The uppermost part of the Rus formation is a medium strong to strong, dolomitized, buff grey limestone known as the Khor Limestone (KLS) (LeBlanc, 2008). This is reflected in the drilling behavior within the KLS which exhibits low penetration speed, high specific energy and hard-to-drill values (Figure 2). This unit can be highly fractured and recovered as non-intact when coring, with the typical erratic behavior of the rig measurements observed in this unit indicative of this fracturing. Due to the usually low recovery of samples from the KLS unit, limited tests are usually carried out. Hence, there are usually very limited rock strength data available for KLS. Figure 2 illustrates a sample interpretation for KLS.

The underlying RUS is typically an interbedded weak carbonate sequence, becoming a clayey to sulphate sequence, the latter being absent in the northern and central Qatar. The readings from the MWD reflect the interbedding observed in the carbonate RUS which helps to distinguish it from the MSH and the KLS. Generally, there is an evident increase in the ease-to-drill and penetration speeds, with a decrease in the specific energy and force vs. velocity ratio, reflective of this drop in strength. Where there are increases in the hard-to-drill and specific energy, this usually represents the competent, stronger limestone beds (Figure 2). When the carbonate RUS advances to the clayey layers there

is a significant increase in penetration speed, ease-to-drill and torque, indicative of the lower strength. The stronger gypsum beds tend to have a drop in the penetration speed, and an increase in the specific energy, hard-to-drill, E-method and torque. Figure 2 illustrates a sample interpretation for RUS.

2.3.5 Umm Er Radhuma (UER)

The only available diagraphy data comes from two boreholes in the Lusail City area (Site 1 in Figure 1). The rock was described as a moderately weathered, porous dolomitic limestone with thin siltstone/claystone beds. The UER tends to have low penetration speeds, and relatively uniform specific energy and force vs velocity ratios. The ease-to-drill and torque increases where the siltstone/claystone beds lie.

2.4 Sample interpretation of stratigraphy

Figure 2 illustrates a sample interpretation of stratigraphy based on MWD results from one borehole location in Site 5. Several lithologies have been identified at the location of this specific investigation point: WSL, SL with attapulgitic clay, SL, BSL, MSH, KLS and RUS.

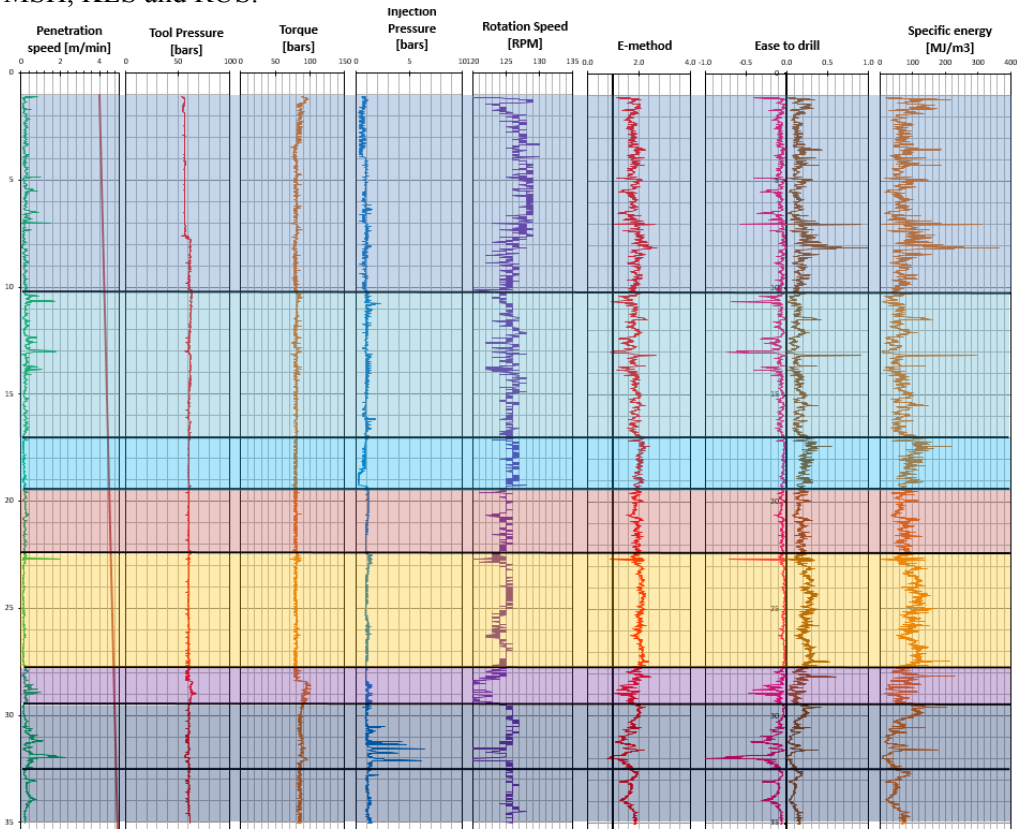

Figure 2: MWD processed results with interpretations for various geologies in Qatar.

The different geologies are represented by various colours from top to bottom: (a) dark blue: WSL, (b) blue: SL with attapulgitic clay; (c) cyan: SL, (d) red: BSL, (e)

orange: MSH, (f) purple: KLS, (g) dark purple: RUS.

In Figure 2, there are notable differences in the drilling parameters (i.e., penetration speed, tool pressure, torque, injection pressure and rotation speed) as well as in the calculated values for the E-method, hard-to-drill and specific energy, the values of which were studied to aptly provide stratigraphical interpretations. For comparison purposes, the numerical values for specific energy from Figure 2 are summarized in this paper, as follows:

- The calculated specific energy values for Simsima limestone (Umm Bab formation) are as follows: (a) WSL has specific energies ranging between 20 MJ/m3 to 360 MJ/m3, with an approximate average of 50 MJ/m3, (b) SL with attapulgitic clay has specific energies generally ranging between 20 MJ/m3 to 140 MJ/m3, with an approximate average of 50 MJ/m3, (c) SL has specific energies generally ranging between 60 to 160 MJ/m3, with an approximate average of 100 MJ/m3, and (d) BSL has specific energies generally ranging between 40 to 120 MJ/m3, with an approximate average of 70 MJ/m3.
- MSH has higher specific energy values than the BSL, with values generally ranging between 60 to 140 MJ/m3.
- KLS has lower specific energy values than the MSH, with values generally ranging from 20 to 120 MJ/m3, while RUS has very variable values of specific energy values, which range from 0 to 200 MJ/m3, due to the presence of interbeds in the carbonate RUS.

It should be noted that the specific energies are only applicable to Figure 2 only. Laterally, these can be correlated on the same investigative site, however, an investigation conducted at another geotechnical site elsewhere in Qatar may exhibit different numerical ranges.

3 CONCLUSION

Through the use of MWD it is possible to discern the geological stratigraphy, to aid in the interpretation, knowledge of the local geology, and correlation either from previous coring boreholes or a coring borehole drilled adjacent to a diagraphy borehole. A geotechnical investigation using the conventional coring methods can limit and bias the project with either over- or under-design. When we do coring, we are dependent on the skill of the driller to recover samples sufficient for laboratory testing; when the geology is difficult to recover, our knowledge of that rock is limited, and we tend to use ‘engineering judgement’ in geotechnical design. As the MWD records at every 1cm intervals, a continuous relative-strength record is produced, determining where the rocks are stronger and weaker through the length of the borehole. This is particularly useful where we do not retrieve samples to ascertain the properties of the rock. We can use the drilling resistance parameter to indicate the relative unconfined compressive strength, and with further research, a correlation with the unconfined compressive strength and shear wave velocity can be done.

If we consider the addition of wireline logging, such as calliper and NGR, it is possible to determine the presence of cavities in rock layers. It also enables more accurate interpretation of the geology and aids in understanding of some rock properties such as

swelling or even the erodibility of the ground in response to the drilling activity.

Instrumented drilling has been a proven technique, with success on several projects in Qatar. The benefits of using MWD have been continuously evident, with a faster project delivery time, borehole data availability within 24 hours of drilling, and more realistic geotechnical design parameters being provided to designers.

Further studies are recommended to be undertaken to derive the correlation between MWD and wireline logging results with Rock Quality Designation (RQD) and hydraulic conductivity. These topics are not touched in this paper.

REFERENCES

Bingham, M. G. (1965). A new approach to interpreting rock drillability. A technical manual reprinted from the oil and gas journal. 93 p.

BS EN ISO 22476-15 (2016). Geotechnical investigation and testing, field testing: measuring while drilling, BSI Standard Publications.

Cagatay, M. & Namik (1990). Palygorskite in the Eocene rocks of the Dammam Dome. *Saudi Arabia Clays and Clay Minerals*, Vol. 38, No. 3, 299-307.

Falconer, I. G., Burgess, T. M. & Sheppard, M. C. (1988). Separating bit and lithology effects from drilling mechanics data. *IADC/SPE Drilling Conference*, Texas, pp. 123-136.

Girard, H., Morlier, P., Puvilland, O. & Garzon, M. (1986). The digital ENPASOL method - exploitation of drilling parameters in civil engineering. *Proc. 39th Canadian Geotechnical Conference*, Ottawa, pp. 59-68.

Gui, M. W., Soga, K., Bolton, M.D. & Hamelin, J. P. (2002). Instrumented borehole drilling for subsurface investigation. *Journal of Geotechnical and Geoenvironmental*, April, pp. 283-291.

LeBlanc, J. (2008). A fossil hunting guide to the tertiary formations of Qatar, Middle East.

Teale, R. (1965). The concept of specific energy in rock drilling. *International Journal Rock Mechanics and Mining Science*, Volume 2, pp. 57-73.

Cite this article as: Gravador-Villamor A. G., Pearce F., "The Use of Measuring While Drilling and Wireline Logging to Identify the Geological Strata in Qatar", *International Conference on Civil Infrastructure and Construction (CIC 2020)*, Doha, Qatar, 2-5 February 2020, DOI: https://doi.org/10.29117/cic.2020.0089

Hydrogen Gas Production from the Injection of Nanoscale Zero-Valent Iron and Sodium Borohydride Solutions: Potential Effects Near Injection Wells

Obai Mohammed
obai.mohammed@queensu.ca
Queen's University, Kingston, Ontario
Current address: Technical Support Section, Ministry of the Environment, Conservation and Parks, Kingston, Ontario

Kevin G. Mumford
kevin.mumford@queensu.ca
Queen's University, Kingston, Ontario

Brent E. Sleep
sleep@efc.utoronto.ca
University of Toronto, Toronto, Ontario

ABSTRACT

The injection of nano-scale zero-valent iron (nZVI) is a remediation technique for the treatment of organic and metal contamination in soil and groundwater. The hydrogen gas (H2) produced during the reaction of nZVI and excess sodium borohydride (NaBH4) used in nZVI synthesis with water can inhibit nZVI transport in the subsurface, potentially limiting solution delivery to the target contaminant zone. Laboratory experiments were completed in a thin flow cell using NaBH4 and nZVI solutions injected into water-saturated medium sands, in which local gas saturations were quantified using a light transmission technique to calculate H2 gas volumes. Hydraulic conductivity, under water-saturated and quasi-saturated conditions, after gas exsolution and throughout gas dissolution, was measured. The results showed that H2 gas volume produced as a result of the reaction of nZVI with water was more than the H2 gas volume produced by the self-hydrolysis of NaBH4 solution regardless of similar NaBH4 concentration used as excess during nZVI synthesis. Pools of H2 gas were formed after injecting nZVI prepared with excess 5 g/L NaBH4 or after injecting 5 g/L NaBH4 without nZVI. Gas accumulated predominantly in a vertical layer of coarse sand, illustrative of a sand pack surrounding an injection well. Lower hydraulic conductivity measurements were linked to higher gas saturations and further reductions were evident as a result of gas pool accumulation at the top of the flow cell. These results show that gas production during the application of nZVI is an important process that must be considered during remediation design and operation to ensure effective delivery to target zones.

Keywords: Nano-scale zero-valent iron (nZVI); Volatile organic compounds; Light transmission

1 INTRODUCTION

In situ chemical reduction with nZVI is a promising technology for the treatment of source-zone and dissolved chlorinated solvents in the groundwater and subsurface soils. Yet, the application of nZVI is challenged by the reduced nZVI solution mobility during injection in some subsurface environments (He et al., 2009). In addition to

concerns regarding agglomeration and sedimentation of nZVI, H_2 gas produced during nZVI implementation can cause changes in groundwater flow patterns (Johnson et al., 2013). Figure 1 is a graphical representation of an nZVI application where H_2 gas exolves during the reaction of nZVI with water near the injection area. In the treatment area, the nZVI reacts with water and volatile organic compounds (VOCs) in the non-aqueous phase liquid (NAPL) source, producing H_2 gas and VOCs that can be mobilized upwards, possibly causing contaminant relocation to the location above the injection area.

Previous field studies have reported complications with nZVI mobility, despite the modification of nZVI with polymers and surface coatings (Kocur et al., 2014, 2013). This indicates that nZVI mobility may be limited for reasons other than nano-particle stability. H_2 gas exsolving from the reaction of freshly synthesized nZVI with water (Chen et al., 2011) is a potential cause of this limitation. Mohammed et al. (2019) performed bench-scale experiments to quantify and determine the consequences of H_2 gas exsolving uniformly during the self-hydrolysis reaction of $NaBH_4$ solution with deionized water in silica sands packed in an acrylic flow cell. Their results showed lower hydraulic conductivity values linked to increased gas saturations associated with increased $NaBH_4$ solution concentrations. Mohammed et al. (2019) concluded that H_2 gas production could decrease the hydraulic conductivity if high concentrations of $NaBH_4$ are added for nZVI synthesis during field application. It is anticipated that nZVI injections will also be affected by heterogeneity in the immediate proximity of an injection well (i.e., the sand pack) which can create a preferential location for gas accumulation.

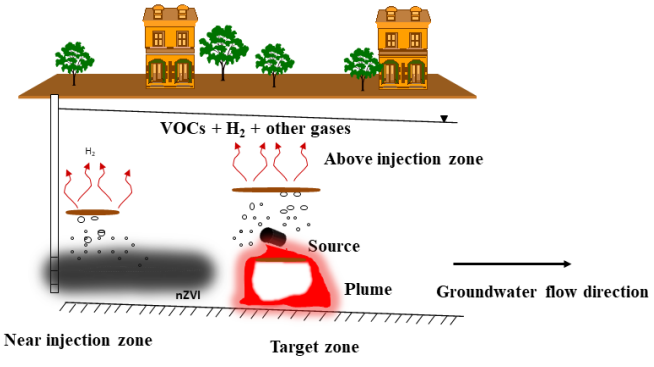

Figure 1: Simplified schematic of a nZVI field injection

In this study H_2 gas exsolving from the nZVI reaction with water compared to $NaBH_4$ self-hydrolysis reaction with water was visualized and quantified, and images were examined to determine the potential of gas mobilization in each case. In addition, the potential effect of H_2 gas exsolution on the effective hydraulic conductivity was investigated, and reductions in hydraulic conductivity were measured as H_2 gas dissolved from a vertical high-permeability layer, representative of a sand pack around a field injection well.

2 MATERIALS AND METHODS

Experiments were completed at the bench-scale by injecting $NaBH_4$ and nZVI solutions into homogeneous medium sand packs. Silica Accusand 20/30 and 12/20 grades, with median particle diameters (d_{50}) of 0.713 mm and 1.105 mm (Schroth et al., 1996), and porosity values of 0.38 and 0.37 to 0.38 (Mohammed et al., 2019), respectively, were used for the experiments performed in a thin acrylic flow cell. Four injection experiments, including two $NaBH_4$ and two nZVI solutions were performed at room temperature (21° C). H_2 gas was produced by the self-hydrolysis of $NaBH_4$, and by nZVI reaction with water. Hydraulic conductivity measurements were determined under water-saturated conditions before gas exsolution, directly after gas exsolution in all experiments, and throughout H_2 gas dissolution. H_2 gas saturations were quantified using a light transmission method.

2.1 Flow Cell

A 22 cm × 34 cm × 1 cm acrylic flow cell (Figure 2), equipped with a top seal to sustain confined conditions, and two clear-wells promoting horizontal water flow, was used to perform the experiments. The flow cell had four bottom drainage ports with water-wet hydrophilic nylon membranes (10 μm pore size, EMD Millipore Corporation) installed to facilitate drainage of sand packs to a residual wetting saturation. A model TJE low range wet-wet (Honeywell International Inc.) differential pressure transducer, attached through water-filled tubes to the clear-wells, was used to measure the differential pressure during the flowing part of the experiments, and the differential pressure data were logged throughout each experiment using a HOBO UX120-006M Analog data logger (Onset Computer Corporation). A vertically oriented layer of 12/20 silica Accusand was packed in the first 6 cm measured from the left inflow clear-well boundary and the remaining part of the cell was packed with 20/30 silica Accusand. This configuration was used to represent a coarse sand pack neighboring an injection well in field applications. In order to remove fines, all sands were washed with deionized water and packed as a slurry into the cell, which was half-way filled with deionized water to create a water-saturated condition to begin with.

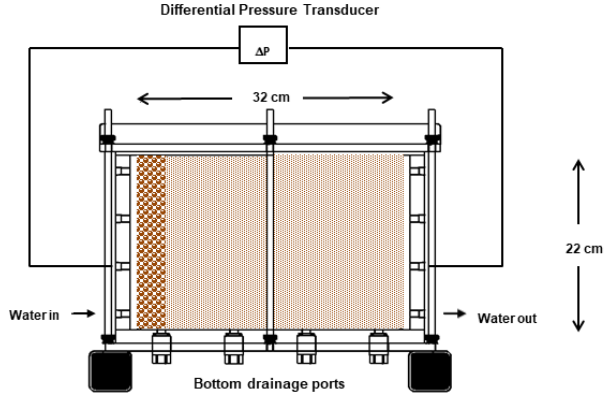

Figure 2: Flow cell sketch

2.2 Gas Visualization and Quantification

A light transmission technique (Tidwell and Glass, 1994; Niemet and Selker, 2001; Mumford et al., 2015; Mohammed et al., 2019) was used to visualize and quantify H_2 gas saturations. Gas saturations(S_g) were calculated from light intensities (I) transmitted through water-saturated conditions (I_s) and residual conditions (I_r). The method assumes uniform diameter pores that are either filled with water or filled with gas and a residual film of water. Effective wetting saturations of an image (I) were calculated using (Niemet and Selker, 2001):

$$S_e = \frac{\ln(I)-\ln(I_r)}{\ln(I_s)-\ln(I_r)} = 1 - \frac{\ln(I/I_s)}{\ln(I_r/I_s)} \quad (1)$$

where I is the light intensity transmitted through the sand, and I_s and I_r are the light intensities transmitted through a fully water-saturated or a residual saturated sand, respectively. Gas saturation was then calculated as:

$$S_g = 1 - (S_e(1 - S_{wr}) + S_{wr}) \quad (2)$$

where S_{wr} is the residual wetting saturation, measured in independent experiments (Mohammed et al., 2019). A light emitting diode (LED) panel (Led Go, CN-1200H) was used as the light source and a single-lens reflex digital camera (Canon, EOS Rebel T3i) was used to capture the images throughout the experiments. The light transmission setup was covered with a black fabric to avoid changes in light while experiments were conducted and the camera settings were held constant.

2.3 Solutions Injection

A volume of 10 mL of $NaBH_4$ or nZVI solution was injected in the flow cell through the left-hand clear-well near the 12/20 Accusand portion of the sand pack. $NaBH_4$ solution concentrations of 1.25 g/L and 5 g/L were carefully chosen since they are representative of concentrations used for 1 g/L nZVI synthesis by means of 2:1 to 4:1 excess $NaBH_4$ ratio described in recent laboratory experiments and field investigation trials (Boparai et al., 2011; Kocur et al., 2013). The nZVI concentration of 1 g/L used during injection experiments has also been reported in field applications and bench-scale experiments (Kocur et al., 2014, 2013; Stefaniuk et al., 2016). The $NaBH_4$ concentrations in experiments E-1 and E-2 correspond to the excess $NaBH_4$ concentrations used for nZVI synthesis in experiments E-3 and E-4 to allow direct comparison between pairs of experiments (Table 1). The experiments were conducted mainly in two parts. The first part (exsolution) was conducted in a static batch mode, with no water flowing through the cell (E-1 to E-4). During gas exsolution, water was displaced out of the cell through one open outflow port, and was recorded using a laboratory balance (Mettler Toledo MS6002S with Mettler Toledo LabX Direct software). Images were captured throughout exsolution every 2 to 5 minutes. The gas volumes calculated from the digital images were obtained by considering the 12/20 and 20/30 sand packed areas separately during image processing and summed to get the total H_2 gas volume. Gas volumes calculated from the captured images using light transmission were related to the displaced water volumes to obtain a best-fit value of (I_r/I_s) in Equation 1 (Mumford et al., 2015; Mohammed et al., 2019). In the second part of each experiment (water flow), deionized water was pumped

through the sand packs at 36.8 mL/min, equivalent to a pore water velocity of 4.4 cm/min (F-1 to F-4). The measured pressure difference between the inflow and outflow boundaries was used to calculate the effective hydraulic conductivity across the entire flow cell. The flow rate was selected to produce high pressure drops with measurable differences between water-saturated and exsolved gas conditions, but was maintained within the Darcy flow regime with Reynolds number of 0.5 in the 20/30 Accusand. The water flow part was sustained for 12.5 to 19 pore volumes for experiments F-3 and F-4, but continued for 189 to 225 pore volumes for experiments F-1 and F-2, respectively (Table 1), to further examine the dissolution of H_2 gas trapped within the 12/20 Accusand (i.e., the coarse sand pack).

Table 1: Solution injection experiments

Exsolution	Water flow	$NaBH_4$ (g/L)	nZVI (g/L)	Pore-volumes Flushed
E-1	F-1	1.25	-	189.0
E-2	F-2	5.00	-	225.0
E-3	F-3	1.25*	1.0	14.0
E-4	F-4	5.00*	1.0	18.0

*excess $NaBH_4$ used during nZVI synthesis

3 RESULTS AND DISCUSSION

3.1 Gas Exsolution

Exsolved gas volumes in the four experiments are shown in Figure 3. $NaBH_4$ solution was used in experiments E-1 and E-2, and nZVI solution (which includes excess $NaBH_4$) was used in experiments E-3 and E-4. The best-fit values of (I_r/I_s) in the 12/20 and the 20/30 sand packed experiments E-1 to E-4 were found to be 0.79 ± 0.03 and 0.58 ± 0.06, respectively, consistent with 0.69 and 0.56 I_r/I_s values reported by (Mohammed et al., 2019) using a similar light transmission set-up and image processing technique. The lower concentration $NaBH_4$ solutions or nZVI solutions synthesized with lower $NaBH_4$ concentrations (E-1 and E-3) produced less H_2 gas compared to injecting higher concentration $NaBH_4$ solutions or nZVI solutions synthesized with higher concentrations of $NaBH_4$ (E-2 and E-4) (Figure 3). This is consistent with the findings reported by Mohammed et al. (2019). Importantly, similar $NaBH_4$ solution concentrations produced more H_2 gas when paired with nZVI. The H_2 gas exsolution rate decreased with increasing time in all experiments (Mohammed et al., 2019). Gas volumes reached a plateau after 250 min in experiment E-1, but did not reach a plateau after greater than 600 min in experiment E-2, which used a higher $NaBH_4$ concentration. In contrast, gas volumes reached a plateau after 100 min in experiment E-3, and 200 min in experiment E-4, which also used a higher $NaBH_4$ concentration in excess for nZVI synthesis (Figure 3). This shorter time to reach the plateau in the nZVI injection experiments (E-3 and E-4) was expected due to the high reactivity of the nanoparticles associated with high nZVI surface area. A relatively similar reaction time for H_2 exsolution from nZVI of about two hours was reported by (Huang et al., 2016).

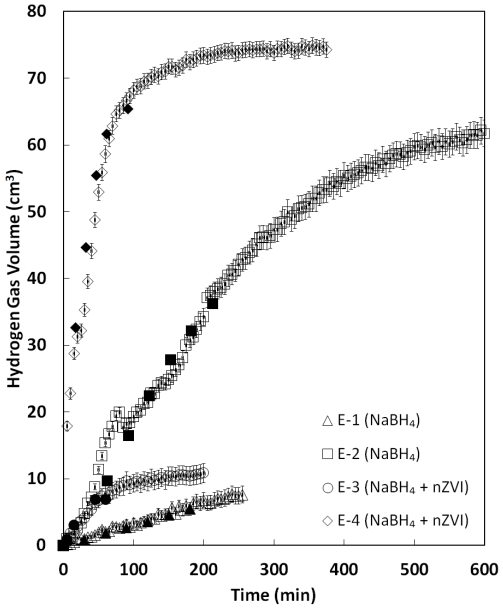

Figure 3: H_2 gas volume produced with time. Open symbols signify volumes of H_2 gas calculated by image processing and closed symbols signify the volumes of gas equivalent to the displaced water volumes during H_2 gas exsolution.

3.2 H_2 Gas Production and Mobilization

Figure 4 illustrates the distribution of gas images processed for gas saturations at different times as H_2 exsolved throughout the experiments. Consistent behavior is evident in all of the performed experiments. H_2 gas is produced mainly in the coarse sand (12/20 Accusand) near the clear-well in which the solution is injected. In all experiments, the volume of gas exsolved was sufficiently high to result in buoyant gas mobilization, resulting in higher gas saturations at the top of the coarse sand. Intermediate gas saturations were also evident at the bottom of the coarse sand, due to exsolution from injected solution that was transported downwards due to its higher density. The lowest gas saturations occurred in the middle of the coarse sand due to gas exsolution and trapping. At later time, H_2 gas progressed into the 20/30 Accusand pack, either driven by gas invasion at the top or by the exsolution of gas from the dense solution at the bottom. In experiments E-2 and E-4, where higher $NaBH_4$ solution concentrations were injected, higher gas saturations and mobilized gas formed a gas pool at the top of the coarse sand that was able to enter and advance to form a gas pool in the finer 20/30 sand. In experiment E-2, this gas pool in the finer sand was also supplied by discontinuous gas flow from the bottom of the finer sand pack as the gas saturations increased due to the self-hydrolysis of $NaBH_4$ (gas fingers in Figure 4g,h). Although high concentrations were also used in experiment E-4, there was no gas mobilization in the finer sand pack in that experiment. This is attributed to the high reactivity of nZVI, resulting in nearly all of the H_2 gas being formed within the first hour and close to the coarse sand compared to the hydrolysis reaction that lasted more than 2 hours.

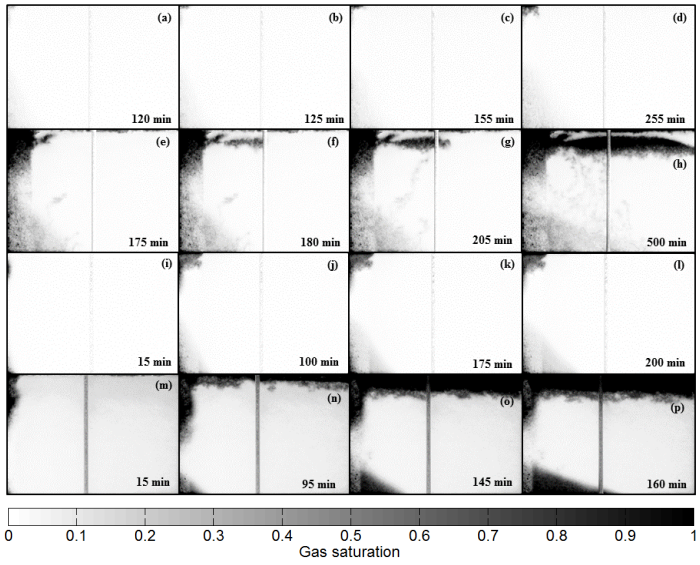

Figure 4: Selected gas saturation images showing H_2 gas exsolution and mobilization from (a)–(d) Experiment E-1, (e)–(h) Experiment E-2, (i)–(l) Experiment E-3, and (m)–(p) Experiment E-4

3.3 Hydraulic Conductivity and Flow

The non-uniform distribution of gas, both vertically and laterally, resulted in substantial spatial variation in aqueous phase relative permeability. The overall relative permeability value (i.e., at the scale of the flow cell) is used here to describe the effect of gas produced in the experiments. The hydraulic conductivity under water-saturated conditions (experiments F-1 to F-4) was 29.8 ± 2.0 cm/min (mean ± one standard deviation). Following H_2 gas exsolution in experiments F-1 and F-3, the hydraulic conductivity was reduced to 26.9 ± 0.3 cm/min and 27.5 ± 0.2 cm/min. This reduction in hydraulic conductivity was associated with H_2 gas volumes of 7.7 ± 1.2 and 11.5 ± 1.4 cm^3, respectively. Replicate experiments conducted under water-saturated conditions were used to calculate standard deviation values in all of the exsolution experiments with the assumption of a constant coefficient of variation based on previously conducted air entrapment and exsolution experiments (Mohammed et al., 2019) used to measure effective hydraulic conductivity. Further reductions in hydraulic conductivity were related to increased $NaBH_4$ solution concentrations (experiments F-2 and F-4). Reduced hydraulic conductivity values of 17.0 ± 3.1 cm/min and 24.1 ± 2.1 cm/min were caused by larger H_2 gas volumes of 62.2 ± 2 and 74.9 ± 1.2 cm^3, respectively. These reductions correspond to overall aqueous phase relative permeability values of 0.62-0.94. However, based on the gas distribution (Figure 4) the reduction in hydraulic conductivity is controlled by large reductions in aqueous phase relative permeability in the coarse sand pack, particularly near the top of the pack for high-concentration injections. As a result, of H_2 gas dissolution due to water flow up to 189 pore volumes in experiment F-1, the hydraulic conductivity value bounced back steadily to the value measured under water-saturated conditions. Yet, dissolution of H_2 gas in experiment F-2 was able to return the

hydraulic conductivity value to only 22.9 ± 0.1 cm/min (82% of the value under water-saturated conditions), even after flushing 225 pore volumes of water through the sand pack. The gas accumulated at the top of the cell in the form of a gas pool exhibited slow dissolution (Figure 4h), with local gas saturations up to 67% remaining.

4 CONCLUSION

The experiments conducted in this study demonstrated that H_2 gas exsolution from the reaction of nZVI prepared with excess $NaBH_4$ with water was more than the H_2 gas exsolved due to the self-hydrolysis of $NaBH_4$ solution alone, despite similar concentrations of $NaBH_4$. Increasing $NaBH_4$ solution concentration resulted in more H_2 gas production, whether the increased $NaBH_4$ solution concentration is injected alone, or is used during nZVI synthesis. Most of the gas exsolved within the coarser sand representative of a sand pack surrounding an injection well, and was mobilized upwards by buoyancy. However, additional gas was produced at the bottom of the sand pack, due to the downward transport of the injected solution driven by density. Vertically mobilized gas channels were created as a result of nZVI solution injection prepared with excess 5 g/L $NaBH_4$ concentration, but was also created in the experiment in which 5 g/L $NaBH_4$ solution was injected alone. In both experiments where 5 g/L $NaBH_4$ was used, the produced gas created H_2 gas pools. Exsolved H_2 gas caused a reduction in the effective hydraulic conductivity, with higher gas saturations resulting in lower effective hydraulic conductivities. Gradual increases in hydraulic conductivity were measured during H_2 gas dissolution, although it did not return to the water-saturated hydraulic conductivity in both experiments due to gas persistence.

In field-scale nZVI applications, H_2 gas produced during the injection of nZVI prepared with excess $NaBH_4$ upstream of a contaminant zone can reduce nZVI mobility and inhibit delivery to the target contaminant zone by blocking pores and reducing the effective hydraulic conductivity, with more reduction expected when using higher concentrations of $NaBH_4$ during nZVI synthesis due to additional H_2 gas production. Gas mobilization can also result in gas pool formation should low permeability layers exist in the injection application area, further decreasing the effective hydraulic conductivity. These impacts can be more severe due to exsolution in the sand pack in the vicinity of the injection well screens, in which H_2 gas can be mobilized upwards in the coarse sand, creating gas pools at the upper portion of the sand pack. While some gas from these pools may flow back into the injection well, depending on the entry pressure of the well screen and the height of the sand pack above the well screen, residual gas that remains in the sand pack will limit subsequent injections. Given that the sand pack is coarser than the surrounding porous medium by design, it is a preferential location for gas accumulation, with the amount of accumulation subject to the displacement pressure of the sand nearby. In these experiments, more than 120 pore volumes of water were required to dissolve the H_2 gas produced by exsolution. This suggests that flow limitations and flow diversion could extend for longer time periods in a field application, including between consecutive nZVI injections. Persistent redirection of groundwater flow is detrimental if repeated nZVI solution injections to the target zone are deemed necessary. Flow diversion can also complicate the analysis of groundwater sampling data collected downgradient if the results are compared to pre-injection conditions.

REFERENCES

Boparai, H. K., Joseph, M., O'Carroll, D. M. (2011). Kinetics and thermodynamics of cadmium ion removal by adsorption onto nano zerovalent iron particles. J. Hazard, *Mater*, 186, 458-465. DOI: 10.1016/j.jhazmat.2010.11.029.

Chen, K. F., Li, S. & Zhang, W. (2011). Renewable hydrogen generation by bimetallic zero valent iron nanoparticles. *Chem. Eng. J.*, 170, 562-567. DOI: 10.1016/j.cej.2010.12.019.

He, F., Zhao, D. & Paul, C. (2010). Field assessment of carboxymethyl cellulose stabilized iron nanoparticles for in situ destruction of chlorinated solvents in source zones. *Water Res*., 44, 2360-2370. DOI: 10.1016/j.watres.2009.12.041.

Huang, Y. X., Guo, J., Zhang, C. & Hu, Z. (2016). Hydrogen production from the dissolution of nano zero valent iron and its effect on anaerobic digestion. *Water Res*., 88, 475-480. DOI: 10.1016/j.watres.2015.10.028.

Johnson, R. L., Nurmi, J. T., O'Brien Johnson, G. S., Fan, D., O'Brien Johnson, R. L. & Shi, Z. et al. (2013). Field-scale transport and transformation of carboxymethylcellulose-stabilized nano zero-valent iron. *Environ. Sci. Technol*., 47:1573-1580. DOI: 10.1021/es304564q.

Kocur, C. M., Chowdhury, A. I., Sakulchaicharoen, N., Boparai, H. K., Weber, K. P., Sharma, P., Krol, M. M., Austrins, L., Peace, C., Sleep, B. E. & O'Carroll, D. M. (2014). Characterization of nZVI mobility in a field scale test. *Environ. Sci. Technol*., 48, 2862-2869. DOI: 10.1021/es4044209.

Kocur, C. M., O'Carroll, D. M. & Sleep, B. E. (2013). Impact of nZVI stability on mobility in porous media. *J. Contam. Hydrol.,* 145, 17-25. DOI: 10.1016/j.jconhyd.2012.11.001.

Mohammed, O., Mumford, K. G. & Sleep, B. E. (2019). Relative permeability measurements during the exsolution and dissolution of hydrogen gas produced by the hydrolysis of sodium borohydride. *Vadose Zone J*., 18:190043. DOI: 10.2136/vzj2019.04.0043.

Mumford, K. G., Hegele, P. R. & Vandenberg, G. P. (2015). Comparison of Two-Dimensional and Three-Dimensional Macroscopic Invasion Percolation Simulations with Laboratory Experiments of Gas Bubble Flow in Homogeneous Sands. *Vadose Zo. J.*, 14. DOI: 10.2136/vzj2015.02.0028.

Niemet, M. R. & Selker, J. S. (2001). A new method for quantification of liquid saturation in 2D translucent porous media systems using light transmission. *Adv. Water Resour.*, 24, 651-666. DOI: 10.1016/S0309-1708(00)00045-2.

Schroth, M.H., Istok, J. D., Ahearn, S. J., Selker, J. S., 1996. Characterization of Miller-Similar Silica Sands for Laboratory Hydrologic Studies. *Soil Sci. Soc. Am. J*., 60, 1331. DOI: 10.2136/sssaj1996.03615995006000050007x.

Stefaniuk, M., Oleszczuk, P. & Ok, Y. S. (2016). Review on nano zerovalent iron (nZVI): From synthesis to environmental applications. *Chem. Eng. J*., 287, 618-632. DOI: 10.1016/j.cej.2015.11.046.

Tidwell, V. C. & Glass, R. J. (1994). X ray and visible light transmission for laboratory measurement of two-dimensional saturation fields in thin-slab systems. *Water Resour. Res*., 30, 2873-2882. DOI: 10.1029/94WR00953.

Cite this article as: Mohammed O., Mumford K. G., Sleep B. E., "Hydrogen Gas Production from the Injection of Nanoscale Zero-Valent Iron and Sodium Borohydride Solutions: Potential Effects Near Injection Wells", *International Conference on Civil Infrastructure and Construction (CIC 2020)*, Doha, Qatar, 2-5 February 2020, DOI: https://doi.org/10.29117/cic.2020.0090

Geotechnical Aspects of Sub-Sea Tunnelling on the Musaimeer Pumping Station and Outfall Tunnel Project

Gary Peach
gary.peach@mottmac.com
Mott MacDonald, Doha, Qatar

Mirjana Hrnjak
mirjana.hrnjak@mottmac.com
Mott MacDonald, Doha, Qatar

Ioannis Papadatos
Ioannis.papadatos@auccqatar.com
HBK-PORR JV, Doha, Qatar

Hernan Vigil
hernan.vigil@auccqatar.com
HBK-PORR JV, Doha, Qatar

ABSTRACT

Musaimeer outfall tunnel is one of the longest storm water tunnels in the world with a total length of 10.2 km. The tunnel is connected via a drop shaft to the main pump station. This system will accommodate surface and storm water received from the drainage networks of 270 km2 of urban areas in southern Doha. Though the geological conditions remain similar to those in Qatar Metro projects, in this project, the tunneling faced new challenges because the outfall tunnel alignment is 40 m deep (25m below the water of Gulf plus 15m under the seabed). This project involves the construction of the outfall tunnel with an internal diameter of 3700 mm sloped at 0.05% upward to the riser shaft. The riser shaft, which is located at the end of the outfall tunnel, is connected to a diffuser field located on the seabed. The tunnel will be excavated by Tunnel Boring Machine (TBM) and is expected to encounter possible water inflows at high pressure, complex mixed ground, weaker ground strata prone to cavities or voids and the presence of vertical and lateral fractures connected to the seabed. The geotechnical parameters in sub-sea tunnelling are being assessed through all main project stages; a) Evaluation b) Verification and c) Application during the execution of this project which is currently in progress. The tunnel alignment traverses through the Rus formation, Midra shale and Simsima Limestone. The TBM will require periodic atmospheric or hyperbaric interventions at the cutter head for cutter tool maintenance. During this process, the face can be mapped and compared to off-shore borehole logs. Geophysical seismic reflection/refraction and resistivity surveys have been carried out along the tunnel alignment. A non-intrusive radar system facility, installed on the TBM cutter-head, able to probe ahead in real time the ground conditions is also presented. By looking at TBM excavation parameters such as, thrust force, torque, penetration, cutter head rotation speed, correlations can be made to the above surveys and a look ahead plan can be developed to aid TBM operation.

Keywords: TBM; Sub-sea tunnel; Hydrostatic pressure; Offshore geophysics; Non-intrusive radar system; Face mapping; TBM parameters

1 INTRODUCTION

The Musaimeer Pumping Station project is governed by the Qatar Construction Specifications (QCS, 2014). The Public Works Authority (PWA) have engaged in two contracts. Firstly Mott MacDonald Ltd., which is the Project Management Consultant (PMC) company, and HBK-PORR JV, which is the Design, Build, Operation and Maintain Contractor for the construction of the MPSO Project, which is the final receiver of the upstream drainage system and located at the end of the Abu Hamour Tunnel, immediately south of the Hamad International Airport (HIA). The outfall tunnel is extending from the pump station, 10 km off-shore discharging drainage system flows into the Gulf. The discharging will be performed through a vertical riser shaft and a marine outfall diffuser field. Figure 1 shows the project location.

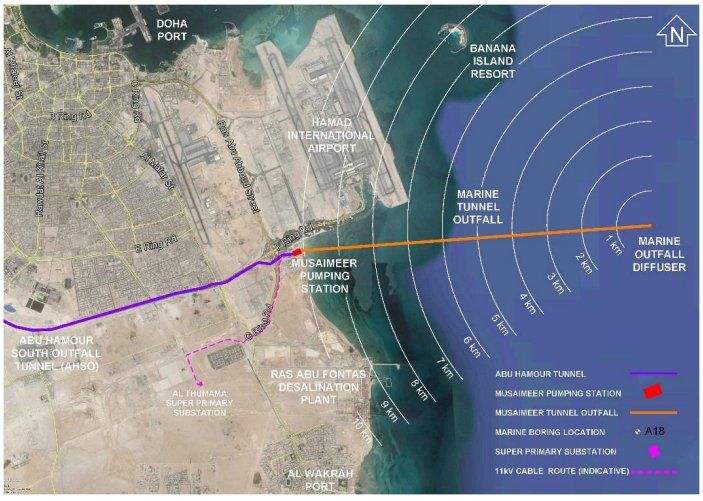

Figure 1: Project Location

2 TENDER GEOTECHNICAL INVESTIGATION – EVALUATION STAGE

PWA (Ashghal) undertook a significant geotechnical investigation program for this particular project prior to tender stage, which consisted of drilling 22 offshore boreholes at 500 m centers, which provided the following geotechnical data:

1. Cores for inspection.
2. In-situ packer tests.
3. Pressure meter tests at each location.
4. Geophysical surveys Sonar Bathymetry,Magnetometer, Seismic Reflection and Seismic Refraction.
5. Laboratory mechanical and chemical tests on soil, rock and water samples.

This geotechnical factual data was available during the early project stage based on which the Contractor made the initial assessment and evaluation of the foreseen tunnel geotechnical conditions. The factual investigation data was combined on a long geotechnical profile which became the basis of the outfall tunnel project, in terms of selection of the TBM machine and tunnel segmental lining, assess the tunnel construction baseline program, evaluate all the tunneling risks and the mitigation measures. Figure 2 shows the long geological profile.

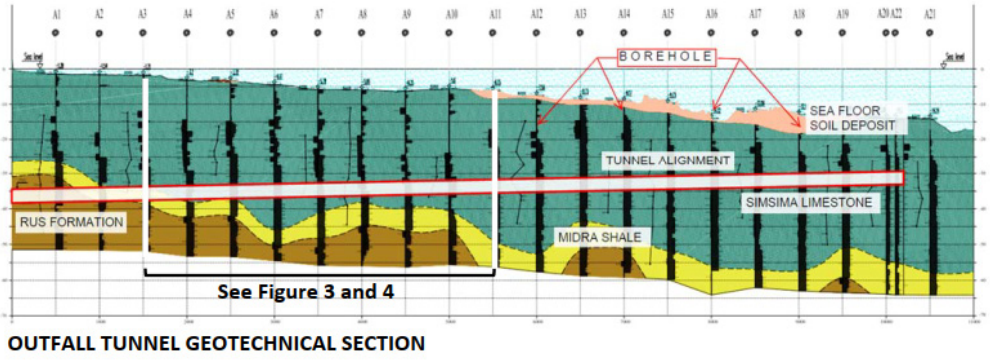

Figure 2: Outfall tunnel geotechnical section

The evaluation of the geotechnical factual data was also a challenge, due to the subsea nature of the tunnel. Although there was a significant experience in TBM tunneling in the Doha area, there was no previous experience on subsea tunneling on the area. The above data indicated the rock quality to be fairly competent along the tunnel alignment, however, there were two major tunnelling risks which required mitigation by the Designer and Contractor. Witnin Figure 2 above are references to two other Figures namely 3 and 4.

2.1 Karstic Features

The first risk the TBM could encounter is karstic features along the tunnel alignment. Although the tender geotechnical investigation has shown no evidence of karstification on the calcareous formations of Rus, Midra and Simsima. However, the risk was still valid. The size of a potential kasrtic feature was also very important and the mitigation possible measures limited, considering that the accessing and intervention from top due to the sea presence was an almost impossible operation. The TBM was desinged and equipted with grouting ports ahead and around the sheild and associated drilling facility, to mitigate this potential hazard which could impede the advancing of the tunnel.

2.2 Hydraulic Connection to Seabed

The second high risk was associated with the hydraulic connection between the seabed and the TBM tunnel. In this case the full hydraulic water pressure, would be directed to the advancing TBM cutterhead, requiring to increase the face pressure and thrust accordingly to balance and advance the tunnel. To mitigate this risk, the TBM was designed to withstand the full hydraulic pressure. However there were significant factual evidences based on the existing geotechnical investigation that along the 85% of tunnel total stretch, competent and low permeability rock would be encountered by the TBM, and at least one tunnel diameter above tunnel crown, providing a safe cover against water infiltration from above. This assessment was based on RQD (Rock Quality Designation) records and the Lugeon field tests performed in the offshore boreholes. Only 15% of the tunnel alignment was rock of poorer quality with increased permeability based on lugeon tests.

3 TUNNEL BORING MACHINED (TBM) SELECTION

The TBM selected took into consideration the requirements of BS 6164:2011 to excavate the the tunnel and was an Earth Pressure Balance (EPB) designed to support a maximum face working pressure of 4.5 bar on the bulkhead to support the maximum working pressure (full hydrostatic) which has been estimated between 0 and 4 Bar. The TBM selcted Typical EPB configuration has a cutterhead, excavation chamber, main bearing or drive, screw conveyor, front, middle and tail shields, man looks, thrust system, articulation, erector and brushes as part of the tail shield seal system. In addition, there are 18 gantries (160 m allocating all electro mechanical parts, additive tanks and rescue chambers among other requirements).

The most important modifications required in this TBM is related to minimize or eliminate the risk uncontrolled water inflow into the tunnel during construction. To prevent this water inflow from the chamber, the TBM has two set of gates, one is located at the end of the screw (double gate) that is being used during normal operation and able to close automatically in case of power shout down. In the event of extraordinary difficult geological conditions like over size voids, the TBM has the facilities to perform drilling for explorations and grouting through the shields by using preventers. The remining set of gates called "guillotine gates" is allocated between screw conveyor and bulkhead and this is considered the final option to be used in case of the gates at the screw conveyor fail.

4 POST TENDER GEOTECHNICAL INVESTIGATION.

The contract requirements specified the implementation of an additional 24 offshore boreholes. However, it was considered that in terms karst identification and possible hydraulic connection to the sea, the drilling of small diameter investigation boreholes would provide minimal benefit to the TBM operation. The drilling of small diameter investigation marine boreholes would only provide additional pin marks on the map, but not a richer picture of the overall hydrogeological and structural conditions along tunnel alignment.

The Contractor has decided to invest on a detailed geophysical investigation survey as a more beneficial approach to mitigate the major geotechnical risks and provided more complete geotechnical information regarding variations in geology, areas of seawater saturation, areas of cavities, weak disturbed zones or other discontinuities under the seabed between the existing 22 boreholes. Thus this geophysical survey was proposed and accepted by the Client.

With the use of a marine geophysical method, it might be possible to get an overall picture of the underground conditions, indicate some critical tunneling areas, schedule the required tunnel interventions and reduce the tunneling risk level further, regarding geotechnical unforeseen hazards.

Based on the above two different types of detail offshore geophysical surveys have been conducted along the outfall tunnel alignment, The Electrical Resistivity Tomography (ERT) and the Seismic Reflection Geophysical Tomography.

4.1 Electrical Resistivity Tomography Survey (ERT)

The objective of Electrical Resistivity Tomography (ERT) is to determine the

subsurface distribution in two or three dimensions (2D and 3D) of resistivity, a physical parameter of the earth that is related to key geological parameters such as soil or rock type and mineral content, as well as the porosity and degree of water saturation in the rock. This ERT survey was performed satisfactorily in good weather conditions and the successive data were processed, analyzed and interpreted. The survey covered more than 10 km of triple parallel ERT marine profiles, aligned along the tunneling corridor (West to East), at 3 m distances between them, integrated by a total of sixteen transversal ERT marine profiles distributed in a crossing direction (South to North) along the 10 km West-East survey tunnelling orientation.

After coducting the offshore survey, the most accurate possible electrostratigraphic model has been developed and refined on the final phase of study and the possible correlation between resistivity value variations and the main three different geologic units have been identified. A number of "conductive anomalies" and "resistive anomalies" have been detected along ERT profiles and documented accordingly. Figure 3 is an extracted section from the whole tunnel survey.

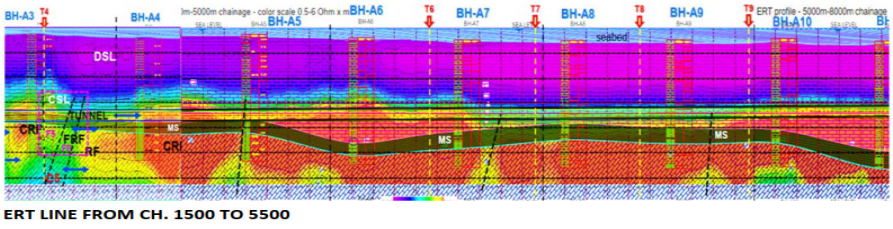

Figure 3: ERT line from 0+200 to 2+200

4.2 Seismic Reflection Geophysical Survey

This process consists of recording the acoustic waves generated at the surface which are reflected by sub-surface structures or interfaces. A reflection will occur when the density and/or the velocity changes at the boundary between two different materials. The acoustic waves are recorded from numerous hydrophones, installed at fixed distance along a seismic cable (streamer).

The seismic reflection geophysical survey is used to correlate the existing borehole defined stratigraphy, confirm the extend of topsoil formations and identified possible vertical weak zones, that may result in excessive water ingress along the TBM tunnel drive. Figure 4 shows a typical section of this survey.

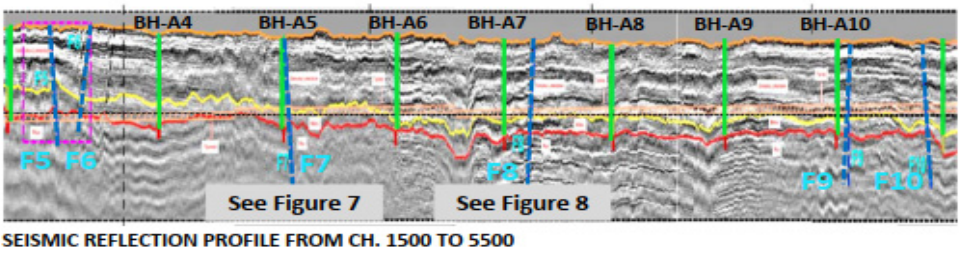

Figure 4: Seismic Reflection Profile

Based on the interpretation of Seismic Reflection Long and Cross Sections certain structural vertical zones/faults were identified indicating possibilities of increased water ingress, these features are marked F5 to F10 and are points on the survey where abrupt changes in the sesismic wave received profiles. Durring this assessment 20 such zones were identified, and thus planning can be instigated to withstand possible full hydrostaic water pressure.

5 FORESEEN GEOTECHNICAL CONDITIONS ALONG THE TUNNEL

To plan ahead and anticipate different ground conditions and hence assess programme impacts on the TBM operation the pretender and additional geotechnical information are combined according to the tunnel chainage. In order to ensure the TBM advances smoothly the cutterhead requires regular inspection, maintenance and repair. The most efficient way to carry this out is in ground conditions which are safe under atmospheric conditions. This operation becomes more complex and time consuming in poorer ground conditions which require hyperbaric support, performed in accordance with Compressd Air regulations (1996/1656). Thus to mitigate the impact of various ground conditions an assessment is made by linear meter of the likelihood of favorable sections where only atmospheric interventions are anticipated, i.e., on Moderate sections where atmospheric interventions are anticipated but hyperbaric may also be required and on Unfavorable sections where TBM interventions should be avoided, unless absolutely required. If required then hyperbaric conditions should be applied. Figure 5 illustrates a typical section of the Foreseen geotechnical profile. The favourable, moderate and unfavourable zones are color coded accordingly.

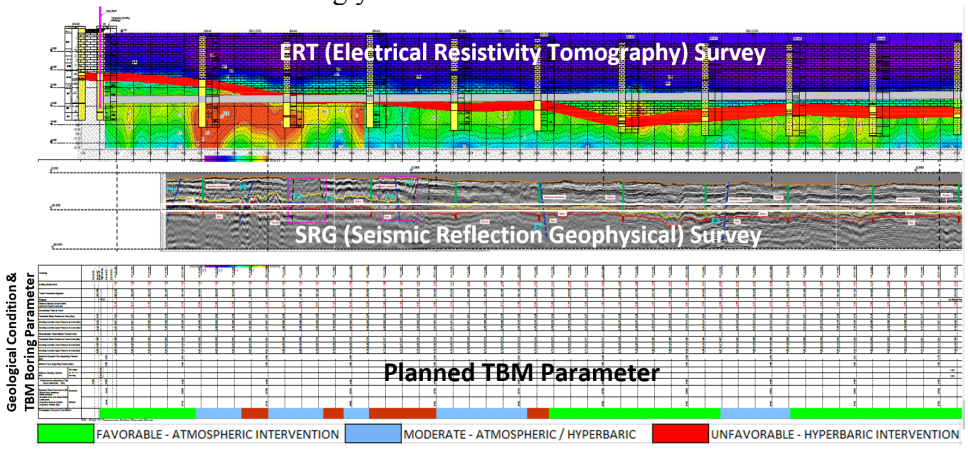

Figure 5: Foreseen geotechnical conditions profile

6 REAL TIME NON-DESTRUCTIVE RADAR STEM (Beam System)

The TBM is provided with a non-intrusive electrical induced polarization prediction system able to provide predictions of the ground conditions and interpretations up to three tunnel diameters ahead and about 3/2 of the tunnel diameter in real time. The Bore-tunneling Electrical Ahead Monitoring (BEAM) System is based on a geotechnical principle that rock mass has different resistivity at varying frequencies, expressed with the Percentage Frequency Effect (PFE). The information is displayed in a matrix, which

combines both resistivity and PFE.

The interpretation of the matrix, which is shown in Figure 6, is based on the columns and rows; factors on the columns refer to the karst interpretation (P1:P4) while factor on the rows (R3:R1) refer to the possibility of water inflow. There is a computer located in the TBM operators' cabin where the information and interpretation are shown on real time as the TBM moves forward, the TBM operator can monitor and correlate with other parameters.

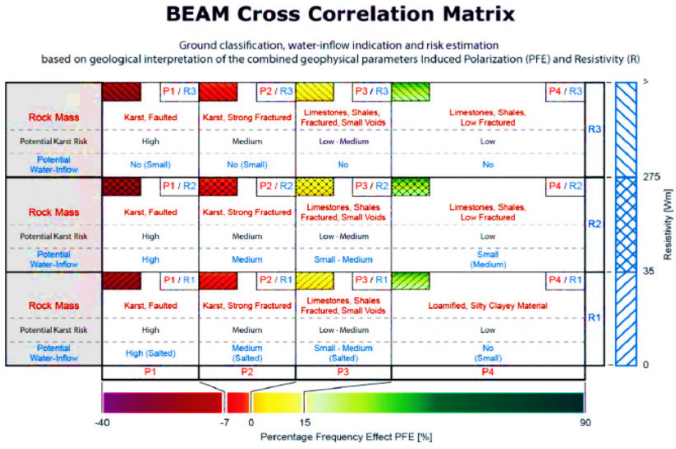

Figure 6: Beam Matrix

Figure 7 shows the real time Beam display, the TBM passing through an area in which the rocks mass is limestone, fracture with small voids, potential karst risk is low-medium and potential aquifer risk is small-medium.

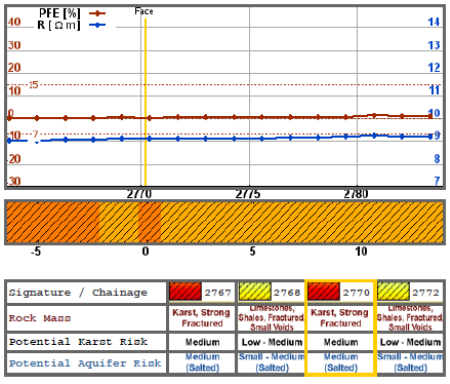

Figure 7: Beam Display

However, in Figure 8 the TBM is shown tunneling in a rock mass with higher potential risk of karts and aquifer, this particular location referes to a previously indentified fault F7. The interpretation coming out from the matrix must be compared with some specific parameters in the TBM, like torque, thrust force, penetration rates, advance speed and cutterhead rotation speed among others.

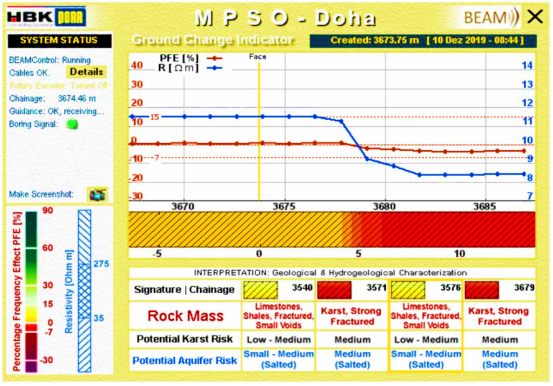

Figure 8: Beam Display for F7

It is important to note that there are limitations on the precision accuracy of the system. The system is not able to identify whether the TBM is passing through Rus formation, Midra Shale or Simsima limestone, it can only identify intrinsic properties of rock mass. It is not also possible to measure the exact amount of water inflow and location. The system can provide an estimation of the possibility that water inflow or aquifers might be encountered. The system can show fractures and cavities that are not found during tunneling because the volume of the tunnel measure is 3/2 of the tunnel volume.

7 TBM PROGRESS TO DATE

TBM tunneling operations commenced February 2019, have encountered so far as foreseen, 1 km of Rus formation, then 0.8 km of Midra Shale formation and 2.0 km of Simsima Limestone, which is expected to continue until the tunnel is completed and reaches the riser shaft. The transition zones between the formation of the tunnel crosses through mixed geological conditions between Rus formation and Midra shale have been characterized by the absence of ground water and presence of limestone bands with gypsum lenses and calcite veins. Those geotechnical factors found along Midra shale constrained the performance of the TBM in terms of advance rates. The torque of the TBM increased up to 75 % of its nominal capacity, the penetration rates were very low around 4 to 5 mm per rpm, the injection of water in the excavation chamber reached 20 m3 per ring and parameters related to foam FIR, FER and CF were duplicated and sometimes triplicated to reach an acceptable soil conditioning. However, it was not possible to avoid scenarios of clogging in the cutter-head and several damages on the cutting tools which required a high number of cutter-head interventions in atmospheric conditions. Logistics in the tunnel were tremendously affected, that required a re-configuration of the trains regarding the number of skips required to dispose the solid due to higher swelling value. The installation of the California switch was anticipated to reduce the idle TBM time during train changing. The encountered geological fracture zones F7 and F8, forced the TBM to operate in full hydrostatics pressure from 3.4 to 3.8 bar, reducing the advance rates.

In both cases, geotechnical engineers and TBM team were monitoring and correlating

the geotechnical profile and BEAM system profiles to adjust and optimize the performance of the TBM via drive instructions.

8 CONCLUSION

As tunneling work is considered as a highly challenging project, because it is constructed in subsea conditions, has a small inner diameter (3700mm), a very long length (10,200m) and has no intermediate access points. The need for comprehensive, accurate and in-depth geotechnical information is critical to a successful tunnel completion. There is no single advance ground investigation method that can completely predict the ground conditions in front of a TBM. There are however several systems that can give an insight into a aspect of the geological conditions that lie in front of the TBM. When the results of these methods are integrated, the prediction can be comprehensive.

On this project, the key issue was the cross correlation with other methods and observed geology in a standard format which allows the identification of patterns and trends. This may well be unique to this project.

REFERENCES

Qatar Construction Specifications (QCS) (2014). Revision IV.

Public Works Authority (2017). *Professional Services Agreement for Professional Consultancy Services - Post Contract Professional Consultancy Services*, Project CP 671/2, Musaimeer Pumping Station and Outfall, Project ID: IA 2016 S 005 G, Contract Number: P2017/22. www.ashghal.gov.qa

Public Works Authority (2017). *Contract Documents for Design, Build, Operate and Maintain of Musaimeer Pumping Station and Outfall*, PROJECT ID: IA 14/15 C 015 G, Contract Number: C2017/109.www.ashghal.gov.qa

The British Standards Institution (2011). *BS 6164:2011 Code of practice for health and safety in tunnelling in the Construction industry*, BSI Standards Publication, London.www.bsigroup.com

Health and Safety Executive (UK) (1996). A guide to work in the Compressed Air Regulations (SI 1996/1656). www.hse.gov.uk

Cite this article as: Peach G., Hrnjak M., Papadatos I., Vigil H., "Geotechnical Aspects of Sub-Sea Tunnelling on the Musaimeer Pumping Station and Outfall Tunnel Project", *International Conference on Civil Infrastructure and Construction (CIC 2020)*, Doha, Qatar, 2-5 February 2020, DOI: https://doi.org/10.29117/cic.2020.0091

Impact of Ionic Strength on Colloid Retention in a Porous Media: A Micromodel Study

Safna Nishad
sn1518223@qu.edu.qa
Department of Civil and Architectural Engineering, Qatar University, Doha, Qatar

Riyadh I. Al-Raoush
riyadh@qu.edu.qa
Department of Civil and Architectural Engineering, Qatar University, Doha, Qatar

ABSTRACT

Release of deposited colloids in the soil porous media during two-phase flow poses potential health hazard due to the facilitated transport of contaminants towards groundwater reservoirs. Considerable uncertainties exist concerning the impact of ionic strength on pore-scale mechanisms of colloid mobilization during transient flow. This study aims to investigate the effect of ionic strength on colloid retention and mobilization using a glass micromodel. The behavior of Carboxylate modified Polystyrene latex particles of 5 μm diameter in saline solution (i.e., 100 mM & 1 mM of NaCl at pH 10) was visualized with an optical microscope during saturated and two-phase flow. We found that colloid aggregation and attachment on Solid-Water Interfaces (SWI) was increased with increase in ionic strength. CO2 injection into the saturated micromodel mobilized the previously attached colloids on SWI, retained at the Gas-Water Interfaces (GWI) due to capillary forces and thus were transported through the micromodel. Imbibition mobilize colloids from GWI and are transported or reattached on SWI depending on the ionic strength of pore water. The greater adhesive forces of colloids at higher ionic strength was resulted in thin film attachment during drainage and reattachment of colloids mobilized from GWI on SWI during imbibition. The acquired images showed the application of a micromodel for the visualization of colloid retention and re-mobilization through the porous media.

Keywords: Colloid retention; Two-phase flow; Drainage and imbibition; Micromodel study

1 INTRODUCTION

Colloid transport and retention in soil porous media has recently attracted significant attention due to its potential impact on various applications including ground water recharge and contamination, filtration in water and wastewater treatment processes (Crist, Zevi, Mccarthy, Throop & Steenhuis, 2005; Saiers & Lenhart, 2003; Sirivithayapakorn & Keller, 2003). Although the colloids themselves rarely pose environmental challenge, the colloid facilitated transport of pathogens and other contaminants occur naturally within the soil and transmit towards the ground water aquifers through the vadose zone (Syngouna & Chrysikopoulos, 2015; Torkzaban, Tazehkand, Walker & Bradford, 2008). Rapid infiltration during rainfall can significantly reduce the ionic strength of pore water, which decreases the colloid retention on Solid-Water Interfaces (SWI) and facilitate its

transport through the soil (Mesticou, Kacem & Dubujet, 2014, 2016; Pazmino, Trauscht & Johnson, 2014). In addition, higher colloid retention was reported in unsaturated porous media with increase in ionic strength (Mitropoulou, Syngouna & Chrysikopoulos, 2013; Zevi et al., 2009; Zhuang et al., 2010). However, the effect on mobilization of the colloid from SWI by the moving Gas-Water Interfaces (GWI) with the changes in ionic strength has not been addressed before.

Previous studies on mobilization of deposited colloids in the porous media reveal the influence of changes in fluid chemistry and flow rate in saturated porous media and transients in flow in unsaturated systems (Molnar, Johnson, Gerhard, Willson & O'Carroll, 2015; Syngouna & Chrysikopoulos, 2015). The force balance considerations on the attached colloids indicate mobilization occur from the solid surface when the detachment force exceed the adhesion force between colloid and the surfaces. This can occur during low salinity flooding (reduced adhesive forces) and at higher injection rates (increased hydrodynamic drag) in saturated flow systems (Gao et al., 2008; Lazouskaya et al., 2011, 2013).

Several laboratory column and microfluidic studies have shown that drainage and imbibition in unsaturated systems promote colloid mobilization by the moving Gas-Water Interfaces (GWI) (Cheng & Saiers, 2009; Lazouskaya et al., 2011, 2013; Saiers & Lenhart, 2003). Column breakthrough curves have shown that pronounced colloid mobilization during imbibition than drainage (Cheng & Saiers, 2009; Flury & Aramrak, 2017; Zhuang, Tyner & Perfect, 2009; Aramrak, Flury, Harsh, & Zollars, 2014). The repulsive capillary force exceeds adhesion force and because of contact angle hysteresis, smaller capillary force exist at advancing interface resulting in less mobilization during drainage. Conversely, visualization experiments on capillary channels reveal comparatively higher mobilization by the advancing interface rather than the receding interface (Aramrak, Flury & Harsh, 2011; Lazouskaya et al., 2013). Strength of colloid attachment on SWI might be contributing to the above contradicting behavior. Visualization study considering different force conditions on a deposited colloid would help to clear the inconsistency in the previous results.

Therefore, the objective of this work is to explore the effect of ionic strength on colloid mobilization during drainage and imbibition in a micromodel. The visualization study was conducted on retention and remobilization of colloids during transient flow conditions at two different ionic strength.

2 MATERIALS AND METHODS

Carboxylate Modified Polystyrene (CMPS) latex mono-spheres was employed in the experiments with diameter of 5-μm and particle density of 1.05 g/cm^3 (MAGSPHERE INC., Pasadena, CA). 0.5 % colloid suspensions were prepared by diluting the stock solution (10% solids) with brine solution. The ionic strength of brine solution was changed by adding NaCl in to deionized water to obtain 1 mM and 100 mM salinity. The pH of the colloid suspension was maintained as 10 by adding 0.1 M NaOH. Colloid suspension was sonicated in a water bath for 30 minutes prior to each experiment using ultrasonic processor (SONICS, Vibra cell) to achieve dispersion. The zeta potential of the colloids in brine solutions was measured by a zetasizer (Nano ZSP, Malvern Panalytical, Southborough, MA) at 22^{0}C and was obtained as -10.40 & -5.28 mV. CO_2 gas was used

as the non-wetting phase in drainage and imbibition studies.

The micromodel used in the experiments was fabricated by Micronit Microfluidics BV on glass plates to represent porous media. The etched area of the micromodel was measured 20 mm x 10 mm with an etch depth of 20-µm. The surface of the microfluidic channel was hydrophilic with an average contact angle 20^0. The pore volume, porosity and permeability of the micromodel are 2.3 µL, 0.58 and 2.5 Darcy, respectively. The micromodel placed inside the holder along with the connections was placed on a microscope stage (Leica Z6, APO).

The experimental set-up used in this study is shown in Figure 1. All the experiments were performed in three stages. The first stage was to saturate the micromodel with colloids in brine solution using a syringe pump (Kats Scientific, NE-1010). Images of micromodel at several locations were captured using a high-resolution camera (Leica MC170) attached to the microscope. The second stage involved the mobilization of the attached colloids by injecting CO2 at constant pressure of 10 kPa using an ISCO pump (Teledyne ISCO 500 HP) and a high-sensitivity diaphragm-sensing pressure-reducing regulator (Swagelok KLF1CFA412A20000 PR regulator) through the outlet port. A commercial CO2 cylinder (Buzwairgas, 99.99%) was supplied the CO_2 gas to the ISCO pump. Maintaining constant pressure, water drainage was initiated by withdrawing water at a constant rate of 50 µL/min using the syringe pump connected at inlet port of the micromodel. The real time visualization of colloid mobilization from SWI was recorded as videos and the images were captured after attaining steady state conditions. The third stage involved the remobilization of the colloids from GWI by initiating imbibition. Colloid free brine solution was injected into the micromodel using another syringe pump connected through the outlet port with a three-way valve. The mobilization of colloids observed and recorded using the camera during and after imbibition.

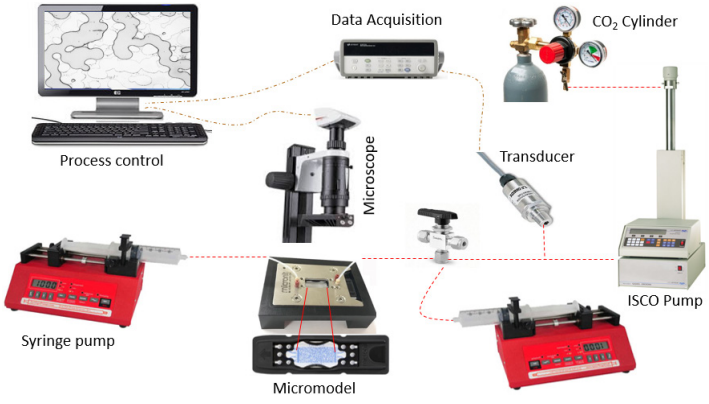

Figure 1: Experimental set-up

3 RESULTS AND DISCUSSION

3.1 Colloid Interaction in Saturated Systems

To examine the role of ionic strength on colloid interaction in saturated porous media, colloid transport experiments were performed at two different ionic strengths; 1 mM and 100 mM of NaCl. The images of the micromodel after first stage are shown in Figure

2 indicate the colloid interaction with other colloids and SWI. The DLVO interaction energies of colloids interacting with other colloids and SWI are calculated as sum of van der Waals and electrostatic forces. The measured zeta potential values are used at two ionic strength conditions. The calculated energy profiles plotted against separation distances and is given in Figure 3.

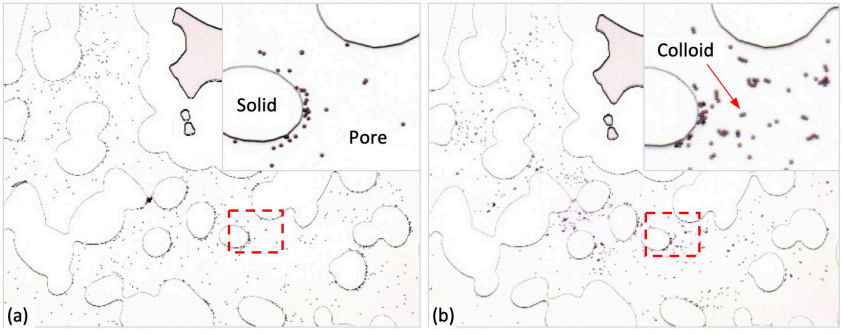

Figure 2: Images of Micromodel saturated with colloids in brine at ionic strength (a) 1 mM and (b) 100 mM

Under saturated conditions, colloid can either attach to SWI or aggregate to form colloid clusters and strain in small pore throats. The aggregation of colloid was observed more at higher ionic strength, whereas attachment on SWI occur irrespective of the ionic strength. Although the DLVO profile shows an energy barrier for colloid interaction with SWI at lower ionic strength, the attachment occurs at a separation distance smaller than 5 nm where primary energy minimum exist (Figure 3). The dispersed colloids in the pore space at lower ionic strength can be explained with the interaction energy profile, where the primary energy minimum exist at very short separation distance. The collision of colloids with previously attached colloids on SWI allow them to interact at these short separation distance and aggregate near the solid surfaces as observed from Figure 2a. Some colloids were attached at the bottom of the micromodel, as the interaction is favorable.

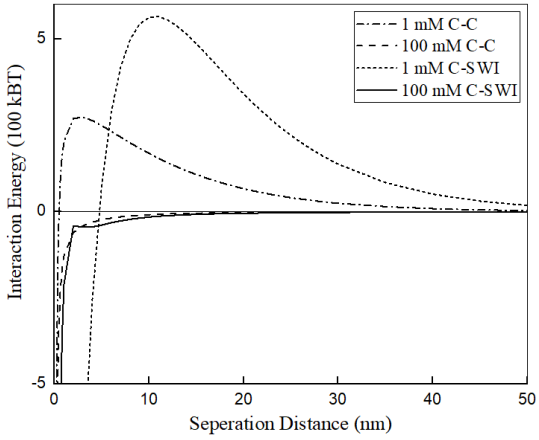

Figure 3: Calculated DLVO energy curve for interaction of colloids with other colloids (C-C) or SWI (C-SWI) at two ionic strengths

3.2 Colloid Mobilization during Drainage

The second stage was started by injecting CO2 at constant pressure and withdrawing pore water at a flow rate of 50 µL/min. Figure 4 shows the images of micromodel captured after attaining steady state CO_2 flow during drainage at two ionic strength. As the interface invade the pore, the porous media was filtered by capturing deposited colloids on GWI as observed from Figure 4. The mobilized colloids remain attached on GWI and were either transported with moving GWI or retained in the porous media with stationary interface. Nevertheless, the random movement of colloids on the interface together with hydrodynamic drag forces rearrange the colloids towards Gas-Water-Solid Interfaces (GWSI) and physically strain there. Further invasion of GWI during drainage was resulted in thin film straining. In addition, colloids are also observed in the gas phase at higher ionic strength (Figure 4b) indicate thin film attachment at top/bottom of the micromodel. The excess particles on GWI shift towards GWSI at top/bottom of the micromodel and retained in thin films as the interface invade the pore. This film retention was observed only at higher ionic strength condition.

The force balance of deposited colloid at GWSI was considered to predict the mobilization from SWI. The adhesion force between the colloids and SWI (DLVO forces) was estimated to be -3 x 10^{-9} and -1.2 x 10^{-8} N for 1 mM and 100 mM ionic strength cases, respectively. The negative sign indicates attraction towards SWI. The drag force on partially saturated media is trivial compared to other forces (Lazouskaya et al., 2013; Shang, Flury, Chen & Zhuang, 2008). The maximum capillary force determined using Equation 1 (Lazouskaya et al., 2013) was 5.5 x 10^{-8} and -1.7 x 10^{-6} for drainage and imbibition front, respectively. Schematic of forces acting on colloid at drainage and imbibition front are shown in Figure 5.

$$F_c = 2\pi r\sigma \sin\varphi \sin(\theta - \varphi) \qquad [1]$$

where r is the radius of colloid, σ is the surface tension, θ is the colloid contact angle and φ is the angle determining position of GWI on colloid surface.

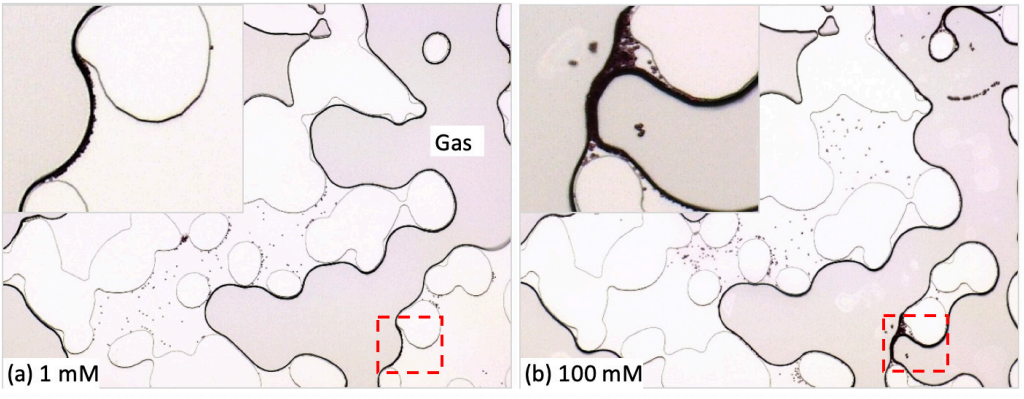

Figure 4: Images of Micromodel after injecting CO2. At lower ionic strength colloids were mobilized by moving GWI while at higher ionic strength, colloids were also retained in thin water films

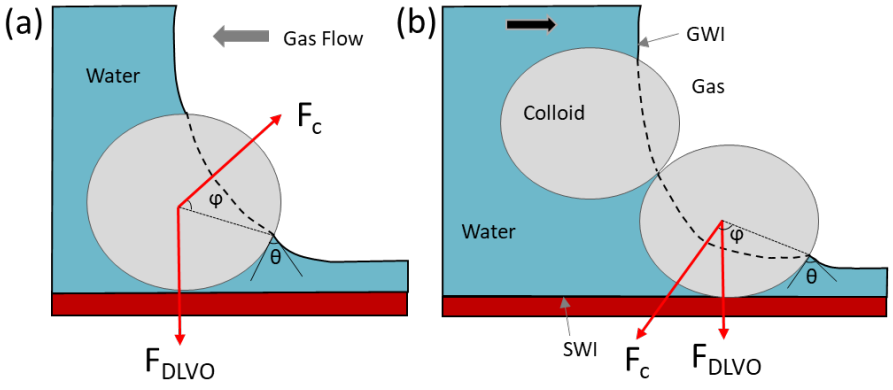

Figure 5: Schematic of forces acting on colloids at GWI: (a) drainage front (b) imbibition front

The above force calculations indicate the lifting of colloids from SWI by the capillary force associated with drainage front for two cases. This is consistent with the reported mobilization of colloids from a surface by capillary forces. Although deposited colloids were mobilized during drainage, the transport occur only with moving GWI. The trapped colloids at stationary gas interfaces can be only mobilized if transients in flow occur.

The colloids more than the GWI capacity shift to GWSI and thin film attachment occur with the advancing interface at higher ionic strength due to the higher adhesion forces, whereas at lower ionic strength those colloids were released back to bulk water. Therefore, breakthrough of colloids at lower ionic strength will be more compared to higher ionic strength due to lower retention on GWSI and thin films.

3.3 Colloid Mobilization from GWI during Imbibition

At the end of second stage, brine was injected into the micromodel at similar flow rate to initiate third stage. The displacement of gas by water (i.e., imbibition) resulted in remobilization of colloids retained on GWI. The advancing front of GWI transports the colloids along with the interface, whereas the receding front releases the excess colloids back to bulk water at lower ionic strength and reattach on SWI at higher ionic strength as shown in Figure 6 & 7. The excess colloids shifted towards GWSI released from the interface due to the horizontal component of the capillary force (Figure 5b). The comparatively lower adhesion forces of colloids at lower ionic strength transport them through the porous media and can deposit on SWI downstream. It is likely that higher ionic strength increase the adhesion force and pose greater affinity towards SWI resulting in reattachment immediately after released from GWI (Figure 7). Thereby reduce the colloid breakthrough after imbibition at higher ionic strength rather than the expected increased release. Our results suggest that the mobilization and retention of colloids were affected by the ionic strength as the adhesive forces play an important role in the detachment of colloid.

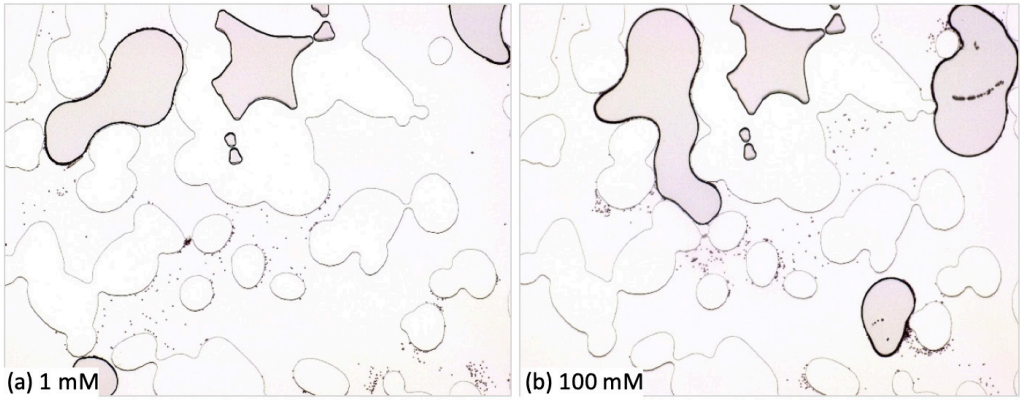

Figure 6: Images of Micromodel after imbibition. At lower ionic strength colloids were released back to bulk water while at higher ionic strength colloids were reattached on solid surfaces

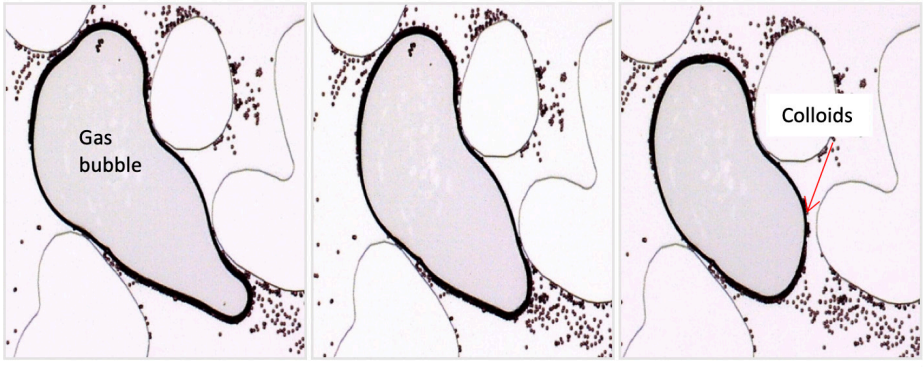

Figure 7: Snapshots of dissolution of Gas bubble (CO_2) during imbibition at higher ionic strength. The excess particles on GWI reattach on SWI (bottom of the micromodel), as the adhesive forces were greater

4 CONCLUSION

This study shows that increasing the ionic strength can be an effective way to control colloid transport and remobilization in porous media. The main conclusions from this study are as follows:

1. The interaction of colloids with other colloids and SWI increases with increase in ionic strength of the solution.
2. Although colloid mobilization by GWI was observed at all ionic strength conditions, immobilization at thin films and stationary GWSIs are more at higher ionic strength due to the higher adhesive forces.
3. Remobilization of colloids from GWI during imbibition was resulted in transport of colloids in the porous media and reattachment on SWI at higher ionic strength.
4. Greater release of contaminants or pathogens attached on SWI or GWI can be expected during drainage or imbibition at lower ionic strength than at higher ionic strength.

ACKNOWLEDGMENT

This publication was made possible by partial funding from NPRP grant # NPRP8-594-2-244 from the Qatar National Research Fund (a member of Qatar Foundation). Any opinions, findings, and conclusions or recommendations expressed in this material are those of the authors and do not necessarily reflect the views of funding agencies.

REFERENCES

Aramrak, S., Flury, M., Harsh, J. B. & Zollars, R. L. (2014). Colloid mobilization and transport during capillary fringe fluctuations. *Environmental Science & Technology*, *48*(13), 7272-7279.

Aramrak, S., Flury, M. & Harsh, J. B. (2014). Detachment of Deposited Colloids by Advancing and Receding Air–Water Interfaces. *Langmuir*, *27*(16), 9985-9993.

Cheng, T. & Saiers, J. E. (2009). Mobilization and transport of in situ colloids during drainage and imbibition of partially saturated sediments. *Water Resources Research*, *45*(8), 1-14. https://doi.org/10.1029/2008WR007494.

Crist, J. T., Zevi, Y., Mccarthy, J. F., Throop, J. A. & Steenhuis, T. S. (2005). Transport and Retention Mechanisms of Colloids in Partially Saturated Porous Media. *4* (2000), 184-195.

Flury, M. & Aramrak, S. (2017). Role of air-water interfaces in colloid transport in porous media: A review. *Water Resources Research*, *53*(7), 5247-5275.

Gao, B., Steenhuis, T. S., Zevi, Y., Morales, V. L., Nieber, J. L., Richards, B. K. … & Parlange, J. (2008). Capillary retention of colloids in unsaturated porous media. *Water Resources Research*, *44*(4).

Lazouskaya, V., Wang, L.-P., Gao, H., Shi, X., Czymmek, K. & Jin, Y. (2011). Pore-scale investigation of colloid retention and mobilization in the presence of a moving air–water interface. *Vadose Zone Journal*, *10*(4), 1250-1260.

Lazouskaya, V., Wang, L.-P., Or, D., Wang, G., Caplan, J. L. & Jin, Y. (2013). Colloid mobilization by fluid displacement fronts in channels. *Journal of Colloid and Interface Science*, 406, 44-50.

Mesticou, Z., Kacem, M. & Dubujet, P. (2014). Influence of ionic strength and flow rate on silt particle deposition and release in saturated porous medium: experiment and modeling. *Transport in Porous Media*, *103*(1), 1-24.

Mesticou, Z., Kacem, M. & Dubujet, P. (2016). Coupling effects of flow velocity and ionic strength on the clogging of a saturated porous medium. *Transport in Porous Media*, *112*(1), 265–282.

Mitropoulou, P. N., Syngouna, V. I. & Chrysikopoulos, C. V. (2013). Transport of colloids in unsaturated packed columns: Role of ionic strength and sand grain size. *Chemical Engineering Journal*, 232, 237-248. https://doi.org/10.1016/j.cej.2013.07.093.

Molnar, I. L., Johnson, W. P., Gerhard, J. I., Willson, C. S. & O'Carroll, D. M. (2015). Predicting colloid transport through saturated porous media: A critical review. *Water Resources Research*, *51*(9), 6804-6845.

Pazmino, E., Trauscht, J. & Johnson, W. P. (2014). Release of colloids from primary minimum contact under unfavorable conditions by perturbations in ionic strength and flow rate. *Environmental Science & Technology*, *48*(16), 9227-9235.

Saiers, J. E. & Lenhart, J. J. (2003). Colloid mobilization and transport within unsaturated porous media under transient-flow conditions. *39*(1). https://doi.org/10.1029/2002WR001370.

Shang, J., Flury, M., Chen, G. & Zhuang, J. (2008). Impact of flow rate, water content, and capillary forces on in situ colloid mobilization during infiltration in unsaturated sediments. *Water Resources Research*, *44*(6), 1-12. https://doi.org/10.1029/2007WR006516.

Sirivithayapakorn, S. & Keller, A. (2003). Transport of colloids in unsaturated porous media : A pore-scale observation of processes during the dissolution of air-water interface. *39*(12). https://doi.org/10.1029/2003WR002487.

Syngouna, V. I. & Chrysikopoulos, C. V. (2015). Experimental investigation of virus and clay particles cotransport in partially saturated columns packed with glass beads. *Journal of Colloid and Interface Science*, 440, 140-150.

Torkzaban, S., Tazehkand, S. S., Walker, S. L. & Bradford, S. A. (2008). Transport and fate of bacteria in porous media: Coupled effects of chemical conditions and pore space geometry. *Water Resources Research*, *44*(4).

Zevi, Y., Dathe, A., Gao, B., Zhang, W., Richards, B. K. & Steenhuis, T. S. (2009). Transport and retention of colloidal particles in partially saturated porous media: Effect of ionic strength. *Water Resources Research*, *45*(12).

Zhuang, J., Goeppert, N., Tu, C., McCarthy, J., Perfect, E. & McKay, L. (2010). Colloid transport with wetting fronts: Interactive effects of solution surface tension and ionic strength. *Water Research*, *44*(4), 1270-1278.

Zhuang, J., Tyner, J. S. & Perfect, E. (2009). Colloid transport and remobilization in porous media during infiltration and drainage. *Journal of Hydrology*, *377*(1-2), 112-119. https://doi.org/10.1016/j.jhydrol.2009.08.011.

Cite this article as: Nishad S., Al-Raoush R. I., "Impact of Ionic Strength on Colloid Retention in a Porous Media: A Micromodel Study", *International Conference on Civil Infrastructure and Construction (CIC 2020)*,DOI:https://doi.org/10.29117/cic.2020.0092

Treatment of Wastewater Using Reverse Osmosis for Irrigation Purposes

MhdAmmar Hafiz
mh1201889@qu.edu.qa
Department of Civil and Architectural Engineering, Qatar University, Doha, Qatar

Alaa H. Hawari
a.hawari@qu.edu.qa
Department of Civil and Architectural Engineering, Qatar University, Doha, Qatar

Radwan Alfahel
ra1404482@qu.edu.qa
Department of Civil and Architectural Engineering, Qatar University, Doha, Qatar

ABSTRACT

This work investigates the performance of reverse osmosis (RO) for the reclamation of treated sewage effluent (TSE) to be used as irrigation water for food crops. The feed water used in this study was a real sample of ultra-filtered tertiary treated sewage effluent (TSE). Reverse osmosis (RO) was evaluated using the following experimental conditions; applied pressure (10 – 20) bar, flow rate 3.5 LPM and (BW30LE) membrane. The performance of RO was evaluated according to the water flux and rejection of dissolved solids. The final water quality was compared with irrigation water standards. The results reported in this study show that reverse osmosis (RO) is capable of reclaiming treated sewage effluent (TSE) to be used as irrigation water for food crops. The maximum average flux was 77.7 LMH achieved using a feed pressure of 16 bar. The permeate water generated using RO had high quality which met the irrigation standards for food crops.

Keywords: Irrigation water; Reverse osmosis; Wastewater treatment

1 INTRODUCTION

Water scarcity is one of the most challenging problems that affect agriculture worldwide, especially in arid areas. The United Nations estimate that agriculture accounts for 70% of water usage around the world (Hafiz et al., 2019). Treated wastewater is an economical solution to be used as irrigation water (Shanmuganathan et al., 2015). However, treated wastewater may damage the soil because of the excessive salts, pathogens, organics, sodium and chloride content. Shanmuganathan et al. (2015) studied the possibility of enhancing the quality of micro-filtered treated sewage effluent using nanofiltration (NF) and reverse osmosis (RO). The study showed that using NF and RO alone could not produce permeate which meets irrigation standards. However, irrigation suitable permeate was produced using a NF-RO hybrid system. In addition, it was found that utilizing NF before RO reduced the RO membrane fouling. Liu et al. (2011) evaluated the effectiveness of nanofiltration and reverse osmosis in the treatment of treated textile effluent in terms of salinity reduction and COD rejection (Liu et al., 2011). The results showed that nanofiltration exhibited more severe flux decline compared to reverse

osmosis (RO) because of the higher porosity and membrane fouling of the nanofiltration membrane. RO showed higher total salts rejection compared to NF. The study evaluated the effect of operating pressure and feed solution pH. The experimental results showed that optimum performance was achieved using a 12 bar pressure, pH = 4 and a flow rate of 8 LPM. Protein-like substances of high molecular weight (MW) are the dominant foulants on the membrane surface (Liu et al., 2011).

Several studies have been performed on the treatment of sewage effluent using reverse osmosis; however, none of the studies have evaluated the performance of reverse osmosis for the reclamation of ultra-filtered tertiary treated sewage effluent to be used in irrigation for food crops. The objective of this paper is to evaluate the feasibility of using reverse osmosis in reclaiming ultra-filtered tertiary treated sewage effluent to be used as irrigation water for food crops.

2 MATERIALS AND SETUP

Tertiary treated sewage effluent (TSE) was used as feed water to the reverse osmosis process. TSE was collected from a wastewater treatment plant located in Doha, Qatar. The characteristics of the collected treated sewage effluent are summarized in Table 1. The water quality was compared with FAO standards (Lejalem et al., 2018; Parlar et al., 2019). TDS of tertiary treated TSE was 1461 ppm which is almost two times higher than the allowable limit. The electrical conductivity was 2.56 mS/cm which is 3 times higher than the allowable limit. Figure 1 shows a schematic diagram for the experimental setup.

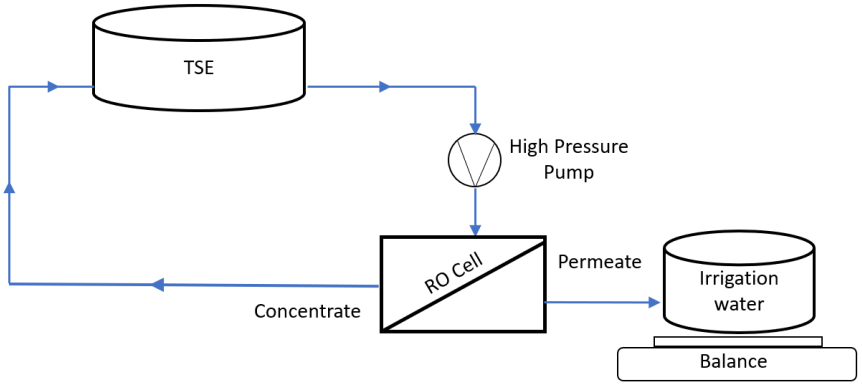

Figure 1: Schematic diagram of reverse osmosis lab scale test skid

Table 1: Characteristics of tertiary treated sewage effluent (feed water)

Parameter	Value	Limit
TDS (ppm)	1461 ± 5	750
Turbidity (NTU)	0.2 ± 0.1	2
EC (mS/cm)	2.56 ± 0.2	0.7

3 RESULTS AND DISCUSSION

The water flux J_w was calculated using the following equation (Thabit et al., 2019):

$$J_w = \left(\frac{V_p}{A_m \times t}\right) \quad (1)$$

Here, V_p is the volume of the permeate (L), A_m is the area of the membrane (m^2), t is the operating time (h). Figure 2 shows the average water flux using different feed pressure. In RO, when the applied pressure was 10 bar, an average water flux of 21.3 LMH was obtained. When the applied pressure increased to 12 bar the water flux increased by 3 times where the average water flux was 68.1 LMH. At a 14 bar applied pressure the water flux increased by 5% compared to the water flux at 12 bar applied pressure where the average water flux was 71.5 LMH. At an applied pressure of 16 bar the average water flux increased to reach an average water flux of 77.7 LMH. As the applied pressure further increased the average water flux decreased. Where at an applied pressure of 18 bar and 20 bar the average water flux was 71.6 LMH and 67.5 LMH, respectively. The average water flux increased as the applied pressure increased until it reached a specific value. The maximum average water flux was obtained at an applied pressure of 16 bar. As the applied pressure increased more than 16 bar the average water flux started decreasing. The water permeability increases as the feed pressure increases; however, applying excessive pressure may result in accumulation of foulants on the membrane surface which results in lower average water flux (Jiang et al., 2017; Qasim et al., 2019).

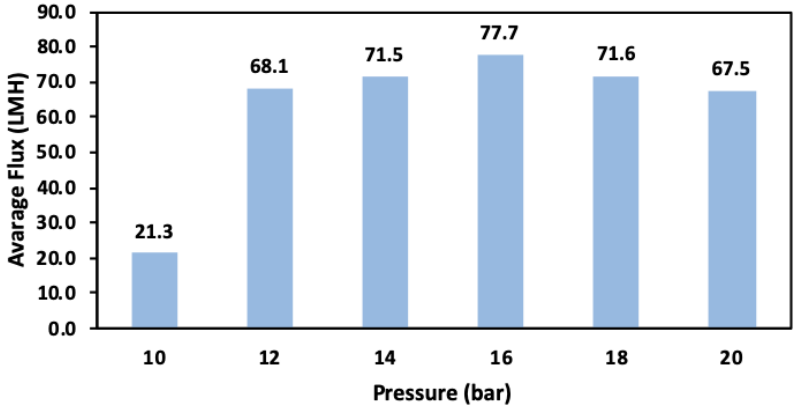

Figure 2: Average water flux using flow rate=3.5 LMP and different feed pressure

Figure 3 shows the total dissolved solids (TDS) concentration in the permeate water. According to Food and Agriculture Organization (FAO), the TDS of irrigation water should not exceed 750 ppm (Ayres & Westcot, 1985). The RO process was effective in reclaiming TSE using feed pressures between 10 -20 bar, where the total dissolved solids was below the allowable limit. The applied pressure has minimal effect on the TDS of permeate water. However, at an applied pressure of 20 bar, TDS increased dramatically to 559 mg/L.

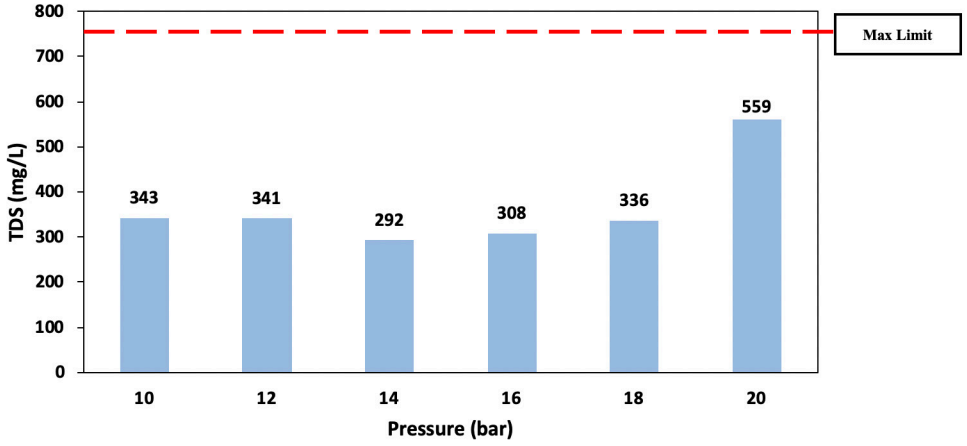

Figure 3: TDS of RO permeate using flow rate=3.5 LMP and different feed pressure

4 CONCLUSION

The results reported in this study show that reverse osmosis (RO) is capable of reclaiming treated sewage effluent (TSE) to be used as irrigation water for food crops. RO is suitable for the reclamation of wastewater because of the high rejection of dissolved ions, where the TDS of permeate water was within the allowable limits recommended by FAO. The most suitable and economical irrigation water was obtained using a feed pressure of 14 bar and flow rate of 3.5 LPM.

ACKNOWLEDGMENTS

This research is made possible by graduate sponsorship research award (GSRA6-1-0509-19021) from Qatar National Research Fund (QNRF). The statements made herein are solely the responsibility of the authors.

REFERENCES

Hafiz, M. A., Hawari, A. H. & Altaee, A. (2019). A hybrid forward osmosis/reverse osmosis process for the supply of fertilizing solution from treated wastewater. *Journal of Water Process Engineering*, 32, 100975.

Jiang, S., Li, Y. & Ladewig, B. P. (2017). A review of reverse osmosis membrane fouling and control strategies. *Science of the Total Environment*, 595, 567-583.

Lejalem, A., Dagnaw, B. C., Zewge, F. & Ababa, A. (2018). Fluoride content of leafy vegetables, irrigation water, and farmland soil in the rift valley and in non-rift valley areas of Ethiopia. *Fluoride*, 50.

Liu, M., Lü, Z., Chen, Z., Yu, S. & Gao, C. (2011). Comparison of reverse osmosis and nanofiltration membranes in the treatment of biologically treated textile effluent for water reuse. *Desalination*, 281, 372-378.

Parlar, I., Hacıfazlıoğlu, M., Kabay, N., Pek, T. Ö. & Yüksel, M. (2019). Performance comparison of reverse osmosis (RO) with integrated nanofiltration (NF) and reverse osmosis process for desalination of MBR effluent. *Journal of Water Process Engineering*, 29, 100640.

Qasim, M., Badrelzaman, M., Darwish, N. N., Darwish, N. A. & Hilal, N. (2019). Reverse osmosis desalination: A state-of-the-art review. *Desalination*, 459, 59-104.

Shanmuganathan, S., Vigneswaran, S., Nguyen, T. V., Loganathan, P. & Kandasamy, J. (2015). Use of nanofiltration and reverse osmosis in reclaiming micro-filtered biologically treated sewage effluent for irrigation. *Desalination*, 364, 119-125.

Thabit, M. S., Hawari, A. H., Ammar, M. H., Zaidi, S., Zaragoza, G. & Altaee, A. (2019). Evaluation of forward osmosis as a pretreatment process for multi stage flash seawater desalination. *Desalination*, 461, 22-29.

Cite this article as: Hafiz M., Hawari A. H., Alfahel R., "Treatment of Wastewater Using Reverse Osmosis for Irrigation Purposes", *International Conference on Civil Infrastructure and Construction (CIC 2020)*, DOI: https://doi.org/10.29117/cic.2020.0093

Impact of Draw Solution Concentration on Forward Osmosis Process: A Simulation Study

Radwan Alfahel
ra1404482@qu.edu.qa
Department of Civil and Architectural Engineering, Qatar University, Doha, Qatar

MhdAmmar Hafiz
mh1201889@qu.edu.qa
Department of Civil and Architectural Engineering, Qatar University, Doha, Qatar

Alaa H. Hawari
a.hawari@qu.edu.qa
Department of Civil and Architectural Engineering, Qatar University, Doha, Qatar

ABSTRACT

In this study, a simulation model was used to evaluate the performance of forward osmosis process. A solution of low salinity was used as the feed solution in forward osmosis to dilute saline solution (i.e. draw solution) for further desalination. The paper evaluated the effect of the draw solution concentration on the recovery rate and energy consumption in forward osmosis. It was found that increasing the concentration of draw solution increased the recovery rate. Also, while increasing concentration of draw solution, energy consumption decreased. The maximum recovery rate of 33% was achieved using (0.5M NaCl) draw solution and a flow rate of 40000 m3/day. The specific power consumption was 0.21 kWh/m3.

Keywords: Forward osmosis; Feed solution; Recovery rate; Power consumption

1 INTRODUCTION

The availability of clean water was one of the sustainable development goals placed forward in the 2030 agenda of the United Nations (Lim et al., 2019). Nowadays, groundwater and seawater are the main sources of water for drinking and irrigation purposes. Membrane technologies have gained much attention for the desalination of seawater and brackish water due to their ability to generate clean water (Greenlee et al., 2009; Hafiz et al., 2019; Heijman et al., 2009; Misdan et al., 2012; Shaffer et al., 2012). Desalination of seawater is usually done using energy intensive processes (i.e., Multistage Flash (MSF) and Reverse Osmosis (RO)) (Elimelech & Phillip, 2011). However, the desalination of wastewater and brackish groundwater consumes a lower amount of energy while using similar technologies. Therefore, low-pressure reverse osmosis and Nano Filtration (NF) have been proposed as convenient technologies for the desalination of brackish water (Phuntsho et al., 2013; Walha et al., 2007). Fouling is considered a major drawback for pressure-driven membrane technologies which increases the operating cost of the process (Guo et al., 2012). Consequently, forward osmosis has attracted more attention because it depends on the osmotic pressure of the draw and feed solution (Lutchmiah et al., 2014). Chen et al. (2017) evaluated the applicability of using the FO process for concentrating wastewater. It was done using

pilot-scale forward osmosis, low strength municipal wastewater as the feed solution and 0.5M NaCl as the draw solution. A spiral-wound membrane module was used to operate the system. 99.8% COD rejection rate, 99.7% total phosphorus rejection rate and 67.8 % of ammonium rejection rate were achieved with a flux of 6 LMH. Phuntsho et al. (2016) evaluated the performance of pilot scale forward osmosis – nano filtration plant which was operated for six months using brackish ground water from the coal mining activities. The study indicate that the hybrid system can produce water quality that meets irrigation standards. The FO feed brine failed to satisfy the discharge effluent standards due to the high concentrations of ammonium and sulfate.

This study investigates the effect of flow rate and draw solution concentration on the performance of forward osmosis process using a numerical simulation model. This was done by estimating the recovery rate and specific power consumption.

2 METHODOLOGY

In forward osmosis, the water flux depends on the osmotic pressure gradient. The osmotic pressure gradient can be estimated by calculating the difference of osmotic pressure between the feed and draw solutions. Therefore, the water flux in the FO process (J_w) can be calculated using equation 1 (Altaee et al., 2016):

$$J_w = A_w \left(\frac{\pi_{Db} e^{\left(\frac{-J_w}{k}\right)} - \pi_{Fb} e^{\left(J_w \frac{S}{D}\right)}}{1 + \frac{B}{J_w}\left(e^{\left(J_w \frac{S}{D}\right)} - e^{\left(\frac{-J_w}{k}\right)} \right)} \right) \quad (1)$$

where, A_w is the membrane permeability coefficient (L/m^2 h bar), π_{Db} and π_{Fb} are the osmotic pressure of the bulk draw and feed solution, respectively (bar); k is the mass transfer coefficient (m/s); B is the solute permeability coefficient (kg/m^2 h); S is the membrane structure (μm), D is the solute diffusion coefficient (m^2/s). The specific power consumption in the FO process, Es, was estimated using equation 2 (Altaee et al., 2016):

$$\text{Es} = \frac{1}{(36 * \eta * Q_p)} \left(P_f Q_{f-in} + P_D Q_{D-in}\right). \quad (2)$$

where, $Q_{f\text{-}in}$ is the feed solution flow rate (m^3/h), P_D is the draw solution feed pressure (bar) and $Q_{D\text{-}in}$ is the draw solution flow rate to the FO membrane (m^3/h). The recovery rate of the forward osmosis process is the ratio of permeate flow rate to the feed flow rate as shown in equation 3 (Altaee et al., 2016).

$$\text{R\%} = \frac{Q_p}{Q_f} \times 100\% \quad (3)$$

where, Q_p is the permeate flow rate (m^3/h), Q_f is the feed solution flow rate (m^3/h).

3 RESULTS AND DISCUSSION

In the simulation study the concentration of the draw solution varied between 0.25 M and 0.5 M NaCl with an increase of 0.05 M for each batch. The feed solution was 0.2 M NaCl. The feed solution flowrate varied between 40,000 m^3/day and 100,000 m^3/day with an increase of 10,000 m^3/day for each batch. DS flowrate was kept at the same flowrate of the feed solution. The effect of draw solution concentration on the recovery rate is shown in Figure 1. The recovery rate was 8.5% using 0.25 M NaCl draw

solution and FS flow rate of 100,000 m^3/day. As the concentration of DS increased to 0.5 M the recovery rate increased to 19.5 %. This is due to the increase in the osmotic pressure gradient. The recovery rate was 29.5% using 0.5 M NaCl draw solution and FS flow rate of 50,000 m^3/day. Generally, the recovery rate increased as the concentration of draw solution increased. The minimum recovery rate was 8.5% using 0.25 M NaCl draw solution and FS flowrate of 40,000 m^3/day, because of the small osmotic pressure gradient between feed solution and draw solution.

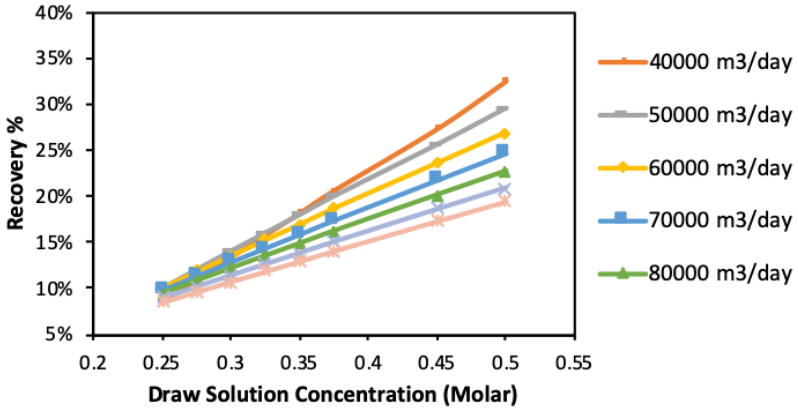

Figure 1: Recovery rate of forward osmosis using different FS flowrate and [0.25 – 0.5 M] NaCl draw solution

The effect of flowrate and draw solution concentration on the specific energy consumption is shown in Figure 2. The maximum specific energy consumption was 0.82 kWh/m^3 using 0.25 M NaCl draw solution and FS flowrate of 100,000 m^3/day. The minimum specific energy consumption was 0.21 kWh/m^3 using 0.5 M NaCl draw solution and FS flow rate of 40,000 m^3/day. Generally, power consumption decreased as the FS concentration increased. The energy consumption decreased as the concentration of draw solution increased.

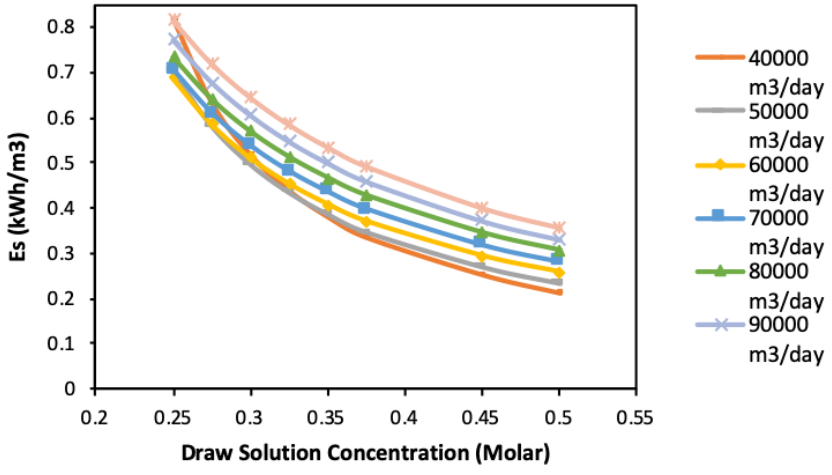

Figure 2: Energy consumption of forward osmosis using different FS flowrate and [0.25 – 0.5 M] NaCl draw solution

4 CONCLUSION

The results reported in this study show that forward osmosis is a promising technology for desalination of saline water. Water recovery of forward osmosis can be enhanced by increasing the DS concentration. Also, the energy consumption can be reduced by increasing the DS concentration.

ACKNOWLEDGMENTS

This research is made possible by Graduate Sponsorship Research Award (GSRA6-1-0509-19021) from Qatar National Research Fund (QNRF). The statements made herein are solely the responsibility of the authors.

REFERENCES

Altaee, A., Millar, G. J., Sharif, A. O. & Zaragoza, G. (2016). Forward osmosis process for supply of fertilizer solutions from seawater using a mixture of draw solutions. *Desalination and Water Treatment*, *57*(58), 28025-28041.

Chen, Z., Luo, J., Wang, Y., Cao, W., Qi, B. & Wan, Y. (2017). A novel membrane-based integrated process for fractionation and reclamation of dairy wastewater. *Chemical Engineering Journal*, 313, 1061-1070.

Elimelech, M. & Phillip, W. A. (2011). The future of seawater desalination: Energy, technology, and the environment. *Science*, *333*(6043), 712.

Greenlee, L. F., Lawler, D. F., Freeman, B. D., Marrot, B. & Moulin, P. (2009). Reverse osmosis desalination: Water sources, technology, and today's challenges. *Water Research*, *43*(9), 2317-2348.

Guo, W., Ngo, H. H. & Li, J. (2012). A mini-review on membrane fouling. Bioresource Technology, 122, 27-34.

Hafiz, M. A., Hawari, A. H. & Altaee, A. (2019). A hybrid forward osmosis/reverse osmosis process for the supply of fertilizing solution from treated wastewater. *Journal of Water Process Engineering*, 32, 100975.

Heijman, S. G. J., Guo, H., Li, S., van Dijk, J. C. & Wessels, L. P. (2009). Zero liquid discharge: Heading for 99% recovery in nanofiltration and reverse osmosis. *Desalination*, *236*(1), 357-362.

Lim, S., Tran, V. H., Akther, N., Phuntsho, S. & Shon, H. K. (2019). Defect-free outer-selective hollow fiber thin-film composite membranes for forward osmosis applications. *Journal of Membrane Science,* 586, 281-291.

Lutchmiah, K., Verliefde, A. R. D., Roest, K., Rietveld, L. C. & Cornelissen, E. R. (2014). Forward osmosis for application in wastewater treatment: A review. *Water Research*, 58, 179-197.

Misdan, N., Lau, W. J. & Ismail, A. F. (2012). Seawater Reverse Osmosis (SWRO) desalination by thin-film composite membrane—Current development, challenges and future prospects. *Desalination*, 287, 228-237.

Phuntsho, S., Hong, S., Elimelech, M. & Shon, H. K. (2013). Forward osmosis desalination of brackish groundwater: Meeting water quality requirements for fertigation by integrating nanofiltration. *Journal of Membrane Science*, 436, 1-15.

Phuntsho, S., Kim, J. E., Johir, M. A. H., Hong, S., Li, Z., Ghaffour, N., Leiknes, T. & Shon, H. K. (2016). Fertiliser drawn forward osmosis process: Pilot-scale desalination of mine impaired

water for fertigation. *Journal of Membrane Science*, 508, 22-31.

Shaffer, D. L., Yip, N. Y., Gilron, J. & Elimelech, M. (2012). Seawater desalination for agriculture by integrated forward and reverse osmosis: Improved product water quality for potentially less energy. *Journal of Membrane Science*, 415-416, 1-8.

Walha, K., Amar, R. B., Firdaous, L., Quéméneur, F. & Jaouen, P. (2007). Brackish groundwater treatment by nano filtration, reverse osmosis and electrodialysis in Tunisia: performance and cost comparison. *Desalination*, *207*(1), 95-106.

Cite this article as: Alfahel R., Hafiz M., Hawari A. H., "Impact of Draw Solution Concentration on Forward Osmosis Process: A Simulation Study", *International Conference on Civil Infrastructure and Construction (CIC 2020)*, Doha, Qatar, 2-5 February 2020, DOI: https://doi.org/10.29117/cic.2020.0094

Utilizing Steel Slag in the Removal of Suspended Solids from Dewatered Construction Water

Alaa Al Hawari
a.hawari@qu.edu.qa
Department of Civil and Architectural Engineering, Qatar University, Doha, Qatar

Abdelrahman Tariq
aa083874@qu.edu.qa
Department of Civil and Architectural Engineering, Qatar University, Doha, Qatar

Ahmed T. Yasir
ay1107095@qu.edu.qa
Department of Civil and Architectural Engineering, Qatar University, Doha, Qatar

Mohamed A. Ayari
arslana@qu.edu.qa
Center for Excellence in Teaching and Learning, Qatar University, Doha, Qatar

ABSTRACT

Construction dewatering is an operation used to remove shallow groundwater that infiltrates construction sites. After recovering this water from the construction sites, the water is either discharged to the sea, injected in deep groundwater aquifers, or treated and reused in some other applications. However, municipal and industrial application of this water is unfeasible due to its poor quality. Thus, in this study, dewatered construction water is being treated utilizing waste steel slag in order to improve the quality of the water. The pH of the dewatered construction water used for this study was 7.59 and the average diameter of steel slag used was 425 nm. For coagulation, the impact of the mass of steel slag and the contact time on the quality of dewatered construction water were studied. By using 5gm/L of steel slag, more than 85% of the total suspended solids and turbidity were removed within 30 minutes.

Keywords: Coagulation; Steel slag; Dewatered construction water; Total suspended solids

1 INTRODUCTION

Deep excavation for construction purposes often results in water seepage from underground reservoirs, especially if the water table is high (Calin, 2017). This water might delay the construction process and damage the infrastructure around the construction site (Serag, 2008). The dewatering process of the construction sites can be done by pumping methods or exclusion methods (Somerville, 2008). Once dewatered, this construction water is generally discharged to the sea (Tchobanoglous, 2001). However, this dewatered construction water has low salinity, low concentration of heavy metals and low concentration of total suspended solid (Hawari, 2018). Thus, this water can be reclaimed by low cost treatment process.

Hawari et al. (2018) treated dewatered construction water using a settling tank and a multimedia sand filter (Hawari, 2018). The dewatered construction water had an initial turbidity of 350 NTU. After 1 hour of settling time, the turbidity reduced to 26 NTU. And

by filtering the dewatered construction water using multimedia sand filter, the turbidity was reduced to 24 NTU (Hawari, 2018). Both technologies showed similar turbidity removal efficiency. The efficiency of the settling process can be improved by adding coagulants. Addition of coagulants would neutralize the surface charge of the colloids and improve coalescence in the water. This will help in forming large flocks of colloids which will settle faster. However, using commercial coagulants will reduce the cost effectiveness of the treatment process. Thus, in this paper the feasibility of using steel slag as a coagulant for the treatment of dewatering construction water was investigated.

Steel slag is a by-product of steel manufacturing industry. Limestone is used as a melting point reducing agent in order to remove the impurities in the iron ore which get deposited as steel slag (Dhoble, 2018). Steel slag is usually generated in large quantities and its disposal poses a significant burden on steel factories (Dhoble, 2018). This waste by-product possesses a porous structure with a high surface area and contains oxides such as FeO-Fe_2O_3-SiO_2-CaO-Al_2O_3. These oxides show characteristics that are similar to coagulants. They have high adsorption capacity and have been used effectively in many studies to remove ammonia, nitrogen, phosphorous and metals from water through adsorption and precipitation (Shilton, 2006; Xiong, 2008; Yi, 2012; Liu, Yuan, 2011). Yin et al. removed 90% of COD from non-degradable organic wastewater using steel slag as a catalyst in an oxidative degradation process (Yin, 2016). Feng et al. used steel slag as an adsorbent to treat acid mine wastewater (Feng, 2004). Since, the density of steel slag is between 3.3 and 3.6 g/cm^3 it can be easily separated from water by gravity settling (Yi, 2012).

Thus, in this study, a coagulation process using steel slag as coagulant is being proposed for reclaiming the dewatered construction water. The effect of concentration of steel slag and the effect of residence time was studied.

2 MATERIAL AND METHOD

2.1 Collection of water samples

Dewatered construction water samples were collected from a construction site located at the Industrial Area, 13 km away from the center of Doha city. Table 1 shows the composition of the dewatering construction water and the method of determination.

Table 1: Properties of the collected dewatering construction water and the determination method

Parameter	Unit	Sample	Testing methods
pH		7.59	SMWW 4500 H+.B
Turbidity	NTU	350	SMWW 2130 B
Total Solids (TS)	ppm	3,015	SMWW 2540 B
Total Suspended Solid (TSS)	ppm	91.2	Hach Method 8006
TDS (Calculated: TS -TSS)	ppm	2,924	SMWW 2540

2.2 Steel slag

The steel slag used in this study was provided by Qatar Steel. The composition of steel slag was analyzed using EDAX. The EDAX analysis in Figure 1 shows that 40% of the total weight of steel slag is made up of iron oxides and calcium oxides. In addition, other metals such as Magnesium (Mg) and Aluminum (Al) are present in small quantities. The steel slag particles have gravel like texture and a blackish color. Moreover, white dust particles are found within the steel slag. In order to remove the dust particles, the slag particles were washed with distilled water. Subsequently, the slag particles were grinded using a Planetary Ball Mill (PM 100 cm, Retsch) for 5 minutes at 500 RMP and then passed through 40-micron filter. Thus, collecting steel slag particles with an average size of 425 µm. The grinded steel slag can be seen in Figure 2.

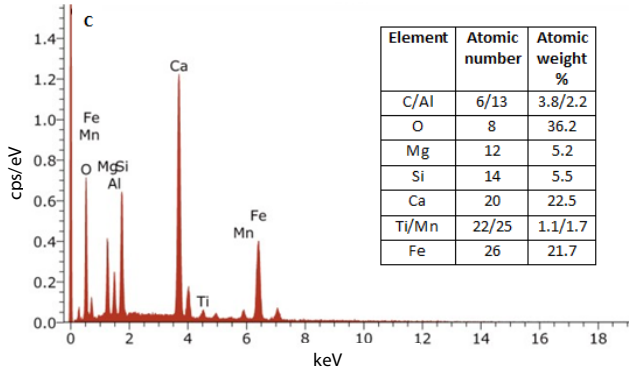

Element	Atomic number	Atomic weight %
C/Al	6/13	3.8/2.2
O	8	36.2
Mg	12	5.2
Si	14	5.5
Ca	20	22.5
Ti/Mn	22/25	1.1/1.7
Fe	26	21.7

Figure 1: EDAX analysis of the slag sample prior to EC

Figure 2: Grinded steel slag sample

2.3 Experimental setup

After collecting the dewatered construction water and characterizing them, the removal of suspended solids was done to improve the turbidity of the water. It was done using jar test apparatus (PHIPPS & BIRD STIRRER 7790-402). The jar test apparatus can accommodate up to 6 beakers at the same time. 600 ml of water sample was added to each beaker in the beginning, this volume is enough to ensure that the stirrers is submerged in the water. After adding the steel slag, the sample was stirred for a fixed amount of time. During this process, the pH of the solution was maintained at 12. After mixing, the samples were allowed to stay still for few minutes for the suspended particles to settle down. After the coagulation process, the turbidity and total suspended solid concentration of the water was measured. The mass of steel slag and the contact time was optimized by repeating the experiment with varying the mass of steel slag

and contact time. After optimizing the process, the coagulation process was repeated with commercial chemical coagulants and its performance was compared with the performance of the proposed coagulant (steel slag).

After the experiment the total suspended solids removal and turbidity removal were calculated as (Hafiz, 2019):

$$TSS\ Removal\ \% = \frac{Original\ Sample\ TSS - Treated\ Sample\ TSS}{Original\ Sample\ TSS}\ x\ 100\% \quad (1)$$

$$Turbidity\ Removal\ \% = \frac{Original\ Sample\ Turbidity - Treated\ Sample\ Turbidity}{Raw\ Sample\ Turbidity}\ x\ 100\% \quad (2)$$

3 RESULTS AND DISCUSSION

3.1 Effect of steel slag concentration

The effect of steel slag concentration on the removal efficiency of total suspended solids (TSS) and turbidity was investigated. The pH of the dewatered construction water was 7.59. The used steel slag particles had a diameter of 425 nm. The test was run for 60 minutes and the TSS removal and turbidity removal were calculated after 60 minutes. The concentration of steel slag used was 5, 10, 15, 20 and 50 mg/L. As seen in Figure 3, when the concentration of steel slag was 5 g/L, the suspended solids removal rate was almost 97%. As the concentration of steel slag increased, the removal rate of suspended solids remained constant. When the concentration of steel slag was 50 mg/L, the removal rate of suspended solids decreased to reach 93.8%. Initially, the removal efficiency of suspended solid was high due to reduction of zeta potential of the water. Reduction of zeta potential reduced the surface charge of the colloids and made Van der Walls's force more dominant in the water. This caused faster agglomeration of colloids and increased TSS removal efficeincy was observed (Shilton, 2006; Xiong, 2008; Yi, 2012; Liu, 2011). Using 5 g/L of steel slag resulted in turbidity removal rate of 97%. The turbidity removal rate did not improve by increasing concentration of the steel slag. On the contrary, increasing the steel slag concentration to 50 gm/L decresed the turbidity removal efficiency to 91.21%. This is because addition of excess steel slag increases the turbidity of the water.

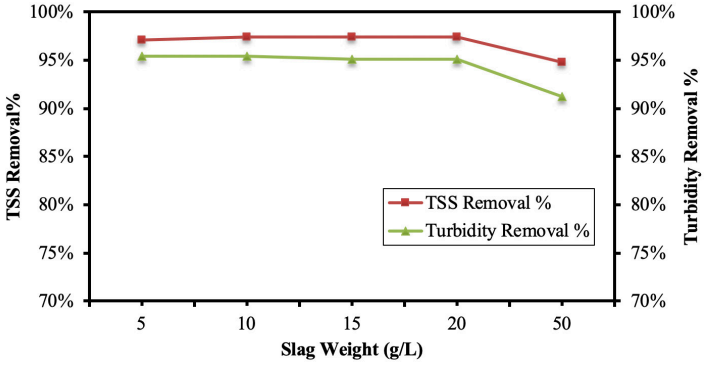

Figure 3: Different weights (g) of 425 nm steel slag turbidity and TSS removal % values

3.2 Effect of contact time

The impact of contact time on total suspended solid (TSS) and turbidity removal rate was also investigated. The concentration of the steel slag was kept constant at 5g/L. The TSS and turbidity removal rates were calculated after 5 minutes, 15 minutes, 30 minutes and 60 minutes of coagulation. Figure 4 shows the TSS and turbidity removal rate at different contact times. It can be seen, that after 5 minutes of contact time, the suspended solids removal rate was almost 60%. As the contact time increased, the removal rate of suspended solids also increased. As the contact time approached 60 minutes, the removal percentage of suspended solids reached about 91.6%. Similar trend can be seen for the turbidity removal rate. After 5 minutes of coagulation, the turbidity removal was 6.1%. The turbidity removal increased and reached 89.6% after 60 minutes of operation. It can be noticed that after 30 minutes of contact time, the TSS and turbidity removal rates do not improve significantly. This is mainly because, all the steel slag added has been used already and to improve TSS and turbidity removal rate, the concentration of steel slag in the water has to be increased.

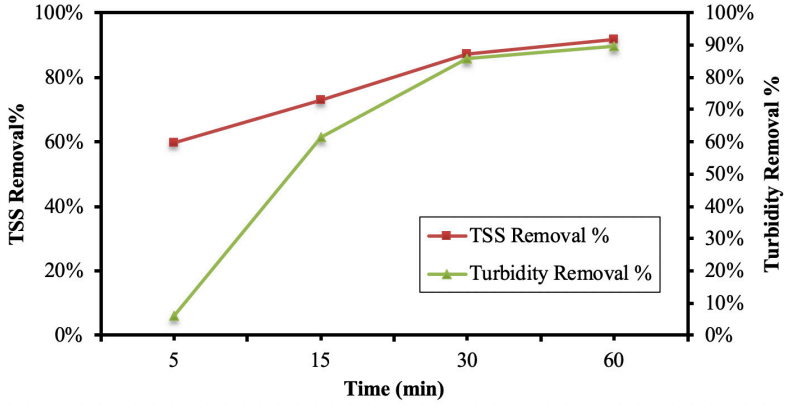

Figure 4: Turbidity and TSS removal % over time range (min) of 425 nm steel slag

4 CONCLUSION

In this study, a coagulation process has been proposed that utilizes steel slag as coagulant for treatment of dewatered construction water. The effect of concentration of the steel slag and contact time for the process on total suspended solid and turbidity removal rates have been studied. The pH of the dewatered construction water was 7.59 and the average radius of steel slag used for this study was 425 nm. The study showed that, by adding 5 gm/L of steel slag, 85% of TSS and turbidity can be removed within 30 minutes. In future, the size of steel slag particle and pH of the water would be studied to improve the performance of the coagulation process. Moreover, the performance of steel slag as coagulant would be compared with commercially available coagulants.

ACKNOWLEDGMENT

The authors would like to thank Qatar University for the financial support. In addition, the authors would like to thank Qatar Steel for the supply of the steel slag samples.

REFERENCES

Calin, N., Radu, C. & Bica, I. (2017). Dewatering system of a deep of excavation in urban area – Bucharest case study. *Procedia Engineering, 209*, 210-215. DOI: https://doi.org/10.1016/j.proeng.2017.11.149.

Dhoble, Y. N. & Ahmed, S. (2018). Review on the innovative uses of steel slag for waste minimization. *Journal of Material Cycles and Waste Management, 20*(3), 1373-1382. DOI: 10.1007/s10163-018-0711-z.

Feng, D., van Deventer, J. S. J. & Aldrich, C. (2004). Removal of pollutants from acid mine wastewater using metallurgical by-product slags. *Separation and Purification Technology, 40*(1), 61-67. DOI: https://doi.org/10.1016/j.seppur.2004.01.003.

Hafiz, M. A., Hawari, A. H. & Altaee, A. (2019). A hybrid forward osmosis/reverse osmosis process for the supply of fertilizing solution from treated wastewater. *Journal of Water Process Engineering, 32*, 100975. DOI: https://doi.org/10.1016/j.jwpe.2019.100975.

Hawari, A. H., Al-Qahoumi, A., Ltaief, A., Zaidi, S. & Altaee, A. (2018). Dilution of seawater using dewatered construction water in a hybrid forward osmosis system. *Journal of Cleaner Production, 195*, 365-373. DOI: https://doi.org/10.1016/j.jclepro.2018.05.211.

Serag, E., Oloufa, A. & Malone, L. (2008). Reconciliation of owner and contractor views in heavy construction projects. *Journal of Professional Issues in Engineering Education and Practice, 134*(1), 128-137. DOI:10.1061/(ASCE)1052-3928(2008)134:1(128).

Shilton, A. N., Elmetri, I., Drizo, A., Pratt, S., Haverkamp, R. G., & Bilby, S. C. (2006). Phosphorus removal by an 'active' slag filter–a decade of full scale experience. *Water Research, 40*(1), 113-118. DOI: https://doi.org/10.1016/j.watres.2005.11.002.

Somerville, S. H. (2008). *Control of Groundwater for Temporary Works*. Retrieved from Construction Industry Research and Information Association (CIRIA).

Tchobanoglous, G., Burton, F. L. & Stensel, H. D. Wastewater Engineering: An Overview. In Wastewater Engineering, Treatment and Reuse (Fourth Edition ed.): Metcalf & Eddy, Inc.

Xiong, J., He, Z., Mahmood, Q., Liu, D., Yang, X. & Islam, E. (2008). Phosphate removal from solution using steel slag through magnetic separation. *Journal of Hazardous Materials, 152*(1), 211-215. DOI: https://doi.org/10.1016/j.jhazmat.2007.06.103.

Yi, H., Xu, G., Cheng, H., Wang, J., Wan, Y., & Chen, H. (2012). An Overview of Utilization of Steel Slag. *Procedia Environmental Sciences, 16*, 791-801. DOI: https://doi.org/10.1016/j.proenv.2012.10.108

Yin, S., Gao, B. & Chen, X. (2016). *Treatment of non-degradable organic wastewater with steel slag catalyst* (Vol. 10).

Yu Liu, S., Yuan Xu, Y., Gao, J., Wei Lu, C. & Jin Yang, Y. (2011). *Preparation and Characterization of Steel Slag Adsorbent* (Vol. 48-49).

Cite this article as: Al Hawari A., Tariq A., Yasir A. T., Ayari M. A., "Utilizing Steel Slag in the Removal of Suspended Solids from Dewatered Construction Water", *International Conference on Civil Infrastructure and Construction (CIC 2020)*, Doha, Qatar, 2-5 February 2020, DOI: https://doi.org/10.29117/cic.2020.0095

Influence of Aspect Ratio on the Bearing Capacity and Correlated Modulus of Subgrade Reaction for Shallow Foundations on Dense Sand

Ramez Alchamaa
ramez.alchamaa@dorsch.com
Dorsch Gruppe, Doha, Qatar

ABSTRACT

One of the most fundamental problems in the field of geotechnical engineering is the prediction of bearing capacity and settlement of shallow foundations on cohesion-less soil subjected to vertical central loading. The fact is that commonly used "SHAPE FACTORS" in the current design practice for estimating the bearing capacity and modulus of subgrade reaction of a shallow foundation are partially empirical values proposed by (Terzaghi, 1943). On the other hand, the current design of shallow foundation on cohesionless soil does not take into consideration the scale effect between the soil particles and foundation geometry. This may result in an excessively conservative design, which in turn results in unnecessary costs of the foundation. Therefore, and to take into account the realistic effect of the three-dimensional mechanism of soil deformation for foundations with various aspect ratios B/L on the shape factor in the classical formulas and theories of ultimate bearing capacity of shallow foundation, a series of small-scale model foundation tests were carried out on a practical type of sand (Toyoura sand) and the three-dimensional mechanism of deformation has been closely monitored and recorded at the end of each performed test. This research presents the main observations and results of the square, rectangular and strip model tests with constant foundation base width B conducted on compacted sand. Finally, the results are presented and compared to those from literature and preliminary conclusions and recommendations are drawn.

Keywords: Model foundation test; Shape factors; Normalized foundation pressure

1 INTRODUCTION

The main objective of this paper is to investigate the bearing capacity of rough and rigid foundations with various shapes and aspect ratios placed on cohesion-less soil (sand) and correlate the modulus of subgrade reaction that is being commonly used for the flexible foundation design. To determine any differences in the behaviors of foundations with various shapes and aspect ratios and quantify these differences, the shape effect was investigated using model-scale square, rectangular and strip foundations with constant width B and various lengths for given homogenous sand properties. The observed behavior from model tests on dense (compacted) sand was presented and the obtained values of the normalized foundation pressure from the model tests results were compared with the commonly used values of bearing capacity factor $N\gamma$ from traditional theories that consider the factor as a dimensionless factor and only related to the unit weight of soil γ and its friction angle φ, where some recent studies by (De Beer, 1970) suggest that $N\gamma$ factor appears to be a dependant factor on other parameters such as the aspect ratio B/L of foundations, foundation width and some other soil properties.

2 MODEL SCALE FOUNDATION TESTS SET-UP AND USED APPARATUS

To fulfill the main goals of this research, a new methodology for testing model-scale of foundations with various shapes was conducted and new mechanical apparatus' was developed in the soil mechanics laboratory at Tokyo Metropolitan University in the period between 2005 and 2007 (Alchamaa et al., 2005). The model foundation tests were all performed on uniformly fine-grained (Toyoura sand) in a test container; having internal dimensions of 60cm in width, 180cm in length and 60cm in-depth and the lateral surfaces made of a transparent material namely (Acrylic-glass) with a thickness of 30mm. To eliminate any potential influence of the friction between the side acrylic walls and the tested sand within the test container on the model test results (especially the case of strip foundation), the sidewalls were well lubricated using a thin transparent film; smeared with a thin layer of waterproof grease; namely, silicone grease as shown in Figure 1.

Figure 1: Lubricating the sidewalls of the test container before forming the sand bed

Moreover, the vertical loads were applied constantly to the foundation models using a loading frame connected to a manually controlled piston as it is shown in Figure 2, the relationship between load and displacement was measured and recorded digitally and saved on a computer utilizing the load and displacement transducers as illustrated in Figure 3.

It is worth to note that the width of foundation models remained constant $B=72\ mm$ in all tests and the aspect ratios were ($L/B=1,\ 1.5,\ 2\ and\ \infty$) respectively in which the distance between the model foundation edge and the sidewalls is 12B in the long direction of the test container. The foundation models were given a rough base and loaded at a constant rate of 0.5mm/minute until a settlement of 0.5B=36mm occurred. Furthermore, the number of formed layers of sand in the test container in each test was about 20 layers on average. To form each layer, the sand was sifted and filtered during pouring into the test container layer by layer using standard test sieve (No. 0.85 mm) to assure that the model foundations are placed on homogenous and uniformly fine-grained layers of sand in the test container. As a next step, each layer was completely prepared flat using some particular apparatus with a thickness of 18 mm and then compacted equally using

a manual vibrator over a thin acrylic plate with no target of specific relative density as demonstrated in Figure 4. Besides, thin layers of black-dyed sand with a thickness of (2 mm) were created to allow a better observation of the vertical displacements at each layer.

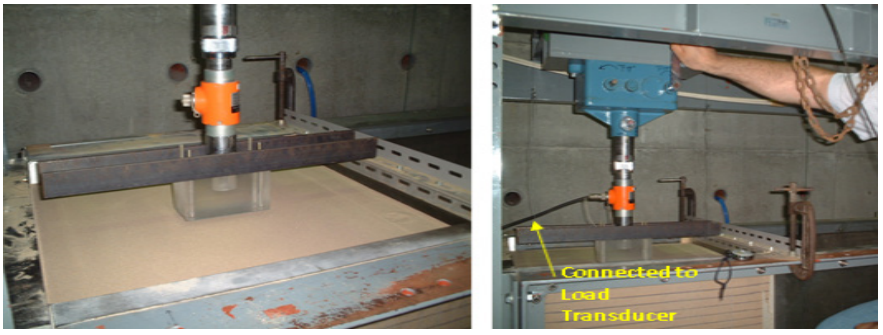

Figure 2: Loading frame and manually controlled piston used for applying vertical loads Constantly to model foundations

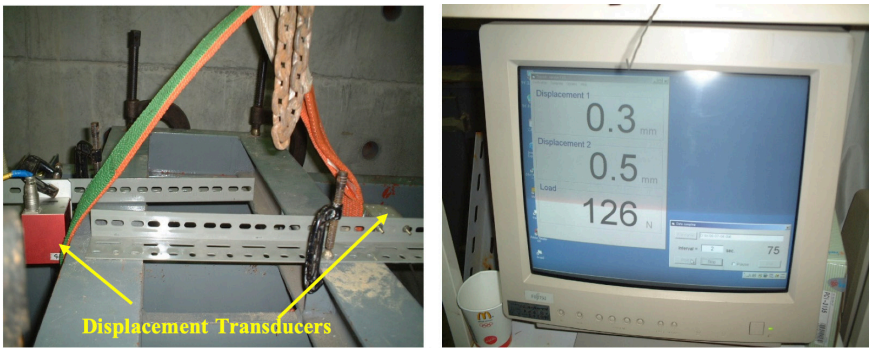

Figure 3: Installation of displacement transducers for measuring and recording the applied loads and resultant displacements

Figure 4: Manually-controlled instrument to form flat sand layers in the test container

3 RESULTS OF LOADING TESTS ON FOUNDATION MODELS, OBSERVATIONS AND DISCUSSION

Theoretically, (Terzaghi, 1943) was the first one who suggested the general equation for determining the ultimate bearing capacity of a centrally loaded strip foundation on the surface of a uniform cohesion-less soil (without overburden soil stress effect) and that with zero cohesion can be simplified from three terms to one term to take the following form:

$$q_{ult} = \frac{1}{2}\gamma B N_\gamma S_\gamma \qquad (1)$$

where: q_{ult} = ultimate bearing capacity; B = foundation width; γ= unit weight of soil; N_γ= bearing capacity factor; and S_γ= foundation shape factor.

For small scale model foundation tests of known geometry, for which an assumed value of S_γ is used (S_γ=1 for strip foundations with L=∞) the only unknown in the previous equation is the bearing capacity factor N_γ, which is considered in the literature by (Meyerhof, 1951) as a dimensionless factor and dependent on the friction angle φ of the soil as stated previously. Moreover, for the series of model foundation tests carried out in this study, the peak point in foundation pressure - foundation penetration curves was simply defined and adopted for the back calculations of the normalized foundation pressure, N_γ.

A summary of the testing conditions and results for each of these model tests is given in Table 1 while the loading test results are shown in Figure 5. The value of (the normalized bearing capacity factor) is used in order to compare all results from different model tests, where $N\gamma_{max}$ is equal to the Nγ at the maximum value of ($2q_{peak}/\gamma B$) vs. the settlement (S) obtained from the model tests, where the maximum settlement S_{max} was about 36mm at the end of all tests as mentioned formerly.

Contrasting the proposed shape factors by (Terzaghi, 1943) that reveal that rectangular foundation capacity should take place between those of the square and strip foundations of the same width, the foundation pressure versus the foundation settlement curves for the series of model tests on sand have evidently demonstrated in Figure 5 that the rectangular foundation with aspect ratio L/B=2 has the highest bearing capacity. Additionally, the results in Table.1 indicate that the square and rectangular foundations with various aspect ratios, namely, L/B=1, 1.5 and 2 have higher bearing capacities than strip foundation of the same width of about 19%, 26% and 61% respectively.

Table 1: Summary of model-scale foundation test results on compacted sand

Foundation shape	**L/B ratio for constant foundation width B=72mm**	**Ultimate bearing capacity $q_{ult=peak}$ (kPa)**	**Settlement at $q_{ult=peak}$ (m)**	**Relative settlement S/B (%) at $q_{ult=peak}$**	**Observed failure condition (Shear failure/ Maximum allowable settlement)**
Square Foundation	1.0	86	0.0033	4.6%	Punching **shear** failure
Rectangular Foundation	1.5	91	0.0045	6.2 %	Local **shear** failure with deformed mass
Rectangular Foundation	2.0	116	0.0050	6.9 %	**Shear** failure with extended deformation
Strip Foundation	∞	72	0.0038	5.3 %	**Shear** failure with many slip surfaces and surface heave

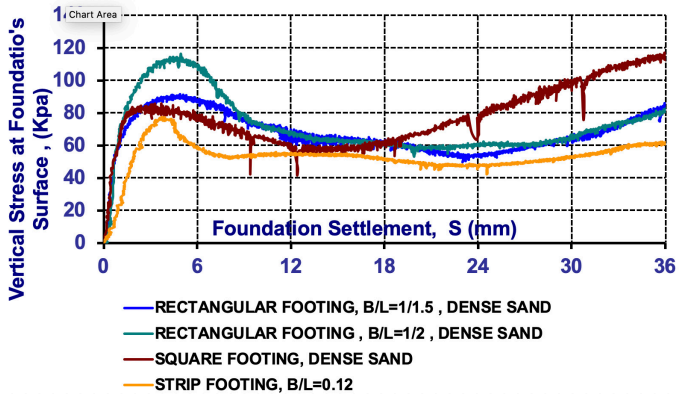

Figure 5: Vertical stress (pressure) at the foundations' surface vs. foundation settlement for model foundation tests on sand

The main observations and results from the model scale foundation tests on dense (compacted) sand are presented as following:

a) Square foundation, (L/B=1):

The major observations from square foundation is that the trace of deformation mechanism was extremely clear. Additionally, a minor heave surface is observed while the deformed mass of soil extends horizontally to a distance (less than 3B) and for about (B) in depth below the foundation; as shown in Figure 6(a).

b) Rectangular foundation, (L/B=1.5):

In this case, the slip surfaces were defined clearly which indicates that the resultant mode of failure (deformation) is about local shear failure. In addition, the slip surfaces extend horizontally up to (2.5 B) and for about (B) in depth below the foundation model, more to the point, a surface heave is observed as demonstrated in Figure 6(b).

c) Rectangular foundation, (L/B=2):

The main observations from this case is that the deformed mass of soil extends laterally to a distantance longer than (3B), while it extends in depth to a shallower distance in comparison to the previously presented cases for about (B). In addition, a significant surface heave is observed and many slip surfaces are defined below and around the foundation model surface; as shown in Figure 6(c).

d) Strip foundation, (L/B= ∞):

The most important observations from the case of strip foundation on dense (compacted) sand, where the plain strain condition was considered as a boundary condition of this model scale foundation test, can be presented as follows:

1. Numerous slip surfaces appeared within the passive wedge of the tested soil and the rigid soil wedge below the foundation as illustrated in Figure 6(d).
2. The observed slip surfaces extend horizontally to a length more than (4B) as shown in Figure 6(d).

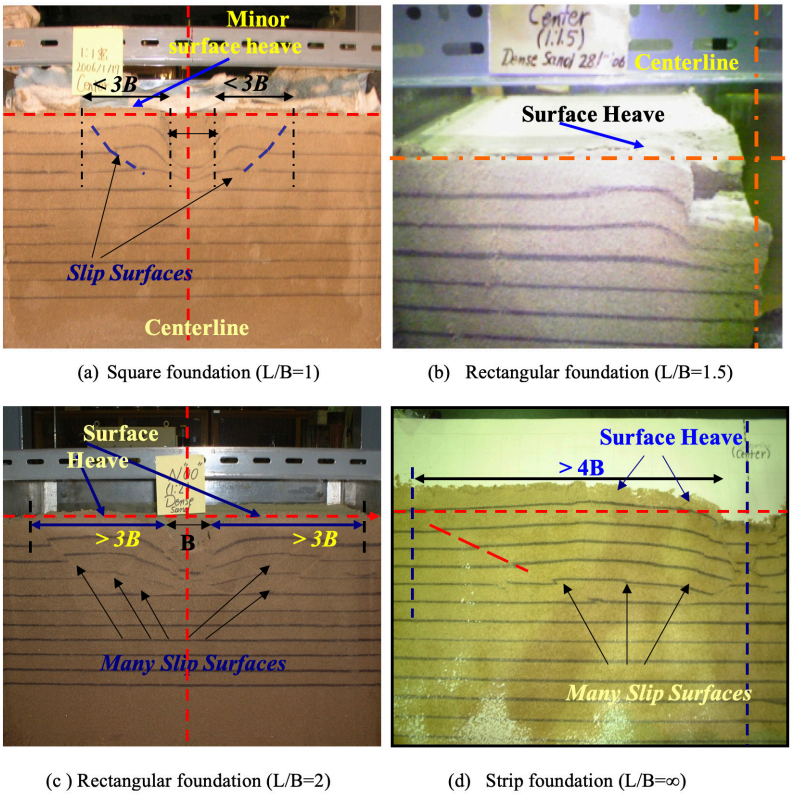

(a) Square foundation (L/B=1) (b) Rectangular foundation (L/B=1.5)

(c) Rectangular foundation (L/B=2) (d) Strip foundation (L/B=∞)

Figure 6: Vertical cross-section at the center of the tested Toyoura sand for (L/B=1, 1.5, 2 and ∞)

However, the bearing capacity of a square foundation (L/B=1) was remarkably larger than that purely under plain strain conditions for (L/B=∞). Furthermore, the observed shapes of triangle wedges (case of strip foundations) and the extension of the deformed volumes of soil from the performed cross-sections were different from those proposed by Terzaghi.

And as a matter of fact, (Terzaghi, 1943) did not consider the existence of the deformed volume of soil that extend widely and deeply around and beneath the foundation in (3D sense) in his theory, which it seems somewhat reflects the influence of foundation shape (foundation behaviour) on the bearing capacity. This would suggest the introduction of new bearing capacity and shape factors that differ from those conservative ones proposed in the literature in addition to a potential correlation to the modulus of subgrade reaction that is widely used in the design of flexible foundations or the slab at grade type of foundation. Stating that the rigid foundation models in this paper are tested under central loads and remained plane when it settled, the modulus of subgrade reaction can be estimated for them by utilizing the soil reaction on the whole surface of the tested foundations as shown in Table 2.

Table 2: Summary of base pressure, displacement, and modulus of subgrade reaction of model-scale foundations from literature and test results

Foundation shape	L/B ratio for constant foundation width B=72mm	Ultimate bearing capacity $q_{ult=peak}$ (kPa)	Settlement at $q_{ult=peak}$ (m)	Ratio ($q_{ult=peak}$ /S) at q_{ult} (kN/m²/m)	Modulus of subgrade reaction (Ks) by Bowles (1997) Ks= 40*q_{ult} (kN/m³)	Governing Failure Criteria
Square Foundation	1.0	86	0.0033	26060	3440	Shear failure
Rectangular Foundation	1.5	91	0.0045	20222	3640	Shear failure
Rectangular Foundation	2.0	116	0.0050	23200	4640	Shear failure
Strip Foundation	∞	72	0.0038	18947	2880	Shear failure

Table 2 provides an attempt to conclude that the modulus of subgrade reaction is about the bearing capacity (pressure) per unit settlement that means soil capacity to withstand pressure for a given settlement in addition to a comparison between the estimated modulus of subgrade reaction based on the obtained test results on the foundation model tests and the presented equation in literature by (Bowles, 1997) for this purpose as follows:

$$Ks = 40\, q_{ult} \qquad kN/m^3 \qquad (2)$$

where: q_{ult} is the ultimate bearing capacity for an assumed 1 inch or 25 mm settlement

However, it is obvious that there is a significant difference in the magnitude between the estimated values of the modulus of subgrade reaction for all foundation shapes in which the calculated values based on the previous equation are conservative and might have substantial cost implication on some construction projects as the equation has also limitations related to the governing failure criteria, so it cannot be applied to foundations where shear failure occurs before reaching the allowable settlement limit which is the reported case in this study as illustrated in Table 2.

4 CONCLUSION AND RECOMMENDATIONS

The following conclusions can be drawn from the results presented in this study:

- The mode of failure was found to be significantly influenced by the boundary conditions and the foundation shape.
- In contrast to what concluded in literature, that the foundation length does not influence the bearing capacity, 'the maximum pressure on square foundation on sand is equal to that on long strip of the same width' (Golder, 1941), the test results suggest that the square foundation has a higher capacity than the strip foundation of the same width with an evident impact of the foundation length and (L/B) ratio.
- The performed physical model tests conducted on compacted sand show obviously that the least ultimate capacity was obtained from strip foundation tests where the plain strain conditions are purely applied, whilst the square and rectangular foundations have higher capacities.
- In all model tests for foundations placed on compacted sand, the load-settlement curves reached their peak point at values of relative settlement (S/B) less than 10% in which the shear failure governs.
- It is also proved that observed trace on the soil top surface extends widely and deeply

around the foundation edges proportionally with the increase in (L/B) ratios.

- Finally, it is always recommended that engineers should exercise caution before using such equations, also, the structural engineers should consult a geotechnical engineer proficient prior to finalizing soil stiffness and bearing capacity values and probably the selection of the best type and shape of shallow foundations to utilize the maximum capacity of the designed foundations.

REFERENCES

Alchamaa, R., Masaya, Y. & Mitsutoshi, Y. (2005). Deformation and bearing capacity of foundations with various shapes under static loading. *The proceeding of the 60th JSCE Japan Society of Civil Engineers*. (III-174, pp.495-496).

Bowles, Joseph E. (1997). *Foundation analysis and design.* (5th Edition), 1997.

De Beer, E.E. (1970). Experimental determination of the shape factors and the bearing capacity factors of sand. *Géotechnique*, *20*(4), 387-411.

Golder, H.Q. (1941). The ultimate bearing pressure of rectangular footings. *J. Int. Civil Engrs*, 17:161-174.

Meyerhof, G.G. (1951) The Ultimate Bearing Capacity of Foundations. *Geotechnique*, 2, 301-332.

Terzaghi, K. (1943). *Theoretical Soil Mechanics*. Wiley, New York.

Cite this article as: Alchamaa R., "Influence of Aspect Ratio on the Bearing Capacity and Correlated Modulus of Subgrade Reaction for Shallow Foundations on Dense Sand", *International Conference on Civil Infrastructure and Construction (CIC 2020)*, Doha, Qatar, 2-5 February 2020, DOI: https://doi.org/10.29117/cic.2020.0096

Predicted and Back-calculated Coefficients of Permeability of Randomly Fractured Rock Mass: A Case Study

Hisham Eid
heid@qu.edu.qa
Department of Civil and Architectural Engineering, Qatar University, Doha, Qatar

Barry O'Sullivan
bsullivan@hydroservint.com
Hydroserv, Doha, Qatar

Mohammed Elshafie
melshafie@qu.edu.qa
Department of Civil and Architectural Engineering, Qatar University, Doha, Qatar

Reiner Stollberg
r.stollberg@fugro.com
Fugro, Doha, Qatar

Robert Kalin
robert.kalin@strath.ac.uk
Department of Civil and Environmental Engineering, University of Strathclyde, the UK

ABSTRACT

This paper presents the discrepancy between the coefficients of permeability measured for randomly fractured limestone using field falling-head tests and that back-calculated for the same rock mass based on the actual discharge yielded from a dewatering system designed for a typical construction site in Doha, Qatar. The study results showed that the back-calculated coefficient of permeability is outside the range of the values measured from the falling-head tests and almost seven times higher in magnitude than the falling-head tests average. The need of having a reliable correlation that can be used to predict the actual permeability of randomly fractured rock in terms of its rock quality indices and the results of the commonly conducted field falling-head test is highlighted.

Keywords: Dewatering; Field tests; Fractured limestone; Permeability; Rock mass

1 INTRODUCTION

Construction dewatering is an essential activity required for many civil engineering projects. The performance of such activity is mainly dependent on the suitability of the dewatering system to the existing hydrogeological conditions and the accuracy of estimating the permeability of the matrix or material to be dewatered. Design of dewatering systems has become a major task in the construction of hundreds of infrastructure projects built as part of the very rapid and significant development of Greater Doha and along the eastern coast of Qatar. This inevitably involved dewatering of a randomly fractured limestone of Eocene age. Field falling-head permeability tests are commonly used for estimating the permeability of such limestone. This paper presents the subsurface and hydrological conditions of a construction site in Doha, the results from twenty falling-head permeability tests conducted on the site as well as the rock mass permeability that has been back-calculated from the water discharge pumped

out of the designed dewatering system on the site. The project site is located in Lusail, approximately 15 Km north of the centre of Doha, capital of Qatar.

2 CASE DESCRIPTION AND SUBSURFACE CONDITIONS

The case study presented herein involved the design of a dewatering scheme required for constructing a boulevard tunnel and associated excavation. An open excavation with width, length, and depth of 73 m, 884 m, and 14.9 m, respectively, was to be constructed in dry conditions. The groundwater table was encountered at a depth of 7.29 m below ground surface that is located at 3.50 m above Qatar National Height Datum (QNHD). As a result, a drawdown level of -12.40 m was targeted (Fig. 1). The distance to open water (i.e., to the Gulf coast) was about 750 m from the edge of the excavation.

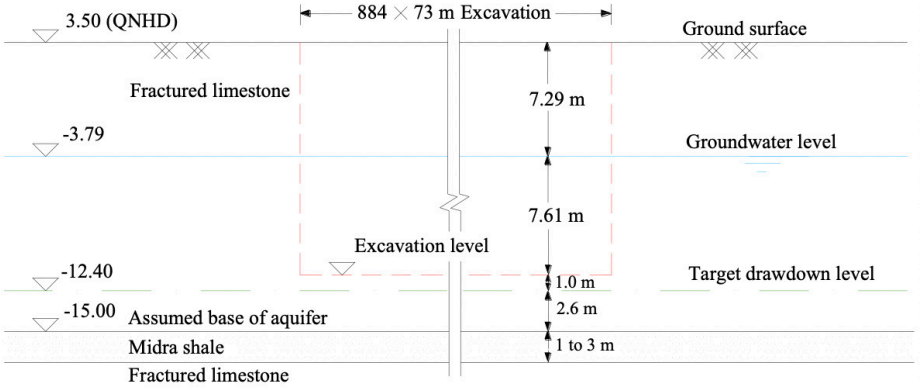

Figure 1: General profile of the dewatering scheme

The subsurface exploration program comprised the excavation of thirty two boreholes and seventeen trail pits located across the project area. Depths of boreholes ranged from 3.5 m to 35 m while the trial pits had a width of 1.5 m and depths ranging between 0.6 m and 1.2 m. The exploration showed that the subsurface profile in the project area starts with 0.5 m of residual soil (typically, silty sand with some gravel and cobbles of limestone) underlain by an extended layer of fractured limestone. The limestone is frequently interrupted at depths between 18 and 20 m by a layer of Midra shale that varies in thickness from 1.0 m to 3.0 m. Because of its low permeability, the shale acts as a confining stratum, preventing large scale vertical water movement into and out of the underlying limestone (Eid 2007). Consequently, the top of the shale layer was considered as the base of an unconfined aquifer from which water was pumped out using the dewatering system described in a subsequent section.

As indicators of the degree of rock fracturing that is related to its permeability, values of rock quality designation (RQD), solid core recovery (SCR), and total core recovery (TCR) measured in twenty four boreholes for the aquifer depth (i.e., between elevations -3.79 m and -15.00 m QNHD) are shown in Figure 2. The three indices (RQD, SCR, and TCR) are defined in BS 5930 (1999) as the sum length of all core pieces that are 10 cm or longer, the length of core recovered as solid cylinders, and the total amount of core sample recovered, respectively, expressed as a percentage of the length of core run. Table 1 shows the result of a statistical analysis on these measured indices.

3 FIELD PERMEABILITY TESTS

As part of the geotechnical investigation, falling-head permeability tests were carried out in selected boreholes. Dissipation tests were also carried out in some trail pits. All of these tests were performed according to the procedures described in BS 5930 (1999). The coefficient of permeability values estimated for the rock located at each falling-head and dissipation test are shown in Figure 3. It can be seen that the wide range of the measured coefficient of permeability revokes the possibility of having one representative value. For example, the measured coefficients of permeability for fractured rock near the excavation level range between 2.1 x 10^{-5} and 5.57 x 10^{-4} m/sec with an average value of about 1 x 10^{-4} m/sec.

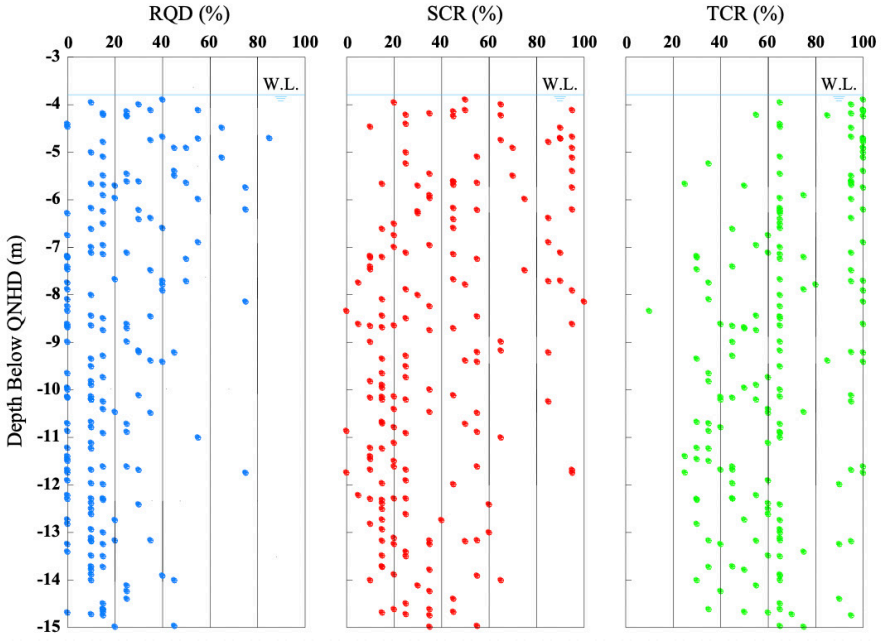

Figure 2: Changes of rock quality indices with depth

Table 1: Statistical parameters for rock quality indices

Index	Statistical Parameters			
	Average (%)	Median (%)	Standard Dev. (%)	Coefficient of Variation
RQD	19.77	15.00	18.55	0.94
SCR	38.61	30.00	26.77	0.69
TCR	65.46	65.00	23.44	0.36

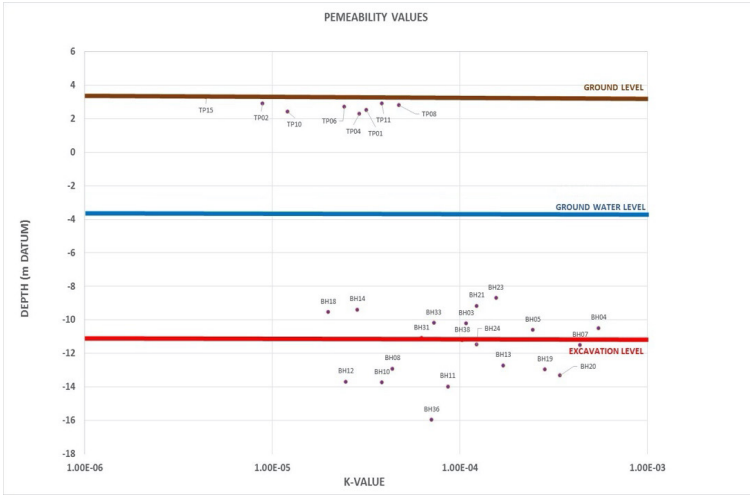

Figure 3. Coefficients of permeability of fractured rock measured in boreholes and test pits

4 BACK-CALCULATED PERMEABILITY

The coefficient of permeability of the rock mass in the project site was back-calculated using the water discharge pumped out of the employed dewatering system. The system consisted of 77 deep wells supplemented with a perimeter and cross trench system to achieve the required drawdown (Figure 4). The project dewatering system began operation in March 2014 and was completed by October 2015. Figure 5 shows the project site after completion of excavation.

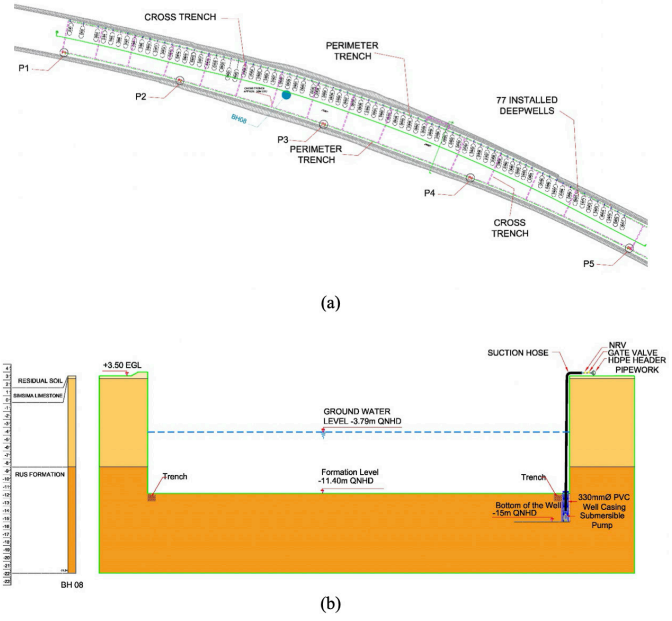

Figure 4: Schematic drawing for the excavation and the employed dewatering system: (a) plan; (b) cross section

Figure 5: Completed excavation at the project site

A summary of the actual flowrate encountered is presented in Figure 6. The steady-state flow was recorded once the final excavation level was reached. This was in mid-December, 2014. Such flow rate (i.e., 465 litre/sec or 0.465 m^3/sec) was used to back-calculate the coefficient of permeability of the rock mass (k) utilizing the following equation for pumping an unconfined aquifer (Preene et al. 2016)

$$Q = \frac{k\ x\ (H^2 - h_w^2)}{L_o}$$

Where Q, x, H, h_w, L_o are the system inflow [taken as 0.465 m^3/sec], the linear length of slot [taken as the perimeter of excavated area = 1914 m], the aquifer depth [taken as 11.21 m], the residual depth of aquifer [taken as 2.6 m], and the radius of influence [taken = $1500(H\text{-}h_w)(k)^{0.5}$ as recommended by Mansur and Kaufman (1962)], respectively. This yielded a back-calculated coefficient of permeability of 6.96 x 10^{-4} m/sec.

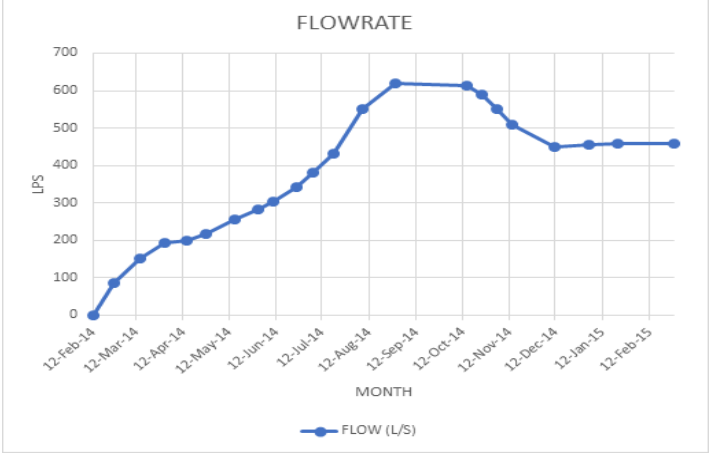

Figure 6: Change of flow rate (in litre/sec) with time

5 ANALYSIS AND CONCLUSION

Considerable discrepancy can be noticed when comparing the values of the coefficient of permeability measured from the falling-head permeability tests to that back-calculated for the rock mass using the discharge pumped out of the dewatering system employed on site. The magnitude of the latter is outside the range of the measured values and almost seven times higher than their average. The studied limestone does not encompass any jointing system but is consistently and randomly fractured. The degree of such fracturing changes with depth showing a significant scatter in the measured rock quality indices (Figure 2 and Table 1). This may be contributed to the discrepancy between the measured and back-calculated coefficients of permeability for the rock mass.

The selection of permeability values is recognized as a critical impute parameter for the design of a successful dewatering scheme. Poor permeability estimates can result in large errors in the flow rate and consequently significant loss of time and money. A better estimate for the rock mass permeability can be made through conducting pumping tests. However, this occurs in rare occasions because of the relatively higher cost and longer execution times for such hydraulic tests. The common practice is to conduct a series of field falling-head permeability tests. Results of these tests frequently lead to poor estimation of the rock mass permeability as shown in the current study. To have a better technique for estimating the permeability of randomly fractured rock, considerable number of similar studies are needed. This effort could include attempts to develop a reliable relationship that correlates such permeability with the results of field falling-head permeability tests and the commonly determined rock quality indices.

ACKNOWLEDGMENT

The funding provided by the Qatar National Research Fund (QNRF), Qatar, under Project No: NPRP12S-0314-190366, for this research work is deeply appreciated.

REFERENCES

BS 5930 (1999). Code of Practice for site investigations, British Standards.

Eid, H. T. (2007). "A technique for estimating permeability of a randomly fractured rock mass", *Acta Geotechnica*, Vol. 2, No. 2, pp. 97-102.

Mansur, C. I. & Kaufman, R. I. (1962). Dewatering. In G. A. Leonards (Ed) *Foundation Engineering*, McGraw-Hill, New York, pp. 241-350.

Preene, M., Roberts, T. O. L., Powrie, W. & Dyer, M. R. (2016). *Groundwater control — design and practice*, Second Edition, CIRIA Publication C515, London, 185 p.

Cite this article as: Eid H., O'Sullivan B., Elshafie M., Stollberg R., Kalin R., "Predicted and Back-calculated Coefficients of Permeability of Randomly Fractured Rock Mass: A Case Study", *International Conference on Civil Infrastructure and Construction (CIC 2020)*, DOI: https://doi.org/10.29117/cic.2020.0097

Fully Softened and Residual Shear Strengths of Midra Shale

Hisham Eid
heid@qu.edu.qa
Department of Civil and Architectural Engineering, Qatar University, Doha, Qatar

ABSTRACT

This paper presents a comparison of the fully softened shear strengths measured using the triaxial and torsional ring shear devices for a shale that possesses noticeably high plasticity and induration. The residual shear strength measured using the torsional ring shear device was also introduced for a supplementary comparison. It was shown that the mode of shear (e.g., the triaxial mode or the torsional ring mode) slightly affects the measured fully softened shear strength of Midra shale. The fully softened strength failure envelopes associated with the two shearing modes exhibit a moderate degree of nonlinearity that is in turn higher than that of the residual shear strength envelope. The measured classification indices of Midra shale are significantly sensitive to the sample preparation procedure. As a result, care should be taken when predicting the fully softened and residual shear strengths of Midra shale using relationships that correlate shear strength to such indices.

Keywords: Failure envelope; Fully softened strength; Residual strength; Shear strength; Shale

1 INTRODUCTION

Layers of Midra shale are frequently encountered in subsurface investigations of construction projects in Doha, capital of Qatar. The shale usually interrupts a continuous layer of fractured limestone (Figure 1). Midra shale is a highly indurated attapulgitic clay and silty material. The percentage of clay varies with the project site location and consequently changes the shale plasticity and colour. In most of these locations, the shale is light green to gray and has a clay-size fraction (i.e., quantity of particles smaller than 0.002 mm) higher than 50%.

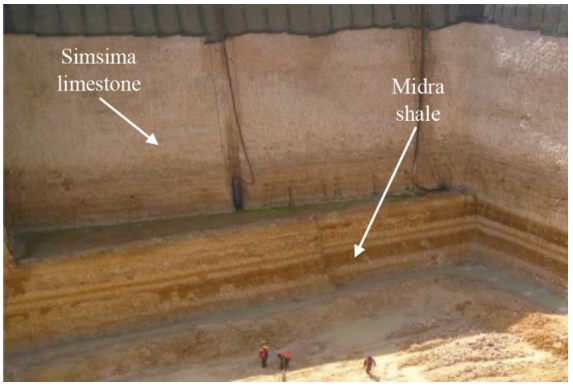

Figure 1: Vertical cut showing the subsurface stratification at one of construction sites in Doha

Because of its high induration, Midra shale has been dealt with, by most of practitioners, as a rock. Consequently, they only measure and report its physical properties, rock quality indices (e.g., RQD), unconfined compressive strength, and modulus of elasticity. Shear strength that controls friction along the cracks of Midra shale (i.e., the fully softened strength) as well as its strength that is mobilized at large displacements (i.e., the residual strength) are usually not measured. Instead, these strengths are typically predicted using published relationships that correlate shear strength to soil classification indices such as the liquid limit, plasticity index, and clay-size fraction. It is commonly known that the fully softened and residual shear strengths are directly relevant to stability assessment of anchor walls, nailed excavations, and slopes.

The measured classification indices of Midra shale are significantly sensitive to the sample preparation procedure due to the material induration. For example, following the standard sample preparation procedures described in ASTM D4318 (1999a) and ASTM D422 (1999b), liquid limit, plastic limit, and clay-size fraction of 158%, 67%, and 63%, respectively, were measured. On the other hand, liquid limit, plastic limit and clay-size fraction of 231%, 74%, and 79%, respectively, were measured when the disaggregation of Midra shale particles was maximized through ball-milling until the entire sample passes the U.S. standard sieve No. 200. Such change in the measured classification indices was also experienced for Oahe Firm shale utilizing the facilities of the soil mechanics lab at Qatar University to have ASTM derived liquid limit, plastic limit, and clay-size fraction of 97%, 40%, and 52% and ball-milled derived values of 140%, 41%, and 79%, respectively. Similar ball-milling derived classification indices were measured for Oahe firm shale by Stark and Eid (1994) utilizing the facilities of the soil mechanics lab at the University of Illinois at Urbana-Champaign. This similarity supports the sensitivity of the measured classification indices of Midra shale to the sample preparation procedure. The factors influencing determination of shale classification indices and their correlation to shear strength properties were comprehensively presented in the literature by the author of this paper (e.g., Eid 2001 and 2006; Eid et al. 2016; Eid and Rabie 2017).

2 TESTING METHODS AND RESULTS

Three consolidated drained triaxial compression tests and seven torsional ring shear tests were performed on normally consolidated remoulded specimens of Midra shale to determine the fully softened shear strength. Triaxial tests were conducted at consolidation stresses (σ'_3) of 60, 120, and 240 kPa following the procedure described in ASTM D7181-11 (2011). The ring shear tests were conducted at effective normal stresses of 10, 25, 50, 100, 200, 300, and 400 kPa as described in Eid and Rabie (2017) and ASTM D7608-10 (2010). The residual shear strength was determined using a ring shear remoulded specimen overconsolidated and presheared at 700 kPa. The multistage shearing process as described in Stark and Eid (1993 and 1994) and ASTM D6467 (1999c) was followed for shear testing at the seven lower effective normal stresses.

Figure 2 shows the shear strengths measured using the torsional ring shear device and their associated failure envelopes. It can be seen that the fully softened friction angle measured for such mode of shear ranges between 18.8° and 12.8° at effective normal stress of 10 and 400 kPa, respectively. Less than half of these values were measured for residual friction angles at the same effective normal stresses.

Mohr's circles yielded from the three triaxial compression tests conducted on different remoulded specimens of Midra shale are shown in Figure 3. The corresponding fully softened shear strength failure envelope for such mode of shear is developed and presented on the same figure. It can be seen that the curvature of this envelope is almost similar to that of the fully softened strength envelope developed using the ring shear test results. However, the triaxial shear mode seems to yield slightly higher strength values.

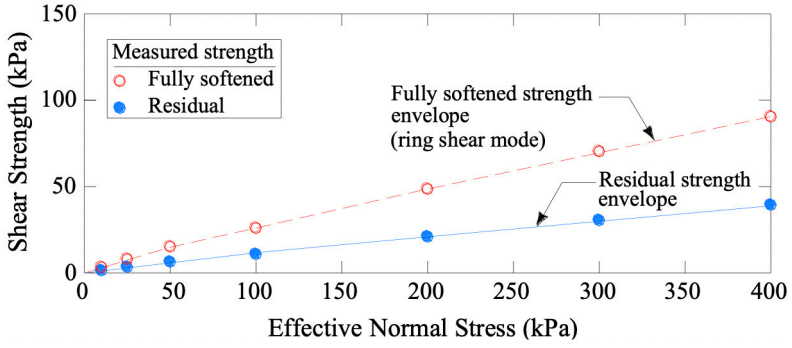

Figure 2: Shear strength of Midra shale based on the results of torsional ring shear tests

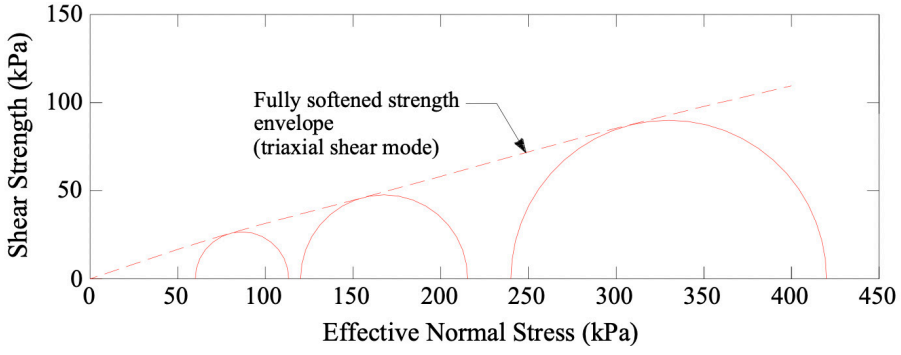

Figure 3: Fully softened shear strength of Midra shale based on the results of triaxial compression tests on remoulded specimens

3 ANALYSIS AND CONCLUSIONS

As shown in Figure 2, Midra shale exhibits a significant difference between the fully softened strength and residual strength. The difference decreases with increasing the effective normal stress. This reveals that the fully softened shear strength failure envelope has a larger nonlinearity than the drained residual failure envelope. A similar behaviour was reported and interpreted by Stark and Eid (1997) for several plastic soils.

In practice, residual shear strength envelopes of soils are frequently considered as straight lines that go to the origin of the shear strength versus effective normal stress plot. As a result, the residual shear strength can be simply expressed in terms of one friction angle. If such practice is applied to the residual strength data presented in Figure 2, an average residual friction angle of 6.5° can be assigned to Midra shale. Such significantly low friction angle reflects the shale mineralogical composition and mandates having an

extra care in stability assessments that involve dealing with large displacements along Midra shale.

A comparison was made between the fully softened angles obtained from the consolidated drained triaxial compression tests $(\phi'_{fs})_{tri}$, and drained torsional ring shear tests $(\phi'_{fs})_{ring}$ as shown in Figure 4. The nonlinear failure envelope shown in Figure 3 was used to estimate $(\phi'_{fs})_{tri}$ at effective normal stresses of 100, 200, 300, and 400 kPa for comparison with $(\phi'_{fs})_{ring}$ measured at the same effective stresses.

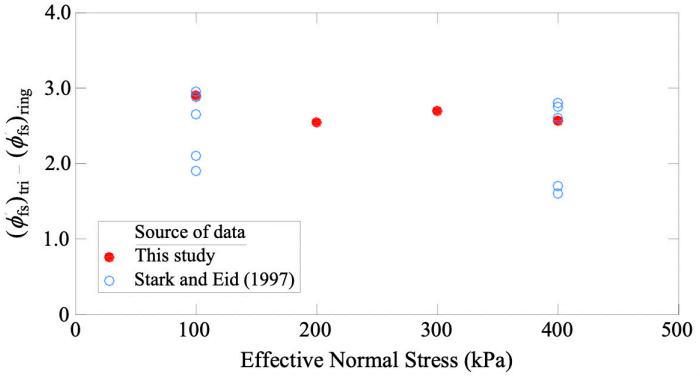

Figure 4: Comparison of fully softened friction angles obtained for different modes of shear

Figure 4 shows that the triaxial compression tests on Midra shale yields a fully softened friction angle that is approximately 2.5° to 2.9° higher than that obtained from the torsional ring shear test. The results of this study are in agreement with the data published in Stark and Eid (1997) showing that the average difference between $(\phi'_{fs})_{tri}$ and $(\phi'_{fs})_{ring}$ is about 2.5°. This difference is attributed to the effect of the shear mode that should be considered by the designers for simulating the mode that would be developed in the field with that of the shear tests.

REFERENCES

ASTM. (1999a). "Standard test method for liquid limit, plastic limit, and plasticity index of soils." D4318, *Annual Book of ASTM Standards*, West Conshohocken, PA, 526-538.

ASTM. (1999b). "Standard test method for particle-size analysis of soils." D422, *Annual Book of ASTM Standards*, West Conshohocken, PA.

ASTM. (1999c). "Standard test method for torsional ring shear test to determine drained residual shear strength of cohesive soils." D6467, *Annual Book of ASTM Standards*, West Conshohocken, PA.

ASTM. (2010). "Standard test method for torsional ring shear test to determine drained fully softened shear strength and nonlinear strength envelope of cohesive soils (using normally consolidated specimen) for slopes with no preexisting shear surfaces." D7608-10, *Annual Book of ASTM Standards*, West Conshohocken, PA.

ASTM. (2011). "Method for consolidated drained triaxial compression test for soils." D7181-11, *Annual Book of ASTM Standards*, West Conshohocken, PA.

Eid, H.T. (2001). "Correlation between Shale Index Properties Derived from Different Sample Preparation Procedures." *Proceedings of the 15th International Conference on Soil Mechanics and Geotechnical Engineering,* Istanbul, Turkey, Vol. 1, pp. 77-80.

Eid, H.T. (2006). "Factors influencing determination of shale classification indices and their correlation to mechanical properties." *Geotechnical and Geological Engineering Journal*, Vol. 24, No. 6 , pp. 1695-1713.

Eid, H.T., Rabie, K.H., and Wijewickreme, D. (2016). "Drained residual shear strength at effective normal stresses relevant to soil slope stability analyses." *Engineering Geology*, Vol. 204, pp. 94-107

Eid, H.T., and Rabie, K.H. (2017). "Fully softened shear strength for soil slope stability analyses." *International Journal of Geomechanics*, ASCE, Vol. 17, Issue 1, 04016023-1to10.

Stark, T.D., and Eid, H.T. (1993). "Modified Bromhead ring shear apparatus." *Geotechnical Testing Journal*, ASTM, Vol. 16, No. 1, pp. 100-107.

Stark, T.D., and Eid, H.T. (1994). "Drained residual strength of cohesive soils." *Journal of Geotechnical Engineering*, ASCE, Vol. 120, No. 5, pp. 856-871.

Stark, T.D., and Eid, H.T. (1997). "Slope stability analyses in stiff fissured clays." *Journal of Geotechnical and geoenvironmental Engineering*, ASCE, Vol. 123, No. 4, pp. 335-343.

Cite this article as: Eid H., "Fully Softened and Residual Shear Strengths of Midra Shale", *International Conference on Civil Infrastructure and Construction (CIC 2020)*, Doha, Qatar, 2-5 February 2020, DOI: https://doi.org/10.29117/cic.2020.0098

Theme 4:
Sustainability, Renovation, and Monitoring of Civil Infrastructure

Steel Reinforced Grout for Strengthening of RC T-section Beams Deficient in Shear

Tadesse Wakjira
twakjira@qu.edu.qa
Department of Civil and Architectural Engineering, Qatar University, Doha, Qatar

Usama Ebead
uebead@qu.edu.qa
Department of Civil and Architectural Engineering, Qatar University, Doha, Qatar

ABSTRACT

Reinforced concrete (RC) beams are bound to lose their strength while in service due to numerous causes. Thus, proper strengthening and rehabilitation techniques are required to restore the strength and extend the service life of the structures. Steel reinforced grout (SRG) has recently been introduced as an efficient and economical strengthening solution, however, the study on its application for the strengthening of shear-deficient RC beams is scarce. Thus, this paper is aimed to investigate the efficacy of SRG for shear strengthening of RC beams with the focus on SRG/stirrups interaction. Six T-cross section beams were grouped into three series based on their internal shear reinforcement ratio and tested under three-point bending. Each series comprised of one reference and one SRG-strengthened beam. The test results revealed that SRG laminates are an effective technique to increase the shear capacity of RC beams. Up to 71% increase in the load-carrying capacity of the strengthened beams was achieved. The increase in the internal shear reinforcement has shown to reduce the shear-strengthening performance of SRG.

Keywords: Strengthening; Steel reinforced grout (SRG); Beam; Shear; SRG/stirrups interaction

1 INTRODUCTION

The geographical location and weather of Gulf countries, including Qatar, expose their key infrastructure to severe deterioration due to the proximity to seawater, humidity, and high temperatures. Therefore, deterioration due to such factors necessitates the need for effective strengthening techniques to extend the service life of the infrastructure. Different strengthening methods were developed through time with advanced strengthening material gaining popularity over traditional ones owing to their favorable advantages such as high strength-to-weight ratio, high resistance to corrosion, and speed and ease of installation. In this context, fiber-reinforced polymer and recently fabric reinforced matrix have shown to be effective strengthening techniques for both reinforced concrete and masonry structures (Al-Saadi et al., 2019; Carozzi et al., 2017; Elsanadedy et al., 2019; Koutas et al., 2019; Marcinczak & Trapko, 2019; Oller et al., 2019; Wakjira & Ebead, 2018; Younis et al., 2017). However, the high cost associated with these materials limits their widespread use. An alternative strengthening system using steel reinforced grout has recently developed as a cost-effective strengthening solution. Steel reinforced grout has shown to be an effective strengthening solution for

RC beams in flexure and shear. The first study on the use of SRG/SRP as a strengthening solution dated back to 2004 for flexural strengthening of RC beams (Barton et al., 2005; Huang et al., 2005; Wobbe et al., 2004). Since then, successful applications of SRG/SRP have been reported in various experimental studies for strengthening of different structural members, including RC beams (Napoli & Realfonzo, 2015; Prota et al., 2006; Wakjira & Ebead, 2019), RC slabs (Annalisa et al., 2015; Hadad & Nanni, 2018), column confinement (Thermou & Hajirasouliha, 2018), and masonry structures (De Santis et al., 2018; De Santis & De Felice, 2015). Theoretical prediction of flexural strengthened RC beams using SRG/SRP system was also presented in a previous research contribution (Bencardino & Condello, 2015). With regard to the RC beams strengthened with SRG, the experimental studies to date are mainly dedicated to the strengthening of beams in flexure (Napoli & Realfonzo, 2015; De Santis et al., 2016). However, the studies devoted to the strengthening of shear deficient RC beams are very limited (Thermou et al., 2019; Wakjira & Ebead, 2019).

Thus, the proposed research investigates the application of SRG for the strengthening of RC beams in shear. The work will contribute to enriching the relatively limited research available on the application of SRG for strengthening of RC structures. The main focus is to investigate the shear behavior of SRG strengthened T-beams and the SRG/stirrups interaction. With this in aim, three control beams and three SRG-strengthened RC T-section beams were prepared and tested under three-point loading. The experimental results confirmed the potential application of SRG for shear strengthening of RC beams.

2 EXPERIMENTAL PROGRAM

2.1 Material

The beams were cast using ready-mixed concrete with an average compressive strength of 34 MPa as obtained from the direct compressive test.

The beams were internally reinforced with 25 mm diameter deformed top bars and 16 mm diameter deformed bottom bars as tensile and compressive reinforcements, respectively. The shear reinforcement outside the shear span was 8 mm diameter stirrups spaced at 75 mm, while outside the shear span three different shear reinforcements were used (none, 6 mm at 300 mm, and 6 mm at 150 mm). The properties of the reinforcement bars are listed in Table 1.

Table 1: Properties of the steel reinforcement bars

Description	**Longitudinal reinforcement bars**		**Stirrups**	
Bar diameter	16 mm	25 mm	6 mm	8 mm
Yield strength	562	588	234	535
Yield strain (%)	0.233	0.241	0.117	0.258
Modulus of elasticity, GPa	241	244	207	207

The SRG system was composed of geo-mortar reinforced with steel fabrics. Figure 1 shows the steel fabrics used in this study, which were made of high strength steel cords obtained by assembling five filaments. Two of the filaments were wrapped around

another three straight filaments to form the steel fabrics, as shown in Fig. 1. The average mechanical properties of the steel fabrics and the associated geo-mortar are listed in Table 2.

Figure 1: Geometry of the steel fabric used in the study

Table 2: Properties of steel fabrics and mortar

Description	Thickness (mm)	Cord area (mm^2)	Weight of fiber (g/m^2)	Density (cords/cm)	Tensile strength (MPa)	Elastic modulus (GPa)	Compressive strength (average of 28 d), MPa	Bond strength (average of 28 d), MPa
Steel fabrics	0.169	0.538	1200	3.14	3000	190	-	-
Geo-mortar	-	-	-	-	8*	22	50	2

*average of 28 d

2.2 Test beams

In total, six test beams of the same T-section and span were prepared and tested. Figures 2a–2c show the reinforcement details and geometry of the test beams. The beams had the following geometry: the cross-section height of 400 mm; the flange width of 450 mm; the flange thickness of 100 mm; the web thickness of 300 mm; the total beam length of 2500 mm; and the critical shear span of 950 mm, as shown in Figs. 2a–2c. The longitudinal reinforcement consisted of five 25 mm diameter bars placed in two rows at the bottom and six 16 mm diameter bars on the top of the beam. The shear reinforcement involved 8 mm diameter stirrups spaced at 75 mm outside the critical shear span, as shown in Figs. 2a–2d.

The beams were grouped into three series based on the number of stirrups within the shear span. The first series was internally unreinforced in shear within the test span, while the second and third series were reinforced with 6 mm diameter stirrups placed at 300 mm and 6 mm stirrups placed at 150 mm, respectively, as shown in Fig. 2c.

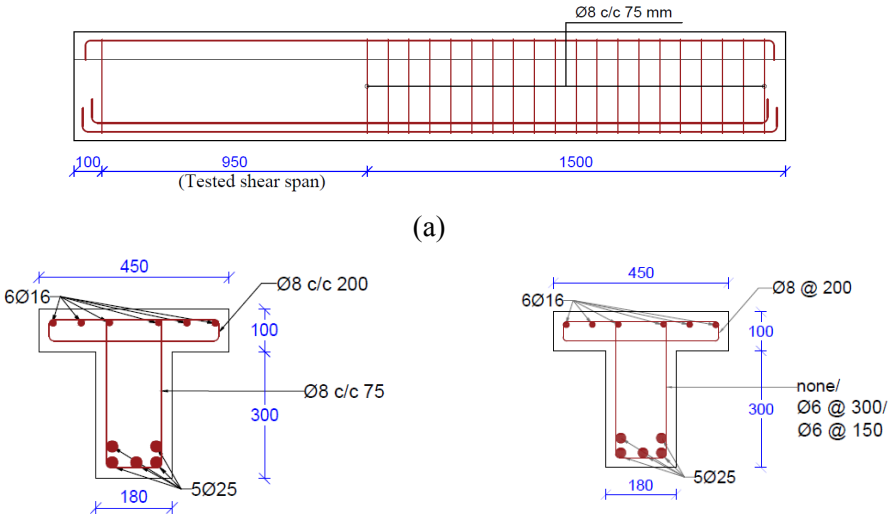

Figure 2: Reinforcement details and geometry of the test beams: (a) longitudinal detail, (b) cross-sectional detail outside the CSS, and (c) cross-sectional detail within the CSS. (Dimensions: mm)

2.3 Strengthening procedures

Each beam was strengthened with two layers of externally bonded SRG applied in the U-wrapped scheme. The strengthening technique is composed of the following procedures: i) the surface of the test beams was sandblasted and cleaned, ii) the SRG fabrics were cut with the desired length and bent in U-shape, iii) the first layer of mortar was applied on the prepared concrete surface, iv) the first layer of the steel fabrics was installed and fully impregnated with the underlying mortar layer, v) second mortar layer was followed by installation of second fabric layer, and vi) the final mortar layer covered the second layer of the steel fabrics and the SRG final surface was finished. To guarantee proper curing of the SRG composite, at least one month passed between the beam strengthening and test dates.

The details of the tested beams are given in Table 3. Each test beam is designated using Si-X, where, “S” stands for beam series, numeral “I” indicates the beam series, “X” identifies if the beam is strengthened or control beam (“C” for control beam, “ST” for strengthened beam).

Table 3: Test matrix

Designation	Beam series	Beam depth (mm)	Beam web width (mm)	Critical shear span (mm)	Steel stirrups within the CSS	SRG wraps
S1-C	1	400	180	950	-	Control
S1-ST	1	400	180	950	-	U-wrap
S2-C	2	400	180	950	6 mm @ 300 mm	Control
S2-ST	2	400	180	950	6 mm @ 300 mm	U-wrap
S3-C	3	400	180	950	6 mm @ 150 mm	Control
S3-ST	3	400	180	950	6 mm @ 150 mm	U-wrap

2.4 Test setup

The beams were tested under three-point bending using the Instron UTM loading frame, as shown in Fig. 3. The applied load (P) at the loading point was recorded by the load cell. The displacement under the loading point was monitored by using two linear variable displacement transducers placed under the load application point, as shown in Fig. 3. In addition, strain gauges were used to measure the strains in the tensile reinforcement and compressive strains in concrete.

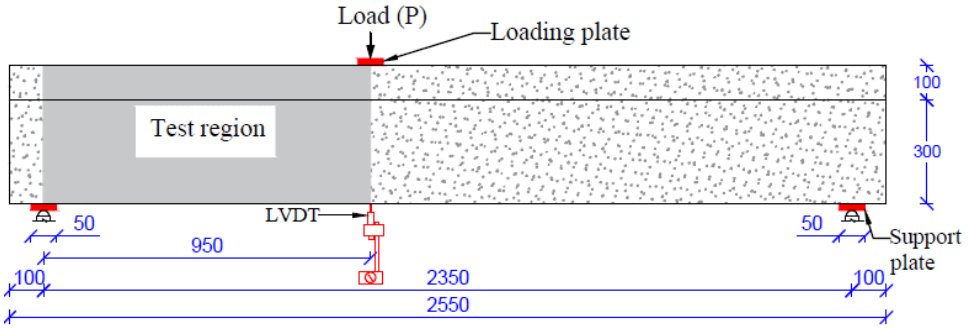

Figure 3: Test setup

3 RESULTS AND DISCUSSION

The main test results including the ultimate load (P_u), gain in P_u, deflection at P_u, the strains developed in concrete and tensile bars at P_u are listed in Table 4 and discussed in the following sections.

Table 4: Test results

Desig-nation	Ultimate load (P_u) (kN)	In-crease in P_u (%)	De-flection at P_u (mm)	Concrete strain at P_u (‰)	Tensile strain in the longitudinal bar at P_u (‰)
S1-C	204	–	2.39	0.430	0.789
S1-ST	349	71	6.17	1.124	1.356
S2-C	283	–	6.78	0.679	1.154
S2-ST	385	36	10.0	0.817	1.513
S3-C	331	–	8.13	2.142	1.312
S3-ST	403	22	11.4	0.497	1.762

3.1 Load-deflection responses

Figure 4 shows the response of load versus deflection under the loading point. Figure 4 and the results included in Table 4 show that the adopted SRG system provided an increase in the beam's shear capacity. The increase in the shear capacity ranged between 22% and 71%, as listed in Table 4. The strengthened specimens, namely, S1-ST, S2-ST, and S3-ST failed at the ultimate load of 349 kN, 385 kN, and 403 kN, respectively. The

control beams S1-C, S2-C, and S3-C failed at ultimate load of 204 kN, 283 kN, and 331 kN, respectively.

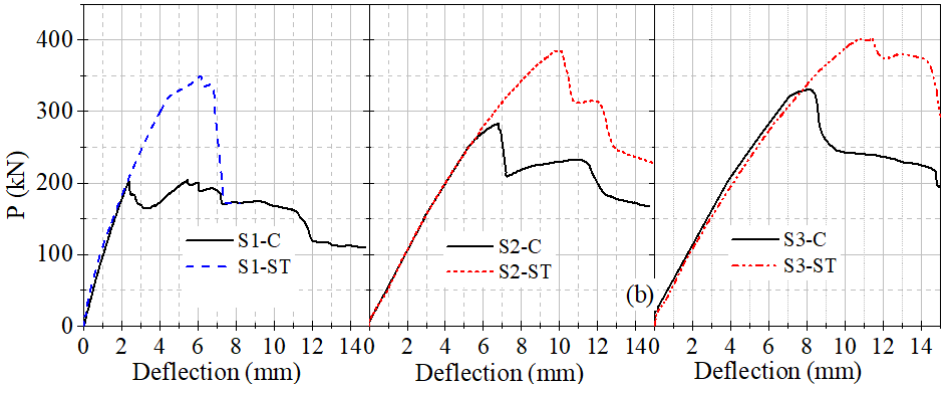

Figure 4: Plots of load versus deflection

3.2 Failure modes

The control beams showed a typical shear failure mode of slender beams, as shown in Fig. 5a for Specimen S1-C. The failure in the strengthened beams was characterized by shear failure caused by shear cracks and premature debonding of SRG laminate off the concrete substrate, as can be seen in Fig. 5b for Specimen S2-ST.

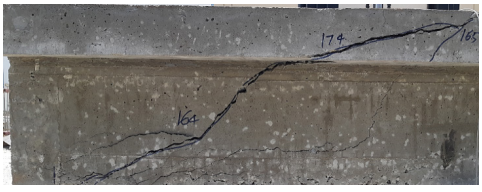

(a) S1-C

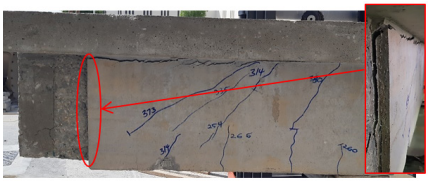

(b) S2-ST

Figure 5: Crack patterns and failure modes observed in the control and strengthened beams

3.3 Interaction between SRG and steel stirrups

The strengthened beam without stirrups within the critical shear span, namely Specimen S1-ST, failed at an ultimate load of 349 kN corresponding to 71% gain in the load-carrying capacity relative to the control beam, S1. The provision of internal shear reinforcement in Specimen S2-ST reduced the gain in the load-carrying capacity due to SRG system compared to Specimen S1-ST with no shear reinforcement in the shear span. Moreover, the gain in the load-carrying capacity was further dropped to 22% by an increase in the internal shear span within the shear span due to the load sharing between the stirrups and SRG reinforcement. Furthermore, the strengthening system has reduced the strains in the stirrups within the critical shear span compared to that for the corresponding control beam.

4 CONCLUSION

The test results of six T-cross section RC beams strengthened in shear with U-wrapped

SRG system were presented in this paper. The effects of SRG/stirrups interaction were analyzed and compared in terms of load-carrying capacity and failure modes. The test results showed that SRG can be used to substantially increase the load-carrying capacity of RC beam shear-strengthened with SRG U-wraps. The increase in the load-carrying capacity ranging from 22% to 71% was observed. The highest increase in the load-carrying capacity was observed for Specimen S1-ST, without stirrups within the critical shear span. Shear interaction exists between SRG and stirrups. The provision of stirrups within the critical shear span reduced the percentage gain in the load-carrying capacity of the strengthened beams. Further reduction in the percentage gain in the load-carrying capacity was observed with an increase in the internal shear reinforcement within the critical shear span. The strengthened specimens failed in shear caused by premature debonding of SRG laminates.

REFERENCES

Al-Saadi, N. T. K., Mohammed, A., Al-Mahaidi, R. & Sanjayan, J. (2019). A state-of-the-art review: Near-surface mounted FRP composites for reinforced concrete structures. *Construction and Building Materials*, 209, 748-769.

Annalisa, N., Roberto, R., Massimo, P. & Casadei, P. (2015). Flexural strengthening of RC Slabs with SRP/SRG : An experimental-numerical comparison. *Applied Mechanics and Materials*, 847(October 2017), 381-390.

Barton, B., Wobbe, E., Dharani, L. R., Silva, P., Birman, V., Nanni, A., Alkhrdaji, T., Thomas, J. & Tunis, G. (2005). Characterization of reinforced concrete beams strengthened by Steel Reinforced Polymer and Grout (SRP and SRG) composites. *Materials science and Engineering: A*, 412, 129-136.

Bencardino, F. & Condello, A. (2015). Reliability and adaptability of the analytical models proposed for the FRP systems to the steel reinforced polymer and steel reinforced grout strengthening systems. *Composites Part B: Engineering*, Elsevier Ltd, 76, 249-259.

Carozzi, F. G., Bellini, A., D'Antino, T., de Felice, G., Focacci, F., Hojdys, Ł., Laghi, L., Lanoye, E., Micelli, F., Panizza, M. & Poggi, C. (2017). Experimental investigation of tensile and bond properties of Carbon-FRCM composites for strengthening masonry elements. *Composites Part B: Engineering*, 128, 100-119.

Elsanadedy, H., Abbas, H., Almusallam, T. & Al-Salloum, Y. (2019). Organic versus inorganic matrix composites for bond-critical strengthening applications of RC structures – State-of-the-art review. *Composites Part B: Engineering*, 174.

Hadad, H. & Nanni, A. (2018). Structural performance of SRG strengthened RC slabs. (August).

Huang, X., Birman, V., Nanni, A. & Tunis, G. (2005). Properties and potential for application of steel reinforced polymer and steel reinforced grout composites. *Composites Part B: Engineering*, 36, 73-82.

Koutas, L., Tetta, Z. C., Bournas, D. & Triantafillou, T. (2019). Strengthening of concrete structures with textile reinforced mortars : State-of-the-art review. *Journal of Composites for Construction*, *23*(1), 03118001.

Marcinczak, D. & Trapko, T. (2019). Shear strengthening of reinforced concrete beams with PBO-FRCM composites with anchorage. *Composites Part B: Engineering*, 158(August 2018), 149-161.

Napoli, A. & Realfonzo, R. (2015). Reinforced concrete beams strengthened with SRP/SRG systems: Experimental investigation. *Construction and Building Materials*, Elsevier Ltd, 93, 654-677.

Oller, E., Pujol, M. & Marí, A. (2019). Contribution of externally bonded FRP shear reinforcement to the shear strength of RC beams. *Composites Part B: Engineering*, 164, 235-248.

Prota, A., Tan, K. Y., Nanni, A., Pecce, M. & Manfredi, G. (2006). Performance of shallow reinforced concrete beams with externally bonded steel-reinforced polymer. *ACI Structural Journal*, *103*(2), 163-170.

De Santis, S. & De Felice, G. (2015). Steel reinforced grout systems for the strengthening of masonry structures. *Composite Structures*, Elsevier Ltd, 134, 533-548.

De Santis, S., De Felice, G., Napoli, A. & Realfonzo, R. (2016). Strengthening of structures with Steel reinforced polymers: A State-of-the-art review. *Composites Part B: Engineering*, Elsevier Ltd, 104, 87-110.

De Santis, S., Roscini, F. & De Felice, G. (2018). Full-scale tests on masonry vaults strengthened with steel reinforced grout. *Composites Part B: Engineering*, Elsevier, 141(December 2017), 20-36.

Thermou, G. E. & Hajirasouliha, I. (2018). Compressive behavior of concrete columns confined with steel-reinforced grout jackets. *Composites Part B: Engineering*, Elsevier, 138(April 2017), 222-231.

Thermou, G. E., Papanikolaou, V. K., Lioupis, C. & Hajirasouliha, I. (2019). Steel-Reinforced Grout (SRG) strengthening of shear-critical RC beams. *Construction and Building Materials*, Elsevier Ltd, 216, 68-83.

Wakjira, T. & Ebead, U. (2018). Hybrid NSE/EB technique for shear strengthening of reinforced concrete beams using FRCM: Experimental study. *Construction and Building Materials*, Elsevier Ltd, 164, 164-177.

Wakjira, T. & Ebead, U. (2019). Experimental and analytical study on strengthening of reinforced concrete T-beams in shear using Steel Reinforced Grout (SRG). *Composites Part B: Engineering*, 177, 107368.

Wobbe, E., Silva, P., Barton, B. L., Dharani, L. R., Birman, V., Nanni, A., Alkhrdaji, T., Thomas, J. & Tunis, G. (2004). *Flexural capacity of RC beams externally bonded with SRP and SRG*. Proceedings of Society for the advancement of material and process engineering Symp., Long Beach, CA, the USA.

Younis, A., Ebead, U. & Shrestha, K. C. (2017). Different FRCM systems for shear-strengthening of reinforced concrete beams. *Construction and Building Materials*, 153, 514-526.

Cite this article as: Wakjira T., Ebead U., "Steel Reinforced Grout for Strengthening of RC T-section Beams Deficient in Shear", *International Conference on Civil Infrastructure and Construction (CIC 2020)*, Doha, Qatar, 2-5 February 2020, DOI: https://doi.org/10.29117/cic.2020.0099

Near Surface Embedded Application for FRCM Strengthening of RC Beams in Flexure

HossamEldin El-Sherif
hossameldin.elsherif@qu.edu.qa
Department of Civil and Architectural Engineering, Qatar University, Doha, Qatar

Usama Ebead
uebead@qu.edu.qa
Department of Civil and Architectural Engineering, Qatar University, Doha, Qatar

ABSTRACT

In this paper, the efficacy of a recent strengthening technique, referred to as Near Surface Embedded (NSE), has been investigated for flexural strengthening of Reinforced Concrete (RC) beams using Fabric Reinforced Cementitious Matrix (FRCM). The process of applying NSE-FRCM strengthening technique involves removing the concrete layer at the beam's soffit (being the most deteriorated), which is then replaced by the FRCM composite. In this study, seven RC beams were constructed and tested under four-point loading considering two test variables, namely, (a) FRCM material (Polyparaphenylene Benzobisoxazole (PBO)/carbon/glass), and (b) strengthening configuration (NSE/ Externally-Bonded (EB)). Amongst the three FRCM materials, the PBO-FRCM system offered the highest strengthening effectiveness (i.e., highest gain in the load carrying capacity). The average gain in the load-carrying capacity was 45% and 58% for the NSE- and EB-FRCM strengthened beams, respectively, compared to the reference (i.e., non-strengthened) specimen. Nonetheless, the results showed a clear advantage for NSE-FRCM strengthening systems over those externally bonded in terms of ductility performance. The advantage of NSE over EB strengthening was also demonstrated by the improved FRCM/concrete bond associated with NSE-FRCM application.

Keywords: Reinforced concrete; Near surface embedded; Fabric reinforced cementitious matrix; Flexural strengthening; Externally bonded

1 INTRODUCTION

Fabric Reinforced Cementitious Matrix (FRCM) systems have been recently introduced as a viable solution for strengthening Reinforced Concrete (RC) structures. FRCM systems are consisted of high strength fabrics embedded in inorganic cementitious matrices and Externally Bonded (EB) to the RC structures to enhance the performance. The use of inorganic matrices has favored FRCM systems with advantages such as the ability to be applied on wet surfaces and compatibility with the concrete substrate (Lee et al., 2013; Raoof et al., 2017). FRCM is also known as Textile Reinforced Concrete (TRC) (Yin et al., 2014), and Textile Reinforced Mortar (TRM) (Younis et al., 2017a).

FRCM has been proven successful in strengthening RC beams in shear (Gonzalez-Libreros et al., 2017; Younis et al., 2017b), and flexure (Ebead et al., 2016; Koutas et al., 2019). It has also been noticed that the substrate surface preparation technique implemented could have a significant effect on the performance of FRCM strengthening

(Ebead & Younis, 2019). The most commonly implemented substrate surface preparation technique is sandblasting the surface and removing a thin layer of fine grain concrete to avoid any bond deficiencies caused with the FRCM composite and provide a rough surface for bonding as recommended by the ACI 549 guidelines (ACI Committee 549, 2013). This technique however, poses safety risks during sandblasting and necessitates protective action (United States Department of Labor, 2014). Wakjira & Ebead (2018) introduced a new surface roughening method allowing the safe and easy application of FRCM embedded within the concrete cover called Near Surface Embedded FRCM (NSE-FRCM) (Wakjira & Ebead, 2018). The NSE technique involves embedding the FRCM into a prepared groove, thus, preserving the RC beam dimensions and enhancing the shear capacity. The results of NSE compared favorably to the traditional EB strengthening and provided improved bonding with the concrete substrate.

It is interesting therefore to study the efficacy of the NSE-FRCM technique in enhancing the flexural capacity of RC beams. To achieve this, seven RC beams were prepared and tested under four-point loading. Three different FRCM fabric materials were employed in preparing the test specimens, namely, carbon, PBO, and glass. Six RC beams were strengthened using EB and NSE techniques to facilitate comparison between these techniques.

2 METHODOLOGY

2.1 Material properties

Seven specimens were cast with the same ready-mixed concrete batch with 28-day compressive strength of 39.5 MPa. The longitudinal reinforcement of the beams had a yield strength of 520 MPa and a corresponding strain of 0.27%. The transverse reinforcement had a yield strength of 535 MPa with a 0.26% strain value. The materials employed in the strengthening procedure were three different FRCM systems, which are: PBO-FRCM, Carbon-FRCM (C-FRCM), and Glass-FRCM (G-FRCM). Each FRCM system is composed of textile with an accompanying mortar mixed according to the manufacturers' recommendations (Ruredil, 2016a, b; SIKA, 2016). The mechanical properties and geometric information for the different FRCM systems are presented in Table 1 provided by their manufacturers (Ruredil, 2016a, b; SIKA, 2016). Table 1 lists the mechanical and geometric properties of the FRCM fabrics consisting of the center-to-center spacing between fabric strands in warp direction, fabric area per unit width (A_f), fiber modulus of elasticity (E), fiber tensile strength (F_{tu}), and ultimate strain (ε_{ult}) for each type of FRCM used.

Table 1: Mechanical and Geometric properties of FRCM textiles

Material	c/c spacing (mm)	A_f (mm²/ mm)	E (GPa)	ε_{ult} (%)	F_{tu} (GPa)
Carbon	10	0.0470	240	1.8	4.8
PBO	10	0.0455	270	2.15	5.8
Glass	18	0.0470	80	3.25	2.6

2.2 Test specimens and preparation

A total of 7 RC beams were cast with a cross section of 150 × 260 mm, and 2500 mm in length. Two 10 mm bars were used as tension reinforcement in all beams and two 8-mm bars were used as top reinforcement. The transverse reinforcement was 8 mm diameter stirrups spaced 100 mm along the length of the beam. The reinforcement details are shown in Figure 1. One beam served as a control specimen with no strengthening, three beams were strengthened using two layers of FRCM fabric 150 mm wide applied as EB and three beams were strengthened using the NSE technique with two layers of FRCM fabric 90 mm wide over the span of the beams. The EB strengthened specimens had the soffit of the beam sandblasted first to remove the fine grain concrete. In order to prepare the NSE strengthened beams, a 90 mm wide groove was prepared using a slitting machine at the soffit of the beam and the concrete was manually chipped away with a chisel resulting in a rough surface. The depth of the groove was selected based on the manufacturers' recommended mortar thickness that accommodates two layers of FRCM fabrics. The test matrix is shown in Table 2. Both NSE, and EB strengthening schemes are shown in Figure 2.

Table 2: Test matrix

No.	ID	Strengthening	Fabric
1	R	-	-
2	P-N	NSE	PBO
3	C-N	NSE	Carbon
4	G-N	NSE	Glass
5	P-E	EB	PBO
6	C-E	EB	Carbon
7	G-E	EB	Glass

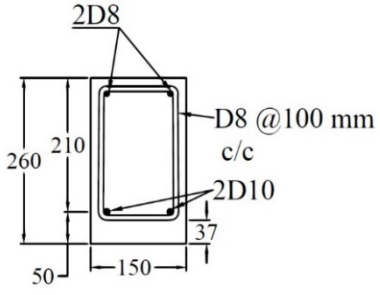

Figure 1: Reinforcement configuration and dimensions (mm)

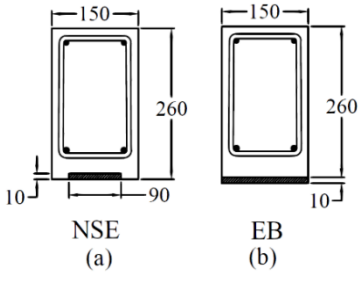

Figure 2: Strengthening configurations (mm)

2.3 Test setup

The specimens were tested under four-point loading using a monotonically applied hydraulic load at two points on the beam as shown in Figure 3. The loading was displacement controlled at a rate of 1 mm/min. The load and midspan deflection measurements were recorded along with the concrete strain at the top, and tension steel strain at the center of the beam.

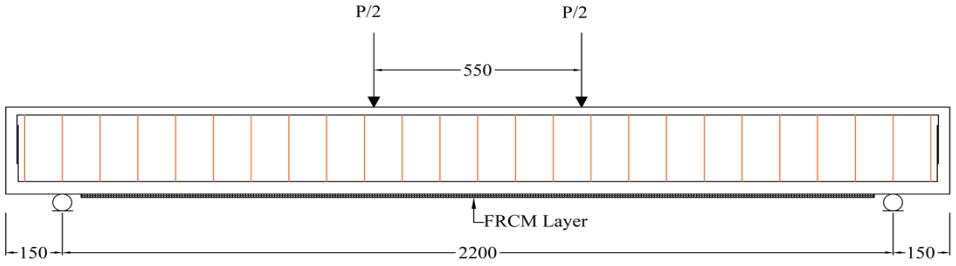

Figure 3: Test setup

3 EXPERIMENTAL RESULTS

Table 3 summarizes the experimental results listing the beam names, equivalent axial stiffness (κ^f), ductility index (ΔI), ultimate load (P_u), percentage gain in ultimate load ($P_u\ gain$), and failure mode.

Table 3: Test results summary

Beam	κ^f κ^f (MPa)	ΔI	$\delta_u\delta_u$ (mm)	P_u (kN)	$P_u\ gainP_u\ gain$ (%)	Failure Mode
R	-	15.31	27.2	40.0	-	A + B
P-N	24.0	5.73	28.1	62.7	56.8	C
C-N	29.9	3.21	16.1	59.2	48.1	C
G-N	13.3	5.56	22.9	52.5	31.0	D
P-E	38.5	4.53	25.7	68.9	72.3	E
C-E	47.9	3.04	16.1	68.7	71.8	C
G-E	21.3	3.03	13.1	51.9	29.8	D

A = steel yielding, B= concrete crushing, C = mid-span delamination, D = fabric rupture, and E = plate-end delamination.

3.1 FRCM composite equivalent axial stiffness

In order to facilitate the comparison, the equivalent axial stiffness (κ^f) is used, which utilizes the amount of FRCM fabric through the given eq. (1) (Ebead et al., 2016):

$$\kappa^f = \rho_f E_f = \frac{N A_f b E_f}{b d_f} \quad (1)$$

where ρ_f = fabric reinforcement ratio, N = number of layers of fabric, A_f = equivalent area of fabric, b = FRCM fabric width (150 mm for EB and 90 mm for NSE), d_f = effective depth of FRCM fabric (265 mm for EB and 255 mm for NSE), and E_f = cracked FRCM composite modulus of elasticity. Table 4 lists the ultimate tensile stress (σ_{fu}), ultimate strain (ε_{fu}), and cracked tensile modulus of elasticity (E_f) acquired from tensile characterization tests on FRCM coupons (Younis et al., 2017b). The highest κ^f values were observed in the C-FRCM strengthened specimens, followed by PBO-FRCM and then G-FRCM strengthening specimens. This is due to the high mechanical properties of the C- and PBO-FRCM composites compared to the G-FRCM. The graph

shown in Figure 4 displays the plots of the gain in P_u vs. the stiffness factor, A linear trend is observed.

Table 4: FRCM tensile characterization results

FRCM	(%) ε_{fu}	(MPa) σ_{fu}	(GPa) E_f
Carbon	1.04	1178	135
PBO	1.06	1235	112
Glass	0.93	767	60

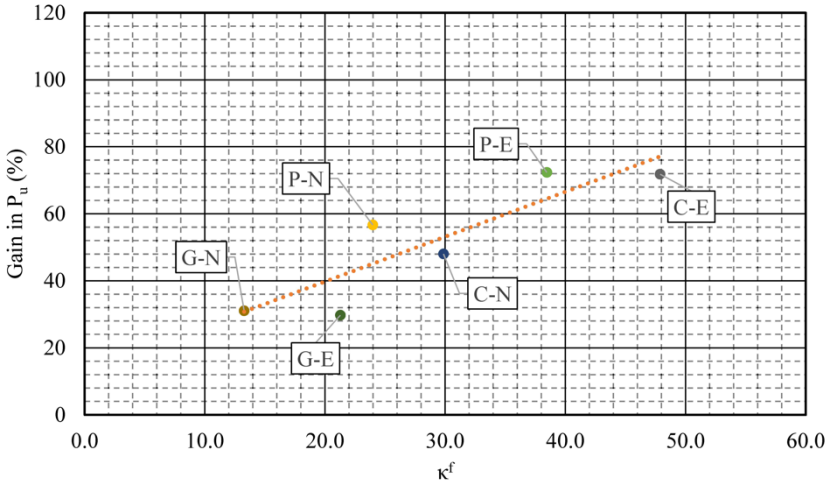

Figure 4: Gain in P_u -κ^f κ^f plots

3.2 Ultimate load carrying capacity

It was observed that PBO resulted in the highest P_u with an average value of 64.6 kN for PBO-FRCM strengthened beams (P-N and P-E) which is 64.6% higher than that of the benchmark specimen R which had a P_u value of 40 kN. As for the C- and G-FRCM strengthened specimens, the average P_u values were 64 kN and 52.2 kN, respectively, providing an increase in P_u of 60% and 30.4%, respectively. Upon comparing the different strengthening techniques, it is shown that the average capacity enhancement is close between both NSE and EB strengthening. The average P_u of NSE-FRCM and EB-FRCM strengthened specimens was 58.1 kN and 63.2 kN, respectively, with a difference of about 8% between them. This shows that NSE strengthening can be a valid alternative to EB strengthening.

3.3 Ductility performance

The load-deflection relationships for the beams are represented in Figure 5 and Figure 6 for NSE and EB strengthened beams respectively. The ductility index (ΔI) which is defined as the ratio of the ultimate deflection (δ_u) to yield deflection (δ_y) shows an advantage towards NSE strengthening. The average ΔI values were 4.8 and 3.5 for

the NSE strengthened specimens and the EB strengthened specimens, respectively. The increased ΔI caused by the NSE strengthening compared to the EB strengthening is attributed to the preserved section dimensions and the lower amount of FRCM composite implemented in NSE strengthening. This allowed NSE strengthened specimens to reach higher deflections at ultimate load. As for the fabric type, the average ΔI values were 5.1, 3.1, and 4.3 for PBO-, C-, and G-FRCM strengthened specimens, respectively, showing the highest ductility for PBO-FRCM followed by G-FRCM and then C-FRCM.

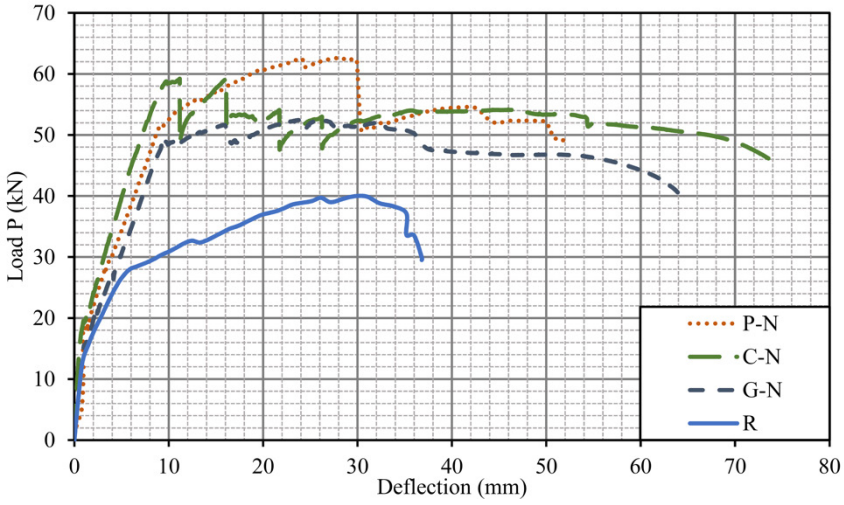

Figure 5: NSE strengthened beams load-deflection graphs

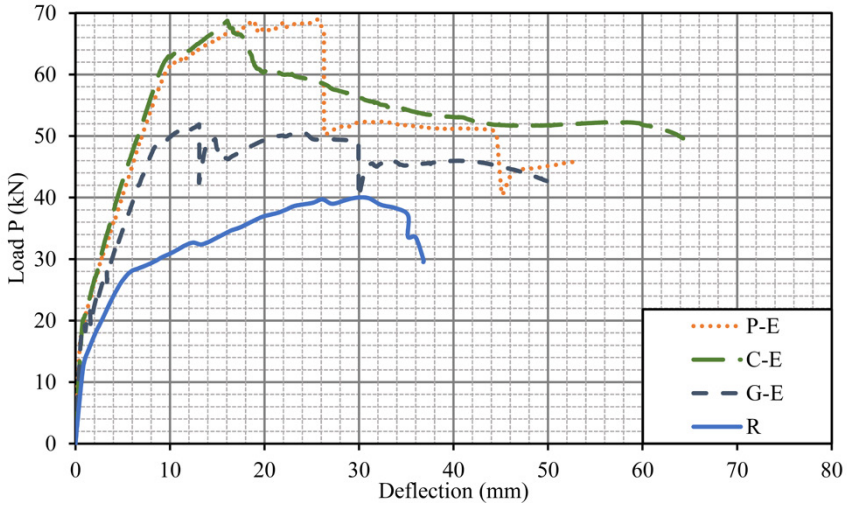

Figure 6: EB strengthened beams load-deflection graphs

3.4 Failure modes

The reference specimen R failed in the typical un-strengthened manner of steel yielding followed by concrete crushing at midspan. The failure mode depended on the FRCM fabric type and strengthening technique. Specimen P-N failed due to midspan

delamination while its EB counterpart (P-E) failed due to plate end debonding which indicated increased bond efficiency between concrete substrate and FRCM composite due to the NSE strengthening. As for the carbon strengthened specimens (C-N and C-E) the failure was due to midspan delamination, and the glass strengthened specimens (G-N and G-E) failed due to complete fabric rupture indicating maximum FRCM utilization.

4 CONCLUSION

This study investigates the efficacy of NSE-FRCM strengthening in enhancing the flexural performance of RC beams. A total of 7 RC beams were prepared and tested in four-point loading. The test parameters were the FRCM fabric material and the strengthening technique. Based on the test results, the following can be concluded:

- The surface roughening of NSE allowed the original section dimensions to be preserved and eliminate the safety risks involved due to sandblasting.
- The average P_u values were 58.1 kN and 63.2 kN for NSE and EB strengthened specimens, respectively, indicating favorable performance for NSE strengthening.
- Specimens strengthened using NSE-FRCM exhibited improved ductility performance compared to their EB-FRCM strengthened counterparts.
- NSE strengthening alleviated the plate end debonding in specimen P-N due to the increased bonding performance between FRCM and concrete substrate.
- Glass FRCM strengthened specimens exhibited maximum FRCM fabric utilization, indicated by the failure due to complete fabric rupture.

This study enriches the literature with promising results about the NSE-FRCM technique that can be helpful for future studies on the applications of FRCM strengthening for concrete and masonry structures.

ACKNOWLEDGEMENTS

This paper was made possible by NPRP grant # NPRP 7-1720-2-641 from the Qatar national research fund (a member of Qatar Foundation). The findings achieved herein are solely the responsibility of the authors.

REFERENCES

ACI Committee 549 (2013). *Guide to Design and Construction of Externally Bonded Fabric-Reinforced Cementitious Matrix (FRCM) Systems for Repair and Strengthening Concrete and Masonry Structures*.

Ebead, U., Shrestha, K. C., Afzal, M. S., El Refai, A. & Nanni, A. (2016). Effectiveness of fabric-reinforced cementitious matrix in strengthening reinforced concrete beams. *Journal of Composites for Construction*, *21*(2), 04016084.

Ebead, U. & Younis, A. (2019). Pull-off characterization of FRCM/Concrete interface. *Composites Part B*, Elsevier, 165, 545-553.

Gonzalez-Libreros, J. H., Sneed, L. H., D'Antino, T. & Pellegrino, C. (2017). Behavior of RC beams strengthened in shear with FRP and FRCM composites. *Engineering Structures*, Elsevier Ltd, 150, 830-842.

Koutas, L. N., Tetta, Z., Bournas, D. A. & Triantafillou, T. C. (2019). Strengthening of concrete structures with textile reinforced mortars : State-of-the-art review. *Journal of Composites for Construction*, *23*(1), 03118001.

Lee, D., Cheng, L. & Yan-Gee Hui, J. (2013). Bond characteristics of various NSM FRP reinforcements in concrete. *Journal of Composites for Construction*, *17*(1), 117-129.

Raoof, S. M., Koutas, L. N. & Bournas, D. A. (2017). Textile-Reinforced Mortar (TRM) versus Fibre-Reinforced Polymers (FRP) in flexural strengthening of RC beams. *Construction and Building Materials*, The Authors, 151, 279-291.

Ruredil. (2016a). *Ruredil X Mesh Gold Datasheet*.

Ruredil. (2016b). *Ruredil X Mesh C10 Datasheet*.

SIKA. (2016). *SikaWrap -350G Grid Datasheet*.

United States Department of Labor (2014). *Protecting Workers from the Hazards of Abrasive Blasting Materials, OSHA FS 3697 - 2014*.

Wakjira, T. G. & Ebead, U. (2018). Hybrid NSE/EB technique for shear strengthening of reinforced concrete beams using FRCM: Experimental study. *Construction and Building Materials*, 164, 164-177.

Yin, S., Xu, S. & Lv, H. (2014). Flexural behavior of reinforced concrete beams with TRC tension zone cover. *Journal of Materials in Civil Engineering*, *26*(2), 320-330.

Younis, A., Ebead, U. & Shrestha, K. C. (2017a). Tensile characterization of textile reinforced mortar. *Proceedings of the Ninth International Structural Engineering and Construction Conference, Resilient Structures and Sustainable Construction*, ISEC Press, Valencia, Spain.

Younis, A., Ebead, U. & Shrestha, K. C. (2017b). Different FRCM systems for shear-strengthening of reinforced concrete beams. *Construction and Building Materials*, Elsevier Ltd, 153, 514-526.

Cite this article as: El-Sherif H., Ebead U., "Near Surface Embedded Application for FRCM Strengthening of RC Beams in Flexure", *International Conference on Civil Infrastructure and Construction (CIC 2020)*, Doha, Qatar, 2-5 February 2020, DOI: https://doi.org/10.29117/cic.2020.0100

Life Cycle Assessment for Fiber-Reinforced Polymer (FRP) Composites Used in Concrete Beams: A State-of-the-Art Review

Mohamed Ibrahim
mohamed.amin@qu.edu.qa
Department of Civil and Architectural Engineering, Qatar University, Doha, Qatar

Usama Ebead
uebead@qu.edu.qa
Department of Civil and Architectural Engineering, Qatar University, Doha, Qatar

Mohammed Al-Ansari
m.alansari@qu.edu.qa
Department of Civil and Architectural Engineering, Qatar University, Doha, Qatar

ABSTRACT

Fiber-reinforced polymer (FRP) composites have become popularly utilized in structural engineering applications. The common use of the FRP composites is related to their economic benefits that can be observed right away or in a long-time period. With increasing concern about global warming and the shortage of natural resources, it is essential to study the environmental implications of the use of FRP composites. Life cycle assessment (LCA) is one of the most common techniques that can be used to take the environmental impact of the FRP into consideration. This paper presents a literature review about the LCA of FRP composites in concrete beams. The LCA results reported in the literature confirmed the use of FRP composites for reinforcing the RC beams instead of conventional steel rebars or that the strengthening of RC beams instead of demolishing and reconstruction is a more environment-friendly approach.

Keywords: Life cycle assessment; Fiber-reinforced polymer; Reinforced concrete; Beams

1 INTRODUCTION

Fiber reinforcement polymer (FRP) composites have been popular within the construction industry, owing to their favorable features, including the superior durability against corrosion, versatility for in-field applications and enhanced strength-to-weight ratio as compared to their counterpart traditional materials. FRPs are commonly used for reinforcing the structural elements in place of steel reinforcement and for the structural strengthening of in-service reinforced concrete (RC) members. (Guadagnini et al., 2006, Abdel Baky et al., 2007, Kim et al., 2008, Rizzo & Lorenzis, 2009, Chen et al., 2012, Ebead & Saeed, 2017). Commonly, FRP composites are composed of different fiber types, such as glass FRP (GFRP), carbon FRP (CFRP), aramid FRP (AFRP), and basalt FRP (BFRP). However, the most commonly used ones are the CFRP and GFRP because of their excessive tensile strength and ductility performance, respectively. Furthermore, FRP can be made by combining varied substances to generate a hybrid FRP composite that gather the advantages of the involved materials. The FRP composites are usually used in the shape of laminates, plates, strips, sheets, and rods (rebars). The internal

reinforcement and the external reinforcement (strengthening) of the concrete members can be easier, faster, and more effective with the use of the FRP composites. (Mohamed Ibrahim, 2019).

The growing awareness about climate change and global warming increased the attention of scholars towards analyzing the environmental impacts associated with products or services. FRP composites have some in-service environmental benefits. The light-weight of the FRP composites and its strong ability to resist corrosion enable them to decrease the energy combustion, green-house emissions associated with installation, transportation, and maintenance. However, to analyze the environmental impacts of FRP composite, it is important to consider the entire FRPs' life cycle from the raw material acquisition through production, operations until the end-of-life treatment. Life cycle assessment (LCA) is an approach used to analyze the impacts of a product or service on the environment from the stage of retrieving the raw materials from the planet until the products are recycled or wasted (Cradle-to-Gate) as per (International Organisation for Standardisation, 2006). The capability of LCA in analyzing the impacts of the industrial systems on the environment is broader and more comprehensive, compared to other cycles, where each stage is considered alone and the interrelation of the products with other activities is ignored. LCA enables the evaluation of a product's impact on global warming (mainly the CO_2 emissions), ozone depletion, eco-systems, energy consumption and human toxicity. Figure 1 shows the flow process of LCA as per the International Organisation for Standardisation (2006).

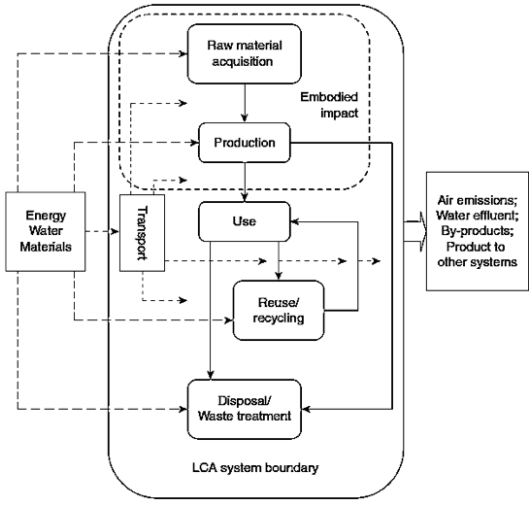

Figure 1: Flow process of LCA (International Organisation for Standardisation, 2006)

The process of practicing a LCA is considered a systematic approach, which consists of four phases: Goal Definition; Inventory Analysis; Impact Assessment; and Interpretation of Results (Zhang, 2013). The Goal Definition phase includes defining the scope of the assessment by clearly defining the boundaries that are in the scope of interest and the environmental effects which are considered in the assessment of the defined product or service. The Inventory Analysis phase is about the quantification

of the product's material and energy usages throughout its life cycle, such as carbon dioxide CO_2 emissions, solid waste disposal, and wastewater discharges. The Impact Assessment phase includes the use of the data in the inventory analysis to assess the impact of the product on several aspects of the environment such as human toxicity, ozone depletion, global warming, Acidification potential and Eutrophication potential. However, the scope of the LCA will define what impacts are going to be considered in the analysis. In the Interpretation of Results phase, the assessments of the emissions and energy usage due to the production of the material in its life cycle are evaluated. The evaluation provides a clear interpretation and understanding of the environmental impacts associated with the product under study. The four components of the LCA are summarized in Figure 2. In the literature, there are several LCA studies about using the FRP composites in the construction applications (Bakis, 2009, Russell-Smith & Lepech, 2009, Mara et al., 2013, Zhang, 2013, Dong et al., 2015, Inman et al., 2017, Cadenazzi et al., 2019, Van Loon et al., 2019).

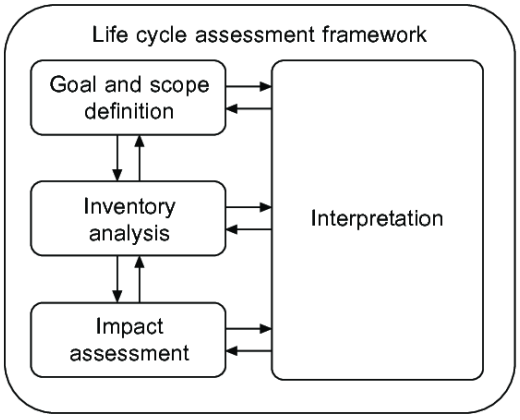

Figure 2: LCA Framework (based on ISO, 2006)

This paper aims to explore the results of existing literature about the environmental impact of using FRP composites in concrete beams either to replace the internal reinforcement (steel rebars) or to strengthen the RC beams by external reinforcement.

2 LCA OF FRP REINFORCED CONCRETE BEAMS

This section provides the environmental impact of using the FRP rebars for reinforcing the concrete structural elements instead of steel rebars, as summarized in Table 1. Garg and Shrivastava (2019) have conducted an analytical study to compare the CO_2 emission and energy consumption resulting from using three types of FRP rebars (CFRP, GFRP, and BFRP) to replace the traditional steel reinforcement rebars for rectangular concrete beams. The LCA environmental impact is determined using Cradle-to-Gate data of each type of reinforcement. Generally, the results showed that the FRP rebars have a better impact on the environment than that of steel rebars. In terms of CO_2 emissions, the GFRP, BFRP, and CFRP reinforced beams showed 43%, 40%, and 39% less CO_2 emissions compared to the steel reinforced beams, respectively, as shown in Figure 3. In terms of energy consumption, the GFRP, BFRP, and CFRP reinforced beams showed

47%, 50%, and 32% less energy consumption than that with steel reinforced beams, respectively as shown in Figure 3. Van Loon et al. (2019) have conducted research to reduce the environmental-economic (shadow) costs of precast RC beams. The authors have studied the impact of partial replacement of the conventional steel rebars by FRP tubes. The authors have considered FRP tubes made of different types of fibers namely, E-glass, Flax, and Kenaf. Results revealed that replacing 46%, 46% and 39% of the steel reinforcement by E-glass, Flax, and Kenaf FRP decreases the shadow costs by 28%, 39%, 36% keeping the capacity unaltered, respectively (Figure 4). Inman et al. (2017)Inman et al. (2017) have performed mechanical and environmental assessments to compare the BFRP rebars and steel rebars in the concrete beams. The results showed that there is 62% saving in the CO2 emissions when the BFRP reinforcement was chosen over the conventional steel rebars. In terms of ozone depletion, and human toxicity, the use of BFRP rebars showed an average reduction of 21% and 78%, respectively. The authors have also studied other environmental impacts such as Terrestrial acidification, Freshwater eutrophication, Marine eutrophication, Photochemical oxidant, Formation, Particulate matter formation, Terrestrial eco-toxicity, Agricultural land Occupation, and Natural land transformation. The results of these environmental impacts were observed to be minimal or less important.

Table 1: Comparison of LCA results from different studies of replacement of the conventional steel reinforcement by FRP composites

Reference	Type of FRP	FRP Replacement % to Steel Rebars	Environmental Impact Category	Reduction % in the Environmental impact due to using FRP rebars
Garg and Shrivastava, (2019)	GFRP	100%	Global Warming (CO_2 emissions)	43%
Garg and Shrivastava, (2019)	GFRP	100%	Energy Consumption	47%
Garg and Shrivastava, (2019)	BFRP	100%	Global Warming (CO_2 emissions)	40%
Garg and Shrivastava, (2019)	BFRP	100%	Energy Consumption	50%
Garg and Shrivastava, (2019)	CFRP	100%	Global Warming (CO_2 emissions)	39%
Garg and Shrivastava, (2019)	CFRP	100%	Energy Consumption	32%
Van Loon et al. (2019)	E-glass	46%	Shadow Cost	28%
Van Loon et al. (2019)	Flax	46%	Shadow Cost	39%
Van Loon et al. (2019)	Kenaf	39%	Shadow Cost	36%
Inman et al. (2017)	BFRP	100%	Global Warming (CO_2 emissions)	62%
Inman et al. (2017)	BFRP	100%	Ozone Depletion	21%
Inman et al. (2017)	BFRP	100%	Human Toxicity	78%

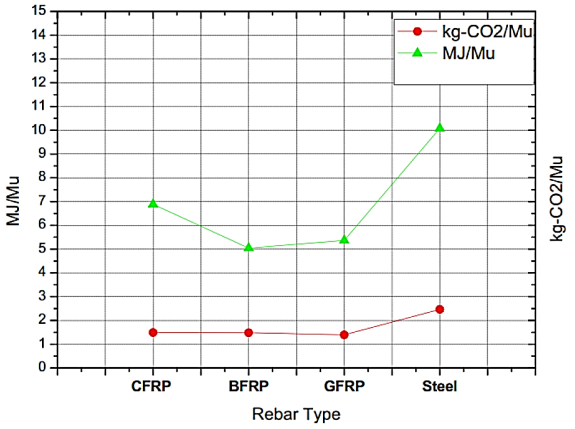

Figure 3: LCA results in terms of energy consumption (at the left side) and the CO_2 emissions (at the right side) for different types of reinforcement rebars in concrete beams, as per (Garg & Shrivastava, 2019)

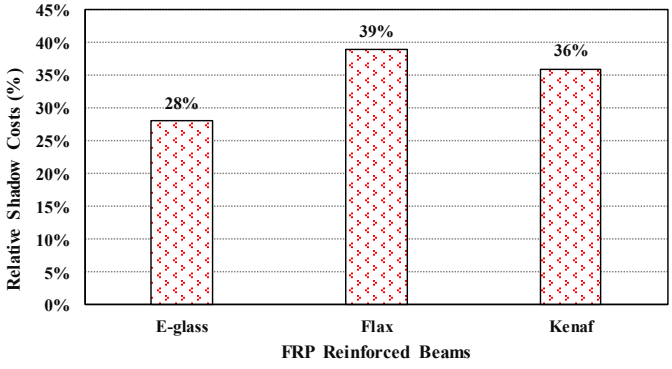

Figure 4: Reduction % of using E-glass, Flax, and Kenaf FRP tubes as partial replacement to the conventional steel rebars (Van Loon et al., 2019)

3 LCA OF FRP USED FOR STRENGTHENING OF RC STRUCTURES

There are various causes of the deterioration of the RC structures including the excessive corrosion of steel reinforcement (especially in the severe weather regions), improper or flawed maintenance, unaccounted carrying load augmentation, increase of the life service load, changing of the original structure's purpose, and mistakes on the design or construction development. Deteriorated and deficient structures require an effective and immediate strengthening application to ensure the users' safety. Strengthening and rehabilitation can be an economical and environmentally possible alternative to demolition/reconstruction of the deteriorated and deficient structures. In the construction sector, FRP can be used for strengthening of existing buildings, thus creating the possibility of avoiding the environmental problems resulting from demolishing these structures and constructing new ones. Several studies have investigated the LCA using FRP composites for the strengthening of RC beams compared to demolish and

reconstruction, as summarized in Table 2. Maxineasa et al. (2015) conducted a LCA to compare the environmental impacts resulting from the strengthening of an existing RC beam with FRP and the environmental impacts resulting from constructing a new RC beam. The study includes different strengthening techniques using CFRP strips. The authors used the cradle-to-gate LCA type to assess the impact categories, namely, global warming, human toxicity, and ozone depletion. Results releveled that the strengthening techniques using FRP can increase the ultimate capacity of the RC beam from 60 kN to 184.3 kN (207%). Moreover, the total CO_2 emissions resulting from the strengthening process was reported 69% less than that for constructing a new RC beam. Similarly, the reduction in the human toxicity and the ozone depletion were reported 73% and 48% compared to the reference beam, respectively. These results were confirmed by (Palacios-Munoz et al., 2018). The authors have reported that the total CO_2 emissions due to strengthening the RC beam by CFRP and due to demolishing and reconstruction new RC beam through a comparative LCA study. The authors observed a 65% reduction in the CO_2 emission from the strengthened beam than that from the reconstructed beam. Maxineasa et al. (2018) have compared the total CO_2 emissions resulting from the construction RC beam and the environmental impact resulting from strengthening an existing RC beam using CFRP and GFRP. The LCA study was Cradle-to-Gate type for the involved materials in global warming (CO_2 emissions) and the ozone depletion. The authors reported 76% and 67% lower in the CO_2 emissions due to strengthening by GFRP and CFRP, compared to the CO_2 emissions resulting from construction of new RC beams, respectively. In addition, the ozone depletion was reduced by 14.2 % by using both FRP types.

Table 2: Comparison of LCA results from different studies about the strengthening of in-service RC structures compared to demolishing and reconstruction of new RC structure

Reference	Type of FRP	Increase % in the load-carrying capacity due to strengthening	Environmental Impact Category	Reduction % in the Environmental impact due to Strengthening
Maxineasa et al. (2015)	CFRP	207%	Global Warming (CO_2 emissions)	69%
Maxineasa et al. (2015)	CFRP	207%	Human Toxicity	73%
Maxineasa et al. (2015)	CFRP	207%	Ozone Depletion	48%
Palacios-Munoz et al. (2018)	CFRP	50%	Global Warming (CO_2 emissions)	72%
Palacios-Munoz et al. (2018)	CFRP	50%	Energy Consumption	60%
Maxineasa et al. (2018)	GFRP	N/A	Global Warming (CO_2 emissions)	73%
Maxineasa et al. (2018)	GFRP	N/A	Ozone Depletion	14.2%
Maxineasa et al. (2018)	CFRP	N/A	Global Warming (CO_2 emissions)	14.2%
Maxineasa et al. (2018)	CFRP	N/A	Ozone Depletion	66%

4 CONCLUSION AND RECOMMENDATIONS

This paper has provided a literature review on the LSA for FRP composites that have been used either for reinforcing concrete beams instead of the conventional steel rebars or for strengthening the old RC beams instead of demolishing and reconstruction of new

ones. Overall, the results reported in the existing literature were found to be consistent with each other and confirming that the utilization of FRP composites is a preferable approach towards reducing the environmental impacts. From the literature, the most important environmental impacts that are commonly assessed are the potential of global warming due to CO_2 emissions, the ozone layer potential, and the human toxicity potential through the life cycle of the product e.g., FRP. Although several scholars have investigated the LCA of FRP in RC structures, the literature still lacks in this context. A limited number of LSA studies have been conducted on replacing the steel rebars of completed structural building projects. Moreover, some authors have not mentioned the increase in percentage due to strengthening although it is essential to assess the performance of FRP with their environmental impact. Therefore, the authors of this paper recommend conducting a comprehensive LSA of using GFRP, CFRP and BFRP rebars as a replacement to the conventional steel rebars for various structural members' designs such as columns, beams, slabs and footings for completed RC high-rise building projects. Furthermore, the authors recommend enriching the literature by conducting a grade-to-gate LCA of using different strengthening techniques such as near-surface mounted and near-surface embedded, using different types of FRP namely, rods, sheets, or laminates for strengthening RC structural members. Finally yet importantly, authors suggest exploring the interaction between the economic impacts and the environmental impacts of the use of FRP in the concrete structural elements in order to help the decision-makers with a widespread overview.

REFERENCES

Abdel Baky, H., Ebead, U. A. & Neale, K. W. (2007). Flexural and interfacial behavior of FRP-strengthened reinforced concrete beams. *Journal of Composites for Construction*, *11* (December), 629-639.

Bakis, C. E. (2009). Life cycle analysis issues in the use of Frp composites in civil infrastructure. *Life Cycle Assessment of Sustainable Infrastructure Materials*, 21-22.

Cadenazzi, T., Dotelli, G., Rossini, M., Nolan, S. & Nanni, A. (2019). Life-cycle cost and life-cycle assessment analysis at the design stage of a fiber-reinforced polymer-reinforced concrete bridge in Florida. *Advances in Civil Engineering Materials*, *8*(2), 20180113.

Chen, G. M., Chen, J. F. & Teng, J. G. (2012). On the finite element modelling of RC beams shear-strengthened with FRP. *Construction and Building Materials*, *32*, 13-26.

Dong, J. F., Jia, P., Yuan, S. C. & Wang, Q. Y. (2015). Compressive behaviours of square timber columns reinforced by partial wrapping of FRP sheets. *Materials Research Innovations*, *19*, S1465-S1468.

Ebead, U. & Saeed, H. (2017). FRP/stirrups interaction of shear-strengthened beams. *Materials and Structures/Materiaux et Constructions*, *50*(2), 1-16.

Garg, N. & Shrivastava, S. (2019). Environmental and economic comparison of frp reinforcements and steel reinforcements in concrete beams based on design strength parameter. *In*: Dr B R Ambedkar National Institute of Technology, ed. *UKIERI Concrete Congress*, Jalandhar (Punjab), India.

Guadagnini, M., Pilakoutas, K. & Waldron, P. (2006). Shear Resistance of FRP RC Beams: Experimental Study. *Journal of Composites for Construction*, *10*(6), 464-473.

Inman, M., Thorhallsson, E. R. & Azrague, K. (2017). A Mechanical and Environmental Assessment and Comparison of Basalt Fibre Reinforced Polymer (BFRP) Rebar and Steel Rebar in Concrete Beams. *Energy Procedia*, *111*(1876), 31-40.

International Organisation for Standardisation, (2006). *Environmental management – Life cycle assessment – Principles and framework*. ISO 14040. Geneva, Switzerland.

Kim, G., Sim, J. & Oh, H. (2008). Shear strength of strengthened RC beams with FRPs in shear. *Construction and Building Materials*, *22*(6), 1261-1270.

Van Loon, R. R. L., Pujadas-Gispert, E., Moonen, S. P. G. & Blok, R. (2019). Environmental optimization of precast concrete beams using fibre reinforced polymers. *Sustainability (Switzerland)*, *11*(7).

Mara, V., Haghani, R., Sagemo, A., Storck, L. & Nilsson, D. (2013). Comparative study of different bridge concepts based on life-cycle cost analyses and life-cycle assessment. *Proceedings of the 4th Asia-Pacific Conference on FRP in Structures, APFIS 2013*, 1-6.

Maxineasa, S. G., Isopescu, D. N., Entuc, I. S., Taranu, N., Lupu, L. M. & Hudisteanu, I. (2018). Environmental performances of different carbon and glass fibre reinforced polymer shear strengthening solutions of linear reinforced concrete, *11*(1).

Maxineasa, S. G., Taranu, N., Bejan, L., Isopescu, D. & Banu, O. M. (2015). Environmental impact of carbon fibre-reinforced polymer flexural strengthening solutions of reinforced concrete beams. *International Journal of Life Cycle Assessment*, *20*(10), 1343-1358.

Mohamed Ibrahim (2019). *Externally Bonded and Near-surface Mounted FRP Strips For Shear Strengthening of RC Deep Beams*. Qatar University.

Palacios-Munoz, B., Gracia-Villa, L., Zabalza-Bribián, I. & López-Mesa, B. (2018). Simplified structural design and LCA of reinforced concrete beams strengthening techniques. *Engineering Structures*, *174* (July), 418-432.

Rizzo, A. & Lorenzis, D. L. (2009). Behavior and capacity of RC beams strengthened in shear with NSM FRP reinforcement. *Construction and Building Materials*, *23*(4), 1555-1567.

Russell-Smith, S. V & Lepech, M. D. (2009). Life cycle assessment of frp seismic retrofitting. *Life Cycle Assessment of Sustainable Infrastructure Materials*, 21-22.

Zhang, C. (2013). Life cycle assessment (LCA) of fibre reinforced polymer (FRP) composites in civil applications. *Eco-Efficient Construction and Building Materials: Life Cycle Assessment (LCA), Eco-Labelling and Case Studies*, 565-591.

Cite this article as: Ibrahim M., Ebead U., Al-Ansari M., "Life Cycle Assessment for Fiber-Reinforced Polymer (FRP) Composites Used in Concrete Beams: A State-of-the-Art Review", *International Conference on Civil Infrastructure and Construction (CIC 2020)*, Doha, Qatar, 2-5 February 2020, DOI: https://doi.org/10.29117/cic.2020.0101

Verification of ACI- 549 Code for Flexural Strengthening of Reinforced Concrete Beams Using FRCM

Muhammad Shekaib Afzal
shekaib@qu.edu.qa
Department of Civil and Architectural Engineering, Qatar University, Doha, Qatar

Usama Ebead
uebead@qu.edu.qa
Department of Civil and Architectural Engineering, Qatar University, Doha, Qatar

ABSTRACT

This paper presents an analytical study to verify the ACI 549-4R-16 code for experimentally tested Reinforced Concrete (RC) beams, which were strengthened to enhance the flexural capacity using Fiber-Reinforced Cementitious Mortars (FRCM). Twelve RC beam specimens having 2500 mm length, 150 mm width, and 260 mm depth were prepared with two different reinforcement ratios (ρ_s^D12=0.72% and ρ_ s^D16=1.27%), and were then strengthened with two different FRCM systems, namely carbon and polyparaphenylene-benzobisoxazole (PBO) FRCM systems. Two RC beams were tested as control specimens. Six beams were externally reinforced using single, double and triple layers of carbon FRCM system, while the remaining four beams were repaired with one and two layers of PBO FRCM system. The strengthened RC beams were tested in flexural under four-point monotonic loading. The experimental results revealed that a reasonable gain in flexural strength was achieved for both FRCM systems, with up to 78% increase in flexural capacity for carbon FRCM systems and up to 27.5% for PBO FRCM system over that of their control specimens. Further, the results obtained from the theoretical approach using the ACI 549 code conform well with the experimental load-carrying capacities. Moreover, the values obtained for experimental to theoretical ratio ($\frac{P_U}{P_T}$) are quite close to 1.00 which somewhat shows satisfactory computational results.

Keywords: Fabric-reinforced cementitious mortar; Flexural strengthening; Reinforced concrete beams; Reinforcement ratios; FRCM systems

1 INTRODUCTION

Recently, several studies on strengthening of Reinforced Concrete (RC) structures have been focused on the application of Fiber Reinforced Polymer (FRP) Externally Bonded (EB) with polymer-based pastes (Abdel Baky et al., 2007; Aidoo et al., 2006; Almassri et al., 2014; Barros & Fortes, 2005; Capozucca, 2014; Ebead & Saeed, 2013; Ebead & Saeed, 2014; Elsayed et al., 2007; Elsayed et al., 2009; Kotynia et al., 2008; Kreit et al., 2010; Neale et al., 2006; Teng et al., 2006; Ebead, 2011). Recently, a new strengthening technique has been introduced, that uses Fabric Reinforced Cementitious Matrix (FRCM) systems for reinforced concrete structures (Arboleda et al., 2015; Babaeidarabad et al., 2014; Loreto et al., 2015; Ombres, 2011; Ombres, 2015; Tetta et al., 2015; Triantafillou & Papanicolaou, 2006). The existing studies have shown great success of FRCM in improving the performance of repaired RC elements as an external

strengthening system. This relatively new technique (FRCM strengthening technique) is a viable repair/strengthening solution in the Gulf where extremely elevated heat, severe humidity, and elevated salt amounts round the concrete foundations that can severely deteriorate the concrete and steel reinforcement (Ebead et al., 2016).

This paper presents the analytical method to verify the ACI 549-4R-16 code (ACI 549, 2016) for experimentally tested Reinforced Concrete (RC) beams, which were repaired to enhance their flexural performance using Fiber-Reinforced Cementitious Mortars (FRCM). Twelve RC beams were tested under four-point monotonic loading. The beams were externally reinforced with two different FRCM systems, namely, carbon and polyparaphenylene-benzobisoxazole (PBO) FRCM systems. The test matrix involves two different reinforcement ratios and several combinations of fabric plies. The experimental results were compared with those of the analytical approach (using ACI 549 code).

2 EXPERIMENTAL INVESTIGATION

2.1 Materials

2.1.1 Concrete

Ready mix concrete was used to cast the beam specimens. The design mix proportions per each cubic meter of concrete were 1,100 kg of gravel, 370 kg of ordinary Portland cement and 800 kg of sand. The water-to-cement ratio was kept at 0.45.

2.1.2 Reinforcing Steel Rebar's

Grade B (BS 4449, 2005) steel bars were used as reinforcement for RC beams: 8 mm diameter bars were used for all the transverse steel reinforcement and also for the compression reinforcement, while 12 and 16 mm bars were used for the main flexural reinforcement. The yield stress and elastic modulus of these steel rebars are 520 MPa and 200 GPa, respectively.

2.1.3 Textile Reinforced Mortar (FRCM)

Two commercially available FRCM systems have been utilized in this study. The first system consists of PBO textile with Ruredil X Mortar M750 and the second one includes carbon textile with Sika Mono top-612 Mortar. Table-1 reports the mechanical properties for each textile, provided by the manufacturer.

Table 1: Textile geometric and mechanical properties in warp direction (data adopted from Ruredil, 2016 & S&P, 2016)

Textile Type	Area per unit width (A_f), (mm^2/mm)	Elastic Modulus (GPa)	Tensile strength (GPa)	Ultimate Strain (%)
PBO	0.05	270	5.80	2.15
Carbon	0.157	240	4.30	1.75

Further, FRCM test coupons (410 × 50 × 10 mm) were tested after 28 days curing period to obtain the tensile properties for each FRCM composite in accordance with AC434 (ICC, 2013). The tensile characterization test results are presented in Table 2.

Table 2: FRCM composite tensile characterization properties

Textile composite Type	Elastic modulus of cracked specimen, (E_f), (GPa)	Ultimate Tensile strength, f_{fu} (GPa)	Ultimate Strain (%)
PBO	121	2.59	2.30
Carbon	151	2.10	1.25

2.2 Test Specimens

Twelve (12) beam specimens (2500 mm long, 260mm deep and 150 mm wide) were tested in this research. The parameters investigated were: i) reinforcement ratios (ρ_s^{D12} =0.72% and ρ_s^{D16}=1.27%), ii) FRCM strengthening systems, and iii) number of textile/ fabric layers. Out of 12 beam specimens, 2 beams were used as control specimens (not repaired), one each with the main reinforcing bars of 2D12 (ρ_s^{D12} =0.72%) and 2D16 (ρ_s^{D16} =1.27%), respectively. The effective depth of the beam was fixed at 210 mm for all of the tested specimens. Four beams were repaired with two different PBO-FRCM strengthening schemes (one and two layers of textiles). The remaining six beams were repaired with three different Carbon-FRCM strengthening schemes (one, two and three layers of textiles).

The procedure of FRCM strengthening includes the following steps: first, the soffit of the beam was roughened/sandblasted to a level where the smooth outer layer concrete was removed up to 2-3 mm depth and some fine aggregates were exposed. Next, the beams were covered with hessian cloth and water was sprinkled over the beam for at least 30 minutes prior to application of FRCM strengthening technique. Figure 1 shows a typical FRCM-repaired beam specimen.

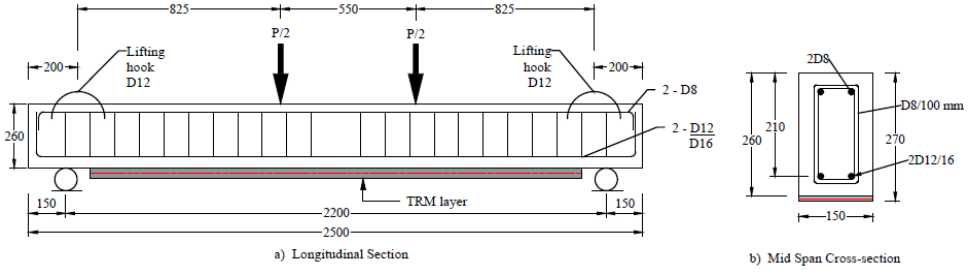

Figure 1: Longitudinal and cross-sectional details of typical FRCM repaired beam specimen *(All dimensions are in mm)*

Table-3 shows the test matrix, in which each specimen is identified using the "*T-R-L*" nomenclature, where: "*T*" denotes the FRCM strengthening scheme (CR for Carbon and PB for PBO); "*R*" denotes the main reinforcement bar ratio (R12 for ρ_s^{D12} =0.72% and R16 for ρ_s^{D16}=1.27%); and "*L*" denotes the number of textile layers (L1 for single layer, L2 for two layers, and L3 for three layers).

Further, the amount of FRCM composite layers is expressed in terms of equivalent stiffness for FRCM composite, κ^t given by $\kappa^t = nA_f E_f / b_s$, as listed in Column 2 of Table

3, where A_f is the equivalent area of each yarn of textile/fabric per unit width (Table 1), b_s is width of the tensile characterization coupon sample, n is the number of yarns of fabric within the width of the coupon sample, and E_f is the cracked elastic modulus of the FRCM composite in N/mm^2 (Table 2). This equivalent stiffness parameter is important as the values of A_f, n, and E_f are different for carbon and PBO FRCM systems. The comparison between the two FRCM systems was made based on their equivalent values. For instance, the normalization of to a single layer of carbon FRCM (κ = 1422 MPa) gives following expressions for each FRCM system: κ for 1 layer of carbon, 2×κ for 2 layers of carbon, 3×κ for 3 layers of carbon, 0.42×κ for 1 layer of PBO, and 0.85×κ for 2 layers of PBO. These normalized values clearly suggest that the equivalent stiffness of the PBO FRCM is approximately half that of the Carbon FRCM system.

2.3 Test Setup and Instrumentation

The test setup for the beam specimens is shown in Figure 2. Displacement control mode with a loading rate of 1mm / min was used for testing the beam specimens. The tested beam was mounted in Instron 1500HDX Static Hydraulic Universal Testing machine as shown in Figure 2.

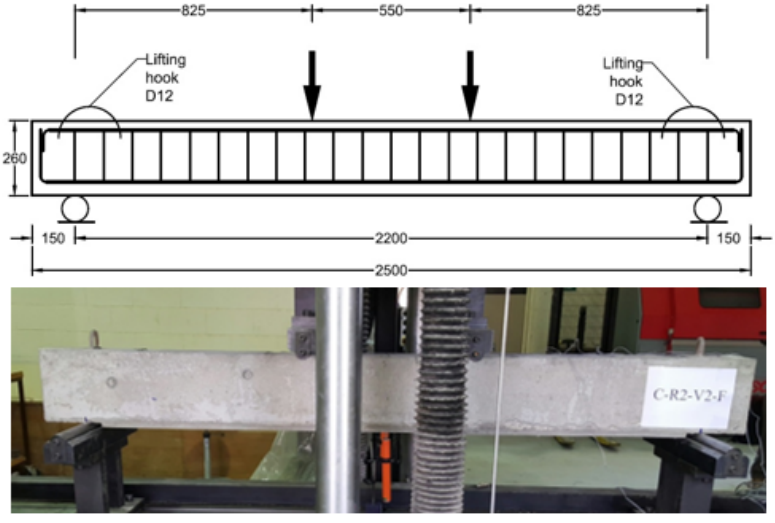

Figure 2: Instron Universal Testing Machine with loading pattern

3 EXPERIMENTAL FINDINGS

The test findings include the plots for load versus mid span-deflection, along with maximum load and deformation characteristics. The cracking patterns and failure mode characteristics are also discussed. Table 3 summarizes the experimental results for all tested specimens. Columns 4 and 5 of Table 3 list the maximum capacity (P**u**) for each beam and the increase in P**u** with respect to the corresponding reference specimen.

Table 3: Test Matrix and summary of Experimental Results (Ebead et al., 2016)

Beam ID*1	κ^t (MPa)	Normalized κ^t	Pu (kN)	Gain in Pu (%)	P_{Th} (kN)	$(\frac{P_U}{P_T})$	Mode of failure at Pu*2
R12	-	-	69.14	-	67	1.03	SY+CC
R16	-	-	110.32	-	109	1.01	SY+CC
CR- R12-L1	1422	κ	85.15	23.16	78	1.09	FS+FC
CR- R12-L2	2845	2 κ	89.12	28.90	91	0.98	FS+FC
CR- R12-L3	4267	3 κ	122.71	77.48	104	1.18	FS+D
CR- R16-L1	1422	κ	126.17	14.37	125	1.01	FS+D
CR- R16-L2	2845	2 κ	142.29	28.98	137	1.04	FS+D
CR- R16-L3	4627	3 κ	161.93	46.78	150	1.08	FS+D
PB- R12-L1	605	0.42 κ	84.68	22.48	72	1.18	FRCM(C+D)
PB- R12-L2	1210	0.85 κ	88.15	27.49	79	1.11	FRCM(C+D)
PB- R16-L1	605	0.42 κ	118.92	7.80	113	1.05	FRCM(C+D)
PB- R16-L2	1210	0.85 κ	123.86	12.27	119	1.04	FRCM(C+D)

*[*1]CR represents Carbon–FRCM, PB represents PBO–FRCM; R12 is for 2–D12, and R16 is for 2–D16 main reinforcement; L1 is for 1 layer, L2 for 2 layers, and L3 is for 3 layers of textile*

*[*2]SY– steel yielding, CC – concrete crushing, FS – fabric slippage, FC – flexural cracks, D – FRCM delamination, FRCM(C+D) – Cracking plane within FRCM and FRCM delamination*

3.1 Carbon Textile Reinforced Beams

Figure 3-a shows mid-span deflection plot against the load for repaired beams with D12 as flexural steel reinforcement. Significant gain in load carrying capacity was observed for the carbon FRCM system with gains in P_u of 23% for CR-R12-L1, 29% for CR-R12-L2, and 77% for CR-R12-L3. Similarly, for D16 main steel reinforcement, the load-deflection plots are shown in Figure 3-b. The associated gains in maximum load for the specimens were 14% for CR-R16-L1, 29% for CR-R16-L2, and 47% for CR-R16-L3.

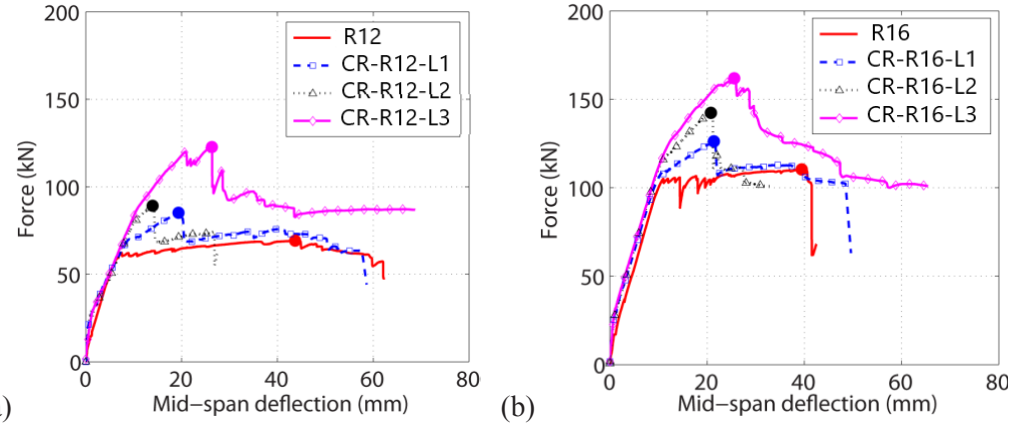

(a) (b)

Figure 3: Load-deflection graphs for Carbon FRCM repaired specimens: (a) D12 specimens, (b) D16 specimens

3.2 PBO Textile Reinforced Beams

The mid span deflection plots for PBO repaired FRCM system having D12 and D16 as main longitudinal reinforcement are shown in Figure 4-a and 4-b, respectively. The observed gains in *P*u (expressed as Specimen – Pu increase) were (PB-R12-L1 – 22%, PB-R12-L2 – 27%) and (PB-R16-L1 – 8%, PB-R16-L2 – 12%). This also showed a considerable increase in maximum capacity compared to the unstrengthened specimens R-12 and R-16.

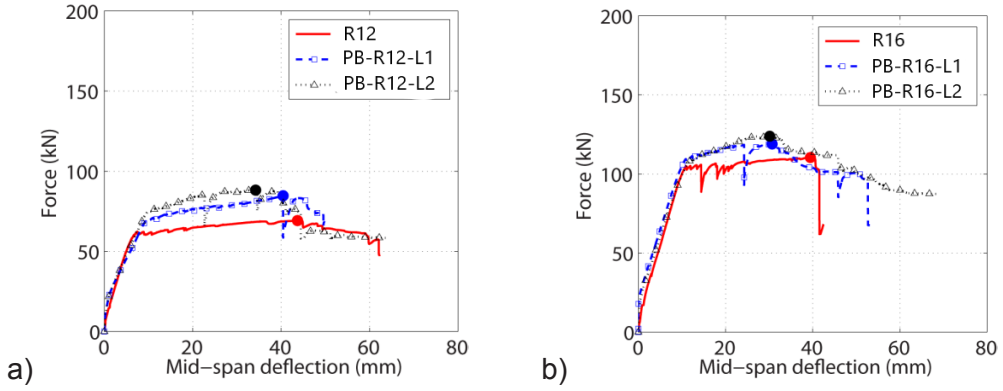

Figure 4: Load-deflection graphs for PBO FRCM repaired specimens: (a) D12 specimens, (b) D16 specimens

4 THEORETICAL FORMULATION

The experimental results for flexural repaired beam specimens are compared with the analytical approach to verify the ACI 549-4R-16 code (Afzal, 2016). The profiles for the stresses and the associated strains for a repaired RC are shown in Figure 5. Here, T_s is the tension force provided by the steel reinforcement; T_f is the tensile force provide by the FRCM reinforcement; C is the compressive total internal force provided by the concrete; A_s is the area of tensile steel reinforcement; and A_s‘ is the area of compression steel reinforcement.

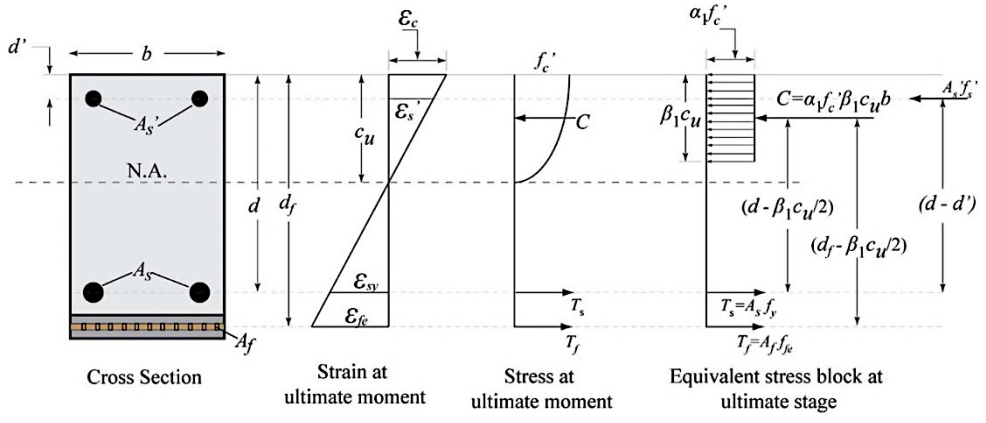

Figure 5: Internal stress and strain profile for a beam section repaired with FRCM under flexure at ultimate limit state

Figure 6 presents a flow chart prepared according to the ACI - 549 code that was used to compute the theoretical load values for all the experimentally tested specimens, which are listed in Column 6 of Table 3. Column 7 of Table 3 shows the experimental-to-theoretical ratios for load-carrying capacity ($\frac{P_U}{P_T}$), which were close to 1.00, indicating satisfactory computational results.

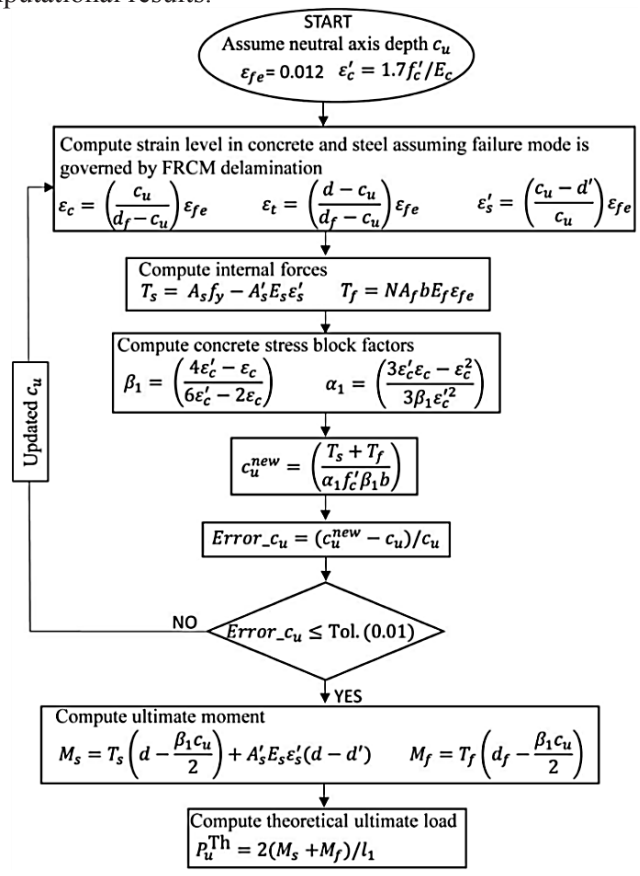

Figure 6: Flowchart for calculating the theoretical load-carrying capacity (Ebead et al., 2016)

5 CONCLUSION

An analytical approach to validate the ACI 549 code on experimentally tested beam specimens repaired in flexure with FRCM is presented in this study. The experimentally tested beam specimens had two different main steel reinforcement ratios and repaired with two different FRCM systems (carbon and PBO). The effect of the number of textile layers were also investigated. The following general conclusions can be drawn from the reported experimental and analytical approaches:

- The experimental results revealed that a reasonable gain in flexural strength was achieved for both FRCM systems, with up to 78% increase in flexural capacity for carbon FRCM system and up to 27.5% for PBO FRCM system over that of their control specimens.

- Theoretical formulation to validate the ACI-549 code for these experimentally tested beam specimens showed satisfactory computational results: the values obtained for experimental to theoretical ratio ($\frac{P_U}{P_T}$) were quite close to 1.00.
- The equivalent stiffness factor κ^t used in the theoretical formulation is an important factor which directly influences the maximum capacity of the repaired beams. The two FRCM systems, with similar equivalent stiffness values, showed approximately similar increase in Pu values.

ACKNOWLEDGMENT

This paper was made possible by NPRP grant # NPRP 7-1720-2-641 from the Qatar National Research Fund (a member of Qatar Foundation). The findings achieved herein are solely the responsibility of the authors.

REFERENCES

ACI (American Concrete Institute) (2016). *Guide to design and construction of externally bonded fabric-reinforced cementitious matrix (FRCM) systems for repair and strengthening concrete and masonry structures*. (ACI 549). Farmington Hills, MI.

Abdel Baky, H. M., Ebead U. A. & Neale, K. W. (2007). Flexural and interfacial behavior of FRP-repaired reinforced concrete beams. *ASCE Journal of Composites for Construction*, 11: 629-39.

Afzal, M. S. (2016). *Strengthening of reinforced concrete beams With Textile-Reinforced mortars* (Master dissertation).

Aidoo, J., Harries, K. A. & Petrou, M. F. (2006). Full-scale experimental investigation of repair of reinforced concrete interstate bridge using CFRP materials. *ASCE Journal of Bridge Engineering*, 11: 350-58.

Almassri, B., Kreit, A., Mahmoud F. A. & François, R. (2014). Mechanical behavior of corroded RC beams repaired by NSM CFRP rods. *Composites Part B: Engineering*, 64: 97-107.

Arboleda, D., Carozzi, F. G., Nanni, A. & Poggi, C. (2015). Testing procedures for the uniaxial tensile characterization of fabric-reinforced cementitious matrix composites. *ASCE Journal of Composites for Construction*: 04015063.

Babaeidarabad, S., Loreto, G. & Nanni, A. (2014). Flexural strengthening of RC beams with an externally bonded fabric-reinforced cementitious matrix. *ASCE Journal of Composites for Construction*, 18: 04014009.

Barros, J. A. O. & Fortes, A. S. (2005). Flexural strengthening of concrete beams with CFRP laminates bonded into slits. *Cement and Concrete Composites*, 27: 471-80.

Ebead, U., Shrestha, K. C., Afzal, M .S., El Refai, A. & Nanni, A. (2016). Effectiveness of fabric-reinforced cementitious matrix in strengthening reinforced concrete beams. *Journal of Composites for Construction*, *21*(2), p.04016084:1-14.

Ebead, U. A. (2011). Hybrid externally bonded/mechanically fastened fiber-reinforced polymer for RC beam strengthening. *ACI Structural Journal*, 108: 1-10.

Ebead, U. A. & Saeed, H. (2014). Flexural and interfacial behavior of externally bonded/mechanically fastened fiber-reinforced polymer repaired reinforced concrete beams. *ACI Structural Journal*, 111: 741-51.

Ebead, U. A. & Saeed, H. (2013). Hybrid shear strengthening system for reinforced concrete beams: An experimental study. *Engineering Structures*, 49: 421-33.

Elsayed, W. E., Ebead, U. A & Neale, K. W. (2009). Studies on mechanically fastened fiber-reinforced polymer strengthening systems. *ACI Structural Journal*, 106: 49-59.

Elsayed, W. E., Ebead, U. A. & Neale, K. W. (2007). Interfacial behavior and debonding failures in FRP-repaired concrete slabs. *ASCE Journal of Composites for Construction*, 11: 619-28.

ICC (International Code Council) (2013). Acceptance criteria for masonry and concrete strengthening using fabric-reinforced cementitious matrix (FRCM) composite systems. AC434, Washington, D.C.

Kotynia, R., Abdel Baky, H. M., Neale, K. W. & Ebead, U. A. (2008). Flexural strengthening of RC beams with externally bonded CFRP systems: Test results and 3D nonlinear FE Analysis. *ASCE Journal of Composites for Construction*, 12: 190-201.

Kreit, A., Al-Mahmoud, F., Castel, A. & François, R. (2010). Repairing corroded RC beam with near-surface mounted CFRP rods. *Materials and Structures*, 44: 1205-17.

Loreto, G., Babaeidarabad, S., Leardini, L. & Nanni, A. (2015). RC beams shear-repaired with fabric-reinforced-cementitious-matrix (FRCM) composite. *International Journal of Advanced Structural Engineering (IJASE)*, 7: 341-52.

Neale, K. W., Ebead, U. A., Abdel Baky, H. M., Elsayed, W. E. & Godat, A. (2006). Analysis of the load-deformation behavior and debonding for FRP-repaired concrete structures. *Advances in Structural Engineering*, 9: 751-63.

Ombres, L. (2015). Structural performances of reinforced concrete beams repaired in shear with a cement based fiber composite material. *Composite Structures*, 122: 316-29.

Ombres, L. (2011) Flexural analysis of reinforced concrete beams repaired with a cement based high strength composite material. *Composite Structures*, 94: 143-55.

Ruredil (2016) Technical datasheet, Ruredil X mesh gold data sheet. Retrieved from

(http://english.ruredil.it/SchedeProdottoENG/RuredilXMeshGOLD_ing_1.pdf) (Jul. 16, 2016).

S&P (2016). Technical datasheet, S&P ARMO-mesh technical data sheet. Retrieved from

(http://www.spreinforcement.ch/sites/default/files/field_product_col_doc_file/tds_sp_armo-mesh_ver08_2015.pdf) (Jul. 16, 2016).

Teng, J. G., De Lorenzis, L., Bo, W., Rong Li, Wong, T. N. & Lik, L. (2006). Debonding failures of RC beams repaired with near surface mounted CFRP strips. *ASCE Journal of Composites for Construction*, 10: 92-105.

Tetta, Z. C., Koutas, L. N. & Bournas, D. A. (2015). Textile-reinforced mortar (TRM) versus Fiber-Reinforced Polymers (FRP) in shear strengthening of concrete beams. *Composites Part B: Engineering*, 77: 338-48.

Triantafillou, T. C. & Papanicolaou, C. G. (2006). Shear strengthening of reinforced concrete members with Textile-Reinforced Mortar (TRM) jackets. *Materials and Structures*, 39: 93-103.

Cite this article as: Afzal M. S., Ebead U., "Verification of ACI- 549 Code for Flexural Strengthening of Reinforced Concrete Beams Using FRCM", *International Conference on Civil Infrastructure and Construction (CIC 2020)*, Doha, Qatar, 2-5 February 2020, DOI: https://doi.org/10.29117/cic.2020.0102

Effects of Using Seawater and Recycled Coarse Aggregates on Plain Concrete Characteristics

Adel Younis
adel.younis@qu.edu.qa
Department of Civil and Architectural Engineering, Qatar University, Doha, Qatar

Usama Ebead
uebead@qu.edu.qa
Department of Civil and Architectural Engineering, Qatar University, Doha, Qatar

ABSTRACT

Using seawater and/or recycled coarse aggregates (RCA) for concrete mixing is deemed advantageous from a sustainability perspective. This paper reports on the results of an experimental study on fresh and hardened properties of concrete mixed with seawater and RCA. Three concrete mixtures were investigated, namely, Mix A (traditional concrete), Mix B (concrete made with seawater), and Mix C (concrete made with seawater and RCA). It was concluded that the use of seawater and/or RCA had a notable effect on fresh concrete properties. Mix B concrete showed a slightly lower strength performance than that of Mix A (<15%), whereas the strength of Mix C concrete had a significant drop (~30%) compared to the reference (Mix A). The permeability performance of hardened concrete for Mixes A and B was similar, whereas Mix C concrete showed 60% increase in water absorption and 100% increase in chloride permeability as compared to Mix A.

Keywords: Sustainable Concrete; Seawater concrete; Recycled concrete aggregate; Workability; Strength; Permeability

1 INTRODUCTION

Concrete is the most commonly used construction material worldwide (Monteiro & Miller, 2017), whose production from its traditional raw ingredients typically results in negative impacts on the environment (Miller et al., 2016). Recently, there has been an increasing interest in other sources of concrete mixing ingredients so as to achieve more ‘‘green’’ concrete (Alnahhal & Aljidda, 2018; Rahal, 2007). In this context, seawater and recycled coarse aggregate (RCA) have increasingly emerged as alternative mixing ingredients for concrete, bearing in mind the increasing global concerns of freshwater scarcity (Mekonnen & Hoekstra, 2016), the accumulation of construction and demolition waste, as well as the possible depletion of natural aggregate resources (Tam et al., 2018). However, steel reinforcement corrosion potentially associated with such concrete mixtures (as a result of seawater chloride ions) makes an undeniable challenge that mitigates the use of seawater in concrete. Yet, this can be basically addressed by using the proposed mixtures in non-reinforced concrete applications or with the use of non-corrosive reinforcement in concrete structures (Younis et al., 2018a). Given that, the current paper reports on the results of an experimental campaign carried out to investigate the effects of using seawater and RCA in concrete. The paper establishes a comparison among three concrete mixtures, namely, (i) Mix A (reference), which

represents the conventional mix produced with freshwater and natural coarse aggregate (NCA); (ii) Mix B, which is produced with seawater and NCA; and (iii) Mix C, which is produced with seawater and RCA.

2 EXPERIMENTATION

2.1 Materials

Seawater was brought from Al-Khor coastal area in Qatar to be used for concrete mixing. Chemical characterization test results obtained for the two water types can be found in (Younis et al., 2018b). The negative effects of seawater mixing are expected to arise due to the high presence of sulfate and chloride ions: the concentration of these ions in seawater was higher than the allowable limits for concrete production. As for fine aggregates, washed sand was used in all concrete mixtures. As for coarse aggregates, Gabbro crushed rock was used in Mixes A and B. Recycled coarse aggregates - that are often produced in Qatar from demolished concrete structures (Al-Ansary & Iyengar, 2013) - were used in Mix C. Physical and mechanical characterization test results obtained for the aggregates used can be found in (Younis et al., 2020). In general, RCAs showed higher water absorption as well as lower density and mechanical strength compared to NCAs, which can be basically attributed to the adhered porous mortar on the surface. As for cementitious materials, ordinary Portland cement (OPC) and blast furnace slag (at 65% replacement level) were used in all concrete mixtures. The use of slag is actually known to improve the performance of concrete mixed with seawater or RCA (Etxeberria et al., 2016). Chemical characterization test results obtained for both cementitious materials can be found in (Younis et al., 2018b).

2.2 Concrete Mixture Proportions

Ready-mix concrete with a 60-MPa 28-day design compressive strength was used to cast the test specimens. The mix design proportions for concrete mixtures (as per BS EN 206) are presented in Table 1. As shown in the table, the mix proportions were the same for Mixes A and B (i.e., the difference was only in the water type). In Mix C, natural coarse aggregates were fully replaced by RCAs on a volume basis. Additional mixing water was considered in Mix C in order to account for the higher water absorption of RCAs. A commercial superplasticizer was incorporated with a 3.8-kg/m^3 dosage in all concrete mixtures.

Table 1: Concrete Mixture Proportions (as kg/m^3 of Concrete).

Constituent	Mix A	Mix B	Mix C
OPC	158	158	158
Slag	292	292	292
Gabbro 20 mm	700	700	-
Gabbro 10 mm	490	490	-
5-20 mm RCA	-	-	990
Washed sand	750	750	750
Freshwater	165	-	-
Seawater	-	165	205

2.3 Assessment Methods for Concrete

Physical characteristics and workability performance of fresh concrete were compared among the three mixtures. For this, two tests were performed: (a) slump flow test as per ASTM C143, and (b) density, yield, and air content tests as per ASTM C138. As for hardened concrete, compressive strength test was conducted on concrete cylinders (150 by 300 mm) as per ASTM C39 considering two test variables: (i) concrete mixture (A, B, or C); and (ii) test time (Days 3, 7, 28, or 56 following mixing). Moreover, rapid chloride permeability (RCP) test was performed as per ASTM C1202 to measure the chloride penetration resistance of hardened concrete. Also, water absorption (WA) test was conducted according to BS 1881-122, to measure the water ingress through the concrete surface.

3 RESULTS AND DISCUSSIONS

3.1 Fresh Concrete

Table 2 presents the density, yield, and air content measurements for the three concrete mixtures. As intuitively expected, the measured density of fresh concrete for Mix A and Mix B was the same (2555 kg/m^3). However, the density of Mix C concrete (2400 kg/m^3) was approximately 5% lower than that of Mixes A and B. Using 100% RCA in Mix C reduced the concrete density: this is attributed to the RCAs being naturally less dense than NCAs as a result of the adhered porous mortar on their surface (Behera et al., 2014). Previous studies concerning recycled-aggregate concrete conform with the results herein (Silva et al., 2018), showing around 5–8% inferior density of concrete as a result of using 100% RCA.

As shown in Table 2, a slight increase in the air content was observed on the fresh concrete while mixing with seawater (1.40% for Mix A and 1.65% for Mix B). However, combining seawater and RCA in Mix C resulted in a notable increase in the air content (more than 30%) as compared to that of the conventional Mix A. In principle, RCAs have higher porosity as well as rougher surface caused by recycling processes (Silva et al., 2018) and therefore, air could have easily become trapped in the aggregates' surface. Bearing in mind the fact that RCAs were not pre-saturated in this study, it is possible that the test method has measured the additional part of the air content inside the RCA.

Table 2: Physical Characteristics of Fresh Concrete.

Characteristic	Mix A	Mix B	Mix C
Density	kg/m³ 2555	kg/m³ 2555	kg/m³ 2400
Yield	101.6%	101.6%	99.9%
Air content	1.4%	1.65%	1.85%

Figure 1 depicts the slump flow versus the time elapsed for concrete mixtures. As shown in the figure, the use of seawater in Mix B reduced the slump flow of fresh concrete to be (initially) 20% lower than that of Mix A. Using seawater also led to lower slump retention, where the slump loss in Mix B was faster than that of Mix A. However, combining seawater and recycled coarse aggregates in Mix C resulted in a more significant reduction in the workability of the resulted concrete. Not only did the

concrete of Mix C show an initial slump 25% lower than that of Mix A, but also it remained flowable for only half the period (i.e., 60 minutes in Mix C versus 120 minutes in Mixes A and B).

The reduction in workability of Mix B concrete can be attributed to the accelerating effects induced by seawater ions (Li et al., 2019). As for Mix C, incorporating RCA resulted in a slump loss greater than that of Mix B. In principle, RCAs have harsh/ granular texture (due to crushing of parent concrete) as well as higher porosity (because of the adhered porous mortar on the surface). Accordingly, more water (or energy) is required for compaction on account of the inter-particle friction (Behera et al., 2014).

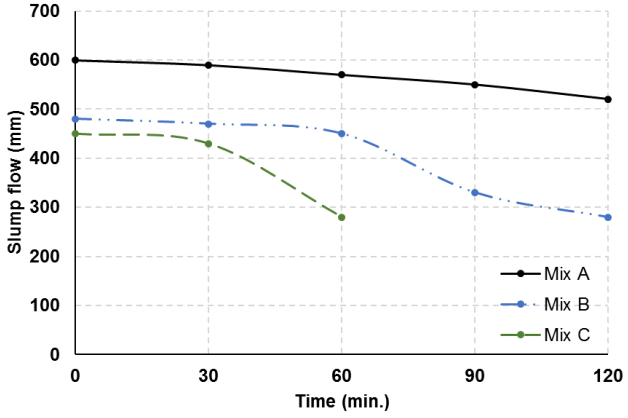

Figure 1: Slump Flow Measurements as a Function of Time.

3.2 Hardened Concrete

Figure 2 depicts the compressive strength results for concrete mixtures. Comparing Mix A and Mix B concretes, a slight increase (3–5%) was generally observed in the compressive strength at early age (i.e., up to 7 days) with the use of seawater. This higher early-age strength of Mix B concrete can be connected with its lower porosity due to the acceleration of cement hydration (Kaushik & Islam, 1995). However, at later ages (i.e., 28 days or later), Mix B showed compressive strength lower than that of Mix A, with an approximate difference of 7–10% reported at Day 56. Kaushik & Islam (1995) suggested that the lower long-term strength of seawater concrete can be attributed to the leaching of hydration products.

Mix C, however, showed lower compressive strength compared to the other two mixtures at all ages. As of Day 56, the compressive strength of Mix C concrete was ~30% lower than that of the conventional Mix A. The negative effects from seawater and RCA were simultaneously combined in Mix C and reflected on its strength performance. In principle, recycled aggregate concrete is more likely to have lower strength performance due to the inferior mechanical performance of RCA as well as the weak interfacial bond between RCA and the matrix (Rahal & Alrefaei, 2017, 2018)such as the shear resistance. This paper presents the results of an experimental investigation of the effects of the use of RCA on the shear strength of longitudinally reinforced concrete (RC.

The 28-day and 56-day results for RCP and WA tests are presented in Table 3. In general, the test results showed a higher permeability performance of 56-day hardened

concrete than that reported at Day 28, mostly because of improvements in concrete due to the ongoing hydration. RCP test results for all concretes lied within the acceptable limits as per Qatar Construction Specifications (QCS, 2014). However, WA test results revealed a deprived permeability performance for Mix C compared to the other two mixtures or even the standard limits - 2.5% max. as per (QCS, 2014).

Whilst seawater mixing showed almost no effect on the permeability performance of hardened concrete (results of Mixes A and B were comparable for all tests), incorporating RCA in Mix C had evidently reduced its permeability performance. This indeed is attributed to the high porosity of RCA that makes concrete more susceptible to permeation (Guo et al., 2018).

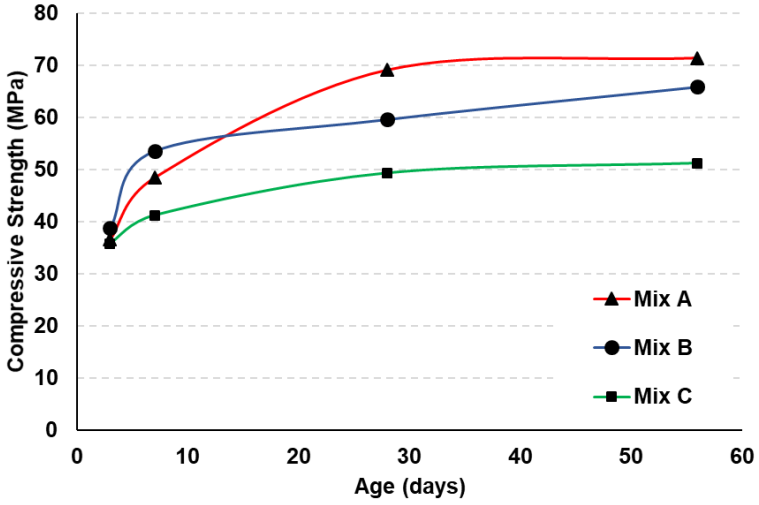

Figure 2: Compressive Strength Results.

Table 3: Summary of Permeability Test Results.

Specimen	RCP (as charge (passed in coulombs	(%) WA
Mix A – 28d	407	1.79
Mix A – 56d	369	1.58
Mix B – 28d	439	1.69
Mix B – 56d	349	1.56
Mix C – 28d	1100	2.87
Mix C – 56d	844	2.63

4 CONCLUSION

This paper compared three concrete mixtures, namely, Mix A (conventional concrete), Mix B (seawater-mixed concrete), and Mix C (seawater-mixed recycled-aggregate concrete). Based on the results of this study, the following conclusions were drawn:

- The concrete density and air content did no notably change with seawater mixing. However, using 100% seawater and RCA reduced the concrete density (by ~5%) and

increased the air-content measurements of Mix C.

- Seawater mixing led to a noticeable reduction in the slump flow of fresh concrete (~20%). Using 100% seawater and RCA in Mix C led to a more significant decrease in the slump flow (~ 25%) as well as the workability retention.
- Seawater mixing initially led to a slight increase in strength performance (till Day 7), followed by a reduction of 7–10% in the long term. Combining seawater and RCA in Mix C, however, resulted in a significant reduction in strength performance of concrete (~30%).
- Seawater mixing showed almost no effect on the permeability performance of hardened concrete. However, using 100% seawater and RCA in Mix C led to a significantly reduced permeability performance.

ACKNOWLEDGMENT

The authors would like to acknowledge the fund received by the NPRP grant # NPRP 9-110-2-052 from Qatar National Research Fund (a member of Qatar Foundation). The findings of this study are solely the responsibility of the authors. The authors would like to thank Readymix Qatar (as a part of LafargeHolcim) for providing the expertise that greatly helped in completing this research.

REFERENCES

Al-Ansary, M. & Iyengar, S. R. (2013). Physiochemical characterization of coarse aggregates in Qatar for construction industry. *International Journal of Sustainable Built Environment*, *2*(1), 27-40.

Alnahhal, W. & Aljidda, O. (2018). Flexural behavior of basalt fiber reinforced concrete beams with recycled concrete coarse aggregates. *Construction and Building Materials*, Elsevier Ltd, 169, 165-178.

Behera, M., Bhattacharyya, S. K., Minocha, A. K., Deoliya, R. & Maiti, S. (2014). Recycled aggregate from C&D waste & its use in concrete - A breakthrough towards sustainability in construction sector: A review. *Construction and Building Materials*, 68, 501-516.

Etxeberria, M., Gonzalez-Corominas, A. & Pardo, P. (2016). Influence of seawater and blast furnace cement employment on recycled aggregate concretes' properties. *Construction and Building Materials*, 115, 496-505.

Guo, H., Shi, C., Guan, X., Zhu, J., Ding, Y., Ling, T. C., Zhang, H. & Wang, Y. (2018). Durability of recycled aggregate concrete – A review. *Cement and Concrete Composites*, 89, 251-259.

Kaushik, S. K. & Islam, S. (1995). Suitability of sea water for mixing structural concrete exposed to a marine environment. *Cement and Concrete Composites*, *17*(3), 177-185.

Li, L. G., Chen, X. Q., Chu, S. H., Ouyang, Y. & Kwan, A. K. H. (2019). Seawater cement paste: Effects of seawater and roles of water film thickness and superplasticizer dosage. *Construction and Building Materials*, 229, 116862.

Mekonnen, M. M. & Hoekstra, A. Y. (2016). Four billion people facing severe water scarcity. *Science Advances*, *2*(2), e1500323.

Miller, S. A., Horvath, A. & Monteiro, P. J. M. (2016). Readily implementable techniques can cut annual CO2 emissions from the production of concrete by over 20%. *Environmental Research Letters*, IOP Publishing, *11*(7), 74029.

Monteiro, P. J. M. & Miller, S. A. (2017). Towards sustainable concrete. *Nature Materials*, *16*(7), 698-699.

QCS. (2014). *Qatar Construction Specifications*. Qatar General Organization for Standards and Metrology, Qatar.

Rahal, K. (2007). Mechanical properties of concrete with recycled coarse aggregate. *Building and Environment*, *42*(1), 407-415.

Rahal, K. N. & Alrefaei, Y. T. (2017). Shear strength of longitudinally reinforced recycled aggregate concrete beams. *Engineering Structures*, 145, 273-282.

Rahal, K. N. & Alrefaei, Y. T. (2018). Shear strength of recycled aggregate concrete beams containing stirrups. *Construction and Building Materials*, 191, 866-876.

Silva, R. V., De Brito, J. & Dhir, R. K. (2018). Fresh-state performance of recycled aggregate concrete: A review. *Construction and Building Materials*, 178, 19-31.

Tam, V. W. Y., Soomro, M. & Evangelista, A. C. J. (2018). A review of recycled aggregate in concrete applications (2000–2017). *Construction and Building Materials*, 172, 272-292.

Younis, A., Ebead, U. & Judd, S. (2018a). Life cycle cost analysis of structural concrete using seawater, recycled concrete aggregate, and GFRP reinforcement. *Construction and Building Materials*, Elsevier, 175, 152-160.

Younis, A., Ebead, U., Suraneni, P. & Nanni, A. (2018b). Fresh and hardened properties of seawater-mixed concrete. *Construction and Building Materials*, *190*(C), 276-286.

Younis, A., Ebead, U., Suraneni, P. & Nanni, A. (2020). Performance of sewater-mixed recycled-aggregate concrete. *Journal of Materials in Civil Engineering*, *32*(1), 04019331.

Cite this article as: Younis A., Ebead U., "Effects of Using Seawater and Recycled Coarse Aggregates on Plain Concrete Characteristics", *International Conference on Civil Infrastructure and Construction (CIC 2020)*, Doha, Qatar, 2-5 February 2020, DOI: https://doi.org/10.29117/cic.2020.0103

Long-Term Cost Performance of Corrosion-Resistant Reinforcements in Structural Concrete

Adel Younis
adel.younis@qu.edu.qa
Department of Civil and Architectural Engineering, Qatar University, Doha, Qatar

Usama Ebead
uebead@qu.edu.qa
Department of Civil and Architectural Engineering, Qatar University, Doha, Qatar

ABSTRACT

Corrosion, which leads to the premature deterioration of reinforced concrete (RC) structures, is increasingly an issue of global concern. Accordingly, corrosion-resistant materials have emerged as alternative reinforcement solutions in concrete structures. Yet, the high initial cost of such materials may mitigate their potential use. This paper reports on the results of two life-cycle-cost-analysis (LCCA) studies that aim at verifying the long-term cost performance of corrosion-resistant reinforcements in structural concrete. The first study conducted a 100-year-based LCCA study to evaluate the relative cost savings of structural concrete that combines seawater, recycled coarse aggregates, and glass fiber-reinforced polymer (GFRP) reinforcement in high-rise buildings as compared to a traditional reinforced concrete (i.e., freshwater-mixed, natural-aggregate, black-steel-reinforced). In the second study, a life-cycle-cost comparison was established among four reinforcement alternatives, viz., conventional steel, epoxy-coated steel, stainless steel, and GFRP for a RC water chlorination tank considering a 100-year study period. The results of these two studies suggest that the use of corrosion-resistant reinforcement (especially GFRP) in structural concrete may potentially lead to significant cost savings in the long term: the net present cost of GFRP-RC structures was generally 40–50% lower than that reinforced with black steel.

Keywords: Sustainably; Alternative materials; Reinforced concrete; Life-cycle costing

1 INTRODUCTION

Nowadays, there has been a growing interest among researchers to achieve sustainability goals in reinforced concrete (RC) structures, mostly by introducing alternative "greener" materials for construction and repair. Steel reinforcement corrosion is deemed a significant factor hindering sustainable development by causing premature deterioration of reinforced concrete structures. In an attempt to address this issue, non-corrosive materials (e.g., glass fiber-reinforced polymer (GFRP) and stainless steel) have been suggested by researchers as alternative reinforcement solutions for concrete. However, the higher initial cost of such materials (compared to that of the conventional black steel) imposes a long-term economic investigation to evaluate their actual cost performance during an RC structure's service life. In view of that, the current paper presents two studies on the long-term cost performance of corrosion-resistant reinforcements in structural concrete. In Study 1 (Younis et al., 2018), a life cycle cost

analysis (LCCA) was performed to verify the cost savings associated with using seawater, recycled coarse aggregates (RCA), and GFRP reinforcement in structural concrete. For this, two design alternatives were compared for a high-rise building, namely, RC1 that represents the conventional design (i.e., freshwater-mixed natural-aggregate concrete with black steel reinforcement), and RC2 (seawater-mixed, recycled-aggregate, GFRP-reinforced concrete). Likewise, Study 2 (Younis et al., 2020) compared the long-term cost performance among four reinforcing materials (viz., black/epoxy-coated/stainless steels and GFRP) for a concrete water chlorination tank using LCCA.

2 METHODOLOGY

Typically, the life cycle cost model included 4 main elements (Figure 1), namely, material cost, construction cost, maintenance/repair cost, and end-of-life/disposal cost. Further details and assumptions regarding each component of the cost model can be found in (Younis et al., 2018, 2020). Material characterization and structural design details of the buildings considered can be found in (Foraboschi et al., 2014)of the components, per net rentable area for Study 1 and in (Mohamed & Benmokrane, 2014)but also to durability and crack control. This paper presents the design procedures, construction details, leakage testing, and monitoring results for the world's first RC water chlorination tank totally reinforced with glass-fiber-reinforced polymer (GFRP for Study 2. Unit costs used in LCCA calculations are provided in (Younis et al., 2018) for Study 1 and in (Younis et al., 2020) for Study 2. All costs were allocated for a functional unit of 1 m^2 of the building floor in Study 1, whereas the functional unit considered in Study 2 was 1 m^3 of the water tank capacity. Life-365 software (Ehlen et al., 2009) was used to predict the repair activity timing as well as the service life of RC structures. A life cycle period of 100 years was considered in both studies, at which end, it was assumed that the structure would be demolished regardless of any potential remaining service life. Finally, the Net Present Cost (NPC) was obtained as the sum of all partial costs incurred over the entire life cycle, not overlooking the opportunity value of time, calculated as follows (ISO 15686-5, 2008):

$$NPC = \sum_{t=0}^{T} \frac{C_t}{(1+r)^t} \qquad (1)$$

where t is the time (in years), T is the analysis period, is the cost incurred at year t, and r is the real discount rate.

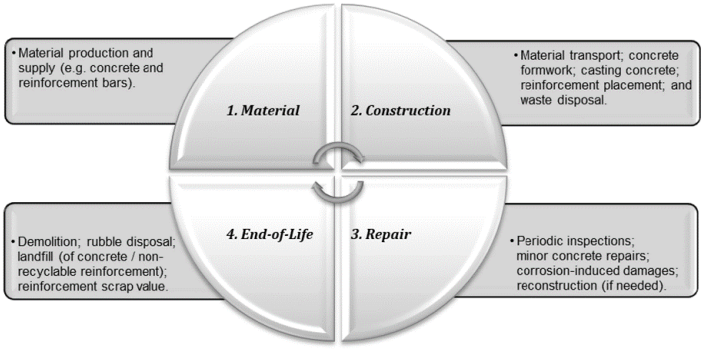

Figure 1: Components of the Life Cycle Cost Model (Younis et al., 2020).

3 RESULTS AND DISCUSSIONS

Table 1 presents the LCCA outcomes for Study 1. As shown in the table, the proposed design alternative RC2 had a 50% lower NPC compared to that of the conventional design (RC1), indicating the economic advantage of the former in the long term. Previous cost studies on GFRP reinforcement generally show an agreement with the results herein (Cadenazzi et al., 2019). It is to be noted that the alternative materials in concrete mixtures (i.e., seawater and RCA) ultimately had little-to-no effect on the long-term cost performance of RC structures. The life-cycle-cost difference between the two design alternatives (RC1 and RC2) was actually realized with altering reinforcement material. Yet, it is emphasized that these findings are solely realized from the financial perspective of the building's owner: the use of seawater and/or RCA in concrete mixtures actually has an environmental significance that reaches far beyond (Arosio et al., 2019; Hossain et al., 2016).

Table 1: LCCA results of Study 1.

Design alternative	Present Costs ($/m²)					NPC ($/m² floor area)
	Material	Construction	Repair	Reconstruction	End-of-life	
RC1	90	135	183.9	230.7	50.8	690.4
RC2	174	108	-	-	54.3	336.3

Figure 2 summarizes the LCCA results for Study 2. As shown in the figure, epoxy-coated and stainless steel reinforcements had NPC values 11% and 25% less than that of the conventional steel, respectively. GFRP reinforcement showed the most saving potential, with a 43% less NPC compared to conventional steel. Evidently, the higher initial cost associated with corrosion-resistant reinforcements may be recouped in the long term as a result of reducing repair costs (Figure 2) and extending service lives of RC structures. These results are in conformity with previous research studies concerning the cost effectiveness of corrosion-resistant reinforcements (Grace et al., 2012; Mistry et al., 2016).

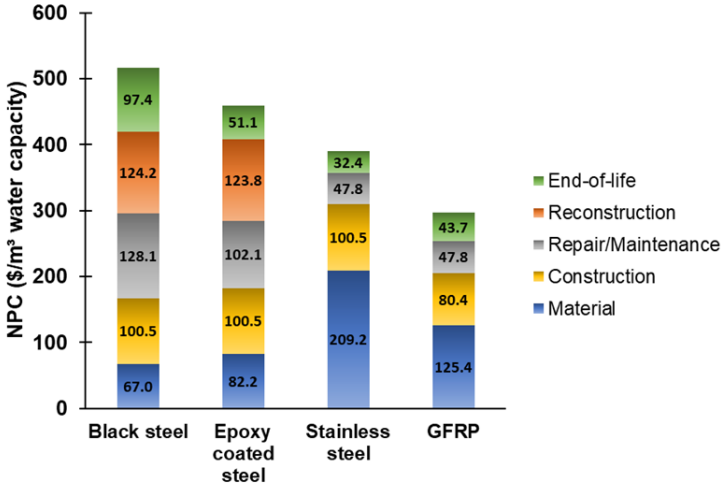

Figure 2: Summary of LCCA results for Study 2 (Younis et al., 2020).

4 CONCLUSION

This paper reports two LCCA studies pertaining to the economic viability of corrosion-resistant reinforcement in structural concrete. In Study 1, a potential long-term cost saving of ~50% was determined for a high-rise RC building when combining seawater, RCA, and GFRP reinforcement in structural concrete (compared to a conventional RC design): the reinforcement material was actually the relevant factor in realizing the cost difference between the two design alternatives. Study 2 had more focus on the application of corrosion-resistant reinforcements in concrete structures: a comparative life-cycle cost analysis was performed to verify the economic viability of using epoxy-coated steel, stainless steel, and GFRP in lieu of black steel to reinforce a concrete water chlorination tank. The life cycle cost obtained for epoxy-coated steel, stainless steel, and GFRP reinforcements was approximately 11, 25, and 43% lower than that of the conventional steel. Nonetheless, the findings achieved herein are only based on the assumptions, the data, and the methods that are specific to the case of these two studies. Future studies are encouraged to enrich the archival literature with more data concerning the cost implications of using alternative materials in RC structures.

ACKNOWLEDGMENT

The authors would like to acknowledge the fund received by the NPRP grant # NPRP 9-110-2-052 from Qatar National Research Fund (a member of Qatar Foundation). The findings of this study are solely the responsibility of the authors.

REFERENCES

Arosio, V., Arrigoni, A. & Dotelli, G. (2019). Reducing water footprint of building sector: concrete with seawater and marine aggregates. *IOP Conference Series: Earth and Environmental Science*, IOP Publishing, *323*, 12127.

Cadenazzi, T., Dotelli, G., Rossini, M., Nolan, S. & Nanni, A. (2019). Life-cycle cost and life-cycle assessment analysis at the design stage of a fiber-reinforced polymer-reinforced concrete bridge in Florida. *Advances in Civil Engineering Materials*, *8*(2), 20180113.

Ehlen, M. A., Thomas, M. D. A. & Bentz, E. C. (2009). Life-365 service life prediction model TM Version 2.0. *Concrete International*, *31*(05), 41-46.

Foraboschi, P., Mercanzin, M. & Trabucco, D. (2014). Sustainable structural design of tall buildings based on embodied energy. *Energy and Buildings*, *68*, 254-269.

Grace, N. F., Jensen, E. A., Eamon, C. D. & Shi, X. (2012). Life-cycle cost analysis of carbon fiber-reinforced polymer reinforced concrete bridges. *ACI Structural Journal*, *109*(5), 697-704.

Hossain, M. U., Poon, C. S., Lo, I. M. C. & Cheng, J. C. P. (2016). Comparative environmental evaluation of aggregate production from recycled waste materials and virgin sources by LCA. *Resources, Conservation and Recycling*, 109, 67-77.

ISO 15686-5. (2008). *Buildings and constructed assets–Service-life planning–Part 5: Life-cycle costing*. International Organization for Standardization.

Mistry, M., Koffler, C. & Wong, S. (2016). LCA and LCC of the world's longest pier: A case study on nickel-containing stainless steel rebar. *International Journal of Life Cycle Assessment*, *21*(11), 1637-1644.

Mohamed, H. M. & Benmokrane, B. (2014). Design and performance of reinforced concrete water chlorination tank totally reinforced with GFRP bars: Case study. *Journal of Composites for Construction*, *18*(1), 05013001.

Younis, A., Ebead, U. & Judd, S. (2018). Life cycle cost analysis of structural concrete using seawater, recycled concrete aggregate, and GFRP reinforcement. *Construction and Building Materials*, Elsevier, *175*, 152-160.

Younis, A., Ebead, U., Suraneni, P. & Nanni, A. (2020). Cost effectiveness of reinforcement alternatives for a concrete water chlorination tank. *Journal of Building Engineering*, Elsevier Ltd, 27, 100992.

Cite this article as: Younis A., Ebead U., "Long-Term Cost Performance of Corrosion-Resistant Reinforcements in Structural Concrete", *International Conference on Civil Infrastructure and Construction (CIC 2020)*, Doha, Qatar, 2-5 February 2020, DOI: https://doi.org/10.29117/cic.2020.0104

Positively Shifting the Mindset in Construction Using Non-Biodegradable Materials for Sustainable Construction: An Experimental Study

Faheem Memon
faheemquest@hotmail.com
Quaid-e-Awam University of Engineering Science & Technology
Nawabshah, Pakistan

ABSTRACT

Disposing of the non-biodegradable material, scrap Tire rubber specifically, has always been a bone of contention for the municipalities around the world. Not only the land that it covers is the major issue, but also the environment is always at risk because the scrap tire being non-biodegradable, takes ages in decomposition. It is always prone to fire, which may cause disastrous situation around as it is not so easy to extinguish the scrap tire fire by whatever the resources available to the firefighters. To deal with this modern-day issue which rapidly became a serious concern of many governments in terms of social, economic & environmental sustainability, many researches started working on the effective use of scrap tire rubber by using it in different infrastructure elements, for instance, road pavements, waterproofing of underground utilities, shotcrete for tunnel wall lining, floor coverings of the playgrounds. Keeping in mind the sustainability issues, this study was conducted to assess the change in the fundamental structural properties of the concrete by mixing scrap tire rubber as an additive material. Four batches of the concrete were designed to be tested in the laboratory with the first batch as plain concrete with no scrap tire rubber to be kept as a reference point, 10%, 20% and 30% addition of scrap tire rubber by weight of cement. Results showed drastic improvement in Cylinder Crushing Strength, Modulus of Elasticity, the Poisson's ratio and the Ultimate Flexural Strength of beams.

Keywords: Scrap tire rubber; Concrete; Ultimate flexural strength; Modulus of elasticity; Poisson's Ratio

1 INTRODUCTION

Fibre-reinforced concrete is a composite material consisting of cement paste, mortar or concrete with the fibre of asbestos, glass, plastic, polypropylene, steel etc. such a fibre reinforcement may be useful under explosive loading where high strength in tension zone and reduced hair cracking is desired. Different fibres are used for reinforcing concrete and still research is underway to introduce some new and better ones.

Steel (carbon, stainless), glass (alkali-resistant) has a higher value of elastic moduli, and they contribute both to impact resistance and to flexural strength. Again, natural fibres like asbestos and vegetable fibres and polypropylene improve impact resistance but flexural strength may remain unaffected. A few of the advantages of such type of concrete are; high tensile and impact resistance, high compressive strength, very good and satisfactory flexural strength, increase in ultimate load carrying capacity, improvement of ductility, shear strength, torsion strength, splitting resistance, bearing

strength, resistance against wear and abrasion, high resistance to freezing and thawing and fatigue loading.

The compressive strength of concrete is very high but due to its brittleness, it cannot resist sufficient tensile stress. Therefore, steel bars are used to strengthen concrete in situations where tensile stresses are developed. Another form of reinforcement is random dispersal of short, discontinuous and discrete fine fibres called fibre reinforcement. The fibre can be imagined as an aggregate with an extreme deviation in shapes from the rounded smooth aggregate. The fibres interlock and entangle around aggregate particles and considerably reduce the workability while mix becomes more cohesive and less prone to segregation. The fibre suitable for reinforcing the concrete has been produced from steel, glass and organic polymers.

In contrast to reinforcing bars in reinforced concrete which are continuous and carefully placed in the structures to optimize their performance, the fibres are discontinuous and are generally randomly distributed throughout the concrete matrix. Thus, the reinforcing performance of steel fibres, for example, is inferior to that of reinforcing bars. Also, the fibres are likely to be more expensive than conventional steel bars, thus, fibre reinforced concrete is not likely to replace conventional reinforced concrete. However, the addition of fibres makes the conventional plain concrete more versatile, more flexible in method of production and more competitive as a construction material.

Essentially, fibres act as crack arrestors, restricting the development of cracks and thus transforming an inherently brittle matrix, i.e., Portland cement with its low tensile and impact resistances into a strong composite with superior cracks resistance, improved ductility and distinctive post-cracking behaviour before failure. Steel fibres are probably the best suited for structural applications. Due to the superior properties like increased tensile and bending strengths, shear and torsional strengths, improved ductility, resistance to cracking, high impact strength and toughness, spalling resistance and high energy absorption capacity, fibre-reinforced concrete has found special application in hydraulic structures, airfield pavements highways, bridge decks, heavy-duty floors and tunnel linings.

Since all the types of fibre tried so far are quite expensive to achieve economy of construction but without sacrificing the better and improved strength properties of fibre reinforced. Initially, at Quide Awam University of engineering Science & Technology, this was done by micro-concrete using machine shop scrap. However, the study that is being presented in this paper has an enhanced scope of the addition of scrap tire rubber with normal concrete consisting of Ordinary Portland Cement, hill sand and coarse aggregates.

2 LITERATURE REVIEW

In general, the concrete used with fibre reinforcement requires higher cement concrete, lower coarse aggregate content and smaller size of coarse aggregate. A very large number of investigators have conducted systematic research on various aspects of fibre reinforced concrete for more than three decades. A few of application areas in which significant field trials took place include overlays for bridge decks and pavement (highway and airfield), mining and tunnelling application, slope stabilization, refractory application, concrete repair, industrial floors and precast concrete products.

Samarai, 1974 studied experimentally the influence of fibres upon crack development in reinforced concrete subject to uniaxial tension. Gopalan et al., 1974 studied the effect of steel fibres on the strength of concrete beams. Aligned continuous fibres, aligned discontinuous fibres and random discontinuous fibres were within the domain of their extent of experimental investigations. The durability of fibre with the cement matrix is one of the most important aspects. Therefore, Hannant et al., 1975 undertook to assess experimentally the resistance of steel fibre to corrosion in normal weight and lightweight concrete cylinders in the cracked state and also studied the performance of fibres in normal grade concrete beams exposed after initial loading which induced cracks with widths of 0.1 mm to 0.3mm. The cylinders were placed on three sites covering relatively mild exposure, marine conditions and polluted industrial atmosphere. Observation for 4.75 years suggests that the corrosion of fibres within the concrete is unlikely to cause major problems. The cracked beams were exposed to the marine environments for eleven months during which significant carbonation and fibre corrosion occurred. The failure loads of the specimens tested at this age did not decrease below the initial cracking loads. The failure of steel fibre reinforced concrete composites is generally attributed to the failure of the bond between fibres and matrix. Thus, the strength of the fibres is not fully utilized. Attempts have been made to improve the efficiency of fibre reinforcement by increasing the shear strength of the fibre-matrix interface by chemical or mechanical means as well as by aligning the fibres in the direction of the principal tensile stress. The influence of increased bond strength by chemical or mechanical means is generally measured by a pull-out test on a single fibre. The peak load required to pull out fibre is often expressed at average bond strength by dividing its value by the embedded surface area. The post cracking tensile strength of fibre reinforced concrete has been studied by Gasparini, et al., 1989. Nammur George et al. 1989 investigated the bond stress for fibre reinforced concrete based on the bond stress-slip relationship.

3 EXPERIMENTAL DETAILS

The behavior of concrete is affected by different parameters. Therefore, before starting the project it is necessary to decide the parameter of the study. Since, it is supposed to compare the properties of the concrete, mixed with different proportions of fibre fragments, hence the percentage of fibre fragments in the mix is kept as variable and all other parameters as fixed. Tire fibres with Approximate dimension of 40x2x2 mm from the sidewall of the scrap tire were prepared for the study reason.

3.1 Ratio of Tire fibre

It is expected that Tire fibre scrap would increase the strength of concrete with an increase of percentage in mix. So, the ratio of 10% to 30% of tire fibre is used.

In this regard, a standard mix with a design strength of 15 N/mm^2 is taken and the effect of the ratio of Tire fibre added as reinforcement, on the fundamental structural properties have been investigated. The ratio of this fibre is 10% to 20% to 30% by weight of the cement. The tire fibre is added randomly during the mixing of the ingredients of the fresh concrete.

3.2 Mix Proportions

To get comparable results, any type of concrete can be used, e.g., Normal concrete (i.e., with fine and coarse aggregates) or micro concrete (i.e., with fine aggregate only). For this study, normal concrete is used, prepared with fine sand (i.e., red hill sand) passed through No: 16 sieve and coarse aggregate passed through 10 mm sieve mixed with cement and potable water. The ratio of mix is kept as 1: 2: 4: by weight (i.e., 1 for the cement, 2 for the fine aggregates and 4 for the coarse aggregates) and w/c ratio is 0.5.

3.3 Compaction

The compaction of concrete may result in large variations between selected batches, if not maintained properly. The compaction is usually done by table vibrators in the' laboratories. In our structures laboratory, the available vibrator is table type and its maximum intensity is 10 oscillation/min.

To get the same degree of compaction in all the batches, the vibrator was maintained at 5 oscillation/min. and kept it on for 20 minutes.

3.4 Curing

As discussed earlier in detail, that the strength of concrete increases with age if properly cured. Since for design purposes, 28-day strength is used, therefore, all the batches were submerged in the pond for 28-days.

3.5 Cubes

Cubes are used for determining crushing (compressive) strength of concrete. However, they contribute to determining the modulus of elasticity and Poisson's ratio too. The latest size as prescribed by BS 1881 is 100mm x 100mm x 100mm. Due to the restraining effects of platens, it is expected that the results obtained at such size are more reliable than any other size at uncharged factors.

3.6 Cylinders

Cylinders are used especially for determining the indirect tensile strength tests, and on the other hand, they help a lot to determine the modulus of elasticity. Cylinders give tensile strength by using cylinders of 150 mm height and 75mm diameter.

4 EXPERIMENTAL PROCEDURE

The experimental procedure is different for different types of tests. For this study, different tests were performed and various purposes served by these tests are as follows;

4.1 Compression Tests for Crushing Strength

For compression tests, the cube is concentrically placed between the platens of universal load testing machine and then load is applied gradually till the cube is crushed. The ultimate load at the crushing failure is divided by the cross-sectional area of the cube to give ultimate compressive stress. At least three cubes from each batch are crushed and tested for values. Average of the three is taken as the representative value of ultimate compressive stress.

Figure 1: Forney Universal Load Testing Machine

4.2 Test for Modulus of Elasticity

4.2.1 Immediately before the test, the cube crushing strength of concrete is determined and one-third of the value is taken as Cm, i.e. Elastic limit stress. DEMEC pads are stuck on the opposite sides of cylinder specimen with the help of Magic Depoxy steel (or Araldite) in such a fashion that gauge points are symmetrically about the middle of the specimen. DEMEC gauge is used to measure the strain at different loading stages.

4.2.2 Initially, no-load readings of the gauge are noted and this specimen is placed under compression in the universal load testing machine, the load is gradually applied up to (Cm). The load is maintained here for one minute approximately and DEMEC gauge readings are measured on either side of the specimen. The load is then released to measure the strain values again before the second step of loading.

4.2.3 The load is then reapplied at the same rate until the average stress of (Cm+ 1) is reached. Strains are measured once again and load is hold up till the gauge readings are taken safely. The no-load readings are again noted after releasing loads.

4.2.4 The load is applied once again at the same rate and strains are measured at a point when the average stress of (Cm+2) is reached and after releasing the load, the value of strain is measured.

4.2.5 The load is applied fourth time at the same rate and DEMEC gauge readings are taken in approximately ten equal increments of stresses up to (Cm).

Modulus of elasticity, $E = \frac{Stress}{Strain}$

Where $Stress = \frac{Force}{Cross\ sectional\ area\ of\ a\ cylinder}$

For each case and finally the average of all represents the actual modulus of elasticity for that particular concrete mix.

4.3 Test for Poisson's Ratio

Tests for Poisson's ratio are performed on cubes, keeping in mind the principle that axial strain is always accompanied by lateral strain. For the very purpose, DEMEC pads are stuck on two opposite sides of the cube in a set of four, two are horizontal and two are vertical. They are kept at the same distance from the centre of the cube. The strain gauge readings are measured horizontal and vertically simultaneously for lateral strain and axial strain respectively.

The load is applied in the same manner as was done for the computation of modulus of elasticity.

Poisson's Ratio, $v = \frac{Lateral\ micro\ strain}{Axial\ micro\ strain}$

5 GENERAL DESCRIPTION

In all Twelve Cubes were tested for 4 batches of concrete with 0%, 10%, 20% & 30% tire rubber.

Poisson's Ratio, as well as Cube crushing strength, were determined. Twelve Cylinders were tested to find the modulus of elasticity and cylinder crushing strength. Four beams with no reinforcement Steel bars were tested by applying a single point load at the center. The effective span of the beam was 900mm and the load was applied gradually with small increments till failure; the purpose was to determine tensile strength and its improvement due to the presence of Tire rubber.

6 SUMMARY OF RESULTS

Table 1: Summary of Results

Property	**Fibre Percentage**			**Remarks**
	10%	**20%**	**30%**	
Cube Crushing Strength N/mm^2	*	*	24	Concrete Grade M15
Cylinder Crushing Strength N/mm^2	18.35	21.26	28.41	Concrete Grade M15
Modulus of Elasticity KN/mm^2	*	28	36.05	
Poisson's Ratio	0.382	0.37	0.1185	B/W 1.1 For High Strength 1.2 For Weak Mixes
Ultimate Flexural Stress N/mm^2	4.9	8.69	12.42	Increasing with the fibre increase

* Due to experimental inaccuracies, some of the results were discarded.

7 CONCLUSION

- Cube crusting strength does not show appreciable improvement of strength except when the Tire Fibre ratio is in the range of 30%.
- Cylinder crushing strength shows substantial improvement with the increase of the ratio of Tire Fibre at every percentage.
- Modulus of elasticity also shows a drastic increase only in the case of 30% Tire Fibre.
- Poisson's ratio decreases quite a lot when the Tire Fibre is 30%. Otherwise, at lower percentage, the effect is negligible.
- The improvement of ultimate flexural stress is quite good at every percentage.

REFERENCES

Gasparini, D. A., Verma, D. & Abdallah A. Post cracking Tensile Strength of Fiber Reinforced Concrete. *ACI's Materials Journal*, Volume 86, Issue 1, 10-15.

George Nammur Jr. & Antoine E. Naaman. (1989). Bond Stress Model for Fiber-Reinforced Concrete Based on Bond Stress-Slip Relationship. *ACI's Materials Journal*, Volume 86, Issue 1, 45-57.

Hannant, D. J. (1976). Additional data on fiber corrosion in cracked beams and theoretical treatment of the effect of fiber corrosion on beam load capacity. *RILEM*, Volume 2, 533-538.

Rajagopalan, K., Parmasivam & Ramaswamy G. S. (1974). Strength of Steel Fiber Reinforced Concrete Beams. *Indian Concrete Journal*, Volume 48, Issue 1, 17-25.

Samarrai, Mufid A. & Elvery Robert H. (1974). The influence of fibers upon crack development in reinforced concrete subject to uniaxial tension. *Magazine of Concrete Research*, Volume 26, Issue 89, 203-211.

Cite this article as: Memon F., "Positively Shifting the Mindset in Construction Using Non-Biodegradable Materials for Sustainable Construction: An Experimental Study", *International Conference on Civil Infrastructure and Construction (CIC 2020)*, Doha, Qatar, 2-5 February 2020, DOI: https://doi.org/10.29117/cic.2020.0105

Dune Sand Mortar Effects on Deflections of Repaired Steel Bars-Reinforced Concrete Beams

Madina Djeridane
mad.djeridane@lagh-univ.dz ; djeridanemadina@yahoo.fr
Rehabilitation and Materials Laboratory (SREML), University of Laghouat , Laghouat, Algeria

Ali Zaidi
a.zaidi@lagh-univ.dz ; Ali.Zaidi@USherbrooke.ca
Rehabilitation and Materials Laboratory (SREML), University of Laghouat, Laghouat, Algeria

Mohammed Fatah Lakhdari
mf.lakhdari@lagh-univ.dz
Rehabilitation and Materials Laboratory (SREML), University of Laghouat, Laghouat, Algeria

ABSTRACT

This paper presents theoretical and experimental investigations to analyze the flexural behavior of reinforced concrete beams repaired with mortars based on dune sands. The beams supposedly damaged were repaired using mortars based on dune sand varying the mortar cover thickness and the reinforcement ratio. After a suitable cure of beam specimens in the laboratory, they submitted to progressive loading until failure. The results obtained show that the repaired dune sand mortar could be used to enhance the flexural capacity and the ductility of damaged reinforced concrete beams, repaired with dune sand mortars. Comparisons between theoretical and experimental results in terms of deflections are also presented.

Keywords: Dune sand mortar; Repaired concrete beam; Theoretical and experimental deflections; Reinforcement ratio

1 INTRODUCTION

Several works were conducted for strengthening reinforced concrete structures (Prabhat et al., 2015; Attari et al., 2012; Carlo et al., 2011; ACI, 2008; Park & Yang, 2005; Dong-Suk Yang & Sun-Kyu Park, 2002; Hollaway & Leeming, 1999). However, to valorize the local materials such as the dune sand, which covers 60% of the Algerian territory at one hand, and to develop the new repair mortar based on the dune sand on other hand because of the high cost of reparation and rehabilitation of concrete buildings. An experimental study is carried out to investigate the flexural behavior of concrete beams reinforced with steel bars repaired with mortars based on the dune sand varying the mortar cover thickness and the reinforcement ratio. Comparisons between experimental and theoretical results in terms of deflections of repaired reinforced concrete beams are presented.

2 EXPERIMENTAL INVESTIGATION

2.1 Parameters

The present research examines the flexural behavior of reinforced concrete beams repaired with cementitious repair materials using the normal Portland cement mortar

based on the dune sand applied in the tensile zone. The studied parameters of reinforced concrete beams are the steel reinforcement ratio and the repair mortar cover thickness as shown in Table 1.

Table 1: Studied parameters of steel bars-reinforced concrete beams.

Reinforcement ratio	Series Beam	Cover thickness
ρ= 0.0122	PTA1	1.5 cm
	PRA1	
ρ= 0.0125	PTA2	2 cm
	PRA2	
ρ= 0.0085	PTB1	1.5 cm
	PRB1	
ρ= 0.0087	PTB2	2 cm
	PRB2	
ρ= 0.0056	PTC1	1.5 cm
	PRC1	
ρ= 0.0058	PTC2	2 cm
	PRC2	

2.2 Materials

The mechanical properties of concrete used to fabricate concrete beams were determined experimentally on concrete cylinders 16 cm x 32 cm according to French Standards (NFP 18-406 and NFP 18-408). The compressive strength and the tensile strength of concrete at 28 days (f_{c28}) were found to be equal to 30 MPa and 3 MPa, respectively. The different rates of the normal Portland cement and fine aggregates used for the repair mortar are shown in Table 2. The mechanical properties of the repair mortar such as the compressive strength and the tensile strength at 28 days of curing were found equal to 18.13 MPa and 5.82 MPa, respectively.

Table 2: Composition of cement repair mortar (MSDA4)

Cement (Kg/m^3)	Water (Kg/m^3)	Fine aggregate (Kg/m^3)	Coarse aggregate (Kg/m^3)
400	200	623.57	1148.71

2.3 Beams description

A total of 12 reinforced concrete beams were cast having overall dimensions of 150 mm in width, 200 mm depth, 1500 mm length, and 1300 mm span between supports. Two types of 12 and 10 mm diameters of steel bars were used as tensile and compression reinforcements. 6 mm diameter of steel bar was used as stirrups. Shearing bars were arranged with an interval of half of the effective depth to minimize the effect of the shearing force.

The beams after casting were removed from their moulds after 1 day, and stored in water cured at ambient temperature of 20°C for 28 days.

3 RESULTS AND DISCUSSION

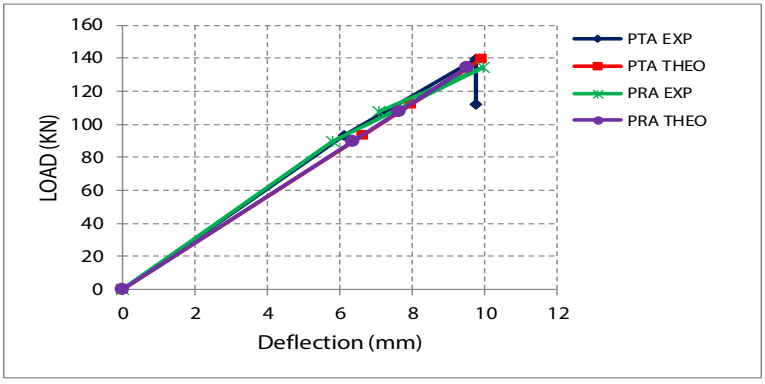

Figure 1: Load-Deflection curves of A-type beams- Comparison between theoretical and experimental results.

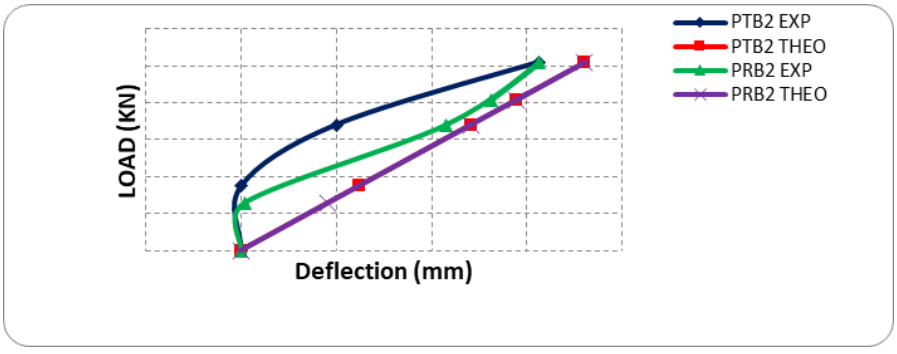

Figure 2: Load-Deflection curves of B-type beams- Comparison between theoretical and experimental results.

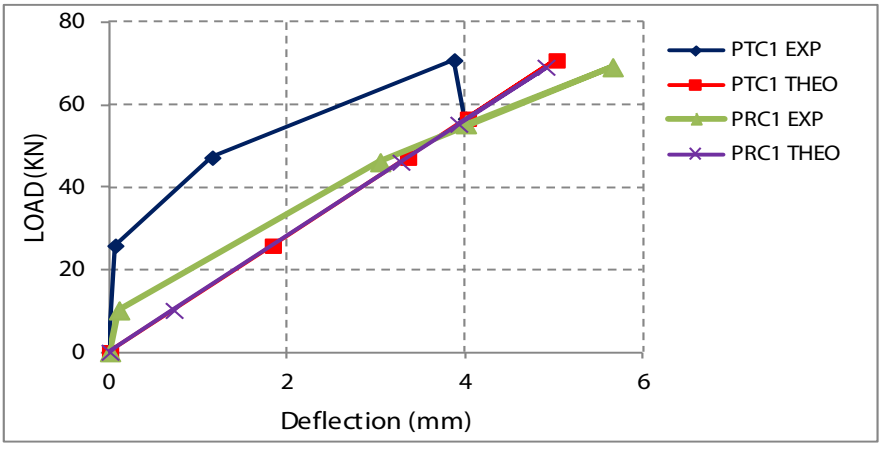

Figure 3: Load-Deflection curves of C-type beams- Comparison between theoretical and experimental results.

As shown in figures 1 to 3, the theoretical and experimental deflections are almost

similar for A-series beams (over reinforced section) because the cracks in this series did not reach the reparation mortar. B2 and C1-series beams show in general experimental values relatively close to those predicted from theoretical models (Jean-Pierre Mougin, 2004; Lim & Hong, 2016; Smarzewski, 2019). However, certain B2 and C1 beam specimens (under reinforced section) show disturbance in deflection results because probably of the lack of the sensibility of certain LVDTs (displacement instrument).

4 CONCLUSION

Analysis results in terms of deflections of concrete beams reinforced with steel bars repaired with cementitious mortar based on dune sand, permit to draw the following conclusions:

- The cementitious mortar based on the dune sand can be used to enhance the flexural capacity of damaged concrete structures reinforced with steel bars.
- Deflections of reinforced concrete beams repaired with the mortar based on the dune sand are generally reduced compared to those of control beams, and consequently the beam stiffness is increased.
- The ductility of reinforced concrete beams repaired with the mortar based on the dune sand is 20% greater than that of the control beam for under-reinforced beams (with low reinforcement ratio). However, for over-reinforced beams, the ductility of repaired beams is close to that of the control beams. This proves that the concrete beam repaired with the dune sand mortar is able to absorb the load during deformation after the appearance of the first crack. As a consequence, the ductility enhancement particularly for under-reinforced beams is due to the repair dune sand mortar contribution.
- Deflections of reinforced concrete beams predicted from theoretical models are in general close to those obtained from experimental tests.

REFERENCES

American Concrete Institute (ACI) Committee 440 (2008). *Guide for the design and construction of externally bonded FRP systems for strengthening concrete structures,* (ACI 440-2R-08, ACI). Michigan, the USA.

Association Française de Normalisation (AFNOR) (1981*). Concrete Compression Test, French Standard* (NFP 18-406, AFNOR). Paris, France.

Association Française de Normalisation (AFNOR) (1981). *Concrete tensile test, French Standard* (NFP 18-408, AFNOR). Paris, France.

Attari, N., Amziane, S. & Chemrouk, M. (December 2012). Flexural strengthening of concrete beams using CFRP, GFRP and hybrid FRP sheets*. Construction and Building Materials*, 37, 746-757.

Carlo Pellegrino, Francesca Da Porto & Claudia Modena (March 2011). Experimental behavior of reinforced concrete elements repaired with polymer-modified cementitious mortar. *Materials and Structures*, *44*(2), 517-527.

Dong-Suk Yang & Sun-Kyu Park (March 2002). An Experimental study on the flexural behavior of RC Beams with cementitious repair materials. *KSCE Journal of Civil Engineering*, *6*(1), 11-17.

Hollaway, L. C. & Leeming, M. B. (1999). *Strengthening of reinforced concrete structures: using externally bonded FRP composites in structural and civil engineering*, CRC Press, Florida.

Jean-Pierre Mougin (2004). *Béton armé-BAEL 91 modifié 99 et DTU associés [Reinforced concrete-BAEL 91 modified 99 and DTU associated]*, Eyrolles, Paris.

Lim, W. Y. & Hong, S. G. (2016). Shear tests for ultra-high performance fiber reinforced concrete (UHPFRC) beams with shear reinforcement. *International Journal of Concrete Structures and Materials*, 10, 177-188.

Prabhat Ranjan Prem, Ramachandra Murthy, A., Ramesh, G., Bharatkumar, B. H. & Nagesh, R. Iyer (2015). *Flexural Behaviour of Damaged RC Beams Strengthened with Ultra High Performance Concrete*. Springer, India V. Matsagar (ed.) Advances in Structural Engineering.

Park, S. K. & Yang, D. S. (2005). Flexural behavior of reinforced concrete beams with cementitious repair materials, *Materials and Structures*. *38*(3), 329-334.

Smarzewski, P. (2019). Analysis of failure mechanics in hybrid fiber-reinforced high-performance concrete deep Beams with and without Openings. *Materials, MDPI*, 12, 1-24.

Cite this article as: Djeridane M., Zaidi A., Lakhdari M. F., "Dune Sand Mortar Effects on Deflections of Repaired Steel bars-Reinforced Concrete Beams", *International Conference on Civil Infrastructure and Construction (CIC 2020)*, Doha, Qatar, 2-5 February 2020, DOI: https://doi.org/10.29117/cic.2020.0106

Water Supply from Turkey to Cyprus Island with Suspended Marine Pipeline

Izzet Ozturk
ozturk@itu.edu.tr
Istanbul Technical University (ITU), Istanbul, Turkey

Necati Agiralioglu
necati.agiralioglu@antalya.edu.tr
Antalya Bilim University, Antalya, Turkey

Omer Ozdemir
omeroz@dsi.gov.tr
General Directorate of State Hydraulic Works, Ankara, Turkey

Nasir Akinci
nakinci@kalyongrup.com
Kalyon Group, Turkey

ABSTRACT

More than 90% of the water requirement for the Turkish Republic of Northern Cyprus (TRNC/KKTC) was being supplied from groundwater resources, while the rest was being provided from surface waters and seawater until the 1990s. Due to excessive water abstractions above their natural feeding levels, most of the aquifers had salinization as a result of sea water interference with electrical conductivity (EC) value exceeding 7000 mmho/cm. In order to provide a permanent and long-term solution to the water problem in TRNC, a sea-crossing suspended water transmission pipeline (TRNC Water Supply) project has been developed for sustainable water transfer from Turkey to the Cyprus Island. While the initial feasibility and conceptual design studies have been prepared for State Hydraulic Works (DSI) in 1998-1999, the implementation projects and tender documents have been completed in 2006-2009, and the construction of the suspended marine pipeline has started in 2011 as commissioned by DSI. The engineering supervision and consultancy services of the project have been provided by a team from Istanbul Technical University (ITU). The project, which has been fully completed in October 2015 had a total cost of 1.6×10^9 TL (600×10^6 $), including expropriation costs. The unit cost of the water with flowrate 75×106 m^3/year is calculated to be 0.6 $/$m^3$ (n=15×50 years, i=0.08), and the investment is expected to be repaid in 5.3 years. In this article, design details of the suspended marine pipeline and its critical components of this unique project are presented.

Keywords: Cyprus Island; TRNC; Water supply; Suspended marine pipeline; Innovative construction technologies

1 INTRODUCTION

The TRNC had been experiencing an increasing water stress –in terms of both quantity and quality- for the last 30 years. Drinking and potable water requirements were met solely from the groundwater resources prior to completion of this project. Due to the excessive water extraction from aquifers, seawater intrusions had occurred in Mağusa, followed by Güzelyurt region, causing the salting of groundwater. The high quality

groundwater obtained from Beşparmak Mountains served only a limited population. In the meantime, available dams and water ponds, alongside groundwater resources, had become insufficient with regards to significant population increase (Agiralioglu et al., 2018). In order to solve the major problem of water supply in the TRNC, a number of studies have been carried out including water transportation from Turkey to the island, however they could not be implemented at the time due to technological and/or financial difficulties (Agiralioglu, 2016). Finally, in 2011, the first step was taken towards the realization of Cyprus Water Supply Project, which was symbolically regarded as the *Peace Water project*.

As Cyprus is an island country having limited water resources, supplying water from Turkey to TRNC for human consumption, as well as for irrigation purposes, is expected to provide significant contribution to the development of the TRNC in general. Potable water need of the country will be met up to year 2045, and approximately 16000 ha of agricultural land will be irrigated. The climate of the region requires long and hot summers versus short and temperate winters alongside very fertile agricultural lands, thus, the provided water enables nearly 2-3 harvests in a year through irrigation.

This paper aims to review the main construction, economic and operation features of the TRNC Water Supply Project, putting forth certain comments that may be useful for the future of water resources management of the island.

2 WATER SUPPLY PROJECT FROM TURKEY TO CYPRUS

The implementation projects and tender documents of the water supply project from Turkey to Cyprus have been completed during 2006-2009 by Intech Engineering BV & Alarko Contracting Group (2008), and the construction of the suspended marine pipeline has started in year 2011 as commissioned by DSI. The engineering supervision and consultancy services relating to the sea-crossing component of the project has been provided by Istanbul Technical University (ITU, 2008).

The facilities built in the scope of project are gathered in three main groups, namely "Turkish Side Land Structures", "Sea Crossing Pipeline" and "TRNC Side Land Structures". These are;

Turkish Side Land Structures:

- Alaköprü Dam with 130.5 million m^3 reservoir capacity and HEPP,
- 22.646 km long Turkish side transmission line with 1.500 mm nominal diameter,
- Anamur Balancing Chamber with 10.000 m3 capacity.

Sea Crossing Pipe Line:

- 80 km long HDPE pipeline with 1.600 mm nominal diameter.

TRNC Side Land Structures:

- Güzelyalı Pumping Station,
- 3.7 km long TRNC side force main with 1.400 mm nominal diameter,
- Geçitköy Dam with 26.5 million m^3 reservoir capacity,
- Geçitköy Pump Station.

Turkish side land structures are located in the Anamur district in southern Türkiye and Sea crossing pipeline established in the Mediterranean Sea extending from Anamur to the Güzelyalı region located in west of Girne district of TRNC and the land structures of

TRNC side also situated around the Geçitköy region. The general layout of the facilities built in the scope of this project is given in Figure 1 and the longitudinal section of the whole system is shown in Figure 2.

2.1 Turkish Side Land Structures

Alaköprü Dam. Alaköprü dam is the source of water transferred to the TRNC. It has been established on Dragon creek which has an annual water capacity of approximately 600 million cubic meters. The dam is concrete faced rock fill type with storage capacity of 130.5 million m^3 and height of 94 m from thalweg of the creek. The image of the Alaköprü dam and the reservoir is shown in Figure 3.

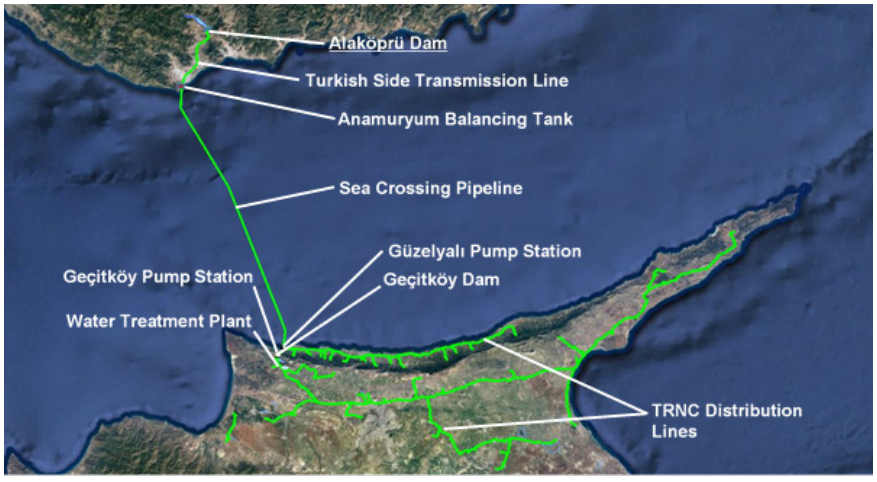

Figure 1: The General Layout of the Project

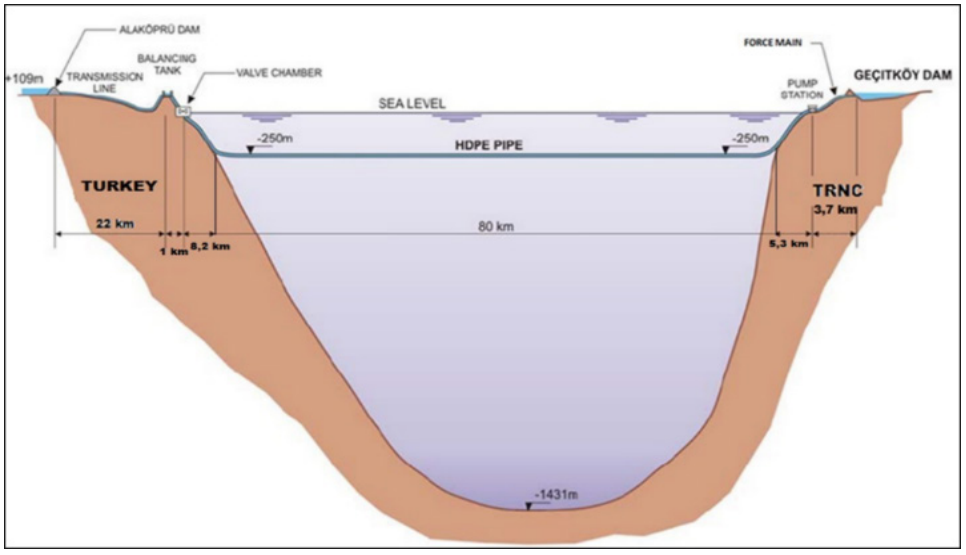

Figure 2: Longitudinal section of the whole system

Figure 3: Alaköprü Dam and reservoir

Transmission pipeline. This pipeline is composed of ductile pipes with a diameter of 1,500 mm and a total length of 22.646 km which enables the water taken from the Alaköprü dam to be transferred first to the Anamur balancing tank and then to the sea crossing transmission line (see Figure 4).

Anamur balancing tank. Water taken from the Alaköprü Dam is delivered to this reservoir, which was built near the sea in Anamur. As the pressure of the water coming from the dam needs to be balanced due to the special hydraulic characteristics of the sea crossing pipeline, the name of the reservoir has the expression 'balancing'. The storage capacity of the tank is 10.000 m^3.

Figure 4: Pipeline and balancing tank

2.2 TRNC Side Land Structures

Güzelyalı Pumping Station. Water transmitted to the TRNC by gravity from Türkiye is pumped to the Geçitköy Dam by means of Güzelyalı Pumping Station situated on the route of sea crossing pipeline. The Pumping Station has 2 primary and 1 spare pumps

with the total capacity of 2.38 m^3/h. The elevation height is H_m = 101.45 m.

Force Main. The main has a length of 3.7 km and a nominal diameter of 1,400 mm, which provides the transmission of water from the Güzelyalı Pumping Station to Geçitköy Dam. Pipe type is mechanically connected ductile iron.

Geçitköy Dam. The water transferred from Turkey is stored in the reservoir of Geçitköy dam and is the source of water transferred to the TRNC. The dam is clay core rock fill type with storage capacity of 26.5 million m^3 and height of 58 m from thalweg. The image of the Alaköprü dam and the reservoir is shown in Figure 5.

Geçitköy Pumping Station. The water stored in Geçitköy Dam is raised to a treatment plant with a capacity of 200.000 m3 / day through this pumping station. There are 5 original and 1 spare pumps at the Station with a capacity of 2.38 m^3 /h. The elevation height is H_m = 233.61 m.

Figure 5: Geçitköy Dam and reservoir

3 CRITICAL SYSTEM COMPONENTS OF SUSPENDED MARINE PIPELINE

The Cyprus Water Supply (CWP) pipeline system will have a nominal capacity of 2.38 m^3/s (75 mill m^3/yr) and will operate by gravity flow. The HDPE pipeline outer diameter is 1,600 mm with a PE100 material grade. The pipeline has an approximate true length of 80 km. A wall thickness of 63mm corresponding to SDR=26 is used along most of the route, with the exception of the Turkish on-bottom section where SDR=21 (corresponding to a wall thickness of 76mm). The battery limits (boundary conditions) for the offshore section of the CWP Pipeline System are shown in Figure 6.

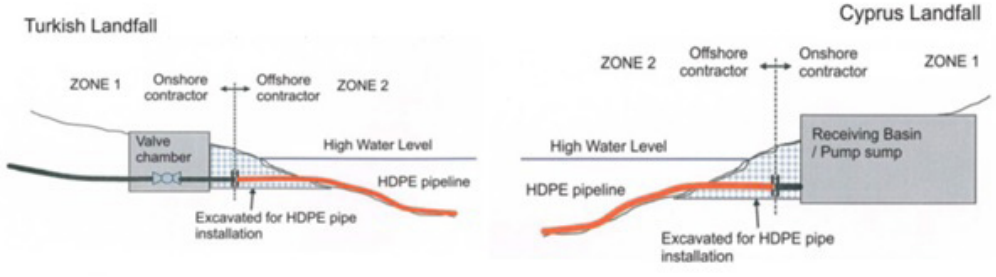

Figure 6: Battery Limit Definition –Turkey (a) Cyprus (b)

On-Bottom Section Design. The on-bottom sections of the CWP pipeline system extend from the shore crossings up to a water depth of 280m on both the Turkish and Cyprus sides. Figure 7 shows general layout of the on-bottom sections and names the main components.

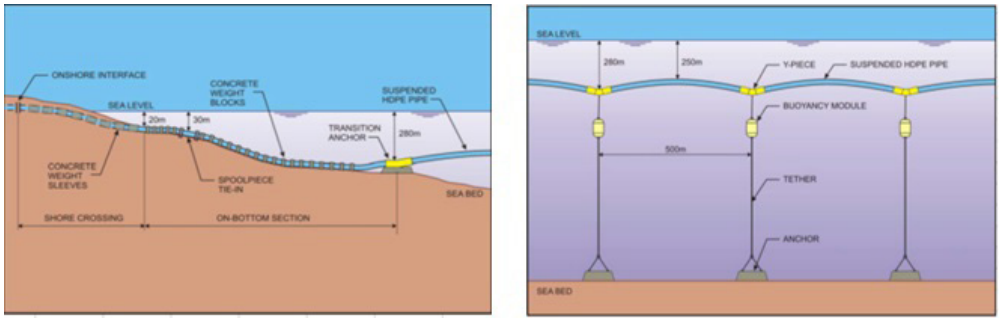

(a) (b)

Figure 7: Schematic of On-Bottom Sections (a) Suspended Section General Arrangement (b)

Shore Crossing: In the shore crossing areas, the pipeline is to be installed in a pre-cut trench. After pipeline installation into the trench, backfilling will be performed using suitable and approved materials either from the dredged materials or from materials imported from elsewhere. The Pipeline Shore Crossing Detailed Design Report prepared by Intec Eng. BV contains the following information: pipe deflection analysis, concrete weighting sleeve design, trenching and backfilling, liquefaction assessment.

Suspended Section Design: The suspended pipeline system extends from the 280m water depth contour at the Turkish side to the 280m water depth contour at the Cyprus Side. The main components of the suspended pipeline systems were shown in Figure 7.

System Configuration: Analysis has been performed during both the preliminary design and detailed design phases to define the overall suspended system configuration and to evaluate its behavior over a wide range of design conditions. It is noted that design reports address both the normal operating conditions of the pipe (including extreme environmental loading events) and several contingency / failure events. The failure events addressed include seabed instability resulting in anchor movement, tether failure above the buoyancy module, and tether failure below the buoyancy module. A basic principle of the suspended system design is that the pipeline shall be able to withstand all defined operating and environmental loads without failure. Furthermore, the system design shall be robust to withstand earthquake loads and accidental loads such as external impact.

The System Configuration and Dynamic Analysis Final Report prepared by Intec Eng. BV –recommended that confirmation of the fatigue properties of the material be performed. The fatigue resistance of the material is of critical importance due to the potential for vortex induced vibrations of the pipeline spans. A test program was initiated at Becetel Laboratories in Belgium during 2008 to assess both the fatigue and fracture properties of full-scale HDPE pipe wall samples (AES Engineering and Consultancy Ltd., 2014).

Anchors: The Anchor Detailed Design Report presents detail design of the seabed anchors required to maintain the position of the suspended portion of the CWP pipeline. The basic function of each seabed anchor is the same; namely to react to the vertical and horizontal loads imposed by the buoy and suspended pipeline. The two anchors at the ends of the suspended configuration (called Transition Anchors) must also react to a significant horizontal load in addition to the vertical load. Four types of anchors have been designed: Type 1 is a basic gravity type anchor that reacts to the vertical load of the suspended system using its own self-weight. Type 2 is a gravity anchor with "skirts" along the bottom perimeter to penetrate into the seabed. The Type 3 anchor is an embedded drag anchor from a major anchor supplier. The final type of anchor, Type 4, is applied at the transitions from on-bottom to suspended configuration.

Tether System: The system configuration and Dynamic Analysis report defines the mooring requirements for the CWP suspended pipeline system. The Det Norske Veritas code for permanent offshore mooring systems has been used as the basis for the design. Requirements for corrosion allowance, minimum break loads, component details and minimum lengths are determined.

Buoyancy Module. The buoyancy modules will be made of syntactic foam material with an outer protective shell and an inner steel core for load transfer.

Y-piece. The Y-pieces will join the adjacent HDPE pipe spans to each other and to the buoy/tether/anchor system (Figure 8). This system must be robust to transfer the system loads during the entire design life, must interface with the adjacent components such as the buoy/tether/anchor system, and must allow for future diverless subsea intervention in the event of repairs. The Y-part that has been proposed as joining 3 pieces of stainless steel pipes in the preliminary design made by Intec Eng. BV, has indeed been manufactured without welding through the method of heat-bending (ITU, 2008 & 2015) by the Salzfilter Mannesman Grobblech Incorporation in accordance to the American Bureau of Shipping's Guide for Building and Classing of Subsea Pipeline Systems ((ABS, 2006). In the HDPE pipe joints of the Y-part, stress/deformation analysis has also been performed with respect to the loading scenarios of both construction & operation phases by the finite element method in order to show that the flanged connection is safe & sufficient (AES Ltd., 2014).

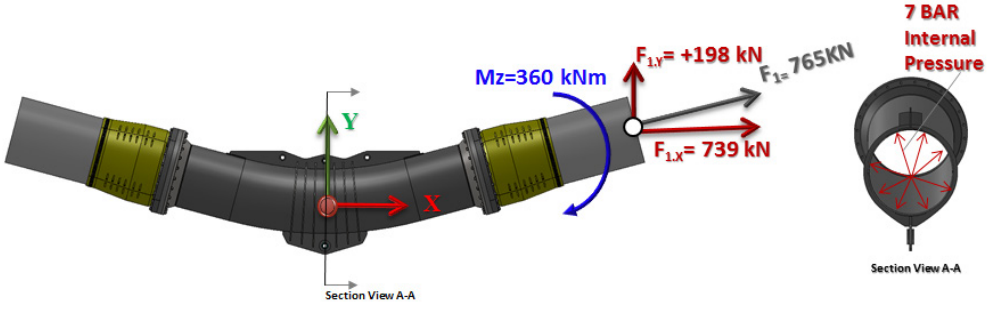

Figure 8: Operation Loads of the Turkey-side (TR #1 Load Situation given as an example)

4 PROJECT COST

The total cost (excluding expropriation costs) of the Cyprus Water Supply Project equals to 1,320 x 10^9 TL (480 x 10^6 $). The cost distribution of the project with respect to the facilities on both Turkey and Cyprus sides along with the suspended marine pipeline are given in Table 1.

Distribution of each project component in terms of construction works and equipment costs, along with account details of annual investment cost are also included in the same table. In the calculation of the annual investment cost, the interest and depreciation ratio is taken as i = 0.08, and the useful life value of the project is taken as n=50 years (averagely) for construction components and n=15 years (averagely) for equipment & installation.

Table 1. Cyprus Water Supply Project Cost Data (in 2015 Prices)

Costs (x 10^6 TL)	Initial Investment Cost	Construction Cost *(n=50, i=0,08 A/P=0,08174)*	Equipment Cost *n=15, i=0,08 A/P=0,11683*	Annual Investment Cost
Alaköprü Dam HEPP	91	61	30	8.49
Buildings (Turkey)	60	54	6	5.11
Sea Transition Line	885	865	20	73.04
Land Constructions (in Cyprus)	35	25	10	3.21
Geçitköy Dam	29	23	6	2.58
Water Treatment Plant	29	14	15	2.90
Water Distribution Line	191	170	21	16.35
Total Costs	1320 ***(480 ×10⁶ $)***	1212	108	111.69 ***(40.6 × 10⁶ $)***

Annual Investment Cost

Annual investment cost of the project is calculated as 40.6 x10^6 $/year with the above-given assumptions (Table 1).

Operation and Maintenance Cost

The annual operation and maintenance costs of the Cyprus Water Supply Project have been found as follows with two different approaches;

$OMC_1 \cong$ 0.03 x Total Investment Cost = 14.4 x 10^6 $/year

$OMC_2 \cong$ 1/3 x Annual Investment Cost = 40.6 / 3 = 13.5 x 10^6 $ / year

Total Annual Cost

The total of annual investment and operation & maintenance costs equals to;

(40.6 + 13.5) x $10^6 \cong$ 54 x 10^6 $/year

In this case, the gross unit cost of the project (per m^3 water delivered) is 54 x 10^6 $/year / 75 x 10^6 m^3/year = 0.72 $/$m^3$. Considering the energy generation income at Alaköprü Dam, 26.5Í10^6kWÍ180daysÍ24hÍ0.08$/kWh=9.16Í$10^6$$/year (0.12 $/$m^3$), the net unit cost of the project equals to 0.72-0.12 = 0.6 $/$m^3$.

With the assumption that 60% of the water delivered through Cyprus Water Supply Project will be used for drinking/municipal use and the remaining 40% for irrigation

purposes, the total benefit to be obtained from the project can be calculated as 90 x 10^6 $/year (Beaumont, 2000):

Revenue from sales of municipal water : 0.60 Í 75 Í10^6 Í 0.8 $/$m^3$ = 36Í10^6 $/year

Value added with irrigation in agriculture : 0.40 Í 75 x 10^6 Í 1.8 $/$m^3$ = 54Í10^6 $/year

In this case, the repayment period of the project investment can be taken as 480Í10^6 / 90Í10^6 = 5.3 years. Therefore, Cyprus Water Supply Project provides a solution 33% cheaper compared to water supply of sea water with RO (Reverse Osmosis) technology (0.9 $/$m^3$).

5 WATER MANAGEMENT AND OPERATION STUDIES

The Republic of Turkey (TR), and the Turkish Republic of North Cyprus (TRNC) have signed an agreement regarding the water management and operational studies within the scope of the TRNC Water Supply Project in March 2016, as the highlights of the agreement are given below:

The provided water from Turkey and local water of Cyprus are regarded as a whole in terms of management, planning, and allocation of water in the TRNC. The provided drinking-potable water is operated by a single operator in the TRNC. While the operation of the supplied water is carried out under the supervision of the TRNC, the agricultural areas to be irrigated with the provided water is decided upon with both the TR and the TRNC.

The enterprises responsible for both drinking-potable water, wastewater & rainwater, and the agricultural irrigation are operated through separate tenders. Existing facilities and networks belonging to the public institutions & municipalities in TRNC are delivered to the project operator upon contract. Investments that will be needed during the operation period specified for all drinking-potable water, wastewater & rainwater, and agricultural irrigation facilities are made entirely by the operators.

The facilities on the Turkey side are managed by the General Directorate of State Hydraulic Works (DSI) with respect to operation, maintenance-repair, and all other technical issues. In addition to this, the DSI provides technical support in the facilities of the Cyprus side when required as well.

6 CONCLUSION AND RECOMMENDATIONS

Water supply from Turkey to Cyprus with the suspended marine pipeline remains to be the first and only project of its kind in this area. Since October 2015, 75Í10^6 m^3/year of water has been delivered to the TRNC, and the total construction cost equals to 480Í10^6 $, while the unit cost of water remains to be 0.60 $/$m^3$. It is clear with the project that an important step has been taken in terms of mitigating the effects of climate change (rainfall and river flow) which is becoming more apparent in the region on Cyprus side (Eastern Mediterranean). It is expected that there will be significant improvements in the quality of life of the residents with the efficient use of water delivered to the TRNC, especially in the municipal and agricultural sectors. In this context, loss/leakage (non-revenue water) control in the water distribution networks, use of modern irrigation techniques, and reduction of evaporation losses in the Geçitköy Dam through floating solar energy panel system, along with the fact that these important facilities should be

sustainably operated at full cost-based water tariffs are all considered to be important measures to be taken for the sustainability of water supply.

ACKNOWLEDGMENTS

First, we would like to thank Prof Veysel Eroğlu, the TR Minister of Forestry and Water Affairs of the time, for his great contributions in the realization of this unique project, and his bold vision. Due to the efforts and contributions in the project design, planning and construction phases, we are thankful to Alarko Contracting Group, Intec Engineering DV, Artı Project, Danish Hydraulic Institute (DHI), AES Engineering Ltd, Firat Plastic Inc., and Kalyon - Sigur Ros Joint Venture, together with all stakeholders working on design and construction of the land structures of the project. We also extend our gratitude to the managers & employees of the General Directorate of State Hydraulic Works (DSI) for their efforts in this project.

REFERENCES

ABS (2006). Guide for Building and Classing Subsea Pipeline Systems, s.25, Section 3.15.

AES Engineering and Consultancy Ltd. (2014). *Cyprus Water Supply Project, Structural Analysis Report with HDPE and Steel Pipe Connections*, Project Report. AES Engineering and Consultancy Ltd., Istanbul.

Agiralioglu, N. (2016). Cyprus Water Supply Project and Their Effects on Region, Project Report. Kalyon Construction, İstanbul.

Agiralioglu, N., Danandeh Mehr, A., Akdegirmen, Ö. & Tas, E. (2018). Cyprus Water Supply Project: Features and Outcomes, *13th International Congress on Advances in Civil Engineering*. 12-14 September 2018, Izmir/TURKEY.

Beaumont, P. (2000). The Quest for Water Efficiency - Restructuring of Water Use in the Middle East. *Water, Air, and Soil Pollution*, Vol: 123, 551-564.

Intech Engineering BV & Alarko Contracting Group (2008). Cyprus Water Supply Project, Vol: 1-6.

ITU (2008). Supervising and Consultancy (Scientific Support and Expert Inspection) Studies on Cyprus Water Supply Project, Alarko Contracting Group and General Directorate for State Hydraulic Works.

ITU (2015). The Assessment Report of Suspending Pipeline and Y-Piece at Cyprus Water Supply Project.

Cite this article as: Ozturk I., Agiralioglu N., Ozdemir O., Akinci N., "Water Supply from Turkey to Cyprus Island with Suspended Marine Pipeline", *International Conference on Civil Infrastructure and Construction (CIC 2020)*, Doha, Qatar, 2-5 February 2020, DOI: https://doi.org/10.29117/cic.2020.0107

Utilizing Recycled Polypropylene Fibers as Reinforcement for Concrete Beams

Khadra Bendjillali
bendjilalik@yahoo.fr
Laboratory of Structures Rehabilitation and Materials, University Amar Telidji, Laghouat, Algeria

Mourad Hadjoudja
hadjoudja_m@yahoo.fr
Laboratory of Civil Engineering Research, University Amar Telidji, Laghouat, Algeria

Mohamed Chemrouk
mchemrouk@yahoo.fr
Faculty of Civil Engineering, University of Science and Technology Houari Boumediene, Algiers, Algeria

ABSTRACT

Polypropylene (PP) fibers are among numerous plastic waste materials, which are generated by the different industrial and domestic activities. Due to its low biodegradability, plastic waste constitutes a real environmental problem. The valorization of recycled PP fibers in the fabrication of concrete is one of the efficient solutions to cater for the environmental problems induced by plastic waste. In this experimental work, the workability and the mechanical properties of concrete are examined with different content ratios of recycled PP fibers. The mechanical behavior and the failure mode of concrete beams reinforced with recycled PP fibers are also studied. The used PP fibers are recycled from plastic waste of PLAST BROS factory in BordjBouArreridj, in Algeria. The fiber's diameter varies between 0.7 and 0.9mm. The various fiber content ratios tested in this investigation are 0.25, 0.5 and 1%. Based on the results of this study, the presence of recycled PP fibers in concrete decreases its workability; the addition of an adequate superplasticizer to the concrete mix becomes then necessary. Nevertheless, a positive effect is observed on its mechanical behavior. Indeed, in the presence of steel bars, reinforcing concrete beams with recycled PP fibers improves greatly their ductility and delays the appearance of cracks.

Keywords: Recycled fibers; Polypropylene fibers; Workability of fresh concrete; Mechanical strength; Ductility

1 INTRODUCTION

The greatest benefit obtained by utilizing fibers as reinforcement of concrete elements is the improvement of the long-term serviceability of constructions. The presence of fibers into concrete is a very effective technique to control cracking and to improve the tensile behavior, the ductility and the durability of structures. Many types of fibers such as in metals, in synthetic and in vegetables have been used in concrete. Synthetic fibers of polypropylene (PP) are the most common commercial products in fiber reinforced concrete (Yin et al., 2015). Recently, numerous reports and papers investigating the use of PP fibers in concrete were published. PP fibers which are produced from homo-polymer polypropylene resin are flexible and hydrophobic materials possessing excellent chemical and wear resistances; compared to other types of fibers, they have a lower

coast. PP fibers are very effective in controlling plastic shrinkage cracking in concrete (Banthia & Gupta, 2006). In addition to reducing the shrinkage of concrete (Sun & Xu, 2009) and improving its cracking resistance (Zhang & Zhao, 2012), PP fibers reduce the permeability of concrete that can significantly affect the lifespan of structures and delay their degradation (Kakooei, 2012). Reinforcing beams by PP fibers gives them the capability to support further loads beyond the first cracking (ACI 544.1R-96, 2002). With a minimal conventional steel reinforcement, the use of 0.5% of PP fibers can offer a better mechanical behavior in shear and in flexion of concrete beams (Bendjillali & Chemrouk, 2018). For small crack opening ranges, PP fibers exhibited a high post-cracking toughness (Caggiano, 2016). In Algeria, a large quantity of plastic fibers is wasted in certain factories and can be recycled by the construction industry to improve the concrete properties. In addition, the recycling of this waste participates successfully to solve some environmental problems and then protect the nature. Several researchers have tested the use of some plastic waste fibers in concrete and the results were very encouraging.

The main objectives of this paper are first to study the influence of the addition of recycled PP fibers on the fresh as well as hardened properties of concrete. The paper looks particularly at their role in the improvement of the mechanical behavior of concrete beams having a conventional steel reinforcement.

2 CONCRETE MIXING INGREDIENTS

Limestone crushed aggregates coming from OUAZANE crushing station in Laghouat (Algeria) and consisted of sand (0/3mm) and two fractions of gravel (3/8 and 8/16mm) are used for the fabrication of tested concrete specimens. Portland cement CEM II/B-42.5N produced by LAFARGE of Hammam Dalaa factory in M'Sila (Algeria) is used with potable water and high-range water-reducing admixtures, type SIKAVISCORETE TEMPO 12 fabricated by SIKA EL DJAZAIR. The polypropylene fibers used as reinforcement of the tested concrete are recycled from plastic waste (Figure 1) of PLAST BROS, a factory situated in BordjBouArreridj (Algeria). Fibers have a length of 50mm and diameters between 0.7 and 0.9mm. The sand has a fineness modulus of 2.73 and a sand equivalent of 74%. The water absorption varies between 3.8, 1.5 and 1.8% for sand, gravel 3/8 and gravel 8/16 respectively.

Figure 1: Polypropylene fibres used in the present tests

3 PREPARATION AND CURING OF THE CONCRETE SPECIMENS

The concrete mixture is prepared using Pierre Rossi optimization based on Baron-Lesage method; with a water to cement W/C ratio of 0.6 and a sand to gravel ratio S/G of 0.65. The superplasticizer is added for improving the concrete workability (slump = 9cm). The composition of the control concrete is as follows:

Cement: 350kg/m^3, Sand: 663kg/m^3, Gravel 3/8: 105kg/m^3, Gravel 8/16: 916kg/m^3, Water: 210kg/m^3, Superplasticizer: 2.3kg/m^3.

The same composition is used for making the recycled PP fibers concrete, where three fractions of fibers (by weight) are used: 0.25, 0.5 and 1%. Firstly, the cement and aggregates are dry mixed in a drum concrete mixer, secondly half of the water content with the admixture are added, the fibers then are introduced and dispersed manually into the mix (Figure 2) and the remaining half of the water is added gradually at last. After demolding, the concrete specimens are cured under plastic sheets until the testing day.

Figure 2: Adding of PP fibers

4 FRESH CONCRETE CHARACTERISTICS

Test results show that the concrete workability decreases as the content of recycled PP fibers is increased, especially when the fibers content is more than 0.5% (Figure 3).

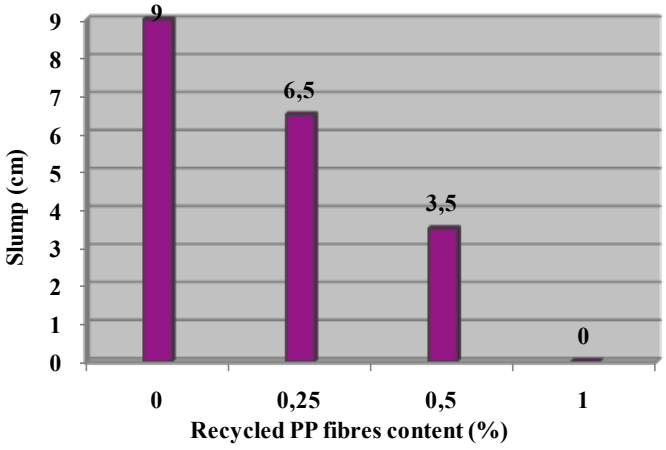

Figure 3: Variation of concrete slump

This is due to the presence of fibers which imprison cement paste and making concrete more viscous (Figure 4) and difficult to place in the formwork. In this case, the superplasticizer amount must be increased to obtain a better workability and facilitate the concreting. Similar result was previously observed in several studies (Hsie et al., 2008; Söylev & Özturan, 2014; Bendjillali et al., 2018). Vairagade and Kene (2013) have reported that fibers can form a network structure in concrete, which restrains mixture from segregation and flow.

Figure 4: Slump test realized on recycled PP fibers concrete

5 HARDENED CONCRETE CHARACTERISTICS

The mechanical strength (flexural and compressive strength) of prismatic samples 70x70x280mm is measured after 28 days of age, the results are presented in Figure 5.

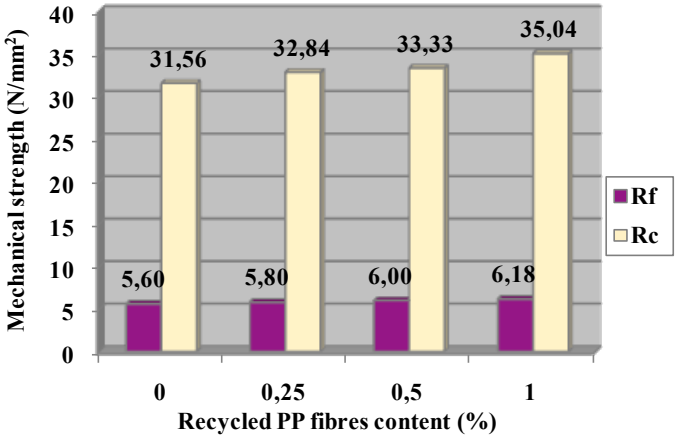

Figure 5: Mechanical strength of recycled PP fiber concrete

The improvement of the flexural strength was 3.6, 7.2 and 10.4% respectively when 0.25, 0.5 and 1% of recycled PP fibers were used as reinforcement in concrete. As shown in other works (Zhang & Zhao, 2012; Suji et al., 2007), the increase of the flexural strength is proportional to amount of PP fibers. There is usually an optimum amount of PP fiber which results in an effective distribution of fibers in concrete and consequently

leads to a better flexural strength (Alamshahi et al., 2012; Dharan & Lal, 2016). For the compressive strength, the improvement ratio reaches 4.1, 5.6 and 11% in 0.25, 0.5 and 1% recycled PP fibers concrete respectively.

As reported by Naraganti et al. (2019), the compressive strength increases proportionately with the increase in the PP fibers content. This is in contradiction with some of the findings in the literature, reporting a decrease of the compressive strength with an increase in the fibers content (Meddah & Bencheikh, 2009; Ramezanianpour et al., 2013; Sadiqul Islam & Gupta, 2016; Das et al., 2018). However, while the effect of recycled PP fibers on the compressive strength of concrete may not seem to be considerable, nor widely accepted, their effect on the failure mode in flexure as well as in compressive, is very significant, as shown in Figure 6. Thanks to the presence of recycled PP fibers, concrete specimens failed in a noticeable ductile manner (Figure 6-b), whereas the control concrete specimens containing no fibers failed in a brittle manner (Figure 6-a). Ductility of concrete expresses the ability of the material to absorb energy in the post cracking state. Such ductile behavior exhibited by PP fibers concrete is mainly attributed to the extension of fibers and at the same time to the restraint of the crack widening by these fibers. As a result, a number of fine cracks would form at the post cracking state before failure. Such behavior was reported in several works, using numerous types of fibers (Soutsos et al., 2012; Cifuentes et al., 2013; Sahoo et al., 2015).

After flexural test

After compressive test

a: Control concrete **b: Recycled PP fibers concrete**

Figure 6: Failure mode in concrete specimens

6 FLEXURAL BEHAVIOUR OF POLYPROPYLENE FIBERS CONCRETE BEAMS HAVING CONVENTIONAL STEEL REINFORCEMENT

Four-point bending tests are carried out on 100x100x500mm beams having conventional reinforcement according to the schematic diagram given in Figure 7-a. The cross-section of the beam specimens is as shows in figure 7-b.

From Figure 8, the effect of recycled PP fibers is appreciated not only through the failure load of the different tested beams, but also through their first cracking load. In effect, concrete beams containing 0.25% recycled PP fibers have their first cracking load increased by 13% compared to control beam. This percentage increase reaches almost 27% for concrete beams containing 0.5% recycled PP fibers and 48% for concrete beams containing 1% recycled PP fibers. This result is of an enormous practical importance since it reveals the high efficiency of fibers to delay the first cracking in concrete beams. Recycled PP fibers have also played an important role in increasing the failure load of concrete beam, compared to beams without fibers.

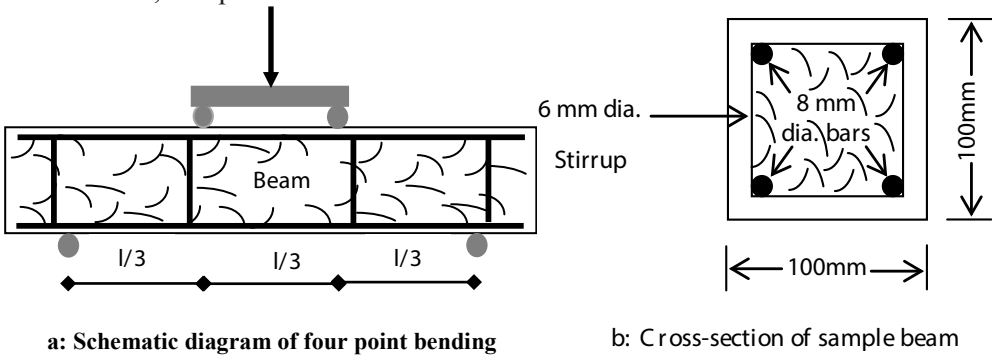

Figure 7: Four point bending tests

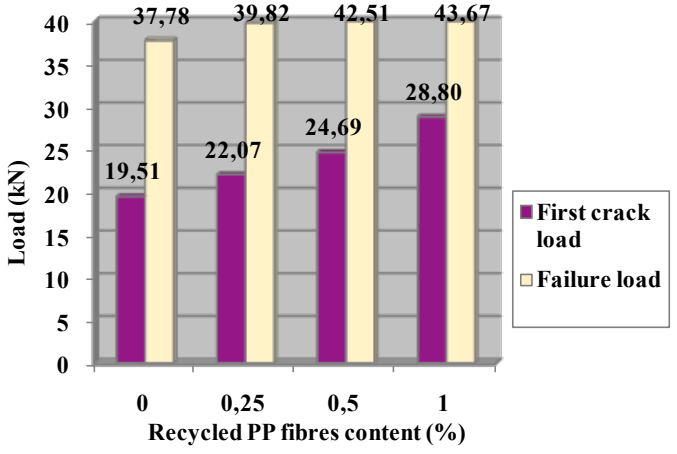

Figure 8: Variation of first cracking load and failure load of reinforced concrete beam

In effect, the failure load increased by 6% for beams containing 0.25% recycled PP fibers. For fibers contents of 0.5% and 1%, the ultimate load increased by 13% and 16% respectively. Although, the reinforcement of structural elements by PP fibers improves the first cracking behavior, the efficient contribution of fibers in general appears at the

post cracking state (Ghosni et al., 2013). When recycled PP fibers are added to concrete, the shear capacity of beams is increased (Figure 9). The recycled PP fibers concrete beams show more ductile behavior with relatively more restrained diagonal cracks (figure 9-b) compared to the control beam (figure 9-a). The used fibers have significantly reduced the width and number of shear cracks, which improves the mechanical performance of reinforced concrete beams. Some researchers (Baskar et al., 2018; Tahenni et al., 2015) have reported that with the addition of fibers, the strength and stiffness of concrete beams increase, while the cracks decrease in width and in length. The incorporation of fibers in concrete increases the cohesion of the matrix and hence the failure becomes more ductile and gradual in fiber reinforced beams (Madhavi et al., 2014). Combining PP fibers and stirrups improves the behavior of reinforced concrete beams and changes its failure mode (Ghallab & Badr, 2006).

a: Control beam. **b: Recycled PP fibers concrete beam**

Figure 9: Typical shear failure of the beams tested

7 CONCLUSION

Based on the results obtained in this investigation, the following conclusions can be made:

- The workability of concrete is negatively affected by the addition of recycled PP fibers.
- For compressive as well as flexural strength, the strength's optimum is reached at 1% of recycled PP fibers content.
- Both, the first cracking load and the failure load are significantly increased by the presence of recycled PP fibers in concrete beams.
- Beams reinforced with recycled PP fibers have exhibited higher shear strengths and showed more ductility before failure than the control beams.

REFERENCES

ACI 544.1R-96 (2002). State of the art report on fiber reinforced concrete.

Alamshahi, V., Taeb, A., Ghaffarzadeh, R. & Rezaee, M. A. (2012). Effect of composition and

length of PP and polyester fibres on mechanical properties of cement based composites. *Construction and Building Materials*, 36, 534-537.

Banthia, N. & Gupta, R. (2006). Influence of polypropylene fiber geometry on plastic shrinkage cracking in concrete. *Cement and Concrete Research*, 36, 1263-1267.

Baskar, K., Elangovan, G. & Mohan Das, K. (2018). Flexural behaviour of fibre reinforced concrete beams with different aspect ratios. *FIBRES & TEXTILES in Eastern Europe*, *26, 1*(127), 59-66.

Bendjillali, K. & Chemrouk, M. (2018). Study of the reinforcement of structure members by polypropylene fibres waste. *MATEC Web of Conferences*, 149, 01022.

Bendjillali, K., Chemrouk, M. & Boulekbache, B. (2017). Recycled synthetic waste fibres for the reinforcement of concrete. WASTES–Solutions, Treatments and Opportunities II, 1st Edition, *CRC Press*, 9-15.

Caggiano, A., Gambarelli, S., Martinelli, E., Nisticò, Ni. & Pepe, M. (2016). Experimental characterization of the post-cracking response in hybrid steel/polypropylene fiber-reinforced concrete. *Construction and Building Materials*, 125, 1035-1043.

Cifuentes, H., García, F., Maeso, O. & Medina, F. (2013). Influence of the properties of polypropylene fibres on the fracture behaviour of low-, normal- and high-strength FRC. *Construction and Building Materials*, 45, 130-137.

Das, C. S., Dey, T., Dandapat, R., Mukharjee, B. B. & Kumar, J. (2018). Performance evaluation of polypropylene fibre reinforced recycled aggregate concrete. *Construction and Building Materials*, 189, 649-659.

Dharan, D. S. & Lal, A. (2016). Study the effect of polypropylene fiber in concrete. *International Research Journal of Engineering and Technology*, *3*(6), 616-619.

Ghallab, A. & Badr, A. (2006). Flexural behaviour of polypropylene fibers reinforced concrete beams. *Housing and Building National Research Centre Journal*, *2* (3), 50-63.

Ghosni, N., Samali, B. & Vessalas, K. (2013). Ductility and strength of reinforced concrete beams intrinsically reinforced with polypropylene fibers. *The Thirteenth East Asia-Pacific Conference on Structural Engineering and Construction* (EASEC-13), Sapporo, Japan.

Hsie, M., Tu, C. & Song, P. (2008). Mechanical properties of polypropylene hybrid fiber-reinforced concrete. *Materials Science and Engineering A*, 494, 153-157.

Kakooei, S., Akil, H. M., Jamshidi, M. & Rouhi, J. (2012). The effects of polypropylene fibers on the properties of reinforced concrete structures. *Construction and Building Materials*, 27, 73-77.

Madhavi, T. Ch., Raju, L. S. & Mathur, D. (2014). Polypropylene fiber reinforced concrete- A Review. *International Journal of Emerging Technology and Advanced Engineering*, *4*(4), 114-119.

Meddah, M. S. & Bencheikh, M. (2009). Properties of concrete reinforced with different kinds of industrial waste fiber materials. *Construction and Building Materials*, 23, 3196-3205.

Naraganti, S. R., Pannem, R. M. R. & Putta, J. (2019). Impact resistance of hybrid fibre reinforced concrete containing sisal fibres. *Ain Shams Engineering Journal*, *10*(2), 297-305.

Ramezanianpour, A. A., Esmaeili, M., Ghahari, Seyed-Ali & Najafi, M. (2013). Laboratory study on the effect of polypropylene fiber on durability, and physical and mechanical characteristic of concrete for application in sleepers. *Construction and Building Materials*, 44, 411-418.

Sadiqul Islam, G. M. & Gupta, S. D. (2016). Evaluating plastic shrinkage and permeability

of polypropylene fiber reinforced concrete. *International Journal of Sustainable Built Environment*, 5, 345-354.

Sahoo, D. R., Maran, K. & Kumar, A. (2015). Effect of steel and synthetic fibers on shear strength of RC beams without shear stirrups. *Construction and Building Materials*, 83, 150-158.

Soutsos, M. N., Le, T. T. & Lampropoulos, A. P. (2012). Flexural performance of fibre reinforced concrete made with steel and synthetic fibres. *Construction and Building Materials*, 36, 704-710.

Söylev, T. A. & Özturan, T. (2014). Durability, physical and mechanical properties of fiber-reinforced concretes at low-volume fraction. *Construction and Building Materials*, 73, 67-75.

Suji, D., Natesan, S. C. & Murugesan, R. (2007). Experimental study on behaviors of polypropylene fibrous concrete beams. *J Zhejiang Univ Sci A*, *8*(7), 1101-1109.

Sun, Z. & Xu, Q. (2009). Microscopic, physical and mechanical analysis of polypropylene fiber reinforced concrete. *Materials Science and Engineering A*, 527, 198-204.

Tahenni, T., Chemrouk, M. & Lecompte, T. (2016). Effect of steel fibers on the shear behavior of high strength concrete beams. *Constructions and Building Materials*, 105, 14-28.

Vairagade, V. & Kene, K. (2013). Strength of normal concrete using metallic and synthetic fibers. *Procedia Engineering*, 51, 132-140.

Yin, S., Tuladhar, R., Shi, F., Combe, M., Collister, T. & Sivakugan, N. (2015). Use of macro plastic fibres in concrete: A review. *Construction and Building Materials,* 93, 180-188.

Zhang, S. & Zhao, B. (2012). Influence of polypropylene fibre on the mechanical performance and durability of concrete materials. *European Journal of Environmental and Civil Engineering*, *16*(10), 1269-1277.

Cite this article as: Bendjillali K., Hadjoudja M., Chemrouk M., "Utilizing Recycled Polypropylene Fibers as Reinforcement for Concrete Beams", *International Conference on Civil Infrastructure and Construction (CIC 2020)*, Doha, Qatar, 2-5 February 2020, DOI: https://doi.org/10.29117/cic.2020.0108

High and Ultra-high Performance Concretes: A Solution to Reinforced Concrete Durability under Harsh Climate of Arabian Gulf

Muazzam Ghous Sohail
muazzam.ghous@qu.edu.qa
Center for Advanced Materials, Qatar University, Doha, Qatar

Ramazan Kahraman
ramazank@qu.edu.qa
Department of Chemical Engineering, Qatar University, Doha, Qatar

Nasser Al Nuaimi
anasser@qu.edu.qa
Center for Advanced Materials, Qatar University, Doha, Qatar

Wael Alnahhal
wael.alnahhal@qu.edu.qa
Department of Civil and Architectural Engineering, Qatar University, Doha, Qatar

Muhammad Wasee
wasee.ahmed@qu.edu.qa
Center for Advanced Materials, Qatar University, Doha, Qatar

ABSTRACT

Reinforced concrete (RC) infrastructure in the Arabian Gulf region deteriorates under severe environmental conditions after only short service life. To overcome this problem, it is imperative to employ high-quality concretes and reinforce them with rebars that are corrosion resistant. This paper investigates the durability performance of newly developed high performance concretes (HPC) and ultra-high performance concretes (UHPC). The HPC and UHPC were manufactured using locally available materials in Qatar without employing any special treatment. The durability characteristics of HPC and UHPC in comparison to a normal strength concrete (NSC) were determined. Durability indicators such as concrete resistivity, sorptivity, porosity and resistance to chloride permeability were evaluated in order to access the durability of these concretes. These parameters were also compared to the concrete core samples taken from 30 to 50 years old RC structures in Doha city. The electrical resistivity of HPC and UHPC was 11 and 20 times higher than NSC, respectively. Sorptivity was 2 and 3 times less than NSC, respectively for HPC and UHPC. While the porosity of HPC and UHPC was 2.45 and 1.43% respectively. These newly fabricated concretes showed higher performance in durability testing than the concretes from real structures. With such attributes, the UHPC will be a useful tool in arresting the rapid deterioration of RC structures especially under harsh-climatic conditions of the Arabian Gulf.

Keywords: Durability of reinforced concrete infrastructure; High-performance concrete; Ultra-high-performance concrete; Durability indicators of RC structures

1 INTRODUCTION

The civil infrastructure including low and mid-rise residential construction, high rises, bridges, and harbors in Arabian Gulf and around the world are mostly reinforced concrete (RC). The RC structures in the Arabian Gulf are constantly subjected to extremely hot and humid environmental conditions (Al-Samarai, 2015). In global classification, the

Gulf Region lies in an arid and subtropical climate with a total precipitation of 5 cm/year while the evaporation is 124 cm/year (Bazaraa, 1989). The temperature reaches 50 °C frequently in summer while the relative humidity (RH) ranges between 60% to 100%. In comparison with other seas, the Gulf water shows higher salinity with an average of 38.9 g/lit (Sohail et al., 2018a), while the groundwater chloride contents in Qatar range from 43 g/l to 68 g/l (Qatalum, 2006). The above mentioned environmental conditions cause RC structures to deteriorate well before their designed service lives (Sohail et al., 2019). Authors carried out a field study on 30 to 50 years old RC structures in the Arabian Gulf region in order to determine the environmental load and resistance factors. A serious deterioration was observed after 30 to 50 years of service life. It was observed that in most of the cases the chloride ion concentration was 4-6 times higher than the threshold to initiate the corrosion of mild steel reinforcing bars. The carbonation depth was up to 70 mm in some concretes. The average and maximum carbonation rates were calculated to be 6 $mm/\sqrt{year}$ and 10.8 $mm/\sqrt{year}$, respectively. The concrete resistivity to electrical charge, rapid chloride permeability, and sorptivity were measured (Sohail et al., 2018a). It was observed that, given the severe environment, the quality of concrete was not sufficient to fulfil the intended function over the design life. It was concluded that new construction materials and practices need to be adopted for future construction and repair to minimize the damage caused by these aggressive hot and humid conditions with high concentrations of chlorides both airborne and in groundwater.

High-performance concretes (HPC) and ultra-high performance concrete (UHPC) exhibit dense microstructure and low porosity, which make them suitable materials to arrest the degradation of RC structures subjected to harsh climatic conditions. HPC is defined as concrete with a compressive strength of up to 100 MPa and workability equal to a self-compacting concrete (SCC). On another hand, the UHPC is defined as the concrete with a compressive strength above 150 MPa and very high workability (Fehling et al., 2014a; Graybeal & Tanesi, 2007; Sohail et al., 2018b). To be able to attain such high strength, flowability, and lower porosity, it is required to employ a water-to-cement (w/c) ratio between 0.2 to 0.3, addition of pozzolanic supplementary cementitious materials (SCM), and high amount of superplasticizers are employed (Russel, G & Graybeal, 2013; Wille et al., 2011a). Development of UHPC has been through several stages over time; first of kind was low-porosity-concrete (Yudenfreund et al., 1972) manufactured with finely ground cement and by applying external pressure on the paste to achieve lower porosity. Bache (1981) developed a concrete with higher compressive and flexural strength by adding micro-silica and a high amount of steel fibers, it was called a Densified concrete matrix (DCM). The matrix was very ductile with higher compression and flexural strengths. During the early manufacturing of UHPC, special treatments such as vacuum mixing, external pressure on fresh concrete, and heat curing are applied to achieve higher compressive strengths. However, these specific materials and special techniques were not practical for large scale applications. That is why the progress and use of UHPC was restricted. The latest form of UHPC was first developed by (Richard & Cheyrezy, 1995), known as reactive powder concrete (RPC) with compressive strengths of 200MPa and 800MPa. Ingredients were proportioned by employing a compressible packing model (CPM) presented by de Larrard and Sedran (1994). The homogeneity of RPC matrix was achieved by using micro-silica and heat curing at 95^{o}C.

In this study, the high-performance and ultra-high-performance concrete were cast using locally available materials in Qatar. The mixture proportions were established to achieve 100 MPa. HPC and above 150 MPa of UHPC. The durability indicators such as resistivity, sorptivity, porosity, and rapid chloride permeability were studied. These durability indicators were compared to normal concrete employed in the construction industry in recent times and to those concretes that were used to build RC structures in the 1970s, 1980s, and 1990s presented by Sohail et al. (2018a).

2 EXPERIMENTAL DETAIL

2.1 Fabrication of HPC and UHPC; materials and mix proportion

The manufacturing of UHPC was carried out by trial and error following the methods employed by (Wille et al., 2011b) and (Wong & Kwan, 2008). Where the flow and strength are optimized by changing the quantities of cement, fine secondary cementitious materials, sand, water, and high range water reducers (HRWR). Flow cone tests in accordance with (ASTM C230/C230M14, 2014) were used to measure the flow of UHPC. The initial mixture proportion for trials was selected after performing an extensive literature review which has been published elsewhere (Sohail et al., 2018b), the mixture proportions that employs commonly available materials were selected to initiate the trials. A ratio of cement (C): silica fume (SF): fly ash (FA) of 1:0.25:0.25 was initially employed. All the materials are readily available in the construction market of Qatar. The trial mixtures were carried out by using 5L Pan Mixer. After several trials, the required strength and acceptable flow for UHPC were achieved, the finalized mixture proportions are shown in Table 1. In case of HPC the trial was also carried out by hit and trial, coarse aggregates of up to 10 mm were added in the mixture proportion. The mixture proportion for HPC and NSC are also presented in Table 1. The ordinary Portland cement (OPC) CEM I 42.5 R was used to cast all types of concretes; it was acquired from a local cement company. For NSC and HPC the gabbro aggregates with a maximum size of 10 mm and washed sand with 0/4.75 mm size were employed. For UHPC, two sand sizes were used, i) passing through 1180 μm retained at 600 μm and ii) passing through 600 μm retained at 300 μm sieves sizes, respectively. Finer than 300 μm sand was removed to reduce the amount of fines in order to minimize the water demand. In case of HPC and UHPC, the addition of fly ash and silica fume is necessary. These two products are mostly imported to Qatar from India and China. The fly ash type F and Grey silica fume were used as secondary cementitious materials.

In the case of UHPC, the mixing procedure is as important as the ingredients selection. For UHPC, the ingredients were first dry mixed for 5 minutes in order to obtain a homogeneous mixture. Then half of the HRWR was added in one minute. The other half of HRWR was mixed with the water. This water containing HRWR was then poured into the mix slowly for 1 minute. The mixing was continued until a uniform flow able UHPC was obtained. The same procedure was adopted for trials mixes in 5 L PAN mixer and in 95 L PAN mixer to cast 65 liters of UHPC to prepare cylindrical (100x200mm) and prism (100x100x350mm) samples. The NSC and HPC were mixed using Gravity Mixers.

The flow of NSC and HPC were measured according to (ASTM C1611 / C1611M - 14, 2014) and for UHPC it was measured according to (ASTM C230/C230M14, 2014)

without lifting and dropping the table. The total flow of the NSC for HPC in Abraham Cone was 535 and 586 mm and T50 was 7.8 and 6.8 seconds, respectively, in accordance with (ASTM C1611/C1611M-14, 2014). No vibration was applied during the casting of samples for durability testing. After 28 days, the maximum compressive strengths of NSC, HPC, and UHPC were 38 MPa, 93 MPa, and 161 MPa, respectively.

Table 1: The mixture proportions of NSC, HPC, and UHPC

Ingredients	**NSC**	**HPC**	**UHPC**
	Kg/m^3	**Kg/m^3**	**Kg/m^3**
Cement	410	640	820
Silica Fume	-	128	190
Fly Ash	-	128	148
Sand (0/4 mm)	962	700	-
Fine sand 1(retained at 600 μm)	-	-	718
Fine sand 2 (retained at 300 μm)	-	-	308
Coarse (0/10 mm)	965	550	-
Water	159	200	172
SP	5.2	10	25
Flow (mm)	535~	586~	280*
T_{50} (sec)	7.8	6	NA
7 days compressive strength (MPa)	23.5	54	86
28 days compressive strength (MPa)	**37.5**	**93**	**161**
90 days compressive strength (MPa)	48	105	**163**
~ASTM C1611-14, *ASTM C230/C230M			

The failure mode of NSC, HPC, and UHPC is distinctly different in compression test. The NSC cylinders failed in cement matrix with failure lines passing throughout the lengths. While in case of HPC and UHPC, the failure was abrupt with a blast of cylindrical samples. The failure in HPC was through the aggregates and matrix, the failure shape was conical in both HPC and UHPC.

Durability Testing

2.1.1 Concrete resistivity

Concrete's electrical resistivity is an indicator of its quality, a high-quality concrete shows very high electrical resistance, while porous and low-quality concrete shows easy flow of electrical currents. Lower the value of concrete resistivity, higher is the risk of corrosion. Concrete resistivity higher than 20,000 Ohm.cm would present negligible corrosion risk to the reinforcing steel rebars. Concrete resistivity was measured on three cylindrical concrete samples of 100x200 mm at 28 days of curing in accordance with (AASHTO TP 95, 2011). The samples were kept in saturated stat to eliminate the humidity effects on the resistivity values.

2.1.2 Rapid Chloride Permeability Test (RCPT)

Rapid chloride penetrability was measured on 100x50 mm in accordance with (ASTM C1202-12, 2012). These disk samples were taken from 100x200 cylinders after testing for resistivity. The disk samples were kept in oven at 50°C for three days, then immersed underwater and a vacuum of 50 mm Hg was applied for 18 hours. After this conditioning, the samples were placed between two chambers with 3.5 % $NaCl^-$ in one and 0.3 NaOH in the other. A voltage of 60V was applied on two terminals and current passing through the concrete samples was measured. Total charge transfer was measured over a period of 6 hours.

2.1.3 Sorptivity

Sorptivity is a very relevant indicator of long-term durability of concrete. It measures the amount of moisture that could be transported and contained into an unsaturated concrete (Dias, 2013; Patel, 2009). ASTM C1585-13 (2013) was followed to measure the sorptivity of concrete core samples (100 x 50 mm). The samples were placed in an environmental chamber with 50°C and RH of 80% for 3 days, and then kept in a laboratory environment for 15 days before being used for sorptivity tests. The samples were immersed into distilled water and the change in weight was measured at time intervals mentioned in (ASTM C1585-13, 2013).

2.1.4 Porosity

The porosity of NSC, HPC, and UHPC was measured according to ASTM C1754/ C1754M-12. Cylindrical concrete samples of 100 mm x 200 mm were cut to a height of 50 mm size. Samples were dried at 38°C and weight was measured after 24 hours. The samples were kept in the oven until the weight became constant or change is about 0.5%. Then samples were completely submerged into the water for 30 minutes and submerged weight was recorded. Total void contents were calculated by the formulas provided by ASTM C1754/C1754M-12.

3 RESULTS AND DISCUSSION

3.1 Resistivity

Average concrete resistivity values from three old RC structures and of newly fabricated NSC, HPC and UHPC are shown in Figure 1. The RC structures had resistivity less than 10000 Ohm-cm, a higher risk of steel corrosion is associated with such lower resistivity values. The NSC, HPC, and UHPC after 28 days of curing had a resistivity of 25041, 336006, and 457483 Ohm-cm respectively. These are considered very high resistivities and indicate no-corrosion risk present in RC. The HPC and UHPC have 6 to 10 time's higher resistance to electric current than conventional concretes. In addition, about 45 times higher resistivity than the practiced concrete until 1990s in the Middle Eastern region. With such high resistance, the ingress of chlorides and carbon dioxide will be minimized and the corrosion process will be hindered.

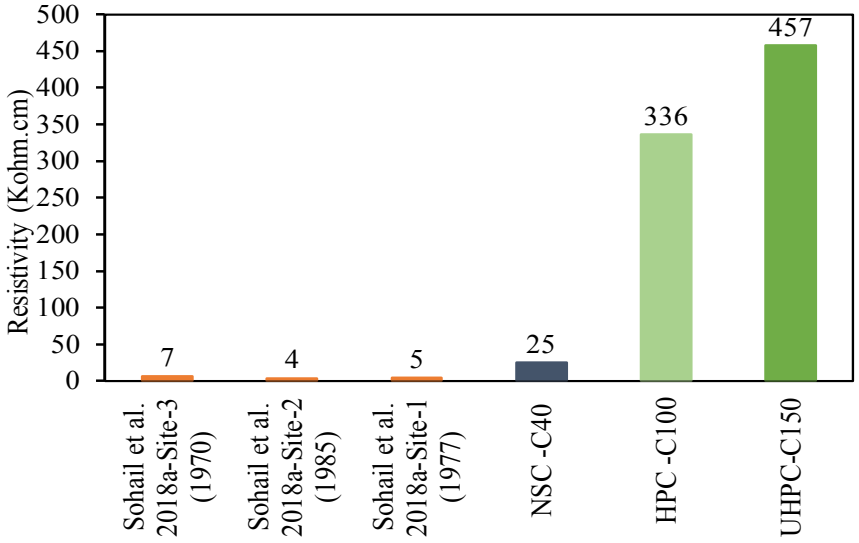

Figure 1: Concrete resistivity from columns of old reinforced concrete structures against the resistivity from cylinders of NSC at 90 days, HPC at 90 days and UHPC at 60 days

3.2 Sorptivity

A comparison between initial sorptivity of old concretes (the values of which are presented by (Sohail et al., 2018a) and newly fabricated NSC, HPC, and UHPC are shown in Figure 2a. The average initial sorptivity values for columns of three studied structures were up to 680×10^{-4} mm/s$^{1/2}$. While for NSC it was 43×10^{-4} mm/s$^{1/2}$, for HPC and UHPC it was found to be 25×10^{-4} mm/s$^{1/2}$ and 11×10^{-4} mm/s$^{1/2}$, respectively. The sorptivity for HPC and UHPC is significantly lower. Such lower sorptivity will considerably reduce the ingress of deleterious materials like Cl^- or carbonation in concrete and hence will improve the durability for longer periods. Lower initial sorptivity indicates the dense microstructure and disconnected capillary pores in case of HPC and UHPC.

3.3 RCPT values

The average RCPT values were observed to be 5148, 120 and 45 Coulombs for NSC, HPC, and UHPC, respectively (Figure 2b), while these values were up to 1000 Coulombs in concrete from RC structures built from the 1970s,1980s, and 1990s. The sorptivity and RCPT for NSC are relatively higher, this could be due to no vibration applied and might have interconnected pores. The HPC and UHPC are expected to increase the durability of RC structures with such lower RCPT values.

3.4 Porosity

The porosity of NSC, HPC and UHPC were respectively 5.5, 2.4 and 1.43%. Such lower porosity will restrict the amount of water to be absorbed into the concrete volume.

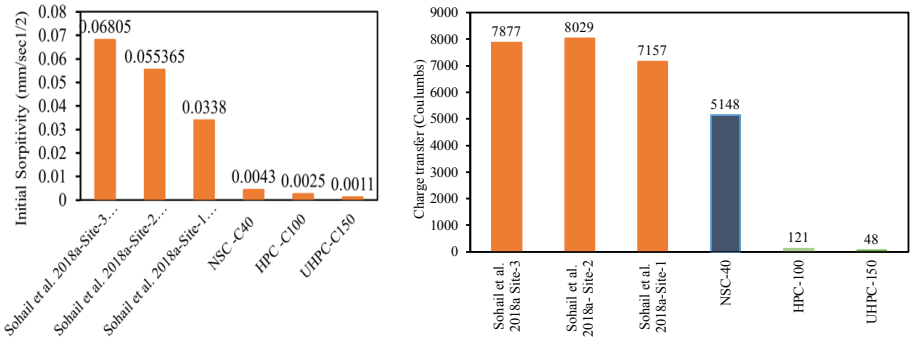

a) b)

Figure 2: a) Sorptivity values, b) RCPT values of NSC, HPC and UHPC in comparison to values from old concrete

4 CONCLUSION

High and ultra-high performance concretes were cast using locally available materials in the Qatari construction market. These concretes are expected to arrest the deterioration of reinforced concrete (RC) infrastructure under the action of severe environmental conditions. The durability indicators are compared against normal strength concrete and to those concretes that were used to build RC structures in 1970, 1980, and 1990s. The following are some major conclusions:

- The concrete resistivity of HPC and UHPC was 11 and 20 times higher than normal strength concrete. This shows a dense microstructure of HPC and UHPC. Ingress of deleterious agents will take a longer time to reach the steel-concrete interface, hence delayed corrosion initiation. Also once the corrosion is initiated the movement of Fe2+ and OH- ions will be hindered and the corrosion process will be retarded.
- HPC and UHPC shoed negligible passage of charge transfer in RCPT, which indicated the less pore volume and their disconnectivity.
- HPC and UHPC showed a porosity of 2.4 and 1.43% respectively. With such lower porosity, the ability to absorb water is reduced. Hence no ingress of deleterious agents.
- The sorptivity of these newly developed concretes is also very low, in comparison to normal strength concrete, HPC and UHPC showed 2 and 3 times lower values, respectively. While compared to core samples from old RC structures, these values were up to 60 times lower.

With such attributions, the HPC and UHPC could a very useful tool to overcome the durability issues, especially in the region of the Arabian Gulf, where very harsh climatic conditions are encountered.

ACKNOWLEDGMENTS

The funding for this research was provided by the National Priorities Research Program of the Qatar National Research Fund (a member of the Qatar Foundation)

under the award no. NPRP 7-410-2-169. The statements made herein are solely the responsibility of the authors and do not necessarily reflect the opinions of the Sponsor.

REFERENCES

AASHTO TP 95 (2011). *Standard Method of Test for Surface Resistivity Indication of Concrete's Ability to Resist Chloride Ion Penetration*. American Association of State Highway and Transportation Officials, Washington, D.C.

Al-Samarai, M. (2015). Durability of Concrete in the Arabian Gulf. *Journal of Materials Science and Engineering A*, 5, 11-12.

ASTM C1202-12. (2012). *Standard Test Method for Electrical Indication of Concrete's Ability to Resist Chloride Ion Penetration*. ASTM International, West Conshohocken, PA, 2012.

ASTM C1585-13. (2013). *ASTM C1585-13 Standard Test Method for Measurement of Rate of Absorption of Water by Hydraulic-Cement Concretes*.

ASTM C1611/C1611M-14. (2014). *Standard Test Method for Slump Flow of Self-Consolidating Concrete*. West Conshohocken, PA.

ASTM C1754/C1754M-12. (2012). *Standard Test Method for Density and Void Content of Hardened Pervious Concrete*.

ASTM C230/C230M14. (2014). *Standard Specification for Flow Table for Use in Tests of Hydraulic Cement*. ASTM International, West Conshohocken, PA.

Bache, H. (1981). Densified cement/ ultra fine particle based materials. *The second International conference on superplasticizers in Concrete*, Ottawa, Ontario, Canada June 10-12, 1981.

Bazaraa, A. S. (1989). Estimates of potential evapotranspiration over The State of Qatar. *Qatar University*, 2.

Dias, W. P. S. (2013). Reduction of concrete sorptivity with age through carbonation.

Fehling, E., Michael, S., Joost, W. & et al. (2014). *Ultra-High Performance Concrete UHPC: Fundamentals, Design, Examples*.

Graybeal, B. A. & Russell, H. G. (2013). *Ultra-High Performance Concrete: A State-Of-The-Art Report for The Bridge Community* (FHWA-HRT-13-060).

<https://www.fhwa.dot.gov/publications/research/infrastructure/structures/hpc/13060/> (Nov. 9, 2015).

Graybeal, B. & Tanesi, J. (2007). Durability of an Ultrahigh-Performance Concrete. *Journal of Materials in Civil Engineering*, *19*(10), 848-854.

de Larrard, F. & Sedran, T. (1994). Optimization of ultra-high-performance concrete by the use of a packing model. *Cement and Concrete Research*, *24*(6), 997-1009.

Patel, V. N. (2009). *Sorptivity testing to assess durability of concrete against freeze-thaw cycling*. The Department of Civil Engineering and Applied Mechanics McGill University Montreal, Canada.

Qatalum. (2006). *Environmental Impact Assessment*. Doha.

Richard, P. & Cheyrezy, M. (1995). Composition of reactive powder concretes. *Cement and Concrete Research*, *25*(7), 1501-1511.

Sohail, M. G., Kahraman, R., Ozerkan, N. G., Alnuaimi, N. A., Gencturk, B., Dawood, M. &

Belarbi, A. (2018a). Reinforced Concrete Degradation in the Harsh Climates of the Arabian Gulf: Field Study on 30-to-50-Year-Old Structures. *Journal of Performance of Constructed Facilities*, *32*(5), 04018059 (1-12).

Sohail, M. G., Salih, M., Al Nuaimi, N. & Kahraman, R. (2019). Corrosion performance of mild steel and epoxy coated rebar in concrete under simulated harsh environment. *International Journal of Building Pathology and Adaptation*, Emerald Group Publishing Ltd., *37*(5), 657-678.

Sohail, M. G., Wang, B., Jain, A., Kahraman, R., Ozerkan, N. G., Gencturk, B., Dawood, M. & Belarbi, A. (2018b). Advancements in Concrete Mix Designs: High-Performance and Ultrahigh-Performance Concretes from 1970 to 2016. *Journal of Materials in Civil Engineering*, *30*(3), 04017310.

Wille, K., Naaman, A. E. & El-Tawil, S. (2011a). Optimizing Ultra-High Performance Fiber-Reinforced Concrete. *Concrete International*, *33*(9), 35-41.

Wille, K., Naaman, A. E., El-Tawil, S. & Parra-Montesinos, G. J. (2012). Ultra-high performance concrete and fiber reinforced concrete: achieving strength and ductility without heat curing. *Materials and Structures*, Springer Netherlands, *45*(3), 309-324.

Wille, K., Naaman, A. E. & Parra-Montesinos, G. J. (2011b). Ultra-High Performance Concrete with Compressive Strength Exceeding 150 MPa (22 ksi): A Simpler Way. *Materials Journal*, *108*(1), 46-54.

Wong, H. H. C. & Kwan, A. K. H. (2008). Packing density of cementitious materials: part 1—measurement using a wet packing method. *Materials and Structures*, Springer Netherlands, *41*(4), 689-701.

Yudenfreund, M., Skalny, J., Mikhail, R. S. & Brunauer, S. (1972). Hardened portland cement pastes of low porosity II. Exploratory studies. Dimensional changes. *Cement and Concrete Research*, *2*(3), 331-348.

Cite this article as: Sohail M. G., Kahraman R., Al Nuaimi N., Alnahhal W., Wasee M., "High and Ultra-high Performance Concretes: A Solution to Reinforced Concrete Durability under Harsh Climate of Arabian Gulf", *International Conference on Civil Infrastructure and Construction (CIC 2020)*, Doha, Qatar, 2-5 February 2020, DOI: https://doi.org/10.29117/cic.2020.0109

Accelerated Corrosion Tests on Lapped Spliced Joints in Concrete

Sara Eltayeb-Onsa
saronsa93@gmail.com
Civil Engineering Department, Faculty of Engineering, University of Khartoum, Khartoum, Sudan

Amged O. Abdelatif
Amged.Abdelatif@uofk.edu
Civil Engineering Department, Faculty of Engineering, University of Khartoum, Khartoum, Sudan

ABSTRACT

This paper presents a new test setup of experiments to investigate corrosion at lapped spliced joints using accelerated corrosion test. The experiments were carried out on two set of samples: cylinders and beam blocks. Corrosion current readings were recorded with time and samples monitored for cracking pattern during the test. The results show that the cracks appearance and severity depend mainly on the cover diameter ratio. Also, the paper shows how the corrosion cracks propagate at lapped splice joints in concrete. The comparison of the results with previous literature was satisfactory.

Keywords: Corrosion; Lapped spliced joints; Accelerated corrosion test; Cracks; Current time relationship

1 INTRODUCTION

1.1 General

Reinforced concrete structures in severe environments may experience an unacceptable loss in serviceability earlier than anticipated due to corrosion of their steel reinforcement. Corrosion leads to the deterioration of structures by causing a remarkable reduction at the cross sectional area of the reinforcing steel bars and by causing cracking and spalling of the concrete cover due to expansive forces from corrosion products, and hence leading to a loss of structural bond between the reinforcement and concrete (Shihata A, 2011). The main problem of deterioration of reinforced concrete due to corrosion is not the reduction of reinforcement strength, but rather that the corrosion products induce stresses within the concrete, and the concrete therefore cracks leading to weakening the bond and anchorage between concrete and reinforcement which directly impairs the durability and ultimate strength of concrete elements (Shihata A, 2011).

1.2 Effect of Corrosion on Bond between Reinforcing Steel and Concrete:

Corrosion can be considered as one of the main causes leading to the reduction of the bond and thus reduction of member strength. A number of researchers indicated that the loss of strength in a corroded reinforced concrete member can be due to three factors which are: 1) losses in the effective cross-sectional area of concrete member because of the cracks in the concrete cover developed due to corrosion; 2) losses in the mechanical performance of reinforcing steel bars due to the losses in their cross-sectional area; and 3) losses in the bond performance of concrete with reinforcements. “Studies made by Auyeeung confirmed that the loss of bond strength for unconfined reinforcement is much

more critical than cross-section loss; that is, a low percent diameter loss could lead to 80% bond reduction. Auyeeung's study also showed that confinement provides excellent means to counteract the bond loss (Fang C., Lundgren K., Chen L., & Zhu C, 2004).

1.3 Corrosion at lapped spliced joints

Limited studies similar on the corrosion of steel reinforcement at lapped spliced joints in concrete were found. Previous studies investigated the corrosion at lapped spliced joints either experimentally using the accelerated corrosion test, or by using a finite element (FE) modelling.

An experimental study conducted by (Shihata A. & Soudki K., 2011) examined the effect of confinement provided by CFRP on the bond strength of corroded tension lap splices in concrete beams under static loading. An accelerated corrosion test on 9 beams at different corrosion level and different cover diameter (c/d) ratios was conducted. The results showed that the highest bond strength reduction occurs at a cover diameter ratio of 1.5.

The finite element study by Abdelatif AO et al. presented a numerical study of the chloride induced corrosion process in lap splice joints in concrete (Abdelatif A. O., Ozbolt, J. & Gambarelli S, 2018). The study was conducted using 3D chemo-hygro-thermo-mechanical FE model developed to simulate the corrosion of lapped spliced joint. The results obtained from the model were compared with the results obtained from Shihata experiment (Shihata A. & Soudki K., 2011). The comparison showed that the model results indicate an acceptable similarity to the results obtained from the experimental tests. Figure 1 shows the cracks results obtained from the model in comparison with the actual cracks from the experiment.

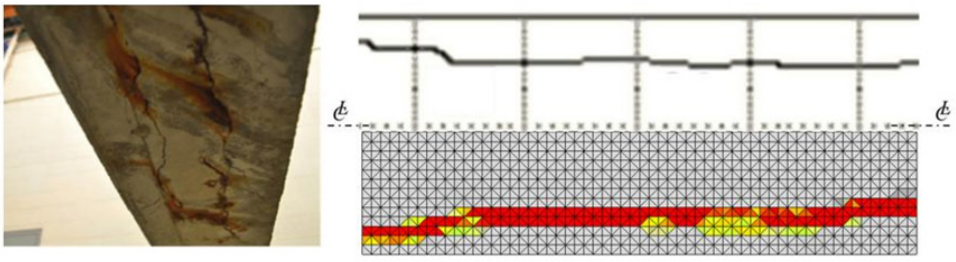

Figure 1: Cracks Pattern from the Model and from the Experiment (Abdelatif A. O., Ozbolt, J. & Gambarelli S, 2018)

2 EXPERIMENTAL PROCEDURE:

The aim of the experimental work in this study is to achieve better understanding of corrosion at lapped spliced joints and the processes related to it. In this study two set of groups were tested, the first group consists of 4 cylinders with 2 steel bars embedded at their center, the second group consists of 2 blocks with reinforcement representing the lapped spliced joint zone on each beam.

2.1 First group (Cylinders):

All samples of this group have an average 28 days compressive strength of 24 MPa.

A 10% NaCl of cement weight was added to the mix to help accelerate the corrosion process. Table 1 shows the dimensions of the cylinders.

Table 1: Cylinder samples dimensions

Sample ID	Diameter of rebar (mm)	Added length in the middle (mm)	Cover (mm)	Cover/Diameter Ratio (c/d)
C-16-42	16	16	42	2.6
C-25-37.5	25	25	37.5	1.5

2.1.1 Accelerated Corrosion Test:

In this study impressed voltage technique was used due to its simplicity to perform the test. The general layout of the test is shown in Figure 2. The first step of the sample preparation was wrapping the samples with stainless steel mesh to assure equal distribution of current around the cylinders. The test was started by applying a constant voltage of 12 volts to the system, after the test started current reading was taken twice a day using a digital multi-meter. Also the samples were checked about thrice a day to monitor the crack appearance and progression.

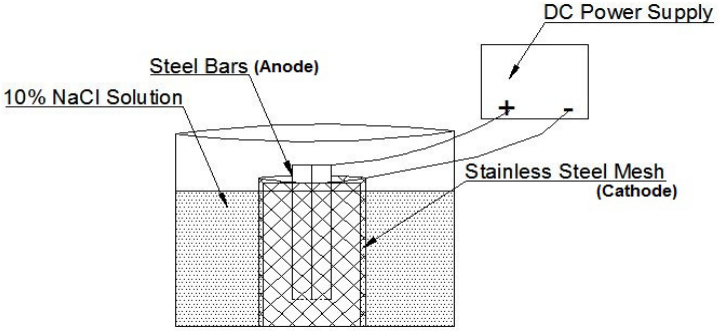

Figure 2: General Layout of the Test

2.1.2 Test results of corrosion of lapped spliced joints in cylinder specimens:

The results of the test show that all samples started to show cracks after short period of time but the development of crack was different for each sample according to its c/d ratio. The test was continued until the crack became very sever. For each cylinder sample, both crack patterns (Figure 3) and time-current relationship (Figure 4) was presented.

(a) Cylinder C 16-42, c/d = 2.6 (b) Cylinder C 25-37.5, c/d = 1.5

Figure 3: Crack pattern at lapped spliced joint in cylinder samples in: a) c/d = 2.6; b) c/d = 1.5.

The results show that the cracks were more developed in the cylinder C 25-37.5, c/d 1.5 compared to C 16-42, c/d 2.6. This could be due to the larger diameter and small cover. Also, it is noted that the first cylinder only shows longitudinal crack failure (Figure 4a) while in the second cylinder spalling of a concrete wedge is observed at the top (Figure 4b).

(a) (b)

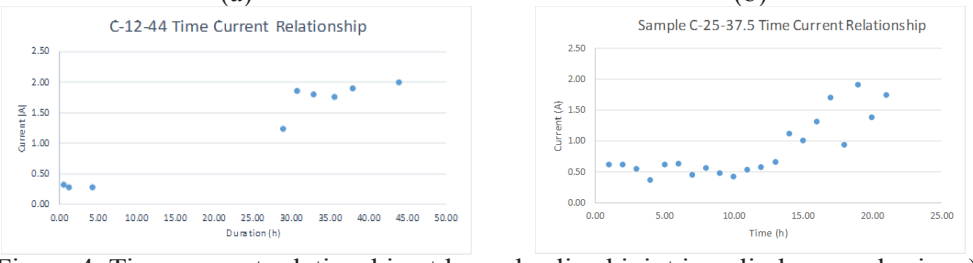

Figure 4: Time-current relationship at lapped spliced joint in cylinder samples in: a) c/d = 2.6; b) c/d = 1.5.

2.2 Second Group (Beams):

The average 28 days strength of the block samples was 20 MPa. In these samples, a stainless-steel tube with diameter 10 mm was embedded in concrete as cathode. Steel bars diameters of 16 mm and 20 mm were used. The group consisted of 2 beam samples with dimension (200×200×150) mm; each beam is reinforced with 4 steel bars at its bottom 2 at each end and equipped with a stainless steel tube with diameter 10 mm at the center as shown in Figure

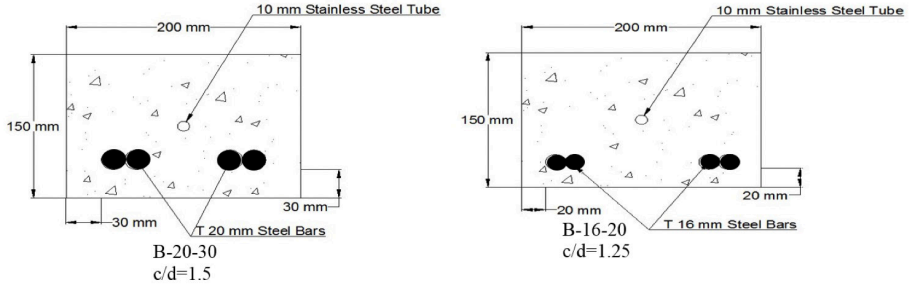

Figure 5: Beam specimens.

2.2.1 Test setup of lapped spliced joints in beam specimens

In this group, 10% NaCl solution was sprinkled at the samples using a water pump connected with a hose with 2 sprinklers installed above the beams. figure shows the test setup. The test was started by applying constant voltage of 12 volts, the current readings were taken once or twice a day and the time and duration of the reading were also recorded. Moreover, the samples were visually inspected to monitor the cracks development.

Figure 6: Test setup for beams group.

2.2.2 Test results of corrosion of lapped spliced joints in beam specimens

Both results of crack pattern and the relation of the corrosion current with time for these specimens were presented in Figure 7 and Figure 8. As an example, only the results for the beam block reinforced with 16 mm bars are presented.

Concrete cracks due to corrosion started to appear at different durations for each sample, the cracks were longitudinal and parallel to the steel bars. With time, the cracks became wider, and other cracks appeared between the bars and around the stainless-steel tube, Figure 7. These findings were also observed in the experiment conducted by Shihata (Shihata A. & Soudki K., 2011) as shown earlier in Figure 1 and similar to the finite element results by Abdelatif, AO et al. (Abdelatif A. O., Ozbolt, J. & Gambarelli S, 2018), The experiment was stopped after 544 hours of being subjected to the voltage.

Figure 7: Crack pattern in a block specimen compared to previous FE results.

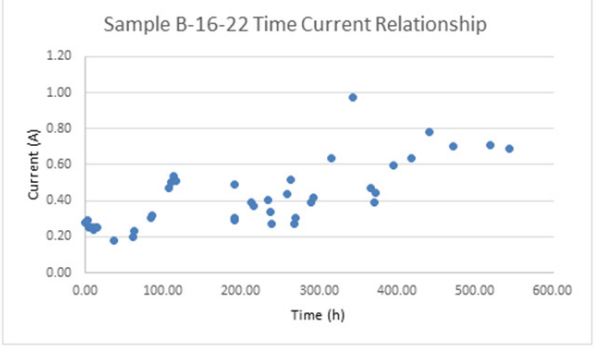

Figure 8: Time Current Relationship in a Block sample

Time current relationship was plotted for each beam as shown in Figure 8. It is noted from the Time Current Relationship that the current reading increases significantly after the cracks appear; this happens due to the diminution of the concrete resistance to the voltage causing more current in the electrical circuit leading eventually for more and wider cracks.

3 CONCLUSION

This study developed an accelerated corrosion test to investigate the corrosion at lapped spliced joints in concrete. Both experimental results are matched with previous findings in the literature. The developed test was found to be able to study the corrosion at lapped splice joints and could be used in the future to bring more light on this topic.

For future studies in this field it is recommended to study the effect of corrosion of lapped spliced joints on the bond between the steel bars and the bond between the steel reinforcement and concrete utilizing both pull out test and finite element modelling.

REFERENCES

Abdelatif A. O., Ozbolt, J. & Gambarelli S. (2018). 3D finite element modelling of corrosion of lap splice joints in concrete. *Construction and Building Materials*, *169*, pp. 124-131.

Fang C., Lundgren K., Chen L. & Zhu C. (2004). Corrosion influence on bond in reinforced concrete. *Cement and Concrete Research*, *34*, pp. 2159-2167.

Shihata A. (2011). *CFRP Strengthening of RC Beams with Corroded Lap Spliced Steel bars*, Univercity of Waterloo.

Shihata A. & Soudki K. (2011). *Corroded Tension Lap-Spliced RC Beams with FRB Wraps*, Waterloo, Canada.

Cite this article as: Eltayeb-Onsa S., Abdelatif A. O., "Accelerated Corrosion Tests on Lapped Spliced Joints in Concrete", *International Conference on Civil Infrastructure and Construction (CIC 2020)*, Doha, Qatar, 2-5 February 2020, DOI: https://doi.org/10.29117/cic.2020.0110

Technologies Serving Concrete for Economy, Durability and Sustainability

Yahia Alhassani
Yahia.alhassani@parsons.com
Parsons International LLD, Doha, Qatar

ABSTRACT

Concrete comes as the second most used material after water in the world, but it is the first used construction material especially in Middle East. World population is increasing while resources are decreasing. Therefore, construction industry needs to find a way to produce more by consuming less. Currently, concrete production results in significant carbon dioxide emissions creating an environmental hazard. On the other hand, usable sand for concrete in many countries is short in supply. Hence, science and technology need to be used at the earnest to prevent unrecoverable environmental damage associated with elevated costs. This paper describes a recently developed technology that converts desert sand into construction sand and aggregates when combined with another technology of dual mixing scheme capable of providing up to 40% of cement savings in concrete production; remarkable results are achieved. Those revolutionary, economical and environment friendly technologies are now available. We will introduce the outlines of the said technologies and then we shall present the possible applications of these technologies for efficient, sustainable and durable construction especially for the area.

1 INTRODUCTION

Concrete exhibits many advantages for the construction industry such as excellent resistance to water and fire, is generally a durable material, flexible for molding and shaping, usually made of local ingredients and relatively inexpensive. The idea of mixing water, binder and stones to formulate such plastic material with ability to be casted in predefined shape is very old and could go back to 20 centuries. Such composite called concrete was developed with time and according to needs along with the available technologies. Of course, the invention of Portland Cement and after that the admixtures are considered revolutionary in concrete industry. These developments enabled concrete to be a widely recognized and highly standardized construction building material, used several times more than steel or timber in many countries. Precast technologies helped much to have concrete products with higher quality and quick erection. Despite all these developments, one critical feature of concrete production remained unchanged over centuries; the mixing process. Mixing such composite of multi-scales (few micrometers to several millimeters) in conventional way presents a limitation to optimize concrete properties as still not complying to produce fully homogenous mixture. Dual Mixing is our first technology to speak about in this paper.

Other challenge or obstacle is to have enough resources for construction and concrete in order to have the required housing and infrastructure and follow the boom in such developments is finding enough suitable aggregates. This problem is faced in most of the countries that are laying in desert zones. The solution of importing the aggregates from other countries usually imposes additional challenges and issues with logistics, extra

cost, less control on sources and sometimes internal relationship restrictions in addition to environmental adversity (Dredging Activities if Applied).

As we know, the world's population is increasing, and most of that increase will be in our area (Asia, Middle East and Africa). So, we need to find a way to produce more in order to satisfy the needs and at the same time should be economical and environment friendly/sustainable. Since the desert sand is widely available, and we usually remove it from construction sites. New technology was developed to convert desert sand into aggregates in palletization process with the help of Dual Mixing technology as mentioned before. This technology will be presented in the second points in our paper.

2 MATERIALS AND METHODS

2.i Dual Mixing

The idea of Dual Mixing came over by questioning the way of conventional concrete mixing. By mixing water, cement and aggregates with a low speed mixer (tens rpm) for several minutes will not enable all cement particles to get in touch with needed water, hence, more water and cements are used to achieve the target slump and strength. It is well known that the water cement ratio needed for the hydration process is in the order of 0.15, whereas the rest of the water is needed for plastic consistency, i.e. slump for workability. In other words, to increase the probability of having cement particles meet with water, higher dosage of cement is usually used requiring higher water consumption. In order to devise an optimum concrete, the function of water is split into two by changing the mixing process to a dual mixing strategy patented by Multicon GmbH. The idea of Dual Mixing consists of mixing the slurry components (Water, binder and admixture) in very high-speed mixer ranging 1500 rpm) and added to the aggregates (coarse & fine). To show the difference between the two ways of producing concrete and achievements we will prepare a mix presenting each of them. The first mix is prepared with water, cement, cement replacing inert fines and admixtures by using an advanced high-speed mixer at 1500 rpm at about 20 seconds. The water binder ratio is kept at about 30% and cement replacing inert materials (for example limestone powder) with a maximum size of 100 micrometer is used to reduce cement consumption up to 40%. The use of high-speed mixing improves liquefaction of concrete, disperses the cement particles effectively, further breaks the particles by abrasion and allows obtaining a highly homogenized mix with an optimum w/c ratio. The second mix is conducted like the conventional concrete mixing with the slurry from the first mix, aggregates and additional water, if needed, for the target slump. The flowchart of the dual mixing process is summarized in Figure 1. a and 1.b. An example mix design and obtained savings are presented in Figure 1.c. It can be observed that the cement saving, and by consequence carbon dioxide emission reduction is (about 30%) with a cost saving of about 15%.

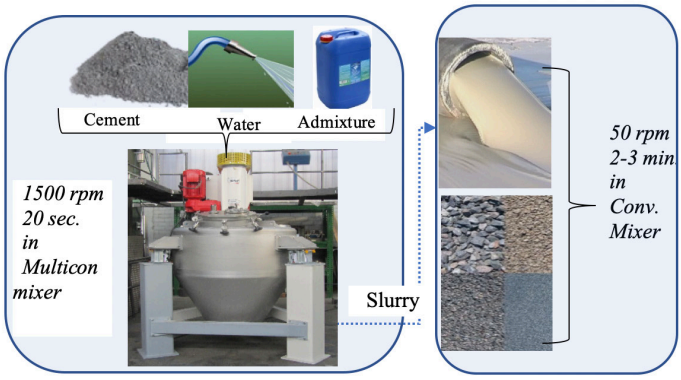

Ingredients/Perf.	Conv. Concrete	Optimized Concrete with Dua Mixing
Sand 0-4 mm	794 kg	794 kg
Agg. 4-8 mm	397 kg	397 kg
Agg 8-16 mm	793 kg	793 kg
Admixture	1.6 kg	1.6 kg
Water	167 kg	150 kg
Cement	320 kg	220 kg
Limestone Powder	-	100 kg
Spread	54 cm	57 cm
Comp Str (MPa)	27.6	30.2

a) Stage 1- High Speed Mixing. b) Stage 2- Conv. Mixing c) Mixes (typical improvement)

Figure 1: Dual Mixing Methodology and Benefits

The dual mixing technology does not only provide economical and sustainable concrete but also allows the realization of lightweight concrete in an efficient manner. The researchers of Multicon invented perlite lightweight concrete produced by using perlite, cement, water and admixtures mixed with the advanced high-speed mixing technology. The technology allows producing concrete with a specific weight of about 1500 kg/m^3 and a strength of 30 MPa (Figure 2.a). Such a concrete can reduce gravity and earthquake forces thereby providing economical and more efficient transportation of precast elements. In the case of using aluminum powder as the expansion agent, we may produce aerated concrete with a specific weight of 700 kg/m^3 and strength of about 6 MPa. In this way non-structural lightweight concrete block can be produced without needing any expensive autoclaving process (Figure 2.b).

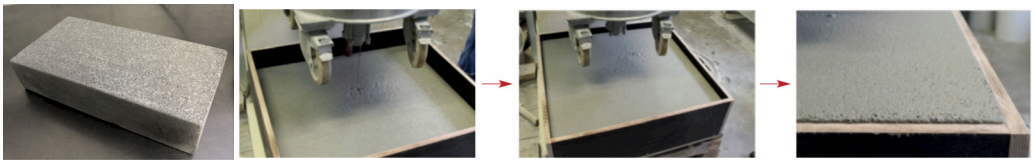

a) Lightweight concrete b) Lightweight aerated concrete

Figure 2: Lightweight concrete with high speed mixing

The other good advantage of Dual Mixing technology is helping to produce Self Compacting Concrete (SCC) easily and with less cost.

2.2 Sand Aggregates

Despite the wide availability of concrete ingredients, some countries, especially those having large deserts, lack quality aggregate necessary for concrete production. The transportation of aggregates is almost never a feasible option; hence sand is usually extracted from river or sea basins with consequential irreversible environmental damage. Multicon GmbH recently developed a procedure to address the needs of the society. With this patented technology, the abundant useless desert sands can be converted into usable construction sands or aggregates such as sand and gravel. With this technology,

the fine or desert sand is first pulverized with grinding mills into finer particles (Figure 3). This sand powder is then granulated on pelletizing plates with the addition of the slurry similarly obtained in the first stage of the Dual Mixing Technology. More than 90% of grains have a sphericity above 0.9 (GmbH 2018), and sizes vary between 0.1 to 16 mm with a compressive strength of 10 to 100 MPa made with a 5 to 15% cement consumption. In this way, man-made natural aggregates are prepared from dessert sand and slurry from the high-speed mixing process. Properties of pellets concrete were investigated by an accredited institution (IAB, 2019).

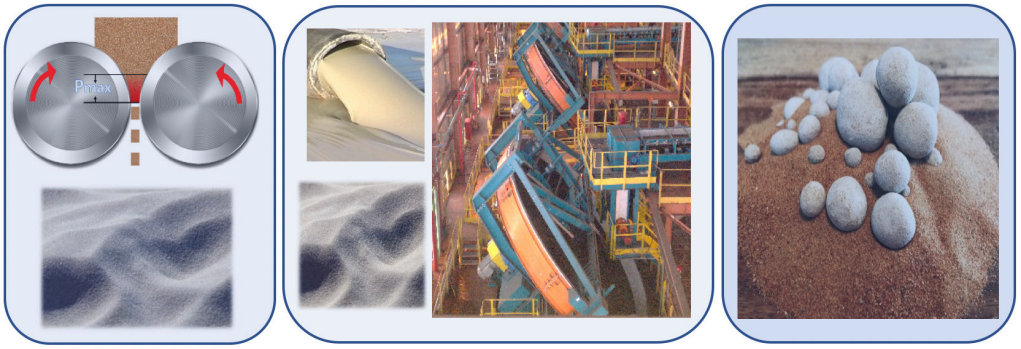

a) Pulverization b) Pelletization c) Sand-aggregates

Figure 3: Production of Sand Aggregates

Figure 4 shows the Sand aggregates (pellets), and cross section of concert made of. The spherical shape is very helpful for flowability and pumpability of concrete.

a) Pellets b) Concrete Cross section

Figure 4: Sand aggregates and Concrete.

3 CONCLUSION

The conventional way of mixing concrete is a serious barrier in improving the properties of concrete, providing economy and increasing sustainability. Thanks to the

invention of the dual mixing strategy with the advanced high-speed mixer of Multicon GmbH, new frontiers are now wide open for better concrete. The future vision of the technology places the high-speed mixer at the heart of concrete production. The slurry produced from the high-speed mixer provides the binder to produce pelletized aggregates utilizing abundant desert sand while preserving river basins and environmental damage. Afterwards, pelletized aggregates and slurry from the first stage high speed mixing are conventionally mixed to produce cement optimized environment friendly, sustainable concrete. The reinvention presented herein not only reduces cement consumption in concrete production, reduces emissions and protects the environment with the utilization of desert sand but also increases sustainability and brings a new vision for the future of concrete.

REFERENCES

DIN EN 12620 (Feb. 2019). IAB – Institut für Angewandte Bauforschung Weimar gemeinnützige GmbH.

Pelletizing of desert sand (October 2018). *Technical Report*, HAVER ENGINEERING GmbH.

Prüfbericht PB 1916, Untersuchung von Sand-Zement-Agglomeraten auf Eignung als Gesteinskörnung für Beton nach.

Cite this article as: Alhassani Y., "Technologies Serving Concrete for Economy, Durability and Sustainability", *International Conference on Civil Infrastructure and Construction (CIC 2020)*, Doha, Qatar, 2-5 February 2020, DOI: https://doi.org/10.29117/cic.2020.0111

Cantilever Beam Metastructure for Passive Broadband Vibration Suppression

Ratiba Fatma Ghachi
rg1408372@qu.edu.qa
Department of Civil and Architectural Engineering, Qatar University, Doha, Qatar

Wael Alnahhal
wael.alnahhal@qu.edu.qa
Department of Civil and Architectural Engineering, Qatar University, Doha, Qatar

Osama Abdeljaber
osama.abdeljaber@lnu.se
Department of Building Technology, Faculty of Technology, Linnaeus University, Vaxjo, Sweden

ABSTRACT

This paper presents a beam structure of a new metamaterial-inspired dynamic vibration attenuation system. The proposed experimental research presents a designed cantilevered zigzag structure that can have natural frequency orders of magnitude lower than a simple cantilever of the same scale. The proposed vibration attenuation system relies on the masses placed on the zigzag structure thus changing the dynamic response of the system. The zigzag plates are integrated into the host structure namely a cantilever beam with openings, forming what is referred to here as a metastructure. Experimental frequency response function results are shown comparing the response of the structure to depending on the natural frequency of the zigzag structures. Results show that the distributed inserts in the system can split the peak response of the structure into two separate peaks rendering the peak frequency a low transmission frequency. These preliminary results provide a view of the potential of research work on active-controlled structures and nonlinear insert-structure interaction for vibration attenuation.

Keywords: Vibration attenuation; Metastructures; Cantilever beam; Frequency-response-function

1 INTRODUCTION

For decades a special interest has been given to vibration control (F. Casadei, Beck, Cunefare, & Ruzzene, 2012), noise reduction (Filippo Casadei, Dozio, Ruzzene, & Cunefare, 2010), and wave guiding (Vasseur et al., 2007). Passive vibration suppression is when a system is designed to operate independently from external force or controller. An example of a single DF vibration absorber is if the desired system is modeled as a single degree of freedom oscillator. With the estimation of the stiffness and mass matrix, a single DOF absorber is chosen with stiffness and mass matrix that allows the resonant frequency to be reduced or eliminated (Abdeljaber, Avci, Kiranyaz & Inman, 2017; "Engineering vibration," 1994). Later, researchers expanded the concept of the single absorber to a series of distributed absorbers distributed along with the structure. These structures are mentioned here as metastructures as their behavior is reminiscent of this of matematerials. The purpose of this research is to reduce the vibration in the structure while allowing it to perform to its original function.

Zhu et al. (2014) proposed a metastructure design using chiral oscillators (Zhu, Liu, Hu, Sun, & Huang, 2014). Sun et al. (2010) conducted a numerical and analytical study of beam metastuctures (Sun, Du, & Pai, 2010). In applied mechanics research, Chen et al. (2011) performed experiments on sandwiched beams damped with spring-mass resonators (Chen, Sharma & Sun, 2011).

In this paper, we will report experiments on a cantilever beam including zigzags and present the gain in vibration attenuation compared to a cantilever beam of the same scale. The masses placed at the end of the zigzag approach the zigzag's natural frequency to this of the beam, which will change the overall system response.

2 EXPERIMENTAL ANALYSIS

The zigzag plates are integrated into the host structure namely a cantilever beam with openings, forming what is referred to here as a metastructure. Experiments were performed on a cantilever beam with zigzags and beams with zigzags and end masses (Figure 1).

Table 1: Geometry and mechanical properties for the host structure

Material properties	Symbol	Value	Units
Young's Modulus	E	69	GPa
Shear modulus	G	26	GPa
Density	ρ	2.7	g/cm^3
Channel Dimensions			
Length	L	80	cm
Base Width	O_1	5	cm
Leg Length	O_3	2.6	cm
Thickness	O_4	3.75	mm
Cutout Dimensions			
Length	O_5	7.1	cm
Width	O_6	3.4	cm
Number of cut-outs	N_c	10	-

Table 2: Geometry for the zigzag inserts

Zigzag Parameters	Symbol	Value	Units
a-beam Length	a	5.21	mm
a-beam Width	ω_a	1.24	mm
b-beam Length	b	1.73	mm
b-beam Width	ω_b	0.89	mm
Thickness	h	1.9	mm
Number of a-beams	N_a	7	-

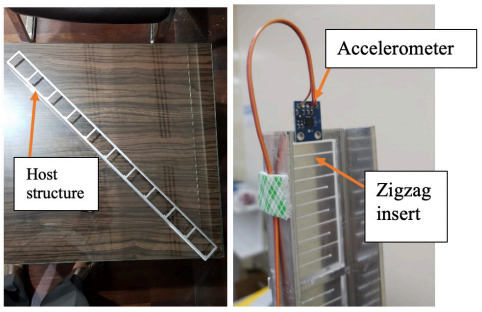

Figure 1: Experimental setup

All components of the cantilever beam were fabricated from 1100-H24 (ASTM, 2019). The host structure consists of a u-channel with openings cut with CNC high-pressure waterjet. The waterjet was also used to cut the zigzags out of a 1.9 mm plate. A Cyanoacrylate has been used to glue the inserts to the frame. Beam and insert geometry are specified in Tables 1 and 2.

3 RESULTS

The beam has been subjected to a sweep vibration at its base 1-50 Hz. The input and output signals have been measured using accelerometers. The shaker vibration is perpendicular to the zigzag surface. The shaker is controlled by an amplifier. Given the two signals, a frequency response has been computed and illustrated in Figure 2. The solid line represents the host structure with empty inserts. The dotted line represents the host structure with inserts with an end mass of eight grams. 23 15

$$FRF(\omega) = \frac{|A_{out}(\omega)|}{|F_{in}(\omega)|} \qquad (1)$$

In the no mass FRF there is one peak at 23Hz. Compared to a split in peaks in the with mass FRF we can clearly see two peaks one at 15Hz and another at 23 Hz.

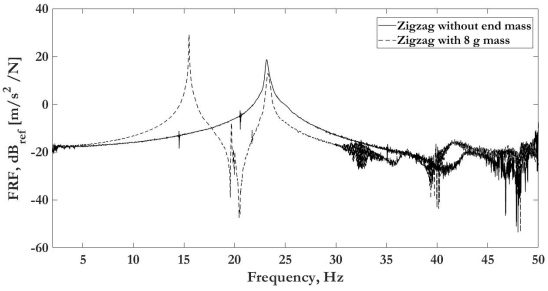

Figure 2: Comparative frequency response function

The phenomenon of the split of the frequency in the no mass FRF is that there is one peak at 23Hz. Compared to a split in peaks in the with mass FRF, we can clearly see two peaks one at 15Hz and another at 23 Hz. The phenomenon that occurs here is that the closer the mass and stiffness of the insert approach the structure own mass and stiffness, the more change we can see in the frequency response peak. This can be achieved by

controlling the end mass weight for instance. The potential of this observation is that the stiffness and mass of the insert can be optimized to produce a low-frequency zone on the exact frequency the beam normally resonates.

4 CONCLUSION

In this paper, we present an experimental investigation on the transmission behavior of a cantilever beam with inserts. Ten inserts have been placed on a 0.8 m beam with openings. Transmission behavior has been measured by accelerometers under the external force of a shaker vibrating in a sweep signal. Experimental frequency response function results are shown comparing the response of the beam to depending on the natural frequency of the zigzag structures. Results show that the host with inserts system can split the peak response of the structure into two separate peaks rendering the peak frequency a low transmission frequency. These results show the promising potential of research endeavors on active-controlled structures and nonlinear insert-structure interaction for vibration attenuation.

REFERENCES

Abdeljaber, O., Avci, O., Kiranyaz, S. & Inman, D. J. (2017). Optimization of linear zigzag insert metastructures for low-frequency vibration attenuation using genetic algorithms. *Mechanical Systems and Signal Processing*, 84, 625-641. https://doi.org/10.1016/j.ymssp.2016.07.011.

ASTM (2019). ASTM B209-14: Standard specification for aluminum and aluminum-alloy sheet and plate. *ASTM International*, *8*(2), 2019. https://doi.org/10.22201/fq.18708404e.2004.3.66178.

Casadei, F., Beck, B. S., Cunefare, K. a. & Ruzzene, M. (2012). Vibration control of plates through hybrid configurations of periodic piezoelectric shunts. *Journal of Intelligent Material Systems and Structures*, *23*(10), 1169-1177. https://doi.org/10.1177/1045389X12443014.

Casadei, F., Dozio, L., Ruzzene, M. & Cunefare, K. A. (2010). Periodic shunted arrays for the control of noise radiation in an enclosure. *Journal of Sound and Vibration*, *329*(18), 3632-3646. https://doi.org/10.1016/j.jsv.2010.04.003.

Chen, J. S., Sharma, B. & Sun, C. T. (2011). Dynamic behaviour of sandwich structure containing spring-mass resonators. *Composite Structures*, *93*(8), 2120-2125. https://doi.org/10.1016/j.compstruct.2011.02.007.

Engineering vibration (1994). *Choice Reviews Online*, *31*(08), 31-4381-31–4381. https://doi.org/10.5860/choice.31-4381.

Sun, H., Du, X. & Pai, P. F. (2010). Theory of metamaterial beams for broadband vibration absorption. *Journal of Intelligent Material Systems and Structures*, *21*(11), 1085-1101. https://doi.org/10.1177/1045389X10375637.

Vasseur, J. O., Hladky-Hennion, A. C., Djafari-Rouhani, B., Duval, F., Dubus, B., Pennec, Y. & Deymier, P. A. (2007). Waveguiding in two-dimensional piezoelectric phononic crystal plates. *Journal of Applied Physics*, *101*(11). https://doi.org/10.1063/1.2740352.

Zhu, R., Liu, X. N., Hu, G. K., Sun, C. T. & Huang, G. L. (2014). A chiral elastic metamaterial beam for broadband vibration suppression. *Journal of Sound and Vibration*, *333*(10), 2759-2773. https://doi.org/10.1016/j.jsv.2014.01.009.

Cite this article as: Ghachi R. F., Alnahhal W., Abdeljaber O., "Cantilever Beam Metastructure for Passive Broadband Vibration Suppression", *International Conference on Civil Infrastructure and Construction (CIC 2020)*, Doha, Qatar, 2-5 February 2020, DOI: https://doi.org/10.29117/cic.2020.0112

Sustainability in Construction: Reduce, Reuse and Recycle for a Greener Qatar

Mohamed Tolba
mtolba@ashghal.gov.qa
Public Works Authority (Ashghal), Doha, Qatar

Lavinia Melilla
Lavinia.melilla@arcadis.com
Arcadis, Doha, Qatar

Khaled Al Nassa
kalnaas@ccc.net
CCC, Doha, Qatar

ABSTRACT

In this paper, an innovative Engineering Sustainability Policy (ESP) and a new Sustainable Engineering Index (SEI) is proposed on the basis of testing results obtained within the context of the DN16 project in the State of Qatar, the largest project of the existing C2 Programme which represents the biggest sewage, drainage, and roads development programme worldwide. The ESP has been developed through a joint effort and active participation by the authors from Ashghal (PWA), the government entity, Arcadis, the consultant (acting from a design and site supervision perspective) and contractor (CCC). The policy refers to the general pillars for sustainable engineering defined by the Institution of Civil Engineers (ICE), which are environmental, financial, and social. Also, it fully aligns and complies with Ashghal and Qatar Vision 2030 regarding sustainability. The proposed policy takes into account a number of areas and aspects across all distinct phases of a project life-cycle, from master-planning to the design phase, from construction to handing over phases. During the testing phase for both the policy and index, the project's CAPEX and OPEX have been monitored throughout and, by adopting the new proposed approach, a decrement of the overall costs has been observed. The new proposed policy and index shall comply with international regulation over sustainable engineering, however they have been primarily designed to integrate existing Ashghal policies and procedures based over the on-going interaction process between major parties involved. Next step will be to define a refined calibration of the suggested SEI using data from a wider pool of projects from a holistic perspective, i.e. from concept to the handing over phase. The newly proposed SEI may be used as an initial effective tool to monitor the sustainability status of every project by means of qualitative interviews with key project people and managers.

Keywords: Sustainability; Sustainable engineer; Sustainability index; Environmental policies; Engineering sustainability policy

1 INTRODUCTION

Looking at most common and recently developed policies and procedures present in the literature in terms of sustainable engineering, the proposed Engineering Sustainability Policy (ESP) and Sustainable Engineering Index (SEI) aim at factoring in theoretical and practical solution elements for sustainable designing and construction used as part of the C2 Programme, in particular for the DN16 Project.

Extrapolating data and information for the DN16 project, the SEI intends to provide

a synthetic measure for the overall project sustainability, and it has been developed and calibrated based on interviews and a factor comparison with the teams from Ashghal (Ashghal, 2017), Arcadis and CCC on a joint effort and participation basis.

Given the substantial index independency from any country reference and project type and specifications it can be used globally as well. After a testing phase over the above mentioned C2 programme, a summary log for the key follow-up actions brought to define a new policy (the ESP) that aims at integrating Ashghal Corporate Environmental and Sustainability Policy (1).

Ashghal policy provides statements and guidelines to establish, deploy and maintain a robust and viable environment and sustainability management system across PWA that is compliant with local and international regulations. The purpose of existing Ashghal policy is in fact to provide clear directions to the senior management team and ensure that compliance with local and international standards is achieved and maintained.

The existing Ashghal policy must be followed by all Ashghal team and engaged parties, affairs, projects, PMC, GEC, contractors and subcontractors.

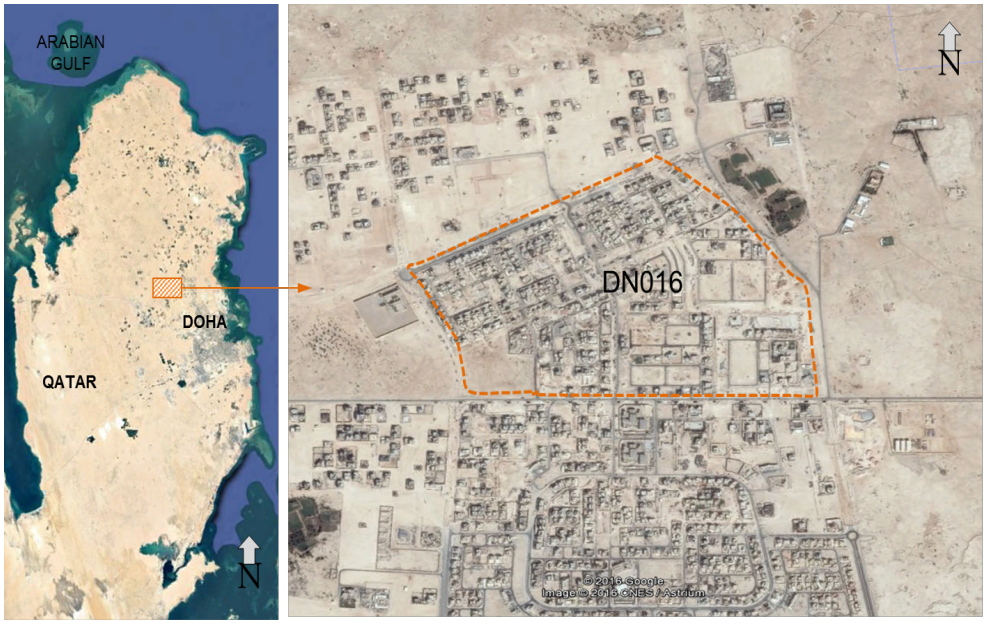

Figure 1: Qatar, Doha- Ashghal DN016 Project, located north east of Celebration Road

2 SUSTANABILE ENGINEERING IN DESIGN SOLUTIONS

Best practices framework and innovative design solutions have been implemented and adopted to maintain the main pillars of sustainable engineering looking at both environmental, economic and social issues (ICE, 2005). The framework provides options and specific action drivers for both installation and on-going maintenance across different areas.

Arcadis has developed the following design principles meant at supporting the highest level of sustainable engineering from a holistic perspective within the project design phase:

1. Sustainable and innovative design based on value engineering fundamentals, with no major design changes associated.
2. Since master-planning stage, minimized design changes over existing utilities and roads in order to minimize noise and disruption for the residents.
3. Reduced material quantities and preferential usage of locally produced or sourced materials in line with Qatar Sustainability Vision 2030 (Qatar Vision, 2008).
4. Optimized water usage across the overall system (focusing on drainage and sewage in particular) minimizing dredging and micro-tunneling structures, and adopting selected open cut solutions and shallower drainage system.
5. Use of gravity systems wherever possible, in order to reduce wide energy consumption.
6. Adopting cost efficiency and optimization tools for roads design and sewage drainage aiming at implementing green design elements whenever / wherever possible, subject to Ashghal design standards.
7. Use of recycled materials, again subject to Ashghal standards.

3 SUSTANABILE ENGINEERING IN CONSTRUCTION

CCC, the contractor, defined the following areas and action points to be referenced to increase sustainability across the project construction phases:

1. Energy efficiency and conservation.
2. Water, wastewater systems and re-use (site has a re-using structure for sewage grey water).
3. Green building (contractors are using sustainable materials on site where cost does not increase, as ecological concrete, low VOC paint, bamboo flooring).
4. Waste reduction and recycling (full paper / paper printing recycling policy on site).
5. Climate-friendly air circulation (air conditions on site are eco-friendly).
6. Renewable energy & low carbon fuels (using sustainable distances and recyclable material).
7. Efficient transportation.
8. Land use and community design (open spaces adopted) and carbon emissions/CO2 offsetting.
9. Common and individual behavior (sustainability and innovative design with value engineering exercises, subject to no major design changes).

In particular, in DN16 the following initiatives are being implemented aimed at maximizing development sustainability and overall programme efficiency during the various project phases, which also enable significant cost savings. Amongst them:

1. Energy savings (installation of solar flashing lights, traffic signs; units and offices being provided with high density insulation to save HVAC units; fully synchronized power houses for energy and power savings).
2. Water and wastewater systems (use of ground water for testing the water structures; use of gravity water supply by building water towers for office premises).
3. Use of air test instead of water test wherever possible.

4. Waste reduction and recycling.
5. No printing on Thursdays.
6. All internal correspondences via e-mailing.
7. Pool transportation.
8. Use of green pickups to reduce carbon emissions.
9. Smart planning for extended hour requirements.

From Table 1, an example of CO2 reduction, using recycled material, has been extrapolated. “Road – general filling to make up levels” has been evaluated. Two options were studied:

1. Using new material imported from Oman.
2. Crushing and recycling the excavated material directly from the same site DN16.

It is worth mentioning that 140,482 m3 of filling materials for the road levels corresponds to 224.771 tons (t). Using crushing and screening CO2 factor equal to 0.003, and considering 12km transportation between DN16 and the plant, emissions of CO2 was calculated as 998 t CO2.

Using completely new materials from Oman, the CO2 emission was much higher, as it was calculated at 2303 t CO2. This resulted in a 1367 T CO2 saving, or 60% of CO2 reduction. This example is used to promote the use of recycled material and/or locally produced abnd sourced materials.

4 THE SUSTAINABLE ENGINEERING INDEX (SEI) AS A KEY ENABLER

In agreement with all parties involved, a Sustainable Engineering Index (SEI) has been developed with matrices and weights for each area in scope (from design to construction) to standardize the quantification of the sustainability value of each project.

Data were calibrated by testing the index in several DN projects, aiming at ensuring robustness and effective validity for the tool, and the objectiveness and efficiency of the tool itself go along its interconnected lines with the Engineering Sustainability Policy (ESP).

A holistic strategy was adopted, new policy elements have been factored in and a scorecard like structure and design used as a starting point with maximum score to be assigned for full sustainable project standing at 100.

Table 1: Qatar, Doha- Ashghal DN016 Project: Minimization example of surplus material on site

Project	Excavated Materials			Fill Materials (IFC Drawings)		Remarks
	Suitable (IFC drawings)			Filling (m3)	Excess Material to be disposed (m3)	
	Disposed of Site (m3)	To be Disposed (m3)	Total (m3)			
DN016						
Roads		68,232	68,232			Road Works Quantities
Utilities for Trenches		198,077	198,077			SWD, FWD & TSE Quantities
Attenuation Tanks		44,194	44,194			Attenuation Tanks
Manholes		44,433	44,433			Manholes, Shafts & Chambers for SWD, FSD & TSE
Roads - General Filling to Make up levels				140,482		Road Works Quantities
Filling for Replacement of Subgrade Material				Included in General Filling above		
General Backfilling in trenches				31,362		Net volume of Filling for All Trench Works
General Backfilling around Manholes				13,384		Net volume of Filling for All Manhole Works
General Backfilling around Attenuation Tanks				8,035		Net volume of Filling for All Attenuation Tanks Works
Filling used for the specified bedding and Surrounds				99,849		
Filling used for the specified granular filling around Manholes				10,951		
Filling used for the specified granular filling around Attenuation Tanks				9,271		
			A	**B**		
			354,936	**313,334**		
				(A - B)	**41,602**	**Surplus Materials On-site**

Table 2: Sustainable Engineering Index (SEI): Structure and design

	AREA	Weight	PWA	Ar-cadis	CCC	Partial Score	Client	Con-sultant	Con-tractor	Partial Index Green
1	Design phase	8	7	7	6	53.33	10	10	10	80
2	Sustainable Design	10	8	9	6	76.67	10	10	10	100
3	Innovative Design	7	6	6	6	42	10	10	10	70
4	Value Engineering in design	9	7	7	6	60	10	10	10	90
5	Design of site office	6	6	6	6	36	10	10	10	60
6	Working remotely	6	6	6	6	36	10	10	10	60
7	Using local resources	10	10	7	6	76.67	10	10	10	100
8	Land use and Community design (Open spaces) Carbon Emissions	5	7	7	6	33.33	10	10	10	50
9	Dust suppression and irrigation water	6	7	7	10	48	10	10	10	60
10	Energy efficiency and Conserva-tion	6	6	6	8	40	10	10	10	60
11	Water and Waste water re-use	7	7	7	10	56.00	10	10	10	70
12	Green building Ecological con-crete, low VOC paint, bamboo floor)	7	7	9	9	58.33	10	10	10	70
13	Waste reduction and recycling (paper recycling policy on site)	9	7	7	7	63	10	10	10	90
14	Climate-friendly air circulation	5	7	6	6	31.67	10	10	10	50
15	Renewable energy & low carbon fuels (using sustainable distances and recyclable material)	7	7	6	8	49	10	10	10	70
16	Efficient transportation	5	7	6	8	35.00	10	10	10	50
17	Common and individual behavior	7	7	7	7	49	10	10	10	70
18	Energy Savings	7	9	9	9	63	10	10	10	70
19	Solar flashing lights and traffic signs	6	6	6	6	36	10	10	10	60
20	high density insulation	6	8	8	6	44.00	10	10	10	60
21	Fully synchronized power houses	6	6	6	6	36	10	10	10	60
22	Use of gravity water supply by building water towers for office	7	6	7	8	49	10	10	10	70
23	Use of air test instead of water test if possible	6	7	7	9	46	10	10	10	60
24	Waste Reduction and Recycling	9	9	9	9	81	10	10	10	90
25	No printing on Thursdays	6	6	8	6	40	10	10	10	60
26	Internal correspondence by email	5	7	6	6	31.67	10	10	10	50
27	Pool transport	5	6	9	6	35.00	10	10	10	50
28	Use of green pickups to reduce Carbon Emissions	6	7	9	9	50	10	10	10	60
29	Smart Planning for extended hour requirements	5	7	7	8	36.67	10	10	10	50
30	Value engineering in construction	8	9	9	9	72	10	10	10	80
		202				48.81				67.33
	Sustainability index =	**72.49**								
		0-39	40-69	70-100						

The SEI is based upon 30 factors that influence the most sustainability engineering objectives and drivers. This applies to the specific DN16 project but ultimately to all other projects in Qatar, and eventually worldwide, given the independence from country risk / country specifications.

The factors were selected and reviewed based on the best practice largely in use across the DN16 project. Each party (i.e. Ashghal, Arcadis, CCC) was interrogated first of all over the weight to assign to each factor and driver, and, in order to make the process as easy as possible, the correspondent scores were set within a 0 to 10 range, and calibrated on a subsequent stage to a "perfect" project where all scores were supposed to be 10.

In such a way, the weights of the factors were set, and they should remain fixed, subject to further enhancement for the scoring formula that can be achieved through recalibrating the tool with a larger data / projects set. After that, at the presence of the all three parties involved, it was assigned a score (that can be changed for each phase of the project, or if any major change will be happening) to Ashghal, Arcadis and CCC for each factors line.

Results ranging from 70 to 100 would assign a Green status / flag to the project as it was the case in this particular testing.

5 CONCLUSION

In summary, using data collected from the DN16 Project as a starting point and a scorecard like approach, a Sustainable Engineering Index (SEI) was developed, and a new Engineering Sustainability Policy (ESP) defined to integrated current guidance embedded in Ashghal policy and standards.

Input from many parties engaged in the project across its al life-cycle was factored in and current industry best practices and local and international regulations and standards, together with cost management aspects, adopted as a reference for both.

DN16 project had a resulting SEI score of 72.49 demonstrating that DN16 is in the range of Green projects, this mainly, thanks to the number of initiatives adopted during the design and construction project phases as to consolidate and sustain sustainable engineering throughout.

Future step would be testing the index on other C2 projects and double check if there is any need for extending or recalibrating the model in terms, for example, of factor weights and score aggregation criteria.

The SEI is meant to provide a high-level quanti-qualitative based measure to evaluate any civil project and mark main sustainability factors to be referenced through the project development and deployment phases.

Moreover, Ashghal is developing an advanced software to capture the reduction in CO2 emission per activity, tailor made for the Middle East, which could also be integrated as part of the proposed index.

REFERENCES

Ashghal QSD03 Corporate Environmental and Sustainability Policy (2017). PWA, Doha, Qatar.

ICE Sustainability Pillars (2005). ICE Institution Civil Engineers, London, the UK.

Qatar Vision 2030 (2008). Doha, Qatar.

Cite this article as: Tolba M., Melilla L., Al Nassa K., "Sustainability in Construction: Reduce, Reuse and Recycle for a Greener Qatar", *International Conference on Civil Infrastructure and Construction (CIC 2020)*, Doha, Qatar, 2-5 February 2020, DOI: https://doi.org/10.29117/cic.2020.0113

Concrete Hydration Model Characterization Using Evolutionary Optimization

Qianchen Sun
qs217@cam.ac.uk
Department of Engineering, University of Cambridge, Cambridge, UK

Mohammed Z.E.B. Elshafie
melshafie@qu.edu.qa
Department of Civil and Architectural Engineering, Qatar University, Doha, Qatar

Yi Rui
yr228@cam.ac.uk
Department of Engineering, University of Cambridge, Cambridge, UK

ABSTRACT

Pile thermal integrity assessment by means of temperature measurement has received increasing attention in recent years. The thermal integrity testing method measures temperature changes during the concrete curing process; using an appropriate concrete hydration model together with tracking temperature development during the curing process, defects within piles could be detected. However, the implementation of thermal integrity testing in practice faces, potentially, many uncertainties including undocumented concrete mixes, lack of knowledge of ground thermal properties, uncertain boundary conditions for pile, etc... These uncertainties increase the complexity of determining appropriate parameters for the hydration model, which directly affects the defect detection capacity of the method. This paper presents an inverse approach using differential evolution (DE) algorithms to determine the concrete hydration model. With this approach, the finite element (FE) analysis is integrated into the DE algorithm to generate approximate solutions that match a controlled dataset instead of approximating the concrete hydration parameters with limited prior knowledge as currently used in practice. Firstly, a field test temperature dataset with a well-defined boundary condition is selected. The temperature development corresponding to the selected dataset is then numerically simulated using an uncalibrated general hydration model. Finally, the hydration model parameters are determined using DE algorithms based on the measured and simulated temperature development as inputs. A field case study is presented in the end of this paper. The results indicate that the proposed inverse approach using DE algorithms can be used effectively in thermal integrity testing.

Keywords: Differential evolution; Thermal integrity test; Pile anomaly detection; Finite element modelling; Structural health monitoring

1 INTRODUCTION

Pile foundations provide support for structures by transferring the load into deeper layers of stiff soil or rock. Although pile foundations have been widely used in construction, there are still challenges about pile inspection and quality assurance. Due to practical construction issues and/or lack of knowledge of ground conditions, anomalies such as voids, soil inclusion, necking and poor concrete quality can exist inside pile

concrete body. These integrity problems could severely affect the load bearing capacity of concrete piles. Whereas, it is not possible to inspect the pile visually during or after installation. Therefore, pile quality control and quality assurance has been an important but challenging task.

A new thermal integrity testing method has been proposed recently for pile defect detection. The fundamental mechanism is that early age concrete release heat during the hydration process, temperature signatures within the concrete body will change if defects exist. Distributed temperature sensors are used for temperature measurement; the method then employs concrete hydration model and finite element analysis to predict temperature development, which is then compared with field test temperature data. The comparison between thermal integrity testing data and numerical data can provide further insights to identify the nature and geometry of anomalies. Details of this method can be found in Rui et al. (2017) and (Sun & Elshafie, 2019).

The capacity of the thermal integrity method to detect defect depends on the accuracy of the hydration model. The general practice is to use a general hydration heat generation graph based on limited knowledge of concrete mixes and ground conditions to predict the theoretical concrete temperature development. In this paper, an inverse approach is proposed which uses measured temperature data to analyze the actual hydration development. The finite element (FE) analysis is integrated into a differential evolution (DE) algorithm to generate approximate solutions that match a controlled dataset.

In this paper, the fundamental mechanism of concrete hydration will be presented first, followed by the proposed evolutionary optimization for the hydration model. Then a field case study will be presented to demonstrate the proposed method. Conclusions will be drawn at the end of the paper.

2 CONCRETE HYDRATION MODEL

The concrete hydration reaction is a thermally activated and exothermic process. The amount of heat, which is liberated within the first few days of concrete casting, plays a crucial role in temperature development of early age concrete. Temperature abnormities can be a good indication of concrete anomalies.

An early classic hydration model is developed by (De Schutter & Taerwe, 1995), based on a series of isothermal cement calorimetry tests and concrete adiabatic tests. In this model, the heat production rate $\dot{Q}$ is expressed as a function of temperature and degree of hydration:

$$\dot{Q}(t) = q_{max,20}.c.[\sin(\alpha_t \pi)]^a.e^{-b\alpha_t}.e^{-\left[\frac{E}{R}\left(\frac{1}{T_c}-\frac{1}{T_r}\right)\right]} \quad (1)$$

where a, b and c are the material constants controlling the distribution of hydration heat production; α_t is the degree of hydration, defined as the fraction of the heat of hydration that has been released ($Q_{released}/Q_{total}$); E is the apparent activation energy, R is the universal gas constant, $q_{max,20}$ is the is the maximum heat production rate at 20 °C, T_c is the temperature of concrete (K), and T_r is the is the reference temperature (293 K). This model has a simply mathematical expression and gives a relatively accurate

hydration heat prediction, but it has limitation for simulating Type Ⅲ cement. Another hydration model is shown below to tackle this issue.

Another hydration model is developed based on the equivalent age maturity theory and Arrhenius rate theory (Schindler, 2004; Schindler & Folliard, 2005; Riding et al., 2006). The main advantages of this model are suitability of various cement types and better representation of temperature effect by applying equivalent age (t_e) (Malhotra & Carino, 2003). The model is mathematically expressed as follows:

$$t_e = \sum_0^t exp\left(\frac{E}{R}\left(\frac{1}{273+T_r} - \frac{1}{273+T_c}\right)\right).\Delta t \tag{2}$$

$$\dot{Q}(t) = H_u.\left(\frac{\tau}{t_e}\right)^{\beta}.\frac{\beta}{t_e}.\alpha_u.exp\left(-\left[\frac{\tau}{t_e}\right]^{\beta}\right).exp\left(\frac{E}{R}\left(\frac{1}{273+T_r} - \frac{1}{273+T_c}\right)\right) \tag{3}$$

where τ = hydration time parameter, β = hydration shape parameter, and α_u = ultimate degree of hydration, H_u = total heat of hydration.

Using the hydration models above, the heat generation, transient heat flow and boundary conditions could be implemented using FE analysis through MATLAB. It would predict temperature profiles of early age concrete of different mixes and element geometries. However, the hydration model application in practice faces many uncertainties, including undocumented concrete mixes, lack of knowledge of ground thermal properties, uncertain boundary conditions for piles, etc... These uncertainties increase the complexity of determining appropriate hydration parameters, which directly affects the defect detection capacity of the method. The next section introduces an inverse approach using evolutionary algorithms to better estimate the concrete hydration model parameters.

3 DIFFERENTIAL EVOLUTION

An optimization algorithm known as differential evolution (DE) is adopted for this purpose. DE is an efficient optimization algorithm first introduced by (Storn & Price, 1997) for global optimization over continuous parameter spaces. It is conceptually similar to other evolutionary algorithms such as genetic algorithms and is not prone to converging at local maxima. The DE algorithm has been effectively used in many recent engineering applications, such as geotechnical modelling (Uchida et al., 2016), damage detection (Jena et al., 2013; Liu & Mao, 2016) and superstructure-foundation interaction (Leung et al., 2017).

3.1 Randomize Initial Population

In this process, NP initial random solutions (parameter sets) are first generated, where NP is the population size. The solutions are expressed in vectors form $\boldsymbol{\theta}_i$ as sown in Equation 4, known as target vector, which is evolved over G generations to reach an optimal solution. Each target vector component has D-dimension element, where D is

the number of variables which equals to six corresponding to hydration parameters in this study $(a, b, c, E, q_{max_{\infty}}, Q_{total})$. Storn and Price (1997) suggested that a reasonable population size NP should be between 5 to 10 times of the number of variables$D$.

$$\boldsymbol{\theta}_{i,G} = \{\theta^1_{i,G}, \theta^2_{i,G}, \ldots, \theta^D_{i,G}\},\ i = 1, 2, \ldots, NP \tag{4}$$

In the concrete hydration problem, the search space of each variable is bounded by cement and concrete mix properties. The upper and lower bounds of these variables are defined as $\boldsymbol{\theta}_{min} = \{\theta^1_{min}, \theta^2_{min}, \ldots, \theta^D_{min}\}$ and $\boldsymbol{\theta}_{max} = \{\theta^1_{max}, \theta^2_{max}, \ldots, \theta^D_{max}\}$ respectively. The maximum and minimum values can be found in (De Schutter & Taerwe, 1995, 1996). The initial value of jth variable for ith solution at generation zero ($G = 0$) can be expressed by the Equation 5, where $\mathbf{rand}$ stands for a uniformly distributed random number in the interval $(0,1)$:

$$\theta^j_{i,0} = \theta^j_{min} + \text{rand} \cdot (\theta^j_{max} - \theta^j_{min}) \tag{5}$$

3.2 Mutation

At each subsequent generation, mutant vectors $\boldsymbol{v}_i$ are formed by adding the amplified differential variation from two target vectors to a third one, expressed by the following equation:

$$\boldsymbol{v}_{i,G+1} = \boldsymbol{\theta}_{r1,G} + F \cdot (\boldsymbol{\theta}_{r2,G} - \boldsymbol{\theta}_{r3,G}) \tag{6}$$

where $r1, r2, r3$ are mutually different random indexes chosen from integer set $\{1,2,3, \ldots, NP\}$ and F is a factor with range $[0,2]$ controlling the amplification of the differential variation. A larger F enables the algorithm to search in a wider scope within the domain of each parameter, thus empowering it with a better exploration ability. In the optimization later stage, as the solutions converge, the population variation becomes smaller. Thus, a smaller F value empowers the algorithm with a better local exploration and amendatory ability. Figure 1 is a schematic representation of the mutation process for a simple two-dimensional objective function.

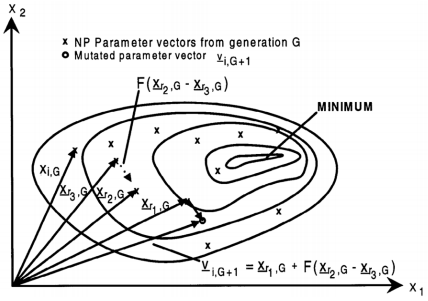

Figure 1: Illustration of operation process of mutation (Storn & Price, 1997)

3.3 Crossover

To increase the population diversity, "crossover" is introduced to determine the trial vectors $\boldsymbol{u}_i$ ($\mathrm{i} = 1, 2, \ldots, \mathrm{NP}$). The operation is carried out by randomly exchanging components of mutation vectors $\boldsymbol{v}_{i,G+1}$ and the target vectors in the preceding generation $\boldsymbol{\theta}_{i,G}$, which produces the trail vectors $\boldsymbol{u}_{i,G+1} = \{u^1_{i,G+1}, u^2_{i,G+1}, \ldots, u^D_{i,G+1}\}$. The chosen for each component of $\boldsymbol{u}_i$ is formulated as follows:

$$u^j_{i,G+1} = \begin{cases} v^j_{i,G+1} & \text{if } (\text{rand} \le \text{CR}) \text{ or } j = j_{\text{rand}} \\ \theta^j_{i,G} & \text{otherwise.} \end{cases} \tag{7}$$

where CR is the crossover constant within the range $[0, 1]$, and j_{rand} is a random integer from $[1, \mathrm{D}]$. Figure 2 illustrates an example crossover operation for 7-variable vectors.

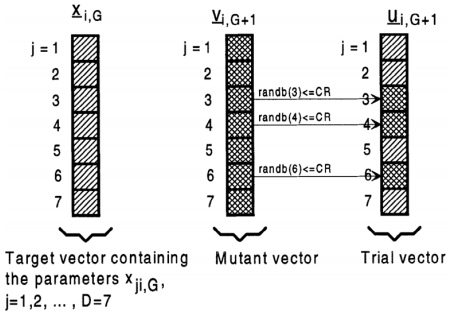

Figure 2: Illustration of operation process of crossover (Storn & Price, 1997)

3.4 Selection

The fitness of target vector $\boldsymbol{\theta}_{i,G}$ and trail vector $\boldsymbol{u}_{i,G+1}$ are compared and evaluated through an objective function $\boldsymbol{f}$. If $\boldsymbol{u}_{i,G+1}$ yields a smaller function value, then $\boldsymbol{\theta}_{i,G}$ $\boldsymbol{\theta}_{i,G}$ is replaced by $\boldsymbol{u}_{i,G+1}$; otherwise the original value $\boldsymbol{\theta}_{i,G}$ is retained in $(G+1)$ generation. The selection process is operated over the entire $\boldsymbol{NP}$ population.

3.5 Objective function

Heat generation of early age concrete is controlled by hydration model. Variations of hydration model parameters make changes in concrete temperature prediction. In this study, the field test temperature development is simulated with a finite element (FE) program, which employs De Schutter's hydration model for predicting concrete curing heat. The objective function $\boldsymbol{f}$ for determining a suitable hydration model is treated as an optimization problem. The optimal set of hydration parameters $\boldsymbol{\theta}^*$, as shown in Equation 8, is obtained by minimizing the total difference between the field test temperature data ($\boldsymbol{T_{test}}$) and the FE model simulated temperature ($\boldsymbol{T(\theta)}$).

$$\boldsymbol{\theta}^* = \arg\min_{\theta} f(\boldsymbol{\theta}) = \arg\min_{\theta} \textstyle\sum_t || T(\boldsymbol{\theta}) - T_{test} || \tag{8}$$

4 FIELD CASE STUDY

A field case study of thermal integrity testing has been conducted in London. This project involved the construction and monitoring of a test CFA pile. The test pile is used for validating the thermal integrity method and the proposed concrete hydration evolutionary optimization. The length of the pile was 20m with a nominal diameter of 900mm and a reinforcement cage diameter of 750mm. Three temperature cables were vertically attached to the reinforcement cage and measured the temperature at 15-minute intervals. Three one-meter long engineering inclusions were placed inside the reinforcement cage at depths of 3m, 6m and 9m. The inclusions were made of sandbags or containers with sand in order to simulate the defects such as loss of concrete cover and soil inclusions. More details on the test site and instrumentation used can be found in (Sun et al., 2019).

In this study, the measured temperature dataset between 14m and 18m depth was selected as the baseline temperature for calibrating the hydration model. No engineering defect was placed at this depth and the temperature profiles were consistently relatively stable. The average temperature data of three cables along 14m - 18m were selected as the baseline temperature ($\boldsymbol{T_{test}}$) for optimization.

For efficient optimization of the hydration parameters, DE algorithms were employed for characterizing the hydration model. The concrete hydration heat is defined by a total of six parameters, grouped as a vector $\boldsymbol{\theta} = \{a, b, c, E, q_{max_{28}}, Q_{total}\}$. Firstly, 30 candidate solutions, known as 'target vectors', were first generated randomly in the optimization process as the initial generation population $\boldsymbol{G_0}$. At each generation, 'mutant vectors' were formed by linear interpolation and multiplication of target vectors randomly selected from the population. A new set of 'trial vectors' was then generated by random mixture of the mutant vectors and the trial vectors in the previous generation.

Fitness of target vectors and trial vectors from the old and the new generations were compared through an objective function, which evaluates the discrepancies between FE model simulated temperature data and the temperature profiles obtained from field test results in 14-18m depth. This discrepancy was defined as an objective function $\boldsymbol{f(\theta)}$. The fitter solutions remain in the new population, while the weaker ones are discarded. The procedures above were continuously iterated until a global optimum solution was achieved.

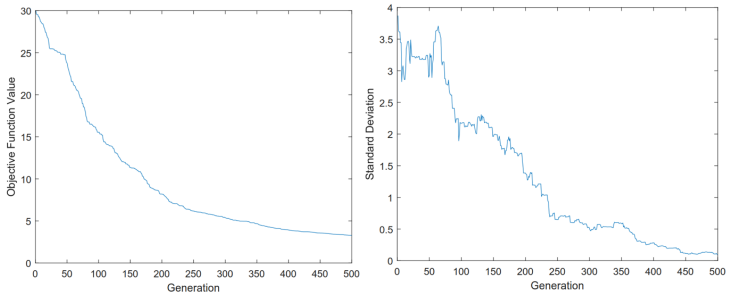

Figure 3: (a) Objective function value evolution (b) Standard deviation evolution

Figure 3 (a) and (b) show the changes of average objective function value $f(\theta)$ and changes of the standard deviation of objective function values of each iteration. The function value rapidly reduced in the first 350 generations, and then became steady at a function value of around 5. The standard deviation of candidate solutions in each generation also continuously decreased and then maintained around 0.1 after 400th generation. At 500th generation, the global optimum was achieved, and the optimized hydration model parameters were obtained as shown in Table 1. The temperature prediction from the calibrated hydration parameters and the baseline temperature can be found in Figure 4. The temperature in the figure represent the temperature change compared to the initial baseline temperature 23°C. It shows a good agreement with field test average temperature between 14-18m depth.

Table 1 Optimized hydration model parameters

Parameters	a	b	c	E kJ/mol	$q_{max\ 20}$ J/gh	Q_{total} J/gh
Cement	0.787	3.3	3.0	28.0	9.91	161

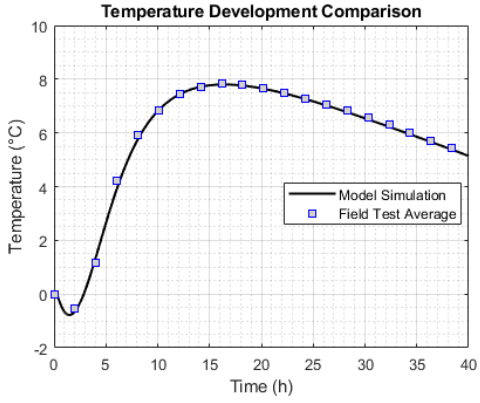

Figure 4: Temperature comparison between optimized model simulation and field test

5 CONCLUSION

The key element in thermal integrity testing is to determine an accurate concrete hydration model which controls temperature prediction and directly affects the capacity of defect detection of this method. In this paper, we proposed an inverse method to characterize concrete hydration model parameters using evolutionary optimization. With this approach, the finite element analysis is integrated into the differential evolution algorithm to generate approximate solutions that match a controlled dataset instead of approximating hydration parameters with limited prior knowledge as currently used in practice. The method overcomes the uncertainties of concrete mixes and material thermal properties. The field case study further verifies that the proposed inverse approach using DE algorithms can be used effectively in thermal integrity testing.

ACKNOWLEDGEMENT

This work was performed in the framework of ITN-FINESSE, funded by the European Union's Horizon 2020 research and innovation program under the Marie Skłodowska-Curie Action grant agreement n° 722509.

REFERENCES

De Schutter, G. & Taerwe, L. (1995). General hydration model for Portland cement and blast furnace slag cement. *Cement and Concrete Research*, *25*(3), 593-604.

De Schutter, G. & Taerwe, L. (1996). Degree of hydration-based description of mechanical properties of early age concrete. *Materials and structures*, *29*(6), 335.

Jena, P. K., Thatoi, D. N. & Parhi, D. R. (2013). Differential evolution: an inverse approach for crack detection. Advances in Acoustics and Vibration, 2013.

Leung, Y. F., Klar, A., Soga, K. & Hoult, N. A. (2017). Superstructure–foundation interaction in multi-objective pile group optimization considering settlement response. *Canadian Geotechnical Journal*, *54*(10), 1408-1420.

Liu, G. & Mao, Z. (2017). Structural damage diagnosis with uncertainties quantified using interval analysis. *Structural Control and Health Monitoring*, *24*(10), e1989.

Malhotra, V. M. & Carino, N. J. (2003). *Handbook on non-destructive testing of concrete*. CRC press.

Riding, K. A., Poole, J. L., Schindler, A. K., Juenger, M. C. & Folliard, K. J. (2006). Evaluation of temperature prediction methods for mass concrete members. *ACI Materials Journal*, *103*(5), 357-365.

Rui, Y., Kechavarzi, C., O'Leary, F., Barker, C., Nicholson, D. & Soga, K. (2017). Integrity testing of pile cover using distributed fibre optic sensing. *Sensors*, *17*(12), 2949.

Schindler, A. K. (2004). Effect of temperature on hydration of cementitious materials. *Materials Journal*, *101*(1), 72-81.

Schindler, A. K. & Folliard, K. J. (2005). Heat of hydration models for cementitious materials. *ACI Materials Journal*, *102*(1), 24.

Storn, R. & Price, K. (1997). Differential evolution–a simple and efficient heuristic for global optimization over continuous spaces. *Journal of global optimization*, *11*(4), 341-359.

Sun, Q. & Elshafie, M. Z. E. B. (2019). A new thermal integrity method for pile anomaly detection. *The 12th International Workshop on Structural Health Monitoring*. September 10-12, 2019, Stanford, California, the USA.

Sun, Q., Elshafie, M. Z. E. B., Backer, C., Fisher, A. & Rui, Y. (2020). Thermal integrity testing of cast in-situ piles using a new interpretation approach. *Structural health monitoring*, journal in progress.

Uchida, S., Xie, X. G. & Leung, Y. F. (2016). Role of critical state framework in understanding geomechanical behavior of methane hydrate-bearing sediments. *Journal of geophysical research: solid earth*, *121*(8), 5580-5595.

Cite this article as: Sun Q., Elshafie M. Z.E.B., Rui Y., "Concrete Hydration Model Characterization Using Evolutionary Optimization", *International Conference on Civil Infrastructure and Construction (CIC 2020)*, Doha, Qatar, 2-5 February 2020, DOI: https://doi.org/10.29117/cic.2020.0114

Experimental Study on the Performance of Circular Concrete Columns Reinforced with GFRP under Axial Load

Sherif El Gamal
sherif@squ.edu.om
College of Engineering, Sultan Qaboos University, Muscat, Oman

Othman Alshareedah
othman.alshareedah@wsu.edu
College of Engineering, Washington State University, USA

ABSTRACT

Corrosion of steel reinforcement in concrete structures subjected to severe environments is a big challenge and requires huge repair and maintenance costs. Glass fiber reinforced polymer (GFRP) reinforcement with its corrosion resistance and good mechanical properties is a promising solution to replace steel in such structures. This paper investigates the efficiency of using GFRP bars and spirals in concrete columns instead of conventional steel reinforcement. Five circular concrete columns of 230 mm diameter and 1500 mm height reinforced with different types and ratios of reinforcement were constructed and tested under concentric load. Test parameters included the type and ratio of the longitudinal reinforcement. The results showed that the columns reinforced with GFRP behaved in a similar way as the reference columns reinforced with steel, however, they showed slightly lower nominal capacity. It was also found that increasing the GFRP longitudinal reinforcement ratio enhanced the nominal capacity of the columns.

Keywords: GFRP reinforcement; Circular concrete column; Reinforcement ratio; Concentric load

1 INTRODUCTION

Corrosion of steel reinforcement is the main reason for concrete structures deterioration in harsh environments. In 1998, steel corrosion-related problems caused a direct cost of $276 billion in the United States (Koch et al., 2002). Fiber Reinforced Polymers (FRP) with their non-corrosive nature, high strength, and lightweight encouraged their use instead of steel reinforcement in concrete structures to avoid the steel corrosion problems (Al-Salloum et al., 2013; El-Gamal et al., 2016; El-Gamal et al., 2019). This includes several field applications such as bridge deck slabs, parking garages and concrete pavements (Benmokrane et al., 2007; El-Gamal et al., 2009; Thébeau et al., 2010; Bouguerra et al., 2011; Benmokrane et al., 2008). However, most of the FRP bars in these field applications were used in flexural members and there is a need to extend their use in compression members such as columns as well.

In recent years, researchers started to investigate the behavior of concrete columns reinforced with FRP (FRP-RC columns). Maranan et al. (2016) studied the behavior of Glass FRP (GFRP) RC columns under concentric load. Circular columns with 1000 mm height and 250 mm diameter were cast with 38 MPa geopolymer concrete and reinforced with longitudinal GFRP bars and stirrups. The test results showed that before the spalling

of concrete cover, the GFRP bars' contribution in the axial capacity varied from 6.6% to 10.5% for the columns with a 2.43% reinforcement ratio. Moreover, considering stirrups configuration, specimens with less spacing revealed more ductile failure mode and higher confinement efficiency compared with columns reinforced with higher stirrups spacing. Tobbi et al. (2014) explored the behavior of concrete columns reinforced with GFRP under concentrated axial load. Rectangular columns with 350 mm cross-section and 1400 mm height were constructed with 30 MPa grade concrete. The research parameters were longitudinal reinforcement ratio, transverse reinforcement spacing, reinforcement material, and diameter. It was observed that modes of failure depended on the lateral reinforcement configuration and spacing as well as the material of longitudinal bars. Columns reinforced with GFRP failed by bar crushing or buckling and stirrups rupture while steel-RC columns failed by excessive bar buckling. Furthermore, increasing the reinforcement ratio increased the peak load before the activation of confinement. The study stated that the steel-RC columns achieved higher peak loads compared to the GFRP-RC columns with the same reinforcement ratio. Also, the axial strain of the GFRP-RC columns was lower than the steel-RC columns by 30%. Similar conclusions were reported by Afifi et al. (2013) where they tested circular columns with 300 mm diameter and 1500 mm height and 42.9 MPa concrete compressive strength. The study revealed that GFRP-RC columns with low stirrups spacing failed by either concrete crushing or stirrups rupture. Besides, GFRP-RC columns reached an ultimate capacity lower than steel RC columns by about 7% on average. Higher ductility and lower post-peak strength decay were exhibited by GFRP-RC columns. The contribution of GFRP bars in the peak load was between 5 to 10% while the contribution of steel bars was 16% of the peak load. Tavassoli (2013) showed that GFRP-RC columns can accommodate more axial cyclic loading than the same columns reinforced with steel. This is due to the large buckling of steel reinforcement after the yield strain, unlike GFRP reinforcement where it can reach larger strain values before failure. Lotfy (2010) found that increasing the FRP longitudinal reinforcement ratio from 0.72% to 1.08% resulted in higher loading capacity with a magnitude larger than increasing the reinforcement ratio from 1.08% to 1.45%. Castro et al. (1995) found that the FRP contribution in the ultimate capacity of low-grade concrete columns subjected to buckling was more significant than high-grade concrete columns.

It can be noted that previous studies concentrated on investigating the behavior GFRP-RC columns with normal strength concrete and there is a lack of research studies that investigate the behavior of GFRP-RC columns with low strength concrete. This is covered in this research study where the behavior of low strength concrete GFRP-RC columns under concentric axial load is investigated. The study parameters include the type of reinforcement (Steel and GFRP) and the longitudinal reinforcement ratio.

2 EXPERIMENTAL WORK

2.1 Test Specimens

Five circular concrete columns of 230 mm diameter and 1500 mm height were constructed. The specimens were divided into two groups based on each study parameter as shown in Table 1. The first group was designed to study the effect of reinforcing material. The S1 column was reinforced with steel bars and spirals while S2 was reinforced with steel bars and GFRP spirals. G1 column was fully reinforced with GFRP

bars and spirals. Group 2 columns were designed to investigate the effect of the GFRP longitudinal reinforcement ratio. The reinforcement ratio was increased from 1.63% in G1 to 2.17% and 3.87% in G2 and G3, respectively. The spirals spacing was fixed to 75 mm in all columns. At the top and bottom 250 mm portion, the spacing of the spirals was reduced to 50 mm to provide more confinement at the ends and avoid premature failure.

2.2 Materials

Ready-mix concrete with an average compressive strength of 25.6 MPa and average tensile strength of 2.3 MPa was used. GFRP bars and spirals fabricated by a company in Dubai (Pultron Composites) were used in this study. Figure 1 shows photos of both the GFRP longitudinal bars and spirals. The longitudinal bars and the spirals were fabricated using two different techniques. The longitudinal bars and straight bars of the spirals were tested in tension to obtain their mechanical properties. The tensile tests were conducted according to ACI 440-3R guide (ACI 440, 2004) as illustrated in Figure 2. Table 2 shows the mechanical properties of GFRP bars and spirals.

Table 1: Details of Test Specimens

Group	Specimen	Longitudinal Reinforcement		Spirals
		Material	Size (Ratio %)	Material (size)
I	S1 (6S12-S75)	Steel	6 φ12 (1.63%)	Steel (φ10@75 mm)
	S2 (6S12-G75)	Steel	6 φ12 (1.63%)	GFRP (φ10@75 mm)
	G1 (6G12-G75)	GFRP	6 φ12 (1.63%)	GFRP (φ10@75 mm)
II	G1 (6G12-G75)	GFRP	6 φ12 (1.63%)	GFRP (φ10@75 mm)
	G2 (8G12-G75)	GFRP	8 φ12 (2.17%)	GFRP (φ10@75 mm)
	G3 (8G16-G75)	GFRP	8 φ16 (3.87%)	GFRP (φ10@75 mm)

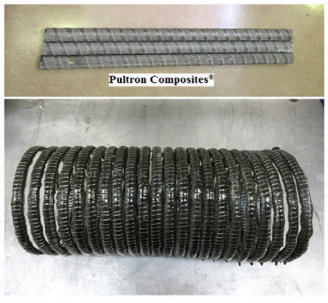

Figure 1: GFRP reinforcement used in this study

Figure 2: Tensile testing of GFRP bars

Table 2: Tensile test results for GFRP specimens

Type of GFRP	Nominal Diameter (mm)	Exterior Diameter (mm)	Cross-sectional area (mm^2)	Fracture Strain	Tensile Strength (MPa)	Elastic Modulus (GPa)
Longitudinal Bar	12	12.8	128.6	1.8%	1191	63.3
Longitudinal Bar	16	15.9	198.56	1.8%	1102	61.2
Spirals	12	12.8	128.6	2.2%	1345	60.9

Deformed steel bars and spirals were purchased from a local supplier in Oman. The longitudinal bar diameter was 12 mm while the spiral stirrups diameter was 10 mm. Tensile tests were performed on steel specimens of both diameters to obtain their yield strength and tensile modulus. The results of the test are illustrated in Table 3.

Table 3: Tensile test results for steel bars and stirrups

Type	Nominal Diameter (mm)	Cross-sectional area (mm^2)	Tensile Strength (MPa)	Elastic Modulus (GPA)
Longitudinal bars	12	113	451	209
Stirrups	10	78.5	446	210

2.3 Construction of Test Specimens

The reinforcement cages were prepared using two wooden holders to align the bars straight in their positions inside the spirals. The spirals were stretched to the desired spacing and then fixed with the longitudinal bars via steel binding wires. Plastic pipes with an internal diameter of 230 mm and 1500 mm height were used as formworks. The pipes were placed in a wooden structure designed to stabilize the columns during construction and concrete casting as shown in Figure 3. The reinforcement cages were placed inside the pipes and concrete cookies were used to maintain the concrete cover. After the concrete was cast and hardened, the pipes were cut using an electrical saw to remove them and take out the concrete columns to start the curing process for 28 days before testing.

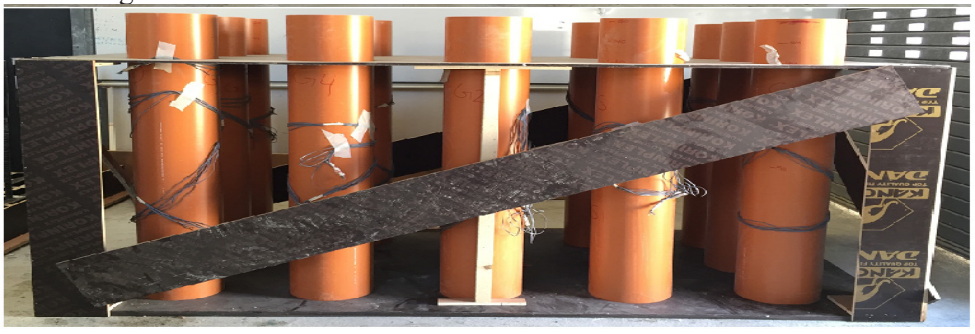

Figure 3: Formwork ready for concrete casting

2.4 Test Setup and Instrumentation

Several strain gauges were installed on the longitudinal and transverse reinforcement to measure the strains in the reinforcement during testing. In addition, six strain gauges were installed on the surface of the concrete at mid-height of the columns in the longitudinal and hoop direction to measure concrete strains. Furthermore, a Linear Variable Differential Transformer (LVDT) was used to measure the total axial deformations of the columns. Two steel caps were used to confine both ends of the columns to prevent premature failure at the ends due to high stresses. The axial loads were applied using a 4000 kN testing machine under a displacement control of 1 mm/min loading rate until failure. Figure 4 shows a schematic drawing of the locations of strain gauges and the testing set-up.

3 TEST RESULTS AND DISCUSSIONS

All tested columns experienced three different stages. The first stage starts with the initial loading until reaching the first peak load and hairline cracks appear on the surface of the concrete. The first peak load will be considered the nominal capacity (P_n) of the columns. The second stage starts after reaching the P_n until reaching the maximum load (P_{max}). The third stage starts after reaching the P_{max} until the total collapse of the columns. Figure 5 shows the three stages and Table 4 summarizes the test results of all tested columns.

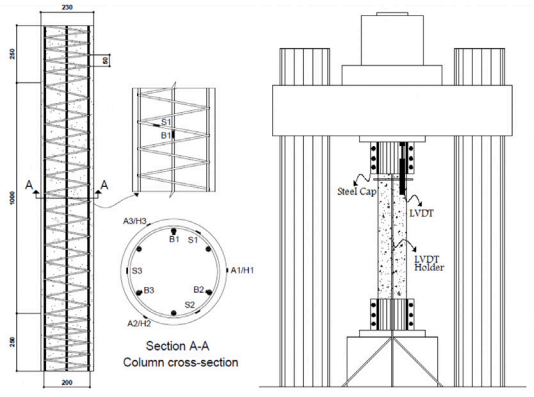

Figure 4: Instrumentation and testing set-up

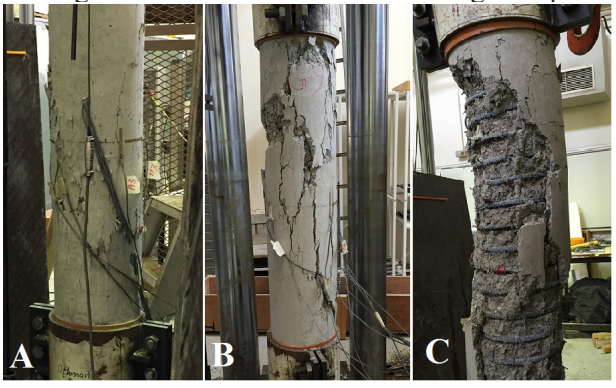

Figure 5: (a) First phase; (b) Second phase; (c) Third phase

3.1 Effect of Reinforcement Type

Test results of Group I specimens that have the same amount but different types of reinforcement show that columns S1 (totally reinforced with steel) and column S2 (reinforced with longitudinal steel bars and GFRP spirals) had the same nominal capacity. Columns G1 (totally reinforced with GFRP) showed about 6.7% lower nominal capacity compared to both S1 and S2. This lower capacity can be attributed to the lower elastic modulus of GFRP bars compared to steel bars, which results in less contribution of the GFRP longitudinal reinforcement to the capacity of the columns. The G1 column, however, showed almost similar maximum capacity as S1 and S2 columns. This can be attributed to the linear behavior of the GFRP reinforcement, which continues to support loads until reaching their ultimate strain.

Table 4: Test results of all specimens

Group	Spec-imen	P_n (kN)	P_{max} (kN)	Δ_{Pn} (mm)	Δ_{Pmax} (mm)	ε_t (μ)	Reinforcement Strains (at P_n)		Concrete strains	*Failure Mode*
							ε_{bar}* (μ)	$\varepsilon_{stirrups}$* (μ)	ε_c** (μ)	
I	S1	1139	1203	3.2	5.5	2133	2163	493	2465	Buckling of Bars → CC
	S2	1140	1183	4.0	10.8	2666	2041	521	2769	
	G1	1063	1197	4.6	7.1	3066	4985	3818	2127	Crushing of Long. Bars → CC
II	G1	1063	1197	4.5	7.1	3000	4985	3818	2127	
	G2	1190	1536	6.6	17.6	4400	3997	2001	2035	
	G3	1227	1457	5.5	10.7	3666	3670	2321	2149	CC

*Values were taken corresponding to P_n.
** The values of ε_c is taken at the load just before severe cracking and concrete spalling.
CC = concrete crushing

Figure 6(a) shows that column G1 exhibited lower initial axial stiffness compared to S1 and S2, which resulted in higher axial displacement at P_n. In addition, it is worth noting that the G1 column showed less ductile behavior compared to the steel-reinforced columns. Figure 6(b) shows that the strains in the longitudinal bars of S1 and S2 were similar up to steel yielding. The longitudinal steel bars in S1 and S2 columns yielded at load values very close to their P_n (about 1140 kN). The corresponding longitudinal strains in the bars were about 2163 and 2041 microstrain (Table 4), which are very close to the yield strain of the steel bars. After steel yielding, columns S1 shows a slight increase (5.6%) in the axial load while column S2 shows only a 3.7% increase in the P_{max} compared to its P_n. Figure 6(b) shows also that G1 exhibited higher axial compressive strains in the longitudinal bars compared to S1 and S2 columns. The maximum recorded bar compressive strains at failure were about 10000 micro-strain in G1, which were about 55% of the ultimate tensile strain of the GFRP bars.

Table 4 shows that columns S1 and S2 had almost similar strains in the spirals (493 and 521 micro-strain) at P_n. These strains were less than 25% of the yield strain of steel. They were also much lower than the spirals strains recorded in G1column (3818 micro-strain) which were only 18% of the ultimate tensile strain of the GFRP bars. This indicates that the stirrups were not actively utilized at this stage of loading. The spirals strains in the three columns increased significantly after exceeding the P_n where concrete cores expand and dilate thus applying more tensile stresses on the transverse reinforcement. At collapse, spirals strains of about 6500 to 6800 micro-strain were recorded in S2 and G1, respectively. These values were twice the strains recorded in the steel spirals in S1 and were about 30% of the ultimate strain of the GFRP reinforcement. The higher recorded strains in the GFRP spirals accompanied by the increase in the axial load mean that the spirals continued to confine the columns until failure.

3.2 Effect of Reinforcement Ratio

Table 4 shows that the nominal capacities of G1, G2, and G3 were 1063, 1190 and 1227 kN respectively. This indicates that increasing the longitudinal reinforcement ratio increased the P_n of the columns. However, this increase was not linear. Increasing the reinforcement ratio from 1.63% in G1 to 2.17% in G2 increased the P_n by 11.9% while

increasing the ratio to 3.87% in G3 increased the P_n by only 15.4% compared to G1 column and by only 3% compared to G2 column. The results of the P_n reveal that it is not efficient or economical to use very high GFRP reinforcement ratios in RC columns.

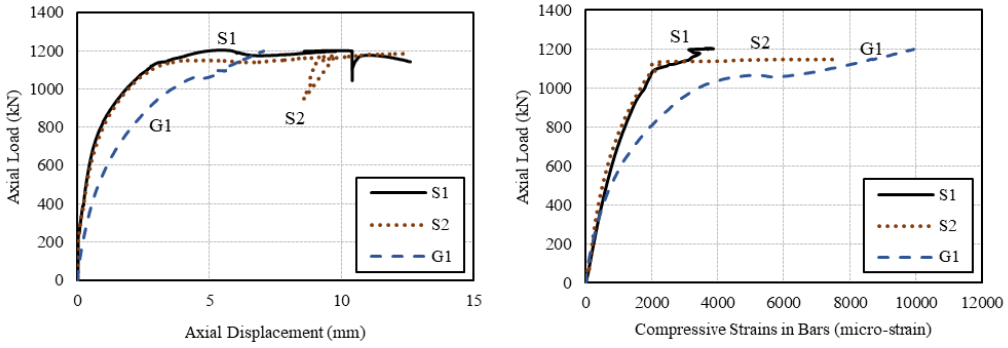

(a) (b)

Figure 6: Effect of reinforcement type; (a) load-vertical displacement; (b) load-compressive strains in longitudinal bars

Crushing of longitudinal bars was recorded in G1 and G2 columns while G3 failed by concrete core crushing. This could be attributed to the larger reinforcement ratio and the larger diameter of GFRP bars used in G3 (16 mm) compared to the 12 mm diameter bars used in G1 and G2. Figure 7(a) shows the load-vertical displacement curves of G1, G2, and G3. The three columns showed almost similar behavior until reaching the P_n of each column. Column G2 showed the highest P_{max} (1457 kN) among the three specimens while specimen G1 showed the lowest P_{max} (1197 kN).

Figure 7(b) and Table 4 shows that the strains corresponding to P_n of each column decreased as the reinforcement ratio increased. The strains in longitudinal bars increased rabidly after exceeding the P_n. At failure, the highest longitudinal bars strains in the three columns were recorded in the G2 column with more than 16200 micro-strain, which were about 90% of the ultimate tensile strain of the GFRP bars. It was observed that the G3 column showed the lowest longitudinal bars strain at P_n (3670 microstrain) among all GFRP-RC columns due to its higher reinforcement ratio compared to other columns.

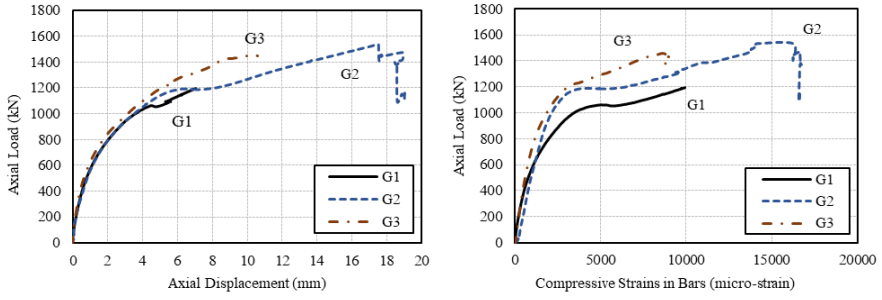

(a) (b)

Figure 7: Effect of reinforcement ratio; (a) load-vertical displacement; (b) load-compressive strains in longitudinal bars

4 CONCLUSION

Steel-RC columns failed by steel buckling followed by concrete crushing, while most of the GFRP-RC columns failed by crushing of GFRP bars accompanied with concrete crushing. The nominal capacity (P_n) of the GFRP-RC column was about 6.7% lower than the nominal capacities of the steel-RC columns whereas the maximum capacities (P_{max}) were almost similar. Increasing the longitudinal reinforcement ratio in the GFRP-RC columns resulted in higher P_n. The steel-RC columns sustained approximately constant load after the first peak while the axial deformations and strains increased gradually. On the contrary, GFRP-RC columns showed a continuous increase in the load after the first peak coupled with an increase in the axial deformations and strains until failure.

REFERENCES

Afifi, M. Z., Mohamed, H. M. & Benmokrane, B. (2013). Axial capacity of circular concrete columns reinforced with GFRP bars and spirals. *Journal of Composites for Construction*, *18*(1).

Al-Salloum, Y., El-Gamal, S., Almusallam, T., Alsayed, S., Aqel, M. (2013). Effect of Harsh Environmental Conditions on the Tensile Properties of GFRP Bars. *Composites: Part B*, *45*(1): 835–844.

American Concrete Institute Committee 440 (2004). *Guide Test Methods for Fiber-Reinforced Polymer (FRP) Composites for Reinforcing or Strengthening Concrete and Masonry Structures.* (ACI 440.3R-04). American Concrete Institute, Farmington Hills.

Benmokrane, B., El-Salakawy, E., El-Ragaby, A. & El-Gamal, S.E. (2007). Performance evaluation of innovative concrete bridge deck slabs reinforced with fiber-reinforced-polymer bars. *Canadian Journal of Civil Engineering*, *34*(3), 298-310.

Benmokrane. B., Eisa. M., El-Gamal, S. E., Denis Thébeau & El-Salakawy. E. (2008). Pavement System Suiting Local Conditions. *ACI Concrete International Magazine*, November, pp. 34-39.

Bouguerra, K., Ahmed E. A., El-Gamal, S. E. & Benmokrane, B. (2011). Testing of full-scale concrete bridge deck slabs reinforced with fiber reinforced polymer (FRP) bars. *Construction and Building Materials Journal*, Vol. 25, 3956-3965.

Castro, P. F., Howie, I. & Karbhari, V. (1995). Concrete columns reinforced with FRP rods. *International Journal of Materials and Product Technology*, *10*(3-6), 338-343.

El-Gamal S. E., Al-Nuaimi A. S., Al-Saidy A. H. & Al-Lawati A. (2016) Efficiency of Near Surface Mounted Technique Using Fiber Reinforced Polymers for the Flexural Strengthening of RC Beams. *Construction and Building Materials Journal*, Elsevier, Vol. 118: 52-62.

El-Gamal S. E., Al-Nuaimi A. S., Al-Saidy A. H. & Al-Shanfari K. (2019) Flexural behavior of RC beams strengthened with CFRP sheets using different strengthening techniques. *The Journal of Engineering Research*, Vol. 16 (1): 35-43.

El-Gamal, S. E., Benmokrane, B. & El-Salakawy, E. F. (2009). Cracking and deflection behavior of one-way parking garage slabs reinforced with CFRP bars. *ACI Special Publication*, SP-264-3, 33-52.

Koch, G. H., Brongers, M. P., Thompson, N. G., Virmani, Y. P. & Payer, J. H. (2002). Corrosion cost and preventive strategies in the United States. FHWA-RD-01-156.

Lotfy, E. M. (2010). Behavior of reinforced concrete short columns with Fiber Reinforced

polymers bars. *International Journal of Civil and Structural Engineering*, *1*(3), 545-557.

Maranan, G. B., Manalo, A. C., Benmokrane, B., Karunasena, W. & Mendis, P. (2016). Behavior of concentrically loaded geopolymer-concrete circular columns reinforced longitudinally and transversely with GFRP bars. *Engineering Structures*, 117:422-436.

Tavassoli, A. (2013). *Behavior of GFRP-reinforced concrete columns under combined axial load and flexure*. (M.Sc. degree dissertation, University of Toronto).

Thébeau, D., Benmokrane, B. & El-Gamal S. E. (2010). Three-year performance of continuously reinforced concrete pavement with GFRP bars. *11th International Symposium on Concrete Roads*, Seville, Spain, October 13-15, p. 11.

Tobbi, H., Farghaly, A. S. & Benmokrane, B. (2014). Behavior of concentrically loaded Fiber-Reinforced Polymer Reinforced Concrete Columns with varying reinforcement types and ratios. *ACI Structural Journal*, *111*(2).

Cite this article as: El Gamal S., Alshareedah O., "Experimental Study on the Performance of Circular Concrete Columns Reinforced with GFRP under Axial Load", International Conference on Civil Infrastructure and Construction (CIC 2020), Doha, Qatar, 2-5 February 2020, DOI: https://doi.org/10.29117/cic.2020.0115

An Innovative Structural Solution to Failed Stabilized Earth Embankment in Multilevel Interchange

Ali Kara
akara@ashghal.gov.qa
Highway Projects Department, Public Works Authority (Ashghal), Doha, Qatar

Tamer Tahoun
tamer.tahoun@parsons.com
Parsons International, Doha, Qatar

ABSTRACT

This paper summarizes a case study of a failure in a mechanically stabilized earth retaining wall ramp heading to a multilevel interchange. The failure was caused by a washout cavity resulting from a long-term leakage from unknown existing wet utilities adjacent to the mechanically stabilized earth retaining wall. The interchange is located within a very congested traffic area and has limited right of way and working space. The methodology of investigation, root cause of the failure, evaluation of the existing structure and innovative solution to the problem within fast-track design and construction are studied in this paper. Due to the necessity of maintaining the existing traffic movements at the interchange which is located at one of the most important expressway routes, timely rectification methodology was conceived, designed and implemented. This paper is prepared only to evaluate the technical innovative alternatives, solutions and fast-track construction without mentioning the interchange and project area.

Keywords: Embankment failure in MSE wall; Fast track rectification; Wet utility damages

1 INTRODUCTION

The major objective of this paper to outline the rectification method of the partial failure on the Mechanically Stabilized Earth Wall (MSE) Embankment ramp heading the bridge in addition to the evaluation of all bridge ramps, pavement, service roads considering a major constraint which is the time limitation to execute the work since the project under study is located in one of the critical traffic flows. The country and the region of the project area are not mentioned in this paper.

The multilevel interchange is located within a traffic congested area and having multi direction movements providing expressway functionality and local access. One of the MSE ramp heading bridge had pavement failure, which was observed by local commuters. The relevant traffic department stopped the traffic and detour the traffic movement to local roads. Relevant authority professional team visited the site and initiated a fast track investigation of the failure along with ultimate design and construction solution proposals.

The failure was in the pavement along a deep crack in the backfilling of the ramp embankment as shown in figure 1.

Figure 1: Partial Failure

The site investigation started with a field geophysical survey. However, due to the necessity of maintaining the existing traffic, the geotechnical and geophysical report was delivered progressively in parallel to the construction.

Following field investigations were carried out:

- Geotechnical and Geophysical survey using MASW covering all the embankments,
- Intrusive works at locations identified from the MASW investigation and complemented with a GPR survey,
- Pavement evaluation using destructive and non-destructive evaluation.

Destructive testing included pavement cores and trial to evaluate the material the layer thickness properties. The non-destructive testing using Falling Weight Deflectometer (FWD) was carried out on the bridge ramps and the service road. The purpose of FWD was to evaluate the existing structural capacity of the pavement.

2 PROJECT DESCRIPTION

The Project investigation area was limited within the interchange embankments approach ramps, Mechanically Stabilized Earth Walls (MSE), and service road at ground along MSE walls.

The MSE wall of embankment approach ramp was deflected by 50mm horizontally measured from top within 50m length. Deep cracks were observed in the asphalt and embankment fill. A vertical settlement of 30mm was observed at the MSE wall. The directly affected area within the ramp is an open crack of around 16m length and 2m

depth. This crack is suspected to extend around 14m. Geotechnical investigation and geophysical survey were undertaken to obtain detailed information about the surface and subsurface strata allowing the condition assessment of the MSE wall embankment.

3 GEOTECHNICAL INVESTIGATION AND DESIGN

3.1 Geotechnical Investigation and Geophysical Survey

The geotechnical investigation and geophysical survey undertaken to MSE wall embankment approach include:

- Walk-over survey and gathering of chronological data of the affected zone,
- Geophysical survey (MASW) to determine the weak areas and zones of risk within the MSE wall and adjacent road formation.
- Based on results of walk-over and geophysical survey, the below geotechnical investigation was undertaken:

i. Drilling of 4 diagraph boreholes down to 15m below ground level (BGL) in the close vicinity of MSE wall along services road.
ii. Drilling two geotechnical boreholes down to 15m BGL on the embankment in the close vicinity of MSE wall. Carrying out SPT tests in boreholes.
iii. 3 DCPT within crack area.

3.2 Findings from Geotechnical Investigation and Geophysical Survey

Based on the investigations carried out for the MSE wall of embankment, the following conclusions are drawn:

1. The identified velocities within the embankment backfill corresponds to generally medium dense to dense material with shear wave velocities between 180m/s and 360m/s (SPT results also show the similar conditions) while the rock is identified at around +7.0m to +8.0m where the shear wave velocities exceed 600m/s which is line with the conditions revealed from the geotechnical boreholes.
2. The rock contains some weak areas, which are attributed to existing utilities. The backfill exhibits some lower SPT values close to the service road elevation (within limited thickness of 0.5m).The service road top 1.5m to 2.0m near the MSE wall contains loose sandy material susceptible to wash out if in contact with moving water (rain or broken wet utilities). This effectively resulted in the partial failure of the MSE wall of the south-west embankment. The MSE wall is intact with no apparent face distortion or horizontal movement within the strips zone.
3. The repetitive migration of dune sand under the adjacent service road due to several leaks and movement of water, resulting in partial loosening of the foundation ground under the outer part of the MSE wall is the likely cause of bearing capacity failure of the MSE wall in addition to the washout cavities as shown in figure 2.

Figure 2: Washout Cavities

Accordingly, it was concluded that the partially failed section in the MSE wall at the side is typical to tilt/bearing capacity failure mode as described by (Bobet, 2002), see Figure 3

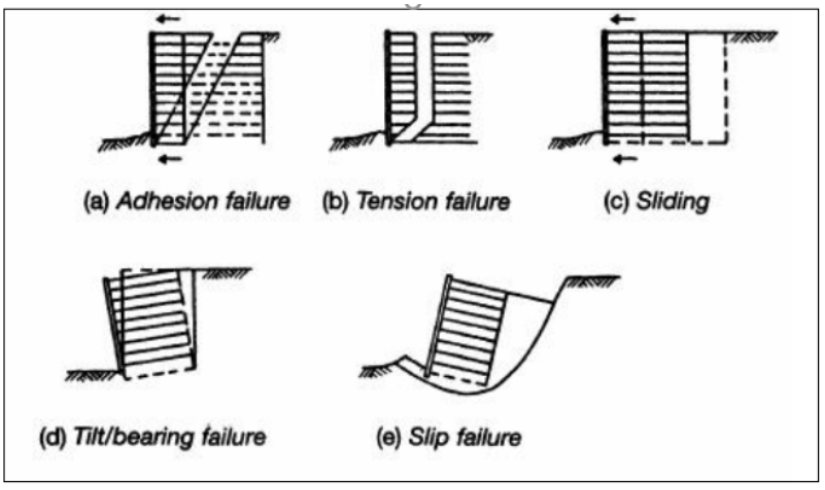

Figure 3: MSE Walls Typical Failure, adapted from (Bobet, 2002)

The likely cause of the bearing capacity failure is the repetitive migration of dune sand under the adjacent road due to several leaks and movement of water, resulting in partial loosening of the foundation ground under the outer part of the MSE wall. The movement took place at the current location since the foundation fill, because of loosening, could not carry anymore the load/height of the MSE wall. On the other hand, the sections towards the lower level of the embankment, which are mostly affected by the migration of the sand with several wash out cavities, did not fail due to their reduced height (less than 2m).

Although all the MSE walls (except the partially failed section) are in good condition, there was a risk of washout and material loosening along the service road adjacent to the MSE walls foundation, spotted from the various trial pits, boreholes, MASW survey and the GPR survey.

3.3 Geotechnical Design Parameters & Recommendations

Based on the above investigation, the recommendations for the subsurface properties and solutions are given below:

1. The rock-head below MSE wall is at level varying from +8.0m to +9.5m whereas it is around +7.75m below service road.

2. Table 1 depicts the design parameters as recommended in the geotechnical report:

Table 1: Design Parameters of Limestone Rock

RQD (%)	GSI	Density (kN/m3)	PLI (MPa)	UCS (MPa)*	E (MPa)
20	30	20.5	0.7	7.0	2000
*taking into account the point load index values with a ratio of 10 to the UCS					

3. The pile ultimate skin friction is recommended at 1000 kPa.
4. The piles should be tested in accordance international specifications.
5. The pile socket into bedrock should be verified on site through monitoring of the cutting and logging of boring speed.

3.4 Rectification Structural Design

The structural design was carried out using BS 5400 and BD 347/01. Multiple options were investigated to provide a rectification of the MSE walls partial failure. Further investigations of the design studies resulted in three viable options.

The first option was to provide grout injection at the MSE wall along with rebuilding the top two meters that experienced a deep pavement crack, please refer to Figure 4.

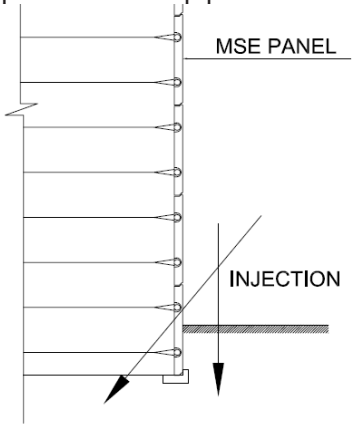

Figure 4: Proposed First Option

This option was not utilized due to the associated uncertainties of the size of the washout cavities that the geophysical surveys indicated. The second option was to rebuild an independent structure consisting of piles and pile cap that carries out the backfilling at the 90 meters length that experienced most of the cavities, Figure 5.

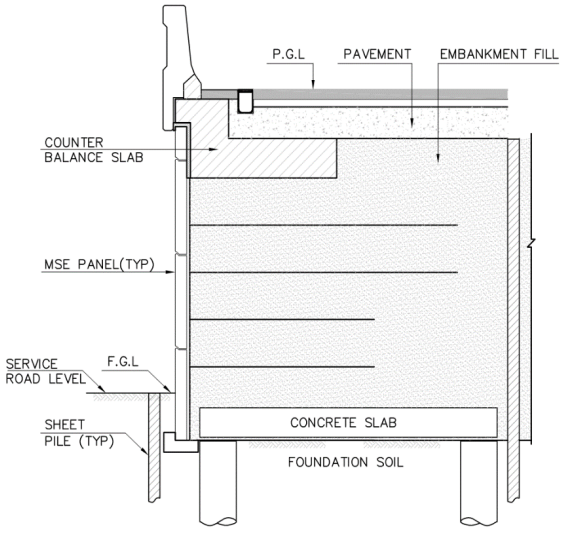

Figure 5: Proposed Second Option

This option was not utilized due to the time limitation which was set as one month for the design and construction. The time constraint for the rectification was the biggest constraint that did not allow to excavate significant depth, build piles and pile cap, then backfill the area under consideration.

Due to the observations of the large cavities at the MSE service road level right below the MSE walls and the partial loosening of the foundation ground under the outer part of the MSE wall, a complete independent structure at this area has been introduced as a third option. The structural system consists of slab supported on two rows of piles. These piles at the outer part have been casted contiguously from the external side to retain the MSE wall fill and relieve any earth pressure transfer to the MSE walls under study while the piles at the other side of MSE wall have been casted at 2.1 meters center to center. This work has been selected to be carried out for the affected area. The advantage of this option is the time saving of deep excavation along with high backfilling, Figure 6, 7, and 8.

The construction sequence has been selected and implemented at site considering the necessity of supporting the MSE wall panels during the piles casting due to the expected damage of MSE walls straps resulting from the piling work.

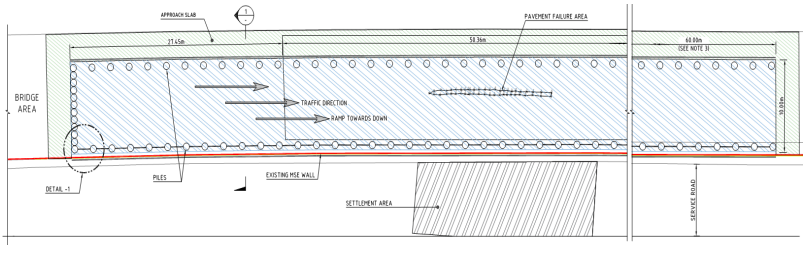

Figure 6: Utilized Option - Layout

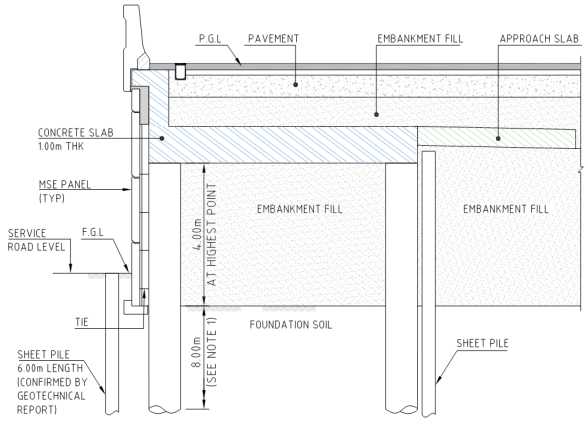

Figure 7: Utilized Option – Section 1-1

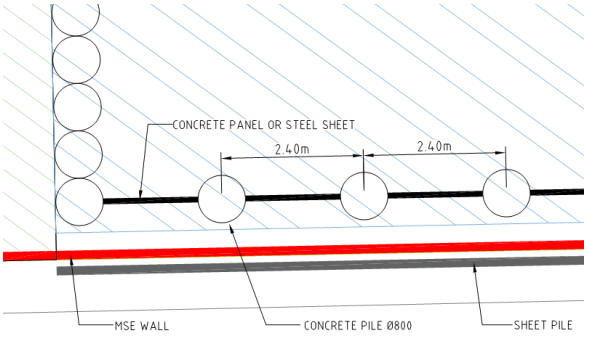

Figure 8: Utilized Option – Detail -1

4 PAVEMENT

The Pavement Design is done keeping in view the future anticipated traffic volumes. This included the bridge ramps and service roads. For the upgradation of existing pavement, two options are considered; full reconstruction option and mill/overlay option. The upgradation option for a given pavement section was selected based on the existing road quality (surface distress) and structural capacity of the pavement section. The existing pavement structural capacity was evaluated using both destructive and non-destructive approaches.

Pavement study was carried out based on the condition of the existing pavement and to provide an estimated overlay requirement to extend the structural life of the pavement for 20 years. In addition, FWD testing was also used for the identification of the weak areas.

Coring of the existing pavement for the estimation of asphalt thickness along with Falling Weight Deflectometer (FWD) analysis was carried for the embankments ramp up and ramps down. Towards the direction failed pavement because of the partial movement of MSE wall. For this section full depth pavement, section was proposed.

5 CONCLUSION AND RECOMMENDATIONS

Although the rectifications for the affected areas have been carried out, the below recommendations are being shared to avoid the reoccurrence of the MSE walls partial failure in the future:

- The repair was carried out by the contractor for the service road at the areas where poor backfilling was captured, it was recommended to divert the utilities away from the MSE walls considering the limitation of the boreholes, trial pits, and geo-physical survey to capture every single area that had poor backfilling in the past.
- Any leakage of the wet utilities at the MSE wall or nearby should be treated immediately.
- As another level of mitigation, vertical permanent shoring could take place adjacent to the MSE wall at the service road level to assure that there will be no impact from the service road backfilling on the MSE walls.
- Regular inspection of the MSE wall to observe any deformation that might occur.
- Regular inspection of the pavement to report any deformation at the bridge level or at the service road if took place.

REFERENCES

Bobet, A. (2002). *Design of MSE Walls for Fully Saturated Conditions* (Report No. FHWA/IN/JTRP-2002/13). Perdu University, Indiana, the USA.

British Standards Institution (1990). BS5400-4. Steel, Concrete, and Composite Bridges: Code for Practice for Design of Concrete Bridges, the UK.

Design Manual for Road and Bridges (2001). BD37/01. Load for Highway and Bridges: Highway Structures: Approval Procedures and General Design, the UK.

Cite this article as: Kara A., Tahoun T., "An Innovative Structural Solution to Failed Stabilized Earth Embankment in Multilevel Interchange", *International Conference on Civil Infrastructure and Construction (CIC 2020)*, Doha, Qatar, 2-5 February 2020, DOI: https://doi.org/10.29117/cic.2020.0116

Modelling Catchments in Qatar to Assist in Operations

Shirish Gokhale
sgokhale@ashghal.gov.qa
Public Works Authority (Ashghal), Doha, Qatar

Anil Kumar Gupta
agupta@ashghal.gov.qa
Public Works Authority (Ashghal), Doha, Qatar

Nasser Yousef Fakhroo
nfakhroo@ashghal.gov.qa
Public Works Authority (Ashghal), Doha, Qatar

Kapil Devang
kdevang@ashghal.gov.qa
Public Works Authority (Ashghal), Doha, Qatar

Tim Kelly
tkelly@ashghal.gov.qa
Public Works Authority (Ashghal), Doha, Qatar

ABSTRACT

Qatar is experiencing unprecedented growth and infrastructure is being developed at a rapid pace. The infrastructure is served by storm water systems which are under development and need to be resilient in case of storms. The storm water systems serving Doha and nearby areas are complex in nature. They include passive, positive drainage systems and also connect critical locations such as underpasses and a number of ancillaries. The two main reasons adding to the complexity are asset creation work ongoing at multiple locations and various temporary and permanent systems operating simultaneously. A standardized approach for operating this complex storm drainage network becomes essential. Also, while solving problems such as flooding during a rainfall event, at times root cause of a problem may be at a different geographical place than that of the actual location of the problem. It is difficult to arrive at a root cause without an overall understanding of the system. This along with a standardized approach is useful in taking better informed decisions before, during and after storm events. A coordinated effort between Ashghal Design and Operation & Maintenance Departments resulted into an operational philosophy. Hydraulic modelling supported by comprehensive GIS information played an important role in developing this. The work consisted of considering issues encountered during recent major storm events and simulating multiple scenarios. The recommended actions are currently under implementation. The next stage will be to set up a near real time operation system which would include SCADA data linked to and hydraulic models.

Keywords: Reclaimed asphalt pavement; Mix design; Rutting; Fracture; Optimum RAP content

1 INTRODUCTION

The State of Qatar has experienced exceptional levels of economic and population growth over the past three decades. Exponential increase has been observed in last two decades. Population has grown from 700,000 in year 2000 to 2.5 million currently. Figure

1 shows the population increase over the years (United Nations, 2017). This population growth has translated into an ever-increasing demand for housing, commercial, institutional and recreational development. Rapid growth in the infrastructure has changed the urban landscape drastically. Open land which was relatively permeable has been converted into a built-up area with high impermeability (Shandas et al., 2017). This has resulted into changed runoff patterns.

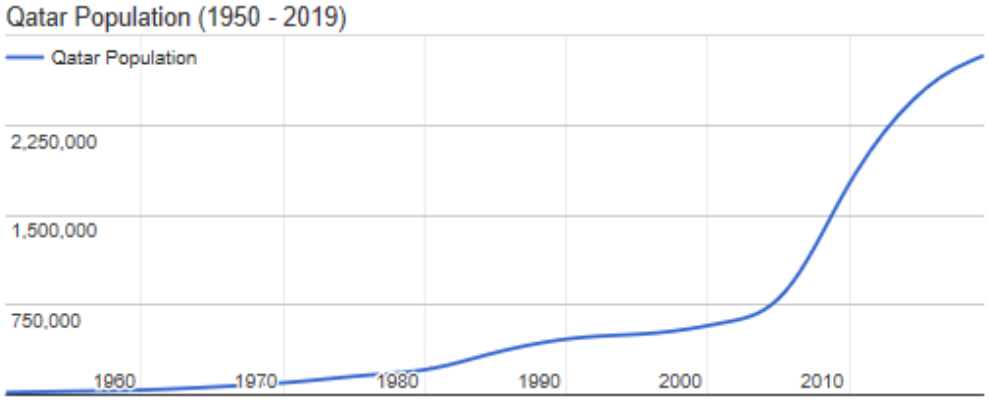

Figure 1: Population growth (data source: 2019 United Nations, DESA, Population Division)

Urban flash floods can be devastating for the population, assets and can bring a city to standstill. The storm water systems are not currently proportionately developed to cater to such events (Salvan, et al., 2016). Frequency of floods has increased in recent years in Qatar primarily due to an increase in the frequency of occurrence of extreme storm events. Real Time Controlled (RTC) operations have been tested with multiple approaches all over the world (Jafari et al., 2018). There is therefore a strong need to optimize current assets for changed rainfall and rapid development scenarios.

This paper focusses on hydraulic model developed to represent ever changing existing storm water systems and its use for understanding current and future performance issues and identifying mitigation measures. The model uses design storm events as well as measured rainfall events. It was further used to develop an operational philosophy for planning and optimizing the level of service.

2 STORM WATER MANAGEMENT SYSTEM IN QATAR

Storm water catchments in Qatar comprise of three main areas:

- Asian Games Outfall (AGO) & Musaimeer Pump Station Outfalls (MPS).
- North District of Doha (NDoD - including Lusail and West Bay).
- Wakra (includes southern areas).

The NDoD and Wakra catchments are under the subject of separate detailed outfall studies and drainage strategies for these catchments will be developed in the next two years. Currently there are a few outfalls including AGO operational. The Musaimeer tunnel has been constructed and a terminal pumping station is under construction. Figure 2 shows storm water catchments in Qatar.

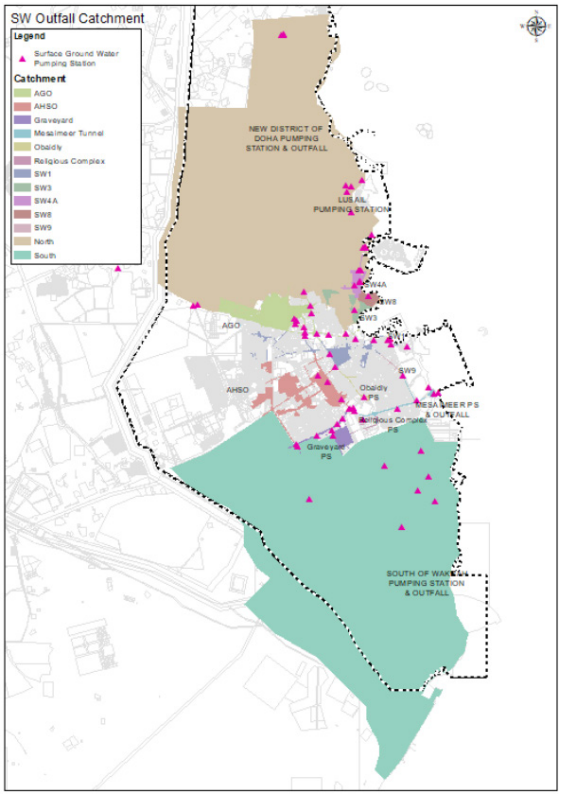

Figure 2: Storm water catchments in Qatar and locations of pumping stations

There are two main types of surface water collection and disposal systems in Qatar:

2.1 Piped systems

This type of system is known as a positive system in Qatar. The main principle of the positive drainage system is to remove rainwater as quickly as possible from where it falls. Surface water from certain paved and roof areas is collected and directed straight into an underground network of pipes to convey the water by gravity to a disposal point. These disposal points are currently either the marine environment or inland emergency flood areas.

2.2 Passive systems

These are full or partial infiltration drainage systems which help manage surface water by replicating natural drainage. A network of infiltration trenches decreases the rate at which water drains by storing and infiltrating or releasing at a controlled rate. This is typically designed for return periods up to 10 years. During extreme events capacity is exceeded and runoff is conveyed through overland flow paths.

2.3 Challenges in level of service

Both the systems have a finite capacity which, if exceeded, will cause the system firstly to surcharge and ultimately overflow and cause flooding. Subsequent infill development

or redevelopment/expansion of urban areas that replaces permeable ground results in increased peak flows and the potential need to upsize the drainage system to continue to provide the prescribed level of service.

As the permanent measures are being constructed e.g. the terminal MPS, there is a need to address storm water in the interim. There are major areas connected to the tunnel and runoff from these areas needs to be managed till the MPS is operational. There are also a number of other construction projects ongoing at various stages of execution. Interim measures are required to manage storm water from these areas.

Increased ground water levels have posed a challenge in some areas making the passive systems ineffective.

While solving flooding problems, at times root cause of a problem may be at a different geographical location than that of the problem. It is difficult to arrive at a root cause without an understanding of the overall system.

3 HYDRAULIC MODELLING

A surface drainage includes underground positive/ passive systems as well as overland flows. Interaction between underground (1D) and overland (2D) flows is complex. This can be reasonably modelled during normal storms, however, during extreme events to understand how the overall system works, can be challenging due to operational issues such as clogging of gullies and blockages. The complexity is further increased by the features on ground such as buildings, walls, sidewalks and curbs etc.

Comprehensive Geographic Information System (GIS) data which includes asset data and LiDAR digital terrain models, was processed and used for building 1D-2D catchment models. Assets in ground were modelled using InfoWorks ICM. There are a number of temporary measures taken till permanent measures become fully operational. These include pumps and emergency flooding areas or lagoons and storages. These were included in the model to represent the current catchment. Details were included in the model for overland features around critical locations such as underpasses.

The catchment models were calibrated based on flow and depths survey data and information available in SCADA records.

4 RESULTS

The models were simulated for 5, 10, 25, 50 and 100 year design storm events as well as recorded storm events that occurred in the year 2018. The results were validated for various areas based on historical flooding records, flood extents and operations feedback. Mitigation measures were identified for priority areas and where permanent measures will be in place in future.

An operational philosophy was derived with the help of the models. This included works to be done when there is business as usual, during storm event alert status, during storm and after a storm event. This helps in optimizing the existing network including storages to get maximum level of service in the interim and longer-term scenarios making it more sustainable.

Figure 3 shows examples of model results where the model shows good representation of flood paths, extents and potential low-lying areas needing attention. Example results also show a tunnel top water level during a real time operation scenario.

Improved understanding of the system using detailed models helped in identification of controls in the AGO - MPS catchment which would help in optimizing the system operation in ever changing short term as well as long term scenarios. Figure 4 shows the locations of flow controls.

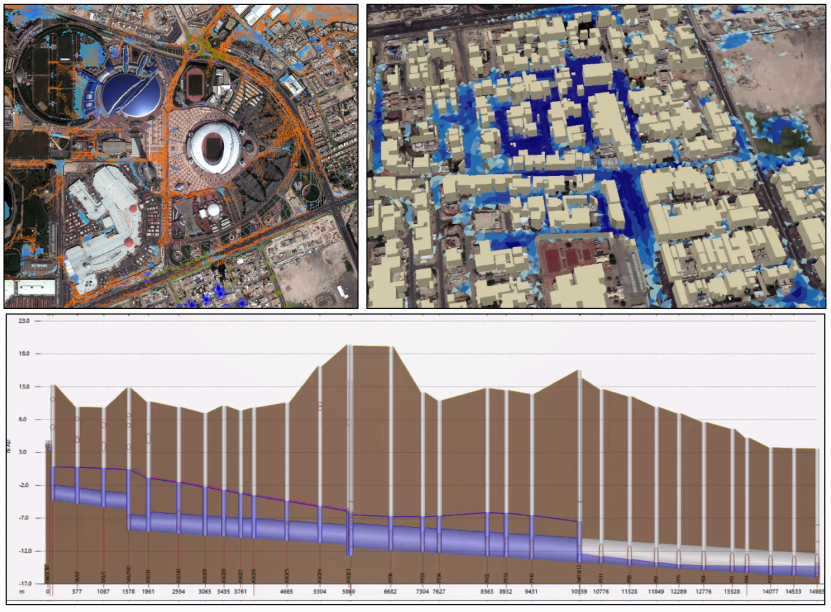

Figure 3: Examples of model results showing overland flow paths, flood depths and underground tunnel hydraulic performance

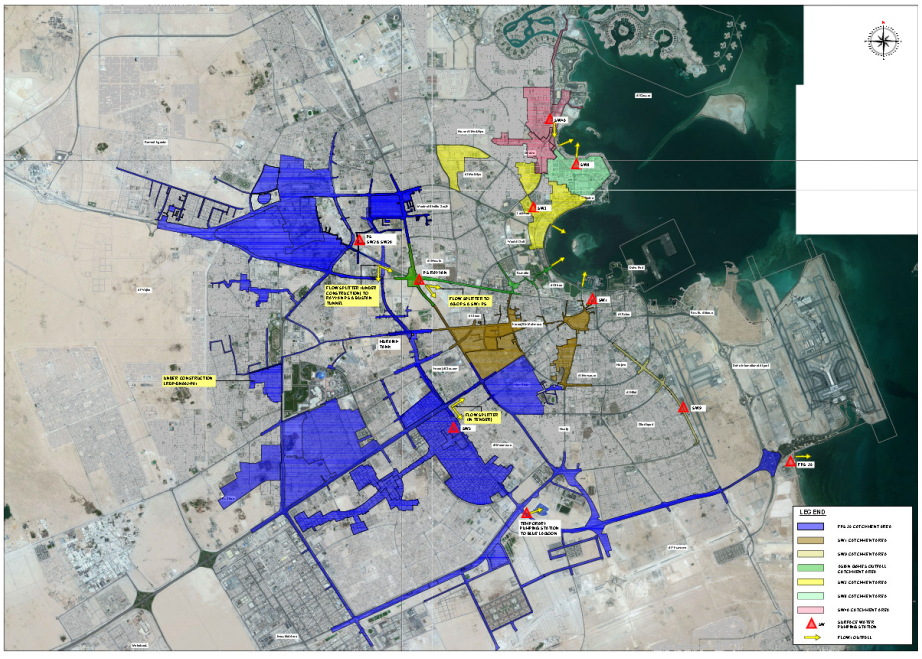

Figure 4: Locations of controls identified in the catchments for optimized operation

5 CONCLUSION

Rapid pace of development in Qatar along with a significantly changed rainfall pattern has posed a major challenge in terms of managing storm water. Due to the evolving storm-water network, there are a number of temporary and permanent systems operating that play a major role in storm water management in Qatar. A dynamic hydraulic model was prepared and maintained in InfoWorks ICM to help in decisions and to plan temporary and permanent flood mitigation measures. The model was simulated for a number of scenarios and locations of flow controls were identified. This was used in defining operational procedures which would help in sustainable and optimized use of existing infrastructure in ever changing short term scenario and the long term as well. The system is evolving and the set philosophy is under implementation. The next stage of this is the near real time decision making involving a link with SCADA data.

ACKNOWLEDGMENT

Authors would like to thank the Ashghal Drainage Networks Operation and Maintenance Department for their inputs in preparing the model and operational philosophy. Authors would also like to thank the Ashghal Engineering Services Department and Ministry of Municipality and Environment for supplying the LiDAR data.

REFERENCES

Jafari, F., Mousavi, J. & Joong, K. (2018). A Real-time Optimal Gate Operation Model for Urban Drainage Systems. 10.29007/ktzw.

Salvan, L., Abily, M., Gourbesville, P. & Schoorens, J. (2016). Drainage system and detailed urban topography: Towards operational 1D-2D modelling for storm water management. *Procedia Engineering*, 154. 890-897. 10.1016/j.proeng.2016.07.469.

Shandas, V., Makido, Y. & Ferwati, S. (2017). Rapid urban growth and land use patterns in Doha, Qatar: Opportunities for sustainability. *European Journal of Sustainable Development Research*, *1*(2), 11. DOI: 10.20897/ejosdr.201711.

United Nations (2019). DESA, Population Division, World Population Prospects.

Cite this article as: Gokhale S., Gupta A. K., Fakhroo N. Y., Devang K., Kelly T., "Modelling Catchments in Qatar to Assist in Operations", *International Conference on Civil Infrastructure and Construction (CIC 2020)*, Doha, Qatar, 2-5 February 2020, DOI: https://doi.org/10.29117/cic.2020.0117

Eco-friendly Concrete Using Local Materials From Sudan

Salma Yahia Mohamed Mahmoud
salmaymm@gmail.com
College of Engineering, University of Science and Technology, Omdurman, Sudan

El Tahir Abualgasim Mohammed Alshiekh
schoolcivil@yahoo.com
College of Engineering, Sudan University of Science and Technology, Khartoum, Sudan

ABSTRACT

This study is aimed at investigating the potentiality for utilizing some locally available eco-friendly materials to replace some concrete constituents as a possible opportunity to introduce sustainable construction in Sudan. Six suggested scenarios were explored to visualize the possible outcomes : (1) 100% recycled aggregates (RA) and natural pozzolana in replacement of coarse aggregates (2) steel slag replacing fine aggregate or cement (3) treated sawdust replacing fine aggregates (4) sawdust ash in partial replacement of cement (5) meta-kaolin (MK) in partial substitution for ordinary Portland cement (OPC) (6) quarry dust (QD) in partial replacement of sand or cement. Laboratory experiments were conducted and concrete workability and compressive strength were determined. The results confirmed the suitability of RA for full replacement of natural coarse aggregates. Steel slag was more appropriate in replacing sand than cement when added in small percentages not exceeding 15%. Sawdust needed treatment to eliminate the unfavorable properties before using it as a substitute for sand but when the ash was used to replace cement, it was not possible to achieve the required strength at early ages and better results were achieved in 28 days. With a chemical composition comparable to cement, MK showed impressive results when used in partial replacement of OPC. The addition of QD in replacement of 15% of sand offered a reasonable workability but the compressive strength was only approaching the targeted value. According to these results, it could be inferred that the tested options offer reasonable evidence to confirm their potentiality for producing green concrete in Sudan.

Keywords: Green concrete; Meta-kaolin; Sudan; Sustainability

1 INTRODUCTION

Concrete is a heavy, rough building material made from a mixture of cement, fine and coarse aggregates, water and maybe some additives. For the negative impacts resulting from its production, concrete has been classified as environmentally unfriendly. Its production consumes natural resources such as river sand, clays and rocks which are normally not returned back and involves the emission of huge amounts of CO_2 during the production of cement-as one of its major constituents. Accordingly, sustainable trails in the building industry called for preserving these natural resources through the production of eco-friendly concrete. This is concrete where waste materials are used as at least one of its components or its production does not lead to environmental destruction through the reduction, reuse or recycling techniques.

2 SUSTAINABILE ALTERNATIVE BUILDING MATERIALS

The call for cement and concrete production sustainability was stressed in several previous studies. Green concrete is thought to be one of the solutions leading to sustainable construction because it "... uses waste material as at least one of its components, or its production process does not lead to environment destructions" (Akbarnezhad et al., 2013; De Brito & Saikia, 2013). They evaluated the physical and mechanical properties of different material options when used in substitution for some of the main components of concrete. Durga and Andira (2016) tested the use of construction debris and demolition waste, for partial or entire replacement of virgin aggregate when making new concrete and argued that it "… could save about 60% of limestone resources and reduce CO_2 emissions by about 15%–20%". It has been reported though that there are some limitations recorded on its use pertaining to its long-term durability. It was found that variation in the RA properties, different environmental conditions in addition to the crushing process, contamination and impurities, affect the new concrete properties (El Shiekh et al., 2012; Mahmoud & El Shiekh, 2018; Juenger et al., 2012; McNeil & Kang, 2013; Mehta, 2010; Pachipala, 2017).

The use of alternative materials to replace aggregates was another option to avoid depleting the natural aggregates. Silica sand, a by-product of the glass industry, is an alternative incorporated to partially replace natural sand in concrete mixtures (Pimraksa et al., 2018; Silva et al., 2015). The results showed up to 32% increase in compressive strength and 13% improvement on tensile strength upon replacement of natural sand by 60% and 40% respectively (Ulloa et al., 2013).

The behavior of concrete with supplementary cementitious materials (SCM) has been investigated in many studies. "Natural supplementary materials such as volcanic rock and limestone are used for their economic benefit and early-strength and durability improvements" (Vishnumanohar, 2014). Among the commonly used SCM are coal fly ash, silica fumes, metakaolin and blast furnace slag (Xiao et al., 2014). Calcined clays, municipal solid waste incinerator residues and limestone fillers are few examples cited in the literature where their use as alternative supplementary materials was outlined.

3 TRIALS TO PRODUCE ECO-FRIENDLY CONCRETE IN SUDAN

Initially, the chemical and physical properties of the different materials used in these trials were determined, different mix designs considering several options were developed then the concrete was prepared and casted in cubes. The fresh concrete mixtures were tested for workability and the hardened concrete was tested for compressive strength after 7, 14 and 28 and in some instances for 90 in all trials.

3.1 100% recycled aggregates (RA) and natural pozzolana in replacement of coarse aggregates

This study built on a preliminary study conducted by the authors on the reuse of building demolition wastes and their potential usefulness in producing new concrete. More investigation scenarios were included. The physical properties of fresh and hardened RCA included concrete were investigated with and without natural pozzolana being added to the mixtures. OPC conforming to (BS–8112-1996) was used with 32.5% normal consistency, 2 hours and 25 minutes initial setting time, 3 hours and 30 minutes

final setting time, 2% fineness and 2mm stability size. Specific gravity and absorption were determined as shown in table 1.

Table 1: Aggregates Characteristics

Characteristics	**Natural Coarse Aggregates (NCA)**	**Recycled Coarse Aggregates (RCA)**
Specific Gravity	2.76	2.66
Absorption	0.44	0.98

The recycling process involved crushing, separation of metals by a magnet, manual removal of other impurities (plastic, wood, etc.), and classification of aggregates to different grades based on particle size as illustrated in Figures 1a, 1b, 1c respectively.

Figure 1a: Aggregates crashing

Figure 1b: Metals separation

Figure 1c.: Aggregates classification

Proportions for 8 different mix trials were considered and the materials proportions are presented in table 2. The targeted compressive strength value was (25MPa).

Table 2: Mix Trials materials proportions

Trial	Cement (Kg)	Water (Kg)	Fine Aggregate (Kg)	NCA (Kg)	RCA (Kg)	Pozzolana (Kg)
1	325	195	641	1189	-	-
2	325	195	641	891.8	297.3	-
3	325	195	641	594.5	594.5	-
4	325	195	641	297.3	891.8	-
5	325	195	641	-	1189	-
6	292.5	195	641	-	1189	32.5
7	260	195	641	-	1189	65
8	227.5	195	641	-	-	97.5

Slump test values ranged between 60-180mm. However, workability was noticed to decrease in the range of 4.2-14.3% with increasing replacement ratios of RCA up to a maximum of 20.2% with 100% RCA in comparison to NCA. Contrary wise, an increase in the range of 3.2-7.4% was reported with the inclusion of pozzolana with 100% RCA concrete. In its fresh state, the optimum ratio was achieved with the full replacement with RCA and 20% pozzolana. Compressive strength results depicted in figure 2 showed a strength decrease as the RCA replacement percentage increases. The target strength was achieved with 10% pozzolana and 100% RCA.

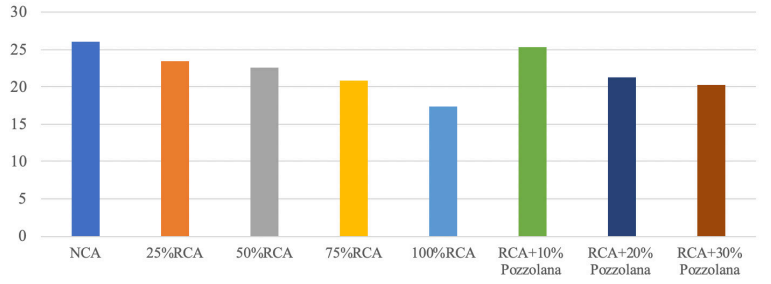

Figure 2: 28-Days compressive strength results for the different mix trials

The results for the durability test presented in Figure 3, revealed a drop in the wave speed value (Km/sec) when the NCA were completely replaced by RCA while an increase was witnessed with the different percentages of Pozzolana added to mix.

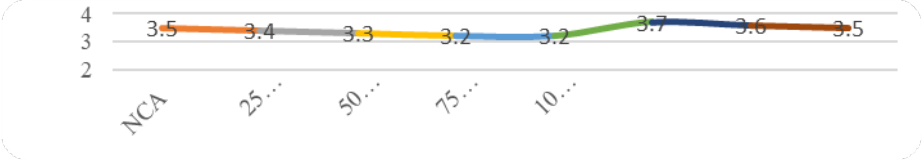

Figure 3: Durability Test Results (Wave speed Km/sec)

3.2 Steel slag replacing fine aggregate or cement

Blast furnace slag (BFS), a by-product from the production of steel at Giad Factory south of the city of Khartoum – Sudan was used. Both chemical analysis and XRD test were conducted on a BFS sample and the results showed similar oxides in comparison to OPC but with different proportions (SiO_2, 33%; Al_2O_3, 7%; Fe_2O_2, 11%). It was incorporated in partial substitution for sand then cement in concrete mixtures.

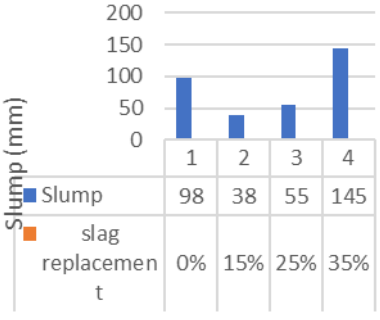

Figure 4a: Workability Results for mixtures containing Steel Slag in Replacement for Sand

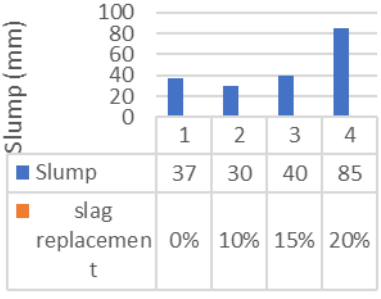

Figure 4b: Workability Results for mixtures containing Steel Slag in Replacement for Cement

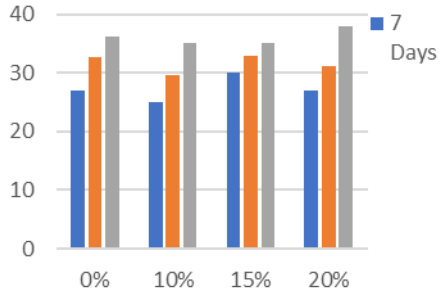

Figure 5a: Compressive Strength Results for Concrete with the Inclusion of Steel Slag in Replacement for Sand

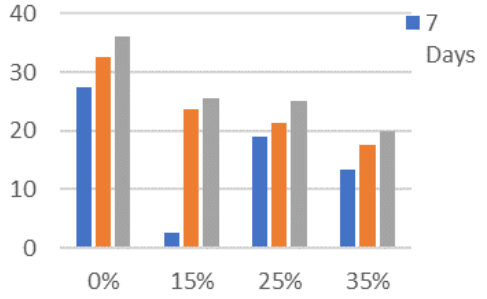

Figure 5b: Compressive Strength Results for Concrete with the Inclusion of Steel Slag in Replacement for Cement

A standard mix and 3 others where the slag replaced (10%, 15%, and 20%) of the sand weight and (15%, 25%, and 35%) of the cement weight. The slump and compressive strength results are shown in figures 4a, 4b, and 5a, 5b. The results for slag replacement for sand confirmed that both the workability and the compressive strength have increased. Alternatively, in the case of replacing the slag with varying percentages of the cement weight, the results showed an increase in workability parallel with the increase in the slag amount while the compressive strength has dropped.

3.3 Treated sawdust replacing fine aggregates

Samples of the abundantly available sawdust (SD) from the local furniture market on Khartoum State, Sudan were collected, treated then used in concrete mixtures. Seven cases, shown in table 3, were analyzed. Compressive strength at the different curing ages was as illustrated in table 3.

Table 3: Compressive strength results for treated Sawdust included in replacement of fine Aggregates Concrete mixtures

Scenario	Streangth (MPa)		
	7 Days	14 Days	28 Days
Untreated Sawdust	34.5	37.03	38.96
Unsoaked Sawdust with 10% repalcement	8.77	9.31	9.8
Unsoaked Sawdust with 20% repalcement	2.08	3.9	6.3
soaked Sawdust with 10% repalcement	16	15.9	18.07
soaked Sawdust with 20% repalcement	11.5	13.8	17.8
Sawdust treated with calcium hydroxide + 10% MC	15.13	11.3	18.1
Sawdust treated with calcium hydroxide + 20% MC	3.24	5.5	12.3

The unfavorable properties of SD made if hardly possible to approach the targeted strength. With unsoaked SD, 10% replacement offered better results and when the dust was soaked nearly equal results were obtained for 10 and 20% replacement which are also equal to the strength value 10% replacement when the SD was treated with the calcium hydroxide and coated with varnish.

3.4 Sawdust ash in partial replacement of cement

The ash was prepared as depicted in figures 6a, 6b, 6c and 6d and the mix trials were prepared with the proportions shown in table 4

Figure 6a: Raw Sawdust

Figure 6b: Sawdust burning

Figure 6c: Sawdust ash sieving

Figure 6d: Hardened sawdust concrete mix

Table 4: Compressive strength results for Sawdust ash included in replacement of cement in Concrete mixtures

Mix Trial (% replaced)	Compressive strength (MPa)		Slump (mm)
	7 days	28 days	
0%	24.1	37.67	37
10%	18.14	22.04	35
20%	15.87	24.9	34

Better results are achieved when the ash was used in replacement for cement. Slump values are within the designed for limit (30-60mm) and the compressive strength is just as the targeted value with 20% replacement ratio.

3.5 Meta-kaolin (MK) in partial substitution for ordinary Portland cement (OPC)

A two stages process was followed. The first stage was concerned with the kaolinite clay (KC) collected from different locations in Sudan. The chemical composition was determined using X-Ray florescence where the major oxides were identified then compared to the major constituents of OPC. KC was transformed to Meta-Kaolin (MK) through a calcination process then tested according to the ASTM-C618 to determine its pozzolanicity. The evaluation of the pozzolanic activity of the MK was conducted via chemical and mechanical tests. The former comprised measurement of the amount of the three major oxides (SO_2+Al_2O_3+Fe_2O_3), Loss on ignition percent and the later was concerned with assessing the strength properties of MK included concrete. The results shown in table 5, confirmed the pozzolanicity of the MK.

Table 5: The evaluation of the pozzolanicity activity of the Meta-Kaolin from Sudan

Elements	Meta-kaolin from different locations in Sudan				Pozzolanicity
	Site 1	Site 2	Site 3	Site 4	Limits according to ASTM C618 (%)
$SiO_2+Fe_2O_3+Al_2O_3$	93.05	88.42	97.30	97.60	≥70%
LOI	4.08	5.65	0.68	1.3	≤6%

MK was then added to concrete mixtures in (0, 5, 10, 15, 20, 30) % replacement for cement. Workability of the fresh concrete samples was tested through the slump test where all results were conforming to the required limit (60-180mm) then a set of 56 (150×150×150)mm cubes were casted and cured for 7,14,28,90 days. The results depicted in figure 7 show an increase in the strength with the MK inclusion with an optimum limit of 20% yielding 35.8MPa in 28 days. It was also evident that very promising results could be achieved at long ages as shown in 20 and 30% MK which yielded 40.1 and 42.3MPa respectively exceeding by that the targeted strength and indication the pozzolanic reactivity of the MK at longer ages.

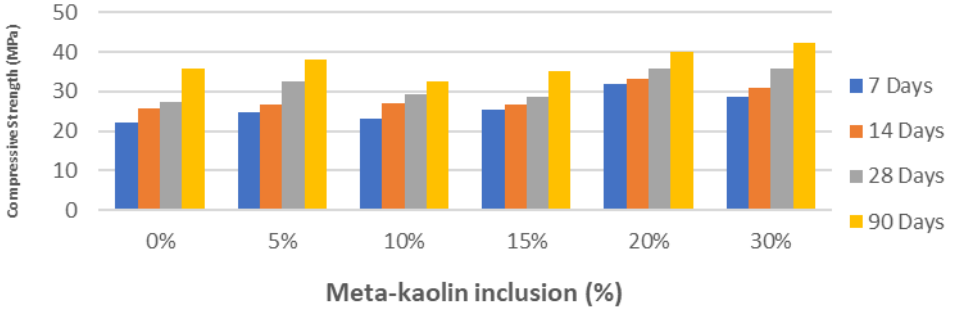

Figure 7: Compressive strength of meta-kaolin included concrete mixtures

3.6 Quarry dust (QD) in partial replacement of sand

Quarry dust is a sediment or residue from the process of extracting and treating rocks. For this study, the dust was obtained from two locations; (Toureah) Mountain, south of Omdurman, and Algabaleen. When collected its physical appearance is as depicted in figures 8a and 8b.

Figure 8a: Quarry Dust Collection

Figure 8b: Collected Dust

In replacement for sand, concrete mixtures containing (15%, 25%, 35%) of the QD and in replacing cement (15%, 25%, 50%) were designed and prepared then cured in water. Workability of fresh concrete was measured for all mixtures and the compressive

strength of hardened concrete was defined for 7 and 28 days. The results showed that the target strength was nearly achieved in the two cases. The replacement of sand by 15% QD yielded the best results among the mixing ratios while further increase in the dust reduced the compressive strength. In replacing cement, the optimum results were achieved with 25% replacement for cement, refer to figures 9a and 9b).

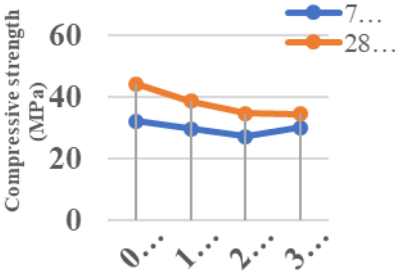

Figure 9a: Quarry Dust inclusion (%) from Omdurman-Sudan

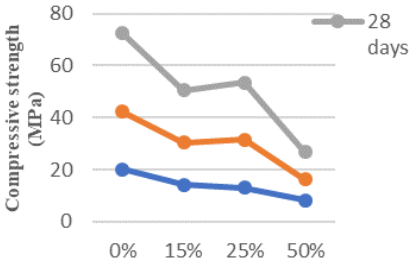

Figure 9b: Quarry Dust inclusion (%) from Algabaleen-Sudan

4 CONCLUSION

The results confirmed the suitability of RA for full replacement of natural coarse aggregates. Steel slag was more appropriate in replacing sand than cement when added in small percentages not exceeding 15%. Sawdust needed treatment to eliminate the unfavorable properties before using it as a substitute for sand but when the ash was used to replace cement, it was not possible to achieve the required strength at early ages and better results were achieved in 28 days. With a chemical composition comparable to cement, MK showed impressive results when used in partial replacement of OPC. The addition of QD in replacement of 15% of sand offered a reasonable workability but the compressive strength was only approaching the targeted value. According to these results, it could be inferred that the tested options offer reasonable evidence to confirm their potentiality for producing green concrete in Sudan.

REFERENCES

Akbarnezhad, A., Ong, K. C. G., Tam, C. T. & Zhang, M. H. (2013). Effects of the parent concrete properties and crushing procedure on the properties of coarse recycled concrete aggregates. *Journal of Materials in Civil Engineering*, Vol. 25, No. 12, pp. 1795-1802.

De Brito, J. & Saikia, N., (2013). *Recycled aggregate in concrete: Use of industrial, construction and demolition waste*. London, the UK: Springer.

Durga, B. & Andira, M. (2016). Experimental study on various effects of partial replacement of fine aggregate with silica in cement concrete and cement mortar. *International Journal of Engineering Trends and Technology (IJETT)*, Vol. 33, no. 5.

El Shiekh, A. A., Mahmoud, S. Y. & Attaalmanan, M. (2012). Study of the effect of steel slag on some of the properties of concrete. *Sudan Engineering Society Journal*, Vol. 57, No.1, pp1-8.

Juenger, M., John, L. P., Elsen, J., Winnie, M. & Doug, H. R. (2012). Supplementary cementitious materials for concrete: Characterization needs, *Materials research society symposium proceedings*. Vol. 1488.

Mahmoud, S. & Elshiekh, E. (2018). The potential usefulness of recycled aggregates and pozzolana in producing green concrete in Sudan. *International Journal of Structural and Civil Engineering Research*. Vol. 7, No.2.

McNeil, K. & Kang, T. H. K. (2013). Recycled concrete aggregates: A review. *International Journal of Concrete Structures and Materials*, Vol. 7, No.1, pp. 61-69.

Mehta, P. K. (2010). Sustainable cements and concrete for the climate change era – a review, *Proceedings of the 2nd International Conference on Sustainable Construction Materials and Technologies*. Ancona, Italy, pp. 28-30.

Pachipala, S. (2017). A study on mechanical properties of concrete using silica sand as partial replacement of cement. *International Journal of Civil Engineering* (SSRC-IJCE), Vol. 4, No. 5, pp. 34-39.

Pimraksa, K. P., Chindaprasirt, J. S. & Ling, T. C. (2018) Alternative cementitious materials and their composites. *Advances in Material Science and Engineering*, Vol. 2018, article 50746.

Silva, R. V., de Brito, J. & Dhir, R. K. (2015). Prediction of the shrinkage behavior of recycled aggregate concrete: A review. *Construction and Building Materials*, Vol. 77, pp. 327-339.

Ulloa, V. A., García-Taengua, E., Pelufo, M. J., Domingo, A. & Serna, P. (2013). New views on effect of recycled aggregates on concrete compressive strength. *ACI Materials Journal*, Vol. 110, No. 6, pp. 1-10.

Vishnumanohar, A. (2014). Performance of normal concrete with eco sand (finely graded silica) as fine aggregate. *International Journal of Engineering Science Invention*, Vol 3, No. 5, pp. 27-35.

Xiao, J., Li, L., Tam, V. W. & Li, H. (2014). The state of the art regarding the long-term properties of recycled aggregate concrete. *Structural Concrete*, Vol. 15, No. 1, pp. 3-12.

Cite this article as: Mahmoud S. Y. M., Alshiekh E. T. A. M., "Eco-friendly Concrete Using Local Materials From Sudan", *International Conference on Civil Infrastructure and Construction (CIC 2020)*, Doha, Qatar, 2-5 February 2020, DOI: https://doi.org/10.29117/cic.2020.0118

Mechanical Properties of Concrete Made with Electric Wires, Steel Fibers, Basalt Fibers and Polypropylene Fibers

Yasmin Zuhair Murad
y.murad@ju.edu.jo
University of Jordan, Amman, Jordan

Haneen Abdel-Jabbar
eng.haneen.20@hotmail.com
University of Jordan, Amman, Jordan

ABSTRACT

An experimental program is conducted in this research to investigate the mechanical properties of concrete made with electric wires, steel fibers, basalt fibers, and polypropylene fibers. Fibers are added to the concrete mix in three different percentages (48, 32 and 16 kg/m3 for steel and wire fibers) and (2, 4 and 8 kg/m^3 for basalt and polypropylene fibers). Fifty two concrete cylinders are tested under compression and splitting tensile strength tests to investigate the compressive and tensile behaviors of the fibrous concrete. Test results have shown that steel fiber is superior over the other types of fibers in increasing the compressive and tensile strengths of concrete. The addition of 48 kg/m3 steel fiber has increased the compressive strength of concrete up to 9% and has duplicated its tensile strength compared to the control specimen. The addition of 2 kg/m3 polypropylene fibers has increased the compressive and tensile strengths of concrete up to 8.6% and 10.3% respectively. Increasing the percentage of polypropylene fibers to 8 kg/m^3 has resulted in increasing the tensile strength of concrete up to 22.8% while it has reduced its compressive strength by 9.6% compared to the control specimen. The addition of basalt fibers and wire fibers has resulted in decreasing the compressive and tensile strengths of concrete. The maximum reduction in concrete compressive strength is measured with 48 kg/m3 wire fibers where concrete compressive strength is reduced by 32.6%. The lowest tensile strength is measured with 8 kg/m^3 basalt fibers where the tensile strength is reduced by 27.7%.

Keywords: Concrete mechanical properties; Recycled electric wires; Steel fibers; Basalt fibers and Polypropylene fibers

1 INTRODUCTION

Several experimental programs have been recently conducted to investigate the mechanical properties of concrete made with several types and percentages of natural and synthetic fibers. Natural fibers are fibers that found in the nature such as coconut, horse tail etc. while synthetic fibers are prepared by humans such as carbon, glass, steel, and basalt fibers, etc. Few studies have recently investigated the mechanical behavior of concrete made with waste materials such as plastic, iron filling, rubber etc. (Murad, Abu-Haniyi, Alkaraki & Hamadeh, 2018) have investigated the compressive and tensile behaviors of concrete made with iron fillings. Researchers have shown that steel fibers have limited effect on the compressive strength of concrete (Ou, Tsai, Liu & Chang,

2012) while they can reduce the width and quantity of cracks in concrete elements (Amin & Foster, 2016). The compressive strength of concrete has been increased up to 21.67% due to the addition of 0.2% pvc fibers at 28 days (Nidhish & Arunima S, 2017). Other researchers have sown that the use of 0.8% of pvc fibers is an optimum percentage and they have also recommended that pvc concrete can be used as an alternative to plain concrete (Varghese & Boby, 2017). Gull et al. have shown that pvc can enhance the mechanical behavior of concrete (Gull & Balasubramanian, 2014).

Alnahhal et al. have shown that concrete compressive strength has not been changed due to the addition of basalt fibers (Alnahhal & Aljidda, 2018). Other researchers have shown that the mechanical properties of concrete has been improved due to the addition of fiber (Jaysing & Joshi, 2014). Sahoo et al. (Sahoo, Solanki & Kumar, 2015) have shown that the compressive and tensile strengths of concrete have not been improved due to the addition of polypropylene fibers while they have shown that the addition of steel and polypropylene fibers can improve the concrete tensile strength about 25-100% .

This research investigates the compressive and tensile behavior of concrete made with electric wires, steel fibers, basalt fibers and polypropylene fibers. Fibers are added in three different percentages (5%, 10% and 15% for steel and wire fibers) and (0.6%, 1.3% and 2.5% for basalt and polypropylene fibers) of the total cement weight. The research suggests the preferable type and percentage of fibers that can improve the mechanical properties of concrete.

2 MATERIAL PROPERTIES

The proportions of the plain concrete mix which used in this research are shown in Table 1 where the compressive and tensile strengths of the plain concrete are 41.7 MPa and 3.4 MPa respectively. Four different types of fibers, shown in Figure 1, are added solely to the concrete mix in three different percentages; (48, 32 and 16 kg/m^3 for steel and wire fibers which equal to 5%, 10% and 15% fibers of the total cement weight) and (2, 4 and 8 kg/m^3 for basalt and polypropylene fibers which equal to 0.6%, 1.3% and 2.5% fibers of the total cement weight). The selected percentages are close to the proportions proposed by the manufactures for each type of fiber. It should be noted that copper is removed from the electric wires and then the electric pvc plastic wires are cut into pieces with fixed length of 60 mm. The properties of the utilized fibers are shown in Table 2.

Table 1: Concrete mix proportions

Materials	Weight (Kg/m^3)
Cement	325
Water	190
Fine aggregate	1070
Sand	690
Super – Plasticizer	1.195

Table 2: Fiber properties

Fiber type	Length mm	Diameter	Aspect ratio (L/D)	Density g/cm^3
Steel fiber	60	0.75 mm	80	7.8
Polypropylene	54	0.80 mm	76.5	0.91
Basalt	60	22 µm	2727.3	2.7
Wires	60	0.75 mm	80	1.38

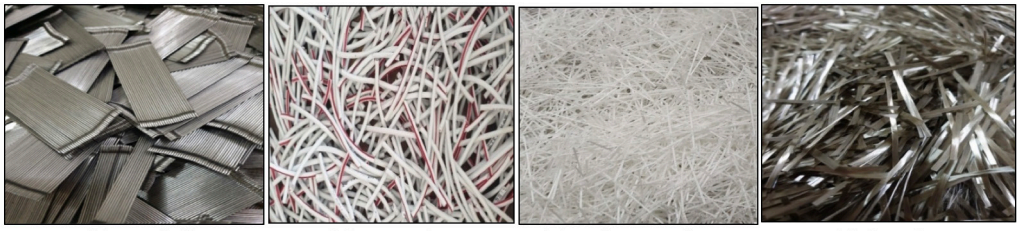

(a) steel fibers (b) pvc wires (c) polypropylene (d) basalt

Figure 1: The utilized fibers

3 EXPERIMENTAL PROGRAM

Fifty two cylinders are tested in this research in order to investigate the compressive and tensile behavior of concrete made with electric pvc wires, polypropylene fibers, steel fibers and basalt fibers. Twenty six cylinders are tested under compression strength test while the other twenty six cylinders are tested under splitting tensile strength test. The dimensions of the concrete cylinders are 150mm x 300mm. The test setup is shown in Figure 2.

(a) Compression test (b) splitting tensile test

Figure 2: Test setup

4 TEST RESULTS AND DISCUSSION

Test results are listed in Table 3. Steel fibers and electric wires are added in three different percentages 5%, 10% and 15% of the total cement weight. The addition of 15% steel fibers has duplicated the tensile strength of concrete and it has increased its compressive strength up to 8.9% compared to the control plain concrete. The addition of 5% and 10% steel fibers has insignificant effect on the compressive strength of concrete while it has increased its tensile strength up to 59% and 35% respectively.

Electric pvc plastic wires are recycled into concrete in three different percentages.

The addition of wires has an adverse effect on the compressive and tensile strengths of concrete. The addition of 5%, 10% and 15% wires has reduced the compressive strength of concrete by 15%, 19% and 32.6% respectively. The tensile strength of concrete is also reduced by 20%, 15% and 25% due to the addition of 5%, 10% and 15% wires respectively. A comparison is made between the compressive and tensile strengths of the plain concrete and the concrete made with electric wires and steel fibers as shown in Figure 3 and Figure 4.

Basalt and polypropylene fibers have been added to the concrete mix in three different percentages 0.6%, 1.3% and 2.5% of the total cement weight. The addition of basalt fibers in any percentage has an adverse effect on the compressive and tensile strengths of concrete. The addition of 2.5% basalt fibers has reduced the compressive and tensile strength of concrete by 7% and 27.6% respectively. Decreasing the percentage of basalt fibers to 5 % and 10% has reduced the compressive strength of concrete by 12% and 11% respectively moreover it has decreased the tensile strength of concrete by 11.6% and 11% respectively.

The effect of basalt fibers on the tensile and compressive strengths of concrete is still unclear. Previous experimental results have shown the addition of basalt fibers increased the tensile and compressive strength of concrete while other studies have shown the opposite. Abdulhadi et al. (Abdulhadi, 2014) have shown that the addition of 0.3% and 0.6% volume of basalt fiber increased the splitting tensile strength of concrete by 2.6% and 22.9% respectively; while the addition of 0.9% and 1.2% volume reduced the splitting tensile strength of concrete by 11.3% and 19.8% respectively. Sarkar et al. (Sarkar & Hajihosseini, 2018) have shown that the addition of basalt fiber increased the concrete compressive strength in a range of 4.3% and 9.4%. Niu et al. (Niu et al., 2019) have shown that the addition of basalt and polypropylene fibers in high percentage has an adverse effect on the mechanical properties of concrete. Gnanasundar et al. (Gnanasundar.V.M & Palanisamy.T, 2017) have shown that the addition of basalt fiber can increase the strength of concrete when they are added in a low dosage up to 0.3% of concrete volume, while the addition of high percentage of basalt fibers has resulted in reducing the concrete strength. Murad et al. (Murad & Abd Aljabbar, 2019) have shown the addition of basalt fibers can increase the flexural strength of RC beams.

Thus, the percentage of basalt fibers has a significant effect on the compressive and tensile strength of concrete. In addition, the mechanical properties of concrete are significantly influenced by the orientation of fibers. In this test, the adopted percentages of basalt fibers are 0.6%, 1.3%, 2.5% where the addition of fibers have reduced the compressive and tensile strengths of concrete. Test results agree with the previous results found in the literature.

The addition of polypropylene fibers in any dosage has increased the tensile strength of concrete up to 22.8% where the maximum enhancement is measured with 2.5% fibers. The addition of 0.6% polypropylene fibers has increased the compressive and tensile strength of concrete up to 8.6% and 10.3% respectively. The compressive strength of concrete has reduced by 9.6% and 2.16% due to the addition of 2.5% and 1.3% polypropylene fibers. Figure 5 and Figure 6 compares between the compressive and tensile strengths of concrete made with basalt and polypropylene fibers.

Table 3: Test results

Name	Fiber	Fiber weight (Kg/m^3)	Average compressive strength (MPa)	Increment or decrement Fc· percentage (%)	Average tensile strength (MPa)	Increment or decrement Ft percentage (%)
Control	Control	0	41.7		3.44	
S16	Steel	16	41.3	-0.96	5.473	+59.1
S32	Steel	32	42	+0.72	4.65	+35.17
S48	Steel	48	45.4	+8.9	6.909	+100.8
V16	Wires	16	35.5	-14.9	2.732	-20.58
V32	Wires	32	33.8	-18.9	2.913	-15.32
V48	Wires	48	28.1	-32.6	2.577	-25.08
P2	Polypropylene	2	45.3	+8.6	3.794	+10.3
P4	Polypropylene	4	40.8	-2.16	3.442	+0.06
P8	Polypropylene	8	37.7	-9.6	4.225	+22.8
B2	Basalt	2	36.6	-12.2	3.042	-11.6
B4	Basalt	4	37.3	-10.55	3.058	-11.1
B8	Basalt	8	38.7	-7.19	2.489	-27.65

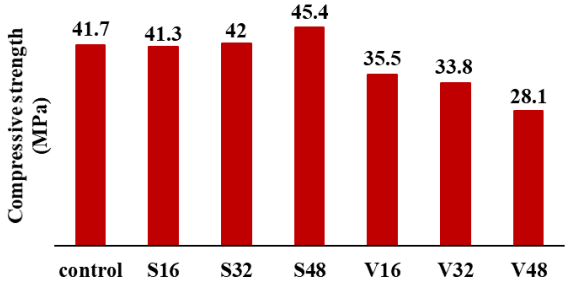

Figure 3: The compressive strength of steel fiber concrete and electric wire concrete

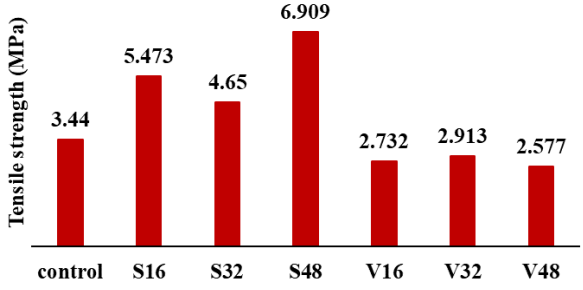

Figure 4: The tensile strength of steel fiber concrete and electric wire concrete

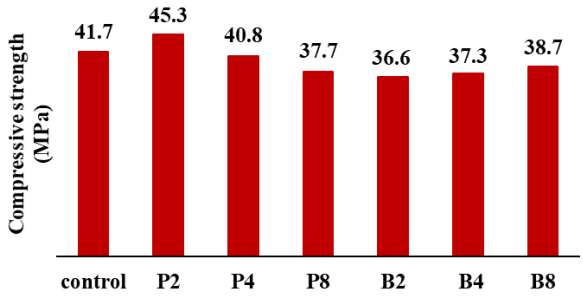

Figure 5: The compressive strength of steel basalt concrete and polypropylene concrete

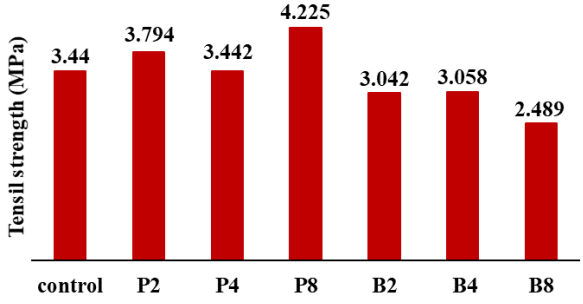

Figure 6: The tensile strength of steel basalt concrete and polypropylene concrete

5 CONCLUSION

Fifty two concrete cylinders are tested under compression and splitting tensile strength tests to investigate the compressive and tensile strength of concrete made with electric wires, steel fibers, basalt fibers, and polypropylene fibers. Fibers are added to the concrete mix in three different percentages (5%, 10% and 15% for steel and wire fibers) and (0.6%, 1.3% and 2.5% for basalt and polypropylene fibers) of the total cement weight. The following points summarize the test results:

- The addition of 15% steel fibers has duplicated the tensile strength of concrete and it has increased its compressive strength up to 8.9% compared to the control plain concrete.
- The addition of 5% and 10% steel fibers has insignificant effect on the compressive strength of concrete while it has increased its tensile strength up to 59% and 35% respectively.
- The addition of wires has an adverse effect on the compressive and tensile strengths of concrete. The addition of 5%, 10% and 15% wires has reduced the compressive strength of concrete by 15%, 19% and 32.6% respectively.
- The tensile strength of concrete is reduced by 20%, 15% and 25% due to the addition of 5%, 10% and 15% wires respectively.
- The addition of basalt fibers in any percentage has an adverse effect on the compressive and tensile strength of concrete.

- The addition of 2.5% basalt fibers has reduced the compressive and tensile strength of concrete by 7% and 27.6% respectively.
- Decreasing the percentage of basalt fibers to 0.6% and 1.3% has reduced the compressive strength of concrete by 12% and 11% respectively moreover it has decreased the tensile strength of concrete by 11.6% and 11% respectively.
- The addition of polypropylene fibers in any dosage has increased the tensile strength of concrete up to 22.8% where the maximum enhancement is measured with 2.5% fibers.
- The addition of 0.6% polypropylene fibers has increased the compressive and tensile strength of concrete up to 8.6% and 10.3% respectively.
- The compressive strength of concrete has reduced by 9.6% and 2.16% due to the addition of 2.5% and 1.3% polypropylene fibers.

REFERENCES

Abdulhadi, M. (2014). A comparative Study of Basalt and Polypropylene Fibers Reinforced Concrete on Compressive and Tensile Behavior. *International Journal of Engineering Trends and Technology (IJETT)*, *9*(6). Lokaliseret fra http://www.ijettjournal.org.

Alnahhal, W. & Aljidda, O. (2018). Flexural behavior of basalt fiber reinforced concrete beams with recycled concrete coarse aggregates. *Construction and Building Materials*, *169*, s. 165-178. DOI: 10.1016/j.conbuildmat.2018.02.135.

Amin, A. & Foster, S. J. (2016). Shear strength of steel fiber reinforced concrete beams with stirrups. *Engineering Structures*, *111*, s. 323-332. DOI: 10.1016/j.engstruct.2015.12.026.

Gnanasundar, V. M. & Palanisamy, T. (2017). Evaluation of mechanical properties of basalt fiber reinforced concrete. *International Journal of Intellectual Advancements and Research in Engineering Computations*, *5*(1), s. 857-861. Lokaliseret fra www.ijiarec.com.

Gull, I. & Balasubramanian, M. M. (2014). A New Paradigm on Experimental Investigation of Concrete for E-Plastic Waste Management. *International Journal of Engineering Trends and Technology (IJETT)*, *10*(4). Lokaliseret fra http://www.ijettjournal.org.

Jaysing, G. P. & Joshi, D. A. (2014). Performance of Basalt Fiber in Concrete. *International Journal of Science and Research*, *3*(5). Lokaliseret fra www.ijsr.net.

Murad, Y. & Abd Aljabbar, H. (2019). The Influence of Basalt and Steel Fibers on the Flexural Behavior of RC Beams. *International Journal of Civil and Environmental Engineering*, *13*(9), s. 548-551. Lokaliseret fra https://www.researchgate.net/publication/335665848_The_Influence_of_Basalt_and_Steel_Fibers_on_the_Flexural_Behavior_of_RC_Beams.

Murad, Y., Abu-Haniyi, Y., Alkaraki, A. & Hamadeh, Z. (2018). An experimental study on cyclic behavior of RC connections using waste materials as cement partial replacement. *Canadian Journal of Civil Engineering*, *46*(6), s. 522–533. DOI: 10.1139/cjce-2018-0555.

Nidhish & Arunima, S. (2017). Parametric study on fibrous concrete mixture made from e-waste pvc fibers. *International Journal of Advance Engineering and Research Development*, *4*(4).

Niu, D. et al. (2019). Experimental study on mechanical properties and fractal dimension of pore structure of basalt–polypropylene fiber-reinforced concrete. *Applied Sciences*, *9*(8), s. 1602. DOI: 10.3390/app9081602.

Ou, Y.-C., Tsai, M.-S., Liu, K.-Y. & Chang, K.-C. (2012). Compressive behavior of steel-fiber-reinforced concrete with a high reinforcing index. *Journal of Materials in Civil Engineering*,

24(2), s. 207-215. DOI: 10.1061/(ASCE)MT.1943-5533.0000372.

Sahoo, D. R., Solanki, A. & Kumar, A. (2015). Influence of steel and polypropylene fibers on flexural behavior of RC beams. *Journal of Materials in Civil Engineering*, *27*(8). DOI: 10.1061/(ASCE)MT.1943-5533.0001193.

Sarkar, A. & Hajihosseini, M. (2018). The effect of basalt fiber on the mechanical performance of concrete pavement. *Road Materials and Pavement Design*. DOI: 10.1080/14680629.2018.1561379.

Varghese, V. M. & Boby, L. N. (2017). Studies on the effect of fiber size on strength of fibrous concrete mixture made from recycled electronic waste fibers. *International Research Journal of Engineering and Technology*. Lokaliseret fra www.irjet.net.

Cite this article as: Murad Y. Z., Abdel-Jabbar H., "Mechanical Properties of Concrete Made with Electric Wires, Steel Fibers, Basalt Fibers and Polypropylene Fibers", *International Conference on Civil Infrastructure and Construction (CIC 2020)*, DOI: https://doi.org/10.29117/cic.2020.0119

Climate Change and the Structural Resilience of the Doha Metro

Georgios Nikolis
gnikolis_dbi@qr.com.qa
DB Engineering & Consulting, Doha, Qatar

Petros Chronopoulos
pchronopoulos_dbi@qr.com.qa
DB Engineering & Consulting, Doha, Qatar

Marin Griguta
mgriguta@qr.com.qa
Qatar Rail, Doha, Qatar

ABSTRACT

In recent years, the Doha Metro has been the spearhead of Qatar's effort to expand and upgrade its transportation infrastructure. In its current phase it will comprise three lines of an approximate overall length of 76 km and 37 stations. It is self-explanatory that such a significant infrastructure project should be a resilient one. The requirement for a 120 years design life for its permanent civil works structures implies that they should be resilient not only against the current environmental conditions, but also against future conditions due to the ongoing climate change. Resilient means that they will be able to serve their purpose under foreseen climatic changes during their design life. It is expected that climate change will increase the occurrence and intensity of weather events, especially in the Middle East and North Africa region. As per the AR5 assessment report of the Intergovernmental Panel on Climate Change "Climate change will have profound impacts on a broad spectrum of infrastructure systems..." transport being one of them. Furthermore, since transportation is interconnected with the economic and social welfare of an area, it is evident that the metro is a critical infrastructure system of Doha. In this paper, the climate change related main hazards on the Doha Metro permanent assets are presented along with the mitigation measures that have been adopted through provisions in the structural design and the materials used. Furthermore, suggestions for future contingency measures are made.

Keywords: Climate change; Doha metro; Hazards; Resilience; Mitigation

1 INTRODUCTION

The ongoing climate change in the Middle East region is expected to impact the rainfall, the wind, the ambient temperature, the air humidity and the groundwater composition. The risk of climate change becomes more prominent by the considerably long design life of 120 years of the network.

From a structural point of view, resilience means reliability, robustness and durability. Leaving robustness aside (see §3.1) as it is not in the scope of this paper, climate change can affect reliability in terms of loads and durability in terms of deterioration mechanisms. To this end, an assessment of the current resilience level is performed and its results are compared with the possible effects of the expected climate change. At the

end, conclusions are made on the resilience of the Doha Metro against expected changes to environmental conditions in its design service life.

2 CLIMATE CHANGE PHENOMENA CONSIDERED

The main civil structure assets of the Doha Metro are underground (Stations, Tunnels), at grade (Stations' Shelters, Depots, Stabling Yards, Troughs) and elevated (Viaducts, Stations). These can be affected by the frequency and intensity of the following phenomena influenced by the climate change:

2.1 Rainfalls / Floods

Changes in precipitation intensities and frequencies significantly influence many design parameters, e.g. groundwater table levels, volume of run-off water, etc. The most important risk associated with increased rainfall is that of flooding of underground civil works. Heavy and intensive rainfalls, in combination with an increasing groundwater table or sea level, can potentially lead to flooding with disproportionate consequences for the serviceability of the affected structures. For this reason, the flooding risk has been thoroughly investigated during the design stage of the Doha Metro, aiming to minimize all associated risks by planning and implementing several "lines-of-defense" (both construction and operational measures, see §3.3).

2.2 Winds

It is expected that climate change will affect the wind intensity around the globe. Winds are generally expected to decline in speed, but storms are expected to bring stronger winds with them as they are "fed" by the warmer air and water of the oceans. Qatar might not be directly exposed to the ocean, but the phenomenon of increased winds during storms cannot be excluded as a remnant of a strong storm, without further research.

2.3 Rising temperatures

The temperature around the globe is rising and so does the sea level. But it does not stop there: scientists all over the world are confident that temperatures will continue to rise in the future. For the Middle East in particular, as per Pal and Eltahir (2015) and Coffel et al., (2017), it is predicted that until the end of the century the temperatures will be rising to levels that the wet-bulb temperature threshold of 35^{o}C will be exceeded several times (compared to none until the date of that study). Moreover, the maximum dry-bulb temperature might reach 60^{o}C in some places (e.g Kuwait City). While most of the Gulf countries are vulnerable to one of the two temperature indexes, Qatar, due to its unique geographical location, is vulnerable to both.

2.4 Humidity

Due to the expected increase of the temperatures in the area, it is expected that the humidity levels in the atmosphere will also rise as increased volumes of water will be evaporating.

2.5 Groundwater composition alteration

It is expected that climate change will increase in the long term the salinity of the sea water due to the increased intensity of the precipitation – evaporation cycle. In addition, increased air pollution due to anthropogenic activities will further burden the groundwater with chemicals through rain. The possible result will be a more aggressive groundwater, with some chemicals (e.g., sulphates and chlorides) present in the form of a solution in the groundwater.

All the above, isolated or combined, might affect the civil works assets of the Doha Metro. Below it is presented how the structural and civil designs and selection of materials are to provide structurally resilient structures against the above phenomena.

3 STRUCTURAL/CIVIL DESIGN PROVISIONS TO ACHIEVE RESILIENCE

For the Doha Metro, Qatar Rail specified a 120 years design life for its permanent structures and the use of the Eurocodes for their design (see Qatar Rail reliability and durability assessment reports). The Eurocodes are in power in many countries within, as well as outside, the European Union. They emphasize on advanced concepts for the design of civil engineering. The most important of them are reliability, robustness and durability. Robustness is not in the scope of this paper (it was achieved through several strategies, the basic of them being tying, alternative load paths analysis and consideration of key elements). Furthermore, special mention will be made to the flood protection of Qatar Rail assets, as per Qatar Rail Empl0yer's Requirements (ER) and Public Works Authority – Qatar Sewerage and Drainage Design Manual.

3.1 Reliability

In order to achieve the required reliability, all the necessary measures listed under Clause 2.2 (5) of EN 1990 have been taken (with further guidance from ISO2394, (Tanner et al., 2007; Tanner & Hingorani, 2010). The ones covered in this paper are:

a) The choice of partial factors for 120 years design life, and
b) Durability.

3.1.1 Determination of the target reliability index

According to a structure's Reliability Class, EN 1990 provides minimum values for the reliability index β for 1 year reference period as well as for 50 years reference period. It does not however provide any values for a reference period greater than 50 years, so the target minimum reliability index for the reference period of 120 years must be calculated. We know that:

$$P_f = \Phi(-\beta) \tag{1}$$

P_f is the probability of failure of a structure; Φ is the cumulative distribution function of the standardized normal distribution and β the reliability index. Equation (1) can be written for 1 year reference period:

$$P_{f,1} = \Phi(-\beta_1) \tag{2}$$

From the elementary probability theory we know that the probability of success P_s is:

$$P_s = 1 - P_f \tag{3}$$

Combining equations (2) and (3) we have:

$$P_{s,1} = 1 - P_{f,1} = 1 - \Phi(-\beta_1) = \Phi(\beta_1) \tag{4}$$

For *n* years of reference period:

$$\Phi(\beta_n) = [\Phi(\beta_1)]^n \Rightarrow P_{s,n} = \left[P_{s,1}\right]^n \tag{5}$$

Also, for *n* years of reference period equation (1) can be written as follows:

$$P_{f,n} = \Phi(-\beta_n) \Rightarrow \beta_n = -\Phi^{-1}\left(P_{f,n}\right) = \Phi^{-1}\left(1 - P_{f,n}\right) = \Phi^{-1}\left(P_{s,n}\right) \Rightarrow \beta_n = \Phi^{-1}\left(\left[P_{s,1}\right]^n\right) \tag{6}$$

The results of equation (6) are compared in the following Table 1 to the values of β provided in Annex B of EN 1990 for 50 years reference period and values are provided for 120 years.

Table 1: Comparison of minimum values for reliability index β (ultimate limit states) for 50 years and values for 120 years reference period

Reliability Class	Minimum values for β - *ULS*			
	1 year reference period	50 years reference period [EN 1990]	50 years reference period [equation (6)]	120 years reference period
RC3	5.2	4.3	4.42	4.22
RC2	4.7	3.8	3.83	3.60

3.1.2 Partial factors calibration

Based on the above reliability index, all the partial factors for actions and resistances have been calibrated. This has been done by multipliers that were the ratio of the design value of each variable for the reliability index for 120 years to the value for the reliability index for 50 years.

In the case of variable actions, especially the ones that are related to the climate and thus possibly affected by the climate change, their expected maximum values might increase during the design life. Assuming that the standard deviation remains the same over the considered design life, the increase of the mean value $\mu_{q,n}$ of the maxima of a variable load q for a reference period of 120 years is:

$$\frac{\boldsymbol{\mu_{q,120}}}{\boldsymbol{\mu_{q,50}}} = \frac{\mathbf{1} + \frac{\sqrt{\mathbf{6}}}{\boldsymbol{\pi}} \cdot \boldsymbol{V_q} \cdot \boldsymbol{ln}(\mathbf{120})}{\mathbf{1} + \frac{\sqrt{\mathbf{6}}}{\boldsymbol{\pi}} \cdot \boldsymbol{V_q} \cdot \boldsymbol{ln}(\mathbf{50})} \tag{7}$$

The same methodology was followed for the rest of the loads and resistances and it finally led to an increase of the partial factors for the variable loads (with the exception of traffic loads on railway bridges) from 1.50 to 1.60. All the remaining partial factors did not change compared to the ones for 50 years design life.

3.2 Durability

The Doha Metro is located in a very aggressive environment with high concentrations of chlorides and sulphates present in soil and groundwater, high air and groundwater temperatures, high humidity and wind borne salts. Special measures that ensure the durability have been taken for concrete structures and steel structures.

3.2.1 Concrete structures

The fib Bulletin 34 adopts two different strategies that can be followed, sole or combined, to ensure the durability of concrete structures:

- Strategy A: Avoid the deterioration due to the type and aggressiveness of the environment, e.g. by use of stainless steel, steel fibers, cathodic protection, etc.
- Strategy B: Select an optimal material composition and structural detailing to resist for the specified design service life the deterioration threatening the structure.

Bored Tunnels

For the TBM tunnels Strategy A has been followed by implementing Steel Fiber Reinforced Concrete (SFRC) for the segmental lining (see also ACI 5441.R). The possible deterioration mechanisms during their service life and their mitigations are shown in Table 2 below. Based on Table 2, it is believed that the bored tunnels will not be affected by the climate change.

Table 2: Deterioration mechanisms and mitigations for the Doha Metro bored tunnels

Deterioration mechanism	**Mitigation**
Chloride-induced steel corrosion	Chloride threshold of steel fibres 5 to 10 times higher than that of traditional reinforcement, depending on concrete composition and fibre geometry; fibres follow the setting of concrete, thus no voids; fibres are manufactured by cold drawing steel, thus reduced roughness and imperfections.
Carbonation-induced corrosion (internal surface only)	No/minimum carbonation in saturated/near saturated concrete; could happen at the internal surfaces (rust stains) due to availability of carbon dioxide. However, for water/cement ratios below 0.4, the thickness of such regions is not more than a few millimetres.
Stray current-induced corrosion (from the metro power traction)	As per the American Concrete Institute *"Since the fibres are short, discontinuous, and rarely touch each other,* ***there is no continuous conductive path for stray or induced currents*** *from electromotive potential between different areas of the concrete".*
Sulphate attack	The CS 163 recommendations for the concrete composition and type of cement binder have been followed for the sulphate class S3.
Alkali aggregate reactions	Selection of non-reactive/inert aggregates.

Other Underground Structures (Stations, Troughs, Shafts, In-situ Tunnels, Foundations of Elevated Structures), Viaducts and Elevated Stations.

For these structures both Strategies A and B were combined (with more guidance based on (CS 163; Dauberschmidt, 2006; JCSS, 2001; QCS, 2010; Tang, 1996). The possible deterioration mechanisms during their service life and their mitigations are shown in Table 3 below:

Table 3: Deterioration mechanisms and mitigations for other underground structures, viaducts and elevated stations of the Doha Metro

Deterioration mechanism	Mitigation
Chloride-induced steel reinforcement corrosion	Strategy B: performance based durability modelling for carbon steel reinforced concrete to restrict the risk of corrosion to an acceptable limit.
Carbonation-induced corrosion (internal surface only)	Strategy A: Same as in bored tunnels..
Stray current-induced corrosion (from the metro power traction)	Strategy A: The provisions of relevant standards were followed (BS EN 50122-2, BS EN 50162 etc.)
Sulphate attack	Strategy A: Same as in bored tunnels..
Alkali aggregate reactions	Strategy A: Same as in bored tunnels..
Salt weathering	Strategy A: Properly consolidated and cured concrete with low water/ binder ratio (< 0.40)

For the performance based durability modelling mentioned under Strategy B in Table 3 above, the *fib* Bulleting 34 model has been selected as service life design model. The key input parameters are quantified as probabilistic distributions.

As per *fib* Bulleting 34, the target reliability index towards reinforcement depassivation has been selected as 1.3 for the elevated structures and 0.5 for the underground ones has been considered as the waterproofing membranes are expected to provide a reliable protection for quite some years and they have been successfully used at similar projects in the region.

In order to verify the results of this probabilistic approach provided by the Design Consultants we have followed the approach in the second Strategic Highway Research Program (SHRP2) of the Federal Highway Administration of the U.S. Department of Transportation: we have carried out several Monte Carlo simulations with 10,000 (ten thousand) trials per simulation and the results matched the ones of the Design Consultants. This simulation was used to approximately predict the possible effects of the climate change. A conservative approach for the temperature was made, as we assumed that the average ambient and groundwater temperature is already 10ºC higher than the current average (32ºC). Then in our models we considered the most conservative chloride migration coefficients from the approved concrete mix designs. The results are presented in Table 4:

Table 4: Increase in temperature due to climate change - Monte Carlo simulation results for the reliability index for durability

Structure	Target Reliability Index	Predicted Reliability Index
Underground (except tunnels)	0.5	≈ 0.7
Elevated	1.3	≈ 1.0

These results show that for the underground structures there is no impact, while for the elevated structures the possibility that the reinforcement will start corroding after 120 years has increased from 10% to 15%. It is worth noting that the considered chloride concentrations in the groundwater are in the range of 22,000 to 25,000 mg/l which is higher than the salinity of the Mediterranean Sea. These higher values are data from only a few boreholes, whereas the majority of the boreholes tests provided values in

the range of 2,000 to 5,000 mg/l. It is reasonably believed that any future groundwater contamination due to the climate change is covered by the chloride concentrations considered in the models.

3.2.2 Structural steel structures

The steel structures of the Doha Metro are located in a C2, C3 or C5-M environment (ISO 12944-2) and are protected with duplex coating. Based on the design, the minimum expected service life of the duplex coating system is 440 years for the C2 environment, 135 years for the C3 environment and 53 years for the C5-M environment.

The coating of the steel structures in C5 environment might start deteriorating at around 53 years, even earlier if the average air humidity and the number of humid days increase due to climate change. Although the situation is better with steel structures in C3 environment (current expectance of coating deterioration is at 135 years), climate change might reduce the expected service life of the coating. Therefore, regular inspections are expected.

The elastomeric bearings comprise stainless steel for the sliding surfaces and carbon steel parts that are classified under C5-M environment.

3.3 Flood protection of Qatar Rail assets

While flooding is not directly connected with the structural issues discussed above, it is a major threat to any metro. The Doha Metro is not an exception. Doha has undergone a very rapid development during the past years. As a result, many open areas, where previously permeable surfaces existed, have been paved, substantially affecting the storm water runoffs situation. Consequently the past flood records would have proved insufficient to assess the risk of flooding of Metro underground structures.

In addition to providing a design that meets Qatar Rail Employer's Requirements (ER) the Contractors were requested to perform assessments of the flooding risks at multiple locations for all the structures and establish design flood levels derived from external and internal flood sources (see Qatar Rail flood risk assessment reports).

Storm scenarios were studied assuming functional effective storm water drainage (Scenario 1) and, non-functional storm water drainage (Scenario 2). In addition, the consequences of utility bursts were also reviewed along with hazards posed due to rise in seawater and ground water levels. The critical flood levels at each asset were defined as the worst case predicted flood level of all of these sources for both Scenarios (1) and (2).

Considering the design life time of Doha Metro of 120 years, in order to account for predicted climate changes over the next century, the flooding models have taken into account the results of Ministry of Municipality and Urban Planning (MMUP) study on regional design rainfall in Qatar and of United Nation's Intergovernmental Panel on Climate Change (IPCC) Assessment Report 5 (AR5), by applying a defined climate factor.

A holistic approach was required for the modelling, as various flood elements could interact and/or occur simultaneously. Combined events were investigated, such as:

- Interaction: surface drainage system and coastal flooding,
- Interaction: surface drainage system and groundwater,
- Combination event: utility burst and rainfall event, and

- Internal flooding: caused by water tank leakage/overflow, water pipe leakage, sprinkler/fire water discharge and drainage system malfunction.

Simulations of surface water hydraulic behavior for a selection of storm profiles representing different storm duration and return period, as defined by the Qatar Rail ER, were carried out. The hydraulic models covered areas of interest in adequate detail to investigate the potential flooding at each asset site in both Scenarios (1) and (2). No modifications or options have been applied to the base model provided. The hydraulic models created allowed any predicted flooding from the surface water network to be mapped as it flows overland, modelled and quantified any ponding in the vicinity of the assets and defined the worst case flood elevation as the Design Flood Level. In alignment with industry best practice, a minimum asset level (freeboard) above the Design Flood Level has been defined in Qatar Rail ER in order to take account of:

a) Contingency for uncertainties in modelling data, and
b) Dynamic effects such as wind-blown effects and minor wave effects.

The urban development of the city of Doha is a very fluid environment and the coordination with interested Stakeholders required a constant re-iteration and update of the flooding models and entrance levels. This was feasible up to a point in time where the construction of the Metro assets progressed to an extent where the changes of the structures were not feasible anymore. Later developments of the city infrastructure may have altered, at particular locations, the flood prediction and, consequently, the established Design Water Level at the same locations. Nevertheless, in order to ensure the protection against the flooding risk, Qatar Rail performed simulations of the impact of changes on the entire Metro network combined with jointly inspection with interested Stakeholders. As a result, assets potentially exposed to a defined gradual flood risk, as consequences of changes, were identified and construction measures by Qatar Rail and/or interested Stakeholders combined with operational measures were defined and implemented.

It is worth mentioning that the city of Doha is still under development, especially near the Metro assets, and future changes would require revisiting today's configuration, followed by construction and operational measures to ensure a continuous flood protection of the Metro assets.

4 CONCLUSION

The major structural/civil design provisions against the effects of climate change for the Doha Metro have been presented in this paper. The combination of considered reliability requirements, durability modelling and conservative values for the loads (climatic or not) dictated by Employer's Requirements (e.g. groundwater level at ground level for the permanent structures) safeguards the resilience of the Doha Metro against the climate change from a structural point of view.

However, it should be noticed that all the work presented in this paper has been carried out based on tools and data that we have in our hands today. Sophisticated climate models and tools are being constantly developed and will continue to do so. Weather data should be collected, analyzed, evaluated and compared to the assumptions regarding climate in this paper. Additionally, regular inspections and structural monitoring would be of utmost importance for such an important project.

REFERENCES

ACI 544.1R (2002). *State-of-the-Art Report on Fiber Reinforced Concrete*. (Report 544.1R-96 (Reapproved 2002)). American Concrete Institute (ACI), Farmington Hills, MI, the USA.

BS EN 50122-2 (2010). Railway applications. Fixed Installations. Part 2: Protective provisions against the effects of stray currents caused by d.c. traction systems.

BS EN 50162 (2004). Protection against corrosion by stray current from direct current systems.

Coffel, E., Horton, R. & Sherbinin, A. (2017). Temperature and humidity based projections of a rapid rise in global hear stress exposure during the 21st century. *Environmental Research Letters*, 13.

The Concrete Society (2008). *Guide to the Design of Concrete Structures in the Arabian Peninsula* (CS 163), the UK.

Dauberschmidt, C. (2006). *Untersuchungen zu den Korrosionsmechanismen von Stahlfasern in chloridhaltigem Beton* (Doctoral dissertation). RWTH Aachen University, Aachen, Germany.

European Committee for Standardization, CEN. Eurocodes EN1990, EN1991-1-1, EN1991-2, EN1992-1-1, EN1992-2, EN1993-1-1, EN1993-2, EN1998-1, EN1998-2. CEN, Brussels.

Fib (2006) Model Code for Service Life Design, fib Bulletin 34. International Federation for Structural Concrete (fib), Lausanne, Switzerland, 1st edition, 126 pp.

International Organization for Standardization. ISO2394:1998. General principles on reliability for structures. Geneva.

International Organization for Standardization. ISO12944-1 to ISO12944-8, Paints and varnishes - Corrosion protection of steel structures by protective paint systems. Geneva.

Joint Committee on Structural safety (JCSS) 2001. Assessment of Existing Structures, RILEM publications S. A. R. L., edited by D. Diamantidis.

Joint Committee on Structural safety (JCSS) (2001). Probabilistic Model Code.

Ministry of Municipality and Urban Planning (MMUP). Study on regional design rainfall in Qatar. Doha.

Pal, J. & Elathir, E. (2015). Future temperature in southwest Asia projected to exceed a threshold for human adaptability. *Nature Climate Change*, 6, 197-200.

Public Works Authority and Ministry of Environment, State of Qatar. Qatar Construction Specifications. Doha.

Public Works Authority, State of Qatar. Qatar Sewerage and Drainage Design Manual. Doha.

Qatar Rail & Contractor JVs (ISG, RLR, QGD, FYAP, ALYSJ, SOQ, PSH, SPH). *Flood risk assessment reports for the Doha Metro Projects*. Doha.

Qatar Rail & Contractor JVs (ISG, RLR, QGD, FYAP, ALYSJ, SOQ, PSH, SPH). *Durability and reliability assessment reports for the Doha Metro Projects*. Doha.

Qatar Rail. Qatar Integrated Railway Project, Employer's Requirements.

Tanner, P. & Hingorani, R. (2010). Development of risk-based requirements for structural safety, Joint IABSE – fib Conference on Codes in Structural Engineering, Dubrovnik, 2010, ISBN 978-953-7621-05-6.

Tanner, P., Lara, C. & Hingorani, R. (2007). Seguridad estructural. Una lucha con incertidumbres, Hormigón y Acero, No. 245, pp. 59-78, Madrid, 2007, ISSN 0439-5689.

Tang, L. (1996). *Chloride Transport in Concrete – Measurement and Prediction, Chalmers University of Technology*, Dept. of Building Materials. ISSN: 1104-893X

U.S. Department of Transportation, Federal Highway Administration, second Strategic Highway Research Program (SHRP2), Service Life Design for Bridges (R19A).

Cite this article as: Nikolis G., Chronopoulos P., Griguta M., "Climate Change and the Structural Resilience of the Doha Metro", *International Conference on Civil Infrastructure and Construction (CIC 2020)*, DOI: https://doi.org/10.29117/cic.2020.0120

Towards Sustainable Public Open Spaces for Promoting Human Comfort, Health and Well-Being: The Case of Oxygen Park in Doha, Qatar

Eman Al-Fadala
200558264@student.qu.edu.qa
Architecture and Urban Planning Department, Qatar University, Doha, Qatar

Fodil Fadli
f.fadli@qu.edu.qa
Architecture and Urban Planning Department, Qatar University, Doha, Qatar

ABSTRACT

Public Open Spaces (POS) are an important and necessary component of the urban city design. Well-designed and well-functioning public open spaces provide a variety of social, economic, environmental, physical and psychological advantages for populations, and thus play a substantial role in improving the quality of city life and contributing to livability. Doha city, the capital State of Qatar, has encountered a rapid urbanization which brought with it an increasing number of inhabitants and the implementation of many urban projects (Salama & Wiedman, 2013); these changes demand well-designed and well-functioning public open spaces. Responding to this need, this paper aims to develop design guidelines for a sustainable public open space by exploring the physical and non-physical characteristics of a few key public open spaces as well as the ways in which environmental conditions impact user comfort, health and well-being—with an eye for accessibility, sociability, activities and user's comfort—in these POS. To achieve this aim, a combined methodology based on quantitative and qualitative techniques was developed and used to encompass the multi-dimensionality of the POS. Expected outcomes state that POS can become catalyst for healthy urban spaces if a series of multi-dimensional parameters are considered at all design stages.

Keywords: Sustainable urban development (SUD); Public open spaces (POS); Sustainable city design; Oxygen park

1 INTRODUCTION

Qatar has recognized the need to concentrate on Sustainable Urban Development (SUD) goals expressed through developing sustainable cities. SUD directives significantly focus on treating factors that affect human comfort, health and well-being. Research has shown that Public Open Spaces (POS) are a necessary component of urban city design (Habitat, 2014). Well-designed and well-functioning POS, provide a variety of social, economic, environmental, physical and psychological advantages for populations, and thus play a substantial role in improving the quality of city life and contributing to livability.

Cities worldwide are becoming larger, more complicated as the urban areas experiencing rapid urban growth and the increase in the population. This accelerated change, in turn, has led to emergence problems related to the urban design qualities of POS. Most POS are rather uncomfortable because they were not designed to adapt to

different environmental conditions.

Oxygen Park is considered a new POS developed for serving as an outdoor green oasis in education city that invited the students of the QF and the general public to refresh their bodies, minds and emotions by walking, engaging in sports and discovering the symbiotic relationships between plants, oxygen and healthy living. Thus, the aim of this study is to develop a set of design guidelines for sustainable POS to ensure that Doha POS promote comfort, health and well-being and, in turn, achieve SUD. The main objectives are to assess the physical and non-physical characteristics of these POS and examine how environmental parameters impact user comfort.

In order to do so, an evaluation criteria framework has been developed. Accordingly, combined methodologies were adopted to realize the main aim. More specifically, this study used both quantitative and qualitative techniques to encompass the multi-dimensionality of the POS. These approaches are rooted in the four aspects of a sustainable POS, namely: accessibility, sociability, activity, and user comfort, that is, the evaluation criteria, in order to then proceed to evaluate the abilities of Oxygen park and their impact on users' comfort, health and well-being.

The outcomes outline that the major physical factor of Oxygen park influencing is user comfort. Furthermore, the findings reveal that comprehending the mutual relations among environmental conditions and psychological adaptation factors may prove significant for evaluating the design qualities of POS. Notably, the study found that the microclimate, noise level and air quality significantly affected psychological adaptation, user comfort and health.

2 PUBLIC OPEN SPACES AND USER COMFORT, HEALTH AND WELL-BEING

Public Open Spaces (POS) is any land open into outdoor space which is accessible by all and it includes parks, plazas, squares, etc. where these spaces are normally publicly owned and can be used by all on daily basis for various activities (Nochian, Tahir, Maulan & Rakhshanderoo, 2015). The term 'comfort' is synonymous with 'well-being' and defined as 'the immediate state of being strengthened through catering the needs for relief, ease, and transcendence addressed in the four contexts of comprehensive human experience: sociocultural, environmental, physical, and psycho-spiritual' (Kolcaba, 2003). Meanwhile, 'health', as defined by the World Health Organization (WHO), signifies 'a state of complete physical, mental and social well-being and not merely the absence of disease or infirmity' (WHO, 1948). Comparatively, 'well-being' signifies 'the presence of positive emotions and effects (e.g. happiness), the absence of negative emotions (e.g. anxiety), and satisfaction with life' (Pintoa, Fumincellic, Mazzoc, Caldeirad & Martins, 2017).

In this context, POS yields socio-cultural, environmental, physical psychological benefits by enhancing social interaction (socio-cultural well-being), fostering physical activity (physical well-being) and enhancing relaxation and reducing stress (psychological mental well-being). Furthermore, POS have a great political and economic significance, and the degree to which any town has livable open grounds is a depiction of civilization (Brook, 2014). Several advantages accrue to an urban settlement with POS within the built environment. The most common benefits relate to health and wellbeing, tolerance,

learning, and economic. POS grounds can provide health gains as they act as arenas for inhabitants and employees to enjoy fresh air, lessen sedentary lifestyle, and exercise. Thus, open places are significant for residents' physical and mental health. Such spaces can further give social learning openings. They aid people to directly meet other people with different cultures and lifestyles. Thus, it is important to ensure that POS is accommodating the sustainable aspects.

2.1 Aspects of Sustainable Public Open Spaces

There are four aspects of an efficient POS which incorporate creative activities and stimulate use such as those that of accessibility, sociability, activities and user comfort (Ageing, 2009). The following Table 1 show these aspects as evaluation criteria that have used for the identified POS.

Table 1: Aspects of Sustainable POS

1	**Accessibility**	- Integrated diverse land with transportation systems. - Good signage system. - Space visually connected with adjacent buildings. - Equal access for all people.
2	**Sociability**	-Accessible for everyone. - High proportion of users in groups. - Emphasizing local identity. - People meet and see friends. - Feeling comfortable speaking with strangers.
3	**Activities**	-Lively, attractive environment for visitors. - Utilized by everyone (high proportion of users in groups). - Recreational places that activate the space and enable diverse activities.
4	**User Comfort**	- Meeting expectations to satisfy user groups. - Safety: by installing lighting oriented towards faces, CCTV and security personals. - Provision of places to sit. - Air temperature, humidity and wind. - Noise and air quality.

2.2 Physical Public Open Spaces Characteristics

POS physical characteristics can be studied through usage and perception. The framework of the identified physical elements of a POS includes vegetation, water features, lighting and safety, urban furniture, general bins, signage, and floorscapes (Madanipour, 1996). Meanwhile, a questionnaire can be used to determine users' perceptions of particular elements and their influence.

2.3 Non-Physical Public Open Spaces Characteristics

Psychological variables affect user perceptions of comfort. There are five variables constitute the framework for evaluation, namely: environmental stimulation, time of exposure, perceived control, naturalness of the space and expectations and experience (Nikolopoulou & Steemers, 2003).

2.4 Environmental Conditions Impacting User Comfort

Microclimatic conditions refer to the sets of atmospheric elements that connect the climate of metropolitan areas and civil activities (BojinSki & VerStraete, 2014). Relative humidity, air temperature, and wind velocity are variables of the microclimate that have focused on this study. In other respect, noise is an important public environmental problem. It signifies undesirable sounds in outdoor environments that negatively impact human comfort. A noise level is measured by decibels (dB) (Table 2) (Audiology, 2009).

Table 2: Level of Noise in Decibels (Audiology, 2009)

Category	Faint	Soft	Moderate	Loud	Over 85 dB for long period can cause loss	Very loud	Uncomfortable	Painful and dangerous
Decibel	20	30 – 40	50 – 60	70 – 80		90 – 100 - 110	120 (Dangerous over 30 seconds)	130 – 140

Meanwhile, air quality refers to the condition of the air and the degree to which it is free from harmful pollutants that impact human health and generate many environmental problems (Lanzafamea, Monfortea, Patanèa & Stranoa, 2015). Due to the emergence of several environmental problems, in 1999, the Environmental Protection Agency (EPA) developed the Air Quality Index (AQI) to estimate and monitor the overall state of the level of air pollution and human health (EPA, 1999) (Table 3). This index enables daily reports of air quality by measuring the concentrations of pollutants in urban areas and showing their associated health effects.

Table 3: Air Quality Index (EPA, 1999)

Levels of Health Concern	AQI Values	Colors and Meaning
Good	0 to 50	Air quality is good.
Moderate	51 to 100	Air quality is acceptable; a moderate health concern may exist.
Unhealthy for Sensitive Groups	101 to150	The public is not likely to be affected; sensitive people may experience health effects.
Unhealthy	151 to 200	Every person may start to experience some harmful health effects.
Very Unhealthy	201 to 300	Every person may experience serious health effects (health alert).
Hazardous	301 to 500	This is an emergency condition that demands health warnings.

3 STUDY METHODS, STAGES AND TOOLS

The study explores the POS of Oxygen Park through a particular focus on studying the POS design qualities to understand how their design provides sustainable POS aspects and which in turn promoting comfort, health, and well-being. To fulfil this aim, the overall research methods has adopted three steps (Fig. 1):

(1) Determination of the aspects of a sustainable POS directing the Oxygen Park through a review of the literature and research studies; (2) The quantitative method has been used to produce objective measurements that are fundamentally utilized to measure POS microclimatic variables, noise and air quality. This method helps to comprehend the overall environmental conditions, which are important in determining how to realize external psychological adaption and user comfort. Further, on-site measurements were done by using data devices. The Multifunction Environment Meter (CEM DT-8820)

utilized for air temperature, humidity and sound. The Kestrel 4500 (Pocket Weather Tracker), utilized for measuring wind velocity. The iPhone, fitted with an application called the Airvisual App (IQAir), which measured the air quality. Measurements were done on weekdays and weekends, from 8 am to 9 pm and logged every hour; (3) Qualitative method has been used to produce subjective measurements of a real-time situation. The authors carried out several site visits to understand the studied POS and the physical design elements. Furthermore, these measurements are conducted in order to obtain a better understanding of the design aspects of POS, comfort levels, perceptions, and human behavior. Hence, the main techniques were a questionnaire and observation.

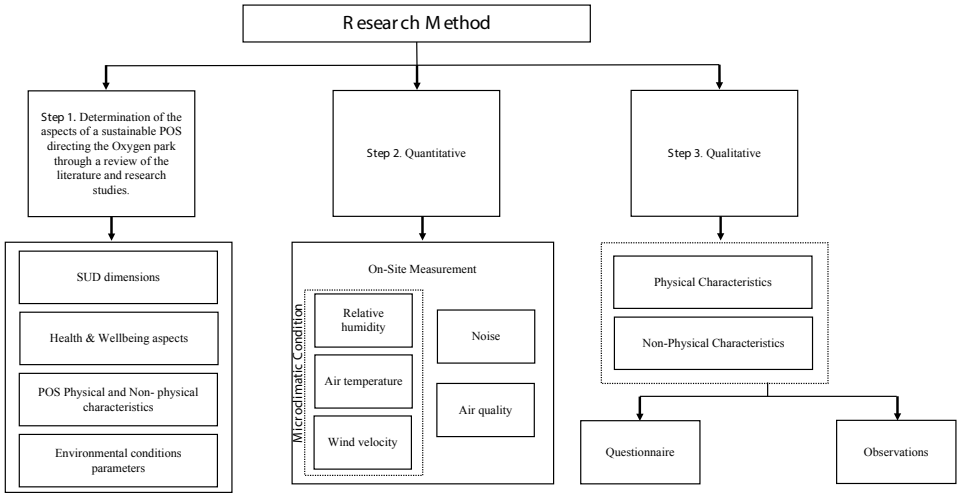

Figure 1: Research Method Used for This Study

4 OXYGEN PARK

4.1 Overview of the Study Area

Oxygen Park is considered a newly developed park in the Al Rayyan area (Fig. 2), and located within the boundaries of education city, where it was implemented by the Qatar Foundation (QF). The POS of Oxygen Park opened in the 2016 and occupied 130,000 m2 with the aim of serving as an outdoor green oasis in education city that invited the QF students and the general public to refresh their bodies, minds and emotions. The Park is accessible to people of all ages and is connected by Huwar Street, and Al Huqoual Street. Currently, the POS of Oxygen Park has no gates, or fences; it can thus be accessed from everywhere. Oxygen Park is divided into two zones. The first zone was allocated for sports constitutes two levels: upper and lower and the second for recreation (Fig. 3).

Figure 2: The Location Map of Oxygen Park

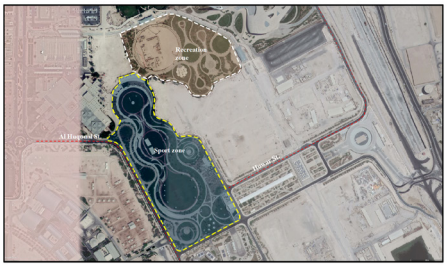

Figure 3: The Zones Map of Oxygen Park

4.2 POS Physical Characteristics Assessment

Oxygen Park, demonstrated some of the physical characteristics and elements, discussed in the literature review. The existing physical elements and related observations are as follows:

- Oxygen park has a variety of native plants, trees, shrubs and grass banks (Fig. 4).
- In terms of water features, over the edge of the pathway covering there are cascading waterfalls, which offer a beautiful sight, sound and water spray (Fig. 5).
- The lighting system is plentiful in different zones throughout the park (Fig. 6). There is spotlighting, column and 14 big lighting poles that provide better illumination at night. The park is also equipped with surveillance equipment such as CCTV and security personals.
- The lower level involves seats in sun and in shade. The upper level also provides seats for all users (Fig. 7). Further, there is amphitheater with grassy banks that provide space to gather, sit and see the sporting activities. Additionally, the park is equipped with trash and recycling bins (Fig. 8).
- The Oxygen park has a good signage system inside the park (Fig. 9).
- The surface of the ground in Oxygen Park is of a mixture of artificial hills and flat land. It has light concrete pavement, soft walking mats (rubber) and sand trails.

Figure 4: Vegetation

Figure 5: Water Feature

Figure 6: Lightings

Figure 7: Seats

Figure 8: Recycle Bins

Figure 9: Signage

4.3 POS Non-Physical Characteristics Assessment

4.3.1 User Physical Well-Being: Activities

Both social and optional activities were observed. Users were found sitting on the green hills enjoying their time and relaxing, or walking around the POS. There is a certain spot very attractive to adults and children: the circular multi-use sports courts, which is offer a running path and pitches.

4.3.2 User Psychological Well-Being: Psychological Adaptation

On day 1: questionnaire assessment (24-04-2019)—weekday: during the morning from (8am to 11am), based on the survey results, 100% of users did not desire any change in the humidity level or wind velocity (Fig. 10). However, 33% of users were not satisfied with air temperature at (9am). Between (4pm and 5pm), the users began to endure overall weather conditions. During the evening period, from (6pm to 8pm), users were able of enduring general weather condition. It is important to note that at (1pm, 2pm and 9 pm), no users filled out the survey; this gap is evident in the graph. While on day 2: (27-04-2019)-weekend: from (10am to 12pm), users were unable to endure the weather conditions. Over the afternoon, at (1pm and 3pm), all users preferred low air temperature with low humidity, with 75% not pleased with the wind velocity. Time from (6pm to 9pm), the results show that users desired no changes into air temperature, humidity and wind velocity (Fig. 11).

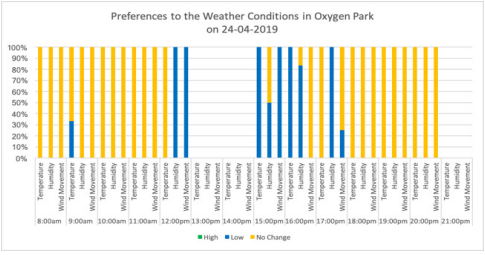

Figure 10: Preferences to Weather Conditions on 24-04-2019

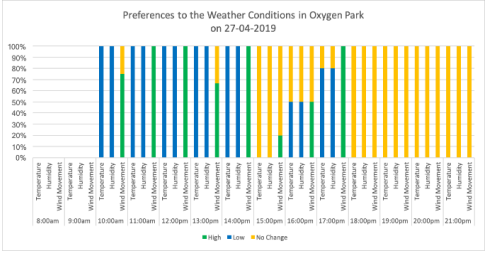

Figure 11: Preferences to Weather Conditions on 27-04-2019

Regarding duration of stay, 23.53% of visitors were able to stay in the POS for over an hour on weekday. It is significant to note that, on this day, there was a total of 34 visitors surveyed. While on weekday, 41 users in total were surveyed in the park.

Environmental stimulation is a unique feature that distinguishes this space. These features are evident in the beautiful landscape, the sound of the waterfall, and the greenery that encourage people to visit the POS. Furthermore, on weekday, it was observed that individuals and groups used the park between (8am and 3pm); individuals, groups, and families frequented it between (4pm and 8pm) and families constituted the highest percentage of visitors after (6pm). While on the weekday during the time between (10am and 12pm), it was noticed that the POS was occupied more by individuals. In contrast, between (3pm and 9pm), the park was primarily used by individuals and groups, including a few families.

4.4 Environmental Conditions Assessment

Day 1: microclimate condition (24-04-2019): the hottest peak was recorded during the afternoon period at 3pm at 26°C, whereas, the humidity was found at one of its lowest levels at 25% and wind velocity was one of the highest recorded readings at 25.9 km/h (Fig.12). In other respect, the coolest peak was at 8pm at 22°C with one of the highest humidity levels at 33% and the highest wind velocity at 25.2km/h. Based on these readings, the sum temperature reached 17°C as per the outdoor comfort online calculator. For the day 2 (27-04-2019): the hottest peak was logged in between (1pm and 3pm), with 29°C, during which time low humidity was logged at 21% and moderate wind velocity was recorded at 21.6 km/h (Fig 13). Accordingly, the sum temperature reached 23°C.

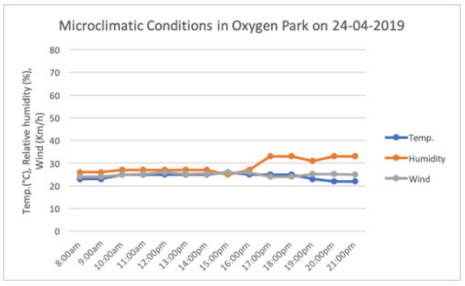

Figure 12: Microclimate Condition (24-04-2019)

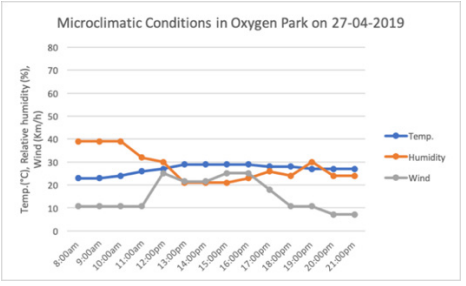

Figure 13: Microclimate Condition (27-04-2019)

On the other hand, the noise level readings on (24-04-2019) demonstrate that the highest sound level occurred between (5pm and 7pm) at 74dB (Fig. 14). Comparatively, the noise was low at (2pm) at 35dB (soft). Meanwhile, day 2: (27-04-2019): the noise level was between 30–40dB and 50–60dB. The high sound level was logged in the morning (9am) and (10am) at 56dB (Fig.15).

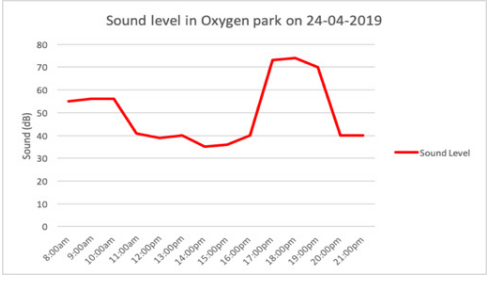

Figure 14: Sound level on 24-04-2019

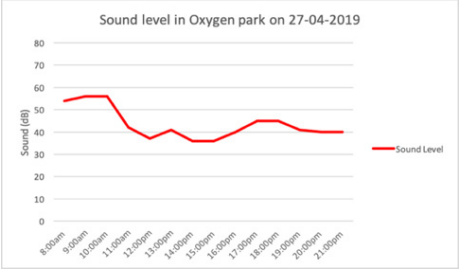

Figure 15: Sound level on 27-04-2019

The air quality readings of weekday were in an AQI range between 51–100 (yellow), signifies that the air quality was 'moderate' and acceptable (Fig. 16). Whereas, the air quality readings on weekend were between 101–150, that is, 'unhealthy air for sensitive groups' (Fig. 17).

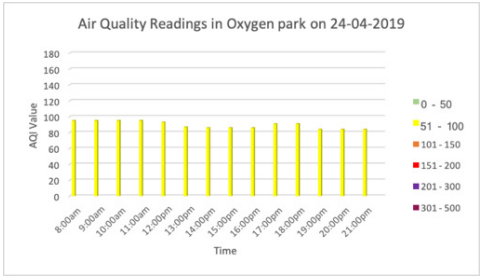

Figure 16: Air quality on 24-04-2019

Figure 17: Air quality on 27-04-2019

5 CONCLUSION

POS are essential ingredients of SUD and healthy cities. In this paper, it has been reviewed the POS Of Oxygen park—by unpacking three factors (physical, non-physical characteristics and environmental conditions) to deepen existing knowledge about sustainable specification. The findings affirmed that Oxygen Park relies on the promoting of the user comfort, health and well-being through sustainable urban design qualities. The study also confirmed that the physical characteristics significantly impact the comfort level experienced. In addition, the study assured the need to highlight the importance of non-physical characteristics that impact user psychological adaptation and comfort. According to the data of POS that have been obtained supported the conclusions of this study and its development of design guidelines for Doha's POS. These guidelines can be summarized as follows: (1) different types of vegetation and trees should be introduced; (2) Water features are beneficial and should be provided in all sorts of forms; (3) Lighting and safety elements should be provided; (4) Adequate furniture should be available throughout the space; and (5) Signage should be readable and well distributed. Through consideration, all of that POS can promote user comfort and well-being.

REFERENCES

Ageing, A. G. D. o. H. a. (2009). *Health Spaces & places: a national guide to designing places for healthy living*. Retrieved from Planning Institute of Australia: https://www.healthyplaces.org.au/userfiles/file/HS&P%20An%20overview.pdf

Audiology, A. A. O. (2009). *Level of noise in decibel*. In: American Academy of Audiology.

Brook, D. A. (2014). *History of Future Cities*. New York: W. W. Norton & Company.

BojinSki, S. & VerStraete, M. (2014). *The concept of essential climate variables in support of climate research, applications, and policy,* (vol. 95): Bulletin of american meteorological society.

EPA. (1999). Guideline for reporting of daily air quality – air quality index (AQI). In. Office of Air Quality Planning and Standards: Research Triangle Park, NC 27711.

Habitat, U. N. (2014). *Public Space in the Global Agenda for Sustainable Urban Development*. Retrieved from Nairobi GPO Kenya: www.unhabitat.org

Kolcaba, K. (2003). *Comfort theory and practice: a vision for holistic health care and research*. Ottawa: Springer Publishing Company.

Lanzafamea, R., Monfortea, P., Patanèa, G. & Stranoa, S. (2015). Trend analysis of Air Quality

Index in Catania from 2010 to 2014. ATI 2015 - *70th Conference of the ATI Engineering Association*, *Energy Procedia, 2015*(82), 708-715.

Madanipour, A. (1996). *Design of Urban Space*. In. London: Wiley.

Nochian, A., Tahir, O., Maulan, S. & Rakhshanderoo, M. (2015). A comprehensive public open space categorization using classification system for sustainable development of public open spaces. In (Vol. 8). Serdang: Universiti Putra Malaysia.

Nikolopoulou, M. & Steemers, K. (2003). Thermal comfort and psychological adaptation as a guide for designing urban spaces. *Energy and Buildings*, 95-101.

Pintoa, S., Fumincellic, L., Mazzoc, A., Caldeirad, S. & Martins, J. (2017). Comfort, well-being and quality of life: Discussion of the differences and similarities among the concepts. *2*(1), 6-12.

Salama, A. & Wiedman, F. (2013). *Demystifying Doha*. London, UK: Ashgate Publishing Limited.

WHO. (1948). *WHO definition of health (online)*. Retrieved from https://www.who.int/governance/eb/who_constitution_en.pdf

Cite this article as: Al-Fadala E., Fadli F., "Towards Sustainable Public Open Spaces for Promoting Human Comfort, Health and Well-Being: The Case of Oxygen Park in Doha, Qatar", *International Conference on Civil Infrastructure and Construction (CIC 2020)*, Doha, Qatar, 2-5 February 2020, DOI: https://doi.org/10.29117/cic.2020.0121

Development of a Software for Design and Design Comparison of Prestressed I-Beam for Highway and Railway Bridges Based on International Standards

Mustafa Can Yücel
mustafacan@bridgewiz.com
Bridgewiz Engineering R&D Co., Ankara, Turkey

Dilara Akdoğanbulut
dilara@bridgewiz.com
Bridgewiz Engineering R&D Co., Ankara, Turkey

Alp Caner
acaner@metu.edu.tr
Middle East Technical University, Ankara, Turkey

ABSTRACT

New computer software is being developed within Bridgewiz R&D Co. for the aim of rapidly comparing design solutions for a prestressed I-beam (highway or railway bridge) according to different international specifications. The software will perform a series of beam designs based on user inputs and then make a comparison in terms of dimensions, material quantities, and total costs (using either user-defined or auto-acquired unit prices). The design and comparison results will be presented to the user in the form of a PDF report (as well as an on-screen window) which includes tables and charts for easy visualization. The initial specifications that are planned to be included in the software are AASHTO-LRFD, EUROCODE, and Turkish Highway Bridge Specifications for highway bridges and AREMA, EUROCODE, and Turkish Railway Bridge Specifications for railway bridges. Fresh engineers will be able to use the program for verifying their designs and experienced engineers can utilize the program for staying up-to-date with requirements of contemporary specifications. The parameters that will be designed by the software are the optimum number of girders, their geometry, girder lateral spacing, number of prestressing tendons and jacking forces (taking the losses into account), prestressing tendon distribution, deck reinforcement area, and deck section stresses. The development is supported by KOSGEB – a Turkish government organization for supporting micro and small companies on research and development projects.

Keywords: Bridge; Design; Prestressed I-beam; Design comparison; Software

1 INTRODUCTION

Even though new technologies and construction techniques are continuously being developed for building bridges, most of the time these methods are used for bridges having an extraordinary feature such as long spans, increased heights, heavy loads…etc. For simpler and more common requirements, prestressed I-beam bridges are still widely preferred due to their standardized manufacturing process and ease of construction that result in lower costs and faster completion times. This trend can be seen in the ratio of I-beam bridges to the overall stock; the 97% of the bridges in Turkey and 75% of the bridges in the world are of I-beam (Figure 1).

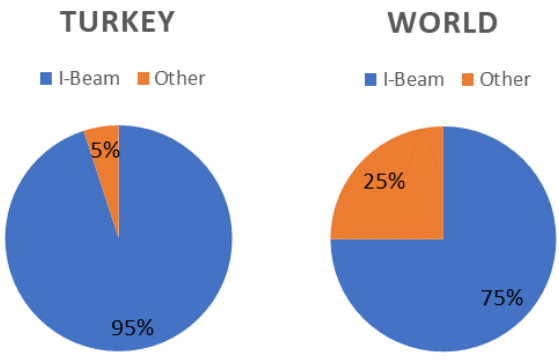

Figure 1: Quantity Distribution of Bridge Types in Turkey and the World

The common internationally-used specifications for these bridges are not beginner-friendly and sometimes lead to confusion among inexperienced engineers. Moreover, if a foreign standard is used in a country (for example, AASHTO and EUROCODE are the most commonly used specifications in Turkey), the risk for miscalculations increases due to the language gap and the differences in engineering practices.

There are advanced software suites that can design a bridge according to the aforementioned specifications, however, most of the time these are sophisticated finite element programs that require extensive amounts of information, knowledge, and expertise on the subject as well as time-consuming model creation and analysis definitions. They are not optimized to be used for quick and simple partial designs, single item design verifications (such as the number of tendons needed) and education of fresh engineers on bridge design approaches. To close this lack of tools in the market, a new application that performs I-beam design according to the common specifications and compares the results is being developed. The application also aims to supply basic information on design practices for educational purposes, allowing fresh engineers to sharpen their skills in design practices. More experienced designers can also use the software to initiate a new design basis before proceeding to advanced computations. The software is developed using C# language for Windows operating systems.

2 SOFTWARE INPUT PARAMETERS, CALCULATION FLOW AND REPORTING

For keeping the user experience non-complicated, the software is designed to ask the minimum number of necessary parameters from the engineer.

In the current development stage of the program, the following parameters are expected from the user to start a new design or design comparison:

1. Bridge type: The software is being developed to support two main bridge types according to their target vehicles: a highway bridge and a railway bridge. The selected type of bridge determines the available specifications that can be used in the design.
2. Specification: Based on the bridge type chosen in step 1, the available specifications

are presented to the user. The currently available codes are given in Table 1. The selection of specification determines the live load vehicles (design trucks or trains) that will be available in the further steps, the design equations and the limits to be verified.

3. Unit system: To ensure the usability of the program in different regions, both the SI and Imperial unit systems are supported. Users may select either one of them, and it will change all the units within the app.
4. Span length: The total span that will be crossed by the I-girders. This parameter determines the geometrical properties of the girder cross-section as well as several prestressing properties.
5. Deck width: The total width of the deck. This parameter influences the total number of girders needed along the deck.
6. Girder type: The user is asked to select a starting girder type. There are several commonly used sections are predefined into the software, and a user-defined section option is added for custom I sections.

Table 1: Available Specifications for Bridge Types

Highway Bridge	**Railway Bridge**
AASHTO	AREMA
EUROCODE	EUROCODE
Turkish Bridge Design Guidelines	

Once these six parameters are defined, the user can continue with the design. In the next phase, the minimum and the maximum number of girders that can be used in the deck section are presented, and the user is asked the following parameters:

7. The number of girders: The user needs to select the number of girders, which has to be between the minimum and the maximum limits.
8. Slab thickness: The thickness of the slab.
9. Deck compressive strength: The concrete quality of the deck.
10. Strand properties: The physical properties of the pretensioning strands should be defined. This section includes diameter, spacing, and modulus of elasticity, ultimate strength, and minimum yield strength.
11. Enforce debonding limit: This option is to enable and disable the upper limit for the ratio of debonded strands to the overall number of strands.

Once these parameters are defined, the program can calculate the total number of strands, the number of debonded strands, and a preliminary strand distribution (Figure 2).

If the user wants to calculate an approximate cost of the total bridge, the following additional parameters are needed:

12. Pier information: The height and diameter of every pier.
13. Total bridge length: The total length of the bridge (not a single span length).
14. Unit price information: The software is shipped with default unit pricing for the

construction materials, but these initial values should be revised based on regional market prices.

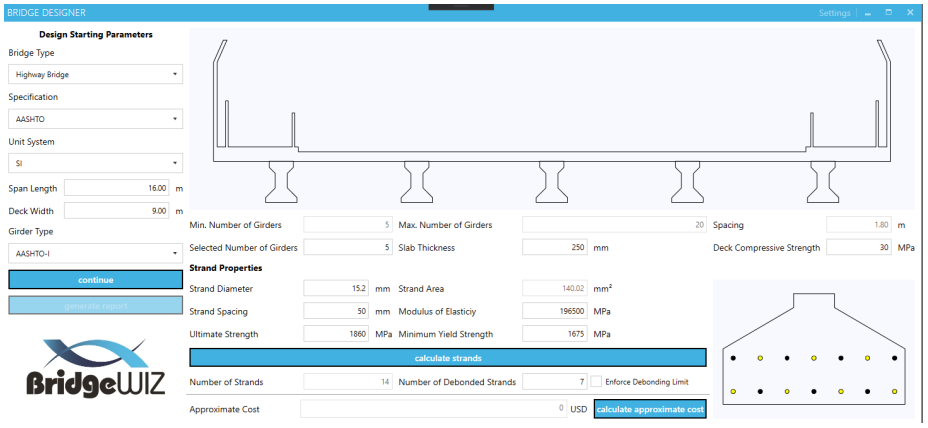

Figure 2: Strand Calculation Results

Once these additional parameters are entered, the software can calculate the approximated price for the bridge based on several assumptions, details of which are explained in further sections.

After performing the calculations, the user can get a PDF report which includes;

- Input parameters
- Section details
- Calculation details (such as dead and live load moments, prestressing forces after losses, single strand forces…etc.).
- Coarse cost estimation breakdown (concrete for superstructure and substructure, prestressing cable, reinforcement).

In the further development stages of the program, additional design calculations such as stress controls are planned to be implemented.

3 CALCULATION DETAILS

3.1 Dead, Superimposed Dead and Live Loads

The total moment generated by the dead load of the structure is assumed to be the maximum moment in a simply supported beam (1). The total dead load is calculated using the self-weight of girders and deck as well as weights of the sidewalk, wearing surfaces, barriers, and fences (superimposed).

$$M_{dl} = {}^{w_{dl}L^2}/_{8} \tag{1}$$

The live load moment is determined considering the user-selected vehicle. The live load distribution on one girder is calculated according to the selected specification. For example, while using AASHTO, Article 4.6.2.2.2b is used (AASHTO, 2017). The impact factor is also determined according to the selected specification and the most critical effect of the live load is calculated (considering both the interior and the exterior girders).

3.2 Stress Limits for Concrete

Stresses in concrete are checked at two phases; at the transfer of prestressing and at service condition with expected losses (2):

$$f_{bc} = -\frac{P_p}{A_g} + \frac{P_p * e}{S_t} - \frac{M_{gdl}}{S_t} - \frac{M_{slabw}}{S_t} - \frac{M_{sdl} + M_{llg}}{S_{tc}}$$
$$f_{bt} = -\frac{P_p}{A_g} + \frac{P_p * e}{S_b} - \frac{M_{gdl}}{S_b} - \frac{M_{slabw}}{S_b} - \frac{M_{sdl} + M_{llg}}{S_{bc}} \quad (2)$$

The limiting values for the tensile and compressive stresses in concrete will be taken from the selected specification; for AASHTO Article 5.9.4.1 and 5.9.4.2 are used (AASHTO, 2017). Usually, girders cracked at construction stages are rejected to be used at the site and girders cracked at service times will decrease the economic life of the structure. Immediately after prestressing, the end zones of prestressed precast girder can crack due to excessive prestressing. At the service state, a section at mid-span can crack due to some overloading of the section. As known, cracking can reduce the economic life of the structure. Gravity loads developed over the time of construction and service typically results in downward deflection. Usually, compression develops at top fibers and tension develops at bottom fibers in the absence of prestressing. Prestressing reverses the gravity effects. Components of stresses induced by different load cases can be superimposed on to each other to determine cumulative stresses at the top and bottom fibers of the element at any section. At mid-span usually, top fibers are in compression and bottom fibers may or may not be in tension depending on the level of prestressing. Longitudinal cracks can develop due to excessive compression that can decrease the durability of the concrete. Therefore, it is better to limit the compression stresses to a limit. The prestressed precast girder design requires a crack-free design to maintain the durability of the element. The selected tensile stress limits are lower than a tensile strength of concrete that will not allow any cracking.

3.3 Estimation of Minimum Required Number of Strands

The quick assessment of the number of strands is based on a computation of tensile stresses induced by gravity loads that need to be balanced by prestressing. Prestressing will not only overcome tensile stresses but can deflect the girder upwards as it will happen at some stages of construction. Maximum tensile stresses develop at the service stage. The amount of prestressing steel needs to overcome these maximum tensile stresses. Combined gravity stresses and prestressing stresses at mid-span needs to be less than concrete stress limits. As expected, gravity loads will deflect the girder downward and prestressing effects will deflect it upwards. Gravity loads will develop compressive stresses at top fiber and tensile stresses at bottom fiber at the mid-span. These tensile stresses need to be balanced by the counteracting prestressing forces. The deck is made composite to the girder through extended ties of the girder that usually work as shear connectors. The effective width of the deck needs to be computed that will be part of the composite section. The specifications allow some tension at the bottom flanges

of the section. Therefore, the tensile stresses that need to be balanced can be reduced by specification allowance. Total prestressing force can be computed from the tensile stresses that need to be balanced. The final stresses at the bottom will not reach the tensile stress limit of the specification. The number of strands that will develop the needed prestressing force can be computed based on the tensile stress limits of the strands. In the software, an approximate ratio of 20% losses is assumed for simplicity.

3.4 Estimation of Approximate Cost

The approximate cost of the bridge is calculated using the material quantity equations developed by statistical analyses (Hewson, 2003). In his study, Hewson proposed lower and upper limits for material quantities in terms of bridge type and deck area. In the software, only the upper limit is considered to prevent underestimation problems.

4 ACCESSING THE SOFTWARE AND FUTURE PLANS

The software is currently still under development and it is not open to closed or open testing yet. New specifications are being added and several new design checks will be added before any public release.

Any parties that are interested in the software can register their contact information to Bridgewiz to keep informed on any progress. The software is planned to be licensed per user for either limited or unlimited time.

5 CONCLUSION

A simple-to-use Windows PC software is being developed to establish preliminary design starting points or quick design checks/verifications as well as comparison of designs for different specifications. The software is targeted both to fresh engineers for preventing design errors and increasing their knowledge and senior engineers for quick calculations and getting up to date with new specification releases and code comparisons. The major aim of the software is to add a simple yet powerful tool to the engineer's arsenal for minimizing design starting errors and increasing efficiency of design processes. The software is still in development and will be available in near future to be sold using per-user licensing.

REFERENCES

American Association of State Highway and Transportation Officials (2017). *AASHTO LRFD Bridge Construction Specifications*, 4th Edition.

Hewson, N. (2003). *Prestressed Concrete Bridges: Design and Construction*. ICE Publishing.

Cite this article as: Yücel M. C., Akdoğanbulut D., Caner A., "Development of a Software for Design and Design Comparison of Prestressed I-Beam for Highway and Railway Bridges Based on International Standards", *International Conference on Civil Infrastructure and Construction (CIC 2020)*, DOI: https://doi.org/10.29117/cic.2020.0122

Vibration Prediction Model for Building Developments Adjacent to Railways

Martin Seiner
Seiner@vce.at
VCE Vienna Facility Management LLC, Doha, Qatar

Elisabetta Pistone
pistone@vce.at
VCE Vienna Consulting Engineers, Vienna, Austria

Günther Achs
achs@vce.at
VCE Vienna Consulting Engineers, Vienna, Austria

Hanno Töll
toell@vce.at
VCE Vienna Consulting Engineers, Vienna, Austria

ABSTRACT

This paper presents the experimental and computational evaluation of ground-borne noise and vibration impacts at sensitive receivers in the vicinity of existing track sections. Vibration problems occur as an effect of train passings adjacent to buildings and structures, thus needing to satisfy stringent vibration and ground-borne noise criteria. Therefore, it is necessary to quantify comprehensively the vibration impact in the design of new developments and the compliance with the provided criteria. Test measurements of vibration propagation through the structure are often possible only under certain circumstances since, based on the construction work progress, many relevant parts of the analyzed structure have not yet been completed. In such cases, measurement data is combined with computation data applying the Finite-Element-Method (FEM). The structure is modelled as a basis for dynamic analyses and the subsequent tuning of damping systems. The paper presents a semi-empirical prediction model on the basis of measurements and computational models that was applied to international projects. One of the projects is in close vicinity of one of the metro stations in Doha, including a six-level underground parking structure with various facilities and a large development with numerous towers of different use on top. Another project that will be presented in the paper is a luxury hotel located adjacent to another station along one of the Doha metro lines. Outcomes summarize the state of the art aforementioned topic.

Keywords: Vibration tests; Measurement data; FEM; Railways; Damping systems

1 INTRODUCTION

Inner-city railway sections are highly frequented, and they happen to be cross densely populated urban areas. Besides all benefits of modern mass transport systems, the generation of annoyance due to noise and vibration that impacts people living close by is an aspect that needs to be studied and possibly solved.

In general, human beings in buildings are relatively sensitive to structural vibrations. Particularly in places where people sleep, it is essential to prevent the interference of vibration.

Compared to car traffic, railways and trains are generating a much higher level of vibrations due to wheel-rail interface. Those vibrations are transferred via the track structure, the tunnel structure and subsoil to the adjacent buildings. Within those buildings, vibrations are often amplified and transferred directly to sensible locations.

The ground-borne noise and vibration problem occurs as an effect of train passings adjacent or below future developments, thus needing to satisfy stringent vibration and ground-borne noise criteria. Therefore, it is necessary to quantify comprehensively the ground-borne noise and vibration impact in the future developments and to verify the compliance with the provided criteria.

Such aspects need to be considered in an early design stage of both railway sections or developments, that are planned to be built close to existing tracks. In this case, semi-empirical spectral prediction models as presented in the FTA-manual are applied [FTA, 2018]. These models are based on the principle that vibration impact is a product of the source input (train emission), the vibration transfer through the ground, the coupling at the foundation (transfer soil-structure) and the amplification inside the building (transfer structure – receiver). All these spectra can be determined independently. Figure 1 shows the general prediction model of vibration and ground-borne noise.

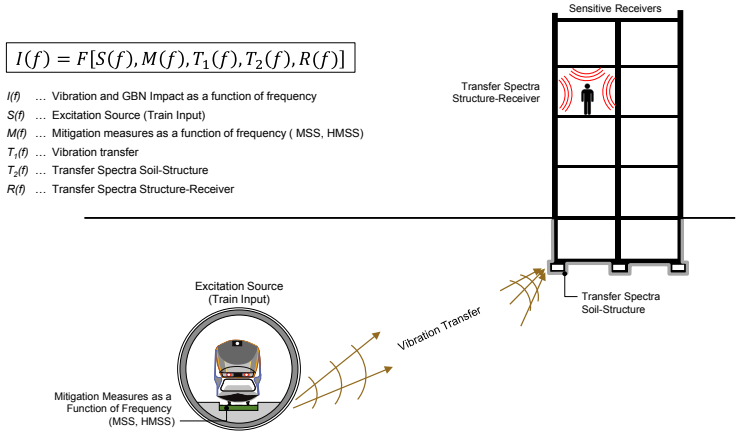

Figure 1: General prediction model of vibration and ground-borne noise

2 PREDICTION BASED ON MEASUREMENTS

Vibration propagation tests through the structure are one of the most valid tools for predicting future consequences. However, measurements are often not possible as the future structure does not exist yet. In such cases, measurements are limited to specific parts of the prediction chain, for instance:

- Measurement of the vibration emission with transducers placed on the rail, on the sleeper or on ballast less track, on the tunnel foundation or on the tunnel wall. The requirement is that similar trains running on similar track sections and speeds are accessible to measurements.
- Measurement of the ground transfer with transducers placed inside the tunnel and close to the future foundation. The requirement is that tunnel and excavation pit are already existing and accessible at the exact site, other measurement results can hardly be applied due to different soil conditions.

- Measurement of soil-structure interaction with sensors placed on bottom / on top of foundation.
- Measurement of building transfer with sensors placed at the foundation and at various locations inside the building.

Based on the construction work progress, many relevant parts of the analyzed structure have not yet been completed. In such cases, measurement data is combined with computation data applying the FEM.

3 PREDICTION BASED ON FEM

Vibrations due to train operations excite the structure at the base in the vertical direction. For this reason, the structure needs to be modelled and analyzed without any mitigation measures to quantify for the requirement to damp out vibrations caused by traffic. Each substructure needs to be modelled in detail regarding geometric and structural properties, i.e., properties of major structural elements, such as thickness and span of slabs, or material parameters, i.e., strength and stiffness properties that are associated with structural members. For the calculation of the vibration transmission through the building, a steady-state analysis is used. The numerical model is created using commercial software, such as Sofistik or SAP2000, and it consists of:

- Soil-structure interaction
- Foundation
- Basement
- Superstructures

Often it is not required to model the entire structural model. The finite element size strongly depends on the structural properties, but also on the settings of the dynamic analysis. The need for a fine FE mesh results in a very high number of nodes and model complexity. To avoid very long computational time, the model is subdivided into more sub-models based on the locations of expansion joints.

For the calculation of the transfer function the model is excited at the foundation with a uniform acceleration in the vertical direction. The response amplitude at specific points is compared to the uniform loading amplitude, thus not requiring train emission data as input.

Generally, a train can be approximated as a line source that generates vibrations at the wheel-rail interface. It is therefore useful to apply several concentrated impacts based on the train's wheelset location to consider a line source as input to the model. Please see Figure 2 for details.

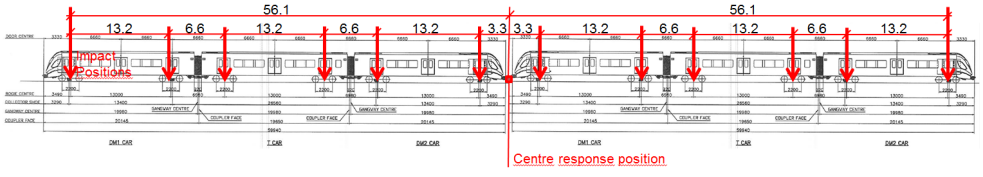

Figure 2: View of a typical load pattern for a passenger train

By defining as input nodes the ones at the locations of the running train or at the

foundation and as output nodes the ones at the locations of the future sensitive receptors (inside the apartments), the transfer function between these nodes can be determined. Transfer functions are the ratio of output and input and are unitless. They can be determined for each of the parameters displayed in Figure 1.

4 IMPLEMENTATION EXAMPLES IN DOHA

VCE has completed the ground-borne noise and vibration assessments for numerous major construction projects. Two related developments will be presented in Chapter 4. Measurements of transfer functions have been carried out by third party in order to ensure transparency and super partes results.

4.1 Metro station development

This area is characterized by the crossing of two lines, and several future developments, including a six-level underground parking structure with various facilities and a large development with numerous towers of different use on top. All future developments aforementioned need to satisfy very stringent vibration and ground-borne noise criteria. Thus, it was necessary to comprehensively quantify the vibration impact in the future developments and to verify compliance with the provided criteria.

Test measurements of vibration propagation through the structure of this station were not possible in the planning stage because, based on the construction work progress, many relevant parts of the structure were not yet completed. Figure 3 shows overviews during the construction condition. For this reason, a numerical approach using a spatial FEM to describe the vibration propagation in the structure was applied.

Figure 3: Overviews of construction condition during the planning stage

A comprehensive numerical model representing this area has been defined using commercial structural-analysis software Sofistik [VCE, 2018]. Buildings, basements, and the foundation system have been modeled in detail to identify dynamic characteristics of noise and vibration in structural members. Figure 4 shows the complete FEM model of the structure. Comprehensive parameter studies have been applied to verify settings, such as finite element size, time step size and the damping model assigned to the structure. Dynamic analysis has been conducted by means of direct integration methods for different load patterns, which represent metro trains passing at various locations on different tracks. Subsequently, transfer functions have been determined to transform predefined spectra of trains from the tunnel-level to specific floor levels. The ramping function as illustrated in Figure 3 is used to define the time dependent excitation for

Response History Analysis (RHA). Therefore, a Dirac impulse will be approximated by a rectangle ramping path. At time instances t>0.004 the ramping function remains zero, implying the structural response represents a free damped vibration.

Safety factors depending on location of the metro have been used to take into account possible uncertainties. At representative floor positions, floor velocity spectra have been compared to predefined velocity spectra of performance targets.

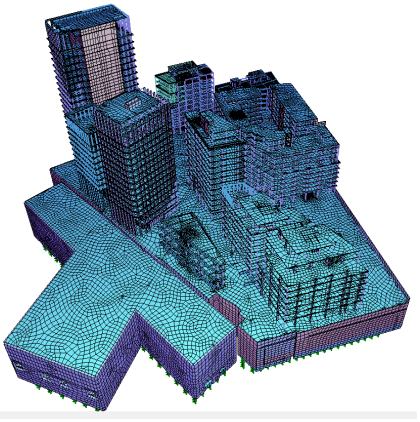

Figure 4: Finite element model of station development

The assessment resulted into the installation of mitigating track systems (mass-spring systems) in the track underneath the development. This very efficient method of mitigating track-borne impacts was made possible because the metro tunnels and the development on top were both at planning stage and so the issue of noise and vibration came to attention at the very right time. Figure 5 summarizes the results for ground-borne noise with and without mitigation measures.

Ground-Borne Noise Levels					Overview of the locations with exceeded limits (without mitigation measures)
Building output node & location	Use	Worst case floor	$L_{A,max,s}$ [dB ref. 5 x 10^{-8}]		
			without measures	measures included	
LC01-20011	office	4	65	35	
LC02-18131	residential	6	66	32	
LC03-18011	residential	6	63	30	
LC04-14001	commercial	4	47	32	
LC05-19091	office	12	59	34	
LC06-13071	office	3	69	29	
LC07-13071	office	3	69	27	
LC08-12101	office	2	64	23	
LC09-14001	commercial	4	53	41	
LC10-14001	commercial	-1	48	37	
LC11-13992	prayer room	-3	67	42	

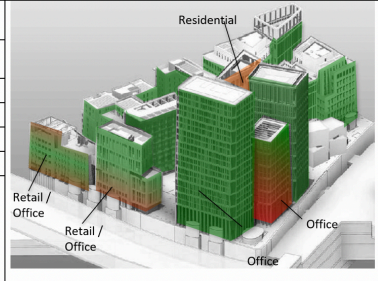

Figure 5: Summary of results and graphical overview

4.2 Hotel development

The Hotel development is 5 a stars hotel located adjacent to one of the metro stations. The site area is 11.184 m². The project is composed of three basement levels, ground floor, mezzanine, and seven stories with 257 guest rooms and amenities.

For this assessment, extensive measurement data could be used for the prediction [VCE, 2013]. The train emission was determined by a set of tests and the transfer through the soil was determined in the area adjacent to the project. The missing link was the coupling of the foundation and the vibration propagation through the building. For this calculation, a 3D model was generated in the commercial structural-analysis software SAP2000. Figure 6 shows the whole FEM model.

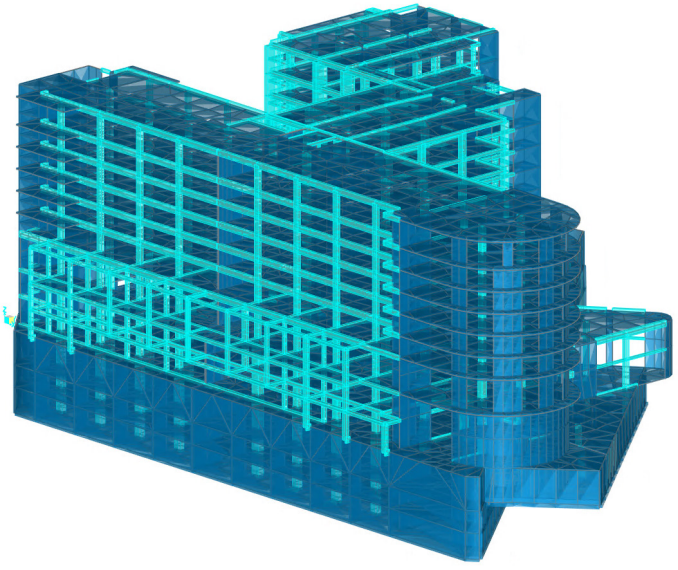

Figure 6: Finite element model of the hotel structure.

The prediction included the determination of the impact levels of vibration and ground-borne noise. For the calculation of the transfer function, the model is excited at the foundation with a uniform acceleration in the vertical direction. The response amplitudes at certain points are compared to the uniform loading amplitude. The result of this computation is the transfer function which denotes the amplification of the input amplitudes at an output node.

To verify the impact criteria, the levels were predicted in absence of any mitigation measures at specific points in the structure. The fact that the adjacent metro section included a mass-spring system as mitigation measure helped to have already ground-borne noise and vibration limits fulfilled. For this reason, additional mitigation measures were not required under the development foundations.

5 VALIDATION

In order to validate the outcomes of numerical models, validation measurements are often applied. Such measurements can include:

- Determination of track insertion loss: an in-situ determination of the insertion loss within the framework of a measurement campaign according to DIN SPEC 45673-3 to be conducted by a competent measurement engineer.
- Validation of building transfer (after completion) with artificial force impacts: the vibration amplitude caused by mechanical impacts generated by a falling mass (input) can generally be measured at all output locations at mid-span in vertical direction and compared to the transfer functions determined with the model. It is essential to select an input force with enough energy input, such as a standard soil sampling hammer, as shown in Figure 7.

Figure 7: Falling weight machine

- Validation measurements of ground-borne noise and vibration limits at sensitive receptors: usually vibration or acceleration transducers are placed on the floor of the sensitive receptor. Ground-borne noise is determined on the basis of vibrations according to international standards and is then compared to national limit values.

6 CONCLUSION

This paper presents a study relative to the evaluation of ground-borne noise and vibration impacts at sensitive receivers in the vicinity of existing track sections. Integration between experimental and computational information are presented here. Where test measurements were not possible, computation data applying the FEM were considered and developed. Structures were modelled as a basis for dynamic analyses and the subsequent tuning of damping systems.

The results stem from a semi-empirical prediction model on the basis of measurements and computational models that have been applied to international projects. The first project is relative to one of the metro stations in Doha, including a six-level underground parking structure with various facilities and a large development with numerous towers of different use on top. The analysis evidenced the necessity of the installation of additional mitigation measures. The second project was a luxury hotel located adjacent to another

station along one of the Doha metro lines. The analysis did not evidence the necessity of the installation of additional mitigation measures.

REFERENCES

Office of planning and environment, Federal Transit Administration (2018). *FTA-report: Transit noise and vibration impact assessment*. Ed (September).

VCE (2018). Doha Metro – Track Works TRK03: Ground-Borne Noise and Vibration Prediction for Msheireb Station, M010-MSI-TRK-DET-32940, November.

VCE (2013) N&V Assessment for Al Matar Dream Hotel, February.

Cite this article as: Seiner M., Pistone E., Achs G., Töll H., "Vibration Prediction Model for Building Developments Adjacent to Railways", *International Conference on Civil Infrastructure and Construction (CIC 2020)*, Doha, Qatar, 2-5 February 2020, DOI: https://doi.org/10.29117/cic.2020.0123

The Investigation of an Efficient and Effective Proactive Pipeline Integrity System

Masoud Forsat
m.forsat@qu.edu.qa
Department of Mechanical and Industrial Engineering, Qatar University, Doha, Qatar

Abdelmagid S. Hamouda
hamouda@qu.edu.qa
Department of Mechanical and Industrial Engineering, Qatar University, Doha, Qatar

ABSTRACT

In this paper, we propose the investigation of an efficient and effective proactive pipeline integrity system that uses multi-sensors for monitoring and inspection of the pipeline. Although the focus is on the pipeline, the methodologies will also be applicable for other systems including other energy infrastructure elements. The investigation focuses on the integration of multi-sources of data as well as multi-types of data for the same location (section) of the pipeline. The data include imaging, acoustic signals, electromagnetic flux system, and others. Moreover, the data could be obtained using continuous monitoring of the pipeline sections or through time intervals. In both cases, the data may also include censored observations. We develop several approaches to filter the data for noise and identify outliers, integrate the data streams into one degradation path and determine the optimum time to maintain or replace the pipeline sections being monitored. It will utilize extensive mathematical modeling for condition-based maintenance and repair, which will be developed by the investigators of this proposal. Following the suggestions of one of the reviewers of the last year's submission, we plan to validate and modify the model using standard or artificially developed defects such as corrosion, cracks, stress cracking, etc. to understand the output of the proposed methodology and validate the models accordingly.

Keywords: Pipeline; Infrastructure; Integrity system; Crack detection

1 INTRODUCTION

Regarding that the use of pipelines in the industries has been widened, and any leakage of their valuable or hazardous liquids could result in serious environmental problems, the attention to the faults and damages types and reason are compulsory for users and authorities. Structural damages caused by fault action are attracting much attention from engineers and researchers in recent years. The reasons for the pipelines damage are corrosion, cracks, vibration (Forsat, 2019), loads (Mirjavadi, Forsat et al., 2019) and etc. Also, a wide variety of damage detection and health monitoring of them have been used which including fiber optical sensors and piezoceramic transducer (Zeng, Dong et al. 2019). A lot of investigation on the pipeline damages detection and dynamic responses of the metals has been done (Mirjavadi, Forsat et al., 2019) and the results can be categorized to two overall sections, Visual Inspection and Computerized Inspection. Visual inspection mostly done by the some methods like NDT or ultrasonic (Lowe, Alleyne et al., 1998; Chang, Zi et al., 2017) and another method is computer

vision that has developed these days, is by the use of computer software and different kinds of analyzing (Jin, Zhang et al., 2014; Chen, Zhou et al., 2019; Mirjavadi, Forsat et al., 2019). The computerized inspection method is an economical and more appropriate replacement to the traditional and dangerous techniques of inspection of a pipeline, especially if a pipeline carrying dangerous liquids, flammable or be too small for human entry (Bahadori, 2017; Hawari, Alamin et al., 2018). In some industries that they have deep-water pipeline, the use of computer vision method is undeniable. The investigations on the marine deep water pipeline showed the importance of using internal damage detector machine controlling by the computers (Mao, Chu et al., 2015). The use of wireless sensors networks (WSN) for designing of the cost-effective leak detective system has been investigated. The experimental results showed the improvements of the WSN to other techniques in the context of damage detection in the monitoring water pipeline process (Ayadi, Ghorbel et al., 2019). The problem of pipe damaging is more important in gas transportation industries because any leakage in this system is hard to see by normal methods and most of them are dangerous liquids. An investigation on the acoustic wave detection system has been done in many researches (Sousa, Cruz et al., 2009; Xu, Zhang et al., 2013; Liu, Li et al., 2017; Zajam, Joshi et al., 2019). At the first stage, the phonation principle of the leakage and the characteristic of the sound source has been investigated and then the simulation of the leakage acoustic field has been done. The results showed the detection system could identify small gas leakage effectively and avoids false-alarms which caused by running conditions with a good prospect (Xu, Zhang et al., 2013). Specific routine and special operations are essential in order to maintain an efficient, reliable, and economic pipeline operation. These operations may be caused by hydrate formation, formation of inorganic deposits, transported product contamination and etc. (Stewart, 2016). The development of the many different monitoring devices and their modification and improvement over time have allowed the pipeline industry to be able to monitor all of the metal pipes and structures desired (Singh, 2017).

2 EXPERIMENTAL WORK

For the starting of the experimental works and testing of the robot and our simulation works, a circulate pipeline setup has been prepared (Fig 1). The setup consists of a water pump, 16cm thickness of pipes, three L bolts, and one water tank. The pipes were held by the hanging rods (Pipeline holder) to avoid any vibration on them and make them stable at their position. In addition, the temperature of the tanker is controlled by a thermostat for different water temperatures.

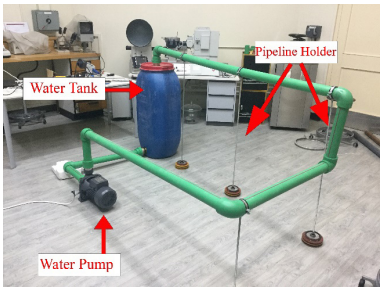

Figure 1: Pipeline setup details

The main robot will move through the pipeline while it takes data like images, recorders and etc. from whole sides of the pipe (Fig 2). After that, the collected data will exposure to several different image processing to classify in their own group. The different groups of images will be categorized by the type and shape of the damages on the pipe. As a result, the damages on the pipeline will be clear to identify and make a good decision for their maintenance.

The main components of the machine are: C arm, Gearwheel, Gear holder, and Robot holder

These parts help the image capturing robot to move through the pipeline system so they act as the mechanical part of the system that are responsible for controlling the movements.

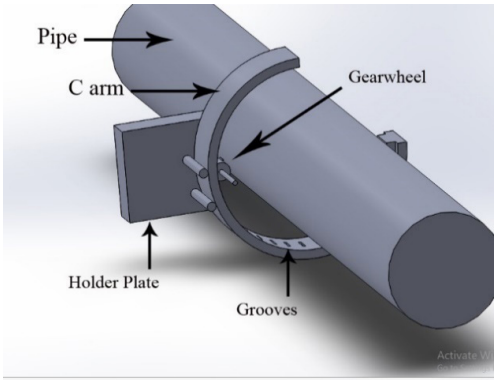

Figure 2: The components of the system

The first part of the machine is the arm that entitled C arm because of its shape that is the 3/4 a circle (Fig 3). With this arm, the camera can rotate around the pipe to capturing the images. It is consist of a cylindrical gear wheel that doing the rotating duty. In addition, it has two lockers in the ends of the circle to avoiding getting out of the ring the movement of this arm is along the pipeline system. Moreover, there are four ratchets on the gearwheel to lock with the grooves on this C arm. Also in each grooves of C arm, the light entitled SMD LED is placed for increasing the brightness and get a better quality of images (Fig 4). The C arm is constant and not rotating around the pipeline.

Another part of the device is the Gearwheel. In one side, the gearwheel is connected to C arm and on the other side is connected to the holder plate. With the rotating of this gearwheel, the holder plate will move around the pipe and the capturing robot can collect its data. The rotating clockwise and vice versa can control the direction of plate movement. The rotation speed of gearwheel is constant but the direction of movement will change automatically to cover all aspects of the pipeline. Also, there are two cylindrical shafts behind the C arm to keep the holder plate away from the probable vibration.

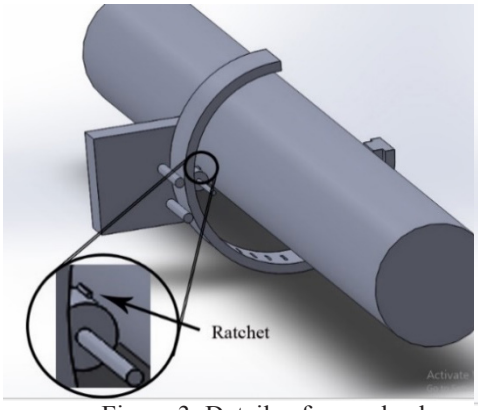

Figure 3: Details of gearwheel

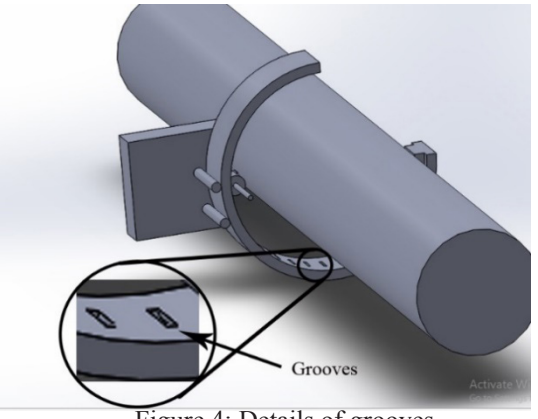

Figure 4: Details of grooves

The last part of the machine is the holder plate, which the camera will be placed on this plate. This plate has connected to the C arm by two cylindrical shafts and one gearwheel. The camera has a flexible place and it is capable to change its degree of capturing based on the situation of the plate. By this, the pipeline always will be in the vision of the camera lens. The plate movement is perpendicular to the pipeline direction.

3 FINITE ELEMENT METHOD SIMULATION

At the first stage, for simulation of the cracks and defects on the pipes and the verification process, we considered a metal material with some probable cracks and defects on it. For this purpose, we used a punched piece of the magnesium alloy that is common to use on for aerospace industries or gas and oil industries to the lightweight and high efficiency (A. NourollahiI, Farahani et al., 2013; Mirjavadi, Forsat et al., 2019). These parts of the pipe were analyzed by SEM and finite element methods. The dies and punches utilized in the setup for shear–punch test geometry for the sample in Fig.1 consists of a flat end punch of 1.38 mm diameter and a die of 1.51mm diameter (W=9 mm). Both of these were made of hardened steel (RC 58). The machine and punch compliance was minimized [11] by coupling a linear variable differential transformer (LVDT) to the moving punch. The punch is attached to a load cell having a capacity of 3000 N. An LVDT with a travel range of 3 mm measures the displacement of the punch. All shear–punch tests were performed at room temperature using a screw driven ATS machine with a constant crosshead speed of 3×10^{-3}mm/s. The cracked in in the specimen is considered as voids or hollow pathway to control the three dimensional meshing feature. The elements employed in the whole process has 8 nodes, all of which has three degree of freedom. Since the force exerted on the specimen is vertical, for applying the load we suppose that the elements which are in direct contact with the load will be subjected to the normal force on the surface. The amount of force exerted on the top plane might be considered as the average amount of the force on the last stage in the shear punch testing.

Near the crack region, which can be considered as volumetric flaw, the stress analysis shows that the region around the sideline of the crack should contain more elements with aspect ratio, while the region far from the crack can be considered as regions, which is

not necessary to contain fine elements.

Regarding the boundary conditions, it is suggested that the whole perimeter including the three-degree-of-freedom nodes around the sample of shear punch should be fixed, it means that the amount of displacement in three main axis equals to zero.

4 RESULTS

Based on the simulations on the samples it can be seen in Fig. 5 that demonstrates some macro cracks occurred on the surface of the punch area. These cracks are formed due to the stress concentration at the edge of the cross-section area of the cylinder and on its height. Moreover, the cracks propagate in 3 main direction and also created a junction of the crack with more depth. This is because of the crack paths reaching together and then stopped propagating.

It is clear from Fig. 5, all the crushes and separated pieces, have a gradient to the down side of the picture that it states there were not equal force on the surface of the specimen.it can be induced from inequality of load balancing on its surface or the height of both dies were not equal exactly.

Another problem might happen when the dies were not parallel to each other and it is led to uneven force deviation. Fig5 shows that there is a color contrast throughout the picture because of the above-mentioned reasons. It is also worth mentioning that there is no crack and crush on the top side of the picture. Furthermore, cracks could exist before the shear punch test as a defect of the specimen and during the test started propagating.

Also, it can be considered, presence of intermetallic compounds caused to initiate the crack because of their hardness (Fig. 6). It is obvious when some crack paths combine; they reinforce each other and then propagate with a higher rate than before.

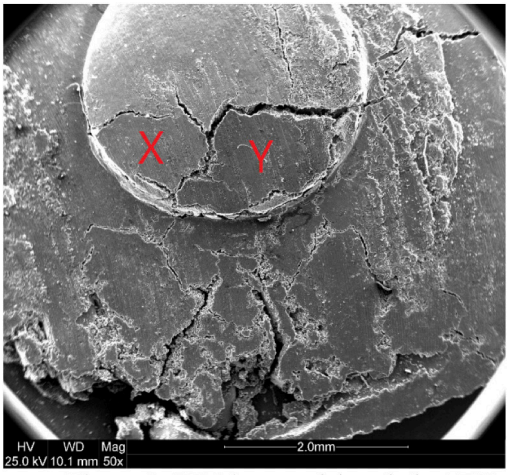

Figure 5: SEM image of the whole AZ81 shear punch surface

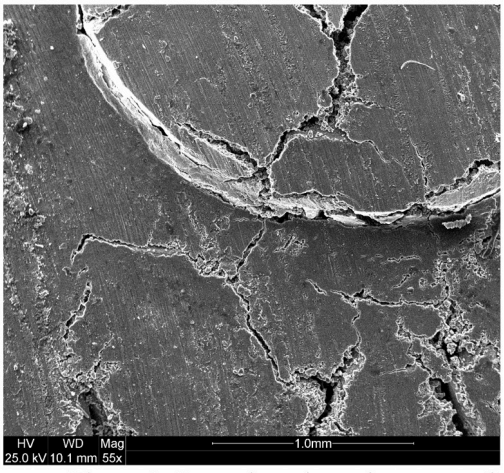

Figure 6: Created cracks at the corner of the punch effected zone (AZ81)

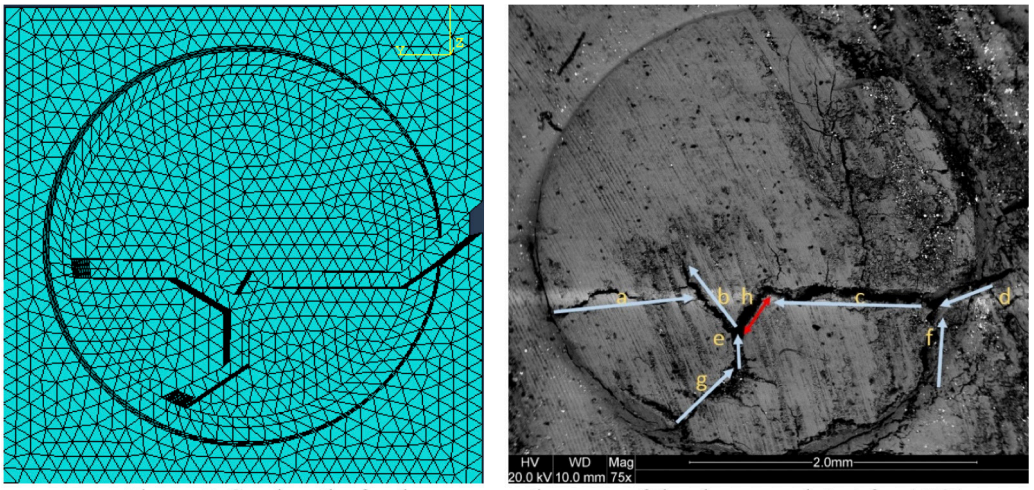

Figure 7: Crack paths for the cross-section area of the shear punch test for AZ81

Fig. 7 shows that the entire crack initiated from the zones with more stress intensity factor. As the result of this function a, d, f and also g (‘g’ itself is a combination of 2 other macro cracks). By considering Fig. 3 can understand that the width of c vector is much more than d and f vectors which induced from joining former vectors.it seems that h vector is created from 2 vectors (e and c) which cause to make a line of joining instead of junction mode. From the viewpoint of color contrast at h vector, it comes that a fully brittle zone (h) bring into being and there is no specific point of joining. Another issue is that the most width and depth occurred in this part because of associating 2 other vectors with high energy.

It must be noticed that ‘a’ vector ended with a very low width because of the crack path ended with another crack that leads to separation of two different areas. Another issue is the crushing behavior on the top of the shear punch sample to the right side and it is due to the material properties that are not dispersed throughout the sample and maybe because of accumulation of brittle secondary phases on the sample.

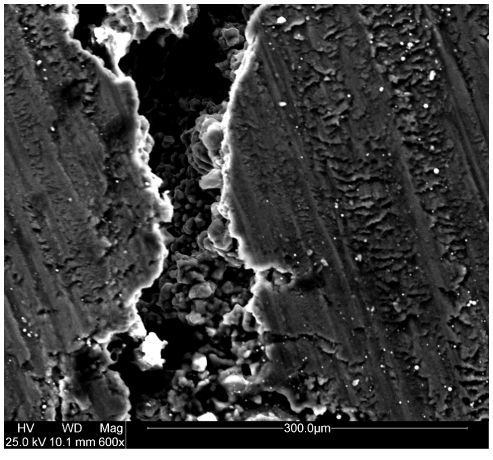

Figure 8: Macrostructure of the ‘e’ crack path in AZ81

It is obvious from Fig. 8 that a shear crack occurred in this part because of the depth of the macrocrack is not completely dark this time. Another probability is that this shear crack shape made as a result of pieces slope to the down side of the picture(X and Y area in Fig 1) in the fracture area.

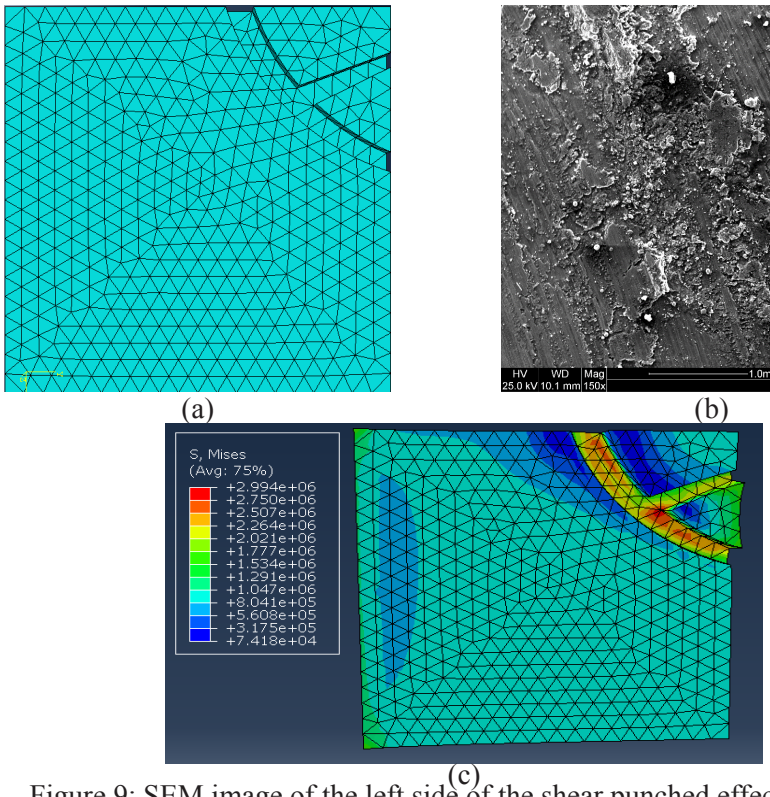

Figure 9: SEM image of the left side of the shear punched effect for AZ81 specimen. (a) Finite element meshes (b) SEM photo (c) finite element result

Regarding Fig. 9, likely, there is some dust and there are some ups and downs on the surface of the specimen. It was maybe due to the specimen damage before the test or casting defect on the Mg FSPed sheet. As it can be seen from fig. 9 that the exerted force leads the stress to increase rather than the region far from the cracks. It is also worth mentioning that maximum amount is 100 times greater than the minimum counterpart due to the fact that

5 CONCLUSION

In this paper, the investigation on the crack and defect detection of the metals for the pipelines has been done. The experimental setup consists of a circulation water system for the pipelines and the finite element simulation has been done on the metal samples. The achieved results based on the simulation and SEM are as bellow:

- Finite Element simulation for post processing indicate that the maximum load at the final step size in the simulation plays an important role in distribution of maximum

stress around the cracks.

- As it was clear from Fig. 9, the amount of maximum stress distribution varies through the circular crack and the amount of this maximum is approximately 3 MPa.
- Crack initiation and growth will occur in the regions with highest intensity factor.
- Numerical simulation indicates that in the region with minimum stress field, the crack initiation will not occur and the experiment validate this phenomenon in Fig. 9.

REFERENCES

A. NourollahiI, G., Farahani, M. A., Babakhaniii & Mirjavadi, S. S. (2013). Compressive Deformation Behavior Modeling of AZ31 Magnesium Alloy at Elevated Temperature Considering the Strain Effect.

Ayadi, A., Ghorbel, O., BenSalah, M. S. & Abid, M. (2019). Kernelized technique for outliers detection to monitoring water pipeline based on WSNs. *Computer Networks,* 150: 179-189.

Bahadori, A. (2017). Chapter 1 - Transportation Pipelines. Oil and Gas Pipelines and Piping Systems. A. Bahadori. Boston, *Gulf Professional Publishing***:** 1-27.

Chang, Y., Zi, Y., Zhao, J., Yang, Z., He, W. & Sun, H. (2017). An adaptive sparse deconvolution method for distinguishing the overlapping echoes of ultrasonic guided waves for pipeline crack inspection. *Measurement Science and Technology*, *28*(3): 035002.

Chen, X., Zhou, F., Chen, X. & Yang, J. (2019). Mobile visual detecting system with a catadioptric vision sensor in pipeline. *Optik*, 193: 162854.

Forsat, M. (2019). Investigating nonlinear vibrations of higher-order hyper-elastic beams using the Hamiltonian method. *Acta Mechanica.*

Hawari, A., Alamin, M., Alkadour, F., Elmasry, M. & Zayed, T. (2018). Automated defect detection tool for closed circuit television (cctv) inspected sewer pipelines. *Automation in Construction,* 89: 99-109.

Jin, H., Zhang, L., Liang, W. & Ding, Q. (2014). Integrated leakage detection and localization model for gas pipelines based on the acoustic wave method. *Journal of Loss Prevention in the Process Industries*, 27: 74-88.

Liu, C., Li, Y., Fang, L. & Xu, M. (2017). Experimental study on a de-noising system for gas and oil pipelines based on an acoustic leak detection and location method. *International Journal of Pressure Vessels and Piping*, 151: 20-34.

Lowe, M. J. S., Alleyne, D. N. & Cawley, P. (1998). Defect detection in pipes using guided waves. *Ultrasonics*, *36*(1): 147-154.

Mao, D., Chu, G., Yang, L. & Li, Z. (2015). Deepwater Pipeline Damage and Research on Countermeasure. *Aquatic Procedia*, 3: 180-190.

Mirjavadi, S. S., Forsat, M., Barati, M., Abdella, G., Mohasel afshari, B., Hamouda, A. M. S. & Rabby, S. (2019). Dynamic response of metal foam FG porous cylindrical micro-shells due to moving loads with strain gradient size-dependency.

Mirjavadi, S. S., Forsat, M., Hamouda, A. M. S. & Barati, M. R. (2019). Dynamic response of functionally graded graphene nanoplatelet reinforced shells with porosity distributions under transverse dynamic loads. *Materials Research Express*, *6*(7): 075045.

Mirjavadi, S. S., Forsat, M., Nikookar, M., Barati, M. R. & Hamouda, A. M. S. (2019). Nonlinear

forced vibrations of sandwich smart nanobeams with two-phase piezo-magnetic face sheets. *The European Physical Journal Plus*, *134*(10): 508.

Singh, R. (2017). *5 - Hazards and Threats to a Pipeline System. Pipeline Integrity Handbook* (Second Edition). R. Singh, Gulf Professional Publishing, 35-88.

Sousa, E. O., Cruz, S. L. & Pereira, J. A. F. R. (2009). Monitoring pipelines through acoustic method. Computer aided chemical engineering. De Brito Alves, R. M., do Nascimento, C. A. O. & Biscaia, E. C. *Elsevier*, 27: 1509-1514.

Stewart, M. (2016). *14 - Pipeline operations. Surface Production Operations*. M. Stewart. Boston, Gulf Professional Publishing**:** 961-979.

Xu, Q., Zhang, L. & Liang, W. (2013). Acoustic detection technology for gas pipeline leakage. *Process Safety and Environmental Protection*, *91*(4): 253-261.

Zajam, S., Joshi, T. & Bhattacharya, B. (2019). Application of wavelet analysis and machine learning on vibration data from gas pipelines for structural health monitoring. *Procedia Structural Integrity*, 14: 712-719.

Zeng, X., Dong, F.-F., Xie, X.-D. & Du, G.-F. (2019). A new analytical method of strain and deformation of pipeline under fault movement. *International Journal of Pressure Vessels and Piping*, 172: 199-211.

Cite this article as: Forsat M., Hamouda A. S., "The Investigation of an Efficient and Effective Proactive Pipeline Integrity System", *International Conference on Civil Infrastructure and Construction (CIC 2020)*, Doha, Qatar, 2-5 February 2020, DOI: https://doi.org/10.29117/cic.2020.0124

Integration of Environmental and Sustainability Management Practices into Construction Industry: A Case Study

Gary Peach
gary.peach@mottmac.com
Mott MacDonald, Doha, Qatar

Dila Ersenkal
dila.ersenkal@mottmac.com
Mott MacDonald, Doha, Qatar

George Daoutis
george.daoutis@mottmac.com
Mott MacDonald, Doha, Qatar

Sotirios Koropoulis
s.koropoulis@auccqatar.com
HBK-PORR JV, Doha, Qatar

Pavel Zuzula
pavel.zuzula@auccqatar.com
HBK-PORR JV, Doha, Qatar

Biliana Karamukova
b.karamukova@auccqatar.com
HBK-PORR JV, Doha, Qatar

ABSTRACT

Integration of environmental and sustainability management into the construction industry has become essential as a result of a need to improve financial performance, adopt international protocols in a global marketplace, address stakeholder interests, and attain high environmental performance. Communities also expect organizations to comply with environmental standards and reduce the environmental impacts in their daily operations. That may be a challenge, but it is also an opportunity for the organizations to demonstrate their commitment to environmental responsibility and sustainability. Environmental impacts arising from the construction industry and the consequences could be challenging if appropriate practices are not in place. Therefore, adopting responsible approach to management of environmental matters and embedding the environmental and sustainability principles into the full lifecycle of the projects, starting as early as conceptual design, is crucial for long-term success. Responsible environmental management and commitment to sustainability has been central to Public Works Authority (PWA)'s success as a leading government organization. This is evident from the manner in which PWA is requesting all contractors and consultants working on behalf of PWA projects to develop and implement Environmental Management System (EMS) and comply with international sustainability rating schemes for their projects. This paper provides information on a case study; namely the Musaimeer Pumping Station and Outfall (MPSO) project and discusses the strategies, systems, procedures, and tools

developed and implemented by the Project Management Consultant (PMC) and the Contractor to achieve and exceed PWA's environmental and sustainability requirements for the project.

Keywords: Construction innovation; Manufacturing innovation; Road construction; Case study; Project management; Plastic bags; Glass bottle

1 INTRODUCTION

Musaimeer Pumping Station and Outfall (MPSO) project area is located nearshore to the southwestern area of Doha, in-between the RAF Desalination Plant and Hamad International Airport. This particular area has experienced rapid expansion of growth in recent years, with ongoing developments. Therefore, the need to increase drainage capacity in order to accommodate additional storm water runoff and constructional activities has become critical. PWA has developed and implemented multiple projects, including the MPSO Project.

The MPSO project comprises a pumping station to handle a peak flow rate of 19.7 m^3/s; a 10 km long 3.7 m diameter marine tunnel outfall, an offshore riser shaft and 84 port diffuser field. HBK-PORR JV is the Design, Build, Operation and Maintain Contractor for the construction of the MPSO Project, and Mott MacDonald Ltd. is the Project Management Consultant (PMC) Company.

Construction activities of the MPSO project comprise a wide range of activities including but not limited to excavation and dewatering, tunneling, marine and offshore works including dredging, and drilling. These activities have the potential to affect a broad spectrum of environmental aspects. Environmental concerns associated with the MPSO project include, but are not limited to:

- Releases of airborne particulate matter and air emissions.
- Impacts on aquatic ecosystems.
- Impacts on terrestrial ecosystems.
- Impacts on local and regional surface water and groundwater flow.
- Wastewater from site runoff.
- Waste generation.
- Noise.
- Planned and accidental releases of pollutants.
- Social impacts.

The objective of this paper is to provide an overview of the environmental and sustainability practices implemented at the MPSO project site in order to facilitate and encourage continual improvement in the environmental performance of the project throughout the project life cycle.

2 ENVIRONMENTAL REQUIREMENTS FOR THE PROJECT

Responsible environmental management and commitment to sustainability has been central to PWA's success as a leading government organization. This is evident from the manner in which PWA is requesting all contractors and consultants working on behalf of PWA projects to develop and implement an Environmental Management System (EMS) and comply with international sustainability rating schemes for their projects. PWA is

defining project requirements, setting public tenders for the execution of works, and defining the requirements for environmental management and sustainability.

It is also a requirement of Qatar Construction Specifications (QCS, 2014) that all companies engaged to undertake work on behalf of the PWA and PWA, have an existing or working towards the development and implementation of an Environment, Health and Safety Management System (EHSMS). Sections below provide information on the contractual requirements set forth for the Consultant and the Contractor by PWA for the MPSO project.

2.1 Requirements for PMC

PWA has set forth environmental management requirements for the MPSO project in the Professional Services Agreement (PSA) (PWA, 2017) signed with the Project Management Consultant (PMC) – Mott MacDonald. The contract is comprehensive and provides detailed information on the necessary actions to be implemented by the PMC to ensure that the environmental impacts associated with the MPSO project are managed effectively. These include but are not limited to the following:

- Appointment of a Senior Civil/Environmental Engineer.
- Requirements for Core Team Design and Construction Supervision Team to have experience in environmental protection aspects of the construction and operation of similar large diameter tunneling projects and deep below ground pumping stations/ structures; demonstrated knowledge of environmental regulations; demonstrable experience of environmental management and permitting; and knowledge of Qatar environmental legislation.
- Undertaking an environmental assessment during the planning and implement of the project.
- Instigation of an Environmental Management System.
- Development of an Environmental Management Plan and associated procedures.
- Compliance with environmental obligations.
- Adherence to the requirements of applicable environmental specifications, codes and other requirements.
- Monitoring the Contractor's compliance with environmental management requirements.
- Coordination of environmental activities including but not limited to environmental permit applications, review of Contractor's environmental submissions, and undertaking environmental surveys.
- Ensuring submission of necessary documentation for environmental permits.
- Conducting EMS audits to verify the implementation and maintenance of Contractor's EMS.
- Submission of monthly progress reports that include a section on environmental management.
- Identifying and keeping a record of project lessons learned, including environmental issues.

2.2 Requirements for the Contractor

Similar to the PSA made with the PMC, environmental management requirements

for the Contractor has been extremely well defined in PWA's contract made with the Contractor HBK-PORR JV (PWA, 2017). There is a detailed chapter on 'Environmental Management' to furnish the Contractor with the Authority's fundamental requirements for environmental management to be delivered by the Contractor throughout all stages of the project. A summary of these requirements includes, but is not limited to the following:

- Mobilization of a dedicated Environmental Manager, with a minimum of 5 years' experience in an environmental manager role, located permanently in Doha for the duration of the project and with the authority to enable the discharge of all environmental requirements.
- Proactively demonstrating implementation of a close working interface between the engineering and environmental technical and management disciplines.
- Designing, implementing and effectively resourcing a comprehensive Environmental Management System (EMS), compliant with Authority, Government, International standards and recognized best practice, that will include a range of management plans specific to Engineering / Environmental design integration, environmental impact / risk assessment, construction environmental management planning, site supervision, project environmental / sustainability performance and auditing.
- Establishing an ISO 14001 compliant (or an equivalent, internationally recognized system EMS) to be audited at least twice a year to ensure ongoing compliance.
- Obtaining all necessary permits for the MPSO project, and preparing all reports required by the permits.
- Compliance with the requirements of the Authority, national legislation of the State of Qatar, the international legislation / conventions ratified by the State of Qatar, and industry recognized best practice.
- Compliance with all requirements of the Ministry of Municipality and Environment and in particular the requirements of the project environmental permit obtained for the MPSO Project.
- Adherence to the requirements of applicable environmental specifications, codes and other requirements.
- Application of international standards where (i) Qatar National Standards have not been developed for a particular parameter, or (ii) there is agreement with the Engineer that use of an international standard provides greater environmental security, without compromising compliance with Qatar National Standards.
- Submission of construction environmental management plan and safety management plan.
- Ensuring that all mitigation measures necessary, including those identified in the Environmental Impact Assessment are implemented during the project.
- Conducting all necessary environmental surveys and collect environmental data; i.e. detailed topographic survey, detailed bathymetric surveys of the diffuser area, condition survey of access roads to the site, marine geotechnical investigations, etc.
- Establishing an environmental monitoring programme that includes on site air quality monitoring, monitoring ground water levels on the site, noise monitoring, seawater quality sampling and analysis programme, continual online seawater quality monitoring via buoys.

- Developing a protocol, designing and implementing systems for sharing seawater quality analysis and online monitoring data, with third parties in consultation with MME, Kahramaa and Ras Abu Fontas Power and Water Desalination Plant.
- Implementing risk management to cover all project risks not restricted only to health and safety matters; but also risks to the environment, the design, the program for design, the cost of design, the construction of the tunnel and shafts and the associated works, the program for construction and cost of construction.
- Developing a detailed Environmental Risk Assessment (ERA) Programme all environmental aspects and impacts of all works.
- Conducting hazard and operability (HAZOP) and control hazard and operability (CHAZOP) studies.
- Identifying and registering the project with CEEQUAL International (CEEQUAL, 2015) and achieve a score of 'GOOD' under 'CEEQUAL lnternational' scheme.
- Provision of monthly environmental progress reports that include environmental issues.
- Conducting bi-weekly site inspections and semi-annual audits.
- Delivering environmental management performance to international standards.

3 ENVIRONMENTAL PRACTICES AT MPSO PROJECT SITE

Comprehensive definition of the environmental management requirements in the contract has significantly contributed to the high environmental performance of the MPSO project. Moreover, the appointment of consultants and contractors that have international best practice experience in environment and sustainability field, with mature management systems in place, has definitely been important contributor for the continual improvement of the environmental and sustainability performance of the project and raising the bar in the construction industry. Table 1 presents a summary of the selected environmental practices being implemented at the MPSO project site.

Table 1: Summary of Environmental Practices at MPSO Project Site

Subject	Practices at MPSO Site
Leadership	Both the PMC and the Contractor demonstrate leadership and commitment for the implementation of an effective environmental management system for the MPSO project and enhancing the project's environmental performance.
Environmental Policy	A project environmental policy has been developed and is being implemented. The policy is displayed at various locations at the site and communicated to all staff and relevant other parties involved in the MPSO project.
Environmental Assessment	PWA as the project owner has consulted with the Ministry of Municipality and Environment (MME) early in the project planning process to determine whether the proposed project would require an environmental assessment. A credible environmental consulting company, following the MME requirements, has undertaken an Environmental Impact Assessment (EIA) for the project in 2014.
Baseline Studies	Environmental data such as water quality, air quality, soil quality, terrestrial ecosystems, and groundwater quality is collected as part of the baseline studies associated with the EIA undertaken for the project. Environmental monitoring program is currently in place to allow for comparison of baseline environmental data with monitoring data that is being collected through the project life cycle to identify long-term trends and fluctuations.

Environmental Design	Environmental design criteria have been established and integrated into the project design. The following have been considered for establishing the design criteria: • Consideration of climate change impacts. • Inclusion of future projections. • Coastal management and protection. • Discharging storm water back into the water cycle in a controlled manner. • Minimizing impacts on marine water quality and ecosystem. • Achieving required dilution and mixing levels under all current scenarios for full range of operating conditions and flows. • Minimizing changes in ambient concentrations and impacts on sensitive habitats such as corals and seagrass.
Environmental Management System	Both the PMC and the Contractor has established an environmental management system (EMS) for the project in accordance with international best practice, such as ISO 14001:2015.
Risk Management	Project risks are identified, analyzed, and evaluated to ensure that the risks are effectively managed through the application of a robust risk management process. Project risk workshops are undertaken at planned intervals with the involvement of various project stakeholders, an overarching Project Risk Register is maintained to capture the risks, and the mitigation measures identified. Risk management is part of the responsibilities of management and an integral part of all project processes and disciplines. In addition, a separate Environmental Risk Assessment Register is being maintained throughout the project lifecycle to identify, monitor, and manage the environmental impacts associated with the project activities.
Environmental Management Plans	Construction Environmental Management Plan and associated environmental aspect-specific management plans are developed for the MPSO project. These plans are implemented and updated throughout the project life cycle to ensure continual improvement.
Compliance Obligations	Compliance obligations applicable for the project's environmental aspects have been identified and the project's compliance is being evaluated through the review and update of the Environmental Compliance Matrix established for the project. Moreover, a project Permit Register is established and maintained to track all the applicable permits for the project, including but not limited to environmental related permits such as project environmental permit, dewatering permit, dredging and offshore works permit, chemical storage permit, water treatment plant permit.
Training and Awareness	Toolbox talks, topic-specific trainings, and environmental awareness sessions are being provided at the MPSO project site to raise the awareness of the project staff on environmental matters.
Communication	Weekly and monthly progress meetings are held with the attendance of the PMC, Contractor, and PWA to discuss the project progress with respect to each project discipline, including environment. In addition to these meetings, discipline-specific internal meetings (i.e. environment, HS, marine, tunneling, commercial, etc.) are held between the PMC and the Contractor to evaluate the status of the project and to identify any issues of concern.) Progress reporting and presentations are also done both by the PMC and the Contractor in accordance with the contractual requirements.
Performance Evaluation	Environmental performance of the project is monitored and evaluated through the use of various tools such as site inspections, internal and external audits, and monthly management review meetings. Daily, weekly, and monthly site inspections are completed by both the PMC and the Contractor at all project sites. Internal and external, PMC, Contractor, and PWA EMS audits are conducted in accordance with ISO 14001: 2015 standard, to determine (a) whether the project site is operating in adherence to compliance obligations (b) whether the EMS and other environmental plans have been properly implemented and maintained. Monthly, integrated health, safety, and environmental (HSE) management review meetings are conducted with the presence of PMC and the Contractor representatives to ensure the continuing suitability, adequacy and effectiveness of the project EMS.
Environmental Monitoring	Environmental monitoring program is in place for monitoring and measurement of environmental aspects such as air quality, noise, groundwater quality, wastewater quality, seawater quality, waste generation, and excavated materials.

Emergency Planning	Site-specific environmental emergency plan has been developed and implemented, tested and updated on a regular basis. The scope of the emergency plan is comprehensive in nature, and goes beyond the compliance obligations, particularly with respect to hazard identification, risk analysis and consequence as well as communications.
Sustainability	PWA has set a target for the MPSO project to achieve 'good level' for CEEQUAL, the evidence-based sustainability assessment, rating and certification scheme (CEEQUAL, 2015). The Contractor understands the importance of delivering a sustainability-driven strategy for the MPSO project and conducts regular CEEQUAL workshops to ensure that the desired level of achievement will be realized by addressing the requirements of each CEEQUAL category that includes management, resilience, communities and stakeholders, land use and ecology, landscape and historic environment, pollution, resources, and transport.

3.1 Environmental performance evaluation – site inspections

Environmental performance of the MPSO project is monitored and evaluated through the use of various tools such as site inspections, internal and external audits, and monthly management review meetings. Daily, weekly, and monthly site inspections are completed by both the PMC and the Contractor at all project sites. Environmental site inspection sheets cover a wide range of topics such as air quality, water quality, noise & vibration, biodiversity, carbon footprint, emergency planning, record keeping; and permit-specific inspection sheets to evaluate the project's compliance against the conditions set forth in the environmental permits obtained.

Figure 1 below shows the environmental site inspections conducted by the PMC within the past year. As can be seen from the graph, the frequency of the site inspections is increased depending upon certain construction activities. As an example, the dredging works were completed during the month of May 2019, thus the frequency of the site inspections were increased to ensure that the mitigation measures to reduce the potential environmental impacts were implemented adequately and effectively by the Contractor.

It is paramount to adopt a systematic and integrated approach in implementing management systems for a project and MPSO project is a proof of the importance given for environmental management as much as H&S and quality management for the overall success of the project.

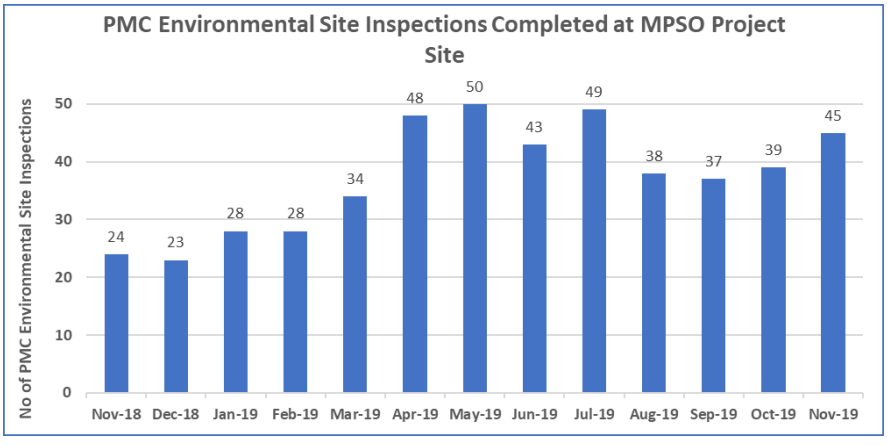

Figure 1: PMC Environmental Site Inspections Completed at MPSO Project

3.2 Environmental monitoring – seawater quality monitoring

Site-wide environmental monitoring is being implemented at specified representative sensitive receptor locations around the project site, for monitoring and measurement of environmental aspects such as air quality, noise, groundwater quality, wastewater quality, seawater quality, waste generation, and excavated materials. As the MPSO project includes the construction of a 10km outfall chamber below the seabed, it is of crucial importance to establish the baseline data for the seawater quality to allow for comparison of baseline environmental data with monitoring data that is being collected through the project life cycle to identify long-term trends. With that regard, PWA has clearly defined in the Contract, the requirements for establishing a seawater quality programme that includes monthly seawater sampling and analysis and continual online monitoring of seawater quality through installation of oceanographic buoys. The Contractor prepares and submits monthly analysis reports to present the results of this monitoring exercise. Figure 2 is a demonstration of the results of the seawater quality monitoring at the MPSO project site, from the buoys along with the monthly sampling undertaken.

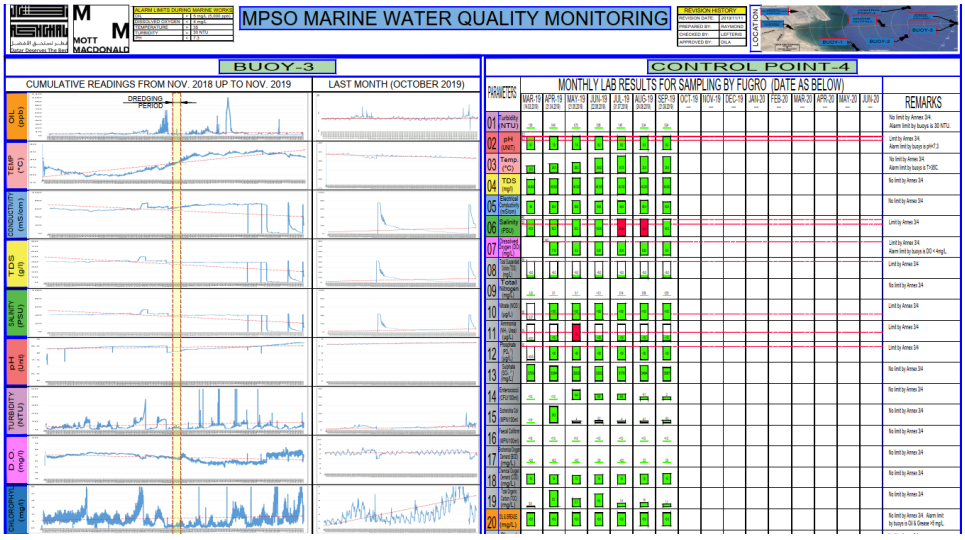

Figure 2: Results from the Seawater Sampling and Online Buoys Monitoring

4 CONCLUSION

MPSO project is a proof of PWA's thought-leadership in sustainability and environmental management. PWA's organizational culture that supports the integration of environmental management and sustainability into the project lifecycle has led to the achievement of high/enhanced environmental performance for the MPSO project and also resulted in various other benefits, including but not limited to the following:

- Better use of energy and resources.
- Compliance with legislation.
- Management of environment aspects effectively.
- Protecting the environment by preventing or mitigating adverse environmental impacts.
- Reduced risks.

- Improved sustainability performance.
- Improved stakeholder confidence and trust.

The recipe for success in achieving high standards for environmental management and sustainability is also dependent on the commitment by all parties involved in the project, including the PMC and the Contractor. PMC and Contractor management also plays a significant role in the successful implementation and maintenance of the established systems by providing adequate financial resources and intangible resources such as support, commitment of time, encouragement of employees that facilitate the adoption and maintenance of the systems. The recipe for success for the MPSO project has been the collaborative approach and the open dialogue between all project stakeholders, including PWA, PMC, and the Contractor, creating solutions together.

REFERENCES

CEEQUAL Ltd. (2015). *CEEQUAL Version 5.2 Assessment Manual for Projects, Qatar International Edition.*

Public Works Authority (2017). *Professional Services Agreement for Professional Consultancy Services - Post Contract Professional Consultancy Services*, Project CP 671/2 Musaimeer Pumping Station and Outfall, Project ID: IA 2016 S 005 G, Contract Number: P2017/22.

Public Works Authority (2017). *Contract Documents for Design, Build, Operate and Maintain of Musaimeer Pumping Station and Outfall*, Project ID: IA 14/15 C 015 G, Contract Number: C2017/109.

Qatar Construction Specifications (QCS) (2014). Revision IV.

The British Standards Institution (2015). *BS EN ISO 14001:2015 Environmental management systems — Requirements with guidance for use*, BSI Standards Publication, London.

Cite this article as: Peach G., Ersenkal D., Daoutis G., Koropoulis S., Zuzula P., Karamukova B., "Integration of Environmental and Sustainability Management Practices into Construction Industry: A Case Study", *International Conference on Civil Infrastructure and Construction (CIC 2020)*, Doha, Qatar, 2-5 February 2020, DOI: https://doi.org/10.29117/cic.2020.0125

Cut Carbon, Cut Cost – Feasibility of Applying PAS 2080

Lakshmi Suryan
Lakshmi.suryan@mottmac.com
Mott MacDonald, Doha, Qatar

George Daoutis
GeorgeDaoutis@mottmac.com
Mott MacDonald, Doha, Qatar

Lisa Girrbach
Lisa.Girrbach@mottmac.com
Mott MacDonald, Doha, Qatar

ABSTRACT

State of Qatar is committed to delivering its Intended Nationally Determined Contributions (INDC) submitted to the United Nations Framework Convention on Climate Change (UNFCCC) secretariat. (Ministry of Environment, 2015). Though the INDC are voluntary, without any specific target threshold to commitments, Qatar has over the years developed robust policies and action plans with the intention to reduce greenhouse gas (GHG) emissions by 2030. As a host country for the World Cup 2022, sustainable tourism and carbon neutral tournament are already high priority on the agenda. Meeting GHG emission reduction targets by 2030 will be a challenge for all sectors across Qatar and reduction of emissions from Qatar's infrastructure will soon be a regulatory requirement. The paper will be based on a literature review of the standard available in the industry, such as PAS 2080, for carbon management in infrastructure. The feasibility of applying such standards in Qatar will be reviewed in detail, with the objective of managing whole life carbon in infrastructure and achieve reduction in carbon and cost. The study will also detail how carbon reduction can not only be achieved by quantifying carbon and addressing carbon hotspots to improve efficiency but also by including changes in behaviors/culture, processes and systems, in addition to implementation of low carbon solutions.

Keywords: Climate change; Infrastructure carbon; PAS 2080; Low carbon solutions

1 INTRODUCTION

State of Qatar is committed to delivering its Intended Nationally Determined Contributions (INDC) submitted to the United Nations Framework Convention on Climate Change (UNFCCC) secretariat (Ministry of Environment, 2015). Even though the INDCs are voluntary, Qatar has over the years making efforts to reduce its national greenhouse gas emissions. As a host country for the World Cup 2022, sustainable tourism and carbon neutral tournament are already high priority on the agenda (The Penninsula, 2019). Infrastructure is the backbone of Qatar's economy, providing essential services to the society. The INDCs report issued by the Ministry of environment in 2015, specially identifies infrastructure as a potential mitigation measure against climate change impacts and reduction of emissions from Qatar's infrastructure will soon be a regulatory requirement.

1.1 Infrastructure carbon

Infrastructure refers to transport, energy, water, waste and communications sectors, as defined in the UK National Infrastructure Plan 2014 and support the essential societal services of a country (bsi, 2016). Typically, infrastructure projects are energy and carbon intensive and studies indicate approximately 70% of global greenhouse gas emissions (GHGs) come from infrastructure construction and operations (World bank blogs, 2018).

Carbon in infrastructure will be used as the short-hand for GHGs as defined by the UNFCC Kyoto Protocol. Carbon is a key concern for infrastructure assets and the term is split into three: capital carbon which refers to emissions associated with creation of an asset, operational carbon which refers to the emissions associated with the operation and maintenance of an asset and whole life carbon which is a collective term for both capital and operational carbon. (UK Green Building Council, 2017).

1.2 Drivers for carbon reduction

There are number of drivers for opting carbon reduction measures in infrastructure. As climate change impacts are exacerbating and climate talks are gaining momentum, globally, it is crucial that carbon mitigation actions are captured locally via reducing carbon footprint and improving resilience. Other than the environmental consideration, cost of energy and material prices are key drivers for adopting a low carbon approach as carbon is a proxy for material / energy used during the construction and operation of assets (Okereke, 2007). As majority of the carbon emissions are from the construction, operation and maintenance of the asset, focusing on these key areas have demonstrated that considerable carbon and cost reduction can be achieved. Carbon reduction from end user (usecarb) is attributed to behavioral changes, though can be influenced by the infrastructure asset owners /value chain, will require buy in from other stakeholders (Infrastructure Working Group, 2013). A study that explores the motivations, drivers and barriers to carbon management in businesses, (Okereke, 2007), identified that market shift, technological changes and governmental regulations can push the envelope to kick start the carbon management process.

For carbon foot printing of an asset or an organization, there are tools available in the industry to assist in quantifying emissions and reporting. With a complex structure of delivery and interrelations with multiple stakeholders, carbon assessment in infrastructure had a dearth for a common platform that connects the entire value chain and maximize efforts (HM Treasury, 2013).

In alliance with the Paris agreement, UK government has specific climate change commitments and infrastructure carbon review (ICR) undertaken in 2013, indicated that 16% of UK's total carbon emissions were from the construction, operation and maintenance of the infrastructure assets (UK Green Building Council, 2017). The ICR alluded various carbon reduction opportunities that support UK's emission reduction target and it included a recommendation to create a specification that integrates the entire value chain involved in creating infrastructure assets (HM Treasury, 2013). This led to the development of PAS 2080.

2 WHAT IS PAS 2080

Typically, publicly available specification (PAS) are a precursor to development of a

standard and aims to fulfil an immediate requirement in the industry for such a process. PAS 2080 was driven by the need in the construction industry to streamline the carbon management process in infrastructure projects. PAS 2080 came into effect in May 2016 (bsi, 2016), commissioned by the Green Construction Board (GCB) and facilitated by BSI standards limited. It was supported by technical experts in the field of construction (including the team from Mott MacDonald and Arup) and supported by the organizations and stakeholders during the development and deployment phase of the document. It is world's first specification that details the process to be adopted for managing carbon reduction in infrastructure projects and provides general guidance to promote carbon management in infrastructure delivery on a whole life basis (bsi, 2016). It aims to provide a consistent methodology for gathering data, benchmarking, setting baseline, quantification and reporting of infrastructure carbon and cannot be regarded as a carbon assessment tool for quantifying GHG emissions. Acknowledging the responsibility of asset owner / managers as well as the parties involved in the design, construction of the assets, PAS 2080 aims to integrate and align the work of the value chain to push boundaries for innovation. A new culture of design and construction that challenges the current practices and innovates to reduce cost and carbon are the expected outcomes, when PAS 2080 is applied.

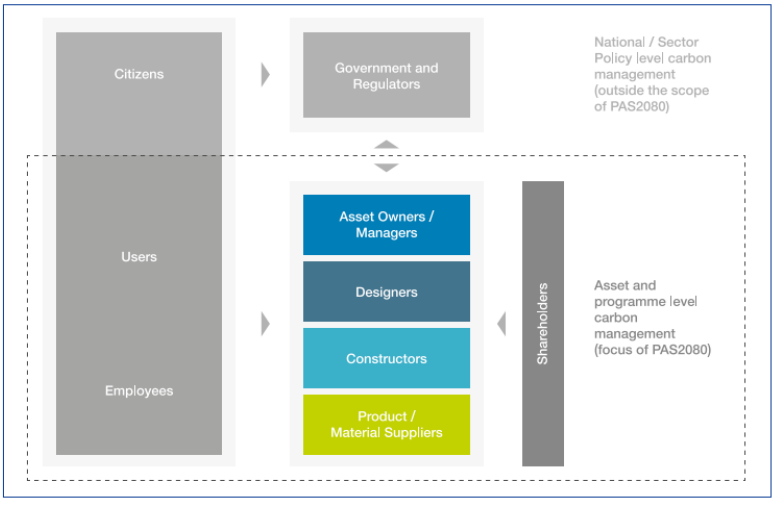

Figure 1: Infrastructure value chain members responsible for carbon management (bsi, 2016)

2.1 Key enablers

PAS 2080 is based on key principles that underpin the whole life carbon management and provides a comprehensive set of responsibilities for each party in the value chain, via specific clauses. As indicated in the below Figure 2, the whole life carbon reduction can be applied across 8 work stages that denote the infrastructure delivery. A separate guidance document which should be read in conjunction with PAS 2080, provides guidance, case studies and support for better understanding and efficient application of the specification (The Green Construction board , 2016) .

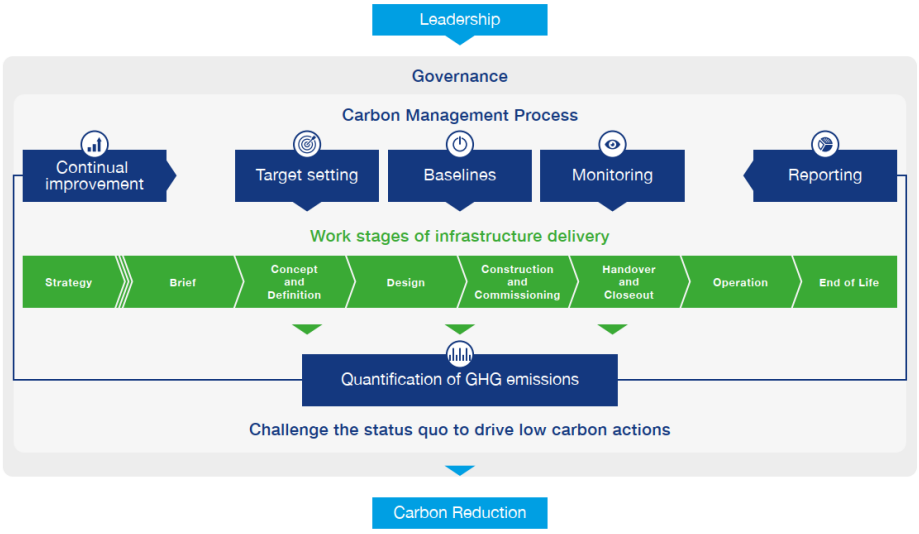

Figure 2: PAS 2080 Carbon management process (bsi, 2016)

3 FEASIBILITY OF CARBON MANAGEMENT

The feasibility of applying carbon reduction measures can be demonstrated through two key case study examples.

3.1 Case study example-1 Cut carbon, cut cost

As early adopter of PAS 2080, Anglian water in the UK has demonstrated the causal link between carbon and cost by analyzing its data for 8 years and establishing correlation between reduced carbon and reduced cost. Understanding this, Anglian Water is the first water company to set a target of becoming carbon neural by 2050. Their annual integrated report for 2019 states that they are on track to achieve this, demonstrates the reduction in capital carbon from their 2010 levels by 58% and operational carbon emission by 29% (Anglian water services limited , 2019). Attention to design, material, installation and commissioning techniques has contributed to the 58% reduction in capital carbon and focus on carbon has been commercially beneficial , achieving a capital cost saving of more than 20%, measured against a 2010 baseline (Davide Stronati, 2019). This is a fine example of how a top down approach, with the right leadership and governance, has contributed to the successful delivery of reduced carbon targets.

3.2 Case study example-2 Carbon foot printing

In the context of wider interest in carbon reduction in the UAE, including national reduction targets, one of the government entities wanted to understand its carbon footprint and how to reduce the climate change impact of operations, cut costs and provide carbon performance data to internal and external stakeholders. The exercise identified potential carbon savings of over 2.3 million tCO2e/year by 2030 by developing a carbon footprint calculation tool and forecasting scenarios. The project also helped to identify reductions in emissions of 35-54% as well as operational cost savings. The roadmap included significant quick wins that could be implemented in the short term as well as

investments over the medium/longer term. The project also built carbon management capacity within the company and enabled to develop a carbon reduction and energy efficiency investment program for the short and medium term, across all similar assets.

4 CONCLUSION

As Qatar aspires to transition into a low carbon economy, it is imperative to understand that change will be required when managing infrastructure assets (Ronan Bolton, 2015). Taking cue from the list of perceived and actual barriers in the UK for the uptake of low carbon infrastructure (HM Treasury, 2013), based on professional expertise, the authors note the same set is applicable in Qatar as well.

In-depth studies will be required to verify and establish the veracity of these observations and will be helpful to understand the preferred route for stakeholders in response to a potential market shift (Okereke, 2007). Hence based on the literature review, the below set of recommendations have been drafted to support the way forward for adopting PAS 2080 in Qatar for infrastructure projects.

Leadership is key

As demonstrated by various case studies, leadership is of paramount importance while aiming to adopt PAS 2080 in infrastructure. Government organizations should aim to take lead in setting strategy for managing carbon in infrastructure assets, understand the baseline and aim to improve against those baselines through targets setting and monitoring (Granoff, 2016). Prior to that it is important to note that main ingredients of carbon reduction include shift in behaviors/culture, processes and systems in addition to implementation of low carbon solutions. Typically carbon reduction is not embedded in the current mindset of organizations, therefore having a clear vision and communicating the objective within the organization, as a core value, and percolating it to the supply chain and wider industry partners will assist in quicker acceptance and adoption of the specification (HM Treasury, 2013).

Capacity building

Carbon awareness is not a skill that is viewed as a requirement for the team managing and creating infrastructure assets and appropriate training are not typically provided to assist in building the skill set. It also needs to be acknowledged that with a plethora of carbon tools, models etc., and carbon management can be viewed as a complex and daunting process (HM Treasury, 2013). Nevertheless, it is imperative to note that carbon management is the responsibility of the entire value chain and only when the whole value chain is aligned, then the maximum potential for cost and carbon reduction can be realized. (Institution of Civil Engineers, 2016) . Development of carbon skills at all levels and tiers of the supply chain, from class room to board room, is critical and investment in human capital will add value to the infrastructure industry.

Mindset for innovation

Innovation triggers change in technology and application of unique solutions to achieve the desired carbon reduction. This may include novel designs, products or practices which are new and can be perceived as ‘risky’ in comparison to tried and

tested carbon intensive solutions (Granoff, 2016). The perception of increased cost or reduced level of service can be a hindrance to adoption of low carbon solutions by clients and discourage new thinking in the supply chain (UK Green Building Council, 2017). Early engagement with the supply chain to provide low carbon solutions at the project onset and having a dialogue with the service providers, product suppliers, designer and contractors on the possibilities to reduce cost and carbon , can foster creativity and innovation (HM Treasury, 2013).

REFERENCES

Anglian water services limited (2019). *Annual integrated report 2019*, London: Anglian water services limited.

Bsi (2016). PAS 2080- Carbon Management in Infrastructure, London: The British Standards Institution.

Davide Stronati (2019). Why carbon is key to success. [Online] Retrieved from https://www.mottmac.com/views/why-carbon-is-key-to-success [Accessed 15 December 2019].

Granoff, I. H. J. &. M. (2016). Nested barriers to low-carbon infrastructure investment. *Nature Climate Change*, 14 November, pp. 1065-1071.

Treasury, H. M. (2013). Infrastructure carbon review, London: Government of the UK.

Infrastructure Working Group (2013). Infrastructure Carbon Review Technical Report, London: The Green Construction board.

Institution of Civil Engineers (2016). PAS 2080: World's first specification for cutting carbon dioxide emissions in infrastructure. *Briefing: Standards*, 169(CE3).

Okereke, C. (2007). An exploration of motivations, drivers and barriers to carbon management: The UK FTSE 100. *European Management Journal*, Vol. 25(No. 6), pp. 475-486, 2007.

Ronan Bolton, T. J. F. (2015). A socio-technical perspective on low carbon investment challenges – Insights for UK energy policy. *Elsevier*, Volume 14, pp. 165-181.

The Green Construction board (2016). Guidance document for PAS 2080, London: The Green Construction board.

The Peninsula (2019). SC sign agreement to deliver carbon-neutral FIFA World Cup in Qatar. Retrieved from https://www.thepeninsulaqatar.com/article/04/11/2019/SC-sign-agreement-to-deliver-carbon-neutral-FIFA-World-Cup-in-Qatar [Accessed 15 November 2019].

UK Green Building Council (2017). Delivering Low Carbon Infrastructure, London: UK Green Building Council.

World Bank blogs (2018). Low-carbon infrastructure: an essential solution to climate change? Retrieved from https://blogs.worldbank.org/ppps/low-carbon-infrastructure-essential-solution-climate-change [Accessed Dec 2019].

Cite this article as: Suryan L., Daoutis G., Girrbach L., "Cut Carbon, Cut Cost – Feasibility of Applying PAS 2080", *International Conference on Civil Infrastructure and Construction (CIC 2020)*, DOI: https://doi.org/10.29117/cic.2020.0126

Regulatory Frameworks for the Successful Implementation of Construction and Demolition Waste Treatment Infrastructure

Sam Dowding
sam.dowding@mottmac.com
Mott MacDonald, Doha, Qatar

George Daoutis
george.daoutis@mottmac.com
Mott MacDonald, Doha, Qatar

ABSTRACT

In an ever expanding world, our constant need to construct and to support a constantly growing population is resulting in significant increase in construction waste. Rapid expansion is a trend that can be seen throughout the Middle East therefore the need to manage the resulting construction waste should be seen as critical. According to the Qatar National Development Strategy (QNDS, 2018), construction waste was recorded at 3,796,540 tonnes per year in 2016 with a total of 11.5% successfully treated. The QNDS indicates that construction waste increase is expected to peak at approximately 6.6 million tonnes per annum by the year 2030 as a result of future development plans within the Qatar. A requirement exists to manage this material in a sustainable manner to minimise the quantities sent for final disposal at landfill sites which can be achieved through the treatment and reuse of the waste materials which arise form construction processes. This paper provides an overview of the methods considered suitable for the treatment of construction waste within the middle east region and describes in detail the regulatory frameworks that are typically required to support the successful implementation of construction waste treatment technology.

Keywords: Regulatory frameworks; Construction; Demolition

1 INTRODUCTION

Construction waste comprises the materials arising from the construction or demolition process. These materials are highly dependent upon the type of project being carried on. In the Middle East region, it is common to find significant quantities of concrete and other aggregate materials within the waste stream. These materials typically arise from temporary site structures, erroneous concrete works and temporary site roads. A typical construction waste composition is shown in Figure 1. Figure 1 shows that significant quantities of concrete and aggregate are expected to be present within the construction waste stream. These materials are suitable for recovering and restoring back to a usable aggregate and suitable for a variety of construction uses) (Globex-City Consult, 2001, National Development Strategy, 2018).

Processing the construction waste into a reusable recycled concrete aggregate requires a line of plant machinery designed to crush large pieces of waste concrete into specific grade aggregates whilst removing contaminated waste materials such as wood, plastic, metals, cement and sand.

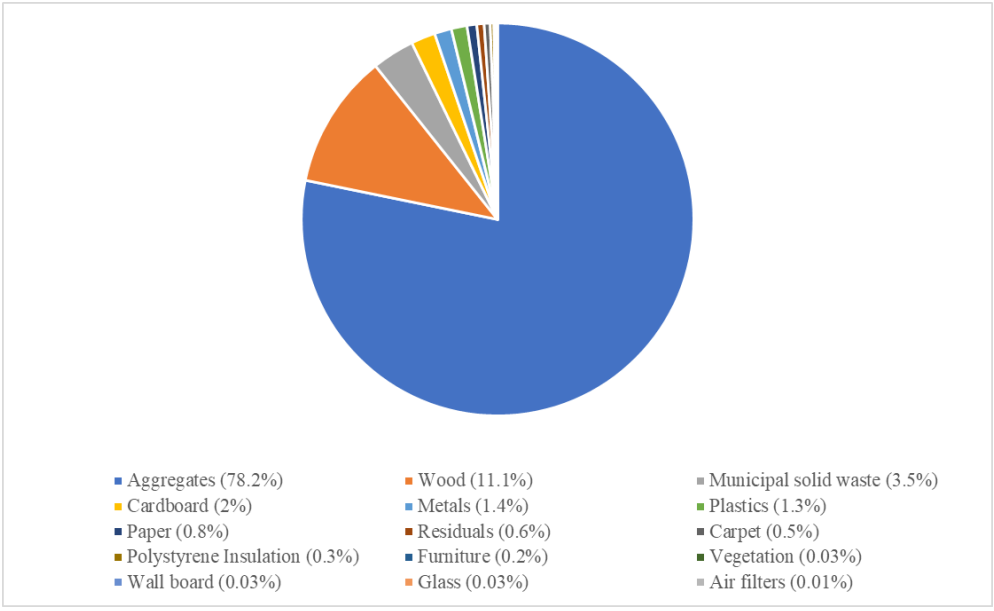

Figure 1: Construction waste composition

2 RECYCLED CONCRETE AGGREGATES

The aggregate material produced from a construction and demolition waste recycling facility is produced at a variety of different size grades suitable for use in various construction works. The potential uses include:

- Sub-base material under roads
- Drainage networks and standpipe filler
- Landscaping material
- Non load bearing concrete such as pavements and flooring
- Non load bearing concrete blocks

The quality of the output aggregate material is dependent upon the process used to remove contaminants from the input waste material. To reach a higher quality output product, washing is typically incorporated into the recycling process to remove sands and cement that can remain under a dry crushing system. A lower quality product can be used as a road sub-base material whilst a higher quality product can be used for landscaping works and non-load bearing concrete applications. Achieving a higher output quality is also dependent upon the quality of the input material that is received at the facility.

3 REGULATORY FRAMEWORK

3.1 Input material

Control of the input material arriving at the facility should be considered to maximise the throughput of potentially recyclable aggregates and increase the quality of the output aggregate product. Controls on the input material also prevent these recyclable materials from being disposed to landfill. Control of the input material is achieved by controlling the types of waste that arrive at the recycling facility and through the prevention of landfilling of concrete and aggregate waste.

3.1.1 Construction site controls

A successful way of promoting the arrival of a cleaner concrete and aggregate waste material at the construction waste recycling facility is to promote source segregation at construction sites. Source segregation can be achieved through specific government regulations that require developers and construction contractors to segregate waste at the site with a focus on the segregation of concrete and aggregate wastes from other materials. Segregation on site should be followed by segregated transport of the waste to the construction waste recycling facility.

3.1.2 Landfill charges

A second way of promoting the segregation of concrete and aggregate wastes from other waste materials is to implement a higher landfill gate fee for mixed waste and a lower gate fee at the recycling facility for vehicles containing segregated concrete waste. With this regulation in place it is in the interest of the developer, construction contractor and delivery vehicle to make sure that only segregated concrete and aggregate are transported to the facility. Any mixed waste arriving at the gate is redirected to the landfill and charged a higher fee. A mixed material gate fee based on weight would be a successful way of reducing instances of mixing of construction waste with concrete. Concrete has a significantly heavier weight that other construction materials meaning weight based charges systems would be costly if the segregation requirements were not adhered to.

When a financial deterrent is put into place for the management of a waste stream, it is important to recognize that this act may result in increased instances of illegal dumping as delivery vehicles try to avoid the high mixed waste landfill charges by illegally disposing of the waste on unused remote ground. A system of fines and penalties enforced by the regulatory body can assist in the prevention of illegal dumping activities and should be seen as helpful when used in combination with a tiered gate fee system.

3.2 Output product regulations

The successful development of a construction and demolition waste recycling facility requires a demand for the output product that is produced. The demand for the output product can be increased through the development of product specifications which provide a guarantee to the quality of the product. Typically, different end use applications require the product to conform to different specifications which may indicate the quality, strength or grade of the product for its intended use. The requirement for a construction and demolition waste recycling facility to conform to various product specifications means the product can readily be used for a wider number of uses.

To support the product uses, regulatory mandates can be issued which require certain entities to enforce the use of a certain percentage of the recycled concrete aggregate for certain uses. An example of this is the use of the aggregate as a sub base material within road projects. The Abu Dhabi Waste Management Center has released a mandate which requires 40% of the total aggregate used in a road construction project to comprise recycled concrete aggregate.

4 CONCLUSION

It can be seen that regulatory changes can have significant positive impact upon the success of construction and demolition of waste recycling facilities. These regulations are focused around either the input of concrete and aggregate material into the recycling facility or the output use of recycled aggregate in new construction projects.

REFERENCES

Globex-City Consult (2001). *Construction waste composition – Abu Dhabi*.

National Development Strategy (2018). *Qatar Second National Development Strategy*.

Cite this article as: Dowding S., Daoutis G., "Regulatory Frameworks for the Successful Implementation of Construction and Demolition Waste Treatment Infrastructure", *International Conference on Civil Infrastructure and Construction (CIC 2020)*, Doha, Qatar, 2-5 February 2020, DOI: https://doi.org/10.29117/cic.2020.0127

An Analytical Review of Sustainable Green Buildings in Qatar: Implementations in the Architecture, Engineering and Construction (AEC) Sector

Diala Al Midani
dalmidani@qu.edu.qa
Department of Architecture and Urban Planning, Qatar University, Doha, Qatar

Fodil Fadli
f.fadli@qu.edu.qa
Department of Architecture and Urban Planning, Qatar University, Doha, Qatar

ABSTRACT

Sustainable buildings and related construction techniques are becoming increasingly recognized within the urban planning development in Qatar. The study aims to develop an analytical review of sustainable green projects in several countries to highlight the main sustainable green buildings principles and techniques. In addition, the study aims to propose a set of recommendations that facilitate and improve the green building principles implementation in Qatar. The methodology is based on qualitative approach in collecting data about the sustainable green buildings besides highlighting existing relevant projects from different countries. Moreover, analyzing the green building assessments systems to review their classification and technique. The analysis reveals that sustainability is witnessing a growing awareness in the construction domain in Qatar and many countries, which is leading to a prominent attention to develop green buildings and sustainable construction industries. The discussion indicates some perplexed opinions related to green buildings issues, such as the cost. Therefore, the present paper mentions that green building approaches still need further knowledge across stakeholders to demonstrate the various benefits of green buildings, primarily the energy efficiency to promote best practices. Consequently, the paper addresses the need for a governmental legislation to ensure implementing green buildings as a step forward on sustainability implementation in the AEC (Architecture, Engineering and Construction) sector in Qatar.

Keywords: Green buildings; Sustainability; AEC sector; Qatar

1 INTRODUCTION

Sustainable Green Buildings are one of the most effective construction techniques that is used in the world. It is widely used in the last few years in some Arab countries, especially in Qatar and United Arab Emirates (UAE). It is becoming more common because of its outstanding efficiency in consuming the resources such as energy and water supplies. It, also, uses environment friendly construction materials that produce less amount of carbon dioxide. The construction technique of sustainable green buildings includes the design, implementation, operation, removal and recycling of the building materials and it takes into consideration the basics of environment friendly construction in each phase. It has the least effect on the surrounding environment compared to regular buildings. Using this construction technique has helped the Qatari government's plan to ensure saving the power resources by 50% and the water usage by 40%. The construction

materials used in green buildings helped reducing the harmful emissions by 35% (Schulz, 2018). All of the previous gives a good explanation why the international market of green buildings is expected to grow from 7 billion $ in 2015 to be 36 billion $ in 2020 (Waked, 2018). The Qatari government is paying more attention and doing serious studies in the field of sustainable construction and green buildings as it is adopting that technique in its future construction projects. The GSAS (Global Sustainability Assessment System) was developed in association with the Pennsylvanian University to create a sustainable urban environment that reduces the environmental impact of the buildings. The spread of the implementations of the sustainable construction in Qatar is benefiting the environment as it reduces the consumption and produces less air pollution. This spread helps to make a high standard building with a great architectural design, which in return creates the modern urban environments. (X.L. Zhao, 2016).

There is a split in opinions of whether the sustainable green buildings construction technique is very effective. The pretense was that this technique costs a lot of money compared to the regular types of buildings. It is, indeed, much more expensive than regular types of construction, but we should also consider how much of the resources consumption it reduces, and then, we could tell how efficient it is.

In this study three existing examples of sustainable green buildings from different countries has been highlighted in order to produce a comprehensive and analytical review of the sustainable green building's technique.

The objective of this study is to determine the effect of sustainable construction on the AEC sector in Qatar, the neutralization of the relationship between the cost of sustainable green buildings and the saving in the resources consumption and finally how the implementations of that technique in Qatar is being subdued to an accredited system or code of specifications.

2 BACKGROUND

Sustainable green buildings technique is considered a visionary trend that sooner or later many countries will adopt. This technique was developed gradually over many years. In the engineering fields, the ideas are generated from problems, that is how the sustainable construction technique started. There was a persistent need to solve problems such as the increasing demand and consumption of the resources like energy and water. The studies mentioned that the regular building materials are responsible for a huge amount of the carbon dioxide generated in the air (Meadows, 2010). Then the idea of finding an alternative techniques and materials was developed to mitigate these problems. The cost is much more expensive than usual, but the results was significantly positive.

The following are some examples of the implementations of the sustainable green buildings and a brief review of each one:

2.1 BedZED:

The Beddington Zero Energy Development (BedZED) is a great existing example of sustainable construction implementations. It is an environmentally friendly housing development that is located in England, in Hackbridge, London. It was the first large scale community in the United Kingdom. The project started in 2000 and it was completed in 2002. The project belongs to Peabody Group which has more than 66000 homes in London

Peabody Group made partnership with architect Bill Dunster in order to carry out the project of building the first large-scale community in the United Kingdom. The building was designed to be carbon neutral by creating zero carbon dioxide emission, which helps being an environmentally friendly building. BedZED project is also distinguished by being the first construction project where the government of the United Kingdom sold the land at a lower price than the market in order to encourage sustainable development economically viable. The BedZED project consists of 82 homes and about 1405 square meters of workspace.

In order to be a zero-carbon emission facility, private transportation is discouraged. The project encourages public transportation (like the provided rail and bus routes), cycling and walking beside having a very limited parking space. BedZED project's buildings uses only renewable energy resources which is generated on site. The main source of energy is the 777 square meters of solar panels. There are many systems that provide different forms of energy such as Cogeneration or Combined Heat and Power (CHP) system, which is fueled by the tree waste to provide electricity. Everything was taken into consideration while the construction process, even the building materials were selected from renewable or recycled sources. The materials were selected within maximum 50 miles around the construction site in order to minimize the required energy for transportation. The architectural design stated that the houses were oriented to face the southern direction so that it faces the sun most of the day and have the maximum possible thermal insulation. The water system also was selected to rely on the rainwater, which is collected and treated to be reused, and the recycled water. In the terms of the urban appearance, the apartments finishing was done to a high standard to satisfy the residents. Private cars were discouraged while public transportation and walking were encouraged. (Peabody, n.d.)

One year after the start of the operation, the project achieved distinguished records as an environmentally friendly project. The space heating was not as much needed as usual. More than the half reduced the hot water consumption. The use of electricity was also, reduced thanks to the smart systems and the solar power panels. Special vehicles had less mileage than usual as planned after encouraging using public transportation, cycling and walking. The cost of the apartments in the project is very expensive hoping that would change in the near future. A while after the start of the operation, a few problems were found such as the dysfunctional problems in many of the systems used to generate electricity and to recycle the water. The maintenance costs a lot of money and that made the problem harder to cure. (Peabody, n.d.)

BedZED project was a significant example of the sustainable construction and green buildings. It gained many awards from 2000 till 2005 such as: Housing Design Award for sustainability from the Royal Institute of British Architects in 2001 - Evening Standard New Homes Awards in 2001 - Office of the Deputy Prime Minister Award for sustainable communities in 2003 - Stirling Prize in 2003 - Bremen Awards Special Commendation in 2004 - Sutton and Cheam Society Design award in 2005.

2.2 Chorlton Park Apartments:

The Chorlton Park Apartments is a green apartment building, in England. It was designed by Roger Stephenson, an architect, and built as part of collaboration between

Urban Splash and Irwell Valley in the year 2002. The project collected several awards such as the Housing Design Award in 2001, Roses Design Awards - best residential project in 2002 and in 2003 in the residential section; it won the MSA Design Award as well. (Colquhoun, 1999)

Natural light is maximized by the orientation of its living rooms with bedrooms located on the inner side of the building to have the minimum noise from the street. Each apartment has a balcony with louvered screens on rollers to provide shade and privacy. They are designed to be an extension of the living space and are constructed using a frame of green-oak posts and beams which were reclaimed from a wind-damaged forest in France. The standards of the green buildings were considered while the phases of the design, implementation and operation of the facilities of the project. Low heating and maintenance costs and sustainable construction were among the priorities in developing the site.

2.3 Green Building Principles:

There are some principles that the green buildings should have in the terms of design, implementation, operation and recycling. These principles are considered the most important as they are the elements that make a green building. (Seville, 2013)

• **Zero Energy:** The design of the project considered that only energy from renewable sources generated on site or near the construction site will be user. Usual types of energy like gas that runs cars are not encouraged because of the environment harmful gases it causes. Also, energy resources need transportation and that idea is not encouraged, in order to minimize the harmful gases in the site area.

• **Energy Smart:** the house is preferred to face the sun most of the time if it's possible, to help the solar panels absorb the sunlight and produce clean energy. The houses also have the most thermal insulation, so facing the sun most of the time is not considering a problem.

• **Water Efficient:** the water used in the projects of green building is not relying on the regular resources of water, it uses the rainwater which is collected after the rain and used. Also, the reclaimed water is used since the projects have water recycling units.

• **Low-Impact Materials:** The building materials are selected from renewable sources or recycled ones. It is preferred to collect building materials within 80 km from the construction site, to minimize the energy required for transportation.

• **Waste Recycling:** Waste is collected in facilities that are designed to support recycling.

• **Transportation:** Private cars are discouraged in many ways such as awareness campaigns, car free zones in specific areas and by reducing the parking areas. Otherwise, public transportation, cycling and walking are encouraged and supported.

• **High Quality of Life**.

These and others are the most common principles of green building construction that every green building design should consider. It delivers a high-quality building that ensures the high class and high standard lifestyles and being an environmentally friendly building (Seville, 2013).

3 METHODOLOGY

The study is based on qualitative approach in collecting data about the sustainable

construction and green buildings. Firstly, it highlights existing sustainable projects from different countries, then analyzing the green building assessments to review the assessment classification and technique. Consequently, addressing certified green and sustainable projects in Qatar and gulf region. The study adopts data from the United Nations Environment Program (UNEP) about the effect of the regular building on the environment, in addition to the statistics from the United States Green Building Council (USGBC) to highlight the importance of the sustainable green buildings system.

The collected data is mainly gathered from certified websites like the United Nations Environmental Program (UNEP) official website, Peabody and IES LTD.

4 ANALYSIS

The sustainable green buildings construction is based on some well-known concepts that every building must achieve. The buildings are subjected to the evaluation by one of the international evaluation systems such as LEED or BREEAM. These two systems are examples for the systems that determine whether the building is a green building or not. But at first it is necessary to overview the GSAS and QSAS. They are also green building evaluation systems. In Arab countries, the sustainability of the buildings is greatly required to not only cope with the growing needs of comfort and high standard apartments, but also to respond to the nature whining about how cruel the humanity is dealing with the resources and wasting it. Green buildings may cost more than regular buildings in the implementation phase, but once the building is ready for operation, almost every single resource consumption is reduced by a great percentage. It is called "green" buildings for an obvious reasons, it reduces the harmful effect of the regular buildings on the environment, as in usual the regular buildings are responsible for about 35% of the carbon produced in the air (Schulz, 2018). The building materials, the public transportation and all other elements of the construction process are taken into a. The GSAS is considered as the most comprehensive green building assessment system in the whole world. It was set after the precise analysis of over 40 green buildings codes of specifications from all over the world. One of the most important advantages of the GSAS is that it considers the social, economic, environmental and cultural features of the society, which mainly differ from one country to another around the world. Many of the Middle Eastern and North African (MENA) countries such as, Saudi Arabia, Kuwait, Jordan and Sudan paid great attention about considering the GSAS a unified green building certification in the MENA region. (Schulz, 2018)

In 2010, Qatar included the Qatar Sustainability Assessment System (QSAS) in Qatar construction code of specifications. Recently every single project whether it is a public or private sector must have a GSAS certificate. The 140 building rating system of GSAS includes a sustainability assessment mechanism and it divides into 8 sections: urban communication, site, energy, water, urban environment, economic value, cultural value management and operation. Every section of the system is measuring a specific criterion of the environmental impact of the project. The sections are well illustrated and clear. The sections of the project are evaluated and given degrees that match comply with the specifications. (Waked, 2018)

The government in Abu Dhabi made an initiative to improve the life of residents in Abu Dhabi throughout concentrating on the cultural habits and the social values, so it

initiated the Pearl Rating System (PRS). The PRS is Abu Dhabi Emirate green building assessment system. It was designed to support the sustainability of buildings from the beginning in the design phase until the operation including the building and the villas. It states some requirements to evaluate the expected performance of the project from the sustainability perspective. The PRS is made with precision to consider the common climate in Abu Dhabi that requires a high need of energy to satisfy the air conditioning systems, high evaporating rate and low rate of rain flow and lack of drinking water. The PRS has many levels of certifications starting form one pearl reaching up to 5 pearls. To develop any project inside Abu Dhabi Emirate, it is required to have a certificate with at least 1 pearl. The PRS is divided into 7 sections, which are getting between compulsory credits and optional credits. To get the 1 pearl certificate it is required that all the compulsory credits are achieved (Aigbavboa, 2019).

Unlike the GSAS there is a less famous system to rate the green buildings in Lebanon which is called the ARZ Rating System. It is the first Lebanese green building assessment system as an initiative to create an international code of specifications with a credential system managed by Lebanon Green Building Council (LGBC). That council was created to support the implementations of the sustainable green buildings in Lebanon. ARZ Rating System was developed by Lebanese experts from the LGBC in association with the National Finance Corporation. The system aims to achieve the most efficiency in operation and reducing the environmental impact. ARZ Rating System is a curriculum based on evidence to evaluate the sustainability of buildings. The system includes some techniques, procedures and energy-consuming levels that the LGBC expect to see in the future in the Lebanese sustainable green buildings. An evaluator certified by the LGBC performs an inventory of the energy consumption, the water consumption and the procedures and techniques applied in the building, then the LGBC gives a rating degree to the building based on how it is corresponding with the techniques and procedures related to the ARZ Rating System (Islam, 2019).

4.1 GSAS:

GSAS refers to the Global Sustainability Assessment System, which is based on performance and developed for rating sustainable green buildings and infrastructures. Its main and primary objective is to create a sustainable environment that minimizes ecological impacts and reduces the consumption of resources, like energy and water, while addressing the local needs and environmental conditions of the region. It adopts an integrated lifecycle approach for the assessment of the environment including the phases of the design, construction and operation (Sillitoe, 2017). The GSAS started in 2007 by reviewing more than 140 building rating systems and codes of specifications, tools, and guidelines from all over the world and narrowed down to the 40 whole building rating systems. The study then focused on the review and the assessment of the best practices adopted by international green buildings rating systems. The system aims to improve the human wellbeing, protecting natural environment and conserving natural resources (GORD, 2019).

4.2 QSAS:

It might be said that Qatar Sustainability Assessment System (QSAS) is the Qatari

specialized Global Sustainability Assessment System. It is a green building certification system developed for the State of Qatar. The primary objective of QSAS is similar to the GSAS objective, which is to create a sustainable environment that minimizes ecological impact while addressing the specific regional needs and environment of Qatar and Qatari people. It was developed in 2010 by the Gulf Organization for Research & Development (GORD) in association with the University of Pennsylvania to achieve the objective of the GSAS/QSAS to create a sustainable modernized environment to reduce the buildings' ecological impact and in the same time achieving the needs of the society (Sillitoe, 2017).

4.3 UN Environment Program:

The United Nations gives strong attention to the sustainability of the environment, the United Nations Environment Program (UNEP) took seriously the issue of sustainable buildings after the increasing rates of pollution and resources consumption. Studies showed a clear relationship between public health and buildings in terms of being harmfully affecting. Meanwhile, the built environment developed based on a huge amount of energy which is about 40% of the global energy consumption, greenhouse gas (GHG) emissions which is about 30%, the generated waste and natural resources consumption that are threatened to run out (Meadows, 2010).

UNEP started the Sustainable Buildings and Climate Initiative (SBCI) in 2006 in order to address these issues. It supports the practices of sustainable buildings on a wide scale with a focus on the efficiency of energy and emission reduction of Greenhouse Gas (GHG). SBCI gather around stakeholders who are involved in the process of planning, building and policy making on the local, national and international levels by providing a space for discussion and well-studied teamwork decisions. The initiative develops strategies of a better evaluation and implementations of the sustainable building practices. Pilot projects show how important is the role of green buildings for adaptation to different climate changes. Sustainable Social Housing Initiative (SUSHI) is one of those pilot projects in UNEP. It enhances the sustainability in the green social housing projects. Another project to test the available tools and construction strategies is the Sustainable Buildings Policies in Developing Countries (SPOD). It aims to help governments at both of the national and the local fields in order to develop policy tools to support the practices of the green buildings and the mainstreaming sustainable construction. In two pilot cities, Ouagadougou 'Burkina Faso' and Nairobi 'Kenya', a 'Quick Scan Tool' to evaluate the policies in the building branch and also scenarios to improve the state are being tested (Sustainable Buildings, n.d.).

4.4 Green Building Projects in Qatar and Gulf region

There are several projects in the Gulf region that adopted the sustainability construction techniques of green buildings. Some of them are in, Qatar and others in Gulf region as the following:

Qatar Museums Authority (QMA) Tower:

Qatar Museums Authority (QMA) Tower is a Grade (A) 16 floor commercial office buildings in Doha. The building is used as the Qatari Museums Association head office in Qatar. The project managed to achieve the requirements of the LEED Silver Certified

level of sustainability in construction under the United States Green Building Council's (USGBC), Leadership in Energy and Environmental Design (LEED™) and Green Building Rating System for Commercial Interiors 2009. (Oxford Business Group, 2014)

Sowwah Square:

This project is covering an area of 500000 square meters and is located in Abu Dhabi in the United Arab Emirates (UAE). It is a multibillion-dollar project, a mixed-use waterfront development, comprise of four commercial towers ranging from 33 to 36 stories, as well as two buildings with six story car parks and the iconic Abu Dhabi Securities Exchange, alongside a luxury retail and restaurants. It obtained the LEED Gold certification of sustainability in 2014 (Location Group Research, 2014).

Lusail Marina District:

Lusail Marina District is a 21+ story residential building located in Lusail City, which is one of the most groundbreaking concepts of Qatari Diar Real Estate Investment Company. Lusail City is a futuristic project, which will deliver a modern and ambitious society in Qatar. The smart and inspirational environment combines artistic elements of architecture with various practical and versatile services in order to deliver perfect products that satisfy all the needs of its residents (Oxford Business Group, 2014).

Al Ain Ladies Club:

The implementation of the project took about 2 years, from 2012 until 2014. The project provides ladies-only sports facility in the City of Al Ain and is part of the Abu Dhabi Sports Council's mission to ensure the provision of such facilities within the Abu Dhabi Emirate. The project has a net floor area of around 13,500 square meters with two floors. It has been designed to achieve a 2-Pearl rating from the PRS (Jane Stark, Trident Press, 2006).

5 DISCUSSION

From the previous brief review of opinions and projects related to sustainable green buildings then following it by reviewing existing sustainable projects. It became obvious how important to spread the approach of sustainable construction technique and green buildings. These are, the future of construction around the world. Qatar took that important step forward on the way to achieve its own individuals' prosperity and welfare, also to achieve the criteria of creating a sustainable environment with less harmful building materials, cleaner air and less energy resources consumption. The only problem that may face the projects of sustainable green buildings and sustainable is the cost. It has seen that the cost of a green building shall be divided into smaller sections or categories: Design, implementation, operation, maintenance and recycling. The high cost of green building is just until the implementation phase, and then the cost is less than regular buildings. The cost of the operation, maintenance and recycling is much less than usual as well. Thus, if a financial study were performed, investors would get encouraged to invest their money in the sustainable green building projects as it is not only a lower cost investment, but it is also a money saving investment that could, after few years, generate energy and have renewable resources. In order to ensure spreading this technique in the state of Qatar, the need for a governmental legislation is necessary. Ensure implementing green buildings is a step forward on sustainability implementation in the AEC. The study suggests additional recommendation to enhance the sustainable

green buildings implementation in Qatar as the following:

a. Expand green building education and awareness by providing educational campaigns.
b. Outreach to the financial and real estate community about the criteria and benefits of Green Building.
c. Continue and expand the professional development opportunities and requirements for staff by providing internal and external training.
d. Involve experts that can guide the project and implementation.
e. Share best practices with other companies/stakeholders.
f. Use water conservation products and practices when building.
g. Practice sustainable storm water management at building sites.
h. Recycling and reusing materials, on and off site.
i. Use local materials as much as possible to reduce transportation needs.
j. Design for the use of disassembly and reuse/recycling.

6 CONCLUSION

Finally, it is obvious that the sustainability techniques are important. As shown in the previous background, there are many existing examples of the sustainable green buildings in MENA region, especially in Qatar and United Arab Emirates. The climate state in those countries tempted its governments to think of alternative ways of construction, saving energy resources and deliver the high standard buildings and apartments that are also depend on the renewable energy resources. The sustainable construction satisfied all these needs and gave hope to a sustainable environment. It uses only renewable resources of energy, have special units and solar panels to generate electricity, have units that collect rainwater and recycle the used water, use environmentally friendly building materials that produce less carbon to the air. After a while of using the sustainability construction technique, the statistics from the Press Room of the United States Green Building Council (USGBC) showed that the electricity consumption was reduced by 30%, the hot water consumption is less by 57%, the private cars mileage was less by 65% and the most important for the environment, the carbon in the air was measured to be less by 40% in the green building areas (Press: Benefits of green buildings, 2018). Therefore, the study highlights the need of integrating the sustainable green buildings in the AEC sector in Qatar, which are seeking for a sustainable environment. The paper proposes a set of recommendations that contributes to enhance and improve the sustainable green buildings implementation.

REFERENCES

Aigbavboa, O. D. (2019). *Sustainable Design and Construction in Africa: A System Dynamics Approach*. New York, Abingdon: Routledge.

Colquhoun, I. (1999). *RIBA Book of British Housing*. Elsevier.

Fox, W. (2000). *Ethics and the Built Environment*. London: Routledge.

GORD. (2019). Retrieved from GORD: http://www.gord.qa/trust-gsas-resource-center-overview.

Islam, M. N. (2019). *Silk Road to Belt Road: Reinventing the Past and Shaping the Future*. Springer International.

Jane Stark & Trident Press. (2006). *United Arab Emirates Yearbook 2006*. Trident Press, Ministry of information and technology.

Kalle Kähkönen, J. P. (2005). *Global Perspectives on Management and Economics in the AEC Sector*. Technical Research Centre of Finland.

Location Group Research (2014). Retail Market Study Worldwide, 2014.

Meadows, R. S. (2010). *Green Building Materials: A Guide to Product Selection and Specification*. New Jersey: Wiley.

Oxford Business Group (2014). The Report: Qatar 2014.

Peabody. (n.d.). Retrieved from BedZED: https://www.peabody.org.uk/about-us/our-performance/sustainability/case-study-bedzed.

Press: Benefits of green buildings. (2018, Nov. 13). Retrieved from USGBC: https://www.usgbc.org/articles/green-building-accelerates-around-world-poised-strong-growth-2021.

Schulz, J. A. (2018). *Green Building Transitions*. Springer International Publishing.

Seville, A. K. (2013). *Green Building: Principles and Practices in Residential Construction*. Delmar.

Sillitoe, P. (2017). *Sustainable Development: An Appraisal from the Gulf Region*. New York, Oxford: Berghahn.

Sustainable Buildings. (n.d.). Retrieved from UN Environment Program: https://www.unenvironment.org/explore-topics/resource-efficiency/what-we-do/cities/sustainable-buildings.

Waked, T. (2018, 11 11). نظم تقييم المباني الخضراء في الشرق الأوسط. Retrieved from EcoMENA: https://www.ecomena.org/green-rating-mena-ar/.

X. L. Zhao, W. L. (2016, November 7). A Framework for the Integration of Performance Based Design and Life Cycle Assessment to Design Sustainable Structures. SAGE.

Cite this article as: Al Midani D., Fadli F., "An Analytical Review of Sustainable Green Buildings in Qatar: Implementations in the Architecture, Engineering and Construction (AEC) Sector", *International Conference on Civil Infrastructure and Construction (CIC 2020)*, Doha, Qatar, 2-5 February 2020, DOI: https://doi.org/10.29117/cic.2020.0128

East Industrial Pedestrian Bridge: A Case Studyof Value Engineering and High Performance Material

Theodoros Tzaveas
ttzaveas@ashghal.gov.qa
Public Works Authority (Ashghal), Doha, Qatar

ABSTRACT

East Industrial Road, a main arterial for the city of Doha with high average daily traffic, made crossing by foot being not only challenging, but also dangerous. Authorities proposed to build a pedestrian bridge over East Industrial Road which would allow for easy, safe travel over this busy roadway. As part of initiatives towards reduced cost of road construction and maintenance, alternative materials for the bridge were considered. For the construction phase, quick installation and utilization of prefabricated units, and for the operational phase, solutions not requiring periodical maintenance were favored. The primary objective of this paper is to describe the potential of aluminum in competition with common steel solutions for this pedestrian bridge. Collaborative design work remains a key aspect in projects that addresses not only technical efficiency but also human experience. Cross-disciplinary collaboration requires a language that allows exchanges across disciplinary boundaries. This paper also discusses the design process of the first pedestrian bridge built in Qatar made of structural aluminum. As engineering and building challenges increase in complexity due to environmental and political factors inherent in the modern age, as well as ever accelerating changes in technology, project clients are seeking ways for effective management. The purpose of value engineering is to improve the value of the project designs and to demonstrate to the client that the objective of "value" has been achieved. The process is documented to illustrate the range of considerations required in the design/construction team to ensure a successful project implementation.

Keywords: Pedestrian bridge; Structural aluminum; Aerodynamic effects; Vibration control; Value engineering

1 INTRODUCTION

In 2013, Public Works Authority (PWA) developed a program to deliver grade-separated pedestrian bridges in different parts of Qatar to provide a complete separation of pedestrian and vehicular traffic and make it easier and safer for pedestrians to walk to a variety of destinations such as schools, shopping centers and public transport.

Early 2014 the program was launched, initiating a procurement phase for high-priority locations mostly in terms of pedestrian safety based on traffic fatality figures. From the priority list, a specific location at East Industrial Road was selected for the first pedestrian bridge to be built by PWA. Value engineering principles applied to produce meaningful results within a reasonable schedule encouraging owner, contractor and stakeholder participation in the assessment in order to take advantage of experience and knowledge, which significantly increases the value of the ideas presented, and the

implementation of recommendations. In August 2014, PWA awarded a design & built contract to a joint venture of specialized contractors for the design and construction of an aluminum pedestrian bridge across the East Industrial Road. Work on site was completed late in the spring of 2015. This paper will demonstrate how the design has been developed specifically for its context; how it overcomes the challenging site constraints, the conflict between the design aspirations for a fully enclosed, air conditioned corridor, limited site access, and clearance constraints, and key design constraints for quick installation and utilization of prefabricated units, not requiring periodical maintenance for the operational phase while enhancing connectivity between the two development sites on either side of the road. Wind tunnel testing was required to demonstrate aerodynamic stability of the footbridge and detailed vibration computations carried out to ensure comfort levels to end users. The pedestrian counter installed on the bridge justifies the need and significant use of the bridge.

2 SITE

The bridge is located in the Industrial Area of Doha, on East Industrial Road at about chainage 123+560 along the main carriageway. East Industrial Road is a busy expressway serving the industrial area. There is a high percentage of HGVs along the route. It is a dual carriageway with a narrow median and the mainline consists of three (3) lanes in both directions. The service roads are 2 lanes. The industrial area is located to the south of East Industrial Road and commercial and residential areas are located to the north of road. Considering the development of the area, pedestrian desire lines were clearly defined between these areas that the bridge would ultimately serve.

Figure 1: Location map with the position of the bridge (in green)

3 VALUE ENGINEERING (VE)

Projects tend to be initiated based on linear, generic thinking that mostly consider the primary functions. For the particular project, additional requirements and constraints were merged as the concept was developing. Value engineering takes a step back and looks at the project from a functional perspective rather than how it is originally conceived. VE helps organizations improve the delivery of a project or product by reducing cost, improving performance, improving quality, saving time during construction, solving problems and using resources effectively.

Value considerations are not necessarily priorities in the planning of a project when compared with project cost analysis. Often, the design effort does not address life cycle cost. Scoping constraints, design standards and stakeholder demands often override any

initiative in the planning process to optimize the design or to manage costs. Often there is little time in the planning process for creativity and innovation in design. The risk associated with project delivery, schedule and operations may not be apparent in the project planning phase. For these reasons, lowest price option is not always the best value solution, which can be achieved in design. The project team reviewed the project functions and identified key components, as listed below:

- Design standards.
- Space for assembly but limited access and maneuvering.
- Congested area with services and utilities – limited scope for diversions.
- Continuous (& heavy) traffic 24/7.
- Limited space for staircase landings.
- Foundation footprint shall be limited to median.
- Limited road closures.
- High durability demand due to environmental exposure conditions.
- Options for dismantling and re-usability.
- Minimum inspection and maintenance requirements.
- Enclosed deck - Air Conditioned.
- Elevators.
- CCTV, fire safety, internal/external lighting.

Options comprising both steel and aluminum were assessed against an initial baseline concept of an open steel bridge configuration originally proposed for the particular site. Performance criteria were established as a basis of comparing options including safety, quality, aesthetics, new technologies, constructability, convenience, schedule and whole life cost. At the end of the process, a modular type aluminum enclosed truss as illustrated in Figure 2 was the preferred option to be developed to a detailed design.

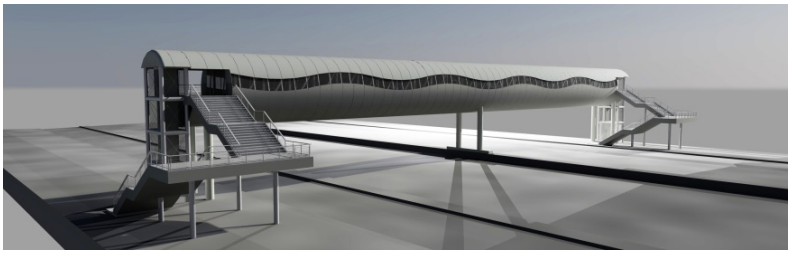

Figure 2: Rendering of the preferred option in aluminum

4 FOOTBRIDGE FORM AND DEVELOPMENT OF DESIGN

The proposed footbridge is a two span aluminum bridge with a total length of approximately 84m. The bridge is located within the right of way in the industrial area providing a safe crossing point over the East Industrial Road. The deck is enclosed with a cladding made of 4mm thick aluminum panels attached to a circular aluminum frame with double-glazing on the sides to provide the necessary transparency while maintaining air conditioning and ventilation of the enclosed footbridge deck. Access onto the bridge is provided by a staircase and lifts at both ends. The footbridge is equipped with air condition and ventilation system, CCTV, lighting both inside and outside, fire alarm and fire extinguishing devices, and a counter device which together with the lifts, are all

integrated into a Building Management System (BMS) to allow various types of control during the operation phase.

4.1 Concept design

The bridge comprised of a pre-engineered aluminum (Howe) trusses consisting of two simply supported spans measuring 40.15m & 38.15m. An expansion joint is introduced only at the middle over the central pier as illustrated in Figure 3. The pre-engineered solution developed further to improve the stiffness and capacity to accommodate the added loads as a result of the enclosures as well as adhering to deflection requirements of L/400. The bridge is designed to satisfy the requirements of BS5400-DMRBs, BS EN 1991-2 & 1999 and AASHTO LRFD. Adherence to PWA Interim Advice Notes 009 (Design Criteria for Highway Structures) and 006 (Specification for Bridge Bearings) and QCS are ensured through the various design phases.

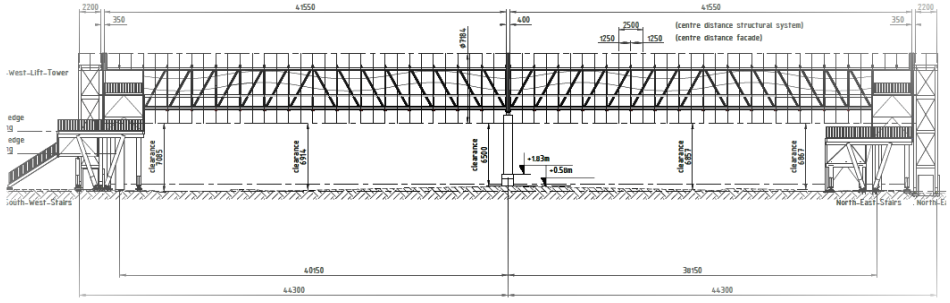

Figure 3: Elevation and span arrangement

4.2 Superstructure

The trusses are 4.80 m high and spaced at 4.75 m. The overall height of the bridge including the cladding is 7.18m. Effective deck width for the movement of pedestrians is 4.00 m with a total width of 6.55 m to include the maintenance corridors for access into the enclosure. Figure 4 illustrates the details of a typical truss.

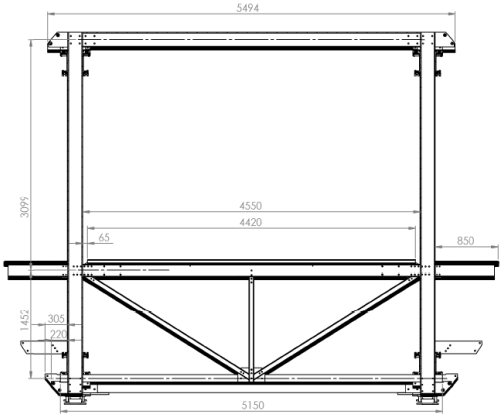

Figure 4: Cross section of typical truss

One of the big advantages of aluminum when compared to steel is ease of forming and the possibility of extruding complex profiles. This gives the possibility to design a multi-functional profile without extra costs. Truss members comprise of open channel section for the truss chords, hollow sections for the transverse frames and the diagonal members and T-sections for the cladding frames all made of alloy EN-AW 6082 T6 with an ultimate strength of 310 Mpa. All connections between aluminum members are bolted with stainless steel bolts of grade A4-70 to BS EN ISO 3506-1. When significant contact areas between dissimilar metals present in a joint location insulating washers or pads are introduced to isolate the different metals, aluminum extruded deck panels, 50mm thick, with a roughened surface oriented perpendicular to the traffic direction and the top of the transverse frames act as the walking surface.

4.3 Foundations and substructures

The exploratory holes conducted at support locations indicated that the subsurface stratigraphy is generally consisting of quaternary deposits and generally consists of slightly dense light brown, slightly silty, very sandy fine to coarse gravel of limestone. The Simsima limestone was encountered in all boreholes and generally consists of weak to medium strong, very thickly bedded, light grey, fine grained dolomitic limestone with few voids and few inclusions of very weak light greenish grey fine grained calcareous siltstone. Due to the lightweight features of the superstructure, it was possible to optimize the foundation footprint. The bridge supports consist of twin circular concrete columns with a diameter of 0.90 m resting on rectangular concrete footings, with plan dimensions 10x1.6m in the median and 10x1.8m at the two ends. With these optimized sizes impact, it was made possible to get around existing/future utilities corridors and minimize disruption during the excavation in the median.

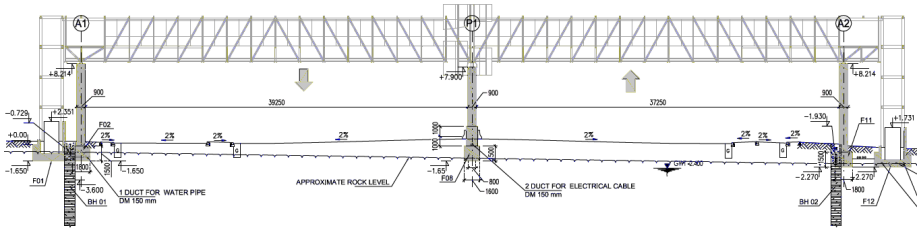

Figure 5: Foundation configurations

4.4 Articulation

The aluminum deck is supported on the columns through spherical bearings. Both spans are restrained transversally, and only allowed to slide longitudinally over the middle support. To accommodate the movements in the middle, both columns have a steel bracket to efficiently provide space for the pair of bearings for each span as illustrated in Figure 6.

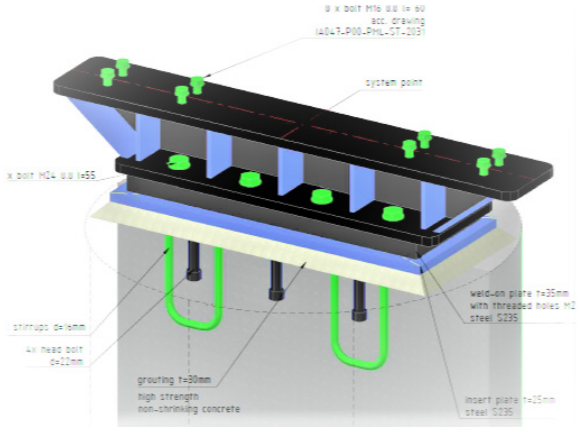

Figure 6: Steel brackets on intermediate piers

4.5 Aerodynamic assessment

The aerodynamic Susceptibility Parameter (Pb) was calculated as per BD 49 and resulted in a value of 0.26, which is within the scope of the rules specified in BD 49. Assessment of the bridge against the given criteria and limitations, suggested that, whilst the footbridge satisfies the limits for vortex excitation, but it could not comply with the divergent amplitude response checks for galloping and stall flutter. It was therefore necessary to demonstrate by other means that the wind speed required to induce the onset of galloping was in excess of the critical wind speed limit (calculated as 53m/s). A wind tunnel test illustrated in Figure 7 was subsequently commissioned and the footbridge was found to have sufficient stability against galloping and flutter. Resonant vortex shedding effects were excluded within the range of expected wind speeds at project site.

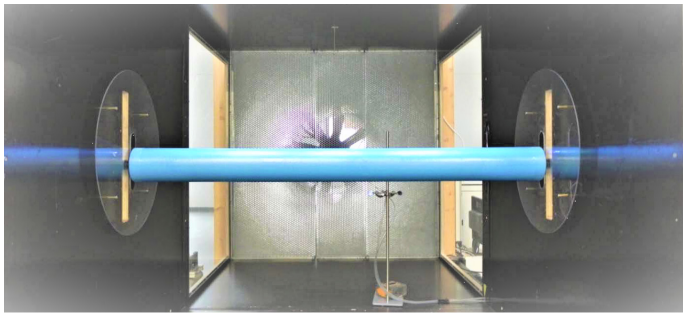

Figure 7: Section model in the wind tunnel test

4.6 Vibrations

The footbridge was also checked for vibration serviceability to ensure that the structure was not excessively excited by pedestrian use in reference to BD37 and BS EN 1991-2. The determination of natural frequencies and analysis of induced vibrations was made by a special software using 3D model as shown in Figure 8.

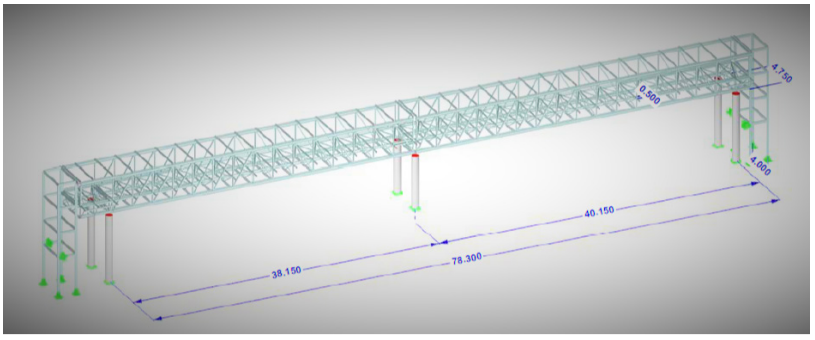

Figure 8: Isometric view of analytical model

In vertical direction the fundamental natural frequency was found to be 2.23Hz. Therefore, maximum vertical acceleration had to be assessed. The assessment based on the provisions of NA to BS EN 1991-2 and carried out for walking and crowded, resulted in values of 0.585m/s2 and 1.485m/s2 respectively. When compared with the maximum design acceleration limit of 2.0m/s2 was found satisfactory. The natural frequency in horizontal direction satisfies the threshold of 1.50Hz.

5 CONSTRUCTION

Adopting a configuration with bolted connections and manageable lightweight member lengths may pose some difficulties and risks during the assembly process but on the other hand proved to be advantageous in the construction logistics and the delivery schedule. Aluminum was fabricated off site in fabrications workshops overseas under well controlled and monitored conditions. The members delivered to site section sizes suitable to be transported in standard container sizes. The area adjacent to the bridge site was made available to the construction team for assembly of the bridge. This removed significant health and safety risks associated with erecting and assembling large bridge modules and transporting them to the bridge site. Carriageway possessions for footbridge erection and construction were clearly very limited for such a busy corridor. The reduced weight that the aluminum offers, allowed spans to be constructed progressively, including cladding and finishes supported on temporary trestles and then positioned on the piers during only two overnight possessions using a pair of mobile cranes for each span. Figure 9 shows a typical span being assembled including the cladding and subsequently erected using mobile cranes. When the 41m long span module was lifted for installation it was weighing approximately 24 tons.


Figure 9: Off-site assembly and erection of typical span

6 CONCLUSION

The design and construction of the East Industrial Pedestrian Bridge, from inception to final handover was challenging. End users prove the success of the project when considering the recorded number of passages over the bridge which was just over two (2) million by the end of 2018. By applying value engineering principles even in a slightly informal way opened the opportunities for non-conventional approaches to be adopted and new materials to be utilized. The primary objective of this paper is to present the potential of aluminum solutions within pedestrian bridges based on a case study in the State of Qatar. As a construction material, aluminum contains several advantages; high specific strength, high corrosion resistance, and no need of periodic maintenance. Concerning manufacturability of aluminum, smart and creative use of manufacturing methods and pre-engineered solutions give the material an advantage to implement a tight design and construction programme.

Communication is paramount to handling the challenges on a project of this scope and magnitude. The project team is large, the scope of work often widens to adopt client's aspirations and stakeholder requirements, things happen fast, and everything must get underway with a minimum of lead-time. Effective communication mostly comes from hard work, interpersonal interaction and controls guiding the conduct of the communication process throughout the project. Understanding this and the principals that govern effective communication the project team collaborated with the construction team to develop an effective communication path between the designer, the independent checker, the contractor and the subcontractors and material suppliers which resulted in the successful implementation of the project.

REFERENCES

British Standards Institution. Eurocode 9: BS EN 1999 - Design of Aluminium Structures. BSI, London, the UK.

British Standards Institution. Eurocode 1: BS EN 1991-2 – Actions on Structures. BSI, London, the UK.

British Standards Institution. BS EN ISO 3506-1 - Mechanical properties of corrosion-resistant stainless steel fasteners. Bolts, screws and studs. BSI, London, the UK.

British Standards Institution. BS5400: Steel Concrete and Composite Bridges. BSI, London, the UK.

Highways Agency. Design Manual for Roads and Bridges, BD49 - Design Rules for Aerodynamic Effects on Bridges. Highways Agency, London, the UK.

Highways Agency. Design Manual for Roads and Bridges, BD37 – Loads for Highway Bridges. Highways Agency, London, the UK.

Highways Agency. Design Manual for Roads and Bridges, BD29 – Design Criteria for Footbridges. Highways Agency, London, the UK.

Save International. Value Standard and Body of Knowledge (2007). SAVE, New Jersey, the US.

Cite this article as: Tzaveas T., "East Industrial Pedestrian Bridge: A Case Study of Value Engineering and High Performance Material", *International Conference on Civil Infrastructure and Construction (CIC 2020)*, Doha, Qatar, 2-5 February 2020, DOI: https://doi.org/10.29117/cic.2020.0129

Mechanical Performance and Thermo-Physical Properties of Cement Mortar Incorporating Hybrid Slags

Mahad Baawain
msab@squ.edu.om
Department of Civil and Architectural Engineering, Sultan Qaboos University, Muscat, Oman

Hamada Shoukry
aboshoukry2020@gmail.com
Housing and Building National Research Center (HBRC), Building Physics Institute, Cairo, Egypt

Khalifa Al-Jabri
aljabri@squ.edu.om
Department of Civil and Architectural Engineering, Sultan Qaboos University, Muscat, Oman

ABSTRACT

Owing to the growing environmental pressure to reduce waste and pollution, the effective utilization of industrial solid wastes in construction applications has gained notable attention. This study investigates the mechanical and thermal properties of cement mortars incorporating two types of waste slags. Ferrochrome (FeCr) slag aggregate was used as a replacement for sand at the ratios of 25, 50, 75 and 100 wt. %. Ground granulated blast furnace slag (GGBS) has been used as a partial replacement of cement at the ratio of 25 wt. %. Compressive strength, permeable voids content and thermal conductivity tests have been conducted after 28 days of curing. The microstructure characteristics have been investigated by scanning electron microscope (SEM) equipped with energy dispersive analytical x-ray unit (EDAX). The experimental results revealed that FeCr waste aggregates could satisfactorily replace for natural fine sand in cement mortars up to 25 wt. % without a remarkable degradation of the compressive strength. Furthermore, Increasing replacement ratios of FeCr aggregates over 25 wt. % have resulted in noticeable decrease in thermal conductivity and an increase in the permeable voids content of cement mortars. The integration of GGBS with FeCr aggregates leads to enhanced compressive strength, reduced voids content and contribute to improved microstructure. The developed mortars with comparatively improved thermal resistance can be recommended for several structural and non-structural applications especially in hot weather regions.

Keywords: Ferrochrome slag; Blast furnace slag; Compressive strength; Thermal conductivity; Microstructure

1 INTRODUCTION

The utilization of industrial solid waste materials as aggregates in concrete structures has become of great importance in terms of saving landfill space and reducing the consumption and demand for extraction of natural aggregates (Rao & Prasad, 2002; Taha & Nounu, 2008; Borhan, 2012). Various types of waste metallurgical slags like steel slag (Nadeem & Pofale, 2012), copper slag (Al-Jabri et al., 2009), ferronickel (FeNi) slag (Saha & Sarker, 2017) and recently ferrochrome (FeCr) slag (Al-Jabri et al.,

2018a) have been utilized for fine and coarse aggregates replacements in the production of cement mortar and concrete for various construction applications. Nadeem and Pofale (2012) investigated the use of granular slag as a partial replacement of natural sand in masonry and plastering applications. In this study, cement mortars in various (cement : sand) proportions of 1:3, 1:4, 1:5 and 1:6 by volume were prepared with granular slag replacing 25, 50, 75 and 100 wt.% of sand. The compressive strength increased with increasing the replacement level up to 75 wt. %. An enhancement by about 15% has been attained relative to the ordinary mortar. An experimental study conducted by Al-Jabri et al. (2011) in which various mortar and concrete mixtures were prepared with different proportions of copper slag ranging from 0% to 100% as fine aggregates replacement. The results obtained for cement mortars revealed that all mixtures with different copper slag proportions achieved comparable or higher compressive strength than that of the control mixture. The results obtained for concrete indicated that the substitution of up to 40-50% copper slag as a sand replacement yielded comparable strength to that of the control mixture. Increasing copper slag over 50% resulted in strength reduction. The mechanical performance of cement mortar incorporating 25, 50, 75 and 100 wt. % of FeNi slag as a replacement of natural sand has been studied by (Saha & Sarker, 2017). The compressive strength of the hardened mortars increased with the increase of FNS up to 50% and then declined with further increase of FNS. The study also revealed that the use of fly ash as 30% cement replacement together with FNS as replacement of sand decreased the strength of hardened mortars. Ferrochrome (FeCr) slag is a by-product from the production of ferrochrome.

The production of 1 ton of FeCr alloys yields about 1.1 to 1.6 ton of slag (Niemela & Kauppi, 2007). In Oman, there are two FeCr plants producing about 355,000 t of FeCr slag annually Al-(Jabri, 2018a). The majority of this by-product is not reused in an effective manner and is currently being dumped. Dumping of FeCr slag in the landfills induces environmental problems in terms of the risk of leaching of hazardous elements like Cr (VI) causing contamination of the soil and ground water. Panda et al. (2013) studied the properties of normal and high-strength concrete made with FeCr slag as an alternative for aggregate. The results indicated that replacement of fine aggregate with FeCr slag up to 75% has improved the strength of concrete compared with conventional concrete. The influence of elevated temperature on concrete incorporating 50 wt. % FeNi slag as sand replacement and 30% fly ash as cement replacement has been recently studied by (Saha & Sarker, 2019), the use of 30% fly ash showed significant improvement in residual compressive strengths of all the mixtures for exposure up to 600°C. Although, the use of supplementary cementitious materials (SCMs) like silica fume (SF), Fly ash (FA), Ground granulated blast-furnace slag (GGBS), metakaolin (MK), etc., was proved to be very helpful in improving physical, mechanical and microstructural properties of conventional concrete; in addition, the use of SCMs in the production of blended cement can reduce carbon dioxide emissions by approximately 22% and improve sustainability in construction (Flower & Sanjayan, 2007), few studies investigated the influence of SCMs on properties of cement mortar and concrete containing high amounts of recycled waste slag aggregates. The aim of this study is to investigate the combined effects of FeCr slag fine aggregates and GGBS (a by-product of steel making industry) as partial replacement for cement on the properties of cement mortar.

2 EXPERIMENTAL DETAILS

2.1 Materials

The cement used in this study was ordinary Portland cement, OPC (CEM I: 42.5 N). Two types of slags have been used in this study including FeCr and GGBS slags. FeCr slag granules were collected from the plants of ferrochrome industry, situated in Al Tamman Indsil Company (ATIC), Sohar city, Oman. GGBS is a byproduct of iron and steel manufacturing; it is also locally available in Oman. The chemical compositions of both FeCr and GGBS are demonstrated in table (1). The type of sand used is natural siliceous. The specific gravity of FeCr is (2.97) which is slightly higher than that of the sand (2.77). The FeCr grains are angular in shape; while, the sand grains are semi-rounded. The grain size distribution for the sand, FeCr-slag aggregate (as received) and their combinations in various proportions along with the lower and upper acceptable limits of grading according to ASTM C33 is presented in Fig. 1. It can be seen that the sand possessed the optimum gradation. The FeCr grading curve has exceeded the upper limit of ASTM C33; in addition, the grading is curve is approximately flat especially in the mid-size range, this indicates that the grains are not well-graded; i.e., they can be prone to segregation during mixing. The combination of FeCr with natural sand has relatively improved the gradation. The replacement of sand by 25% FeCr possessed a grading comparable to that of the natural fine sand.

Table 1: Chemical compositions of used slags (mass, %)

Material	SiO_2	Al_2O_3	Fe_2O_3	CaO	MgO	Na_2O	K_2O	Cr_2O_3	SO_3	TiO_2	Cl^-	L.O.I.
FeCr	37.29	22.50	1.91	1.46	31.10	0.23	0.04	4.64	0.50	0.17	0.06	0.10
GGBS	35.10	10.60	0.38	42.00	5.95	0.15	0.31	--	2.75	0.76	--	2.00

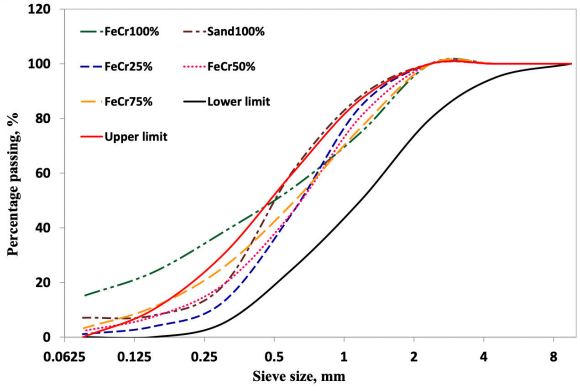

Figure 1: Gradation of sand, FeCr slag and their combinations

2.2 Samples preparation, identification and testing

The mortar samples were prepared using binder-sand ratio of 1:2.75. Fine sand was replaced with FeCr-slag aggregates at the ratios of 0, 25, 50, 75 and 100 wt. %. These mixtures were termed as (FeCr0, FeCr25, FeCr50, FeCr75 and FeCr100) respectively. Two groups of samples were prepared using different binders; a group made of OPC and the other made of 25 wt. % GGBS blended-OPC. The GGBS replacement ratio of 25 wt. % was proved to be the optimum by (Oner & Akyuz, 2007). The blended mortars were prepared using the water of standard consistency in order to attain a constant workability

degree among different samples. The compressive strength and volume of permeable voids tests were conducted on 50 mm cube samples at the age of 28 d in accordance with ASTM C109 and ASTM C642 respectively. Thermal properties analyzer (model: KD2 Pro) was used to evaluate the thermal conductivity of 50 mm cube dried samples in accordance with ASTM D 5334. The analytical scanning electron microscope, (JEOL JSM-7500F) equipped with EDAX unit for phase analysis was used to examine the microstructural characteristics of the freshly fractured samples.

3 RESULTS AND DISCUSSION

3.1 Compressive strength

Figure 2 shows the variations in compressive strength of the mortars incorporating various percentages of FeCr fine aggregates prepared with plain and GGBS-blended cements at the age of 28 day of curing. The mortar incorporating 25 wt. % of FeCr slag aggregates showed slight insignificant decrement in strength by about 5.70 %; whilst, the compressive strength considerably decreases by 23.74, 28 and 41.54 % for the use of FeCr aggregates at higher percentages 50, 75 and 100 wt., % respectively. This is attributed to the variation in grading characteristics of Fine sand and FeCr slag aggregates. Based on the grading analyses, the fine sand exhibited better grain size distribution than FeCr slag, which showed lesser proportion of finer aggregates passing 1.18mm. This is in line with previous studies reported that the use of slag with poor grading inversely affects strength (Saha et al., 2019). The grading that contains small percentages of aggregates in the mid-size range negatively affects the particle packing quality and result in the creation of permeable voids inside the structure. As it was expected, the use of GGBS as a SCM replacing 25 wt. % of OPC has satisfactorily compensated for the loss in compressive strength. The FeCr25 mortar attained a gain of strength by 10% and exceeded the compressive strength of the reference mortar made with natural sand and without GGBS. The maximum enhancement caused by GGBS incorporation is obtained for the mortar containing 50 wt. % FeCr slag aggregates; i.e., FeCr50 mixture has retrieved about 19% of the loss of strength relative to the reference ordinary mortar. The pozzolanic activity of GGBS explains the reason of enhanced strength. GGBS is classified as one of the active pozzolanic materials which consumes $Ca(OH)_2$ crystals liberated during cement hydration and creates additional cementing calcium silicate phase (CSH) and results in refining the pore structure and providing compact microstructure (Oner & Akyuz, 2007).

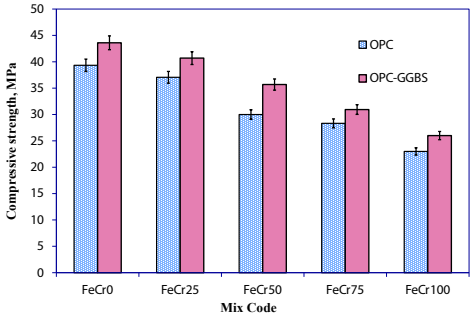

Figure 2: Compressive strengths of mortars containing various amounts of FeCr aggregates prepared with OPC and GGBS-blended OPC binders at the age of 28 day of curing

3.2 Volume of permeable voids

Figure 3 presents the permeable voids content (vol. %) for the mortars incorporating various percentages of FeCr slag aggregates prepared with plain and GGBS-blended cements at the age of 28 day of curing. The remarkable increase of volume of permeable voids (VPV) with increasing FeCr slag aggregates is consistent with the reduction in compressive strength. The VPV has been increased by about 8, 33.6, 40 and 49% relative to the reference mortar with the inclusion of 25, 50, 75 and 100 wt. % FeCr slag aggregates respectively. The increase of VPV points to the poor packing of FeCr grains inside mortar structure as compared with fine sand. Due to its ultrafine size and high pozzolanic activity, GGBS has considerably reduced VPV for all of FeCr slag-blended mortars by improving the physical packing; furthermore, the additional CSH produced by its pozzolanic reaction gets deposited in the inter-grain space and results in denser microstructure (Babu & Kumar, 2000). Although GGBS has relatively reduced VPV of the FeCr slag blended mortars, the mixtures that containing high percentages 50, 75 and 100 wt. % of FeCr recorded permeable voids contents higher than that of the reference mortar which indicates that there is still void spaces not filled with any hydration products.

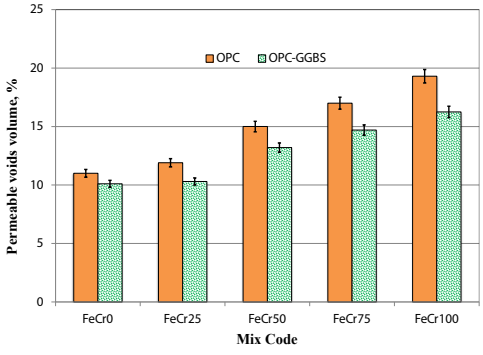

Figure 3: Volume of permeable voids of mortars containing various amounts of FeCr aggregates prepared with OPC and GGBS-blended OPC binders at the age of 28 day of curing

3.3 Thermal conductivity

Figure 4 presents the variation in thermal conductivity of the developed mortars containing FeCr and GGBS hybrid slags. It can be seen that the thermal conductivity decreases with increasing FeCr slag aggregates in the mortar. The thermal conductivity coefficients have been decreased by about 2.9, 7, 10.6 and 15.5% for the mortars incorporating 25, 50, 75 and 100 Wt. % of FeCr respectively as compared with the reference mortar. This is assigned to the increase of the voids content and the decrease of the bulk densities of the FeCr slag-blended mortars. These results are in line with findings of a previous study on the use of waste glass as sand replacement (Sikora et al., 2017). Due to its very low thermal conductivity, the static air entrapped in the voids between aggregates caused by the poor packing is responsible for the reduced conductivity coefficients (Krishnamoorthy & Zujip, 2013). The use of GGBS generally increases the thermal conductivity coefficients of the mortars with and without FeCr slag aggregates;

however, the maximum increase was found for the mortar made with fine sand (i.e., without FeCr). The increase of thermal conductivity is attributed to the improvement in the physical packing and the relative compactness of the microstructure achieved by incorporating GGBS. The compactness of solid structures facilitates the heat flow by conduction; therefore, increases thermal diffusivity and hence thermal conductivity (Al-Jabri & Shoukry, 2018b). The pozzolanic reaction induced by GGBS and the produced CSH affects the porosity of blended mortar and may alter the size, distribution, shape, and connectivity of the pores; this is the reason behind the considerable variation in the thermal conductivity attained upon the loading of GGBS (Gori & Corasaniti, 2014).

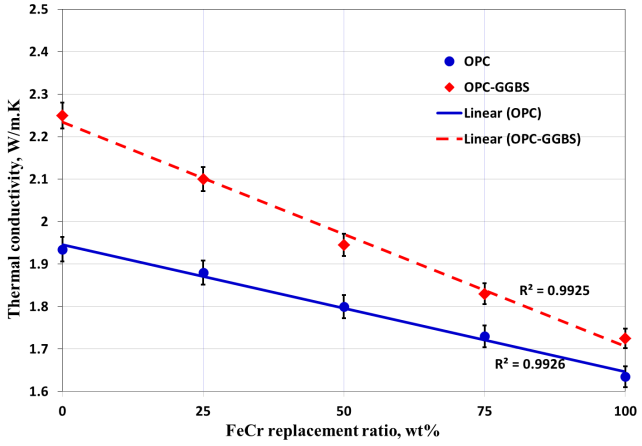

Figure 4: Variations in thermal conductivity of mortars containing various amounts of FeCr aggregates prepared with OPC and GGBS-blended OPC binders at the age of 28 day of curing.

3.4 Microstructure characteristics

SEM investigation was conducted to provide visual evidence of the change in microstructure characteristics responsible for the variation in the mechanical and thermal properties of the mortars incorporating hybrid slags. Figs. 5 and 6 Present SEM micrographs and EDAX spectra for the mortars incorporating 0 and 25 wt. % of FeCr slag aggregates made of plain and GGBS-blended cements. The SEM in Fig. 5(a) displays the most common hydration products of OPC including gel-like CSH and CH hexagonal crystals, these phases are not uniformly distributed through the hardened cement matrix; in addition, capillary micro pores are obvious. The inclusion of GGBS has remarkably improved the microstructure, denser and compact microstructure has been observed; furthermore, CH big crystals are absent; instead, gel-like CSH is predominant because of the pozzolanic reaction as shown in fig.5b. Fig.6a shows a FeCr aggregate embedded within the cement matrix the EDAX confirm the growth of CSH over FeCr aggregate surface; although, good binding is evident between aggregate and hydrated cement, big voids are present owing to the relatively less packing. The use of GGBS resulted in the production of additional honeycomb-shaped CSH networks in the inter-particle space and relatively improves the packing efficiency as depicted in fig.6b and confirmed by EDAX analysis.

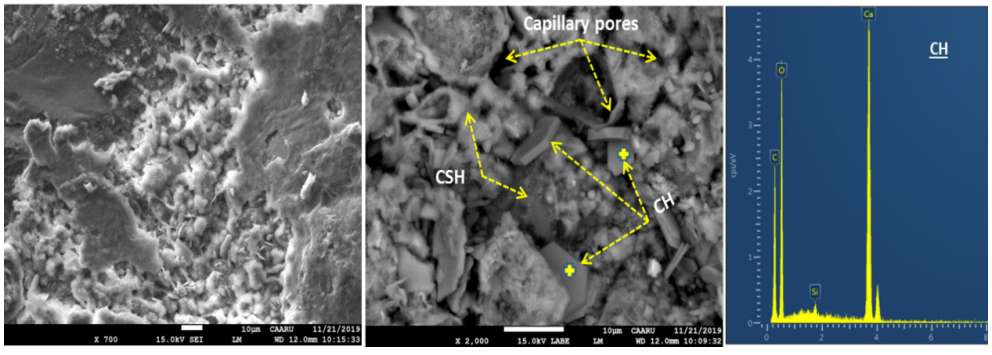

(a)

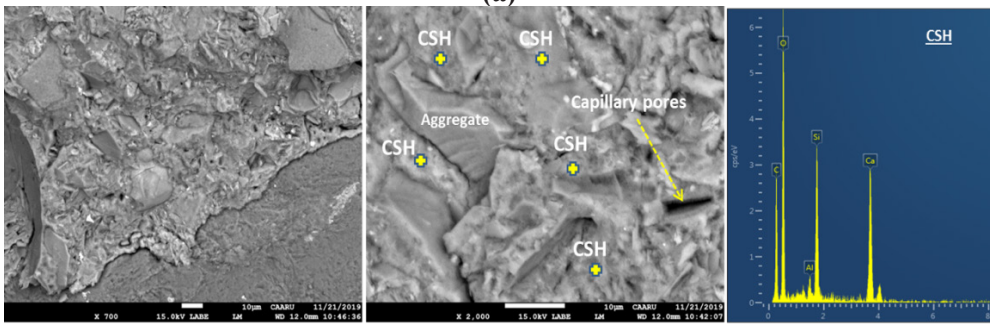

(b)

Figure 5: SEM micrographs and EDAX spectra of selected areas for mortars containing 0 wt.% FeCr made of (a) OPC and (b) GGBS-blended OPC

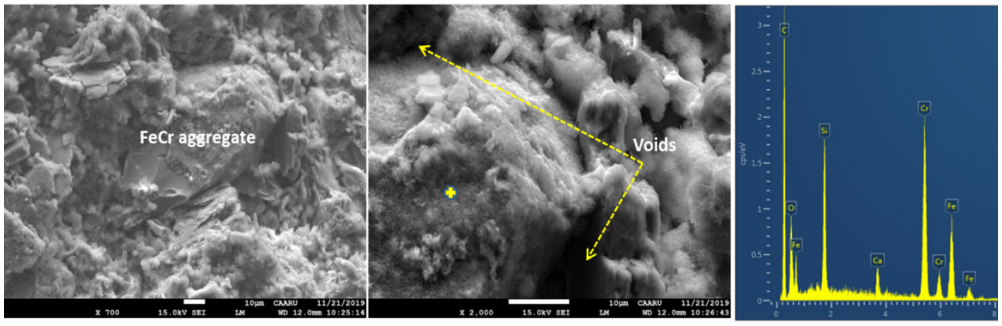

(a)

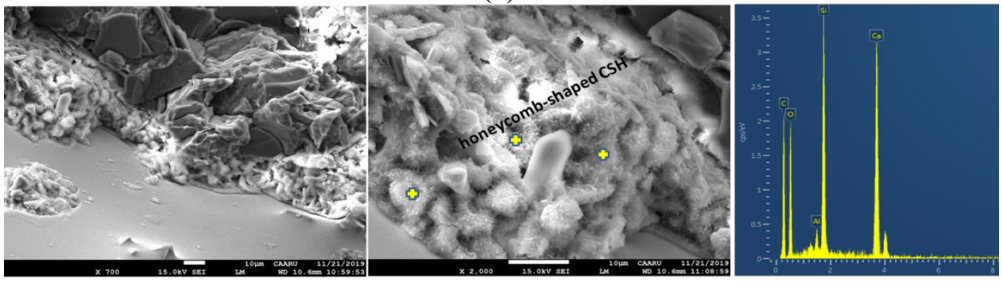

(b)

Figure 6: SEM micrographs and EDAX spectra of selected areas for mortars containing 25 wt.% FeCr made of (a) OPC and (b) GGBS-blended OPC

4 CONCLUSION

The combined/hybrid effects of FeCr slag together with GGBS on compressive strength, permeable voids content, thermal conductivity and microstructure of cement mortar have been investigated. The experimental results of this study warranted the following conclusions:

- The FeCr slag has a potential to be used as a substitute for fine natural sand in cement-based construction materials.
- The grading characteristics of FeCr fine aggregates affect to a great extent the mechanical strength and thermo-physical properties of mortar and play important role in determining the optimum replacement levels for natural sand. The inadequate gradation of the as received FeCr slag samples has restricted its utilization as sand replacement at higher percentages more than 25%.
- Controlling the grain size distribution of FeCr slag could help in improving the strength of the mortars incorporating high percentages of FeCr slag.
- The use of SCMs like GGBS is very helpful in enhancing strength, reducing voids content and improving microstructure of the FeCr-slag blended mortars.
- The use of FeCr slag at percentages higher than 25% reduces compressive strength and thermal conductivity, this may recommend these mortars (containing high amount of FeCr) for plastering applications where the high strength is not an important factor; however, the reduced thermal conductivity is useful for reducing heat transfer by conduction and hence improving thermal performance of exterior walls of buildings especially in hot weather regions.

ACKNOWLEDGEMENT

The authors would like to acknowledge the financial support provided by Sohar Port and Free Zone Company under Sultan Qaboos University Grant No. CR/ENG/CAED/18/07.

REFERENCES

Al-Jabri, K. S., Hisada, M., Al-Oraimi, S. K. & Al-Saidy, A.H. (2009). Copper slag as sand replacement for high performance concrete. *Cement and Concrete Composites*, *31*(7), pp. 483-488.

Al-Jabri, K. S., Al-Saidy, A. H. & Taha, R. (2011). Effect of copper slag as a fine aggregate on the properties of cement mortars and concrete. *Construction and Building Materials*, *25*(2), pp.933-938.

Al-Jabri, K., Shoukry, H., Khalil, I. S., Nasir, S. & Hassan, H. F. (2018a). Reuse of Waste Ferrochrome Slag in the Production of Mortar with Improved Thermal and Mechanical Performance. *Journal of Materials in Civil Engineering*, *30*(8), p.04018152.

Al-Jabri, K. & Shoukry, H. (2018b). Influence of nano metakaolin on thermo-physical, mechanical and microstructural properties of high-volume ferrochrome slag mortar. *Construction and Building Materials*, 177, pp. 210-221.

Babu, K. G. & Kumar, V. S. R. (2000). Efficiency of GGBS in concrete. *Cement and Concrete Research*, *30*(7), pp.1031-1036.

Borhan, T. M. (2012). Properties of glass concrete reinforced with short basalt fiber. *Materials &*

Design, 42, pp. 265-271.

Gori, F. & Corasaniti, S. (2014). Effective thermal conductivity of composites. *International Journal of Heat and Mass Transfer*, 77, pp. 653-661.

Krishnamoorthy, R. R. & Zujip, J. A. (2013). Thermal conductivity and microstructure of concrete using recycle glass as a fine aggregate replacement. *International Journal of Emerging Technology and Advanced Engineering*, *3*(8), pp. 463-471.

Nadeem, M. & Pofale, A. D. (2012). Replacement of natural fine aggregate with Granular Slag-A waste industrial by-product in cement mortar applications as alternative construction materials. *International Journal of Engineering Research and Applications*, *2*(5), pp. 1258-1264.

Niemelä, P. & Kauppi, M. (2007). Production, characteristics and use of ferrochromium slags. INFACON XI, pp. 171-179.

Oner, A. & Akyuz, S. (2007). An experimental study on optimum usage of GGBS for the compressive strength of concrete. *Cement and Concrete Composites, 29*(6), pp. 505-514.

Rao, G. A. & Prasad, B. R. (2002). Influence of the roughness of aggregate surface on the interface bond strength. *Cement and Concrete Research*, *32*(2), pp. 253-257.

Saha, A. K. & Sarker, P. K. (2017). Compressive strength of mortar containing ferronickel slag as replacement of natural sand. *Procedia engineering*, 171, pp. 689-694.

Saha, A. K., Sarker, P. K. & Majhi, S. (2019). Effect of elevated temperatures on concrete incorporating ferronickel slag as fine aggregate. *Fire and Materials*, *43*(1), pp. 8-21.

Sikora, P., Horszczaruk, E., Skoczylas, K. & Rucinska, T. (2017). Thermal properties of cement mortars containing waste glass aggregate and nanosilica. *Procedia engineering*, 196, pp. 159-166.

Taha, B. & Nounu, G. (2008). Properties of concrete contains mixed color waste recycled glass as sand and cement replacement. *Construction and Building Materials*, *22*(5), pp. 713-720.

Cite this article as: Baawain M., Shoukry H., Al-Jabri K., "Mechanical Performance and Thermo-Physical Properties of Cement Mortar Incorporating Hybrid Slags", *International Conference on Civil Infrastructure and Construction (CIC 2020)*, Doha, Qatar, 2-5 February 2020, DOI: https://doi.org/10.29117/cic.2020.0130

Structural Efficiency of Steel Stiffening Deck Systems in Suspension Bridges Due to Gravity Loads

Ahmed Gasim M. Hussein
ahmedgasim@gmail.com
Faculty of Engineering Sciences, Omdurman Islamic University, Omdurman, Sudan

Mohamed Faisal F. Mohamed
fadla_faisal@hotmail.com
Faculty of Engineering Sciences, Omdurman Islamic University, Omdurman, Sudan

ABSTRACT

In this paper, suspended stiffened decks in suspension bridges are considered. Three steel deck-stiffening systems are compared structurally; the plate girder, the box girder and the stiffening truss. A three-span continuous suspension bridge model is considered. Analysis is made by the second order non-linear deflection theory in its linearized form. Developed software is used for the analysis to determine the induced tension in the cable, moments, shears and deflections of the girders for any general live load case. AASHTO criteria for steel girders are adopted. AASHTO highway live loads -HL 93- are applied to Khartoum–Tuti Suspension Bridge in Khartoum, Sudan for each type of the stiffening systems. Ten load cases are considered and discussed. Results have shown that the most efficient type to resist gravity loads is the stiffening truss, followed by the box girder and last is the plate girder.

Keywords: Suspension bridges; Steel deck systems; Deflection theory; AASHTO

1 INTRODUCTION

The principal structural elements of a three-span suspension bridge are as shown in Figure (1):

- Two or more high-strength steel main cables, and which support the traffic-carrying deck and transfer it's loading by direct tension forces to the supporting towers and anchorages.
- A deck structure together with a longitudinal stiffening system to distribute concentrated traffic loadings on the deck, and control local deflections. An economical overall design requires the lightest practicable deck structure which is supported from the main cables by hangers of high-strength wire ropes or strand that are spaced at regular intervals throughout the spans.
- Towers to support the main cables at a level determined by the main span cable sag
- Anchorages to secure the ends of the main cables against movement.

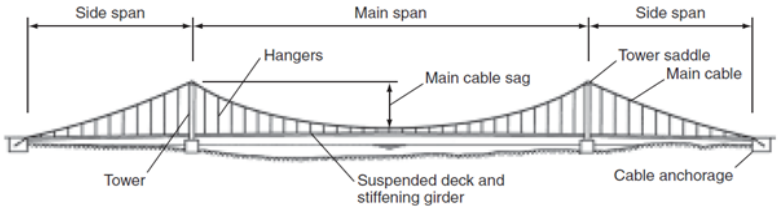

Figure 1**:** Suspension Bridge Elements. (Barker & Pucket, 2007)

2 REVIEW OF THEORIES OF ANALYSIS OF SUSPENSION BRIDGES:

The different approaches that have been introduced for the analysis of externally-anchored

suspension bridges (Pugsley, 1968; Arzoumanidis & Bieniek, 1985; Jennings, 1987 & Hussein, 1998) can be summarized as follows:

i) The classical elastic theory: Derived on strain energy basis and yields higher bending moments and shears than the actual. The method is used for approximate analysis and preliminary designs.

ii) The deflection theory: Based on non- linear fourth order differential equation. The method is accurate but difficult to apply practically due to cumbersome work required to evaluate the solution parameters.

iii) The Linearized deflection theory: Based on the linearization of the basic differential equation of the deflection theory. The theory was treated in different ways such as the flexibility coefficient method, the Fourier series treatment, etc…. The method is less accurate than the deflection theory but permits the use of superposition and influence lines techniques.

iv) Matrix form solutions: In which the computer was used primarily. These solutions include the finite difference formulation; based on the Linearized deflection theory, and the finite element methods, based on the elastic stiffness of the members. These methods are easier but less accurate than the deflection theory.

In this research paper, a new treatment to the deflection theory will be introduced analytically and in computer form, yielding capability of solving any type of static loading. This, computerized treatment will be extended to the linearized deflection theory to make use of the superposition advantage.

3 THE DEFLECTION THEORY AND ITS LINEARIZED FORM

Steinman (1935), Pugsley (1968), Choi et al. (2013) and Hussein (1998)]

3.1 Assumptions of the Deflection Theory

a. Cable is parabola and sag span ratio is 1.8 or lesser.

b. Initial dead load is carried by the cable only, causing no stresses in stiffening deck.

c. Suspenders elongation are negligible, i.e. the girder vertical deflection at any point is the same as that of the corresponding point on the cable.

d. The deflection of any point on the cable, v(x), due to applied live load “P” per unit length of girder, is sensible compared with the initial dead load ordinate y(x) of that point.

3.2 Fundamental Equations of the Deflection Theory

If the distortion of structural geometry of the span of a suspension bridge under the action of live loads is neglected, and if *y* describes the cable ordinate from the horizontal line joining the two towers, the bending moment at any point of a simple suspended span, *M* is given by the basic formula of the elastic theory (Pugsley, 1968) See Figure (2).

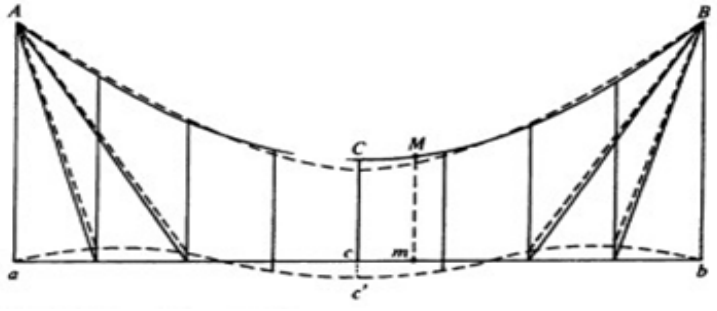

Figure 2: Elastic Theory

$$M = M_0 - hy \tag{1}$$

Due to the fact that distortions might be very large, especially for long spans, the deflection theory accounts for the effects of these changes in geometry. For amount of deflection v, the bending moment will be reduced to

$$M = [M_0 - hy] - (H + h)v \tag{2}$$

Where M_0 is the dead load Moment; h and H is the horizontal components of cable tension due to live and dead loads respectively.

For continuous suspended middle span, accounting for continuity moment at the tower *T,* equation (2) will take the form

$$M = [M_0 - hy] - (H + h)v + T \tag{3}$$

From Euler's equation for flexure

$$M = -EIv`` \tag{4}$$

The following equation, eq. (5), called the fundamental equation of the girder is describing the deflection of

the girders according to the deflection theory

$$v`` = C^2 v - \frac{C^2}{H+h}(M_0 + T - h) \tag{5}$$

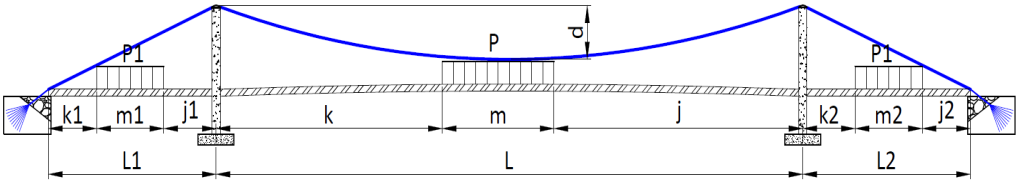

Figure 3: Deflection Theory Parameters for 3-Spans symmetrical Suspension Bridge

The nonlinear differential equation (5) can be solved as follow:

$$v = \frac{h}{h+H}\left\{C_1 e^{cx} + C_2 e^{cx} + \left[\frac{M_0}{h} + \frac{T}{h} - y\right] + \frac{1}{C^2}\left(\frac{8d}{L^2} - \frac{P}{h}\right)\right\} \quad (6)$$

It can be shown that:

$$H = \frac{wl^2}{8d} \quad (7)$$

Where *w* is the total dead load per unit length of cable; and

$$C^2 = \frac{H+h}{EI} \quad (8)$$

The coefficients C_1 & C_2 can be obtained from the boundary conditions. The effect of continuity moment T can be obtained by

$$T = T_1 - (T_1 + T_2)\frac{x}{l} \quad (9)$$

Where the girder continuity moments at the left and right towers, $T_1 \& T_2$, are evaluated by equating slopes at the towers.

Equation (6) is the first fundamental equation; known as the girder equation. There are two unknowns; namely the deflection v and the induced tension "h ". The other fundamental equation, known as the cable equation, is:

$$\frac{hl}{A_c E_c} \pm \propto L_c t - \frac{w}{H}\int_0^L v dx = 0 \quad (10)$$

in which *l* is the horizontal projection of cable length L_c, α is the coefficient of linear thermal

expansion, *t* is the temperature difference, θ is the cable inclination, A_c is the cable x-sectional area, E_c is the cables' modulus of elasticity, and

$$l = \int_0^L \left(\frac{ds}{dx}\right)^3 dx \approx L\left(\sec^3\theta + 8\frac{d^2}{L^2}\sec\theta\right) \quad (11)$$

$$L_c = \int_0^L \left(\frac{ds}{dx}\right)^2 dx \approx L\left(\sec^2\theta + \frac{16}{3}\frac{d^2}{L^2}\right) \quad (12)$$

The cable equation is derived in detail and the solution of equation (5) are as shown by Hussein (1998), yielding the general formula for deflection of the girder or truss

$$v = \frac{h}{h+H}\left[C_1 e^{Cx} + C_2 e^{-Cx} + \left(\frac{M_0}{h} + \frac{T}{h} - y\right) + \frac{1}{C^2}\left(\frac{8d}{L^2} - \frac{p}{h}\right)\right] \qquad (13)$$

Where p is the intensity of the live load at the section, x, and C_1 and C_2 are integration constants; and all other symbols are as defined previously.

3.3 The Linearized Deflection Theory

The only different assumption of the linearized deflection theory from those of the deflection theory is that: since the live load p is small as compared to the dead load w, then h is small as compared to H, and accordingly, the term (H+h) in the first fundamental equation of the deflection theory, can be replaced only by H. This will yield the general solution to be:

$$v = \frac{h}{H}\left[C_1 e^{Cx} + C_2 e^{-Cx} + \frac{M_0}{h} + \frac{T}{h} - y + \frac{1}{C^2}\left(\frac{8d}{L^2} - \frac{p}{h}\right)\right] \qquad (14)$$

i.1 Developed Algorithm:

The solution above has been put in a general form to enable applying any gravity load case as shown in Figure (3). The steps to solve for any loading case are as follows:

1. Enter bridge data: L, L1, I etc.
2. Enter load data: p, p_1, p_2, k, m, etc.
3. Assume initial values for the main span continuity moments as $T_1 = TM1 \; and \; T_2 = TM2$.
4. Assume an initial value for the induced tension $h = h^{(1)}$.
5. Calculate integration constants C_1 & C_2 corresponding to all bridge loaded & unloaded segments.
6. Calculate an improved value of h= $h^{(2)}$.
7. Go back to step (4) using $h^{(2)}$ as $h^{(1)}$ and repeat the procedure till convergence, i.e. $h^{(i)} = h^{(i-1)} = h^f$
8. For the assumed pair (TMI, TM2), and using the last computed value of h =h^f in step (7), compute the corresponding values of integration constants C_1&C_2 ,and then calculate new values of continuity moments TN1&TN2.
9. Check if TN1=TM1 & TN2=TM2. If not, go back to step (3) assuming another initial set of continuity moments, and repeat the procedure till convergence; i.e. TN1=TM1 & TN2=TM2.
10. The last set of values: h^f, TN1 & TN2 of step (9) represent the correct values. Use these values then to compute moments, shears, deflections and suspender tensions.

4 KHARTOUM-TUTI SUSPENSION BRIDGE CASE STUDY WITH VARIOUS STEEL DECK SYSTEMS

In this section the developed software based on the linearized deflection theory will

be applied to Khartoum –Tuti Suspension Bridge in Sudan. Three steel deck systems will be used for the analysis, the existing plate girder system, a proposed box girder system equivalent in area to that of the original plate girder, and a stiffening truss system equivalent in area to the other alternatives. AASHTO criteria for each system is checked, and AASHTO (HL 93) live load will be applied to the bridge for different load cases as shown.

4.1 Tuti Suspension Bridge with its original plate girder system

4.1.1 Bridge Data; (Dorman Long Technology (2007))

With the reference of the parameters in Fig. (3):

$L1 = 50m, L = 210m, D = 25m, W = 130kN/m$

Modulus of Elasticity for the steel $= 200 \times 10^6 kN/m^2$

Cable Inclination angle at the tower $= 20.8°$, Camber $(CM) = 1.5m$

Thermal Expansion Coeficient $= 11.7 \times 10^{-6}/°C$

Plate girder x-sectional Area =0.1588 m^2 (see Figure 4), A=0.1588 m^2 Ixx= 0.1257 m^4

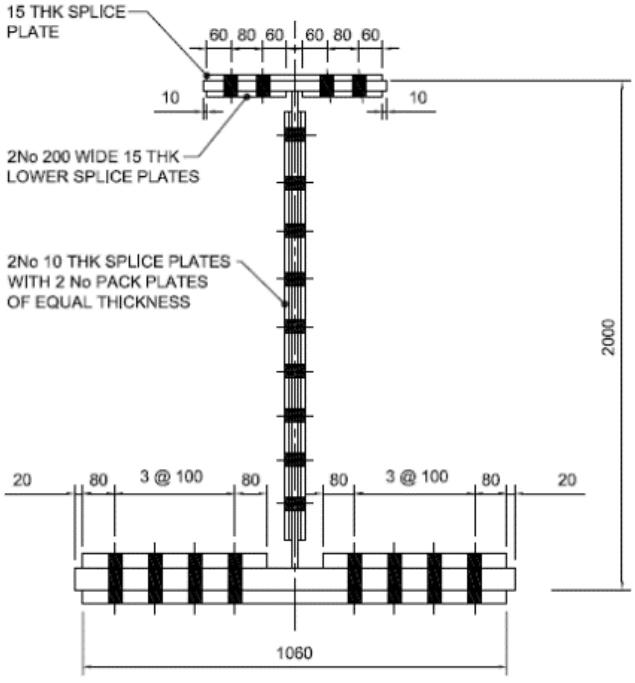

Figure 4: X-section of Tuti Br. Plate Girder

4.1.2 AASHTO requirements for Plate Girders

This as AASHTO (2012) section (6.7.3) states:

"Structural steel, shall not be less than 8.0mm, in thickness". Also as AASHTO section (6.10.2), for I section (rolled and plate girder), for webs without longitudinal stiffeners: $\frac{D}{t_w} \leq 150$ and for webs with longitudinal stiffeners: $\frac{D}{t_w} \leq 300$) compression and tension flanges shall be proportioned to: $\frac{b_f}{2t_f} \leq 1$; $b_f \geq \frac{D}{6}$, $t_f \geq 1.1t_w$; $0.1 \leq \frac{I_{yc}}{I_{yt}} \leq 1.0$

4.2 Tuti Suspension Bridge with box girder system

4.2.1 Selected Box Girder section (see Figure 5)

$A = 0.159m^2$, $I_{XX} = 0.1571m^4$, $I_{YY} = 0.0433m^4$

Check:

$\frac{D}{t_w} \leq 150$,$\frac{D}{t_w} = \frac{2.7}{0.02} = 135 \leq 150$ OK

$b_f \geq \frac{D}{6}$ $\frac{D}{6} = \frac{2.7}{6} = 0.45$ …… $1.2 \geq 0.45$ OK

And:

$t_f \geq 1.1t_w$ $1.1t_w = 1.1 \times 0.02 = 0.022$ OK

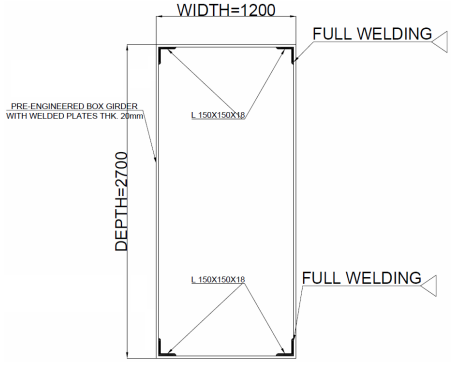

Figure 5: Proposed Box Girder

4.2.2 AASHTO requirements for Box Sections

As per AASHTO (2012) section (6.11.2), Webs without longitudinal stiffeners shall be proportioned such that:

$\frac{D}{t_w} \leq 150$; And for webs with longitudinal stiffeners: $\frac{D}{t_w} \leq 300$

The flanges of tub sections subjected to compression or tension shall be proportioned such

That: $b_f \geq \frac{D}{6}$; And $t_f \geq 1.1t_w$

4.3 Tuti Suspension Bridge with Stiffening Truss system

4.3.1 Selected Truss section (see Fig. 6)

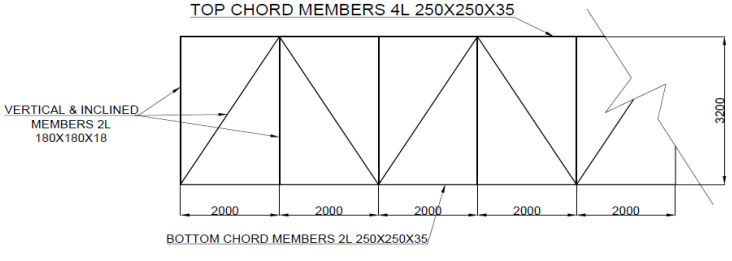

Figure 6: Proposed Stiffening Truss

The calculated section properties are as follows: $A=0.14m^2$ $Ixx=0.41m^4$

4.3.2 AASHTO requirements for Trusses

As described in AASHTO (2012) section (6.14.2) Trusses should have inclined end posts. Effective depths of the truss shall be assumed as follows:

- The distance between centers of gravity of bolted chords, and
- The distance between centers of pins.
- Members shall be symmetrical about the central plane of the truss.

5 LIVE LOAD CASES: (As shown in Fig. 7)

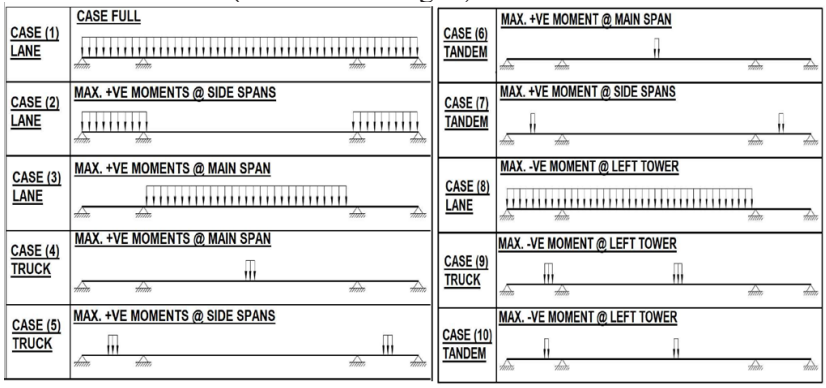

Figure 7: All Live Load Cases

6 RESULTS AND DISCUSSION

The results obtained -as in Figures 8, 9 and 10- shows clearly that for the different load cases considered the minimal deflections are obtained when using the stiffening truss choice, followed by the box girder and then the plate girder with maximum deflections. For maximum bending moments, although the truss is not the optimum but due to its larger depth the bending stresses in the top and bottom chords are far low from limiting stresses. Fabrication difficulties encountered in trusses can be minimized by making use of new technologies. It is clear that this comparison is for gravity loads only, and assuming one stiffening member per each cable.

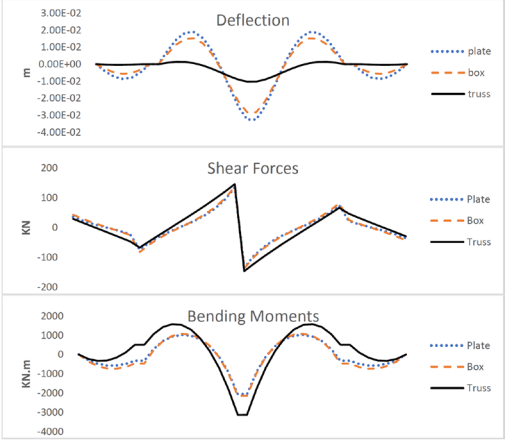

Figure 8: Results of Analysis of Tuti Suspension Bridge for load case (4)

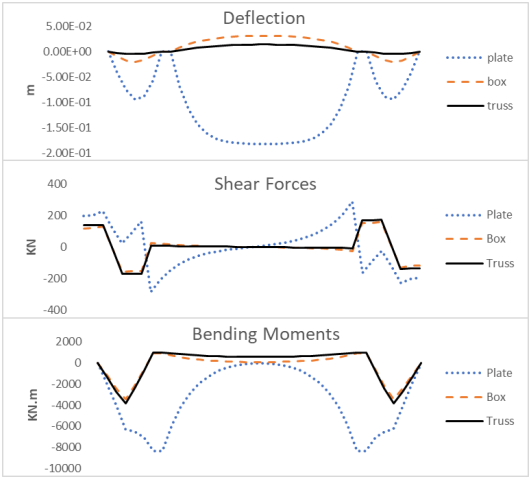

Figure 9: Results of Analysis of Tuti Suspension Bridge for load case (5)

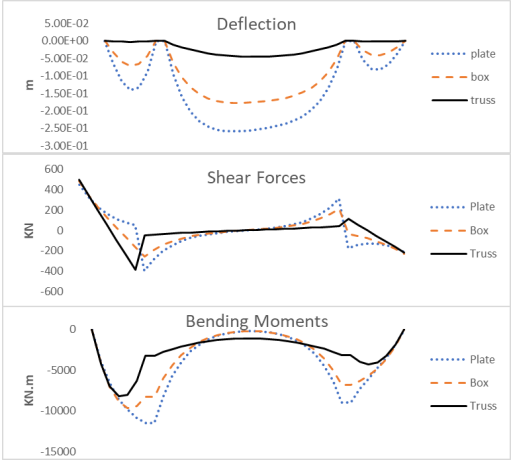

Figure 10: Results of Analysis of Tuti Suspension Bridge for load case (8)

7 CONCLUSION

For the three selected steel deck-stiffening systems to suspension bridge decks, the stiffening truss has been the optimum, structurally to resist gravity loads. The box girder is found to be the second and the plate girder system to be the third. Of course, the optimum deck choice has to consider other loads than gravity ones; like dynamic wind and earthquake loads.

REFERENCES

American Association of State and Highway Transportation Officials (2012). AASHTO LRFD Bridge Design Specifications, Chapter 6, AASHTO Executive Office, Washington, D.C.

Arzoumanidis, S. G. & Bieniek (1985) M. P. Finite Element Analysis of Suspension Bridges. *Computers & structures*, Vol. 21, No. 6, PP 1237-1253.

Barker, R. M. & Puckett, J. A. (2007). *Design of Highway Bridges an LRFD Approach*. John

Wiley & Sons, Inc., New Jersey.

Choi, D., Gwon, S. & Yoo, H. (2013). Nonlinear static analysis of continuous multi-span suspension bridges. *Int. J. Steel Struct*, *13*(1), 103-115.

Dorman Long Technology (2007). Khartoum-Tuti Suspension Bridge Design Drawings. London.

Hussein, Ahmed G. (1998). *Static and Free Vibration Analysis of Suspension Bridges* (Ph.D. Thesis to Baghdad University). Baghdad.

Jennings, A. (1987) Deflection Theory Analysis of Different Cable Profiles for Suspension Bridges. *Engineering structures*, V. 9, No.2, April 1987, P (84-94).

Pugsley, Sir Alfred (1968). *The Theory of Suspension Bridges*. Edward Arnold, 2nd ed. 1968.

Shin, S., Jung. M., Park, J. & Kim, M. (2013). A deflection theory and its validation of earth-anchored suspension bridges under live loads. *KSCE J.*

Steinman, D. B. (1935). *A Generalized Deflection Theory for Suspension Bridges*; Transactions, ASCE, Vol.100, 1935, P (1113-1170).

Cite this article as: Hussein A. G. M., Mohamed M. F. F., "Structural Efficiency of Steel Stiffening Deck Systems in Suspension Bridges Due to Gravity Loads", *International Conference on Civil Infrastructure and Construction (CIC 2020)*, Doha, Qatar, 2-5 February 2020, DOI: https://doi.org/10.29117/cic.2020.0131

Numerical Study of Four Bolts End-Plate Joint Behaviour for Robustness Assessment

Bashir Saleh
b.Saleh@il.pw.edu.pl ; bashiak2003@gmail.com
Libyan Academy, Tripoli, Libya and High Institute of Engineering Technology, Ghryan, Libya

ABSTRACT

The paper presents new studies on numerical modeling (FEM) for beam-to-column behavior under sagging and hogging bending moment when the framework is exposed to service and unexpected loads that may cause a column loss scenario. This investigation is focused on four bolts end-plate joints with 10 mm thickness which are proven experimentally to have more ductile behavior than other end-plates joints (6, 8 bolts), spite of their weakness to transfer the unexpected loads from the initial state to a residual state of the stable equilibrium, that leads to a failure of limited floor area to adjacent joints when tested experimentally (Saleh, 2014). FEM technique used in this research is an extension of the previous technique and is characterized by the use of a more sophisticated technique than the previous, discovered from the result of continuous research and the use of all the options available in the new version of commercial ABAQUS/CAD software. The elements are designed using multiple layers of specific elements of a brick arranged in such a way that the mesh nodes of the tiles should coincide with certain layers with the top of the shear inlay and in line with reinforcement, not as the former study that used thick shell elements to model the reinforced concrete slab with total negligence of reinforcing steel and bolts between the slap and the beam. This investigation is very complex because of highly nonlinear effects associated with the prediction of joint performance, such as structural imperfections, huge displacements and large rotations, inelastic properties of steel and concrete, bonding effects between steel and concrete, friction between end-plate and column flange and focus on the slip between concrete and structural steel, among others which is the most difficult modelling application. The paper addresses all these problems in addition to an evaluation of the joint with four bolts end-plate and provides recommendations for new computer simulation techniques (FEM). With these satisfactory results, this technique can be used to solve many problems and difficulties facing the steel and steel-concrete composite frames due to extraordinary events (explosions and hurricanes).

Keywords: Flush end-plate; Robustness; Catenary action; Implicit; Explicit

1 INTRODUCTION

In the context of continuous scientific research on the establishment of static bases for numerical analysis using modeling, this paper presents a numerical investigation of the joint behavior in steel and steel-concrete, composite frameworks using end-plate joints with 10 mm thickness and four bolts connection (flush end-plate). However, codes do not cover the beam-to-column joints design when subjected to sagging bending moment with the effect of axial forces. When considering the structural robustness and the design

requirements for cases of unexpected events. The most important issue is the structural ability to internally redistribute new forces from the initial state to the adjacent joints and in this way might stop damage propagation. The generation of so-called alternative loading paths is predominantly carried out through the joint ductility, i.e. by ensuring that joints possess a sufficient rotational capacity. In the analysis, the robustness of a structure is most often evaluated by considering a notional removal of the key structural elements and by checking whether the local damage may be absorbed by the deteriorated structural system. This requires investigations into the behavior of joint reactions when exposed to a negative and positive bending moment at the same time, linking these moments and comparing them to axial forces. Current modeling techniques are extended to the joints under a complex procedure that appears in the case of gradual collapse and validation through comparisons with experimental test results conducted before. (Saleh, 2014). The aim of this contribution is to enhance knowledge in the numerical research (FEM) of structures with unexpected loads resulting from the collapse of a part of the building (column lose) and to create the basis for the global assessment of the structural fragility of the disproportionate collapse through static and nonlinear analysis based on energy.

2 FE MODEL DEVELOPMENT

According to previous studies, it was recognized that nonlinear static and dynamic analysis yields the most realistic results for the numerical simulation of considered commercial finite element programs, ABAQUS/CAD. And for the accurate results, in the present study, the analysis is used for two different types of studies namely static and quasi-static and the finite element joint model adopted is different from previous study and defined in the following: the reinforced concrete slab of composite joint is modeled using several layers of brick finite elements arranged in such a way that the slab mesh nodes of certain layers must coincide with the top of shear studs and in line with the reinforcement. The use of FEM in this study simply means that an inelastic constitutive model for concrete is included in the structural analysis process. Therefore, as cited in the previous section, it means the use of two models of concrete: concrete smeared cracking and concrete damage plasticity process. Lately, the concrete damaged plasticity model has been the choice of researchers for doing various researches mainly due to its incredible preciseness and the fact that it captures the reaction of concrete remarkably well. Hence, it has been included in this study and thoroughly described below. Nevertheless, note, the main two failure mechanisms according to this model are tensile cracking and compressive crushing. Cracking is believed to take place when the stresses reach a failure surface and repeatedly, it reaches the point of crushing and collapse. The reinforcement of concrete slab is modeled with truss elements and located in the same place as in the tested specimens. This allows the real stud length to be modeled matching end nodes of the connected shell elements of the beam flange and brick elements of reinforced concrete slab. The effect of profiled sheeting is included. Sheeting is modeled with use of thin shell elements. 3D beam elements type B31, which is based on Timoshenko beam theory allowing for transverse shear strain, are employed to model bolts. The concrete ribs are modeled with use of brick finite elements in the form of cubes and other shapes. A circular cross section is used to model the bolt section

profile. Small sliding contact interface is applied between the end-plate and the column flange. This refined numerical model of common behavior shows better accuracy than previous models that were created in the past. It was therefore used to represent the physical framework that was tested to simulate global behavior for the purpose of this research. It should be noted that; this investigation is an extension of previous studies on the possibility of developing simulation in such a way that the results of the analysis correspond to a large proportion of the results obtained from the experimental tests results. It is also pointed out that this study is unprecedented, in addition to its accuracy; therefore, very accurate results are expected that can be used to solve many construction-related problems.

3 TEST SCENARIOS

The most important thing of this study is to obtain highly consistent results between numerical analysis and experimental test results. The specimen with those recorded for full-scale experiments, which were carried out before (SALEH B. Thesis) on actual structural bare steel framework, for which the details are shown in Figure 1. Tested specimens had the same arrangement of steel part of beam-to-column joints that were equipped with flush end-plates of thickness 10 mm and four M20 bolts, one that is a bare steel specimen and the second one the specimen with the steel-concrete composite framework of effective non uniform width of the reinforced concrete slab and composite beam-to-column joints. Two types of loading programmed were applied. In the first case, the pushdown displacement is applied on the middle joint gradually until collapse. The second specimen composite test is different where it needs two stages of application loads: the application of loads on the slab to simulate the service loads in the first stage using concrete blocks 1.20×1.20×1.00 meters were steeply placed in two layers on the composite slab prepared specifically for the experimental test. In this stage, all the beam-to-columns composite joints were subjected to hogging bending. And the second step is to apply the pushdown displacement on the middle of the specimen vertical direction by suspending it to the actuator until the collapse. The idea of the gravity loads and the displacement application is applied as in the use of ABAQUS/ CAD documentations, with some precision in selecting the specific points in the position of the displacement and the gravity loads that are applied to the length of the slab according to what is contained in experimental test.

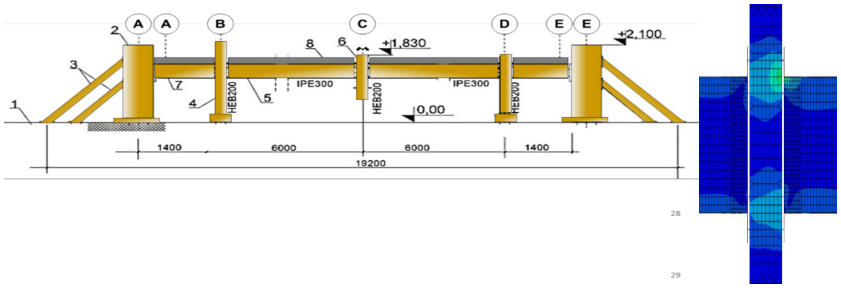

Figure 1: Frame specimen , 2 – stand resistance elements, 3- stand stabilizing elements, 4 –column, 5 –beam, 6 –middle column, 7 – pin joint between frame side and column, 8 - reinforced concrete slab

4 VALIDATION OF FE MODEL

4.1 Steel flush end-plate joints

The modified static general analysis is adopted for all subsequent numerical simulations. The results of the FE analysis are presented in terms of load-deflection curves corresponding to the internal column displacement and the applied load at the same point, and in terms of the characteristics corresponding to the joint rotation and the bending moment. The results of the FE simulation and experimental investigation of the analysis of steel flush end-plate joint are presented in Figure 2. The comparison of load-displacement curves shows compatible agreement for the initial elastic stage of the joint behavior as predicted numerically and measured experimentally, after that the FE curve separated gradually from the experimental curve when it reached the plastic phase and specifically when the force reached a value of 72.9 kN-385.2 mm, after which it began to rise until reaching the point of failure at 109.1 kN force and 621.9 mm displacement. The joint M-ϕ curves are presented in Figure 3. For the same test, the maximum value of applied load and the ultimate moment obtained from the tests and FE models are almost the same 41.93kNm – 93mm and 46 kNm - 90 mm in the range of moderate deformation then the FE results are slightly different from the results of experimental test until the point of collapse.

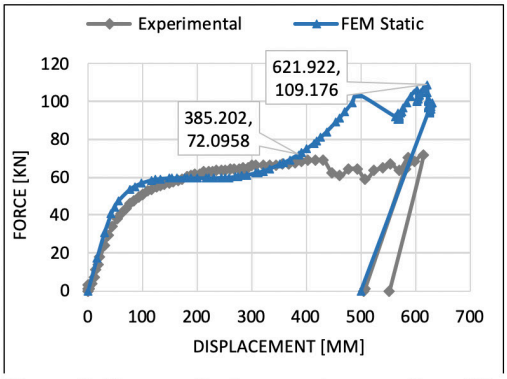

Figure 2: Force – displacement curves from FE and test for flush end-plate steel joints

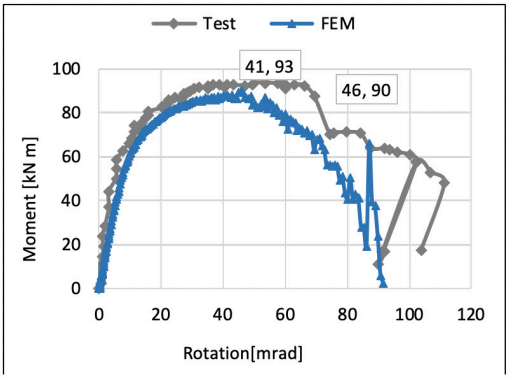

Figure 3: Moment-rotation curves from FE and test for flush end-plate steel joints

This is clearly observed in both curves of load-displacement and the moment-rotation. Because of the specimen symmetry, the sagging and hugging bending moment-rotation characteristics are almost the same. Figures 4 and 5 show a comparison between the deformed shapes of the flush end-plates obtained experimentally and numerically. The shape of flush end-plates is such that the most deformed part is located between the most distant bottom bolt rows of the inner joint at the adjacent of end-plate welded connection to the bottom flange of the beam. This is seen clearly in the joint that was subjected to sagging bending moment. For the external joint subjected to the hogging bending moment, the flush end-plate deformed shape is located above the most distant top bolt rows of the joint, at the adjacent of end-plate welded connection to the top flange of the beam.

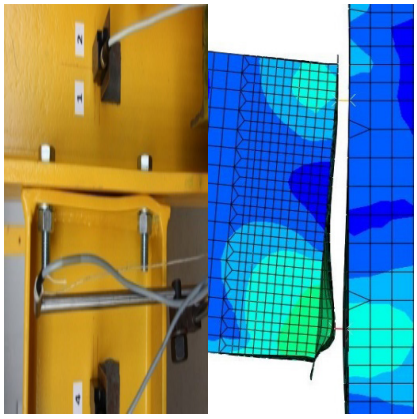

Figure 4: Deformed shape of steel joints with flush end-plates from test and FE–joint, sagging bending

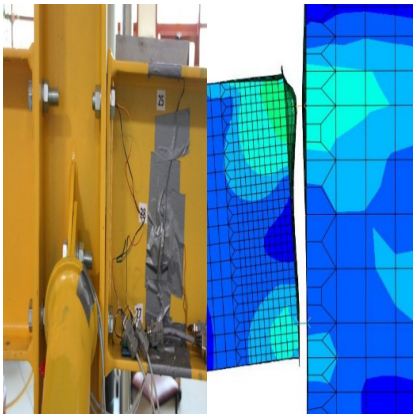

Figure 5: Deformed shape of steel joints with flush end-plates from test and FE joint, hogging moment

4.2 Composite flush end-plate joints of inner and outer columns

The test for the steel-composite specimen was conducted in two stages. In the first stage of numerical analysis, the gravity loading is applied including the application of uniform loads on a regular full slab (similar to the concrete cubes in the experimental test) in terms of weight, with the prevention of vertical movement by using the middle column as a support. This caused a vertical reaction in this column equal to an absolute value of 136.0 kN, then immediately the second phase began which was the application of displacement on a regular basis to the middle column. During this phase, the support was removed by lowering the middle column and leaving the specimen free in the vertical direction. This was done automatically until the end of the analysis when the specimen reached the point of failure. The data from the history output was collected, which is referred to displacement, rotation and stress data. This was then analyzed and kept in order to calculate the load-disablement, and the moment-rotation relationship of the data related to the joints that were later used to assess the global behavior of the framework and for the evaluation of local joints in terms of their degree of robustness. In the initial curve phase, there is a large consensus between FE and the test, both in the relationship between the loads-displacement curves as shown in Figure 6 and in the relationship between the moments-rotation curves as shown in Figure 7. At this stage, all the joints were subjected to positive bending moment. Compatible agreement between the experimental and numerical results for the first stage was reached, then compatibility continued to be shown between the curves (FEM and the test) at the elastic stage, and perhaps a little later, in the plastic phase, the FE curve starts to begin a gradual downward separation from the experimental curve and continues in this manner until the end of the analysis. In all the stages, agreement is observed. The only discrepancy is that these ultimate values are reached at different displacements of the load-displacement curve. There was no sign of failure in the first stage. It can be seen from the results using steel and composite joints that there are similar deformation mechanisms of the end-plates in the first stage of loading, and there is a good correlation between experimental and numerical characteristics. In the second stage, it was observed that there is a faster

deterioration of rigidity with successive displacement application in the numerical simulation than in the test. This can be attributed to the fact that the effect of end-plate material fracture could not be represented in numerical simulations as precisely as in the experimental test. This also caused a discrepancy in the way load-displacement curves approach the zero level of loading. Moreover, in some of the investigations into the mesh shape configuration and its impact on results in the search, it turns out that fine mesh may also create these differences when FE analysis is carried out with the use of ABAQUS/ CAD software.

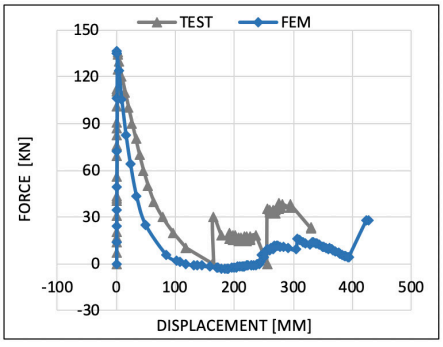

Figure 6: Force [kN]–displacement [mm] curves from FE and test for flush end-plate specimens

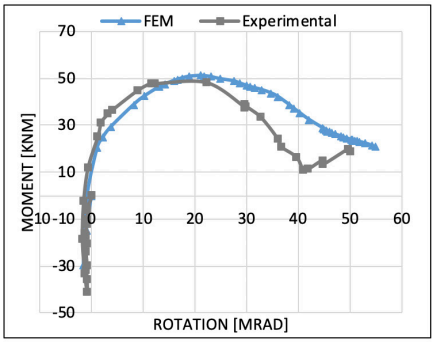

Figure 7: Moment-rotation curves from FE and test for flush end-plate composite specimens

Figure 8 shows a similarity between the end-plate deformation shape in the experimental test and that of the FEM simulations in the outer joint when this joint is subjected to hogging bending moment. Figure 9 shows the comparison of experimental and the FE results for the end-plate deformation of the inner joint when the joint is subjected to sagging bending moment. It can be clearly seen that there is considerable similarity between the end-plate deformations in the shapes that have been obtained experimentally and numerically.

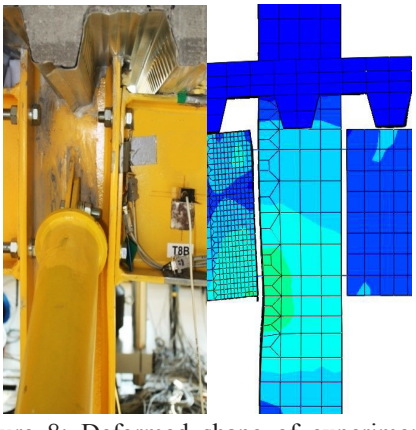

Figure 8: Deformed shape of experimental and FEM of outer composite joint

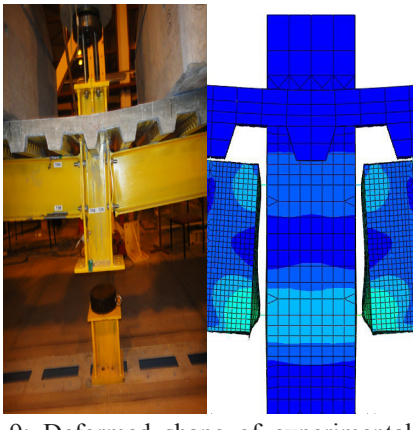

Figure 9: Deformed shape of experimental and FEM of inner composite joint

5 CONCLUSION

In the process of computer simulation (FEM), investigating the joint moment-rotation characteristic, the results of tests conducted elsewhere on joints were considered. It has been obvious that for the symmetric arrangement of bolts, like for flush end-plates, the moment-rotation characteristics of steel joints are the same in cases of both hogging and sagging bending. The results obtained for composite joints are more complex. The moment-rotation characteristics are different for hogging and sagging bending moments for flush end-plate joint with symmetric bolt arrangement on both sides according to the results obtained numerically.

The most important property for the robustness of a structure is its resistance to progressive collapse scenarios. For robust structural systems, both tests and FE modeling simulations should prove that the structure could sustain the applied load in case of a deteriorated static scheme after the removal of its critical structural element as a result of the expected local damage simulation.

Robust joints have to have a sufficient balance between the rotation capacity and strength. FEM simulation and tests on steel and steel-composite frameworks have shown that end-plate joints with four bolts are not robust since their low strength, despite good ductility proven in tests and FE modeling simulation on joints does not allow for the sufficient development of catenary action in the beam when tested in the framework.

Tests relating to the global behavior of frameworks conducted in previous studies and in this study should be repeated with respect to simulation of fixed column removal taking into account the dynamic effects associated with column removal. This would need more sophisticated measurement devices, more of a high-speed visual recording nature that of the mechanical nature, including the fast speed video camera and laser technology.

There is a need for continued research on Finite Element Modeling (FEM) of the local and global behavior of frameworks, especially with reference to dynamic situations. Initial investigations presented in this study on the dynamic simulations of static behavior of joints have shown that there are a number of difficulties in terms of numerical stability, this causes the non-continuity of the analysis and early termination of numerical analysis as a result of severe nonlinearities appearing in the finite element formulation of physical phenomena, especially related to modeling of the inelastic behavior and cracking phase of concrete.

REFERENCES

Eurocode 3: EN 1993-1-8: Design of steel structures (2005). Part 1-8: Design of joints. CEN, Brussels.

Gizejowski, M. A., Kwasniewski, L., Saleh, B. & Balcerzak, M. (2012). Numerical Study of Joint Behavior for Robustness Assessment, Applied Mechanics and Materials, Yantai, Peoples R CHINA, vol. 166-169, pp. 3114-3117.

Gizejowski, M., Saleh, B., Kozlowski, A., Pisarek, Z. & Sleczka, L. (2012). Experimental investigations of frame behavior subjected to exceptional actions. *85th Annual Conference on Scientific Problems of Civil Engineering*, Krynica- Rzeszow, Poland.

Hibbit, Karlsson, and Sorenson Inc (2006). ABAQUS/ CAD, User's Manual, Version 6.10,

Providence, RI.

ABAQUS, User's Manual, version 6.10, Hibbit, Karlsson and Sorenson Inc., Providence, RI, (2006).

Saleh, B. (2015). Moment-rotation characteristic of joints of steel-concrete composite frame under exceptional events. *IABSE, Nara*, Japan, pp. 504-505.

Saleh, B. (2014). *Modelling of beam-to-column joint of steel-concrete composite frames subjected to standard and extreme load combinations* (Warsaw University of Technology, Warsaw, Poland).

Saleh, B. (2016). Experimental investigation for the steel-concrete composite joints subjected to in exceptional load. *6th Conference of Building Materials and Construction*, Ghryan, Libya.

Cite this article as: Saleh B., "Numerical Study of Four Bolts End-Plate Joint Behaviour for Robustness Assessment", *International Conference on Civil Infrastructure and Construction (CIC 2020)*, Doha, Qatar, 2-5 February 2020, DOI: https://doi.org/10.29117/cic.2020.0132

Latest Advances in Smart Components and Monitoring for Civil Structures

Thomas Richli
trichli@mageba-group.com
Mageba Group, Bulach, Switzerland

Antonios Chrysovergis
achrysovergis@mageba-group.com
Mageba Group, Bulach, Switzerland

Achilleas Athanasiou
aathanasiou@mageba-group.com
Mageba Group, Bulach, Switzerland

Niculin Meng
nmeng@mageba-group.com
Mageba Group, Bulach, Switzerland

ABSTRACT

Rapid technical advances and the increasing demand for long design lives of civil structures of any kind make Structural Health Monitoring (SHM) increasingly popular for owners and designers for the valuable information it provides about structural performance. SHM offers a wide range of benefits including increased service life, improved maintenance planning, construction optimization, and risk minimization. For example, it can be used to verify design assumptions or to provide actual measurements in advance of upgrading and repair work. Depending on the objective to be achieved by SHM on any particular structure, systems can be simple and "portable", or sophisticated and comprehensive. SHM can be especially efficient and useful when the sensors that measure data are pre-integrated in the design and fabrication of a bridge's key components – in particular, its bearings, expansion joints and dampers/shock transmission units. The benefits are further enhanced by ongoing developments in the communication technologies used to transmit data from the sensors on the bridge to the user's online interface. This paper briefly illustrates the use of this modern technology on bridges in Qatar, Switzerland, Norway, Canada, and India.

Keywords: Structural health monitoring; SHM; Smart components; Bearings; Expansion joints

1 INTRODUCTION

The use of modern structural health monitoring systems can be very beneficial in the construction, inspection, maintenance and renovation of structures in general, and of bridge structures in particular. By automatically measuring, recording, summarizing and analyzing key variables – 24 hours a day and seven days a week with little or no manual effort – it can play a key role in the overall monitoring and maintenance of a structure. It can even provide automatic notification (e.g. by SMS or email) to the responsible engineers when a measured value exceeds a pre-defined threshold value, providing confidence in a structure's ongoing condition and serviceability at any time. Useful data can also be provided during the construction stage, or to assist the planning

of renovation or replacement works, making SHM useful throughout the complete life cycle of a structure or a component.

Recent technological developments in the field of structural health monitoring, particularly in relation to sensors and data logging, have greatly increased the potential of such technology to play a valuable role in civil and structural engineering – especially as it relates to critical infrastructure such as road and railway bridges. Continually progressing research work and the innovations of suppliers have resulted in the development of systems and solutions, which can greatly increase the effectiveness and efficiency of bridge construction, inspection, maintenance and renovation work (Treacy et al., 2019; Meng & O'Suilleabhain, 2018).

In particular, there is a great potential to benefit from bringing together the key modern technologies that each can contribute so much to enhancing the life-cycle performance of structures – on the one hand, the SHM that so efficiently provides key data relating to movements, loads, etc., on the other hand, the high-tech components that accommodate, support, or control the same movements and loads. By integrating suitable sensors in the design and fabrication of key structural components such as bridge bearings, expansion joints, and seismic protection devices – giving rise to the development of so-called "smart" components – the long-term functioning and effectiveness of both the SHM and the key component can be optimized (Spuler et al., 2011; Islami et al., 2016).

Recent and ongoing examples of the use of such technology in various countries around the world are referenced below.

2 APPLICATION EXAMPLES

The following brief references to uses of the type of technology described above indicate the great diversity of application possibilities for this technology.

2.1 Al Majd Road (Orbital Highway) Junction Bridges, Doha, Qatar

This project highlights the benefits of incorporating SHM technology in the design and fabrication of a structure's bearings – components that are critically important for the structure's proper long-term performance. Qatar's new Al Majd Road (formerly known as the Orbital Highway) was opened to traffic in 2019, greatly improving traffic conditions around the country's capital, Doha. At one of the highway's main intersections shown in Figure 1 (left), a spaghetti junction where it crosses the Dukhan Road, it was decided to install an SHM system to monitor the condition of the various structures. The system is based on measurement of data from the bearings that support the various superstructures. All the sensors on 28 of these bearings, of the spherical type, are connected to 14 sensor nodes, as shown in Figure 1 (right).

Figure 1: Construction of the main junction of the new Al Majd Road (formerly known as the Orbital Highway) in Qatar (left), and main sensor node of the project's SHM system, connected to bearings above (right)

The SHM system is designed to continuously monitor the load acting on each monitored bearing, around the clock. This enables it to immediately identify any change in loading conditions – e.g. should the load on any bearing increase or decrease due to structural damage/deterioration or ground settlement, either rapid or gradual? With threshold values defined (above or below, which the responsible engineers should be notified), risks to structure users can be minimized, and any structural damage or deterioration arising can be addressed before it develops into a bigger problem. An example of the data presentation on the system's secure online portal is shown in Figure 2.

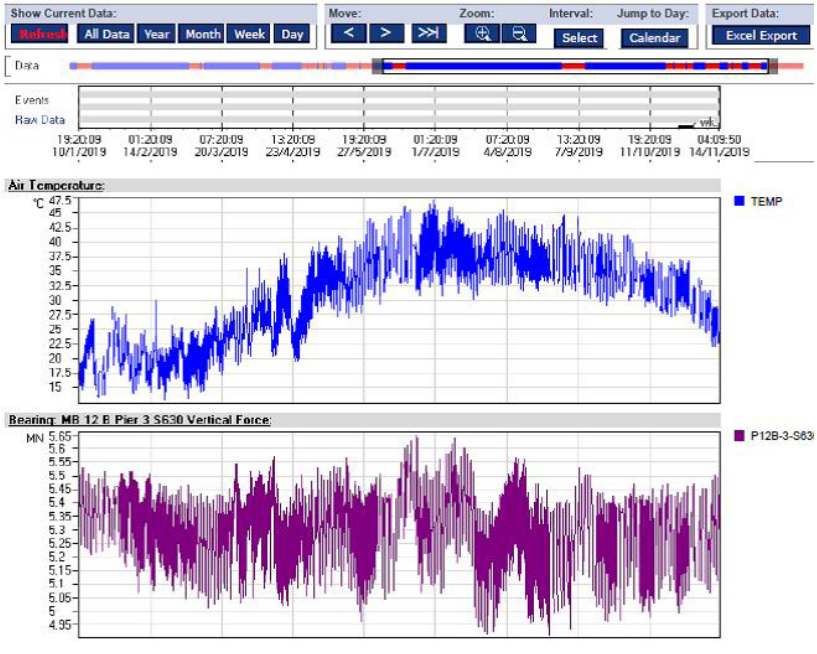

Figure 2: Sample presentation of recorded data relating vertical force carried by a particular bearing to temperature over a period of ten months

2.2 Al Bustan South Viaduct, Doha, Qatar

Doha's Al Bustan South viaduct (Figure 3, left), currently being constructed as a key

element of the Qatar Expressway Programme, is a highway viaduct consisting of twin parallel structures, each carrying four lanes of traffic. Each of the parallel structures has a length of approximately 1.9 km, with 34 spans – each typically 57 m long, but with lengths of up to 72 m at intersections. Entry/exit ramps at four locations comprise an additional length of 863 m of structure – here also multi-span viaducts with typical spans of 57 m. The superstructures are supported by a total of 214 Reston-Spherical bearings (Figure 3, right), designed to support vertical ULS loads of up to 45,250 kN, to resist horizontal ULS loads of up to 15,600 kN and to accommodate longitudinal sliding movements of up to +/-260 mm. In compliance with the local specification for bridge bearings, IAN 2006 (Rev. A2 Clause 3.6), two free-sliding spherical bearings were selected to be "smart bearings", with pre-integrated SHM sensors for connection to an SHM system.

To maximize the efficiency of data transfer, this is done by means of Lo-Ra (long-range) technology, avoiding the need for cabling work on the structure – an ideal solution when data is measured at low frequency (such as temperature-induced bridge movements).

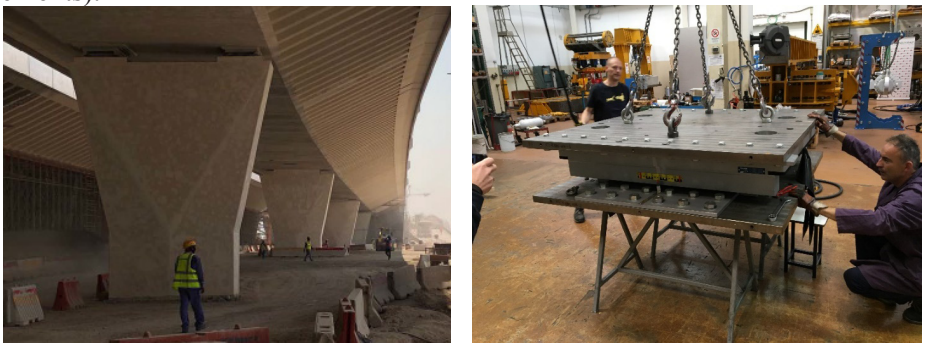

Figure 3: A small part of Doha's Al Bustan South viaduct (left), and one of the spherical bearings that support its superstructures – two of which are equipped with SHM sensors

2.3 Lutrive River Bridge, Vaud, Switzerland

The *Ponts sur la Lutrive* bridges over the River Lutrive in Vaud, Switzerland are parallel concrete bridges with a length of 395 m (Figure 4, left). As part of a recent bridge renovation project, it was decided to monitor the bridge's movement behavior, providing detailed information in support of maintenance and renovation works, particularly relating to the bridge's bearings and expansion joints. Due to the bridge's static design and nature – with traffic and wind having been found to have practically no effect on the bridge's movements, which thus depend primarily on thermal expansion and contraction – a low-frequency SHM system was proposed, to record just one measurement every 30 minutes. The low frequency of data transmission made this project another good candidate for the use of wireless Lo-Ra technology to transmit the measured data from four longitudinal and four transverse displacement sensors – one of each at each superstructure abutment (Figure 4, right). An example of the movement data recorded at one abutment during a six-month period is presented in Figure 5.

Figure 4: Lutrive River Bridge, Switzerland (left), and use of Lo-Ra wireless technology to transfer measured data from a sensor node to a gateway (right)

The use of wireless Lo-Ra technology avoided the need to install cabling between sensors and data acquisition unit, substantially reducing costs. Furthermore, the sensor nodes can be easily repositioned on other parts of the structure at a later stage. Here, data is transmitted wirelessly, from the sensors to the data acquisition unit, over a distance of approximately 400 m. In good conditions – without significant obstacles – this technology can enable data to be sent wirelessly up to 15 km.

Figure 5: Longitudinal movements at abutment of Lutrive River Bridge during a six-month period

2.4 Hålogaland Bridge, Norway

The Hålogaland Bridge, located within the Arctic Circle in northern Norway, opened to traffic in 2018, forming part of the European Route E6 highway. The suspension bridge has a main span of length 1.1 km, crossing one of Norway's many fjords. Its design required the installation of a Shock Transmission Unit (STU) at each of the bridge's towers (Figure 6).

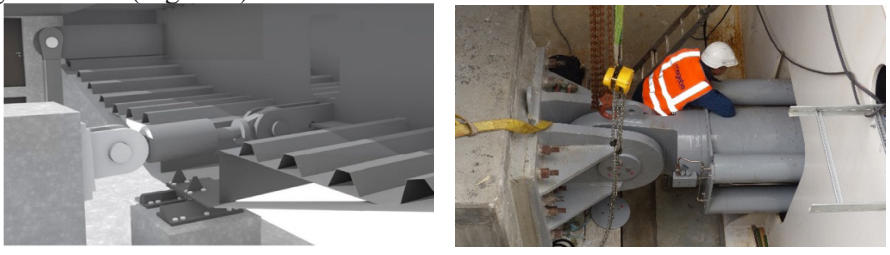

Figure 6: An STU at each tower of the Hålogaland Bridge controls superstructure movements – design representation (left) and during installation (right)

To minimize the risks associated with the advanced structural engineering methods applied in the construction of this bridge, it was decided to install an SHM system. The system is initially based on measurement of data from the STU devices at the towers. An SHM system was designed to measure the longitudinal movements of the STUs, which have a stroke of +/- 450 mm, and to also measure pressure and temperature inside these hydraulic devices. Each STU is equipped with one sensor for measuring movements, two sensors for measuring oil pressure within the device, and one sensor for measuring internal temperature. All sensors were integrated in the design and fabrication of the STUs at the production facility, maximizing durability and ensuring reliability. The system measures the pressure inside the STUs at a frequency of 100 Hz, correlating the data against similarly monitored temperature and deck vibration data. This enables STU condition to be checked at any time, and for additional peace of mind, the system is also designed to provide immediate notifications should any predefined threshold values for movement or differential pressure be exceeded. In addition, the system also correlates the pressures inside the STUs against recorded seismic data in order to enable the actual seismic performance of the STUs to be evaluated following an earthquake.

The performance of these "smart" STUs is illustrated by the data shown in Figure 7 relating to temperature, displacement and force at the STU at one end of the bridge. This demonstrates how these variables are correlated, and analyses have shown that these devices are also sensitive, for example, to vehicle movements on the bridge, further showing how this use of STUs can help protect the structure against excitations.

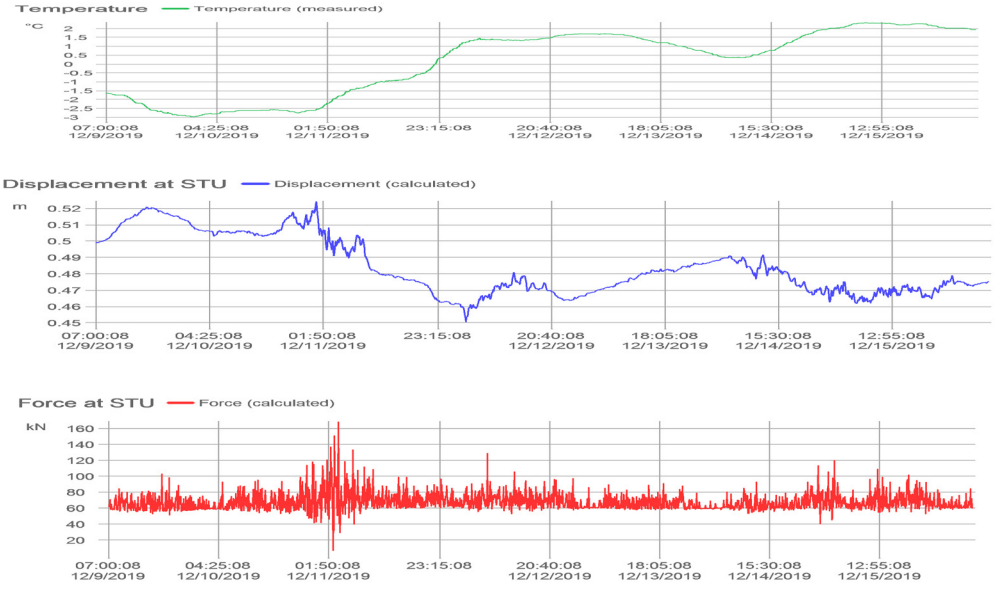

Figure 7: Data showing correlation between temperature, displacement and force at an STU of the Hålogaland Bridge

2.5 The New Champlain Bridge, Montreal, Canada

An example of the implementation of a far more extensive SHM system on a bridge

construction project is the monitoring system of the New Champlain Bridge (Figure 8, left) in Montreal, Canada. The SHM system recently installed on this bridge over the St. Lawrence River and the neighboring Île-des-Soeurs Bridge is a comprehensive system that will conduct real-time monitoring of critical aspects of the two bridges, recording displacements, corrosion, strains and environmental conditions at carefully selected locations on the structures (Treacy et al., 2019). The numerous sensors include:

- 141 metal foil strain gauges (48 embedded and 93 surface-mounted to capture local strains);
- 44 draw wire displacement sensors (at expansion joints and bearings);
- 15 accelerometers (on deck/piers and cables);
- 6 tiltmeters (on pylon and piers) to capture rotations associated with horizontal movements;
- 22 corrosion sensors within reinforced concrete elements (Figure 8, right);
- Global Positioning System (GPS) units (incl. one at tower base and two at tower tops);
- Weather stations capable of measuring air pressure, temperature, humidity, rainfall, wind speed, wind direction and pyranometers, which measure solar radiation;
- 18 temperature sensors (8 for pavement, 10 for structure).

Figure 8: Construction of the New Champlain Bridge in Montreal, Canada (left), and one of the many corrosion sensors installed in the structures' concrete to monitor long-term deterioration (right)

The system includes 26 Data Acquisition Units (DAUs), which act as substations within the SHM network – 22 on the New Champlain Bridge and four on the Île-des-Soeurs Bridge. Each DAU receives data from a cluster of sensors and is positioned accordingly. The DAUs, in turn, are connected to the master station by fibre optic cabling. This sensible use of modern SHM technology will help to optimize bridge maintenance efforts and will enable unexpected deterioration or changes in behavior to be immediately recognized and optimally addressed, for many years to come.

2.6 The Kota Chambal Bridge, India

Another recent example of the implementation of a comprehensive SHM system on a major bridge is that of the Kota Chambal Bridge (Figure 9, left) – recently constructed in Rajasthan, India, to carry a bypass highway of the city of Kota over the Chambal River. In this case, the sophisticated SHM system was designed to serve different purposes at different stages in the bridge's life cycle – first, during the construction stage to support the bridge's construction (incorporating a new approach to measuring displacement of

the bridge's pylons) and subsequently, permanently, for inspection and maintenance purposes (Islami et al., 2018). This required the system to be modified, in particular in relation to sensor specifics and layout, following completion of construction. The permanent system is designed to continuously record the dynamic movements and stresses in the bridge (including in its stay cables – see Figure 9, right) along with the environmental factors (including traffic, seismic, wind, etc.) that may cause or affect these. It is also designed to, in real time, process, analyze and interpret the data, as well as to display the data and analysis results. The graph in Figure 10, for example, shows the accumulated movements from thermal effects alone (measured at a frequency of one measurement every two minutes, excluding micro-movements due to traffic or wind) to be about 25 m per year at one expansion joint location, or 70 mm per day. The system is also set up to provide a warning should a predefined "safe" value for any measured variable be exceeded.

Figure 9: Construction of Kota Chambal Bridge (left), with monitoring of many variables including stay cable vibrations (the picture on the right shows forced vibration of a stay cable with an accelerometer)

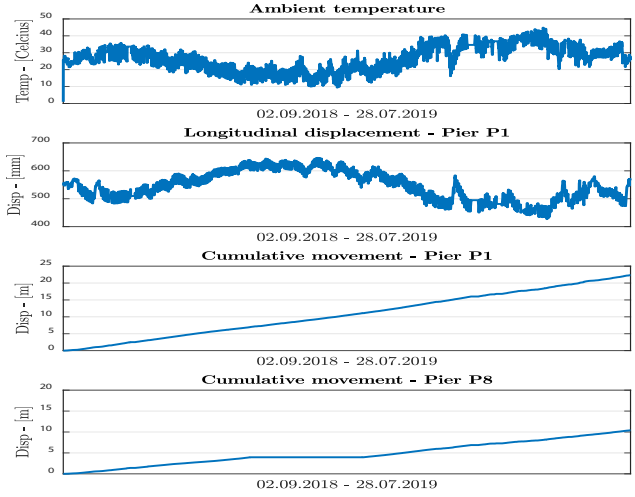

Figure 10: Example of recorded data from selected sensors on the Kota Chambal Bridge, showing clear correlation between low-frequency measurements of temperature and longitudinal displacement, as well as accumulated longitudinal movements at one location

3 CONCLUSION

The use of SHM systems on bridges and other structures can offer great benefits to their asset management programs, efficiently providing data required for almost any purpose, at any stage of a structure's life cycle. The benefits of using such systems continue to increase as the technology is continually developed – with recent innovations including the use of wireless Lo-Ra (Long Range) transmission technology where low-frequency data measurements are required – e.g. to record temperature-induced bridge movements.

Integrating sensors in key bridge components – especially mechanical ones that accommodate or control bridge movements – offers several benefits. With sensors pre-installed, in factory conditions, work on site is reduced, the quality of installation work can benefit, and potential problems can be identified at an earlier stage. Such sensors, detailed and installed by the manufacturer of the key component with its specialist knowledge of the component, can be optimally implemented to provide not only data on the bridge's movements, condition and performance, but also on those of the component itself. Designing key bridge components to be "smart" in this way is surely, therefore, the future of this critical part of the bridge construction and maintenance industry.

REFERENCES

Islami, K., Meng, N. & O'Suilleabhain, C. (2016). Smart bridge components (expansion joints, bearings and seismic devices) for intelligent infrastructure. *Proc. 19th IABSE Congress*, Stockholm, Sweden.

Islami, K., Savioz, P. & Malekzadeh, M. (2018). Integration of SHM at an early stage in the design and construction of long-span bridges. *Proc. IABSE Conference*, Kuala Lumpur, Malaysia.

Meng, N. & O'Suilleabhain, C. (2018). Automated monitoring of exceptional civil structures – Case studies. *Proc. IABSE Conference*, Copenhagen, Denmark.

Spuler, T., Moor, G. & Berger, R. (2011). Automated monitoring systems for bridge bearings and expansion joints. *Proc. 7th World Congress on Joints, Bearings and Seismic Systems*, Las Vegas, the USA.

Treacy, M., Meng, N. & Paciacconi, A. (2019). What added value can SHM bring to my construction project or structure maintenance programme?. *Proc. SMAR Conference*, Potsdam, Germany.

Treacy, M., Moor, G., Baillés, B. & Paciacconi, A. (2019). A comprehensive Structural Health Monitoring System for the New Champlain Bridge. *Proc. 9th International Conference on Structural Health Monitoring of Intelligent Infrastructure (SHMII)*, St. Louis, Missouri, the USA.

Cite this article as: Richli T., Chrysovergis A., Athanasiou A., Meng N., "Latest Advances in Smart Components and Monitoring for Civil Structures", *International Conference on Civil Infrastructure and Construction (CIC 2020)*, Doha, Qatar, 2-5 February 2020, DOI: https://doi.org/10.29117/cic.2020.0133

Derivation of the Governing Differential Equation of Vibrating Host Plate with Two Piezoelectric Patches

Wasim Barham
wsbarham@just.edu.jo
Civil Engineering Department, Jordan University of Science and Technology, Irbid, Jordan

Khaldoon Bani-Hani
khaldoon@just.edu.jo
Civil Engineering Department, Jordan University of Science and Technology, Irbid, Jordan

Mutaz Mohammad
mmmohammad16@eng.just.edu.jo
Civil Engineering Department, Jordan University of Science and Technology, Irbid, Jordan

ABSTRACT

One of the most difficult challenges facing researchers these days is making industrial applications (e.g. engines, automobiles, and aircraft) run on renewable energy and reducing the use of fuel as much as possible. One approach to achieve this goal is the use of smart materials such as piezoelectric materials which produce mechanical stress or strain under the application of an electrical field. Vice versa, if this material is subjected to a mechanical strain, an electrical field will result. Piezoelectric materials are used as sensors or actuators for the structural control of smart structures. In this paper, a mathematical model represented by the governing differential equation for a host plate containing two piezoelectric patches has been developed to predict the displacement of a plate excited by the piezoelectric patches and transverse loads.

Keywords: Renewable energy; Piezoelectric material; Piezoelectric patches; Electric field; Host plate

1 INTRODUCTION

Piezoelectric materials are smart materials used in many applications such as sensor and actuator for active health monitoring (Tzou & Tseng, 1990), aircraft morphing wing technology (Jha & Kudva, 2004), voltage generators (Yando, 1970), and accelerometers (Scheeper et al., 1996). Piezoelectricity idiom from the Greek word "piezo" (Ueberschlag, 2001) denotes to the pressure of electricity. It is a character of some materials to produce a mechanical stress or strain on the application of an electrical field (Cheng et al., 2007), referred to as inverse piezoelectric effect, Figure 1-b. Vice versa, if this material is subjected to a mechanical strain, an electrical field will result, this is called the direct piezoelectric effect (Munjal, 2015), Figure 1-a. The direct piezoelectric effect was discovered by the two brothers Curie (1880). In 1910, Woldemar Voigt published a book named Lehrbuch der Kristallphysik which depicted many natural crystal classes that have piezoelectricity property and provided the piezoelectric constants using tensor analysis (Voigt, 1910). For a period, a lot of research was conducted to examine the crystal structure that shows piezoelectricity. The piezoelectricity can be obtained in some materials through polarization process such as ceramic, Lead Zirconate Titanate

PZT, polyvinylidene fluoride (Ueberschlag, 2001), and Barium Titanate (Balmes E, Deraemaeker, 2013).

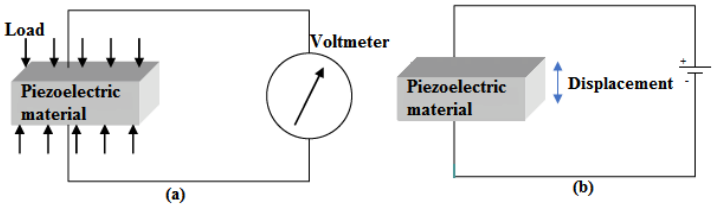

Figure 1: (a) Direct piezoelectric effect (b) Inverse piezoelectric effect

A hysteresis of piezoelectric actuators was studied and modelled mathematically by (Singh & Apte, 2006). Gharib et al. (2008) analyzed functionally graded beam comprising two piezoelectric patches used as sensor and actuator. Sun et al. (2001) examined the effect of controlling beams vibration with piezoelectric patches used as sensors and actuators. Energy harvesters driven by vibration effectively convert vibration energy into electrical energy using three electromechanical transduction processes: piezoelectric (Behjat et al., 2011), electrostatic (Song et al., 2016), and electromagnetic (Singh & Apte, 2006).

In this paper, piezoelectric patches are bonded to a host plate and used as sensors and actuators. A static analysis for a piezoelectric plate has been conducted to evaluate the displacement induced by an electric field. Furthermore, mathematical model of the host plate contained piezoelectric sensor and actuator has been developed to predict the displacement of a plate excited by piezoelectric patches, subject to any function of electric field and load.

2 PARTIAL DIFFERENTIAL EQUATION OF A PLATE WITH TWO PIEZOELECTRIC PATCHES

In this section, the governing differential equation for the thin plate with piezoelectric sensor and actuator will be derived. Consider a rectangular plate with *a* and *b* dimensions and thickness *h*. The plate has piezoelectric sensor and actuator patches as shown in Figure 2 and Figure 3.

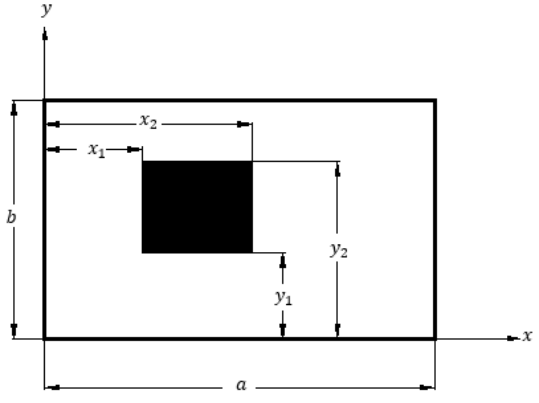

Figure 2: Rectangular plate with piezoelectric patches

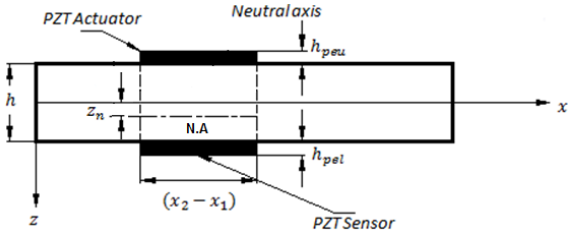

Figure 3: Elevation view

The displacement components of the host plate at a point located at a distance z from the mid-surface are given by:

$$u = -\left(z - z_n S(x,y)\right)\frac{\partial w}{\partial x}$$
$$v = -\left(z - z_n S(x,y)\right)\frac{\partial w}{\partial y} \quad (1)$$
$$w = w(x,y)$$

The displacement components of the piezoelectric patches at a point located at a distance z from the mid-surface are given by:

$$u = -(z - z_n)\frac{\partial w}{\partial x}$$
$$v = -(z - z_n)\frac{\partial w}{\partial y} \quad (2)$$
$$w = w(x,y)$$

Where z_n is the distance between mid-plane and neutral surface.

The shift of the neutral surface can be calculated as follows:

$$\sum F_x = 0 \quad (3)$$

Assuming that the slope of flexural stress for each material equals to the modulus of elasticity as shown in Figure 4 below:

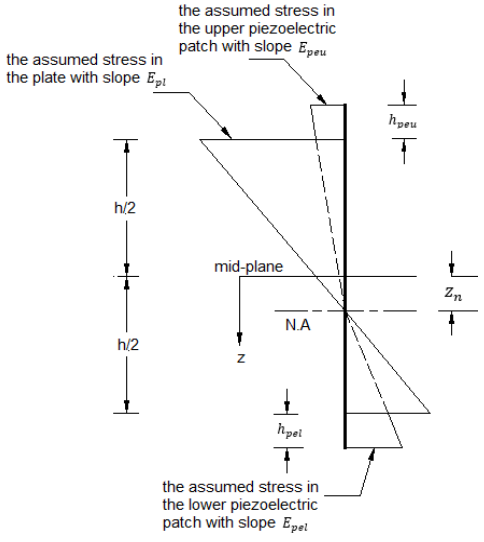

Figure 4: The assumed stress diagram to compute z_n

One can write,

$$\begin{Bmatrix} \int_{-(h/2+h_{\mathrm{peu}})}^{-h/2} E_{\mathrm{peu}}(z-z_n)\,dz \\ \int_{-h/2}^{h/2} E_{\mathrm{pl}}(z-z_n)\,dz \\ \int_{h/2}^{h/2+h_{\mathrm{pel}}} E_{\mathrm{pel}}(z-z_n)\,dz \end{Bmatrix} = 0 \tag{4}$$

Where,

$$z_n = \frac{\begin{Bmatrix} E_{pel}h_{pel}\left(h+h_{pel}\right) \\ -E_{peu}h_{peu}\left(h+h_{peu}\right) \end{Bmatrix}}{2(E_{pl}h + E_{pel}h_{pel} + E_{peu}h_{peu})} \tag{5}$$

and,

$$S(x,y) = \begin{bmatrix} H(x-x_1)H(x-x_2) \\ -H(x-x_1)H(x-x_2) \end{bmatrix} \tag{6}$$

$H(x)$ is a Heaviside unit step function. For the host plate, strain functions can be written in terms of the plate deflection w as follows:

$$\begin{aligned} \boldsymbol{\epsilon_x} &= \boldsymbol{z_n}\frac{\boldsymbol{\partial S(x,y)}}{\boldsymbol{\partial x}}\frac{\boldsymbol{\partial w}}{\boldsymbol{\partial x}} - \left(\boldsymbol{z - z_n S(x,y)}\right)\frac{\boldsymbol{\partial^2 w}}{\boldsymbol{\partial x^2}} \\ \boldsymbol{\epsilon_y} &= \boldsymbol{z_n}\frac{\boldsymbol{\partial S(x,y)}}{\boldsymbol{\partial y}}\frac{\boldsymbol{\partial w}}{\boldsymbol{\partial y}} - \left(\boldsymbol{z - z_n S(x,y)}\right)\frac{\boldsymbol{\partial^2 w}}{\boldsymbol{\partial y^2}} \\ \boldsymbol{\gamma_{xy}} &= \begin{Bmatrix} \left(\dfrac{\boldsymbol{\partial S(x,y)}}{\boldsymbol{\partial y}}\dfrac{\boldsymbol{\partial w}}{\boldsymbol{\partial x}} + \dfrac{\boldsymbol{\partial S(x,y)}}{\boldsymbol{\partial x}}\dfrac{\boldsymbol{\partial w}}{\boldsymbol{\partial y}}\right) \\ \boldsymbol{-2\left(z - z_n S(x,y)\right)}\dfrac{\boldsymbol{\partial^2 w}}{\boldsymbol{\partial x \partial y}} \end{Bmatrix} \end{aligned} \tag{7}$$

On the other hand, for the piezoelectric patches, the strain functions can be written in terms of the plate deflection w as follows:

$$\begin{aligned} \boldsymbol{\epsilon_x} &= \boldsymbol{-\left(z - z_n S(x,y)\right)}\frac{\boldsymbol{\partial^2 w}}{\boldsymbol{\partial x^2}} \\ \boldsymbol{\epsilon_y} &= \boldsymbol{-\left(z - z_n S(x,y)\right)}\frac{\boldsymbol{\partial^2 w}}{\boldsymbol{\partial y^2}} \\ \boldsymbol{\gamma_{xy}} &= \boldsymbol{-2\left(z - z_n S(x,y)\right)}\frac{\boldsymbol{\partial^2 w}}{\boldsymbol{\partial x \partial y}} \end{aligned} \tag{8}$$

Finally, the stresses in the plate and in the piezoelectric patches are respectively.

$$\begin{bmatrix}\boldsymbol{\sigma_x}\\ \boldsymbol{\sigma_y}\\ \boldsymbol{\tau_{xy}}\end{bmatrix}_{\boldsymbol{pel}} = \frac{\boldsymbol{E_{pel}}}{\boldsymbol{1-\nu_{pel}^2}}\begin{bmatrix}\boldsymbol{1} & \boldsymbol{\nu_{pel}} & \boldsymbol{0}\\ \boldsymbol{\nu_{pel}} & \boldsymbol{1} & \boldsymbol{0}\\ \boldsymbol{0} & \boldsymbol{0} & \boldsymbol{\frac{1}{2}(1-\nu_{pel})}\end{bmatrix} \begin{bmatrix}\boldsymbol{-(z-z_n)w_{xx}}\\ \boldsymbol{-(z-z_n)w_{yy}}\\ \boldsymbol{-2(z-z_n)w_{xy}}\end{bmatrix} - \frac{\boldsymbol{d_{31}E_{pel}}}{\boldsymbol{1-\nu_{pel}}}\begin{bmatrix}\boldsymbol{1}\\ \boldsymbol{1}\\ \boldsymbol{0}\end{bmatrix}\boldsymbol{E_{zl}} \tag{9}$$

Where subscript 'pl', 'peu', and 'pel' indicate for plate, upper piezoelectric patch, and lower piezoelectric patch respectively. The bending and twisting moments of the plate are given by:

$$M = M_{pl} + S(x,y)\left(M_{peu} + M_{pel}\right) \tag{10}$$

Where:

$$\begin{bmatrix}M_x\\ M_y\\ M_{xy}\end{bmatrix}_{pl} = \int_{-h/2}^{h/2}\begin{bmatrix}\sigma_x\\ \sigma_y\\ \tau_{xy}\end{bmatrix}_{pl} z\,dz$$

$$\begin{bmatrix}M_x\\ M_y\\ M_{xy}\end{bmatrix}_{peu} = \int_{-(h/2+h_{peu})}^{-h/2}\begin{bmatrix}\sigma_x\\ \sigma_y\\ \tau_{xy}\end{bmatrix}_{peu} z\,dz \tag{11}$$

$$\begin{bmatrix}M_x\\ M_y\\ M_{xy}\end{bmatrix}_{pel} = \int_{h/2}^{h/2+h_{pel}}\begin{bmatrix}\sigma_x\\ \sigma_y\\ \tau_{xy}\end{bmatrix}_{pel} z\,dz$$

Substituting Equations (9) in Equations (11), the following expressions can be written for the bending and twisting moments in terms of the plate deflection w:

$$\begin{aligned} M_x &= \begin{matrix}-D\left(w_{xx}+\nu_{pl}w_{yy}\right)\\ -S(x,y)\begin{pmatrix}\gamma_l-\gamma_u+\\ \left(w_{xx}+\nu_{peu}w_{yy}\right)\beta\\ +\left(w_{xx}+\nu_{pel}w_{yy}\right)\alpha\end{pmatrix}\end{matrix}\\ M_y &= \begin{matrix}-D\left(\nu_{pl}w_{xx}+w_{yy}\right)\\ -S(x,y)\begin{pmatrix}\gamma_l-\gamma_u+\\ \left(\nu_{peu}w_{xx}+w_{yy}\right)\beta\\ +\left(\nu_{pel}w_{xx}+w_{yy}\right)\alpha\end{pmatrix}\end{matrix}\\ M_{xy} &= \begin{pmatrix}-D\left(1-\nu_{pl}\right)\\ -S(x,y)\begin{pmatrix}\left(1-\nu_{\mathrm{peu}}\right)\beta\\ +\left(1-\nu_{\mathrm{pel}}\right)\alpha\end{pmatrix}\end{pmatrix}w_{\mathrm{xy}}\end{aligned} \tag{12}$$

Where β, α, γ_u, and $\gamma_l$are constant expressions defined as follows:

$$\beta = \frac{E_{peu}h_{peu}\begin{pmatrix}4h_{peu}^2 + 6h_{peu}(h+z_n)\\ +3h(h+2z_n)\end{pmatrix}}{12\left(1-\nu_{peu}^2\right)}$$

$$\alpha = \frac{E_{pel}h_{pel}\begin{pmatrix}4h_{pel}^2 + 6h_{pel}(h-z_n)\\ +3h(h-2z_n)\end{pmatrix}}{12\left(1-\nu_{pel}^2\right)}$$

$$\gamma_u = \frac{6E_{peu}h_{peu}d_{31u}\left(h+h_{peu}\right)}{12\left(1-\nu_{peu}\right)}E_{zu} \qquad (13)$$

$$\gamma_l = \frac{6E_{pel}h_{pel}d_{31l}\left(h+h_{pel}\right)}{12\left(1-\nu_{pel}\right)}E_{zl}$$

$$D = \frac{E_{pl}h^3}{12\left(1-\nu_{pl}^2\right)}$$

By substituting the moment expressions Equation (12) into the differential equation of equilibrium for bending of thin plate Equation (14) below:

$$\frac{\partial^2 M_x}{\partial x^2} + 2\frac{\partial^2 M_{xy}}{\partial x \partial y} + \frac{\partial^2 M_y}{\partial y^2} + q_z = \rho h \frac{\partial^2 w}{\partial t^2} \qquad (14)$$

The governing differential equation in terms of the displacement w can be expressed as:

$$\begin{aligned}
&-D\nabla^4 w + \left(S_{xx} + S_{yy}\right)(\gamma_u - \gamma_l)\\
&-\beta\begin{bmatrix}S\nabla^4 w + 2S_x\left(w_{xxx} + w_{xyy}\right)\\ +2S_y\left(w_{yyy} + w_{xxy}\right)\\ +S_{xx}\left(w_{xx} + \nu_{peu}w_{yy}\right)\\ +2\left(1-\nu_{peu}\right)S_{xy}w_{xy}\\ +S_{yy}\left(w_{yy} + \nu_{peu}w_{xx}\right)\end{bmatrix} + q_z\\
&-\alpha\begin{bmatrix}S\nabla^4 w + 2S_x\left(w_{xxx} + w_{xyy}\right)\\ +2S_y\left(w_{yyy} + w_{xxy}\right)\\ +S_{xx}\left(w_{xx} + \nu_{pel}w_{yy}\right)\\ +2\left(1-\nu_{pel}\right)S_{xy}w_{xy} +\\ S_{yy}\left(w_{yy} + \nu_{pel}w_{xx}\right)\end{bmatrix}\\
&\qquad = \rho h\frac{\partial w^2}{\partial t^2}
\end{aligned} \qquad (15)$$

It is worth mentioning here that the first term represents the effect of the host plate, the second term represents the effect of the electric field difference between the two patches, and the third and the fourth terms account for the effect of the upper and lower piezoelectric patches' properties respectively. Various methods for analysis of plates

were developed for arbitrary shapes. However, in many cases, the exact solution cannot be obtained, therefore, numerical methods such as finite element method, finite divided difference, and Galerkin method can be used to get approximate solution.

3 CONCLUSION

An analytical model for a host plate with two piezoelectric patches under the condition of free vibration has been developed and the governed partial differential equation has been derived. The model can be applied to a rectangular plate with any boundary conditions. One of the most important features of this model is that the neutral axis for the host plate is represented by Heaviside step function since it shifted by z_n at patches location. It can also be concluded that if the electric field is zero in both patches then the governing partial differential equation (15) becomes identical to Kirchhoff equation with the effect of material properties of the patches included.

REFERENCES

Balmes E. & Deraemaeker A. (2013). Modeling structures with piezoelectric materials. *SDT tutorial*.

Behjat B., Salehi M., Armin A., Sadighi M. & Abbasi M. (2011). Static and dynamic analysis of functionally graded piezoelectric plates under mechanical and electrical loading. *Scientia Iranica*, *18*(4):986-94.

Cheng L., Zhang H. & Li Q. (2007). Design of a capacitive flexible weighing sensor for vehicle WIM system. *Sensors. 7*(8):1530-44.

Curie J. (1880). Développement par compression de l'électricité polaire dans les cristaux hémièdres à faces inclinées. *Bull Soc Fr Mineral*, 3:90.

Gharib A., Salehi M. & Fazeli S. (2008). Deflection control of functionally graded material beams with bonded piezoelectric sensors and actuators. *Materials Science and Engineering*, A. *498*(1-2):110-4.

Jha A. K. & Kudva J. N. (2004). Morphing aircraft concepts, classifications, and challenges. *Smart Structures and Materials: Industrial and Commercial Applications of Smart Structures Technologies*, International Society for Optics and Photonics.

Munjal B. S. (2015). *Finite element analysis design development of smart skin spacecraft antenna reflectors using intelligent smart materials structural systems*, Gujarat University.

Scheeper P., Gulløv J. O. & Kofoed L. M. (1996). A piezoelectric triaxial accelerometer. *Journal of Micromechanics and Microengineering, 6*(1):131.

Singh A. & Apte D. (2006). Modelling and analysis of hysteresis in piezoelectric actuator. *Defence Science Journal*, *56*(5):825.

Song Y., Yang C. H., Hong S. K., Hwang S. J., Kim J. H., Choi J. Y., et al. (2016). Road energy harvester designed as a macro-power source using the piezoelectric effect. *International Journal of Hydrogen Energy*, *41*(29):12563-8.

Sun D., Tong L. & Atluri S. N. (2001). Effects of piezoelectric sensor/actuator debonding on vibration control of smart beams. *International Journal of Solids and Structures, 38*(50-

51):9033-51.

Tzou H. & Tseng C. (1990). Distributed piezoelectric sensor/actuator design for dynamic measurement/control of distributed parameter systems: a piezoelectric finite element approach. *Journal of sound and vibration*, *138*(1):17-34.

Ueberschlag P. (2001). PVDF piezoelectric polymer. *Sensor review*, *21*(2):118-26.

Voigt W. (1910). *Lehrbuch der kristallphysik*: BG Terebner. Leipzig, 964.

Yando S. (1970). *Piezoelectric voltage generator*. Google Patents.

Cite this article as: Barham W., Bani-Hani K., Mohammad M., "Derivation of the Governing Differential Equation of Vibrating Host Plate with Two Piezoelectric Patches", *International Conference on Civil Infrastructure and Construction (CIC 2020)*, Doha, Qatar, 2-5 February 2020, DOI: https://doi.org/10.29117/cic.2020.0134

Index of Authors

A.

Abd Rahman N. R., 25, 26, 126, 132, 134, 257, 263, 264
Abdelaal A., 27, 356, 363
Abdelatif A. O., 24, 33, 94, 97, 846, 847, 850, 851
Abdeljaber O., 33, 857, 860
Abdel-Jabbar H., 34, 909, 916
AbdelZaher M., 26, 252, 256
Abdi A. M., 25, 122, 125
Abiad M., 29, 487, 494
Abotaleb M. M., 26, 252, 256
AbuTaqa A., 21, 26, 298, 306, 307
Achs G., 34, 943, 950
Afzal M. S., 23, 32, 775, 785, 790, 792, 793
Agiralioglu N., 33, 818, 819, 827
Ahmad H. H., 29, 528, 536
Ahmed T., 28, 452, 461
Aiash A., 26, 288, 297
Akdoğanbulut D., 34, 937, 942
Akhtar H. M., 25, 98, 107
Akinci N., 33, 818, 827
AlAbdulmuhsen S. A. N., 31, 672, 679
Al Alawi M., 24, 65, 74
Al Ansari M., 26, 298, 307
Al Farabi A., 28, 477, 486
Al Ghafri A., 24, 65, 74
Al Kheder S., 26, 288, 297
Al Mamoon A., 30, 621, 627
Al Mamun A., 26, 273, 280
Al Masri Z. A. B., 29, 487, 488, 493, 494 Al Midani D., 35, 979, 988
Al Nass K., 25, 116, 121
Al Nassa K., 33, 861, 868
Al Nuaimi N., 22, 27, 33, 306, 372, 376, 377, 381, 837, 845
Al Rawi N., 30, 609, 618
Al Rukaibi F., 26, 288, 297
Al Shahri M., 24, 65, 74
Alabbasi Y., 27, 308, 310, 314, 315
Al-Ansari M., 22, 32, 777, 784
Alara S. A., 26, 232, 241, 242
Al-Buenain A., 26, 199, 207
Alchamaa R., 32, 740, 741, 747
Al-Emadi K., 29, 30, 553, 559, 560, 565, 574, 581
Al-Emadi K. M. I., 29, 411, 502, 511, 512, 521
Al-Fadala E., 34, 927, 936
Alfahel R., 32, 724, 728, 729, 733
Alfarra M., 30, 628, 633
Al-Gasim Z., 24, 39, 50, 54
Alhajyaseen W., 22, 27, 356, 363
Alhassani Y., 33, 852, 856
Ali M. H. M.M., 29, 502, 511, 512, 521
Al-Jabri K., 35, 997, 998, 1004, 1005
Al-Kheetan M. J., 27, 324, 325, 327, 330, 331, 333
Al-Kuwari M. B.-S., 29, 553, 559
Al-Muhanadi S., 26, 199, 207
Alnahhal W., 33, 794, 799, 837, 845, 857, 860, 910, 915
Alnuaimi N. A., 29, 547, 552, 844
Al-Raoush R., 22, 31, 32, 640, 643, 644, 645, 648, 649, 653, 654, 658, 715, 723
Al-Refaei S., 28, 452, 461
Al-Saudi A., 28, 431, 440
Alshareedah O., 34, 877, 885
Alshibli K., 31, 640, 643, 644, 648
Alshiekh E. T. A. M., 34, 900, 908
Altaher R. S., 28, 452, 461
Al-Tamimi S. A., 28, 403, 412
Al-Tarawneh M., 28, 413, 415, 417, 419
Al-Tawalbeh A., 26, 281, 287
Arewa A., 25, 67, 73, 122, 125
Arewa A. O., 24, 25, 84, 86, 93, 98, 107
Athanasiou A., 35, 1024, 1032
Ayari M. A., 32, 734, 739

B.

Baawain M., 35, 997, 1005
Badri Y., 31, 666, 671
Bani-Hani K., 35, 1033, 1040
Barham W., 35, 1033, 1040
Bawa S., 30, 582, 587
Bendjillali K., 33, 828, 829, 831, 835, 836
Bhuyan M. R.-U.-K., 27, 334, 343
bin Yusoff M. E., 24, 39, 54

C.

Caner A., 34, 937, 942
Cardiño C., 24, 75, 83
Chakraborty T., 28, 477, 486
Chehab G., 21, 29, 487, 493, 494, 495, 500, 501
Chemrouk M., 33, 828, 836
Chronopoulos P., 34, 917, 926
Chrysovergis A., 35, 1024, 1032
Chung H.-W., 27, 316, 323
Cwirzen A., 30, 566, 573

D.

Daoutis G., 35, 960, 968, 969, 974, 975, 978
Dehdezi P., 29, 522, 527
Devang K., 34, 894, 899
Dias C., 21, 27, 356, 363
Djeridane M., 33, 813, 817
Dora G., 31, 659, 665
Dowding S., 35, 975, 978

E.

Ebead U., 3, 5, 20, 32, 33, 761, 762, 768, 769, 770, 772, 775, 776, 777, 783, 784, 785, 786, 789, 791, 792, 793, 794, 800, 801, 805
Eid H., 3, 5, 20, 32, 748, 749, 753
El Gamal S., 34, 877, 884, 885
El Hussien O., 29, 560, 565
Elbeltagi E., 26, 208, 216, 217, 231
El-Hussain O., 29, 30, 553, 559, 574, 581
Elkaseem A., 30, 582, 587
Elmosalmi D., 25, 151, 152, 153, 160, 161
Elshafie M., 22, 32, 748, 753
Elshafie M. Z.E.B., 34, 869, 870, 876
Elshaikh E., 25, 191, 198
Elsherbeny H. A., 24, 55, 56, 62, 63
El-Sherif H., 32, 769, 776
Elshikh M., 26, 208, 216, 217, 231
Eltayeb-Onsa S., 33, 846, 851
Emborg M., 30, 566, 573
Ersenkal D., 35, 960, 968

F.

Fadli F., 34, 35, 927, 936, 979, 988
Fahmy M., 26, 265, 269, 429
Fakhreddine M. N., 29, 487, 494, 495, 501
Fakhroo N. Y., 34, 894, 899
Falamarzi M., 26, 199, 207
Faqih F., 25, 162, 171
Fayyad E. M., 29, 547, 552
Forsat M., 34, 951, 952, 954, 958, 959
Freija O., 30, 609, 618

G.

Ganguli A., 25, 143, 150
Ghachi R. F., 23, 33, 857, 860
Ghaffar S. H., 27, 324, 330, 333
Ghanim M. S., 30, 588, 591, 594, 595, 596, 599, 602, 603
Ghosh S., 27, 28, 382, 392, 393, 402
Girrbach L., 35, 969, 974
Gokasar I., 28, 468, 469, 470, 471, 475, 476
Gokhale S., 34, 894, 899
Gravador-Villamor A. G., 31, 690, 696
Griguta M., 34, 917, 926
Gunay G., 28, 468, 469, 470, 471, 475, 476
Gunduz M., 3, 5, 20, 24, 55, 56, 57, 63, 67,
Gupta A. K., 34, 894, 899

H.

Hadjoudja M., 33, 828, 836
Hafiz M., 32, 724, 727, 728, 729, 732, 733
Haider M., 27, 382, 392
Hamidy M. M., 25, 108, 115
Hamouda A. S., 34, 951, 958, 959
Hannun J., 31, 643, 644, 646, 648
Hashem S., 24, 75, 83
Hassan K. E., 21, 29, 30, 553, 554, 558, 559, 560, 565, 574, 579, 580, 581
Hassan M. K., 29, 547, 552
Hawari A. H., 21, 32, 724, 727, 728, 729, 732, 733, 734, 735, 739, 951, 958
Hedlund H., 30, 566, 573
Himpel F., 28, 431, 440
Hodgson R. J., 28, 412, 448, 451
Hrnjak M., 31, 706, 714
Huang Y., 28, 348, 413, 415, 417, 419
Humza M., 31, 659, 663, 664, 665
Hussein A. G. M., 35, 1006, 1007, 1010, 1015
Hussein M., 3, 5, 20, 27, 31, 308, 315, 666, 671

I.

Ibrahim A., 24, 94, 97
Ibrahim M., 32, 777, 778, 784
Ibrahim M. M., 25, 151, 161
Idris O. E. M., 29, 411, 502, 511, 512, 521
Inuwa I. I., 26, 232, 233, 234, 235, 236, 240, 241, 242
Irshidat M. R., 22, 27, 29, 372, 376, 377, 381, 547, 552
Ismail R., 31, 649, 653, 654, 658

J.

Jarrar Z., 31, 640, 641, 643, 644, 648
Jung J., 31, 640, 643, 644, 648

K.

Kahraman R., 33, 837, 844, 845
Kajewski S., 29, 537, 546
Kalin R., 32, 748, 753
Kara A., 21, 25, 28, 34, 135, 142, 143, 150, 448, 451, 886, 893
Karama A., 26, 243, 251
Karamukova B., 35, 960, 968
Kelly T., 34, 529, 536, 894, 899
Khattak M. J., 27, 28, 334, 342, 343, 420, 430
Khnaizer J., 27, 344, 348, 349, 355
Koluksuz A. F., 25, 172, 177
Konstantis S., 25, 31, 182, 183, 190, 680, 689
Koropoulis S., 35, 960, 968
Kose-Mutlu B., 30, 634, 639
Koyuncu I., 30, 634, 639
Kumar A., 29, 394, 398, 401, 537, 546

L.

Lakhdari M. F., 33, 813, 817
Lakys R., 28, 452, 461

M.

Mahmoud S., 25, 191, 198
Mahmoud S. Y. M., 34, 900, 901, 907, 908
Maina J., 27, 349, 355
Manickam S., 27, 382, 392
Masad E., 21, 26, 28, 273, 274, 279, 280, 441, 447, 494, 509, 510
Mashali A., 26, 208, 216, 217, 231
Massinas S., 25, 31, 182, 183, 190, 680, 689
Mchaweh A., 25, 178, 181
Melilla L., 25, 33, 116, 121, 861, 868
Memon F., 33, 806, 812
Meng N., 35, 1024, 1025, 1032
Meyer L., 25, 135, 142
Miqdad M., 30, 588, 595
Mohamed M. F. F., 35, 1006, 1015
Mohamedain M. H., 30, 574, 581
Mohammad A., 30, 609, 618
Mohammad M., 35, 1033, 1040
Mohammed O., 31, 697, 698, 699, 700, 701, 703, 705
Mohsen M., 26, 159, 160, 298, 299, 306, 307
Motawa I., 26, 208, 216, 217, 231
Muley D., 21, 28, 462, 467
Mumford K. G., 31, 697, 700, 705
Murad Y. Z., 34, 909, 912, 915, 916

N.

Naeem M., 31, 659, 665
Nikolis G., 34, 917, 926
Nishad S., 32, 715, 723
Nosheen A., 25, 98, 107
Nunoo C. N., 28, 403, 405, 412

O.

O'Sullivan B., 32, 748, 753
Oad P., 29, 537, 546
Omar B. A.-S., 28, 452, 461
Ozdemir O., 33, 818, 827
Ozturk I., 33, 818, 827

P.

Papadatos I., 31, 706, 714
Pasaoglu M. E., 30, 634, 639
Peach G., 31, 706, 714
Pearce F., 31, 690, 696
Pistone E., 34, 943, 950

R.

Rabie M., 27, 372, 376, 377, 381
Rabie M. H., 29, 547, 552
Rahman M. M., 27, 324, 330, 331, 333, 486

Rahman N. R. A., 25, 26, 126, 132, 134, 257, 263, 264
Rahman S. S., 28, 296, 420, 430
Renno J., 31, 666, 671
Richli T., 35, 1024, 1032
Roja K. L., 28, 441, 447
Ronald M., 29, 495, 501
Rp R., 28, 393, 402
Rui Y., 34, 869, 870, 876

S.

Saab E., 26, 252, 256
Sadek H., 26, 30, 281, 287, 628, 633
Sadeq M., 26, 30, 274, 280, 281, 287,628, 633
Saleh B., 35, 1016, 1017, 1018, 1022, 1023
Salim S., 27, 372, 376
Santagata E., 29, 502, 503, 504, 508, 510, 511, 512, 517, 521
Sarvi M., 27, 356, 358, 363, 363
Sarwar G., 31, 659, 665
Sassi S., 31, 666, 671
Sayahi F., 30, 566, 567, 568, 569, 570, 571, 573
Sebaaly H., 29, 512, 521
Seiner M., 34, 943, 950
Senin A. A., 24, 39, 54
Senouci A., 26, 298, 307
Shaaban K., 21, 30, 588, 589, 591, 595, 596, 599, 602, 603
Shafieiyoun S., 31, 649, 651, 653, 654, 658
Shoukry H., 35, 997, 1002, 1004, 1005
Sirin O., 3, 5, 20, 26, 273, 280, 505, 511
Sleep B. E., 31, 697, 705
Sohail M. G., 33, 837, 838, 839, 842, 843, 844, 845
Soliman E., 25, 162, 171
Stelmarczyk M., 30, 566, 573
Stollberg R., 32, 748, 753
Subgranon T., 27, 316, 323
Sun Q., 34, 869, 870, 874, 876
Suryan L., 35, 969, 974
Swai L. P., 24, 84, 93

T.

Taha R., 26, 298, 306, 307, 429, 997, 1004
Tahmasseby S., 22, 27, 28, 364, 371, 462, 467
Tahoun T., 34, 886, 893
Tariq A., 32, 734, 739
Tarlochan F., 27, 28, 356, 363, 462, 467
Tia M., 27, 316, 321, 323
Tolba M., 25, 33, 116, 121, 861, 868
Töll H., 34, 943, 950
Tyrer M., 25, 122, 125
Tzaveas T., 35, 989, 996

U.

Ugulu R. A., 24, 25, 84, 93, 122, 125

V.

Vigil H., 31, 706, 714

W.

Wakjira T., 32, 761, 762, 768, 770, 776,
Wasee M., 33, 837, 845
Wink B. W., 28, 462, 467

Y.

Yasir A. T., 32, 734, 739
Yassin M. H., 28, 452, 461
Yeganeh S., 29, 502, 511
Younis A., 33, 761, 769, 772, 794, 795, 800, 801, 802, 803, 805
Yücel M. C., 34, 937, 942
Yuksekdag A., 30, 634, 636, 639

Z.

Zaidi A., 33, 813, 817
Zaki M., 30, 604, 608
Zayed T., 18, 24, 25, 162, 171
Zeytuncu B., 30, 634, 635, 637, 639
Zuzula P., 35, 960, 968

International Conference on Civil Infrastructure and Construction (CIC 2020)

This is the proceedings of the CIC 2020 Conference, which was held under the patronage of His Excellency Sheikh Khalid bin Khalifa bin Abdulaziz Al Thani in Doha, Qatar from 2 to 5 February 2020. The goal of the conference was to provide a platform to discuss next-generation infrastructure and its construction among key players such as researchers, industry professionals and leaders, local government agencies, clients, construction contractors and policymakers.

The conference gathered industry and academia to disseminate their research and field experiences in multiple areas of civil engineering. It was also a unique opportunity for companies and organizations to show the most recent advances in the field of civil infrastructure and construction.

The conference covered a wide range of timely topics that address the needs of the construction industry all over the world and particularly in Qatar. All papers were peer reviewed by experts in their field and edited for publication. The conference accepted a total number of 127 papers submitted by authors from five different continents under the following four themes:

Theme 1: Construction Management and Process
Theme 2: Materials and Transportation Engineering
Theme 3: Geotechnical, Environmental, and Geo-environmental Engineering
Theme 4: Sustainability, Renovation, and Monitoring of Civil Infrastructure

Editors

ISBN 9789927139109

www.cic.qa